ENGINEERING TRANSPORTATION
LIBRARY Indexes

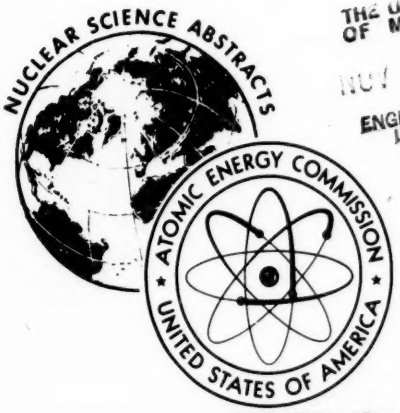

THE UNIVERSITY OF MICHIGAN
NOV 29 1966
ENGINEERING LIBRARY

NUCLEAR SCIENCE ABSTRACTS

Volume 20 Number 20

Abstracts 36542–38541

October 31, 1966

UNITED STATES ATOMIC ENERGY COMMISSION
Division of Technical Information

DEPOSITED BY THE
UNITED STATES OF AMERICA

USAEC DEPOSITORY LIBRARIES

Collections of USAEC reports are maintained in the libraries of the organizations listed below for reference use by the general public. Facilities for making photocopies are available. The USAEC also makes available through these libraries atomic energy reports of countries other than the U. S. that are abstracted in *Nuclear Science Abstracts*.

ALABAMA
Auburn, Auburn University
ALASKA
College, University of Alaska
ARIZONA
Tucson, University of Arizona
ARKANSAS
Fayetteville, University of Arkansas
CALIFORNIA
Berkeley, University of California
Davis, University of California
Los Angeles, University of California
San Diego, Public Library
Stanford, Stanford University
COLORADO
Boulder, University of Colorado
Denver, Public Library
CONNECTICUT
New Haven, Yale University
DELAWARE
Newark, University of Delaware
DISTRICT OF COLUMBIA
Washington, Library of Congress
FLORIDA
Coral Gables, University of Miami
Gainesville, University of Florida
Tallahassee, The Florida State University
GEORGIA
Atlanta, Georgia Institute of Technology
HAWAII
Honolulu, University of Hawaii
ILLINOIS
Chicago, John Crerar Library
Chicago, University of Chicago
Evanston, Northwestern University
Urbana, University of Illinois
INDIANA
Bloomington, Indiana University
Lafayette, Purdue University
IOWA
Ames, Iowa State University
KANSAS
Manhattan, Kansas State University
KENTUCKY
Lexington, University of Kentucky
Louisville, University of Louisville
LOUISIANA
Baton Rouge, Louisiana State University
New Orleans, Tulane University
MARYLAND
Baltimore, Johns Hopkins University
College Park, University of Maryland
MASSACHUSETTS
Cambridge, Harvard University
Cambridge, Massachusetts Institute of Technology
MICHIGAN
Ann Arbor, University of Michigan
Detroit, Public Library
East Lansing, Michigan State University
MINNESOTA
Minneapolis, University of Minnesota
MISSISSIPPI
State College, Mississippi State University
MISSOURI
Kansas City, Linda Hall Library
Rolla, University of Missouri School of Mines and Metallurgy
St. Louis, Washington University
MONTANA
Bozeman, Montana State College
NEVADA
Las Vegas, Nevada Southern University
Reno, University of Nevada
NEW JERSEY
Princeton, Princeton University
Teaneck, Fairleigh Dickinson University
NEW MEXICO
Albuquerque, University of New Mexico
NEW YORK
Albany, The University of the State of New York
Buffalo, State University of New York at Buffalo
Ithaca, Cornell University
New York, Atomic Industrial Forum, Inc.
New York, Columbia University
New York, New York University
Rochester, University of Rochester
Schenectady, Union College
Syracuse, Syracuse University
Troy, Rensselaer Polytechnic Institute
NORTH CAROLINA
Charlotte, Public Library of Charlotte and Mecklenburg County
Durham, Duke University
Raleigh, North Carolina State College
NORTH DAKOTA
Grand Forks, University of North Dakota
OHIO
Cincinnati, University of Cincinnati
Cleveland, Public Library
OHIO (CONT.)
Columbus, Ohio State University
Toledo, University of Toledo
Youngstown, Youngstown University
OKLAHOMA
Norman, University of Oklahoma
Stillwater, Oklahoma State University
OREGON
Corvallis, Oregon State University
Portland, Reed College
PENNSYLVANIA
Philadelphia, University of Pennsylvania
Pittsburgh, Carnegie Library
University Park, Pennsylvania State University
PUERTO RICO
Rio Piedras, University of Puerto Rico
RHODE ISLAND
Providence, Brown University
SOUTH CAROLINA
Columbia, University of South Carolina
TENNESSEE
Knoxville, University of Tennessee
Memphis, Public Library
Nashville, Joint University Libraries
Oak Ridge, Oak Ridge Associated Universities
TEXAS
Austin, University of Texas
College Station, Texas A & M University
Dallas, Southern Methodist University
Houston, Rice University
Lubbock, Texas Technological College
San Antonio, Public Library
UTAH
Salt Lake City, University of Utah
VIRGINIA
Blacksburg, Virginia Polytechnic Institute
Charlottesville, University of Virginia
Norfolk, Old Dominion College
WASHINGTON
Pullman, Washington State University
Seattle, University of Washington
WEST VIRGINIA
Morgantown, West Virginia University
WISCONSIN
Madison, University of Wisconsin
Milwaukee, Public Library
WYOMING
Laramie, University of Wyoming

DEPOSITED BY THE
UNITED STATES OF AMERICA

Volume 20, Number 20, October 31, 1966

NUCLEAR SCIENCE ABSTRACTS

A semimonthly publication of the USAEC Division of Technical Information, Edward J. Brunenkant, Director. Published by the USAEC Division of Technical Information Extension, Robert L. Shannon, Extension Manager.

Nuclear Science Abstracts covers the international literature on nuclear science and technology and provides the only comprehensive abstracting and indexing of this body of information. Published twice each month since 1947, *NSA* covers technical reports of the U. S. Atomic Energy Commission and its contractors, technical reports of U. S. Government agencies and other governments, universities, industrial and research organizations, as well as patents, books, and journal literature on a world-wide basis. Nearly 350,000 abstracts have appeared in *NSA* through Volume 19. The subject matter covered in *NSA* is described in issue Number 1 and in TID-4552, *Subject Scope of Nuclear Science Abstracts*, available free from the U. S. Atomic Energy Commission, Division of Technical Information Extension, P. O. Box 62, Oak Ridge, Tennessee 37830.

Abstracts are arranged according to a number of subject categories and subcategories. Definitions of categories appear in issues Number 1 and 13. If the language of the original item is not English, the language will be indicated. Translations are not abstracted where an abstract of the original item has appeared in *NSA*.

INDEXES TO NSA

Corporate author, personal author, subject, and report number indexes appear in each issue and are cumulated quarterly, semiannually, and annually. Multi-volume cumulations have been issued as indicated on the following page. Report number indexes for all volumes (1–18) were issued at the end of Vol. 18. At the end of Vol. 19, the indexes for Vols. 1–15 were reissued to include additional public availability information. This cumulation will be a permanent shelf item and will not be reissued. Report number indexes for Vol. 19 are included as a cumulation beginning with Vol. 16.

AVAILABILITY OF PUBLICATIONS ABSTRACTED

The public availability of all U. S. Atomic Energy Commission reports is indicated in the report number indexes. The availability of other reports, when known, is also indicated. The availability of some unnumbered reports is given in the abstract.

Dissertations abstracted in *Dissertation Abstracts* and included in *NSA* are available from University Microfilms, Inc., 315 N. First Street, Ann Arbor, Michigan 48103.

Most of the published literature abstracted in *NSA* is on deposit at the Library, Oak Ridge Associated Universities, Oak Ridge, Tennessee, (a USAEC depository library) and is available through interlibrary loan. When requesting papers from this source, it is important that *NSA* volume and abstract number be cited.

HOW TO OBTAIN NUCLEAR SCIENCE ABSTRACTS

NSA is available on an exchange basis to universities, research institutions, industrial firms, and publishers of scientific information. Inquiries should be directed to the U. S. Atomic Energy Commission, Division of Technical Information Extension, P. O. Box 62, Oak Ridge, Tennessee 37830.

Government agencies may obtain *NSA* free of charge.

NSA is available to the general public on a subscription basis from the Superintendent of Documents, U. S. Government Printing Office, Washington, D. C. 20402, as follows:

For the 24 regular issues, $30.00 domestic, $37.00 foreign. A single issue costs $1.75, plus 25 per cent for foreign mailing. Domestic rates apply to the United States, Canada, Mexico, and Central and South American countries except Argentina, Brazil, Guyana and French Guiana, Surinam, and British Honduras. Foreign rates apply to the countries excepted above and to all other countries throughout the world.

For the quarterly, semiannual, and annual indexes, $22.00 domestic, $25.00 foreign.

Multivolume subject and author indexes are available as follows:

Vols. 1–4 (1948–1950) Johnson Reprint Corporation, 111 Fifth Avenue, New York, N. Y. 10003, $30.00.

Vols. 5–10 (1951–1956) Superintendent of Documents, U. S. Government Printing Office, Washington, D. C. 20402, $5.25.

Vols. 11–15, Subjects, Superintendent of Documents, U. S. Government Printing Office, Washington, D. C. 20402, $19.00.

Vols. 11–15, Personal Authors, Superintendent of Documents, U. S. Government Printing Office, Washington, D. C. 20402, $14.25.

Vols. 11–15, Corporate Authors, Superintendent of Documents, U. S. Government Printing Office, Washington, D. C. 20402, $2.50.

Cumulative Report Number Index, Vols. 1–15, Revised, is available from the Superintendent of Documents, U. S. Government Printing Office, Washington, D. C. 20402, $4.00.

Cumulative Report Number Index, Vols. 16–19, is available from the Superintendent of Documents, U. S. Government Printing Office, Washington, D. C. 20402, $2.50.

Annual Indexes are available separately from the U. S. Government Printing Office as follows:

Vol. 16, Subject and Authors, $9.75.
Vol. 17, Subject and Authors, $12.25.
Vol. 18, Subject and Authors, $12.50.
Vol. 19, Subject and Authors, $12.50.

ACKNOWLEDGMENTS

Agreements between the United States Atomic Energy Commission and the following organizations with regard to providing continuing services and specific literature coverage for *Nuclear Science Abstracts* are gratefully acknowledged:

American Institute of Physics; Atomic Energy of Canada Limited; Atomic Energy Research Establishment, United Kingdom; European Atomic Energy Community (EURATOM); Gmelin Institute; International Atomic Energy Agency; Japan Atomic Energy Bureau — Japan Atomic Energy Research Institute; Netherlands Patent Office; Reactor Centrum Nederland.

TABLE OF CONTENTS

Volume 20, Number 20, October 31, 1966

Category	Page
BIOLOGY AND MEDICINE	4421
General	4421
Ecology	4422
Metabolism, Tissue Distribution, and Toxicology	4423
Radiation Effects on Biochemicals	4427
Radiation Effects on Tissues	4430
Radiation Effects Therapy and Countermeasures	4440
Radiation Hazards and Protection	4441
Radiotherapy and Radiodiagnosis	4442
CHEMISTRY	4446
General	4446
Analytical Procedures	4446
Inorganic and Physical Chemistry	4454
Organic Chemistry	4462
Radiation Chemistry	4463
Radiochemistry	4471
Separation Processes and Procedures	4473
ENGINEERING	4477
General	4477
Applications of Nuclear Explosions	4477
Facilities and Equipment	4479
Heat Transfer and Fluid Flow	4480
Materials Testing	4482
Protective Structures	4482
Space Propulsion	4482
Vacuum Engineering	4482
GEOLOGY, METEOROLOGY, AND MINERALOGY	4483
General	4483
Meteorology	4483
Natural Radioactivity and Fallout	4483
Techniques and Equipment	4484
HEALTH AND SAFETY	4487
INSTRUMENTATION	4490
General	4490
Radiation Detection	4492
Radiation Effects	4500
ISOTOPE TECHNOLOGY	4501
General	4501
Industrial Applications	4501
Power Application	4503
Separation and Production	4504
MATHEMATICS AND COMPUTERS	4505
METALS, CERAMICS, AND OTHER MATERIALS	4506
General	4506
Corrosion	4507
Fabrication	4509
Properties and Structure	4510
Radiation Effects	4518
PHYSICS	4522
General	4522
Accelerators	4523
Astrophysics and Cosmology	4526
Atomic Physics	4536
Cosmic Radiation	4541
Direct Energy Conversion	4574
Elementary Particles and Radiations	4575
Field Theory, Scattering Theory, and Symmetries	4584
Fluid Physics and Thermodynamics	4588
Geophysics	4590
Gravitation, Quantum Mechanics, and Relativity Theory	4595
Low Temperature Physics	4597
Neutron Physics	4603
Nuclear Properties and Reactions	4606
Plasma Physics and Thermonuclear Processes	4628
Shielding	4647
Solid State Physics	4648
REACTOR TECHNOLOGY	4656
General	4656
Auxiliaries and Components	4656
Criticality Studies	4657
Design and Feasibility	4661
Fuels	4662
Power and Power-Breeder Reactors	4665
Process Heat Reactors	4670
Propulsion and Space	4670
Research and Test Reactors	4670
WASTE DISPOSAL AND PROCESSING	4672
GENERAL AND MISCELLANEOUS	4673
CORPORATE AUTHOR INDEX	INDEX-1
PERSONAL AUTHOR INDEX	INDEX-7
SUBJECT INDEX	INDEX-55
REPORT NUMBER INDEX	INDEX-134

STAFF OF NUCLEAR SCIENCE ABSTRACTS

MANAGING EDITOR

John W. Norris

ASSISTANT MANAGING EDITOR

Donald D. Davis

ASSOCIATE EDITORS

Lawrence T. Whitehead
David E. Bost
Robert C. Kelly
Lee M. Thompson

SUBJECT INDEX EDITOR

Everett J. Hoffman

EVALUATORS

William D. Matheny
John H. Mitchell
Mary H. Newman

ABSTRACTORS

F. S. Armstrong (AECL)
Jane G. Buchanan
D. Lamar Cason
Bennie G. Di Bona
Helen G. Donald
James R. Dulaney
Wells L. Green
Mary Catherine Grissom
Fernando J. Hamilton
Phyllis C. Hansen
Carolyn D. Houston
Rose V. Jermain
Betty L. McDowell
Jean F. Peckham
Mona H. Raridon
Julia S. Redford
Francis L. Sachs
Lila B. Smith
Charles E. Stuber
Martha J. Thomas
Anne G. Ward
David C. West
Milton O. Whitson
Gabriel O. Ycaza

SUBJECT HEADING SPECIALIST

Robert E. Upchurch

CORPORATE AUTHOR SPECIALIST

Clara L. Fox

DESCRIPTIVE CATALOGING SPECIALIST

J. Paul Meredith

SCHEDULING AND PUBLISHING COORDINATOR

Brainard L. Patton

Communication concerning the editorial policy and content of *NSA* should be addressed to the Managing Editor, *Nuclear Science Abstracts*, AEC Division of Technical Information Extension, P. O. Box 62, Oak Ridge, Tennessee 37830.

Use of funds for printing this publication approved by the Director of the Bureau of the Budget, June 28, 1966.

Volume 20, Number 20 October 31, 1966

NUCLEAR SCIENCE ABSTRACTS

BIOLOGY AND MEDICINE

General

36542 DETERMINATION OF SILICON BY ACTIVATION ANALYSIS, USING A NEUTRON GENERATOR, IN THE SPUTUM OF SILICOTIC PATIENTS. Sardi, Andras; Tomcsanyi, Attila. Atomtech. Tajek., 9: 301-6(1966). (In Hungarian).

It was assumed, although not yet proven, that the sputum of tubercular and silicotic patients differ sufficiently to allow diagnosis on the basis of silicon content. A method was developed to determine silicon by activation analysis, using the 14-Mev neutrons from a neutron generator and taking advantage of the 220-mbarn cross section $^{28}Si(n,p)^{28}Al$ nuclear reaction. The complete fast-neutron activation analysis may be carried in about 15 minutes, under conditions of high sensitivity. The sputum specimens were treated with trypsin and formic acid, acidified with trichloroacetic acid, taking care to remove all of the soluble phosphorus. The treated samples were placed in a polyethylene cylinder and activated at a dose rate of 2×10^9 n/sec for 2.3 minutes, measuring the activity by means of a NaI(Tl) crystal and a 128-channel analyzer at the 1.78 peak. The activity of Si in the specimens obtained from silicotic patients was more than twice higher than that of other patients. In view of the small number of patients tested, no definite conclusions were drawn. (TTT)

36543 CRITICAL VARIABLES IN THE RADIOIMMUNOASSAY OF SERUM INSULIN USING THE DOUBLE ANTIBODY TECHNIC. Soeldner, J. Stuart; Slone, D. (Harvard Medical School, Boston). Diabetes, 14: 771-9 (Dec. 1965).

A modification of the double antibody immunoassay method using ^{131}I-insulin, as described by Morgan and Lazarow, confirmed the presence of an inhibitor in serum and plasma which delays the rate at which the ^{131}I-insulin-insulin antibody complex is rendered insoluble by rabbit serum containing antibodies to guinea pig globulin. Serum dilution reduces the effect of the inhibitor but increases dilutional error. Heparin similarly reduces the effect of the inhibitor, but excess heparin produces falsely low values for immunoreactive insulin (IRI). Data are presented for serum which show that if sufficient time (72 hr) is allowed to elapse after the addition of the precipitating antibody (rabbit anti-guinea pig globulin serum), the precipitating system reaches equilibrium. Employing this modification, additional data are presented, showing excellent recovery of human insulin added to serum, good duplication of respective serum IRI values in repeat assays, and constancy of fasting serum IRI in any one individual on repeated sampling. Normal adults exhibit fasting values of serum IRI from 1 to 20 μU/ml with a mean of 8.4 μU/ml, and after rapid intravenous injection of glucose, serum IRI usually reaches max levels in one to two min. (BBB)

36544 TRACER THEORY: A REVIEW. Bergner, Per-Erik E. (Oak Ridge Associated Universities, Inc., Tenn.). Isotop. Radiat. Technol., 3: 245-62(Spring 1966).

The theory, methods, and problems of tracer applications are reviewed with emphasis on biomedicine, although many of the conclusions may be valid for other scientific fields and for industry. The mathematics for general cases and the approach to some applications are outlined. Attempts are made to recognize basic problems rather than to give laboratory methods. The communications gap between theory and practice is discussed; several fundamental problems are described, which require solutions before completely reliable methods can be developed. (auth)

36545 BIOSYNTHESIS OF HIGHLY LABELED ACTINOMYCINS. Katz, Edward; Mauger, Anthony B.; Weissbach, Herbert (Georgetown Univ. Schools of Medicine and Dentistry, Washington, D. C.). Mol. Pharmacol., 1: 107-9(July 1965).

Recent interest in the mechanism of action of actinomycin as an inhibitor of the DNA-dependent RNA synthesis and its use as an antitumor agent indicate the need for actinomycin of high specific activity for use in biochemical and pharmacologic studies. The synthesis of tritiated actinomycin having a specific activity of 80,000 cpm/μg was accomplished by growing Streptomyces antibioticus in the presence of methyl labeled L-methionine. L-Methionine was selected as precursor since it is the source of the methyl groups of sarcosine, N-methyl-L-valine and the actinomycin chromophore. There are 2 moles each of sarcosine and N-methyl-L-valine per mole of actinomycin as well as two methyl groups per mole of the chromophore; thus 6 moles of methionine are required for synthesis of 1 mole of antibiotic. Mycelial suspension was used to inoculate 250-ml Erlenmeyer flasks containing 100 ml of glutamic acid-galactose-mineral salts medium, which was incubated for 42 hr at 30°. Chloramphenicol was then added to inhibit protein synthesis and to enhance actinomycin formation. Immediately afterward, 0.5 ml of L-methionine-methyl-^3H (750 μC, 3 μmoles) was added to the flasks, and the cultures were reincubated for an additional 2 hr. The same concentration of radioisotope was then added again followed by a similar incubation period. Extraction of the culture medium with ethyl acetate under neutral or slightly alkaline conditions was used as a highly specific method for the isolation of actinomycin. This was established by paper chromatographic and crystallization procedures. No radioactive substances other than actinomycins I, IV, and V were detected. The high specific activity of the material should be of value in elucidating the mechanism of action, tissue distribution, and metabolism of this agent. (BBB)

36546 VIABILITY OF PRESERVED BONE MARROW CELLS. Nicolau, C. T.; Apateanu, V.; Grigoriu, G. (Centrul de Hematologie, Bucharest). pp 239-42 of

Proceedings of the 10th Congress International Society of Blood Transfusion, Stockholm, 1964. Basel, S. Karger, 1965. (In French).

The viability of bone marrow cells was studied in 15 cancer patients in whom hematopoiesis had been depressed by chemotherapy. To measure the regenerative capacity of autologous marrow stored in glycerin at –80°C, four tests were used: motility of stored ram spermatozoa frozen and thawed at the same time as the samples of autologous bone marrow; rat-mouse heterotransplantation with frozen rat myelocytes thawed at the same time as the samples of autologous human marrow; failure of living cells to stain with trypan blue; and increase in the number of leukocytes and reticulocytes after readministration of stored autologous marrow. In the second method the rat bone marrow cells, frozen in 15% glycerin, were injected intravenously in mice given 900-R whole-body doses of radiation. In seven patients hematologic values were studied intensively to assess restoration of hematopoiesis. In six of the seven patients, a post-transfusion rise in megakaryocytes was noted and in three cases a rise in leukocyte levels was seen 10 to 14 days after the transfusion. Techniques for preservation of bone marrow at low temperatures are described. (BBB)

36547 SVERKHSLABYE SVECHENIYA PRI BIOKHIMICHESKIKH REAKTSIYAKH. (Very Faint Luminescence in Biochemical Reactions). Vladimirov, Yu. A. Moscow, Izdatel'stvo Nauka, 1966. 103p.

A survey is given of molecular mechanisms in bioluminescence, and of chemiluminescence in base-catalyzed autoxidation reactions and in the oxidation of organic substances. Mitogenetic radiation and very faint luminescence of homogenates and mitochondria are discussed as well as the luminescence produced by reverse photochemical reactions in generation of quanta in biological systems. (215 references.) (R.V.J.)

Ecology

36548 (TID–23036) BIOCLIMATIC AND SOILS INVESTIGATIONS IN FOREST ENVIRONMENTS. VIII. RADIOLOGICAL INVESTIGATIONS AT NEOTOMA. Gilbert, Gareth E.; Laughlin, Ronald L. (Ohio Agricultural Experiment Station, Wooster. Dept. of Botany and Plant Pathology. Ohio State Univ., Columbus). Aug. 1964. Contract AT(11-1)-552. 28p. Dep. mn. CFSTI $2.00 cy, $0.50 mn.

Data are presented on the content and distribution of ^{90}Sr in soil samples collected at depths of 1 to 3 in. or 6 to 9 in. at various habitats of Neotoma Valley, Hocking County, Ohio, in 1958, 1959, 1962, and 1964. Data are included on the total γ activity and content of fallout fission products in samples of lichens, herbaceous plants, woody plants, fruits, and leaf litter collected in 1962 and 1964. (C.H.)

36549 FRACTIONATION OF THE STABLE ISOTOPES OF CARBON AND OXYGEN IN MARINE CALCAREOUS ORGANISMS: THE ECHINOIDEA. PART I. VARIATION OF ^{13}C AND ^{18}O CONTENT WITHIN INDIVIDUALS. Weber, Jon B. (Pennsylvania State Univ., University Park); Raup, David M. Geochim. Cosmochim. Acta, 30: 681-703 (July 1966).

A systematic study of the distribution of ^{13}C and ^{18}O in the calcite skeletons of recent sea urchins and sand dollars has demonstrated that these animals fractionate both carbon and oxygen isotopes to a considerable extent. Systematic variation of $\delta^{13}C$ within a single skeleton may amount to as much as 13 per mil. In general, the coronal plates of the test are greatly enriched in ^{12}C with respect to the spines, but the isotopic compositions of the spines are similar to those of most other marine invertebrates, such as the mollusk, foraminifera etc. The different morphological parts of the echinoid lantern differ in $\delta^{13}C$ and $\delta^{18}O$ values to the extent of several per mil; $\delta^{13}C$ and $\delta^{18}O$ for these parts are strongly correlated, suggesting incorporation of varying amounts of CO_3^{2-} of different isotopic composition from different sources, perhaps from mixtures of metabolic CO_2 and seawater bicarbonate in varying proportions. Variation in the degree of isotope fractionation during growth appears to be relatively small. (P.C.H.)

36550 FRACTIONATION OF THE STABLE ISOTOPES OF CARBON AND OXYGEN IN MARINE CALCAREOUS ORGANISMS: THE ECHINOIDEA. PART II. ENVIRONMENTAL AND GENETIC FACTORS. Weber, Jon N. (Pennsylvania State Univ., University Park); Raup, David M. Geochim. Cosmochim. Acta, 30: 705-36 (July 1966).

The carbon and oxygen isotopic composition of the calcite skeletons of recent sea urchins and sand dollars has been determined for representatives of all major taxonomic groups. The specimens comprise a world-wide sampling of the class Echinoidea in which polar to tropical and littoral to abyssal dwellers are included. Although the spines differ relatively little in isotopic composition, large variations in $\delta^{13}C$ (up to 13 per mil) and $\delta^{18}O$ for the tests and parts of the echinoid lantern are apparent. $^{13}C/^{12}C$ and $^{18}O/^{16}O$ for individuals of a single species from a given locality, for different species from the same locality, and for the same species from different localities, in conjunction with depth and temperature data, show that the degree of isotope fractionation is largely genetically controlled, although the effect of temperature is detectable, especially in the case of $^{18}O/^{16}O$. Carbon and oxygen isotope ratios are correlated with crystallographic data and the application of this information to phylogenetic problems is discussed with two examples: the question of a polyphyletic ancestry of the order Echinoida, and inhomogeneity in the order Cidaroida. (auth)

36551 PREDICTED SEASONAL RADIOSENSITIVITY OF SOUTHEASTERN TREE SPECIES. Taylor, F. G. Jr. (Oak Ridge National Lab., Tenn.). Contract W-7405-eng-26. Radiat. Bot., 6: 307-11 (Aug. 1966). (ORNL-P-1870).

Vegetative shoot apices of 14 tree species at Oak Ridge, Tennessee, were studied for 1 year (1964). The average interphase nuclear volumes, estimated interphase chromosome volumes and ratios of volumes in actively growing to dormant plants were determined. Results indicate that the predicted range in sensitivity between species for any month, approximately a 17-fold range, is constant even though the predicted sensitivity of individual species changes with respect to time. (auth)

36552 DISTRIBUTION OF CHROMIUM IN MARINE ORGANISMS. Fukai, Rinnosuke; Broquet, Daniele (IAEA, Monaco). Radioact. Sea, No. 16, 1-19(1965).

Trace amounts of chromium were determined in various types of marine organisms, and on the basis of the results some conclusions were drawn about the behavior and distribution of chromium in marine biota. In the majority of cases, the chromium content for various seaweeds was in the range of 0.4 to 2.5 μg Cr per gram of dry matter. Variations in the chromium content of seaweeds did not exhibit any definite dependence on species, seasons, or locations. Polychaetes, in general, seemed to have a high chromium content. With some exceptions, at least part of the chromium in crustacea, mollusks, echinoderms, and fish may be considered as having been introduced into their metabolic cycles. The "standard abundance" of chromium was estimated for various groups of marine organisms. (auth)

36553 CHEMICAL COMPOSITION OF SHALLOW-WATER SEDIMENTS IN THE BAY OF ROQUEBRUNE. Fukai, Rinnosuke (IAEA, Monaco). Radioact. Sea, No. 17, 1-15(1965).

In order to obtain basic data for the dynamic study of the behavior of radionuclides in marine environments, chemical analyses of various constituents were carried out on marine sediments taken from the Bay of Roquebrune. On the basis of the results obtained, some considerations were made on the main chemical components of the sediments and the behavior of trace elements in marine environments. At the same time leaching experiments were carried out on the sediments with a view to obtaining preliminary information about mineralogical forms of some of the metallic ele-

ments in the sediments. The sediments distributed in the Bay of Roquebrune can be considered to be composed of organic matter and the debris of silicate (accompanied by aluminum, iron, and potassium) and carbonate (associated with calcium, magnesium, and sodium) minerals, the latter of which includes those of biological origin. There are some indications that iron is accompanied by chromium, and manganese by copper and zinc, and probably by cobalt. (D.H.M.)

Metabolism, Tissue Distribution, and Toxicology

Refer also to abstracts 36643 and 36921.

36554 (LA-DC-7305) COMPARATIVE METABOLISM OF RADIONUCLIDES IN MAMMALS. III. RETENTION OF ^{54}Mn BY FOUR MAMMALIAN SPECIES. Furchner, J. E.; Richmond, C. R.; Drake, G. A. (Los Alamos Scientific Lab., Univ. of California, N. Mex.). [1964]. Contract W-7405-eng-36. 32p. Dep. mn. CFSTI $2.00 cy, $0.50 mn.

Radiomanganese (^{54}Mn) was administered to mice and rats by the oral, intravenous, and intraperitoneal routes and to dogs and monkeys by the oral and intravenous routes. Whole-body counting techniques, utilizing 4π liquid scintillation counters, were used to determine whole-body retention parameters. Retention functions consisting of the sum of three or four exponential expressions were adequate descriptions of retention until the body burden was less than 1 percent of the administered dose. The longest effective half-times after intravenous injections were 119, 146, 99, and 68 days for mice, rats, monkeys, and dogs, respectively. Tissue distribution studies in rats showed that, for most tissues, concentration as a function of time roughly paralleled whole-body retention. Both bone and brain were found to have a slower rate of loss than other tissues. Using a parabolic relation between body weights and the integrals of the retention functions, it was estimated that 7×10^{-3} μCi/ml was the maximum permissible concentration in water for man. This value is in good agreement with the current ICRP recommended value of 8×10^{-3}. (auth)

36555 (NYO-2643-22) AN INVESTIGATION ON THE MECHANISMS AND REGULATIONS OF NUCLEIC ACID AND PROTEIN SYNTHESIS, AND THEIR POSSIBLE RELATIONSHIP TO RADIATION DAMAGE. Progress Report, September 1, 1965–August 31, 1966. Zamecnik, Paul C.; Gardella, Joseph W. (John Collins Warren Labs., Massachusetts General Hospital, Boston). June 22, 1966. Contract AT(30-1)-2643. 51p. Dep. mn. CFSTI $3.00 cy, $0.50 mn.

Progress is reported in tracer studies of control mechanisms and regulators of nucleic acid and protein synthesis. Topics discussed include the structure of transfer RNA; activation reactions for protein synthesis; the chemical modification of enzyme systems controlling nucleic acid and protein synthesis; the fractionation of transfer RNA; the effects of uv radiation on the formation of transfer RNA in E. coli; the synthesis of RNA in regenerating rat liver; and effects of virus infection on the synthesis of RNA in cultured chick embryo cells. A list is included of 17 publications during the period covered by this report. (C.H.)

36556 DECORPORATION OF RADIOSTRONTIUM: RADIOACTIVE ASSAY TECHNIQUES. AN EXPERIMENTAL STUDY ON MICE. Setaelae, Kai (Univ. of Helsinki). Acta Radiol., Suppl. 241, 1-61(1965).

A description is given of assay techniques designed for long-term quantitative follow-up determination of radiostrontium (^{90}Sr, and ^{85}Sr + ^{89}Sr) accretion into, topographic distribution within, and removal from, the bone of live mice. The assemblies and different radiation detector systems that were constructed for quantitative determination of radiostrontium are also described. Both in vitro and in vivo investigations are discussed. The in vivo calibration studies revealed that intragastrically instilled radiostrontium spontaneously and in a rapid manner declines below the detection limit of the assemblies. (77 references). (P.C.H.)

36557 ACTION OF HISTAMINE LIBERATORS ON CALCIFICATION PRODUCED BY VARIOUS METALS. Serafimov, N.; Tuchweber, B.; Gabbiani, G.; Jean, P.; Selye, H. (Univ. of Montreal). Arch. Int. Pharmacodyn., 154: 251-62(Apr. 1965).

The relation between various histamine liberators (dextran, dextrin, Compound 48/80, polymyxin, viomycin) and calcergens (lead, cerium, lanthanum, indium, and zinc compounds) were studied in rats by varying doses and injection sites. Rats were injected intravenously with $CeCl_3$ (3 mg), $InCl_3$ (0.5 mg), $LaCl_3$ (7.5 mg), Pb acetate (7.5 mg), and $ZnCl_2$ (2 mg) dissolved in 1 ml of water. Immediately afterwards, three different doses of polymyxin were administered in 0.2 ml of Tyrode solution subcutaneously in the right dorsal (1 μg), left lumbar (10 μg), and right lumbar (50 μg) regions. Of the five calcergens, only lead acetate induced calcification at the polymyxin injection sites. Following treatment with this compound, as little as 1 μg of polymyxin produced massive calcification in the skin and subcutis. When calcergens and other histamine liberators were injected systemically, only lead acetate elicited a calcifying anaphylactoid reaction. Similarly, in rats given subcutaneous injections of various histamine liberators, topical calcification at the injection site occurred only following intravenous injection of lead acetate, not of other calcergens. It could be shown that, after intravenous administration of lead acetate, calcinosis occurred in different parts of the body, depending upon the type of histamine liberator administered systemically and the route of its administration. Presumably, systemically administered histamine liberators can act selectively upon certain regions and thereby elicit specific organotropic effects, depending upon the type of agent used and the route of administration. (BBB)

36558 ^{90}Sr EXCRETION FROM THE BLOOD STREAM INTO THE GASTRO-INTESTINAL TRACT IN RATS. Zalikin, G. A. Byull. Eksp. Biol. Med., 61: No. 5, 67-9 (May 1966). (In Russian).

Experiments were carried out on 49 albino rats subdivided into three groups: in rats of the first group excretion was determined under normal conditions, in the other two groups laparotomy was carried out before poisoning and ligatures were applied, without damaging the mesenteric vessels, to provide artificial obstruction between various portions of the digestive tract. It was found that in the case of a single intravenous injection of strontium-90 to rats the most intensive excretion took place in the small intestine within 2–6 hours after injection of the isotope. (auth)

36559 NATURAL RADIOACTIVITY OF SKELETONS IN LEUKEMIA CASES. Leonov, V. A.; Pavlova, M. P. (Minsk Inst. of Medicine). Dokl. Akad. Nauk BSSR, 10: 339-40(May 1966). (In Russian).

The radioactivity of portions of the skeletons of 39 patients, including 7 children, who died of leukemia was determined by a highly sensitive instrument. It was found that the β and γ activity of the sternum of traumatized individuals amounted to an average of 132.4 pulses/min, or 0.543×10^{-10} C/100 g, while the sternum of leukemia victims, especially children, exhibited a higher activity. For children, the activity was 431.6 pulses/min, or 1.9×10^{-10} C/100 g and for the 22 to 54-year old group, 202.6 pulses/min, or 0.91×10^{-10} C/100 g. For aleukemic leukemia cases, the activity was reduced to 93.5 pulses/min, or 0.35×10^{-10} C/100 g, exhibiting similarities with the panmyelophthysis group. There are thus two separate groups of leukemia patients, depending on whether the β and γ activity of the skeleton is increased or decreased; this is probably related to mitotic activity in bone marrow. (TTT)

36560 ROOT EXTENSION IN A LONGLEAF PINE PLANTATION. Ferrill, Mitchell D. (Univ. of Connecticut, Storrs); Woods, Frank W. Contract AT(40-1)-2790. Ecology, 47: 97-102(Winter 1966).

A radioisotope method employing ^{131}I was developed to measure root extension, without disturbing the tree roots by excavation, at different depths in a longleaf pine plantation in the sandhills of North Carolina. Root extension is the straight line distance from the tree to the point of isotope application and not the total root length. Radioiodine was applied at three soil depths. Surrounding trees were monitored with a portable scintillation counter to determine whether roots had absorbed ^{131}I from the volume of soil treated at the point of application and translocated it to the tree in sufficient quantities to be detected. If the tree became radioactive, it was assumed that it had root connections with the volume of soil treated. The soil was sterilized with methyl bromide gas to kill roots at the point of application before the isotope was applied. Isotopes are absorbed much more rapidly by dead than by living roots, apparently because of the increased amount of passive absorption which results after destruction of the differentially permeable membranes. After application of 10 mC of ^{131}I directly to the soil, on the surface, or at depths of 1 or 3 ft, surrounding trees were monitored with a portable scintillation counter. Within 10 ft of the point of application, all trees above 3.0 in. dia. absorbed ^{131}I in sufficient quantities to be detected. Beyond 22 ft for surface applications, and 33 ft for 1- and 3-ft depths, no ^{131}I was detected in any trees. Regressions were computed to determine whether root extension could be predicted. When distance from the point of application was used as the dependent variable, an index of competition and the angle from the tree row proved to be the most useful, to the exclusion of the various measures of tree size. (BBB)

36561 RADIATION DOSE TO THE RAT THYROID FROM SEVERAL RADIOIODINE NUCLIDES. Rhodes, B. A.; Buddemeyer, E. U. (Johns Hopkins Medical Institutions, Baltimore). Int. J. Appl. Radiat. Isotop., 17: 447-52(Aug. 1966).

Radiation dosages to the rat thyroid during radioiodine tracer and equilibrium studies were estimated for ^{125}I, ^{129}I and ^{131}I. The total dose-rate constants for each of these isotopes in 10, 15, and 20 mg thyroids were calculated. An equation for the concentration of radioactivity in the thyroid as a function of time after the beginning of radioiodine equilibration, was derived by assuming a steady state of iodine metabolism. This gave rise to a general dose equation which was programmed on a computer. Tables of radiation dose estimates were generated which give the dose as a function of time and level of daily iodine intake. A comparison of the three isotopes was made, based on the radiation dose required to produce a given sensitivity in a particular isotopic equilibrium study. (auth)

36562 ISOTOPE DILUTION METHOD FOR DETERMINING THE ABSOLUTE AMOUNTS AND SPECIFIC ACTIVITIES OF PROLINE AND HYDROXYPROLINE IN TISSUES. Stanley, Elizabeth M.; Dawson, K. B.; Field, E. O.; Glicksman, A. S. (Royal Marsden Hospital, Sutton, Eng.). Int. J. Appl. Radiat. Isotop., 17: 467-77(Aug. 1966).

A method is described for estimating the absolute amounts and the specific activities of proline and hydroxyproline in tissue collagen, following the in vivo administration of ^{3}He-labelled proline. The method depends on an isotope dilution procedure, ^{14}C-labeled imino acids being added to tissue hydrolysates and recoveries, on chemical analysis, computed by reference to calibration curves prepared with a series of standard imino acid solutions. The chemical analysis is adapted from that of Peterofsky and Prockop and preliminary experiments for establishing the optimal conditions for each individual step in the separation, appropriate to this type of biological material, are described. Some cross-contamination between the assay fractions results in small over-estimates of the specific activities of both imino acids and of the absolute concentration of proline, but appropriate correction factors can be applied. Rat skin collagen contained 1.5 times as much proline as hydroxyproline; the specific activities obtained 48 hr after injection of ^{3}He-labeled proline are approximately equal. (auth)

36563 EFFECT OF FEEDING THIOCYANATE TO DAIRY COWS ON ABSORPTION AND CLEARANCE OF INTRAMAMMARY IODINE. Miller, J. K.; Swanson, E. W.; Cragle, R. G. (Univ. of Tennessee, Oak Ridge). J. Dairy Sci., 48: 1118-21(Aug. 1965).

The effects of thiocyanate on passage of radioiodine from the udder to blood plasma of dairy cows were investigated. Cows used to compare the metabolism of oral and intramammary radioiodine each received 4 mC ^{131}I through the streak canals into the gland cisterns of two quarters and 1 mC ^{125}I orally. Dosed and nondosed udder halves were milked and sampled separately for five days. Additional cows were given ^{131}I by intramammary infusion of 1.2 mC per quarter. Each cow was given 10 g sodium thiocyanate orally 64 hr later, and 60 μC of ^{125}I per quarter was then injected into each cow's udder 8 hr later. Twice daily thereafter for three days, 5 g NaSCN was given. The metabolism of oral and intramammary iodine did not differ appreciably, as shown by plasma levels and protein binding or urinary and fecal excretion. Two milkings were required to remove residual ^{131}I from dosed udder halves to a level comparable to that in nondosed halves. After the second milking following the intramammary dose, the milk contained primarily radioiodine secreted after absorption into the blood. Thiocyanate reduced iodine passage from the mammary gland to the blood; 50% more radioiodine was recovered in milk 16 hr after intramammary infusion following thiocyanate administration compared to the control period. Despite high urinary values, total three-day radioiodine excretion was only slightly increased when thiocyanate was administered, due to reduced fecal excretion. The milk/plasma exchangeable ^{131}I ratio dropped sharply from an average of 1.5 immediately before thiocyanate feeding to less than 0.5 after thiocyanate administration, indicating that passage of plasma ^{131}I, administered three days before thiocyanate feeding, was reduced. The lower milk/plasma ^{131}I ratio persisted for the duration of thiocyanate feeding. Both total and protein-bound radioiodine in plasma were reduced by thiocyanate. (BBB)

36564 AFFINITY OF MELANIN FOR CHLOROQUINE. Sams, W. Mitchell Jr.; Epstein, John H. (Letterman General Hospital, San Francisco). J. Invest. Dermatol., 45: 482-7(Dec. 1965).

By the use of pigmented hairless mice which developed a darkly melanotic plaque at the site of uv irradiation, it was possible to demonstrate the affinity of dermal melanin for chloroquine. The uv source was an Hanovia air-cooled high-pressure mercury contact lamp, which emits 2.12×10^5 erg/cm^2/sec. of mid-uv energy (2800-3200 Å) at a distance of 3.4 cm. Each mouse received a 5-sec exposure of uv radiation to the posterior third of the back three times a week. By 10 weeks the pigmented mice had developed deeply melanotic plaques, and the albino animals developed erythematous nonmelanotic plaques at the uv-irradiated sites. The uv radiation was discontinued at this time, and each of the animals was given a single intraperitoneal injection of 0.5 mg chloroquine diphosphate. Histologic examination of uv-irradiated skin revealed hyperkeratosis, hypergranulosis, acanthosis, and a thickened dermis, with an increased number of mast cells, fibrocytes, and inflammatory cells in both the amelanotic and melanotic plaques. The tissues of the pigmented mice differed from those of the albino mice only in the dense accumulation of dermal melanocytes and melanin in the pigmented areas. The nonirradiated skin of these animals showed an epidermis of 2-3 cell layers and a thin dermis with degenerating hair follicles, epithelial cysts, and some mast cells. In contrast to the normal skin of the albino, the normal skin of the pigmented mice contained a few scattered dermal melanocytes. The chloroquine levels in the albino control mice, which developed nonmelanotic plaques at the uv-irradiated sites, fell rapidly to zero within one week after a single intra-

peritoneal injection of the drug. The melanotic plaques of the pigmented mice, on the other hand, contained high levels of chloroquine for at least three weeks. Thus, the hairless mouse provides a model for studying the binding of drugs to melanin. (BBB)

36565 GLUCOSE PRODUCTION RATES IN DOGS DETERMINED BY TWO DIFFERENT TRACERS AND TRACER METHODS. Hetenyi, G. Jr.; Ninomiya, R.; Wrenshall, G. A. (Univ. of Toronto). J. Nucl. Med., 7: 454-63(June 1966).

The rate of endogenous glucose production was calculated in fasting conscious dogs utilizing data obtained simultaneously with two different tracers (6-^{3}H) glucose and glucose uniformly labeled with ^{14}C, and by two methods, A and B. Method A utilized successive measured injections of tracer (quantity dilution), while in Method B the rate was calculated by rate dilution employing the primed infusion of the tracer at a constant rate. Statistical analysis of the results demonstrated that both tracer methods yield equal rates for glucose production. However, 6-^{3}H glucose as a tracer yielded glucose production rates significantly higher than when ^{14}C glucose was used as tracer. Since with Method A the use of ^{14}C glucose had been shown to yield valid glucose production rates as eviscerated dogs, 6-^{3}H glucose is rejected as a tracer for glucose transfer rate studies in dogs. (auth)

36566 EFFECT OF INTESTINAL DAMAGE PRODUCED BY EIMERIA NECATRIX INFECTION IN CHICKS UPON ABSORPTION OF ORALLY ADMINISTERED ^{65}Zn. Turk, D. E.; Stephens, J. F. (Clemson Univ., S. C.). J. Nutr., 88: 261-6(Mar. 1966).

Experiments were undertaken to determine the effects of infection of the intestinal protozoan Eimeria necatrix upon absorption of radiozinc. E. necatrix infections result in damage to the wall and musculature of the mid-portion of the small intestine. These trials were designed to follow ^{65}Zn absorption rates throughout the coccidial disease cycle, from one until 35 days postinoculation. In chicks severely infected with coccidiosis, absorption rates of ^{65}Zn exceeded those of uninfected birds on the first day postinfection, decreased on the third day, decreased severely by the sixth day, and afterward began to return to levels observed in uninfected birds. By 21 days postinoculation, ^{65}Zn absorption rates were near control levels, and at 28 and 35 days postinoculation, absorption rates were much greater than control levels. Mild intestinal damage with slight inflammation was found to increase absorption, whereas severe damage and hemorrhaging decreased or stopped absorption. This absorption pattern explains the observations, previously reported, of nutrient deficiency symptoms appearing in chicks early in a coccidial attack, and of increased growth rates occurring during the recovery phase of the disease. Inconsistencies in the data from trial to trial appear to be explainable on the basis of the effects of varying amounts of cellular damage upon absorption. Slight damage and inflammation noted at some stages of the infection and at lower levels of inoculation appear to increase absorption rates, whereas more severe cellular damage occurring at other stages of infection tends to greatly decrease absorption rates. (BBB)

36567 EFFECT OF CALCIUM, STRONTIUM, AND MAGNESIUM ON THE POSITIVE INOTROPIC ACTION OF FLUORIDE. Berman, David A. (Univ. of Southern California, Los Angeles). J. Pharmacol. Exp. Therap., 152: 75-89(Apr. 1966).

Frequency-force experiments were used to study the effects of calcium, strontium, and magnesium on the positive inotropic action of fluoride. In rat ventricle strips fluoride stimulated the basal contractions. The effect on the first poststimulation contraction was biphasic; it was stimulated and then depressed. The positive inotropic effect was greater when the tissue was exposed to fluoride in the presence of calcium, strontium, or magnesium than in the absence of these ions. Fluoride potentiated the effect of calcium on the basal contractions and antagonized the effect of increasing calcium concentration on the first poststimulation contraction. The calcium in the medium was replaced by 3.3 mM strontium, and the tissues were stimulated at a constant frequency of 1 every 2 min. Frequency-force relations were not studied, for strontium markedly prolonged the contraction cycle and utilization of the stimulation frequency patterns used in the previous experiments resulted in fusion of contractions during the 100/min stimulation period. It was evident that fluoride markedly stimulated contractions in a medium in which the calcium was replaced by strontium. Inasmuch as fluoride also exerts a positive inotropic effect when the tissue is incubated in media in which the calcium is replaced by strontium or magnesium, fluoride may also exert its effect as a magnesium or strontium complex. However, it is also possible that these cations are complexed to the cell surface or elsewhere, and that the presence of this complex is essential for the action of fluoride. It is concluded that fluoride exerts its effects as a complex, and its effect on contractility is not simply an increased sensitivity of the tissue to calcium. (BBB)

36568 PHOTOSYNTHESIS AND UPTAKE OF ^{85}Sr IN FRESHWATER PLANKTON. Patten, Bernard C.; Iverson, Richard L. (Oak Ridge National Lab., Tenn.). Nature, 211: 96-7(July 2, 1966). (ORNL-P-1622).

Studies were made on light and dark uptake of ^{85}Sr by organisms in water obtained from a depth of 2 ft. in Melton Hill Lake, Oak Ridge, Tennessee, on Aug. 26, 1964, and incubated in a controlled environment chamber (temperature about 25°C, light about 1,000 ft. candles, photoperiod 12 hr). Initial phytoplankton concentration was 36.6×10^{3} cells/ml. Initial uptake of ^{85}Sr proceeded rapidly in both light and dark, but assimilation in light became greater after 6 hr. Both light and dark samples showed a decrease in cell radioactivity for about 24 hr, after which the dark material remained approximately constant while the illuminated samples showed a linear increase with time. It was concluded that ^{85}Sr assimilation by natural plankton material is independent of temperature except possibly at abnormally high temperatures. Mechanisms are suggested to explain how the assimilation of ^{85}Sr can be dependent on light yet independent of photosynthesis. (P.C.H.)

36569 IN VIVO AND IN VITRO ASSAYS WITH ^{59}Fe IN GALLUS DOMESTICUS WITH REFERENCE TO THE TRANSPORT OF IRON IN SERUM. Martin-Mateo, M. C.; Sebastian, M. F.; Planas, J. (Univ., Valladolid, Spain). Rev. Espan. Fisiol., 21: 179-85(Dec. 1965). (In Spanish).

Localization of ^{59}Fe in various serum protein fractions was studied in chickens. In in vivo tests ^{59}Fe was injected intravenously in doses of 12 to 35 μC/kg body weight. In vitro tests were conducted by adding 0.032 to 12 μC ^{59}Fe per ml serum. Paper electrophoresis and immunoelectrophoresis were used to localize the radioactivity in serum protein fractions. In the tests carried out in vivo it was shown that radioactivity was selectively fixed at the level of the β-globulins, independent of the degree of saturation of the transferrin. The in vitro experiments carried out with increasing proportions of ^{59}Fe showed different distributions of the radioactivity, shifting toward the zone of the α-globulins. Two fractions associated with ^{59}Fe were clearly seen in some specimens. It was not possible to establish any relation of ^{59}Fe distribution with the sex or with the laying phenomena in the females. By obtaining transferrin from the serum of this species, together with the use of commercially available conalbumin, some tests of immunological relations (immunoelectrophoresis and diffusion in agar gel) were made which showed the close relation between the two proteins. Thus reactions of identity were obtained with conalbumin and transferrin by using their respective antiserums. This result confirms earlier reports of the relation of these serum proteins. (BBB)

36570 PHYSIOLOGY AND CLINICAL COURSE OF IODINE METABOLISM. Kutzim, Heinrich (Univ., Cologne). Strahlentherapie, Sonderbaende, 52: 252-7(1963). (In German).

The metabolism of inorganic iodine, triiodothyronine,

and thyroxine is outlined and illustrated by autoradiographies of whole mice. The high concentration of triiodothyronine and thyroxine in the lacrimal gland and the occurrence of exophthalmos were correlated by an hypothesis. (J.S.R.)

36571 ORIGIN OF THE SECONDARY EFFECT OF IODATED X-RAY CONTRAST MEDIA ON THE THYROID. Schuessler, Richard (Univ., Saarlandes, Hamburg). Strahlentherapie, Sonderbaende, 52: 258-62(1963). (In German).

The effects of iodated x-ray contrast media on the thyroid were investigated, and the results are discussed. It was found that even purified x-ray contrast material containing no iodide inhibited the iodine uptake by the thyroid. (J.S.R.)

36572 EFFECT OF IODINE-CONTAINING X-RAY CONTRAST MEDIA ON THE SERUM IODIDE CONCENTRATION AND ON THE IODIDE UPTAKE AND ENDOCRINE FUNCTION OF THE HUMAN THYROID. Fitting, Wilfried (Evangelische Krankenhauses, Cologne). Strahlentherapie, Sonderbaende, 52: 263-71(1963). (In German).

The magnitude of the absolute iodide uptake of the thyroid depends on two factors: the concentration of the inorganic iodine in the serum and the iodide uptake capacity of the thyroid. Iodine containing x-ray contrast material leads to an increase of the concentration of the inorganic serum iodide. It causes therefore the reduction of the iodide uptake capacity; this is expressed in radioiodide test by a reduction of the iodine-131 clearance or the iodide-131 uptake rate. It also causes an increase of the absolute iodide uptake of the thyroid which is limited by the reduction of the iodide uptake capacity. The application of iodine-containing x-ray contrast media does not inhibit the endocrine function of the thyroid but it can increase these quantitatively so that hyperthyrosis or exophthalmic goiter of a previously hyperplastic thyroid results. Such an undesired secondary effect must be avoided by antithyroidal medications. (P.C.H.)

36573 RESULTS OF THE ^{131}I-TRIIODOTHYRONINE TEST WITH AN ION EXCHANGE RESIN. Doering, Paul; Schmele, Rolf (Univ., Goettingen, Ger.). Strahlentherapie, Sonderbaende, 52: 272-82(1963). (In German).

In methodic studies the effects of resins (amberlite), serum fractions, temperature, incubation time, and wash procedures on the size of the ^{131}I-triiodothyronine storage were tested. Women have a significantly lower storage value than men. Hyperthyrosis shows a significantly increased value and hypothyrosis is lower. A statistical evaluation was not possible because of the few data. Extrathyroidal increases of the T_3 storage were found in strong dysproteinemia, principally the nephrotic syndrome, liver cirrhosis, and primary chronic polyarthritis. They were also observed in skin decompensations and polyglobulia. Decreases were also found in pregnancies beyond the sixth to eighth week. Additional studies were concerned with the effects of serum albumin factors, antithyroidal substances, and iodides. (tr-auth)

36574 INCORPORATION OF 2-^{14}C-ACETATE IN MUSCLE AND SERUM PROTEINS OF INTACT AND IRRADIATED RABBITS. Zhurbin, G. I. (Inst. of Biochemistry, Kiev). Ukr. Biokhim. Zh., 38: 235-40(1966). (In Russian).

The rate and intensity of incorporation of the radioactive label in aldolase, glycerophosphate dehydrogenase (GPD), and glyceraldehyde-3-phosphate dehydrogenase (GAPD) of the muscles, in water-soluble proteins of muscle extract and tissue, as well as in gamma-globulin, albumin, and serum proteins of intact rabbits were established at various intervals after injection of the isotope indicator. Different renewal rates were found for various proteins: GPD is renewed almost 1.3 times as fast as aldolase and 2.3 times as fast as GAPD; aldolase, 1.76 times as fast as GAPD; gamma-globulin, 1.5 times as fast as crystalline serum albumin. Different doses of ionizing radiation have different effects on the intensity of renewal of rabbit blood and serum proteins. The quantity of muscle extract and serum protein is interchanged in rabbits irradiated with 400–850 R. Irradiation of the animals with a dose of 1000 R raises the quantity of protein in muscle extract and serum by 45.4 and 19.5%, respectively. (auth)

36575 INFLUENCE OF GENOTYPE ON RATE OF STRONTIUM ABSORPTION BY BARLEY. Pinkas, Leonard Lieber Hirsch. Minneapolis, Univ. of Minnesota, 1965. 63p.

Thesis.

Large differences in accumulation of strontium in the grain were observed between the barley varieties Regal and Tregal, Regal accumulating higher concentrations than Tregal. Twelve-day old seedlings selected for uniformity in size were placed in nutrient solutions containing strontium labelled with ^{89}Sr for absorption periods ranging from 30 to 150 minutes. Accumulation of strontium in the shoot was used as a measure of absorption of strontium by the root from the ambient solution, active transfer into the transpiration stream in the xylem, and subsequent accumulation in the shoot. Rates of strontium absorption from nutrient solutions containing eight concentrations of strontium indicate a definite trend towards higher rates of strontium absorption by Regal as compared to Tregal. To determine if passive processes were involved in strontium absorption, measurements were made of transpiration rate, distance from epidermis to endodermis, and number of cortical cell layers. It was concluded that differential strontium absorption was not due to variation in path length for ion movement through the free space to sites of active transport. No relationship was observed between transpiration rate and rate of strontium absorption in either variety. Rates of strontium absorption increased approximately two-fold in both Regal and Tregal as the temperature was increased 10°C, thereby indicating that strontium absorption is dependent on metabolic processes. The metabolic inhibitors cyanide and dinitrophenol significantly inhibited strontium absorption in both varieties. Generally, Regal and Tregal did not differ in amounts of strontium absorbed in the presence of inhibitor concentrations that significantly suppressed strontium absorption. However, in the presence of cyanide or dinitrophenol concentrations that did not significantly affect strontium absorption, differences between Regal and Tregal in amounts of strontium absorbed were highly significant. This information, combined with the similarity of the Q_{10} values for the two varieties, suggests that differential strontium absorption between Regal and Tregal is due to quantitative rather than qualitative differences in the metabolic processes associated with strontium absorption. (TCO)

36576 INCREASED RADIOISOTOPE UPTAKE BY MALIGNANT CELLS IN A HIGH OXYGEN ENVIRONMENT RESULTING FROM H_2O_2 BREAKDOWN. Finney, J. W.; Balla, G. A.; Mallams, J. T. (Baylor Univ., Dallas). 21p. (CONF-660212-10). ORAU. Gmelin, AED-CONF-66-016-10.

From Radiation Research Society, 14th Annual Meeting, Coronado, Calif.

It was found that both ^{131}I labeled human serum albumin and [3-(chloromercuri)-methoxypropyl] urea-^{203}Hg will localize preferentially in the area of malignant tumor tissue when given intraarterially during the intraarterial infusion of dilute hydrogen peroxide in either tumor bearing animals or human beings. Autoradiographic and electron-photomicroautoradiographic data indicate the intracellular distribution of the isotope. The time of the scan in either experimental animals or humans is not critical. The best tumor outline is obtained at 48–72 hours after the infusion. This time interval is sufficient to allow a decrease in the intravascular background radiation in the scan area. The technique is of value in outlining tumor size and extent in involvement as a diagnostic aid as well as a procedure whereby the results of therapy might be followed. (auth)

36577 DEUTERIUM ISOTOPE EFFECTS IN THE MUTAROTATIONS OF α-D-GLUCOSE AND β-D-FRUCTOSE. Wade, Clarence W. R. Washington, D. C., Georgetown Univ., 1965. 70p.

Thesis.

The rates of mutarotation were studied of α-d-glucopyranose and of β-d-fructopyranose in H_2O, and of the corresponding O-deuterium analogs in D_2O, in the presence of sulfuric acid (0.015M, 0.0025M, and 0.00125M), potassium acid phthalate (0.001M), and o-nitrophenol (0.01M), at 3.90 and 20.00°C. The rates of mutarotation of α-d-glucopyranose in 0.0006M sodium hydroxide, in H_2O and D_2O, were also studied. From the rate constants, the activation energies, acid-base catalytic effects, and isotope effects for the mutarotation of each sugar were calculated. The results were then examined and interpreted as functions of α ⇌ β-pyranose or Type I interconversions (for d-glucose) and pyranose ⇌ furanose or Type II interconversions (for d-fructose). The activation energies, catalytic effects, and rate constants clearly show differences between Type I and Type II interconversions in both solvent systems. However, both the measured and the calculated (catalytic) isotope effects show three distinct but similar mechanisms for the two types of reaction. Consequently, it is concluded that Type I and Type II interconversions proceed via similar mechanisms. The isotope effects show that, in strongly acid solutions, α ⇌ β-pyranose and pyranose ⇌ furanose interconversions must occur by the rapid formation of the conjugate acid of the sugar, followed by the rate-determining step. Measurements of pH and isotope effects show that, in basic solutions, both types of interconversions consist of the initial formation of the sugar anion, followed by the rate-determining step. However, for catalysis by H_2O, the evidence indicates that the proton transfers occur during the rate-determining step. (Dissertation Abstr.)

Radiation Effects on Biochemicals

See also CHEMISTRY — Radiation Chemistry

36578 (ORNL-P-2240) REPAIR OF DNA. Setlow, R. B. (Oak Ridge National Lab., Tenn.). [1966]. Contract W-7405-eng-26. 31p. (CONF-660620-1). Dep. mn. CFSTI $2.00 cy, $0.50 mn.

From International Symposium on Regulatory Mechanisms in Nucleic Acid and Protein Biosynthesis, Lunteren, Netherlands.

Biological and physico-chemical evidence for the existence of repair systems for DNA is reviewed. Results of studies of the response of viruses, bacteria, and mammalian cells to uv and x radiation are summarized. It is concluded that the biological data indicate that repair systems operate to remove damage from DNA. Reaction mechanisms involved are discussed and the biological systems and the physico-chemical lesions that have been related to the various steps involved in repair by excision are cataloged. (66 references.) (C.H.)

36579 THE ACTION OF ROENTGEN AND γ RAYS ON HYDRATION OF PROTEIN IN BLOOD SERUM. Marczewski, Stanislaw. Arch. Immunol. Therap. Exp., 14: 239-42 (1966).

In experiments using a personal method it was found that irradiation of serum with x or γ rays at first raises the index of hydration of serum protein and then lowers it. Irradiation with a mercury-quartz lamp had a similar effect. Since the light of the mercury-quartz lamp contains short electromagnetic waves (ultraviolet rays) and long waves (infrared rays), the similar effects of Roentgen and γ rays and mercury-quartz light indicate that long electromagnetic waves are emitted together with x and γ rays. (auth)

36580 REGULATION OF LIPID TRANSPORT AND RADIATION-INDUCED HYPERLIPEMIA. Paoletti, R.; Berti, F. (Univ. of Milan). Atompraxis, 12: 285-90 (June 1966).

Information on triglyceride synthesis, composition and breakdown in mammalian adipose tissue and the hormonal, nervous and metabolic mechanisms regulating free fatty acids (FFA) mobilization from adipose tissue is reviewed, as background information necessary to understanding the mode of action of ionizing radiations in inducing hyperlipemia. Several possible mechanisms have been considered: increased mobilization of FFA, increased synthesis of liver lipids, deficiency of specific enzymes such as lipoprotein lipase in peripheral tissues, and synthesis of abnormal lipoproteins by the liver of irradiated animals. Evidence is presented supporting the last possibility and indicating an important role for the reticulo-endothelial system in the regulation of plasma lipids in the irradiated mammalian organisms. (120 references). (auth)

36581 STUDY ON THE PLASMA PROTEINS OF PATIENTS WHO SURVIVED THE A BOMB INCLUDING THOSE WHO SUFFERED FROM THE REMAINING RADIOACTIVITIES. Makidono, J.; Takanashi, S.; Yoshimoto, T.; Yoshimoto, K.; Kai, T.; Matsutani, M.; Miura, M. (Makidono Radiology Clinic and Clinical Radiology Research Inst., Hiroshima). Atompraxis, 12: 291-4(June 1966).

The plasma proteins of A-bombed survivors, healthy persons, long term x-ray workers (radiologists and x-ray technicians), cancer patients, and tumor-therapy cancer patients were examined by electrophoretic tests. Attempts were made to solve the problem of the biological mechanisms of irradiation immunology. The results for each group are discussed. (P.C.H.)

36582 PROTEIN ELECTROPHORETIC CHANGES FOLLOWING TOTAL-BODY IRRADIATION OF NORMAL AND TUMOR-BEARING RATS. Sikov, M. R.; Chapman, B. B.; Hissong, D. E.; Pringle, B. H. (Wayne State Univ., Detroit. Veterans Administration Hospital, Dearborn, Mich.). Atompraxis, 12: 297-300(June 1966).

Total serum protein determinations and electrophoretic and ultracentrifugal separations were accomplished on fresh and lyophilized serum samples from normal and tumor-bearing rats at sequential times after irradiation. The concentrations of the beta and alpha-2-globulins were altered by the presence of a tumor, by irradiation, and by lyophilization of the sample. These changes occurred at times which correlated with those in which plasma from irradiated animals was found to enhance the oncolytic effect of local irradiation of transplanted tumors. A specific relation between the two phenomena is tentatively proposed. (auth)

36583 ENZYMATIC BREAKDOWN OF UV-IRRADIATED DNA BY THE EXTRACT FROM MICROCOCCUS LYSODEICTICUS. Moriguchi, Etsuko; Suzuki, Kenshi (National Inst. of Radiological Sciences, Chiba, Japan). Biochem. Biophys. Res. Commun., 24: 195-202(July 20, 1966).

The extract of M. lysodeicticus was found to possess at least three kinds of nuclease activity for DNA; very high activity for degrading denatured DNA and weak activities on uv- and native-DNA. Evidence was found that suggests that the breakdown of uv-DNA is catalyzed by a new enzyme which has a specific afinity for uv-DNA and that the coexisting enzymes that act on native- and denatured-DNA are different ones. (P.C.H.)

36584 EFFECTS OF γ IRRADIATION ON THE STRUCTURE OF RIBONUCLEASE. Slobodian, F· elyn; Fleisher, Martin (New York Univ.). Biochemistry, 5: 2192-2200 (July 1966).

The effects of γ irradiation on aqueous solutions of ribonuclease A (polyribonucleotide 2-oligonucleotidotransferase, EC 2.7.7.16) were studied using the techniques of viscometry and tritium–hydrogen interchange measurement. Irradiated samples showed a progressive increase in viscosity with increased enzymic inactivation; the most highly inactivated sample had a viscosity approaching that of native enzyme in 8 M urea. Ultracentrifuge patterns demonstrated the absence of aggregates in a heavily irradiated sample. Tritium–hydrogen exchange studies, carried out using Bio-Gel P-2 column fractionation, also demonstrated the progressive loss of tightly bound, slow-exchanging hydrogens with increased radiation effect. Kinetic analyses of the exchange-out data

confirmed that the loss of slow-exchanging hydrogens reflected the progressive unfolding of helical structure and the loss of intramolecular side chain hydrogen bonds. The results clearly demonstrate that irradiation causes extensive disorientation of the native ribonuclease A conformation. (auth)

36585 EFFECT OF RADIATION ON COLLAGEN. I. ELECTRON-SPIN RESONANCE SPECTRA OF 2537-A-IRRADIATED COLLAGEN. Forbes, W. F.; Sullivan, P. D. (Univ. of Waterloo, Ont. Univ. of Rochester, N. Y.). Biochim. Biophys. Acta, 120: 222-8(June 8, 1966).

Samples of human collagen, when irradiated with 2537-Å light, afford electron-spin resonance spectra which differ markedly from the electron-spin resonance spectra reported after exposure of collagen samples to x rays. The signals from ultraviolet light-irradiated collagen are tentatively associated with unpaired electrons located predominantly on the aromatic nuclei of the tyrosine and phenylalanine residues. The collagen signals show characteristic decay rates which also suggest the existence of two distinct radical sites. The decay rates are different for collagen, gelatin and molecular mixtures of approx. the same amino acid composition. The intensities and decay rates of the signals show changes which can be related to the age of the individual samples. On standing, a new electron-spin resonance signal was formed in several cases, which may be due to a trapped ·CHO radical. (auth)

36586 THEORY OF LOW-ANGLE SCATTERING OF X RAYS BY RNA MOLECULES IN SOLUTION. Fedorov, B. A. (Leningrad State Univ., Zhdanov, USSR). Biophysics (USSR) (Engl. Transl.), 10: 5-9(June 1966).

Translated from Biofizika, 10: 7-10(1965).

Low angle scattering of x-rays by solutions of RNA (with an ionic strength of 0.14M) in light of the recently developed theory of electromagnetic radiation scatter by branched macromolecules points to considerable branching of the RNA molecules with relatively small interhelical zones. An expression was obtained for the indicatrix of scatter by the starfish taking into account the fact that adjacent helices may be separated by flexible unspiralized zones. The possibility of determining the size of the interhelical regions from the indicatrix of scatter with central scatter of x rays was examined. (auth)

36587 LINK BETWEEN LUMINESCENCE OF RHODOPSIN AND THE VISIBILITY OF X RAYS. Avakyan, Ts. M. (Agricultural Research Inst., Echmiadzin, Armenian SSR). Biophysics (USSR) (Engl. Transl.), 10: 215-18(June 1966).

Translated from Biofizika, 10: 189-91(1965).

Studies on luminescence of rhodopsin extracted from frogs confirmed the theoretical assumptions that substances present in the retina may give luminescence on exposure to x rays and that the eye receptors may react to light quanta formed by secondary physical processes in the retina. (P.C.H.)

36588 QUANTITATIVE CYTOPHOTOMETRIC STUDIES OF NUCLEAR PROTEIN IN VICIA FABA FOLLOWING ACUTE IRRADIATION. Alvarez, M. R.; Cowden, R. R. (Univ. of Florida, Gainesville). Exp. Cell Res., 42: 578-84(June 1966).

Germinating seeds of Vicia faba were exposed to 1000 R of x rays. Nuclei from the primary root meristems of the irradiated seedlings as well as from non-irradiated controls were isolated, smeared on slides, and air dried. Total nuclear protein was stained with pH 2.8 fast green FCF and by the ninhydrin-Schiff method. Histones were visualized by staining with pH 8.2 fast green FCF and sulfhydryl and disulfide containing proteins by staining with mercury orange. Cytophotometric measurements of irradiated nuclei indicated an increase in total nuclear protein over controls during the post-irradiation period in which chromosomal rejoining occurs. No change in the amount of histones was noted. Protein-bound sulfhydryl and disulfide groups increased slightly during the restitution period with a subsequent return to control level at the close of this time interval. The rise in total nuclear protein was attributed primarily to proteins of the nucleoplasm rather than to those of the chromosomes. (auth)

36589 EFFECTS OF DIETHYL PYROCARBONATE ON BARLEY SEEDS. Natarajan, A. T.; Fedorcsak, I.; Ehrenberg, L. (Univ. of Stockholm). Exp. Cell Res., 42: 617-24(June 1966).

Barley seeds (karyopses) were treated with solutions of diethyl pyrocarbonate (DEP), and the biological effects during germination were observed. With increasing concentration of DEP, an increasing fraction of the seeds shows complete inhibition of germination. The surviving seedlings show practically no inhibition of growth rate. On the cellular level the following effects were observed: chromosome breaks (low frequency), no exchanges, cells with single-stranded chromosomes, haploid cells, aneuploid cells, tripolar spindles, and chromosome contraction. Post-irradiation treatment with DEP was found to increase the frequencies of γ-ray and neutron induced chromosome breaks, and to decrease the frequency of γ-ray induced two-hit effects. Neutron induced two-hit effects were not affected. These effects are similar to those of such antimetabolites as Myleran, FUDR, and aminopterin. The results are briefly discussed considering the biochemical effects of DEP: a general reactivity towards proteins leading to enzyme inactivation, whereas nucleic acids are left intact under the same conditions of treatment. (auth)

36590 EFFECT OF X IRRADIATION ON THE NICOTINAMIDE ADENINE DINUCLEOTIDES (NAD-NADH) CONTENT OF RAT THYMOCYTES. Campagnari, F.; Whitfield, J. F.; Bertazzoni, U. (EURATOM-CCR, Ispra, Italy). Exp. Cell Res., 42: 646-56(June 1966).

Isolated rat thymocytes, treated with x rays (1500 R) or subjected to sham irradiation, were incubated at 37°C for 4½ hr. Samples were taken at different time intervals for cytological examination and nicotinamide adenine dinucleotide (NAD and NADH) measurements. In normal thymocytes NAD decreased slightly after 1½ hr of incubation and then remained constant, while NADH declined slowly throughout the experimental period. The findings may be the result of the isolation procedure and of the natural aging of cultures. X rays caused a severe drop of NAD and NADH in the cells, the decrease being much greater than in normal cultures. However, in both cases (irradiated and unirradiated thymocytes) the change occurred at the same time and to approximately the same degree as the disappearance of nuclear structure (nuclear homogenization) which is considered the symptom of cell death. The losses of pyridine nucleotides by x-ray treated thymocytes accompanied rather than caused the death of cells. Therefore they should not be regarded as early and prevailing events in the process of radiation injury, but as unspecific and late effects of cellular damage. In fact at all the phases of experiment, the irradiated thymocytes with regularly stained nuclei seemed to contain a normal amount of pyridine nucleotides. The cytological and NAD–NADH changes in irradiated cultures are not necessarily associated or closely linked together. In fact, the proper addition of nicotinamide or spermidine to the incubation medium allowed them to occur independently. (auth)

36591 CONTRIBUTION TO THE STUDY OF DNA FROM IRRADIATED TISSUES. Janik, B. (Inst. of Biophysics, Brno). Folia Biol. (Prague), 12: 189-98(1966).

After whole-body irradiation of rats with a dose of 600 R only the effects of degradation processes were observed with bound thymus DNA, i.e., with DNA which remained in the DNP complex after irradiation. These effects became manifest in a decrease of the average molecular weight (to about one-half) and in an increase of the heterogeneity of the preparation with regard to molecular weight. Free thymus DNA of irradiated rats is considerably degraded and heterogeneous: the average molecular weight is more than 5 times or 3 times as low as that of the bound DNA from irradiated and nonirradiated rats, respectively. In addition to degradation, considerable denaturation occurs with free DNA. These changes occur probably as a result of the re-

lease of DNA from the complex of nuclear DNP caused by irradiation. The observed changes are ascribed to the effect of enzymes on the nuclear DNP complex or on the DNA released from it. (auth)

36592 CONSEQUENCES OF UV-MICROBEAM IRRADIATION OF THE NUCLEOLI OF LIVING CELLS. Sakharov, V. N.; Voronkova, L. N. (Inst. of Chemical Physics, Moscow). Genetika, No. 6, 144-8(June 1966). (In Russian).

Experiments on tissue culture cells are described. Local irradiation of certain sites of a mitotic cell was shown to result in a disturbance of the nucleoli formation in cells of the next generation. As long as nucleoli exist in the mitotic cell, i.e., in the early and middle prophase, this effect is due solely to damage of the nucleolus. However, after the nucleolus becomes dissolved in the late prophase, the effect becomes a consequence of damage of any site of the nucleus. At later stages of mitosis this effect occurs as a result of chromosome damage. The experiments show the localization of the mitotic cell substances responsible for formation of nucleoli in cells of the next generation. As a result of damage of these substances, a high number of small dense bodies are formed in telophase cells. (auth)

36593 EFFECT OF IRRADIATION ON DNA SYNTHESIS IN THE REGENERATING LIVERS OF RATS. Lehnert, S. M.; Okada, S. (Univ. of Rochester, N. Y.). Contract AT(30-1)-1286. Int. J. Radiat. Biol., 10: 601-8(July 15, 1966).

Cells of regenerating livers require at least two steps preparatory to entering S stage to start the DNA-synthesis. One of the steps is synthesis of enzymes involved in DNA-synthesis, and the other is an alteration of the structure of deoxyribonucleoprotein, which is reflected by the priming ability in vitro. Irradiation interferes with these two processes, thus preventing the cells from synthesizing the DNA. The rate of DNA-synthesis in the S stage cell in vivo is related to the level of DNA-synthesizing enzymes estimated in vitro studies. However, the priming ability of nuclei, estimated in vitro, had little relationship to the rate of DNA-synthesis in vivo. (auth)

36594 CYTOKINETICS AND REGULATION OF PROGENITOR CELLS. Lajtha, L. G. (Christie Hospital and Holt Radium Inst., Manchester, Eng.). J. Cell. Physiol., 67: Suppl. 1, No. 3, 133-47(June 1966).

Four different assay methods of bone marrow stem cells were examined with regard to the kinetic pattern following perturbation of the steady-state system, e.g., by irradiation. Basically, the stem cell assays fall into two categories: those depending on grafting hemopoietic cells into suitably treated recipients, and those in which recovery of the population is allowed in the animal in which the perturbation was produced, without handling the cells. Evidence is accumulating which indicates that in the grafting techniques, a selective loss of stem cells may occur, especially stem cells in cell cycle; hence, in early stages of recovery of the population, unduly low numerical values might be noted. In view of this evidence, the concept of the colony-forming cell may have to be replaced by the concept of the colony-forming property of the stem cell. (auth)

36595 EFFECT OF ULTRAVIOLET IRRADIATION ON SKIN COLLAGEN. Bottoms, Eva (Royal Victoria Infirmary, Newcastle upon Tyne, Eng.); Cater, C. W.; Shuster, Sam. Nature, 211: 97-8(July 2, 1966).

The degree of crosslinkage of mouse skin and kangaroo tail tendon collagen before and after uv irradiation was measured. Radiation exposures were for 19 or 44 hr. The results indicated that uv irradiation produces an increased molecular crosslinkage between the collagen fibrils both of hairless mouse skin and kangaroo tail tendon. The reduced capacity of the irradiated collaged to take up water is presumably related to this increase in crosslinkage. It is now clear that uv irradiation in vitro produces collagens with properties resembling those found in aging skin, which result from the production of intermolecular crosslinks. (P.C.H.)

36596 ENZYMATIC DEGRADATION OF ULTRAVIOLET-IRRADIATED DEOXYRIBONUCLEIC ACID. Dellweg, H.; Wacker, A. (Univ., Frankfurt am Main). Photochem. Photobiol., 5: 119-26(Jan. 1966).

After uv irradiation of DNA, thymine dimer and other photoproducts can be found in the enzyme-resistant fraction. Thus enzymatic hydrolysis can be used for distinguishing between uv-damaged and undamaged sequences in native DNA. The analysis of the mixture of oligonucleotides containing photoproducts was also performed to elucidate the action mechanism of enzymes on irradiated DNA. This is of interest in relation to repair mechanisms in irradiated or otherwise damaged cells by scission of the damaged sequence together with the neighboring nucleotides in the double helix. Attempts were made to separate the enzyme-resistant fraction by chromatography. Double-stranded DNA after uv irradiation was degraded by the action of deoxyribonuclease and snake-venom phosphodiesterase. In addition to mononucleotides a number of nuclease-resistant oligonucleotides, containing photochemically altered bases, could be detected and separated by column chromatography. The phosphorus contents indicated the existence of some photoproducts other than dimers of pyrimidines, especially within the trinucleotide fraction. Comparison of the DNase action on irradiated and on unirradiated DNA suggests that DNase is hindered from splitting the chain next to a photoproduct, tetranucleotides being the smallest and octanucleotides the most frequent degradation products bearing an altered base. (BBB)

36597 DEHYDRATION OF UV-IRRADIATED URIDINE AND ITS DERIVATIVES. Logan, D. M.; Whitmore, G. F. (Univ. of Toronto). Photochem. Photobiol., 5: 143-56 (Jan. 1966).

The uv irradiation of uridine, oligonucleotides, and long-chain polyuridylic acid (Poly U) produces a variety of photoproducts including a hydrated base arising from the addition of water to the 5,6 double bond. Both the hydration and dehydration reactions in a nucleotide are sensitive to the position of the phosphate linkage. The 5′-mononucleotide is less easily hydrated than the 3′. Conversely, the dehydration process in the nucleoside and the nucleotides is most rapid for uridine and decreases progressively in rate as a phosphate is added to the 2′, 5′, or 3′ position respectively. In the compound uridylyl-5-uridine the dehydration is a two-component reaction with the two dehydration rates similar to those of 5′ and 3′ mononucleotides respectively. In higher order oligonucleotides the dehydration rate is slower than any of the rates for 5′ and 3′ monophosphate or 3′,5′ diphosphates. The dehydration rate decreases rapidly for oligonucleotides up to chain lengths of 6 or 8 and then decreases at a diminishing rate. Long-chain Poly U (>200 nucleotides) dehydrates at $\frac{1}{5}$ the rate of the monomer. In addition, the initial alkaline treatment to dehydrate irradiated Poly U may result in chain breakage but this effect is not seen in subsequent cycles of irradiation and dehydration. The chain length effect on dehydration rate is only slightly decreased by the presence of 7M urea in the dehydration mixture. Quantitative data are presented on the effect of temperature and pH on the rate constant for dehydration of uridylic acid and its derivatives. (BBB)

36598 CHANGES IN THE CONTENT OF UNSATURATED HIGHER FATTY ACIDS IN THE FREE LIPID FRACTION OF IRRADIATED LEAVES AND AN INVESTIGATION OF TOXIC PROPERTIES OF THIS FRACTION. Boudnitskaya, E. V. (Bach Inst. of Biochemistry, Moscow). Radiat. Bot., 6: 351-5(Aug. 1966).

The action of ionizing radiation upon the content of oleic, linoleic, and linolenic acids in the free lipid fraction isolated from bean (Latvia) seedling leaves irradiated with doses of 1–50 kR was studied. It was found that the irradiation of plants with doses of 10, 30, and 50 kR led to a considerable increase (30–50%) in the content of unsaturated higher fatty acids in a free lipid fraction. The irradiation with 1 kR caused a decrease in the quantity of these acids in the fraction tested (20–40%). The irradiation of bean leaves that had been steamed in order to inactivate enzymic

systems showed either a clearly manifested increase or a decrease in the content of the acids investigated (some 7–10%), which proved the enzymic character of the storage of unsaturated higher fatty acids and their peroxides in a free lipid fraction isolated from x-irradiated plants. It was also found that a free lipid fraction isolated from irradiated and unirradiated bean seedlings and containing a large quantity of unsaturated higher fatty acids and their peroxides has a strong toxic effect, inhibiting the growth and development of germinating wheat seeds (Moscovskaya 24II). This is in good agreement with the data of others carried out in the same line. (auth)

36599 EFFECT OF GAMMA-RAYS ON POTATO STARCH IN RELATION TO ITS WATER CONTENT. Reuschl, H.; Guilbot, A. Staerke, 18: No. 3, 73-7(1966). (In German).

The effects of gamma radiation with a dose of 30 Mrad on potato starch as a function of its water content was investigated by studying the degradation of the carbohydrate chains and the formation of various oxidation and dehydration products. The glucose formed in starch as well as the presence of hydroxymethylfurfural imply that hydrolytic fission has taken place through intermolecular reaction. Water was found to interfere with starch radiolytic reactions in three ways: by a protective effect against oxidation reactions which are most evident when hydration is low; by a protective effect against chain rupture when the water content is above 21%; and by influence on the formation of glucose whose yield depending on hydration increases by degrees with intermediate stages. This reaction is related to the characteristic points concerning the bound state of water in starch of 10, 17–18, and 33%. (P.C.H.)

36600 INTENSITY OF RENEWAL OF RABBIT MUSCLE AND SERUM PROTEINS IN THE DYNAMICS OF RADIATION SICKNESS. Zhurbin, G. I. (Inst. of Biochemistry, Kiev). Ukr. Biokhim. Zh., 38: 241-6(1966). (In Russian).

Sharp changes in the metabolism of muscle and serum proteins occur during radiation sickness. The changes are of a wave nature. The renewal intensity of muscle enzymes, such as glycerophosphate dehydrogenase (GPD), aldolase, and glyceraldehyde-3-phosphate dehydrogenase (GAPD), decrease by 59–83% within three hours after irradiation. Twelve hours later the renewal returns to the normal level, and after 18 hours renewal of muscle proteins exceeds the control. Afterwards the intensity of muscle protein renewal gradually falls. After 120 hours the specific radioactivities (SR) of aldolase, GPD, and GAPD comprise 39.6, 58.4, and 28.3% of the control, respectively. The SR curves of serum protein are almost a mirror image of the muscle protein SR curves. Within three hours after irradiation the SR of gamma-globulin and albumin exceed the control by 80 and 86%, respectively. During the 12th hour the serum protein SR falls to the control level and lower (gamma-globulin). By the 18th hour the SR of gamma-globulin and albumin exceed the control by 88.3 and 121.5%, respectively. During the 120th hour after irradiation the SR of gamma-globulin exceeds the control by 44.2%, while the albumin SR is 13.0% short of the control level. The SR of muscle tissue and summary serum proteins, as well as the percent of protein in muscle extract and serum of the irradiated rabbits, did not differ from those of the control animals during the entire period of the investigation. (auth)

36601 EFFECT OF NEUTRON IRRADIATION ON THE AMINOTRANSFERASE ACTIVITY OF THE CENTRAL NERVOUS SYSTEM AND SKELETAL MUSCLE. Pikulev, A. T.; Konyaeva, M. P. (Belorussian State Univ., USSR. Inst. of Physiology, Minsk). Ukr. Biokhim. Zh., 38: 258-63(1966). (In Russian).

Total irradiation of albino rats with neutrons of intermediate energies in doses of 13 rad leads to changes in the activity of aspartate-aminotransferase and alanine-ketoacid aminotransferase in the cerebral cortex, cerebellum, spinal cord, and skeletal muscle at the end of the 1st, 3rd, 15th, and 30th days. These changes are characterized not only by a rise or fall in transaminizing enzymes, but also by discoordination in this enzyme system. This is corroborated by the change in the calculated value of K, which expresses the relationship of aspartate-aminotransferase activity to alanine-ketoacid aminoferase. (auth)

36602 CONTENT AND METABOLISM OF PHOSPHOPROTEINS IN DENERVED AND INTACT MUSCLES AFTER X-RAY IRRADIATION. Sokolov, I. I. (Dnepropetrovsk State Univ., Ukrainian SSR). Ukr. Biokhim. Zh., 38: 264-8(1966). (In Ukrainian).

Studies were made on changes in content and metabolism of phosphoproteins (PP) in denerved rabbit muscles after a single whole-body irradiation with an x-ray dose of 1200 R. The method of radioactive indicators was used. The investigations show that at later periods after denervation the PP content falls and metabolism in the muscles rises. A single whole-body irradiation induces a valid fall in the PP content in the intact muscles both during the initial period (16–20 hours after irradiation) and during the acme of radiation sickness (10–12 days). The rate of ^{32}P incorporation and PP phosphorus metabolism intensity is considerably elevated. In the denerved muscles the effect of radiation does not lead to substantial changes in the content or metabolism of PP. The results indicate the essential role of the central nervous system in the formation of the muscle tissue reaction to ionizing radiation. (auth)

36603 METHYLATION OF GUANIDINACETIC ACID IN LIVER SECTIONS OF RATS SUBJECTED TO X-RAY IRRADIATION. Zelinskii, V. G. (Odessa Medical Inst.). Ukr. Biokhim. Zh., 38: 314-17(1966). (In Ukrainian).

The process of guanidinacetic acid methylation in surviving liver sections of albino rats sacrificed at various periods after x irradiation (800 R) was studied. A rapid, profound, and prolonged depression of guanidinacetic acid methylation was found. Inhibition of the biosynthesis of creatine is possibly due to the effect of ionizing radiation on enzymes involved in remethylation. The observed disturbance may be partially explained by the fall in ATP level in the tissue, for the addition of ATP in the incubation mixture considerably raises the quantity of synthesized creatine. (auth)

36604 INFLUENCE OF IONIZING RADIATION ON THE DISCHE-POSITIVE MATERIAL IN URINE AND BLOOD OF IRRADIATED ANIMALS. Zicha, B.; Pospisil, J. Vet. Med. (Prague), 7: 431-42(1965). (In Czech).

The excretion of desoxyribosides by means of the Dische-reaction in urine of pigs, sheep, and dogs following whole-body irradiation was traced. Excretion of the Dische-stuffs significantly increased in pigs and sheep 6 hours after irradiation. No statistically important increase was observed in dogs. The D-stuffs were traced in the perchloric filtrate of blood in dogs and rats after whole-body irradiation. A statistically significant increase after irradiation was ascertained. From the methodical point of view the most accurate evaluation of the D-stuffs appeared to be the extinction-difference between the maximum and minimum of the absorption curve within the range of 400–550 nm. Subtracting at one wavelength does not seem suitable for evaluating the D-stuffs in urine because of its considerable nonspecific interference. (auth)

Radiation Effects on Tissues

Refer also to abstract 37025.

36605 (COO-1119-5) X IRRADIATION OF THE DEVELOPING AVIAN EMBRYO AS A FACTOR OF AGING. Period Covered: January 1, 1962–December 31, 1965. Muller, Harry D. (Colorado State Univ., Fort Collins. Dept. of Poultry Science). Jan. 10, 1966. Contract AT (11-1)-1119. 52p. Dep. mn. CFSTI $3.00 cy, $0.50 mn.

The effects of a single dose of 85 R x radiation de-

livered on the 3rd, 8th, or 13 day of embryonic development were followed for 48 months in chickens. Emphasis was placed on reproductive performance, egg production, aging, and other pertinent biological factors. A synopsis of previous progress reports is included. (C.H.)

36606 (NYO–1864-23) THE EFFECT OF X-RAY IRRADIATION ON PHOSPHOLIPID METABOLISM. Progress Report, October 1, 1965–May 31, 1966. Schwarz, Henry P. (Philadelphia General Hospital, Pa.). Contract AT(30-1)-1864. 18p. Dep. mn. CFSTI $1.00 cy, $0.50 mn.

Progress is reported in studies on the phospholipid content and chemical composition of phospholipids in blood plasma of men and rats; the effects of x radiation doses of 2000 to 3000 R on the total phospholipids in rat liver fractions and blood plasma; and the effects of stress caused by acceleration of healthy men at 3 to 4 G for 10 sec on total phospholipid and phosphatidylglycerol content in plasma. The syntheses of phosphatidylglyceral, tritium-labeled phosphatidylglycerophosphate, and a new cardiolipin are described. (C.H.)

36607 (TID–23114) A STUDY OF THE EFFECTS OF RADIATION ON HOST-PARASITE RELATIONSHIPS. Progress Report, June 1954–June 1966. Jones, Arthur W. (Tennessee Univ., Knoxville. Dept. of Zoology and Entomology). June 15, 1966. Contract AT(40-1)-1749. 12p. Dep. mn. CFSTI $1.00 cy, $0.50 mn.

Progress is reported in studies of the effects of x radiation on host-parasite relationships. The effects of radiation on six species of cestode, seven species of final vertebrate hosts and a number of intermediate invertebrate hosts of these parasites were investigated. Data are summarized on the life cycle, cytology, histopathology in intermediate hosts, effects of whole-body radiation on final hosts, the survival of heavily irradiated larvae, and immune reactions of hosts to the dog tapeworm, cat tapeworm, rat tapeworm, salamander tapeworm, mouse tapeworm, and other related studies. (C.H.)

36608 STUDIES ON RENAL CLEARANCE. PART III. CHANGES OF KIDNEY AND RENAL CLEARANCE FOLLOWING NEUTRON IRRADIATION OF THE KIDNEY. Hamada, Kunihiko (Hiroshima Univ. School of Medicine). Acta Urol. Jap., 10: 237-52(May 1964). (In Japanese).

In preliminary studies, ddN strain male mice were whole body irradiated with 200-rad doses of either 14.1-Mev neutrons or 150-kv x rays and radiation damage to the kidney due to these relatively small doses of irradiation was observed. Macroscopic and microscopic examinations of the tissue were made at various intervals from 24 hours to two months following irradiation. No changes were observed macroscopically. Mild changes in the glomerulus and tubules, with inflammatory cell infiltration in the interstitial tissue, were observed during initial and middle stages. All of these alterations were much less severe than expected. The death rate was much higher in the neutron-irradiated mice and the histological changes occurred slightly earlier in this group than in x-irradiated mice. In other experiments, male mice were irradiated with 100-rad doses of neutrons to study the changes in macro- and microscopic findings in the kidney and to observe the interrelation of the values of glomerular filtration rate and tubular clearance of p-aminohippuric acid. As in the preliminary studies, only slight changes, which disappeared soon, were observed macro- and microscopically. However, distinct changes were obtained in the renal clearance rates. These results indicate that such small doses of radiation cause transient morphological changes in the kidney at the earlier stage postirradiation, followed by rapid regeneration to give an apparently normal picture. However, different results might be obtained if the observations were followed for longer periods. (TCO)

36609 RADIATION-INDUCED PREMATURE AGING IN LEAVES AND AUTUMNAL EVENTS IN NATURE. Krebs, Adolph T. (Walter Reed Army Inst. of Research, Washington, D. C.). Beitr. Biol. Pflanzen, 41: 157-74 (1965).

Ionizing radiation was shown to produce autumn-like effects (color changes and fall of leaves) as demonstrated in field experiments and in lab studies. The field experiments were done with mixed neutron-γ radiation from an unshielded (air-shielded) 10-Mw reactor and in a natural-environment γ field, using a cesium-137 radiation source. The 10-Mw bare reactor in Georgia is surrounded by mixed evergreen-deciduous forests and covers a radiation field of several hundred acres when operated at full power. In this radiation field, two systems were studied for radiation effects: a hardwood stand (oak-hickory) for measurement of forest litter production, and loblolly pines for general appearance of radiation damage. It was found that 15,000 rad absorbed during summertime, when the foliage was matured, caused initiation of litter fall seven weeks earlier than normal litter fall; 4000 rad induced earlier leaf fall by one week as compared to normal leaf shedding. The leaves receiving 4000 rad followed a normal, but accelerated, autumnal change in color patterns, while high doses caused the leaves to turn brown before falling. Loblolly pine trees within 500 ft of the reactor changed from green to reddish-brown one week after about 8000 rad, and turned brilliant red-brown one month after exposure to a total dose of about 12,000 rad. Pine trees were killed by exposure to 20 R/day, while hardwood species were more radioresistant. The effects of 50-kv x rays on single leaves, entire plants, and leaf extracts were also examined. Leaves responded to irradiation with distinct color changes in the irradiated area, varying with dose from bleaching to grey-green over yellowish-green to red, and, as in the case of Sassafras leaves, to red-purple. Chlorophyll-ether solutions from fresh leaves and from pure chlorophyll a and chlorophyll b were irradiated under identical conditions at a dose rate of 11,400 rad min. Absorption curves as a function of radiation dose showed a decrease in the characteristic chlorophyll peaks at 663 and 430 mμ and formation of a new compound in the 500 mμ region. The relation between natural autumnal events and radiation-induced responses in leaves and plants is discussed. (TCO)

36610 THE RESISTANCE OF MICROCOCCUS RADIODURANS TO ULTRAVIOLET RADIATION. III. A REPAIR MECHANISM. Boling, M. E.; Setlow, Jane K. (Oak Ridge National Lab., Tenn.). Biochim. Biophys. Acta, 123: 26-33(July 20, 1966). (ORNL-P-1635).

The thymine-containing pyrimidine dimers in the DNA of ultraviolet-irradiated Micrococcus radiodurans are excised at exponential rates from the DNA and appear in the medium outside the cells rather than in the acid-soluble fraction of the cells. The dimers extruded into the medium are apparently almost all in oligonucleotides smaller than tetranucleotides, as judged by chromatographic mobilities, and some of the oligonucleotides contain a terminal phosphate. The excision process depends on the presence of some nutrients in the medium, but glucose is not required. It is inhibited by iodoacetamide but not by chloramphenicol. The rate of excision, but not cell sensitivity, is considerably greater in log-phase cells than in stationary cells. (auth)

36611 THE EFFECT OF UNILATERAL LIMB SHIELDING ON THE HEMOPOIETIC RESPONSE OF THE GUINEA PIG TO GAMMA IRRADIATION (150 r.). Osmond, D. G.; Roylance, P. J.; Lee, W. R.; Ramsell, T. G.; Yoffey, J. M. (Bristol Univ., Eng.). Brit. J. Haematol., 12: 365-75(July 1966).

Guinea-pigs were exposed to 150 R gamma irradiation while approximately one-fifth of the total bone marrow was protected by shielding two limbs. Quantitative cell counts of both the shielded and irradiated marrow were combined with observations on the thymus, spleen, and blood during the recovery period, and compared with the effects of whole-body irradiation. Following whole-body irradiation (150 R) the thymus showed a delayed secondary cellular depletion coinciding with a marked splenic hyperplasia. Both phenomena were eliminated by limb shielding. The lymphocytes in the irradiated marrow of partially shielded animals continued to show both the overshoot and the secondary fall in numbers which characterize recovery from whole-body irradiation. After an initial fall

in numbers of erythroid and granulocytic precursors, the shielded marrow showed a temporary increase in granulocytopoiesis coinciding with an abortive phase of granulocytopoiesis in the irradiated marrow. There was no evidence of any effective colonization of irradiated marrow by cells from the shielded marrow. The significance of these findings is discussed. (auth)

36612 LASERS AND ULTRASONICS. Mellerio, J. (Inst. of Ophthalmology, London). Brit. Med. J., 1: 978-9(Apr. 16, 1966).

The role of ultrasonic, electromagnetic, and thermal effects in laser-produced lesions in the eye is considered. Recordings were made of mechanical pulses produced in the eye by laser coagulation. These pulses have large amplitudes and complex waveforms with a fundamental frequency of the order of 200 kcps, hence ultrasonic. These mechanical events are produced only when a lesion is at once visible ophthalmoscopically and travels outwards from the lesion site. This ultrasound is a form of shock wave generated by the explosive formation of a lesion. Preliminary results indicate that the amplitude of these wave trains is of the order of 1 g/cm^2 peak to peak, 12 mm from the site of origin. The question of whether lesion formation is due to electromagnetic disruption is discussed. If this effect occurs it is unimportant. If the temperature around a lesion site during its formation is measured carefully, large temperature changes are recorded. Retinal pigmentation effects the size of lesion produced. It can only do so if lesion formation depends on the amount of energy absorbed, for this absorbed energy is degraded directly into heat which can then damage retinal tissue. If electromagnetic disruption were a prime force in lesion formation, pigmentation would not effect lesion size. (BBB)

36613 ON THE THYMUS ORIGIN OF LYMPHOMATOSES OBSERVED IN MICE OF DIFFERENT STRAINS AFTER GENERALIZED IRRADIATION BY X RAYS. Riviere, M. R.; Chouroulinkov, I.; Guerin, M. (Institut de Recherches Scientifiques sur le Cancer, Villejuif, France). Bull. Ass. Franc. Etude Cancer, 52: 267-78(July-Sept. 1965). (In French).

Mice of various strains (Swiss, AKR, C57B1, XLII, and C3H) aged 1½ to 8 months were given whole-body exposures to x rays, either in single doses of 150, 300, or 600 R, or 4 weekly doses of 150 R each. The mice were sacrificed at intervals after irradiation varying from two to 12 months, and mediastinal tissue was examined histologically. Among the 166 C57B1 mice examined leukemia was found in four, and in an early stage in two of these mice. It could be traced to an origin in the thymus. Similarly, of 233 AKR mice, 31 had leukemia, and in 8 cases it could be traced to the thymus. Swiss mice developed leukemia in 48 out of the 532 individuals examined; in 20 thymic origin could be traced. Of 108 nonirradiated Swiss mice, five developed leukemia and of these, three showed its thymic origin. Four of 276 XLII mice were found to have leukemia, but none of 79 C3H mice became leukemic. It is emphasized that in the susceptible strains of mice, leukemia could be shown to arise in most cases in the thymus, often in only one of the two lobes of the gland. The mediastinal lymph nodes contained leukemic cells, but only secondarily, and in only two instances were they the origin of the leukemic process. (BBB)

36614 CERTAIN PECULIARITIES OF NERVE TRUNK REGENERATION IN RELATION TO THE PHASE OF ACUTE RADIATION LESION. Ryss, Ya. I. (Rostov-on-Don Medical Inst., USSR). Byull. Eksp. Biol. Med., 61: No. 4, 115-19(Apr. 1966). (In Russian).

An experiment was carried out on dogs in which the right sciatic nerve was severed and sutured during the latent period (30 animals) and in the period of climax (30 animals) of acute radiation sickness of moderate severity. The single dose of total irradiation was 350 R. The animals were killed at different times after the operation (from one day to one year). Analysis of histological material showed that in animals operated upon when the disease was at its height the processes of nerve degeneration and regeneration slowed down, particularly in the early period after the operation, with heavier and denser neuromas forming in the region of the suture. Histopathological changes in the cerebrospinal ganglia were more manifest than in the spinal cord. Long-term observations revealed no appreciable difference in the state of the damaged nerves in animals of both groups. Dystrophic disorders in animals operated upon in the period of climax of radiation sickness took a longer course and were more severe. (auth)

36615 EFFECTS OF X RAYS ON THE YOUNG EMBRYO OF THE BLINDWORM (ANGIUS FRAGILIS L.). Pieau, Claude (Institut Pasteur, Sannois, France). Compt. Rend. Soc. Biol., 160: 59-62(1966). (In French).

Preliminary results obtained in a study on the effects of x rays on young embryos of the blindworm are reported. The results showed that the embryo is capable of surviving, at least for about 12 days, the administration of x-ray doses of the order of 780 to 1300 R. These doses however exercise appreciable destructive effects on the majority of the organ rudiments. (J.S.R.)

36616 EFFECT OF IONIZING RADIATIONS ON THE HeLa CELL. II. ELECTRON MICROSCOPIC STUDY. Driessens, J.; Dupont, A.; Demaille, A.; Cappelaere, P.; Giaux, G.; Puvion, E. (Institut de Recherches sur le Cancer, Lille). Compt. Rend. Soc. Biol., 160: 91-3(1966). (In French).

The irradiation of HeLa cells causes numerous morphological modifications affecting principally the nucleus, nucleolus, and organelles (particularly the mitochondria). Multiple cytoplasmic inclusions appear similar to those observed in a culture of old HeLa cells. A 4-day delay is necessary for the lesions to become evident. These progress in 8 days to the appearance of numerous giant cells. The cytoplasmic lesions depend less on the dose received than on the time after its administration. (J.S.R.)

36617 INCREASE IN THE PROPORTION OF VIRUS-PRODUCING CELLS AND OF SEVERAL MUTANTS IN K12λ CULTURES EXPOSED TO ULTRAVIOLET LIGHT, TRIETHYLENE MELAMINE, OR HYDROGEN PEROXIDE. Northrop, John H. (Univ. of California, Berkeley). Enzymologia 30: 131-4(Feb. 28, 1966).

The effect of triethylene melamine (TEM), uv light, and hydrogen peroxide on the proportion of virus-producing cells, neomycin-resistant cells, penicillin-resistant cells, P_1 phage-resistant, and T_2 phage-resistant cells in Escherichia coli K12λ cultures was determined. All the mutagens tested increased the proportion of all the mutants, as well as the virus-producing cells, from 2 to 30 times. Prolonged exposure to uv light followed by growth at 25° caused small increases in all the types of cells. The mutagen TEM can cause the mutations to occur without any cell growth or cell division. Under the conditions of these experiments, therefore, the occurrence of the virus-producing cells increases to about the same relative extent as does that of recognized mutants. This result confirms the assumption that the change from virus-free to virus-producing cell is a mutation. Continuous culture in the presence of TEM or repeated exposure to uv light, however, has a different result. Under these conditions a great increase in λ virus first occurs with little change in the proportion of mutants. Several days after this, an entirely new virus appears which infects and lysogenizes the parent culture that produced it. The result is that the original culture that produced λ phage is replaced by a different strain that produces the TEM phage. These latter experiments are similar to the production of polyhedral silk worm virus after exposure of the larvae to various mutagens as described earlier. (BBB)

36618 SOME COMPONENTS OF THE GENETIC LOADS IN IRRADIATED EXPERIMENTAL POPULATIONS OF DROSOPHILA MELANOGASTER. Sankaranarayanan, K. (Rockefeller Univ., New York). Contract AT (30-1)-3096. Genetics, 54: 121-30(July 1966).

Three experimental populations, kept under conditions designed to minimize the larval competition and crowding, received each 120,000 R of x rays during 20, 30, and 60

generations, respectively. The egg-to-adult viability decreased sharply, but, after the radiation was discontinued, the egg-to-adult viability recovered rapidly for several generations and then reached a plateau. This plateau is, however, 15 to 20% below that in the control, unirradiated, population. The frequencies of the second chromosomes which were lethal or semilethal when homozygous declined after the cessation of the radiation, without however in any case reaching the control level. The frequency of alleles among the lethals has increased. Some particular lethal chromosomes have become more frequent, probably owing to heterotic effects under the conditions obtained in the experiments. (auth)

36619 AGE DEPENDENCE OF LOCATIONS OF X-RAY-INDUCED SOMATIC CROSSING-OVER IN DROSOPHILA. Tokunaga, Chiyoko; Arnheim, Norman Jr. (Univ. of California, Berkeley). Genetics, 54: 267-76(July 1966). (UCRL-16687).

Radioinduced somatic crossing over was studied in the left arm of the second chromosome in Drosophila melanogaster. In experiments with the genes Tufted (Tft, 48.5–54.5) or Bristle (Bl, 54.8), x irradiation given early in development resulted in more somatic exchanges to the left of these loci than to the right of them. Later in development the opposite was true, with more crossing over occurring to the right than to the left. It would appear that both the Bl and Tft loci lie between two chromosome regions which differ in the time during ontogeny at which they are maximally sensitive to x-ray induced somatic crossing over. (auth)

36620 MUTATIONS OBTAINED IN SPRING WHEAT LUTESCENS 62 TREATED WITH FAST NEUTRONS AND GAMMA RAYS FOLLOWED BY PARTIAL REMOVAL OF DAMAGING IRRADIATION EFFECT. El'shuni, K, A.; Khvostova, V. V. (Inst. of Biological Physics, Moscow). Genetika, No. 6, 37-46(June 1966). (In Russian).

Additional treatment decreasing chromosome damage caused by γ irradiation did not reduce mutation frequency in M_2 of wheat; it caused an increase of more than 50% at a dose of 10 kR. An irradiation dose equal to 40 kR followed by treatment yielded up to 40% mutations per 100 M_2 progenies. Additional treatment with fast neutrons did not influence mutation rate. A series of mutations which can serve as initial material for wheat breeding (for instance mutants 56, 68, 73, 75, 93, with a cylindrical ear, erectoids 171, 191, 209, form with a large ear 432, bluish high yielding plants, etc.) were obtained. (auth)

36621 CYTOGENETIC ANALYSIS OF THE MUTAGENIC EFFECT OF IONIZING RADIATION AND ALKYLATING COMPOUNDS IN PEAS. Akhund-zade, A. I.; Khvostova, V. V. (Inst. of Biological Physics, Moscow). Genetika, No. 6, 47-54(June 1966). (In Russian).

A comparative study of mitosis in rootlets and apex buds of seedlings in garden peas of the variety Pioneer treated with fast neutrons, gamma rays, ethylenimine, ethylmethansulfonate, as well as a study of meiosis in anthers of M_1 plants, of the number of seeds formed by M_1 plants and of the frequency of chlorophyll mutations in M_2 is reported. A correct registration of the number of chromosome rearrangements in the first mitosis of the meristem of seedlings is possible only when they are analyzed during the whole first mitotic cycle, because the maximal number of rearrangements arising after treatment with different mutagens is found at different hours of fixation. Treatment with chemical mutagens induces rearrangements of the isochromatid type which are eliminated during mitosis and are lost before meiosis. Symmetrical translocations, inversions, and micro-nuclei are found in tetrads during meiosis after irradiation. Decrease of the number of seeds in M_1 was observed only after irradiation. A maximal number of chlorophyll mutations of the broadest spectrum was obtained after treatment with ethylmethanesulfonate, then follows ethylenimine, gamma rays, and fast neutrons. The RBE of fast neutrons is 25–30 compared with gamma rays. The data show that chemical mutagens induce as many chromosome rearrangements as ionizing radiations; however, isochromatid deletions which predominantly arise are eliminated in mitosis and do not reach the germ cells. The ratio of chlorophyll mutations in M_2 to the maximal number of chromosome rearrangements in rootlets of M_1 seedlings equals 0.25 for neutrons, 0.5 for gamma rays, and 0.75–1.4 for ethylenimine and ethylmethanesulfonate. (auth)

36622 INFLUENCE OF PARTIAL REPARATION OF THE DAMAGING EFFECT OF IRRADIATION ON THE FREQUENCY OF CHLOROPHYLL MUTATIONS IN BARLEY. Khvostova, V. V.; El'shuni, K. A. (Inst. of Biological Physics, Moscow). Genetika, No. 6, 55-61 (June 1966). (In Russian).

Additional treatment which diminishes radiation damage led to a decrease in the number of cells with chromosome rearrangements during the first mitotic cycle in meristematic cells of seedling roots obtained from seeds irradiated at 10 kR; the highest influence was observed at the beginning of the cycle. An analysis of the dosage dependence of chlorophyll mutations rate showed that irradiation followed by an an additional treatment induced a nearly linear increase of mutation rate whereas irradiation at 10–30 kR without additional treatment gave a plateau. Thus, a decrease of damaging effect led to recovery of such M_2 mutations which would have been lost without additional treatment. (auth)

36623 THE FIRST ATTEMPT OF OBTAINING MUTATIONS OF THE FINE FIBER COTTON PLANT OF THE SPECIES GOSSYPIUM BARBADENSE L. Fursov, V. N.; Konoplya, S. P. (Turkmen Research Inst. of Agriculture, Iolotan Plant Breeding Station, USSR). Genetika, No. 6, 62-9(June 1966). (In Russian).

Irradiation of air dried seeds of fiber cotton varieties of the G. barbadense L. species with γ rays and slow neutrons revealed the possibility of obtaining plants possessing an increased number of various valuable characters. The basic characteristics of the selected mutants are not any worse than those of the initial variety while some of them present a stressed advantage. (P.C.H.)

36624 CHLOROPHYLL MUTATIONS AS AN INDICATION OF DIFFERENCES IN THE MUTABILITY OF PEA VARIETIES. Sidorova, K. K. (Inst. of Cytology and Genetics, Novosibirsk, USSR). Genetika, No. 6, 81-7(June 1966). (In Russian).

The frequency and spectrum of chlorophyll and morphological mutations were studied in seven pea varieties under the influence of ethylenimine–0.03%, ethylmethanesulfonate 0.15%, and γ rays 10 kR. It was found, that chlorophyll mutations in peas can be an indication of the mutability in the varieties. Positive correlation was observed between the frequency and spectrum of the chlorophyll and morphological mutations. The wider the chlorophyll mutation spectrum in the variety, the higher the variability of morphological mutations. (auth)

36625 ON THE ROLE OF GAMMA TREATMENT OF OOCYTES IN THE REALIZATION OF RADIATION INJURY OF DROSOPHILA SPERM CELLS. Karimov, A. L.; Malinovsky, O. V. (Pavlov Inst. of Physiology, Leningrad). Genetika, No. 6, 140-3(June 1966). (In Russian).

Hatching of eggs obtained from irradiated and non-irradiated females crossed with irradiated and non-irradiated males was studied. It was found that the radiation effect in the case when both oocytes and sperm cells were irradiated simultaneously equals the sum effect of separate irradiation of the female and male sex cells. It follows that oocytes' irradiation does not influence the yield of radiation injured sperm cells. (auth)

36626 EFFECT OF ULTRAVIOLET IRRADIATION ON THE FUNCTIONAL CONDITION OF BASIC CEREBRAL NERVOUS PROCESSES IN MAN. Albitskaya, E. F.; Gorkin, Z. D. (Kharkov Medical Inst.). Gig. Sanit., No. 6, 17-20(June 1966). (In Russian).

The effects of ultraviolet radiation on the higher nervous activity of 15–16-yr-old technical school students were studied. The motor-speech method and the method of directed speech reactions (association test) were used to estimate the function of both signal systems. The ra-

diation source was a PRK-2 mercury-quartz lamp with a wavelength of 136–400 mμ. Biodoses were determined for each student, since individual sensitivity to uv radiation varies widely. Doses were given singly (1½, 1, and ½ biodose) or repeatedly (1 ½ and 1 biodose). The subjects, placed 75 cm from the source, were exposed (to the waist) to uv rays simultaneously from two sides. Indexes of higher nervous activity employed included the accuracy of conditioned reflexes, the length of the latent period of motor and speech reactions, the quality of responses, absence of responses or repetition of words, and errors in pressing buttons. Ten students were studied in 500 experiments with repeated irradiation with 1½ biodose (237.9 $\mu v/cm^2/min$). Experiments showed no change in the accuracy of conditioned reflexes or in the length of the latent period of a motor reaction to a word stimulus. However, repeated irradiation with this dose improved the functional condition of the second signal system in the following ways: the latent period of the speech reaction decreased in length; response reactions improved; and the number of avoidance reactions dropped. The incompleteness of this improvement in the functional condition of the second signal system was demonstrated by the number of repetitive or erroneous responses. It was concluded that this second signal system, based on speech, is more excitable than the first system (sensory), since it can be stimulated by ultraviolet irradiation. (ATD)

36627 HAZARD FROM HIGHLY IONIZING RADIATION IN SPACE. Curtis, S. B.; Dye, D. L.; Sheldon, W. R. (Boeing Co., Seattle). Health Phys., 12: 1069-75(Aug. 1966).

In evaluating the hazard from a source of mixed radiation, it is necessary to determine the importance of the highly ionizing component. Calculations are presented that indicate the importance of this component in the solar-particle radiation environment within a space capsule. Shielding thickness and particle spectrum shape both are important in determining the extent of the hazard. The concept of fractional cell lethality (FCL), the fractional number of cells inactivated in an organ, is introduced to circumvent the inherent disadvangages in the Quality Factor concept when applied to the evaluation of the space radiation hazard. It is shown as an example that up to 7 per cent of the kidney cells in a seated astronaut could have been inactivated during the giant solar-particle event of 12 November 1960. Information on accumulated damage to critical nonreproducing cells, such as neural or retinal cells, is lacking. Perhaps such damage will constitute the bulk of the hazard for space missions of long duration, in which case the FCL concept may provide a sound basis for evaluating the hazard on these missions. (auth)

36628 GASTRIC EMPTYING IN RATS AFTER PART-BODY IRRADIATION. Hulse, E. V. (Medical Research Council, Harwell, Eng.). Int. J. Radiat. Biol., 10: 521-32 (July 15, 1966).

The effects of part-body x irradiation on gastric emptying were studied in rats, mainly using a dose of 100 R. Irradiating the head and shoulders did not delay gastric emptying. Irradiating the abdomen delayed emptying as much as whole-body irradiation, but the delay after irradiation of the cranial, caudal, dorsal, or ventral halves of the abdomen was less. The cranial half of the abdomen was more sensitive than the caudal half. The right side of the body was as sensitive as the whole body but the left side was less sensitive. Irradiation of a small part of the abdomen through a 1 in. lateral port delayed emptying only slightly less than whole-body irradiation. Anatomical studies led to the conclusion that irradiation of the small intestine and associated structures is the most important factor in producing the delay. Possible mechanisms whereby intestinal irradiation could delay gastric emptying are discussed. (auth)

36629 THE RADIATION SENSITIVITY OF A CYTOPLASMIC MUTANT OF ASPERGILLUS NIDULANS. Arlett, C. F. (Wantage Research Lab., Eng.). Int. J. Radiat. Biol., 10: 539-49(July 15, 1966).

A cytoplasmic mutant of Aspergillus nidulans produced two classes of conidia, mutant and non-mutant. The mutant conidia were more resistant to uv than the non-mutant, and this difference was found to be attributable entirely to the cytoplasm. There were no differences between the two classes of gamma irradiation. It was not practicable to examine the possibility of differences in a cytoplasmic target in this system, and an attempt was made to test whether cytoplasmically determined differences in repair capacity might account for the different uv sensitivities. The chemical inhibitors of repair processes, acriflavine and caffeine, which are effective in some bacteria did not reduce but enhanced survival in the fungus. Some other treatments which enhanced survival also delayed germination, and an explanation based on a prolonged period for repair is suggested. (auth)

36630 EFFECT OF X RAYS ON THE METABOLISM OF THE RETINA. Lucas, D. R. (Medical Research Council, Harwell, Eng.). Int. J. Radiat. Biol., 10: 551-65(July 15, 1966).

The effect of x rays on respiration and glycolysis was studied in organ cultures of the retina of the guinea-pig and the rat. With the guinea-pig there was a rapid depression of respiration after doses of 2000 rad or more. The magnitude of the depression was proportional to the amount of histological damage in the visual cell layers. No effect on aerobic or anaerobic glycolysis was detected. With the rat there was a moderate depression of both respiration and glycolysis after doses of 5000 rad or more. But the magnitude of the depression was not proportional to dose or to the amount of histological damage in the visual cell layers. The differences in behavior of the retinas of the two species is attributed to different metabolic and vascular patterns. (auth)

36631 THE ACRIDINE ORANGE AND DYE EXCLUSION VIABILITY TESTS APPLIED TO IRRADIATED EHRLICH TUMOR CELLS. Seydel, H. Gunter; Lawson, Noel S. (Univ. of Maryland, Baltimore). Int. J. Radiat. Biol., 10: 567-76(July 15, 1966).

Mice bearing an Ehrlich ascites tumor were given whole-body x irradiation and sacrificed at intervals of one hour to three days after treatment. Specimens of ascites were removed and stained supravitally with acridine orange, eosin yellow, or nigrosin. The viability of the ascites cells was assayed by observing their ability to produce new growths. The percentage of cells which showed unaltered cytoplasmic fluorescence after staining with acridine orange, or which did not absorb eosin or nigrosin, was significantly different from the percentage of cells which produced tumors. On the other hand, there was a good correlation between the results obtained with the two methods of assay when the cells were killed by treatment with formalin, alcohol, or centrifugation. Fixed irradiated Ehrlich tumor cells showed a change in the cytoplasmic acridine orange fluorescence from red to orange or green. The percentage of cells showing this change increased with increasing dose, but did not correlate with the percentage tumors produced by the irradiated ascites after subcutaneous injection. (auth)

36632 SENSITIVITY OF RAT OOCYTES TO X RAYS. Mole, R. H.; Papworth, D. G. (Medical Research Council, Harwell, Eng.). Int. J. Radiat. Biol., 10: 609-15(July 15, 1966).

A re-analysis of already published data (Mandl A. M., Proc. Roy. Soc. B, 150: 53(1959)) showed that normal stage 1 oocytes of the young mature rat survived irradiation according to a typical exponential dose-response relation with $D_{37} = 91$ r and $n = 2.3 \pm 1.1$. When the data for normal plus atretic oocytes are combined, the dose-response relationship for stage 1 is not simple. Oocytes at later stages of follicular development were very much more radioresistant. Large doses of radiation increased the proportion of atretic follicles in the earlier stages even as late as 30 days after exposure. In contrast at stages 5–6 doses of radiation too small to affect the number of normal oocytes reduced the number of atretic oocytes to levels much below those in unirradiated controls. (auth)

36633 THE EFFECT OF IRRADIATED MEDIUM ON THE GROWTH OF L5178Y LYMPHOMA CELLS. Scott, O. C. A.; Diss, Carol; Sturrock, Jean (Mount Vernon Hospital, Northwood, Eng.). Int. J. Radiat. Biol., 10: 617-19(July 15, 1966).

Unirradiated lymphoma cells were inoculated into irradiated medium and variations in growth rate were investigated. When exposed to 850 rad, the growth expressed as a percentage of growth in unirradiated medium after 3 days incubation was 42% (mean of 8 experiments), using the radiosensitive strain of cells. The radioresistant line was also susceptible to the effect of irradiated medium. Cells from old cultures (~10^6 cells/ml) were found to be more sensitive to irradiated medium than cells from younger cultures (10^5 cells/ml). Other factors affecting growth inhibition are also discussed. (P.C.H.)

36634 COMPARATIVE STUDIES OF PHYSICAL AND CHEMICAL MUTAGENS ACCORDING TO THE FREQUENCY OF MUTATIONS IN THE SECOND GENERATION. Sharma, B. Izv. Timiryazevsk. Sel'skokhoz. Akad., No. 4, 127-40(1965). (In Russian).

The determination of the efficiency of mutagens with respect to the frequency of mutations in the M_2 generation of Krupnoplodny G-20 peas showed that from three methods of calculation of the frequency of mutations the percentage of mutations appears more precise for the determination of the mutagen efficiency. Chemical mutagens cause more changes in M_2 than exposure to ^{60}Co γ and fast neutrons. Of the three chemical mutagens (ethylenimine, diethyl sulfate, and nitrosomethylurea), the nitrosomethylurea shows the most effectiveness; it can give 100 mutations per 100 M_2 seeds. Non-chlorophyll mutations reflect a general mutability or more precision than chlorophyll mutations. As the quantity of mutants increases, the spectrum of the characteristics becomes broader. Different combinations of exposures and concentrations of mutagens give different results and the efficiency of the dose depends on this. Each mutagen has its specific mutations, which appear often with this mutagen and very rarely with others. The determination of the effects of concentrations and exposures on the number of mutations with ethylenimine and diethyl sulfate indicates that different mutagens control themselves in this relation and this question is in great need of investigation. (tr-auth)

36635 CHROMOSOMAL MAPPING BY MEANS OF MUTATIONAL INDUCTION IN SYNCHRONOUS POPULATIONS OF STREPTOCOCCUS FAECALIS. Stonehill, E. H.; Hutchison, Dorris J. (Sloan Kettering Inst. for Cancer Research, New York. Cornell Univ., New York). J. Bacteriol., 92: 136-43(July 1966).

A new method for mapping genetic loci on the bacterial chromosome, based on the linear progression of the deoxyribonucleic acid-replicating enzyme (replicase) in synchronous cultures of Streptococcus faecalis, is described. Ultraviolet irradiation was used to induce mutations to drug and to bacteriophage resistance at various intervals during the progress of the replicase along the chromosome. The time of duplication of the gene in synchronous populations was determined from reductions in the rates of radio-induced mutation. After the replication of various genes, the rates fell to half their former values. The resulting data made possible the construction of a 1-hr time-map indicating the sequence of replication of five genes in S. faecalis. (auth)

36636 ULTRAVIOLET MUTAGENEIS IN BACTERIOPHAGE T4. II. PHOTOREVERSAL OF MUTATIONAL LESIONS. Drake, John W. (Univ. of Illinois, Urbana). J. Bacteriol., 92: 144-7(July 1966).

T4r mutations were induced by ultraviolet irradiation of extracellular phage particles, using a phage mutant, v, which is particularly susceptible to photoreactivation. Most of the induced r mutations could be subsequently photoreversed intracellularly with white light. Ultraviolet irradiation induces both transitions and sign mutations, and both were susceptible to photoreversal. The results suggest that two very different types of mutational lesions may arise from a common type of photochemical lesion. (auth)

36637 HISTOLOGIC CHANGES IN THE LOCALLY IRRADIATED SPLEEN RELATED TO THE IMMUNE RESPONSE. Simic, Miroslav M. (Boris Kidric Inst. of Nuclear Sciences, Belgrade). J. Cell. Physiol., 67: Suppl. 1, No. 3, 129-32(June 1966).

Rat spleens were surgically exteriorized and x irradiated with 10,000 R during different phases of the hemolysin response. The aim was to correlate histologic changes in the spleen with the specific modifications of the hemolysin formation due to localized irradiation of the spleen. The results strongly indicate that the immunologic recovery of the heavily damaged spleen must be due to repopulation by circulating lymphocytes. Furthermore, the view is supported that the large pyroninophilic cells, and consequently antibody-forming cells, originate from circulatory lymphocytes rather than from fixed reticular or endothelial cells. Finally, it appears that macrophages must be extremely radioresistant in initiating antigen-antibody response. (P.C.H.)

36638 PERSEVERATION LEARNING SET FORMATION TO NONREWARDED CUES BY NORMAL AND PREVIOUSLY IRRADIATED RHESUS MONKEYS. McDowell, A. A.; Brown, W. Lynn (Univ. of Texas, Austin). J. Genet. Psychol., 107: 309-11(Dec. 1965).

Excitation is the propotent mechanism of response-perseveration learning set for nonrewarded cues. Normal male and female rhesus monkeys do not differ significantly from each other, and irradiated female monkeys do not differ significantly from normal female monkeys. Attempts were made to determine if previously irradiated male monkeys differ from normal male monkeys with respect to the acquisition of the same learning set, i.e., with respect to the acquisition of two-trial response-perseveration learning set for nonrewarded cues. Nine rhesus monkeys, aged 7 to 9 yr served as subjects. Five years earlier, four had been exposed to chronic fast-neutron radiation: 24-hour whole-body exposure every four days at 87.2 mrep/hr to a total dose 583 rep. The five controls had been sham-exposed during the same period. Testing was done in a modified version of the Wisconsin General Test Apparatus, with a stimulus tray holding two food wells 12 in. apart. The stimuli for testing were 336 test objects differing in multiple dimensions: i.e., in size, shape, and color. Each day for 16 days each monkey was tested on 24 two-trial object-quality discrimination problems. The results showed irradiated male monkeys to be significantly more capable than normal monkeys in the utilization of the excitatory properties of nonrewarded cues. They reflect possibly the narrowed scope of attention that has been reported for irradiated male monkeys. High-dose irradiated monkeys, more frequently than normal and low-dose subjects, showed discrete trial associations with the discriminable stimulus reinforced but not with the position reinforced. (BBB)

36639 SOCIAL DISTRACTIBILITY OF PREVIOUSLY IRRADIATED FEMALE RHESUS MONKEYS. McDowell, A. A.; Brown, W. Lynn (Univ. of Texas, Austin). J. Genet. Psychol., 108: 35-8(Mar. 1966).

Male monkeys exposed in the lab to mixed γ and neutron radiations, male monkeys exposed in the field to nuclear radiations, and male monkeys exposed in the lab to neutron radiation have exhibited decreased social distractibility accruing to prior radiation exposure. A study was made to determine if previously irradiated adult female rhesus monkeys show a similar decrease in social distractibility. As a social stimulus a female monkey of a different species, a Stump-tailed Macaque of the speciosa group, was used. Four control monkeys and 11 whole-body irradiated monkeys served as subjects. They were the female survivors of an exposure to nuclear radiations more than six years earlier. The six irradiated monkeys that had been exposed to estimated total doses of 273, 299, or 355 rem were considered in one group and the five that had been exposed to estimated total radiation doses of 397, 439, or 512 rem in another. Each monkey, over a three-day period, was first

observed with no social stimulus present; next, with the adult-female Stump-tailed Macaque present; and again, with no social stimulus present. The social stimulus was visually but not physically accessible in a well-lighted holding cage at a distance of three ft. Behavioral stability was considered in terms of the maintenance of the balance between total directed activities and total nondirected activities as manifest during the first observation. Total nondirected activity was used to measure that stability. The presence of the social stimulus disrupted the free-cage behavior of control subjects significantly more than it did that of irradiated subjects. The control subjects showed significantly greater direct responsiveness to the social stimulus than did the irradiated subjects. The results demonstrate a decrease in social distractibility for female monkeys previously exposed to nuclear radiations. Such results, considered together with the previous findings on irradiated male monkeys, demonstrate the generality of the phenomenon of decreased social distractibility in irradiated rhesus monkeys. (BBB)

36640 LONGEVITY IN NEUTRON-EXPOSED GUINEA PIGS. Kimeldorf, Donald J.; Phillips, Richard D.; Jones, Dave C. (Naval Radiological Defense Lab., San Francisco, Calif.). J. Gerontol., 21: 265-7(Apr. 1966).

Young adult guinea pigs were exposed to a single total-body exposure of fast neutrons. Then they were maintained in a duration-of-life study to observe the effects on the life span. Exposure to 100 rad was sublethal for the 30-day postirradiation period. Doses of 120 to 160 rad yielded 30-day mortality rates of 11 to 72%. The median life span of sham-exposed controls was 828 days, or 28 months. The animals subjected to 100 rad had a median life span of only 730 days, or a 12% reduction from the controls. For survivors of exposure in the lethal dose range, the median life span was 698 days, or about 23 months. The reduction of five months from the control value represents a 16% decrease in median life span. Groups were matched for body weight at the time of exposure, and one month postirradiation a mean deficity of 100 g was apparent in the group exposed to 120 to 160 rad. In a related study, young adult male rats (94 to 110 days old) were irradiated with 215 to 230 rad with the same neutron source. In terms of 30-day survival, this dose was sublethal for rats, but in terms of median life span there was a reduction of about 22% relative to controls. Thus a dose range which produces some acute mortality in the guinea pig has less effect on life span in this species than does a dose which is sublethal in the rat. In terms of radiation dose, the extent of reduction in median life span per rad seems comparable for the two species under the same conditions. (TCO)

36641 HOMOTRANSPLANTATION STUDIES IN DOGS FOLLOWING SELECTIVE RADIOISOTOPIC LYMPHATIC ABLATION. Winchell, H. S.; Pollycove, M.; Loughman, W. D.; Richards, V.; Kim, L.; Lawrence, J. H. (Univ. of California, Berkeley). J. Nucl. Med., 7: 416-23(June 1966).

A selectivity method for radiating lymphatic tissue was used for preparing dogs for renal tissue homografting. The results showed that selective lymphatic ablation using the methods described produces generalized suppression of the hosts' immunologic competence. The animals thus treated are less able to resist infection as well as being less able to reject homografts than untreated animals. In the case where homologous bone marrow saved the lives of lethally irradiated animals, it appeared that long term survival of the animal was accompanied by eventual return of host immune response and eventual rejection of homologous tissue. (P.C.H.)

36642 KINETIC REGULARITIES IN THE POSTRADIATION RECUPERATION OF CELLS. Korogodin, V. I. (Inst. of Medical Radiology, Moscow). Med. Radiol., 10: 17-24(Aug. 1965). (In Russian).

Experiments, carried out with yeast cells that were irradiated at different doses, and also with yeast cells that were irradiated repeatedly after an initial recovery, showed that the recovery was practically constant after each irradiation and did not depend on the dose D_0. On comparing the experimental results with theoretical recovery values it was found that the decrease of the reversible component of radiation damage with time corresponded to a statistical model, where the aftereffects of separate hits were independently eliminated from the irradiated cells. The recovery in yeast cells can be represented by the following equation: $D_t = D_0 [K + (1 - K) \exp(-\beta t)]$. Here D_t is the effective dose; D_0 is the administered dose; K is the irreversible component of the radiation damage; t is the time interval between the occurrence and realization of potential damage in a cell, and β is the recovery constant, which is proportional to the probability of eliminating a single elementary hit from a cell per unit time. It was estimated that 75 to 80% of the primary hits were potential in character and could be considered as reversible as long as the cell did not undergo division. The transfer of potential damage to an irreversible state became more probable with decreasing time t, that is, if cell division took place a short time after the hit occurred. (TTT)

36643 HEMATOLOGICAL AND HISTOLOGICAL STUDIES IN THE OFFSPRING OF WISTAR STRAIN ALBINO RATS TREATED WITH ANTICANCER DRUGS OR X IRRADIATION. III. HEMATOLOGICAL STUDIES IN THE DESCENDANTS OF WISTAR STRAIN ALBINO RATS TREATED WITH 6-MERCAPTOPURINE OR X IRRADIATION. APPENDIX: SUMMARY AND COMMENTS ON THE RESULTS OF THE PRECEDING EXPERIMENTS. Ito, Taturo (Kyoto Univ.). Naika Hokan, 12: 105-12(Mar. 1965). (In Japanese).

Wistar rats of both sexes at three months of age were whole-body irradiated with a single dose of 300 R of x ray. Seven of the F_1 rats were examined as offspring of these treated rats 100 days after irradiation. In these F_1 rats, the white blood cell counts in the blood tended to decrease gradually as they matured. In one of the F_1 rats which had marked leukocytopenia there was a less marked degree of induced neutrophilia in peripheral blood after a single intramuscular injection of a chemical hematopoietic stimulant, indicating decreased bone marrow activity. In another of the F_1 rats, growth was impaired and early death occurred. Wistar rats of both sexes also were injected intramuscularly with 6-mercaptopurine in a daily dose of 5 mg/kg of body weight for 30 days. A slight decrease of the red blood cell counts was observed in the treated rats 10 days after beginning the injections. Mating was carried out between the treated male and female rats to obtain the two litters of F_1 rats, composed of seven and six rats each. No marked changes were found in the blood cell counts and blood pictures of these F_1 rats. It is concluded that anemia or leucocytopenia occurring in the F_1 rats obtained among the cytostatic agent-treated or x-irradiated male and female rats is probably related to congenital hematopoietic disturbances, and that cryptorchidism occurring in the descendants of the cytostatic-treated rats might be caused by mutagenic action of the chemical agent upon the germ cells of the parent rats. (TCO)

36644 EFFECT OF THERMAL NEUTRON IRRADIATION ON MITOSIS. Rao, C. U.; Sen, S. K. (Banaras Hindu Univ., India). Naturwissenschaften, 53: 335(1966).

The effects of thermal neutron irradiation on seeds of Pisum sativum in the rate of mitosis and also in the integrity of the mitotic chromosomes when observed in 120 hr growing root tip cells were studied. The irradiation was done in thermal neutron flux of 2.2×10^7 n/cm^2/sec for 6, 8, 10, and 12 min. Lengthening the duration of prophase was marked with higher doses resulting in a delay in completion of the cycle. Chromosomal breakages were observed only in the cases of 12 and 8 min treatments at 2.7 and 2.04% frequency, respectively. Single as well as double chromatid breakages were noted. (P.C.H.)

36645 RADIATION-RELATED LEUKEMIA IN HIROSHIMA AND NAGASAKI, 1946–1964. I. DISTRIBUTION, INCIDENCE AND APPEARANCE TIME. Bizzozero, O. Joseph Jr. (Atomic Bomb Casualty Commission,

Hiroshima); Johnson, Kenneth G.; Ciocco, Antonio. New Engl. J. Med., 274: 1095-1101(May 19, 1966).

The occurrence of leukemia in Hiroshima and Nagasaki for the period 1946-1964 is reported. During this period leukemia developed excessively in persons exposed within 1500 meters from the hypocenter. A decreased appearance time, defined as the interval between exposure to radiation and the clinical or symptomatic onset of leukemia, was noted in patients exposed within 1500 meters. Attention is directed to the role of age as a covariable to distance in the appearance time of acute leukemia developing in such persons. In this group chronic granulocytic leukemia developed in persons up to twenty-nine years of age at the time of the bombings in the period 1946–1955 at a disproportionate rate as compared to the distally exposed and the pattern of spontaneous leukemia for this age group. (auth)

36646 EFFECTS OF MOISTURE CONTENT OF IRRADIATED SEEDS OF LUPINUS ANGUSTIFOLIUS L. Brusse, M. J. (Dept. of Scientific and Industrial Research, Lincoln, New Zeal.). New Zeal. J. Agr. Res., 4: 197-202(Feb.-Apr. 1961).

An explanation was sought for differences which have been observed in irradiation injury in different lots of treated seeds of Lupinus similarly irradiated in different years. Survival rates of plants varied from 15% to 70%. Such erratic results decrease the efficiency of projects designed to produce beneficial mutations. Seeds were conditioned to five different moisture contents and irradiated at three different doses (20, 49.9, 86 kR) with ^{60}Co. Germination was reduced in irradiated seeds only at the highest moisture content (24%). Rate of germination was retarded in the irradiated seeds of low moisture content (6% and 9%). Growth was retarded in all irradiation treatments. The effect increased with higher dose. Within any irradiation dose it was least at 12% and 16% moisture. Death rate increased with increasing dose in each moisture treatment. It decreased in each irradiation treatment with increase in moisture up to 16%. These results show that the critical dose and LD_{50} can be raised by appropriate conditioning of the seeds. These observations suggest a complexity of the nature of irradiation injury, consisting of at least two types of effects: (1) The main (acute) effect is to cause physical damage to the embryo. Increase in susceptibility to the acute effect may be brought about by decreasing the moisture of the seed. (2) Chronic effects upset the metabolic system of seedling and plant. Increase in susceptibility to chronic effects may be produced by increasing seed moisture. (BBB)

36647 FURTHER NOTES ON THE IRRADIATION OF GROUNDNUTS. van der Walt, W. J. (Univ. of Pretoria). S. Afr. J. Sci., 58: 152-3(May 1962).

Attempts were made to develop a resistant mutant to a virus disease called rosette, which can cause tremendous losses in yield of peanuts. In 1957, 70 lb of peanut seed of the Natal Common variety, was irradiated with γ rays from a ^{60}Co source. The doses were: 6000, 9000, 10,800, and 12,600 R. One year later two more samples were irradicated with doses of 15,000 and 18,000 R. This report mainly deals with the results obtained in the γ-2, γ-3, and γ-4 generations and an outline is given of the present and future programs. Observations and counts were made in the first generation of the visible mutations, germination, and emergence. The whole progeny was planted out the next season and the plants were infected with the rosette virus every season by infected aphids. The plants that remained healthy were selected. The results showed that the percentage of mottled plants and dwarfs increased with increasing doses, while the germination and emergence as well as the yield were not decreased significantly. In the γ-3 generation seven single plant families that remained healthy were selected, but in the following season when a more severe infection was produced all turned out to be susceptible. Up to this stage no resistant mutants have been obtained. Several families, however, appeared promising in spite of their showing the disease symptoms, and are being tested in yield trials. The progeny of a blue-green mutant developed the rosette symptoms at a later stage than the rest of the field, giving the impression of some resistance. Several other mutants being studied include a dark green color mutant which differed from Natal Common in several characteristics. This was probably not a genuine mutation but rather the result of an outcross with another variety in an adjacent field. Male sterility, commonly found after irradiation, might have played a part. Another single plant family segregated for normal and variegated plants in a 3:1 ratio. Further investigation will show whether this was due to a gene mutation. One of the families in the 18,000-R group had several yellowish plants, which turned out to be largely sterile. (BBB)

36648 RADIOSENSITIVITY IN PLANTS. VII. RELATION BETWEEN POLYPLOIDY AND RADIOSENSITIVITY UNDER CHRONIC CONDITION. Matsumura, Seiji; Fujii, Taro (National Inst. of Genetics, Misima, Japan). Seiken Ziho, No. 17, 17-23(Dec. 1965).

The effects of chronic γ irradiation on cultivated and wild types of di-, tetra-, and hexaploid wheats were studied. Total irradiation time was 2844 hours, and radiation intensity was 0.31 ~ 30.6 R/hr. Therefore, total dosage was 880 R at the minimum and 8700 R at the maximum. Survival rates in the highest dosage lot of two hexaploid species and T. dicoccoides were low. But the rates in the highest dosage lot of the other species were fairly good, and all seedlings in other dosage lots matured. Number of culms was examined at maturity. In each species, mean number of culms per plant increased roughly with increasing dosage; this was clear in tetra- and hexaploids. Plant height was also measured at the same time. Radiation damage was noticeable in the inhibition of plant height with increasing dosage. Decrease of fertility was clear in each species with increasing dosage, and unexpectedly, these were no marked differences among the three ploids. However, when the decreasing rate was compared between the cultivated and wild types at each ploidy level, in general the rate for the wild type was slightly lower than for the cultivated type. Differences in radiation tolerance among the ploidy levels and between cultivated and wild types are discussed. (auth)

36649 DIFFERENCES IN EFFECTS OF γ RAYS AND FAST NEUTRONS FROM Po–Be SOURCE ON PADDY RICE. Matsumura, Seiji; Mabuchi, Tomoo (National Inst. of Genetics, Misima, Japan). Seiken Ziho, No. 17, 37-9(Dec. 1965).

Fast neutrons in doses ranging from 158 to 440 rad were given to rice seeds for 2 to 10 weeks. For comparison gamma rays were used acutely a day before sowing at 5 ~ 25 kR and 10 kR/hr. Seedlings were measured 17 days after sowing. No clear inhibiting effects were noticed on seed germination, seedling growth, and survival in the field in the neutron irradiated lots. However, seedling growth was delayed with the increase of gamma doses. For seed fertility showing a 25% depression the RBE value of fast neutrons from a Po–Be source against gamma rays became almost 19. The RBE value was also calculated as 19 for chlorophyll mutation rate amounting to 3%. (P.C.H.)

36650 DEVELOPMENT OF MUTATED CELLS IN WHEAT EMBRYO. Fujii, Taro (National Inst. of Genetics, Misima, Japan). Seiken Ziho, No. 17, 39-43(Dec. 1965).

Young embryos of einkorn wheat were exposed to gamma rays 24 to ~96 hr after pollination and the appearance of mass mutation was scored. Doses of 500 R were given at 1 kR/hr. Seed setting in all irradiated lots was almost as good as that of non-irradiated control, namely about 90% of pollinated flowers set seeds. Germination in all irradiated lots was lower than in the control and that of the 24 hr lot was as low as 35%. Also, longitudinal chlorina and necrotic stripes caused by somatic mutations were detected in young seedlings having one or two leaves. Survival of the seedlings is also discussed. (P.C.H.)

36651 FUNCTIONAL RADIODAMAGE OF THE BRAIN. Oeser, Heinz; Ruebe, Werner (Freie Univ., Berlin).

Strahlentherapie, Sonderbaende, 52: 63-73(1963). (In German).

Changes in the EEG obtained during and after irradiation in human and animal studies were investigated. The relation of the observed immediate effect, 1-to-3 day effect, and the subsequent normalization of the brain action potential for the pathogenesis of radioencephalopathy are described. The significance of the end of the observation for knowledge of the dose-effect relations was developed. The detection of an all-or-nothing behavior in the EEG indicates the existence of a threshold value, which can be determined for the 1-to-3-day effect with 200 R. (tr-auth)

36652 EFFECTS OF SMALL IRRADIATION DOSES AND LOW-DOSE OUTPUTS. Langendorff, Hanns (Univ., Freiburg i. B. Heiligenberg-Institut, Ger.). Strahlentherapie, Sonderbaende, 52: 188-96(1963). (In German).

A review is given of the results of studies on the effects of small irradiation doses with respect to mutation induction, increase of leukemia incidence, and mean life span. Studies made with mice and rats are summarized. The paucity of the experimental results for low radiation dose effects prevents the derivation of any conclusions or hypotheses. (J.S.R.)

36653 RADIOINDUCED BACK MUTATIONS IN DEPENDENCE ON THE CHROMOSOME ACTIVITY AND THE MILIEU. Fritz-Niggli, Hedi (Kantonsspitals, Zurich). Strahlentherapie, Sonderbaende, 52: 197-203(1963). (In German).

The extinction of reversions of individual subgenes of Schizosaccharomyces pombe induced by radiation is dependent on the mitotic activity of the irradiated cell. The dividing cell is very radiosensitive with respect to its mutability. The mutability of the radioinduced mutations was not affected by treatment with dinitrophenol before, during, and after irradiation. In chemically induced mutations a preliminary treatment with chloramphenicol produced a significant protective effect. This protective effect can be traced under some circumstances to the reduction of the vitality of remutated cells by chloramphenicol. The mutations induced by nitrite behaved quantitatively different with respect to irradiation and environmental factors from the mutations induced by uv and x irradiation. The principal differences are the incomplete reversion and frequent occurrence of suppressors. It appears improbable that the nitrite-induced mutant occurs through simple conversion of a single base pair. (tr-auth)

36654 THE QUESTION OF THE BIOLOGICAL DOSE EQUIVALENT OF ^{60}Co γ AND 200-kv X RADIATION. Linden, Walfried (Univ., Goettingen, Ger.). Strahlentherapie, Sonderbaende, 52: 204-12(1963). (In German).

A comparison was made of the biological effectiveness of 200-kv x radiation and ^{60}Co γ radiation. 60 Wistar rats were used as research animals. 30 animals received a dose of 9000 R fractionated over 9 days, 20 animals received corresponding x irradiation, and 10 animals remained unirradiated as controls. The build-up effect of ^{60}Co γ irradiation was avoided by a covering with a 5-mm thick tissue equivalent paraffin plate in front of the irradiated object. Special value was placed on the uniformity of both radiation qualities with respect to dose and dose output. The results showed low biological effectiveness of γ radiation which was explained through its smaller differential ionization. (tr-auth)

36655 EFFECT OF IONIZING RADIATION ON DELAYED HYPERSENSITIVITY. Benassi, Enrico (Univ., Turin). Strahlentherapie, Sonderbaende, 52: 228-34(1963). (In German).

A brief review is given of a series of experiments made to determine the effects of ionizing radiation on delayed hypersensitivities in guinea pigs and rabbits. The two factors studied were the sequence followed in the propagations of antigens and irradiations and the time between these two treatments. A hypothetical scheme for the effects of ionizing radiation on the immunity process is given. (J.S.R.)

36656 EARLY AND LATE EFFECTS OF X IRRADIATION ON THE CEREBRAL CORTEX OF THE MONKEY. Caveness, William F. (Columbia-Presbyterian Medical Center, New York); Roizin, Leon; Carsten, Arland; Schade, J. P. Trans. Amer. Neurol. Ass., 89: 126-7 (1964).

The effects from the exposure of a portion of the head to 3500 R (x radiation) were determined in 14 Macaca mulatta, irradiated at 12 months of age. A single exposure, at a rate of 350 R/min, was delivered to the right portion of the head to provide comparison with the left. It was limited to the cerebral cortex, its coverings, and the immediately subjacent white matter, to a total depth of 1 cm (to avoid secondary influences from alteration of large vascular beds and midline nuclear masses). Following irradiation there were intermittent functional alterations, as expressed by electroencephalography (EEG), that began as early as 24 hr. The first changes consisted of amplitude asymmetries between the irradiated and the contralateral cortex, more readily recorded during drowsiness and sleep than in the waking state. This was observed in 6 to 8 animals by 4 weeks, and all from 12 to 16 weeks. A more subtle alteration was the diminution or absence of sleep spindles over the irradiated area. Beyond the 18th week there were alterations in rate as well as amplitude. Contralateral paresis was noted in two of the three animals followed beyond the 20th week, and focal seizures in one of these. All of the EEG changes were episodic, becoming more constant as the postirradiated course extended. Structural changes of questionable significance in the irradiated cortex, i.e., glial alteration or proliferation, were noted as early as the third day. Inflammatory reactions, circumscribed or perivascular, were seen as early as the first week. Degenerative, chromatolytic, or pyknotic cellular alterations were seen as early as the fourth week. Necrobiotic changes were noted in none of the animals sacrificed up to 16 weeks. Electron microscopic study of the synapses showed an increase in vescles and greater density of the pre- and postsynaptic membranes, as well as a decrease and variation in the size of the vesicles, less distinctness in the membranes, and occasionally the inclusion of osmiophilic material. Quantitative analysis of the dendritic plexus of pyramidal cells showed a progressive loss in dendritic ramifications, with accompanying decrease in synaptic surface, as the postirradiation period lengthened. (BBB)

36657 PATHO-ANATOMICAL FINDINGS IN PIGS WHOLE-BODY IRRADIATED WITH GAMMA RAYS. Otoupal, Pavel; Pawel, Otto; Kalousova, Vilma (Veterinarni Vyzkumne Stredisko, Prague). Vet. Med. (Prague), 11: 641-6(1965). (In Czech).

Typical patho-anatomical findings in pigs after whole-body irradiation by ^{60}Co at a dose of 700 R are described, along with the acute stage of radiation sickness. A dose of 450 R applied to 16% of the animals did not evoke the disease. Less or more expressed hemorrhagic diathesis was ascertained in all organs and tissues of animals with acute radiation sickness. Skin of the caudal area of the ventral part of the body and the medial area of pelvic extremities are considered to be the places of comparatively typical localization of hemorrhages. Further, hemorrhages were often observed in mucous membrane of epiglottis, epicard, and gastrointestinal and urogenital tracts. Diphtheroidally necrotic changes were found in gastrointestinal tract in 20% and in the mucous membrane of the large intestine and cecum in about half of the dissected cases. (auth)

36658 INFLUENCE OF MODIFYING FACTORS ON THE ACTION OF IONIZING RADIATION ON PLANT CELLS. Micke, A. (Univ., Goettingen, Ger.). Z. Pflanzenzuecht., 55: 29-6(Feb. 1966). (In German).

The possibility of modifying radioinduced effects in resting seeds of sweet clover (Melilotus albus) and barley (Hordeum sativum) was investigated using plant development and survival as criteria for radiation damage. In general, the results showed that the effect of x irradiation is extremely dependent on the action of secondary factors, but that there are important differences between the two spe-

cies. When the radiosensitivity of barley seeds was tested in the moisture range 23.6 to 5.1%, radiation damage was lowest between 12.5% and 18.8%, and increased below and above this range. Postirradiation storage for 24 hr in air at equilibrating humidities increased damage to seeds with less than 7.4 and more than 18.8% moisture. There was a slight indication of recovery for seeds with a moisture between 7.4 and 9.6% during the postirradiation period. The radiosensitivity of sweet clover seeds diminished linearly with decreasing moisture form 31.4 to 5.2%. A slight sensitizing effect could be achieved by drying to 1.63% moisture. Postirradiation storage of sweet clover seeds at equilibrating humidities increased the damage for seeds with more than 11.8% moisture, but decreased the damage to seeds with 5.2 and 10.9% moisture. Postirradiation storage of these seeds at 98% relative humidity in all cases led to an increased damage. Postirradiation storage of seeds with 31.4% moisture (in equilibrium with 98% relative humidity) led to a marked increase of the survival if the humidity during the storage was less than 90%. It is concluded that the oxygen content of sweet clover seeds diminishes with decreasing water content, so that seeds with less than 10.9% moisture are effectively free of oxygen. In sweet clover seeds with 1.63% moisture, radiation damage can be doubled by pregermination soaking in oxygenated water even 820 days after the irradiation. This suggests, that oxygen-sensitive free radicals can persist in sweet clover seeds with extremely low moisture for more than two years after irradiation. For seeds with 5.2% moisture this was not the case. The different behavior of sweet clover and barley seeds under the action of modifying factors may be caused by a different amount of radicals produced in the tissue, a different rate of decay of the radiation-induced radicals, the different dose level, or a mechanism which inhibits the reaction of oxygen in sweet clover seeds. The demonstrated possibility of modifying radiation effects by various factors points out the importance of controlling the experimental conditions before, during, and after the irradiation, even in work on practical plant breeding. (BBB)

36659 GENETIC VARIABILITY INDUCED BY IONIZING RADIATIONS IN QUANTITATIVE TRAITS OF HABROBRACON. Dalebroux, Marc Augustin. Raleigh, N. C., North Carolina State Univ., 1965. 95p.

Thesis.

An investigation of the importance of radiation-induced mutations was carried out with quantitative characters in Habrobracon juglandis by means of an analysis of genetic variances. The traits studied were adult female body weight, adult male body weight, and fecundity. Females from an inbred line were irradiated and their parthenogenetic sons were mated individually to virgins from the same as well as from a different inbred line, in order to obtain families with homozygous and heterozygous genetic backgrounds. The analysis of the data on female body weight and fecundity was done on the basis of the means of the above families. The male body weight character was studied among individual grandsons within families and among family means. A dose of 1.5 kR was chosen on the basis of a preliminary investigation. The radiation source used was cobalt-60 delivering gamma rays at the rate of approximately 250 kR per hour. When the analysis was made on family means, the most significant findings were as follows: in both genetic backgrounds, a highly significant increase in genetic variation was detected for female body weight; insofar as fecundity is concerned, there was only a tendency towards increasing the genetic variability in the treated materials as compared to their respective controls; there seemed to be no evidence of nonallelic interactions between induced mutations and their genetic backgrounds. When the analysis was carried out on individual male body weight, the increase in genetic variance induced by radiations was much larger under the homozygous genetic background than that found under the heterozygous background. The reliability of the dosage-response curve and possible explanations of the results are discussed. (TCO)

36660 STUDY OF THE HEMODYNAMIC PARAMETERS IN EXPERIMENTAL HEART FAILURE, PRODUCED BY EMBOLIZATION AND IONIZING RADIATION. Bishop, Vernon S. Jackson, Miss., Univ. of Mississippi, 1964. 138p.

Thesis.

The functional status of the heart prior to embolization and at different stages of progressive embolization was determined by measuring cardiac function curves. Progressive injections of small quantities of microspheres over a period of 2–3 hrs were used. Both the maximum cardiac output and maximum minute work output decreased approximately proportionately after each individual injection of incremental quantities of microspheres. Chronic heart failure was produced by giving 20,000 R Co-60 irradiation to either the right or left ventricle in nine closed-chest animals. Measurements of right and left atrial pressures, arterial pressure, pulse rate, body weight, and blood volume were made before and after irradiation. The right and left atrial pressures rose progressively until death in three animals irradiated on the right side. In six animals irradiated on the left side, the left atrial pressure rose progressively, but the right atrial pressure either did not rise or rose only during the latter stages of failure. Declining arterial pressure and increasing pulse rate were common to both groups. Increases in blood volume were significant only in the group irradiated on the left side. At autopsy, seventy to one hundred per cent of the right ventricular muscle was damaged in dogs irradiated on the right side, and forty to seventy per cent of the left ventricle in dogs irradiated on the left side. Hydrothorax and liver congestion were found in the right-sided group and pulmonary congestion in the left-sided group. Different types of ventricular function curves were determined over a period of several weeks in seven conscious dogs. Ventricular output was measured continually by chronically implanted electromagnetic flow probes. Right and left ventricular minute volume output curves, stroke volume output curves, left ventricular minute work curves, and left ventricular stroke work curves were obtained every few days on all animals. (TCO)

36661 DETAILED STUDY OF THE LETHAL EFFECTS OF X RAYS AND ULTRAVIOLET LIGHT ON TWO CILIATE PROTOZOANS. Calkins, John Claud. Austin, Tex., Univ. of Texas, 1963. 139p.

Thesis.

The survival of Paramecium aurelia and Tetrahymena pyriformis was studied. The radiation dose that prevents 50% of an irradiated population from producing mass cultures (LD-50) was determined. The LD-50 of x-irradiated P. aurelia was observed to be about 270 kilorads and T. pyriformis about 450 kilorads. The LD-50's of these animals for ultraviolet irradiation were found to be about 800 ergs/mm^2 for T. pyriformis and 4000 ergs/mm^2 for P. aurelia. The following properties of individual irradiated animals were determined: the length of division inhibition following irradiation, the growth rate following irradiation when growth resumes, the number of divisions, if any, before death, and the average day irradiated animals die. Radiation doses were separated by different time intervals to investigate the time course of recovery from sublethal radiation damage. X-ray damage, as judged by survival, is essentially completely repaired in 24 hours while the repair of ultraviolet-induced damage is more complex and still incomplete after two days. Significant differences are observed in the response of P. aurelia and T. pyriformis to ultraviolet light and photoreactivating light. While photoreactivation increases the LD-50 of P aurelia only a small amount (about 40%), the LD-50 of T. pyriformis increases 400%. Also it was observed that letheally irradiated T. pyriformis could be photoreactivated even after one or two post-irradiation divisions. The radiation sensitivity of P. aurelia to both ultraviolet and x rays at various times in the interdivision cycle was determined. The sensitivity to x rays showed little variation through the interdivision cycle while sensitivity to ultraviolet was slightly greater shortly after division. No marked relation between radiation sen-

sitivity and DNA synthesis was observed. Consideration of the lethal and associated radiation responses in two groups, termed early death type damage and late death type damage, suggests that early death might be the response to predominantly cytoplasmic damage while nuclear damage alone tends to produce the late death. (TCO)

36662 X-RAY-INDUCED ABNORMALITIES AND RECOVERY IN HYMENOLEPIS MICROSTOMA. Tan, Bian Djoen. Knoxville, Tenn., Univ. of Tennessee, 1965. 73p. Thesis.

To study the injurious effects of x rays and the presumed possession of a recovery mechanism in adult cestodes, 7-day old Hymenolepis microstoma were subjected to single doses of 2,500, 5,000, and 7,500 R respectively in vitro. These were then transplanted into new hosts. Similarly, unirradiated worms were transplanted into mice for controls. After intervals of 2, 4, 6, 8, and 32 days, respectively, the hosts were sacrificed and the worms collected for study. Migration of the transplanted parasites from the duodenum to the bile duct of the host was observed. Although the x irradiation did not affect the overall transplantation yield, it tended to slow down the process of migration. Results of the length measurement indicated that x irradiation at the above doses caused a primary stimulation of growth during the first 2–4 days, a temporary inhibition between day 4 and day 8, and a return to normal rate afterward. Three conclusions were drawn from the results of morphological analysis. First, the germinal neck region is highly radioresistant, and the pregravid proglottids are very radiosensitive. Second, x irradiation affected not only the radiosensitive embryonic pregravid proglottids but also, to a lesser degree, a portion of the germinal neck region. In both cases the effects were proportional to dose. Third, recovery from the injurious effects of x radiation was shown to have already started 8 days post-irradiation and to have been completed before the thirty-second day of incubation. The results are discussed in relationship to similar results obtained by other workers in mammalian testes, mammalian and avian embryos, and certain cestodes. Recovery can be explained in terms of the survival of radioresistant germinal cells capable of regenerating the injured tissue or repropagating the destroyed strobila, the latter in the case of the cestode. (Dissertation Abstr.)

Radiation Effects Therapy and Countermeasures

36663 POSSIBLE MECHANISM OF THE PROTECTIVE EFFECT OF S-β-AMINOETHYLISOTHIOURONIUM-BROMIDE (AET). Pisarevskii, A. N.; Seleznev, A. F. (Lenin State Univ., Belorussian SSR). Biophysics (USSR) (Engl. Transl.), 10: 202-5(June 1966).

Translated from Biofizika, 10: 179-81(1965).

The process of transfer of electron excitation energy to AET by external quenching was studied in a model consisting of a liquid scintillator. The results showed that AET is a good quenching agent of radioluminescence in a dioxane liquid scintillator. This quenching effect of AET observed may manifest itself as one of the protective mechanisms in the form of transfer of energy of electron excitation from biologically important structures of the cell. (P.C.H.)

36664 PERTURBATIONS IN X-RAY DOSE RESPONSE IN VITRO WITH TIME AFTER PLATING: A PITFALL IN THE COMPARISON OF RESULTS OBTAINED BY DIFFERENT LABORATORIES USING ASYNCHRONOUS CELL SYSTEMS. Berry, R. J.; Evans, H. J.; Robinson, D. M. (Medical Research Council, Oxford. Medical Research Council, Harwell, Eng.). Exp. Cell Res., 42: 512-22(June 1966).

Removal of clone A Chinese hamster and HeLa $S\text{-}3_{oxf.}$ cells from monolayer cultures into suspension, followed by replating, produces a partial synchronization of the population in both cell lines. This is reflected by changes in the sensitivity of the cells to the killing effects of x rays. In Chinese hamster cells, trypsinization was shown to produce a transient suppression of the incorporation of ^{3}H-thymidine into DNA. In the early hours following trypsinization the perturbations in x-ray response are consequences of the trypsinization procedure and are qualitatively similar in both cell lines. Later changes in response reflect the increasing importance of the most resistant fraction of the cell population in determining the survival curves. (auth)

36665 THE ROLE OF CYSTAMINE–NUCLEIC ACID INTERACTIONS IN PROTECTION AGAINST X-RAY-INDUCED DAMAGE OF DNA. Jellum, Egil (Univ. of Oslo). Int. J. Radiat. Biol., 10: 577-94(July 15, 1966).

The ability of different disulfides to protect solutions of calf-thymus DNA against x-ray-induced damage was compared. Degradations of the DNA were followed by determining shifts of the T_m value and changes in the ability of DNA to act as primer for the enzymic synthesis of RNA. Diamino-disulfides such as cystamine, which readily interact with DNA, offered significantly better protection of the DNA than diacetyl cystamine and oxidized glutathione. The difference proved to be due, at least in part, to the cystamine-nucleic acid interaction. The data suggest that diamino-disulfides are efficient protectors of DNA because they contain a disulfide group, stabilize the DNA-helix, and a substantial amount of the disulfide is localized on the DNA molecule. Radiation damage of the priming activity of DNA was only partially prevented by the disulfides. No difference in the (weak) protective effect of cystamine and diacetyl cystamine was observed. The possible significance of the cystamine-DNA interaction for radioprotection of DNA in vivo is discussed. (auth)

36666 INFLUENCE OF CYSTAMINE ADMINISTERED BY MOUTH TO MICE IRRADIATED WITH GAMMA RAYS AT A LOW DOSE-RATE. Bacq, Z. M.; van Caneghem, P. (Univ. of Liege). Int. J. Radiat. Biol., 10: 595-9(July 15, 1966).

Mice fed on a diet containing 1% cystamine (2HCl) were exposed to gamma radiation from a ^{137}Cs source at dose-rates varying from 10 to 0.026 R/min; the total dose was 700–900 R. Cystamine in these conditions not only failed to protect but increased mortality. The deleterious effect of cystamine increased with the decrease in dose-rate and prolongation of its administration. Cystamine increased greying of hair of C57Bl. mice irradiated at low dose-rate. (auth)

36667 CURRENT STATUS OF THE USE OF BONE MARROW TRANSPLANTS IN THERAPEUTICS. Nicolau, C. T.; Apateanu, V.; Grigoriu, G. (Centrul de Hematologie, Bucharest). Med. Interna, 17: 129-39(Feb. 1965). (In Rumanian).

This review examines the experimental and clinical data relating to the use of homologous and autologous bone marrow grafts in the treatment of radiation disease and depressed hematopoiesis induced by other agents. Techniques for obtaining, preserving, and administering marrow cells are given. Detection of successful takes of bone marrow cells in the recipient is discussed, as is the immunologic response of the recipient to the donor cells and its sequelae (homologous disease). Possibilities of the use of autologous cells in clinical situations (radiotherapy, chemotherapy) are discussed. The literature relating to the clinical use of bone marrow grafting in heavily irradiated persons (accidentally or for treatment of leukemia) is critically examined. The authors' results in the use of bone marrow infusions in patients with aplastic anemia and hemorrhagic disorders are also recounted. It is concluded that, while some successful results have been reported, in general, much more knowledge is needed before routine success can be obtained with bone marrow transplantation. (73 references) (BBB)

36668 PARTICIPATION OF THE HYPOPHYSEAL-ADRENAL SYSTEM IN DEVELOPMENT OF SYMPTOMS OF RADIATION-INDUCED PATHOLOGY (REVIEW).

Kondror, V. I. Probl. Endokrinol. Gormonoterap., 9: No. 5, 109-17(Sept.-Oct. 1963). (In Russian).

Experiments on shielding or on extirpating the adrenals are reviewed. Shielding the adrenals softens the effect of irradiation, while surgical removal of the adrenals decreases the radiation resistance of the animal. The effects of giving cortisone, ACTH, and other hormones on the physiology of protein, carbohydrate, and lipid exchange in irradiated animals is also reviewed. The decrease in arterial pressure with irradiation is related to a decrease in adrenal activity. Lymphopenia and eosinopenia are shown to be stress reactions of the irradiated organism whose adrenals are in an activated state. (195 references.) (TTT)

36669 WHOLE-BODY IRRADIATION AND IMPLANTATION OF ALLOGENIC BONE MARROW IN MAN. Mathe, Georges. Strahlentherapie, Sonderbaende, 52: 213-27 (1963). (In German).

The results of whole-body irradiation of man and treatment of the consequent radiation sickness are considered. Graphs illustrate the effect of radiation dose on reticulocytes, granulocytes, lymphocytes, and thrombocytes. The relation between radiation dose and aplasia is discussed. The symptomatic treatment of radiation sickness is briefly considered but the emphasis is on therapy by bone marrow implantation. The results obtained are summarized. (J.S.R.)

36670 AUTORADIOGRAPHIC STUDIES WITH A RADIATION PROTECTION MATERIAL. Pliess, Guenther; Franke, Herbert (Univ., Hamburg). Strahlentherapie, Sonderbaende, 52: 295-301(1963). (In German).

Young rats received intraperitoneal injections of 150 mg/kg of the radiation protective material β-aminoethylisothiuronium (AET) labeled with ^{35}S. 24 animals were irradiated 30 min later with 100, 500, or 1000 R (single irradiation of the head with a dose output of 70 R/min). Extensive autoradiographic studies showed that after 1 to 24 hr activity was detectable in numerous organs. The distribution model in the liver and the incisor basis of the rat was altered by head irradiation. Early investigations with AET showed morphologically an amplification of karyorrhexis in the basel pulp of the rat incisor, only the young odontoblasts were protected. A considerable homogeneous distribution of the ^{35}S-AET was found in all tissues of the rat tooth basis. It was concluded that the local protective effect of radiation protective materials represents less a quantitative distribution problem and is dependent on the specific biological interference between tissue and radiation protective material. (tr-auth)

Radiation Hazards and Protection

See also HEALTH AND SAFETY

Refer also to abstract 37144.

36671 ^{90}Sr IN MECKLENBURG HAY. Keil, R.; Randow, F.; Schulze, H.-A. (Univ., Rostock, Ger.). Arch. Tierernaehr., 16: 125-30(1966). (In German).

Samples of hay (pure meadow hay or clover hay as well as mixtures of both) were obtained from the first cut in 1962 from the districts of Rostock, Neubrandenburg, and Schwerin and found to be contaminated with an amount of ^{90}Sr averaging 27 pC per gram of ash (proportional to 1750 pC per kg dry matter) and 290 pC per gram of calcium. (auth)

36672 DOSE DISTRIBUTION DURING IRRADIATION WITH A PULSED SCANNING ELECTRON BEAM. Gruenewald, Th. (Bundesforschungsanstalt fuer Lebensmittelfrischhaltung, Karlsruhe, Ger.). Atompraxis, 12: 308-9 (June 1966). (In German).

The problem of dose distribution at the irradiation of lineary moved samples with a pulsed scanning electron beam can be simplified by separate consideration of the inhomogeneity in the direction of motion of the samples and in the direction of motion of the beam. The formulas for the critical values of the transport velocity and the pulse frequency at a constant beam diameter as well as constant scanning amplitude and scanning frequency for achieving optimal homogeneity of dose distribution are stated. (auth)

36673 PROTECTIVE ACTION OF BACILLUS SUBTILIS ON X-IRRADIATED MICE. Bellack, Stephen. Lab. Dig., 28: 5-6(Nov.-Dec. 1964).

A study of the influence of antigens prepared from gram-positive bacilli on the radiation syndrome is reported. In an earlier study on the effect of environmental uv irradiation upon bacterial contamination, it was found that Bacillus subtilis frequently persisted, whereas viable bacterial contaminants of other species diminished after uv irradiation. This resistance of the organisms to uv irradiation and the ease of culture, general availability, and known nonpathogenicity, suggested the use of B. subtilis for experimental determination of the radioprotective effect of prepared suspensions on test animals. Pathogenicity tests showed no gross evidence of pathogenicity during periods up to 5 months. Two different injectants were prepared from a suspension of living bacilli, constituting two different bacterial factors. Injectant A, an aliquot of 50 ml of the stock suspension sterilized in an autoclave, was filtered through a Seitz apparatus and the bacteria-free filtrate was used for the protection studies. Injectant B was prepared in the same manner as A but was not filtered after sterilization. Consequently it contained the factors present in A plus the cellular material from the dead bacteria. The injections were made at various time intervals before x irradiation with 700-R (90–100% lethal dose). The greatest decrease in mortality is achieved with B given 24 hr before irradiation. Solution A was consistently less effective than B. Multiple injections at 24 and 48 hr before irradiation were less effective. Injection one hr prior to irradiation was not found to protect as effectively as injection 24 hr prior to irradiation, which gave 90% 30-day survival compared to 10% in uninjected, irradiated controls. It is concluded that the gram-positive bacterial preparations described are able to decrease radiation mortality in x-irradiated mice. The mechanism by which this protection is achieved may be related to an antigen-antibody response, a heat-stable enzyme, a chemical by-product from the bacilli, a bacterial-cellular factor, or a combination of any of these. (BBB)

36674 ^{90}Sr IN MILK. Randow, F.; Schulze, H.-A. (Univ., Rostock, Ger.). Nahrung, 9: 705(1965). (In German).

Data on ^{90}Sr contents in milk from June 1962 through December 1964 are presented. The average activity for 1964 was $^{48}pC/10$ g of ash. (M.C.G.)

36675 RADIATION BURDEN THROUGH ^{131}I AND THYROID FUNCTION. Numberger, Josef (Univ., Munich). Strahlentherapie, Sonderbaende, 52: 283-94(1963). (In German).

The mean specific radiation on dose of ^{131}I, which is the mean whole-body dose in rad/100 mC of injected radioactivity without consideration of the radioactivity in the thyroid, was determined in six women. The path of the activity concentration in the thigh after incorporation of a test dose of ^{131}I was used as the basic measurement for the calculation. The specific radiation dose is strongly dependent on the thyroid function. The lowest value in a healthy thyroid was 4 rads/100 mC and the highest value of 80 rads/100 mC was in a low hyperthyrosis. (tr-auth)

36676 RADIATION PROTECTION IN THE FRAMEWORK OF THE ATOMIC LAW OF THE GERMAN REPUBLIC. Pfaffelhuber, Josef. Strahlentherapie, Sonderbaende, 52: 316-25(1963). (In German).

The basic provisions of the German Atomic Law with respect to radiation protection are outlined. (J.S.R.)

36677 PRESENT EXPOSURE OF THE POPULATION THROUGH MEDICAL RADIATION USES AND ITS SIGNIFICANCE. Seelentag, Walter (Bundesgesundheitsamt,

Berlin). Strahlentherapie, Sonderbaende, 52: 326-33 (1963). (In German).

The genetically significant doses administered medically are tabulated by countries. The genetic significant dose received is then discussed with respect to the body area irradiated. Data are presented from German hospitals and clinics to show the wide variation in the gonad dose as a result of irradiation techniques used. (J.S.R.)

36678 QUESTION OF ENDANGERING THE ENVIRONMENT BY THE APPLICATION OF RADIOACTIVE MATERIALS IN MEDICINE. Aurand, Karl (Bundesgesundheitsamt, Berlin). Strahlentherapie, Sonderbaende, 52: 334-40(1963). (In German).

The dangers of water contamination in the medical use of unsealed radioactive preparations are discussed. The amount of activity introduced, permissible concentrations in water, and theoretical waste water volumes are compiled for radioisotopes most often used in unsealed sources. These figures are correlated with the use of isotopes in various German cities to illustrate the amount of radioactivity being discharged into waste water. (J.S.R.)

36679 POSSIBILITIES OF LEGAL CONTROL OF RADIATION PROTECTION OF PATIENTS FROM THE VIEWPOINT OF THE X RADIOLOGIST. Beck, Hans R. Strahlentherapie, Sonderbaende, 52: 341-6(1963). (In German).

A survey on the possibilities of legislation on the radiation protection of patients showed that these are generally limited to professional radiation protection. The legislation can be supported only by some basic principles whose development could be sought. (tr-auth)

Radiotherapy and Radiodiagnosis

Refer also to abstract 36919.

36680 STUDIES ON THERAPEUTIC SHORT-DISTANCE AND INTRACAVITARY GAMMA BEAM TECHNIQUES. PHYSICAL CONSIDERATIONS WITH SPECIAL REFERENCE TO RADIATION PROTECTION. Walstam, Rune (Karolinska Sjukhuset, Stockholm). Acta Radiol., Suppl. 236, 1-129(1965).

Developments in therapeutic short-distance and intracavitary gamma beam techniques over a period of more than 10 years are reviewed. The design of two kinds of apparatus for radiotherapy and the development of techniques for their clinical application are included. Special attention is given to radiation protection and to methods for measuring personnel exposure. The therapy units described include a short-distance gamma beam device and a remotely controlled afterloading apparatus, mainly intended for gynecological applications. The design, physical properties, and application of a special type ionization chamber dosemeter for radiation protection measurements are also given. (135 references). (P.C.H.)

36681 PRIMARY INTERACTION WITH ^{131}I-LABELED ANTIGENS AS AN APPROACH TO DETECTING TUBERCULOSIS. Farr, Richard S. (Scripps Clinic and Research Foundation, La Jolla, Calif.). Amer. Rev. Respirat. Dis., 92: No. 6, 94-103(Dec. 1965).

Exploratory techniques in the development of a method using ^{131}I-labeled antigens to measure serum antibody levels for various diseases are described. If an antigen can be labeled with ^{131}I and is soluble in 50% saturated ammonium sulfate, the ^{131}I-labeled antigen can be added to normal serum, and when 50% saturated ammonium sulfate is added, the ^{131}I radioactivity remains in the supernatant. If, on the other hand, the ^{131}I-labeled antigen is added to an antiserum, soluble antigen-antibody complexes are formed. Part of the complex is antibody globulin and, consequently, the complexes precipitate upon the addition of 50% saturated ammonium sulfate. Thus, under these circumstances, it is possible to differentiate between the amount of antigen complexed to antibody and the amount of antigen free in solution. The concept of interfering with or blocking the interaction between ^{131}I-labeled antigen and antibody by the addition of unlabeled antigen is useful to detect unlabeled antigen, to detect antigenic similarities between two antigen solutions, and to measure the avidity of the antibody-antigen interaction. A test for antibodies in serum of patients with tuberculosis was devised, wherein bacterial cells (H37Rv strain) were labeled with ^{131}I and reacted with antiserum. To 0.5 ml of a 1:40 dilution of the test serum in borate buffer, 0.5 ml of plain borate buffer was added. One-half ml of the ^{131}I labeled antigen, containing 0.5 μg of nitrogen, was then added, and the mixture was incubated overnight at 4°C. Thereafter, anti-human-globulin serum prepared from rabbits was added in order to precipitate the ^{131}I-H37Rv-antibody complexes. The precipitation reaction was allowed to proceed for two hours; the preparations were then centrifuged, the supernatant decanted, and the precipitate washed with cold borate buffer. The amount of radioactivity present in the precipitate was divided by the total number of antigen counts added to give the percent of ^{131}I-H37Rv antigen in the precipitate. Results indicated that the sera from one-half of the persons with active tuberculosis tested contained antibodies that would specifically bind with antigens in the heterogeneous ^{131}I-labeled antigen mixture employed. This binding was specific in that the addition of unrelated antigens such as sonicated E. coli, sheep erythrocytes, and bovine serum albumin failed to interfere with the binding of ^{131}I-H37Rv. (BBB)

36682 CLINICAL STUDIES IN LASER PHOTOCOAGULATION. Campbell, Charles J.; Koester, Charles J.; Curtice, Vonda; Noyori, Kimiharu S.; Rittler, M. Catherine (Coll. of Physicians and Surgeons of Columbia Univ., New York). Arch. Ophthalmol., 74: 57-65(July 1965).

The technique of laser photocoagulation, a description of instrumentation which has been used clinically, and the advantages and problems of this procedure are discussed. In experimental animals, a study of intraocular temperature changes produced by photocoagulation showed that the thermal effects are smaller in magnitude, shorter in duration, and more narrowly confined to the site of the coagulation in the laser than in the xenon arc. An investigation of the histologic characteristics of laser coagulations, and their relation to the ophthalmoscopic appearance of the lesions, indicated that lesions of therapeutic intensity are not accompanied by profound intraocular damage. Destructive necrosis and scar formation are confined to the site of the coagulation and destructive changes of significant magnitude are not evident in either the choroid or the sclera. These preclinical studies indicate that photocoagulation of the retina with a properly controlled laser can be performed safely. Clinical lesions produced by the laser photocoagulator could be divided into four categories depending on the intensity of the burn. The appearance of the lesion is identical in humans and experimental rabbits. A grade 2 lesion appears to be of optimum therapeutic intensity. Results in 220 patients treated with the laser photocoagulator are described. Complications encountered consisted of damage to the iris, an inadequate treatment barrier surrounding a retinal tear, inadequate delimiting barriers in retina detachments, and transitory corneal changes. About 25% of the patients exhibited fine punctate corneal staining. (TCO)

36683 PROPHYLACTIC PHOTOCOAGULATION OF RECURRENT TOXOPLASMIC RETINOCHOROIDITIS: A PRELIMINARY REPORT. Spalter, Harold F.; Campbell, Charles J.; Noyori, Kimiharu S.; Rittler, M. Catherine; Koester, Charles J. (Columbia Univ., New York). Arch. Ophthalmol., 75: 21-31(Jan. 1966).

Effects and side-effects of laser irradiation in 24 patients are reported. In the choice of a photocoagulator, the laser was employed for several reasons. Histologic study of laser coagulators in the animal and human eye reveals that the maximum destructive effect occurs in the retina rather than in the choroid. In a disease characterized by primary retinal inflammation, maximal energy delivered to this tissue level would be desirable. The laser beam because of its coherent characteristics and single wavelength emis-

sion gives little scattering effect in the vitreous. Furthermore, the laser beam can be focused in the plane of the retina. The vitreous is not heated to any significant degree. One reason for photocoagulation in the prophylactic treatment of ocular toxoplasmosis is the amount of heat generated by laser energy. At the site of coagulation, an evaluation of 40°C above body temperature is reached in the rabbit eye. This degree of temperature evaluation is adequate to affect the toxoplasma cysts since they are apparently destroyed by heating to 60°C. None of the 24 patients developed recurrent retinitis in the photocoagulated areas during a 6- to 33-month follow-up period. In two patients the location of the healed focus prohibited a complete encircling photocoagulation barrier. No complications were encountered as a result of laser coagulation. Specifically, no retinal breaks or detachments were produced, no significant increase in vitreous pathology noted, and no inflammatory activity was produced by photocoagulation. (BBB)

36684 INTRALYMPHATIC ISOTOPE THERAPY WITH A NEW RADIOACTIVE PHOSPHATE COMPOUND (^{32}P) IN FAT SOLUBLE RADIOPAQUE CONTRAST MEDIA. (PRELIMINARY NOTE). Onnis, A.; Romagnolo, A.; Bresadola, S.; Colombini, C. (Univ., Padua). Attualita Ostet. Ginecol., 10: 617-23(Sept.-Oct. 1964). (In Italian).

Preparation and therapeutic evaluation of a new radioactive compound for use in treating metastatic cancer are reported. Steps in the synthesis of this new ^{32}P-labeled compound, the tri-n-octyl ester of phosphoric acid, are described. Synthesis precedes via $Ag_3{}^{32}PO_4$, prepared from $AgNO_3$ and H_3PO_4, and reaction of this silver salt with n-octyl bromide. The product has a sp act. of 200 mC/mM, allowing a low-viscosity solution to be prepared of the lipid-soluble agent with a sp act. of 432 mC/ml. The LD_{50} of the compound tested in animals was 5 mg/kg. The relatively high sp act. of solutions of the compound make it suitable for intralymphatic treatment of lymph node metastases. Its dispersion in the lymph node allows homogeneous irradiation of the node. Advantages of this compound over ^{131}I-labeled lipids, used for the same purpose, are enumerated. Its use in treating gynecologic cancer patients is proposed. (BBB)

36685 CLINICAL EVALUATION OF THE TREATMENT OF ADVANCED HEAD AND NECK CANCERS WITH HIGH-ENERGY ELECTRON BEAMS. Perry, Harold; Chu, Florence C. H.; Kitagawa, Toshio; Glicksman, Arvin S.; Nickson, James J. Cancer, 19: 1081-7(Aug. 1966).

Cases of head and neck carcinoma (210) were reviewed following treatment with high-energy electrons, 6 to 24 Mev. The ease of altering the electron beam energy allows for rapid replanning of treatment when tumor size diminishes. The primary aim of treatment in most cases was palliation. Doses greater than 5,500 rads in 5 weeks were necessary for control of the primary and recurrent tumors as well as the metastatic nodes. The intervening normal tissue tolerated the dosage schedules quite well. In the material reported the number of complete regressions was modest and the duration of continued control was short. The obvious reason for this finding is that the material was advanced or recurrent in 90% of cases. Other factors may account in part for the failures. The RBE of electrons is still uncertain. Consideration of tissue heterogeneity which was not done with these cases may produce different dose distributions. It was concluded that high-energy electrons are a safe and convenient source of ionization for the treatment of head and neck cancers. (auth)

36686 STUDY OF THE DISTRIBUTION OF DOSE IN RADIOTHERAPY WITH THE AID OF ELECTRONIC COMPUTERS. Da Rocha, A. F. G.; Probst, W. G. (IASEG Hospital, Rio de Janeiro. Brazilian Red Cross Hospital, Rio de Janeiro). J. Coll. Radiol. Austral., 10: 140-4(May 1966).

The utilization of electronic computers as a means of obtaining, quickly and efficiently, the distribution of dose in radiotherapy, with consequent facilitation of the planning procedure is discussed. The plan of operation and its flow chart is described. (auth)

36687 NEW REMOTELY CONTROLLED UNIT FOR TREATMENT OF UTERINE CARCINOMA. O'Connell, D.; Howard, N.; Joslin, C. A. F.; Ramsey, N. W.; Liversage, W. E. (Charing Cross Group of Hospitals, London). Lancet, 2: 570-1(Sept. 18, 1965).

Intracavitary radium therapy is at present the major cause of stray radiation exposure of staff and patients in hospitals. The technique and apparatus described are designed to eliminate this hazard by using a remotely controlled afterloading intracavitary method. The high dose-rate reduces the treatment time to only a few minutes instead of several hours or days, and allows the use of a fully protected treatment room with a rapid turnover of patients. This technique for treatment of uterine carcinoma has been made possible by a device known as the Cathetron. It utilizes three stainless-steel catheters, one in the uterine canal and one in each lateral fornix. Flexible-drive tubes are connected from the catheters to a protective storage safe. This safe contains up to nine different ^{60}Co sources which may be individually selected for use in a particular catheter. The use of dose rates 100 times greater than those now used in routine radium treatments raises the questions whether there is likely to be any change in the relative biological efficiency, and whether this change is likely to vary with the type of tissue irradiated (tumor, uterus, rectum, colon, bladder, or small intestine). The radiobiological effects on different tissues in animals were studied at different dose rates, by whole-body irradiation of mice using a ^{60}Co source to establish possible changes in LD_{50} with dose rate. The results show that the $LD_{50(30)}$ for 24-hr irradiation is 1250 rad, while for 15 min irradiation it is 725 rad. These mice died as a result of radiation injury to normal tissues, mainly intestine or hemopoietic tissue. These results indicate an increased sensitivity at the higher dose rate by a factor of 1.7. For a tumor, a 24-hr dose of 2000 rad would be equivalent to an acute dose of about 1700 rad, an increased sensitivity at the higher dose rate by a factor of only 1.2. It is concluded that it is advisable to increase the number of fractions when treating carcinoma of the cervix at a high dose rate. (TCO)

36688 DETERMINATION OF THE ISODOSE CURVES WITH THE USE OF THE "DOSE GRADIENT" LINES (IN THE CASE OF THE USE OF ^{60}Co RAY BEAM). Dezsi, Zoltan. Magyar Radiol., 166-9(June 1966). (In Hungarian).

In telecobalt deep therapy with apparatus of Gravicert type, the lines of the dose gradient form straight lines and by using them the isodose curves are promptly determined. (auth)

36689 SIMPLE DETERMINATION OF THE FLUX DENSITY DISTRIBUTION OF FAST ELECTRONS AND ITS USE IN RADIATION THERAPY AND RADIOBIOLOGY QUESTIONS. Hagemann, Gerd (Univ., Marburg, Ger.). Strahlentherapie, 130: 73-80(May 1966). (In German).

A simple method for determining the relative flux density of fast electrons is described; based on the Tscherenkow effect, flux density distribution in acrylic glass can be obtained. By comparing the results with energy dose measurements, the LET can be determined and details concerning the energy spectrum of secondary electrons can be obtained. Examples in radiobiology and radiation therapy are discussed. (auth)

36690 THE YEAR BOOK OF NUCLEAR MEDICINE. VOLUME 1, 1966. Quinn III, James L. (ed.). Chicago, Year Book Medical Publishers, Incorporated, 1966. 384p. $10.00.

Information is included on: radionuclide dosimetry in nuclear medicine; radiation physics and instrumentation; radiochemistry and radiopharmacology; health physics and radiobiology; and various systems including endocrine, hemopoietic and lymphatic, genitourinary, central nervous,

gastrointestinal, heart and great vessels, pulmonary, and osseous and cartilaginous systems. (P.C.H.)

36691 STRAHLENFORSCHUNG UND STRAHLENBEHANDLUNG. Vortraege aus den Gebieten der Strahlenphysik, Strahlenbiologie und Strahlentherapie, der Nuklearmedizin und des Strahlenschutzes. Band IV. 43. Tagung der Deutschen Roentgengesellschaft in Koeln vom 7. bis 10. Mai 1962. (Radioresearch and Radiotherapy. Contribution from Areas of Radiophysics, Radiobiology and Radiotherapy, Nuclear Medicine and Radiation Protection. Volume IV. Forty-Third Meeting of the German X-Ray Society, Cologne, May 7–10, 1962). Meyer, Hans; Becker, Josef (eds.). Strahlentherapie, Sonderbaende, 52: 1-372(1963). (CONF-620502).

Forty-one papers are included. Subjects covered include: radiology and space research; treatment of malignancies; thyroid therapy; weak x radiation; radiobiology and radiopathology; radiobiological studies in nuclear medicine; radiation protection in medicine; techniques in medical irradiation; the physicist in hospitals; and measurement and determination of ionizing radiation. Separate abstracts were prepared for 35. (tr-auth)

For abstracts of individual papers see: 36570–36573, 36651–36655, 36669, 36670, 36675–36679, and 36692–36710.

36692 OPERABILITY LIMITS AS INDICATION FOR RADIOTHERAPY IN BRAIN TUMORS. Toennis, Wilhelm (Univ., Cologne. Max-Planck-Instituts fuer Hirnforschung, Cologne). Strahlentherapie, Sonderbaende, 52: 21-7(1963). (In German).

Factors affecting the operability or radiotherapy of brain tumors are principally the site and type of tumor. The diagnostic methods used for determining these two factors are reviewed. (J.S.R.)

36693 EXPERIENCE IN THE RADIOTREATMENT OF 242 BRAIN TUMORS. Friedmann, Gerhard; Gaebel, Eva (Univ., Cologne. Allgemeinen Ortskrankenkasse, Cologne). Strahlentherapie, Sonderbaende, 52: 28-33(1963). (In German).

The results obtained in radiotherapy of 242 cases of brain tumors, both without and with complete or partial extirpation of the tumor, are reported in tabular form and discussed. (J.S.R.)

36694 IRRADIATION OF BRAIN TUMORS. Cocchi, Umberto (Univ., Zurich). Strahlentherapie, Sonderbaende, 52: 34-46(1963). (In German).

On the basis of experience with 457 brain tumors and of results reported in the world literature, the radiation consequences of different operable and non-operable brain tumors are reported. A brief review is given of experiences with the irradiation of hemangiomas, arterio-venous aneurisms, brain metastases, and hypophysis tumors. Radiation techniques and the danger of delayed damage in the brain are also briefly considered. (tr-auth)

36695 MORPHOLOGICAL CHANGES IN TUMORS AFTER IRRADIATION AND THE POSSIBILITY OF INJURIES IN THE NORMAL BRAIN. Zuelch, Klaus J. (Max-Planck-Instituts fuer Hirnforschung, Cologne. Staedt. Krankenanstalt, Cologne). Strahlentherapie, Sonderbaende, 52: 47-62(1963). (In German).

Morphological changes induced in tumors by irradiation are briefly summarized with respect to the type of tumor. The delayed damage caused in healthy brain tissue by irradiation is described and illustrated. It is shown that injuries can result from conventional radiation doses. Delayed necrosis can give space through cystic transformation and a type of "internal discharge" of the brain can occur. (J.S.R.)

36696 DETECTION OF CEREBRAL RADIATION DAMAGE WITH RADIOACTIVE ISOTOPES. Wende, Sigurd (Freie Univ., Berlin). Strahlentherapie, Sonderbaende, 52: 74-80(1963). (In German).

Studies were made to determine whether a brain edema caused by x radiation could be detected with γ encephalography. The γ encephalograms were made 2 and 24 hrs after i.v. injection of radioactive iodine-labeled serum albumin. In a clinically evident, radioinduced brain edema the γ encephalography shows a clearly increased level of the pulse curve over the entire brain. If at the beginning of the x-ray therapy there is no support for a nascent brain edema, the pulse curve of γ encephalography shows the same value as the brain before irradiation. The results of γ encephalography are parallel with the clinical findings. (J.S.R.)

36697 TELE-X-RAY AND TELECOBALT THERAPY IN METASTASES. Quack, Guenter (Allgemeinen Ortskrankenkasse, Cologne). Strahlentherapie, Sonderbaende, 52: 81-92(1963). (In German).

The results of the tele-x-ray and telecobalt therapy of 56 cases of metastases following mammary carcinoma are reported and analyzed. (J.S.R.)

36698 TREATMENT OF CANCEROUS METASTASES WITH SMALL DOSES. Heilig, Walter (Krankenhauses Lainz, Vienna). Strahlentherapie, Sonderbaende, 52: 93-106(1963). (In German).

The results obtained in whole-body x irradiation at small doses to 2913 patients with generalized dissemination of cancerous tumors are reported. The observation period covered a time span of 20 yrs from 1938 to 1957. The indication for whole-body irradiation is given in all cases by generalized carcinosis or sarcomatosis, in which there is no leukopenia under 2500 and no erythrocyte drop under 2,500,000. The therapeutic results of whole-body x irradiation are dependent on the site of the metastases. (tr-auth)

36699 DETERMINATION AND LOCALIZATION PROBLEMS IN THE RADIOTHERAPY OF CARCINOMA OF THE CERVIX UTERUS. Frischkorn, Rolf (Univ., Goettingen, Ger.). Strahlentherapie, Sonderbaende, 52: 107-16(1963). (In German).

Radium therapy is usually carried out by the use of the milligram element hour so that data on the dose distribution are not possible in individual cases. Therefore there is no possibility of correlating a given effect of radiation with definite doses and a given time dose distribution. A method is proposed that makes it possible to establish exactly the dose distribution in each individual case by introduction of a physical dose magnitude. By avoiding the milligram element hour all irradiation effects can be related to definite doses. The necessary personnel, material, and time expenditure are basically the same as in other radiological and operative methods. There exists a possibility of additional improvements in the therapeutic results not only by earlier identification but also by individualization of the radium therapy. (tr-auth)

36700 QUESTION OF THE SUBTLE ADAPTATION OF THE IRRADIATION FIELD IN FAST ELECTRONS. Breitling, Gerhard; Vogel, Karl-Heinz (Univ., Tuebingen, Ger.). Strahlentherapie, Sonderbaende, 52: 117-26(1963). (In German).

Studies on a material called Plastilin showed that it is suitable for the subtle adaptation of the radiation field to tumor shape in fast electron therapy. Plastilin also has low bremsstrahlung yield and is economical. (P.C.H.)

36701 EVALUATION OF THE GROWTH ACTIVITY OF BONE METASTASES. Schermuly, Willi (Univ., Marburg, Ger.). Strahlentherapie, Sonderbaende, 52: 127-41 (1963). (In German).

Clinical results and x-ray findings of bone metastases are frequently in disaccord. The calcium and phosphorus values in the urine and blood determined under given diet conditions can show an increase with increasing osteolysis in patients with bone metastases in mammary carcinoma. Often increased calcium precipitation was found in the urine of such patients, but it was only after weeks or months that the metastasization was clinically evident and could be de-

tected by x radiology. The growth active process in clinically latent stages was therefore made probable. In almost half the patients with x radiological osteolytic metastases the alkali serum phosphastase increases as a sign of the restoration process. With x-ray detectable recalcification in the area of early osteolytic metastases there is generally an increase of the alkaline serum phosphatase. This can decrease as a sign of perturbation of local restoration at the time point of a renewed growth before the renewed osteolysis can be detected by x rays. In x rays the metastatic destruction process can be detected according to its location in various bones according to whether this process occurs in recalcified or normal structured bones. The parallel occurrences of the recalcified osteolytic areas do not signify that in both places a renewed tumor growth is in process. (tr-auth)

36702 UNDESIRED CO-IRRADIATION OF THE ORGANISM IN DEEP THERAPY OF MALIGNANT TUMORS. Schoen, Detlev (Univ., Tuebingen, Ger.). Strahlentherapie, Sonderbaende, 52: 142-7(1963). (In German).

Charts and graphs showing the dose received by the organism during deep therapy of malignant tumors are presented. (J.S.R.)

36703 FREQUENCY OF RADIOFIBROSES IN SOUND LUNG TISSUE AFTER INTENSIVE RADIOTHERAPY OF BRONCHIAL CARCINOMAS. Eichhorn, Hans-Juergen; Mateev, Botjo. Strahlentherapie, Sonderbaende, 52: 149-5(1963). (In German).

Cases of bronchial carcinomas (139) that were irradiated with focal doses of 4000 to 9000 R were investigated with respect to the frequency of radiofibroses occurrence in the co-irradiated healthy lung tissue outside the tumor area. The effects of the dose and dose distribution were also studied. The results showed that almost 50% of all cases showed radiofibroses 5 months after the beginning of radiotherapy. This value is only slightly higher in the upper range of doses than in the lower dose regions. 12 months after irradiation the fibrosis quota is only slightly higher than 4 months after irradiation. A division of the dose into two series leads to an increase of the fibrosis quota when in the first series a dose of 5000 R was administered. The pure irradiation effect is sharply limited to the area of radiation absorption. (tr-auth)

36704 IN VIVO INVESTIGATIONS WITH ^{3}H-THYMIDINE FOR THE STUDY OF TUMOR CELL KINETICS IN PUNCTATES. Chone, Bruno; Frischbier, Hans-Joachim. Strahlentherapie, Sonderbaende, 52: 156-65(1963). (In German).

In 10 patients with metastatic body cavity discharges in vivo, incubations of the exudates were made with 0.5 to 2 mC of ^{3}H-thymidine. The subsequent investigation controls covered a time period of 14 days. The results obtained showed a resulting corresponding path in the tendencies according to individual radiotherapy. However, the data obtained is not sufficient for a valid hypothesis. (tr-auth)

36705 INVESTIGATIONS WITH A TRITIUM-LABELED N-MUSTARD GAS DERIVATIVE IN CARCINOMA TREATMENT. Bolt, Wilhelm; Ritzl, Friedrich; Nahrmann, Hans (Univ., Cologne. Kernforschungsanlage, Juelich, Ger.). Strahlentherapie, Sonderbaende, 52: 166-70(1963). (In German).

The results of studies carried out on inoperable tumors are described. Labeled cyclophosphamide, cyclophosphamide labeled in the nitrogen mustard gas group, and endoxan labeled in the molecule ring were used. It was found that 90 minutes after injection of the radioactive compounds various new radioactive components could be clearly detected in the serum and urine. However, after injection of cyclophosphamide labeled only in the molecule ring, a homogeneous distribution was observed in the body; after injection of completely labeled cyclophosphamide, an enrichment was found in the malignant tissue. This selection of radioactivity in the tumor tissue was increased considerably after injection of the compound labeled in the nitrogen mustard gas group. The radiation burden of the patient is described and discussed. (tr-auth)

36706 INDICATION OF THYROID THERAPY BY RADIOIODIDE LOCALIZATION. Tosch, Reinhard; Schumacher, Werner (Staedt. Rudolf-Virchow-Krankenhauses, Berlin). Strahlentherapie, Sonderbaende, 52: 171-9(1963). (In German).

From studies on radioiodide localization using the scanning method, indications were obtained for desired therapy. The demarcations of the individual thyroid disorders and the possibility of being able to limit within the thyroid functional and non-functioning regions gives the surgeon, the radiotherapist, and the internist indications that can make possible a satisfactory treatment. The individual indications are described by various examples. (tr-auth)

36707 X-RAY THERAPY WITH SMALL DOSES WITH SPECIAL CONSIDERATION OF THE TREATMENT OF CHILDREN. Pape, Rudolf (Wilhelminenspitals, Vienna). Strahlentherapie, Sonderbaende, 52: 180-7(1963). (In German).

Low x irradiation with doses of 1 to 20 R can be used with good results for inflammations, degenerative diseases of the motor apparatus, in conditions of pain, and in functional therapy in the narrow sense. Clinical observations of early reactions showed the efficiency of irradiation. Recommendations are given with respect to gonad protection in children in inflammation therapy with diagnostic radiation. Recommendations are also given for orientating studies that leave no detectable effect. (tr-auth)

36708 CONSEQUENCES OF IRRADIATION TO THE FACE, ESPECIALLY TO THE DENTURES. Korkhaus, Gustav; Jung, Till (Univ., Bonn). Strahlentherapie, Sonderbaende, 52: 235-51(1963). (In German).

A review is given of the most frequently occurring delayed consequences of the use of radiation therapy in infants and small children. Emphasis is on damage to the teeth, jaw bone, and face. Specific cases are used as illustrations and examples. (J.S.R.)

36709 RESPONSIBILITY OF THE DOCTOR IN THE RADIATION DETECTION OF PATIENTS. Glauner, Rolf (Marienhospital, Stuttgart). Strahlentherapie, Sonderbaende, 52: 302-7(1963). (In German).

Only the doctor can differentiate between the uses and damages of a radiodiagnostic or radiotherapeutic treatment. All theoretical studies are not sufficient to provide guidelines. This is valid for both somatic and genetic damages. The genetic burden for medical treatments is approximately $\frac{1}{3}$ of the natural radiation level. It is therefore suggested that the doctor be as sparing as possible in the use of ionizing radiation. (tr-auth)

36710 CONSTRUCTION CHARACTERISTICS OF CESIUM TELECURIE DEVICES. Walter, Erich (Siemens-Reiniger-Werke AG, Erlangen, Ger.). Strahlentherapie, Sonderbaende, 52: 347-52(1963). (In German).

The construction and design characteristics of cesium telecurie devices are based on the properties of the cesium decay scheme and medical requirements. These are briefly indicated and discussed. (tr-auth)

CHEMISTRY

General

Refer also to abstract 37279.

36711 COMPUTATION OF RADIOACTIVE ISOTOPE CONCENTRATION IN AN ENCLOSED TANK DURING ISOTOPE ADSORPTION BY THE BOTTOM LAYER. Prokhorov, V. M. At. Energ. (USSR) 20: 448-9(May 1966). (In Russian).

The adsorption of radioactive isotopes by the bottom layer of a tank was described by a kinetic equation obtained from natural conditions and applied to the concentration of isotopes in water. A more accurate description of radioactive contamination at the bottom was obtained by determining the rate of isotopic diffusion at the tank's surface layer. Adsorption curves for the case of single and of constant influx are presented. (G.O.Y.)

Analytical Procedures

See also Separation Processes and Procedures

Refer also to abstracts 36542, 36562, 37018, 37019, and 37151–37153.

36712 (IS–1335) BIBLIOGRAPHY OF MASS SPECTROSCOPY LITERATURE, COMPILED BY COMPUTER METHOD. Capellen, J.; Svec, H. J.; Sage, C. R. (Ames Lab., Iowa State Univ. of Science and Tech.). Mar. 1966. Contract W-7405-eng-82. 399p. Dep. mn. CFSTI $4.25 cy, $1.75 mn.

More than 1500 articles in the field of mass spectroscopy are listed as a result of computer searching of more than 340,000 scientific articles during late 1964, 1965, and early 1966. The 108 papers presented at the 13th Annual Conference on Mass Spectrometry and Allied Topics held in St. Louis, Missouri, May 16–25, 1965 are included in the listing. A bibliography, an author index, and a permuted title (KWIC) index are contained in the report. An explanation of how to use each section is presented. (auth)

36713 (LA–3402) THE POTENTIOMETRIC TITRATION OF CERIUM AND MANGANESE FOLLOWING SEPARATION FROM PLUTONIUM AND COBALT. Bryan, R. G.; Waterbury, G. R. (Los Alamos Scientific Lab., Univ. of California, N. Mex.). Aug. 23, 1965. Contract W-7405-eng-36. 16p. Dep. mn. CFSTI $1.00 cy, $0.50 mn.

Cerium in ternary alloys consisting of plutonium, cerium, and cobalt, and cerium and manganese in quaternary alloys consisting of plutonium, cerium, cobalt, and manganese are separated and then determined by potentiometric titration. In the analysis of the ternary alloy, the plutonium is separated by an anion exchange resin method, and the cerium, in the presence of cobalt, is oxidized with silver(II) to cerium(IV) which is titrated with iron(II) solution. The relative standard deviation is 0.3% for a single measurement of cerium. In the analysis of the quaternary alloy, plutonium is separated by the anion exchange resin method, and then cerium is separated from manganese and cobalt using mixed mineral acid-organic solvent eluant solutions and strongly basic anion exchange resin columns. Then the cerium and manganese are oxidized to cerium(IV) and manganese(VII), respectively, with silver(II) oxide, and each is titrated with iron(II) solution. The average cerium found in 52 solutions, corresponding to 11 to 36% cerium in quaternary alloys that also contain 50% plutonium, was 99.9% with a relative standard deviation of 0.4%. The average manganese found in 44 solutions, corresponding to 8 to 27% manganese in the quaternary alloys, was 100.0% with a relative standard deviation of 0.4%. For manganese concentrations of 3% or less, an established spectrophotometric method is recommended. High concentrations of aluminum, chromium, lanthanum, nickel, sodium, and vanadium interfere in the method. (auth)

36714 ACTIVATION ANALYSIS OF TRACES OF IMPURITIES IN URANIUM. I. DETERMINATION OF COBALT. Travesi, A.; Galiano, J. A. (Atomic Energy Commission, Madrid). An. Real Soc. Espan. Fis. Quim. (Madrid), Ser. B, 62: 247-57(1966). (In Spanish).

When neutron activation analysis is applied to uranium samples, interferences arise because of the fission products of uranium. To avoid them there are two possibilities. One is to remove the uranium with an adequate treatment before the irradiation. The second one is to irradiate samples without previous treatment but using specific radiochemical separation procedures for the elements to be analyzed. The advantages and disadvantages of both procedures are considered, and to show their feasibility, determination of cobalt traces in uranium compounds was carried out by both procedures and the results obtained are compared. In the first case, the uranium was removed from the samples by extraction with a mixture of TBP and cyclohexane. The uranium extraction conditions were determined by a previous study. By using radioactive tracers it was shown that cobalt is not lost during the extraction process. In the case of the samples irradiated without previous treatment, the earlier methods of cobalt radiochemical separation had to be improved to avoid fission-product interference. Results obtained by both procedures were compared with those earlier obtained with the same samples using other analytical techniques (colorimetry and emission spectrography) and excellent agreement was found. (auth)

36715 ACTIVATION ANALYSIS OF TRACES OF IMPURITIES IN URANIUM. II. DETERMINATION OF COPPER, CHROMIUM, AND MANGANESE. Travesi, A.; Galiano, J. A. (Atomic Energy Commission, Madrid). An. Real Soc. Espan. Fis. Quim. (Madrid), Ser. B, 62: 259-73(1966). (In Spanish).

Activation analysis using reactor neutrons (JEN-1) was applied to determining traces of copper, chromium, and manganese in uranium samples involving methods without chemical treatment for the removal of uranium previous to the irradiation. By combining chemical separation techniques of high specificity and gamma spectrometry measurements it was possible to determine trace amounts of these elements without interference from fission products. The radiochemical methods developed include addition of isotopic carrier and a coarse initial separation by precipitation, followed by purification using liquid-liquid extraction. In this way satisfactory decontamination is obtained in a relatively short time. The sensitivities obtained in the methods used were between 1 ppM in the worst case (chromium) and 0.003 ppM in the determination of manganese. The results were compared with those earlier obtained with the same samples using other analytical techniques (colorimetry and emission spectrography) and excellent agreement was found. (auth)

36716 SPECTROPHOTOMETRIC DETERMINATION OF URANIUM WITH ARSENAZO PRIOR TO EXTRACTION AND COLOROMETRIC DETERMINATION IN ORGANIC MEDIA. Palomares Delgado, F.; Vera Palomino, J.; Petrement, J. An. Real Soc. Espan. Fis. Quim. (Madrid), Ser. B, 62: 275-92(1966). (In Spanish).

The determination of uranium with arsenazo is hindered by a great number of cations that form stable complexes with the reagent and may give rise to interferences. By studying the optimum conditions of uranium extraction by means of tributyl phosphate solutions dissolved in methylisobutyl ketone, under conditions for previous masking of the interfering cations, an organic extract was obtained containing all the uranium together with small amounts of iron. The possible interference derived from the latter

element is avoided by reduction with hydroxylammonium chloride followed by complex formation of the Fe(II)-o-phenanthroline compound in alcohol. The determination of uranium is carried out by taking an aliquot of the organic extract and developing the color in alcoholic medium. The relative stabilities of the complexes involved by the o-phenanthroline and arsenazo reagents with the cations Fe^{2+} Fe^{3+}, and UO_2^{2+} were studied under these conditions. (auth)

36717 SOLVENT EXTRACTION METHODS APPLIED TO THE CHEMICAL ANALYSIS OF URANIUM. II. STUDY OF EXTRACTION WITH TRIBUTYL PHOSPHATE-ETHYL ACETATE. Vera Palomino, J.; Palomares Delgado, F.; Petrement, J. An. Real Soc. Espan. Fis. Quim. (Madrid), Ser. B, 62: 293-9(1966). (In Spanish).

The extraction of uranium on the trace level was studied by means of the solvent system tributyl phosphate–ethyl acetate under conditions of constant acidity by using aluminum, calcium and ammonium nitrates as salting-out agents. For calcium nitrate, which gave optimum results, an equation was obtained which relates the percent of extracted uranium with the concentrations of tributyl phosphate in ethyl acetate c and calcium nitrate in the aqueous phase n. The curves of equal extraction are obtained in the c, n plane, where from the optimum extraction conditions may be easily inferred for any given case. (auth)

36718 SOLVENT EXTRACTION METHODS APPLIED TO CHEMICAL ANALYSIS OF URANIUM. III. STUDY OF EXTRACTION WITH INERT SOLVENTS. Vera Palomino, J.; Palomares Delgado, F.; Petrement, J. An. Real Soc. Espan. Fis. Quim. (Madrid), Ser. B, 62: 301-15(1966). (In Spanish).

The extraction of uranium on the trace level was studied by using tributyl phosphate as the active agent under conditions aiming at the attainment of quantitative extraction by means of a single step process using a number of salting-out agents. Two inert solvents were investigated, benzene and cyclohexane, which allowed the corresponding empirical equations describing the extraction process to be derived and the results obtained were compared with those previously reported for solvents which, like ethyl acetate and methyl isobutyl ketone, favor the extraction of uranium. (auth)

36719 ANALYSIS OF SURFACES BY SCATTERING OF ACCELERATED ALPHA PARTICLES. Peisach, Max; Poole, Darrell O. (Southern Univ. Nuclear Inst., Faure, South Africa). Anal. Chem., 38: 1345-50(Sept. 1966).

Elastic scattering of monoenergetic alpha particles was used for qualitative and quantitative analysis of surface layers nondestructively. Energy spectra were obtained with surface barrier semiconductor detectors. Surface concentrations of films were measured between 0 and 40 $\mu g/cm^2$ with a precision of ± 0.2 $\mu g/cm^2$ over an area of 0.5 mm^2. The method was also applied to thick coatings and to geological samples. A monogram is presented for selecting experimental conditions and for the rapid interpretation of experimental data. (auth)

36720 LIMITATIONS OF TRITIUM MEASUREMENTS BY LIQUID SCINTILLATION COUNTING OF EMULSIONS. Benson, Royal H. (Monsanto Co., Texas City, Tex.). Anal. Chem., 38: 1353-6(Sept. 1966).

Considerable error can result from the use of the emulsion counting technique when applied to undefined systems. Important variables are shown to be phosphor concentration, sample concentration, temperature, agitation, sample distribution, cooling time, chemical nature of the sample, and methods used for quench correction. Two methods of sample preparation are given and the errors associated with each are defined. The toluene-Triton X-100 phosphor gives a solubilized system with a discontinuous transition to a soluble plus emulsion system as water sample size is increased. (auth)

36721 A SIMPLE IN-VIAL COMBUSTION METHOD FOR ASSAY OF ^3H, ^{14}C, AND ^{35}S IN BIOLOGICAL, BIOCHEMICAL, AND ORGANIC MATERIALS. Gupta, Gopi N. (Rockefeller Univ., New York). Anal. Chem., 38: 1356-9 (Sept. 1966).

A simple in-vial combustion method is described for radioactivity determination of ^3H, ^{14}C, and ^{35}S in biological and organic materials. The sample is combusted and counted in the same vial. The tritiated water and ^{14}C and ^{35}S gaseous combustion products are counted in liquid scintillator. In this system, counting efficiency (count rate of combusted sample/count rate of directly counted standard sample) for both ^3H and ^{14}C is about 90% with 24 and 73% of machine efficiency, respectively. The quenching remains minimum and constant. The counting efficiency of ^{35}S is about 12 to 17% higher than with direct counting with about 70% of machine efficiency. The method is simple, rapid, and inexpensive. (J.G.B.)

36722 SPECTROFLUOROMETRIC ANALYSIS OF RARE EARTH CHELATES OF THENOYLTRIFLUOROACETONE, BENZOYLACETONE, AND DIBENZOYLMETHANE BY COMPUTER SPECTRUM STRIPPING TECHNIQUES. Stanley, Elizabeth C.; Kinneberg, Bruce I.; Varga, Louis P. (Oklahoma State Univ., Stillwater). Anal. Chem., 38: 1362-7(Sept. 1966).

Fluorescence studies of rare earth tetrakis chelates with the β-diketone ligands thenoyltrifluoroacetone, benzoylacetone, and dibenzoylmethane in acetonitrile solution indicated the feasibility of a general method for rare earth analysis. By choosing a ligand having the proper chelate triplet state energy level, selective excitation of the resonance levels of the rare earth ions was observed allowing controlled elimination of some overlapping spectral features. Emission data from the single beam spectrofluorometer were corrected, normalized, machine plotted, and a spectrum stripping program was found capable of identifying the components of a rare earth mixture by systematic search and identification of the maximum peak wavelengths. The long wavelength cut-off of the spectrofluorometer limited observation of intense fluorescence to samarium, europium, and terbium chelates, but the wavelengths of possible intense line fluorescence are presented for all rare earths studied. Phosphorescence was observed for gadolinium and lutetium thenoyltrifluoroacetone chelates at 0°C. (auth)

36723 OXYGEN-TUBE COMBUSTION METHOD FOR LIQUID SCINTILLATION ASSAY OF ^{14}C AND TRITIUM. Scott, Benjamin F.; Kennally, James R. (New England Nuclear Assay Corp., Boston). Anal. Chem., 38: 1404-5 (Sept. 1966).

Two methods for liquid scintillation assay of carbon-14 and tritium in non-volatile organic compounds were combined in order to minimize disadvantages of each. Samples undergo sealed tube combustion at high temperature prior to being dissolved in scintillation solution. The procedure is relatively simple, producing high yields. Disadvantages center around tube size which limits sample size. (J.G.B.)

36724 DETERMINATION OF COPPER IN HYDROGENATED FATS BY NEUTRON ACTIVATION ANALYSIS. Hoegdahl, Ove. T.; Melsom, Sigurd (Central Inst. for Industrial Research, Blindern, Norway). Anal. Chem., 38: 1414-15(Sept. 1966).

A procedure that avoids the use of hydrolysis or wet decomposition of the fat in which copper is to be determined by neutron activation analysis was developed. Induced copper activity was extracted from a toluene solution of the fat with hydrochloric acid, then removed from the aqueous solution with carbon tetrachloride containing Zn-dibenzyldithiocarbamate. The method is rapid, giving results comparable to those of the wet decomposition method. (J.G.B.)

36725 COLORIMETRIC DETERMINATION OF GOLD, PLATINUM, AND CERIUM. Hashmi, M. H.; Rashid, Abdur (Pakistan Council of Scientific and Industrial Research, Lahore). Anal. Chem., 38: 1423-4(Sept. 1966).

An equimolar mixture of isonicotinic acid hydrazide and 2,3,5-triphenyltetrazolium chloride was used as the color producing agent in the determination of gold, platinum, and cerium. The method is simple and accurate. The visual limit of identification is 2, 15, and 6 μg per ml of gold,

platinum, and cerium, respectively. The maximum tolerable limit of various metal ions which do not interfere is reported. (J.G.B.)

36726 DETERMINATION OF TRACE AMOUNTS OF COPPER IN NIOBIUM AND TANTALUM BY ATOMIC-ABSORPTION SPECTROSCOPY. Kirkbright, G. F.; Peters, M. K.; West, T. S. (Imperial Coll. of Science and Technology, London). Analyst, 91: 411-17(July 1966).

Copper may be determined in niobium and tantalum at the 1 to 10 ppm level by extraction of copper 8-hydroxyquinolinate from a fluoride medium into ethyl acetate at pH 4.5, and by direct atomic-absorption spectroscopy of the extract in an air-propane or air-acetylene flame at 3247 Å. Optimum conditions of pH, reagent concentration, and solvent composition were established, and a study of the effect of other cations and anions is presented. Only titanium(IV) and molybdenum(VI) caused interference when present in 100-fold excesses, but even these could be masked by the addition of hydrogen peroxide. (auth)

36727 PRIMARY ANALYTICAL STANDARDS FOR PLUTONIUM: QUANTITATIVE SEPARATION OF PLUTONIUM FROM DICESIUM PLUTONIUM HEXACHLORIDE. Miner, F. J. (Dow Chemical Co., Golden, Colo.). Analyst, 91: 464-5(July 1966).

Separation of plutonium from dicesium plutonium hexachloride, proposed as a primary analytical standard for plutonium, was studied using the slurry-column procedure. Removal of cesium with HCl before separation and recovery of plutonium eliminated the difficulties that are inherent in the use of dicesium plutonium hexachloride. Stirring for 20 min before adding to the ion exchange column produced no breakthrough of plutonium during washing to remove cesium. Recovery of plutonium was 99.99% with a standard deviation of 0.03%. (P.C.S.)

36728 (n,γ) ANALYSIS OF HUMAN BLOOD AND HAIR. Asai, Takuo; Meren, Eiichiro; Iwai, Mineko; Sato, Yuji; Azuma, Toshio. Ann. Rep. Radiat. Center Osaka Prefect., 6: 111-14(1965).

The elements in human blood and hair were measured by (n,γ) activation. Three samples of blood and hair, respectively, and four standard NaCl samples were irradiated for 20 minutes in a neutron flux 4×10^{12} n/cm^2 sec of a reactor. The gamma spectra from these activated samples were then measured. The contents of Cl, Ni, Zn, Mn, Ca, and K were estimated from gamma-ray energies on the strong background of Na activities. (auth)

36729 SPECTROGRAPHIC DETERMINATION OF TRACE AMOUNTS OF RARE EARTHS. III. DETERMINATION OF ALL RARE EARTH ELEMENTS BY THE CARRIER DISTILLATION METHOD. Strzyzewska, B.; Radwan, Z.; Minczewski, J. (Inst. of Nuclear Research, Warsaw). Appl. Spectros., 20: 236-40(July-Aug. 1966).

A carrier distillation method was used for quantitative determination of trace amounts of rare earths in hydrochloric acid solution evaporated on graphite matrix. The method can be applied to all rare earth elements. The detection limit obtained for individual elements was from 0.02 to 0.16 μg per sample (except for Yb, it was 0.0008 μg per sample). The deviations of the position of the analytical curves for the individual rare earth elements were investigated as affected by addition of all other rare earth elements in concentrations at the upper limit of the procedure. The influence of additional elements was different for various elements and for different lines of the same element. The interpolation error for maximal difference in composition between the sample and spectrographic standards was calculated. (auth)

36730 SPECTROGRAPHIC DETERMINATION OF FLUORIDE IN PLUTONIUM NITRATE SOLUTIONS. Johnson, A. J.; Vejvoda, E. (Dow Chemical Co., Golden, Colo.). Appl. Spectros., 20: 262-3(July-Aug. 1966).

Semiquantitative determination of fluoride in plutonium nitrate solution using the green system of the CaF band spectrum was developed. The method is applicable to fluoride concentration ranging between 0.20 and 10.0 g/l, is rapid, and provides a quick estimate of the fluoride concentration during the course of metal-nitric acid dissolutions. Criteria for the selection of the green CaF (5291.0 Å) over the green BaF (4950.8 Å) and the yellow SrF (5772.0 Å) systems are given. General enhancement of background and spectral intensities was observed for a corresponding increase in the plutonium concentration of the sample. To minimize this effect, the plutonium concentration was adjusted to fall within 50 to 125 g/l range. Standard deviation obtained was ±0.45 g/l with a relative standard deviation of 21.4%. (P.C.S.)

36731 CALCULATION METHOD FOR AZEOTROPIC STEAM FRACTIONATION, APPLIED TO THE TBP–CCl_4 SYSTEM. Zil'berman, B. Ya.; Komarov, V. N.; Pushlenkov, M. F. At. Energ. (USSR), 20: 419-21(May 1966). (In Russian).

The propagation principle of uniform molar flow for stratified systems was used to investigate the azeotropic distillation of the ternary system TBP–CCl_4–H_2O. This propagation principle leads to the concentration of "fictive" components in the sum of the liquid phases. The equation for the system is analogous to that of a homogeneous two-component system; the difference is that in the homogeneous condensate phase a concentration of fictive components appears. (G.O.Y.)

36732 UTILIZATION OF FAST CHARGED PARTICLE INELASTIC SCATTERING FOR ANALYSIS OF COMPOSITION OF MATERIALS. Vasil'ev, S. S.; Mikhaleva, T. N.; Vorob'ev, Yu. A.; Chuprunov, D. L. At. Energ. (USSR), 20: 432-4(May 1966). (In Russian).

The impurities in Al samples were analyzed by using a 6.6-Mev proton beam and a 100-channel scintillation spectrometer with Cs(Tl) as a proton recorder. The recording time for each angle of the scattered proton spectrum was ~10 min at 2.0 to 6.5 Mev. The spectra obtained were then analyzed, and the proton elastic and inelastic scattering peaks from the Al nuclei were determined along with the scattering maxima of other nuclei. Impurities consisting of Ca, Mn, Si, and Na were found. The results were compared with neutron activation data on the Si impurity. (G.O.Y.)

36733 RAPID ANALYSIS OF RaA AEROSOL CONCENTRATION AND OF LATENT ENERGY IN THE AIR. Kartashov, N. P. At. Energ. (USSR), 20: 444-8(May 1966). (In Russian).

An efficient method for determining the concentration of RaA and the energy liberated during the complete decay of the short-lived radon contained in one liter of air (latent energy) is proposed. The theory for the method is discussed, and an experimental formula that fits this theory is derived from previous data. (G.O.Y.)

36734 RANDOM ERRORS IN NEUTRON-ACTIVATION ANALYSIS. Rakovic, M.; Martincova, Z. (Charles Univ., Prague). Atompraxis, 12: 306-7(June 1966).

A general approach permitting the appraisal of the errors with which the various operations of neutron activation analysis are burdened is described. Results obtained experimentally are presented by means of an example of such an evaluation. (auth)

36735 DETERMINATION OF POTASSIUM IN BIOLOGICAL MATERIALS BY VARIOUS METHODS OF NEUTRON-ACTIVATION ANALYSIS. Rakovic, M.; Langerova, I.; Talpova, H. (Charles Univ., Prague). Atompraxis, 12: 344-6(July 1966).

Three methods for the determination of potassium in biological material by neutron activation analysis were investigated. Nondestructive methods, based on single or double filtration, proved to be unsuitable, whereas incineration of the material and separation of potassium in the form of $KClO_4$ lead to good results. (auth)

36736 BEHAVIOR OF POLONIUM EVAPORATED FROM FUSED SALT. Kamemoto, Yuichiro; Yamagishi, Shigeru (Japan Atomic Energy Research Inst., Tokyo). Bull. Chem. Soc. Jap., 39: 1160-3(June 1966).

Studies were made of the evaporation of polonium from a fused potassium chloride-lithium chloride mixture and of the deposition of the evaporated polonium on several metal plates under different temperatures. Approximately 100% of the polonium evaporates, probably as polonium tetrachloride, from the fused salt at the fused salt temperature higher than 500°C when heated for 3 hr in an argon atmosphere. The evaporated polonium was deposited on copper, platinum, palladium, and silver plates which were held over the fused salts. The relationship between the percentage of polonium evaporated from these metal plates and the temperature shows that the polonium deposits on these metal plates are elementary polonium or polonide. (auth)

36737 SENSITIVE GAS CHROMATOGRAPHY OF PARA-, ORTHOHYDROGEN, HYDROGEN DEUTERIDE AND DEUTERIUM. Yasumori, Iwao; Ohno, Seigo (Tokyo Inst. of Tech.). Bull. Chem. Soc. Jap., 39: 1302-6(June 1966).

A sensitive gas chromatograph of the reduced-pressure type was devised to analyze hydrogen nuclear spin isomers and isotopes, and its characteristics were studied in order to obtain the optimum conditions for analysis. It was found that the para and ortho composition of 0.01 ml S. T. P. of normal hydrogen could be determined within an accuracy of 1% by employing an alumina column cooled at −196°C, while the composition of 0.02 ml S. T. P. of the equilibrated mixture of hydrogen, hydrogen deuteride, and deuterium at 25°C could be determined within the same accuracy by employing an alumina column coated with manganese chloride. The alumina column was no longer capable of separating the spin isomers when it was treated above 350°C. Kinetic studies of the hydrogen-deuterium equilibration (21°C) and of the orthohydrogen conversion (−196°C), using the alumina as a catalyst, revealed that this strong activation creates active sites for the equilibration and the magnetic conversion which makes the peak separation obscure. The nature of these active centers is briefly discussed. (auth)

36738 SHEET SCINTILLATION COUNTING OF TRITIUM IN SURFACE FILMS. Muramatsu, Mitsuo; Tokunaga, Noboru (Tokyo Metropolitan Univ.). Bull. Chem. Soc. Jap., 39: 1331-3(June 1966).

An attempt was made to develop a scintillation method that does not require a flowing gas and where the space for the sample is not limited. The counting probe consisted mainly of a sheet of plastic scintillator and a photomultiplier tube. The effects of scintillator sheet and sample thickness on counting characteristics were studied. It was found that temperature dependence of the background is decreased markedly by a decrease in the applied voltage and by a narrowing of the window width. The method shows promise in determining the amount of a tritiated substance present in very thin layers at the air/water interface of any size sample. (J.G.B.)

36739 T-E_γ CHARTS OF SHORT-LIVED NUCLIDES FORMED BY NEUTRON ACTIVATION. Okada, Minoru (Government Chemical Industrial Research Inst., Tokyo). Bull. Chem. Soc. Jap., 39: 1340-1(June 1966).

Previously uncharted γ-active radionuclides of short half lives are presented for identification purposes. The half life, T, is plotted against the γ energy, E_γ. Nuclides from various types of nuclear reactions are included. (J.G.B.)

36740 PRELIMINARY STUDY OF THE DETERMINATION OF HYDROGEN CONTENT IN HEAVY WATER BY MEANS OF NEUTRON TRANSMISSION. Ono, Masayoshi; Kiso, Yoshiyuki (Kyoto Univ.). Bull. Chem. Soc. Jap., 39: 1594-5(July 1966).

The difference in total cross sections of thermal neutrons between light and heavy water was studied in relation to determining the hydrogen content in heavy water. Curves obtained by experiments and calculations based on the neutron linear attenuation formula were discussed. In high neutron flux, i.e., from nuclear reactors, this procedure promised high accuracy and rapidity. (P.C.S.)

36741 DETERMINATION OF OXYGEN IN ALUMINUM AND ZIRCONIUM BY IRRADIATION WITH ^{3}He IONS. Albert, Philippe; Deyris, Michele; Revel, Gilles (CNRS, Vitry-sur-Seine, France). Compt. Rend., Ser. C, 262: 1774-7(June 20, 1966). (In French).

During a study of the nuclear reactions of Al, Zr, Fe, Cu, Cr, and Mg produced by irradiation with ^{3}He ions, the conditions permitting the nondestructive analysis of O in Al and Zr were defined. (tr-auth)

36742 THORIUM-MELANOXETIN COMPLEX: A SPECTROPHOTOMETRIC STUDY. Katyal, M.; Prakash, S.; Singh, R. P.; Malik, K. K. (Univ. of Delhi). Curr. Sci. (India), 35: 388-9(Aug. 5, 1966).

The complex formation between thorium and melanoxetin (7,8,3′,4′-tetrahydroxyflavonol) is described. The complex was found to obey Beer's law from 0 to 7 ppm of thorium at pH 2.0. Sensitivity of the reaction was found to be 0.011 γ Th/cm^2 $\equiv \log I_0/I = 0.001$. The average value of the stability constant was calculated to be 4.8×10^3 at pH 2.0 and in 40% alcoholic medium. The ligand, though quite sensitive for thorium, can not be used for its determination without a prior separation of accompanying ions. (M.C.G.)

36743 AUTOMATIC COMPENSATION OF FLUORESCENCE EXTINGUISHING AND OTHER DISTURBING FACTORS, WHICH APPEAR IN THE SCINTILLATION COUNTING OF RADIOACTIVE SUBSTANCES IN SOLUTIONS. Jordan, P.; Kaczmar, U. (Technische Hochschule, Zurich). Experientia, 22: 482(1966). (In German).

A procedure is described, based on the use of an external γ or α source, that allows the automatic correction, up to a few tenths of a percent, of most perturbing factors impairing the liquid scintillation counting of ^{14}C and ^{3}H, such as spectrometer instability, chemical and color quenching, as well as turbidity effects. (auth)

36744 SODIUM DISTRIBUTION IN THERMAL OXIDE ON SILICON BY RADIOCHEMICAL AND MOS ANALYSIS. Yon, E.; Ko, W. H.; Kuper, A. B. (Case Inst. of Tech., Cleveland). IEEE (Inst. Elec. Electron. Eng.), Trans. Electron. Devices, 13: 276-80(Feb. 1966).

Direct comparison was made between Na distribution determined radiochemically and electrically in 6000 Å thermal oxide on 10Ω-cm n-type Si. Na within $\gtrsim$ 1000 Å of Si/SiO_2 interface correlates in most cases with MOS flat band voltage shift, i.e., $N_{Na}(\gtrsim 1000\ Å) \approx + \Delta Q_{MOS}$. Appreciable Na, which does not appear to affect Si surface potential, is found through the bulk of the oxide. Neutron activation of "clean" oxide (grown in wet or dry oxygen) showed ~1 ppm Na throughout, ~10 ppm at free surface. Gold was also identified at ppm concentrations but did not correlate with ΔQ_{MOS}. The U-shaped profile seen after diffusion (300 to 1000°C in dry N_2) or indrift (~200°C, 5×10^5V/cm) is believed due to rate limitation at the free surface; electrostatic binding plus enhanced solubility at the Si/SiO_2 interface. Time dependence was observed in diffusion at 500 and 800°C, which is not expected from the fast diffusion of Na. This is also attributed to the surface rate limitation. The anion significantly affects Na diffusion kinetics and distribution in contamination experiments with radiotracer ^{24}NaOH, ^{24}NaCl, and $^{24}Na^{82}Br$. Br is found to accompany Na diffusion, suggesting anion neutralization of Na within the bulk oxide. P_2O_5 SiO_2 is seen to "getter" Na from the oxide. These results support the suggestion of Snow et al. that Na is responsible for uncontrolled drift of surface potential in oxidized Si devices. (auth)

36745 POLAROGRAPHIC STUDIES ON URANIUM COMPOUNDS IN DIMETHYLFORMAMIDE AND DIMETHYLSULFOXIDE. Michlmayr, M.; Gritzner, G.; Gutmann, V. (Technische Hochschule, Vienna). Inorg. Nucl. Chem. Lett., 2: 227-31(Aug. 1966).

Polarographic behavior of uranium salts in dimethylformamide (DMF) and dimethyl sulfoxide (DMSO) was studied. DMF was found to be a suitable solvent for the polarographic analysis of U(IV), but DMSO was found superior to DMF if uranyl ions are studied. (D.H.M.)

36746 NONDESTRUCTIVE DETERMINATION OF NITROGEN IN DIAMOND BY PHOTOACTIVATION. Rocco,

G. G.; Garzon, Oro Lucy (Wentworth Inst., Boston). Int. J. Appl. Radiat. Isotop., 17: 433-40(Aug. 1966).

A photonuclear radioactivation technique is described for the non-destructive determination of total nitrogen in diamonds. Activation of ^{13}N is produced by the (γ,n) reaction on ^{14}N. The activating bremsstrahlung is produced from a linear accelerator. The bremsstrahlung flux distribution was determined by irradiating solid boron nitride (BN) cubes in a variety of well-defined positions. BN of approximately the same weight and shape of the sample diamonds was used as the standard. Corrections for the flux nonhomogeneity were applied. A curve of ^{13}N activity versus nitrogen content of known weighed amounts of BN, $NaNO_3$, and quinaldic acid confirmed the expected linear relationship. Three non-semiconducting type diamonds were found to contain total nitrogen in the range of 0.15–0.28 percent. If all adjustable parameters are optimized, then this method has an ultimate sensitivity, using the present instrumentation, of 0.2 ppM. (auth)

36747 LIQUID SCINTILLATION DETERMINATION OF ^{45}Ca AND ^{89}Sr IN UNICELLULAR ALGAE. Yarbrough, J. D.; Findeis, A. F.; O'Kelley, J. C. (Univ. of Alabama, University). Int. J. Appl. Radiat. Isotop., 17: 453-8(Aug. 1966).

A simple rapid procedure is described for determining ^{45}Ca and ^{89}Sr simultaneously in whole algal cells using a single-channel Packard Liquid Scintillation Spectrometer System, Model 314-F. The cells are dehydrated and decolorized with ethyl or methyl alcohol and dispersed in toluene containing PPO, dimethyl POPOP, and thixotropic gel (Cab-O-Sil). Counts are made with gain and tap settings adjusted for maximum detection of ^{45}Ca and again with settings for maximum ^{89}Sr detection. No detectable leaching of ^{45}Ca radioactivity was noted after cell dehydration, as evidenced by lack of activity in the alcohols after extraction. Counting of a graded series of cell suspensions revealed little internal quenching at algal concentrations of 63.0 mg/ml, but measurable quenching at 75.6 mg/ml. The Ca/Sr ratio within algal cells obtained using the cell dehydration–suspension procedure agreed with the Ca/Sr ratio obtained following oxidation of the algal cells to the inorganic state and counting the wet ash produced. (auth)

36748 SEPARATION OF ^{90}Sr AND ^{137}Cs FROM FISSION-PRODUCT SOLUTIONS BY ANION EXCHANGE PAPER CHROMATOGRAPHY. Hilton, D. A. (Central Electricity Generating Board, Berkeley, Eng.). Int. J. Appl. Radiat. Isotop., 17: 483-5(Aug. 1966).

Strontium-90 and cesium-137 were separated from nitric acid solutions of fission products by descending chromatography, using the hydroxide form of a weakly basic anion exchange paper (WB-2). The R_F values are 0.84 for cesium and 0.59 for strontium. From these separations, ^{90}Sr and ^{137}Cs can be determined by end window β-counting and γ-scintillation spectrometry, respectively. (J.G.B.)

36749 PREPARATION, PROPERTIES, AND USES OF KRYPTONATES IN CHEMICAL ANALYSES. Carden, Joan E. Isotop. Radiat. Technol., 3: 206-14; 228(Spring 1966).

^{85}Kr was stably incorporated into a wide variety of solids. These solid sources, termed Kryptonates, prepared by bombardment of solids with ionized krypton and by diffusion of krypton into solids at high temperature and pressure. Sources prepared by either method display essentially the same useful and unique properties. They are stable over extended periods of time at room temperature, and they are remarkably stable at elevated temperatures. The Kryptonates are sensitive to chemical disturbances at the surface, and such disturbances lead to proportional losses of ^{85}Kr. This property is the basis of the use of Kryptonates in chemical analyses. (auth)

36750 DETERMINATION OF CHROMIUM AND SOME OTHER ELEMENTS BY ANALYSIS OF THE γ SPECTRA FROM THE (n,γ) REACTION. Lobanov, E. M.; Aripov, G. (Inst. of Nuclear Physics, Academy of Sciences, Uzbek SSR). Izv. Akad. Nauk Uz. SSR, Ser. Fiz.-Mat. Nauk, No. 6, 64-7(Nov.-Dec. 1965). (In Russian).

Some preliminary experimental data are presented on a method for determinating chromium, which could be used for continuous monitoring of the chromium content in a chromium ore. A 2-g ore sample was irradiated in a reactor with neutrons at a flux of 107 $n/cm^2 \cdot sec$, but other sources could be used, e.g., a polonium–beryllium source, to supply the neutrons. The ore samples were irradiated in cylindrical polyethylene containers. Energies below 8.3 Mev, from sodium, silicon, iron, aluminum, and potassium, were filtered out with 5 mm of lead in front of the recorder. The remainder of the spectrum, which is due to chromium, was approximately a straight-line function of the chromium content. A scintillation spectrometer was used to measure the activity. With heavier samples, the neutron source activity may be decreased. (TTT)

36751 DETERMINATION OF IRIDIUM IN COPPER AND NICKEL MUDS AND PLATINUM CONCENTRATES BY NEUTRON ACTIVATION ANALYSIS USING COINCIDENCE SPECTROMETRY. Lobanov, E. M.; Khusnutdinov, R. I. (Inst. of Nuclear Physics, Academy of Sciences, Uzbek SSR). Izv. Akad. Nauk Uz. SSR, Ser. Fiz.-Mat. Nauk, No. 6, 72-6 (Nov.-Dec. 1965). (In Russian).

Iridium was determined in the muds and platinum concentrates from polymetallic ore processing by γ-γ coincidence measurements of the ^{192}Ir produced in 50 to 100 g of mud and in 10 mg of platinum concentrate by neutron irradiation in the reactor at a flux of 1.2×10^{12} $n/cm^2 \cdot sec$. The samples also contained gold, silver, copper, nickel, cobalt, iron, selenium, tellurium, and antimony. Of these, only selenium, as ^{75}Se, interfered with the approximately 300-kev ^{192}Ir peak under the conditions used. Calculation of the relative error from deviation of the results from average iridium contents determined 67 days after irradiation, when only ^{192}Ir remains, indicated that the results are satisfactory 7 to 12 days after irradiation. However, a clear coincidence spectrum was obtained even on the second and fourth day, indicating the possibility of determining iridium sooner if, for example, standards with similar iridium contents can be prepared. The sensitivity of the method depends on the background. (TTT)

36752 RADIOACTIVATION METHOD FOR DETERMINING POTASSIUM IN ROCKS USING MAGNETIC β SEPARATOR. Lobanov, E. M.; Abarov, U. (Inst. of Physics and Technology, Academy of Sciences, Uzbek SSR). Izv. Akad. Nauk Uz. SSR, Ser. Fiz.-Mat. Nauk, No. 1, 77-80(Jan.-Feb. 1966). (In Russian).

A method was developed for determining potassium with a simplified beta spectrometer, a "beta separator." With this equipment, electrons emitted by a sample pass through a vacuum chamber and are deflected by a magnetic field. Those with a certain energy are focused in an end-window counter at the chamber outlet. The impingement of electrons with the desired energy is controlled by regulating the current in a magnetic coil. The basic components of the system are a constant-current electromagnet and a vacuum chamber, which provides the vacuum necessary to decrease electron absorption and dispersion in the space between the equipment and detector and is between the poles of the magnet. For determining potassium in rocks, 50-mg samples in polyethylene containers were irradiated with thermal neutrons. For potassium contents between 0.1 and 0.01%, irradiation with a flux of 1.8×10^{12} $n/cm^2 \cdot sec$ for 2 hr and counting the ^{42}K after 24 hr decay gave a precision of 0.01%. About 5 min was then required for a determination. (TTT)

36753 THIN-LAYER CHROMATOGRAPHY OF INORGANIC IONS. Lesigang-Buchtela, Margrit (Univ., Vienna). Mikrochim. Acta, No. 3, 408-14(1966). (In German).

A description is given of the separation of the following mixtures on thin layers of cellulose powder or silica gel: Pb, Cd, Bi, Cu, and Hg or As, Sb, and Sn, also Ni, Co, Fe, Mn, Al, Cr, Zn, U. The mobile phase consisted especially

of mixtures of alcohols or ketones with dilute acids. Detection of the transported substances was by means of oxine or suitable spot test reagents. Excellent separations were obtained in 1 to 4 hours. (auth)

36754 CHELATE EXCHANGE ON THE BASIS OF 8-HYDROXYQUINOLINE AND ITS USE FOR ANALYTICAL SEPARATIONS. **Bernhard, H.; Grass, F. (Univ. Vienna). Mikrochim. Acta, No. 3, 426-46(1966). (In German).**

A chelate ion exchanger is described with 8-hydroxyquinoline as chelate-forming group. It was possible to obtain the exchange resin by direct condensation of metal chelates with resorcinol and furfuraldehyde, whereby the arrangement of the planar 8-hydroxyquinoline groups became dependent on the method of preparation. Al-oxinate (octahedral), Ba-oxinate (planarquadratic) and Na-oxinate were cross linked with the matrix in this way. The resins obtained showed good stability toward acids and alkaline solutions and could be used for separations on the column. A separation of Ru, Zr, U, and Ce was accomplished, in which carrier-free Ru-106, Zr-95, and Ce-144 were present. Furthermore a far-reaching separation of uranium from its fission products and neptunium is described. In addition, the stability against radiation of the exchange resins makes it likely that they may be employed for working up solutions that are highly radioactive. (auth)

36755 NEUTRON ACTIVATION ANALYSIS OF LUMINOPHORESCENT ZINC COMPOUNDS. PART I. INFLUENCE OF INTERFERING REACTIONS IN DETERMINATION OF Cu, Ni, Co, Fe, AND Mn IN $ZnSO_4$ AND ZnS. Pfrepper, G.; Koch, H. (Institut fuer Angewandte Radioaktivataet, Leipzig. (Deutsche Akademie der Wissenschaften, Berlin). Mikrochim. Acta, No. 3, 481-7(1966). (In German).

Interfering side reactions occur in the activation determination of Cu, Ni, Co, Fe, and Mn in $ZnSO_4$. The interference coefficients were determined experimentally and the analytical error evaluated. (auth)

36756 NEUTRON ACTIVATION ANALYSIS OF LUMINOPHORESCENT ZINC COMPOUNDS. PART II. DETERMINATION OF Cu AND Ni. **Pfrepper, G.; Koch, H. (Institut fuer Angewandte Radioaktivataet, Leipzig. Deutsche Akademie der Wissenschaften, Berlin). Mikrochim. Acta, No. 3, 488-94(1966). (In German).**

Preliminary accumulation of impurities in $ZnSO_4$ through the use of ion exchangers yield samples whose Cu- and Ni-content can be determined by activation analysis. The sensitivity of the determination is 10^{-5}% Ni and 10^{-6}% Cu. (auth)

36757 NEUTRON ACTIVATION ANALYSIS OF LUMINOPHORESCENT ZINC COMPOUNDS. PART III. DETERMINATION OF MANGANESE, IRON, AND COBALT. **Pfrepper, G.; Koch, H. (Institut fuer Angewandte Radioaktivitaet, Leipzig. Deutsche Akademie der Wissenschaften, Berlin). Mikrochim. Acta, No. 3, 495-500(1966). (In German).**

The comparison procedure with chemical processing of the samples was employed to determine Co, Fe, and Mn in zinc compounds free of luminophors by means of neutron activation methods. The separation was made by anion exchange chromatography on Dowex 1 (Cl^-) or Wof. SBW (Cl^-). The sensitivity of the method, at a neutron flow of 10^{12} n/sec cm^2, is 10^{-8}% Mn, 5×10^{-7}% Co, and 5×10^{-6}% Fe. The standard deviation of the individual results is about ±5%. (auth)

36758 DETERMINATION OF ^{137}Cs IN IRRADIATED URANIUM AND IRRADIATED THORIUM USING ANION-EXCHANGE PAPER AND THE RING OVEN TECHNIQUE. **Hilton, D. A.; Reed, D. (Berkeley Nuclear Labs., Gloucestershire, Eng.). Mikrochim. Acta, No. 3, 508-12 (1966).**

By using a strongly basic anion-exchange resin paper in the hydroxide or carbonate forms, cesium-137 was separated from irradiated uranium solutions on a ring oven. A ring oven separation of cesium-137 from irradiated thorium can also be achieved by using an oxalate-hydroxide form resin paper. In each case the cesium-137 was washed to the ring zone with water and determined by γ spectrometry. The coefficient of variation of the methods was less than 2 per cent. (auth)

36759 ION EXCHANGE METHOD OF ESTIMATING ^{90}Sr AND OTHER RADIONUCLIDES IN RAINWATER. Brenan, C.; Lovatt, J. H.; Smith, H. (United Kingdom Atomic Energy Authority, Annan, Scotland). Nature, 211: 68-9(July 2, 1966).

A method is described for collecting rain water that incorporates a method for separating ^{137}Cs from ^{90}Sr. The various components of the apparatus are separated at the end of each sampling period (1 month) and analyzed for ^{90}Sr. Gamma spectrometric analyses of the activity on column components showed that most of the ^{137}Cs is retained by an ammonium-12-molybdophosphate/asbestos pad in the apparatus, although in some cases part of it is retained by a particulate filter. However, if the ammonium-12-molybdophosphate stage were omitted, it seems reasonable to suggest that almost all the ^{90}Sr would be retained by the cation resin. In the circumstances the method would be specific for ^{90}Sr. (P.C.H.)

36760 ACTIVATION ANALYSIS OF TITANIUM IN IRON BY PHOTONUCLEAR REACTIONS. Abe, Shigeki (Yamagata Univ., Yonezawa, Japan). Nippon Kagaku Zasshi, 87: 710-14(July 1966). (In Japanese).

A method for nondestructive determination of titanium in iron oxide was developed. Titanium and iron oxides were irradiated for an hour with a 20-Mev bremsstrahlung generated from a linear electron accelerator. The γ spectrum of titanium showed prominent photopeaks at 0.16 and 0.51 Mev. Those photopeaks were attributed to ^{47}Sc($T_{\frac{1}{2}}$ = 3.43 day) and ^{45}Ti($T_{\frac{1}{2}}$ = 3.07 hr), which were produced by (γ,p) and (γ,n) reactions of titanium, respectively. With the iron, three photopeaks were observed at 0.85, 1.81, and 2.13 Mev. These were attributed to ^{56}Mn which was produced from ^{57}Fe by (γ,p) reaction, the half life of which was 2.58 hr. For the determination of titanium in iron oxide, the ^{56}Mn activity was used as an internal monitor for photon flux intensity. The activity ratios of ^{47}Sc, (0.16 Mev)/^{56}Mn, (0.85 Mev) at photopeaks vs the weight ratios of Ti/Fe were plotted for various synthetic samples and a linear relationship was obtained. Thus titanium in iron oxide was determined nondestructively to about 0.1%. (auth)

36761 MICROCHEMICAL DETECTION OF CESIUM USING ION-EXCHANGE RESIN PARTICLES. Murase, Takeo (Atomic Fuel Corp., Tokyo); Kakihana, Hidetake. Nippon Kagaku Zasshi, 87: 721-4(July 1966). (In Japanese).

Cation-exchange resin particles absorbing cesium ions showed a red coloration in potassium bismuth iodide solution because of the formation of red crystalline precipitate on the surface. This coloration was used for detection of small quantities of cesium. One or two drops of the neutral sample solution on the pot plate was adjusted to weakly basic with a few particles of strongly basic anion-exchange resin(OH form), and a particle of the strongly acidic cation-exchange resin(OH form) was added. Cesium ions were effectively absorbed by the particle of cation-exchange resin, which was then transferred to a drop of potassium bismuth solution in the glass plate. A red precipitate appears on the particle. The limit of detection is 1.2 μg, and the dilution limit is $1:5 \times 10^4$. A considerable amount of Na or K ions interfere with this confirmatory test and the limit of detection becomes 100 μg Cs/ml. (auth)

36762 AN AUTOMATED ANION-EXCHANGE METHOD FOR THE SELECTIVE SORPTION OF FIVE GROUPS OF TRACE ELEMENTS IN NEUTRON-IRRADIATED BIOLOGICAL MATERIAL. Samsahl, Knut (Aktiebolaget Atomenergi, Nykoeping, Sweden). Nukleonik, 8: 252-6(June 1966).

An anion-exchange method based on fast selective sorption steps from mixtures of sulfuric, hydrobromic, and hydrochloric acid solutions was developed for the separation of five different groups of radioactive trace elements in neutron-irradiated biological material. The separations

are performed automatically with a simple proportioning pump apparatus. The apparatus allows the exact adjustment of influent solutions to the series of ion-exchange columns. The practical application of the method is described in detail. The successful use of the method is practically independent on the level of ^{24}Na activity present in the samples. (auth)

36763 METHOD FOR PREPARING SPECIMENS SUITABLE FOR LIQUID SCINTILLATION COUNTING FROM ^{3}H-LABELED BIOLOGICAL MATERIAL BY MEANS OF COMBUSTION. Tsurufuji, Susumu; Takahashi, Jun (Tokyo Univ.). Radioisotopes (Tokyo), 14: 146-7(Mar. 1965). (In Japanese).

For combustion of samples for scintillation counting, about 20 mg of a mixture of 2–20 mg ^{3}H-labelled biological material and sucrose or filter paper and about 100 mg Ni_2O_3 are placed in a hard-glass tube about 25 cm long and 12 mm in inside diameter having wall thickness about 1.5 mm. One end of the tube is sealed and the other part is made into a tube of 5–6 cm in length and 10 mm in outside diameter. Residual pressure is evacuated to 5–10 mm mercury and the tube is sealed. The whole is heated at 450–500°C for 5 hrs with an electric furnace. After the furnace temperature has fallen to 120–150°C, about 20 cm of the tube length is drawn out of the furnace to allow it to cool. Then, the tube is taken out completely and again cooled with an acetone-dry ice mixture. The content in the tube is eluted with 18 ml of scintillator and is centrifuged at 3000 rpm for 2–3 min. The supernatant is used for liquid scintillation counting. The recovery obtainable by the method is 97.5% and the reproducibility is very satisfactory. (NSA of Japan)

36764 DETERMINATION OF ^{14}C AND ^{3}H BY LIQUID SCINTILLATION SPECTROMETER. VI. APPLICATION OF OXYGEN FLASK COMBUSTION TECHNIQUE TO DETERMINATION OF ^{14}C IN PLANT TISSUE. Kashida, Yoshihiko; Yamazaki, Mikio (National Inst. of Radiological Scisson, Chiba, Japan). Radioisotopes (Tokyo), 14: 331-4(July 1965). (In Japanese).

The use of the oxygen flask combustion technique for the destruction of organic tissues in the liquid scintillation spectrometric method for examining ^{14}C metabolism in plants is described. A 10 to 50-mg sample of plant tissues is burned in a platinum gauze box in a combustion flask (300 to 500 ml) with an electric ignitor. The carbon dioxide formed is collected by 10 ml of Hyamine–ethanol mixture with PPO and POPOP toluene solution. The β radiation is measured directly with a scintillation spectrometer. The data and some discussion on Orthodon japonicum benth et oliv. and Ipomaea batatas lam. are given. (NSA of Japan)

36765 X-RAY SPECTROANALYSIS USING A ^{147}Pm BETA SOURCE. Enomoto, S. (Japan Atomic Energy Research Inst., Tokyo); Tanemura, T. (Rigaku Denki Co., Tokyo). pp 97-105 of STI-PUB-112(Vol.1).

The capability of a device for x-ray spectroanalysis using a ^{147}Pm beta source is compared with that of a beta-excited x-ray source. Since precision of the x-ray spectroanalysis is determined by the background due to the matrix in the specimen rather than the background due to the element of interest, background intensities were observed for materials of different atomic numbers. Ratios of the intensity of K x rays from chromium, iron, and nickel to background in matrices of low and intermediate atomic numbers when bombarded by the beta source are higher than or comparable with those bombarded by the beta-excited x-ray source. These ratios are lower for the beta source in matrices of high atomic numbers. The ratios of the intensity of molybdenum K x rays to background excited by the beta source are lower than those excited by the beta-excited x-ray source except for very light matrices such as paraffin. (G.O.Y.)

36766 CONTINUOUS GAS ANALYSES BY MEANS OF X-RAY FLUORESCENCE. Stoeppler, M.; Wiesner, L.; Kuehn, W. (Isotopen-Studiengesellschaft, Kernforschungszentrum, Leopoldshafen, Ger.). pp 147-156 of STI-PUB-112(Vol.1).

A device for continuous gas analyses using x-ray fluorescence is described. The results of concentration measurements of SO_2, H_2S, and HCl as well as the intensity response of different targets are presented. (G.O.Y.)

36767 ADVANCES IN THE GAMMA-ABSORPTIOMETRIC DETERMINATION OF URANIUM AND PLUTONIUM IN SOLUTION. Whittaker, A.; Green, G.; Garnett, J. E. (United Kingdom Atomic Energy Authority, Windscale Works, Sellafield, Eng.). pp 271-99 of STI-PUB-112(Vol.1).

Light elements, such as hydrogen, nitrogen, and oxygen, give rise mainly to incoherent and coherent scattering of the gamma photons which are then lost from a narrow beam. Photoelectric absorption events, on the other hand, are comparatively rare. Hence, it is concluded that the use of a detection system subtending a solid angle of 4π steradians at the source ought to result in reduced light element interference. To confirm this, two experimental 4π gamma absorptiometers were built using ionization chambers with cylindrical and spherical geometry, respectively. A 40-mg ^{241}Am source, emitting 59.6-kev gamma rays, was used in each case. An appreciable reduction in nitric acid interference by a factor of up to 16 was observed, thus confirming the theory. Brief details of a single-beam gamma absorptiometer, which is used to measure and control the in-stream plutonium concentration of several large titanium evaporators in a nuclear fuel reprocessing plant, are given. (G.O.Y.)

36768 IONIZATION GAS ANALYSER. Czernecki, A. (Inst. for Nuclear Research, Warsaw). pp 301-16 of STI-PUB-112(Vol.1).

A 6-electrode ionization chamber irradiated by an active tritium β-source with titanium absorbers is used to measure the mobility of the gas filling the chamber. The chamber is polarized by a direct current of about 1000 v and by a sinusoidal oscillation generator with a frequency varying from a few to a few hundred cps. The current in this chamber at a set generator oscillation frequency depends solely on the number of ions with accurately determined mobility. The mobility is measured by determining the maximum ionization current depending on frequency. The nature of the dependence of current on frequency in a chamber constructed in this way makes it possible to carry out quantitative and qualitative analysis of the composition of the gas filling the chamber. (G.O.Y.)

36769 ON-LINE NUCLEAR ANALYSIS SYSTEM. Martin, T. C.; Hall, J. D.; Morgan, I. L. (Texas Nuclear Corp., Austin). pp 411-23 of STI-PUB-112 (Vol.1).

A closed-loop system for on-line continuous elemental measurements is described. The system is housed in a pilot plant facility that includes a variable speed coal-type conveyer belt, a 1000-ft^3 storage tank for solids such as coal, and the necessary screw conveyers to complete a closed loop system. A liquid loop system for continuous analysis of liquids will be installed also. Data are presented on the utilization of this system in the continuous measurement of Al, C, O, and Si in coal. Data obtained with the data analysis system reveal that the Compton subtraction techniques used in the data analysis system work satisfactorily and that these data agree very well with spectral data obtained at the same time with a multichannel analyzer. (G.O.Y.)

36770 THE ANALYSIS OF SULFURIC ACID SOLUTIONS USING THE METHOD OF BACKSCATTERED β RADIATIONS. Marcu, Gheorghe; Tolea, Florian. Stud. Univ. Babes-Bolyai, Ser. Chem., 11: No. 1, 7-14(1966). (In Rumanian).

Sulfuric acid solutions were analyzed using the method of backscattered β radiations. This method permits determination of the sulfuric acid concentration for solutions of 9 to 100% concentration with an error of +0.5%. For 1% sulfuric acid there are about 200 pulses/min, indicating a good efficiency for the method. This method also permits rapid determination of the density of sulfuric acid solutions

from 1.065 to 1.832. It is also suited for a continual control in the process of producing the sulfuric acid. (auth)

36771 INSTRUMENT COMPENSATION OF THE QUENCHING EFFECTS IN DETERMINATION OF ^{14}C AND ^{35}S. Kainz, Gerald; Wachberger, Eugen (Univ., Vienna). Z. Anal. Chem., 220: 15-20(1966). (In German).

After combustion of the organic sample a quenching effect is observed, due to several combustion products as NO_2, halogens, SO_2, and SO_3. Quenching of the combustion products in the determination of ^{14}C and ^{35}S was eliminated, if the high voltage of the data-photomultiplier was raised to a certain level (compensation point) and if the counting was performed in a window. The compensation point was calculated graphically by determining the counting rate of the pure absorbant and the absorbant plus the highest expected amount of combustion products. The relation between instrumental compensation and the energy spectrum of ^{14}C is elucidated. It was not possible to compensate quenching in the determination of tritium, because the energy spectrum of ^{3}H is influenced in a different way than the spectrum of ^{14}C and ^{35}S. (auth)

36772 CALIBRATION-CURVE-OBTAINED EMISSION SPECTROGRAPHIC ^{15}N DETERMINATION WITH THE Q24-ZEISS SPECTROGRAPH. Sommer, K.; Kick, H. (Univ., Bonn). Z. Anal. Chim., 220: 21-6(1966). (In German).

Spectrographic ^{15}N determination in the range from 0.38 to 20.0% was studied. The method can be used with normal spectrographic equipment. The relative isotopic abundance was determined by means of a calibration curve. The relative standard deviation of the isotope determinations was between 2.0 and 3.0%. (auth)

36773 ELECTROLYTIC SEPARATION OF LEAD FROM MICROQUANTITIES OF THORIUM AND URANIUM AND THEIR PHOTOMETRIC DETERMINATION. Starodubskaya, A. A.; Kovalenko, P. N.; Bagdasarov, K. N. (Rostov-on-Don State Univ., USSR). Zh. Anal. Khim., 21: 663-8(1966). (In Russian).

Conditions were studied for the electrolytic precipitation of lead on the cathode from solutions containing hydroxylamine hydrochloride and Complexone III. Lead can be electrolytically separated from thorium and uranium at the ratios of $Pb:Th = 120-800$, $Pb:UO_2 = 126-945$. An electrophotometric method was developed for determining lead, thorium, and uranium. Lead is separated electrolytically on the cathode, and thorium and uranium are determined photometrically. (auth)

36774 DETERMINATION OF MICROQUANTITIES OF URANIUM IN SOILS, ROCKS, AND MINERALS BY MEANS OF ARSENAZO III. Nemodruk, A. A.; Glukhova, L. P. Zh. Anal. Khim., 21: 688-93(1966). (In Russian).

A rapid photometric method was developed for determining small amounts of uranium in soils, rocks, and minerals using Arsenazo III. The method includes uranium extraction with tributyl phosphate from an aqueous solution at pH 1.0 in the presence of ammonium nitrate and Complexone III, then back extraction with a solution of Arsenazo III. The stripping solution is diluted with an equal volume of concentrated HNO_3, treated with urea, and its optical density is measured on a photoelectrocolorimeter using a red light filter. With 0.1- to 1-g samples the method permits determination of $1 \times 10^{-4}-1.5 \times 10^{-2}$% of uranium in soils, rocks, and minerals with a mean square error of ~10%. With 5-g samples the sensitivity of the method is $2 \cdot 10^{-5}$% of uranium. One determination (excluding decomposition of the sample) takes 45 to 50 min. (auth)

36775 PREPARATION OF IRIDIUM AND RHODIUM STANDARD SOLUTIONS FOR RADIOACTIVATION ANALYSIS BY ELECTROLYTIC DISSOLUTION WITH THE ALTERNATING CURRENT. Lobanov, E. M.; Khusnutdinov, R. I. (Inst. of Nuclear Physics, Tashkent). Zh. Anal. Khim., 21: 743-5(1966). (In Russian).

A method of electrolytic dissolution of metals with the alternate current was used for preparing standard iridium and rhodium solutions applied as reference solutions in activation analysis. Optimum conditions for dissolution were found with HCl and HNO_3 solutions used as electrolyte. The titer of a solution is found by the amount of metal dissolved in a definite electrolyte volume, which is determined by weighing electrodes before and after the dissolution. (auth)

36776 ANALYSIS OF MIXTURES OF OXIDES OF RARE EARTHS AND ALKALINE EARTHS. Nazarchuk, T. N.; Boremskaya, S. F. (Inst. of Problems in Material Studies, Kiev). Zh. Anal. Khim., 21: 745-7(1966). (In Russian).

A method was developed for the complexometric determination of rare earth and alkaline earth elements when they are present together (without their separation) using arsenazo as as indicator. The method was used for the analysis of a number of samples. A comparison was made of the results obtained by the method suggested with those of the gravimetric method. It was established that the accuracy and reproducibility of the suggested method are quite satisfactory. (auth)

36777 DYNAMIC MASS SPECTROMETERS. Blauth, Erich W. New York, Elsevier Publishing Co., 1966. 196p. $13.75.

Translated from Dynamische Massenspektrometer.

The classic static mass spectrometer is described briefly. A systematic and detailed description of the basic principles of dynamic mass spectrometers is then given. This is followed by a comprehensive review of actual dynamic spectrometers in which the different instruments are treated separately and reference is made to analogies to particle accelerators. (M.O.W.)

36778 ARSENAZO III. METODY FOTOMETRICHESKOGO OPREDELENIYA REDKIKH I AKTINIDNYKH ELEMENTOV. (Arsenazo III. Methods of Photometric Determination of Rare Earth and Actinide Elements). Savvin, S. B. Moscow, Atomizdat, 1966.

A brief review is given of the theoretical and practical aspects of Arsenazo III and its analogs used in determining U, Zr, Hf, Sc, La, rare earth elements, Pu, Np, Cm, Pa, Nb, Ba, Sr, and S. Topics covered include: complexing and color reactions; composition and structure of compounds; selectivity; and other properties of the Arsenazo-thoron group reagents. Most of the described methods were developed for a certain material; however, with some alterations they can be used for other types of materials. (R.V.J.)

36779 MASS SPECTROMETER. Noeller, Hans-Georg (to E. Leybold's Nachfolger). German Patent 1,219,255. June 16, 1966. Filed Oct. 9, 1962.

A mass spectrometer comprises in combination a cylindrical condenser, electric field, and a uniform magnetic field (the lines of force of which are parallel to the axis of symmetry of the condenser). The ions to be analyzed are generated in front of an entrance slit in the outer condenser electrode by means of electron bombardment, and the ion beam is directed on the axis of symmetry of the condenser. The beam axis is perpendicular to the axis of symmetry. Because of the force exerted by the magnetic field the ions follow a path around the central electrode of the condenser into the exit slit in the outer electrode. (Gmelin Inst.)

36780 IMPROVED ACCURACY IN DETERMINATION OF RADIONUCLIDE CONCENTRATIONS IN SOLUTIONS CONTAINING FAST-DECAYING ISOTOPES BY LEAST-SQUARES RESOLUTION OF THE GAMMA-RAY SPECTRA. Schonfeld, E. (Oak Ridge National Lab., Tenn.). 5p. of Modern Trends in Activation Analysis, Proceedings 1965 International Conference.

Two extensions to the least-squares resolution method, that improve the accuracy of the quantitative analysis of solutions containing several isotopes with short half life are described. (D.C.W.)

36781 HAIR INDIVIDUALIZATION STUDIES. Perkons, A. K.; Jervis, R. E. (Univ. of Toronto. Attorney-General's Lab., Toronto). 32p. (CONF-650405-26). ORAU. Gmelin, AED-CONF-65-040-37.

From International Conference on Modern Trends in Activation Analysis, College Station, Tex.

A large-scale activation analysis study of human hair individualization was carried by the Ontario Attorney General's Crime Laboratory in conjunction with the University of Toronto. The program was essentially completed and more than 1100 hair samples from over 750 different persons were analyzed by a routine instrumental neutron activation analysis procedure. The major findings from the large body of results obtained are presented and discussed, and the feasibility of individual hair matching is appraised. (auth)

36782 USE OF AN AUTOMATED SYSTEM INCLUDING A RADIOCHEMICAL STEP IN ACTIVATION ANALYSIS. Girardi, F.; Guzzi, G.; Pauly, J.; Pietra, R. (EURATOM, Ispra, Italy). 24p. (CONF-650405-23). ORAU. Gmelin, AED-CONF-65-040-36.

From International Conference on Modern Trends in Activation Analysis, College Station, Tex.

The problems related to setting up of a system for automation in activation analysis are discussed. It is hoped that a system, in which the task of the analyst will be the choice of the sequence of operation required and the actuation of the operations themselves will be the task of machines, will be devised. The problems related to the complete radiochemical separation are considered. The problem of constructing safe and reliable machines to do the separations is being solved. (D.H.M.)

36783 PLUTONIUM AND URANIUM MASS SPECTROMETRY MEASUREMENTS ON IRRADIATED FUELS. Chenouard, J.; Lucas, M.; Bir, R. (CEA, Paris). 26p. (CONF-650602-86). ORAU. Gmelin, AED-CONF-65-125-127.

From American Nuclear Society 11th Annual Meeting, Gatlinburg, Tenn.

Measurements on some samples of irradiated fuels were made, dealing with: the isotopic composition of the plutonium produced; the concentration of this plutonium in the fuel; the ^{235}U depletion; and the amount of ^{236}U produced. All measurements were made using mass spectrometry after extensive studies of analytical procedures and more particularly of an improved isotopic dilution method using a double tracer for the $^{238}U/^{239}Pu$ ratio determination. Measurement of isotopic composition of the plutonium is performed by surface ionization mass spectrometry. It was necessary to eliminate the greatest amount of uranium from the solution. The separation takes place on an ion exchange resin. The precision obtained for the 240/239 ratio is about 1%. Information on ^{235}U depletion is a relative value, therefore UF_6 mass spectrometry is often used. The precision obtained was about 0.05% for the depletions expressed as ratios of isotopic ratios. The ^{236}U concentration measurement could be done either on a solid mass spectrometer or on a UF_6 one. The precision obtained was about 2%. (D.H.M.)

Inorganic and Physical Chemistry

Refer also to abstracts 36850, 37176, 37179, 37243, and 38314.

36784 (AD-636054) CRYSTAL CHEMISTRY STUDIES. Fourth Quarterly Report, February 14–May 13, 1966. Roy, Rustum; McCarthy, G. J.; Muller, O.; White, W. B. (Pennsylvania State Univ., University Park. Materials Research Lab.). July 1966. Contract DA-28-043-AMC-01304(E). 50p. (ECOM-01304-4). CFSTI $2.00 cy, $0.50 mn.

The results of studies on preparation and characterization of $Sm_4(SiO_4)_3$ and complex rare earth oxides in the systems $Ln_2O_3-ReO_2$ are reported. $Sm_4(SiO_4)_3$ was identified by means of electron microprobe analysis and emission spectroscopy. Its powder pattern was indexed, with the aid of single crystal photographs on a hexagonal cell of parameters a = 9.497 and c = 6.949 Å. The formation and magnetic properties of compounds in $Ln_2O_3-ReO_2$ systems are discussed. (P.C.H.)

36785 (ORNL-P-2202) THE SOLUBILITIES OF HF AND DF IN MOLTEN FLUORIDES. Field, Paul E. (Virginia Polytechnic Inst., Blacksburg. Dept. of Chemistry); Shaffer, James H. (Oak Ridge National Lab., Tenn.). [1966]. Contract W-7405-eng-26. 17p. (CONF-660907-1). Dep. mn. CFSTI $1.00 cy, $0.50 mn.

From American Chemical Society Meeting, New York.

The solubilities of HF and DF in molten $LiF-BeF_2$ (66 to 34 mole %) were determined over the temperature range from 500 to 700°C and at solute gas pressures between 1 and 2 atm. Using previously established experimental methods, the solubilities of both gases were found to obey Henry's Law. The Henry's Law constants, K_H (10^{-4} moles HF/mole melt-atm) for HF and DF respectively at 500, 600, and 700°C were: 3.37 ± 0.13, 2.96 ± 0.07; 2.16 ± 0.05, 1.83 ± 0.03; and 1.51 ± 0.06, 1.25 ± 0.03; where the values given were obtained by a linear least squares fit of the experimental data as in K_H vs 1/T and the uncertainties are at the 95% confidence interval. The heats of solution, ΔH^s, obtained from the least squares evaluation were −5.98 ± 0.19 and −6.43 ± 0.15 kcal/mole for HF and DF, respectively. Comparison of ΔH^s for HF in this melt composition with those obtained previously in melts ranging from 54 to 89 mole % LiF in BeF_2 revealed linear dependence of ΔH^s on the mole fraction of LiF above and below 67% with a maximum at 67% LiF. Interpretation of the isotope effect was made by comparison of the difference in the entropies of solution between DF and HF with the difference in the calculated values of the entropies of the two gases at 600°C. (auth)

36786 (ORNL-TM-1558) INVESTIGATION OF DENITRATION OF HIGH-NITRATE PLUTONIA SOLS BY BAKING. Lloyd, M. H.; Kosiancic, Eugene J. (Oak Ridge National Lab., Tenn.). June 22, 1966. Contract W-7405-eng-26. 16p. Dep. mn. CFSTI $1.00 cy, $0.50 mn.

The denitration of high-nitrate plutonium(IV) polymer sols by baking to produce low-nitrate plutonia sols was investigated. A plutonia sol with a nitrate to plutonium ratio as low as 0.4 was obtained, and extrapolation of the data indicate that lower ratios should be obtained by further baking. Two temperatures were investigated and in both cases a linear plot of the data was obtained by assuming the reaction was second order with respect to residual nitrate concentration. Experimental rate constants were determined from the plots. Additional data are required to determine if the rate remains constant when baking to lower nitrate values. (auth)

36787 (YALE-2723(Vol.1)) BINARY PHASE DIAGRAMS OF HALIDE SALTS. Robertson, William D. (Yale Univ., New Haven, Conn. Hammond Lab.). June 13, 1966. Contract AT(30-1)-2723. 333p. Dep. mn. CFSTI $7.00 cy, $1.50 mn.

A compilation of available information on phase diagrams of halide salts is presented. A summary of information contained in 690 papers published from 1900 to 1964 is given in 337 binary phase diagrams. The scope is confined to the binary halide systems having either a common cation or common anion. All combinations of fluorides, chlorides, bromides, and iodides of metallic cations in Periodic Groups IA, IIA, IIIA, IVA, VA, and IB and IIB for which information is available on at least one phase boundary are included. All systems and tabulated data are arranged in alphabetical order of the conventional chemical notation. (M.C.G.)

36788 (YALE-2723(Vol.2)) BINARY PHASE DIAGRAMS OF HALIDE SALTS. Robertson, William D. (Yale Univ., New Haven, Conn. Hammond Lab.). June 13, 1966. Contract AT(30-1)-2723. 344p. Dep. mn. CFSTI $7.00 cy, $1.75 mn.

36789 PRECIPITATION AND HYDROLYSIS OF METALLIC IONS. II. STUDIES ON THE SOLUBILITY OF ZIRCONIUM HYDROXIDE IN DILUTE SOLUTIONS AND IN 1 M $NaClO_4$. Bilinski, Halka; Branica, Marko; Sillen, Lars Gunnar (Inst. Ruder Boskovic, Zagreb. Royal

Inst. of Tech., Stockholm). Acta Chem. Scand., 20: 853-61(1966).

The variation of the solubility of zirconium hydroxide with pH was studied in dilute solution at 20 and 40°C, and in 1M $NaClO_4$ at 20°C, using a tyndallometric method. The results are compared with the scanty and widely diverging literature data. The data could be fitted to a power series which indicated that complexes of charges 0, +1, and +4 predominate (in 1M $NaClO_4$). For dilute solutions, better agreement was obtained with equations with non-integral powers of h. (auth)

36790 CRYSTAL STRUCTURE OF $Nb_{12}O_{29}$(mon). Norin, Rolf (Chalmers Inst. of Tech., Goteborg. Univ. of Goteborg. Univ. of Stockholm). Acta Chem. Scand., 20: 871-80(1966).

The crystal structure of monoclinic $Nb_{12}O_{29}$ was studied using single crystal x-ray methods. The unit cell has the dimensions: a = (31.32 ± 0.05); b = (3.832 ± 0.006); c = (20.72 ± 0.04) Å; β = (112.93 ± 0.07)°; and V = (2290 ± 10) Å^3. It contains 4 formula units of $Nb_{12}O_{29}$. The structure proposed has the symmetry A2/a and may be described in terms of NbO_6-octahedra which share edges and corners to form an infinite three dimensional framework. (auth)

36791 HYDROTHERMAL PREPARATION OF SOME RARE EARTH TRIHYDROXIDES AND RARE EARTH OXIDE HYDROXIDES. Christensen, A. Noerlund (Univ. of Aarhus, Denmark). Acta Chem. Scand., 20: 896-9 (1966).

Hydrothermal methods were used to prepare the hydroxide oxides of dysprosium, erbium, holmium, and ytterbium. Microcrystals of the trihydroxides of cerium, dysprosium, erbium, holmium, terbium, and thulium were prepared using similar methods. Unit cell parameters were calculated from powder patterns using a Guinier camera of 114.6-mm diameter, giving good precision. The data were compared with results of others. (J.G.B.)

36792 INVESTIGATION OF THE CHEMICAL FORMS OF CARRIER-FREE ^{131}I BY PAPER ELECTROPHORESIS. Nagy, A. G. (Central Research Inst. for Physics, Budapest). Acta Chim. Acad. Sci. Hung., 48: 331-41(1966).

A method based on paper electrophoresis was developed for qualitative and quantitative determination of the chemical forms of carrier-free iodine isotopes of high specific activity. The chemical forms present in carrier-free ^{131}I preparations, and the chemical changes taking place in such preparations on the effect of various parameters, such as the pH, presence of oxygen, light, radiation, etc., were investigated. Results showed that the chemical behavior of iodine in solutions of ultramicro concentration differs from its normal reactions in macro concentration. Conditions were established under which the carrier-free ^{131}I isotope can be preserved in a defined chemical form during the storage period. (auth)

36793 PROCEDURE FOR THE CONTINUOUS RECORDING OF THE ISOTOPIC EXCHANGE BETWEEN SOLUTION AND SOLID PHASE. Sauerbeck, D. (Univ., Bonn). Atompraxis, 12: 341-4(July 1966). (In German).

For kinetic investigations on heterogeneous isotopic exchange between solids and solution the reaction curves have to be determined rather accurately. An apparatus is described that avoids the lack of precision when numerous separate samples must be run and counted. The device was designed especially for the treatment of very finely dispersed suspensions (e.g., soils). It makes it possible to withdraw small aliquots of the liquid from the suspension at frequent intervals, to record the radioactivity by integration, and to return them to the reaction vessel. (auth)

36794 COPRECIPITATION BEHAVIOR OF RARE EARTH ELEMENTS WITH CALCIUM OXALATE UPON PRECIPITATION FROM A HOMOGENEOUS SYSTEM. Matsui, Masakazu (Kyoto Univ.). Bull. Chem. Soc. Jap., 39: 1114-19(June 1966).

The effects of the pH value, concentration of organic acid, and several other variables upon the distribution coefficient were studied for the coprecipitation process of the calcium-lanthanide oxalate system. The logarithmic distribution law was followed in all cases of the coprecipitation of rare earth elements. Of the several variables studied which affected the logarithmic distribution coefficient, the most important were the pH value and the concentration of an organic acid. The coefficient decreased as the acid anion content increased. This can be attributed to the fact that the acid anion formed complex compounds with lanthanide and calcium. The distribution coefficients of several rare earth elements in producing the precipitate from a similar solution were closely related to their basicity or to the solubility of their oxalate salts. The order of the magnitude of the distribution coefficient was as follows: Lu > Y > Eu > Ce; this was in the reverse order of the basicity of rare earth elements or of the solubility of their oxalate salts. (auth)

36795 PHYSICOCHEMICAL PROPERTIES OF THORIUM FORMATES WITH DIFFERENT DEGREES OF HYDRATION. Claudel, Bernard; Mentzen, Bernard (Institut National des Sciences Appliquees, Lyon). Bull. Soc. Chim. France, No. 5, 1547-52(May 1966). (In French).

Conditions for the preparation of the trihydrate of thorium formate and the thorium formate anhydride are defined. Dehydration of the trihydrate produced a hydrate at $\frac{2}{3}$ H_2O, which constituted a distinct crystalline phase. It gave, with the two other salts and water vapor, monovariant equilibrium. The solubility of the trihydrate in different solvents is given. The ternary diagram water–formic acid–formate was established and the 3 salts were characterized by their x-ray-diffraction diagram. (tr-auth)

36796 INCORPORATION OF URANYL CATIONS IN CARBONATES DURING FORMATION. Lauffenburger, Ivan; Wey, Raymond (Ecole Superieure de Chimie, Mulhouse, France). Bull. Soc. Chim. France, No. 5, 1743-9 (May 1966). (In French).

Carbonates of Ca and Fe^{2+} were precipitated in the presence of uranyl complexed in the form of the anions $[UO_2(CO_3)_2(H_2O)_2]^{2-}$ and $[UO_2(CO_3)_3]^{4-}$. Analysis of the products showed that it is possible to make the UO_2^{2+} ions insoluble in these carbonates. Whether the precipitation conditions are favorable for the formation of calcite or aragonite, the presence of UO_2^{2+} cations always favors the formation of vaterite; however, the lattice of the siderite remains unchanged. (tr-auth)

36797 INCORPORATION OF URANYL CATIONS IN SILICATES DURING FORMATION. Lauffenburger, Ivan; Siffert, Bernard; Wey, Raymond (Ecole Superieure de Chimie, Mulhouse, France). Bull. Soc. Chim. France, No. 5, 1749-53(May 1966). (In French).

The possibility of making uranyl cations insoluble in a silicate during formation was studied. A saturated solution in silica monomer containing magnesium chloride, uranyl nitrate, and ammonium carbonate evolved at room temperature. The ammonium carbonate complexed the uranium in solution in the form of the anions $[UO_2(CO_3)_2(H_2O)_2]^{2-}$ and $[UO_2(CO_3)_3]^{4-}$. The medium was made alkaline by the addition of ammonia. Either a magnesium silicate of the sepiolite type or a uranium silicate of the boltwoodite type was precipitated according to the conditions. (tr-auth)

36798 PREPARATION OF PROTACTINIUM PENTACHLORIDE AND OBSERVATIONS ON THE ABSORPTION SPECTRA IN THE ULTRAVIOLET AND THE VISIBLE OF THE COMPOUND IN CERTAIN MEDIA. Pissot, Anne-Marie; Muxart, Roland; Ferreira de Miranda, Carlos (Institut de Physique Nucleaire, Arcueil, France). Bull. Soc. Chim. France, No. 5, 1757-60(May 1966). (In French).

A method for preparation of protactinium pentachloride, with good yield and under excellent safety conditions, is described. The absorption spectra in the ultraviolet and the visible regions of the halogenide dissolved in methanol, carbon tetrachloride, and hydrochloric acid 11M were obtained. The effect of aging was examined. (tr-auth)

36799 CESIUM–GRAPHITE SORPTION ISOTHERMS DETERMINED BY A STATIC METHOD. Milstead, C. E.; Riedinger, A. B.; Zumwalt, L. R. (General Atomic Div., General Dynamics Corp., San Diego, Calif.). Contract AT(04-3)-167. Carbon, 4: 99-106(May 1966). (GA–6415; CONF-650632–1).

The sorption of Cs by nuclear-grade graphite at 800 to 1100°C and at partial pressures of 1×10^{-8} to 7×10^{-3} atm has been determined by static method. Approximately 0.5 g of graphite, having a known BET surface area, is placed in the horizontal leg of a pyrex-stainless steel, L-shaped, evacuated tube, and Cs metal tagged with ^{137}Cs is distilled into the other leg. The entire system is thoroughly outgassed and sealed off at a pressure of $\sim 10^{-5}$ mm Hg. During a run the Cs pressure is fixed by maintaining the Cs metal source at a constant temperature. The amount of Cs on the graphite specimen is monitored with a calibrated gamma scintillation counter until an equilibrium condition has been established at the desired specimen temperature and Cs pressure. The data obtained indicate chemisorption at concentrations below that corresponding to a monolayer of coverage of internal (BET) surface area. Under these conditions, the Cs pressure was found to be proportional to the Cs concentration to the nth power, where n is approximately 3 to 6, depending on temperature. Isosteric heats of sorption are of the order of 40 to 90 kcal/mole, depending on concentration. More complex isotherms and less strong sorption are found for concentrations corresponding to greater than a monolayer of coverage. (auth)

36800 SORPTION OF SMALL AMOUNTS OF RADIOIODINE AS IODIDE ANIONS ON HYDRATED FERRIC OXIDE CONTAINING SILVER. Kepak, F. (Inst. of Nuclear Research, Rez, Czech.). Collect. Czech. Chem. Commun., 31: 1493-1500(Apr. 1966).

The sorption of the radioisotope ^{131}I as the iodide anion from the aqueous phase on hydrated ferric oxide containing 1% silver was studied. The dependence of sorption on the pH of the medium and the effects of surface active substance, of temperature, and other factors on the sorption equilibrium were studied in order to determine the suitability of a sorbent for the removal of radioiodine from aqueous solutions. Addition of silver increased the sorption efficiency of ferric oxide, high values of the distribution coefficient were attained and a sorbent activated in this way showed properties suitable for the decontamination of radioactive waters from ^{131}I. (auth)

36801 EFFECT OF SOME PREPARATION CONDITIONS ON THE SURFACE AREA AND STRUCTURE OF AMMONIUM POLYURANATE. Jakes, D.; Landspersky, H.; Sedlakova, L.; Sulc, J. (Inst. of Nuclear Research, Rez, Czech.). Collect. Czech. Chem. Commun., 31: 1677-84(Apr. 1966).

The relationship between the preparation conditions of ammonium polyuranate used on the technological scale, the changes in the surface area, structure, and composition of the precipitate were investigated. Two maxima of the surface area of the precipitates were observed at pH 5 or 7 to 8. All four structural types reported in literature were found and their dependence on pH was determined at the technologically used concentration of the solution. The possibilities of correlating the composition, structure, and surface area of ammonium polyuranate are discussed. (auth)

36802 EQUILIBRIUM ULTRACENTRIFUGATION OF HYDROLYZED THORIUM(IV) SOLUTIONS. Hentz, Forrest C. Jr.; Johnson, James S. (Oak Ridge National Lab., Tenn.). Inorg. Chem., 5: 1337-44(Aug. 1966). (ORNL-P–1979).

The hydrolytic aggregation of Th(IV) in 1 M total perchlorate media was investigated by equilibrium ultracentrifugation (interference optics) from hydroxyl number n (hydroxyls bound per thorium) of 0–3. Concentrations of Th(IV) were 0.025–0.1 M over most of the range. The solutions appeared to reach chemical equilibrium up through n = 2.5. All hydrolyzed solutions contained polymeric species, and the weight-average degree of polymerization, N_w, increased with degree of hydrolysis. Comparison of centrifugations at the same n but different thorium(IV) concentrations indicated that the charge per monomer unit z' on the polymeric species was not the maximum, 4–n, i.e., that there was some complexing of perchlorate ions by the polymers. At n = 2, for example, N_w was about 3.6 and z' appeared to be about 1.3, instead of the maximum 2. For n = 3, chemical equilibrium was not attained, and molecular weights were much higher and increased with time. Hydrolyzed thorium(IV) chloride solutions did not reach chemical equilibrium and, if aged for a few weeks, contained much more highly aggregated species than perchlorate solutions of the same degree of hydrolysis. Volumes and refractive index increments of hydrolyzed thorium(IV) perchlorate solutes are presented. Approximate molecular weight determinations of some highly aggregated Th(IV) dispersions are described. (auth)

36803 REACTIVITY OF TRANSITION METAL FLUORIDES. II. URANIUM HEXAFLUORIDE. O'Donnell, T. A.; Stewart, D. F.; Wilson, P. (Univ. of Melbourne). Inorg. Chem., 5: 1438-41(Aug. 1966).

Reactions were studied between uranium hexafluoride and a series of lower fluorides of other elements. The study included reactions with a wide range of covalent chlorides. The reactivity of uranium hexafluoride is compared with that of the higher fluorides of d-transition elements, chromium, molybdenum, and tungsten, and considered in the light of uranium as an f-transition element. (auth)

36804 REACTIVITY OF TRANSITION METAL FLUORIDES. III. HIGHER FLUORIDES OF VANADIUM, NIOBIUM, AND TANTALUM. Canterford, J. H.; O'Donnell, T. A. (Univ. of Melbourne). Inorg. Chem., 5: 1442-6 (Aug. 1966).

A series of oxidation–reduction and halogen-exchange reactions was used to compare the chemical reactivities of the pentafluorides of vanadium, niobium, and tantalum. Vanadium pentafluoride is extremely reactive and its reaction pattern with many reagents is extremely complex, depending largely on relative proportions of reagents and other experimental conditions. The pentafluorides of niobium and tantalum are very much less reactive than that of vanadium and are similar to each other. There is some evidence that of the two, the niobium compound is slightly more reactive. The reactivities of these three pentafluorides are discussed in terms of their physical properties and in relation to the higher fluorides of neighboring transition elements. (auth)

36805 ATOMIC PARAMETERS IN THE LANTHANUM TRIFLUORIDE STRUCTURE. Zalkin, Allan; Templeton, David H.; Hopkins, Ted E. (Univ. of California, Berkeley). Inorg. Chem., 5: 1466-8(Aug. 1966). (UCRL–16752).

The structure of synthetic lanthanum trifluoride crystals was determined to be trigonal. Each lanthanum atom is on a twofold axis and has nine neighbors at nearly equal distances. Final positional and thermal parameters are presented. (J.G.B.)

36806 REACTION OF OH RADICALS WITH NUCLEIC ACID BASES: AN ESR STUDY. Ormerod, M. G.; Singh, B. B. (Royal Military Coll. of Science, Swindon, Eng.). Int. J. Radiat. Biol., 10: 533-8(July 15, 1966).

The reactions of OH radicals with nucleic acid bases were studied in aqueous solutions at pH 1 using ESR spectroscopy. It was found that the pyrimidine bases were more reactive than the purines and free radical products could only be detected in the pyrimidines. In thymine, cytosine, and uracil, the OH radical added to the 5, 6 double bond. This confirms the conclusions of previous radiation chemical studies by others. (auth)

36807 INFRARED ABSORPTION SPECTRA OF CHROMITES OF RARE EARTH ELEMENTS. Matveichuk, V. T.; Shevchenko, A. V.; Skripchenko, N. V. (Inst. of Material Science Problems, Academy of Sciences, Ukrainian SSR). Izv. Akad. Nauk SSSR, Neorg. Mater., 2: 514-16 (1966). (In Russian).

The ir absorption spectra of 13 chromites of rare earth elements were taken. Chromite samples were prepared by two techniques. Single crystals were grown from a melt containing PbO + PbF_2 mixed solvent, the melt was held at 1360°C for 4 hours and then the melt temperature was reduced from 1360°C to 1000°C at a rate of 10 to 30°C per hour. Using the second method, mixtures of chromium oxide were fused with rare earth oxides at 2000°C for 15 minutes in an argon atmosphere. Individual chromite phases were examined by petrographic and x-ray analyses and the chromite compositions were confirmed by chemical analysis. The ir spectra of chromites of the cerium subgroup elements are presented. The ir spectra of chromites of the yttrium subgroup elements are also presented. It was found that chromites of the rare earth elements give a characteristic absorption band at about 600 cm^{-1}, which is connected with valence vibration of the Cr–O bond. The chromites of the cerium subgroup elements have a second band in the 430 to 480 cm^{-1} range. Due to imperfections in the crystal lattice, the second band of the chromites of the yttrium subgroup elements is split into either a doublet or a triplet, or a quadruplet. A linear relation was established between the wave number of the second band and the ionic radii of the rare earth elements contained in the chromites. (ATD)

36808 HIGH-TEMPERATURE CHEMISTRY OF CERIUM IN Al_2O_3, Cr_2O_3, AND Ga_2O_3 WITH CERIUM OXIDE. Leonov, A. I.; Andreeva, A. B.; Shvaiko-Shvaikovskii, V. E.; Keler, E. K. (Inst. of Silicate Chemistry, Academy of Sciences, SSSR). Izv. Akad. Nauk SSSR, Neorg. Mater., 2: 517-23(1966). (In Russian).

The effect of temperature (up to 2600°C) on structural properties of mixed oxide systems composed of CeO_2 and Al_2O_3, Cr_2O_3, or Ga_2O_3 was studied in air and hydrogen atmospheres. The phase relationships in the Ce_2O_3–Al_2O_3 system are shown. The phase relationships in Ce_2O_3–Cr_2O_3 systems are also shown. It was found that CeO_2 does not form chemical compounds with oxides of Al, Cr, and Ga. Above 1650°C in air, mixtures of oxides (e. g., Ce_2O_3–Al_2O_3, Ce_2O_3–Cr_2O_3, and Cl_2O_3–Ga_2O_3) form perovskite-type compounds ($CeAlO_3$, $CeCrO_3$, and $CeGaO_3$) admixed with the corresponding starting oxides. Pure $CeAlO_3$ and $CeCrO_3$ were obtained in a reducing atmosphere. Pure cerium gallite was synthesized by fusing a mixture of CeO_2 with Ga_2O_3 and metallic Ga in a sealed evacuated ampul. $CeAlO_3$ and $Ce_2O_3 \cdot 11Al_2O_3$ form in the Ce_2O_3–Al_2O_3 system. Only one compound with a 1:1 ratio is formed in each of the Ce_2O_3–Cr_2O_3 and Ce_2O_3–Ga_2O_3 systems. (ATD)

36809 THERMODIFFUSIVE INTERACTION OF TANTALUM AND BORON CARBIDE POWDER IN A VACUUM. Meerson, G. A.; Fekhretdinov, F. A.; Kopeikin, V. A.; Medvedev, A. A.; Moiseitseva, Z. K. Izv. Akad. Nauk SSSR, Neorg. Mater., 2: 604-7(Apr. 1966). (In Russian).

The object of the study was to determine the phase composition and arrangement of layers on Ta obtained by thermal diffusion in boron carbide at 1200 to 1700°C in a vacuum of 3×10^{-4} mm Hg. The phase composition and structure of the coatings on Ta were analyzed by x-ray diffraction and microscopic examination. Diffusion coatings consisting of TaB_2, TaB, and Ta_2B up to 4μ thick were found on the surface of the samples at 1200, 1300, and 1400°C. After treatment at 1500, 1600, and 1700°C, the powder patterns show strong lines of TaC, and faint lines of TaB_2 and Ta_3B_4, and indicating that TaC is the main phase in the reflecting layer. A faint line corresponding to the strongest line of Ta_2B also appears. At these higher temperatures, the thickness of the coating increases to 32μ. (auth)

36810 STUDY OF THE CONVERSION OF ZIRCONIUM DODECABORIDE INTO ZIRCONIUM DIBORIDE. Kislyi, P. S.; Kuzenkova, M. A. (Inst. of Materials Science Problems, Academy of Sciences, Ukrainian SSR). Izv. Akad. Nauk SSSR, Neorg. Mater., 2: 617-25(Apr. 1966). (In Russian).

The conversion of ZrB_{12} into ZrB_2 was studied by dilatometric, thermographic, and microstructural methods. It was shown that during heating, ZrB_{12} converts to ZrB_2 at 1530 to 1650°C. The transformation is associated with a decrease in volume, evolution of heat, and increase of porosity. The kinetics of the transformation are determined by diffusion processes. The generation of centers of the new phase is indicated by the volume of the matrix at the site of micropores and by other defects. The diboride formed accretes coherently around the primary grain of diboride increasing its size. Pores are formed in place of the dodecaboride grains. The coefficient of linear expansion of ZrB_{12} was found to be 28×10^{-6} deg^{-1} at 1600 to 2200°C. (auth)

36811 PHYSICAL PROPERTIES OF CERTAIN RARE EARTH DICARBIDES. Paderno, Yu. B.; Yupko, V. L.; Rud, B. M.; Makarenko, G. N. (Inst. of Materials Science Problems, Academy of Sciences, Ukrainian SSR). Izv. Akad. Nauk SSSR, Neorg. Mater., 2: 626-9(Apr. 1966). (In Russian).

The temperature dependence of the electrical resistance at 20 to 1300°C, the thermoelectric emf coefficient, the Hall coefficient at room temperature, and the melting point were measured on the same samples of Y, La, Ce, Pr, and Nd dicarbides. From these measurements, the charge carrier concentrations and mobilities were calculated. An anomalous temperature dependence of the electrical resistance was observed at about 1000°C. The high effective carrier concentration in CeC_2 as compared with the other dicarbides studied is explained on the basis of the electronic structure of the rare earth atoms and the magnetic susceptibility of the dicarbides. The low effective carrier concentration in the case of YC_2 is due to a change in bond character in the C_2 complex, this being supported by data on the hydrolysis of YC_2. (auth)

36812 PHASE TRANSFORMATIONS OF CERTAIN RARE EARTH CHROMITES. Pavlikov, V. N.; Lopato, L. M.; Tresvyatskii, S. G. (Inst. of Materials Science Problems, Academy of Sciences, Ukrainian SSR). Izv. Akad. Nauk SSSR, Neorg. Mater., 2: 679-82(Apr. 1966). (In Russian).

Phase transformations were studied by differential thermal analysis, dilatometric measurements, high-temperature microscopy, and high-temperature x-ray analysis in binary systems formed by chromium oxide reactions with the rare earth oxides, La_2O_3, Pr_2O_3, Nd_2O_3, Sm_2O_3, and Y_2O_3. $LaCrO_3$ was found to have a reversible endothermic transformation at 290 ± 5°C, associated with a change from a rhombic to an orthorhombic structure. This is confirmed by the conservation of anisotropy of high-temperature $LaCrO_3$ single crystals. The effects associated with the transformation of $LaCrO_3$ are slight. No polymorphic transformations were noted at 20 to 900°C in Pr, Nd, Sm, and Y chromites. However, the possibility of polymorphic transformations at higher temperatures is not excluded. (auth)

36813 STRUCTURE OF GLASSES OF THE Na_2O–B_2O_3 SYSTEM ACTIVATED WITH RARE EARTHS. EUROPIUM. Denisov, Yu. V.; Dzhurinskii, B. F.; Kizel, V. A. (Moscow Inst. of Physics and Tech. Kurnakov Inst. of General and Inorganic Chemistry, Academy of Sciences, USSR). Izv. Akad. Nauk SSSR, Neorg. Mater., 2: 693-701(Apr. 1966). (In Russian).

The emission and absorption spectra of glasses of the Na_2O–B_2O_3–Eu_2O_3 system (prepared from Na_2CO_3, H_3BO_3, and Eu_2O_3) were studied at room and liquid N temperatures using apparatus of high dispersion and sensitivity. The absorption spectra undergo little change with temperature. The form of the luminescence spectra depends on the frequency of the exciting light, not on the Eu concentration. It is postulated that two types of luminescence centers of unlike coordination exist. The duration of luminescence was measured for certain lines. As the Na_2O content rises, the transfer of energy to the lattice increases. The strongest interactions between an Eu^{3+} ion and its surroundings take place at the highest and the lowest Na_2O content, at which the homogeneity of the field around the ion is greatest. The asymmetry of the field increases with the Na_2O content. (auth)

36814 GROWING OF BERYLLIUM OXIDE SINGLE CRYSTALS. GROWING CRYSTALS FROM THE GAS-VAPOR PHASE. Budnikov, P. P.; Kushakovskii, V. I.; Sandulov, D. B.; Butra, F. P. (Mendeleev Chemical Engineering Inst., Moscow). Izv. Akad. Nauk SSSR, Neorg. Mater., 2: 829-32(May 1966). (In Russian).

BeO single crystals were grown by the vaporization-condensation method in a stream of moist air at 1400 to 1600°C. The crystals had various forms (prisms, whiskers, plates). X-ray analysis revealed that the direction of growth of prismatic and filamentary crystals coincided with the direction of the crystallographic axis c. High-temperature thermal tests showed that single crystals heated up to 1970, 2000, and 2100°C retained their form and transparency. X-ray diffraction showed that crystals heated to 2200°C lost their transparency and cracked owing to the presence of discrete disoriented blocks in place of the single crystal. Crystallization of fused beryllium oxide from 2450 to 2500°C produced coarse (2 × 2 × 2 mm), transparent grains, which x-ray-diffraction data identified as pseudocrystals. The disorientation of the blocks in the crystals was apparently due to polymorphic transformation of beryllium oxide taking place during cooling of the single crystals. (ATD)

36815 EFFECT OF EUROPIUM OXIDE ADMIXTURES ON THE POLYMORPHISM OF ZIRCONIUM DIOXIDE. Davtyan, I. A.; Glushkova, V. B.; Keler, E. K. (Grebenshchikov Inst. of Silicate Chemistry, Academy of Sciences, USSR). Izv. Akad. Nauk SSSR, Neorg. Mater., 2: 890-5 (May 1966). (In Russian).

The $ZrO_2-Eu_2O_3$ system was studied by using thermal and x-ray analysis. Addition of Eu_2O_3 was found to lower the temperature of the monoclinic–tetragonal transition of ZrO_2 considerably. Crystallization of mixtures of Eu_2O_3 and ZrO_2, coprecipitated in the amorphous state, formed metastable cubic solid solutions of europium oxide and zirconium dioxide. The crystallization temperature and lattice parameter of the cubic solid solution increased with rising Eu_2O_3 content. The decomposition of the metastable solid solution into stable phases was investigated. The minimum addition of europium oxide required for the complete stabilization of ZrO_2 was 7 mole % Eu_2O_3. The addition of only 2% Eu_2O_3 eliminated the cracking of ZrO_2 during heating. A phase diagram was plotted for the phase transitions in the $ZrO_2-Eu_2O_3$ system for the region rich in zirconium dioxide. (ATD)

36816 MOESSBAUER-EFFECT STUDIES OF WEAK NUCLEAR QUADRUPOLE INTERACTIONS IN ^{119}Sn. Stoeckler, Hans A.; Sano, Hirotoshi; Herber, Rolfe H. (Rutgers-The State Univ. of New Jersey, New Brunswick). J. Chem. Phys., 45: 1182-9(Aug. 15, 1966).

Nuclear quadrupole interaction in some tin compounds was investigated by the use of the Moessbauer effect. Stannic oxide showed a partially resolvable quadrupole splitting of 0.49 ± 0.06 mm/sec at 1 atm pressure. The origin of the nuclear quadrupole interaction is attributed to the characteristic rutile crystal structure in SnO_2. The absence of resolvable quadrupole splitting in stannic bromide and diphenyltin indicated that interpretations concerning the electric field gradient tensor based on the Moessbauer effect in ^{119}Sn alone are not always sufficient to warrant definitive conclusions about molecular structures. It was shown that this restriction is largely due to the relatively broad total natural linewidth for ^{119}Sn, $I = 3/2+$. Quadrupole-splitting and isomer-shift data for some phthalocyaninotin complexes indicated that simple correlations between chemical parameters, e.g., electronegativities, and Moessbauer parameters are not generally valid. (auth)

36817 MOESSBAUER EFFECT IN $MnFeO_3$. Banks, E. (Polytechnic Inst. of Brooklyn); Kostiner, E.; Wertheim, G. K. J. Chem. Phys., 45: 1189-91(Aug. 15, 1966).

The Moessbauer spectrum of $MnFeO_3$ was measured at 4.2, 78, and 300°K. At 300°K the spectrum consists of two overlapping sets of resonances with isomer shifts of +0.496 and +0.478 mm/sec and quadrupole splittings of 1.161 and 0.666 mm/sec, respectively. At 4.2°K the isomer shift increases to +0.61 mm/sec and a magnetic hyperfine splitting, corresponding to an effective field of 469 kOe, is observed. The distribution of Fe^{3+} ions over the available cation positions was determined from an analysis of the resonance curves. (auth)

36818 LOW-PRESSURE STUDY OF HETEROGENEOUS HYDROGEN–DEUTERIUM EXCHANGE AT STEADY STATE. Bergsnov-Hansen, Bjorn; Pasternak, R. A. (Stanford Research Inst., Menlo Park, Calif.). J. Chem. Phys., 45: 1199-1204(Aug. 15, 1966).

The hydrogen-deuterium exchange reaction on a clean molybdenum filament was investigated at pressures of 10^{-4} to 10^{-5} torr and temperatures of 25 to 800°C; a steady-state approach was employed, and the exchange rates were measured with a mass spectrometer. The adsorption step was found to be rate determining and characterized by pressure independent total sticking probabilities of about 0.4 at temperature above 200°C, declining to 0.2 at 25°C; the sticking probabilities were identical for the three hydrogen species. The net rates of adsorption and the saturation coverages at 25°C measured for hydrogen and for deuterium showed also that the surface cannot distinguish between the hydrogen species. Both the high value and the pressure independence of the sticking probability indicated that at either temperature, exchange occurs in adsorption states of low population. Surface coverage is immeasurably small at high temperatures. However, since at 25°C the total surface coverage is of the magnitude of a monolayer, exchange apparently involves adsorption states of low coverage, which may be identified with low-energy states observed previously in flash-filament studies. (auth)

36819 IONIZATION OF MOLECULES AT LOW ENERGIES. Berry, R. Stephen (Univ. of Chicago). J. Chem. Phys., 45: 1228-45(Aug. 15, 1966).

A general formal theory was developed for the autoionization of molecules at energies within a few electron volts or less of threshold, specifically to include effects of the interaction of an excited Rydberg electron with the rotating, vibrating molecule–ion to which it is bound. The dominant coupling mechanism involves conversion of vibrational energy to electronic energy and is most efficient when the core can undergo a single quantum jump. A number of simplifications and approximations are discussed. Some of these are used in an application of the theory to the autoionization of H_2. Autoionization rates are computed for a number of vibronic Rydberg states of this molecule, and are consistent with the available data. Model calculations for heteronuclear diatomics are presented to show how the presence of a vibrating dipole in the molecular core enhances the rates of autoionization, in comparison with rates in homonuclear diatomics where vibrating quadrupoles stimulate the process. Several experiments are suggested, particularly the measurement of the angular distributions of electrons detached from heteronuclear diatomics. (auth)

36820 VIBRATIONAL RELAXATION IN CO–D_2 MIXTURES. White, Donald R. (General Electric Research and Development Center, Schenectady, N. Y.). J. Chem. Phys., 45: 1257-8(Aug. 15, 1966).

The vibrational relaxation of 0.1 D_2 + 0.9 CO was observed in a shock tube by means of optical interferometry and infrared photometry. From 940 to 1600°K deuterium and helium were found to be equally effective collision partners for the vibrational excitation of carbon monoxide. From 1600 to 2800°K the data suggest that vibrational exchange from the more rapidly excited D_2 contributes to the excitation of CO. (auth)

36821 MOTIONS OF WATER MOLECULES IN POTASSIUM FERROCYANIDE TRIHYDRATE, WATER, AND ICE: A NEUTRON SCATTERING STUDY. Rush, J. J. (Argonne National Lab., Ill. National Bureau of Standards, Washington, D. C.); Leung, P. S.; Taylor, T. I. Contract AT(30-2)-Gen-16. J. Chem. Phys., 45: 1312-17(Aug. 15, 1966). (BNL–10105).

The motions of H_2O molecules in ferroelectric potassium ferrocyanide trihydrate (KFCT), water, and ice were investigated by total cross section and differential inelastic

scattering measurements with cold neutrons. The results showed no significant change in the average rotational or translational freedom of the water molecules in KFCT at or near its ferroelectric transition. The inelastic neutron spectra for KFCT exhibited broad peaks at about 425 and 160 cm^{-1}, both above and below the transition, which were assigned primarily to the librational and optic translational modes of the H_2O molecules, respectively. Moreover, both the total cross section and inelastic scattering results indicated a greater freedom of motion of the H_2O molecules in the KFCT lattice than in either water or ice. In addition, a decrease in the total cross section of H_2O, and in its variation with neutron wavelength was observed at the water-ice transition, indicating a significant change in the frequency distribution. The neutron results were compared with the results of NMR and infrared measurements. (auth)

36822 ELECTROMETRIC STUDIES ON THE COMPOSITIONS OF THORIUM POLYVANADATES. Saxena, R. S.; Sharma, O. P. J. Indian Chem. Soc., 43: 209-14 (Apr. 1966).

The formation and composition of thorium polyvanadates, obtained by the interaction of thorium salt and different alkali vanadates (ortho, pyro, meta, and poly) were investigated by means of glass electrode and conductometric titrations between the reactants at different pH levels in aqueous solutions, each of the reagents alternatively being used as titrant. The sharp breaks and inflections in titration curves provided definite evidence of formation and precipitation of thorium orthovanadate and pyrovanadate, having the compositions $3ThO_2 \cdot 2V_2O_5$ and $ThO_2 \cdot V_2O_5$ at pH ranges 7.5 to 6.0 and 6.0 to 4.8, respectively. The precipitation of thorium orthovanadate was almost quantitative and the titrations offered a simple means of determining thorium in solutions at suitable concentrations and pH ranges. (auth)

36823 STUDY OF BACK COORDINATION IN IRON CHELATES BY THE MOESSBAUER METHOD. Burger, K.; Korecz, L.; Manuaba, I. B. A.; Mag, P. (Eoetvoes Univ., Budapest). J. Inorg. Nucl. Chem., 28: 1673-8(Aug. 1966).

Magnetic moments of the iron (II)-, iron (III)- and cobalt (II)-dimethylglyoxime and those of the iron (II)-, cobalt (II)-, nickel (II)-complexes of salicylaldoxime and its 5-methyl, 5-chloro, and 5-nitro-derivatives were determined. The iron (II)-complexes of salicylaldoxime and of its derivatives were high-spin complexes; all the others were low-spin complexes. The Mössbauer spectra of the iron complexes showed the existence of back co-ordination. (auth)

36824 FORMATION CONSTANTS OF LANTHANIDE LACTATE COMPLEXES. Gouveia, M. A.; Guedes de Carvalho, R. (Laboratorio de Fisica e Engenharia Nucleares, Sacavem, Portugal). J. Inorg. Nucl. Chem., 28: 1683-8 (Aug. 1966).

The formation constants, β_1 and β_2, of the lactates of six lanthanides (La, Pr, Gd, Dy, Er, and Lu) were determined by a potentiometric method in aqueous medium of 0.1 M ionic strength ($NaClO_4$) at 25°C. Values of β_3 were calculated for Dy, Er, and Lu. (auth)

36825 SUBOXIDES OF NIOBIUM. Niebuhr, J. (Max-Planck-Institut fuer Metallforschung, Stuttgart). J. Less-Common Metals, 11: 191-203(Sept. 1966). (In German).

The lower oxides of niobium can be divided into 4 groups: NbO_x, NbO_y, and NbO_z; NbO and NbO_2; homologous series of oxides $Nb_{3n+1}O_{8n-2}$ with n = 6, 7, and 8, these are $NbO_{2.42}$, $NbO_{2.46}$, and $NbO_{2.48}$; and some lower niobium oxides not yet thoroughly investigated. NbO_x, NbO_y, and NbO_z formed only by oxidation of niobium, or by aging of niobium that was supersaturated with oxygen in definite ranges of temperature and oxygen pressure. NbO and NbO_2 were made by oxidation of niobium or by reduction of Nb_2O_5. They were stable up to the melting point and were present in the vapor phase. $NbO_{2.42}$, $NbO_{2.46}$, and $NbO_{2.48}$ formed within alloys of appropriate composition by long-time tempering at ~1100°C. Probably they were not stable up to the melting point. NbO_x (Nb_6O) formed at 300 to 500°C. According to x ray diffraction it was tetragonal with a = 3.39 Å, c/a = 0.97. According to electron diffraction of thin, single-crystal films in transmission, NbO_x had a superstructure with a = $4a_{Nb}$ = 13.5 Å, c/a = 0.97. NbO_x is isomorphous with TaO_x (Ta_6O). NbO_y formed at 350 to 500°C. According to x-ray studies NbO_y was orthorhombic and isomorphous with TaO_y (Ta_4O); according to electron diffraction of monocrystalline thin films it was cubic with a = $2a_{Nb}$ = 6.9 Å. NbO_y, formula Nb_4O was according to x-ray and electron diffraction tetragonal with a = $2a_{Nb}$ = 6.65 Å, c/a = 0.5. NbO_z formed at 400 to 700°C. It was tetragonal with a = 6.64_5 Å, c/a = 0.72 and isomorphous with $TaO_z(Ta_2O)$. (93 references) (auth)

36826 HOMOMOLECULAR AND ISOTOPIC EXCHANGE OF OXYGEN ON GADOLINIUM OXIDE. Sazonov, L. A.; Sokolovskii, V. D.; Boreskov, G. K. (Inst. of Catalysis, Academy of Sciences, USSR). Kinet. Kataliz, 7: 284-8 (Mar.-Apr. 1966). (In Russian).

The reactions of homomolecular and isotopic exchange of oxygen on gadolinium oxide were studied over a wide temperature range (−78 to 500°C) in relation to the preliminary treatment of the oxide. The catalytic activity of the oxide in this reaction was found to be stable below 200°C. Heating of the catalyst in oxygen above 200°C, where the isotopic exchange of oxygen between the oxide and the gas phase begins, caused a change in catalytic activity at low temperatures. At high temperatures, the two reactions occurred at similar rates and equal activation energies, indicating the presence of a common rate-determining step. Calcining of the catalyst in a vacuum at 700°C causes a high catalytic activity with respect to homomolecular exchange even at −78°C; this activity disappeared after the oxide was heated in oxygen above 200°C. Two temperature regions with different activation energies were found for the low-temperature exchange. (ATD)

36827 KINETIC STUDIES IN ETHYLENE POLYMERIZATION WITH ZIEGLER TYPE CATALYSTS. III. TRANSFER AND EXCHANGE REACTIONS WITH HYDROGEN AND DEUTERIUM IN THE SYSTEM $Et_2AlCl-TiCl_4$. Schindler, A.; Strong, R. G. (Research Triangle Inst., Durham, N. C.). Makromol. Chem., 93: 145-57(1966).

Deuterium was used to investigate the polymerization of ethylene with a catalyst system derived from Et_2AlCl and $TiCl_4$ in the presence of hydrogen. Kinetic equations describing the pressure dependence of the rate of polymerization and the methyl content of the polymers are presented. Infrared analysis revealed the presence of 3 kinds of deuterated groups in the polymer, CH_2D groups resulting from transfer reactions, as well as CHD and CD_2 groups being caused by an exchange reaction involving the β-hydrogen of the growing polymer chain. The easy migration of the β-hydrogen provides an explanation for the high methyl content observed in the presence of deuterium if it is assumed that, due to the relatively long residence time of adsorbed gas molecules, the transfer reaction takes place preferentially with the adsorbed HD molecules resulting from the exchange reaction. The effect of catalyst composition on the participation of deuterium in transfer and exchange reactions was investigated in a range of catalyst ratios from 0.33 to 40.0, the deuterium concentration being kept constant. The results show that only the exchange reaction is strongly influenced by the catalyst composition, its occurrence being completely restricted to low Al/Ti ratios. Thus, migration of the β-hydrogen of the growing chain occurs only if the latter is attached to a catalyst site with a tetravalent titanium center. (BBB)

36828 CALCULATION OF THE r.m.s. JUMP DISTANCE IN LIQUIDS FROM THE INTERMOLECULAR CONTRIBUTION TO NUCLEAR SPIN RELAXATION. Muller, B. H. (Univ. of Nottingham, Eng.). Phys. Lett., 22: 123-4(Aug. 1, 1966).

The r.m.s. jump distance in liquids can be found from the study of nuclear spin relaxation. This distance, of the order of the molecular diameter in each case, is given for benzene, methane, ethane, and helium-3. (auth)

36829 ON THE FORMATION OF COMPLEX COMBINATIONS OF ^{241}Am AND ^{246}Cm IN CITRIC ACID MEDIA BY ELECTROPHORESIS ON PAPER. Marcu, Gheorghe; Samochocka, Krystyna. Stud. Univ. Babes-Bolyai, Ser. Chem., 11: No. 1, 15-20(1966). (In Rumanian).

The formation of americium and curium complexes in citric acid medium, ~0.04M, by electrophoresis on Whatman paper No. 4 was studied. The constants of stability in the case of $[AMCit_2]^{3-}$ and $[CmCit_2]^{3-}$ compounds, $1g\beta_{2(Am)} = 9.66$ and $1g\beta_{2(Cm)} = 10.26$, were determined after establishing the electrophoretic mobilities of these compounds at various pH values for the potential difference of ~925 v. The existence in the solution of the ions of $[CmCit_2]^{3-}$ form was deduced from the behavior of curium, which resembles americium. At the same time, the instability constants, $K_{Am} = 4.5 \times 10^{-11}$ and $K_{Cm} = 1.82 \times 10^{-12}$, were calculated. (auth)

36830 EMF STUDIES OF ELECTROLYTIC DISSOCIATION. PART 9. YTTERBIUM ACETATE, MALONATE AND SULFATE IN WATER AT 25 DEG C. Archer, D. W.; Monk, C. B. (Edward Davies Chemical Lab., Aberystwyth, Wales). Trans. Faraday Soc., 62: 1583-8(June 1966).

H_2–AgCl, glass-calomel and glass-AgCl electrode cells were used to estimate the dissociation constants at zero ionic strength of several ytterbium ion-pairs. The cells were designed so stock solutions could be added and the standard electrode potentials evaluated from the dissociation constants of the ion-pairing acids. Intercomparison indicated that the uncertainties in the primary dissociation constants of $YbAc^{2+}$, $YbMal^{+}$ and $YbSO_4^{+}$ are about ±5%. (auth)

36831 ELECTRON ABSORPTION SPECTRA OF Ce(III) SALTS IN WATER-TRI-N-BUTYL PHOSPHATE MIXTURES AND IN PURE TRI-N-BUTYL PHOSPHATE. Batyaev, I. M.; Palchevskii, V. V.; Zheleznova, L. P. Vestn. Leningr. Univ., Ser. Fiz. Khim. (4), No. 1, 91-7 (1966). (In Russian).

The absorption spectra of $Ce(NO_3)_3$, $CeCl_3$, and $Ce_2(SO_4)_3$ were obtained in aqueous, aqueous dioxane solutions of acids, in TBP, and in H_2O–TBP. The occurrence of complexing between HNO_3 and TBP and between $Ce(NO_3)_3$ and TBP was shown, one complexing being superimposed. (auth)

36832 SOME PROPERTIES OF U_2O_5. Kozhina, I. I.; Osipova, V. V.; Solntsev, V. M.; Tolkachev, S. S. Vestn. Leningr. Univ., Ser. Fiz. Khim. (4), No. 1, 129-32(1966). (In Russian).

It was established that U_2O_5 has a hexagonal cell with size: a = 6.814 ± 0.001 kX and c = 4.118 ± 0.001 kX. At temperatures above 145°C U_2O_5 is disproportionated on two phases: hexagonal and cubic. At low temperature the hexagonal phase of U_2O_5 exists in the range of composition from $UO_{2.50}$ to $UO_{2.64}$. (auth)

36833 SPECTROPHOTOMETRIC STUDIES OF ASCORBIC COMPLEXES. IV. STUDY OF THE EUROPIUM–ASCORBIC ACID SYSTEM. Stolyarov, K. P.; Amantova, I. A. Vestn. Leningr. Univ., Ser. Fiz. Khim. (4), No. 1, 141-5(1966). (In Russian).

The formation of two complexes in the 0.2 to 1.0 M solutions of ascorbic acid (H_2A): EuHA (of pH 2.5 to 4.0) and Eu_2A (at pH 9) was established. The formation of the second complex is connected with the appearance of maximum at 380–390 mμk. This, in turn, may be explained by the opening of the lactonic ring. Molar extinction coefficients were found for EuHA: $E_{380} = 284$ and for Eu_2A: $E_{390} = 3250$. A method for the determination of Eu ($0.5(10)^{-4}$ – $15(10)^{-4}$ M) by means of ascorbic acid at pH 9 was suggested. (auth)

36834 INVESTIGATION OF EVAPORATION OF TUNGSTEN, MOLYBDENUM, AND TANTALUM IN VACUUM. Golubtsov, I. V.; Nesmeyanov, An. N. (Moscow State Univ.). Vestn. Moskov. Univ., Ser. II, Khim., No. 5, 31-3(Sept.-Oct. 1965). (In Russian).

The evaporation rate of W, Mo, and Ta in vacuum at 8×10^{-9} to $2 \cdot 10^{-4}$ mm Hg was investigated. Specimens of zone-melted, high-purity metals marked with radioactive isotopes ^{99}Mo, ^{185}W, and ^{182}Ta were heated at 2063 to 3203°K by passing an electric current or by electron bombardment. It was found that at 10^{-4} to 10^{-6} mm Hg, the evaporation rate of all tested metals increased. A further pressure drop below 10^{-7} mm Hg brought about considerably weaker additional effect. The composition of residual gases also affects the evaporation rate. At a pressure of 10^{-7} mm Hg and lower the evaporation proceeds in the form of molecules; at high pressures, such as 10^{-4} mm Hg, it proceeds in the form of oxides. (auth)

36835 STRUCTURE INVESTIGATIONS ON LANTHANIDE OXALATES. I. SINGLE-CRYSTAL INVESTIGATIONS ON NEODYMIUM(III) OXALATE DECAHYDRATE AND SAMARIUM(III) OXALATE DECAHYDRATE. THE ELEMENTARY CELL OF PROMETHIUM(III) OXALATE DECAHYDRATE. Weigel, F.; Ollendorff, W.; Scherer, V.; Hagenbruch, R. (Univ., Munich). Z. Anorg. Allg. Chem., 345: 119-28(June 1966). (In German).

The unit cell dimensions of the monoclinic lanthanide oxalate decahydrates, $Nd_2(C_2O_4)_3 \cdot 10H_2O$ and $Sm_2(C_2O_4)_3 \cdot 10H_2O$ were obtained from rotating crystal patterns. The data were used to index the powder patterns of both the neodymium and samarium salts, and, by analogy, the powder pattern of the corresponding promethium oxalate decahydrate, $Pm_2(C_2O_4)_3 \cdot 10H_2O$. The values for lattice parameters, unit cell volumes, and calculated densities are reported. In the zero-layer single crystal patterns (rotation about c axis), all reflections 0 k 0 with k odd are absent. This makes space group $P2_1/m$ the most likely. (auth)

36836 p-T-c-REPRESENTATION OF THE NIOBIUM–OXYGEN AND TANTALUM–OXYGEN SYSTEMS. Fromm, Eckehard (Max-Planck-Institut fuer Metallforschung, Stuttgart). Z. Metallk., 57: 540-5(July 1966). (In German).

Gravimetric degassing curves of Nb and Ta containing O in solution were evaluated assuming that only the volatile oxides NbO and NbO_2, and TaO and TaO_2, respectively, evaporate. The rate of evaporation of the volatile compounds was evaluated as a function of O concentration and temperature of the α solid solutions. From these results the equilibrium partial pressures of the oxides and the α solid solution were determined and the p-T-c equilibrium diagrams of the metal rich part of the Nb–O and Ta–O systems were established. (auth)

36837 COMPLEXES OF NEODYMIUM, HOLMIUM, AND ERBIUM WITH PYROGALLOSULFONIC ACID. Tserkasevich, K. V.; Efryushina, N. P.; Poluektov, N. S. (Inst. of General and Inorganic Chemistry, Academy of Sciences, Ukrainian SSR). Zh. Neorg. Khim., 11: 93-8 (Jan. 1966). (In Russian).

Formation of Nd, Ho, and Er complexes with pyrogallosulfonic acid (I) was investigated by using potentiometric and spectrophotometric methods. Results of potentiometric titration, performed with potentiometer LP-58 and glass electrodes, are summarized in graphs. Spectrophotometric study of the reaction was conducted in neutral as well as in strongly alkaline (1N KOH) media and was performed on a recording instrument SF-10. From the data obtained by both methods, it was possible to decide what equations were followed. From the data obtained in the spectrophotometric study in highly alkaline medium it was possible to calculate the apparent reaction constants K. (ATD)

36838 STABILITY OF CATIONIC COMPLEXES OF RARE EARTH ELEMENTS WITH TARTARIC AND TRIHYDROXYGLUTARIC ACIDS. Davidenko, N. K.; Deribon, V. F. Zh. Neorg. Khim., 11: 99-102(Jan. 1966). (In Russian).

Stability constants of cationic complexes of all 13 rare earth elements (except for Pm and Tm) with tartaric and trihydroxyglutaric acids were determined potentiometrically and were compared with those obtained by N. K. Davidenko (Zh. Neorg. Khim., 9: 1781, 1964) for malic acid. Solutions of rare earth chlorides were prepared by dissolving the corresponding oxides in dilute HCl. A potentiometer with a glass electrode and a saturated calomel electrode was used to measure pH. It was assumed in calculating the stability constants that, under reaction conditions, only complexes of equimolecular composition are formed. Results of the statistical treatment of the data

are shown. It was established that the stability of complexes increases in the series of hydroxy acids: tartaric < trihydroxyglutaric < malic. (ATD)

36839 INVESTIGATION OF SOLID SOLUTION REGION BASED ON SCANDIUM OXIDE IN THE SYSTEM Sc_2O_3–Fe_2O_3–MnO_x USING STATISTICAL METHODS. Komissarova, L. N.; Pokrovskii, B. I.; Granovskii, Yu. V.; Shaplygin, I. S. (Moscow State Univ.). Zh. Neorg. Khim., 11: 151-5(Jan. 1966). (In Russian).

A simple mathematical model of a single phase region of a three-component solid solution is examined. The change of the lattice parameter for a solid solution and its magnetic susceptibility as function of the composition were investigated on a solid solution. The latter was formed by oxides of iron and manganese in scandium oxide within the concentration limits of 28 mole % of Fe_2O_3 and 14 mole % of Mn_2O_3. The information is of interest because Sc_2O_3 is used in elements of a magnetic memory based on the system of magnesium-manganese ferrites. The lattice parameter was determined by means of x-ray powder diagrams. It was established that mathematical models can be utilized in describing the properties of Sc_2O_3 solid solutions of binary systems Sc_2O_3–Fe_2O_3 and Sc_2O_3–MnO_x. Investigation of the region of Sc_2O_3 solid solution of the binary system Sc_2O_3–MnO_x showed the solid solution parameter and magnetic susceptibility to be functions of MnO_x concentration. (ATD)

36840 REACTIONS OF LANTHANUM AND NEODYMIUM OXIDES WITH OXIDES OF ELEMENTS OF GROUPS III AND IV OF THE PERIODIC SYSTEM. Andreeva, A. B.; Keler, E. K. Zh. Prikl. Khim., 39: 489-98(Mar. 1966). (In Russian).

The reactions of La_2O_3 and Nd_2O_3 with certain oxides of tri- and tetravalent elements in the solid state were studied and the principal physiotechnical properties of the reaction products were determined. Pressed powder mixtures were prepared in which the molar ratio Ln : Me = 1 : 1 and 1 : 2, where Ln = La_2O_3 and Nd_2O_3, and Me = Al_2O_3, Ga_2O_3, Fe_2O_3, Cr_2O_3, Y_2O_3, SiO_2, TiO_2, ZrO_2, SnO_2, and CeO_2. The pressed pellets were then sintered at 1350, 1500, and 1700°C, and the products were examined by x-ray diffraction. La_2O_3 and Nd_2O_3 were found to form pyrochlore-type compounds with TiO_2, SnO_2, and ZrO_2; perovskite-type compounds with trivalent metal oxides Al_2O_3, Ga_2O_3, Cr_2O_3, and Fe_2O_3; and solid solutions in the region of Y_2O_3 and CeO_2 with the latter oxides. It was established that in La_2O_3- and Nd_2O_3-base compositions, no stability is imparted to the samples by SiO_2, TiO_2, ZrO_2, SnO_2, Y_2O_3, and CeO_2, taken in the proportion of 1 : 1 after firing at 1500°C. In compositions in which this proportion is 1 : 2 (except those containing TiO_2), fired up to 1400°C, ground up with a 1% admixture of mineralizer (B_2O_3 or ZnO), and refired at 1500°C, a good sintering was obtained, the reaction was complete, and the samples were stable both in air and during boiling in ammonium acetate and ammonium nitrate solutions. It was concluded that materials based on Ln_2O_3 and Nd_2O_3 can be used as special-purpose refractories (systems with ZrO_2, Cr_2O_3, Y_2O_3, Al_2O_3, SiO_2) with melting points at 2000°C and above and also as radio ceramics (systems with TiO_2, ZrO_2, Al_2O_3, Y_2O_3, and SnO_2) and semiconductors (systems with CeO_2, Cr_2O_3, ZrO_2, and Fe_2O_3). (ATD)

36841 THERMODYNAMICS OF VAPORIZATION OF REFRACTORY OXIDES AT HIGH TEMPERATURES. Yudin, B. F.; Karklit, A. K. (All-Union Inst. of Refractories, USSR). Zh. Prikl. Khim., 39: 537-44(Mar. 1966). (In Russian).

The thermodynamics of vaporization of SiO_2 (quartz), ZrO_2, MgO, CaO, and Al_2O_3 was studied. The heat of vaporization of SiO_2 at the boiling point, $\overline{\Delta H}_{3050°}$, was calculated to be 167.1 kcal/mole SiO_2. The approximation of partial pressures of the components of vaporization of ZrO_2, MgO, CaO, and Al_2O_3 in the form of equations of the type $\lg P_i = (A_i/T) + B_i$ which gives the coefficient of the Van't Hoff equation, was found to be sufficiently accurate. The heat of vaporization of Al_2O_3 at the boiling point was calculated to be $\overline{\Delta H}_{3990°}$ = kcal/mole Al_2O_3. The main vaporization products of Al_2O_3 are Al and O (pressure one order of magnitude greater than that of Al_2O and AlO). However, as the temperature rises, the stability of aluminum suboxides increases appreciably, and at the boiling point the pressure of Al_2O and AlO vapors becomes comparable to the pressure of Al vapor. (ATD)

36842 FORMULA INDEX TO NMR LITERATURE DATA. VOLUME 2: 1961–1962 REFERENCES. Howell, M. Gertrude; Kende, Andrew S.; Webb, John S. (eds.). New York, Plenum Press Data Division, 1966. 524p. $22.50.

A literature guide to organic compounds whose NMR spectra were described entirely or in part in scientific literature of 1961 to 1962 is presented. Approximately 5700 compounds are identified by empirical formula, structural formula (where known), or by common name. Compounds, fully referenced, are arranged in order of empirical molecular formula to facilitate the search for related compounds. (P.C.S.)

36843 PREPARATION AND ADSORPTIVE PROPERTIES OF THORIUM OXIDE. Davis, Burtron Hamilton. Gainesville, Fla., Univ. of Florida, 1965. 198p.

Thesis.

The preparation of thorium oxide catalysts was studied. Catalysts with a nitrogen B.E.T. surface area greater than 50 m^2/g were prepared by the thermal decomposition of thorium nitrate, thorium oxalate, and the precipitated hydroxide. The effect of the variables concerned with the precipitation and subsequent treatment of the precipitate was extensively investigated. The rate of heating had a great influence on the surface area of the thoria obtained by the thermal decomposition of thorium nitrate and oxalate. The presence of nitrate ions enhanced the surface area of the thoria obtained by the thermal decomposition of thorium oxalate. Crystallite size as determined by x-ray line broadening seemed to be determined by the activation temperature. The surface areas for many of the catalysts were determined by water adsorption. Adsorption isotherms appeared to be type IV according to Emmett's classification. The wide line NMR technique was used to study the adsorption of water on thorium oxide. The line width was measured at room temperature for increasing surface coverage of water adsorbed on thoria samples prepared by different methods. No great difference was observed in the line widths at a particular coverage for the different samples when the surface coverage was based on the nitrogen B.E.T. monolayer. A particular line width was obtained at a lower surface coverage for the larger surface area thoria samples. This increase in line width for a particular coverage appeared to be related to the surface area if the coverage was based on the monolayer calculated from the nitrogen B.E.T. area. A wide and narrow line was observed for a catalyst prepared from colloidal thoria, activated at 600°C, exposed to water vapor, and then reheated to 400°C, before beginning the water adsorption. The protons causing the wide line could be exchanged with D_2O; the ones causing the narrow line could not be exchanged. The temperature dependence of the line width for various coverages was measured. (TCO)

36844 PREPARATION AND THERMODYNAMICS OF EUROPIUM DICARBIDE. Gebelt, Robert E. East Lansing, Mich., Michigan State Univ., 1965. 123p.

Thesis.

Europium dicarbide was prepared by the reaction of europium metal and graphite in a stainless steel bomb. Chemical analysis indicated an average composition of $EuC_{1.87\pm0.07}$. X-ray powder diffraction analysis showed the compound to be of body-centered tetragonal symmetry, space group D_{4h}^{17}–I4/mmm, with lattice parameters a_0 = 4.045 Å and c_0 = 6.645 Å. The analytical data lead to the conclusion that europium dicarbide resembles the alkaline earth dicarbides more than the other lanthanon dicarbides. The vaporization of europium dicarbide over the temperature range 1150° to 1600°K was investigated by the Knudsen effusion method. Gaseous europium and europium dicarbide were both found in equilibrium with solid europium dicarbide in concentra-

tions of 99% and 1% respectively. Calibration of the mass spectrometer with silver permitted the calculation of the pressures corresponding to the observed ion intensities. An empirical equation, fitted to the data for europium by the method of least squares, gave $\ln_e P_{(atm)} = (-23709 \pm 715)/T + 9.270 \pm 0.886$. By means of the second law of thermodynamics the following values were found for the reaction $EuC_{2(s)} \rightleftharpoons Eu_{(g)} + 2C_{(graphite)}$: $\Delta H^{\circ}_{298} = 51.09 \pm 1.42$ kcal/mole and $\Delta S^{\circ}_{298} = 18.43 \pm 1.75$ eu. Values of the free energy function for $EuC_{2(s)}$ were estimated and combined with published data to yield, for the same reaction, the following value calculated from the third law of thermodynamics: $\Delta H^{\circ}_{298} = 51.22 \pm 0.80$ kcal/mole. The enthalpies obtained for the dissociation reaction were combined with published data on the enthalpy of vaporization of europium to yield the following value for the standard enthalpy of formation of EuC_2: $\Delta H^{\circ}_{298} = -9.17 \pm 1.15$ kcal/mole. (Dissertation Abstr.)

36845 ORBITAL ENERGY DIFFERENCES AND CHEMICAL BONDING IN RARE EARTHS. Joergensen, Chr. Klixbuell (Cyanamid European Research Inst., Cologne). 20p. (CONF-650804-24). ORAU. Gmelin, AED-CONF-65-208-24.

From 5th Rare Earth Research Conference, Ames, Iowa.

Recent theoretical interpretations of rare earth absorption and luminescence spectra are used to draw conclusions about the extent of covalent bonding and to understand the conditions for formation of metallic or nonmetallic compounds. The behavior of metallic alloys is discussed and remarks made about the 5f elements. The reluctance of lanthanides to change their odixation state is related to the repulsion between 4f electrons. (D.H.M.)

Organic Chemistry

Refer also to abstracts 37179 and 37305.

36846 (N-66-13499) POLYIMIDAZOPYRROLONES: A NEW CLASS OF RADIATION-RESISTANT POLYMERS. Bell, Vernon L.; Pezdirtz, George F. (National Aeronautics and Space Administration, Langley Station, Va. Langley Research Center). [1965]. 11p. (NASA-TM-X-57034). CFSTI $1.00 cy, $0.50 mn.

Experimental procedures are presented for the preparation of polymers, which are called stepladder (partial ladder) and ladder polyimidazopyrrolones or pyrrones, from the reaction of a dianhydride with a tetraamine in highly polar solvents such as dimethylformamide, dimethylacetamide, and dimethysulfoxide. A method is also given for synthesis of the polymers using the tetrahydrochloride salts of tetraamides. Evidence for the existence of the all-ladder structure of the polymers was deduced from the infrared spectra of thin films. Radiation effect data were obtained on 1 mil films from a PMDATADPO polymer. Preliminary results indicate that the imidazopyrrolones appear to be one of the most radiation-resistant polymers to be developed to date. The results of thermal stability studies are also summarized. (STAR)

36847 PLASTIC SCINTILLATORS. II. THE SYNTHESIS OF SOME DISTYRYLBENZENE DERIVATIVES AS WAVELENGTH SHIFTERS IN PLASTIC SCINTILLATORS. Nakaya, Tadao; Imoto, Minoru (Osaka City Univ.). Bull. Chem. Soc. Jap., 39: 1547-51(July 1966).

Synthesis, absorption spectra, and fluorescence spectra were studied for 2,5-dimethoxy-1,4-distyrylbenzene derivatives and related compounds. Some of the synthesized compounds were better wavelength shifters in plastic scintillators than compounds described in literature. (auth)

36848 PLASTIC SCINTILLATORS. III. THE SYNTHESIS OF SOME ANTHRACENE DERIVATIVES AS WAVELENGTH SHIFTERS IN PLASTIC SCINTILLATORS. Nakaya, Tadao; Tomomoto, Takanori; Imoto, Minoru (Osaka City Univ.). Bull. Chem. Soc. Jap., 39: 1551-6 (July 1966).

Fifteen anthracene derivatives were synthesized, and their absorption and fluorescence spectra were measured. Some of the synthesized derivatives were better wavelength shifters than compounds described in literature. (auth)

36849 THE KINETICS OF HYDROGEN ISOTOPE EXCHANGE REACTIONS. PART XIV. ACID-CATALYSED TRITIUM EXCHANGE AND ITS RELATIONSHIP TO THE DEHYDRATION OF t-BUTYL ALCOHOL. Gold, V.; Gruen, L. C. (London Univ.). J. Chem. Soc., No. 7, 600-3 (1966).

The rate of hydrogen exchange between tritium-containing aqueous perchloric acid and the C–H bond of dissolved t-butyl alcohol was measured at 25°C as a function of acid concentration. The logarithm of the rate constant is a linear function of H_0 with slope, 1.35. On the assumption that exchange takes place by dehydration to isobutene followed by re-addition of labeled water, the results were used to obtain the rate constant for dehydration of t-butyl alcohol in 0.5M-perchloric acid. The value agreed with one calculated by combining the previously determined rate constant for hydration of isobutene with the equilibrium constant for the hydration reaction evaluated from thermodynamic data. This agreement supported the view that the route via olefin is the most significant mechanism of hydrogen exchange of t-butyl alcohol in moderately dilute aqueous acid at 25°C. (auth)

36850 PREPARATION OF URANIUM NITRIDE AND CARBONITRIDES FROM URANIUM OXIDE IN A FLUIDIZED BED. Hyde, K. R.; Landsman, D. A.; Morris, J. B.; Seddon, W. E.; Tulloch, H. J. C. pp 1-18 of Special Ceramics 1964. Popper, P. (ed.). London, Academic Press, 1965. (AERE-R-4650).

Processes for making UN and carbonitrides direct from the oxide were examined. The simplest route involves carbothermic reduction in a stream of N_2 by the reaction $UO_2 + (2+x)C \xrightarrow[1450°C]{N_2} U(C_xN_{1-x}) + 2CO$. The results of two applications of this reaction, using fluidized beds, are presented. In one, the oxide was heated in a stream of N_2 and benzene vapor; in the other the oxide powder and C were intimately and heated in a stream of N_2. Fluidization was carried out in graphite vessels heated by induction. In general, both routes gave products consisting of solid solution of UC in UN. The first method yielded a product $UN_{0.7}C_{0.3}$. Higher N contents could only be obtained if the reaction was stopped before complete conversion of the UO_2. The second method was more flexible and yielded carbonitrides ranging from pure UC to $UN_{0.96}C_{0.04}$. (auth)

36851 THE PREPARATION OF ALKOXIDES OF SOME TRANSITION AND RARE-EARTH METALS AND THE FORMATION OF POWDERS AND COATINGS OF ULTRAHIGH-PURITY ZIRCONIA. Mazdiyasni, K. S.; Lynch, C. T. pp 115-38 of Special Ceramics 1964. Popper, P. (ed.). London, Academic Press, 1965.

The thermal decomposition of organo-metallic compounds in the vapor phase under controlled conditions produces high-purity, fine powders or coatings. Compounds of the type $M(OR)_3$ and $M(OR)_4$ where M is Ti, Zr, Hf, Th, Y, Yb, and Dy, and R various alkyl groups such as C_4H_9 and C_5H_{11} were studied. The metal–O bond in these compounds is very stable and thermal decomposition is complete to the oxides. A method was developed to produce zirconia with average <100 Å and purity >99.9$_5$%. Adherent coatings of ZrO_2 and HfO_2 on graphite were made by thermal decomposition of the alkoxides at the substrate surface. (auth)

36852 SPECTROPHOTOMETRIC STUDY OF ASCORBIC COMPLEXES. V. STUDY OF THE HOLMIUM–ASCORBIC ACID AND ERBIUM–ASCORBIC ACID SYSTEMS. Stolyarov, K. P.; Amantova, I. A. Vestn. Leningr. Univ., Ser. Fiz. Khim. (4), No. 1, 155-9(1966). (In Russian).

The formation of the following complexes in the solutions of ascorbic acid (H_2A) was established. Their molar extinction coefficients and indexes of stability constants were calculated. A spectrophotometric method for the de-

termination of Ho (451 mμ) and Er (378 mμ) in the form of ascorbic complexes was suggested. (auth)

36853 THERMOGRAVIMETRIC STUDY OF SOME GAS-SOLID REACTIONS. Nesbitt, Lyle Edwin. Lubbock, Tex., Texas Technological Coll., 1964. 124p.

Thesis.

A thermogravimetric study of some gas-solid reactions was carried out using a controlled atmosphere deflection type of thermobalance whose transducer was a linear variable differential transformer. Details of the construction and calibration of the thermobalance are presented as well as results from the gas-solid systems studied. Reactions examined were those of isopropylamine with the following solids: $CrCl_3$, $FeCl_2$, $CoCl_2$, $NiCl_2$, $CuCl_2$, $CdCl_2$, YCl_3, $LaCl_3$, $PrCl_3$, $NdCl_3$, $SmCl_3$, and $ErCl_3$. The apparatus was capable of measuring the thermodynamic variables of pressure and temperature as a function of solid composition and was used to derive equilibrium data for systems that proceed to equilibrium in short times. (Dissertation Abstr.)

36854 CRYSTAL FIELD EFFECTS IN ZIRCONIUM OXIDE. Meehan, John Patrick. Philadelphia, Temple Univ., 1965. 93p.

Thesis.

Chromium and vanadium were incorporated into monoclinic zirconium oxide powder at concentration levels of approximately one mole percent. Diffuse reflectance spectra were taken over the range from 10,000 to 50,000 cm^{-1}. Paramagnetic resonance spectra of the powders were obtained. Both the optical and EPR spectra were taken at room temperature (300°K), and at liquid nitrogen temperature (77°K). The spectra were interpreted in the light of ligand field theory. Chromium is present in the ZrO_2 : Cr systems as chromium (III) and chromium (VI). The optical spectra of the ZrO_2 : Cr systems reveal absorption maxima at 16,270, 22,700, 29,400, and 37,000 cm^{-1}. The first three peaks are attributed to crystal field transitions from the $^4A_{2g}$ ground state of chromium (III) to the $^2T_{2g}$, $^4T_{1g}$ (F), and $^4T_{1g}$ (P) excited states, respectively. The crystal field parameters for chromium (III) in ZrO_2 are Dq = 1,627 cm^{-1}, and B = 640 cm^{-1}. The $^4F-^4P$ term separation for the chromium (III) ion is estimated to be 9,900 cm^{-1}. The EPR spectrum of ZrO_2 : Cr exhibits three peaks. The average g value is about 1.95. The peak at 37,000 cm^{-1} is attributed to a charge transfer process involving the species chromium (VI). Vanadium is present in the ZrO_2 : V systems as vanadium (IV) and vanadium (V). The optical spectrum exhibits an intense absorption band, the onset of which is at 19,000 cm^{-1}. This band is attributed to a charge transfer transition from oxygen to pentavalent vanadium. No EPR signal is noted at 300°K, but a 77°K three sets of eight peaks occur. These peaks arise from hyperfine interaction in the VO^{++} ion. The average g value is slightly less than 2, and the hyperfine peaks are separated by 241 gauss. (TCO)

36855 OPTICAL FARADAY ROTATION STUDIES IN PRASEODYMIUM ETHYLSULFATE. Griffiths, David John. Vancouver, Can., Univ. of British Columbia, 1965. 159p.

Thesis.

The technique of detecting EPR spectra and measuring spin-bath relaxation times by the magneto-optical Faraday rotation was applied to carefully grown crystals of praseodymium ethylsulfate (PrES). All experiments were done at liquid helium temperatures ($1.4 \leq T \leq 4.2$°K) and in external magnetic fields up to 12 kilogauss. Successful measurements were made with the optic axis of the crystal aligned parallel to the polarized light beam and the external magnetic field. The EPR spectrum at X band of undiluted PrES is a broad band extending over several kilogauss with no evidence of hyperfine structure. The band decreases at 8400 ϕ and covers 800 ϕ from its maximum to half power point. The relaxation times, measured as a function of temperature over the range 1.40 to 2.18°K and at 4.22°K and as a function of the external magnetic field, range from 0.1 to 10 msec. For $1.40 \leq T \leq 1.80$°K, τ decreases from 0.40 to 0.15 msec, is proportional to $T^{-(3.6 \pm 0.4)}$, and is considered to be the phonon-bath relaxation time. Values of τ show a scatter within 0.20 ± 0.02 msec for $1.80 \leq T \leq 1.95$°K. As the λ-point is approached ($1.95 \leq T \leq 2.18$°K), τ exhibits a very rapid increase, having a value of 0.20 msec at 2.155°K and 0.85 msec at 2.165°K. The magnetic field dependence of τ is interpreted in terms of phonon scattering by the paramagnetic Pr^{3+} ions. The effect is strongest at the lowest temperatures (i.e., ~1.4°K) where there is an increase in τ from 0.5 to 2.0 msec for the magnetic field H increasing from 3.5 to 11.5 kilogauss. The effect of the magnetic field on τ decreases with increasing temperature and at 2.15°K τ appears to be independent of field. An unsuccessful attempt to detect electron spin resonance in neodymium ethylsulfate oriented with its optic axis perpendicular to the light path (and external magnetic field) is described. (TCO)

36856 REACTIONS OF DEUTERIUM ATOMS WITH OLEFINS AT 90 DEG K. Kassal, Thomas Theodore. Syracuse, N. Y., Syracuse Univ., 1964. 78p.

Thesis.

The reactions of deuterium atoms produced on a hot tungsten filament with olefins at 77–90°K were studied in both the solid and liquid states. The peculiar gradation of olefin reactivities in the solid state reported by other workers was confirmed. It was found, however, that any olefin of diene that displayed a low reactivity in the pure state would react rapidly when mixed with solid ethane. The trends in reactivities of olefins dissolved in liquid propane at 90°K are the same as those observed at room temperatures for reactions of olefins with hydrogen atoms and methyl radicals. All vinyl olefins containing the group $R-CH=CH_2$ are equally reactive while isobutene and butadiene 1–3 react 5.5 and 25 times as fast. Pentene-2 and hexene-2 react about one half as fast as the terminal olefins and allene displays a reaction rate slightly slower than these two compounds. The heat of solution of deuterium atoms in liquid propane is calculated to be −1.7 kcal/mole and this quantity has to be added to the measured activation energies in order to obtain the activation energy for the reaction D· (solvent) + olefin → R· (solvent). The activation energies for the terminal olefins as well as pentene-2 and hexene-2 are all about 3.1 ± .1 kcal/mole while that for isobutene seems to be only 2.5 kcal/mole. The concentration of atoms in solution is calculated on the basis of the steady-state diffusion equation $DdC/dx = kC^2$ where D is the diffusion coefficient for deuterium atoms in liquid propane at 90°K and C is the atom concentration. From this equation along with the observed rate of pressure decrease, the absolute rate constant for the addition of deuterium atoms to pentene-1 at 90°K is calculated to be 1.7×10^6 cm^3/mole·sec with a frequency factor of 7×10^{13}. (Dissertation Abstr.)

Radiation Chemistry

See also BIOLOGY AND MEDICINE — Radiation Effects on Biochemicals Radiation Effects on Tissues

Refer also to abstract 36846.

36857 (COO-1088-21) THE ULTRAVIOLET SPECTROSCOPY OF IRRADIATED POLYETHYLENE. [PART] II. Dole, Malcolm; Boehm, G. G. A. (Northwestern Univ., Evanston, Ill.). July 7, 1966. Contract AT(11-1)-1088. 27p. (CONF-660614-3). Dep. mn. CFSTI $2.00 cy, $0.75 mn.

From 3rd International Congress on Radiation Research, Cortina, Italy.

Electron irradiation of polyethylene at liquid N_2 temperatures using a combined irradiation and uv spectrophotometric cell is described. Design of the cell is discussed, along with classification of the uv absorption bands and effects of conjugated double bonds. The effects of heat and light on radioinduced free radicals are also examined. (J.R.D.)

36858 (IFA-CR-73) THE RADIOLYTIC BEHAVIOR OF IRON IONS IN ACETYLENE AQUEOUS SOLUTION. Fiti, Maria (Institutul de Fizica Atomica, Academia R. P. R., Bucharest (Romania)). 1966. 14p. Dep. mn.

The radiolysis of acetylene aqueous solution in the presence of iron ions, led to a considerable increase of the radiolytic oxidation process of both the acetylene and Fe^{2+} ions. Results obtained confirmed the important role for radiolytic processes of the electron transfer reactions taking place in the presence of Fe^{2+} ions and leading to an appreciable sensitizing of some useful radiolytic processes. A mechanism for the sensitizing of the radiolytic oxidation of acetylene in aqueous solutions by Fe^{2+} ions is suggested. (auth)

36859 (N-66-13497) CROSS-LINKING OF POLYVINYLIDENE FLUORIDE BY GAMMA RADIATION. Sands, George D.; Pezdirtz, George F. (National Aeronautics and Space Administration, Langley Station, Va. Langley Research Center). [1965]. 6p. (NASA-TM-X-57037). CFSTI $1.00 cy, $0.50 mn.

Experiments were conducted to determine the effects of high energy gamma radiation on polyvinylidene fluoride. Tensile strength was found to increase as the polymer was irradiated, which is typical of polymers undergoing cross linking. Elongation was found to decrease. Solubility was 74% at a dose of 2 mR and fell rapidly to 4% after a dose of 590 mR. This solubility behavior, indicating cross linking, is consistent with the tensile strength and elongation behavior. As the radiation bonds the polymer chains together into a three-dimensional network, the tensile strength increases because there are more bonds to be broken, but the simultaneous limitation of movement of the chain segments results in a decrease in elongation. The atypical response of polyvinylidene fluoride to radiation, namely cross linking instead of the expected chain scission, is associated with the small size of the fluorine atom and as a result the small fluorine groups are not crowded, produce no strain, and hence cross linking occurs instead of chain rupture. (STAR)

36860 (NP-16150) STRAHLENCHEMISCHE CYCLOMERISATIONEN. Eine Vergleichende Untersuchung Mit Optischen und Ionisierenden Strahlen. (Radiochemical Cyclomerization. Comparative Study with Optical and Ionizing Radiation). Metzner, Wolfgang (Bonn Univ. (West Germany)). 1966. 130p. Dep. mn.

Thesis.

A comparative study was made of the photo- and radio-induced cyclomerization of C_4 compounds. The behavior of benzocyclic olefins such as indene and coumarin and their derivatives were investigated under conditions of photon and radiation sensitization. The photochemical and radiochemical C_4 cyclodimerization, co-C_4-cyclo additions and C_4 cycloisomerization of Diels-Alder adducts of p-benzoquinone to 1,3-diene were investigated. The mechanisms of photosensitized C_4 cyclo addition, radiation-chemical formation of cyclobutanes, and formation of 1,3-dienes from chlorocyclobutanes are discussed. (J.S.R.)

36861 (UJV-1553) THE HYDROGEN FORMATION IN THE RADIOLYSIS OF LIQUID METHANOL. Teply, J.; Habersbergerova, A. (Ustav Jaderneho Vyzkumu, Ceskoslovenska Akademie Ved, Rez). May 1966. 17p. Dep. mn.

Expressions for the kinetics of the scavenging of different precursors of hydrogen formed in the radiolysis of liquid methanol and ethanol are given. The average yield values for different precursors were obtained. In the case of methanol the precursors of hydrogen are solvated electrons ($G_{e^-_s} = 1.1$), hydrogen atoms ($G_H = 1.6-2.7$) and "unscavengeable" hydrogen ($G_{H_2} \pm 1.6$), which consists of hot hydrogen atoms or highly excited methanol molecules ($G_{H^\bullet} \geq 1$) and of molecularly formed hydrogen ($G_{H_2,m} = 0.4 - 0.6$). At high scavenger concentration additional electrons (not solvated) are scavenged ($G_{e^-,add} = 0.5-0.8$). The known differences in the hydrogen yields in pure methanol ($G(H_2)_0 = 4.3-5.4$) are interpreted as caused by suppression of hydrogen atoms formation by an impurity. Similarly, in the ethanol radiolysis $G_{e^-_s} = 1.0$, $G_H \pm 2.6$, $G_{H_2} \pm 1.2$ and $G_{e^-,add.} = 0.75$. The values of rate constants were derived. It was shown that $FeCl_3$ is not an appropriate scavenger in protogenic solvents. (auth)

36862 p-BIS-(o-METHYLSTYRYL)BENZENE, USEFUL SECONDARY FLUOR FOR LIQUID SCINTILLATION COUNTING. Kobayashi, Yutaka (Worcester Foundation for Experimental Biology, Shrewsbury, Mass.). Contract AT(30-1)-2085. Anal. Chem., 38: 1240(Aug. 1966).

An increase in counting efficiency was observed when p-bis-(o-methylstyryl)benzene was substituted as a secondary fluor for p-bis-[2-(4-methyl-5-phenyloxazolyl)] benzene in various solvent systems used in liquid scintillation counting. (D.H.M.)

36863 RELATIVE EFFICIENCY OF A NEW LIQUID SCINTILLATION FLUOR, p-BIS-(o-METHYLSTYRYL) BENZENE. Bush, Elizabeth T. (Nuclear-Chicago Corp., Des Plaines, Ill.). Anal. Chem., 38: 1241-2(Aug. 1966).

A secondary solute for liquid scintillation counting, p-bis-(o-methylstyryl)benzene (bis-MSB), was compared with two previously available fluors, p-bis-2-(5-phenyl-oxazolyl) benzene, (POPOP), and bis-2(4-methyl-5-phenyloxazolyl) benzene, (dimethyl POPOP). The effectiveness of bis-MSB in reducing quenching and wavelength shifting was tested. The three secondaries, each at or near its maximal concentration at 4°C, were compared for effectiveness in samples containing compounds known to quench. With each quencher efficiency was improved by the secondaries in the order bis-MSB > dimethyl POPOP > POPOP. When comparisons were made at equal concentrations by weight of the secondary solute, the order of efficiency was POPOP > bisMSB > dimethyl POPOP. (D.H.M.)

36864 LUMINESCENCE OF FUSED QUARTZ EXCITED WITH PULSED ELECTRONS. Kawabata, Keisuke; Okabe, Shigeru. Ann. Rep. Radiat. Center Osaka Prefect., 6: 71-3(1965).

An intense, rapidly decaying luminescence was observed in fused quartz under irradiation by pulsed high-energy electrons from a linear accelerator. The luminescence was analyzed directly with a prism monochromator from 2000 to 6000 Å and the decay times were determined at several wavelengths. The observed decay times were 9.5 and 60 μsec. The wavelength distribution was shown to have a broad peak around 3500 to 4500 Å for the rapidly decaying component and even for prompt decay during the 2-μsec burst similar distribution was observed. This distribution was the same as that in longer phosphorescence. (auth)

36865 CONDUCTION CARRIERS IN NEUTRON-IRRADIATED ZnS SINGLE CRYSTALS. Kitagawa, Michiharu; Shono, Yoshihiko. Ann. Rep. Radiat. Center Osaka Prefect., 6: 78-9(1965).

The Hall effect in a neutron-irradiated ZnS single crystal was measured at room temperature. Under fast-neutron irradiation, the Hall mobility decreased to 44 cm^2/volt-sec, and the photoelectric sensitivity decreased by three orders of magnitude. These effects may be caused by production of many scattering centers of carrier and recombination centers, which have high recombination probabilities. The sign of the Hall coefficient was negative for both unirradiated and irradiated crystals, indicating that the current carriers are electrons. Hence, it appears that the conduction mechanism is mainly dominated by the behavior of electrons. (auth)

36866 RADIATION-INDUCED ISOTOPE EXCHANGE IN SOME C_6-HYDROCARBONS. Kroh, J.; Hankiewicz, E. (Technical Univ., Lodz, Poland). Bull. Acad. Pol. Sci., Ser. Sci. Chim., 14: 243-4(1966).

The influence of gamma radiation on H-D exchange in gaseous and liquid systems containing $D_2(D_2O)$ and benzene, cyclohexane, or n-hexane was studied using a mass spectrometer. No exchange was observed in the liquid systems. Data proved the exchange most efficient for benzene of the gaseous mixtures. Exchange probably occurred through an excited state mechanism. Non-radical species played an important and direct part. (P.C.S.)

36867 TEMPERATURE EFFECTS IN X-RAY RADIOLYSIS OF FROZEN FRICKE SOLUTIONS. Kroh, J.; Czerwik, Z. (Technical Univ., Lodz, Poland). Bull. Acad. Pol. Sci., Ser. Sci. Chim., 14: 245-8(1966).

Experiments with 40-kev x rays within the temperature range from −196 to −20°C were performed to determine the values of $G(Fe^{3+})$. In the temperature range between −20 and −60°C and below −100°C, $G(Fe^{3+})$ decreases linearly with decreasing temperature at a rate of about 0.3%/°C. Between −60 and −100°C, the value decreases abruptly from 2.95 to 0.65, probably caused by the structural transformation occurring within this range in ice and frozen aqueous solutions. (P.C.S.)

36868 RADIATION-INDUCED H-T EXCHANGE IN AROMATIC HYDROCARBONS SATURATED WITH TRITIATED WATER. Kroh, J.; Plonka, A. M. (Technical Univ., Lodz, Poland). Bull. Acad. Pol. Sci., Ser. Sci. Chim., 14: 331-4(1966).

The results of gamma radiolysis of benzene and toluene, saturated with tritiated water, were examined. No H-T exchange occurred when unirradiated samples of benzene or toluene saturated with tritiated water were stored for any length of time. The activities of the irradiated samples were proportional to the absorbed dose of gamma radiation and increased with the activity of the tritiated water used for saturation. The degree of exchange, defined as the ratio of the final specific activity of benzene or toluene to the initial specific activity of the respective solutions prepared for irradiation, was found to be independent of the activity of the tritiated water. The exchange was more efficient for benzene than toluene. (D.H.M.)

36869 HYDRAZINE FORMATION IN THE γ RADIOLYSIS OF AN AQUEOUS SOLUTION OF AMMONIA. Sakumoto, Akihisa (Japan Atomic Energy Research Inst., Tokyo). Bull. Chem. Soc. Jap., 39: 1349 (June 1966).

Hydrazine formation in the γ radiolysis of a mixture of liquid ammonia and water at a high irradiation dose was studied. At the irradiation temperature of −50°C, the yield of hydrazine increased gradually to a maximum value at about 85 mole %, and then decreased with an increase in the concentration of ammonia. On the other hand, the maximum yield of hydrazine was obtained at about 50 mole % of ammonia. (J.G.B.)

36870 THE ELECTRON SPIN RESONANCE OF γ-IRRADIATED SODIUM POLYPHOSPHATE. I. THE GLASS AND THE SINGLE CRYSTAL. Miura, Masaji (Hiroshima Univ.); Hasegawa, Akinori; Fukui, Tokinori. Bull. Chem. Soc. Jap., 39: 1432-6(July 1966).

Under γ irradiation at room temperature, the glass of sodium polyphosphate or its single crystal doped with sodium sulfate became red, whereas the pure single crystal remained colorless. The glass and the doped single crystal exhibited ESR spectra, which were attributed to the hole trapped in the non-bonding orbital on the oxygen atom. The pure single crystal exhibited no ESR spectra. Polymerization in the aqueous solution of the glass showed a decrease in the length of the main chain caused by the γ radiation. The P−O−P bond ruptured under the radiation and the effect of γ on sodium polyphosphate closely correlated with the local strain of the P−O−P bond. (auth)

36871 PARAMAGNETIC RELAXATION OF TRAPPED ELECTRONS IN IRRADIATED ALKALINE ICES. Zimbrick, John; Kevan, Larry (Univ. of Kansas, Lawrence). J. Amer. Chem. Soc., 88: 2678-9(Aug. 5, 1966).

Paramagnetic relaxation experiments are reported, which support the previously proposed F-center model of trapping sites in which the electron is trapped in a hydroxide anion vacancy. Frozen solutions of 10.0 M NaOH and 7.3 M NaOD were irradiated at 77°K with gamma rays from ^{60}Co. Results indicated that the trapping site is located in a radiation-produced spur. It was found that the trapped electron relaxes via cross relaxation with O^-, which is also formed in irradiated alkaline ices. (D.H.M.)

36872 ELECTRON SPIN RESONANCE ANALYSIS OF A γ-IRRADIATED SINGLE CRYSTAL OF PENTAFLUOROPROPIONAMIDE. Lontz, Robert J. (Army Research Office, Durham, N. C.). J. Chem. Phys., 45: 1339-45 (Aug. 15, 1966).

Electron spin resonance data indicated that irradiation of pentafluoropropionamide at 300°K produces the stable free radical $CF_3\dot{C}FCONH_2$. The hyperfine interaction of the unpaired electron with the alpha-fluorine nucleus has the characteristic values observed in other cases of the CF fragment. The unpaired electron also interacts equally with each of the three methyl-group fluorine nuclei at room temperature, implying free rotation of this group about the $C_\alpha - C_\beta$ bond. Two of the principal elements for the beta-fluorine tensor (36 and 14 G) are located in the plane perpendicular to the maximum alpha-fluorine hyperfine element, and the third (17 G) is perpendicular to this plane. Also presented is evidence that the free rotation of the methyl group may be stopped by cooling the crystal to 77°K. Preliminary room-temperature data indicate attack of the free radical by oxygen to produce the radical $R-O-\dot{O}$, and the possible existence of a second free radical, $CF_3CF_2\dot{C}ONH$, resulting from N−H bond rupture. (auth)

36873 X-RAY PHOTOCONDUCTIVITY OF ANTHRACENE. Kramer, G. (AVCO Corp., Norman, Okla.); Ghalla, M.; Canfield, J. J. Chem. Phys., 45: 1346-51 (Aug. 15, 1966).

The excess current generated in anthracene crystals under x radiation were measured as a function of x-ray intensity, electric field, and temperature. The currents were linear with respect to absorbed dose rate and electric field. A sensitivity of $7.1 \pm 0.7 \times 10^{-12}$ C/cm^2·rad at a field strength of 630 v/cm was obtained. The mobility, lifetime product, $\mu\tau$, was $9.9 \pm 0.9 \times 10^{-8}$ cm^2/v. The photocurrent was observed to increase with increasing temperature and exhibited two different activation energies, one below 250°K and a second above 250°K. The magnitude of these energies decreased with increasing dose rate. The temperature behavior may be explained in terms of exciton theory or may be due to changes in carrier mobility. (auth)

36874 THERMAL ANNEALING OF PARAMAGNETIC DEFECTS INDUCED BY γ IRRADIATION IN $(NH_4)_2SO_4$ AND $(ND_4)_2SO_4$ SINGLE CRYSTALS. II. EXPERIMENTAL VERIFICATION OF THE THEORY OF RECRYSTALLIZATION OF THE HOT ZONE. Calusaru, A.; Barbur, I.; Ursu, I. (Institut de Physique Atomique, Bucharest. Univ., Cluj). J. Chim. Phys., 63: 809-14(June 1966). (In French).

The EPR spectrum of monocrystals of $(NH_4)_2SO_4$ and $(ND_4)_2SO_4$ is the result of the superposition of two radicals: one, assigned I_1, corresponds to a sulfur compound, the other, I_2, is localized on the ammonium group. The kinetics of the recombination of the I_2 radical were studied. This radical shows a hyperfine structure for certain positions, with the C axis parallel to the static magnetic field. The comparison of experimental values with those calculated by means of the spin Hamiltonian indicated that I_2 corresponds to a nitrogen compound. The isothermal recombination as a function of time follows, in this case, the model of recrystallization of the hot zone. At the temperature of activation for the recombination reaction of this radical in $(NH_4)_2SO_4$ the value $T_H = 10{,}250$°K ($E_H = 0.874$ ev) and $(ND_4)_2SO_4$, $T_D = 9{,}500$°K ($E_D = 0.81$ ev). (auth)

36875 RADIOCHEMICAL POLYMERIZATION OF LAURYL METHACRYLATE IN LIQUID AND SOLID PHASES. Chapiro, Adolphe; Perec, Liliana. J. Chim. Phys., 63: 842-4(June 1966). (In French).

The radioinduced polymerization of lauryl methacrylate was studied in the liquid phase at 20 and 0°C, in the crystalline state at −78°C, and in solid mixtures with mineral oil in the form of a glass at −78°C. In the liquid phase the polymerization is complicated by the gel effect; the dose-rate exponent is close to 1 and the temperature coefficient is very small. In the crystalline state the reaction rate is larger. The addition of mineral oil leads to a marked acceleration of the reaction as has been observed with several other vinyl monomers. (auth)

36876 RADIOCHEMICAL COPOLYMERIZATION OF MIXTURES OF STYRENE WITH ACRYLONITRILE IN MEDIA OF DIFFERENT KIND. I. COPOLYMERIZATION IN BULK AND IN SOLUTION. Jendrychowska-Bonamour, Anna-Maria. J. Chim. Phys., 63: 855-62(June 1966). (In French).

The radiochemical polymerization of styrene-acrylonitrile mixtures was studied both in bulk phase and in solution. Experiments were carried out at –78, 0, and 50°C. The dose rates used were in the range from 16.8 to 6,360 rads/mn. The reaction was carried out in bulk, in dimethylformamide solution and in an oil giving a gel at low temperatures. In the liquid phase at the higher temperatures the reaction proceeds by a radical mechanism. At low temperatures and high dose rates an ionic contribution to the mechanism is observed. In a polar solvant such as dimethylformamide two reactions occur simultaneously: an anionic polymerization leading to pure polyacrylonitrile and a free radical copolymerization giving low molecular weight products, which are not precipitated by methanol. (auth)

36877 RADIOCHEMICAL COPOLYMERIZATION OF MIXTURES OF STYRENE WITH ACRYLONITRILE IN MEDIA OF DIFFERENT KIND. II. COPOLYMERIZATION IN GEL MEDIA. GRAFTING ON TO POLYVINYL CHLORIDE. Jendrychowska-Bonamour, Anna-Maria. J. Chim. Phys., 63: 863-80(June 1966). (In French).

The radiochemical grafting of styrene-acrylonitrile mixtures onto PVC was studied in the temperature range from 0 to 50°C at dose rates between 16.8 and 1,180 rads/mn. It was observed that at low temperatures and high dose rates the reaction is controlled by the rates of monomer diffusion into the film being grafted. At sufficiently high rates of diffusion the variation both of the grafting rate and of the composition of the grafted chains with respect to initial monomer concentrations is analogous to that observed in the radical copolymerization of these monomers. Thus the presence of polymer has no particular effect in this system. (auth)

36878 RADIOCHEMICAL COPOLYMERIZATION OF MIXTURES OF STYRENE WITH ACRYLONITRILE IN MEDIA OF DIFFERENT KIND. III. RADIOCHEMICAL GRAFTING TO POLYTETRAFLUOROETHYLENE. Jendrychowska-Bonamour, Anna-Maria. J. Chim. Phys., 63: 881-5(June 1966). (In French).

By studying the grafting of styrene–acrylonitrile mixtures on polytetrafluoroethylene the influence of monomer diffusion rates on the grafting process can be demonstrated. It was observed that at relatively high dose rates (43 rad/min) the reaction is governed entirely by monomer diffusion rates. From this study a curve of reaction rate against composition of monomer mixture was obtained. This curve showed a maximum at the 50-50 monomer mixture. At lower dose rates (17 rad/min) the grafting reaction exhibited features similar to those observed in the free radical copolymerization of these two monomers. (auth)

36879 DEGRADATION OF PECTIN BY γ RADIATION UNDER VARIOUS MOISTURE CONDITIONS. Wahba, I. J.; Massey, L. M. Jr. (Cornell Univ., Geneva, N. Y.). J. Polym. Sci., Pt. A-1, 4: 1759-71(July 1966).

By using D_{50} and D_{37} doses for 50 and 63% decreases in the solution viscosity of pectin, an evaluation was made of the effectiveness of radiation at different moisture levels. The relation between radiation effectiveness, as measured by the D_{50} value, and the pectin : water ratio was expressed in a simplified empirical equation. The indirect effect of radiation in dilute aqueous solutions decreased progressively with increasing pectin concentration. A protective effect was produced by small additions of water to dry pectin and a minimum in degradation (i.e., maximum D_{50} and D_{37} values) was attained at about the 20% moisture level. The relation between the intrinsic viscosity of dilute aqueous solutions of pectin irradiated air-dry and the number-average molecular weight and D_{37} values was determined. By using the former relation, the number of chain scissions per unit of absorbed energy was measured at different moisture levels. The importance of moisture control in comparative radiation studies was emphasized. An approximately 26-fold increase in the radiation sensitivity of pectin was produced by an increase in the moisture content from the 20 to the 99% level. Varying the moisture content therefore provides a good means of altering the sensitivity of pectin and similar materials to radiation damage. (auth)

36880 KINETICS OF RADIATION-INDUCED ALLYL POLYMERIZATION. II. Dolmatov, S. A.; Polak, L. S. (Inst. of Petrochemical Synthesis, Academy of Sciences, USSR). Kinet. Kataliz, 7: 27-32(Jan.-Feb. 1966). (In Russian).

Allyl alcohol was polymerized by irradiation and the effects of solvent, inhibitors, and oxide addition were investigated. The study was made with dose rates of 243 to 850 r/sec and at temperatures of –78, 52, and 300°C. Polymerization is assumed to follow a radical mechanism. Cyclohexane, water, and benzene were used as solvents; the resulting polymer was insoluble in these solvents, which made for an increased rate of conversion (gel effect) when the polymer precipitated. The polymer has a transparent, egg-white appearance. Diphenylpicrylhydrazyl, benzoquinone, hydroquinone, pyrogallol, and atmospheric oxygen were studied as inhibitors. Polymerization with these inhibitors occurred in mass and in an azeotropic mixture of monomer and water. Of the five, DPPH and oxygen failed to show inhibitory effects. Al_2O_3, ZnO, and silica were added in concentrations of 40 to 50 wt % but failed to affect the rate of polymerization. The limiting viscosity number n was determined as a function of polymer yield. There was an abrupt increase in n when the wt % yield reached 80. The increase in n was interpreted as an abrupt increase to 10^3 to 10^4 in the degree of polymerization, $\overline{P}$. Compared to other polymers, a low n of the order of 1 to 10 ml/g was found even at considerable $\overline{P}$ indicating that the polymer molecule is considerably branched and probably spherical in solution. The Huggins constant was found in the region of 1 to 3. Infrared bands for C = C and C – H deformation were reduced in intensity as the yield of polymer is increased. The amorphous polymer formed at doses up to 1.2×10^9 r was completely soluble in a hot mixture of methanol and HCl. (ATD)

36881 NATURE AND KINETICS OF ACCUMULATION OF PRODUCTS FORMED BY THE RADIOLYSIS OF BENZENE IN AQUEOUS SOLUTIONS OF SODIUM NITRATE. Chernova, A. I.; Orekhov, V. D. (Lomonosov Inst. of Fine Chemical Tech., Moscow). Kinet. Kataliz, 7: 49-54 (Jan.-Feb. 1966). (In Russian).

The qualitative composition and kinetics of accumulation of benzene radiolysis products in a 0.5M aqueous solution of sodium nitrate were investigated. ^{60}Co gamma radiation in doses from 0.05 to 1 Mrad was used. In the initial dose range, the stable products are nitrobenzene (which forms only in the absence of oxygen), nitrophenols, phenol, nitrous acid, and hydrogen peroxide. Radioinduced nitration of benzene was observed in the range of pH below 6.0 and the oxidation of its molecules continued at higher pH values. As the dose increased, nitrobenzene in an inert atmosphere converted into dinitrobenzene, and nitrophenol changed into dinitrophenol. The main direction of the conversion of phenol was radiolytic nitration; a side direction was a nonradiolytic reaction with nitrous acid, forming nitroso compounds and nitrophenol. At pH values exceeding 6.0, phenol radiolytically oxidized into hydroquinone and pyrocatechol. At pH values above 7.0, precipitation of insoluble dimerization products was observed. (ATD)

36882 KINETICS OF RADIATION POLYMERIZATION OF ACRYLONITRILE FROM THE GAS PHASE ON A MINERAL SUBSTRATE. Berezkin, V. G.; Kolbanovskii, Yu. A.; Kyazimov, E. A. (Topchiyev Inst. of Petrochemical Synthesis, Academy of Sciences, USSR). Kinet. Kataliz, 7: 187(Jan.-Feb. 1966). (In Russian).

The kinetics of graft polymerization of acrylonitrile initiated with ^{60}Co gamma radiation was studied. The reaction was conducted with a view to modifying the proper-

ties of INZ-600 brick, which is widely used as a carrier in gas-liquid chromatography. A powdered form of this material in a glass ampul was subjected to heat treatment at 300°C and a pressure of 10^{-2} mm Hg for 3 to 4 hr; a second ampul containing the degassed monomer was connected to the first ampul so that during the irradiation the powder was in acrylonitrile vapor (the liquid acrylonitrile was shielded from the radiation with lead). The weight of polymer formed was measured as a function of irradiation time. The kinetics of the process were described by the Roginskiy-Zel'dovich equation for adsorption on an inhomogeneous surface $dq/dt = ae^{-bq}$ or $q = (1/b)[\ln(t + t_0) - \ln t_0]$, where $t_0 = 1/ab$. It was concluded that the surface which actually takes part in the grafting process is inhomogeneous. (ATD)

36883 FORMATION OF RADICALS DURING RADIOLYSIS OF ORGANIC SOLIDS. III. EPR SPECTRA AND RADIATION YIELDS OF RADICALS IN CERTAIN ORGANOSILICON COMPOUNDS. Chkheidze, I. I.; Molin, Yu. N.; Mironov, V. F.; Chernyshev, E. A.; Buben, N. Ya.; Voevodskii, V. V. Kinet. Kataliz, 7: 230-6(Mar.-Apr. 1966). (In Russian).

The EPR method was used to investigate the radical processes involved in the low-temperature radiolysis of certain organosilicon compounds with a view to determining the effect of the silicon atom entering into the aliphatic chain on the effectiveness and direction of primary radiochemical processes. The radiation yields of the radicals (G_R) formed by irradiating the compounds with fast electrons at temperatures from −130 to −180°C were determined by the EPR method. It was found that G_R for saturated and aromatic substituted derivatives of tetramethylsilane did not differ from G_R for hydrocarbons of similar structure and amounted to 4 to 5 $^1/_{100}$ ev and 0.2 to 0.6 $^1/_{100}$ ev, respectively. For compounds of the general formula $(CH_3)_3Si(CH_2)_n CH=CH_2$ (n = 0, 1, 2), the radiation yield was $G_R \simeq 1\ ^1/_{400}$ ev, which is approximately $^1/_4$ that for hydrocarbons with double bond. Analysis of the EPR spectra showed that the introduction of a silicon atom in the aliphatic chain does not produce any appreciable changes in the radiolysis mechanism. (ATD)

36884 ELECTRON SPIN RESONANCE OF AN X-RAY IRRADIATED SINGLE CRYSTAL OF POTASSIUM DIHYDROGEN ARSENATE, KH_2AsO_4. Hampton, Marlene; Herring, F. G.; Lin, W. C.; McDowell, C. A. (Univ. of British Columbia, Vancouver, Can.). Mol. Phys., 10: 565-73(1966).

The electron spin resonance of an x-irradiated single crystal of potassium dihydrogen arsenate was examined and a radical thought to be AsO_4^{4-} identified. Analysis of the spectra for various orientations of the crystal with respect to the external magnetic field led to an axially symmetric hyperfine interaction tensor, which was in agreement with what would be expected for the AsO_4^{4-} radical. Semi-empirical LCAO molecular orbital calculations for the AsO_4^{4-} radical with symmetry D_{2d} trapped in the tetragonal KH_2AsO_4 crystals led to the conclusion that the odd electron enters a molecular orbital with A_1 symmetry. The isotropic part of the hyperfine interaction tensor was calculated from this theory to be 2098 Mc, compared with the experimental value of 3038.6 Mc. The anisotropic part of the hyperfine interaction calculated from the theory, however, was much too low when compared with the value estimated from the experimental data. It is possible that part of this difference is due to the neglect of spin polarization effects. Proton hyperfine structure was resolved on each of the lines due to the ^{75}As nucleus. For the case with the c axis of the crystal orientated parallel to the magnetic field five lines were observed in the intensity pattern of 1:4:6:4:1. This supported the viewpoint that the radical is AsO_4^{4-} hydrogen-bonded to other tetrahedra units in the crystal. (auth)

36885 THE CATALYTIC DECOMPOSITION OF HYDROGEN PEROXIDE ON THE γ-IRRADIATED NICKEL OXIDE. Yamashina, Toshiro; Sano, Masakatsu (Hokkaido Univ., Sapporo). Nippon Kagaku Zasshi, 87: 553-6 (June 1966). (In Japanese).

Catalytic decomposition, surface excess oxygen, and electric conductivity of γ-irradiated nickel oxide as a function of radiation dose were studied. Catalytic activity and surface excess oxygen increased linearly with radiation dose. Electric conductivity decreased with dose, in spite of increasing the excess oxygen of nickel oxide, a p-type semiconductor. The active sites of irradiated nickel oxide are discussed. (auth)

36886 NUCLEAR RECOIL AND RADIATION EFFECTS ON METAL PHTHALOCYANINES. Merz, E. (Kernforschungsanlage, Juelich, Ger.). Nukleonik, 8: 248-52(June 1966). (In German).

Investigations were carried out on the phthalocyanines of 17 metals concerning the influence of nuclear recoil and radiation effects on the yields of separable radioactive metal atoms and their retentions. A broad comparison on many different elements revealed for the (n,γ), (n,2n) and (n,p) nuclear reactions as well as for β decay, isomeric transition and K-capture process characteristic relations of the available recoil energy, radiation chemical influences, charge and excitation of the atoms and molecules on chemical bond rupture and annealing. From the results the part repelling forces due to nuclear processes play in liberating metal atoms out of the phthalocyanine molecules could be realized. It was further established that foreign species present in the samples, particularly oxygen, strongly influence recombination reactions. Heating or prolonged evacuating of the compounds prior to neutron activation causes an increase in retention. Quantum radiation induces a relatively strong radiation decomposition of the phthalocyanine compounds, which is however superimposed by annealing. (auth)

36887 PHOTOCHEMICAL REACTION INDUCED IN BORATE GLASSES CONTAINING ARSENIC AND MANGANESE. Bishay, A.; Arafa, S. (Atomic Energy Establishment, Inshas, Egypt. American Univ., Cairo). Phys. Chem. Glasses, 6: 134-42(Aug. 1965).

The effect of ^{60}Co or reactor radiation on the optical absorption of some alkali borate glasses containing either manganese or arsenic or both was studied and the intrinsic absorption spectrum characteristic of glasses containing manganese is discussed according to the ligand field theory. A photochemical reaction was induced in glasses containing both manganese and arsenic when exposed to ^{60}Co or to reactor radiation and an absorption band characteristic of photo-oxidized Mn^{3+} ions was induced at about 2.4 ev (515 mμ). Growth curves, fading characteristics, and thermal bleaching behavior of the normal color centers and photochemically induced centers were studied. The photochemically induced centers were studied. The photochemically induced absorption band at about 2.4 ev was found to be stable and increased linearly in intensity with increasing total exposure which suggested its use for dosimetry. The effects of glass composition as well as the conditions of irradiation are also discussed. (auth)

36888 LINEAR ENERGY TRANSFER EFFECT IN RADIOLYSIS OF CYCLOHEXANE. Blackburn, R.; Charlesby, A. (Royal Military Coll. of Science, Shrivenham, Eng.). Proc. Roy. Soc. (London), Ser. A, 293: No. 1432, 51-69(July 5, 1966).

The effectiveness of iodine was studied under a range of conditions (concentration of iodine, phase, and temperature of cyclohexane) for γ radiation, and compared with that for α irradiation of liquid cyclohexane. The results showed that iodine is about equally effective in solid and liquid cyclohexane irradiated near the melting point, but is far less effective for low temperature irradiation, followed by warming. It is also less effective for α irradiation. The data are compared quantitatively with calculated values for a one-radical diffusion model, with good agreement. Reaction constants consistent with this model agree with those obtained directly from pulse radiolysis, while the estimates for the dimensions of α ionizing tracks are in conformity with these generally assumed in the radiolysis of water. The much lower efficiency of radical scavenging observed with α radiation is directly related to the linear energy transfer effect frequently observed in radiobiology. The

existence of a nonscavengeable (i.e., non-protected) fraction is explained without any necessity to invoke a different radiation mechanism. (auth)

36889 EFFECT OF GAMMA RADIATION ON NICKEL, ZINC AND SILVER CHELATES OF α, β, γ, δ-TETRAPHENYLPORPHINE. Araki, Chiroru; Yamamoto, Kiyoko; Tokunaga, Chiho (Inst. of Physical and Chemical Research, Tokyo). Rika Gaku Kenkyusho Hokoku, 40: 45-9(1964). (In Japanese).

The γ radiolysis of nickel, zinc, and silver chelates of α, β, γ, δ-tetraphenylporphine (Ni-, Zn-, and Ag-TPP) in dioxane (10^{-4} mole/l) was studied spectrophotometrically in the visible region. Ni-TPP and Zn-TPP were easily reduced, and were decomposed by atomic hydrogen generated from dioxane by γ radiation. However, with Ag-TPP, the silver–nitrogen bond was first broken and α, β, γ, δ-tetraphenylporphine was released. The TPP was then reduced to α, β, γ, δ-tetraphenylchlorine (TPC) and decomposed. With Zn-TPP, products of two kinds were observed and isolated, i.e., zinc chelate of TPC and that of TPC derivative in which the chlorine ring was substituted. In Ni-TPP the first product (nickel chelate of TPC) was easily converted to the TPC derivative and only the second product was isolated. Opening of the porphyrine ring began earlier in Ni-TPP than Zn-TPP. (BBB)

36890 EFFECTS OF PROCESS VARIABLES ON THE TELOMERIZATION OF ETHYLENE WITH CARBON TETRACHLORIDE INDUCED BY γ RADIATION. Takehisa, Masaaki; Yasumoto, Masahiko; Hosaka, Yoshinobu. Tokyo Kogyo Shikensho Hokoku, 61: 169-77(May 1966). (In Japanese).

The telomerization of ethylene with carbon tetrachloride induced by γ radiation is described. The experiments were carried out in a batch system with a reactor of 300 ml and a 2,000-C ^{60}Co radiation source. A series of compounds with the general formula $CCl_3(C_2H_4)_nCl$ was obtained under the following conditions: temperature of reaction –16 to 120°C, initial pressure of ethylene 15 to 80 kg/cm^2, total dose 1 to 10 Mrad. The reaction was inhibited by oxygen contained in commercial ethylene. The induction period was proportional to the inverse of dose rate. The rate of ethylene consumption was nearly proportional to the amount of ethylene in the reaction system, and was proportional to the dose rate in 0.63 power. An increase in the reaction temperature increased the G (telomer) to 200 to 2,000 and the apparent activation energy of this reaction was about 3 kcal/g·mole. Telomers of n = 2 and n = 3 in the general formula were obtained as main products of this reaction, and the reaction period had little effect on the distribution of the products. The products with the same average degree of telomerization had the same distribution of telomers, even if they were formed under different conditions of reaction. (auth)

36891 TELOMERIZATION OF ETHYLENE WITH CARBON TETRACHLORIDE INDUCED BY γ RADIATION UNDER CONSTANT ETHYLENE PRESSURE. Takehisa, Masaaki; Yasumoto, Masahiko; Hosaka, Yoshinobu. Tokyo Kogyo Shikensho Hokoku, 61: 182-9(May 1966). (In Japanese).

The difference between the telomerization of ethylene with carbon tetrachloride induced by γ radiation under a constant ethylene pressure and the same reaction in a batch system was studied. Essentially the same methods were used as in the previous work. The reaction rate was proportional to 0.78 power of the dose rate in place of 0.63 power in a batch system. The initial rate of consumption of carbon tetrachloride was represented by the following experimental equation (initial rate of consumption of CCl_4) = $K\{12 - [CCl_4]/[C_2H_4]\}$. The K in the experimental equation was found to increase with temperature, while the Arrhenius plot of K gave an apparent activation energy of 4.2 kcal/g·mole. As the reaction proceeded, the average degree of telomerization was found to increase by 11%. The maximum yield of n = 2 telomer was increased at a lower reaction temperature over the temperature range of 10 to 100°C. (auth)

36892 REACTION OF BUTENE-1 WITH PHOSGENE INDUCED BY γ RADIATION. Takehisa, Masaaki; Yasumoto, Masahiko. Tokyo Kogyo Shikensho Hokoku, 61: 190-5(May 1966). (In Japanese).

The reaction of butene-1 with phosgene induced by γ radiation was carried out in the temperature range from –78 to 35°C and total dose range of 10 to 50 M rad. The main products were 1-chlorobutane, 2-chlorobutane, 1,2-dichlorobutane, C_8-olefins, and monochlorooctanes. Ketones and acidic substances were also formed in the high boiling fractions. The maximum yield of the crude products was obtained at about 0.5 mole fraction of phosgene. The rate of the reaction was proportional to the 0.93 power of the dose rate, and the temperature dependence of the rate of reaction was equivalent to 1.3 kcal/g·mole of an apparent activation energy. These products and the effect of reaction conditions on the distribution of the products strongly suggests that the reaction proceeds by a free radical mechanism. A telomerization mechanism characterized by a chain transfer to phosgene is unprobable. A high activation energy for abstraction of Cl atoms from phosgene molecules and relatively low activation energy for a degradative chain transfer to butene-1 may be responsible to the results. (auth)

36893 EFFECT OF γ RADIATION ON FLOTATION PROPERTIES OF ANIONIC COLLECTOR AGENTS. Lebedev, A. T.; Orel, M. A.; Uchurkhanov, M. M. Tsapkov, N. T.; Klyueva, E. D.; Kartushin, V. P.; Rozen'fel'd, S. Sh.; Mal'tseva, I. I. (Inst. of Nuclear Physics, Uzbek Academy of Sciences, USSR. Central Asian Scientific Research Inst. for Geology and Mineral Deposits, USSR). Tsvetn. Metal., No. 5, 19-21(May 1966). (In Russian).

Experiments were carried out for improving the capacity of anionic flotation collectors. Samples of sodium oleate, tall oil, and potassium butyl xanthate were irradiated by means of a ^{60}Co γ source at a dose rate of 100 R/sec. Flotation tests were carried out with pure minerals, such as fluorite, calcite, alumite, pyrochlore, ilmenite, chalcopyrite, and bornite and with commercial ores. The results indicated that at total doses within 1000 to 10,000 R the collector capacity of sodium oleate is strongly increased by the irradiation. In the case of oxyhydride type collectors, the increase in capacity was found to be directly proportional to the consumption of the agent; this is probably due to the γ-induced dispersion of the collector and prevention of micelle formation which in turn results in improved extraction of the minerals. Properties of the mercapto-type collectors were not affected by the irradiation. Extraction of phosphates from phosphorite ores by means of tall oil was improved by the irradiation of the latter because micelle formation was reduced or completely prevented. (TTT)

36894 RADIATION-CHEMICAL PRODUCTION AND OPTICAL ABSORPTION SPECTRA OF ORGANIC SULFUR RADICALS IN ORGANIC GLASSES AT-196 DEG C. Wendenburg, J.; Moeckel, H.; Granzow, A.; Henglein, A. (Hahn-Meitner-Institut fuer Kernforschung, Berlin). Z. Naturforsch., 21b: 632-42(July 1966). (In German).

Organic disulfides, mercaptans, sulfides, and hydrogen sulfide were exposed to γ radiation in glasses of methyltetrahydrofuran or hydrocarbons at –196°C. Absorptions were observed, which are attributed to either radicals of the type RS· or to addition complexes of these radicals to S-containing molecules or ions (for example to RS–SR$^-$ radical ions). In the case of disulfides, the S-radicals were produced by dissociative capture of electrons from the ionization of the glassy solvent. In the case of mercaptans, the sulfur radicals were formed via H-abstraction by free radicals from the radiolysis of the solvent, when the irradiated glasses were slowly warmed up. HS was formed this way in H_2S-containing irradiated glasses. The electron capture in benzyl mercaptan, dibenzyl disulfide, and dibenzyl sulfide partially led to the benzyl radical. Several absorption bands were observed, which are tentatively attributed to negative ions: $C_6H_5SH^-$

from phenyl mercaptan (8100 Å), $C_6H_5SC_6H_5^-$ from diphenyl sulfide (broad absorption over the visible range), and $C_6H_5CHS^-$ from dibenzyl sulfide (~3900 Å). Carbon tetrachloride simultaneously present in the glass was found to inhibit all reactions of free electrons, while the reactions of free radicals during warming were not suppressed. Glass of a methylcyclohexane-isopentane mixture containing olefines were found to absorb strongly between 7000 and 9000 Å. These absorptions are attributed to positive ions. The absorption of ionized or protonated olefines occurred at longer wavelengths with decreasing number of H-atoms at the carbon atoms of the double bond. Absorptions of positive ions were also observed in the case of diphenyl disulfide (8500 Å), and of diallyldisulfide (6840 Å). Small amounts of substances that can readily be protonated (such as n-propanol or methyltetrahydrofuran) decrease the intensity of the absorption bands of positive ions. (auth)

36895 ANOMALOUS POSITIVE EFFECTS OF PRELIMINARY IRRADIATION. I. ANOMALOUS EFFECTS OF BACKGROUND RADIATION. Bogomolov, K. S.; Gruz, E. A. Zh. Nauch. Prikl. Fotogr. Kinematogr., 10: 266-72 (July-Aug. 1965). (In Russian).

The light-sensitivity of a fine-grained film (average diameter of 0.34μ) was studied as a function of a previous irradiation dose with x rays, electrons, and light. X rays gave a slight positive effect; electrons gave a slightly larger positive effect, and light increased the film sensitivity by a factor of 3 with a previous, optimum irradiation dose. The light sensitivity attained a value of $S_{0.2}$ = 55 to 60, which was very high. On using a mixed emulsion containing fine-grained and coarse-grained crystals in various ratios, it was found that a slight previous irradiation with light increased the sensitivity as compared to a previous irradiation with x rays or electrons. At high background film densities it was noted that a previous light irradiation acted to decrease the light sensitivity more strongly than x rays and electrons did. This behavior is explained by the greater thickness of the film layer which could be irradiated more uniformly with x rays than with light. (TTT)

36896 THE LIFETIMES OF POSITRONIUM IN POLYMERS IRRADIATED BY GAMMA RAYS. Chandra, Girish; Kulkarni, V. G.; Lagu, R. G.; Thosar, B. V. (Tata Inst. of Fundamental Research, Bombay). 7p. (CONF-650721-16). ORAU. Gmelin, AED-CONF-65-211-16.

From Positron Annihilation Conference, Detroit.

The variation of the slow component of the lifetime of positrons annihilating in Teflon and polyethylene as a function of the dose of gamma irradiation of the samples is reported. The results are shown for each polymer and are qualitatively interpreted in terms of the damage caused to the structure of the polymers by gamma radiation. (J.F.P.)

36897 EFFECTS OF HIGH-ENERGY RADIATION ON INORGANIC SUBSTANCES. A Symposium Presented at the Fifth Pacific Area National Meeting, American Society for Testing and Materials, Seattle, Wash., Nov. 2-3, 1965. Amer. Soc. Test. Mater., Spec. Tech. Pub., No. 400, 1-170 (1966). (CONF-651147).

Each of the eight papers is abstracted separately. (D.H.M.)

For abstracts of individual papers see: 36898—36905.

36898 THERMAL DECOMPOSITION OF IRRADIATED MERCURIC OXALATE. Prout, E. G.; Moore, D. J. (Rhodes Univ., Grahamstown, South Africa). Amer. Soc. Test. Mater., Spec. Tech. Pub., No. 400, 1-16(1966).

The thermal decomposition of unirradiated mercuric oxalate and the effects of pre-irradiation by x rays, γ rays, and sunlight were examined. Pre-irradiation accelerated the subsequent decomposition in all cases. Considerable radiolysis occurred when using γ rays, but there was no detectable loss in weight when using sunlight or x rays. The effects of γ rays and light on the thermal decomposition were similar in that an initial burst of gas preceded the main accelerator and decay periods. The initial reaction was studied in detail in each case and activation energies determined. (auth)

36899 RADIOLYTIC DECOMPOSITION OF CRYSTALLINE ALKALI METAL AND ALKALINE EARTH BROMATES. Chase, John W.; Boyd, George E. (Oak Ridge National Lab., Tenn.). Amer. Soc. Test. Mater., Spec. Tech. Pub., No. 400, 17-43(1966).

Yields from bromate ion decomposition and production of oxidizing fragments, bromide ions, and oxygen gas in the radiolysis of crystalline alkali metal and alkaline earth bromates by ^{60}Co γ rays, neutrons, and ^6Li fission recoil particles were determined as a function of dose, temperature, and dose rate. The oxidizing fragment yields were strongly temperature dependent. At high doses the oxidizing fragment concentrations tended to "steady-state" values dependent on the irradiation temperature. The yields of the radiolytic products were dependent on the nature of the cation of the salt but were independent of the dose rate. Bromate decomposition and oxidizing fragment yields for the alkali metal bromates in the reactor irradiations were the same as observed with ^{60}Co γ rays except for the lithium salt. The production of high LET (linear energy transfer) tritons and α particles by ^6Li fission gave a significantly larger yield for $LiBrO_3$. The initial decomposition mechanism did not appear to change with increasing LET. The data were consistent with the hypothesis that bromide ion, bromite ion, oxygen gas, and possibly BrO_2 were formed directly by the dissociation of excited or ionized bromate, whereas hypobromite and some bromide ions were formed via precursors. At large absorbed doses or at irradiation temperatures above 300°C, the radiolysis of bromate ion went effectively to bromide ion and oxygen gas. (auth)

36900 THERMAL DECOMPOSITION OF GAMMA-IRRADIATED BARIUM AZIDE. Prout, E. G.; Moore, D. J. (Rhodes Univ., Grahamstown, South Africa). Amer. Soc. Test. Mater., Spec. Tech. Pub., No. 400, 45-74 (1966).

The thermal decomposition of ground dehydrated barium azide was examined. The sigmoid pressure-time plots were fitted in the temperature range from 110 to 140°C by the Avrami-Erofeyev equation, $-\ln(1-\alpha) = (k_1t)^4$, and the contracting sphere formula in the acceleratory and decay periods, respectively. Activation energies were determined for the induction, acceleratory, and decay periods. The essential role of barium metal in the thermal decomposition was demonstrated and a theoretical explanation of the decomposition mechanism presented. Preirradiation with γ rays (^{60}Co) drastically reduced the induction period and increased the velocity constants. The effects of increasing the γ dose were studied and activation energies determined. The kinetics of the main decomposition are considered to be the same as for the unirradiated salt. The processes occurring during the induction period with unirradiated and preirradiated BaN_6 are different. Electrical conductivity measurements of irradiated and unirradiated pellets were made in the temperature range from 20 to 60°C. The conductivity increased after irradiation. (auth)

36901 LOW-TEMPERATURE ANNEALING PROCESSES IN ALKALI HALIDES. Royce, B. S. H. (Princeton Univ., N. J.). Amer. Soc. Test. Mater., Spec. Tech. Pub., No. 400, 75-91(1966).

Simple point defect configurations may be produced in alkali halides such as KBr by irradiation with x rays at temperatures attainable with liquid helium. An understanding of their thermal stability aids in interpretation of the mechanisms of radiation damage. Experiments are discussed in which the stability of single negative ion vacancy-interstitial pairs are examined as a function of temperature and the presence of impurities in the KBr lattice. The order of the annealing processes indicates that the first three stages in pure KBr are correlated recombinations between the vacancies and interstitials and a fourth stage, the recombination of more distant defect pairs through a free migration of an interstitialcy. The presence of a Cl^- impurity in KBr stabilizes the x-ray-produced defects and arguments are advanced to show that this is the result of substitution of Cl^- interstitials for Br^- interstitials as a result of radiation damage processes. These ideas are applied to the formation processes of di-negative ion vacancy

centers, and an apparent discrepancy between simple geometrical probability arguments and experiment is resolved. (auth)

36902 ELECTRON SPIN RESONANCE SPECTRA OF RADIATION-DAMAGED INORGANIC CRYSTALS. Morton, J. R. (National Research Council, Ottawa). Amer. Soc. Test. Mater., Spec. Tech. Pub., No. 400, 93-119(1966).

Irradiation of inorganic materials frequently causes paramagnetic fragments to be trapped in the crystalline matrix. These fragments (radicals) may be studied by ESR. This technique is described briefly and isoelectronic radicals are compared. The discussion of diatomic radicals trapped in irradiated alkali halides is followed by that of the more complex species, which may be trapped in irradiated oxy and fluoro salts. (auth)

36903 RADIATION-INDUCED DECOMPOSITION OF SOME INORGANIC SULFATES. Huang, Suei-rong (Long Island Univ., New York); Johnson, Everett R. Amer. Soc. Test. Mater., Spec. Tech. Pub., No. 400, 121-38(1966).

The radioinduced decomposition of Na_2SO_4, $Na_2SO_4 \cdot 10H_2O$, $MgSO_4 \cdot 7H_2O$, $ZnSO_4 \cdot 6H_2O$, $CuSO_4 \cdot 5H_2O$, $Cr(SO_4)_3 \cdot 15H_2O$, $Cr_2(SO_4)_3$ (aq), $NiSO_4 \cdot 6H_2O$, $MnSO_4 \cdot H_2O$, and $CoSO_4 \cdot 7H_2O$ were studied. Oxidation of the cation occurred only in $NiSO_4 \cdot 6H_2O$ and $MnSO_4 \cdot H_2O$. Reduction of the SO_4^{2-} occurred only in $NiSO_4 \cdot 6H_2O$. The remaining sulfate hydrates decomposed to yield H_2 and O_2 only in very low yields. A mechanism is given to explain the observed results. (auth)

36904 ACTIVATION AND SINTERING BEHAVIOR OF CALCIUM OXIDE. THE EFFECT OF COPPER X-IRRADIATION ON THE SURFACE AREA OF THE OXIDE PRODUCED BY THERMAL DECOMPOSITION. Mikhail, R. Sh. (A'in Shams Univ., Cairo). Amer. Soc. Test. Mater., Spec. Tech. Pub., No. 400, 139-54(1966).

The effects of copper x radiation on the activity of the produced oxide in lime-burning was studied. Copper x irradiation of the parent material did not cause any variation of the surface area of the starting material or its decomposition products. But irradiation of partially or completely dehydrated products resulted in measurable changes of the surface area. These changes were traced for products heated under vacuum at different temperatures for fixed durations, and for products heated at constant temperatures for various durations. The results are discussed mainly to show the effect of irradiation on the different stages followed by a solid during thermal decomposition; these stages are dissociation, recrystallization, packing, and sintering, and a possible interpretation is presented. (auth)

36905 DICHROISM IN R-BANDS INDUCED IN γ-IRRADIATED POTASSIUM CHLORIDE CRYSTALS. Damm, J. Z. (Inst. of Physical Chemistry, Wroclaw). Amer. Soc. Test. Mater., Spec. Tech. Pub., No. 400, 155-70(1966).

The dichroism in R-bands is measured by applying various excitation and measurement conditions. The different spectra of R bands indicate that the oscillator strength of the R_F band should be about 50% higher than those of the R_1 and R_2 bands. Kinetic measurements of the dichroism growth showed a good agreement with the first-order kinetic equation, suggesting that this effect appears as a result of simple reorientation of R centers. The distribution of individual optical transition moments of R centers observed in ⟨100⟩, ⟨110⟩, and ⟨111⟩ directions was compared with that resulting from the van Doorn model; the results showed a satisfactory agreement with the latter. Some observations point to the possibility of interaction effects between various trapped-electron centers, leading to a dichroism "forced" in absorption bands of centers not subjected to excitation. (auth)

36906 METHOD FOR GRAFTCOPOLYMERIZING HIGHLY SUBSTITUTED CELLULOSE-MALEATE. Sakaguchi, Jiro (to Nippon Rayon Co., Ltd.). Japanese Patent 1965-8911. May 10, 1965. Filed Aug. 24, 1962.

A method is proposed for obtaining a new graft-copolymer which is different from the usual graft-copolymer of cellulose or cellulose derivatives. The cellulose produced can be used not only as a fiber but also as a moldable resin. Highly substituted cellulose is acetylyzed to the mixed esters of cellulose acetate and maleate. Then, vinyl compounds are graft-polymerized with the initiators of polymerization, or by an ionizing radiation, in organic solvents which swell or dissolve the mixed esters. (NSA of Japan)

36907 METHOD OF PRODUCING IMPROVED POLYCARBONATE. Oya, Shinzo (to Teijin Ltd.). Japanese Patent 1965-9630. May 17, 1965. Filed Feb. 7, 1962.

Either before or after molding, an unsaturated cross-linking agent is added to the polycarbonate, which is then irradiated with an ionizing radiation to yield an efficiently cross-linked polycarbonate. (NSA of Japan)

36908 METHOD FOR PRODUCING GRAFT POLYMERS. Uemura, Kiyoshi (to Furukawa Electric Co., Ltd.). Japanese Patent 1965-9964. May 21, 1965. Filed June 7, 1962.

A method is proposed for graft-copolymerization in the gas phase in which the graft yield and the grafting rate can be increased without enhancing the homopolymerization. The reaction is carried out between vinyl compounds and mixed gases after irradiation in the presence of an oxidizing gas. The substrate consists of a polymeric material. (NSA of Japan)

36909 ELECTRON SPIN RESONANCE STUDIES OF SOME SIMPLE RADICALS TRAPPED IN KRYPTON. Morehouse, Robert Lyman. Durham, N. C., Duke Univ., 1965. 125p.

Thesis.

Three related phenomena are studied: energy migration in inert gas matrices at 4.2°K, transfer of this migration energy to a sample molecule trapped in the matrix, and the nature of the free radicals formed from the molecules by the transferred energy. The molecules chosen for this investigation were the volatile hydrides: diborane, methane, silane, germane, stannane, ammonia, phosphine, arsine, stibine, hydrogen sulfide, and hydrogen selenide. The principal investigations were made with a krypton matrix. A few observations were made with neon, argon, and xenon when these results seemed to be pertinent to the problem. The energy migration was detected by the observation of free radicals produced from these hydrides by the ionizing radiation. A K-band electron-spin-resonance spectrometer was used. The samples were irradiated and studied while immersed in a liquid helium bath. A cobalt-60 γ source was used for the irradiation. The electron spin resonance spectra of several free radicals not previously studied were obtained. These radicals were GeH_3, SnH_3, PH_2, atomic arsenic, and a spectrum from diborane. The hyperfine constants and g factors were determined for these radicals. Evidence was obtained from the study of the CH_3 spectrum on the hindered rotation of the methyl radical at 4.2°K in several matrices. SiH_3, GeH_3, and SnH_3 also gave evidence of rotation at 4.2°K, and the axes of rotation were deduced. Some consideration is given to the nature of the energy migration process. A model that uses excitons to carry the energy through the inert gas crystal lattice is considered in the light of the energy migration observed. Some general properties of the process were determined. (Dissertation Abstr.)

36910 RECOMBINATION OF HYDROGEN AND OXYGEN IN THE PRESENCE OF WATER VAPOR UNDER THE INFLUENCE OF RADIATION. Benjamin, Benny Moses. Minneapolis, Univ. of Minnesota, 1964. 203p.

Thesis.

The gamma-ray induced recombination of hydrogen and oxygen in the presence of large amounts of water vapor at temperatures above boiling was studied using ^{137}Cs γ rays. Water was the reaction product. Mixtures of hydrogen and oxygen were analyzed in amounts less than one micromole by gas chromatography. Ethylene gas was used as the gas dosimeter. The reaction rate was found to be first order in the hydrogen concentration, increased with oxygen concentration though at a decreasing rate and appeared to be linear at low water concentration. At higher concentrations (>0.3 g/l) the rate becomes almost constant decreasing

slightly with water concentration. Increasing dose rates cause the reaction rate to increase though at a decreasing rate. The rate is independent of temperature up to 280°F (138°C) but appears to increase with temperature above this value. The reaction rate could be expressed in terms of either one of two rate equations, one giving a better fit to the experimental data than the other. The initial yields $G^0(H_2O) = G^0(-H_2)$ were found to be 3.0 to 6.0 for most of the runs. $G^0(H_2O)$ increases linearly with hydrogen concentration, is of the Langmuir type for oxygen concentrations, and decreases with absorbed dose rate and with water concentration (>0.3 g/l). Some of the experimental observations were explained in terms of the elementary steps proposed for radical reactions in the hydrogen-oxygen systems. (Dissertation Abstr.)

36911 GAMMA RADIOLYSIS OF AQUEOUS STANNOUS CHLORIDE–HYDROCHLORIC ACID SOLUTIONS. Hatch, Richard Calder. Durham, N. H., Univ. of New Hampshire, 1963. 94p.

Thesis.

Certain important points in connection with the study of the gamma radiolysis of aqueous stannous chloride–hydrochloric acid solutions are brought out. The primary radiation yields, g(H), g(OH), $g(H_2)$, and $g(H_2O_2)$ appear to be essentially constant over the acid concentration range of 0.4 molar to 3.0 molar. Within these concentration limits, g(H) = 3.65, g(OH) = 2.92, $g(H_2)$ = 0.45, $g(H_2O_2)$ = 0.80. The quantitative determination of Sn(IV) in the presence of Sn(II) is feasible employing a polarographic analysis with a supporting electrolyte of 2.0 molar ammonium chloride, 1.0 molar hydrochloric acid, and 0.01% gelatin. The production of hydrogen gas during the radiolysis of aqueous stannous chloride–hydrochloric acid solutions, like that of Sn(IV), is a linear function of the radiation dose. The radiation yields of stannic tin and hydrogen gas, G(Sn(IV)) and $G(H_2)$, are markedly dependent on the initial stannous chloride concentration between 5×10^{-4} molar and 6×10^{-3} molar and independent of this reactant concentration between 6×10^{-3} molar and 10^{-2} molar. The hydrolysis products of Sn(II) play an important role in the radiation-induced reaction when the hydrochloric acid concentration is in the vicinity of 0.5 molar. The observed hydrogen gas yields, $G(H_2)$, are considerably greater than the primary yield, $g(H_2)$. The hydrogen radical reacts in two ways with the Sn(II) species. One involves an oxidation: $Sn(II) + H + H^+ = Sn(III) + H_2$. The other involves a reduction: $Sn(II) + H = Sn(I) + H^+$. The relative effectiveness of these two opposing processes depends on the initial conditions for the reaction. A mechanism is proposed to explain the radiation chemistry of the aqueous stannous chloride–hydrochloric acid system. (Dissertation Abstr.)

36912 EFFECT OF GAMMA RADIATION ON CONDUCTIVITY OF ELECTROLYTE SOLUTIONS. Rosenfeld, Judy Vadasz. Los Angeles, Univ. of California, 1965. 262p.

Thesis.

Experiments were performed to observe changes due to gamma rays in the conductivity of an electrolyte solution during irradiation. These experiments consisted of conductivity measurements before, during, and after insertion into a radiation field. Cupric, zinc, and nickel sulfates, cupric, ferric, and chromic nitrates, and cupric perchlorate in water were investigated. Concentrations varied from 0.005F to 0.02F. The experimental data indicate that the change depends on the cation. Nickel and zinc cause a decrease, and Cu, Fe, and Cr an increase in the resistance during irradiation. The results obtained with Ni and Zn sulfates lend support to Baxendale's interpretation of pulse radiolysis data. The divalent cation is reduced to the unusual univalent cation, most of which is oxidized by the radiation-induced OH radical to the divalent state, and a small fraction is disproportionated to the metal ion in zero valency state. There is a resulting increase in H^+ concentration, causing a decrease in the resistance of the solution. From details of the conductivity change during irradiation, an estimate of the unknown reaction rate constant for the reaction $M^+ + M^+ \rightarrow M^{2+} + M^0$ was made. For Zn, the reaction rate constant is about $5-8 \times 10^3$ liters mole^{-1} sec^{-1}, and for Ni $< 6 \times 10^2$ liters mole^{-1} sec^{-1}. The reaction rate constant for the reaction $M^+ + H^+ \rightarrow M^{2+} + H$ is about $500-650$ liters mole^{-1} sec^{-1} for Zn, and <650 liters mole^{-1} sec^{-1} for Ni. The increase in the resistance of solutions of cupric, ferric, and chromic salts may be understood in terms of a two-electron transfer between the radiation-induced ferrous, cuprous, and chromous ions and hydrogen peroxide, as proposed by Cahill and Taube, and a very small reaction rate constant for the dissociation reaction $M(OOH)^{+n} \rightarrow M^{+n} + HO_2$. (Dissertation Abstr.)

36913 THERMOLUMINESCENCE OF SOME CARBONATES, ThO_2, AND $BaTiO_3$. Angino, Ernest E. (Univ. of Kansas, Lawrence). 19p. (CONF-650637–9). ORAU. Gmelin, AED-CONF-65-151-13.

From International Conference on Luminescent Dosimetry, Palo Alto, Calif.

Thermoluminescent studies suggested the feasibility of utilizing luminescent properties of carbonates, ThO_2, and $BaTiO_3$ for dosimetry purposes in the range from 1×10^5 to 5×10^5 R. Tests beyond this range were attempted and suggest the range may be extended to 2.0×10^6 R. The carbonate minerals of Ca, Ba, Sr, Mg, and Zn (calcite, witherite, strontianite, magnesite, and smithsonite, respectively) are thermoluminescent. $SrCO_3$ is several times more sensitive to radiation than the others. Replicate runs on $MgCO_3$ after irradiation with 470×10^3 R show good reproducibility of peak temperatures and intensities. Preliminary results suggest that the structure of the carbonates may well have considerable effect on the thermoluminescence observed in the different materials. A large symmetrical glow peak was found in unirradiated thoria (ThO_2) at 195 ± 5°C. After irradiation with ^{60}Co γ irradiation of 10^4 to 10^6 R, a smaller peak appeared at 65 ± 5°C. The intensity of the 195 ± 5°C peak is a direct linear function of radiation dosage in the range 10^4 to 10^6 R. No indication of peak saturation was observed up to 10^6 R. Decay studies established the 195°C peak to be the result of a first order reaction. (auth)

36914 METHOD FOR PRODUCING POLYMER OF DIOXASPIROHEPTANE BY IONIZING RADIATION. Tashiro, Shiegeki (to Japan Association for Radiation Research on Polymers). Japanese Patent 1965–19193. Aug. 27, 1965. Filed June 25, 1962.

A method is proposed for producing a polymer of dioxaspiroheptane by irradiating with an ionizing radiation such as from Co-60 at below 100°C without the use of a ring-opening catalyst. Dioxaspiroheptane is a difunctional cyclic oxide and is easily polymerized by ring opening with an ionic catalyst of acidic nature such as BF_3 to give a polymer of high molecular weight with three-dimensional reticulated structure. The poly(dioxaspiroheptane) decomposes at above 800°C without melting due to its high crystallinity and the three-dimensional reticulated structure. In addition, the polymer is insoluble in almost all the organic solvents. (NSA of Japan)

Radiochemistry

See also Separation Processes and Procedures

Refer also to abstract 37041.

36915 (N–66–17678) DESIGN AND APPLICATIONS OF β-EXCITED X-RAY SOURCES. Ezop, J. J.; Stinchcomb, T. G. (IIT Research Inst., Chicago, Ill.). 1966. 10p. CFSTI $1.50 cy, $1.25 mn.

An experimental survey on β-excited x-ray production is summarized which uses sources of several energies, targets of various thicknesses and atomic numbers, and various geometries. Results are interpreted, applied to the design of prototypes, and utilization of strontium-90 and promethium-147 source designs is discussed. These investigations indicate that β-excited x-ray sources are extremely useful complements to presently existing machines. Smallness of size makes the sources very attractive for field and other uses where the use of conventional x-ray equipment

is not feasible. Another advantage is the relative monochromatic output of these sources; limitations are related to the limited photon outputs per unit source area. (STAR)

36916 SYNTHESIS OF SOME TRITIUM-LABELLED MUTAGENIC ALKYL ALKANESULFONATES. Wachtmeister, C. A.; Pring, B.; Osterman, Siv; Ehrenberg, L. (Univ. of Stockholm). Acta Chem. Scand., 20: 908-10 (1966).

Methyl-T, ethyl-2-T, and isopropyl-1,3-T methanesulfonates were synthesized on a semi-micro scale in high yields from commercially available tritiated alcohols, which were allowed to react with methanesulfonic anhydride. The tritiated esters were stored as 0.1% solutions in dry light petroleum to minimize autodecomposition, which was determined, and to facilitate withdrawal of small samples from the stock solution. Gas chromatographic analyses were performed on the esters, and the radiation chemical stability of each was evaluated. (J.G.B.)

36917 THE BEHAVIOR OF ^{131}I IN POLYMETATELLURIC ACID IRRADIATED IN THE NUCLEAR REACTOR. Teofilovski, Cedomir. Bull. Boris Kidrich Inst. Nucl. Sci., 17: 17-27(Jan. 1966).

Polymetatelluric acid, whose composition is $(H_2TeO_4)_n$, was successfully used as a target for obtaining ^{131}I in the reactor. It was prepared by heating orthotelluric acid in air at 160°C or in a stream of water vapor at 208°C. Analysis of the valency states of ^{131}I in irradiated $(H_2TeO_4)_n$ prepared in either of these ways showed a variable ratio of reduced and oxidized forms. A considerable increase of the reduced forms with increasing integral thermal neutron flux during irradiation in the reactor in the given interval was also observed. In order to explain the above phenomenon, $(H_2TeO_4)_n$ was irradiated in the reactor under different conditions, with measurement of the wall temperature of the quartz ampoules containing the target material. Yields of reduced and oxidized forms of ^{131}I were determined immediately after irradiation and after annealing of the target at temperatures from 60 to 150°C. A considerable decrease in the yield of the reduced forms of ^{131}I on target annealing above 100°C was observed. (auth)

36918 INVESTIGATION OF THE INTERACTIONS THAT OCCUR BETWEEN I_2 RADIONUCLIDES AND AN IRON OXIDE AEROSOL IN THE RESPIRABLE SIZE RANGE. Craig, Douglas K. (Univ. of Rochester, N. Y.). Health Phys., 12: 1047-67(Aug. 1966).

Aerosols, whether pre-existing in the atmosphere or generated in a nuclear incident, represent surfaces to which radionuclides that escape into the environment can become attached. The importance of the relationship between adsorbed activity and aerosol particle size is discussed. The conclusions from previous studies, most of which have utilized the decay products of radon and thoron as radionuclides, are contradictory. In the present work, a labeled iron oxide aerosol was allowed to interact with radionuclides consisting of ^{131}I—as molecular iodine. The Goetz Aerosol Spectrometer was used to characterize the adsorption of the iodine onto the aerosol as a function of particle size. Relative radionuclide-aerosol concentrations were varied from 3×10^2 to 3×10^5 molecules per particle. The following conclusions were drawn from these experiments: first, the adsorbed activity appeared to be proportional to the function d^z of the particle diameter, where $2 \leq Z \leq 3$, over the approximate size range $0.06 < d < 1.2\ \mu$; secondly, even at the lowest radionuclide concentration used ($9 \times 10^{-6}\ \mu g\ I_2/1$), some of the iodine seemed to be present in the form of very small particulates ($<0.01\ \mu$), a factor which complicated interpretation of the above result; thirdly, the adsorption of iodine onto surfaces was at least partially reversible; and finally, variation of the experimental conditions over a considerable range did not significantly affect the results. (auth)

36919 AGGREGATED ^{99m}Tc-LABELED ALBUMIN FOR LUNG SCINTISCANNING. Gwyther, Myfanwy M.; Field, E. O. (Royal Marsden Hospital, Sutton, Eng.). Int. J. Appl. Radiat. Isotop., 17: 485-6(Aug. 1966).

The chemical steps involved in labeling albumin with ^{99m}Tc and subsequent aggregation of the particles, were studied in detail. Temperature, pH, and albumin concentration were critical in producing uniform aggregates of the required size. For undetermined reasons, a few massive particles appeared among aggregates that were largely of the correct size. The value of ^{99m}Tc-labeled aggregates for studies of lung pathology is emphasized. Anterior and posterior scans were compared. (J.G.B.)

36920 NEW DIRECT METHOD FOR PREPARING CARRIER-FREE $H_2{}^{35}SO_4$ FROM REACTOR-IRRADIATED POTASSIUM CHLORIDE. Suarez, C. (Junta de Energia Nuclear, Madrid). Int. J. Appl. Radiat. Isotop., 17: 491-3(Aug. 1966).

Sulfur-35 was separated as SO_2 when neutron-irradiated KCl was added to a reducing mixture of H_3PO_4 and mercury. Yields were quite satisfactory. The concentration of hard β-emitters in the product was less than 0.01%. Possible radiochemical impurities were separated from irradiated KCl and distillate. (J.G.B.)

36921 PREPARATIONS OF ^{14}C-LABELED POLYOXYETHYLENE (20) SORBITAN MONOLAURATE AND THEIR METABOLIC FATE IN RATS. Nelson, M. F.; Poulos, T. A.; Gongwer, L. E.; Kirschman, J. C. (Atlas Chemical Industries, Inc., Wilmington, Del.). J. Food Sci., 31: 253-8(Mar.-Apr. 1966).

A method is described for the preparation of both fatty-acid-^{14}C-labeled and polyoxyethylene-^{14}C-labeled polyoxyethylene (20) sorbitan monolaurate, which is known also as Tween 20 and as polysorbate 20 and is referred to as PSML. After optimum conditions were established, fatty-acid-labeled sorbitan monolaurate, the intermediate compound, was prepared by condensing 0.53 g of fatty acid (containing 1.5 mC of dodecanoic acid-1-^{14}C and commercial lauric acid used in production of PSML) and 0.511 g of crystalline sorbitol in the presence of disodium phosphate catalyst for 2 hr at 250°C. The resultant sorbitan monolaurate-^{14}C was then condensed with 2.9 g of nonradioactive ethylene oxide using 6 mg of fused sodium oleate catalyst. The reaction was run at 155°C and 25 psi until all ethylene oxide had reacted (about 6 hr). The product, fatty-acid-labeled PSML-^{14}C, had a specific activity of 0.355 mC/g. Polyoxyethylene-labeled PSML was synthesized by condensing 1.0 g of nonradioactive sorbitan monolaurate from regular production with 2.9 g of ethylene oxide containing 1.5 mC of ethylene oxide-1,2-^{14}C. The reaction was run at 155°C and 25 psi until all ethylene oxide had reacted (about 6 hr). The resultant labeled emulsifier had a specific activity of 0.341 mC/g. Following oral administration in rats the ester bond between the polyoxyethylated polyol and fatty acid moieties undergoes almost complete hydrolysis, with the fatty acid portion being metabolized in a manner similar to that for trilaurin. The ether linkage between the polyoxyethylene chain and the hexitan molecule is not disrupted appreciably, and this polyoxyethylene-polyol emulsifier moiety is only slightly absorbed. None of the polyol moiety is stored in the body of the animal. (BBB)

36922 SYNTHESIS OF 2,4,7-TRIAMINO-6-PHENYLPTERIDINE (TRIAMTERENE) LABELED WITH TRITIUM OR ^{14}C. Blackburn, D.; Burghard, G. (Smith Kline and French Labs., Philadelphia). J. Label. Compounds, 2: 62-6(Jan.-Mar. 1966).

The diuretic drug triamterene was labeled with carbon-14 by condensing the intermediate phenylacetonitrile-1-^{14}C with 2,4,6-triamino-5-nitrosopyrimidine. The tritiated triamterene was prepared by direct synthesis from toluene-3,4-^3H and toluene-3-^3H. The ^3H-toluenes were prepared in excellent radiochemical yield by hydrolyzing the dry Grignard reagent of the appropriate bromotoluene with tritium oxide. (auth)

36923 ADSORPTION OF ^{32}P ONTO GLASS WALL. Suzuki, Hideyo Radioisotopes (Tokyo), 14: 111-15(Mar. 1965). (In Japanese).

Experiments were carried out to investigate factors and conditions that influence the removal of ^{32}P from bottle

walls. Factors and conditions investigated and reported are as follows: storage time, temperature in removal treatment, time consumed in removal, kind of glass, method of washing, use of ultrasonic vibration, use of a surface active agent, solvents (e.g., HCl, H_3PO_4, NaH_2PO_4 and Na_2HPO_4), concentration and pH of the solvents, use of glucose, sucrose, sugar, dextrin, starch, gelatin, active carbon, CMC, etc., instead of the solvents, repeated treatments, removal of carrier-bearing ^{32}P, and concentration of the ^{32}P. Removal efficiencies were calculated from the radioactivities before and after treatment. (TCO)

36924 THE RADIOCHEMICAL MANUAL. SECOND EDITION. Wilson, B. J. (ed.). Amersham, Eng., The Radiochemical Center, 1966. 327p. 50s.

A guide is presented for those who use radioactive substances professionally. The book deals with substantial physical data of the more commonly used isotopes, their properties, and their usefulness for special purposes. Discussions are included on how radioisotopes and related products are made; characteristic problems and features of radioactive materials; safety and waste disposal; packaging and carriage; and regulations of ownership and use. A bibliography to the literature available on radioisotopes is included. (50 tables). (P.C.S.)

Separation Processes and Procedures

See also Analytical Procedures
ISOTOPE TECHNOLOGY — Separation and Production

Refer also to abstracts 36731 and 37166.

36925 (HW–82771(Pt.3)) RECOVERY OF ALUMINUM NITRATE NONAHYDRATE FROM REDOX ACID WASTE. PART 3. MATHEMATICAL DESCRIPTION. Godfrey, W. L.; Dean, R. Y.; Stouffer, J. C. (General Electric Co., Richland, Wash. Hanford Atomic Products Operation). Dec. 1965. Contract AT(45-1)-1350. 33p. Dep. mn. CFSTI $2.00 cy, $0.50 mn.

A rigorous mathematical model was developed for the recovery of aluminum nitrate monohydrate from Redox acid waste by crystallization from a concentrated nitric acid solution. A countercurrent crystallization process was developed, which permits multiple stages of crystallization without requiring the separation of crystals and supernate following each stage. Bench-scale investigations and analog computer studies of the process were performed previously. The major additional contributions of the rigorous model are considerations of shrinkage and expansion due to temperature changes, the volume occupied by crystals, washover from cell-to-cell of crystals during the backwash, dissolution of crystals by unsaturated backwash stream, and inclusion of contaminants within the crystal or as a tightly adsorbed layer. (M.C.G.)

36926 (K-L-6091) FLUID-BED VOLATILITY COMPONENT, ENGINEERING FEASIBILITY, AND SCALE-UP STUDIES AT THE OAK RIDGE GASEOUS DIFFUSION PLANT. Smiley, S. H.; Pashley, J. H.; Brater, D. C. (Oak Ridge Gaseous Diffusion Plant, Tenn.). [nd]. Contract W-7405-eng-26. 31p. (CONF-660905-1). Dep. mn. CFSTI $2.00 cy, $0.50 mn.

From 36th International Congress on Industrial Chemistry, Brussels.

Fluid-bed volatility processes for recovering uranium and plutonium from spent nuclear reactor fuels appear promising because of the relatively low process waste volumes, excellent probable decontamination, and apparent mitigation of criticality problems. Conceptual plant studies and evaluation of plant-scale component designs are being performed at the Oak Ridge Gaseous Diffusion Plant. Equipment items, including the fluid-bed reactors, are tested on a semiworks scale using nonirradiated, uranium materials to confirm design assumptions and to evaluate the scale-up problems. Gas compressors, piping connectors, valves, filter media, sorbent trapping systems, and solids transfer equipment, are also included in the test plans. Preliminary results are given for filter media, compressor, and connector tests; and some construction materials studies are discussed. (auth)

36927 (ORNL-TM-1543) REMOVAL OF PROTACTINIUM FROM MOLTEN FLUORIDE BREEDER BLANKET MIXTURES. Barton, C. J.; Stone, H. H. (Oak Ridge National Lab., Tenn.). June 1, 1966. Contract W-7405-eng-26. 24p. Dep. mn. CFSTI $2.00 cy, $0.50 mn.

Three types of experiments involving removal of protactinium from molten fluoride breeder blanket mixtures were performed. Addition of thorium oxide to an $LiF-BeF_2-ThF_4$ mixture containing a tracer concentration of ^{233}Pa (less than 0.1 ppB) precipitated the protactinium and treatment of the mixture with HF redissolved the protactinium. Equilibration of molten $LiF-ThF_4$ containing 26 ppM of ^{231}Pa with a lead–thorium alloy resulted in removal of 99% of the protactinium from the salt phase but only a fraction of the reduced protactinium was found in the molten metal. A small amount of protactinium was transferred from the molten metal to a salt mixture by hydrofluorination treatment. Exposure of solid thorium metal to molten $LiF-ThF_4$ containing 20 to 30 ppM of ^{231}Pa precipitated 81 to 98% of the protactinium. More than half of the reduced protactinium was found in the unfiltered salt mixture, probably associated with small metal particles produced by the preliminary HF treatment of the mixture followed by hydrogen reduction. Again, hydrofluorination of the mixture redissolved the protactinium. Efforts are continuing to find container materials to improve the retention of protactinium in molten lead or bismuth. (auth)

36928 PREDICTION OF DISTRIBUTION COEFFICIENTS OF Pu(IV) DURING EXTRACTION WITH TBP. Estrada, J.; Diaz Nogueira, E.; Lopez Perez, B. An. Real Soc. Espan. Fis. Quim. (Madrid), Ser. B, 62: 231-45 (1966). (In Spanish).

A method was developed that enables distribution coefficients of Pu^{4+} between aqueous nitric acid and tributyl phosphate to be calculated. Its workability is confined to temperatures between 20 and 30°C and an upper limit for concentration (5g/l) and ionic strength (6). An equation was derived, which gives the mean activity coefficient of $Pu(NO_3)_4$ as a function of the ionic strength of the solution. The mean activity coefficient of $Pu(NO_3)_4$ was determined by applying a correction similar to that of Harned. The influence of extractable and nonextractable nitrate on the mean activity coefficient of $Pu(NO_3)_4$ was studied by introducing a term in an equation deduced by an extension of Harned's rule. This term is a function of the nature of the cations present and the ionic strength of the solution. On the assumption that extraction of Pu^{4+} by TBP is described by the equilibrium: $Pu^{4+} + 4NO_3^- + 2TBP \rightleftharpoons Pu(NO_3)_4 \cdot 2TBP$, a method was worked out to calculate the distribution coefficient of Pu^{4+}. Factors taken into account include: mean activity coefficient of $Pu(NO_3)_4$, concentration of free nitrate ion at equilibrium in the aqueous phase, concentration of free TBP in the organic phase, volume increase of the organic phase once equilibrium is attained and thermodynamic distribution constant. The method was verified by checking calculated values against experimental ones found in the literature. (auth)

36929 DECONTAMINATION OF RADIOACTIVE RUTHENIUM BY CELLULOSE DERIVATIVE–BENTONITE FLOCCULATION. III. Ishiyama, Toshio; Matsumura, Takashi; Mamuro, Tetsuo. Ann. Rep. Radiat. Center Osaka Prefect., 6: 33-6(1965).

The decontamination properties of DEAE cellulose–bentonite flocculation were studied with respect to the removals of radioactive Ru(III), Ru(IV), Ru(VIII), and the complex of nitratonitroruthenium(IV) found in the acid waste stream from the fuel reprocessing of liquid wastes through solvent extraction. It was shown that DEAE cel-

lulose is an effective agent for bentonite–polyelectrolyte flocculation, and increased the removal of Ru(III), Ru(IV), and Ru(VIII) remarkably; the removal increased with oxidation number of Ru; and nitratonitroruthenium(IV) complex was effectively removed through the flocculation using only DEAE cellulose as coagulant. (auth)

36930 DECONTAMINATION PROPERTY OF COAL HUMIC ACID COLUMN. Matsumura, Takashi; Ishiyama, Toshio; Mamuro, Tetsuo. Ann. Rep. Radiat. Center Osaka Prefect., 6: 37-41(1965).

A column filled with coal humic acid extracted from oxidized coal was found to be effective in removing Cs, Sr, and Co from low-level waste water. When only very small amounts of foreign matter are present in the water to be decontaminated, $^{137}Cs-^{137}Ba$, ^{89}Sr, and ^{60}Co are satisfactorily removed by the humic acid column. In the presence of a high concentration of Na ions, however, the removal of $^{137}Cs-^{137}Ba$ and ^{89}Sr decreased quickly with increase in Na ion concentration, while the removal of ^{60}Co did not so much depend on Na ion concentration. In the presence of competing Ca ions, the removal of all these nuclides decreased relatively quickly with increase in volume ratio. (auth)

36931 ION EXCHANGE EQUILIBRIA IN THE SYSTEM OF URANYL SULFATE ION–Cl^- AND NO_3^-. Yano, Takeo; Kataoka, Takeshi (Osaka Univ.). Chem. Eng. (Japan), 29: 381-5(June 1965). (In Japanese).

Ion exchange equilibrium between uranyl sulfate and the Cl^- or NO_3^- type of Amberlite-IRA 400 was studied. The effects of SO_4^{2-} and UO_2^{2+} concentrations and pH on the equilibrium were investigated. If SO_4^{2-}/UO_2^{2+} is smaller than or equal to 15, the equilibrium curve is peculiar, having a discontinuity at the origin. The empirical equations for equilibrium in uranyl sulfate $-Cl^-$ and of $-NO_3^-$ systems are given as $(q/Q)/(1-q/Q)^2 = 590\ pH^{1.66}[SO_4^{2-}]^{-0.58}[UO_2^{2+}](C/C_0)/(1-C/C_0)^2$ and $(q/Q)/(1-q/Q)^2 = 450\ pH^{1.80}[SO_4^{2-}]^{-0.36}[UO_2^{2+}](C/C_0)/(1-C/C_0)^2$, respectively. The equilibrium constant, K_c, is dependent on the SO_4^{2-} concentration, pH, and UO_2^{2+} concentration. Uranyl sulfate ion may be regarded as having the form $UO_2(SO_4)_2^{2-}$ if the SO_4^{2-} concentration is sufficiently large. It was found that when separating and purifying uranium from H_2SO_4 solution with Cl^- or NO_3^- form resins, SO_4^{2-}/UO_2^{2+} must be larger than 15. (NSA of Japan)

36932 EXTRACTION OF ALKALIZED SOLUTIONS OF URANYL SALTS WITH TRIBUTYL PHOSPHATE. Baran, V.; Tympl, M.; Cakrt, E. (Inst. of Nuclear Research, Rez, Czech.). Collect. Czech. Chem. Commun., 31: 2382-8(June 1966).

From results of analyses of aqueous alkalized solutions of uranyl salts before and after extraction (total uranium concentration, concentration of unhydrolyzed uranyl, pH, and concentration of bound hydroxyl ions were determined), as well as from the absorption spectra of the organic phase (30 vol % of tributyl phosphate in hexane) after extraction it was concluded that uranium is extracted from the aqueous phase only in the form of solvates of the uranyl ion (but not of its hydroxo complexes). When extraction is less intensive, the absolute quantity of the hydroxo complexes in the aqueous phase does not change (their relative fraction increases), in the case of more intensive extraction the concentration of the hydroxo complexes increases absolutely as well as relatively. (auth)

36933 APPLICATION OF THE PRINCIPLE OF THE THRESHOLD CENTRIFUGE TO THE SIMULTANEOUS SEPARATION AND CONCENTRATION OF URANIUM COMPOUNDS. Makepeace, C. E. (Eldorado Mining and Refining Ltd., Ottawa). Electrochem. Technol., 4: 393-9(July-Aug. 1966).

Use of a threshold centrifuge for separation of UO_2 from oxides of Al, Ni, Fe, Ti, and Nb suspended in methyl iodide or methanol–NaI solutions is described. Autoradiography was used to determine the concentrations of U particles in relation to other particles in the centrifuge. (J.R.D.)

36934 EXTRACTION OF FISSION PRODUCTS FROM WATER BY FOAMING. Anokhin, V. L.; Zheverzheeva, V. F. Gig. Sanit., No. 3, 64-6(Mar. 1966). (In Russian).

Foaming experiments were run in glass columns 25 to 30 mm in diameter and 50 to 126 cm long with ^{91}Y, ^{144}Ce, ^{89}Sr, ^{90}Sr, ^{134}Cs, ^{106}Ru, ^{131}I, ^{95}Zr, and ^{95}Nb as tracers. An insoluble precipitate such as iron or aluminum hydroxide was formed at a pH of 7.0; a foaming agent such as gelatin, peptone, or sulfanol-B was added to the solution, and air was blown through the solution to create a foam. A total of 1200 experiments was run. The most complete removal of ^{90}Sr (95 to 99%) was obtained by foaming a calcium oxalate precipitate with gelatin. Only 85 to 90% of the ^{90}Sr was extracted with a calcium phosphate precipitate. Almost 100% of the ^{91}Y and ^{144}Ce was extracted with the aluminum and iron hydroxide precipitates. About 90% of the cesium was removed with a manganese ferrocyanide precipitate. Less than 50% of the ^{106}Ru could be removed with any precipitant. The liquid foamed over was 4 to 7% of the volume of the treated solution. (TTT)

36935 CATION EXCHANGE STUDIES OF THALLIUM(I) ON DOWEX 50W-X8: SEPARATION FROM MIXTURES. Rangnekar, Asha V.; Khopkar, S. M. (Indian Inst. of Technology, Bombay). Indian J. Chem., 4: 318-20(July 1966).

The cation exchange chromatographic behavior of milligram amounts of Tl(I) on Dowex 50W-X8(H form) was studied. Sulfuric acid, perchloric acid, sodium sulfate, and ammonium acetate are capable of desorbing 20.35 mg of Tl(I) from 1.4 cm × 19 cm bed. Tl(I) is separated from Cu, Cd, Al, Zn, Mn, Co, Ni, U, V, Ag, and Pb by selective elution. Anionic complexation with EDTA and citric acid is used for the separation of Tl(I) from Zr, Ce, Ba, Th, Bi, and Fe. The separation of Tl(I) from Sb and Sr was effected by taking advantage of the elution of these ions with 5% citric or tartaric acids; Tl(I) is recovered later by elution with 4M sulfuric acid after washing the column free of anions with water. (auth)

36936 PURIFICATION OF CERIUM BY ELECTRIC TRANSPORT COMBINED WITH ZONE MELTING. Amonenko, V. M.; Kruglykh, A. A.; Pavlov, V. S.; Mosova, L. N. (Inst. of Physics and Tech., Academy of Sciences, Ukrainian SSR). Izv. Akad. Nauk SSSR, Neorg. Mater., 2: 578-81(Apr. 1966). (In Russian).

Molten Ce samples were refined by passing a current of 5.3 amp/mm^2 in a vacuum for 50 to 150 hr. Impurities such as Fe, Si, Cu, and O moved to the cathode. The experiments were then repeated in He; after 200 hr, the amount of impurities remaining in the cathodic and middle portions of the sample dropped below the sensitivity limit of spectral analysis. The samples were then subjected to zone melting, whose effectiveness was found to increase when an electric current (6 amp/mm^2) was passed through the metal. The amount of impurities thus dropped from 0.245% in the initial sample to 0.085% in the refined product. Following the refining process, the microhardness of Ce decreased from 28 to 23.8 kg/mm^2. (auth)

36937 SOME ASPECTS OF SYNERGISM IN SOLVENT EXTRACTION. III. Am(III) AND Am(VI) IN NITRIC ACID. Zangen, M. (Israel Atomic Energy Commission, Yavne). J. Inorg. Nucl. Chem., 28: 1693-9(Aug. 1966).

Synergistic extraction of Am(III) and Am(VI) from 0.05 M HNO_3 was studied, using a combination of a monoacidic phosphate or phosphonate ester (the chelating agent) with tributyl phosphate (the synergist) at varying concentrations in carbon tetrachloride. Results are in agreement with previous extraction mechanisms; constants governing the extraction equilibrium are derived. (auth)

36938 STUDY ON THE EXTRACTION OF RARE EARTHS WITH TRIBUTYL PHOSPHATE. II. RARE EARTH EXTRACTION FROM KOLA APATITE. Werner, G.; Geseke, H.; Holzapfel, H. (Karl-Marx- Univ., Leipzig). J. Less-Common Metals, 11: 209-15(Sept. 1966). (In German).

Rare earths were extracted by tributyl phosphate from

concentrated nitric acid solutions of Kola-apatite breakdown. With increasing content of ammonium nitrate the distribution coefficients increased with increasing dilution of the tributyl phosphate they decreased. In an extractor with three ideal plates 76% of the rare earths was recovered by 80% tributyl phosphate. (auth)

36939 INVESTIGATION OF THE MECHANISM OF THE NH_4-LACTATE ELUTION SEPARATION OF TRACE LANTHANIDES. Bruecher, Erno; Szarvas, Pal. Magyar Kem. Foly., 72: 152-8(Apr. 1966). (In Hungarian).

During the separation of trace lanthanides on cation exchange columns, the charge number of the lanthanide ions diffusing in the resin phase changes suddenly from 3 to about 2 at a certain lactate concentration owing to the formation of lactate complexes. This drop of the charge number occurs at decreasing lactate concentrations if the atomic number of the lanthanide is higher. Ion-exchange reactions occurring in the separation process are given. Using an eluent flow rate of about 1 cm/min, the rate of ion exchange is determined by the rate of diffusion across the Nernst boundary layer, which does not affect the separation factors in any appreciable degree. The values of the separation factors are determined by the stability constants of the LnL_2^+ and LnL_3 complexes, and by the affinity of LnL^{2+} ions for the resin phase. (auth)

36940 SOLVENT EXTRACTION OF PROTACTINIUM AND OTHER ELEMENTS AS PHENYLARSONATES. Myasoedov, B. F.; Palshin, E. S.; Molochnikova, N. P. (Vernadskii Inst. of Geochemistry and Analytical Chemistry, Moscow). Zh. Anal. Khim., 21: 673-81(1966). (In Russian).

Solvent extraction of protactinium phenylarsonate with isoamyl alcohol from sulfuric, hydrochloric, and nitric acid solutions was studied. Protactinium is extracted practically completely with a 1% solution of the reagent in isoamyl alcohol from 0.1–9 N acid solutions. The effects of the reagent concentration, nature of the solvent, element concentration, and other factors on protactinium extraction from 5 N H_2SO_4 were investigated. Less than 10 mg/ml of Ni^{2+}, Mn^{2+}, Al, Bi^{3+}, La, Sb^{3+}, Sn(IV), Zr, and U(VI) and less than 1 mg/ml of Cr^{3+}, Fe^{3+}, Ti^{3+}, Ti(IV), and Th do not interfere with protactinium extraction from 5 N H_2SO_4. Solvent extraction of Zr, Nb, Fe, U, Th, La, and other elements was studied. It was found that U, Th, La, and Fe are not extracted under the experimental conditions. Extraction of Zr and Nb depends on their concentration. A new and effective method for separating protactinium from Fe, Zr, Nb, Ti, La, Po, Th and U was developed. The method was also used for purifying milligram amounts of ^{231}Pa from Fe, Nb, Zr, and other elements. (auth)

36941 EXTRACTION OF METALS FROM AQUEOUS SOLUTIONS OF HYDROHALIC ACIDS BY MEANS OF DIALKYLALKYLPHOSPHINATES. Navtanovich, M. L.; Chernyak, A. S.; Shemet, V. V. Zh. Neorg. Khim., 11: 184-90(Jan. 1966). (In Russian).

Investigations of extracting iron and rare earth metals from HCl and tantalum and niobium from HF using dialkyl alkylphosphonates (DAAPh) are reported, and data on the chemistry of DAAPh extraction of scandium are presented. A concept of the "relative effectiveness of extractants" ($RE_e^c = D_{e2}/D_{e1}$, where c = ratio of initial concentrations of solvent and metal, D_{e2} = distribution coefficient of the investigated solvent, and D_{e1} = distribution coefficient of known solvent) was formulated for evaluating new extractants. It was established that the extracting ability of DAAPh with alkyl radicals from C_3H_7 to $C_{12}H_{25}$ is directly related to the electron-donating properties of phosphoryl oxygen. These solvents were found much more effective than trialkyl phosphates in extractions from HF, RE_e^1 for Sc and Fe^{3+} being 2.2 and 1.5, respectively, for rare earth elements RE_e^{10} is ~3.5; for Nb, 1.5; and for Ta, ~1.4 to 2.4. (ATD)

36942 EXTRACTION OF THORIUM WITH DIISOAMYL METHYLPHOSPHONATE FROM NITRIC ACID SOLUTIONS. Ukraintsev, E. V.; Kashcheev, N. F. Zh. Prikl. Khim., 39: 513-22(Mar. 1966). (In Russian).

The extractive properties of diisoamyl methylphosphonate (DAMP) in the extraction of thorium from nitric acid solutions were studied. Since water and nitric acid are integral parts of these systems, their extraction with DAMP was also investigated. The diluents employed for the extracting agent were benzene, p-xylene, and CCl_4. DAMP solutions in xylene and benzene were found to be more effective extractants than tributyl phosphate. Extraction of HNO_3 with DAMP involves the formation of the complex $HNO_3 \cdot H_2O \cdot$ DAMP with K = 0.41 ± 0.03. Extraction of H_2O involves formation of a complex of the composition $n \cdot H_2O \cdot$ DAMP, where n depends on the DAMP concentration in xylene and is equal to 3 for 100% DAMP and 1 for ≤ 30% DAMP. The partition coefficient for the extraction of thorium from nitric acid solutions increases sharply with decreasing HNO_3 concentration; this may be explained by the equation $Th(NO_3)_4 \cdot 2DAMP + DAMP \rightleftharpoons Th(NO_3)_4 \cdot 3DAMP$. A comparative evaluation of the number of theoretical plates required for a 99% extraction of thorium with TBP and DAMP shows that use of the latter leads to a decrease in the size of the extraction apparatus. Water and weak ammonia solutions can be used for the reextraction of thorium from a 0.8 M solution of DAMP in xylene; the number of theoretical plates then varies from 1.2 to 3. (ATD)

36943 METHOD FOR REPROCESSING AN IRRADIATED NUCLEAR FUEL. Iwashita, Fumio (to Tokyo Shibaura Electric Co., Ltd.). Japanese Patent 1965-6680. Mar. 31, 1965. Filed Oct. 19, 1962.

In the proposed reprocessing method, fuel is first admixed with an inorganic adsorbent and then contacted with a previously treated neutral organic solvent containing no water, which has previously been treated with a mineral acid. The admixture is electrolyzed, and the fuel material is directly extracted into the solvent. Fission products are adsorbed onto the inorganic adsorbent at the same time. (NSA of Japan)

36944 REACTOR FUEL PROCESSING. Volume 9. Number 2. Lawroski, Stephen (ed.). One of the five Quarterly Technical Progress Reviews published for the Division of Technical Information, USAEC. Argonne National Lab., Ill., 1966. 77p. GPO $0.70 Domestic, $0.90 Foreign.

Developments in commercial aspects of fuel processing, research on aqueous processing, research on nonaqueous processing, waste disposal, production of uranium and its compounds, production of thorium and plutonium and their compounds, and safety in chemical processing are reviewed. Separate abstracts were prepared for 14 of the papers. (M.C.G.)

For abstracts of individual sections see: 36945–36954, 37205–37207, and 38538.

36945 COMMERCIAL ASPECTS OF FUEL PROCESSING. Mecham, W. J.; Jonke, A. A. Reactor Fuel Process., 9: 65-8(Spring 1966).

Fuel reprocessing plans are reviewed, and economics of the fuel cycle are considered. (13 references). (M.C.G.)

36946 PREPARATION FOR FUEL PROCESSING. Stevenson, C. E. Reactor Fuel Process., 9: 69-71 (Spring, 1966).

Graphite-matrix fuels may be prepared for processing by burning them in a fluidized bed or by oxidation in HNO_3 at high pressures. Sulfuric acid decladding of UO_2–PuO_2 mixed oxide fuels is unsatisfactory because of high losses of uranium and plutonium, but sheared fuel is readily dissolved in HNO_3 without the addition of fluoride. Uranium is readily leached by HNO_3 from the residue left by fluid-bed decladding of stainless-steel-clad UO_2 with HF–O_2 at 600°C. An alloy of uranium–2% zirconium was dissolved satisfactorily for processing in 6.6M HF along with zirconium containing a small amount of uranium. Protactinium is effectively scavenged from $Th(NO_3)_4$ solutions by precipitation of MnO_2. (auth)

36947 RESEARCH AND DEVELOPMENT ON AQUEOUS PROCESSING. Reactor Fuel Process., 9: 69-83(Spring 1966).

Fluid-bed and pressurized aqueous combustion processes for graphite-matrix fuels are described. Shear-leach, electrolytic decladding, and sulfuric acid preparation of oxide fuels are also discussed. Solvent extraction processes are considered. Thermal effects in ion exchange and the sorption kinetics of plutonium on Dowex 1-X4 were found to follow Fick's diffusion law. (31 references). (M.C.G.)

36948 SOLVENT-EXTRACTION PROCESSES. Stevenson, C. E. Reactor Fuel Process., 9: 72-4(Spring 1966).

Limited extraction of nitrosylruthenium nitrato complexes indicated that dibutyl cellosolve (DBC) should be a good diluent for tertiary amine solvents. The presence of nitroalkanes and carbonyl compounds in paraffinic diluents used in TBP processes is indicated. Plutonium may be extracted directly from a uranium–plutonium fuel solution in HNO_3 by extraction with Alamine 336 in DBC. In another process plutonium extracted by a tertiary amine is precipitated directly from the organic phase. Di-2-amyl 2-butyl phosphonate gives decontamination similar to that obtained with TBP in a Purex type process. (auth)

36949 PLANT AND EQUIPMENT DESIGN AND OPERATION. Paige, D. M. Reactor Fuel Process., 9: 75-82(Spring 1966).

Operation of a pilot-plant electrolytic dissolver for stainless steel cladding was demonstrated. An integrated-cell concept was developed for shear-leach processing. A pilot-scale facility for thorium fuel cycle development is described. Diagrams of the equipment are included. (M.C.G.)

36950 VOLATILITY PROCESSES. Barghusen, J. J. Reactor Fuel Process., 9: 84-93(Spring 1966).

The oxidation-fluorination process for treating uranium carbide fuels, pretreatment of carbide fuels for volatility processing, chloride volatility processing of UO_2 fuel, fluoride volatility processing of UO_2 fuel, separation of PuF_6 from UF_6, design of equipment for fluid-bed fluoride volatility processes, and preparation and properties of fluorides are discussed. (M.C.G.)

36951 MOLTEN-SALT FLUORIDE-VOLATILITY PROCESSING OF ALUMINUM-BASE FUEL ALLOYS. Mecham, W. J. Reactor Fuel Process., 9: 93-7(Spring 1966).

The molten-salt fluoride volatility process developed earlier for zirconium-base fuels was adapted to the processing of aluminum-base fuels. Fuel and salt charging, fuel dissolution, uranium fluorination, product purification and recovery, and pilot-plant runs with irradiated fuels are described. Removal of UF_6 and PuF_6 from molten salts is discussed. The chemistry of molten $LiF-BeF_2$ is reviewed. (M.C.G.)

36952 COMPACT PYROCHEMICAL PROCESSES. Burris, L.; Bennett, G. A. Reactor Fuel Process., 9: 97-105(Spring 1966).

Salt-transport processes, continuous extraction processes, salt-cycle processes, conversion of fluorides to oxides in molten-salt media, and dry processes for future fast reactor fuels are described. The EBR-II skull reclamation process and fused-salt electrolysis are also described. Purification and preparation of metals is discussed. (M.C.G.)

36953 EVALUATION OF REMOTE SYSTEMS. Mecham, W. J. Reactor Fuel Process., 9: 105-7(Spring 1966).

Remote systems for fuel-cycle operations are considered and some devices are described. (M.C.G.)

36954 SAFETY IN CHEMICAL PROCESSING. Barghusen, J. J.; Jonke, A. A. Reactor Fuel Process., 9: 132-5(Spring 1966).

Compatibility studies of anion-exchange resins are discussed. The thermal behavior of anion-exchange resin in nitric acid systems under Redox process conditions was investigated. (M.C.G.)

36955 FISSILE FUEL RECOVERY PROCESS. Wagner, J. I.; Singer, R. M.; Schweitzer, D. G.; Katz, H. M. (to U. S. Atomic Energy Commission). U. S. Patent 3,260,466. July 12, 1966.

A method of rupturing pyrolytic cladding on nuclear fuel elements is described, which consists of applying electric energy through the cladding in either wet or dry environment in an amount greater than 45 volt amp with a current density of about 0.6 amp/cm^2. (AEC)

36956 PYROLYTIC CARBON DECLADDING. Hatch, L. P.; Reilly, J. J.; Wirsing, E. (to U. S. Atomic Energy Commission). U. S. Patent 3,260,574. July 12, 1966.

A process is described for recovering uranium from pyrolytic-carbon-clad fuel elements by decladding the element in a fluidized bed of inert particles using a stream of oxygen with a temperature of about 675°C and thereafter reacting the exposed uranium in the bed with fluorine at a temperature ranging between 400 and 450°C. (AEC)

ENGINEERING

General

Refer also to abstracts 37306 and 38232.

36957 (DRI–2327) AXISYMMETRIC THERMOELASTIC PROBLEMS IN BISPHERICAL COORDINATES. Final Report No. 556-6605. Weese, John A. (Denver Research Inst., Univ. of Denver, Colo.). May 12, 1966. Contract AT(11-1)-1092, Subcontract No. 74-0777. 76p. (SC-CR-66-2057). Dep. mn. CFSTI $3.00 cy, $0.75 mn.

For Sandia Corp., Albuquerque, N. Mex.

Steady state, axisymmetric thermoelastic problems defined in the bispherical coordinate system are presented. The four basic types of problems treated are: (1) a half space containing a uniformly heated spherical cavity; (2) an infinite medium containing two heated spherical cavities of arbitrary size; (3) an eccentric, heated spherical shell; and (4) an infinite medium containing two, heated, spherical rigid liners of arbitrary size. An outline of the theoretical analysis, operating instructions for the computer programs developed, and extensive numerical results and a description of the stress distribution for each problem are included. (J.H.M.)

Applications of Nuclear Explosions

Refer also to abstract 37010.

36958 (PNE–511) CLOUD DEVELOPMENT STUDIES, Project PRE-SCHOONER II. Day, Walter C. (Army Engineer Nuclear Cratering Group, Livermore, Calif.); Rohrer, Robert (Lawrence Radiation Lab., Univ. of California, Livermore). Feb. 1966. Contract W-7405-eng-48. 29p. Dep. mn. CFSTI $1.50 cy, $0.50 mn.

Cloud development data are presented for the Pre-Schooner II high explosive cratering event conducted in a rhyolite medium in southwestern Idaho. Early base surge radius dimensions are given as a function of time in several directions, and are related to base surge cloud dimensions from past cratering experiments in alluvium and basalt. Measurements of base surge height, main cloud radius, and main cloud height are also given. Two new methods of cloud delineation are described: (1) a laser-radar technique, and (2) a fluorescent particle tracer technique. (auth)

36959 (PNE-603F) SURFACE MOTION MEASUREMENTS. Project DUGOUT. Terhune, R. W. (Lawrence Radiation Lab., Univ. of California, Livermore). Dec. 1965. Contract W-7405-eng-48. 116p. Dep. mn. CFSTI $2.00 cy, $0.75 mn.

Accelerometers and high-speed motion picture photography were used to measure the motion of the surface as it was thrown up by Dugout—a chemical row-charge cratering experiment in basalt, in which five 20-ton charges spaced 45 feet apart and at a depth of 59 feet were fired simultaneously. The experimental procedure for the surface motion measurements and the results obtained are described. Velocity profiles at various points on the rising "mound" of upthrown material from Dugout are presented and compared with those from another cratering experiment, Pre-Schooner Alpha, in which a single 20-ton chemical charge (equivalent to one of the five Dugout charges) was fired in the same basalt material as Dugout and at the same depth. (auth)

36960 (PNE–717F) ON-SITE RADIOLOGICAL SAFETY REPORT. Project SULKY. McClendon, Leslie (comp. and ed.) (Reynolds Electrical and Engineering Co., Inc., Mercury, Nev.). July 1965. Contract AT (29-2)-162. 59p. Dep. mn. CFSTI $2.00 cy, $0.75 mn.

A nuclear cratering experiment in hard rock, executed as a part of the program for the development of nuclear excavation, is described. The purposes of the experiment were: (1) to determine the distribution of radioactivity produced at a greater scaled depth than Danny Boy, which would provide basic input for the design of follow-on larger yield experiments in a similar medium; (2) to determine the concentration of certain radionuclides airborne at various distances; and (3) to produce crater mechanics information at a greater scaled depth than Danny Boy. Appropriate precautions were taken to protect individuals from unnecessary exposure to radiation. Remote radiation measurements were taken during and after the event by a telemetry system, and monitors with portable instruments surveyed the route into ground zero before other planned entries were made. The following measurements were taken and recorded: telemetry and portable instrument measurements of gamma dose rates, radionuclide concentrations in air, and alpha source, toxic gas, and explosive mixture concentrations. (R.C.K.)

36961 (UCRL–12229) EFFECTS OF UNDERGROUND NUCLEAR EXPLOSIONS ON NATURAL GAS WELL PERFORMANCE. Rodean, Howard C. (Lawrence Radiation Lab., Univ. of California, Livermore). June 23, 1965. Contract W-7405-eng-48. 17p. Dep. mn. CFSTI $1.00 cy, $0.50 mn.

A completely contained, underground nuclear explosion produces a cavity filled with gas (the vaporized nuclear explosive plus the shock-vaporized rock) and lined with a layer of melted rock. Beyond this cavity, the surrounding rock is crushed and fractured out to distances of several cavity radii. The crushed and fractured rock above the cavity generally collapses, forming a chimney several cavity radii in height. These phenomena have potential applications to the natural gas industry in increasing well productivity and in forming reservoirs for gas storage. It is shown that a chimney and fractured zone (with the dimensions and properties measured in and near the Hardhat chimney) increase the effective well radius to such an extent that the gas flow rate at early times may be increased approximately one order of magnitude. The rubble-filled chimney and adjacent fractured zone also add significant capability to a well in meeting intermittent peak load demands, and may be used as a gas storage reservoir. (auth)

36962 SALMON SEISMIC EXPERIMENT. Werth, Glenn; Randolph, Philip (Univ. of California, Livermore). J. Geophys. Res., 71: 3405-13 (July 15, 1966).

The Salmon nuclear detonation of October 22, 1964, had a nuclear yield of 5.3 ± 0.5 kt. The teleseismic magnitude was 4.35. P waves observed out to 2500 km show asymmetries in the propagation, with high amplitudes (mμ/sec), faster apparent velocities, and higher signal frequencies to the north and northeast than to the west. At teleseismic distances, many of the signals were very weak and could be identified with Salmon only because the time of detonation and expected arrival time were known. If a cavity were built of a size to fully decouple 5 kt at the Salmon site, theoretical calculations which include the nuclear shock predict a decoupling factor of about 170 or a magnitude of 2.1. If such a cavity were used for partially decoupling a 25-kt shot, the magnitude is predicted to be 3.1. Drilling back into the Salmon shot region revealed a standing shot cavity of 20,000 m^3, corresponding to a sphere of radius 17 meters. (auth)

36963 FREE-FIELD MOTION NEAR A NUCLEAR EXPLOSION IN SALT: PROJECT SALMON. Rogers, Leo A. (Univ. of California, Livermore). J. Geophys. Res., 71: 3415-26 (July 15, 1966).

Calculations (SOC computer code) of shock pressure, position, velocity, and material displacement were made for the Salmon detonation (design yield of 5 kt) based both

on results from the Gnome event (3.1 kt in salt) and physical properties measurements of the material in the shot region. Comparison of the calculations with experimental data gives agreement for peak pressure and peak velocity within 20 to 50% over the range calculated (1 to 600 meters). Calculations and observations agreed to within 1 to 10% for shock wave arrival times, to 25% for displacement of the salt at 300 meters, and to within 10 to 50% for ground surface motion directly above the shot. The calculations based on physical properties measurements from the shot region generally gave better agreement with the data than those extrapolated from the Gnome event. The central cavity apparently grew to a radius of 24 m during the initial dynamic stage and then contracted back to a radius of 17 meters after the shot. (auth)

36964 NUCLEAR DECOUPLING, FULL AND PARTIAL. **Patterson, Dan W. (Univ. of California, Livermore). J. Geophys. Res., 71: 3427-36 (July 15, 1966).**

An underground explosion in a cavity is said to be fully decoupled if the cavity is large enough for the explosion to produce only elastic motion in the walls; in a smaller cavity where the wall motion is elastoplastic, the explosion is said to be partially decoupled. The pressure histories on the walls of cavities in salt of suitable size for decoupling sources are calculated and used in computing the motions of the walls, including the effect of elastoplastic behavior of salt. From the motion of the cavity walls, seismic displacement potentials are calculated and compared with the measured close-in displacement potentials for the Salmon event (5 kt) and the Gnome event (3.1 kt) scaled to 5 kt, both tamped (tightly coupled) nuclear detonations in salt. The close-in decoupling ratios for salt thus obtained are 350 for Gnome data and 200 for Salmon data. The reduced displacement potential based on the Gnome measurement at 298 m and scaled to the 5-kt size of Salmon is found to be 40% above the measured Salmon value of 300 m; the Gnome measurement may have been in the inelastic region or it may have been influenced by stronger horizontal propagation due to bedding planes. Reduced displacement potentials are also calculated for shots of 100 tons, 0.5 kt, and 1 kt, all in a cavity volume for 100-ton decoupling. They are 0.47, 5.0, and 45 m^3, respectively, as compared with 80 m^3 for a 100-ton fully tamped shot. (auth)

36965 CRUSTAL SEISMIC MEASUREMENTS IN SOUTHERN MISSISSIPPI. **Warren, David H.; Healy, J. H.; Jackson, Wayne H. (Geological Survey, Denver). J. Geophys. Res., 71: 3437-58 (July 15, 1966).**

A seismic refraction survey was made in Mississippi along a line trending north from Ansley to Oxford. About 200 seismograms were recorded from 22 chemical explosions at 5 shot points spaced at intervals of about 50 km between Ansley and Raleigh. The Salmon nuclear event, fired in the Tatum salt dome, was also recorded at several locations. A measured average velocity of 3.0 km/sec, to approximate all of the shallow sedimentary rocks, was used in depth calculations. The first strong refraction arrival represents a layer of 5.0 km/sec at a depth ranging from 3.1 to 3.7 km, just under the unconformable boundary between the Upper and Lower Cretaceous sedimentary rocks. The crustal structure is complex below the Lower Cretaceous sedimentary rocks. A curved line could be fitted to the first arrivals between 15 and 150 km on each travel-time plot, increasing in apparent velocity from 4.9 to 6.9 km/sec. All first arrivals between the 5.0-km/sec lower sedimentary rocks and the higher-velocity lower crust are included in one layer, giving an average velocity of 5.9 km/sec for "basement." The basement structure shows a low point corresponding to the trough of the Mississippi salt basin between the Tatum dome and Raleigh and a broad high feature cresting south of McNeill. First arrivals determine an intermediate layer in which the velocity is 6.9 km/sec, typical of basalt, and which rises from a depth of 19 km at McNeill to 13 km near Raleigh. Strong events are apparently reflected from the M discontinuity at critical distances and beyond, and it is necessary to supplement meager first arrivals with the reflections to arrive at a delineation of the upper mantle. The average velocity in the upper mantle is 8.4 ± 0.3 km/sec, the average crustal thickness is 35 km, and the M discontinuity dips 3° toward the south from Raleigh to Ansley. The complicated crustal structure may be due to the intermingling of two major geotectonic trends, the Appalachian and the Ouachita. Low to zero values of regional free-air gravity anomaly indicate that the region is near isostatic equilibrium. For the crustal model to be in isostatic equilibrium, the density must increase in the upper mantle below southern Mississippi. A hypothesis is made that increasing density in the mantle may be the mechanism of formation of the Gulf Coast geosyncline. (auth)

36966 CALCULATION OF FIRST-ZONE P WAVE AMPLITUDES FOR SALMON EVENT AND FOR DECOUPLED SOURCES. **Springer, Donald L. (Univ. of California, Livermore). J. Geophys. Res., 71: 3459-67 (July 15, 1966).**

Theoretical calculations of the first half-cycle amplitudes of the P wave at 250 to 1000 km are made from source functions representing several types of nuclear explosions in salt. Specifically, they are Gnome scaled to 5 kt; Salmon; theoretical 25 kt detonated in a cavity built to fully decouple a 5-kt explosion; and theoretical 5 kt also detonated in a 5-kt cavity. The calculations consist of a series of convolutions of the source functions plus the attenuation operators plus the instrument response. Amplitude factors are calculated using Zvolinskii's near-front approximation for various assumed crustal models. Experimental amplitudes from Salmon fall below the amplitude curve for the scaled Gnome source. They are consistent with amplitudes for the Salmon source; therefore, head-wave propagation along the M discontinuity may occur in the eastern United States. This is not conclusive, however, since body-wave calculations might give amplitudes of equal consistency. Amplitudes calculated for the fully decoupled 5-kt source show a decoupling of 200. Those from the overdriven cavity source indicate that a partial decoupling of 80 can be gained by overdriving a cavity by a factor of 5. (auth)

36967 TRAVEL TIMES AND AMPLITUDES FROM THE SALMON EXPLOSION. **Jordan, James N.; Mickey, Wendell V.; Helterbran, Wayne; Clark, Don M. J. Geophys. Res., 71: 3469-82 (July 15, 1966).**

Salmon, an underground nuclear explosion in the Tatum salt dome in southern Mississippi, was seismically recorded throughout North America and at some overseas stations. Data are presented from 143 seismograph stations recording signals from the Salmon event. Travel times at smaller distances generally confirm the high upper mantle velocities indicated by Gnome as recorded in the eastern United States. Travel times for the area east of the Rocky Mountain front may generally be represented by the equation $t = \Delta/8.3 + 8$ seconds (Δ in kilometers); however, additional detail is shown indicating apparent velocities of up to 8.7 km/sec. In the 10 to 20° distance range multiple arrivals are apparent, and beginning near 16° late initial arrivals are observed which correspond to Jeffreys-Bullen travel time. Amplitudes were generally higher than expected for regional and for teleseismic distances but lower in the 13 to 22° range in the western United States. A revision to procedures for determining magnitudes is shown to be necessary. (auth)

36968 DETECTION, ANALYSIS, AND INTERPRETATION OF TELESEISMIC SIGNALS. I. COMPRESSIONAL PHASES FROM THE SALMON EVENT. **Archambeau, C. B.; Flinn, E. A.; Lambert, D. G. (Teledyne, Inc., Alexandria, Va.). J. Geophys. Res., 71: 3483-3501 (July 15, 1966).**

The travel times and amplitude spectra of first- and later-arrival P phases from the Salmon event are computed on the basis of polarization filter outputs. The interpretation of the P wave radiation field is made in terms of crust and mantle structure using the first- and later-arrival P phases and their amplitude spectra. The observed seismic field corresponds with that expected from a symmetric, purely compressive source. The essential features of the observed travel times and ampli-

tudes are explained in terms of regional mantle structures. These structures provide first-order fits to the observed data and are characterized by low-velocity zones which terminate with rapid and continuous increases in velocity near depths of 130 km. The velocity structures also show a strong velocity gradient near 330 km. The regional models differ most strongly in the relative extent and magnitude of the velocity decrease in the low-velocity zone. (auth)

36969 EPICENTER DETERMINATION FOR THE SALMON EVENT. Herrin, Eugene; Taggart, James (Southern Methodist Univ., Dallas). J. Geophys. Res., 71: 3503-6(July 15, 1966).

With data obtained from earthquakes and explosions before the Salmon event, it was possible to compute regional travel-time corrections and station corrections which reduced the location error for Salmon by a factor of 10 if times from all (91) stations were used, and by a factor of 2 if times from only distant stations were used. When all stations were used, the error was less than 2 km, and the 0.90 confidence ellipse had an area of about 100 km^2. The computation when times from 23 distant stations ($\Delta > 20°$) were used gave an error of less than 6 km, a 0.90 confidence ellipse of about 900 km^2, and a 0.75 confidence ellipse of 500 km^2. The latter ellipse covered the true location. (auth)

36970 POST-EXPLOSION ENVIRONMENT RESULTING FROM THE SALMON EVENT. Rawson, D.; Randolph, P.; Boardman, C.; Wheeler, V. (Univ. of California, Livermore). J. Geophys. Res., 71: 3507-21(July 15, 1966). (UCRL-14280(Rev.1)).

The Salmon event was a 5.3 ± 0.5 kt nuclear detonation at a depth of 827.8 m in the Tatum salt dome in Mississippi. The explosion created a nearly spherical cavity of radius 17.4 ± 0.6 m and vaporized and melted approximately 5.4×10^6 kg of rock which formed a puddle of recrystallized salt. At the time of penetration the cavity was under a partial vacuum with a pressure of less than 313 mb, and the temperature of its gases was about 205°C. Most of the explosion energy was in the form of heat distributed within 45 m of the shot point. Radioactive melt injected into cracks was observed as far as 37 m from the shot point, and radioactivity increased above background as far as 64 m. The wall rock was highly microfractured and contained some macrofractures. The most broken portion of the rock surrounding the cavity was observed in the region 39 to 50 m below shot point. The puddle at the base of the cavity was highly fractionated, with a high concentration of refractory radioactive species in the bottom few centimeters. Separation of ^{131}Xe in the cavity gas from the parent ^{131}I found in the puddle indicates that the puddle took 24 to 32 days to solidify. It is concluded that the resulting cavity is stable and could be used for an experimental investigation of full or partial decoupling; however, the material surrounding the cavity is less competent than it was before the shot, and the present strength and stress distribution of the rock are not known. (auth)

36971 ELECTRICAL TRANSIENTS OBSERVED DURING UNDERGROUND NUCLEAR EXPLOSIONS. Zablocki, C. J. (Geological Survey, Denver). J. Geophys. Res., 71: 3523-42(July 15, 1966).

Electric transients were recorded from eleven underground nuclear explosions at the Nevada Test Site and from one near Carlsbad, New Mexico. The electric field components are only a few microvolts per meter at distances less than 10 km from the shot point, and they generally decay approximately as the inverse cube of distance. Magnitudes are proportional to about the 0.4 power of yield. Two source mechanisms are considered: the formation of an elementary magnetic dipole by the conductive plasma expanding in the earth's magnetic field and the formation of an elementary electric dipole by radial asymmetry in the generation and absorption of β rays. The data accordingly were interpreted in terms of equivalent buried dipole sources. (auth)

36972 EXCAVATION WITH NUCLEAR EXPLOSIVES. PROMISE AND PROBLEMS. Johnson, Gerald W. (Univ. of California, Livermore). Phys. Today, 38-44(Nov. 1963).

The use of nuclear explosions to provide a crater or ditch for engineering purposes is discussed. The sizes and characteristics of the craters formed were found to depend on the magnitude of the charge, the depth of placement, the nature of the medium, and the spacing between charges. Plowshare events used in these studies are discussed. Problems with radiation release and shock waves are considered. (M.C.G.)

36973 PROJECT GASBUGGY: NUCLEAR APPLICATION FOR INCREASING PRODUCTION. Steen, Hugh F. (El Paso Natural Gas Co., Tex.). Proc. Pac. Coast Gas Ass., 56: 31-3(1965).

Use of nuclear explosions to increase recovery from low-productivity natural gas reservoirs is discussed. It was concluded that the extensive, thick natural gas reservoirs in the Rocky Mountain Region are most favorable for such an application and that a full-scale test should be performed in the Pictured Cliffs sandstone, at a site in the San Juan Basin in Northwest New Mexico. A 12-in.-dia explosive will be placed in a 16-in. cased hole 4,150 ft below the surface. The estimated amount of gas in place in this formation is ~5.28 billion cubic feet. (M.C.G.)

36974 ROCK BREAKING TAKES A GIANT STEP INTO THE SPACE AGE. Hansen, Spenst M.; Toman, John (Univ. of California, Livermore). Rock Prod., 68: 52-9(June 1965).

Use of nuclear explosions for rock breaking to form an "instant quarry" is discussed. Gross effects from underground nuclear explosions at various depths of burial are summarized. Tonnage of rock broken as a function of yield and depth of burst is shown. Some results from the Pre-Schooner Charlie, Neptune, Danny Boy, and Sulky experiments are presented. Fragment size distribution of broken rock was evaluated. Site selection, quarry layout, explosive emplacement, and costs of using nuclear explosives are considered. Shock and seismic effects and radioactivity release are discussed. (M.C.G.)

36975 NUCLEAR BLASTING FOR MINING AND LEACHING. Hansen, Spenst M. (Univ. of California, Livermore). World Mining, 18: No. 10, 53-63(Sept. 1965). (UCRL-14330).

The uses of nuclear explosives in the mineral industry as part of the Plowshare Program is considered. Topics discussed include the effects of deeply buried nuclear explosives, nuclear explosive emplacement and firing, nuclear cave mining, in situ leaching, and safety. (J.F.P.)

Facilities and Equipment

Refer also to abstract 37728.

36976 (DP-MS-66-45) HIGH-TEMPERATURE CARBON FOR IODINE ADSORPTION. Milham, R. C. (Du Pont de Nemours (E. I.) and Co., Aiken, S. C. Savannah River Lab.). Aug. 1966. Contract AT(07-2)-1. 18p. (CONF-660904-3). Dep. mn. CFSTI $1.00 cy, $0.50 mn.

For Presentation at 9th Air Cleaning Conference, Boston.

Adsorbers that reduce the probability of igniting existing types of activated coconut-shell carbon in some reactor confinement systems are being studied. A high-temperature coconut-shell carbon (ignition temperature ~530°C) was developed, and, in preliminary tests, meets specifications for the Savannah River Plant confinement system. A standardized procedure was developed to measure ignition temperature, to evaluate promising new types of carbon, and to evaluate effects of variables (such as air flow, bed depth, impregnants, plant service, and humidity) on ignition temperature. Results of these evaluations are reported. (auth)

36977 (NAA-SR-11944) DIGITAL COMPUTER STUDY OF THE DYNAMICS OF THE COMBINED ROTATING UNIT SHAFT-BEARING SYSTEM. Howard, J. M. (Atomics International, Canoga Park, Calif.). July 15, 1966. Con-

tract AT(11-1)-Gen-8. 38p. Dep. mn. CFSTI $2.00 cy, $0.50 mn.

The objectives, method of approach, and results of a digital computer rotordynamic analysis of the SNAP 2 Combined Rotating Unit-V are summarized. Bearing characteristics are in the form of curve fit equations based on empirical data. The effects of shaft bending, differences in fabrication and balancing tolerances, and varying orientation of the rotating magnetic load are evaluated. (auth)

36978 (NAA-SR-12001) ERRORS IN MEASUREMENTS OF BUILDING LEAKAGE DUE TO DYNAMIC TEMPERATURE EFFECTS. Nelson, C. T.; Greenfield, M. A.; Koontz, R. L. (Atomic International, Canoga Park, Calif.). Aug. 1, 1966. Contract AT-11-1-GEN-8. 19p. Dep. mn. CFSTI $1.00 cy, $0.50 mn.

A reference vessel method was used to analyze sources of errors in determining leakage rates of a containment structure. It was shown that the most serious errors do not arise from lack of precision in measuring absolute temperatures and pressures; rather, the largest errors were shown to be due to a combination of a temperature lag between reference vessel and containment structure, and from temperature fluctuations during the testing period. (auth)

36979 (ORNL-3972) TABLE OF THE RATIO B_0 B_{max} FOR MAGNET COILS WITH RECTANGULAR CROSS SECTION AND UNIFORM CURRENT DENSITY. Garrett, M. W. (Oak Ridge National Lab., Tenn.). Aug. 1966. Contract W-7405-eng-26. 9p. Dep. mn. CFSTI $1.00 cy, $0.50 mn.

The tables are given for coil parameters $1.02 \leq \alpha \leq 10.00$ and $0.05 \leq \beta \leq 10.0$. (M.O.W.)

36980 (TID-23270) DETERMINATION OF GAS BEARING STABILITY BY RESPONSE TO A STEP-JUMP. Elrod, H. G. Jr.; McCabe, J. T.; Chu, T. Y. (Franklin Inst. Research Labs., Philadelphia, Pa.). [1965]. Contract Nonr-2342(00). 49p. (I-A2049-27). Dep. mn. CFSTI $3.00 cy, $0.50 mn.

The stability of a gas bearing is treated by a new procedure in which the bearing film is characterized by its responses to step-jump displacements. Duhamel's theorem is invoked to generalize these step responses in a system of dynamical equations. Stability is determined by calculation of a "growth factor" for each degree of freedom. (auth)

36981 (Y-1546) HIGH-PRESSURE GAS MIXING FACILITY. Heatherly, J. L.; Garland, W. (Union Carbide Corp., Oak Ridge, Tenn. Y-12 Plant). Aug. 8, 1966. Contract W-7405-eng-26. 12p. Dep. mn. CFSTI $1.00 cy, $0.50 mn.

A high-pressure gas mixing facility was constructed in the Y-12 Plant. This facility can be used to prepare both binary and multicomponent gas mixtures with the minor component ranging in concentration from 5 ppm to any percent. A high-pressure pump allows mixtures to be prepared up to a volume of 220 cubic feet at a pressure of 2000 psi. (auth)

36982 MEGAGAUSS MAGNETS USING CAPACITOR DISCHARGES. Bitter, Francis (Massachusetts Inst. of Tech., Cambridge). 6p. (CONF-650922-21). ORAU. Gmelin, AED-CONF-65-285-3.

From 1st International Symposium on Magnet Technology, Stanford, Calif.

Plans are described for producing magnetic fields in the 1 to 5 megagauss range in single turn coils a few millimeters in diameter by the oscillatory discharge of a 20 kilojoule capacitor having a quarter period less than 1μsec. (auth)

Heat Transfer and Fluid Flow

See *also* PHYSICS — Fluid Physics and Thermodynamics

Refer also to abstract 38496.

36983 (ALO-3633-1) DEVELOP 1800-400F FIBROUS-TYPE INSULATION FOR RADIOISOTOPE POWER SYSTEMS. Quarterly Progress Report No. 1, March 1–June 30, 1966. Collins, J. O.; Pusch, W. G.; Davis, E. J.; Brailey, R. H. E. (Johns-Manville Research and Engineering Center, Manville, N. J.). July 1, 1966. Contract AT(30-1)-3633. 163p. Dep. mn. CFSTI $5.00 cy, $1.00 mn.

The development and evaluation of fibrous-type thermal insulation materials for use in radioisotopic power systems in the temperature range of 1800 to 400°F were studied. The theoretical heat transfer analysis of MIN-K-type insulations was completed, indicating in part methods to attain greater thermal efficiency. The initial screening of commercially available fibrous insulations was also completed, and candidates which should be considered further recommended. Thirty-five experimental MIN-K formulations were evaluated in part for handleability, strength, moldability, thermal conductivity, thermogravimetric analysis, and machinability. Processing techniques were a major concern. The equipment required for the final screening and detailed evaluation phases is described. (R.C.K.)

36984 (BNL-963) A SPACE-INDEPENDENT MODEL OF TWO-PHASE FLOW AND ITS APPLICATION TO EXPERIMENT. Shotkin, Louis M. (Brookhaven National Lab., Upton, N. Y.). Jan. 1966. Contract AT-30-2-GEN-16. 28p. Dep. mn. CFSTI $2.00 cy, $0.50 mn.

A space-independent model of a boiling hydraulic channel is presented. The model includes two empirical constants– the single-phase friction coefficient and the K-factor in Bankoff's slip ratio relation– and requires a knowledge of the steady-state relation between heat input and flow rate. Linearized analytical results are compared, with reasonably good agreement, with several transfer functions measured by Zivi, Wright, et al. in a boiling loop at atmospheric pressure using both natural and forced circulation. The necessity of applying a heat source correlation to the experimental data is discussed, and the role that the dynamic pressure plays is presented. The physical mechanism causing the experimentally observed hydraulic instability is shown to be an interaction between the transient flow and friction pressure drop in the two-phase region. The experimentally observed increase in unstable oscillation frequency with inverse boiling length is also shown analytically. The position of the boiling boundary in the channel is shown to be important in stability considerations. By comparing analytical results with experimental data of Wissler et al. and Becker et al., it is concluded that the least stable situation results when the boiling boundary is part-way up the channel. Since the position of the boiling boundary is directly related to the degree of subcooling, the existence of this crucial position is used to explain the influence of subcooling on stability. (auth)

36985 (EURAEC-1088) LIQUID VOLUME FRACTION IN ADIABATIC TWO-PHASE VERTICAL UPFLOW-ROUND CONDUIT. Topical Report No. 15. Alia, P.; Cravarolo, L.; Hassid, A.; Pedrocchi, E. (Centro Informazioni Studi Esperienze, Milan (Italy)). June 1965. Contract 060-61-7-RDI. 103p. (EUR-2040; CISE-R-105). Dep. mn. CFSTI $4.00 cy, $0.75 mn.

Work Performed under United States–Euratom Joint Research and Development Program.

Presented are the results obtained at CISE under the CAN-2 Research Program on liquid volume fraction with vertical upward flow of two-phase (gas + liquid) mixtures in adiabatic conditions. The experiments were carried out under the following conditions: geometry: round conduits 1.5 and 2.5 cm ID; fluids: argon, (gas phase), and water, and ethyl alcohol (liquid phase); gas flow rate: 15–100 g/cm² sec; liquid flow rate: 20–200 g/cm² sec; temperature: ~18–20°C; and pressure: up to 22 kg/cm². The results enable one to outline the dependences of liquid volume fraction upon the following parameters: specific mass flow rate, quality, gas density, surface tension, and diameter. An empirical correlation is discussed and compared with the available data in literature. (auth)

36986 (GEAP–5073) MULTIROD, FORCED-FLOW, TRANSITION AND FILM BOILING MEASUREMENTS. Kunsemiller, D. F. (General Electric Co., San Jose, Calif. Atomic Power Equipment Dept.). Feb. 1966. Contract AT(04-3)-189. 83p. (EURAEC–1657). Dep. mn. CFSTI $3.00 cy, $0.75 mn.

Work Performed under United States–Euratom Joint Research and Development Program.

A three-rod geometry with a triangular pitch was used in tests to obtain heat transfer data at three mass flows (1×10^6, 0.5×10^6, and 0.25×10^6 lb/hr-ft^2), three pressures (1000, 600, and 1400 psia), and a quality range of 19 to 75 percent. The effects of rod spacing and finned heat transfer surface were studied for the above conditions. A new effect was introduced when it was discovered that in Geometry I the portion of the rod facing the unheated channel produced CHF (critical heat flux) data which was approximately 10 percent higher than the data from the portion of the rod facing another heated surface. The effect of Geometry II was to decrease this factor from 10 percent to 6.5 percent without a significant change of the CHF conditions of Geometry I. Over the range of test conditions, the size of the transition region was found to vary from 5 to 15 percent of the CHF. This is a slightly larger range than was observed in the single-rod tests but is still indicative of a stable flow pattern. As predicted by the single-rod tests, the heat transfer coefficients were found to exhibit a strong space dependence until a sufficient dry wall length was attained. Once this dry wall length was attained, a fully developed heat transfer coefficient independent of space was observed. The addition of fins to the rods decreased the maximum temperature oscillation by 40 percent and improved the fully developed heat transfer coefficient by 15 percent or more. Better fin effectiveness may be achieved by increasing the ratio of fin height to hydraulic diameter. A long-term demonstration test with the rods operating in transition and film boiling for 101 hours was completed successfully. The findings of this test and the others are reported in detail. (auth)

36987 (NAA-SR–11949) EFFECTS OF SOME SURFACE AND SYSTEM CONTAMINANTS ON MERCURY POOL BOILING HEAT TRANSFER. Shimazaki, T. T. (Atomics International, Canoga Park, Calif.). July 15, 1966. Contract AT(11-1)-Gen-8. 62p. Dep. mn. CFSTI $3.00 cy, $0.75 mn.

The effects of some surface and system contaminants on mercury pool boiling heat transfer were investigated to: (1) explore the validity of the loss-of-adequate-wetting hypothesis proposed as an explanation for Mercury Rankine Program boiler deconditioning, and (2) determine to which contaminants the loss of wetting is attributable. The results indicate that loss of adequate wetting is the most likely cause of boiler deconditioning, and that the effect of oil contamination on loss of wetting is much more severe and permanent than air or water contamination. (auth)

36988 (TID–23261) SOME HYDRODYNAMIC CHARACTERISTICS OF BUBBLY MIXTURES FLOWING VERTICALLY UPWARD IN TUBES. Technical Report No. 5003-30. Rose, Sewell C. Jr.; Griffith, Peter (Massachusetts Inst. of Tech., Cambridge. Div. of Sponsored Research). Sept. 1964. Contract AT(30-1)-3301. 141p. (DSR–5003). Dep. mn. CFSTI $4.00 cy, $1.00 mn.

An investigation of bubbly flow was conducted in vertical plexiglass tubes using air and water at atmospheric pressure. The bubbly flow pattern is an entrance condition or a non-fully developed flow. A spontaneous changeover to slug or annular flow usually occurs if the channel is long enough. The experiments were performed in turbulent flow with superficial liquid velocities ranging from 5 to 30 ft/sec. The friction, hydrostatic, and momentum pressure drop were separated and analyzed individually with the aid of two new experimental measurements. These measurements were of the wall shear force and the momentum flux. The validity of these measurements was verified with numerous single-phase tests. Several different air–water mixing methods, with the air always being introduced at the wall, had no effect on the results. Recommendations are presented for the use of these results when applied to steam–water mixtures. (auth)

36989 (WAPD-TM–492) PRELIMINARY AIR-WATER MIXING TESTS. Pfennigwerth, P. L.; Steer, R. W. (Bettis Atomic Power Lab., Pittsburgh, Pa.). Aug. 1965. Contract AT-11-1-GEN-14. 26p. Dep. mn. CFSTI $2.00 cy, $0.50 mn.

Eddy diffusivity was measured for mixing in the wide direction of a 3.0×0.100-inch vertical duct with upflow, using a dye tracer in water and a helium tracer in air. Diffusion-type equations based upon a point source were used to analyze the data. Experimental techniques were investigated, and the method using the lateral profile of tracer concentration was found to be most satisfactory. An empirical correlation was obtained between Reynolds Number (V De/ν) and the dimensionless mixing number (E/V De). (auth)

36990 TWO-PHASE FLOW THROUGH APERTURES. Chen, P. C.; Isbin, H. S. (Univ. of Minnesota, Minneapolis). Energ. Nucl. (Milan), 13: 347-58(July 1966).

Analytical and experimental studies involving the discharge of saturated water from a reservoir directly through a variety of apertures are discussed. The inlet dia. of the apertures were $\frac{1}{2}$ and $\frac{1}{4}$ in., and the apertures consisted of short tubes and tapered, diverging sections. One tapered aperture had an inlet dia. of 1 in. The length-to-inlet dia. ratios varied from 2 to 4.6. The discharge of saturated water up to 200 psig was investigated. The test results indicate that no vaporization occurred in the immediate vicinity of the aperture opening and that the accelerating water flows produced a superheated liquid jet within the first portions of the aperture. The flashing that did occur over the length of the aperture produced a back-pressure within the aperture that restricted the discharge rate. For the diverging apertures, the backpressure phenomenon is consistent with estimations made from adaptations of the theory of free turbulent jets and the analysis on the thrusts created by the flows. Using the pressure difference between the initial pressure and the back-pressure in the orifice equation for all liquid flow, the mass flow rates and thrusts can be predicted. (auth)

36991 THE THERMAL CONDUCTIVITY OF HYDROGEN FOR PRESSURES UP TO 660 ATM AND TEMPERATURES BETWEEN 1.6 AND 74.6 DEG C. Hamrin, C. E. Jr.; Thodos, G. (Northwestern Univ., Evanston, Ill.). Physica, 32: 918-32(May 1966).

Thermal conductivity measurements were made for hydrogen using a coaxial cylindrical cell. These measurements were carried out at 1.6, 25.0, 50.2, and 74.6°C and pressures up to 660 atm. To eliminate convective and radiative contributions, the maximum temperature difference across the confined gas layer never exceeded 0.45°C. The accuracy of the resulting thermal conductivity values is estimated to be 2.5%. These values were used to test the available theoretical equations for predicting the effect of pressure on thermal conductivity. These equations result from a rigid spherical model, and all were found to be inadequate for representing the effect of pressure on this transport property for hydrogen. A nonlinear relationship between the residual thermal conductivity, $k - k^*$, and the reduced density, ρ_R, adequately represented the data for the four isotherms of this study for hydrogen and those previously reported in the literature for the gaseous and liquid states of this substance. Another relationship between $k - k^*$ and the quantity $(\partial P_R/\partial T_R)_{\rho R}$ was found to be linear on a log-log basis throughout the gaseous and liquid regions. These residual thermal conductivity relationships adequately define the effect of temperature and pressure on thermal conductivity for hydrogen. (auth)

36992 CRITICAL WATER BOILING IN A ROD-BUNDLE MODEL. Efimov, V. A. Teploenergetika, No. 1, 59-64 (Jan. 1966). (In Russian).

One of the characteristics of rods—division of straight-through cross sections into series of parallel cells with alternate gaps between surfaces—under the given condi-

tions does not introduce noticeable features in the regularity of critical boiling in comparison with pipes. Therefore, the conditions of critical boiling in rod bundles with $\underline{d}$ = 10 mm and $\underline{s}/\underline{d}$ = 1.4 can be calculated by dependence for pipes if, in the bundle, there is no noticeable inequality of the mean values of speed and enthalpy in discrete zones. Previous data make it possible to extend this result in the pressure range from 70 to 210 bar. The probability of the start of critical boiling under plates of remote-controlled lattice or in any portion of lattice boundary is greater than on the free surface. (tr-auth)

36993 NUCLEATE AND FILM BOILING HEAT TRANSFER TO NITROGEN AND METHANE AT ELEVATED PRESSURES AND LARGE TEMPERATURE DIFFERENCES. Park, Efton L. Jr.; Colver, C. Phillip; Sliepcevich, C. M. (Univ. of Oklahoma, Norman). 35p. (CONF-650802-13). ORAU. Gmelin, AED-CONF-65-193-23.

From Cryogenic Engineering Conference, Houston, Tex.

Nucleate and film boiling data, as well as convective heat transfer data near the critical point, were obtained for nitrogen at pressures up to 800 psig and temperature differences up to 1000°F and for methane up to 700 psig and temperature differences up to 700°F. The nitrogen data include burnout heat flux measurements up to 0.9 the critical pressure. An empirical correlation, based on corresponding states theory, predicts the ΔT at burnout for nitrogen remarkably well. The film boiling correlation proposed by Breen and Westwater does not fit the data obtained on nitrogen and methane in this study. The discrepancy is attributed to both the effect of pressure as well as heat flux level. For convective heat transfer above the critical pressure, the heat flux at a given ΔT was found to be independent of pressure for both nitrogen and methane. Higher heat transfer rates are obtained in the convective region than in film boiling. (auth)

Materials Testing

36994 RADIOGRAPHY USING ^{192}Ir. Furuta, Junichiro; Hiraoka, Eiichi; Tsujii, Yukio. Ann. Rep. Radiat. Center Osaka Prefect., 6: 80-2(1965).

The sensitivities of radiographic faults observed using ^{192}Ir sources are reported for steel and aluminum. The sensitivity was good, especially for the thinner samples compared with 30 C of ^{60}Co and 1 C of ^{137}Cs. It was concluded that if ^{192}Ir sources of higher curies can be obtained easily, this will be used more generally. (auth)

Protective Structures

36995 (AD-636794) PRELIMINARY INVESTIGATION OF FIRESTORM START-CRITERIA. Lommasson, T. E. (Dikewood Corp., Albuquerque, N. Mex.). June 15, 1965. Contract OCD-PS-65-53. 41p. (DC-TN-1050-1). CFSTI $2.00 cy, $0.50 mn.

A quantitative hypothesis is developed that relates inrush wind velocity at the edge of a potential firestorm area to the energy release rate of fires within the area and to the size of the area itself. The effects of spread from initial fires are considered and criteria are derived to estimate the way in which the fires are likely to develop with time. The hypothesis was applied to German World War II firestorm and group fire situations and appears to yield reasonable results in predicting the occurrences of each. The hypothesis may be applied to nuclear attacks against urban target areas. (auth)

Space Propulsion

See also ISOTOPE TECHNOLOGY — Power Application
REACTOR TECHNOLOGY — Propulsion and Space

36996 (SC-CR-66-2045) BOOSTER ROCKET ALTITUDE ABORT PROGRAM. Quarterly Progress Report No. 3, January 4–April 4, 1966. Ottinger, R. S.; Van Nice, L. J. (TRW Systems, Redondo Beach, Calif.). Contracts AT(29-1)-789; 48-2223. 32p. Dep. mn. CFSTI $2.00 cy, $0.50 mn.

For Sandia Corp., Albuquerque, N. Mex.

An abort-prediction model, Project Pyro test data, and available accident data were analyzed to establish a basis for predicting the early and late intra-fireball environment resulting from booster rocket aborts at altitudes from 10,000 to 70,000 feet. (R.C.K.)

36997 INTERSTELLAR VEHICLE PROPELLED BY TERRESTRIAL LASER BEAM. Marx, G. (Roland Eoetvoes Univ., Budapest). Nature, 211: 22-3(July 2, 1966).

As a possible realization of the principle of transferring rocket recoil energy to the earth, the following propulsion system is considered: a departing vehicle has an effective cross-sectional area, f, as seen from the earth, and acts as a perfect reflector of light in the backward direction. A light beam of constant intensity, I, coming from a terrestrial source, is reflected by it. If the vehicle moves with a speed $c\beta$, the intensity of the reflected light, I', turns out to be smaller than I. The momentum gained is $c^{-1}f(I + I')dt$, the energy gained is $f(I - I')dt$, and the vehicle is accelerated from the velocity $c\beta$ to $c(\beta + d\beta)$. It is concluded that a range of operation of 0.1 light year would require a coherently radiating surface of the order of 1 km^2 which emits hard x rays, and the vehicle would need an x-ray mirror with an effective cross-sectional area of several km^2. (W.D.M.)

36998 SPACE POWER: THE NEXT STEP. Rappaport, Paul (Radio Corp. of America, Princeton, N. J.). Space/Aeron., 44: No. 4, 76-83(Sept. 1965).

The various approaches to providing power sources for the larger space payloads that will be made possible by the Saturn rockets and other large rockets of the future are discussed. Limitations of the photovoltaic systems are considered. The development and application of thermoelectric and thermionic systems using radioisotopes or reactor heat sources are discussed in some detail. (W.D.M.)

36999 NUCLEAR PROPULSION AND MANNED INTERPLANETARY FLIGHT. Hallet, R. W. Jr. (Douglas Aircraft Co., Inc., Santa Monica, Calif.). 26p. (CONF-651132-3). ORAU. Gmelin, AED-CONF-65-337-28.

From Atomic Industrial Forum, 12th Annual Conference, Washington, D. C.

The activation of a manned interplanetary landing mission is contingent upon two requirements: establishing a mission date consistent with sufficient lead time to permit an orderly progression of mission studies, support programs, research and technology programs, and development of the operational hardware from birth to activation—a total time period of 15 to 20 years, and the acceptance of such a mission as a national goal and the confirmation that related expenditures fall well within our economic means. Two types of missions are described—a 960-day mission employing chemical propulsion, and a 460-day mission employing nuclear propulsion. On the basis of such factors as schedule of critical milestones, effect of mission duration upon physiological and psychological stamina of the astronauts, relation of the launch date to the solar flare cycle, requirement for a new post-Saturn launch vehicle, and annual expenditures, it is concluded that a 460-day mission utilizing nuclear rockets and occurring during the year 1984 is consistent with technological and economic capability. (auth)

Vacuum Engineering

37000 (UCID-4548(Rev.4)) FLANGE DESIGN USING ALUMINUM FOIL FOR UHV APPLICATION. Batzer, T. H. (Lawrence Radiation Lab., Univ. of California, Livermore). Jan. 25, 1966. Contract W-7405-eng-48. 19p. Dep. mn. CFSTI $1.00 cy, $0.50 mn.

Stainless steel flanges and aluminum foil gaskets were developed for bakeable ultra-high vacuum systems. Drawings are included for tube sizes from 1 to 36 inches. (D.L.C.)

GEOLOGY, METEOROLOGY, AND MINERALOGY

General

Refer also to abstract 37057.

37001 THEORETICAL INVESTIGATIONS IN NUCLEAR GEOPHYSICS IN THE USSR. Kozhevnikov, D. A. (Moscow Inst. of Petroleum, Chemical, and Gas Industry). pp 43-68 of STI-PUB-112(Vol.2). (In Russian).

The principal results of theoretical investigations in nuclear geophysics in the Soviet Union are reviewed. The development of methods is emphasized. (227 references). (G.O.Y.)

37002 PHYSICOCHEMICAL REACTIONS AS INDICATORS OF COSMIC PHENOMENA. Chizhevskii, A. L. pp 373-81 of Zemlya vo Vselennoi, Sbornik. Moscow, Mysl, 1964. (In Russian).

Solar activity effects on the precipitation of bismuth compounds is described from previous work. The experiments were conducted at different latitudes, and a relation between the course of the reactions, Wolf's number, the geographical latitude, and movement of the Earth through the galaxy was found. (J.F.P.)

Meteorology

See also Site Survey and Selection

37003 ACTION OF RADIOACTIVITY AND OF POLLUTION UPON PARAMETERS OF ATMOSPHERIC ELECTRICITY. Bricard, J. (Lab. of Cloud Physics and Atmospheric Electricity, Paris). pp 82-117 of Problems of Atmospheric and Space Electricity. Coroniti, S. C. (ed.). Amsterdam, Elsevier Publishing Co., 1965.

The characteristic elements of radioactivity and of atmospheric pollution are considered. It is shown that their actions are, in the first case, the formation of small ions and, in the second case, their disappearance and the formation of large ions. From this the ionic density of the air under given meteorological conditions is deduced, and the ions which correspond to the recoil atoms which come from radioactive disintegrations in the troposphere and in the lower atmosphere are studied separately. Finally, the relations between the radioactivity and the other parameters of the atmospheric electricity close to the ground and in the free atmosphere are introduced. (auth)

Natural Radioactivity and Fallout

See also HEALTH AND SAFETY

Refer also to abstract 37003.

37004 ESTIMATES OF BIOSPHERIC CONTAMINATION AND RADIATION DOSE FROM FALLOUT FOR ALL THE PRE-TREATY TESTS OF NUCLEAR WEAPONS. Vohra, K. G.; Rangarajan, C.; Gopalakrishnan, Sarada; Sadasivan, S. (Atomic Energy Establishment, Bombay). Health Phys., 12: 1087-98(Aug. 1966).

The production and dispersion of fission products and induced radioactivity from nuclear weapon tests are discussed. Estimates are given of the important radionuclides released by the tests conducted up to the end of December 1962. The genetically significant external gamma dose from fission products has been estimated on the basis of mean residence time in the stratosphere. The external gamma dose levels as Srinagar and Bombay are also calculated from the deposited activity. The calculations are based on the measured levels of ground deposition of important gamma-emitting isotopes ^{137}Cs, (^{95}Zr + ^{95}Nb), ^{106}Ru, ^{144}Ce, and ^{125}Sb. The analysis for these isotopes was performed using a 100-channel analyzer and a 3 × 3 in. NaI(Tl) crystal. Results of the calculations show that highest dose rates are due to (^{95}Zr + ^{95}Nb) while the cumulative dose is maximum for ^{137}Cs deposited on the ground. The ratios $^{95}Zr/^{137}Cs$ and $^{140}Ba/^{95}Zr$ have been used to partition the activity from different tests for the purpose of dose evaluation. The external gamma dose values have thus been estimated for important test series, based on ground deposition of fission products up to June 1964. The genetically significant external gamma dose from fallout deposited during the period of measurements has been calculated as 62 mrad and 52 mrad respectively for Srinagar and Bombay. Theoretical calculations, however, show that the total external gamma dose in the 20°N to 50°N latitude band from all tests up to December 1962 is 146 mrad. The corresponding average external gamma dose to the world population estimated by the U.N. Scientific Committee on the Effects of Atomic Radiation is 50 mrad. (auth)

37005 CONDENSATION PHENOMENA AND DECONTAMINATION OF THE GROUND AIR LAYER FROM RADIOACTIVE PRODUCTS. Manolov, L. Izv. Fiz. Inst. Aneb, Bulg. Akad. Nauk, 14: 39-44(1966). (In Russian).

Previous studies led to the idea that in the process of the formation of the various types of hydrometeors on the ground, they may play the role of important decontaminators of radioactive substances. Experiments to prove this were conducted under natural conditions in different seasons of the year. They give a picture of the degree of deactivation of radioactive substances by the various types of liquid and solid hydrometeors. During the experiments the radioactivity freely sedimented per unit of area and that accumulated by the hydrometeors on the same unit are separated. An assessment is made of the quantity of air that can be decontaminated by a given amount of condensate. It was shown that from the standpoint of the decontamination of the atmosphere, the various kinds of condensation phenomena in the ground air layer are decontaminators of considerable importance. (auth)

37006 NATURAL RADIOACTIVITY IN GROUND WATER SUPPLIES IN MAINE AND NEW HAMPSHIRE. Smith, Benjamin M.; Grune, Werner N.; Higgins, Frederick B. Jr.; Terrill, James G. Jr. (Georgia Inst. of Tech., Atlanta). J. Amer. Water Works Ass., 53: 75-88(Jan. 1961).

Approximately 350 water samples were collected in Maine and New Hampshire and analyzed for ^{222}Rn; 85 samples were also analyzed for ^{226}Ra. The experimental value of 3.798 days for the half-life of the gaseous radioactivity encountered in ground waters of Maine and New Hampshire showed that the activity was from ^{222}Rn which has a half-life of 3.825 days. But the nature of the analytic method used did not preclude the existence of other gaseous radioactive isotopes in these ground waters. In Maine, 99.2% of all the water samples from drilled wells and 84% of all those from dug wells contained concentrations of ^{222}Rn and daughter products exceeding 2000 $\mu\mu C/1$. The frequency distributions and average activities of radon in Maine and New Hampshire were not significantly different. For large areas, the depth of a well did not significantly influence the radon activity of well water, but when the area used as a basis for comparison was reduced in size to only a few square miles, radon activity was found to vary linearly with depth. In New Hampshire, the ^{226}Ra activity decreased with increased depth; in Maine, a trend could not be established. The average radon activities of drilled and dug wells in several geographic and geologic zones were found to be statistically different. In Maine, drilled wells contained significantly greater concentrations of radon than did dug wells. A continuing high level of radon activity was associated with the drilled wells within a relatively narrow band of geologic formations following the general outline of the Fitchburg Pluton in New Hampshire and the Waterville Formation in Maine. Limited studies on the variation of radon activity with pumping time showed that radon activity varied with the duration of pumping and the idle

period between pumpings. In both Maine and New Hampshire, ^{222}Rn was found to be in excess of equilibrium with the ^{226}Ra present in the ground waters. (BBB)

37007 DIURNAL OSCILLATIONS OF RADON AND THORON AND THEIR DECAY PRODUCTS. Staley, D. O. (Univ. of Arizona, Tucson). J. Geophys. Res., 71: 3357-67 (July 15, 1966).

Periodic and height-dependent solutions are derived for the disturbances of concentrations of ^{222}Rn, ^{220}Rn, and their first three decay products in the air above the earth's surface, account being taken of turbulent diffusion and radioactive decay. At the surface, sinusoidal oscillations of ^{222}Rn and ^{220}Rn are assumed, but the concentrations of decay products are required to vanish. At large heights, all concentrations are required to vanish. It is shown that the ^{222}Rn (radon) concentration disturbance is influenced mostly by turbulent diffusion and only slightly by decay. The form of the disturbance is very similar to that of the diurnal oscillation of potential temperature for a constant eddy conductivity. Amplitude decreases exponentially upward with constant velocity. Daughter products near the surface are not, by reason of the lower boundary condition, in radioactive equilibrium with ^{222}Rn. At sufficiently large heights, however, all daughter products approach radioactive equilibrium with ^{222}Rn by reason of their rapid decay. The height at which radioactive equilibrium becomes a good approximation increases with each successive decay product and ranges from tens to hundreds of meters in numerical examples. These results suggest that the inference of ^{222}Rn concentrations from experimentally determined concentrations of its decay products is not justified except at great heights. The ^{220}Rn (thoron) concentration is strongly influenced by decay as well as by turbulent diffusion. The concentration disturbance attenuates and propagates rapidly upward at exponential and constant rates. Since ^{210}Po decays even more rapidly than ^{220}Rn, these two approach radioactive equilibrium at sufficiently large heights. ^{212}Pb decays much more slowly than its precursors, so that it is not in radioactive equilibrium with them at any height. Amplitude attenuation and phase propagation are similar in form to those of the enthalpy disturbance. Since ^{212}Bi decays more rapidly than ^{212}Pb, these two approach radioactive equilibrium at great heights. (auth)

37008 MEASUREMENTS OF RADIOACTIVE FALLOUT IN THE YEARS 1963 AND 1964. Keck, Gertrud (Tieraerztliche Hochschule, Vienna). Wien. Tieraerztl. Monatsschr., 52: 967-72(1965). (In German).

Measurements of radioactivity associated with fallout in 1963 and 1964 included studies of its γ spectrum, β activity, and the total long-lived β activity in air. At an alpine observation station located at Weissee at an altitude of 2348 m, β activity was higher on 84 days and lower on 24 days than at a station located at Schneiderau in a valley 7 km away at an altitude of 1041 m. On 8 days the values were equal. During 1963 the values at Schneiderau ranged from 3.3 to 10.8 pC/kg and at Weissee the values ranged from 2.6 to 44.7 pC/kg. During 1964 the values at Schneiderau ranged from 0.3 to 5.0 pC/kg and at Weissee the values ranged from 0.6 to 4.9. The daily values of long-lived activity varied widely and almost synchronously between the two stations. From 238 samples taken it was calculated that the mean increase of total long-life β activity of air was 21% for an altitude difference of 1307 m. (BBB)

37009 ANNUAL REPORT OF THE GERMAN WEATHER SERVICE, NO. 13. Offenbach am Main, Ger., Deutsche Wetterdienst, 1966. 94p. (In German).

In addition to other meteorological data collected for the year 1965 in West Germany, extensive fallout data are summarized. Monthly readings of β activity of air are tabulated for 11 monitoring stations in West Germany. The highest average yearly level was recorded in Regensburg (0.93 pC/m^3) and the lowest in Aachen (0.38). The highest β activities in air were recorded in June, when, for example, the level in Stuttgart reached 1.40 pC/m^3. The maximum value for the year was attained in Regensburg on October 26, 1965 (3.13 pC/m^3). Fallout levels are also given as monthly averages recorded at 16 monitoring stations distributed throughout Germany. The highest yearly average of β activity was found in Obersdorf (118.8 pC/l precipitation) and the lowest in Berlin (22.2). Ground levels of β activity varied from 31 pC/km^2 in Husum to 74 in Essen. The monitoring station in Koenigstein recorded increased atmospheric radioactivity levels from May 27 to July 16 because of the Chinese nuclear detonation on May 14, 1965. The maximum ^{131}I value in fallout was noted on June 23 (19.07 pC/l). A table shows the monthly averages of the following fallout radionuclides as recorded at Koenigstein: ^{90}Sr, ^{89}Sr, ^{137}Cs, ^{140}Ba, ^{141}Ce, ^{144}Ce, ^{91}Y, ^{95}Zr, ^{95}Nb, ^{103}Ru-^{103}Rh, ^{131}I, and ^{125}Sb. (BBB)

Techniques and Equipment

Refer also to abstracts 36962, 36964, 36966–36969, 37060, and 37133.

37010 (AD-631340) PALANQUIN. Long Range Seismic Measurements [of] VELA UNIFORM. Seismic Data Laboratory Report No. 144. (Teledyne Industries, Inc., Alexandria, Va. Earth Sciences Div.). Apr. 18, 1966. Contract AF 33(657)-15919. 37p. CFSTI $2.00 cy, $0.50 mn.

An analysis of seismological data from an underground nuclear explosion is presented as a continuing study to provide information to aid in distinguishing between earthquakes and explosions. A table of travel-times and amplitudes of P, Pg, Lg, and surface waves are included along with other unidentified phases. (auth)

37011 SULFUR ISOTOPES AND THE FORMATION OF ORE STRATA. Gehlen, Kurt V. (Univ., Erlangen, Ger.). Geol. Rundsch., 55: 178-97(1966). (In German).

Sulfur, usually as the sulfide, is widely distributed in ore deposits and, on the basis of the occurrence of its two most frequent stable isotopes (^{32}S and ^{34}S, with average abundances of 95 and 4.2%), data can be obtained on the genesis of the deposits. The possibilities and problems of the genetic interpretation of sulfur isotope ratios in ore minerals are discussed using mainly results from the Goettingen isotope lab. For example, criteria are obtained regarding the question whether a certain deposit can be derived from basaltic magmas from the Earth's mantle, or not. The sulfur isotope data for minerals from the deposits of Meggen and Rammelsberg (Germany) are only consistent with a derivation from the mantle if substantial additional assumptions are made (very strong assimilation of unusual crustal material or extreme fractionation in a secondary magma chamber). Hydrothermal deposits derived from the Earth's crust can show variable (Harz mountains) or also rather uniform isotope ratios (Freiberg/Saxony, Southern Germany). Extreme variations within the deposit of Wiesloch near Heidelberg are interpreted as caused by bacterial fractionation of a limited amount of sulfate. Lead isotope ratios for deposits in Southern Germany are tabulated ($^{206}Pb/^{204}Pb$, $^{207}Pb/^{204}Pb$, $^{208}Pb/^{204}Pb$, and $^{206}Pb/^{207}Pb$). (BBB)

37012 MEASUREMENT OF POTASSIUM BY GAMMA SPECTROMETRY IN SECTIONS OF 5 BORINGS MADE IN THE EVIAN QUATERNARY FORMATIONS. Blavoux, B.; Olive, Ph. (Centre Recherches Geodynamiques, Thonon-Les-Bains, (Haute-Savoie), France). Geol. Rundsch., 55: 216-26(1966). (In French).

Methods are described for assaying ^{40}K, and thereby of total K, by a scintillation detector, and of its use in measuring potassium surface and depth-distribution in morainic formations of quaternary age in the Evian area. Measurements were made on samples collected through 5 core drillings of which a schematic geological section is shown. Detailed study of these drillings is described. According to the results, the potassium content varies with the percentage of fine fraction below 40 μ and in inverse ratio to total calcimetry as expressed in % of sediment. The potassium content varied from 0.7 to 3.4%. It is concluded that this nondestructive method for measuring potassium by ^{40}K assay is rapid, accurate, and enables assay of large amounts of sedimentary materials. (BBB)

37013 $^{18}O/^{16}O$ RATIOS OF MINERALS FROM THE IRON FORMATIONS OF QUEBEC. Sharma, Taleshwar (Indian Inst. of Tech., Kanpur); Mueller, Robert F.; Clayton, Robert N. J. Geol., 73: 664-7(July 1965).

The $^{18}O/^{16}O$ ratios of quartz, magnetite, amphiboles, and pyroxenes were determined in the Quebec iron formations and compared with those of corresponding minerals from Lake Superior iron formations of similar metamorphic rank. The $^{18}O/^{16}O$ ratios of the minerals were very high when compared to similar minerals from other sources. For comparable metamorphic grades, the $^{18}O/^{16}O$ ratios of quartz and magnetite from the Lake Superior iron formation were in the range of +10 to +16 and −1 to +5 per mil, respectively. The $^{18}O/^{16}O$ ratios of quartz and magnetite from the Quebec iron formations were about 22 per mil and 11 per mil, and the $^{18}O/^{16}O$ ratios of the cummingtonites averaged about 17 per mil. The isotopic fractionations between the cummingtonites and pyroxenes were found to be nearly zero. The isotopic fractionation between the single magnetite-pyroxene pair was 5.48, which is higher than the range previously reported for igneous rocks (3.8 to 5 per mil). This is consistent with the expected lower temperature of formation of the Quebec metamorphic rocks as compared with igneous rocks. The $\delta^{18}O$ of the hornblende sample was found to be 9.66 per mil, close to values found for hornblende from the amphibolites from the Black Hills, South Dakota, of comparable or somewhat lower metamorphic grade. The remarkably similar values of the $^{18}O/^{16}O$ ratios from sample to sample in the Quebec rocks indicate that a uniform distribution of isotopes occurred throughout an area of at least several square miles represented by the sample. On the other hand, the fact that the hornblende from the amphibolite associated with the iron formation has a markedly lower $^{18}O/^{16}O$ ratio indicates that no significant large-scale redistribution of isotopes took place during the metamorphism. The uniformity of the $^{18}O/^{16}O$ ratio in the iron formation may date to the period of original chemical sedimentation. (BBB)

37014 $^{230}Th/^{238}U$ AND $^{234}U/^{238}U$ AGES OF PLEISTOCENE HIGH SEA LEVEL STAND. Veeh, H. Herbert (Univ. of California, San Diego). J. Geophys. Res., 71: 3379-86(July 15, 1966).

Unrecrystallized fossil corals occurring in their growth positions between 2 and 9 meters above sea level at many locations in the Pacific and Indian Oceans were dated by the $^{230}Th/^{238}U$ and $^{234}U/^{238}U$ methods. Where possible, recent corals were also collected and analyzed for their uranium and thorium isotopes. The uranium contents of the corals were determined fluorimetrically; the $^{234}U/^{238}U$ ratios and the thorium concentrations were ascertained by alpha spectrometry. The $^{230}Th/^{238}U$ ages of the fossil corals range from 90,000 ± 20,000 to 160,000 ± 40,000 years and the $^{234}U/^{238}U$ ages from 80,000 ± 50,000 to 180,000 ± 60,000 years. Absence of ^{230}Th in the recent corals and absence of ^{232}Th in both the recent and the fossil corals confirm the assumption that the ^{230}Th found in the fossil corals resulted solely from radioactive decay of its parent uranium. Control samples of pre-Pleistocene material showed radioactive equilibrium between the various members in the ^{238}U decay chain. Both the internal consistency of the ages, within experimental error, and the agreement between the $^{230}Th/^{238}U$ and $^{234}U/^{238}U$ ages, strongly support the general validity of these ages. The similarity of the $^{230}Th/^{238}U$ ages of Pleistocene coral reefs to those of like elevations above sea level in many localities suggests a eustatic sea level stand higher than now at about 120,000 ± 20,000 years ago, possibly during an interglacial stage of the Pleistocene. (auth)

37015 ISOTOPE DATING OF ANTARCTIC ROCKS: A SUMMARY. Webb, P. N.; Warren, Guyon (New Zealand Geological Survey, Wellington). New Zeal. J. Geol. Geophys., 8: 221-30(May 1965).

Details of 141 potassium-argon, strontium-rubidium, and lead-uranium isotope dates obtained from Antarctic rocks are listed and their geographic distribution shown. These values were reported in recent literature. Accompanying each date are details of the rock type analyzed, the lab method used, the locality at which the sample was collected, the country in which the sample was processed, and a reference to the original publication. Revised ages are listed for 90 determinations summarized in an earlier report. Of the 231 dates summarized in this and the earlier report, 137 originate from Soviet laboratories. Most Soviet results were obtained by Ar/K analysis of whole rocks. When all previous Antarctic $^{40}A/^{40}K$ and $^{87}Sr/^{87}Rb$ dates were recalculated, using revised decay constants, this had the effect of reducing slightly most of the earlier published ages. The present list, as originally compiled, was revised to the same standard constants; i.e., all ages from Ar/K determination are based on calculations using $\lambda_e K^{40} = 5.85 \times 10^{-11}$ yr^{-1}, and ages from Sr/Rb determinations use $\lambda\beta Rb^{87} = 1.47 \times 10^{-11}$ yr^{-1}. (BBB)

37016 POTASSIUM–ARGON AGES OF SOME DALRADIAN, MOINE, AND RELATED SCOTTISH ROCKS. Brown, P. E. (Univ. of Sheffield, Eng.); York, D.; Soper, N. J.; Miller, J. A.; MacIntyre, R. M.; Farrar, E. Scot. J. Geol., 1: 144-51(May 1965).

Potassium-^{40}Ar contents of minerals of some Scottish rocks were assayed for age determinations. Data for 18 rock samples are tabulated. Potassium-argon ages determined for Moine schists from north and central Sutherland are in general agreement with the age of 415-420 Myr already found to be characteristic of the Moine outcrop. A similar age was obtained on an F_3 pegmatite from the Och Monar area and a Lewisian pelite, with F_3 crumples, from Loch Hourn. Dalradian specimens from Perthshire and Banffshire show a spread of ages from 471 to 420 Myr and are interpreted as overprints of a pre-Arenig metamorphism. It is considered that the F_3 metamorphism was essentially co-eval but that the Banff section, presumably by being at a higher tectonic level, cooled to the threshold temperature for argon retention 15–20 Myr before the Central Highlands area; on this hypothesis the absolute age of the F_3 metamorphism would be more closely approached by the 440 than the 420 Myr age and might be mid-Ordovician. (BBB)

37017 PULSED NEUTRON GENERATOR FOR BOREHOLES AND ITS USE IN NUCLEAR GEOPHYSICS. Alekseev, F. A.; Bespalov, D. F.; Gorbunov, G. V.; Srebrodol'skii, D. M.; Shimelevich, Yu. S. (All-Union Scientific-Research Inst. of Nuclear Geophysics and Geochemistry at the USSR State Geological Commission, Moscow). pp 119-38 of STI-PUB–112(Vol.2). (In Russian).

A pulsed neutron generator used in neutron-neutron logging in oil and gas wells is described, and its operating conditions are defined. The detection of the gas-liquid and the oil-water interphase is discussed for regions in which the mineral content of the stratal water is low. (G.O.Y.)

37018 USE OF NEUTRON-INDUCED GAMMA-RADIATION SPECTROMETRY TO INVESTIGATE THE ELEMENTAL COMPOSITION OF ROCKS IN BOREHOLES. Yakubson, K. I.; Eife, K. (Inst. of Petroleum, Chemical, and Gas Industry, Moscow). pp 159-86 of STI-PUB–112 (Vol.2). (In Russian).

The possibility of analyzing elemental rocks in boreholes by spectrometry of capture γ radiation, induced-activity γ radiation, and inelastic-scattering γ radiation is discussed for rocks irradiated with neutrons from ampoule sources with different energy spectra (Po–Be, Po–B). The investigation of metal ores in the iron group is used as an example. The results of experiments with fast-neutron inelastic-scattering γ spectrometry on model coal strata are given along with the results of some theoretical calculations and model experiments on the use of γ spectrometry to study the activation of rocks irradiated by fast neutrons from ampoule sources. (G.O.Y.)

37019 NEUTRON RADIATIVE CAPTURE GAMMA SPECTROMETRY AS A METHOD OF DETERMINING THE COMPOSITION OF IRON-BEARING ROCKS AND ORES. Blyumentsev, A. M.; Fel'dman, I. I.; Nedostup, G. A.; Zheltikov, A. N. (All-Union Scientific-Research Inst. of

Nuclear Geophysics and Geochemistry at the USSR State Geological Commission, Moscow). pp 187-202 of STI-PUB-112(Vol.2). (In Russian).

The results of studies on the possibility of using capture γ spectrometry to detect and evaluate iron-bearing rocks and ores in borehole cross sections are presented. The limitations of the γ-γ logging methods are described, and the basic principles for assessing the metal content of rocks are given. The results of experimental measurements in boreholes in iron-ore deposits are presented. (G.O.Y.)

37020 COMPARISON OF MONTE CARLO CALCULATIONS OF THE PARAMETERS GOVERNING THE RESPONSE OF THE NUCLEAR SOIL DENSITY GAUGE WITH EXPERIMENTALLY OBTAINED VALUES. Heinz, W. F. (National Inst. for Road Research, Council for Scientific and Industrial Research, Pretoria); Engelbrecht, C. A. (Physics Div., Atomic Energy Board, Pelindaba, South Africa). pp 351-68 of STI-PUB-112(Vol.2).

The Monte Carlo method was used to analyze the response of a backscattering density gage. The parameters governing the response of the gage were studied in detail. The results are in good agreement with experimental observations on the response of the gage. (D.C.W.)

37021 GEOLOGICAL PROSPECTING COMPRISING DIRECTIONAL IRRADIATION AND DETECTION. Caldwell, Richard L. (to Mobil Oil Corp.). U. S. Patent 3,263,082. July 26, 1966. Filed June 17, 1963.

A method for rapid site analysis in prospecting for radioactive minerals may be used for minerals found near the surface or those found in formations transversed by a bore hole. Equipment used includes a low energy radiation source, scintillation counter and photomultipliers, pulse analyzers, and rate meters. (F.S.)

HEALTH AND SAFETY

See also BIOLOGY AND MEDICINE — Radiation Hazards and Protection
GEOLOGY, METEOROLOGY, AND MINERALOGY — Natural Radioactivity and Fallout

Refer also to abstracts 36678, 36995, 37167, 37289, and 38537.

37022 (LA-DC-6942) CHARACTERISTICS OF THE AEROSOL PRODUCED FROM BURNING PLUTONIUM. Ettinger, H. J.; Moss, W. D.; Busey, H. (Los Alamos Scientific Lab., Univ. of California, N. Mex.). June 1966. Contract W-7405-eng-36. 22p. (CONF-660904-1). Dep. mn. CFSTI $1.00 cy, $0.50 mn.

From 9th Air Cleaning Conference, Boston.

Safety analysis of Na-cooled, Pu-fueled, fast reactor plants must be concerned with the possibility of fires involving these materials. Design of an air cleaning system for such a facility requires basic data defining the aerosol characteristics of Na and Pu released during a fire. Size characteristics of the aerosol produced during Pu fires were determined for different atmospheres ranging from 20.8% O_2 and 79.2% N_2 to 0.5% O_2 and 99.5% N_2. Pu–Co–Ce, and alpha- and delta-phase Pu metal were burned. Data were obtained to estimate the fraction of Pu alloy airborne during a Pu fire. Fires simulating a reactor accident involving both fuel and coolant defined the relative airborne concentration of Pu and Na. (auth)

37023 (N-65-33865) TISSUE DOSAGES FROM ALPHA PARTICLES AND HEAVY NUCLEI IN SOLAR PARTICLE BEAMS IN SPACE. Schaefer, Hermann J. (Naval School of Aviation Medicine, Pensacola, Fla.). June 17, 1965. 15p. (NASA-CR-64997; NSAM-933). CFSTI $1.00 cy, $0.50 mn.

Recordings of several large flare events indicate that solar particle beams contain, in addition to H and He, also heavy nuclei. For the November 13, 1960, flare in particular, complete rigidity spectra for H and He and C, N, O, and F nuclei have been reported. Evaluation of these spectra in terms of tissue depth doses behind 0.1 g/cm^2 shielding shows that, while the He component contributes substantially to exposure in near-surface regions, the dose function of the medium heavy component remains, even in the tissue surface, on the level of a few percent. In view of the smallness of this contribution, it seems unnecessary to extend the spectral resolution of LET sensors up to the Bragg peaks of medium heavy nuclei (1000 kev/micron T). (auth)

37024 (NLCO-899) REPORT OF FIRE RESISTANCE TESTS FUEL CORE SHIPPING CONTAINER NO. 1. McKinley, J. C.; Burns, H. M.; Dawson, R. K.; Mead, J. C. (National Lead Co. of Ohio, Cincinnati). Dec. 16, 1963. Contract AT(30-1)-1156. 17p. Dep. mn. CFSTI $1.00 cy, $0.50 mn.

Fire resistance tests were carried out on wood containers used to ship uranium fuel cores for production reactors. The tests were carried out in a furnace at 1300°F for 10 minutes. The results indicate that the containers equipped with double lids are adequate, and that the advantage offered by fire retardant paint is small. (D.L.C.)

37025 (PG-Report-705) HEALTH AND SAFETY RESEARCH AT CHAPELCROSS. Annual Report, 1965. Martin, J. H. (Production Group, United Kingdom Atomic Energy Authority, Annon (Scotland)). 1966. 6p. Dep. BIS $0.30, HMSO 1s. 6d.

A correlation between radiation exposure and thymine metabolism in man was found. Possible use of this system as an index of radiation exposure is discussed. Preliminary studies in rats indicate that early treatment with citrate and carrier Sr followed by salicylate stimulates the urinary excretion of radioactive Sr; citrate stimulates the excretion of ^{237}Pu, and the early administration of BAL stimulates the excretion of ^{203}Hg. Thermal neutron fluxes at depth in tissues were measured in tissue-equivalent phantoms using a plastic phosphor detector, an ionization counter, and a ^{6}LiI scintillation counter and appropriate calculations. The development of a neutron dosimeter is discussed. The development of a proportional counter for use in ^{14}C dating studies and the development of a 5-l proportional counter for the identification of α emitters in marine samples by α spectrometry are reported. Data are included on the radioactivity in pond water and the particle size and isotopes present in the gas circuits of Chapelcross reactors. (C.H.)

37026 (PNRO-SMD-137) ENVIRONMENTAL RADIOACTIVITY AT THE SHIPPINGPORT ATOMIC POWER STATION FOR THE SECOND HALF OF 1965 AND CALENDAR YEAR 1965. (Bettis Atomic Power Lab., West Mifflin, Pa.). Contract AT(11-1)-Gen-14. 8p. Dep. mn. CFSTI $2.00 cy, $0.50 mn.

During the second half of 1965, measurements of radioactivity were made in the Ohio River, atmosphere, and fallout in the vicinity of the Shippingport Atomic Power Station. The results of these measurements indicate that the radioactive material released by the power station into the air and into the Ohio River did not result in a significant change in the naturally occurring radioactivity in the environment. Environmental monitoring data for the year 1965 are summarized. (C.H.)

37027 DISTRIBUTION OF NATURAL RADIOACTIVE AEROSOL PARTICLES. Wieser, P. (Landwirtschaftliche Hochschule, Stuttgart). Atompraxis, 12: 294-6 (June 1966). (In German).

The distribution of natural radioactivity on aerosol particles with radii between 10^{-5} and 3×10^{-4} cm was measured by means of a Goetz aerosol spectrometer. In this investigation the natural aerosol was charged with thoron decay products. The results are consistent with values previously published by others. (auth)

37028 STUDIES ABOUT THE ANALYSIS OF TRITIUM-CONTAINING STEAM IN AIR. Daruschy, P. (Landesinstitut fuer Arbeitsschutz und Arbeitsmedizin, Karlsruhe, Ger.). Atompraxis, 12: 301-2(June 1966). (In German).

A simple and useful method for measuring the tritium content of vapor is described. Hygroscopical salts (LiCl, $CaCl_2$) are allowed to absorb the moisture from the air. The water absorbed will be removed by Xylol-distillation and the watery distillate is used for sample production for measuring radioactivity. Taking into account the results obtained as well as the absolute moisture content of the air, statements are made regarding the relevant activity concentrations of THO and T_2O. (auth)

37029 FUNCTIONAL TEST OF A DECONTAMINATION APPARATUS FOR RADIO-CONTAMINATED RAINWATER. Nagasawa, Kakuma; Kido, Yasumasa; Tokimoto, Yoshiko; Ichiba, Katsuya (National Inst. of Hygienic Sciences, Tokyo). Eisei Shikensho Hokoku, No. 81: 71-3(Oct. 1963). (In Japanese).

The decontamination apparatus consists of a pump for suction of the untreated water into a porcelain filter (10 cm thick). Then the water is passed through an ion exchange resin (Amberlite IR-120, sodium cycle) in a 500-ml column. Standard water for testing was prepared by adding ^{90}Sr and ^{90}Y in 0.1N hydrochloric acid solution to water. A 100-l sample of the water passed through the filter at a rate of 50 l/hr. From 10 to 20 l of treated water, ^{90}Sr and

^{90}Y were separated and assayed. The removal rate for ^{90}Sr by the testing apparatus was more than 99.8% and the rate of ^{90}Y extraction was 1–2% lower than that for ^{90}Sr. (BBB)

37030 ^{210}Po AMOUNT IN TOBACCO. DETERMINATION OF POLONIUM IN THE ENVIRONMENT. Pujic, Zdravko (Institut za Biokemiju i Fiziologiju, Sarajevo, Ys.); Knezevic, Zvonko. Glas. Hemicara Tehnol. Bosne Hercegovine, 12: 75-9(1963). (In Croatian).

The amount of Po-210 in tobacco samples was investigated. It was found that Po-210 quantity varies around 3×10^{-6} μC/100 g. Approximately 35% of total Po-210 was drawn out in tobacco smoke. (auth)

37031 RADIUM, RADON, AND DAUGHTER PRODUCTS IN CERTAIN DRINKING WATERS IN GREAT BRITAIN. Kenny, A. W.; Crooks, R. N.; Kerr, J. R. W. (Ministry of Housing and Local Government, London). J. Inst. Water Eng., 20: 123-34(Mar. 1966).

The possibility that sporadic high cancer incidence in West Devon (England) might be due to high levels of radioactivity in drinking water in certain localities was considered. This study was designed to identify public drinking waters containing high levels of radium or radon; to determine whether there is a correlation between high radon concentrations and geological stratum from which the water derives; and to assess the radiological hazard of waters containing the highest concentrations of radon found in Great Britain. Radon concentrations up to 30,000 pC/l in the supply, and up to 20,000 pC/l in tap water have been found. Radium and radium D, E, and F, when present in these waters, is in concentrations far less than that corresponding to radioactive equilibrium with the radon. These results indicate that all waters drawn from granite contain originally more than 1000 pC/l, possibly as much as 10,000 pC/l or more, and that radon is lost to atmosphere as the water flows through adit, stream, or river, or is stored in a reservoir, so that the concentration of radon in the water put into supply depends on the opportunity given the radon to escape. Only occasional results for the daughter radionuclides were obtained, since these measurements were made only to check that high levels were not generally present. The highest values found are 5.0 pC/l for bismuth-210 and 1.3 pC/l for polonium-210. On the basis of the results, the Medical Research Council has advised that it does not consider there is any need to reduce the level of radon in any of these drinking waters. The radiation dose delivered to the individual by these waters is less than the background radiation dose, and that there is no evidence that exposures of this magnitude are capable of producing any detectable damage. (BBB)

37032 ENERGY ABSORPTION IN CYLINDERS CONTAINING AN AXIAL SOURCE. Widman, J. C.; Powsner, E. R. (Veterans Administration Hospital, Dearborn, Mich.). J. Nucl. Med., 7: 407-15(June 1966).

The absorbed photon energy is the total energy associated with the emitted photons times the absorption fraction. For a cylinder containing a radioactive isotope uniformly distributed along its axis, the absorption fraction is derived analytically assuming only that the linear absorption coefficient is constant throughout the cylinder. Values of the absorption fraction are tabulated as a function of the linear absorption coefficient and cylinder dimensions. (auth)

37033 SNOW AND RAIN WASHOUT COEFFICIENTS FOR PROCESS PLANT RADIOIODINE VAPOR. Engelmann, R. J.; Perkins, R. W. (Battelle-Northwest, Richland, Wash.). Nature, 211: 61-2(July 2, 1966).

Experiments were designed to determine the removal of ^{131}I from a stack plume by comparing the total ^{131}I leaving the stack of the ^{131}I carried down by precipitation in a sampling arc which subtended the plume. The quantity of ^{131}I washed out was used to determine the washout coefficient (fraction scavenged per time) for the rain or snowfall, using the formula $\Lambda = Vy\Sigma\ c/QtA$; where Λ is the washout coefficient, V the wind speed at plume height; y the distance between samplers; Σ c the total material collected in all samplers, less background; Q the source release rate; t the sampling time; and A the area of one sampler. It was concluded that nearly all the inorganic radioiodine gas is captured during the water condensation process, as the stack gas mixes with the atmosphere, and that subsequent scavenging occurs at rates appropriate to tiny water drops. (P.C.H.)

37034 SAFETY ASPECTS OF GROUND TESTING FOR LARGE NUCLEAR ROCKETS. Goldman, Morton I. (NUS Corp., Washington, D. C.). Nucl. Appl., 2: 94-8 (Apr. 1966).

Present effluent prediction techniques are applied to ground tests of advanced nuclear rocket engines that will be forthcoming in several years. If the future fuel performance is assumed to be substantially the same as at present, it is shown that effluent decontamination will be required to maintain the present safety record with longer running times and higher reactor-power levels. (auth)

37035 INVESTIGATION OF OCCUPATIONAL EXPOSURES TO IONIZING RADIATION IN THE CZECHOSLOVAK SOCIALIST REPUBLIC. Chysky, J.; Trousil, J. Prac. Lek., 18: 211-19(May 1966). (In Czech).

Film dosimetry is carried out and organized by the Institute for Research, Production, and Application of Radioisotopes in Prague, in collaboration with the regional hygienic-epidemiological stations and the Institute of Radiation Hygiene. A method of personal film-dosimetry was developed and introduced by which the measurement of gamma radiation is made within the range of 10 mR–1000 R and doses of x radiation within the range of 6 mR–150 R. Films (high and low sensitivity) are carried in a modified film badge. The optical density of the chemically treated exposed films is measured by a modified densitometer within the range S = 0 up to S = 6. The exposures found are reported to the users of the film dosimeters as well as to the respective regional hygienic-epidemiological stations. Exposure exceeding 400 mR are reported also to the Institute of Radiation Hygiene. The causes, or the reliability of the higher exposures are determined by the officers of the hygienic service directly in the workplaces. (P.C.H.)

37036 DEPOSITION OF FALLOUT ^{137}Cs ON FORAGE AND TRANSFER TO MILK. Ward, Gerald M.; Johnson, James E.; Wilson, Daniel W. (Colorado State Univ., Fort Collins). Contract AT(11-1)-1171. Public Health Rep. (U. S.), 81: 639-45(July 1966).

Milk samples were collected from 12 cows on pasture and 100 fed on drylot in 1962, 1963, and 1964 at Colorado State University. Concurrent samples of feed intake and milk production from each cow, daily air samples, and samples of each rainfall were collected. All samples were analyzed for cesium-137 content. Deposition of cesium-137 in rainfall ranged from 300 to 7,000 pC/m^2 and on alfalfa hay from 60 to 1,640 pC/m^2. Deposition coefficients ranged from 0.06 to 0.37. The maximum levels of cesium-137 in milk from cows fed on pasture were about 200 pC/l in 1962 and 1963, while the maximum levels in milk from cows fed on drylot were about 170 pC/l. Levels of cesium-137 in milk were lower during the winter months because third-cutting hay, with low cesium-137 activity, usually was fed to all the cows. Transfer coefficients, the percentage of ingested cesium-137 found per liter of milk, were higher for high-grain diets (0.58) than for predominantly hay diets (0.24). (auth)

37037 EXPERIMENTAL STUDY OF DISPERSION OF FALLOUT NUCLEAR DEBRIS IN SEA WATER. Chesselet, Roger; Lalou, Claude (Centre d'Etudes Nucleaires, Saclay, France. Centre des Faibles Radioactivities, Gif-sur-Yvette, France). Radioact. Sea, No. 13, 1-14(1965). (In French).

Filtrations made directly in situ on great quantities of sea water showed that only a small amount of radionuclides was retained on filters with a porosity of 0.5μ. A very simple experiment was carried out in which sea water was enriched with atmospheric fallout collected under natural conditions. It was found that when this sea water is filtered through a 0.5 micron Millipore mem-

brane, more than 50 per cent of the initial radioactivity due to certain radionuclides is rapidly recovered from the filtrate. This suggests that some fixation process by the living microorganisms for the radionuclides must exist other than the uptake of particles greater than 0.5 microns. Examination of the curves of solution showed two types of solubility of the particles carrying the radioactivity. This observation is in agreement with the finding made at the time of atmospheric nuclear tests that there are two main families of radioactive particles. (P.C.H.)

37038 TRANSFER OF FALLOUT ^{137}Cs FROM SOIL TO DAIRY CATTLE FEEDS. Johnson, James E.; Wilson, Daniel W.; Lindsay, Willard L. (Colorado State Univ., Fort Collins). Soil Sci. Soc. Amer., Proc., 30: 416-17 (May-June 1966).

Corn (Sorghum vulgare) seedlings were grown in a greenhouse in the upper 5 cm of soil taken from a permanent pasture containing a cumulative fallout deposition of ^{137}Cs of 80,000 pC/m^2. No detectable ^{137}Cs(<10 pC/kg) was found in the plants. On the other hand, corn plants growing in local fields contained 1,500 pC/kg of ^{137}Cs. It was concluded that the ^{137}Cs content of dairy cattle feeds resulted largely from direct foliar contamination, and that uptake from the soil reservoir was unimportant. Further, the comparable alfalfa hay crops in years since 1963 have been decreasing in ^{137}Cs level, while the top soil ^{137}Cs concentration has increased steadily during this period. (auth)

37039 POSSIBILITIES OF SURVEILLANCE OF RADIOACTIVE CONTAMINATION OF MEAT AND MEAT PRODUCTS. Maurus, P. (Univ., Munich). Zentralb. Veterinaermed., 12: 600-4(Dec. 1965). (In German).

Contamination from fallout of meat results largely from ingestion by cattle of ^{137}Cs with food. In fresh calf muscle it may range from 4 to 6000 pC/100 g, and in beef it may range from 80 to 120 pC/100 g. In areas of localized fallout there would be less accumulation of ^{137}Cs in the musculature than in the case of worldwide fallout. Close to 25% of the present intake of ^{137}Cs by the human population is obtained from meat, and thus surveillance of meat is particularly necessary when this comes from animals in areas heavily exposed to fallout. Because of the wide range of contamination a variety of methods for detection are necessary. The assessment of the risk of eating contaminated meat cannot be confined within rigid normal limits. (BBB)

37040 STRUCTURE AND EQUIPMENT OF THE RADIOCHEMICAL AND RADIOBIOLOGICAL SECTION IN THE INSTITUTE OF ANIMAL PHYSIOLOGY AND NUTRITION OF THE UNIVERSITY OF MUNICH. Brueggemann, J.; Niesar, K. H. (Univ., Munich). Zentralb. Veterinaermed., 12: 686-90(Dec. 1965). (In German).

Radioprotective measures in operation include special work clothing, gloves, safety glasses, breathing masks, film badges, pocket dosimeters, and when necessary, finger rings. Times of entry and exist from working areas are recorded, and hand and foot monitors are used to detect contamination. Radioprotective measures to be used in transport of a 10-C ^{60}Co sealed source are described. These ensure that the dose level on the outer wall of the room containing the source is no more than 0.75 mr/hr. A 0.3-mC ^{90}Sr irradiator is used for dosimetric studies with a 100-kv x-ray apparatus. A 0.5-mC Ra source is used to control dosimetry with the ^{60}Co source. To avoid air contamination the control area has a ventilation system separate from the working areas. Seven ventilators in all are used to provide sufficient fresh air, prevent venting of contaminated air from the control area, heating of the working areas, and radioactive dust control. From 5 to 12 complete changes of air are made each hr. (BBB)

37041 THEORETICAL INVESTIGATIONS OF FISSION-PRODUCT DEPOSITION FROM FLOWING GAS STREAMS. Venerus, Ernest Ronald. Raleigh, N. C., North Carolina State Univ., 1965. 170p.

Thesis.

The deposition of fission products from an isothermal gas stream flowing in laminar flow through a circular tube is investigated for open and closed loop systems. A source is assumed to release a precursor into the gas stream at the origin of the axial coordinate. The radioactive precursor will decay to a first daughter and both nuclear species are assumed to be transported axially by convection and radially by Fickian diffusion. The boundary value problem, which contains the concentration in the gas stream and on the tube surface, is formulated for both the precursor and the first daughter. Two models are examined: Analysis I is applicable when the surface concentration of the deposited fission product is so small that the effect of surface concentration on desorption is negligible, and Analysis II is applicable for larger surface concentrations such that desorption from the surface is affected by the amount of material deposited. The special case of a noble gas precursor is also examined for both the open and closed loop systems. It is assumed that the noble gas will not deposit. For all cases mentioned the exact solution for the stream and wall concentrations is obtained by the use of transform calculus and complex variable theory. The exact solution for the case of the closed loop system is obtained by induction. The case of the precursor in the open loop system is examined in detail. For zero and infinite wall resistances respectively, it is shown that the problem reduces to the standard constant wall heat flux and constant wall temperature heat transfer solutions. The mass transfer coefficient is obtained for the precursor and for the first daughter in both the open and closed loop systems. Various special cases are compared with the heat transfer coefficients. The theoretical solutions for the precursor concentration on the wall are compared with experimental results obtained at Battelle Memorial Institute. (TCO)

37042 ALASKA RADIOLOGICAL HEALTH ACTIVITIES. Heidersdorf, Sidney D. 12p. (CONF-650838-1). ORAU. Gmelin, AED-CONF-65-241-1.

From American Assn. for the Advancement of Science, 16th Alaska Science Conference, Juneau, Alaska.

Program activities in the two areas of most importance in Alaska radiological health activities are discussed: x-ray control and environmental surveillance. To attack the x-ray problem, the Department of Health and Welfare requires the registration of x-ray equipment and conducts surveys of x-ray installations. The goal is to inspect all x-ray equipment, with particular emphasis on educating the user at the time of the inspection. The environmental surveillance program is stressed because of the unique Arctic food chain which has resulted in Eskimo body burdens of ^{137}Cs significantly higher than those found in the non-native population. Radiation protection guides are also discussed. (P.C.H.)

INSTRUMENTATION

General

Refer also to abstracts 36768, 37020, 37134, 37149, 37150, 37310, and 38163.

37043 RECENT DEVELOPMENTS OF GAS DETECTORS VISUALIZING TRACKS OF CHARGED PARTICLES. Interlenghi, A. M. (CISE, Milan). Energ. Nucl. (Milan), 13: 384-9(July 1966).

A review of gas detectors for visualizing tracks of charged particles, developed in the world from 1962 to 1966 is presented. In the comparison of the properties of the various devices, special consideration is given to the spatial isotropy of detection. (auth)

37044 AMPLITUDE SPECTRUM ANALYSIS BY SECTIONS. Marinov, M. Izv. Fiz. Inst. Aneb, Bulg. Akad. Nauk, 14: 51-5(1966). (In Russian).

A device is suggested to be attached to amplitude analyzers, which allows an analysis of the amplitude spectrum to be made section by section. The block diagram of the device is given. The pulses for analysis are fed to the entrance of the input block of the device which consists of one or several cathode followers. If the amplitude of the pulses is below the threshold of the discriminator and shaper, they will pass through the delay line through the entrance (which is normally open) and by the mixer will be fed to the entrance of the amplitude analyzer. In the amplitude analyzer the pulses will be analyzed and recorded in the first half of the address. The first half of the address includes all possible states of the address trigger when the last trigger is in "zero" position. This device not only allows the performance of amplitude analysis by sections but also cuts by half the dead time of the analyzer. The pulses which are registered in the second half of the address are coded within a period of time equal to the time which pulses of the first half of the address are coded. (auth)

37045 ELECTRON BEAMS FROM A DUOPLASMATRON USING A HOLLOW CATHODE ARC AS ELECTRON SOURCE. Roberts, A. S. Jr.; Cox, James L. Jr.; Bennett, Willard H. (North Carolina State Univ., Raleigh). J. Appl. Phys., 37: 3231-5(July 1966).

A high-density electron source was obtained by a modification of the duoplasmatron which employed a hollow cathode discharge (HCD). An electrostatically shielded and water-cooled Faraday cup probe was developed for use in measuring the radial current density distributions of electron beams obtained from this source. These electron beams, formed in a high-vacuum drift space, were found to have symmetrical current density distributions. Under certain conditions, spherical aberration of the beam was observed. (auth)

37046 CsI AS A HIGH-GAIN SECONDARY EMISSION MATERIAL. Edgecumbe, J.; Garwin, E. L. (Stanford Univ., Calif.). J. Appl. Phys., 37: 3321-2(July 1966). (SLAC-PUB-166).

Some preliminary data are reported on CsI (both bulk and low density) as a high-gain secondary emitting material for use in transmission-type electron multipliers. The data obtained are summarized and indicate that CsI has high-gain properties of great interest in electron multipliers. (J.F.P.)

37047 X-RAY SPECIMEN TEMPERATURE CONTROL WITH GAS STREAMS. Young, R. A. (Georgia Inst. of Tech., Atlanta). J. Sci. Instrum., 43: 449-53(July 1966).

The convenient gas-stream method can be thermodynamically desirable, minimizing thermal gradient problems, providing stable temperatures for isothermal experiments and providing rapid yet well-controlled dynamic response to programmed temperature changes. Inert atmospheres can be employed with some additional advantages concerning protection. Equipment design and use considerations are presented. Experimental configurations effectively used and specimen temperature-control results obtained in the range 90–1000°K are described. (auth)

37048 A 10-MHz LINEAR WINDOW AMPLIFIER. Bayer, Ryszard; Koba, Teresa. Nukleonika, 10: 811-15 (1965). (In Polish).

The amplifier system consists of an initial gain-control switch (100:1), a 10 MHz gain-of-four hundred amplifier with two feedback sections, a 0-30 volt discriminator (lower-level cutoff), a pulse lengthener, and a 2 MHz variable gain amplifier. The fast amplifier produces the required initial amplification of pulses which often includes a very large fraction of small, unwanted pulses. The threshold circuit (discriminator or "rug Sweeper") passes only the upper part of the larger pulses, the part that rises above the discriminator circuit. Having thus rejected the smaller pulses, the truncated larger pulses are lengthened and amplified. They are now suitable as input to an analyzer which views a selected segment of the overall pulse-height spectrum. The selected segment is controlled by discriminator and gain settings. The instability of the discriminator setting was corrected with the use of a precision pulse generator. The amplifier gain stability was within 1% per week. The overall amplifier linearity is 1%. (TTT)

37049 CALIBRATION PULSE GENERATOR WITH NANOSECOND PULSES. Wojtowicz, Stefan; Andrzejak, Ryszard. Nukleonika, 10: 821-7(1965). (In Polish).

A pulse generator is described which produces pulses of 2-100 nanosecond pulse width by means of a mercury switch "step-function generator" and coaxial cable clipping lines. The pulse rise time is less than 0.6 nanosecond, the variable amplitude ranges are 0-0.1, 0-1, 0-10.0, 0-100, or 10-20, 20-30 ....., 90-100 v, and the repetition rate is 20-130 cycles per second. With the use of a helipot, driven at constant speed, an accurate linear ramp generator is also featured, covering the above-mentioned pulse height ranges. The stability is $5.4-6.3 \times 10^{-5}$ for a 10% change of supply voltage, 6×10^{-4} for 7 hours, and 8.6×10^{-5} for 1 hour. The temperature sensitivity is 8.3×10^{-5} v/v°C for +20 to +50°C. The output impedance is 50 ohm. (TTT)

37050 ELECTRON-MICROSCOPIC AUTORADIOGRAPHY. ON DOMESTIC FRESH PHOTOGRAPHIC EMULSIONS AND DEVELOPING METHODS, FOR NUCLEUS STUDIES. Mizuhira, Binchi (Tokyo Medical and Dental Univ.). Radioisotopes (Tokyo), 14: 240-51(May 1965). (In Japanese).

Autoradiography using an electron microscope, allows the observation of an isotope in a molecule. With the electron microscope some special cares must be taken concerning the isotopic species used, the thickness of a specimen, the photoemulsion, and its development technique. The emulsion used must have good uniformity in grain sizes below 0.2 micron, a small gelatin content, good sensitivity to the β rays, and must require short exposures. In development, the latent image from a single β-ray hit must be thoroughly blackened, and must be developed in a single dot. The sensitivity of the emulsion depends on grain size and arrangement and on exposure. In the relation between grain size and resolving power for β rays, the grain sizes must be within 0.1 micron, considering emulsion thickness and β energy loss. The view that enhancement by an intense magnetic field may not be observed at less than 1000 kG (by Caro's experiment) is somewhat questionable. For preparing emulsion the following methods are now available: the emulsion drop, pipetting, bubbling, dipping, wire-looping, silver evaporation, centrifugal, and Perspex slide methods. Methods are included for eliminating the gelatin film, electron dyeing of specimens, and for selecting isotope species. (TCO)

37051 SWITCHING CIRCUIT FOR PHOTOMULTIPLIER TUBES. Poenaru, D.; Ivanov, E. (Inst. of Atomic

Physics, Bucharest). Rev. Roum. Phys., 11: 369-76 (1966).

After a brief analysis of the existing methods of gating photomultipliers, the apparatus and the method suggested and some experimental results are described. The gating pulse of any desired length (above 2 μsec) can be applied to any dynode of the photomultiplier which can be fed either by a positive or a negative high tension supply. (auth)

37052 STEREOSCOPIC VIEWER FOR MEASURING POSITIONS AND ANGLES IN THREE DIMENSIONS. Cowan, E. W. (California Inst. of Tech., Pasadena). Contract Nonr-220(53). Rev. Sci. Instrum., 37: 1004-6(Aug. 1966).

An optical device is described that is used for the measurement of the positions and angular coordinates of lines viewed in stereoscopic photographs, such as the photographs of particle tracks in a cloud chamber or bubble chamber. In addition to the absolute angular coordinates of a line in three dimensional space, the viewer furnishes the relative angular coordinates of a second intersecting line and the three rectangular coordinates of the point of intersection. All coordinates are read directly on linear scales. Applications include the measurement of scattering angles, the angles of secondary particles in an interaction or decay with respect to each other and the primary particle, and the angle of traversal of a particle through an absorber. (auth)

37053 PRECISION TECHNIQUE FOR MEASURING ASYMMETRIC DISTORTIONS IN OPTICAL LENSES. Hohenstein, Jack (Univ. of California, Berkeley). Rev. Sci. Instrum., 37: 1007-10(Aug. 1966). (UCRL-16260 (Rev.)).

Apparatus and techniques were developed for accurately measuring asymmetric distortion in camera lenses. Great care was taken in fabricating the camera, which was made cylindrical so that the lens could be rotated. The experimental setup included a collimating telescope, the cylindrical camera containing the lens to be tested, and the test pattern. By rotation of the cylindrical camera, the same portion of the test pattern could be used for checking asymmetric distortion in different sectors of the lens. The distortion was recorded on film plates, which were then measured with a linear micrometer. Results were obtained to an accuracy of 1 part in 10^5. Causes for distortion were investigated but not quantitatively. (auth)

37054 APPARATUS FOR ELECTRON IRRADIATION STUDIES AT LOW TEMPERATURES. Chaplin, R. L. (Clemson Univ., S. C.). Rev. Sci. Instrum., 37: 1014-18 (Aug. 1966). (TID-22721).

To pursue accurate quantitative studies of radiation effects in crystals, it is necessary to adopt precise experimental techniques for controlling the bombarding electrons and for cooling specimens to very low temperatures. With regards to the irradiating electron beam, measurements were made to determine some of the factors which influence the electron flux density over the irradiated area, and a description is given of a system which ensures precise alignment of the beam with respect to the specimens. A sample holder is described which provides good thermal contact and good electric isolation between specimen and specimen holder at low temperatures. The method used for regulating the temperature of the sample holder depends upon adjusting the rate and the amount of helium vapor flow through the holder and data that indicate how these two adjustments govern the resultant temperature are presented. (auth)

37055 ISOTHERMAL DROP CALORIMETER FOR ALPHA-ACTIVE, PYROPHORIC MATERIALS. Savage, Howard (Argonne National Lab., Ill.). Rev. Sci. Instrum., 37: 1062-4(Aug. 1966).

A copper-block drop calorimeter to measure the heat content of intensely alpha-active materials was constructed. The furnace, calorimeter, and aluminum isothermal jacket are contained within an inert atmosphere glovebox. This permits the use of unencapsulated materials without exposing personnel to an alpha contamination hazard. The inert atmosphere also permits measurements to be made on materials which are pyrophoric in air. The apparatus is equipped with a suppressed range recorder to monitor continuously the resistance thermometer signal with a resolution of ±0.4 cal/μv. Electric calibration of the calorimeter yielded a precision of ±0.08% in the thermometer and recording system. The heat content of a sample of Calorimetry Conference sapphire obtained from the National Bureau of Standards was measured, and the results deviated from the Bureau's reported data a maximum of 1.0% at 1008°K. The useful range of the apparatus extends from 306 to about 1450°K. (auth)

37056 MOESSBAUER SPECTROMETER FOR THE STRUCTURAL ANALYSIS OF MATERIALS. Ruegg, F. C.; Spijkerman, J. J.; Devoe, J. R. (National Bureau of Standards, Washington, D. C.). pp 325-35 of STI-PUB-112 (Vol.1).

A Mössbauer spectrometer, designed to provide high-precision Mössbauer spectra, is described. The instrument uses two electromechanical transducers, one driver and one sensor, in a feedback loop which incorporates an operational amplifier and a power amplifier. The transducer system is coupled to the scaler input of a multichannel analyzer. The spectrometer can be used with a variety of auxiliary equipment to measure spectra at low temperature or high pressure. Some applications of this spectrometer to the analysis of materials are discussed. (G.O.Y.)

37057 SIMPLE RADIOISOTOPE X-RAY TRANSMISSION GAGE FOR MEASURING SUSPENDED SEDIMENT CONCENTRATIONS IN RIVERS. Florkowski, T.; Cameron, J. F. (International Atomic Energy Agency, Vienna). pp 395-410 of STI-PUB-112(Vol.1).

An x-ray transmission gauge for measuring suspended sediment concentrations in rivers is described. The measuring head consists of a radioisotope x-ray source and a scintillation counter between which passes the water containing the sediment. This probe is lowered into the river from the bank or a suitable structure and the detector count rate is registered on a portable scaler. The source holder and detector are ruggedly constructed to withstand the conditions of use and are streamlined so that sediment concentrations in the measured volume are not disturbed. Two versions have been constructed, using ^{109}Cd and ^{241}Am. The source-detector gaps in these probes are 6 cm and 25 cm, respectively. The relative merits of the two systems are compared, and the results of flume tests and field use are described. (auth)

37058 DIGITAL METHODS IN THICKNESS GAUGING. THICKNESS GAGES FOR DISCONTINUOUS SHEETS AND TUBE WALLS. Duftschmid, K. E.; Steidl, J.; Patzelt, R.; Attwenger, W. (Oesterreichische Studiengesellschaft fuer Atomenergie, GmbH, Vienna). pp 467-86 of STI-PUB-112(Vol.1).

Two radiometric instruments for measuring the thickness of discontinuous sheets and the concentricity and wall thickness of tubes, respectively, are described. Both instruments use beta sources and digital counting. The former gage uses plastic scintillation counters, while the latter gage uses Geiger-Mueller counters. (D.C.W.)

37059 HIGH-ACCURACY FLUID-DENSITY GAGE. Tabor, P.; Lakosi, L. (Central Measurement Research Lab., Budapest). pp 487-503 of STI-PUB-112(Vol.1).

A radiometric fluid-density gage using an argon-filled high-pressure ionization chamber is described. Relations between the parameters of the system and the measurement parameters are included, together with an analysis of the origin of errors in the measurements. (D.C.W.)

37060 APPLICATIONS OF RADIOISOTOPE INSTRUMENTS IN GEOPHYSICS. Tittle, C. W. (Southern Methodist Univ., Dallas). pp 3-13 of STI-PUB-112(Vol.2).

A brief survey of nuclear geophysical methods is presented; logging techniques are emphasized. (D.C.W.)

37061 DEVICE FOR ESTIMATING NUCLEAR-EXPLOSION YIELD. Deynega, N. Voennyi Vestn., No. 3, 118-20(1966). (In Russian).

To predict radiation conditions and estimate military losses resulting from a nuclear strike, it is necessary to know the yield of a nuclear explosion. This can be computed from the time lapse of light radiation and the height of the cloud produced by the explosion. A special device was designed for this purpose. It automatically signals (with light or buzzer) the occurrence of a nuclear explosion, determines the yield of detonated nuclear explosives, responds to light impulses from both ground and atmospheric detonations, and ensures the safety of the operator. The device consists of a radiation detector, a control panel with a recorder, and a shielded connecting cord. The basis of the electrical circuit are six photoelectronic multipliers, a d-c amplifier, power sources, and relays. Since the device may be activated by direct sunlight, daytime shielding is required. (ATD)

37062 A NUCLEAR RADIATION SENSITIVE SWITCH. Auerbach, Philip B. (American Bosch Arma Corp., Garden City, N. Y.). 6p. (CONF-650707–23). ORAU.

From IEEE Annual Conference on Nuclear and Space Radiation Effects, Ann Arbor, Mich.

High-intensity pulsed nuclear radiation tends to make back biased semiconductor junctions conduct. The design and development of a circuit which would provide a switch opening in response to nuclear radiation pulses was undertaken. The design objectives for the radiation sensitive switch were that switch response should be fast, triggering should be adjustable, operation should not be impaired at high pulse intensities, reset, or switch closure, should be automatic and at a preset time after triggering and switch status should be indicated. A prototype switch was designed and constructed. A number of tests were conducted in a high energy linear accelerator (LINAC) to investigate circuit performance under irradiation. The results of the tests proved that the radiation sensitive switch met or exceeded all design objectives. Switch opening was sustained to pulse intensities as high as 4.8×10^{10} rad/sec. Switch response times were less than 0.2 microseconds. Reset times were constant throughout the test series. A control range of over 4 to 1 in radiation triggering threshold was achieved without changing components. A radiation sensitive switch, to provide a controlled switch opening in response to a nuclear radiation pulse was shown to be feasible and practical. (auth)

37063 PHOTOELECTRIC RECORDING OF THE PROFILE OF H_β ON A MICROSECOND TIME SCALE. Brown, William A. (Univ. of Michigan, Ann Arbor). 8p. (CONF-650927-11). ORAU. Gmelin, AED-CONF-65-222-19.

From American Physical Society Meeting, Honolulu, Hawaii.

The Stark broadening of the H_β line of hydrogen is often used to measure the electron density in transient laboratory plasmas. A two channel photoelectric device is described which, when used as the detector of a monochromator, measures the integrated intensity of a spectral line over two spectral bands centered on the line. Using the H_β profiles of Kolb, Griem and Shen ratios of numerically evaluated integrals over the emission line are related to the electron density. (auth)

37064 GEMINI CARBON DIOXIDE SENSOR. Vanderschmidt, G. F.; Riley, J. S. (Lion Research Corp., Cambridge, Mass.); Cornish, S. D. (McDonnell Aircraft Corp., St. Louis). 33p. (CONF-660207–15). ORAU. Gmelin, AED-CONF-66-011-17.

From Symposium on Radioisotope Applications in Aerospace, Dayton, Ohio.

An instrument for monitoring CO_2 partial pressure in a closed loop breathing system is described. The results from ground and airborne use indicate that this device has proven to be reliable, rugged, and easy to use. The basic concept can be adapted to the detection of other gases by simply providing an adequate substitute for the ascarite. (auth)

37065 HOLLOW GAS ARC DISCHARGE DEVICE UTILIZING AN OFF-CENTER CATHODE. Flowers, J. W. (to U. S. Atomic Energy Commission). U. S. Patent 3,268,758. Aug. 23, 1966.

The means are described for operating a hollow-gas arc discharge by providing a gas-fed self-heated cathode or cathodes and an anti-cathode or anti-cathodes disposed and mounted off-center of the axis of an evacuated discharge chamber and of an axial magnetic field, and establishing an arc discharge which refluxes between the cathode and the anti-cathode within the chamber and through a hollow anode. The anode provides a sufficiently large radial component of electric field so that there is a large rotational drift of the discharge to produce the hollow discharge symmetrical about the axis of and within the hollow anode. The size or diameter of the hollow discharge thus produced is determined by the distance that the cathode is mounted from the axis of the anode. (AEC)

Radiation Detection

Refer also to abstracts 36556, 36689, 36862, 36863, 37575, 37581, 37656, 37657, 37694, 38158, and 38184.

37066 (AECL–2536) ION CHAMBER DC AMPLIFIER, A-10,080. Campbell, D. J. (Atomic Energy of Canada Ltd., Chalk River (Ontario)). Mar. 1962, Reprinted June 1966. 22p. (ELI–70). Dep. mn. AECL $1.00.

An ion chamber d-c amplifier is described which was primarily designed as a reactor neutron flux safety amplifier. The amplifier may be used to measure low currents from a high impedance source over the range 10^{-12}A to 10^{-4}A full-scale. The circuit consists of an electrometer tube input stage followed by a semiconductor d-c amplifier and alarm circuit. Input current level is determined by the voltage across a feedback resistance which is selected either remotely or internally, through the use of dry-reed switches. The voltage is presented on a 0–10 v meter and is available for recorder indication. A circuit description and the functions of the various controls are presented. The performance of a prototype model is also included. (auth)

37067 (AECL–2578) TIME OF FLIGHT ENCODER USING INTEGRATED CIRCUITS. L'Archeveque, R. V.; Leakey, G. A. (Atomic Energy of Canada Ltd., Chalk River (Ontario)). June 1966. 31p. Dep. mn. AECL $1.00.

A time encoder was designed using monolithic silicon integrated circuits. The instrument is primarily intended for neutron time of flight experiments. It can measure the separation between a start pulse and one or more event signals from about 1 μs to 0.4 s. An internal 8 Mc crystal controlled oscillator is included providing excellent long term stability. Operation from an external clock is also possible up to 16 Mc. Numerous features were added to increase the flexibility of the instrument. A true binary read-out is generated in parallel and selection of the number of bits from 8 to 12 can readily be made from a switch on the front panel. Fourteen different values of channel widths are available from 0.5 μs to 48 μs in two ranges. The encoder can be preset to delay the counting from the start signal by up to 4096 channel widths. Choices of channel widths for the delay and the timing are completely independent. Under one mode of operation, the instrument can be dynamically tested using the light display on the front panel. The complete unit contains six printed circuit boards and it is mechanically conformed to the standard of the USAEC Committee on Nuclear Instrument Modules. A short appendix on the micrologic elements used is also included. (auth)

37068 (BNL–10321) DESIGN FEATURES OF A MIXED RADIATION REM RESPONDING RATE METER. Baum, John W. (Brookhaven National Lab., Upton, N. Y.). [1965]. Contract AT(30-2)-Gen-16. 20p. (CONF-660621–9). Dep. mn. CFSTI $1.00 cy, $0.50 mn.

From Health Physics Society, 11th Annual Meeting, Houston, Tex.

The development of a survey instrument suitable for measurements in mixed radiation fields around nuclear reactors and accelerators is discussed. A four-inch diameter Rossi-type tissue-equivalent spherical proportional counter is used as the radiation detector. Pulses from the counter are amplified by a special operational amplifier which serves to convert the detector output into a pulse spectrum which is weighted for quality factor and thus represents Rem dose. In the preliminary laboratory studies an analog-to-digital converter is employed to transform the operational amplifier output pulses to pulse trains which can be counted or passed through a count-rate meter. The required gain characteristics of the nonlinear operational amplifier were determined by considering theoretical pulse height spectra expected from the detector when exposed to fields of radiation containing particles of both single and mixed LET. Design principles of a circuit which has approximately the required gain are discussed along with preliminary laboratory tests of the overall system response to pure and mixed radiation fields. The amplifier has a wide dynamic range, making it possible to measure dose from particles having LET from 0.2 kev/μm of tissue to about 200 kev/μm of tissue. (auth)

37069 (BNWL-260) PRECISION LONG COUNTER FOR MEASURING FAST NEUTRON FLUX DENSITY. De Pangher, J.; Nichols, L. L. (Battelle-Northwest, Richland, Wash. Pacific Northwest Lab.). June 1966. Contract AT (45-1)-1830. 62p. Dep. mn. CFSTI $3.00 cy, $0.75 mn.

A reproducible version of the Hanson-McKibben long counter was built and a comprehensive experimental investigation of its characteristics was made. The counter is made carefully from polyethylene and strengthened with aluminum instead of being paraffin strengthened with steel. It is called a precision long counter (PLC) because models built from a standard set of drawings have closely reproducible properties. Data are given to show how a PLC can be calibrated to within 1% for measuring neutron flux densities from radioactive sources. This calibration is obtained with a small calibrated PuBe neutron source inserted inside the PLC. The standard counter, H-1, is located at Battelle-Northwest in Richland, Washington and the standard small source, M-1045, is located at Mound Laboratory in Miamisburg, Ohio. One counter, H-3, was selected as a roving counter, was calibrated against H-1, and was sent to the Mound Laboratory and to the Argonne National Laboratory to calibrate the two counters, ML-1 and ANL-1. The problem of using a PLC with accelerator neutrons is discussed and a solution offered. (auth)

37070 (BNWL-SA-537) PERSONNEL NEUTRON DOSIMETER DEVELOPMENTS. Unruh, C. M.; Baumgartner, W. V.; Kocher, L. F.; Brackenbush, L. W.; Endres, G. W. R. (Battelle-Northwest, Richland, Wash. Pacific Northwest Lab.). July 27, 1966. Contract AT(45-1)-1830. 20p. (CONF-660807-1). Dep. mn. CFSTI $1.00 cy, $0.50 mn.

From Symposium on Neutron Monitoring for Radiological Protection, Vienna, Austria.

Three approaches to the problem of personnel neutron dosimetry are discussed. These are thermoluminescence, solid state track detection, and activation analysis. (B.G.D.)

37071 (DP-993) PORTABLE MULTIPURPOSE RADIATION MONITOR. Splichal, William F. Jr. (Du Pont de Nemours (E. I.) and Co., Aiken, S. C. Savannah River Lab.). May 1966. Contract AT(07-2)-1. 13p. Dep. mn. CFSTI $1.00 cy, $0.50 mn.

A basic electronic package for a portable multipurpose radiation monitor was designed, fabricated, and field tested. Transistorized plug-in circuits powered by rechargeable nickel-cadmium batteries, a readout meter, and an electromechanical register are contained in a $4 \times 5 \times 6''$ case. Three rate meter ranges, a battery check position, and a register integrator for low rates are provided. The circuitry contains seven silicon transistors on four plug-in cards. Neutron, alpha, beta-gamma, or alpha-beta-gamma detectors can be individually coupled to the electronic package. Calibration for each detector is simple and stable because the package is unaffected by temperature changes between 20 and 100°F. The monitor weighs about seven pounds, can be carried in one hand, requires no warmup period, and is easy to operate and service. (auth)

37072 (KFK-429) ON THE APPLICATION OF LITHIUM-DRIFTED GERMANIUM DIODES IN NEUTRON CAPTURE GAMMA RAY SPECTROSCOPY. Michaelis, W.; Schmidt, H. (Kernforschungszentrum, Karlsruhe (West Germany). Institut fuer Angewandte Kernphysik). June 1966. 15p. (CONF-660625-2). Dep. mn.

From IAEA Panel Meeting, Vienna.

A status report is presented on the application of lithium-drifted germanium diodes in neutron capture gamma ray spectroscopy. The report includes a summary of the research being done at Karlsruhe on neutron capture. A review of the capabilities and limitations in the application of germanium diodes, and indications of trends in future applications. (B.G.D.)

37073 (NP-16201) GRADUIROVKA RADIOMETROV TEPLOVYKH NEITRONOV V DIFFUZNOM POTOKE. (Calibration of Thermal-Neutron Radiation Meters in Diffuse Flow). Report No. 7. Vasil'ev, R. D.; Dorofeev, G. A.; Petrov, V. I.; Pimenov, M. I.; Shevchenko, V. F. (Gosudarstvennyi Komitat po Ispol'zovaniyu Atomnoi Energii SSSR, Moscow. Soyuznyi Nauchno-Issledovatel'skii Institut Priborostroeniya). 1966. 6p. Dep. mn.

The sources of thermal neutrons needed for neutron radiometer calibration should have a negligible background of γ radiation, offer a near-Maxwellian distribution of thermal neutrons, and allow a rapid change in neutron intensity. None of the existing sources satisfy all of the above requirements. Consequently, a new thermal neutron source consisting of a graphite moderator with a cavity containing a $T(d,n)^4He$ source of fast neutrons driven by a low-voltage cascade accelerator yielding $\sim 5.10^9$ neutr/sec was designed. The device operated satisfactorily and yielded $\sim 10^6$ n/sec cm^2 beams with a Maxwellian velocity distribution corresponding to 293°K. A comparison with directed beam calibration shows that the new source producing diffuse fluxes yields somewhat lower calibration values. However, this should be considered an advantage since the calibrated radiometers are, as a rule, used under diffuse neutron flux conditions. (CFSTI)

37074 (NP-16202) PRIMENENIE METODA PODOBIYA RADIATSIONNYKH POLEI PRI NASTROIKE NEITRONNYKH RADIOMETROV. (Application of the Similarity Method to Radiation Fields During Adjustment of Neutron Radiation Meters). Vasil'ev, R. D.; Dorofeev, G. A.; Petrov, V. I.; Pimenov, M. I.; Shevchenko, V. F. (Gosudarstvennyi Komitet po Ispol'zovaniyu Atomnoi Energii SSSR, Moscow. Soyuznyi Nauchno-Issledovatel'skii Institut Priborostroeniya. Gosudarstvennyi Komitet po Ispol'zovaniyu Atomnoi Energii SSSR, Obninsk. Fiziko-Tekhnicheskii Institut). 1966. 4p. Dep. mn.

Metrological laboratories are recently paying increased attention to the problems of calibration of neutron equipment. The adjustment of neutron radiometers with neutron sources based on the similarity of radiation fields formed by appropriate sources which may differ in intensity but which have identical energy spectra is discussed. The sources used were gamma-beryllium (Sb-, Ra-, Na-), alpha-beryllium (Pu-, Po-, Ac-, Ra-), spontaneous fission (^{240}Pu), and nuclear reaction [$D(d,n)^3He$, $T(d,n)^4He$] sources, and the radiation similarity system was compared with conventional calibration results. While the errors never exceed the calibration tolerances, the adjustment time using the new method is significantly shorter, the working procedures are considerably safer, while the calibration ranges are larger by 2 or 3 orders of magnitude as compared with conventional calibration procedures. (CFSTI)

37075 (NP-16204) K VOPROSU OB ISPOL'ZOVANII YADERNYKH REAKTSII $D(d,n)^3He$ I $T(d,n)^4He$ DLYA GRADUIROVKI RADIOMETROV BYSTRYKH NEITRONOV. (Problem of Utilizing Nuclear $D(d,n)^3He$ and $T(d,n)^4He$ Reactions for Calibration of Fast-Neutron Radiation Meters). Vasil'ev, R. D.; Dorofeev, G. A.; Petrov, V. I.; Primenov,

M. I.; Shevchenko, V. F. (Gosudarstvennyi Komitet po Ispol'zovaniyu Atomnoi Energii SSSR, Moscow. Soyuznyi Nauchno-Issledovatel'skii Institut Priborostroeniya. Gosudarstvennyi Komitet po Ispol'zovaniyu Atomnoi Energii SSSR, Obninsk. Fiziko-Tekhnicheskii Institut). 1966. 4p. Dep. mn.

A detailed theoretical and experimental description is given of the study of radiometer calibration by neutrons with energies of approximately 2.5 and 14 Mev produced, respectively, by the $D(d,n)^3He$ and $T(d,n)^4He$ reactions. A diagram shows the target with the proportional counter which accepts neutrons from the NG-200 generator. The neutron radiometer calibration proved in general feasible, and the calibration error evaluated as the sum of mean square errors in the determination of neutron flow densities and the indicators of the meters were between 5 and 10%. (CFSTI)

37076 (SC-DC-66-1512) A PROCEDURE FOR THE COMPUTATION OF NEUTRON FLUX FROM FOIL ACTIVATION DATA: SPECTRA CODE. Greer, C. L.; Walker, J. V. (Sandia Corp., Albuquerque, N. Mex.). July 1966. Contract AT(29-1)-789. 17p. (CONF-660911-2). Dep. mn. CFSTI $1.00 cy, $0.50 mn.

From Conference on Radiation Measurements in Nuclear Power, Berkeley, England.

A technique is presented for determining the differential flux from foil activation data. The differential flux is represented by a piece-wise linear function in energy and the foil activations equations are reduced to a system of linear equations. An iteration algorithm, based on a minimization of a least squared error, is developed for solving the activation equations and the resulting infinite matrix series is solved explicitly. A computer code, SPECTRA, was written which incorporates the above technique, and which presently computes the differential flux at a maximum of fifty energy points. The code contains a cross section library of twenty-eight reactions and a complete data tape handling program which allows the removal, addition, and/or editing of the data on the cross section tape. Examples are presented which indicate that, with a general knowledge of the spectral shape, one can obtain quite accurate spectral information from activation detectors. (auth)

37077 (UCR-34P107-34) POSSIBLE ROLES FOR EMULSION AS A DETECTOR IN EXPERIMENTS WITH FUTURE HIGH-ENERGY ACCELERATORS. Barkas, Walter H. (California Univ., Riverside). [1966]. Contract AT(11-1)-34. 10p. (CONF-660713-1). Dep. mn. CFSTI $1.00 cy, $0.50 mn.

From 6th International Symposium on Corpuscular Photography, Florence.

The future role of emulsion detectors in high energy experiments is discussed. Topics included are the role in strong interactions in which mesons and other secondaries are produced in jets, peripheral production processes in which the nucleus does not disintegrate and to which there is little momentum transfer, the nuclear physics of extreme energies with beams of known character and energy, studies of hyperfragment production by Σ, Ξ, and Ω, hyperons, use with bubble chambers, electromagnetic cascades, and in weak interactions. (B.G.D.)

37078 X-RAY STANDARDIZATION AND COMPARISON OF THE FINNISH AND SWEDISH X-RAY STANDARDS. Rannikko, Simo; Toivola, Ahti (Inst. of Radiation Physics, Helsinki). Ann. Acad. Sci. Fenn., Ser. A VI, No. 201, 1-15(1966).

The Finnish 100 to 300 kv x-ray standard chamber is described. Factors affecting the accuracy of exposure measurements using a parallel-plate free-air ionization chamber are discussed. The maximum disagreement between the Finnish and Swedish x-ray standards was found to be 0.6%. This was well below the value of 1.2%, which is the maximum possible error in the Finnish standard dose measurement. (auth)

37079 MEASUREMENTS OF LARGE γ-RADIATION DOSES AND FLUXES BY MEANS OF PHOTOACTIVATION OF ISOMERIC NUCLEAR STATES. Abrams, I. A.; Pelekis, Paix, D. (Prince Henry Hospital, Little Bay, Australia). Int. J. Appl. Radiat. Isotop., 17: 486-7(Aug. 1966).
L. L.; Taure, I. Ya. At. Energ. (USSR), 20: 434-5(May 1966). (In Russian).

A method for measuring large γ radiation doses by detecting the exit γ' in reactions of the type $A(\gamma,\gamma')A^m$ is described. The results of an experiment using gamma-activation analysis along with standard well-type crystal detectors are outlined. Since the isomer method does not involve destruction of the material, it lends itself to repeated use. (G.O.Y.)

37080 IONIZATION-MECHANICAL DETECTOR FOR IONIZING PARTICLES. Myazdrikov, O. A.; Demidovich, V. N.; Suslov, A. P. At. Energ. (USSR), 20: 442-4(May 1966). (In Russian).

The self-oscillation region of macrocharges produced in electromechanical-type diodes was used to build a detector for high-flux ionizing-particle beams. The theory, which is based on a graphite-covered spherical charge geometry, is discussed along with some experimental tests of the detector. (G.O.Y.)

37081 DOSIMETRY OF IONIZING RADIATION. Cloos, O.; Pohlit, W. (Max Planck-Institut fuer Biophysik, Frankfurt am Main). Atompraxis, 12: 331-8 (July 1966). (In German).

A general survey is presented of the basic principles of the dosimetry of homogeneous and nonhomogeneous media. Dosimetry is based on the transport theory. The application of the probe method to photons, electrons, heavy ions, and neutrons is discussed, together with the requisite measurement conditions. Some measurement methods in experimental dosimetry are also discussed, and conversion relations for energy doses are given. (auth)

37082 LOW-LEVEL ALPHA-DISINTEGRATION RATE DETERMINATIONS WITH A ONE-MULTIPLIER PHOTOTUBE LIQUID SCINTILLATION SPECTROMETER. Horrocks, D. L. (Argonne National Lab., Ill.). Int. J. Appl. Radiat. Isotop., 17: 441-6(Aug. 1966).

A one-multiplier phototube liquid scintillation spectrometer was found to be capable of measuring a few tenths of a disintegration per minute of α-emitting nuclides. A room temperature counting system which employs one of the new bi-alkali photocathode multiplier phototubes was found to have comparable detection limits, with lower background, compared with one which employs a freezer-cooled conventional multiplier phototube. The different α-disintegration rates in a sample containing more than one α-emitting nuclide can be determined within the 6 percent energy resolution obtained in this work. (auth)

37083 SIMPLE MAGNETIC TAPE RECORDING SYSTEM FOR MEDICAL SCINTISCANNERS. Corry, P. M. (Univ. of Texas, Houston). Int. J. Appl. Radiat. Isotop., 17: 459-65(Aug. 1966).

A relatively simple magnetic tape recording system for recording scintillation scan data was developed. One channel is used for storage of the pulses obtained by the scanning scintillation probe. Another channel is used to record the relative position of the end of each scan line. Scans may be played back, on the scanner itself, with different contrast settings to optimize the presentation of information obtained from radioisotope scans. Storage on magnetic tape also safeguards against instrument failure and human error. (auth)

37084 GLASS VESSELS WITH ROUGHENED SURFACE FOR MEASUREMENT OF LOW-ENERGY β RADIATION IN LIQUID SCINTILLATORS. Schwerdtel, E. (Frieseke und Hoepner GmbH, Erlangen, Ger.). Int. J. Appl. Radiat. Isotop., 17: 479-81(Aug. 1966). (In German).

It was found that by roughening smooth test glasses the counting capacity in the measurement of tritium in liquid scintillators can be increased by 10–15%. The new vessels combine the advantages of glass and of polyethylene flasks. (auth)

37085 DO-IT-YOURSELF EXTERNAL STANDARDIZATION FOR A LIQUID SCINTILLATION COUNTER.

A simple alteration, which allows external standardization of all Packard counters up to the 314 series, is described. A hole is drilled in the baseplate of the sample changing assembly vertically above the position of the vial being counted. A γ source may be placed through this hole on top of the detector unit when required. The procedure for using the device and its reproducibility is described. (J.G.B.)

37086 MEASUREMENT OF BETA RADIOACTIVITY IN GAS SAMPLES USING A PLASTIC SCINTILLATOR CELL. Benson, R. H.; Maute, R. L. (Monsanto Co., Texas City, Tex.). Int. J. Appl. Radiat. Isotop., 17: 488-9(Aug. 1966).

The plastic scintillator cells for precise radioassay of gases in static samples, which are extremely stable and give highly reproducible results over years of use, are described. Polishing of the cell surfaces enhances the light-guiding property of the plastic. The end angles of the inner and outer surfaces were chosen to permit maximum transmission of light to the faces with a minimum number of reflections. High counting efficiencies are obtained even for weak β emitters. A major advantage of this type cell is that counting efficiency is independent of the type of filling gas. (J.G.B.)

37087 SCINTILLATION COUNTING WITH PLASTIC PHOSPHOR FOR DETERMINING TRITIUM RADIOACTIVITY AT SURFACES. Muramatsu, M. (Tokyo Metropolitan Univ.); Tokunaga, N. Int. J. Appl. Radiat. Isotop., 17: 489-91(Aug. 1966).

A device for measuring tritium β-rays using a sheet of plastic scintillator is described. It was found that counting characteristics do not depend on the thickness (0.01–0.25 mm) of the sheets. Background varied with temperature, with little influence on the over-all counting efficiency. Precise investigations were made for finding the optimum combination of phototube potential and discrimination width for obtaining the highest value of counting efficiency/background ratio. (J.G.B.)

37088 SPARK CHAMBER OPERATION AT HIGH VOLTAGE PULSE DELAY. Bostandzhyan, N. H.; Marikyan, G. A.; Matevosyan, K. M. (Inst. of Physics, State Atomic Energy Commission, USSR). Izv. Akad. Nauk Arm. SSR, Fiz., 1: 55-8(1966). (In Russian).

The registration efficiency of large gap spark chambers filled with pure neon, under the pressure of 600 mm Hg, is investigated. (auth)

37089 DOUBLE-PULSE IONIZATION CHAMBER FOR CORRELATION MEASUREMENTS OF THE ENERGY, ANGLE, AND MASS DISTRIBUTIONS IN THE FISSION OF HEAVY NUCLEI. Dragnev, T.; Delchev, M.; Dermendzhiev, E. Izv. Fiz. Inst. Aneb, Bulg. Akad. Nauk, 14: 67-72(1966). (In Russian).

A new method is suggested for the determination of the angle between the electric field direction of the double-pulse ionization chamber and the direction of the movement of the fission fragments. The method provides in principle an accurate determination of this angle and also makes possible the correlated study of the energy, mass, and angle distributions at the fission. (auth)

37090 SECONDARY STANDARDS IN DOSIMETRY. Dutreix, J.; Dutreix, A.; Wambersie, A. (Institut Gustave-Roussy, Villejuif, France). J. Belge Radiol., 49: 157-68 (1966). (In French).

Theoretical, technical, and practical studies were made on secondary standards in dosimetry. Two types are considered suitable for use as secondary reference dosimeters: ionization chamber and chemical $FeSO_4$ dosimeter. In the problem of estimating the dose absorbed in water, according to the dosimeter indicator, two steps are to be considered: determination of the absorbed dose in the detector; and evaluation of the relation between the dose absorbed in the detector and in the irradiated medium (water). Theoretical advantages and disadvantages of the ionization chamber and of $FeSO_4$ are discussed. (P.C.H.)

37091 CURRENT INTENSITY AND FLUX OF X RAYS. Van Caneghem, P.; Dunjic, A. (Univ., Liege. Univ., Louvain, Belg.). J. Belge Radiol., 49: 169-73(1966). (In French).

The evident exceptions to the rule of the proportionality between dose rate and milli-amperage are more frequent than is generally supposed. Methods for distinguishing a real sagging of the dose rate due to a fall of tension from an apparent incurvation caused by over-saturation of the ionization chamber by filtration of the radiation are discussed. In the first case, the incurvation persists or becomes more marked with a possible shifting of the maximum; in the second case it disappears. (auth)

37092 APPLICATION OF PROPANE AS BASIC COUNTING GAS IN PROPORTIONAL COUNTERS. Starcuk, Zenon; Cupak, Miloslav (Research Inst. of Macromolecular Chemistry, Brno). Jad. Energ., 12: 228-9 (June 1966). (In Czech).

The advantageous counting characteristics of counters filled with propane gas are discussed. The counting characteristics of pure propane and its mixtures with 10% CO_2 or with 5% O_2, measured by different input register sensitivities, are described. (auth)

37093 COINCIDENCE CIRCUIT FOR X-RAY SPECTROMETRY. Bayer, Ryszard. Nukleonika, 10: 807-9 (1965). (In Polish).

A 0.1 microsecond time resolution coincidence circuit is described, which consists of two parallel circuits that precede the coincidence function, and a pulse shaper and linear integrator (Cooke-Yarborough count rate circuit) with ranges of 1, 10, 100, 1000, 10,000, and 100,000 counts per second. Each of the two parallel circuits preceding the coincidence function has a pulse-height discriminator, a univibrator type delay generator (relative delay = 2 microseconds), and a pulse shaper. A plot of coincidence counts versus relative delay time yields flat-topped "curve" with a full width at half maximum of 2T = 0.2 microseconds. (TTT)

37094 EXAMINATION OF THE OVERPRESSURE AND UNDERPRESSURE METHODS OF OPERATING A PHOTOELECTRIC NUCLEUS COUNTER. Burke, T. P.; Scott, J. A. (University Coll., Dublin). Proc. Roy. Irish Acad., Sect. A, 64: 115-25(Feb. 1966).

An experimental examination of the effect of pressure on the calibration of a photoelectric nucleus counter is made using overpressures and underpressures. Very good agreement with the theoretical treatment of the problem is obtained with a counter of diameter 3.85 cm. With counters of diameter 2.54 cm the agreement is not good. This is attributed to a lack of mixing in the narrow counters. It is found that the mixing of the sample with the pure overpressure air depends markedly on the diameter of the counter. A number of experiments in support of this are described. (auth)

37095 RESULTS FROM THE NEW DENVER MULTIDIRECTIONAL MESON TELESCOPE. Chasson, R. L.; Iona, M.; Kisselbach, V. J.; Baker, P. Jr.; (Univ. of Denver, Colo.). pp 282-4 of Proceedings of the Ninth International Conference on Cosmic Rays. Vol. I. Stickland, A. C. (ed.). London, The Institute of Physics and The Physical Society, 1966.

The new University of Denver multidirectional meson telescope is described and its characteristics are presented. A program which converts data accumulated on a solar time base to a sidereal time base is given. Preliminary results seem to indicate certain anisotropies in excess of those which can be attributed to statistical fluctuations. (auth)

37096 BAROMETRIC CORRECTION ANOMALY AND NUCLEONIC COMPONENT TIME VARIATIONS DURING IQSY. Kisselbach, V. J.; Chasson, R. L. (Univ. of Denver). pp 471-3 of Proceedings of the Ninth International

Conference on Cosmic Rays. Vol. I. Stickland, A. C. (ed.). London, The Institute of Physics and The Physical Society, 1966.

Apparent anomalies resulting from the customary barometric air pressure correction for n-component monitors are discussed. These consist of slight apparent temporal inconstancy in the attenuation coefficients appropriate to the Denver nucleonic monitor computed according to the customary prescription, a residuum of pressure-correlated variations in corrected data reported for other n-component monitors. Further evidence of deviation from the usually accepted pressure regression for n-component monitors is adduced from the IQSY 1964 data of the Denver, Colorado, monitor (1600 m. altitude, 2.93 Gv/c Quenby-Wenk threshold). Apparent agreement with the results of studies of the altitude dependence of the n-component pressure coefficient conducted by the Rome group is pointed out. (auth)

37097 STUDIES OF THE BAROMETRIC COEFFICIENTS OF IGY AND NM-64 NEUTRON MONITORS. Griffiths, W. K.; Harman, C. V.; Hatton, C. J.; Ryder, P. (Univ. of Leeds, Eng.). pp 475-7 of Proceedings of the Ninth International Conference on Cosmic Rays. Vol. I. Stickland, A. C. (ed.). London, The Institute of Physics and The Physical Society, 1966.

The barometric coefficient of the Leeds IGY neutron monitor is shown to have a variation during the eleven-year cycle such that it has a value of about 6% larger at solar minimum than at solar maximum. No significant differences were found between the barometric coefficients of the Leeds IGY and NM-64 monitors for the first five months of 1965. The need to use both the correct value of the barometric coefficient and the experimentally determined mean station pressure is discussed. (auth)

37098 ON THE MULTIPLICITY EFFECT IN AN IGY NEUTRON MONITOR. Dyring, E.; Sporre, B. (Uppsala Univ.). pp 478-80 of Proceedings of the Ninth International Conference on Cosmic Rays. Vol. I. Stickland, A. C. (ed.). London, The Institute of Physics and The Physical Society, 1966

A transistor device for measuring the multiplicity distribution was attached to: (a) the ship-borne 2-counter neutron monitor mounted on M/S Stratus on the route Gothenburg–Cape Town–Australia–Suez–Gothenburg during 1964 for studying the latitude effect; a marked dependence is found with geomagnetic threshold rigidity explained by increasing mean multiplicity with increasing mean energy of the star-producing radiation; a new indication that muons play a part in the IGY neutron monitor data is found by the equal latitude dependence for both the multiplicities k = 1 and 2; (b) a 6-counter section of the neutron monitor at the Uppsala cosmic ray-station from January 1964–March 1965 for studying the time variations. During this period of little solar activity small variations are observed. A small 1% Forbush decrease is observed in January 1964 and the result from the detected multiplicity distribution indicates that a continuous recording of the multiplicity effect can give valuable results when the solar activity increases. Regression analyses of multiplicity intensities on atmospheric pressure have given reliable estimates of the attenuation coefficient for the multiplicities $k = 1, 2, 3, \geq 4$. (auth)

37099 SOME PROPERTIES OF THE RADIATION RECORDED BY THE IGY NEUTRON MONITORS IN THE LOWER ATMOSPHERE. Bachelet, F.; Balata, P.; Iucci, N. (Univ., Rome). pp 481-2 of Proceedings of the Ninth International Conference on Cosmic Rays. Vol. I. Stickland, A. C. (ed.). London, The Institute of Physics and The Physical Society, 1966.

The results are given of an altitude survey carried out in the autumn 1964 with a mobile neutron monitor mounted on a lorry between sea level and 1800 m above sea level at 6.4 Gv geomagnetic rigidity threshold. Both the attenuation and the multiplicity effect are studied as indexes of the properties of the radiation giving rise to the counting rate of the IGY neutron monitors. Some implications of the results obtained referring to the response of the IGY neutron monitors to primary variations are also discussed. In particular, since a 7% change in the atmospheric attenuation coefficient of the monitor intensity is found from 756 to 650 mmHg, attention is called to the practical interest of a detailed knowledge of the altitude dependence of the attenuation coefficient in view of the exact pressure correction of neutron station data. (auth)

37100 METEOROLOGICAL FACTORS AFFECTING THE COUNTING RATE OF NEUTRON MONITORS. Bercovitch, M.; Robertson, B. C. (Atomic Energy of Canada Ltd., Chalk River, Ont.). pp 489-91 of Proceedings of the Ninth International Conference on Cosmic Rays. Vol. I. Stickland, A. C. (ed.). London, The Institute of Physics and The Physical Society, 1966.

Daily average neutron rates from four high latitude NM-64 monitors situated at Inuvik, Churchill, Deep River and Goose Bay were compared to determine their dependence on atmospheric temperature and water vapor content. For each monitor, the neutron temperature effect was calculated from daily average radiosonde temperatures using the weights given by Dorman. The total amount of atmospheric water vapor was calculated from the radiosonde measurements of relative humidity and temperature. It is found that the minimum variance between the normalized rates of pairs of neutron monitors occurs when the rates are corrected for a negative temperature effect 1.27 ± 0.1 times that calculated from the Dorman formulation, and a water vapor effect of $-0.09 \pm 0.03\%/\text{g cm}^{-2}$. Changes in the neutron rate due to the temperature effect can exceed $\frac{1}{2}\%$ over a period of a few days, while the seasonal effect at these stations is about 1%. The water vapor effect produces a seasonal effect of 0.2–0.3% in the same direction as the temperature effect. (auth)

37101 INTRODUCTION OF METEOROLOGICAL CORRECTIONS INTO MESON MONITOR DATA. Carmichael, H.; Bercovitch, M.; Steljes, J. F. (Atomic Energy of Canada Ltd., Chalk River, Ont.). pp 492-4 of Proceedings of the Ninth International Conference on Cosmic Rays. Vol. I. Stickland, A. C. (ed.). London, The Institute of Physics and The Physical Society, 1966.

A set of regression calculations was carried out correlating the daily average meson intensity with barometric pressure, atmospheric temperature, and neutron monitor intensity. Two complete years of data from a plastic scintillator meson monitor and from a large neutron monitor, operated in a constant-temperature laboratory at Deep River, were used. An exhaustive list of atmospheric temperature parameters was investigated: ground temperature, the heights of the 100, 200, 300, and 400 mb levels, some recommended combinations of isobaric level heights and temperatures, formulations due to Dorman and to Maeda using temperatures at all the standard isobaric levels, a number of arbitrarily distorted versions of these formulations including those recommended by Wada and by Lindgren. It was found that the formulations of Dorman, of Maeda, and of Wada were almost indistinguishable in terms of the available data and yielded by far the best fit among the variables. However, none of the temperature parameters tried was able to fit the day-to-day and the seasonal temperature effects equally well with a single regression coefficient. Use of the following partly empirical temperature parameter resolved the difficulty for routine correction of the Deep River data: $1.045\ T(j) + 0.215\ \overline{T}(j)$, where $T(j)$ is Maeda's temperature correction for day j and $\overline{T}(j)$ is its 31-day running average centered on day j. (auth)

37102 RADIO SYSTEM FOR THE DETECTION OF AIR SHOWERS. Porter, N. A.; Long, C. D.; McBreen, B.; Murnaghan, D. J. B.; Weekes, T. C. (University Coll., Dublin). pp 706-7 of Proceedings of the Ninth International Conference on Cosmic Rays. Vol. 2. Stickland, A. C. (ed.). London, The Institute of Physics and The Physical Society, 1966.

A radio receiving system with broad band helical aerial is in operation, in conjunction with a Cherenkov particle detector which selects showers. The frequency is 70 Mc, and the bandwidth about 20 Mc. The angular beamwidth of the

aerial is 50°, centered at the zenith. In 650 hours of operation, five large bandwidth-limited pulses were observed in association with showers. No such pulses were seen in comparison traces or at times before or after the expected time of arrival. In an analysis of one-third of the data, 16 smaller pulses were observed at the expected time of arrival, with none in a comparison interval slightly later. The rates of pulses observed are lower than expected theoretically, which may indicate some degree of decoherence. Operation of the radio system without a particle detector indicates that while interference pulses do occur, they are easily distinguishable from shower pulses. The use of a wide-band radio detecting system without particle detectors may therefore be feasible. (auth)

37103 BALLOON EXPERIMENT USING SPARK CHAMBERS AND AN IONIZATION SPECTROMETER. Pinkau, K. (Univ., Kiel); Pollvogt, U.; Schmidt, W.; Huggett, R. W. pp 821-3 of Proceedings of the Ninth International Conference on Cosmic Rays. Vol. 2. Stickland, A. C. (ed.). London, The Institute of Physics and The Physical Society, 1966.

An instrument was constructed which permits the determination of time of incidence, direction and location of high energy cosmic ray particles using spark chambers. The energy of the particles is measured using an ionization spectrometer. The experiment will soon be flown in Texas and is designed to measure the flux, composition, time variation, and properties of individual interactions of cosmic rays above 100 Bev. (auth)

37104 UNIVERSITY OF UTAH NEUTRINO DETECTOR. Bergeson, H. E.; Hilton, L. K.; Keuffel, J. W.; Morris, M.; Parker, J. L.; Stenerson, R. O.; Wolfson, C. J. (Univ. of Utah, Salt Lake City). pp 1048-50 of Proceedings of the Ninth International Conference on Cosmic Rays. Vol. 2. Stickland, A. C. (ed.). London, The Institute of Physics and The Physical Society, 1966.

Two novel types of detector elements were developed for a 2000-ton neutrino detector now under construction at Utah. The first, a cylindrical spark counter, resembles a giant Geiger tube 15-cm in diameter by 10-m long. With a filling of 50-cm argon and 25-cm ethylene the discharge is a sharply localized corona spike, which may be located by a simple sonic technique to an accuracy of about 3 mm. Four Cherenkov counters will trigger an array of 500 spark counters and determine the sense of travel of upward-going muons produced by neutrinos. The Cherenkov counter consists of a water-filled concrete tank of dimensions 6m × 10m × 1m painted black inside. Each 6m × 10m surface is covered by an array of 113 light-collector elements. By recording separately the pulses from each face, the sense of travel of the muon may be determined. The complete detector will resemble a multi-plate spark chamber with the spark gaps replaced by trays of cylindrical spark counters and the trigger function supplied by the Cherenkov counters. Measurements of the secondary muon energy spectrum will be possible by range and by Coulomb scattering. (auth)

37105 EXPERIMENTAL STUDY OF SOME OF THE BASIC PROPERTIES OF SPARK CHAMBERS. Meyer, M. A.; Retief, J. J. (Univ. of Stellenbosch, South Africa). pp 1070-4 of Proceedings of the Ninth International Conference on Cosmic Rays. Vol. 2. Stickland, A. C. (ed.). London, The Institute of Physics and The Physical Society, 1966.

An experimental study was made of the dependence of the threshold voltage and sparking efficiency on the pressure, separation between the electrodes, clearing field and delay of the high voltage pulse. The threshold and plateau efficiency depends on the pressure and separation through the product of the pressure and separation only. The effect of the delay and clearing field on the efficiency is in agreement with expressions previously derived. (auth)

37106 THEORETICAL ANALYSIS OF THE PERFORMANCE OF HIGH-RESOLUTION MAGNETIC HODOSCOPES. Bacon, D. F.; Nash, W. F. (Univ. of Nottingham, Eng.). pp 1075-8 of Proceedings of the Ninth International Conference on Cosmic Rays. Vol. 2. Stickland, A. C. (ed.). London, The Institute of Physics and The Physical Society, 1966.

A general theoretical treatment is given for digital hodoscopes used in the magnetic analysis of charged particles, with particular reference to high resolution instruments. It enables the momentum response spectrum of any "category" or combination of "categories," recognized by the hodoscope, to be predicted and thus also permits the accurate assessment of experimental error due to instrumental effects. The purpose of the method is to obtain the mean momentum response spectrum for particles incident within a given range of angles to the axis of the acceptance telescope, in terms of the known spatial resolution function of the individual hodoscope elements. Since the sharpness of this function is found to be an important factor, it is given particular attention. (auth)

37107 LIQUID SCINTILLATION COUNTERS. Ashton, F.; Coats, R. B.; Simpson, D. A. (Univ. of Durham, Eng.). pp 1079-81 of Proceedings of the Ninth International Conference on Cosmic Rays. Vol. 2. Stickland, A. C. (ed.). London, The Institute of Physics and The Physical Society, 1966.

The performance of a thin, large area (1.24 m^2) liquid scintillation counter was investigated both experimentally and theoretically. The maximum nonuniformity (maximum deviation from the average response of the counter to relativistic muons incident normal to its largest area) is 18% and 31 ± 9 photoelectrons are collected by the two 5-in. photomultipliers when a phosphor of paraffin oil, 0.5 g l^{-1} of p-terphenyl and 0.005 g l^{-1} of POPOP is used. The average energy loss to produce one scintillation photon is evaluated and using available measurements of the relative efficiencies of known phosphors the feasibility of producing more efficient liquid phosphors than those known at present is discussed. (auth)

37108 LARGE WILSON CLOUD CHAMBER AND ITS APPLICATION TO IONIZATION CALORIMETRY WORK. Hodson, A. L.; Bacon, T. C.; Pullan, B. R. (Univ. of Leeds, Eng.). pp 1082-4 of Proceedings of the Ninth International Conference on Cosmic Rays. Vol. 2. Stickland, A. C. (ed.). London, The Institute of Physics and The Physical Society, 1966.

A cloud chamber, having a useful illuminated volume of 185 cm × 157 cm × 85 cm, is described. The chamber is at present being operated as a multi-plate chamber with 27 plates (total weight about 11,000 kg including about 5,000 kg of absorber). However, the versatile design would equally permit operation as a magnet chamber in a pulsed field. Other novel features of the design include the expansion arrangement which permits piston accelerations of 100 g and decelerations of 300 g in order to achieve a fast laminar expansion. A technique is being developed for measuring the total energy of a high-energy nuclear cascade produced in the cloud chamber by sampling the ionization at several depths in the chamber. Electron collection by the plates gives a measure of the ionization, while the relatively slow-moving positive ions remain to give the tracks. (auth)

37109 CURRENT SPLITTING IN DIVIDED-ELECTRODE SPARK CHAMBERS. Bacon, D. F.; Nash, W. F. (Univ. of Nottingham, Eng.). pp 1087-9 of Proceedings of the Ninth International Conference on Cosmic Rays. Vol. 2. Stickland, A. C. (ed.). London, The Institute of Physics and The Physical Society, 1966.

During the recent development of prototype divided electrode spark chambers, it was found that the total current conducted through the discharge tended to divide between adjacent elements of the divided electrode. The mean relative proportion of this current splitting was found to be a function of the point of origin of the primary avalanche with respect to the divided electrode sections and the nature of this function was found to depend upon the electrode geometry. The phenomenon is discussed in relation to the printed circuit electrodes used during this work and a general model presented in terms of the streamer theory of spark formation. (auth)

37110 IONIZATION MEASUREMENT IN A STREAMER CHAMBER. Asatiani, T. L. (Inst. of Physics, State Committee for the Utilization of Atomic Energy, Erevan); Gazaryan, K. A.; Yamirov, V. N.; Matevosyan, E. M.; Nazaryan, A. A.; Sharkhatunyan, R. O. pp 1091-3 of Proceedings of the Ninth International Conference on Cosmic Rays. Vol. 2. Stickland, A. C. (ed.). London, The Institute of Physics and The Physical Society, 1966.

The experimental results of ionization measurements in a streamer chamber filled with neon and helium are given. The measurements were carried out with protons of various energies at various angles to the electric field. It is shown that track brightness is the best parameter for ionization measurement of the particles. The change in track brightness, as the ionization changes, is investigated and the results are compared with the calculated data. (auth)

37111 USE OF PULSE SHAPE DISCRIMINATION WITH SCINTILLATION COUNTERS FOR COSMIC-RAY STUDIES. Barton, J. C.; Sanni, A. O. (Northern Polytechnic, London). pp 1094-6 of Proceedings of the Ninth International Conference on Cosmic Rays. Vol. 2. Stickland, A. C. (ed.). London, The Institute of Physics and The Physical Society, 1966.

The dependence of scintillation decay characteristics on ionization density offers a possible technique for distinguishing events involving low energy nucleons or nuclear disintegrations from those due to minimum ionizing particles. A method of pulse shape discrimination was developed which provides the wide dynamic range required for cosmic ray applications. The performance possible with various scintillators is reported. (auth)

37112 DEVELOPMENT OF SCINTILLATION COUNTERS BASED ON MEDICINAL PARAFFIN. Barton, J. C.; Crispin, A. (Northern Polytechnic, London). pp 1097-8 of Proceedings of the Ninth International Conference on Cosmic Rays. Vol. 2. Stickland, A. C. (ed.). London, The Institute of Physics and The Physical Society, 1966.

Medicinal paraffin is preferred as a scintillator solvent because it is cheap, safe, chemically inactive and highly transparent. Its efficiency is relatively poor but can be enhanced by the use of a secondary solvent. It is shown that Shellsol A can be effective without spoiling the natural advantages of the paraffin. Counters based on these solutions have proved to be satisfactory for cosmic ray investigations over long periods. (auth)

37113 CHEMICALLY INAGGRESSIVE LIQUID SCINTILLATORS. Meyer, M. A.; Van Der Westhuizen, P. J. (Univ. of Stellenbosch, South Africa). pp 1099-1104 of Proceedings of the Ninth International Conference on Cosmic Rays. Vol. 2. Stickland, A. C. (ed.). London, The Institute of Physics and The Physical Society, 1966.

The light output and attenuation length of a number of inexpensive liquid scintillators which are stable against Perspex were measured. The light output of some of these scintillators approaches that of toluene scintillators. The attenuation length of the scintillation light in these scintillators is in the region of 50% of the value found for a toluene scintillator. (auth)

37114 PARTICLE COUNTING IN LOCALLY PRODUCED SHOWERS USING VIDICON TELEVISION TECHNIQUES. Briggs, D. A.; Hodson, A. L. (Univ. of Leeds, Eng.). pp 1105-7 of Proceedings of the Ninth International Conference on Cosmic Rays. Vol. 2. Stickland, A. C. (ed.). London, The Institute of Physics and The Physical Society, 1966.

Vidicon techniques with spark chambers are increasingly being used for determining the trajectories of single ionizing particles. The possibility of using such vidicon tubes for counting many simultaneous particles is being studied. Owing to the poor multiple track efficiency of ordinary spark chambers, limited discharge chambers were investigated for this purpose. The low intensity of light from these, however, makes observation difficult and methods of increasing the sensitivity of the system are discussed. One possibility is to observe the vidicon output pulses from two or more adjacent television lines in delayed coincidence in order to discriminate against background noise. Preliminary results appear promising and suggest that the technique, when fully developed, may have applications in many fields where a "simultaneous particle counter" is required. For example, one vidicon could be used to gather information from several different levels in a "discharge chamber calorimeter." (auth)

37115 ANTICOINCIDENCE SHIELDED GAMMA-RAY SPECTROMETER FOR NUCLEAR REACTION STUDIES. Evans, Albert E. (Naval Ordnance Lab., Silver Spring, Md. Univ. of Maryland, College Park); Brown, Bernard; Marion, Jerry B. Rev. Sci. Instrum., 37: 991-9(Aug. 1966).

A scintillation spectrometer was built utilizing a modular liquid scintillation anticoincidence shield for a 12.7-cm diameter by 25.4-cm long NaI(Tl) detector crystal. The effectiveness of the anticoincidence shield is enhanced by storing in one-half of a multichannel analyzer memory those pulses from the NaI(Tl) crystal which are coincident with shield pulses. A fraction of this coincident spectrum is then subtracted from the anticoincident spectrum as a correction for shield inefficiency. A computer system is used for data handling. Spectral response for gamma radiation from 0.35 to 17.6 Mev was measured. (auth)

37116 ELECTRON DENSITOMETER FOR IRRADIATION STUDIES IN ELECTRON MICROSCOPE. Sciacca, T. P. Jr.; Eubanks, A. G. (Goddard Space Flight Center, Greenbelt, Md.). Rev. Sci. Instrum., 37: 1019-20(Aug. 1966).

A probe assembly is described which permits the use of an electron microscope to irradiate materials with low energy (50–150 kev) electrons. The electron beam current produced by the microscope can be monitored quickly and accurately with this unit so that the irradiation rate can be closely controlled. Although developed for use in the Hitachi HU-11 electron microscope, the device can, with but minor modifications, be utilized in other microscopes as well. (auth)

37117 POLYMER DEGRADATION DOSIMETER OF POLYISOBUTYLENE IN HEPTANE. Carriker, A. Wendell (American Machine and Foundry Co., Alexandria, Va.). Contract NAS-5-3740. Rev. Sci. Instrum., 37: 1045-7 (Aug. 1966).

A radiation dosimeter that utilizes a polymer solution is described. The viscosity of the solution is an inverse function of dose, and the dose range for a given range of viscosity can be adjusted by changing the concentration and molecular weight of the polymer solute. Several small vibrating transducers for measuring the change of viscosity were investigated. Since polyisobutylene in heptane is a non-Newtonian solution 1-f transducers were most effective. (auth)

37118 EFFICIENT LIGHT COUPLER FOR THRESHOLD CHERENKOV COUNTERS. Hinterberger, H.; Winston, R. (Univ. of Chicago). Rev. Sci. Instrum., 37: 1094-5(Aug. 1966).

A light funnel which performs a maximum reduction in spot size consistent with high efficiency was designed for use as a light coupler for threshold Cherenkov counters. Restriction is made to a reflecting surface which is taken to be a surface of revolution about the phototube axis. If the aperture of one funnel does not cover the entire light spot the required number of funnels can be clustered in a hexagonally close-packed array. This permits all the Cherenkov light to be collected with high efficiency. (J.F.P.)

37119 MICROWAVE DETECTOR USING PLASMA. Chrenka, A. Sdelovaci Tech., 12: 227-8(1964). (In Czech).

The new plasma detector uses the external magnetic field. Hence not only are eventual losses due to gas diffusion lowered, but at the same time, the sensitivity of the detector is increased. In the presence of a suitable magnetic field the plasma operates under the conditions of the cyclotron resonance of electrons, which increases

the efficiency of the interaction between microwave energy and plasma. The block diagram of the new plasma detector is shown. The plasma is created by impulse discharge in a glass discharge tube. (auth)

37120 SIMPLIFIED 180° FOCUSING β-RAY SPECTROMETER. Mei, J. Y.; Chen, H. F.; Tan, B. L.; Chen, J. F.; Feng, J. Wu Li Hsueh Pao, 22: 547-53(May 1966). (In Chinese).

A 180° focusing beta spectrometer is described in which the average radius of the electron trajectories is 100 mm. The uniform magnetic field of the spectrometer is produced by a single-yoke electromagnet. The resolving power of the spectrometer is 0.7% for a ^{198}Hg K conversion line, with a source width of 0.8 mm. (D.C.W.)

37121 CORRELATIONS OF HIDDEN IMAGE PARAMETERS IN OPTICAL AND NUCLEAR PHOTOEMULSIONS. Kartuzhanskii, A. L. (Engel's Inst. of Soviet Trading, Leningrad). Zh. Nauch. Prikl. Fotogr. Kinematogr., 9: 414-19(Nov.-Dec. 1964). (In Russian).

P. V. Meiklyar's expression concerning the breakdown of the reciprocity law was used for studying the latent-image parameters of 19 nuclear and 10 optical photoemulsions from industrial and laboratory sources. The exposed emulsions were kept at temperatures of 0, 20, 30, and 40°C for periods up to 10^4 and even 10^5 seconds. The iso-opacity curves were related to a density of 0.25 above the fog. Up to the formation of a latent image, the higher the electron levels of the sensitivity specks, the lower the sensitivity of the microcrystals. In the case of crystals with low sensitivity, reduction of the levels to the point at which development is initiated, is reached by adding a larger number of silver atoms than required for highly sensitive crystals. The energies of activation of the optical and nuclear emulsions were found to agree with each other, especially if the large grain size of the crystals in the former is taken into consideration. If there are no differences in the absorption of the radiation energy by the microcrystals, the latent image data may be used for the unequivocal description of the formation of development centers in any type of emulsion. (TTT)

37122 DEVICE FOR ESTIMATING AgBr MICROCRYSTAL ENERGY THRESHOLD SENSITIVITY TO CHARGED PARTICLES. Kuks, I. M. Zh. Nauch. Prikl. Fotogr. Kinematogr., 9: 458-9(Nov.-Dec. 1964). (In Russian).

The sensitivity threshold of AgBr microcrystals may be determined on the basis of the formation of conductivity electrons as the result of slowing down fast and slow particles within the solid; the electron energy which does not result in the creation of development centers is thereby taken as the limiting value. The emulsions tested were exposed to electron beams, increasing gradually the energy of the beam and correlating the developed grain yield with the energy of the electrons. Care was taken to limit the radiation density to 0.1 to 0.2 electrons per microcrystal and to keep the mean free paths of the electron smaller than the dimensions of the crystals, in order to minimize the escape probability. The experimental method used allowed to vary the energy from 0 to 1200 ev and the radiation density from 0 to 10^{10} electrons per cm^2. Sensitivity measurements were carried out with the NIKFI-R type emulsion. (TTT)

37123 NEW METHOD FOR THE REDUCTION OF COMPTON CONTINUA IN γ SCINTILLATION SPECTRA. Geisler, M. Leipzig, Univ., Leipzig, 1965. 120p. $2.00 Gmelin, AED-Diss. 65-294.

A method for the reduction of Compton continua is proposed. Photopeak efficiency in NaI crystals for axis parallel collimated incidence depends on the distance of the collimator from the axis because the number of photons leaving their total energy in the scintillator by more than one interaction depends on the geometrical arrangement. By subtraction of the spectrum with peripheral incidence from the spectrum with central incidence, a pulse-height distribution without the Compton continuum is obtained. Peak efficiencies are calculated by Monte Carlo methods and are compared with experimental data. (Gmelin Inst.)

37124 IONIZATION CHAMBER. Despain, L. G.; Andersen, H. A. (Jet Propulsion Lab., Pasadena, Calif.). 5p. (CONF-650827-2). ORAU. Gmelin, AED-CONF-65-213-2.

From Western Electronics Show and Conference, San Francisco.

An integrating ionization chamber modified for the Mariner IV Mars mission and used along with a G-M counter for measurements of charged particles in interplanetary space is described. The design evolution, calibration, operation, and instrument failure are briefly discussed. (L.B.S.)

37125 BETA SPECTRUM SHAPE MEASUREMENTS WITH A 4π SEMICONDUCTOR SPECTROMETER. Spejewski, E. H. (Indiana Univ., Bloomington). 37p. (CONF-651015-14). ORAU. Gmelin, AED-CONF-65-312-36.

From American Physical Society Meeting, Chicago.

A 4π semiconductor spectrometer employing diffused window lithium-drifted silicon detectors was constructed. It was tested by varying the parameters of the system, so as to eliminate possible sources of distortion. If was further tested by measuring the shapes of two simple β spectra (^{143}Pr and ^{185}W), and two inner-group β spectra (^{198}Au and ^{86}Rb) in coincidence with the subsequently emitted γ-rays. The γ-ray pulse, detected by a NaI well counter that envelops the beta spectrometer, supplied the gate to the 400-channel pulse-height analyzer. In all cases, the results of these measurements are in good agreement with those previously reported. The beta spectrum of the ^{170}Tm decay to the first excited level in ^{170}Yb was measured in coincidence with the 84-kev gamma-ray. The experiment was performed under the same measurement conditions used for the ^{198}Au and ^{86}Rb experiments. The spectrum exhibits a definite nonstatistical energy dependence, falling below any straight line Fermi-Kurie plot fit at low energies. The shape factor was fitted by a polynomial of the form $1 + aW + b/W + cW^2$. A good fit was obtained for a = 1.11, b = −0.85, c = −0.24. The endpoint of this transition was determined to be 879 ± 7 kev. (auth)

37126 MEASUREMENT OF HIGH-ENERGY γ-RAYS WITH Ge(Li) DETECTORS. Berg, R. E.; Kashy, E. (Michigan State Univ., East Lansing). 14p. (CONF-651015-11). ORAU. Gmelin, AED-CONF-65-312-28.

From American Physical Society Meeting, Chicago.

A method of measuring the energy of high-energy gamma rays is described. It utilizes parallel capacitors as an effective energy multiplier of a pulser signal to compare unknown high-energy gamma rays to well-known low-energy standards. This method has also provided an effective tool for measuring the linearity of the energy response of Ge(Li) detectors. This response was found to be linear to better than ±0.03% in the range 662 to 2614 kev, and better than ±0.1% up to 6 Mev. As an example of this capacitor multiplying method the energy of the gamma ray from the 3^- excited level of ^{16}O was measured to be 6127.8 ± 1.2 kev. (auth)

37127 GAS SCINTILLATION. Easton, J. F. Edmonton, Alta., Univ. of Alberta, 1963. 27p.

Thesis.

The building of a gas scintillator and experiments done to measure the effects of impurities are described. It is concluded that a practical neutron counter with a stable lifetime in excess of one week can be built and recommendations are given for the building of such a counter. It is also concluded that for low-energy neutrons the counter would be useful for giving a timing pulse in time-of-flight work and would itself measure the energy of higher energy neutrons (1 Mev) with a reasonable resolution. (auth)

37128 ELEKTRONNYE TSIFROVYE SPEKTROMETRY V EKSPERIMENTAL'NOI YADERNOI FIZIKE. (Electronic Digital Spectrometers in Experimental Nuclear Physics). Mel'nikov, G. P. Moscow, Atomizdat, 1966. 191p.

A brief description is given of the design, performance, and applications of electronic digital spectrometers, which have a purely discrete digital part for use with any elec-

tronic multichannel spectrometric instrument (amplitude analyzers, time analyzers, etc.). Considerable space is devoted to numerical spectrometers with 100 to 1000 channels with sufficiently flexible performance for laboratory investigations in nuclear physics. The book is designed for engineers and physicists. 219 references are included. (L.B.S.)

Radiation Effects

Refer also to abstract 38353.

37129 (SC-DC-66-1820) TRANSIENT ANNEALING IN SEMICONDUCTOR DEVICES FOLLOWING PULSED NEUTRON IRRADIATION. Sander, H. H.; Gregory, B. L. (Sandia Corp., Albuquerque, N. Mex.). July 1966. Contract AT(29-1)-789. 32p. (CONF-660705-1). Dep. mn. CFSTI $2.00 cy, $0.50 mn.

From IEEE Annual Conference, Palo Alto, Calif.

This report supersedes SC-DC-66-1443.

Transient annealing following pulsed neutron exposure was investigated in silicon transistors and solar cells as a function of both irradiation temperature and injection level. In addition, experiments incorporating both x and gamma irradiation have demonstrated that transient annealing is a bulk, not a surface, effect. The observed annealing following neutron irradiation is considerably slower at low temperatures than at room temperature. At 213°K the density of annealable defects remaining at 10^{-4} seconds after exposure is approximately three times that observed at this same time for a 300°K irradiation. The injection studies show that at any temperature from 76 to 300°K the presence of minority carrier injection considerably speeds the transient annealing processes. A model is presented which explains many of the features observed in transient annealing. Various kinetic processes are discussed in the derivation of this model, including diffusion limited and generation limited processes, and the results of the model are compared to experimental data. (auth)

37130 BEHAVIOR OF MOS STRUCTURES IN THE CASE OF AN INDUCED IONIZATION. Giralt, G.; Andre, B.; Simonne, J.; Esteve, D. (Univ., Toulouse). Electron. Lett., 2: 209-10(June 1966). (In French).

Experiments of MOS structures when irradiated by x rays involve distributions of positive charges in the dielectric layer. As an interpretation of the results, including the curing of irradiated devices by annealing, ionic-charge motions in the oxidized silicon, depending on the sense of the applied electric field are proposed. (auth)

37131 RADIATION DAMAGE IN LUMINESCENCE INTENSITY OF ANTHRACENE. Asada, Tsunesaburo; Kawanishi, Masaharu (Osaka Univ.). Radioisotopes (Tokyo), 14: 328-30(July 1965). (In Japanese).

The application of molecular crystals of anthracene to the dosimetry of intense radiations is based on the luminescence being degraded with γ dose. An anthracene specimen for investigation was prepared by chemically purifying and repeatedly distilling with ethylene glycol a commercial anthracene. The specimen was activated with ultraviolet rays from a mercury lamp. After irradiation with intense gamma rays from a ^{60}Co source, the intensities of two peaks at 4240 and 4450 Å in the luminescence spectra of anthracene were reduced while the spectral distribution of luminescence remained nearly unchanged. The change in the emission intensity can be expressed as $I/I_0 = (1 + 1.25 \times 10^{-6}D)^{-1}$, where I_0 and I are the emission intensities before and after irradiation, and D is the radiation dose. The remarkable luminescence degradation caused by γ irradiation is not attributed to the radiation damage in the anthracene molecules, but to some damage in the energy transfer mechanism within the crystal. The luminescence degradation shows a tendency similar to that in the degradation of photoconductivity. The mechanism of luminescence degradation due to γ irradiation was compared with that caused by ultraviolet irradiation. (NSA of Japan)

37132 TRANSIENT RADIATION EFFECTS ON INSULATED GATE FIELD EFFECT TRANSISTORS. Krueger, A. F.; Griffin, E. E. Jr. (Autonetics, Anaheim, Calif.). 5p. (CONF-650707-20). ORAU. Gmelin, AED-CONF-65-152-23.

From IEEE Annual Conference on Nuclear and Space Radiation Effects, Ann Arbor, Mich.

The effects of transient gamma radiation on insulated gate field effect transistors were studied. Both n-channel and p-channel devices on semiconductor substrates and also thin film silicon nonjunction devices on insulating substrates were irradiated in the study. Experiments were performed in which the FET's were subjected to the radiation pulse from a 600-kev flash x-ray unit. The dependence of the observed radiation induced gate and drain currents on the device parameters, drain voltage, gate voltage, channel conductance, and input resistance were measured. These data are compared to transient responses predicted by assuming radiation induced gate voltages and radiation induced changes in conductivity of the source-drain channel. (auth)

ISOTOPE TECHNOLOGY

General

Refer also to abstracts 37001 and 37017.

37133 (STI-PUB-112(Vol.2)) RADIOISOTOPE INSTRUMENTS IN INDUSTRY AND GEOPHYSICS. VOL. II. Proceedings Series. Proceedings of the Symposium held by the International Atomic Energy Agency in Warsaw, 18–22 October 1965. (International Atomic Energy Agency, Vienna (Austria)). May 1966. 486p. (CONF-651023 (Vol.2)). IAEA: $10.00; S210,-; £ 3.0.0; F Fr 40,-; DM 35,-.

Separate abstracts were prepared for 9 of the 26 papers included. For the other 17 papers see CONF 651023 in the Report Number Index. (G.O.Y.)

For abstracts of individual papers see: 37001, 37017–37020, 37060, 37134, 37135, and 37154.

37134 USE OF A SURFACE HYGROMETER FOR CHECKING RESIN INJECTIONS IN SALVAGING THE TEMPLES OF ABU SIMBEL. Caron, C. (Societe Soletanche, Paris); Marcesse, J. (Commissariat a l'Energie Atomique, Cadarache, France). pp 425-33 of STI-PUB-112(Vol.2). (In French).

The method adopted by UNESCO for salvaging the temples of Abu Simbel is to section them and raise them in single blocks of 15 to 30 tons which have been previously reinforced. This indispensable reinforcement will be accomplished by injection of a resin capable of cold polymerization (method advocated by Soletanche). The problem is to avoid any flow of the resin which might endanger the surface, particularly the frescos of the inside rooms. The surface neutron probe (normally used for humidity determination) is an ideal method for locating the resin front at a suitable distance from the wall; the sandstone constituting the basic rock is perfectly dry, whereas the injected polyester resin contains a high proportion of hydrogen atoms. In experiments carried out at Cadarache, the reinforced rock was represented by blocks of polyester sand in different geometric shapes previously prepared and immersed in silica sand. It was possible to simulate the process by which the resin advances, both for the case of a continuous front and for the case of movement along strata of different thicknesses. In the former case, scanning of the surface by means of a probe gave rise to a constant signal which was already perceptible when the resin was 30 cm from the wall and became stronger as the front approached. If the medium is heterogeneous the result of the reading depends on the position of the probe. Analysis of the curves obtained from these geometric models indicates the feasibility of rapid interpretation of the measurements made during in situ injections into the rock. (auth)

37135 OBSERVATIONS ON THE UTILIZATION OF THE SCATTERING OF GAMMA RAYS AND NEUTRONS TO INVESTIGATE UNDERGROUND AQUIFERS. Dietl, H.; Kehrer, R.; Moser, H.; Neumaier, F.; Rauert, W. (Forschungsstelle fuer Radiohydrometrie, Munich). pp 435-47 of STI-PUB-112(Vol.2).

As a supplement to tracer measurements of groundwater currents, the authors have attempted by the $\gamma\gamma$ and nn methods to determine the density and moisture content of an underground aquifer, using filter gauge tubes surrounded by a gravel filter. The parameters varied in the laboratory tests were the diameter and wall thickness of the filter tube, the thickness of the gravel filter, and the density and moisture of the soil material. For the calibration measurements, arbitrary moisture contents were produced by mixing quartzous sand, water and gel-forming SiO_2("Aerosil"). Two different logging tools (5-mC ^{137}Cs or 10-mC Ra at a distance from the detector of 20 and 55 cm, respectively) were used to measure soil density. A method is described that allows calibration curves to be constructed for any gauge tube and gravel filter thickness. In field measurements the density logs obtained with the two probes showed slight differences which can be traced to the differing measuring volumes of the two probes and to the formation of pockets in the vicinity of the gauge tube. (auth)

37136 ISOTOPES AND RADIATION TECHNOLOGY. Volume 3, Number 3. Baker, P. S.; Lafferty, Robert H. Jr.; Gerrard, Martha; Fuccillo, D. A.; Greene, R. E.; McKinney, F. E.; Carden, Joan E.; Rupp, A. F. (eds.). Contract W-7405-eng-26. One of the five Quarterly Technical Progress Reviews published for the Division of Technical Information, USAEC. Oak Ridge National Lab., Tenn., Spring 1966. 116p. GPO $0.70 Domestic, $0.90 Foreign.

The developments in the fields of isotopes and radiation technology are discussed. The work of the Isotopes Information Center at ORNL is described. Separate abstracts were prepared for nine sections to cover the review. (M.C.G.)

For abstracts of individual sections see: 36544, 36749, 37127, 37142–37145, 37163, and 37164.

37137 ISOTOPES AROUND THE WORLD. Isotop. Radiat. Technol., 3: 263-79(Spring 1966).

The activities of the Euratom complex concerned with radioisotopes are described. Work in promoting industrial uses of isotopes and synthesis and uses of radioisotope-labeled materials are discussed. State-of-the-art reports on production and uses of radioisotopes in Yugoslavia and Australia are presented. West German radioisotope imports are compiled, and a recent catalog of stable isotopes from East Germany is reviewed. (auth)

Industrial Applications

Refer also to abstracts 36994, 37058, and 37064.

37138 (AED-C-05-05) BIBLIOGRAPHIES IN NUCLEAR SCIENCE AND TECHNOLOGY. SECTION 05: FOOD IRRADIATION. Tuchscheerer, Th.; Beising, K. (comps.) (Zentralstelle fuer Atomkernenergie-Dokumentation, Gmelin-Institut fuer Anorganische Chemie und Grenzgebiete, Frankfurt am Main (West Germany)). June 1966. 165p. Dep. mn.

Over 600 references on irradiation of food are presented. Author, report number, and subject indexes are included. (auth)

37139 (STI-PUB-112(Vol.1)) RADIOISOTOPE INSTRUMENTS IN INDUSTRY AND GEOPHYSICS. VOL. I. Proceedings Series. Proceedings of the Symposium held by the International Atomic Energy Agency in Warsaw, 18–22 October 1965. (International Atomic Energy Agency, Vienna (Austria)). May 1966. 584p. (CONF-651023 (Vol.1)). IAEA: $12.00; S252,-; £ 3.12.0; F Fr 48,-; DM 42,-.

Separate abstracts were prepared for 16 of the 33 papers included. For the other 17 papers see CONF 651023 in the report number index. (G.O.Y.)

For abstracts of individual papers see: 36765–36769, 37056–37059, and 37147–37153.

37140 INDUSTRIAL USES OF IRRADIATION: A NEW AND PROMISING FIELD. Rondenay, F. Atompraxis, 12: 338-41(July 1966). (In French).

In the chemical industry, reactions resulting from the ionization of irradiated material can be used for improving the characteristics of certain products, as well as for creating new products. Manufacturers of foodstuffs and pharmaceuticals can make use of the biological effects of ionizing radiation, especially for destroying microorganisms. A portable irradiation device was introduced for studying problems arising from the application of laboratory results on an industrial level. The device is described and certain

data on the cost of industrial uses of irradiation are presented. (auth)

37141 NUCLEAR RADIATION: TOOL FOR ANTI-COLLISION GUIDANCE. Wilcox, George E. (Naval Air Development Center, Warminister, Pa.). ISA (Instrum. Soc. Amer.) Trans., 13: 43-8(June 1966).

On account of an urgent need to keep military helicopters in Vietnam from colliding with one another during formation tion flights under adverse weather conditions, short-distance anticollision instrument systems were investigated. Nuclear radiation sources appear best, and several alternative systems were examined. Medium-energy γ radiation (0.5 to 1.5 Mev) suffers only about one % loss due to the most severe weather conditions. An isotope of reasonably long half life stays in calibration for extended periods; its signal is essentially unjammable and undetectable beyond the design range. Various γ sources were tested in four types of guidance systems based on the eclipse method, the collimated detector method, the null method, and the stationary array method. A three-detector stationary array system, which is described, was assembled as airborne equipment, and will be flown to prove its capability for measuring range and bearing in a follow-the-leader configuration, its performance in a helicopter environment providing data upon which to base further work. The lab model has proven the practicality of the method. Various problems which need to be solved in the course of optimization of this system are discussed. The present system fulfills the station-keeping requirements for a range of 75 to 1000 ft, providing information concerning range, bearing, and elevation with respect to a lead plane, and offers possibilities of a display on a scope, an on-the-beam correction mode, or an indication of range and bearing from appropriate analog or digital devices. At present the guidance system requires pilot responses to these readouts. It appears feasible, however, to utilize these indications as inputs to an autopilot. (BBB)

37142 NEW DEVELOPMENTS AND TRENDS IN THE ISOTOPE INDUSTRY. Fowler, E. E. (Atomic Energy Commission, Washington, D. C.). Isotop. Radiat. Technol., 3: 185-92(Spring 1966).

Uses of isotopes and radiations are discussed. The dimensions of the growth of industrial uses in the United States are illustrated. Tracer methodology and applications, radioisotope gaging, radiography, process radiation development, radiation preservation of food, and isotopic power are considered. (M.C.G.)

37143 RADIOISOTOPE INSTRUMENTS IN INDUSTRY AND GEOPHYSICS. Fuccillo, D. A. Jr. Isotop. Radiat. Technol., 3: 214-31(Spring 1966).

The AEC program in radioisotope instrumentation is reviewed. Alpha-excited monoenergetic x-ray sources, beta-excited x-ray fluorescence analyzers, a narrow-band x-ray detector, a sediment density and moisture probe, a methane detector, and a high-head-turbine rating system are described. A summary of the Symposium on Radioisotope Instruments in Industry and Geophysics, Warsaw, Poland, Oct. 18 to 22, 1965, is presented. Analysis, gaging, and logging are emphasized. (M.C.G.)

37144 RADIATION SENSITIZERS IN THE PRESERVATION OR STERILIZATION OF FOOD, DRUGS, AND MEDICAL SUPPLIES. de Proost, M. (CEN, Brussels). Isotop. Radiat. Technol., 3: 232-5(Spring 1966).

Chemicals reported in the literature that enhance radiation inactivation of bacteria are oxygen, alkali halides, halogenophenols, vitamin K_5 and its analogs, N-ethylmaleimide, and iodoacetamide. Their effects on bacteria, spores, and yeasts are compared, and the possible technological importance of radiation sensitizers is discussed. (auth)

37145 IRRADIATED WOOD–POLYMER COMBINATIONS. Ross, S. L.; Hodgins, J. W. Isotop. Radiat. Technol., 3: 236-44(Spring 1966).

Two techniques of producing wood–plastic combinations (WPC) by radiation were developed. One of these involves homopolymerization of a plastic inside the cell spaces of wood, and the other, copolymerization of plastic with the cellulose of wood. To achieve copolymerization, swelling of the wood is required. Improved properties were noted in homopolymerized wood, but the swelling needed to produce copolymerized WPC weakens the wood structure so that any gains in physical properties are offset. Since homopolymerization also can be produced by conventional thermocatalytic techniques, it is suggested that the use of radiation to produce WPC by these methods warrants some further investigation. (auth)

37146 RADIATION STERILIZATION OF SUGAR CANE LEAFHOPPERS OF THE FAMILY DELPHACIDAE. Shipp, E. (Univ. of New South Wales, Kensington); Osborn, A. W.; Hutchinson, P. B. Nature, 211: 98-9(July 2, 1966).

Studies on the possibility of eradicating sugar cane leafhoppers of the genus Perkinsiella saccharicida by the sterile male technique showed that the fifth instar nymph is the most suitable stage to irradiate. The results so far indicate a large safety margin within which sterility can be produced, without significantly affecting sperm motility, mating behavior, or adult longevity. (P.C.H.)

37147 USE OF RADIOISOTOPE INSTRUMENTS IN INDUSTRY IN THE USSR. Savitskii, P. (USSR State Atomic Energy Commission, Moscow). pp 3-14 of STI-PUB–112(Vol.1). (In Russian).

The trends in the development of radioisotope instrument engineering in the USSR and the main fields of application of such devices are described. Data are given to show the economic advantages of using radioisotope instruments in various branches of the extractive and processing industries. (G.O.Y.)

37148 REVIEW OF THE DESIGN AND APPLICATION OF RADIOISOTOPE INSTRUMENTS IN INDUSTRY. Clayton, C. G. (Wantage Research Lab., United Kingdom Atomic Energy Authority, Eng.); Cameron, J. F. (International Atomic Energy Agency, Vienna). pp 15-61 of STI-PUB–112(Vol.1).

The physical principles of thickness and density gages, level gages, and analytical instruments are discussed, and summaries are given of the most important industrial applications. The possible future trends in this branch of radioisotope applications are also discussed. 42 references (auth)

37149 PROBLEMS IN THE PRODUCTION AND DEVELOPMENT OF A WIDE RANGE OF RADIOISOTOPE GAGES. Margolinas, S.; Maugest, J.; Vannier, R. (Nucleometre, St. Denis, France). pp 63-70 of STI-PUB–112(Vol.1). (In French).

The practical problems encountered in designing, producing, and developing a wide range of instruments employing radioisotopes for the measurement and control of physical parameters are discussed. (G.O.Y.)

37150 ADVANCES IN RADIOISOTOPE INSTRUMENTATION DEVELOPMENT: PROGRAMME OF THE UNITED STATES ATOMIC ENERGY COMMISSION. Rotariu, G. J. (Div. of Isotopes Development, U. S. Atomic Energy Commission, Washington, D. C.). pp 73-95 of STI-PUB–112 (Vol.1).

Some progress on the development of isotopic sources for the generation of x rays and for x-ray fluorescence is summarized. The development of various instruments that use these sources is discussed. (G.O.Y.)

37151 CONTINUOUS MEASUREMENT OF GALVANIZATION COATINGS BY MEANS OF X-RAY FLUORESCENCE. Cavailles, J.; Martinelli, P. (Commissariat a l'Energie Atomique, Section d'Applications des Radioelements, Centre d'Etudes Nucleaires, Saclay, France). pp 227-39 of STI-PUB–112(Vol.1). (In French).

The choice of radioactive sources to induce the characteristic K x rays of iron and zinc is discussed along with the choice of the best geometric parameters for an industrial measuring head which makes use of backscattering, some very satisfactory results, and the extension of the

process to measurements of tin coatings on iron. A comparative study of the various methods led to the use of a 30-mC source of ^{241}Am to excite the K line of zinc. Particular attention was paid to the different geometric parameters permitting independent measurement of the position of the sheet in a given area (non-planar sheets) and also the design of a perfectly reproducible gauge head not requiring any adjustment. The prototype of the gauge functioned perfectly in continuous operation for a period of four months without needing calibration. (G.O.Y.)

37152 CONTINUOUS AUTOMATIC ANALYSIS OF DRY POWDERS AND AQUEOUS SUSPENSIONS USING RADIOISOTOPE TECHNIQUES. Starnes, P. E.; Clark, J. W. G. (Mineral and Technical Developments Ltd., London). pp 243-69 of STI-PUB-112(Vol.1).

The design principles of equipment for the continuous, automatic analysis of minerals and ores in the form of dry powders or as suspensions of solid particles in water are discussed. The problem of obtaining representative samples of granular materials and of preparing these to render them suitable for instrumental analysis with a minimum delay is considered, and a practical solution is proposed. Two analytical instruments — one using a radioisotope x-ray absorption technique, the other using radioisotope x-ray fluorescence — are described. (G.O.Y.)

37153 COAL-ASH MONITOR WITH LOW DEPENDENCE ON ASH COMPOSITION. Rhodes, J. R.; Daglish, J. C.; Clayton, C. G. (Wantage Research Lab., United Kingdom Atomic Energy Authority, Eng.). pp 447-63 of STI-PUB-112(Vol.1).

A system of measuring coal ash which is largely independent of ash composition is described. The intensity of x rays from a radioisotope source ($^{3}H-Zr$) backscattered from a smoothed, moving bed of crushed coal is used to measure the ash content. Variations in iron concentration, which cause additional changes in the backscattered intensity, are compensated by simultaneously counting Fe K fluorescent x rays with the same detector. The accuracy of measurement is usually within ±0.3% ash in the range 1 to 15% ash and within ±1% ash in the range 15 to 50% ash. Measurement time is about 100 sec. A brief review of methods of coal-ash measurement and a description of the equipment used in the present system are included. (G.O.Y.)

37154 GRAIN MOISTURE MEASUREMENTS WITH NEUTRONS: APPLICATION TO THE PROBLEMS OF CONDITIONING AND STORAGE. Marcesse, J.; Couchat, P.; Jossoud, M. (Commissariat a l'Energie Atomique, Cadarache, France). pp 415-23 of STI-PUB-112(Vol.2). (In French).

The principle underlying the neutron method of measuring moisture is applied to grains. The fast neutrons are thermalized both by the H atoms in the water and by those in the organic material (viz., starch). The results of experiments to measure the desiccation rates of maize subjected to ventilation are presented. (G.O.Y.)

37155 ISRAEL FOOD IRRADIATION PROGRAM AND PROGRESS DURING 1964–1966. Kahan, R. S.; Eisenberg, E.; Lapidot, M. (Soreq Nuclear Research Center, Yavne, Israel). Vienna, International Atomic Energy Agency, 1966, Preprint SM-73/48, 16p. (CONF-660609-13). ORAU.

From International Symposium on Food Irradiation, Karlsruhe, Ger.

The Israel program on the irradiation of agricultural produce is three-fold: to obtain government approval of crops already licensed elsewhere (potatoes, onions), to work on local problems (apricots, pears), and on items of export importance (citrus, bananas, avocados). A 30,000-C source was installed in a versatile irradiator of novel design. Objects ranging from a few grams to 50 kg are treated with 20 to 5×10^{6} rad doses at dose rates of 1.5 to 800 krad/hour. Various tests were conducted on citrus fruits, potatoes, onions, bananas, avocados, sugar beets, dehydrated vegetables, and fruit flies. (auth)

37156 INTERNATIONAL PROJECT ON THE IRRADIATION OF FRUITS AND FRUIT JUICES. Kaindl, K. (Oesterreichische Studiengesellschaft fuer Atomenergie, Seibersdorf, Austria). Vienna, International Atomic Energy Agency, 1966, Preprint SM-73/1, 20p. (CONF-660609-29). ORAU.

From International Symposium on Food Irradiation, Karlsruhe, Ger.

Fundamental studies of preservation of food by irradiation were made using fruit juice as a model, since the components are representative of most foods and are easily separated, because research was done on yeast, and because it has economic value. Fundamental research dealt mainly with radiosensitization of microorganisms, yeast, and to a certain extent mold. Studies on technological feasibility were undertaken including organoleptic and microbiological, and analysis of volatile and nonvolatile substances. Animal feeding studies on rats, mice, and pigs started with tests of the amounts of apples and apple juice that can be tolerated by the animals. Tissue cultures were cultivated for biological screening of the degradation products. An irradiation plant of a new design for about 30,000 to 40,000 C and 10,000 C ^{60}Co are under construction. (auth)

37157 ECONOMIC ASPECTS OF THE FOOD IRRADIATION PROGRAM IN ISRAEL. Lapidot, M.; Foa, E.; Sivan, Y.; Kahan, R. S. (Soreq Nuclear Research Center, Yavne, Israel). Vienna, International Atomic Energy Agency, 1966, Preprint SM-73/49, 16p. (CONF-660609-12). ORAU.

From International Symposium on Food Irradiation, Karlsruhe, Ger.

A technological-economic survey of radiation-preserved agricultural produce was made in Israel in July 1965. All items that potentially could benefit from irradiation (fruits and vegetables, fodder, cereals and cereal products, fish, meat, poultry, and poultry produce) were examined. Crop sizes and their values for 1962-63 and 1968-69 (based on Ministry of Agriculture data) were considered. Irradiation costs were estimated on the basis of available and extrapolated data for small irradiators in the growth areas and for large irradiators in port or along main highways. Surface treatment by electron accelerators and bulk treatment of ^{60}Co, ^{137}Cs, or x-ray sources were considered. Preliminary results with sprout prevention in irradiated potatoes justified detailed economic surveys of the potato and onion commercial set-up as it is today in comparison to a modified set-up comprising several variants of combined irradiation and controlled temperature storage installations. The suggested set-up would reduce the expenditure for storage and handling from 15 to about 8% of the total crop value, the savings representing a net return of about 24% on the investment. (auth)

37158 UNDERWATER BEACON. Kass, I. E. (to U. S. Atomic Energy Commission). U. S. Patent 3,265,152. Aug. 9, 1966.

This invention relates to a radioisotope powered underwater acoustic generator. An isotopically heated, self-controlled, thermal-fluid-mechanical mechanism is employed to produce a constant steam pressure for intermittently, uniformly flowing hydraulic fluid through a hydroacoustic oscillator to produce the desired acoustic pulses. (AEC)

Power Application

See also ENGINEERING — Space Propulsion

37159 CALCULATION OF THE EFFICIENCY OF THE ^{85}Kr NUCLEAR BATTERY. Rodriguez, Pablo J. (Instituto Venezolano de Investigaciones Cientificas, Caracas). Acta Cient. Venezol., 16: 104-8(1965). (In Spanish).

The construction and operation of the ^{85}Kr battery (manufactured by the Leesona Moos Corp.) is described and diagramed, and theoretical aspects of its operation are examined. The battery has a useful life of ~10 yr; it weighs

3.5g and has an OD of 1.43 cm. Efficiency of the battery was calculated and the results compared with experimental findings. Partial losses due to ionization in the dielectric, back-scattering in both the dielectric and collector, and potential were calculated. A method of superposition was used to obtain the total loss from partial losses. The battery efficiency was calculated for several theoretical operational voltages, and the results tabulated. It was determined that the max efficiency would be 2.5% at a theoretical operational voltage of 65 kv. Nevertheless, experiments showed that the max operational voltage is around 7000 v, which corresponds to an efficiency of 0.194%. The analysis shows that the max voltage is limited by both current leakage and breakdown. Also, it was shown that for the experimental max operational voltage, breakdown does not occur within the battery, but rather outside the battery. (BBB)

Separation and Production

See also CHEMISTRY — Separation Processes and Procedures

37160 (DP–1025) PERFORMANCE OF SIEVE TRAYS UNDER GS HEAVY WATER PROCESS CONDITIONS. PART I. LOW PRESSURE OPERATION. Burgess, Mitchell P.; Garvin, Robert G.; Scotten, William C. (Du Pont de Nemours (E. I.) and Co., Aiken, S. C. Savannah River Lab.). June 1966. Contract AT(07-2)-1. 86p. Dep. mn. CFSTI $3.00 cy, $0.75 mn.

Capacity and entrainment of sieve trays were measured under GS process conditions in a 6½-ft-diameter tower. Blower capacity limited gas flow to a maximum F factor of 1.7 at 225-230 psig operating pressure. Tests will be resumed with the increased blower capacity available at 270–275 psig. (auth)

37161 (K-OA–1313) TABLES OF 10-10 URANIUM UNIT COST COMPONENTS. (Oak Ridge Gaseous Diffusion Plant, Tenn.). [Jan. 27, 1965]. Contract W-7405-eng-26. 94p. Dep. mn. CFSTI $3.00 cy, $0.75 mn.

The tables are to be used in calculations involving gaseous diffusion plant operations. The tables list the natural feed cost component and the separative work cost component of uranium at tails assays from 0.10 to 0.65% ^{235}U for a natural feed unit cost of $10.00/kg U as UF_6 and a separative work unit cost of $10.00/kg U. The tables can be used to calculate the unit cost of uranium at other unit costs of natural feed and separative work. (D.L.C.)

37162 ESTIMATION OF EQUILIBRIUM SEPARATION FACTOR IN ISOTOPIC SEPARATION BY CHROMATOGRAPHY. Azuma, Kunio (Kyoto Univ.); Shimokawa, Junichi. Chem. Eng. (Japan), 29: 395-7 (June 1965). (In Japanese).

The equilibrium separation factor was determined by modifying a theory, proposed by Glueckauf, based on breakthrough curves. If the column volume is V, v the volume of liquid supplied from the start to a certain period, and the concentration of the respective components c_i^0(i = A or B component), the following equation is obtained: $c_i/c_i^0 = \frac{1}{2} - A[(\sqrt{V/\Delta V})(a_iV - v/\sqrt{a_iVv})]$, where $A(\lambda) = 1/\sqrt{2\pi}\int_0^\lambda \exp(-\lambda^2/2)d\lambda$. A break-through curve can be obtained by drawing c_i/c_i^0 vs. v. If N_i is the total mole number of the i–th component, contained in the volume of a liquid from the time a break-through curve begins to appear and to its disappearance, the term $N_B/c_B^0 - N_A/c_A^0$ can be expressed as $\int(c_B/c_B^0 - c_A/c_A^0)dv$. If $v_m \simeq a_AV \simeq a_BV$, $1/y_m(N_B/c_B^0 - N_A/c_A^0) \simeq 1/v_m(a_AV - a_BV) \simeq (a_A - a_B)/a_B = (\alpha - 1)(1 - \theta/a_B)$. From these equations, the equilibrium separation factor α can be obtained. This procedure, compared to the one reported by Glueckauf, makes it possible to reduce the errors in determining α-value, since the over-all concentration ratio E, which is greater than $(\alpha - 1)$ by $1/5\sqrt{n}$ times, is measured. (NSA of Japan)

37163 CHEMISTRY OF ELECTROMAGNETICALLY SEPARATED STABLE ISOTOPES. Greene, R. E.; Baker, P. S. Isotop. Radiat. Technol., 3: 193-200; 203-4 (Spring 1966).

The chemistry associated with the recovery of enriched electromagnetically separated isotopes is described. The general considerations of problems inherent in the handling and analysis of these materials are discussed, and a brief description of the chemistry of charge materials is given. The chemical purification methods for strontium, barium, and lead based on the insolubility of their nitrate salts in strong nitric acid and for zirconium and hafnium with DL-mandelic acid are described. (auth)

37164 PHOTOCHEMICAL SEPARATION OF ISOTOPES. Rozenberg, Jean (Centre d'Etudes Nucleaires, Saclay, France). Isotop. Radiat. Technol., 3: 200-5 (Spring 1966).

A literature review on photochemical separation of mercury isotopes indicated this to be a promising technique. Good separation requires that the isotope bands in the absorption spectrum of the element be widely separated and that the product enriched by photoselective reaction not be contaminated by secondary reactions. Separation of mercury isotopes is a well-developed procedure and is about to become industrial. Lithium isotopes should theoretically be separable by such a technique, but handling of molten lithium is difficult. The failure of the first attempts to separate chlorine and uranium isotopes is considered probably due to misjudgement of the primary mechanisms and the use of too simple techniques. Hydrogen isotopes may be separated with light sources with H (or D) α Lyman sources, but yields are too low for large-scale use. (auth)

37165 THE ADVANTAGES OF ^{60}Co FOR HEAT AND RADIATION SOURCES. Dexter, A. H.; Cornman, W. R.; Hennelly, E. J. (E. I. du Pont de Nemours and Co., Aiken, S. C.). Nucl. Appl., 2: 99-101 (Apr. 1966).

Neither the supply of fission products nor the processing capacity is adequate to meet currently anticipated needs for isotopes. It is shown that for current AEC projections of terrestrial applications ^{60}Co is unique in meeting the needs of potential users, while remaining economically competitive with other isotopes. (P.C.H.)

37166 PRODUCTION OF ^{33}P FROM ^{36}Cl AND ^{33}S BY FAST-NEUTRON IRRADIATION. Lewis, R. E.; Butler, T. A. (Oak Ridge National Lab., Tenn.). Nucl. Appl., 2: 102-5 (Apr. 1966).

Enriched ^{33}S, prepared by electromagnetic separation techniques, and ^{36}Cl, prepared by reactor irradiation of natural Cl, were evaluated as targets for the production of ^{33}P by the $^{33}S(n,p)^{33}P$ and $^{36}Cl(n,\alpha)^{33}P$ reactions. The fission-neutron cross sections of these reactions and those of the $^{32}S(n,p)^{32}P$ and $35Cl(n,\alpha)^{32}P$ reactions were measured in four positions in the Oak Ridge Research Reactor (ORR) at various distances from the fuel elements. Millicurie quantities of ^{33}P were prepared by fast-neutron irradiation of enriched ^{33}S and ^{36}Cl and subsequent aging to deplete the ^{32}P content of the ^{33}P. Chemical procedures for separation of carrier-free P activities from elemental S and KCl are given. (auth)

MATHEMATICS AND COMPUTERS

Refer also to abstracts 38350 and 38431.

37167 (IDO-17151) RSAC: A RADIOLOGICAL SAFETY ANALYSIS COMPUTER PROGRAM. Coates, R. L.; Horton, N. R. (Phillips Petroleum Co., Idaho Falls, Idaho. Atomic Energy Div.). May 1966. Contract AT(10-1)-205. 212p. Dep. mn. CFSTI $6.00 cy, $1.25 mn.

An IBM 7040 computer program is presented which is used to compute the potential radiological doses resulting from either a continuous or instantaneous release of radioactive fission products to the atmosphere. This program, the Radiological Safety Analysis (RSAC) Program, is written in Symbolic Language (MAP). The program has been developed as part of the LOFT and the general nuclear safety programs to provide a generalized computer program for a complete parametric investigation of the radiological hazards from any nuclear power plant or reactor system. The doses considered are cloud gamma, deposition gamma, ingestion, and inhalation, and are based upon the release of up to 200 isotopes, the relative abundance of each isotope being dependent upon the operating history of the nuclear reactor under consideration. Included are the mathematical models, conversion factors, assumptions, flow charts, program listings, and other data considered pertinent to the overall development of this program. (C.H.)

METALS, CERAMICS, AND OTHER MATERIALS

General

Refer also to abstracts 36799, 36850, 36851, and 36936.

37168 (BMI–1771) PROGRESS RELATING TO CIVILIAN APPLICATIONS DURING APRIL 1966. Keller, Donald L. (Battelle Memorial Inst., Columbus, Ohio). May 1, 1966. Contract W-7405-eng-92. 33p. Dep. mn. CFSTI $2.00 cy, $0.50 mn.

Research progress is reported in sections on reactor materials and components, ceramic and cermet fuels, UN–PUN fuel materials, portable smoke photometer, coated particle fuel materials, and corrosion resistance of construction materials used in fluidized-bed fluoride-volatility processes for fuel recovery. (J.R.D.)

37169 (BMI–1774) PROGRESS RELATING TO CIVILIAN APPLICATIONS DURING MAY 1966. Keller, Donald L. (Battelle Memorial Inst., Columbus, Ohio). June 1, 1966. Contract W-7405-eng-92. 26p. Dep. mn. CFSTI $2.00 cy, $0.50 mn.

Research progress is reported in sections on reactor materials and components, ceramic and cermet fuels, UN–PUN fuel materials, smoke photometer, and corrosion resistance of materials used in fluidized-bed fluoride-volatility processes for fuel recovery. (J.R.D.)

37170 EFFECTS OF OXYGEN ON THE MECHANICAL AND CORROSION PROPERTIES OF HAFNIUM. Goodwin, J. G.; Trout, H. E. Jr. Amer. Soc. Metals, Trans. Quart., 59: 384–97(Sept. 1966).

The effects of 50 to 1250 ppM O on the hot and cold fabricability, hardness, tensile properties, weldability, impact strength, and corrosion properties of Hf were studied. The O contents examined presented material ranging from high purity (50 ppM) to approximately the upper limit that can be fabricated (1250 ppM). The properties examined represented those most important to the use of Hf as a control material in nuclear reactors exclusive of its neutron absorption characteristics. The aims of the study were to generate information concerning the effects of O on various properties, and to provide information for the selection of an O level that would assure minimum strength properties without impairment of other properties. (auth)

37171 SYMPOSIUM ON ZIRCONIUM AND ITS ALLOYS. DEFORMATION AND FRACTURE. Electrochem. Technol., 4: 289–377(July–Aug. 1966). (CONF–651017 (Pt. 3)).

The symposium information is presented in 14 papers. Separate abstracts were prepared for each paper. (J.R.D.)

For abstracts of individual papers see: 37172, 37198, and 37226–37237.

37172 ADDITIONAL CRACK PROPAGATION TESTS ON ZIRCALOY-2 REACTOR PRESSURE TUBES. Aungst, R. C. (Battelle Memorial Inst., Richland, Wash.). Electrochem. Technol., 4: 353–8(July–Aug. 1966).

A reproducible drop-weight test was developed to determine the nil ductility transformation (NDT) temperature of Zircaloy-2 pressure tubing using specimens cut from the wall of tubes. The principle of the test is similar to that of the standard drop-weight test for steel. A unique crack starter is used in the form of a small piece of Zircaloy wire embrittled by H and resistance welded to the tension side of the specimen. Results show a dependence of the NDT on H content of the specimen. Results of fracture tests on slotted tube specimens covering a wide range of temperature were used to construct a fracture analysis diagram. Failure occurs for a given defect size at the same fraction of yield strength for all temperatures from below the NDT to above the crack arrest temperature. This behavior differs from that of steel plate in that the latter exhibits a marked rise in failure stress at temperatures above the NDT. An ability to grow cracks in tubing in the laboratory without allowing them to become critical is important in order: to correlate test results between cracks growing from milled slots and from natural sources, to demonstrate leakage at operating stress before attainment of critical length, and to conserve material in conducting crack propagation tests. It was demonstrated that a crack growing under cyclic stress progresses in a series of discrete jumps immediately before reaching critical length. Acoustic, ultrasonic, and eddy current techniques appear, in preliminary tests, to offer feasible methods of detecting incipient failure at that stage and thus to allow controlled growth of cracks to any length. (auth)

37173 TECHNIQUE FOR PREPARING SAMPLES OF SMALL FRAGILE PARTICLES FOR ELECTRON MICROSCOPE EXAMINATION BY MEANS OF REPLICAS. Vitali, R.; Fuhrman, Z. A. (SNAM, Milan). Energ. Nucl. (Milan), 13: 381–3(July 1966).

A preparation technique of small fragile particles for electron microscope examination by means of replicas is described. This method has been used in the study of the microstructure of small spheres (Ø 100 to 2000 μ) of the ceramic fuels used in several advanced nuclear reactors. A rapid replication procedure giving positive relief has also been developed. (auth)

37174 ATOMIC ENERGY MATERIALS. Metal Treat. Drop Forger, 284–90(Aug. 1965).

A description is given of work recently completed at AERE on stainless steel cladding– with respect to fabrication, inspection, and material evaluation; radiation effects on the properties of austenitic steels; oxidation behavior of canning materials; testing of radioactive materials; carbide fuels; cermet fuels; improved graphites; and lasers and their applications. The work being done with a ruby laser capable of delivering 50 joules of light energy at powers up to 10 Mw is described. Four photographs are included. (auth)

37175 ENVIRONMENTAL EFFECTS ON THE DIFFUSION OF ^{182}Ta IN bcc TITANIUM. Askill, J. (Oak Ridge National Lab., Tenn.). Phys. Status Solidi, 16: K63–5(July 1, 1966). (ORNL–P–2270).

Experiments in high vacua were carried out using high purity iodide titanium and ^{182}Ta as the tracer. Various combinations of pre-anneal and diffusion anneal conditions were used. The results are tabularized. (M.O.W.)

37176 PREPARATION OF RARE EARTH SILICIDES. Dvorina, L. A. (Inst. of Problems in Material Studies, Academy of Sciences, Ukrainian SSR). Porosh. Met., Akad. Nauk Ukr. SSR, No. 6, 92–4(June 1966). (In Russian).

The possibility was investigated of obtaining silicides of rare-earth elements by synthesis from components on fusion in an arc furnace in an inert medium and by interaction of the oxides with Si in a vacuum. On the basis of the research, conditions were established for obtaining mono- and disilicides of Sc, Y, La, and Ce. (auth)

37177 REDISTRIBUTION OF OXYGEN AND IRON DURING ZONE REFINING OF ZIRCONIUM. Mills, D.; Craig, G. B. (Univ. of Toronto). Trans. Met. Soc. AIME, 236: 1228–9(Aug. 1966).

Experiments are described in which iodide Zr containing 100 to 200 ppM O and Fe and <10 ppM W was used. Results indicate that segregation of O is typical for solutes with distribution coefficient, $K_{eff} > 1$ and that no redistribution of O takes place at high rates of zone travel. It was also found that the distribution coefficient for O lies between 1.5 and 2.0 and that purification with respect to Fe occurs mainly by evaporation. The focusing cage was found to be effective in preventing W contamination. (J.R.D.)

37178 ANISOTROPY OF THE HALL EFFECT IN GADOLINIUM. Volkenshtein, N. V.; Grigorova, L. K.;

Fedorova, G. V. (Inst. of Physics of Metals, Academy of Sciences, USSR). Zh. Eksp. Teor. Fiz., 50: 1505-9 (June 1966). (In Russian).

The Hall effect in Gd single crystal samples ($\rho(292°K)/\rho(4.2°K) = 20$) is measured at temperatures between 4.2 and 370°K. An anisotropy of the field dependence of the specific Hall emf and of the temperature dependence of the spontaneous Hall coefficient R_s is detected. (auth)

37179 SPECIAL CERAMICS 1964. Proceedings of a Symposium, British Ceramic Research Association, Stoke-on-Trent, England, July 8–10, 1964. Popper, P. (ed.). London, Academic Press, 1965. 353p. 90s. (CONF-640715).

Twenty-two papers were presented at the Symposium. Separate abstracts were prepared for five of the papers. Papers for which no abstracts were prepared are concerned with SiC sintering, preparation and properties of SiC, preparation and properties of $LiPN_2$, properties of inorganic polymers and ceramics, analysis of alumina ceramics, preparation and properties of spinel, high temperature properties of ceramics, metal-ceramic reactions at high temperatures, rutile electric conductivity, electric conductivity of metal borides, carbides, and sulfides, frictional properties of SiC and Si_3N_4, laboratory hot-press design, refractory materials melting, continuous hot press design, and ceramics for gas turbines. (J.R.D.)

For abstracts of individual papers see: 36850, 36851, 37189, 37209, and 37264.

37180 SPECIAL REPORT ON FAILURE OF A BOILER DURING HYDROSTATIC TEST AT SIZEWELL NUCLEAR POWER STATION. Glasgow, West of Scotland Iron and Steel Inst., 1964. 80p.

A metallurgical investigation is reported in which it is shown that the failures were not caused by faulty materials or fabrication, but were due to shock redistribution of stresses in the boiler shell when the chock support gave way because of loose hold-down bolts. Results of laboratory investigations of boiler plate brittle fracture are included. (J.R.D.)

37181 NUCLEAR REACTOR FUEL. Robertson, John A. L. (to Atomic Energy of Canada Ltd.). Canadian Patent 733,890. May 10, 1966.

The thermal conductivity of UO_2 above 400°C was found to be increased if the O/U ratio is below 2. Considerably higher power generation in a nuclear reactor may be secured than from stoichiometric or hyperstoichiometric oxide. The production of the hypostoichiometric oxides of U, Pu, Th, and Zr is described. In another embodiment hyperstoichiometric oxide in fuel is at least partially converted to the hypostoichiometric state within the reactor in which it is utilized as a superior fuel. (F.S.A.)

Corrosion

Refer also to abstract 38499.

37182 EFFECTS OF γ RADIATION ON THE SCALE FORMATION PROCESS. Vasina, V. N.; Aleksandrova, V. N.; Gerasimov, V. V. At. Energ. (USSR), 20: 435-6 (May 1966). (In Russian).

The effects of simultaneous heat flow and gamma irradiation on the scale-forming and corrosion processes were investigated for a Cr–Ni–Ti stainless steel in water. Chemical analysis of the scale revealed that 50% of it was $CaSO_4$, 45% Fe_2O_3, and the rest contained oxides of Cr, Mn, and Ni. The pH factor ranged between 3.8 and 10. (G.O.Y.)

37183 THE OXIDATION MECHANISM OF ZIRCONIUM–COPPER ALLOYS IN CARBON MONOXIDE AT HIGH TEMPERATURES. Darras, Raymond; Loriers, Henri; Baque, Pierre; Caillat, Roger (Centre d'Etudes Nucleaires, Saclay, Gif-sur-Yvette, France). Compt. Rend., Ser. C, 262: 1747-9(June 20, 1966). (In French).

Alloys of Cu–Zr composition containing 1 to 4% Cu have better resistance to oxidation in Co than Zr or the majority of other alloys derived from this metal. The beneficent role of Cu is connected with dissolving a sufficient proportion of this element in monoclinic ZrO_2. ZrO_2 is reduced when the Cu concentration passes the solubility limit of this element in the oxide. (tr-auth)

37184 PASSIVITY OF MOLYBDENUM. Pozdeeva, A. A.; Antonovskaya, E. I.; Sukhotin, A. M. (Inst. of Applied Chemistry, Leningrad). Corros. Sci., 6: 149-58 (Mar.-Apr. 1966).

The potentiostatic anodic polarization curves of Mo in 1 N H_2SO_4 and in 1 N KOH were determined. The Mo passivity region in 1 N H_2SO_4 extends from 0.4 v to –0.15 v, where it adjoins the immunity region. Mo does not become passivated in alkaline solution. The electrochemical properties of all the known Mo oxides were investigated experimentally and by means of thermodynamic calculations and it was shown that passivity of Mo in acid solution is due to the γ oxide. Mo dissolves at an almost constant rate at high anode potentials, whether in acid or alkaline solution: this is due to the formation of a multilayered surface film, the outer layer of which consists of the β, β' and α phases. (auth)

37185 ALLOYING-ELEMENT/DISPERSED-PHASE INTERACTIONS IN TUNGSTEN-BASE ALLOYS. White, J. E. (Aerospace Corp., El Segundo, Calif.). Int. J. Powder Met., 2: No. 3, 19-26(July 1966).

The tendency for alloy additions of Zr, Ta, Nb, Re, Mo, and Hf to interact with ThO_2 particles in W-base alloys during exposure to elevated temperature (>2200°C) was evaluated. The details of this interaction were studied during exposure up to 3000°C. (auth)

37186 HIGH-TEMPERATURE OXIDATION OF DUCTILE Cr–Re ALLOYS. Tedmon, C. S. Jr. (General Electric Co., Schenectady, N. Y.). J. Electrochem. Soc., 113: 769-73(Aug. 1966).

The high-temperature oxidation behavior of ductile Cr-Re alloys containing 32 and 44 at. % Re has been investigated using thermogravimetric, metallographic, electron microbeam probe, and x-ray analytical techniques. The oxidation reactions taking place include the formation of a Cr_2O_3 external scale, a subscale, and volatile Re oxides. The Cr_2O_3 scale which forms on the Cr-32 at. % Re alloy is an effective barrier to loss of Re; on the Cr-44 at. % Re alloy, the Cr_2O_3 scale is quite porous, and Re loss as volatile oxide ensues, giving rise to linear kinetics. Air-oxidized samples showed essentially the same kinetics as samples exposed to O_2; Cr_2N did not form. (auth)

37187 HYDROGEN EMBRITTLEMENT OF α-ZIRCONIUM: A REVIEW. Coleman, C. E.; Hardie, D. (Univ. of Newcastle-upon-Tyne, Eng.). J. Less-Common Metals, 11: 168-85(Sept. 1966).

Hydrogen embrittlement in α-zirconium and zirconium alloys was critically examined and the different hypotheses, invoking hydride solubility, hydride and matrix ductility, and variation of twinning with strain rate and temperature were studied to explain the transition temperature effect and the initiation of unstable fracture. A triaxial stress system was thought to be necessary for initiation of an unstable crack and a suitable criterion for crack instability seemed to be that of a critical local shear displacement at the root of the notch. Data are also presented for Nb–Zr and Ni–Nb–Zr alloys. (P.C.S.)

37188 METALLURGICAL EVALUATION OF VARIOUS INFILTRATED TUNGSTEN MATERIALS IN AIR AND NITROGEN PLASMAS. White, J. E.; Leeds, D. H. (Aerospace Corp., El Segundo, Calif.). Contract AF 04(695)-469. J. Spacecraft Rockets, 3: 1051-7(July 1966).

Tests on infiltrated alloys were conducted in both subsonic air and N plasma arcs, delivering cold-wall heat fluxes of 700, 1200, and 2400 Btu/ft^2-sec. Thermal arrest, recession rate, and mass loss were examined as a function of atmosphere, heat flux, and composition for each material. The material changes were examined metallographically and by electron micro-probe techniques. Surface cooling under oxidizing conditions was almost as effective as observed for nonoxidizing conditions for both brass- and silver-infiltrated structures, with no evidence of pore

blockage or secondary heating by oxidation of the infiltrant. The 80 Sn-20 Al and 90 Cu-10 Si infiltrants, in addition to some vaporization cooling, exhibited oxidation protection because of the formation of Al_2O_3 and SiO_2, respectively. Analysis showed no evidence of compound or intermetallic phase formation between W and any of the infiltrants. (auth)

37189 SILICON CARBIDE COATINGS ON MOLYBDENUM AND TUNGSTEN. Moreton, R. pp 61-77 of Special Ceramics 1964. Popper, P. (ed.). London, Academic Press, 1965.

Coatings of SiC were deposited on Mo and W by pyrolysis of methyl trichlorosilane. Adherent coatings on Mo rods were obtained, provided the coating thickness was not more than 0.002 in. Thicker coatings and those on sheet were unsatisfactory owing to spalling on cooling. No spalling occurred with coatings up to 0.015 in. thickness deposited on W rod and sheet. SiC protected Mo rods in air for up to 10.5 hr at 1540°C, failures being due to coating/metal interaction. Better results were obtained with W rods, the protection being for up to 104 hr at 1540°C. The results with W sheet were comparatively poor owing to failures at the ends of the test-pieces. It is suggested that the spalling of coatings on Mo and the poor results with W sheet are due to thermal expansion differences. (auth)

37190 KINETICS OF Ta_3Si_3 AND Cb_3Si_3 GROWTH IN DISILICIDE COATINGS ON TANTALUM AND COLUMBIUM. Bartlett, R. W. (Stanford Research Inst., Menlo Park, Calif.). Trans. Met. Soc. AIME, 236: 1230-1(Aug. 1966).

Results of studies concerning the growth kinetics of Ta_3Si_3 and Nb_3Si_3 formed as conjugate layers between $TaSi_2$/Ta and $NbSi_2$/Nb diffusion couples respectively. Diffusion reactions leading to growth of disilicide coatings ($MeSi_2$) can be expressed in terms of average diffusion coefficient for both diffusing elements. Since the concentration difference between the $MeSi_2/Me_5Si_3$ and Me_5Si_3/Me phase boundaries is unknown, it cannot be separated from an experimental determination of the average diffusion coefficient. A rate equation for growth of Me_5Si_3 layer is included. (J.R.D.)

37191 KINETICS AND ACTIVATION ENERGY OF OXIDATION OF ALLOYS OF THE Nb–V–Ti SYSTEM. Prokoshkin, D. A.; Vasil'eva, E. V.; Lazarev, E. M. (Baikov, Inst. of Metallurgy, USSR). Zh. Prikl. Khim., 39: 323-7(Feb. 1966). (In Russian).

Ternary Nb–V–Ti alloys containing 1, 3, 5, 8, 10, and 15 wt% V at a constant Ti content of 1, 5, and 10 wt% were melted in an arc furnace in an Ar atmosphere, homogenized at 1400°C for 25 hr in a vacuum of 5×10^{-4} mm Hg, and oxidized in air at 900, 1000, 1100, and 1200°C. Metallographic examination of the alloys in the cast and annealed conditions showed a homogeneous, single-phase structure of a solid solution of Ti and V in Nb. In alloys with a low content of the alloying elements, the oxidation kinetics followed a parabolic rate in the initial stage, and approached a linear rate with prolonged exposure. At higher V contents (10 and 15%), the oxidation kinetics followed a linear rate. Alloys containing 10 and 15% V oxidized more rapidly at 1000 than at 1100 or 1200°C, which can be explained by partial sintering of the scale at higher temperatures. At all test temperatures the most oxidation-resistant were alloys containing 5 wt% V; an Nb–5% V–10% Ti alloy was the best. At all test temperatures the oxidation rate of ternary Nb–V–Ti alloys gradually decreased with increasing content, reached a minimum at V content of 5%, and then increased again to a value higher than that for unalloyed Nb at a V content of 10 to 15%. The temperature dependence of the oxidation rate of Nb–V–Ti alloys (k) was found to follow an exponential law expressed by the equation $k = A \exp(-B/RT)$, where A varied from 2.5×10^5 to 6.92×10^2 and B, from 13,800 to 27,500. (auth)

37192 COATINGS FOR EXTREME TEMPERATURE ENVIRONMENTS. Albom, M. J. (Marquardt Corp., Van Nuys, Calif.). 34p. (CONF-650719-2). ORAU. Gmelin, AED-CONF-65-190-3.

From 4th Annual Reliability and Maintainability Conference, Los Angeles.

The distinction of being material pacesetters in the aerospace industry may rightfully be bestowed upon high temperature oxidation resistant coatings. Refractory metals, commonly used for extreme temperature environments, lack oxidation resistance and are therefore restricted to operating temperatures around 3000°F because of coating limitations. Intermetallic or diffusion type coatings such as silicides and aluminides have been investigated extensively. Major emphasis has been placed on the silicides due to their superior protectiveness of widely used Mo. Aluminide coatings are currently under investigation, particularly for Nb and Ta alloys. Significant coating improvements for the silicides have resulted in increasing the oxidation resistance at 3100°F from 30 minutes to approximately 5 hours. Similar improvements but not to the same degree have been obtained with the aluminides. Three problems which make the evaluation of specific coatings extremely difficult are the questionable accuracy of temperature recording instrumentation, the effect of emittance on temperature and the lack of a standard coating evaluation test procedure. Awareness of the first two problems plus good laboratory practice can minimize their effect. Until such time as a standard procedure is established and accepted, reported test results should be accompanied by a complete set of test conditions. Only in this way can a sound judgement be made about the usefulness of a specific coating. (auth)

37193 OXIDATION OF Nb–Zr AND Nb–Zr–Re ALLOYS IN OXYGEN AT 1000 DEG C. Rapp, Robert A.; Goldberg, G. N. (Ohio State Univ., Columbus). 44p. (CONF-660415-2). ORAU. Gmelin, AED-CONF-66-071-3.

From 22nd Annual Conference of the National Assn. of Corrosion Engineers, Miami Beach, Fla.

The steady-state kinetics and microstructures for simultaneous internal oxidation and external scale formation were investigated for the oxidation of Nb–Zr and Nb–Zr–Re alloys in pure O_2 at 1000°C. For each binary alloy, a constant rate of scale formation was observed at steady-state; the internal oxidation zone reached a steady-state, time-independent thickness. The dependence of the scaling rate on Zr content exhibited a maximum at a low Zr content; more concentrated alloys oxidized at a slower rate than pure Nb. This composition dependence of the scaling rate may be partially attributed to the effect of the internal oxidation process as an internal sink for O_2, with the formation of voluminous, and relatively impermeable ZrO_2 precipitates. The morphologies of the ZrO_2 internal oxide precipitates also affected the scaling rate. The internal oxide precipitates were distributed uniformly in the external scale. The steady-state thicknesses of the internal oxidation zones did not agree with those predicted theoretically from an idealized simple model. However, in this particular alloy system the ideal model is not satisfied experimentally. For ternary Nb–Zr–Re alloys with $N_{Re}^{(0)} = 0.02$ or 0.05, the steady-state thicknesses of the internal oxidation zones were less than those for the corresponding binary Nb–Zr alloys. For ternary alloys with $N_{Re}^{(0)} = 0.05$, the formation of a more adherent and less porous external scale caused a reduction in the kinetics of scale formation. (auth)

37194 METHOD FOR THE PRODUCTION OF ZIRCONIUM ALLOYS OF CONTINUOUSLY HIGHER CORROSION RESISTANCE. Wong, James (to Wah Chang Corp.). German Patent 1,213,629. Mar. 31, 1966. Priority date Apr. 10, 1961, United States.

A method for the production of zirconium alloys of consistently higher corrosion resistance is described. The method comprises the steps of heating the alloy to a temperature in the beta phase region, of converting the alloy into the alpha phase by quenching, and of reducing the thickness of profile by at least 30% while heating in the alpha phase region above the recrystallization temperature. (Gmelin Inst.)

Fabrication

Refer also to abstract 38467.

37195 (ANL–6950) COST ESTIMATE FOR REMOTE REFABRICATION OF METALLIC FUELS. Ayer, J. E.; Jones, D. A.; Ebert, D. D.; Buczwinski, T. A.; Sana, J. V. (Argonne National Lab., Ill.). Mar. 1966. Contract W-31-109-eng-38. 30p. Dep. mn. CFSTI $2.00 cy, $0.50 mn.

Procedures used to estimate the cost of refabrication of two typical metal fast-reactor fuels are described. The estimate is extrapolated from the EBR-II process of close-cycle fuel reprocessing followed by fuel refabrication. A computer program was used to produce refabrication costs against variations in plant throughput and fuel and/or blanket diameter and length. It was found that refabrication costs are particularly sensitive to equipment use factor and fuel- or blanket-pin diameter. The greatest contribution to refabrication cost results from the cost of jacket material. The study is of value as a contributing factor necessary to optimize the cost of reactor system operation. (auth)

37196 PILOT-SCALE EXTRUSION OF GRAPHITE FUEL ELEMENTS FOR HTGRs. Tully, G. R. Jr.; Schwartz, A. S.; Goeddel, W. V. (General Atomic Div., General Dynamics Corp., San Diego, Calif.). Contract AT(04-3)-167. Carbon, 4: 51-8(May 1966). (GA–6439; CONF-650632–2).

A method for extruding graphite tubes, and other bodies with multi-hole sections, that require little or no final machining was demonstrated. Bodies $3\frac{1}{2}$ and $4\frac{1}{2}$ in. OD up to 4 ft long were produced, and tubes 16 ft long were carbonized. The critical factors in the process lie in the area of die design and alignment, extrusion temperature control, preforming the charge to a billet, and carbonization firing. A method of adding rings that effectively increase the diameter of a local area has also been developed. The rings are machined out of green stock, placed in position with a pitch interface, and carbonized, which causes the two sections to fuse together. The present stock is made from pitch, fine graphite flour, stearic acid, ethylcellulose, and is wet-mixed with trichloroethylene. Both pitch and resin impregnations are used to increase density and strength and to lower permeability. For an application where a permeability of $\sim 5 \times 10^{-2}$ cm^2/sec is required, a formulation involving coarser graphite flour gives a stock that requires only a pitch impregnation. (auth)

37197 PREPARATION OF MONOCRYSTALS OF HAFNIUM OXIDE BY THE METHOD OF FUSED SALTS. Loc, Vutien; Anthony, Anne-Marie; Bouaziz, Roger (CNRS, Bellevue, France. Faculte des Sciences, Paris). Compt. Rend., Ser. B, 262: 1715-17(June 27, 1966). (In French).

The preparation of HfO_2 monocrystals from fused $PbCl_2$ baths was investigated. The shape of the liquid-solid equilibrium diagram of the HfO_2–PbF_2 system was established. The curve showed the presence of a eutectic melting at 780°C and a reversible transformation of PbF_2 at 350°C. These confirmed the absence of intermediary compounds between the two constituents. A deposit of HfO_2 can be obtained either by slow cooling of the solution or by concentration of the solution by evaporation of PbF_2. The crystalline properties of the crystals prepared by both methods were determined. (J.S.R.)

37198 THE EFFECT OF HEAT TREATMENT ON THE TEXTURE OF FABRICATED Zr-RICH ALLOYS. Cheadle, B. A.; Ells, C. E. (Atomic Energy of Canada Ltd., Chalk River, Ont.). Electrochem. Technol., 4: 329-36(July-Aug. 1966).

Some aspects of heat-treating on the texture of Zircaloy-2 and Zr-2.5 wt % Nb fabricated tubes and rods were studied. Heating into the β-phase develops a new texture in the materials, and there are consistent differences between the two alloys. The observed textures agree with the orientation relationship between the α- and β-phases where the {0001} basal plane in the α-phase is parallel to the {110} planes in the β-phase and the ⟨1120⟩ direction in the α is parallel to the ⟨111⟩ directions in the β. (auth)

37199 INVESTIGATION OF POROUS TUNGSTEN FORMED FROM SPHERICAL TUNGSTEN POWDERS. Kirkpatrick, M. E.; Mendelson, R. A. (TRW Systems, Redondo Beach, Calif.). Contract AF 33(657)-11726. Int. J. Powder Met., 2: No. 3, 35-44(July 1966).

The characteristics and behavior of porous structures formed from spherical W powders were investigated. A near isostatic powder compaction technique was developed, and the preparation of porous compacts exhibiting uniform porosity parameters was accomplished. Sintering rates, porosity parameters, permeability, and mechanical strength data are reported for a series of compacts prepared from six separate size ranges of spherical W particles. Substantial benefits in the performance of ionizers have been realized from porous structures prepared from spherical W powders via the techniques discussed. (auth)

37200 HIGH PRESSURE CONSOLIDATION OF SUBMICRON TUNGSTEN. Zima, Gordon E.; Lakner, John F. (Univ. of California, Livermore). Int. J. Powder Met., 2: No. 3, 49-57(July 1966). (UCRL–14502(Rev. 1)).

Submicron W powders were consolidated using a belt-type, high-pressure apparatus. In a survey of the densification capabilities of this apparatus, pressures from 22 to 85 kbar were used. Consolidation temperatures were limited to ≦1000°C. Measured densities indicated that virtually full densification was obtained within 10 min under 30-kbar pressure at 500 and 1000°C. Mean grain diameter for as-consolidated material was 0.68 μ. Some crack-free compacts with densities greater than 90% of theoretical were obtained. (auth)

37201 SLIP CASTING OF ZIRCONIUM BORIDE. Dobrovolskii, A. G.; Dobrovolskii, G. G.; Lyudvinskaya, T. A.; Popichenko, E. Ya. (Inst. of Materials Tech., Academy of Sciences, USSR). Izv. Akad. Nauk SSSR, Neorg. Mater., 2: 864-9(May 1966). (In Russian).

Slip casting of profiled ZrB_2 products (crucibles, thermocouple sheaths) was studied as a more convenient and more economic method of producing complex forms than conventional compression molding. The importance of ZrB_2 was stressed for high-temperature technology. Preparation of gypsum molds, preparation of ZrC powder and slip for casting, the slip casting procedure, and sintering of cast ZrB_2 products are described. The optimum slip composition was found to be 78% solids and 22% liquid phase and the optimum liquid phase was a 3% aqueous solution of carboxymethylcellulose. These compositions were the most stable of all studied and the cast products prepared from them had a maximum density and did not crack subsequently. Stability of the slip was increased by preliminary straining of the liquid phase through a sieve. Change of pH of the slip was without effect on the casting. Increasing the temperature of the slip or mold up to 50°C did not affect density of the cast product and tended to produce blow holes. Density of the slip cast products was of the same order as in other molding processes, but slip casting was favored over other methods in respect to uniform distribution of particles in the product. The slip cast products, e.g., crucibles 80 × 60 mm and thermocouple sheaths 250 × 30 mm, displayed considerable shrinkage on sintering at 2200°C and increase in density to 5.4 g/cm^3, which corresponded to a 12% residual porosity. (ATD)

37202 ACTIVATED SINTERING OF UO_2. Landspersky, Hanus (Inst. for Nuclear Research, Czechoslovak Academy of Sciences, Rez). Jad. Energ., 12: 207-12(June 1966). (In Czech).

The effects of additions of Ca, Mg, Al, Ti, V, and Mo oxides on pressing and sintering characteristics of powdered UO_2 with surface area > 10 m^2/g were compared. The additions were introduced into UO_2 either by their coprecipitation during the preparation of ammonium polyuranate or as additives to the mill. Additives introduced by means of coprecipitation did not influence pressing characteristics of UO_2, slight differences were found in the case of additives introduced by milling. Differences resulting

from additions after four-hour-sintering were not found. (auth)

37203 INTERACTION BETWEEN SINTERED ALUMINIUM AND URANIUM DIOXIDE. Roellig, H. E. Metal Powder Rep., 20: No. 3, 43(1965).

Reactions of sintered Al with UO_2 were investigated. Ordinary Al powder was used in one series of experiments, and powder for making sintered Al material (ASW) was used in another series. It was found that compacted ASW is as stable as Al toward UO_2, and both materials were stable at 600°C with the UO_2. Pretreatment of the powders to form Al_2O_3 surface films enhanced the resistance of the Al powders and ASW sinters to reaction with UO_2. (J.R.D.)

37204 DIFFUSION SILICONIZING AND ALUMINIZING OF MOLYBDENUM IN POWDERS. Gebalski, Stanislaw. Prace Inst. Mech. Precyzyjnej, 9: 23-33(1961). (In Polish).

Results of investigations concerning diffusion siliconizing and aluminizing of sintered Mo powders are presented. Powder compositions containing 50 to 70% Si or Al, 50 to 30% kaolin, and 0.0 to 0.5% NH_4Cl were used. Al and Si grain sizes were 0.15 and 0.12 mm, and the kaolin grain size was 0.09 to 0.06 mm. The process temperature was controlled at 1200, 1300, and 1350°C. It was found that Al and Si coatings could be deposited on Mo at these temperatures. Other findings concerning optimum temperatures and repetitious coating procedures are summarized. (J.R.D.)

37205 PRODUCTION OF URANIUM OXIDES. Barghusen, J. J. Reactor Fuel Process., 9: 121-2(Spring 1966).

Production of UO_2 by reduction of higher oxides or by conversion of UF_6 is discussed. (M.C.G.)

37206 PRODUCTION OF URANIUM, THORIUM, AND PLUTONIUM AND THEIR COMPOUNDS. Reactor Fuel Process., 9: 121-31(Spring 1966).

Production of ThO_2 by a sol-gel process, production of ThC_2 and ThC–UC by a sol-gel process or conversion of oxides in a rotating crucible, coating of ThC_2 particles, phase studies of Th–C systems, production and properties of PuO_2, and production and refining of Pu metal are described. (M.C.G.)

37207 PREPARATION AND PROPERTIES OF URANIUM AND PLUTONIUM NITRIDES. Nelson, P. A. Reactor Fuel Process., 9: 128-30(Spring 1966).

A study was made of the conversion of UO_2 and PuO_2 to UN and PuN in the presence of carbon. (M.C.G.)

37208 MANUFACTURE OF FUEL ELEMENTS FOR AN ATOMIC REACTOR. Schneider, G. Schweissen Schneiden, 17: 283-7(1965). (In German).

Information is presented concerning fuel element fabrication and production, end-cap welding to fuel element jackets, x-ray inspection and leak testing of cladding, corrosion testing in autoclaves, and fuel element acceptance standards. (J.R.D.)

37209 INFILTRATED OXIDE CERMETS. Williams, L. S. pp 147-65 of Special Ceramics 1964. Popper, P. (ed.). London, Academic Press, 1965.

The further development of oxide-base cermets prepared by infiltration with Ag and Ag alloys is reported. The aspects covered are infiltration criteria, the dispersion-strengthening and interlocking-networks models, refinement of the alumina-base cermets, extension to other oxides, metallographic studies, and testing under single-stroke bend, bend-creep, and impact loading. Since possible applications for these or other infiltrated composites include gas-turbine components, an objective is to combine adequate impact strength and creep resistance, although there are other likely uses requiring less stringent combinations of properties. Useful impact and creep performances were obtained separately, and suggestions are made for preparing skeletal structures more likely to yield the requisite combination of these properties in the infiltrated composites. (auth)

37210 POWDER METALLURGY OF Al–Al_2O_3 COMPOSITES (SAP) FOR NUCLEAR APPLICATIONS. Gualandi, Dante (Istituto Sperimentale Metalli Leggeri, Novara, Italy); Jehenson, Pierre. 34p. (CONF-650631-4). ORAU. Gmelin, AED-CONF-65-194-4).

From International Powder Metallurgical Conference, New York.

In the powder metallurgy of Al the controlled oxidation of Al powder and the sintering of the oxidized powder are important steps. The best known product of this type is SAP, the properties of which were described. Results of work are reported on thermally stable structural materials, improvement of the quality of the starting powder, development methods for fabrication of straight finned tubes, and elimination of metallic impurities. The structure of SAP materials is analyzed, and a summary is given of a theory concerning the influence of temperature and strain rate on its mechanical properties. (J.R.D.)

37211 DEVELOPMENT OF A PRODUCTION METHOD FOR ThO_2–UO_2 FUEL. Skinner, J. (Canadian Westinghouse Co. Ltd., Port Hope, Ont.). 21p. (CONF-651019-4). ORAU.

From 15th Canadian Chemical Engineering Conference, Quebec City.

The development work to establish a cold pressing and sintering route for ThO_2 pellets containing 1.3 and 1.5 wt % of UO_2 and of density greater than 94% of theoretical is described. Although ThO_2 and UO_2 are completely miscible at elevated temperatures difficulties were expected to be encountered in the formation of a homogenous solid solution. Apart from the solid state diffusion effects during sintering homogeneity would also depend on an even mechanical distribution of UO_2 particles throughout the powder blend. Variables investigated were the influence of precompacting and pelletizing pressures, lubricant additions, oxidation state of U, length/diameter ratio of green pellets, and sintering time and temperature. This work allowed a process to be defined for a pilot production run of pellets containing natural U and for the production of pellets containing fully enriched UO_2. For the handling of the latter pellets special handling and materials accountability procedures were required. Pellet quality and acceptability were judged using a modified version of the existing UO_2 pellet specification. (auth)

37212 METHOD OF PREPARING HIGH-DENSITY, COMPACTIBLE URANIUM DIOXIDE PARTICLES. Morse, L. E.; McCorkle, K. H.; Schilling, C. E. (to U. S. Atomic Energy Commission). U. S. Patent 3,262,760. July 26, 1966.

A patent is described relating to a method of preparing high-density, millimeter-size UO_2 particles which are suitable for fabrication into fuel elements by vibratory compaction. A colloidal hydrous UO_2 precipitate is prepared from a tetravalent U solution under a non-oxidizing atmosphere, separated from the remaining solution while maintaining the U in the tetravalent state, and thereafter heated to dryness under a non-oxidizing atmosphere at a temperature below 130°C. For this heating step, the temperature is maintained below about 100°C. until the precipitate has passed through a pasty stage. The resulting fragments are then fired at a temperature of at least 1050°C. under a non-oxidizing atmosphere. (AEC)

Properties and Structure

See also CHEMISTRY — Inorganic and Physical Chemistry
PHYSICS — Solid State Physics

Refer also to abstracts 36790, 36812, 37209, 38424, 38465–38467, and 38469.

37213 THE CLUSTERING OF OXYGEN IN SOLID SOLUTION IN NIOBIUM. I. EXPERIMENTAL. Gibala, R.; Wert, C. A. (Univ. of Illinois, Urbana). Acta Met., 14: 1095-1103(Sept. 1966).

Elastic after-effect and low frequency internal friction measurements were made on Nb–O alloys containing O in solid solution in the range 0.1–1.5 at.%. The data are analyzed into either three or four distinct relaxation processes, depending upon the O concentration. The rate parameters, τ_{io} and ΔH_i, and the variation of the component relaxation strengths, A_i, with temperature and O concentration are determined for these processes. A comparison of these results with information from other investigations suggests that the relaxation spectrum involves the stress-induced ordering of single unassociated O atoms (the Snoek effect) and the relaxation of small (two-to-four atom) O clusters. (auth)

37214 THE CLUSTERING OF OXYGEN IN SOLID SOLUTION IN NIOBIUM. II. INTERPRETATION. Gibala, R.; Wert, C. A. (Univ. of Illinois, Urbana). Acta Met., 14: 1105-13(Sept. 1966).

Anelastic measurements on Nb–O alloys containing 0.1–1.5 at.% O in solid solution are quantitatively interpreted as showing that O is present partly as single, unassociated atoms and partly, in more than random numbers, as clusters of two atoms (pairs), three atoms (triplets), and possibly four atoms (quadruplets). The interpretation is based on the constancy of the relaxation times of the relaxation processes at a fixed temperature and over a wide range of O concentrations and the behavior of the component relaxation strengths according to the law of mass action when the strengths are used as measures of the concentrations of the clusters. From the variation of the component relaxation strengths with temperature, binding enthalpies (enthalpies required to dissociate the clusters) are determined. These quantities are 0.07 ± 0.03 ev for pairs, 0.18 ± 0.04 ev for triplets, and 0.27 ± 0.05 ev for quadruplets. From the variation of the component relaxation strengths with total O concentration, the specific relaxation strength of each cluster (relaxation strength of O atoms per unit concentration of cluster) is determined. These quantities are used to estimate values of the standard free energies and entropies of dissociation of the clusters. (auth)

37215 STRENGTH OF TANTALUM COLUMBIUM ALLOY SINGLE CRYSTALS. Peters, B. C.; Hendrickson, A. A. (Michigan Technological Univ., Houghton). Acta Met., 14: 1121-2(Sept. 1966).

The critical resolved shear stress of Ta–Nb alloy single crystals over a composition range extending from pure Ta to pure Nb is reported. (J.R.D.)

37216 TWIN-PARTICLE INTERACTION IN BERYLLIUM. Katz, R. N.; Greenspan, J. (Army Materials Research Agency, Watertown, Mass.). Acta Met., 14: 1124-6(Sept. 1966).

An unusual twin precipitate interaction in Be occurring during recrystallization of this metal is reported. Upon passing through a network of M Be_{13} type precipitate particles the twins undergo a severe constriction resulting in a sausage-like appearance. This type of constriction inhibits the twinning mode of deformation and may be regarded as a strengthening mechanism. (J.R.D.)

37217 FAULTING IN COLD-WORKED Ta–10 at. PERCENT Re AND W–20 at. PERCENT Re. Aqua, E. N.; Wagner, C. N. J. (Yale Univ., New Haven). Amer. Soc. Metals, Trans. Quart., 59: 367-73(Sept. 1966).

The line broadening resulting from cold working a Ta–10 at.% Re alloy and a W–20 at.% Re alloy was studied by Fourier analysis, integral breadth measurements, and variance analysis. The observed anisotropic particle size was interpreted in terms of faulting on the (112) family of planes in the bcc lattice. For the W–20 at.% Re alloy, the addition of the Re increased the observed fault probability implying a lowering of the stacking fault energy of the alloy relative to pure W. There was little change in the fault probability of the Ta–Re alloy relative to pure Ta. (auth)

37218 EFFECT OF NITROGEN ON TENSILE AND CREEP-RUPTURE PROPERTIES OF NIOBIUM. Stoop, J.; Shahinian, P. (Naval Research Lab., Washington, D. C.). Amer. Soc. Metals, Trans. Quart., 59: 411-26 (Sept. 1966).

Variations in the mechanical properties of Nb caused by N_2 additions, in amounts to give single-phase and two-phase structures, were investigated at both room and high temperatures. N_2 in solid solution raised room-temperature hardness and tensile strength. Increasing the N_2 content to give two-phase structures however produced no additional strengthening. At elevated temperatures, the effect was different in that, with increase in N_2 content, there was a continued rise in tensile strength through the two-phase region. Creep-rupture strength of Nb was improved by N_2 in solution at temperatures slightly below 0.5 of the melting temperature whereas above this temperature the strength was unaffected. This change in the N_2 effect with temperature appears to be related to a concurrent change in the mechanism controlling creep. An increase in the N_2 content of two-phase alloys produced strengthening throughout the 1700 to 2600°F test range. Ductility was high for all alloys at elevated temperatures and, except for a high N_2 alloy, also at room temperature. (auth)

37219 PREVENTION OF MOLYBDENUM ALLOY INGOT CRACKING BY CAPPING. Chang, W. H. (General Electric Co., Evendale, Ohio). Amer. Soc. Metals, Trans. Quart., 59: 457-67(Sept. 1966).

Mo-3 alloy, nominally containing 1.25% Ti, 0.5% Zr, and 0.1% C, is noted for its excellent combination of high-temperature strength and low-temperature ductility in the worked condition. The alloy serves as an ideal model for this investigation by virtue of its notorious propensity toward solidification cracking, which had previously defied repeated attempts to melt sound 3.5-in.-dia. ingots. The investigation consisted of two phases concerned with establishing the validity and major characteristics of capping on, respectively, 3.5-in.- and 6-in.-dia. heats, the latter as a demonstration of the effectiveness of capping on production-sized heats. (auth)

37220 MELTING POINTS OF HYPOSTOICHIOMETRIC URANIUM DIOXIDE. Bates, J. Lambert (Battelle-Northwest, Richland, Wash.). Contract AT(45-1)-1830. J. Amer. Ceram. Soc., 49: 395-6(July 1966). (BNWL-SA-540).

The melting points of hypostoichiometric $UO_{2.00}$ to $UO_{1.67}$ are reported. The melting point for UO_{2-x} decreases as the O-to-U ratio decreases. The portion of the melting point curve near stoichiometry remains uncertain. (J.R.D.)

37221 EFFECT OF ULTRASOUND ON THE DUCTILITY OF HIGH-BORON STAINLESS STEELS. Al'shevskii, L. E.; Kuz'michev, Yu. S.; Korochkina, L. M.; Lupakov, I. S.; Neymark, V. E.; Teulin, I. I. At. Energ. (USSR), 20: 440-2(May 1966). (In Russian).

The effect of ultrasound on the ductility of various stainless steels containing 2.0 to 3.7% B was investigated. B contents above 1.8% form coarse hypereutectic borides that lower the ductility. It was found that the size and shape of the B inclusions can be improved by applying ultrasonic vibration to liquid steel during cooling and solidification. It was also found that the effect of ultrasound is temperature dependent. At a specific temperature for each type of steel, the ultrasound broke down the boride inclusions into small particles uniformly distributed throughout the metal mass and improved considerably the ductility, especially in rolling. The structure of high-boron stainless steels was refined also by homogenized annealing at 1200 to 1250°C. (G.O.Y.)

37222 GRAIN GROWTH IN ALPHA-URANIUM. Cerovic, Danica. Bull. Boris Kidrich Inst. Nucl. Sci., 17: 39-47(Jan. 1966).

To study grain growth in U, samples were deformed up to 50% by rolling and annealed at 600°C to recrystallize. Fine grains 12 μ in diameter were obtained; they were then annealed at different temperatures and times and changes in the grain size observed. The data obtained allowed calculation of the characteristic parameters of grain growth: rate constants, time exponent, and activation energy. (auth)

37223 TEMPERATURE DEPENDENCE OF THE IRRADIATION-INDUCED CREEP OF GRAPHITE. Jenkins,

G. M. (Univ. Coll. of Swansea, Wales); Stephen, D. R. Carbon, 4: 67-72(May 1966).

An experiment is described in which the irradiation induced creep extensions of helical springs under constant load are recorded continuously at various controlled temperatures at 70 to 350°C. The load can be adjusted without removing the rig. Results are reported for specimens of graphitized E Y 9 graphite. Many well-known features of creep in graphite have been confirmed, and among new data the following are of interest: The continuous creep constant increases by a factor of ~1·6 at 100 to 300°C. Reactor transients causing temperature changes result in strain increments corresponding to substantial internal stresses. These can result in fracture under constant load at low creep strains. (auth)

37224 STRESS DEPENDENCE OF THE CREEP RATE OF A URANIUM-LOADED GRAPHITE. Green, W. V. (Los Alamos Scientific Lab., N. Mex.). Carbon, 4: 81-4 (May 1966). (LA-DC-7382).

The stress dependence of the creep rate of a U-loaded graphite was measured. Each sample was tested at 2500°C and a given stress until the creep curve was well established, and then the stress was suddenly changed to another value. With the assumption that no instantaneous dynamic structural change accompanied the change of stress, the creep rate immediately after the change of stress was compared with the rate immediately before the change and related to the change of stress. In this way, the structural differences that normally complicate the analysis of results from several different samples are eliminated since prior creep time and strain, porosity, etc. were identical. The creep rate was found to be proportional to the six-and-one-half power of stress. From this it is concluded that Nabarro–Herring stress-directed diffusion creep was not the rate-controlling process. Some published tensile creep data for U-free graphite are examined with regard to the stress dependence of the creep rate. This dependence is found to be the same as that for the U-loaded graphite. (auth)

37225 PERMEABILITY RELATIONSHIPS USING DARCY PERMEABILITY, VACUUM DECAY, PRESSURE DECAY, AND PORE SIZE DISTRIBUTION METHODS ON GRAPHITIC MATERIALS. Anderson, W. A. (Great Lakes Carbon Corp., Niagara Falls, N. Y.). Carbon, 4: 107-14(May 1966).

A study has been carried out in an effort to more fully explore the relationships which exist between different methods of permeability measurement on graphitic materials. Linear relationships have been confirmed to exist in the laminar flow region between the Darcy permeability value and the vacuum decay permeability value, and the viscous flow coefficient term from the pressure decay method, as well as the slip flow term from the pressure decay method when considering results from various grades of graphite having markedly different pore size distribution spectra. It was also confirmed that the cumulative pore size distribution spectra may be analyzed to calculate an equivalent Darcy permeability value. The pore distribution analysis included molded and extruded samples, two of which having a permeability value twofold greater than any tested by Wiggs. It is significant that an agreement in permeability values may be obtained using the various methods of measurement. An analysis of the subject relationships has been made in an attempt to evaluate these data using theoretical concepts as applied to the flow of gas through porous media. (auth)

37226 DEFORMATION, CREEP, AND FRACTURE IN ALPHA-ZIRCONIUM ALLOYS. Picklesimer, M. L. (Oak Ridge National Lab., Tenn.). Electrochem. Technol., 4: 289-300(July-Aug. 1966).

The anisotropy of mechanical properties observed in α-Zr alloys can be related to the preferred orientation of the material. The influence of preferred orientation on anisotropy of yield strengths, plastic flow, creep, fracture, their strain rate and temperature sensitivities, and the stability of such textures to further deformation are discussed in terms of the deformation systems observed in single crystals. It is concluded that other deformation systems are forced to operate because of the restraint of neighboring grains in polycrystalline materials. (auth)

37227 ETCHING DISLOCATIONS IN ZIRCONIUM. Mills, D.; Craig, G. B. (Univ. of Toronto). Electrochem. Technol., 4: 300-3(July-Aug. 1966).

A technique was developed for revealing both grown-in and glide dislocations in Zr. The method depends on the presence of a surface oxide film produced by prior etching and is sensitive to the orientation of the surface. Bend tests showed a satisfactory agreement between calculated and measured dislocation densities. Pits separated by 1μ have been resolved optically using this technique. (auth)

37228 SOME EFFECTS OF PRESTRAIN AT 77 DEG K ON THE MECHANICAL PROPERTIES OF ZIRCONIUM AT ROOM TEMPERATURE. Reed-Hill, R. E.; Dahlberg, E. P. (Univ. of Florida, Gainesville). Electrochem. Technol., 4: 303-7(July-Aug. 1966).

Prestrain at 77°K of annealed rolled plate Zr along the transverse plate direction was found to have an appreciable effect on subsequent mechanical properties at room temperature. With approximately 1% prestrain, the elongation is increased nearly 50% when compared with a specimen with no prestrain. A corresponding drop in yield strength with a minor change in ultimate strength was also observed. These changes in mechanical properties are attributed to numerous fine $\{11\bar{2}1\}$ twins which are nucleated during low-temperature prestrain. Evidence is presented which shows that $\{11\bar{2}1\}$ twinning can account for nearly all of the prestrain in the range of 1% or less. Room-temperature anelastic phenomena are also observed for 77°K prestrained material. Both a large mechanical hysteresis and elastic aftereffect are believed to be associated with the small reversible and thermally activated motion of $\{11\bar{2}1\}$ twin boundaries. The elastic aftereffect curve is found to follow the relation $\epsilon = -(RT/\alpha)$ ln tanh $(t + t_0/2\tau_\sigma)$. An activation energy of approximately 23,000 cal/mole was found for the mechanism controlling the anelastic strain recovery. (auth)

37229 YIELD POINT OCCURRENCE IN POLYCRYSTALLINE ALPHA-ZIRCONIUM. Weinstein, D. (Illinois Inst. of Tech., Chicago). Electrochem. Technol., 4: 307-12(July-Aug. 1966).

Abrupt yield points were found to exist during tensile deformation of high-purity Zr having grain diameters smaller than 0.0065 mm. Yield points were favored by air cooling from the recrystallization temperature as compared with water quenching. Specimens cut transverse to the rolling direction showed greater yield drops, and the discontinuity persisted to larger grain sizes. Yield points were favored at temperatures above –22°C, and disappearance of abrupt yield was noted at lower temperatures. Discussion is presented showing that a Cottrell pinning/subsequent-unpinning mechanism does not account for the results; other mechanisms proposed for yield point occurrence are examined in the light of these data. Based on microstraining results and other known deformation characteristics of Zr, the occurrence of a yield point is best explained by the dynamic dislocation model for yielding in body-centered cubic materials. (auth)

37230 MULTIAXIAL PLASTIC FLOW OF ZIRCALOY-2 DETERMINED FROM HARDNESS DATA. Wheeler, R. G.; Ireland, D. R. (Battelle Memorial Inst., Richland, Wash.). Electrochem. Technol., 4: 313-17(July-Aug. 1966). (BNWL-SA-180).

Knoop Hardness Numbers (KHN) representing six orientations of the indenter with respect to the principal directions are proportional to the stress deviation necessary to cause plastic flow in Zr and its alloys. Each of the six indenter orientations represent different deviatoric stress ratios. The orientation of the indenter relative to the specimen determined the direction of the deviatoric-stress vector, and the hardness number determines where this vector touches the flow surface. Knoop Hardness Number-flow surfaces obtained from Zr alloys in a number of mechanically worked and heat-treated conditions predicted a stress

and strain behavior that agreed with results obtained from uniaxial tensile and tube-burst tests. The KHN-flow surface is also used to study strain-hardening effects in Zircaloy-2 uniaxial-tensile and tube-burst tests. The KHN-flow surface is a measure of material anisotropy of resistance to plastic deformation and can be applied to nearly any anisotropic solid. (auth)

37231 STUDIES OF THE TENSILE FRACTURE CHARACTERISTICS OF ZIRCONIUM AND ZIRCONIUM–RARE EARTH SOLID-SOLUTION ALLOYS. Zanner, F. J.; Vennett, R. M.; Clough, W. R. (Rensselaer Polytechnic Inst., Troy, N. Y.). Electrochem. Technol., 4: 317-22 (July-Aug. 1966).

Tensile fracture behavior of iodide Zr, Zr–Nd, and Zr–Ho solid solution alloys was studied after testing at 78, 197, and 373°K. Conventional optical metallographic techniques were used and were supplemented by electron microscopy. The influence of void formation, mechanical twins, and grain boundaries on the ductile fracture characteristics were studied. Explanations of microscopic observations were developed. (auth)

37232 RESEARCH ON THE MECHANICAL ANISOTROPY OF ZIRCALOY-2. Rittenhouse, P. L.; Picklesimer, M. L. (Oak Ridge National Lab., Tenn.). Electrochem. Technol., 4: 322-9 (July-Aug. 1966). (ORNL-P-1675).

The preferred orientation developed in close-packed hexagonal Zr alloys during fabrication causes a strong anisotropy of plastic properties. A reliable system of evaluating and characterizing this anisotropy is a prerequisite to the use of Zr alloys as materials of construction. Studies of the mechanical properties, strain behavior, and preferred orientation of Zircaloy-2 sheet were performed with the purpose of developing such a system. A method that uses only the natural strain data from orthogonal pairs of tensile and compression specimens was developed to describe the plastic anisotropy and preferred orientation. (auth)

37233 SOME ASPECTS OF THE BETA ⇌ ALPHA TRANSFORMATION IN Zr–2.5Nb ALLOY WITH VARIABLE COOLING RATE AND SOAK TEMPERATURE. Slattery, G. F. (United Kingdom Atomic Energy Authority, Springfield Works, Eng.). Electrochem. Technol., 4: 336-41 (July-Aug. 1966).

The effect of cooling rate on the transformation temperatures of the Zr–2.5 wt % Nb alloy was studied using a gas-quenching apparatus for high-speed thermal analysis. Cooling rates and soaking temperature in the alpha + beta and beta-phase regions were varied, and the effect of these on the transformed alpha product was obtained. Both the upper and lower transformation arrests increase in temperature with increasing value of the soaking temperature, but they tended to an upper limit for a soaking temperature of 1273°K. (auth)

37234 THE BASIC FEATURES OF THE ISOTHERMAL PROMONOTECTOID TRANSFORMATION IN A Zr–2,5Nb ALLOY. Higgins, G. T.; Banks, E. E. (Univ. of Liverpool). Electrochem. Technol., 4: 341-6 (July-Aug. 1966).

The morphological features and kinetics of the β(b.c.c.) to α(c.p.h.) transformation were examined in alloys containing 400 and 700 ppm of O by metallographic and resistiometric techniques. The metallographic features indicate a direct parallel with other proeutectoid transformations, the α-phase appearing as grain boundary plates, grain boundary sideplates, and intragranular plates. The mechanisms leading to these various features are considered, with particular reference to the role of temperature. The over-all rates of reaction are discussed on the basis of the Cahn site saturation model, and particular attention is directed to the interpretation of the plate growth rates on the basis of the Zener-Hillert diffusion-controlled model. Surface relief effects associated with the transformation suggest that the phase change occurs by shear in which lattice correspondence is maintained. The difficulties in arriving at a satisfactory transformation mechanism embracing both shear and substitutional diffusion are discussed. (auth)

37235 MULTIAXIAL STRAIN FATIGUE IN ZIRCALOY-4. Schreiber, R. E.; Allio, R. J. (Westinghouse Electric Corp., Pittsburgh). Electrochem. Technol., 4: 347-53 (July-Aug. 1966).

Low-cycle strain fatigue tests were conducted on 10% cold-worked Zircaloy-4 at 1175°R in air and N atmospheres. Circumferential-to-axial stress ratios in cylindrical geometry of 2:1, 1:0, 0:1, and 1:1 were investigated. Buckling strains were successfully analyzed. Results correlate well with a Sachs-type equation of the form $N_f = (\epsilon^1 - \epsilon_0/\Delta\epsilon_t)^n$ where N_f = cycles to failure; ϵ_0 = mean strain; $\Delta\epsilon_t$ = strain range; and ϵ^1, n = constants. (auth)

37236 THE EFFECT OF VARIATIONS IN COMPOSITION AND HEAT TREATMENT ON THE PROPERTIES OF Zr–Nb ALLOYS. Winton, J.; Murgatroyd, R. A. (United Kingdom Atomic Energy Authority, Culcheth, Eng.). Electrochem. Technol., 4: 358-65 (July-Aug. 1966). (TRG-Report-1049).

The heat-treatment response of a series of Zr-base alloys having compositions within the range 1.2–4.9% Nb and 300–2500 ppm O_2 was evaluated. The heat treatment involved quenching from the β or high (α + β) phase fields followed by aging at 773°K. After quenching, the hardening which occurs by the martensitic transformation increases directly with Nb content, but is independent of O_2 level. During aging at 773°K, the hardness increase which results from the precipitation of a Nb-rich phase is a linear function of Nb content above 2.2% Nb. Again, the degree of hardening is independent of O_2 content. During the quenching of 2½% Nb alloy either from below 1073°K, i.e., from the (α + β) region, or at a cooling rate slower than 80°K/sec from the β region, the β phase transforms to ω rather than martensitic α because it has been allowed to attain a Nb content greater than about 7½%. The presence of ω has a deleterious effect on low-temperature aging properties and should be avoided. (auth)

37237 TEXTURE AND MICROSTRUCTURE OF THIN-WALLED ZIRCALOY-2 TUBES. Okada, Takeshi; Hirano, Hiroshi; Kunimoto, Nobuo (Kobe Steel Ltd., Japan). Electrochem. Technol., 4: 365-74 (July-Aug. 1966).

A study was made of texture and microstructures such as grain size and precipitates formed during deformation and heat treatment of thin-walled Zircaloy-2 tubes. Manufacturing processes affect texture and microstructure. Textures of hot extruded tube are assigned the indexes (11$\bar{2}$0) [0001]. Those of cold-reduced and cold-drawn tube are similar to those of cold-rolled sheet, and those of cold-swaged tube are assigned the indexes (0001) [1010] with (0001) rotated ±80° and ±60° out of the surface of tube about the longitudinal and the transverse direction, respectively. Agglomerated hydrides in tubes are oriented in different ways. (auth)

37238 THE STRUCTURE OF $YbSb_2$, A $ZrSi_2$ ISOTYPE. Wang, R.; Bodnar, R.; Steinfink, H. (Univ. of Texas, Austin). Inorg. Chem., 5: 1468-70 (Aug. 1966).

A complete structure determination of $YbSb_2$, a ZrS_2 isotype, was carried out in order to evaluate interatomic distances. Single crystals of $YbSb_2$ were grown from a liquid-liquid reaction of the elements in sealed Ta tubes at 1000°C. A flat single crystal with dimensions 0.038 × 0.053 × 0.008mm was selected. Mo Kα radiation was used to record the hkO reflections in a Weissenberg camera and Okl and hOl reflections in a precession camera. The intensities were measured visually. Calculated and observed structure factors are tabulated along with interatomic distances and their standard deviations. (J.G.B.)

37239 INTERMEDIATE PHASES IN THE CHROMIUM–NIOBIUM SYSTEM. Guseva, L. N.; Rusanova, L. N. (Baikov Inst. of Metallurgy, USSR). Izv. Akad. Nauk SSSR, Neorg. Mater., 2: 589-91 (Apr. 1966). (In Russian).

Cr-Nb alloys were studied in the cast state and after annealing for 129 hr at 1400°C, with particular emphasis on $NbCr_2$. X-ray structural analysis was performed on powder samples. The presence of a polymorphic transformation in the compound $NbCr_2$ was confirmed. The high-temperature modification has an $MgZn_2$-type hexagonal structure with a = 4.93, c = 8.07, and the low-temperature modification has

an $MgCu_2$-type structure with a = 6.96. $NbCr_2$ at 1400°C undergoes a phase transition with the formation of the η phase with a face-centered cubic lattice and a lattice constant of 11.46 Å. It is postulated that the η phase belongs to the O_h^7 space group and has an $NiTi_2$-type structure. The high- and low-temperature structural modification of $NbCr_2$ is stabilized by Ni and V. The attendant transformation of the hexagonal to the cubic structure is thought to be associated with an increase in the electron concentration of the alloy. (auth)

37240 PHASE DIAGRAM OF THE SYSTEM WO_3–Nd_2O_3. Rode, E. Ya.; Karpov, V. N. (Kurnakov Inst. of General and Inorganic Chemistry. Academy of Sciences, USSR). Izv. Akad. Nauk SSSR, Neorg. Mater., 2: 683-7(Apr. 1966). (In Russian).

The phase diagram of the $WO_3-Nd_2O_3$ system was constructed from heating curves of annealed mixtures of initial components of various compositions. Cooling and reheating curves of the latter were also considered. X-ray phase analysis of both the pure compounds formed and their mixtures confirmed the diagram obtained. In addition to the normal neodymium tungstate $Nd_2(WO_4)_3$ and 1:1 oxytungstate Nd_4WO_8 described earlier, three more compounds were found to form in this system: 1:2 oxytungstate $Nd_2W_2O_9$, 2:1 oxytungstate Nd_4WO_9, and 3:1 oxytungstate Nd_6WO_{12}. (auth)

37241 PHASE DIAGRAM OF THE SYSTEM $Nd_2(WO_4)_3$–Na_2WO_4. Rode, E. Ya.; Karpov, V. N. (Kurnakov Inst. of General and Inorganic Chemistry, Academy of Sciences, USSR). Izv. Akad. Nauk SSSR, Neorg. Mater., 2: 688-92 (Apr. 1966). (In Russian).

The phase diagram of the $Nd_2(WO_4)_3-Na_2WO_4$ system was constructed by plotting the heating curves of annealed mixtures of initial components of various compositions. Cooling and reheating curves of the latter were also taken into account. The diagram and the characteristics of the phases formed were confirmed by x-ray phase analysis of the pure compounds formed and their mixtures. The diagram showed that only two compounds, $NaNd(WO_4)_2$ (1:1 compound) and $Na_5Nd(WO_4)_4$ (5:1 compound), are formed in this system. The 1:1 compound melts at 1263°C and forms solid solutions (probably substitutional ones) with $Nd_2(WO_4)_3$. The 5:1 compound melts incongruently at 735°C; with Na_2WO_4, it forms a eutectic close in composition to the ordinate Na_2O_4 with a melting point of 686°C. It is suggested that the addition of Na_2WO_4 to a rare earth tungstate orders the structure of the latter. On the basis of the diagram obtained, the crystallization of $Na_5Nd(WO_4)_4$ from Na_2WO_4 melt occurred at 720 to 680°C. (auth)

37242 THE EFFECT OF CERTAIN RARE-EARTH SOLUTES UPON THE F.C.C./B.C.C. TRANSFORMATION TEMPERATURE OF THORIUM. Uy, J. C.; Burr, A. A. (Rensselaer Polytechnic Inst., Troy, N. Y.). J. Less-Common Metals, 11: 149-56(Sept. 1966).

Individual effects of Nd, Gd, Ho, Er, and Lu solutes upon the fcc/bcc allotropic transformation temperature of Th were determined by an electrical resistance method. At low concentrations, all the rare earth solutes raise the transformation temperature of Th; however, at higher concentrations, the effect reaches a maximum and reverses thereafter. The initial effects at low alloy concentrations were correlated with the atomic numbers and atomic sizes of the rare earth solutes. (auth)

37243 CRYSTAL STRUCTURES OF THE RARE-EARTH COMPOUNDS OF THE FORM R_2Ni_{17}, R_2Co_{17} AND R_2Fe_{17}. Buschow, K. H. J. (Philips' Gloeilampenfabrieken, Eindhoven, Netherlands). J. Less-Common Metals, 11: 204-8(Sept. 1966).

A number of intermetallic compounds of the form R_2Ni_{17}, R_2Co_{17} and R_2Fe_{17} were investigated by x-ray diffraction. The structure of these compounds was shown to depend on the size of the rare earth component and on the temperature. For some compounds a low- and a high-temperature modification was observed. For most compounds the type of structure and the lattice constants of each modification were given. (auth)

37244 GAMMA-PHASE IN THE PLUTONIUM–MERCURY SYSTEM. Berndt, A. F. (Argonne National Lab., Ill. Univ. of Missouri, St. Louis). J. Less-Common Metals, 11: 216-19(Sept. 1966).

Investigation of the Hg–Pu system was undertaken to gain a better understanding of the structure of $PuHg_4$. A chemical analysis of the Hg–Pu alloy gave a Hg-to-Pu ratio slightly larger than 4:1. The powder pattern of this compound, believed to be $PuHg_4$, suggested that the true structure was a distorted bcc structure, namely the γ-brass structure. Observed data for the Hg–Pu compound were compared with published intensity data for the γ-phases Ni_5Zn_{21}, Co_5Zn_{21}, Pd_5Zn_{21}, Ni_5Cd_{21}, Ni_5Be_{21}, and Pt_5Zn_{21}. The excellent agreement between these data, especially for the stronger reflections, as well as chemical analysis, offered proof that the formula of the isomorphous Hg–Pu compound should be Pu_5Hg_{21}. (P.C.S.)

37245 NIOBIUM ALLOYS CONTAINING BERYLLIUM. Bartlett, E. S. (Battelle Memorial Inst., Columbus, Ohio); Bradley, E. F. J. Less-Common Metals, 11: 219-20(Sept. 1966).

Thermodynamic stabilities of some Be compounds were studied as an alternative or supplemental addition to Zr- or Hf-containing Nb alloys for improved structural properties. Alloys studied were Nb–15W, Nb–15W–3Zr, Nb–15W–0.1Be, and Nb–2Cr–0.1Be by weight percent, where the W addition was selected for solid-solution strengthening. Finished alloys contained from 150 to 250 ppm total interstitials. Minor additions (0.1%) of Be markedly augmented the strength of Nb alloys with no apparent degrading effect on low-temperature ductility. Preliminary indications of exceptional stability of a strengthening dispersed phase were noted. Zr also showed strengthening properties. (P.C.S.)

37246 SOME COMPARISONS BETWEEN FIBER-REINFORCED AND CONTINUOUS-SKELETON TUNGSTEN–COPPER COMPOSITE MATERIALS. Krock, R. H. (P. R. Mallory and Co. Burlington, Mass.). J. Mater., 1: 278-92(June 1966).

A comparison was made between the elastic and plastic properties of fiber-reinforced, continuous-skeleton, and dispersed-particle W–Cu composite materials. In the elastic range, the stiffness of the fiber-reinforced materials exceeded that of the other two microstructures by about 20%. The fiber-reinforced materials exhibited Young's moduli values predicted by isostrain considerations, while the continuous-skeleton and dispersed-particle W–Cu composites exhibited isostress behavior. In the plastic range, both fiber-reinforced and continuous-skeleton microstructures obeyed a mixture law strengthening with respect to yield strength and ultimate tensile strength. Most of the improvement in absolute strengthening of the fiber-reinforced materials was due to the superior strength of the reinforcement itself, but some contribution was also due to microstructure. Theory predicts that in the W–Cu system extremely small (~5) aspect ratio filaments may be equivalent in reinforcing effectiveness to continuous-filament-reinforced composite materials. (auth)

37247 DISLOCATION ETCH PITS AND PHASE RELATIONSHIPS IN DIMOLYBDENUM CARBIDE SINGLE CRYSTALS. Vahldiek, F. W.; Mersol, S. A.; Lynch, C. T. (Wright-Patterson Air Force Base, Ohio). Jap. J. Appl. Phys., 5: 663-70(Aug. 1966).

Hexahedral, triangular, and spiral etch pits were brought out on Mo_2C single crystals by etching with dilute HNO_3. These etch pits were correlated with the hexagonal Mo_2C structure and the veining substructure as found on all planes of the crystals. The total dislocation density on as-grown crystals was calculated to be 5×10^6 dislocations/cm^2. Annealing at temperatures ranging from 1600 to 2200°C resulted in a concomitant increase in the number of etch pits present. This increase is associated with the polygonization of the veining substructure during annealing, the increasing dispersion of the veining and impurity precipitate particles within the Mo_2C matrix, and the formation of Mo_2C–MoC within the veins. After annealing at 2200°C, the total dislocation density increased to 1×10^8 disloca-

tions/cm^2. The transition from the veining to the band-type substructure during annealing at 2200°C and above is associated with the formation of the Mo–Mo_2C eutectic and the Mo–MoC within the bands, as determined by electron microprobe and electron diffraction analyses. (auth)

37248 OBSERVATION OF ZIRCONIUM FOIL SPECIMENS UNDER THE ELECTRON TRANSMISSION MICROSCOPE. STUDY OF PLASTIC DEFORMATION. Pollard, J.; Rzepski; Lehr, P. (Centre d'Etudes de Chimie Metallurgique, Vitry-sur-Seine, France). Mem. Sci. Rev. Met., 63: 473-80(May 1966). (In French).

Structural changes in Zr subjected to tension at room temperature were studied. Deformation occurs only by prismatic slip, without the appearance of twins. Deflected slip was not observed. The deformation did not produce stacking faults. (auth)

37249 SELF-DIFFUSION OF BERYLLIUM. Dupouy, J.-M.; Mathie, J.; Adda, Y. (Commissariat a l'Energie Atomique, Saclay, France). Mem. Sci. Rev. Met., 63: 481-7(May 1966). (In French).

Determination of the self-diffusion coefficients in Be at 565 to 1050°C is described. ^{7}Be in the form of $BeCl_2$ is used as tracer. Comparison of the results with those for self-diffusion in other metals with compact hexagonal structure reveals that self diffusion in Be is much more rapid. (auth)

37250 DIFFUSION OF IRON AND SILVER IN BERYLLIUM. Naik, M. C.: Dupouy, J. M.; Adda, Y. (Commissariat a l'Energie Atomique, Saclay, France). Mem. Sci. Rev. Met., 63: 488-94(May 1966). (In French).

Tracer determination of the diffusion coefficients is described for Fe at 700 to 1076°C, and for Ag at 656 to 900°C using ^{59}Fe and ^{110}Ag. Particularly marked diffusion anisotropy exists in the case of the Ag. (auth)

37251 STRESS-RUPTURE PROPERTIES OF TUNGSTEN WIRE FROM 1200 TO 2500 F. McDanels, David L.; Signorelli, Robert A. (Lewis Research Center, Cleveland). Metals Eng. Quart., 6:No. 3, 51-8(Aug. 1966).

The stress-rupture properties of 5-mil dia type 218CS W wire were determined for rupture times up to about 200 hr at testing temperatures from 1200 to 2500°F. Results showed that the rupture properties were superior to those reported for other forms of W, other refractory metals, and superalloys in this temperature range. The onset of primary recrystallization observed between 1800 and 2000°F was indicated by a decrease in micro-hardness, a decrease in ductility, and a coarsening of grain size. The strength superiority of the wire over the other materials was maintained beyond the onset of primary recrystallization. (auth)

37252 CONTRIBUTION TO THE STUDY OF THE INHIBITION OF THE GROWTH OF THE RECRYSTALLIZATION GRAIN AND THE HARDENING BY INTERNAL HYDRATION OF MAGNESIUM–ZIRCONIUM ALLOYS. PART I. Dosdat, Jean. Metaux (Corros.-Ind.), 41: 133-43(Apr. 1966). (In French).

The effect of hydration on the growth of recrystallization grains and on the increase of the hardness was studied in Mg–Zr alloys. The experimental methods used in preparation of samples and the structural studies are described. The preparation of samples, thermal treatment in various atmospheres, micrographic methods, and x-ray and electron diffraction methods are described. (J.S.R.)

37253 EFFECTS OF ADDITIONAL ELEMENTS ON DISCONTINUOUS PRECIPITATION IN COPPER–BERYLLIUM ALLOYS. Murakami, Yotaro; Yoshida, Hiroyuki; Kawashima, Toshihiko; Yamamoto, Satoru (Kyoto Univ.). Nippon Kinzoku Gakkaishi, 30: 508-14(1966). (In Japanese).

The effects of small amounts of additive elements on the discontinuous precipitation in Cu–Be and Cu–Be–Co alloys were investigated. The electrical resistivity, micro-vickers hardness and various tensile properties were measured comparing with the results of metallographic examinations during isothermal ageing at 350 and 250°C after quenching from various solution-treatment temperatures. It was found that the rate and quantity of growth of the discontinuous precipitation at grain boundaries could be estimated from the shape of the curves in which the changes of electrical resistivity of specimens were plotted as a function of aging time. The addition of Mg, Co, or Cd restrained both zone formation and discontinuous precipitation, though the addition of Zn to Cu–Be and Cu–Be–Co alloys accelerated them considerably. When solution-treated at higher temperature, the addition of Fe was also very effective for the retardation. No discontinuous precipitation was found to occur in Cu–Be–Co alloy containing 0.1 at.% Mg. (auth)

37254 THE EFFECT OF UO_2 DENSITY ON FISSION-PRODUCT GAS RELEASE AND SHEATH EXPANSION. Notley, M. J. F.; MacEwan, J. R. (Atomic Energy of Canada Ltd., Chalk River, Ont.). Nucl. Appl., 2: 117-22 (Apr. 1966).

The effects of UO_2 density on fission product gas release and sheath expansion were determined in an irradiation experiment in which the performance of fuel elements with densities between 10.42 and 10.74 g/cm^3 was compared at $\int \lambda d\theta$ values of 39 and 42 W/cm. Diametral sheath strain was less for the lower density elements, but fission product gas release and the extent of grain growth were greater as the density decreased. A correlation between the extent of grain growth in the UO_2 and the fractional gas release was found to exist in this test and to apply to a large number of other irradiations; it is suggested that this relationship may be causal and that the fractional gas release is not solely a function of temperature. (auth)

37255 ELECTRON MICROSCOPE OBSERVATION OF THE FISSION-GAS BUBBLE DISTRIBUTION IN UO_2. Whapham, A. D. (United Kingdom Atomic Energy Authority, Harwell, Eng.). Nucl. Appl., 2: 123-30(Apr. 1966). (AERE-R-4970).

The structure of post-irradiation annealed UO_2 was examined by transmission electron microscopy to try to understand the behavior and release of fission gas. At a dose of 2.2×10^{19} fissions/cm^3, 5×10^{15} small gas bubbles/cm^3 are observed in the material. These precipitate at 1100°C and appear to grow from 25 to 100-Å dia at 1500°C by diffusion of gas atoms from the matrix. Grain-boundary migration sweeps up these bubbles at between 1800 and 2000°C. Re-solution of fission-gas bubbles up to 300-Å dia was demonstrated on re-irradiation. At a dose of 1.6×10^{20} fissions/cm^3, bubbles appear to grow by coalescence and by dislocation sweeping. Precipitates, believed to be solid fission products, are observed. It was concluded that, in a fuel element in which a high-temperature gradient exists, the gas release below 1800°C will be controlled by the migration of bubbles to grain boundaries and by the degree of linking up between the gas-filled voids produced at grain boundaries. At temperatures above 1800°C, large gas-filled voids produced at grain boundaries would be expected to migrate up the temperature gradient by the vapor-transfer mechanism, continuing the process of sweeping up most of the gas started by the initial grown-in porosity. (auth)

37256 DIFFUSION IN DOPED UO_2. Matzke, Hj. (Atomic Energy of Canada Ltd., Chalk River, Ont.). Nucl. Appl., 2: 131-7(Apr. 1966).

UO_2, both pure and doped with tri-, quadri-, and pentavalent ions, was labeled with rare gas by means of ion bombardment and reactor irradiation. The gas release at low gas concentrations occurred by a mechanism little or not dependent on self-diffusion of either O_2 or U. At high gas concentrations, retarded release of gas occurred. This was shown by transmission electron microscopy to coincide with formation and annealing of radioinduced bubbles and dislocation loops. (auth)

37257 DEFORMATION TWINNING IN RHENIUM SINGLE CRYSTALS. Jeffery, R. A.; Smith, E. (Associated Electrical Industries, Ltd., Aldermaston, Eng.). Phil. Mag. (8), 13: 1163-8(June 1966).

Experimental results are reported on the formation of $\{11\bar{2}1\}$ deformation twins in rhenium single crystals. de-

formed in tension at room temperature. The twinning shear is large (~0.6), in agreement with some earlier results for similar twins in zirconium. Low shear twins of the $\{10\bar{1}2\}$ type, which are generally a feature of the deformation characteristics of hexagonal metals, were not observed. A possible reason for the choice of twinning system is proposed. (auth)

37258 PRODUCTION AND PHYSICAL PROPERTIES OF ALLOYS OF THE W–LaB_6 SYSTEM. Samsonov, G. V.; Lapshov, Yu. K.; Podchernyaeva, I. A.; Fomenko, V. S.; Erosov, Yu. I.; Dudnik, E. M. (Inst. of Problems in Material Studies, Academy of Sciences, Ukrainian SSR). Porosh. Met., Akad. Nauk Ukr. SSR, No. 6, 17-23(June 1966). (In Russian).

The physical properties of W alloys with 1 to 53 mol % of LaB_6, were examined and an x-ray and metallographic investigation of these alloys was conducted. It is shown that small additions of LaB_6 (of the order of 1 mol %) lead to a sharp decrease in the work function of W during thermal emission, which permits regarding such alloys as promising cathode materials for medium and high temperatures. A tentative explanation is given for the sharp decrease in work function of W on the basis of the rise in its atoms of the statistical weight of d^5 configurations, which permits the nonlocalized La electrons in LaB_6 to become excited to thermal emission. (auth)

37259 GERMANIDES OF LANTHANUM. Lyutaya, M. D.; Goncharuk, A. B. (Inst. of Problems in Material Studies, Academy of Sciences, Ukrainian SSR). Porosh. Met., Akad. Nauk Ukr. SSR, No. 6, 60-3(June 1966). (In Russian).

The conditions for obtaining $LaGe_2$, LaGe, and La_5Ge_3 by synthesis from elements in an arc furnace and $LaGe_2$ were investigated. Chemical properties of La–Ge alloys such as stability of germanide powders in water and thermal stability in air and in an ammonia medium were studied. It is shown that oxidation of germanides passes through lanthanum oxygermanide formation. During interaction of LaGe with ammonia LaGeN is formed as a product. (auth)

37260 PHYSICAL PROPERTIES OF ALUMINIDES OF TRANSITION METALS. Sinel'nikova, V. S. (Inst. of Problems in Material Studies, Academy of Sciences, Ukrainian SSR). Porosh. Met., Akad. Nauk Ukr. SSR, No. 6, 64-7(June 1966). (In Russian).

The conductivity, thermal e.m.f., Hall's constant, thermal conductivity, and microhardness at room temperature of these materials were investigated. The thermal expansion coefficients were measured, and the temperature dependences of the thermal e.m.f. and resistivity of aluminides of some transition metals were determined. The results are discussed from the standpoint of the formation of stable electronic configurations in aluminides. (auth)

37261 X-RAY DIFFRACTION INVESTIGATION OF Nb–W–B. Kuzma, Yu. B.; Lakh, V. I.; Stadnyk, B. I.; Voroshilov, Yu. V. (Lvov State Univ.). Porosh. Met., Akad. Nauk Ukr. SSR, No. 6, 73-6(June 1966). (In Russian).

The system Nb–W–B was investigated by means of x-ray analyses. The phase equilibria were established at 1500°C. The compound W_2B dissolves 15 at.% Nb; Nb_3B_2, 35 at.% W, and NbB, 40.% W. The dependence of a lattice parameters of the solid solution (Nb, W)$_3B_2$ and (Nb, W)B on the composition are shown in tables. (auth)

37262 HEAT RESISTANCE OF ALLOYS ON A BASE OF TUNGSTEN AND NIOBIUM SILICIDES. Dokukina, N. V.; Shamrai, F. I. (Baikov Inst. of Metallurgy, Academy of Sciences, USSR). Porosh. Met., Akad. Nauk Ukr. SSR, No. 6, 88-91(June 1966). (In Russian).

Results of investigations on the heat resistance of the quasibinary systems WSi_2–$NbSi_2$ and W_5Si_3–Nb_5Si_3, as well as on their resistance to oxidation are reported. It is shown that at a temperature of 1000°C neither WSi_2 and W_5Si_3 nor $NbSi_2$ and Nb_5Si_3 are heat-resistant. All intermediate alloys in the two investigated systems have a higher heat resistance than the initial compounds. The highest resistance against oxidation in the WSi_2–$NbSi_2$ system is exhibited by the alloy in the solid solution region of (Nb, W)Si_2 and in the W_5Si_3–Nb_5Si_3 system by the alloy in the solid solution region of (W, Nb)$_5Si_3$. The rate of oxidation of alloys under these conditions is determined by the structure of the oxide film forming on the surface of the alloy and its physico-mechanical properties. (auth)

37263 APPARATUS FOR DETERMINING CREEP BEHAVIOR UNDER CONDITIONS OF ULTRAHIGH VACUUM. Buckman, R. W. Jr. (Westinghouse Electric Corp., Pittsburgh); Hetherington, J. S. Rev. Sci. Instrum., 37: 999-1003(Aug. 1966).

A system for determining the creep behavior of refractory metals at temperatures up to 1900°C and at environmental test pressures of less than 1×10^{-8} torr are described. Results are presented which show that contamination of a tantalum alloy test specimen is inhibited when tested at 1370°C and 1×10^{-8} torr. (auth)

37264 PHASES IN THE ZIRCONIUM–CARBON–OXYGEN SYSTEM. Henney, J.; Jones, J. W. S. pp 35-43 of Special Ceramics 1964. Popper, P. (ed.). London, Academic Press, 1965.

Two oxycarbide phases having the approximate compositions $ZrC_{0.45}O_{0.55}$ and $ZrC_{0.5}O_{0.5}$ were found in ZrO_2–C mixtures above 1600°C. Both phases gave x-ray-diffraction patterns which could be indexed as face-centered cubic, with lattice parameters of 4.645 and 4.675Å respectively. At very low O_2 contents ZrC was found to exist as a single phase having a C content which varied from 6.8 wt % to about the stoichiometric composition (11.6 wt % C). The lattice parameter changed non-linearly from 4.692 to 4.703Å with increasing C content. (auth)

37265 Th–ThC PHASE DIAGRAM. Takeuchi, Sakae; Honma, Toshio; Satow, Tsuneo; Hirai, Toshio. Trans. Jap. Inst. Metals, 7: 59-67(Jan. 1966).

The partial phase diagram in the Th-C system between pure Th and ThC was studied by metallographic and x-ray techniques and by measurements of electrical resistivity in quenched and slow cooled Th-C alloys. The peritectic point of the reaction, liq. + ThC $\rightleftharpoons$ α-Th, was found at 16 at. % C and about 1875°C and the peritectic composition of ThC was 33 at. % C. The eutectic reaction occurred at 1650°C and its composition of α-Th and β-Th was 6.5 and <0.5 at. % C, respectively. The $\alpha \rightleftharpoons \beta$ transformation temperature rose gradually with the C content up to 2.3 at. % C and rose rapidly between the compositions of 2.3 and 3.7 at. % C. The phase boundaries of α/ThC + α, ThC + α/ThC, ThC/ThC + ThC_2 and liq. + ThC/ThC were also established. (auth)

37266 DETERMINATION OF THE BASAL-POLE ORIENTATION IN ZIRCONIUM BY POLARIZED-LIGHT MICROSCOPY. Larson, L. T. (Univ. of Tennessee, Knoxville); Picklesimer, M. L. Trans. Met. Soc. AIME, 236: 1104-6(Aug. 1966). (ORNL-P-2016).

The relationship between the apparent angle of rotation of monochromatic plane polarized light and the tilt of the basal pole from the surface normal was experimentally determined for Zr at 500 to 655 mμ. This relationship allows the determination of the spatial orientation of the basal pole of an individual grain in a polycrystalline Zr specimen to within ±3 deg by three measurements with a polarized-light metallurgical microscope. The method of measurement is discussed. (auth)

37267 MICROSTRUCTURE AND SUPERCONDUCTIVITY OF A 44.7 AT. PCT NIOBIUM(COLUMBIUM)-54.3 AT. PCT TITANIUM ALLOY CONTAINING OXYGEN. Reuter, F. W. (Univ. of California, Berkeley); Ralls, K. M.; Wulff, J. Trans. Met. Soc. AIME, 236: 1143-51(Aug. 1966).

The superconducting behavior and microstructural characteristics of a nominal Nb–40 wt % Ti–0.239 wt % O alloy were studied as a function of thermomechanical processing treatment. Critical current density vs applied transverse magnetic field was obtained for 0.010-in.-dia wires at 4.2°K in steady fields up to 110 kG. Both

optical metallography and transmission electron microscopy were used to delineate the microstructures of the same wires. It was found that a 1-hr 500°C precipitation heat treatment after cold drawing to final size led to the highest critical current density. Heat treatment at 600°C also led to a high critical current density, but the precipitate differs in kind and form from that at 500°C. The resistive critical field was also found to be sensitive to precipitation heat treatment since the effective composition of the superconducting phase changes. This is discussed in terms of the O in interstitial solid solution. (auth)

37268 HIGH-FIELD SUPERCONDUCTIVITY OF TANTALUM–TITANIUM ALLOYS. Colling, D. A. (P. R. Mallory and Co., Burlington, Mass.); Ralls, K. M.; Wulff, J. Trans. Met. Soc. AIME, 236: 1218-23(Aug. 1966).

Solid-solution alloys of the Ta–Ti system containing up to 70 at.% Ti were melted and fabricated into wire. Steady magnetic-field measurements of cold-worked wires at 4.2°K indicate that the resistive critical field increases smoothly with increasing Ti, reaching a maximum of 93 kG ($J = 1$ amp/cm^2) for a composition of about 50 at.% Ti. The composition dependence of the resistive critical field indicates it is largely paramagnetically limited for alloys containing more than 35 at.% Ti. For cold-worked wires the value of the critical current density, J_c, was found to be insensitive to composition changes for compositions in excess of 20 at.% Ti. It was observed that J_c could be increased by final-size heat treatment at 400°C without altering the value of the resistive critical field. Experimental data are used to calculate the electronic specific-heat coefficient and the upper critical field for the alloys studied. (auth)

37269 STRESS ORIENTATION OF ZIRCONIUM HYDRIDE IN A SINGLE CRYSTAL OF ZIRCONIUM. Westlake, D. G. (Argonne National Lab., Ill.). Trans. Met. Soc. AIME, 236: 1229(Aug. 1966).

An experiment is described which is designed to determine whether tensile stress applied to zone-refined Zr single-crystal specimens during slow cooling is instrumental in causing hydride platelets to lie perpendicular to the tensile axis. It was found that the three $\{10\bar{1}0\}$ planes were of equal importance as hydride habit planes. (J.R.D.)

37270 STRUCTURE OF THE ALLOYS OF THE Zr–C–Ta SYSTEM. Avgustinik, A. I.; Ordan'yan, S. S. Zh. Prikl. Khim., 39: 318-23(Feb. 1966). (In Russian).

The interaction between zirconium carbides and Ta over a wide range of temperatures and concentrations was investigated. Specimens of 13 alloys 10 mm in diameter and 10 mm thick were obtained by compacting a mixture of powdered zirconium carbide, 99.5%-pure Ta, Ca-reduced Zr, and acetylene soot under a pressure of 4 t/cm^2 and vacuum sintering at 2272°K for 1 to 2 hr. Sintered specimens were ground to a particle size of less than 60 μ, and compacted and sintered 3 to 6 times. It was found that with increasing Ta content in solid solution, the solidus temperature decreases, and in the region of two-phase alloys, drops to 2750°K, at which temperature a maximum solubility of Ta of about 35 at.% is reached. On the basis of x-ray-diffraction, metallographic, and chemical analyses, the solidus temperatures for all the alloys tested were determined and the section of the Zr–C–Ta system at 2273°K and the section of the ZrC–Ta system were plotted. No ternary compounds were found. The Zr–C–Ta system may be useful for designing heat-resistant alloys: either single-phase alloys on a base of cubic carbide, or two-phase cermets with metallic Ta as a binding material. (auth)

37271 STUDIES OF Sn AND Sn–In ALLOYS IN SUPERCONDUCTIVE STATE USING MOESSBAUER EFFECT. Pobell, F. Munich, Technische Hochschule, 1965. 49p. $2.00 Gmelin, AED-Diss. 65-305.

Thesis.

Resonance absorption of the recoilless fraction of the 23.8 kev γ line from ^{119}Sn in Sn and Sn–In alloys was measured at 2 to 6°K. Moessbauer factors, Debye temperatures, isomer transfer, upper limit of quadrupole interaction, and electrical field gradient were determined from transmission spectra. The values of these parameters in normal and superconducting state were the same. (auth)

37272 INFLUENCE OF α RADIATION ON THE SELF-DIFFUSION IN LEAD. Frenzel, D. Goettingen, Ger., Univ., Goettingen, 1965. 54p. $2.00 Gmelin, AED-Diss. 65-297.

Thesis.

Self diffusion in lead is studied by measurement of the α rays of the tracer isotope ^{212}Pb. Irradiation with ^{210}Po α rays (5 Ci) results in an increase of the diffusion coefficient. Activation energies are given. Smoothing of the surface by α irradiation was observed by electron microscopy. (auth)

37273 LATTICE DYNAMICS OF TRANSITION METALS. Powell, B. M. 5p. (CONF-660411-15). ORAU. Gmelin, AED-CONF-66-060-46.

From American Physical Society Meeting, Washington, D. C.

The frequency wave vector relations of the normal vibration modes of Nb and Mo were measured using one-phonon scattering of slow neutrons. Discussions of these relations are presented using slide illustrations. Discussions are also included concerning anomalies in phonon dispersion curves for three Nb–Mo alloys of different compositions. (J.R.D.)

37274 EFFECT OF ZIRCONIUM ON THE THERMODYNAMIC AND MECHANICAL PROPERTIES OF NIOBIUM–NITROGEN ALLOYS. de Lamotte, E. (Univ. of Illinois, Urbana); Huang, Y. C.; Altstetter, C. J. 38p. (CONF-651025-13). ORAU. Gmelin, AED-CONF-65-375-18.

From Symposium on Physical Metallurgy of Refractory Metals, French Lick, Ind.

An investigation is described in which partial pressure measurements were used to evaluate the thermodynamic properties of Nb–N systems at temperatures above 1500°C. Results of data evaluations indicate that the effect of Zr on high-temperature behavior is small and that precipitation reactions involving N are a major factor of hardening. Discussions of thermodynamic measurements and factors affecting mechanical properties and microstructure are included. (J.R.D.)

37275 ROLE OF BERYLLIUM AS A DILUTE ALLOYING ADDITION TO GROUP VIII AND GROUP I TRANSITION METALS. Wikle, K. G. (Brush Beryllium Co., Elmore, Ohio). 34p. (CONF-651062-3). ORAU. Gmelin, AED-CONF-65-325-5.

From Metallurgical Society Fall Meeting, Detroit.

A review of the role of Be additives is presented. The information and data are given in sections on Be reactions with group VIII transition metals including oxide scavenging, nitrogen scavenging, solid solution hardening, precipitation hardening, beryllide formation, and BeO skin formation. Beryllium reactions as bonding agent are also summarized along with Be powder metallurgical reactions with group VIII transition metals. Information is also included on Be effects on Cu-base alloys and on Ag and Au alloys. (J.R.D.)

37276 EFFECT OF OXIDATION-PROTECTION COATINGS ON THE TENSILE BEHAVIOR OF REFRACTORY METAL ALLOYS AT LOW TEMPERATURE. Imgram, A. G.; Bartlett, E. S.; Ogden, H. R. (Battelle Memorial Inst., Columbus, Ohio). 22p. (CONF-651062-2). ORAU. Gmelin, AED-CONF-65-325-4.

From Metallurgical Society Fall Meeting, Detroit.

Results of investigations concerning the effects of brittle surface coatings on the tensile properties of refractory metals are presented. Samples of TZM alloy (Mo–0.5Ti–0.1Zr) and D43 alloy (Nb–10W–1Zr–0.1C) were coated by pack-siliconizing in particulate mixtures of Al_2O_3–Si–NaF at 982 to 1093°C. The presence of brittle surface layers was mildly degrading to the ductile-to-brittle transition behavior of TZM. The silicide coating on D43 alloy did not significantly affect tensile properties of the substrate at low-temperatures. (J.R.D.)

37277 CRITICAL TEMPERATURES FOR SURFACE IONIZATION AND WORK FUNCTIONS OF TUNGSTEN–RHENIUM ALLOYS, TUNGSTEN, RHENIUM AND IRIDIUM. Husmann, Otto K. (Hughes Research Labs., Malibu, Calif.). 7p. (CONF-650927-25). ORAU. Gmelin, AED-CONF-65-222-49.

From American Physical Society, Honolulu, Hawaii.

The refractory metals selected for investigation were included because of their high work function and high melting point. Data obtained in work function measurements using filaments of the metals and alloys are presented and discussed. (J.R.D.)

37278 A NEW ADIABATIC CALORIMETER FOR SPECIFIC HEAT DETERMINATION FROM 250 DEG TO 1000 DEG C: ITS USE TO STUDY ORDER-DISORDER REACTIONS IN NICKEL–MOLYBDENUM ALLOYS. Norem, Walter Endre. Knoxville, Tenn., Univ. of Tennessee, 1965. 152p.

Thesis.

The calorimeter developed is adiabatic in that the specimen is surrounded by an envelope composed of three metal foil shields, the temperature of each being maintained at the temperature of the specimen to prevent radiant heat transfer between the specimen and its surroundings. A measured amount of power is continuously dissipated to the specimen from an electrical resistance heater within the sample, with the specific heat given by the equation $c_p = (P\Delta t)/(M\Delta T)$ where P is the electrical power dissipated, M is the mass of the specimen, and Δt is the time required for the temperature of the specimen to be increased by some increment ΔT. Methods were developed to correct this measured specific heat for systematic errors in the power measurement, heat absorbed by the specimen heater, and deviations from ideal adiabatic conditions. The data for the specific heat of Cu obtained in the new calorimeter agree very well with data previously reported for temperatures up to 800°C and are felt to be accurate to ±0.3% in this temperature range. The specific heat of a Ni-10 at. % Mo alloy slowly cooled from 1000°C showed a positive anomalous heat effect above 500°C. Studies of quenched samples of the 10 per cent alloy indicated that upon heating, the sample undergoes short-range ordering between 300 and 500°C immediately followed by disordering. The disordering process is essentially complete at about 900°C at which point the specific heat curve approaches an extrapolation of the low-temperature data. The enthalpy of short-range ordering in this alloy was calculated to be 5.1 joules/gram. The specific heat data for the slowly cooled Ni-20 at. % Mo alloy exhibits a very sharp peak near 871°C corresponding to the dispersion of long-range order. The enthalpy for the disordering reaction is approximately 45 joules/gram. There are two anomalous rises in the specific heat of the 20 % alloy above 880°C. The specific heat of the 20 % alloy quenched from 1100°C exhibits two negative deviations from linear temperature dependence. The first of these, which reaches its greatest magnitude at 600°C, is attributed to the formation of equilibrium short-range order and initial long-range ordering. The second negative heat effect has a minimum at 740°C and corresponds to the intensification of long-range order in the sample. There was strong evidence that vacancies which existed at higher temperatures were frozen into the samples upon quenching and that these vacancies played an important part in the kinetics of the short-range ordering reactions which took place upon heating. (TCO)

37279 MAGNETIC PROPERTIES OF $CeFe_2$, $LuNi_5$, AND SOME 1:2 INTERMETALLIC COMPOUNDS OF LANTHANIDE METALS WITH NICKEL AND COBALT. Farrell, John Joseph. Pittsburgh, Univ. of Pittsburgh, 1964. 99p.

Thesis.

$CeFe_2$, $LuNi_5$, and two groups of intermetallic compounds, the $LnNi_2$ and $LnCo_2$ series, where Ln represents Ce, Pr, Nd, Sm, Gd, Tb, Dy, Ho, Er, and Tm, were prepared by levitation and crucible melting. These compounds were then annealed for several days, under high vacuum and at temperatures of 500° to 800°C. All compounds, except $LuNi_5$, exhibited the $MgCu_2$ structure. $LuNi_5$ exhibited the $CaCu_5$ structure. Saturation moments were obtained at 4.2°K for those compounds that seemed to be ferromagnetic or ferrimagnetic. The variation of the susceptibility with temperature in the paramagnetic region was obtained. Curie temperatures, Weiss constants, effective moments, and compensation points were also obtained where applicable. The apparatus and techniques used to obtain these data are described. The lanthanide moments in the $LnNi_2$ series are lower than the respective free tripositive ion values, presumably due to partial quenching of the orbital angular momentum. The nickel ions are nonmagnetic. The lanthanide moments in the $LnCo_2$ series were found to be higher than in the $LnNi_2$ series. The Co moment varied, but was about 1 μ_B/Co in compounds in which the lanthanide moments ordered. $CeFe_2$ was found to be a simple ferromagnet; and $LuNi_5$ was found to be a Pauli paramagnet. Interpretations are given for the magnitudes of the magnetic moments and Curie temperatures and the nature of the coupling in the ordered magnetic phases. (Dissertation Abstr.)

Radiation Effects

See also CHEMISTRY — Radiation Chemistry

Refer also to abstracts 37182, 38464, 38467, and 38468.

37280 (NYO–3330-11) NUCLEAR RADIATION PROCESSING OF OPTICAL MASER MATERIALS. Sadowski, Henry; Held, Kalman; Beckerley, James (Radioptics, Inc., Plainview, N. Y.). Mar. 17, 1966. Contract AT(30-1)-3330. 107p. Dep. mn. CFSTI $4.00 cy, $0.75 mn.

Investigations were made to determine how nuclear radiation can be used to create new materials for use in solid-state optical masers. Two different types of materials were investigated: rare-earth doped alkaline earth halide mixtures and rare-earth doped glasses. The samples were irradiated with gamma, and their optical properties before and after irradiation were determined. The data indicate that the optical absorption properties of these materials were substantially increased by exposure to gamma radiation. Laser testing was performed on selected materials before and after gamma irradiation. The materials chosen were those shown to be upgraded by irradiation. Three laser rods were tested, namely: ruby, neodymium-doped barium silicate glass, and neodymium-doped soda lime silicate glass. These samples were exposed to a total dose of 2.36×10^7 rad. The post-irradiated performance of the ruby surpassed the pre-irradiated performance. (J.H.M.)

37281 IRRADIATION EFFECTS IN BERYLLIA AND ZINC OXIDE. Cowley, J. M. (Univ. of Melbourne). Acta Crystallogr., 21: 192-6(Aug. 10, 1966).

Electron-diffraction and electron-microscope observations were made on the effects of neutron irradiation and electron irradiation in an electron microscope on BeO flakes and ZnO smoke particles. It is shown that the defects or excitations created in BeO by electron irradiation interact strongly with neutron-induced defects to the extent that electron micrographs obtained with normal electron irradiation give a false impression of the form of the defect aggregates present. It is shown that high-intensity irradiation with electrons can transform normal α-BeO to the high-temperature, tetragonal β-BeO phase. The remnants of crystals partially evaporated by the electron beam may consist of fibers of α-BeO, fibers of β-BeO or plates of β-BeO. From single-crystal and oblique-texture electron diffraction patterns the structure proposed for β-BeO and its orientational relationships with α-BeO are confirmed. The significance of the formation of the β phase by electron irradiation is discussed in relationship to the possible nature of the defects in α-BeO responsible for the anisotropic expansion induced by neutron irradiation. The erosion of thin near-perfect crystal plates of ZnO by neutron irradiation and the corrugation of the surface of such plates by electron irradiation are described. (auth)

37282 DIMENSIONAL CHANGES AND RADIATION CREEP OF GRAPHITE AT VERY HIGH NEUTRON DOSES. Perks, A. J.; Simmons, J. H. W. (Atomic Energy Research Establishment, Harwell, Eng.). Carbon, 4: 85-98 (May 1966).

Results of graphite irradiations carried out in the Dounreay Fast Reactor are presented. The total neutron flux is very high, practically all the neutrons have energies capable of producing damage in graphite, and there is a very long fuel cycle. These circumstances have enabled experiments to be carried out to a maximum dose of $\sim 3.8 \times 10^{22}$ ncm^{-2} 260 to 500°C. The results are discussed in terms of current theories of dimensional changes and radiation creep; the dimensional changes follow the trends expected but a high tensile creep strain (>2%) is observed. (auth)

37283 ENERGY RELEASED AT HIGH TEMPERATURE BY IRRADIATED GRAPHITE. Rappeneau, J.; Taupin, J. L.; Grehier, J. (Centre d'Etudes Nucleaires, Saclay, France). Carbon, 4: 115-24(May 1966). (In French).

The energy (H) stored by graphite under neutron radiation can be released by thermal annealing. It is possible to determine by differential thermal analysis the differential enthalpy $dH/d\theta$(cal/g/°C) as a function of the annealing temperature (θ). Integration of the spectrum obtained gives the overall quantity of energy $H(\theta)$. To determine the form of the energy spectrum at high temperature, a differential thermal analysis apparatus operating up to 1800°C was built. The tests were carried out under vacuum in a graphite resistance furnace and the temperature was measured as a function of time by means of $WRe_{5\%}$/$WRe_{26\%}$ and graphite/boronated graphite thermocouples. The description of the apparatus is followed by an examination of graphites irradiated in the reactors BR.2 (C.E.N. Belgium) and H.F.R. (Petten, Holland) at doses between 1000 and 4000 Mwd/t and at temperatures between 70 and 250°C. The energy spectra obtained show, for all the samples studied, the presence of a healing peak at temperatures of the order of 1200 to 1500°C. This peak was also found in the case of thermal healing of other physical properties of irradiated graphites. (auth)

37284 IN-REACTOR STRESS-RUPTURE PROPERTIES OF A 20Cr–25Ni, COLUMBIUM-STABILIZED STEEL. Venard, J. T.; Weir, J. R. (Oak Ridge National Lab., Tenn.). pp 269-82 of Flow and Fracture of Metals and Alloys in Nuclear Environments. Special Technical Publication No. 380. Philadelphia, American Society for Testing and Materials, 1965.

A Nb-stabilized austenitic stainless steel (20Cr–25Ni–bal Fe) developed for gas-cooled reactor service was tested in-reactor for its stress-rupture characteristics. The tests were performed by internally pressurizing tubes at temperatures of 550, 650, 750, and 850°C in a neutron flux of approximately 5.0×10^{12} nv fast (>2.9 Mev) and 6.0×10^{13} nv thermal. Duplicate tests were performed ex-reactor. Brief details of test procedures and a discussion of the experimental results are presented. Only a small effect of irradiation on material strength was seen, but a strong effect of irradiation and temperature on the fracture ductility was observed. (auth)

37285 INFLUENCE OF HEAT TREATMENTS AND IONIZING IRRADIATIONS ON THE CHARGE DISTRIBUTION AND THE NUMBER OF SURFACE STATES IN THE Si–SiO_2 SYSTEM. Kooi, E. (Philips' Gloeilampenfabrieken, Eindhoven, Netherlands). IEEE (Inst. Elec. Electron. Eng.), Trans. Electron. Devices, 13: 238-45(Feb. 1966).

The number of surface states present at an oxidized Si surface is generally much larger when oxidation or further heat treatment has been carried out in a dry than in a wet environment. Especially at low temperatures (400–600°C) water very much tends to cause their disappearance. As H acts in a similar way, the effect seems to be due to a reaction of centers (probably unsaturated silicon bonds) with H, so that they are no longer able to capture holes or electrons. The H may also be evolved during the reaction of an Al electrode on top of the oxide with hydroxyl or water. Irradiation of oxidized Si by X rays or ultraviolet light can cause charge redistributions, which may be accompanied by the formation of new centers. The latter effect is most pronounced when hydroxyl groups can be supposed to occur in the oxide. In these cases the irradiation may cause a disappearance of n-type inversion on p-type silicon, especially when X-ray irradiation is followed by ultraviolet illumination. Irradiation experiments have been used to detect differences in Si-SiO_2 systems in cases where direct electrical measurements failed. (auth)

37286 RADIATION EFFECTS IN SOME ENGINEERING ALLOYS. Reynolds, M. B. (Vallecitos Atomic Lab., Pleasanton, Calif.). J. Mater., 1: 127-52(Mar. 1966).

The effects of neutron irradiation on structural and pressure vessel steels were studied by the Charpy V-notch impact test and the room temperature tension test. Metals studied included Types 17-4PH, AM-350, and A-286 precipitation-hardening stainless steels, Types 405 and 406 ferritic stainless steels, Types HY-80 pressure vessel steel, and ASTM Types A 212B, A 302B, and A 336 pressure vessel steels. Impact fracture energy of all alloys studied except Type A-286 stainless steel was decreased by fast neutron radiation, and where a well-defined fracture transition existed, the transition temperature was shifted upward. Of the alloys studied, the martensitic-ferritic precipitation hardening stainless steels were least stable under fast neutron radiation, and they exhibited no well-defined fracture transition after radiation. Post-irradiation impact strength of these alloys increased with increasing precipitation aging temperatue. Particularly in those alloys aged at lower temperatures, a significant reduction in impact strength resulted from exposure to the irradiation temperature in the absence of radiation. The austenitic precipitation-hardening stainless steel, Type A-286 was virtually unaffected by fast neutron radiation. Among the ferritic stainless steels and low-alloy C steels exhibiting well-defined impact fracture transitions after irradiation, there was a several-fold variation in sensitivity to fast neutron radiation. This variation is attributed to metallurgical variables, radiation sensitivity increasing with grain size. The quenched-and-tempered ASTM Type A 336 steels were generally less affected by fast neutron radiation than were the conventional Types A 302 B and A 212B steels. (auth)

37287 MEASUREMENTS OF NONDESTRUCTIVE FUEL BURNUP BY MEANS OF γ SPECTROSCOPY OF FISSION PRODUCTS. Dragoun, Otakar; Brabec, Vlastislav; Maly, Ludek; Plajner, Zdenek (Inst. for Nuclear Research, Czechoslovak Academy of Sciences, Rez). Jad. Energ., 12: 201-6(June 1966). (In Czech).

A description is given of a nondestructive burn-up determination of nuclear fuel by measurement of fission product gamma intensity. A relation between the fission product activity and/or the ^{235}U burn-up and the ^{239}Pu amount is calculated in the simplified case of natural U fission by thermal neutrons only. Acceptability of the fission products is discussed for various nuclear fuel irradiation and cooling conditions. The utilization of different types of gamma-ray spectrometers is compared. (auth)

37288 STUDY, BY MEANS OF MAGNETIC COAXING, OF DEFECTS PRODUCED BY IRRADIATION IN IRON. Moser, P. Mem. Sci. Rev. Met., 63: 431-62(May 1966). (In French).

Devices to improve the technique of examining and obtaining, at the same time, an increase in speed and an improvement in the quality of the results are discussed. Demonstration of 5 coaxing bands or groups of bands in an iron torus irradiated by neutrons at 77°K is included. (auth)

37289 RADIATION-DAMAGE EXPOSURE AND EMBRITTLEMENT OF REACTOR PRESSURE VESSELS. Shure, K. (Bettis Atomic Power Lab., West Mifflin, Pa.). Nucl. Appl., 2: 106-15(Apr. 1966). (WAPD-T-1859).

A radiation damage model that accounts for neutron

spectral differences between irradiation locations was applied to pertinent data on the change in ductile-to-brittle transition temperature for A302B pressure vessel steel. The resulting correlation supports the contention that such a damage model provides a physically more meaningful measure of exposure than the usually cited neutron flux above 1 Mev. A physically reasonable estimate of the functional dependence of this correlation was fitted by a least-squares method to these data, and a technique for assigning one-sided tolerance limits is described. (auth)

37290 FISSION-GAS RELEASE FROM UO_2 DURING IRRADIATION UP TO 2000 DEG C. Soulhier, R. (Commissariat a l'Energie Atomique, Paris). Nucl. Appl., 2: 138-41(Apr. 1966).

The fission-gas release from UO_2 samples was studied during irradiation at 150 to 2000°C. Both sintered UO_2 and single crystals were studied. Below 600°C, recoil and knock-out are the mechanisms of release. Between 800 and 2000°C, excluding the evaporational escape above 1800°C, the fractional release follows an Arrhenius law were activation energy decreases with increasing density. The fractional release was found to be independent of neutron flux. (auth)

37291 FISSION-GAS RELEASE DURING FISSIONING IN UO_2. Carroll, R. M.; Sisman, O. (Oak Ridge National Lab., Tenn.). Nucl. Appl., 2: 142-50(Apr. 1966).

The results of in-pile tests on UO_2 specimens of fine-grain and single-crystal structure led to the formation of a defect-trap theory to describe fission-gas release. The theory, which applies only when the UO_2 temperature is below the grain growth region (≈1600°C), is described, and confirming experiments are cited. Experimental results are given to support the contention that a knock-out mechanism accounts for the majority of the fission-gas release at UO_2 temperatures under 600°C. An oscillating experimental technique developed to evaluate the defect-trap theory is described, and the initial results are interpreted in terms of the theory. (auth)

37292 DYNAMIC METHOD FOR IN-PILE FISSION-GAS RELEASE STUDIES. Perez, R. B. (Univ. of Florida, Gainesville). Nucl. Appl., 2: 151-7(Apr. 1966).

A dynamic method to study the release of fission gases from fuel specimens during irradiation is presented. The main purpose of the work is to show how a dynamic method can discriminate between diffusion and diffusion-trapping processes by observing the different behavior of the release rate transfer function, with respect to neutron flux oscillations, for the two models. (auth)

37293 MIGRATION OF XENON THROUGH A UO_2 MATRIX CONTAINING TRAPPING SITES. MacEwan, J. R.; Morel, P. A. (Atomic Energy of Canada Ltd., Chalk River, Ont.). Nucl. Appl., 2: 158-70(Apr. 1966).

Recent developments concerning the mechanism for volume diffusion of Xe in UO_2 and the defects observed in irradiated UO_2 by electron microscopy are reviewed with detailed reference to recent results obtained at Chalk River Nuclear Laboratory (CRNL). An earlier interpretation for Xe diffusion in a matrix containing pre-existing and irradiation induced trapping sites is extended. (auth)

37294 COMPUTER EXPERIMENTS ON THE RADIATION ANNEALING OF FRENKEL DEFECTS DURING NEUTRON IRRADIATION. Lueck, G.; Bradatsch, H.; Sizmann, R. (Technische Hochschule, Munich. Univ., Munich). Nukleonik, 8: 256-63(June 1966).

Radiation annealing during irradiation experiments with fast neutrons was simulated in two-dimensional static models by Monte-Carlo machine calculations. The influence of the geometry of cascade structures on the defect distribution produced in the irradiated solid was studied by using model cascades of heterogeneous and homogeneous structures. The defect distributions were characterized by calculating a correlation function $\gamma(r)$ for various irradiation doses. Concerning the dose curves it became obvious that the primary cascade structure is of great importance, particularly for the curvature and the slope of the differential dose curves. This restricts the evaluation of the recombination volume α_0 from radiation annealing to experiments with single-pair-production (e.g., irradiation with fast electrons). Experiments are proposed to obtain knowledge about the primary cascade structures. Evidence is found that the cascade produced by fast neutrons in aluminum consists of homogeneously distributed, rather than clustered defects. (auth)

37295 EFFECT OF NEUTRON AND γ-RAY IRRADIATION ON THE CARRIER LIFETIME AND DETECTIVITY OF InSb. Euthymiou, P. C. (Univ. of Athens); Tanenbaum, A. L. Phys. Status Solidi, 16: 183-90(July 1, 1966).

Single crystals of p-type InSb were irradiated by 4.5-Mev neutrons or γ-rays at liquid nitrogen temperature. The damage produced by neutron irradiation resulted in a small decrease of the carrier lifetime and a large decrease of the detectivity of the crystal. The damage produced by γ rays resulted in an increase or decrease of lifetime, the change depending on how strongly p-type the crystal was. The detectivity was decreased upon γ irradiation. Annealing experiments show that neutron damage is permanent while γ-ray defects can be completely annihilated near or above room temperature, giving a similar result as electron irradiation. Analysis of the effects on lifetime and detectivity shows that neutron damage effects, although severe and permanent, produce no important decrease of lifetime. (auth)

37296 MODEL FOR CHANGE IN ELASTIC MODULUS OF A SOLID CAUSED BY POINT DEFECTS. Melngailis, J. (Max-Planck-Institut fuer Metallforschung, Stuttgart). Phys. Status Solidi, 16: 247-52(July 1, 1966).

Point defects introduced into Cu at low temperatures by irradiation are known to produce bulk expansion. It is suggested that an external stress might cause the defect (represented as oversized spherical inçlusions) to relax. This would change the expansion produced by the defects so that the deformation due to the stress would be greater and the elastic modulus would thus appear smaller. This relaxation is represented by a small deformation of the spherical inclusions, and elastic energy considerations are used to calculate the change in the elastic modulus of Cu due to such defects. If the radius of the inclusions is chosen to be two lattice constants, the experimentally observed value of 18% for the decrease in the elastic modulus at saturation density of defects is obtained. (auth)

37297 STUDIES AND INTERPRETATION OF STAGE I IN NICKEL IRRADIATED BY ELECTRONS AT 20 DEG K. Peretto, P.; Oddou, J. L.; Minier-Cassayre, C.; Dautreppe, D.; Moser, P. (Centre d'Etudes Nucleaires, Grenoble, France). Phys. Status Solidi, 16: 281-7(July 1, 1966). (In French).

Magnetic after effect and electrical resistivity recovery experiments on electron-irradiated, pure or Fe doped Ni at 20°K give information for a refined model of the point defects which anneal out during stage I. The sub-stages are ascribed to interstitials on groups of equivalent sites. The interstitials can migrate via the different sites of a particular group before being trapped in a vacancy. (auth)

37298 ION EMISSION FROM LASER IRRADIATED TUNGSTEN. Bernal G., E.; Ready, J. F.; Levine, L. P. (Honeywell Corporate Research Center, Hopkins, Minn.). 23p. (CONF-660438-4). ORAU. Gmelin, AED-CONF-66-078-7.

From International Quantum Electronics Conference, Phoenix, Ariz.

The masses, energies, and numbers of ions emitted by a tungsten surface upon irradiation with a laser beam were studied using a time-of-flight spectrometer. For light fluxes of 20 to 70 Mw/cm^2 the ion emission consists primarily of adsorbed species. Ion energies up to 180 ev were measured. It is shown that inverse Bremsstrahlung cannot account for the high energies observed. (auth)

37299 THEORIES OF SWELLING AND GAS RETENTION IN REACTOR MATERIALS. Barnes, R. S.; Nelson, R. S. (Atomic Energy Research Establishment, Harwell,

Eng.). 46p. (CONF-650904-12; AERE-R-4952). ORAU. Gmelin, AED-CONF-65-226-7.

From Symposium on Radiation Effects, Asheville, N. C.

The inert gases produced in nuclear materials during irradiation readily precipitate as small bubbles, and because of their insolubility the subsequent behavior of the gases is determined by the behavior of these bubbles. Thus they determine both how much gas is released and the swelling which is produced by the gas retained. It is shown that bubbles can migrate bodily under the influence of various driving forces and by various mechanisms, and that in most practical cases directed migration due to temperature gradients, stress gradients and moving dislocation lines or grain boundaries are more important than Brownian motion, except in short furnace anneals. Analysis of the various driving forces shows that whereas small bubbles are dominated by the behavior of dislocation lines, as their size increases the temperature gradient becomes more important. Thus it is important for the temperature gradient to be known. (auth)

37300 INFLUENCE OF SURFACE STRUCTURE AND PURITY OF Cu SAMPLES AND OF α IRRADIATION ON THE DIFFUSION OF ^{62}Ni IN Cu. Bonzel, H. P. Goettingen, Ger., Univ., Goettingen, 1965. 60p. $2.00 Gmelin, AED-Diss. 65-298.

Thesis.

Diffusion of ^{63}Ni in Cu is studied at 200 to 520°C. Diffusion coeffients as a function of temperature are given for various surface structures. Diffusion coefficients with simultaneous α irradiation are temperature independent. (auth)

37301 RADIATION-INDUCED PHASE TRANSFORMATIONS IN $BaTiO_3$. Schenk, M. Berlin, Humboldt Univ., 1965. 100p. $2.00 Gmelin, AED-Diss. 65-347.

Thesis.

Phase transformations in $BaTiO_3$ as a function of fast neutron flux are studied. The tetragonal modification is transformed by 4.10^{18} n/cm^2 into the cubical modification. This phase is stable at room temperature while cubical $BaTiO_3$ produced by thermal action is unstable. An atomistic theory of radiation induced phase transformations is given. (auth)

37302 CONTROL OF SWELLING BY NUCLEATION. Brinkman, J. A.; Johnston, W. V. (North American Aviation Science Center, Thousand Oaks, Calif.). 32p. (CONF-650904-13). ORAU. Gmelin, AED-CONF-65-226-4.

From Symposium on Radiation Effects, Asheville, N. C.

The agglomeration of inert gas fission product atoms into bubbles can result in swelling of nuclear fuel. It is shown that the amount of agglomeration may be controlled by introducing small amounts of impurity atoms which, after suitable heat treatments, form fine precipitates throughout the volume of the fuel. These precipitates serve as trapping sites for the moving gas atoms and bubbles. The binding energy between particle and bubble is shown to be $\gtrsim$10 ev. Swelling is therefore greatly reduced if the particle density is greater than 10^{13}/cm^3. The conditions under which radiation induced precipitation and re-solution will take place are defined. These conditions can also result in a radiation enhanced solubility which, in certain cases, may provide an additional means of controlling gas atom mobility and thus nucleation. An application of these concepts to cavitational swelling is suggested. The results of other investigations embodying fine dispersions to control swelling are reviewed. (auth)

37303 EMANATION OF XENON AND KRYPTON FROM OXIDE FUELS DURING REACTOR OPERATION. Dreyer, Howard S. 8p. (CONF-650602-84). ORAU. Gmelin, AED-CONF-65-125-119.

From American Nuclear Society 11th Annual Meeting, Gatlinburg, Tenn.

Irradiated fuel elements were physically examined and the released fission gas was sampled by puncturing the individual pins. An analysis of the mass spectrometry data showed that the ratio of the concentration of ^{134}Xe to ^{86}Kr, for the fuel pins was 3.74 ± 0.23. F-tests were made comparing the data from the different fuel compositions; no significantly statistical difference could be detected. Based on the experimentally measured ratio D_{Xe}: D_{Kr}, a calculation was made of the contributions of release by recoil and a mechanism releasing the gas in the ratio of the fission yields. It is concluded that diffusion, recoil, or a combination of these mechanisms are not the only mechanisms of importance at fuel temperatures up to ~1500°C. The experimental data show that a large proportion of the fission gas is being released in direct proportion to their fission yield ratios. (J.R.D.)

37304 MECHANICAL PROPERTIES OF COLD-WORKED AND NEUTRON-IRRADIATED IRON. Edison, G. E.; Backofen, W. A. 19p. (CONF-651062-4). ORAU. Gmelin, AED-CONF-65-325-12.

From Metallurgical Society Fall Meeting, Detroit.

Radiation effects on mechanical properties and brittle fracture of zone-refined Fe were investigated over a range of grain sizes, pre-strains, and integrated neutron doses. An analysis of results is presented along with data obtained in the investigation. (J.R.D.)

37305 TIME DECAY OF SCINTILLATIONS OF ANTHRACENE AND p-TERPHENYL SINGLE CRYSTALS WITH α PARTICLES AS A FUNCTION OF THE DIRECTION OF INCIDENCE. Brinkmeier, F. Goettingen, Ger., Univ., Goettingen, 1965. 83p. $2.00 Gmelin, AED-Diss. 65-348.

Thesis.

Decay curves in anthracene and p-terphenyl for 4.3-Mev α rays and 0.62-Mev β rays are given as a function of the orientation of the direction of incidence. The main contribution to anisotropy is given by the fast decaying component. Results indicate that the light yield depends on the direction of light emission. (Gmelin Inst.)

PHYSICS

General

Refer also to abstract 37279.

37306 (AD-636408) LABORATORY SIMULATION OF WAVES GENERATED BY UNDERWATER NUCLEAR EXPLOSIONS. Jordaan, J. M. Jr. (Naval Civil Engineering Lab., Port Hueneme, Calif.). June 1966. 51p. (R-424). CFSTI $3.00 cy, $0.50 mn.

The kinematics of surface gravity waves produced in water 2.5-feet deep in a basin 90 feet square by a sudden, localized disturbance was studied through measurements of height and period. The waves were generated by the quick withdrawal or immersion, or combinations of these actions, of a 14-foot-diameter half-paraboloid plunger located near the mid-point of one wall of the basin. Smaller plungers of diverse shapes were also used. Measurements were made both in the constant-depth portion of the basin and over a beach with a uniform slope of 1:13.6, which was directly opposite the plunger. At the shoreline about 80 feet from the plunger, waves produced by a sudden withdrawal, for example, were 3 inches high, with a maximum period of 3 seconds. The waves compare adequately with those predicted by the theory of Kranzer and Keller, although they were 40% smaller and 20% shorter. By extrapolation, it was found that waves were produced which adequately simulated those from the actual underwater detonation of a high-energy explosive (5 tons TNT) and a nuclear device (20 kt equivalent). It is concluded that with proper scaling the plunger can be used to simulate waves from such causes. (auth)

37307 (LA-3509) A STUDY OF SOME OF THE PARAMETERS AFFECTING KNUDSEN EFFUSION. DEVIATIONS FROM THE COSINE LAW AS A FUNCTION OF CELL GEOMETRY, CELL MATERIALS, AND NATURE OF THE EFFUSING SPECIES. Ward, John W. (Los Alamos Scientific Lab., Univ. of California, N. Mex.). Jan. 1966. Contract W-7405-eng-36. 144p. Dep. mn. CFSTI $4.00 cy, $1.00 mn.

Thesis. Submitted to New Mexico Univ., [Albuquerque].

Experimental studies of the distributions of particles effusing from a Knudsen cell at high temperatures (1000 to 2000°K) reveal marked deviations from the cosine law. It would appear that complete thermodynamic equilibrium is seldom achieved in a high-temperature Knudsen experiment; further, in terms of ordinary kinetic theory, descriptions of the behavior of the "gas" inside the cell are oversimplified. The measured distributions show clearly, in a fashion analogous to the formation of an image by a pinhole camera, the effects of geometry and choice of materials for each Knudsen cell. In particular, containment problems which force the use of special cell materials at high temperatures may introduce side effects which can cause serious deviations from theory. In order to augment experimental studies, a Monte Carlo program was formulated for the Los Alamos MANIAC computer to attempt to duplicate mathematically the experimental results. The assumptions used in designing the computer program were derived from the experimental work. A cell model was constructed which allowed assignment of probabilities, on the basis of sample and cell geometries, corresponding to events thought to occur in the real case. It was found that the distributions predicted by the computer agreed very closely with those obtained experimentally. Explanations are offered for the results that were observed, and suggestions are made as to how some of these results might be used to improve the reliability of Knudsen data. (auth)

37308 (NP-16226) ANNUAL REPORT, 1965. (European Organization for Nuclear Research, Geneva (Switzerland)). 184p. Dep. mn.

A progress report is presented for CERN which includes individual reports on the Proton Synchrotron, the Synchrocyclotron, nuclear physics research, track chambers, data handling, theoretical studies, nuclear physics apparatus, accelerator research, site and buildings, finance, personnel, health physics, general safety, and central services. (B.G.D.)

37309 GENERALIZATION OF THE DIRAC CHORD METHOD TO INCLUDE CHARGED-PARTICLE PHENOMENA. Lewis, E. E. Nucl. Sci. Eng., 25: 359-64(1966).

The Dirac chord method is applied to the calculation of the escape probability of heavy charged particles from a uniform isotropic source of arbitrary convex geometry. This leads to the distribution of path lengths traveled by particles before escaping from the source. The path-length distribution, which is a function only of the Dirac chord distribution, may be used to average nuclear characteristics over the source geometry. As an illustration, the standard formula for the neutron-escape probability is reproduced. Expressions are then derived for the spectrum and energy self absorption of heavy-charged-particle sources. Specific results for spherical, slab, and cylindrical sources are obtained with the assumption that the range is proportional to an arbitrary power of the particle energy. (auth)

37310 FLAME-TEMPERATURE MEASUREMENT BY THERMAL NEUTRON PROBE. Doherty, P. D.; Barr, R. E.; Boedeker, R. R.; Delaney, R. M.; Manson, D. J.; Weber, A. H. (Saint Louis Univ.). Phys. Fluids, 9: 1577-80(Aug. 1966).

Thermal neutrons from the CP-5 reactor at Argonne National Laboratory were scattered from an oxyhydrogen flame. Simple analysis showed that the energy distribution of the scattered neutrons depended on the translational motion temperature of the flame nuclei. The energy distribution was calculated assuming Maxwell-Boltzmann statistics in the flame and averaging over the energy distribution of incident thermal neutrons. The measured transmission of the scattered neutrons by thin cadmium foils plotted versus foil thickness (0.001-0.015 in.) was compared with calculated plots yielding the translational motion temperature. The temperature determined in this way for a flame at ambient pressures from 20 to 30 Torr was 2800 ± 400°K. (auth)

37311 MEASUREMENT OF THE TIME EVOLUTION OF A RADIATION FIELD BY JOINT PHOTOCOUNT DISTRIBUTIONS. Arecchi, F. T.; Berne, A.; Sona, A. (Laboratori Centro Informazioni Studi Esperienze, Milan). Phys. Rev. Lett., 17: 260-3(Aug. 1, 1966).

The measurement of the time evolution of a stationary Gaussian field by means of joint photocount distributions, which can be considered as a generalization of the single-time photocount distributions used thus far in previous experiments, is reported. (B.G.D.)

37312 STUDY OF ELECTRON BEAMS AND THEIR FORMATION IN ELECTROSTATIC ELECTRON GUNS. Goud, Paulus Arie. Vancouver, Can., Univ. of British Columbia, 1965. 181p.

Thesis.

A theoretical study is made of the formation of electron beams in electrostatic fields. The electron motion is assumed to be normal, congruent, and regular, so that the equations governing the motion can be set up in terms of the action function. By assuming convenient functional forms of the action function, of the potential, and of the metrical coefficients, some new solutions are found by the method of separation of variables. These solutions are studied in detail, and are shown to have some desirable properties. In order to employ a given space-charge flow solution in electron gun design, a method is developed to take into account the distortion of the field due to the anode aperture. The gun is considered to be made up

of two regions separated outside the beam by an auxiliary anode. The desired space-charge flow is assumed to exist in the cathode region, while in the anode region the effect of space-charge on the electrostatic field is assumed to be negligible. An estimate is made of the accuracy of these assumptions. The fields about four idealized anode geometries are obtained by using Schwarz-Christoffel transformations, and a study is made of the relevant properties of these fields. One of these fields, called the wrap-around field, is shown to have properties very desirable for convergent electron guns. The above design method is illustrated by two examples: a gun producing a beam that is initially parallel and rectilinear, and a gun producing a beam that is initially radial and convergent. The latter incorporates the wrap-around field in the anode region. Physical considerations involved in the determination of the electrodes to maintain a given beam are briefly discussed, and it is shown that the sensitivity of the field conditions at the beam boundary to errors in the field at other locations decreases at an exponential rate with distance. A method is suggested for determining beam-forming electrodes that avoids the need for an auxiliary anode to maintain the beam. (Dissertation Abstr.)

Accelerators

Refer also to abstract 37475.

37313 (BNL–10143) COMBINATION OF CYLINDRICAL CURRENT SHEETS TO CANCEL EXTERNAL FIELD. Beth, R. A. (Brookhaven National Lab., Upton, N. Y.). Mar. 29, 1966. Contract AT(30-3)-Gen-16. 5p. Dep. mn. CFSTI $1.00 cy, $0.50 mn.

It was shown previously that any required finite two-dimensional magnetic field can be produced inside or outside a right circular cylinder by letting the proper current distribution flow along the elements of the cylinder. It is shown that by using two coaxial cylinders, the external magnetic field can be cancelled and an arbitrarily required internal field can be produced. (B.G.D.)

37314 (BNL–10148) FIELDS PRODUCED BY CYLINDRICAL CURRENT ARRAYS. Beth, Richard A. (Brookhaven National Lab., Upton, N. Y.). Mar. 25, 1966. Contract AT(30-2)-Gen-16. 8p. Dep. mn. CFSTI $1.00 cy, $0.50 mn.

A general current sheet theorem is formulated for treating planar fields due to cylindrical current arrays as functions of a complex variable. The theorem is illustrated for the case of an arbitrary distribution of currents flowing along the elements of a right circular cylinder. (B.G.D.)

37315 (BNL–10323) STORED ENERGY AND INDUCTANCE IN TWO-DIMENSIONAL FIELDS. Beth, Richard A. (Brookhaven National Lab., Upton, N. Y.). May 20, 1966. Contract AT(30-2)-Gen-16. 4p. Dep. mn. CFSTI $1.00 cy, $0.50 mn.

The energy stored per unit length in a constant gradient field is determined. (B.G.D.)

37316 (BNL–10324) FORCES ON CURRENTS IN TWO-DIMENSIONAL MAGNETIC FIELDS. Beth, Richard A. (Brookhaven National Lab., Upton, N. Y.). May 23, 1966. Contract AT(30-2)-Gen-16. 3p. Dep. mn. CFSTI $1.00 cy, $0.50 mn.

A discussion is presented on the forces on currents in two-dimensional magnetic fields. (B.G.D.)

37317 (BNL–10341) ELLIPTICAL CURRENT SHEETS TO PRODUCE CONSTANT-GRADIENT FIELD. Beth, Richard A. (Brookhaven National Lab., Upton, N. Y.). June 10, 1966. Contract AT(30-2)-Gen-16. 4p. Dep. mn. CFSTI $1.00 cy, $0.50 mn.

A two-dimensional constant-gradient field, typical of the fields used in an alternating-gradient synchrotron is described. The distribution of currents along the elements of an elliptic cylinder to produce any required nonsingular internal field is discussed. The use of confocal elliptical current sheets to cancel external fields is also discussed. (B.G.D.)

37318 (BNL–10436) FIELDS PRODUCED BY ELLIPTICAL CURRENT SHEETS. Beth, Richard A. (Brookhaven National Lab., Upton, N. Y.). July 6, 1966. Contract AT(30-2)-Gen-16. 9p. Dep. mn. CFSTI $1.00 cy, $0.50 mn.

A general solution is presented for problems dealing with elliptic cylinder current sheets. The problems are how should currents flowing along the elements of an elliptical cylinder be distributed to produce a desired magnetic field inside the cylinder and how should currents be distributed if a second outer chamber is provided to cancel the exterior field while producing a desired interior field. (B.G.D.)

37319 (CEA-R–2976) ETUDE DE LA MODULATION DE FREQUENCE DE DIVERS SIGNAUX U.H.F. EXISTANT DANS UN ACCELERATEUR LINEAIRE D'ELECTRONS. (Study of the Frequency Modulation of Various uhf Signals Occuring in an Electron Linear Accelerator). Bergere, Roland; Veyssiere, Andre; Daujat, Pierre (Commissariat a l'Energie Atomique, Saclay (France). Centre d'Etudes Nucleaires). June 1966. 96p. Dep. mn.

A digest of a series of studies on the frequency modulation of uhf fields and signals associated with the linear electron accelerator at Saclay is presented. The frequency modulation of a uhf pulse before its injection into an accelerating structure and after its subsequent propagation when no accelerated electrons are present is considered. A similar analysis is applied to the frequency modulation due to the direct interaction of the electron beam itself and the accelerating uhf fields. The phase modulation of the elementary electron packet itself is then considered. This phase modulation can be correctly interpreted by considering the dynamics of the electron beam as such. This analysis moreover, gives a correct interpretation of the evolution of the phase modulation with time, as the elementary electron packets move along with the sinusoidal uhf accelerating fields. (auth)

37320 (CONF-660510–19) SYNCHROCYCLOTRON CONVERSION. MacKenzie, K. R. (California Univ., Los Angeles). [1966]. Contract AT-04-1-GEN-12. 20p. Dep. mn. CFSTI $1.00 cy, $0.50 mn.

From International Conference on Isochronous Cyclotrons, Gatlinburg, Tenn.

The possibility of increasing the output of f-m cyclotrons is being explored simultaneously in many laboratories. Space charge seems to be the limiting factor. Practically every laboratory is investigating a form of hooded source known as the Livingston, calutron or Oak Ridge source. The ions must clear such a source so higher dee voltages are needed. The higher dee voltage is desirable in any case since the beam usually increases as some power of this voltage (if the repetition rate is increased correspondingly). The theoretical picture indicates a variation between V and V^2. Some f-m cyclotrons will try to increase performance by this method alone. Others will include all the possible improvements including a complete sector field near isochronism which will provide strong vertical focusing and reduce the frequency swing. The largest machines will probably try to achieve their goal by small sectors near the source and somewhat larger limited radii sectors on the poles (with an unchanged radial profile). The status of these efforts is reviewed and some data on the Berkeley model program is given. It appears that most f-m cyclotrons will eventually be partially or wholly converted to sector focused synchrocyclotrons. (auth)

37321 (NP–16205) SOSTOYANIE RABOT NA POZITRON-ELEKTRONNOM NAKOPITELE VZPP-2. (Status of Operation at the Positron-Electron Accumulator VEPP-2). Auslender, V. L.; Blinov, G. A.; Budker, G. I.; (and others) (Akademiya Nauk SSSR, Novosibirsk. Institut Yadernoi Fiziki). 1965. 12p. Dep. mn.

The progress in the construction of the VEPP-2 device, designated for positron-electron interaction experiments up to 2×700 Mev is reported. During the past two years the personnel was able to put into operation the injector synchrotron, to collect strong electron currents in the accumulator unit, to study the instabilities due to beam-

resonator interactions, and to accumulate positrons. A brief description of the device is presented. The accumulation of electrons and positrons and the deployment of the hardware for the positron-electron beam interaction experiments are discussed. The transmittance will be determined from the positron-electron small-angle scattering. (CFSTI)

37322 TRANSFORMER-TYPE HIGH-CURRENT ACCELERATOR. Abramyan, E. A.; Gaponov, V. A. At. Energ. (USSR), 20: 385-92(May 1966). (In Russian).

A direct-action accelerator that can accelerate electrons up to 1.5 Mev with an efficiency of nearly 90% is described. An installation with a 1.5-Mev electron beam and a mean power of 25 kw is discussed. (G.O.Y.)

37323 EXPERIMENTAL DETERMINATION OF RADIATION QUALITY FACTORS IN THE VICINITY OF HIGH-ENERGY ACCELERATORS. Lebedev, V. N.; Zel'chinskii, M.; Salatskaya, M. I. At. Energ. (USSR), 20: 392-6(May 1966). (In Russian).

The results of some measurements of the effective quality factors for pulsed multicomponent radiation in the vicinity of a 10-Bev synchrophasotron are presented. The quality factors obtained by a recombination method varied from 3 to 11. These values are compared with values from other high-energy accelerators. Some data on values measured during experiments with a 680-Mev synchrocyclotron are also given. (G.O.Y.)

37324 68.5 cm SECTOR-FOCUSED CYCLOTRON. Alekseev, A. G.; Barkovskii, V. N.; Basargin, Yu. G.; Vasil'ev, V. N.; Litunovskii, R. N.; Minyaev, O. A.; Nikolaev, V. N.; Stepanov, A. V. At. Energ. (USSR), 20: 429-30(May 1966). (In Russian).

A sector-focusing cyclotron that can deliver protons of 7.5 to 100 Mev and deuterons of 0.5 to 4.0 Mev is described. The acceleration of molecular H_2^+ ions underscores the essential role of the process of proton dissociation. Under certain conditions intrinsic to the sector-focusing cyclotron where the ions achieve several hundred revolutions, this process can interfere with obtaining the intensity of the ion bean H_2^+ at finite energies, if the vacuum in the accelerator chamber is less than 1.10^{-5} mm Hg cm^{-1}. (G.O.Y.)

37325 WHY BUILD INTERSECTING STORAGE RINGS? CERN Cour., 7: 123-5(July 1966).

A discussion is given of intersecting storage rings and the advantages derived from their use. The design and development of these storage rings at CERN is also described. (J.F.P.)

37326 [INTERSECTING STORAGE RINGS]. DESCRIPTION OF THE PROJECT ITSELF. Johnsen, K. CERN Cour., 7: 126-9(July 1966).

A general description of the CERN intersecting storage rings—their basic parameters, how they work, their expected performance is given—and some of the major difficulties foreseen in the construction are outlined. (auth)

37327 [INTERSECTING STORAGE RINGS]. PREPARATORY WORK. CERN Cour., 7: 130-7(July 1966).

Some of the preparatory work which was done on the ISR project is discussed. Information on the major components of the storage rings (magnet, r-f, vacuum, beam transfer and site work), research using the electron storage ring at CERN and storage rings elsewhere is included. (auth)

37328 INCREASING THE INTERNAL BEAM CURRENT OF THE JINR SYNCHROCYCLOTRON BY ADDITIONAL ELECTROSTATIC FOCUSING. Danilov, V. I.; Enchevich, I. B.; Marchenko, B. N.; Polferov, E. A.; Safonov, A. N.; Shestov, A. V. Izv. Fiz. Inst. Aneb, Bulg. Akad. Nauk, 14: 5-19(1966). (In Russian).

The results of the study of the effect produced on the accelerated proton current by the electrostatic field in the central region of the JINR synchrocyclotron are described. The electrostatic field formed by a system of electrodes situated against the dee partially compensated the defocusing action of the spatial charge of the ion bunch near the center of the synchrocyclotron, as a result of which the proton current in the finite range increased from 1.1–1.2 to 2.1–2.3 μA. (auth)

37329 STABILITY OF CROSSED-FIELD ELECTRON BEAMS. Buneman, O. (Stanford Univ., Calif. Avco Everett Research Lab., Everett, Mass.); Levy, R. H.; Linson, L. M. J. Appl. Phys., 37: 3203-22(July 1966).

The stability of crossed-field electron beams is treated for arbitrary values of the parameter $q = \omega_p^2/\omega_c^2$ = (plasma frequency/cyclotron frequency)^2. The theory bridges a gap between existing theories applicable for $q \ll 1$ and for $q = 1$. For wavelengths longer than about five beam thicknesses an instability occurs with a growth rate not exceeding $\sim\frac{1}{4}q\omega_c$. It can be shorted out by conducting walls, or else one can prevent long wavelengths in closed (cylindrical or toroidal) beam geometries. For wavelengths shorter than roughly 6q beam thicknesses a cyclotron instability occurs with a growth rate $\sim\frac{1}{2}q\omega_c \exp(-2/q)$. This becomes practically unimportant for $q \gtrsim 0.2$. Observations support these theoretical results. (auth)

37330 ELECTRICAL OPTICAL PROPERTIES OF THREE-ELECTRODE ELECTRON LENSES. Kanaya, K. (Electrotechnical Lab., Tokyo); Kawakatsu, H.; Yamazaki, H.; Sibata, S. J. Sci. Instrum., 43: 416-29(July 1966).

The focal properties and chromatic and spherical aberrations of three-electrode lenses represented by Glaser's bell-shaped potential distribution and also by double bell-shaped potential distributions are extended. The results can be expressed simply in terms of the half-width of the potential distribution and the ratio of the potential at the center of the lens to that of the accelerating potential. These parameters and their dependence on electrode geometry are derived approximately from Regenstreif's potential theory modified by the aid of experimental measurements, leading to a lens model which may be considered to be the superposition of four or five aperture lenses. Focal lengths deduced from the theory agree sufficiently closely with experimental values to be immediately applicable for design purposes. (auth)

37331 VOLTAGE CALIBRATION OF A 400-kv VAN DE GRAAFF MACHINE. Jiggins, A. H.; Bevan, J. S. (Borough Polytechnic, London). J. Sci. Instrum., 43: 478-9(July 1966).

A technique is described for the rapid calibration of the terminal voltage of a Van de Graaff machine in the range 0 to 500 kv. The signal from a generating voltmeter fitted to the machine is shown to be proportional to the terminal voltage, as determined by (pγ) resonances in the range 164 to 480 kev. (auth)

37332 POLARIZED ACCELERATOR TARGETS. Shapiro, Gilbert Sci. Amer., 215: 68-78(July 1966).

The effects of nuclear particle spin on nuclear forces is reviewed. Topics discussed include a model which accounts for spin-dependent forces that act on the electron, dynamic nuclear polarization, double- and triple-scattering experiments, the spin-correlation experiment, and polarized proton targets. (J.F.P.)

37333 LOW- AND MEDIUM-ENERGY ACCELERATION OF IONS AND THEIR APPLICATION IN NUCLEAR PHYSICS. Nemenov, L. M. Vestn. Akad. Nauk Kaz. SSR, No. 10, 3-12(Oct. 1965). (In Russian).

The Institute of Nuclear Physics of the Kazakh SSR Academy of Sciences has completed the construction and conducted the trial startup of a one-and-a-half-meter cyclotron. The cyclotron laboratory is housed in a two-story building with a basement. A brief exposition is given of the basic characteristics of the cyclotron, which accelerates protons to 17 Mev, deuterons and ions of molecular hydrogen to ~22 Mev, and alpha-particles to ~44 Mev. All operations are remote-controlled. It is planned first of all to provide short-lived radioactive isotopes for laboratories of the Institute of Nuclear Physics and scientific establishments of the Kazakh SSR Academy of Sciences. It is also planned to use the cyclotron for activation analysis and for the determination of impurities in the manufacture of semiconductor transmitters. The main thrust of the work

to be done on the cyclotron is the study of the mechanism of the interaction of charged particles with nuclei at low and medium energies. Of great interest is the study of fission in a wide range of low and medium excitation energies up to tens of Mev. These investigations are being conducted in conjunction with physicists at Obninsk, who are investigating fissions during neutron bombardment of nuclei. The task of the Institute of Nuclear Physics is to study this same process when a nucleus is acted on by charged particles. First priority will be given to investigating the energy dependence of the kinetic energy of fission fragments of heavy nuclei and to studying the angular distributions of fission fragments. The design of the electromagnet makes it possible to accelerate polarized particles in the cyclotron, and as soon as sources of polarized ions of sufficient intensity have been developed, such experiments will be undertaken. To eliminate rapid obsolescence, much work is being done to modernize the cyclotron as it is being put into operation. This includes redesigning the cyclotron according to the Thomas principle and providing slide control of the energy of the ions being accelerated. (JPRS)

37334 FOCUSING OF BEAMS OF FAST CHARGED PARTICLES IN STELLERATOR TYPE FIELDS. Khapaev, M. M. Vestn. Moskov. Univ., Ser. III, Fiz. Astron, No. 3, 57-63(May-June 1965). (In Russian).

The focusing properties of a high-energy beam of charged particles in a helical magnetic field were studied analytically. A set of equations were derived for the particle trajectory in cylindrical coordinates under certain assumptions, and the solution was obtained by means of a simplified degenerate system of equations with two adiabatic invariant integrals, which describes a periodic motion for the average system. Certain conclusions are made concerning the focusing capabilities of such charged particle beams. It is shown that interactions between transverse motion and longitudinal motion in the beam are very small. (TSS)

37335 THEORY OF STOCHASTIC ACCELERATION I. SOLUTION OF THE PROBLEM OF BURSHTEIN, KOLOMENSKII, AND VEKSLER. Biersack, Jochen (Hahn-Meitner-Institut fuer Kernforschung, Berlin). Z. Phys., 194: 311-22(1966). (In German).

Theoretical investigations on the stochastic acceleration in circular accelerators are discussed. The classical problem of Burshtein, Kolomenskii and Veksler are considered. This problem was formulated in a publication very clearly in 1955, but has not yet found an exact solution. The subject is the calculation of the probability that a charged particle is accelerated from the injection energy to the top energy of the apparatus ("probability of acceleration"), supposing that the particle has an equal chance at every circulation to increase or decrease its energy by a fixed amount eU_0. The following investigation shows that this problem can be solved if properly formulated as a matrix equation, and that the solution is of a relatively simple closed form. This is the case, too, if the primary problem is extended by permitting particle losses during the acceleration process ("absorption"). The results are discussed, especially regarding the influence of absorption. Under certain conditions $[(eU_0)^2/S\Sigma \gg (E_{max} - E_{min})^2]$ the probability of acceleration becomes independent of absorption and of the gap voltage U_0. (auth)

37336 THEORY OF STOCHASTIC ACCELERATION. II. DIFFUSION APPROXIMATION AND DYNAMICAL PROCEDURE. Biersack, Jochen (Hahn-Meitner-Institut fuer Kernforschung, Berlin). Z. Phys., 194: 453-77(1966). (In German).

The original problem of stochastic acceleration was solved in the first part of this work. This second part tries to meet the wishes of practice by changing the matrix equation into a different equation of the diffusion type ("diffusion approximation"). Thus, the mathematical treatment becomes much more simple, and one has the advantage to apply the well known methods of solving differential equations (e.g., Greens function and Laplace transformation). By this it will be possible to treat more difficult problems, especially the dynamical behavior of a stochastic accelerator. Using the diffusion approximation, the output intensity for a time-independent injection current is calculated under more general assumptions. The obtained results include the results of the first part as a special case. Furthermore, the time dependence of output intensity is evaluated for an arbitrarily time-dependent injection current. The appendix deals with the possible influence of stochastic acceleration processes on the energy spectrum of the primary cosmic radiation. As a starting point an equation is chosen which permits to consider simultaneously both a (refined) Fermi process and the stochastic acceleration in quasistationary electric fields. The result shows in agreement with the experience that the exponent γ in the energy spectrum $\varphi \approx E^{-\gamma}$ at first increases with increasing energy, and then approaches the same constant value as given by the sole Fermi process. (auth)

37337 NANOSECOND BEAM BURST PRODUCTION. Carlson, Lorne Edwin. Edmonton, Alta., Univ. of Alberta, 1963. 86p.

Thesis.

The 5.5-Mev Van de Graaff accelerator at the University of Alberta presently employs a preacceleration beam chopper which produces 500-μamp beam bunches of 10 nanoseconds duration. The aim of the present work is to develop a top terminal pulsing device, which produces higher intensity 10-nanosecond pulses, by first pulsing the ion source, producing a beam burst longer than 10 nanoseconds, followed by klystron bunching of this beam to produce the desired 10-nanosecond beam burst. Experimental results indicate that this system (pulsed ion source and buncher) can be employed to produce intense ion beam bursts of 10-nanosecond duration. (auth)

37338 PRINCETON-PENNSYLVANIA ACCELERATOR STANDARD MAGNET CURRENT REGULATORS. Riedel, J. (Princeton-Pennsylvania Accelerator, Princeton, N. J.). 3p. (CONF-650922-22). ORAU. Gmelin, AED-CONF-65-285-2.

From 1st International Symposium on Magnet Technology, Stanford, Calif.

The specifications and development of standard magnet current regulators for the Princeton-Pennsylvania accelerator are briefly discussed. The design and operation of the current transducers, reference source, and the complete regulator circuit are described. (L.B.S.)

37339 ELECTRON ACCELERATOR WITH A PEAK BEAM POWER OF 10^{10} WATTS. Dyke, W. P.; Barbour, J. P.; Grundhauser, F. J.; Charbonnier, F. M. (Field Emission Corp., McMinnville, Ore.). 21p. (CONF-660426-1). ORAU. Gmelin, AED-CONF-66-073-1.

From 8th Annual Symposium on Electron and Laser Beam Technology, Ann Arbor, Mich.

The extrapolation of the field emission beta ray device principle to an electron beam current of 10,000 amp at 2.5 Mv is reported. The electron beam is transmitted through a thin window for external use. An energy density of 100 joules/cm^2 is delivered in a pulse length of 30 nanoseconds. Dose per pulse and dose rate are of the order of 10^7 rads/pulse and 10^{14} rads/sec, respectively. The key features of the generator are described briefly and several applications are noted. (J.F.P.)

37340 MAGNETIC GRADIENT PARTICLE ACCELERATOR. Morley, Morgan J.; Gilbert, David I. (to Aerojet-General Nucleonics). U. S. Patent 3,254,564. June 7, 1966. Filed Dec. 4, 1963.

A magnetic-gradient particle accelerator is provided for accelerating 100–1000 μ particles to velocities of 20 km/sec or higher. The accelerator comprises a metallic particle, a hollow flux concentrator having a tapered inner surface adapted to contain the metallic particle, a hollow conductor concentrically arranged about the flux concentrator, and two inductors with one concentrically arranged about one end of the conductor and

with the second concentrically arranged about the other end of the conductor. The inductors are adapted to establish a magnetic field within the conductor and around the particle. An explosive charge is arranged concentrically about the central section of the conductor and between the inductors. The explosive charge is adapted to implode the conductor upon the flux concentrator so as to converge the magnetic field and thereby accelerate the particle. (B.L.M.)

Astrophysics and Cosmology

Refer also to abstracts 37503, 37528, 37536, 37542, 37547, 37793, and 37916.

37341 (N-66-17354) OBSERVATIONS WITH UNIVERSITY OF IOWA EQUIPMENT ON MARINER IV, FEBRUARY-MAY 1965 (PRELIMINARY). Van Allen, J. A.; Frank, L. A.; Krimigis, S. M.; Hills, H. K. (State Univ. of Iowa, Iowa City. Dept. of Physics and Astronomy). May 24, 1965. Contracts NAS7-100; JPL-950613. 19p. (NASA-CR-70375). CFSTI $1.00 cy, $0.50 mn.

For Jet Propulsion Lab., Calif. Inst. of Tech., Pasadena.

The operation and sensitivity of apparatus aboard the Mariner IV for the detection and measurement of the magnetic moment of Mars is discussed. Measurements of solar cosmic ray events up to May 5, 1965 (Day 125), are reported. A diffusion analysis of a solar cosmic ray event occurring during February 5 to 13, 1965, was performed, and an analytical plot of the intensity-time history for protons ($E_p > 55$ Mev) derived from the corrected differences of counting rates of detectors B and D_1 is given. The best-fit value of the parameter β is 0.9. A similar analysis of data from detector C yields $\beta = 0.67$. The discrepancy is not yet understood. In addition, a weak proton event was found in data from the low energy channel D_1 of the solid state detector ($0.50 < E_p < 11$ Mev) on April 20, 1965. A table of solar cosmic-ray events recorded between November 28, 1964, and May 5, 1965, is given. Count/second logs of events for the various detectors are presented. (STAR)

37342 ADVANCES IN ASTRONOMY AND ASTROPHYSICS. VOLUME 4. Kopal, Zdenek (ed.). Advances Astron. Astrophys., 4: 1-346(1966).

A comprehensive treatment is provided of fundamental positional astronomy, including recent developments. Principles and techniques used in predictions of astronomical phenomena are presented. Topics covered include: objective prisms and measurements of radial velocities, the figure and gravity field of the moon, the relativistic degenerate gas, exchange of matter and period changes in close binary systems, and the cometary origin of meteorites. (J.H.M.)

37343 GASEOUS PRESSURE IN SUNSPOTS. van't Veer-Menneret, Claude; van't Veer, Frans (Institut d'Astrophysique, Paris). Ann. Astrophys., 28: 1026-33(Nov.-Dec. 1965). (In French).

A survey of the literature reveals that no reliable method has been developed to measure the temperature, the gas pressure, and the gradients of these parameters in a sunspot. The methods which were used give contradictory results, especially for the pressure, which was found to be higher or lower than in the photosphere according to different reports. After a critical review of the existing methods, a new way is proposed for determining the gas pressure in a sunspot. The proposed method is based on the measurement of the equivalent width and the intensity in the wings of some metal lines in the sunspot and the photosphere. By processing the information contained in these data, it was possible to define a quantity which is a simple function of the ratio of the gaseous pressure in the sunspot and the photosphere. For the observed sunspot, the pressure of $\tau_{5000} = 0.75$ is about the same or slightly lower than in the photosphere at the same level. (BBB)

37344 NON-RELATIVISTIC EQUATIONS OF BULK MOTION OF A RELATIVISTIC GAS. Lerche, I.; Parker, E. N. (Univ. of Chicago). Astrophys. J., 145: 106-8 (July 1966).

The linearized equations of bulk motion of a gas, in which the pressure cannot be neglected compared to the rest energy of the gas, are deduced by taking moments of the collisionless Boltzmann equation in the absence of external forces. The problem is of interest because of its application to the cosmic-ray gas in the Galaxy. (auth)

37345 GALACTIC COSMIC RAYS IN THE SOLAR SYSTEM. Sarabhai, Vikram; Subramanian, G. (Physical Research Lab., Ahmedabad, India). Astrophys. J., 145: 206-14(July 1966).

A model is postulated for the diffusion of galactic cosmic rays in the solar system based on the zonal character of solar activity. In this model there are two zones on either side of the solar equatorial plane where the density of galactic cosmic rays at any given distance from the Sun is lower than the corresponding density in the equatorial plane or at high heliolatitudes. It is suggested that the time variations of cosmic rays up to 50 Bev should be related to a factor which is dependent on the diffusion of galactic cosmic rays along the spiraling magnetic lines and another factor which is related to diffusion normal to the equatorial plane due to magnetic-field irregularities in interplanetary space, particularly in the neighborhood of Earth. It is also suggested that the deficiency of cosmic rays observed along the garden-hose direction from the Sun and sometimes for high-energy cosmic rays from the anti-garden-hose direction must be attributed not only to scattering of particles into the Sun but also to transverse diffusion across the radial gradients of intensity which are not the same at different heliolatitudes. It is demonstrated how regions of magnetic-field irregularities are related to non-uniformity of solar-wind velocity over local zones of activity on the Sun. The properties of interplanetary space relevant to cosmic-ray diffusion can be described in terms of the value of $\epsilon = K_\perp/K_\parallel$. Interplanetary space has a structure with sectors where diffusion is isotropic ($\epsilon = 1$) alternating with sectors where diffusion is largely anisotropic ($\epsilon \ll 1$). The sectors are contained in an envelope where diffusion becomes increasingly isotropic. It is suggested that the following cosmic-ray effects can be understood in terms of the model: (1) the deficiency (sink) observed in the anisotropy of galactic cosmic rays along the spiraling magnetic lines of force; (2) the 27-day variations and the day-to-day changes of cosmic-ray intensity; (3) events such as some Forbush decreases, where the intensity decreases sharply but recovers only slowly; (4) the occurrence of days on which the energy spectrum of variation of anisotropy has a positive exponent; (5) the observation that cosmic-ray intensity at a given level of solar activity is more depressed during the declining phase than during the rising phase of activity of the Sun. An experimental verification of the principal ideas contained in the model through the measurement of the differential energy spectrum of galactic cosmic-ray intensity arriving along the spiraling magnetic lines outside the magnetosphere is suggested. (auth)

37346 SUNSPOT CONFIGURATIONS AND PROTON FLARES. Warwick, Constance S. (Inst. for Telecommunication Sciences and Aeronomy, Boulder, Colo.). Astrophys. J., 145: 215-23(July 1966).

Practically all solar flares that emit energetic protons occur in sunspot groups with the Potsdam δ-configuration, in which sunspot umbras of opposite magnetic polarity appear close together within the same penumbra. This property is related to the known tendency of flares to occur where the magnetic field has a steep gradient, and to special flare-sunspot configurations identified earlier by other workers. The δ-configuration is a relatively reliable and easily recognizable symptom of major flare activity and particularly of proton emission. (auth)

37347 RELATED FLARES. Dodson, Helen W.; Hedeman, E. Ruth (Univ. of Michigan, Ann Arbor). Astrophys. J., 145: 224-30(July 1966).

Observations of four major flare events between 12.45

and 21.00 U. T. on September 18, 1957, in a great center of activity at N. 20° E. 05° provide additional evidence that certain solar events called "flares" may not be independent phenomena. The events can be interpreted as four flares or as two flares, each with two phases and two maxima. The first interpretation implies that at least two families of homologous flares occurred within the same center of activity. The second organization of the data means that the late phase of each flare is considered to be in some sense a consequence or development of phenomena initiated during the early phase of the complex event. Either interpretation of the observations indicates that major homologous flares can repeat in less than 5 hours. High-magnification spectroheliograms of these flares made with radiation from the centers of Hα and the K line of ionized calcium show detailed correspondence in the location of the flare emission at these two wavelengths. The radio-frequency, ionospheric, and geomagnetic phenomena associated with the flares are considered. (auth)

37348 LOOP PROMINENCES AND CORONAL CONDENSATIONS. III. THE ABUNDANCES OF IRON AND CALCIUM. **Jefferies, J. T.; Orrall, F. Q. (Univ. of Hawaii, Honolulu). Astrophys. J., 145: 231-6(July 1966).**

Measured total intensities of the continuum and of the red, green, and yeliow forbidden coronal lines emitted by discrete features of a sporadic coronal condensation are shown to yield firm lower limits to the abundances of iron and calcium. These strict lower limits exceed the photospheric abundances (derived by curve-of-growth analysis of Fraunhofer lines) by a factor of 3 for iron and 12 for calcium; the actual coronal abundance will be higher still. (auth)

37349 INTERACTION OF THE SOLAR WIND WITH A LARGE-SCALE SOLAR MAGNETIC FIELD. **Pneuman, G. W. (General Motors Defense Research Labs., Santa Barbara, Calif.). Astrophys. J., 145: 242-54(July 1966).**

The influence of a large-scale solar magnetic field upon the solar wind is investigated. It is found that, in a minimum corona, the solar wind cannot sustain a radial magnetic field until it expands to several solar radii. As a consequence, the high-latitude field lines are more or less dipolar close to the Sun but undergo a transition to a radial configuration at about 9 $R_\odot$ when the inertial force of the solar wind becomes able to dominate the magnetic force. The solar-wind properties as well as the coronal density distribution are computed for this flow and field model and the results compared with observation. The comparison of predicted polar density with the observed is good over the whole range of observation. This comparison predicts a polar temperature of 0.85×10^6 °K. The equatorial stream lines are found to converge toward the equator up to a distance of about 2.7 $R_\odot$ where the gas pressure becomes sufficient to sustain a radial field. Beyond 2.7 $R_\odot$, they proceed radially outward. Some aspects of the necessary changes in the model to produce the gross characteristics of a maximum corona are also discussed. (auth)

37350 VISCOUS MODEL OF THE SOLAR WIND. **Whang, Y. C.; Liu, C. K.; Chang, C. C. (Catholic Univ. of America, Washington, D. C.). Astrophys. J., 145: 255-69(July 1966).**

A viscous, thermal conductive model of the solar wind is studied by using the Navier-Stokes equations to describe the motion of the solar wind. The fluid equations are reduced to a system of three first-order non-linear differential equations. The system of equations for this viscous model does not have a singular point at Mach $\sqrt{3/5}$. The asymptotic solution for this model shows that the temperature decreases according to $r^{-4/3}$, which is much faster than the results obtained for the inviscid model and the static model. The exact solution for this viscous model is obtained. For all values of the heliocentric distance r, its physical implication is discussed and compared with the observed data. (auth)

37351 AUTO-IONIZATION-BROADENED RYDBERG SERIES IN THE SPECTRUM OF La I. **Garton, W. R. S.; Wilson, M. (Imperial Coll. of Science and Tech., London). Astrophys. J., 145: 333-6(July 1966).**

Two auto-ionization-broadened Rydberg series have been observed in the ultraviolet absorption spectrum of La I. The lines are interpreted as transitions from the ground state $6s^25d\ ^2D$ to $6s^2np\ ^2P^0$ levels. The series give an improved value for the lowest ionization potential of La I, namely, $44981 \pm 5\ cm^{-1}$. (auth)

37352 SIGNIFICANCE OF THE COSMOLOGICAL ENERGY EQUATION. **Layzer, David (Harvard Coll. Observatory, Cambridge, Mass.). Astrophys. J., 145: 349-50(July 1966).**

It is pointed out that the cosmological energy equation $\{d(\epsilon S^3)/dt + p\ [d(S^3)/dt] = 0\}$ has a strictly kinematical significance. A dustlike distribution of matter (particles of zero rest mass are included as a limiting case) is considered, and it is shown that for such a distribution equation the cosmological energy equation follows from the definitions of ϵ and p and from the law for the composition of velocities in special relativity. (W.D.M.)

37353 DENSITY OF INTERGALACTIC HYDROGEN MOLECULES. **Field, George B.; Solomon, Philip M.; Wampler, E. Joseph (Univ. of California, Berkeley. Princeton Univ. Observatory, N. J. Univ. of California, Mt. Hamilton). Astrophys. J., 145: 351-4(July 1966).**

Observations of 3C9 down to a red-shifted wavelength of 3050 Å (source wavelength 1012 Å) were employed to evaluate the density of intergalactic H_2. The observations of 3C9 were made with the 120-inch telescope of Lick Observatory using a photoelectric spectrum scanner. The nearly unreddened 08V star HD 14633 was observed in conjunction with HD 2020 in order to obtain an accurate determination of the extinction coefficient. (W.D.M.)

37354 OPACITY PROPERTIES OF SUNSPOTS. **Jensen, Eberhart; Maltby, Per. Astrophys. Norv., 10: 17-25 (Jan. 1965).**

Three sunspot models are considered with respect to their transparency properties. The optical radius is calculated as a function of the vertical optical depth. At vertical optical depth 0.7, the three spot models considered give (horizontal) optical radii equal to 130, 0.7, and 0.055, respectively. It is pointed out that the vertical temperature distribution cannot be deduced from the observations of the umbra intensity as function of spot position without taking the finite size of the spot into account, unless the opacity in the spot is relatively high. Results indicate that the umbra is about as opaque as the photosphere. Otherwise the surrounding hotter regions would be observable through the umbra when the spot is situated away from the disk center. (auth)

37355 COOLING AND DETECTABILITY OF NEUTRON STARS. **Tsuruta, Sachiko; Cameron, A. G. W. (National Aeronautics and Space Administration, New York). Can. J. Phys., 44: 1863-94(Aug. 1966).**

Surface properties, temperature effects, cooling, behavior, and observability of neutron stars were studied. For this purpose, the opacity of the surface layers is calculated both for a pure iron and a pure magnesium composition. It is found that the nondegenerate layers are only a few meters thick and in no case exceed 1% of the stellar radius. The star cools mainly through neutrino emission when $T \gtrsim 1-4 \times 10^8$°K, but at lower temperatures the cooling is primarily through electromagnetic radiation. The neutrino cooling mechanisms included were the neutrino plasma process, the URCA process, and the neutrino bremsstrahlung process. The cooling behavior is quite complicated, with the rate of cooling generally depending on mass, nuclear potential, and surface composition, among which the dependence on mass is the most significant. It will be hard to observe low-mass neutron stars because of fast cooling rates. However, medium- and high-mass stars should still have temperatures exceeding about 2×10^8°K on the surface for times of the order of 10^3 to 10^5 years. Hence, it should not be impossible to observe massive neutron stars relatively close to

us, if there is no x-ray emission for larger flux coming from the surrounding region. (auth)

37356 SOME EFFECTS OF NUCLEAR FORCES ON NEUTRON-STAR MODELS. Tsuruta, Sachiko; Cameron, A. G. W. (National Aeronautics and Space Administration, New York). Can. J. Phys., 44: 1895-1922(Aug. 1966).

Two composite equations of state were used in the investigation of the structure of neutron (or hyperon or baryon) stars. These were based upon two forms of the neutron-neutron potential suggested by Levinger and Simmons. In one form, repulsive forces come in quickly at greater than nuclear densities, while, in the other form, the repulsive forces come in slowly. In the former case the maximum stable mass of a neutron star is about two solar masses, whereas in the latter case it is only about one solar mass. This probably represents a measure of the basic uncertainty in the properties of neutron-star models due to our lack of knowledge of nuclear forces. The maximum central density of a stable configuration is similarly uncertain; this density probably lies in the range 10^{15} to 10^{16} g/cm^3. Details of many of the neutron-star models calculated are summarized and discussed. (auth)

37357 DYNAMICS OF THE DENSE ASTROPHYSICAL SHELLS. Nedyalkov, I. P. Izv. Fiz. Inst. Aneb, Bulg. Akad. Nauk, 14: 109-26(1966). (In Russian).

Optically very-dense plasma shells, which contain photon gas in their interior, are studied. The shells are supposed to have very great masses M($M \sim 10^6 - 10^{10}\ M_\odot$). It is shown that such shells may be regarded as absolutely opaque for some time τ, τ being considerably greater than the period of their mechanical oscillations and comparable with the lifetime of the quasars. The opaque astrophysical shells are considered as idealization of the massive stars whereby the adiabatic index n is precisely equal to its value 4/3 in the case of photon gas. For this reason they may also be called photon stars. Although the photon stars are regarded as opaque, their brightness may reach values up to 10^{45} erg/sec at $M = 10^9\ M_\odot$. This has prompted the attempt to identify them with some quasars for which Sundage supposes that they have a constant brightness. The enormous mass of these objects is the cause for cosmic dust and neighboring stars being attracted to them. If it is assumed that on entering the shell the stars explode as supernovae owing to the enormous aerodynamic pressure (100 million atmospheres), it is possible to explain the energetic balance of the quasars with variable brightness. A model for objects of the type of 3C 273 and 3C 48 is based on this idea. The question of whether an explosion of accreted stars is possible is discussed. It is demonstrated that stars probably explode under the action of the enormous aerodynamic pressure. (L.B.S.)

37358 NEW SCINTILLATION HYPOTHESIS FOR THE SUPERSTARS AND THEIR CONNECTION WITH THE GALAXIES. Nedyalkov, I.; Kalinkov, M. Izv. Fiz. Inst. Aneb, Bulg. Akad. Nauk, 14: 127-46(1966). (In Russian).

The results of the calculations of a new scintillation model of superstars are presented. In the nucleus of a galaxy or intergalactic star cluster a body with a large mass is found with the following structure: spherical plasma shell limiting volume, and filled with photon gas. The thickness and density of the shell (the true superstar) are obtained. The temperature of the photon gas and its mass are also given. The mass—luminosity relation was obtained by the approximate integration of the fourth fundamental equation of the theory for the internal structure of stars (for the transfer of energy in the case of radiation equilibrium). Two figure variants are examined. The second is acceptable: $\rho = 5.3 \cdot 10^{-5}$ g/cm^3; $h = 3.3 \cdot 10^{12}$ cm, $T_{shell} = 7.4 \cdot 10^{50}$, $M_{ph} = M_n$ and $L_{shell} = 6.3 \cdot 10^{44}$ ergs/sec. Considerations are set forth for the explosion of accreted stars in the shell of superstars. The aerodynamic pressure on the surface of the stars was evaluated. For the second variant $p_0 = 2.4 \cdot 10^{14}$ dyne/cm^2, a value which is 40 times higher than the pressure produced by the central collision of two stars. The exploded supernovae explain the total energy of the superstars, as well as the variations in the light curve. Conclusions are drawn about the connection of the superstars with the galaxies, especially with the compact galaxies. The facts which support the model examined are summarized. Special attention is paid to the spectral indices of radio emission. The differences between the proposed model and the similar models of Sapleter and Zeldovich are discussed. A possible way of evolution of the galaxies where superstars occupy a natural place is examined. (auth)

37359 THERMOLUMINESCENCE OF METEORITES. Houtermans, F. G.; Liener, A. (Univ., Bern). J. Geophys. Res., 71: 3387-96(July 15, 1966).

The experimental techniques used for measuring thermoluminescence are described. The glow curves of achondrites differ markedly from subclass to subclass in their artificially excited glow curves. A fair correlation exists between the radiation ages and the luminescence intensity. The olivine components of pallasites yield very low luminescence whereas the silicate components of mesosiderites (with the exception of Weatherford) exhibit distinct peaks at about 90°C. To a good approximation the luminescence intensity of the chondrites is proportional to their radiation ages. If a correction for the radiogenic part of the thermoluminescence is applied, approximate radiation ages can be estimated from thermoluminescence data. (auth)

37360 OBSERVATIONS OF HARD X-RAY EMISSION FROM SOLAR FLARES. Chubb, T. A.; Kreplin, R. W.; Friedman, H. (Naval Research Lab., Washington, D. C.). J. Geophys. Res., 71: 3611-22(Aug. 1, 1966).

Spectral measurements of solar x rays with photon energy greater than 20 kev were carried out in 1959 during portions of three class 2^+ solar flares. Two of the flares showed strong fluxes with spectra equivalent to that expected from a thermal plasma with temperature $\sim 10^8$ degrees. The emission spectra obtained on September 1, 1959, were indicative of a rapidly cooling plasma with initial temperature of about 285 million degrees. It is argued that a similar plasma could have explained the observations of Peterson and Winckler in 1958 and that there currently exists no definitive observational evidence for nonthermal solar x-ray emission. Spectra in the 2- to 20-kev spectral region during solar microflare activity are suggestive of the existence of a peaking in the solar x-ray spectrum in the 8- to 15-kev region, presumably caused by Fe line and recombination continuum emissions. (auth)

37361 QUASARS AS THE ORIGIN OF PRIMORDIAL MATTER IN A STEADY-STATE UNIVERSE. Stothers, R. (Goddard Inst. for Space Studies, New York). Mon. Notic. Roy. Astron. Soc., 132: 217-23(1966).

In a steady-state cosmology, the expanding universe must be continually replenished with matter. It is proposed that creation occurs in massive bursts, corresponding to local formations of the ylem of evolutionary cosmology, but on a scale of galaxies or even galaxy clusters. Consequently, creation takes place in a "quasi-steady-state". It is postulated that matter is created where it is lacking (between galaxy clusters) because it is lacking (due to the universal expansion), quasars are the manifestation of such creation, and matter is created sharing the universal expansion. A variety of phenomena may apparently be explained on this picture, including mass loss from the universe, observational characteristics of quasars, primordial element abundances, galaxy formation, and possibly clusters of radio galaxies. (auth)

37362 ORIGIN OF THE MICROWAVE BACKGROUND RADIATION. Sciama, D. W. (Dept. of Applied Mathematics and Theoretical Physics, Cambridge, Eng.). Nature, 211: 277-9(July 16, 1966).

If the CN excitation is collisional in origin it is possible to account for the background microwave radiation field as the integrated effect of a population of radio sources. The required properties of these radio sources are discussed. (M.O.W.)

37363 ROTATION OF NEUTRON STARS. Tsuruta, Sachiko (Smithsonian Astrophysical Observatory, Cambridge, Mass.); Cameron, A. G. W. Nature, 211: 356-7 (July 23, 1966).

A brief review of neutron star rotation hypotheses is presented. A plot is described of the ratio of the central to the mean proper energy density for the Tsuruta-Cameron neutron star model sequences characterized by the Levinger-Simmons potentials V_β and V_γ. Also given are the ratios of central to mean densities for various polytropic indices. It is concluded that there is no assurance that rotational flattening of a neutron star will be responsible for eliminating radial vibrational energy by providing a coupling to the quadrupole oscillation mode. (M.O.W.)

37364 UMBRA INTENSITY OF A LARGE SUNSPOT. Roedberg, Harald (Univ. of Oslo). Nature, 211: 394-5 (July 23, 1966).

The large sunspot which was visible March 15–27, 1966, was observed in several positions on the solar disk. Intensity profiles of the spot were obtained by a pinhole photometer in three wavelength regions. These measurements are discussed. (M.O.W.)

37365 EVIDENCE FOR A SOURCE OF PRIMARY GAMMA RAYS. Duthie, J. G.; Cobb, R.; Stewart, J. (Univ. of Rochester, N. Y.). Phys. Rev. Lett., 17: 263-7 (Aug. 1, 1966).

The existence of an anomalously high count of gamma rays from the direction of the constellation Cygnus is reported. This high count was associated with an energy spectrum which appears to differ significantly from the spectrum of secondary gamma rays generated by cosmic rays interacting in the atmosphere above the balloon-borne detection system. (B.G.D.)

37366 SOLAR NEUTRINOS. Bahcall, John N. (California Inst. of Technology, Pasadena). Phys. Rev. Lett., 17: 398-401(Aug. 15, 1966).

The predicted capture rate in the ^{37}Cl experiment for detecting solar neutrinos is calculated using the results of recent nuclear experiments and solar-model investigations. It is shown that additional experiments (e.g., with ^{2}H, ^{7}Li, ^{11}B, or ν-e scattering) are necessary to establish the relative contributions of the proton-proton chain and the CNO cycle to solar energy generation. (auth)

37367 RELATIVISTIC ASTROPHYSICS. Lasota, Jan Piotr (Univ., Warsaw). Postepy Fiz., 17: 281-315 (1966). (In Polish).

The principal problems of relativistic astrophysics and certain possible methods of solving them are described. A brief description is given of contemporary views on the evolution of stars from the moment of their origin. Particular attention is paid to the final stage of evolution. The classical theory of white dwarfs is presented. There also is a more detailed presentation of the problems of stability of systems in hydrostatic equilibrium. Following a short description of the process known as "neutronization" there is a discussion on the "singularity" of the Schwartzschild metric and the relativistic equations of hydrostatic equilibrium. The Oppenheimer and Volkoff solutions, which describe a star composed of ideal neutron gas, are presented. The results are given of trials of a more accurate description of the matter of dense stars. Owing to the more realistic approach to neutron gas (and barions in general) new interesting results have developed which bear influence on the theory of star evolution. The death of stars is next discussed. A description is presented of the process leading to creation of the white dwarf state and also the hypothetical reactions causing a supernova explosion. Finally, the problem of observation of neutron stars is discussed. The notions of maximum mass and critical mass are explained. A criterion for hydrostatic equilibrium is given for a certain class of equations of state. A qualitative description of the contraction process is given. It is based on the quantitative results of Oppenheimer and Snyder. There is also mention of the problem of discovering stars cut off from the Universe. (M.O.W.)

37368 MAGNETIC FIELDS IN THE GALAXY AS DEDUCED FROM RADIO MEASUREMENTS. Davies, R. D. (Nuffield Radio Astronomy Labs., Cheshire, Eng.). pp 35-9 of Proceedings of the Ninth International Conference on Cosmic Rays. Vol. I. Stickland, A. C. (ed.). London, The Institute of Physics and The Physical Society, 1966.

Synchrotron emission from relativistic electrons moving in the magnetic field of the galaxy provides information about the strength and distribution of galactic magnetic fields. The fields and cosmic rays are concentrated in the disk and weakly distributed in the galactic halo. The mean disk field is estimated as around 10^{-5} gauss if account is taken of the irregular distribution of synchrotron emission. The emission is linearly polarized in the vicinity of the sun indicating that the local field is directed towards $l^{II} = 50°$. Attempts to measure the Zeeman splitting of the narrow spectral features of neutral hydrogen have shown that the magnetic field inside interstellar clouds is less than 10^{-5} gauss. A new technique for studying the galactic magnetic field is provided by observations of the Faraday rotation in the galaxy of the polarized radiation of distant radio sources. The magnetic field in the local quadrant of the galaxy appears to be tangential to the radius vector from the galactic center. Its magnitude is estimated to be about 5×10^{-6} gauss. (auth)

37369 SOME ASPECTS OF ASTROPHYSICAL STUDIES BASED ON OBSERVATIONS OF ISOTOPIC CHANGES. Lal, D. (Tata Inst. of Fundamental Research, Bombay). pp 81-91 of Proceedings of the Ninth International Conference on Cosmic Rays. Vol. I. Stickland, A. C. (ed.). London, The Institute of Physics and The Physical Society, 1966.

Some special aspects of investigations based on studies of isotopic composition in terrestrial and extraterrestrial materials are reviewed. The discussions are confined to isotopic changes in materials caused by high energy nuclear active particles and solar wind in interplanetary space and on earth. Early irradiation history of the solar system, the origin of meteorites, the prehistory of cosmic radiation, the intensity of cosmic rays of solar origin and the influx of solar wind are examples of some of the astrophysical problems which are being attacked using the isotope method. Essentially the great triumph of studies of this type lies in the fact that prehistoric quantities can be evaluated—a point of great value in astrophysical studies. It seems obvious that as space technology advances and a greater variety of extraterrestrial samples can be obtained, for example material from the surface of the moon, the scope of the isotope method will be extended considerably. (auth)

37370 QUASI-STELLAR OBJECTS, RADIOGALAXIES AND THE ORIGIN OF COSMIC RAYS. Burbidge, E. M.; Burbidge, G. R. (Univ. of California, San Diego, La Jolla). pp 92-6 of Proceedings of the Ninth International Conference on Cosmic Rays. Vol. I. Stickland, A. C. (ed.). London, The Institute of Physics and The Physical Society, 1966.

A discussion is given of the properties of the quasi-stellar radio sources and quasi-stellar objects. The methods by which they can be identified and their spectroscopic properties are described. If these objects are at cosmological distances, as has commonly been supposed because of their large red shifts, then they form a population of exploding galaxies which probably contribute a significant flux of high energy particles to the intergalactic cosmic ray flux. The contribution is likely to be considerably greater than that estimated from the frequency of strong radio sources by one of us at the Jaipur meeting. If the objects are extragalactic but local (at distances of 1–10 Mparsec), as has recently been considered by Hoyle and Burbidge, then they will make a large contribution to the cosmic ray flux in the area of the local super-cluster. It is concluded that there are no serious objections to supposing that the cosmic ray flux outside the galaxy may be comparable with that inside the galaxy. (auth)

37371 PROTONS AND HELIUM NUCLEI WITHIN INTERPLANETARY MAGNETIC REGIONS WHICH CO-

ROTATE WITH THE SUN. Fan, C. Y.; Gloeckler, G.; Simpson, J. A. (Univ. of Chicago). pp 109-11 of Proceedings of the Ninth International Conference on Cosmic Rays. Vol. I. Stickland, A. C. (ed.). London, The Institute of Physics and The Physical Society, 1966.

From IMP-I measurements it was shown in 1964 that fluxes of protons of greater than 1 Mev energy appeared for several days in a sequence of six consecutive 27-day intervals. It was concluded that these protons were confined within a region co-rotating with the sun which modulates the galactic cosmic radiation at the orbit of earth with the same 27-day recurrence period. This region has persisted for more than 20 solar rotations and was observed with the IMP-I magnetometer by Ness and Wilcox to possess special characteristics. The energy spectrum of the protons in the leading and trailing sides of the co-rotating region was measured. A helium component continuously associated with the protons was found with an energy spectrum of the form proportional to E^{-2} Mev/nucleon in the energy range 2 to 30 Mev/nucleon. Evidence from the OGO-I satellite indicates that the proton and helium fluxes are not only present within co-rotating regions, but are also present at lower intensity and with different spectra at all times throughout a two and a half month period. The source for continual acceleration of these protons and helium nuclei is discussed. (auth)

37372 EFFECT OF COSMIC-RAY FRICTION ON THE SOLAR WIND. Axford, W. I.; Newman, R. C. (Cornell Univ., Ithaca, N. Y.). pp 173-5 of Proceedings of the Ninth International Conference on Cosmic Rays. Vol. I. Stickland, A. C. (ed.). London, The Institute of Physics and The Physical Society, 1966.

The results are presented of some model calculations which illustrate some of the effects of cosmic ray friction on the solar wind. It is shown that in some circumstances the mechanism might be important in limiting the extent of the solar wind cavity, thus supplementing the effect of the galactic magnetic field. However, if the radius of the cavity is as small as 15–20 A.U. some entirely different mechanism might have to be considered. (auth)

37373 SOLAR DAILY VARIATION RECORDED AT A LOW-LATITUDE STATION BY EAST AND WEST POINTING TELESCOPES DURING PERIODS OF MAXIMUM AND MINIMUM SOLAR ACTIVITY. Ahluwalia, H. S.; Escobar, V. I.; Zubieta, M.; Anda, R.; Schreier, M.; Troncoso, O. (Univ. Mayor de San Adnres, La Paz, Bolivia). pp 190-2 of Proceedings of the Ninth International Conference on Cosmic Rays. Vol. I. Stickland, A. C. (ed.). London, The Institute of Physics and The Physical Society, 1966.

The characteristics of the solar daily variations recorded by east and west pointing directional telescopes at Mt. Chacaltaya (altitude = 5200 m, geomagnetic latitude = −4.8°) during the years of maximum (1958) and minimum (1964) solar activity in the last solar cycle were examined. It was found that the amplitude of the diurnal component, both in the east as well as in the west direction, is lower in 1964 compared with its value in 1958. The time of maximum of the diurnal component in the two directions has, however, the same value in the two years within errors of observations. The results for the diurnal component are compared with those obtained with neutron monitors at the other equatorial mountain-level stations of Huancayo and Mt. Norikura for the same period as well as with the parameters defining the diurnal component at Huancayo in the years 1937 to 1954, as obtained by an ion chamber. It is concluded that the basic periodicity in the parameters defining the diurnal component of solar daily variation is one of 22 years rather than 11 years. (auth)

37374 INTERGALACTIC PHOTON DENSITY. Garmire, G. (Massachusetts Inst. of Tech., Cambridge). Contract NAS 5-3205. pp 315-17 of Proceedings of the Ninth International Conference on Cosmic Rays. Vol. I. Stickland, A. C. (ed.). London, The Institute of Physics and The Physical Society, 1966.

The intergalactic starlight photon density was estimated using several cosmological models and is found to be between about 0.002 and 0.007 ev cm^{-3}. This estimate is based on the luminosity function for galaxies obtained by Kiang, and Van den Bergh. The 3.5°K radiation from space obtained by Penzias and Wilson at 4080 Mc is shown not to produce a measurable flux of x rays from bright radio sources at the present level of x ray detector sensitivities. But in the future it may be possible to test for the presence of a 3.5°K energy density of 0.6 ev cm^{-3} through x ray measurements. (auth)

37375 FAST NEUTRONS OF SOLAR ORIGIN. Apparao, M. V. K. (Tata Inst. of Fundamental Research, Bombay); Daniel, R. R.; Vijayalakshmi, B.; Bhatt, V. L. pp 358-9 of Proceedings of the Ninth International Conference on Cosmic Rays. Vol. I. Stickland, A. C. (ed.). London, The Institute of Physics and The Physical Society, 1966.

An experiment was made to observe neutrons emitted by the sun using nuclear emulsion plates flown at an altitude of 10 mb by means of balloons over Hyderabad, India (geographic latitude 17.3°N and longitude 78.5°E), on 23rd March 1962. The neutrons were detected by observing the protons recoiling from elastic collisions of the neutrons with hydrogen nuclei in the nuclear emulsion. After correcting for various backgrounds, a residual flux of 147.6 ± 59.7 solar neutrons/m^2 sec sterad with energy between 20 and 160 Mev was observed. The balloon flight was made on a day when the sunspot number was at the peak of its 27-day variation. Furthermore, there was a visual solar flare of magnitude 3 a few hours before the balloon flight; it is possible that the neutron flux observed is associated with a disturbed region of the sun. (auth)

37376 CELESTIAL SOURCE OF X RAYS IN THE ENERGY RANGE 20 TO 58 kev. McCracken, K. G. (Southwest Center for Advanced Studies, Dallas). pp 449-52 of Proceedings of the Ninth International Conference on Cosmic Rays. Vol. I. Stickland, A. C. (ed.). London, The Institute of Physics and The Physical Society, 1966.

An experiment designed to search for celestial sources of x rays in the energy range 20–58 kev is described. A source of x rays was observed in the constellation Cygnus, and a tentative identification with Cygnus XR-1 is made. The x ray and radio data indicate that the spectrum of the Cygnus XR-1 source is significantly different from that of the x ray/radio emitter Taurus A. (auth)

37377 SOLAR NEUTRINOS. Kocharov, G. E. (Ioffe Inst. of Physics and Tech., Leningrad). pp 1020-2 of Proceedings of the Ninth International Conference on Cosmic Rays. Vol. 2. Stickland, A. C. (ed.). London, The Institute of Physics and The Physical Society, 1966.

Nuclear reactions in the stellar interiors over the temperature range $(5-30) \times 10^6$ deg K are considered. The probabilities of different proton-proton (p-p) chain reactions are calculated. The solar neutrino fluxes at the earth for the point source solar model are obtained. Experimental possibilities of detecting solar neutrinos are considered. (auth)

37378 NEUTRINO SPECTROSCOPY OF THE SUN. Kuzmin, V. A.; Zatsepin, G. T. (Lebedev Inst. of Physics, Moscow). pp 1023-4 of Proceedings of the Ninth International Conference on Cosmic Rays. Vol. 2. Stickland, A. C. (ed.). London, The Institute of Physics and The Physical Society, 1966.

The detection of the solar neutrino radiation is a rather effective way of studying the internal structure of the sun. For the derivation of internal structure parameters it is necessary to separate the contributions to effects observed at the earth induced by neutrinos from various reactions. To do this one needs to use a set of integral neutrino detectors with different threshold energies of differential detectors. The program of neutrino investigations with the set of the detectors ^{71}Ga, ^{71}Li and ^{37}Cl used in radiochemical methods similar to that of Pontecorvo-Davis, and detectors of electrons from the solar neutrino induced β processes on ^{2}H, ^{7}Li, etc. and/or recoil electrons in a neutrino-electron elastic scattering process is discussed. Detectors of the second type may permit separation of the ^{8}B and ^{3}He, p neutrino contributions. Detectors of the first group may be exploited to separate the ^{7}Be, pp and ^{13}N, ^{15}O neutrino con-

tributions. For the separation of the ^{13}N, ^{15}O neutrino contribution and for the determination of the CNO cycle role it was found reasonable to use a radiochemical method with ^{7}Li as a detector. The sequence of the experiment performance and the information obtained about the internal structure parameters of the sun are briefly discussed. (auth)

37379 EXPERIMENTAL POSSIBILITIES OF THE OBSERVATION OF NEUTRINOS FROM COLLAPSING STARS. Domogatskii, G. V.; Zatsepin, G. T. (Lebedev Inst. of Physics, Moscow). pp 1030-1 of Proceedings of the Ninth International Conference on Cosmic Rays. Vol. 2. Stickland, A. C. (ed.). London, The Institute of Physics and The Physical Society, 1966.

According to Zeldovich and Guseinov a collapsing star in the galaxy will give rise to $10^{11}-10^{13}$ neutrinos/cm^2 on the earth during a time period of $10^{-3}-10^{-2}$ sec. It should be possible to observe these neutrinos through the emission of electrons in β processes induced by them in detectors consisting of many tons of target material. (auth)

37380 THERMOMETRY OF THE SOLAR INTERIOR BY NEUTRINO EXPERIMENTS. Kuzmin, V. A. (Lebedev Inst. of Physics, Moscow). pp 1032-3 of Proceedings of the Ninth International Conference on Cosmic Rays. Vol. 2. Stickland, A. C. (ed.). London, The Institute of Physics and The Physical Society, 1966.

Possibilities for determining the temperature of the interior regions of the sun using high threshold (^{37}Cl, ^{7}Li, etc.) and low threshold (^{71}Ga) solar neutrino detectors are considered. The thermometry of the central solar regions can be carried out by the detection of ^{8}B neutrinos in the first case, and ^{7}Be neutrinos and ^{13}N, ^{15}O neutrinos in the second. It is found that on the basis of the results of the Davis experiment one can set an upper limit for the central temperature of the sun, namely $T_C \leq (18 \pm 2) \times 10^{6}$°K. Uncertainties in the fluxes and absorption cross sections of solar neutrinos and related limitations on the accuracy in determining the central solar temperature are discussed. It is shown that the accuracy of temperature estimation using the Pontecorvo-Davis method of neutrino detection is determined by uncertainties in the parameters of the nuclear reactions and the structure of the sun, and is about ±5% in the vicinity of $T_C \simeq 16 \times 10^{6}$°K. In the case of thermometry using ^{71}Ga there is a greater uncertainty in the neutrino absorption cross section, but the temperature dependence of the effect is less. (auth)

37381 REMARKS ON THE SYNCHROTRON RADIATION SPECTRUM OF THE CRAB NEBULA. Shklovskii, I. S. Soviet Astron. AJ (Engl. Transl.), 10: 6-8(July-Aug. 1966).

Translated from Astron. Zh., 43: 10-12(Jan.-Feb. 1966).

Arguments are advanced for a unified synchrotron spectrum for the Crab Nebula, extending from the radio to the x-ray range. The spectral index $\alpha \approx 0.8$ over the range $10^{12} < \nu < 3 \cdot 10^{16}$. The maximum at $\nu \approx 10^{12}$ cps arises from accumulation of relativistic electrons in the nebula. Relativistic electrons are permanently injected at a rate of $\approx 10^{38}$ erg/sec, and their energy-spectrum index $\gamma = 1.6$ for $10^{8} < E < 3 \cdot 10^{12}$ eV. Plasma oscillations in the injection region generate the low-frequency radiation of sources of small angular size. (auth)

37382 STATISTICAL PROPERTIES OF THE OPTICAL VARIABILITY OF THE QUASISTELLAR RADIO SOURCE 3C 273. Ozernoi, L. M.; Chertoprud, V. E. (Lebedev Inst. of Physics, Moscow). Soviet Astron. AJ (Engl. Transl.), 10: 15-25(July-Aug. 1966).

Translated from Astron. Zh., 43: 20-33(Jan.-Feb. 1966).

A statistical reduction was made for observations of cyclical light variations in the quasistellar radio source 3C 273. Analysis of the random departures of the signal from the statistical mean yields parameters for the system expressed by the simple vibration equation with one degree of freedom. The dynamical period $T \approx 9$ yr; the mean rigidity, characterizing the asymptotic stability of the limiting cycle, is $\tilde{N} \approx 1$ yr^{-1}. The material available reveals no effect of synchronism. The phase dispersion increases with time by the diffusion law. The random velocity component, according to the limiting cycle, approximates the regular component. The chief models for the central region of a quasistellar source, in which the cyclic flux variations are discussed, are analyzed from the viewpoint of requirements for a variability mechanism. Preliminary considerations favor an oscillatory model — in particular, circulatory motion in a magnetoid. (auth)

37383 CRITICAL MASS OF A HOT ISOTHERMAL WHITE DWARF WITH GENERAL RELATIVISTIC EFFECTS TAKEN INTO ACCOUNT. Bisnovatyi-Kogan, G. S. Soviet Astron. AJ (Engl. Transl.), 10: 69-74(July-Aug. 1966).

Translated from Astron. Zh., 43: 89-95(Jan.-Feb. 1966).

The critical mass of a hot isothermal white dwarf was determined taking into account general relativistic effects. The thermodynamic functions of matter in a white dwarf near the critical point are discussed. The equilibrium equation and other relations for the critical state of a hot white dwarf are found by an energy method which is asymptotically exact in the given case. The solution of these equations is given in the form of graphs of $\rho_{cr}(T_{cr})$, $T_{cr}(M)$, $\rho_{cr}(M)$. The evolutionary tracks of stars with masses of $1.19M_{\odot}$, $1.20M_{\odot}$, and $1.36M_{\odot}$ immediately before the onset of instability or complete cooling are obtained. (auth)

37384 VARIATION OF THE MOMENT OF INERTIA OF A STAR DURING ACCRETION. Doroshkevich, A. G. Soviet Astron. AJ (Engl. Transl.), 10: 83-4(July-Aug. 1966).

Translated from Astron. Zh., 43: 105-7(Jan.-Feb. 1966).

It is shown that due to the effects of the general theory of relativity the moment of inertia of a rotating star decreases during accretion. The rate of decrease is computed and found to be very rapid for a collapsing star. The effect is absent in Newton's theory. (auth)

37385 SOME PROPERTIES OF THE PHASE OF SOLAR ACTIVITY. Gudzenko, L. I.; Chertoprud, V. E. (Lebedev Inst. of Physics, Moscow). Soviet Astron. AJ (Engl. Transl.), 10: 89-96(July-Aug. 1966).

Translated from Astron. Zh., 43: 113-23(Jan.-Feb. 1966).

An analysis of the statistical properties of the phase of solar activity leads to the conclusion that the changes of solar activity are caused by an autonomous generator with one degree of freedom, synchronized with a weak periodic force. (auth)

37386 COMETS IN THE SOLAR WIND. Ioffe, Z. M. (Gorkii State Univ., USSR). Soviet Astron. AJ (Engl. Transl.), 10: 138-42(July-Aug. 1966).

Translated from Astron. Zh., 43: 175-80(Jan.-Feb. 1966).

A comet nucleus is treated as a source, in the hydrodynamic sense, located in a supersonic, stationary, solar plasma stream. Newton's formula yields the pressure at the source-stream interface. The plasma-head configuration and the cylindrical shape of a type I tail can be explained. The recession distance of the shock wave is estimated by comparison with the solution for a source in an incompressible medium. (auth)

37387 DISCONTINUITIES IN THE SOLAR WIND. Colburn, D. S.; Sonett, C. P. (Ames Research Center, Moffett Field, Calif.). Space Sci. Rev., 5: 439-506(June 1966).

The nonuniform emission of the solar wind from the sun means that conditions are established which favor the development of discontinuities in the plasma parameters. Since the solar wind is in rapid proper motion with respect to the sun and the earth, examination of these discontinuities requires that the wind velocity be transformed away. Then it is found that they satisfy the conditions of magnetohydrodynamics and can be treated as shock waves and the stationary contact surfaces consisting of either tangential or contact discontinuities. The collision-free structure of the solar wind suggests that the tangential

discontinuity is the more likely contact surface as it is more capable of inhibiting diffusion which is required for a lifetime sufficient for the structure to be carried to the neighborhood of the earth. Either the shock wave or the contact surface can create signals that are detectable at the surface of the earth. The simplest surface signal to detect is the sudden impulse (SI) but other signals may be found. The existence of a field of MHD discontinuities in the solar wind should make possible the generation of ensembles of shocks and contact surfaces. Various possibilities are explored and these are discussed from the standpoint of combinations of sudden impulses at the earth's surface which are both positive and negative. Some of these are recurrent with a 27-day period; the interplanetary M region shock ensemble associated with this is discussed and the development of these structures in space is reviewed. Lastly, observational evidence for interplanetary shock waves is given, together with the analytic technique for establishing their geometry and comparing the derived and measured jump parameters. The applicability of the geometrical construction of the general class of MHD discontinuity to their analysis is indicated and shows the way in which the structural content of the solar wind can be classified by the use of magnetometers and plasma probes. A parametric study of the jump conditions through a shock wave can be used to verify the correctness of field measurements because of the redundancy in measurements. This also allows the details of shock structure to be examined including the intrinsic partitioning of the internal energy of the shocked plasma. (auth)

37388 ORIGIN OF COSMIC RAYS. Ginzburg, V. L.; Syrovatskii, S. I. (Lebedeva Inst. of Physics, Moscow). Usp. Fiz. Nauk, 88: 485-504(Mar. 1966). (In Russian).

It is argued that cosmic rays cannot be of metagalactic origin and that plasma effects are of fundamental importance to the further development of the astrophysics of cosmic rays; this also pertains to the quasars. According to the authors, the principal sources of cosmic rays in the Galaxy are the bursts of supernovae and possibly also explosions of the galactic nucleus. Emphasis is placed on the role of instability in the formation of the boundary of the galactic halo and in the isotropicization of the cosmic rays emerging from the Galaxy into the Metagalaxy. Allowance is made for the new knowledge that was gained following the Jaipur Conference on Cosmic Rays in 1963. The Ninth International Conference on Cosmic Rays held in London (September 1965) is critically evaluated; at this conference no new proofs in favor of the theory of the metagalactic origin of galactic cosmic rays—unless the highest energies are concerned—were presented. It is shown that studies of the electron spectrum provide a means of verifying the hypothesis that a large part of cosmic rays (or more exactly, their electron component) is generated during powerful explosions of the galactic nucleus. Any proofs refuting this hypothesis would serve as a strong argument in favor of the local metagalactic theory of the origin of cosmic rays, but no such proofs have yet been presented; nevertheless, this theory merits further discussion. (auth)

37389 DYNAMICS OF THE SOLAR ATMOSPHERE. Pikel'ner, S. B. Usp. Fiz. Nauk, 88: 505-26(Mar. 1966). (In Russian).

Small periodic vertical motions in the photosphere and horizontal motions in large nucleus-like formations were observed on the solar surface. Large motions occur in meridional circulations and in differential rotation where the angular velocity increases from the poles to the equator. Motions in the photosphere create waves whose energy dissipates. Those waves deliver little energy by radiation and heat the upper layers causing the high coronal temperature. The coronal heat generates the solar wind or outflow of ionized gas. Deviations from thermodynamic equilibrium are caused by the emanation of thermal and mechanical energy from the photosphere. Studying the convective motions in the solar atmosphere facilitates understanding of stellar atmospheric phenomena. The transformation of radiative solar energy into mechanical energy causes convection. Convective instability occurs in layers of ionized hydrogen in which the logarithmic gradient of radiation is greater than the algebraic one. Granules are not caused by convection; their mean size is about 700 km and their lifetime is about 8 to 10 minutes. Bright granules move upward and the maximum speed is attained 40 seconds after the maximum brightness. The period of upward motion is 2.5 minutes. Very large granules have horizontal motions and are found deeper than normal granulation. The horizontal motion in large granules, or supergranules, may be caused by the magnetic field. In addition to convective motions, a regular solar motion covers large areas of the surface. This motion consists of the differential rotation and the meridional circulation. The motion in the solar atmosphere is also caused by its magnetic field. A strong magnetic field exists in sunspot groups where individual spots have their own polarities. The spot polarities of the solar Northern Hemisphere are opposite to those of the Southern Hemisphere; but the polarities are reversed in both hemispheres at the beginning of a new solar activity cycle. Before the magnetic field appears on the surface, action motions take place in the solar photosphere. Outside magnetically-active regions a weak magnetic field covers the whole solar surface. This field is stronger in near-polar regions and polarities are opposite in each hemisphere. In the period of maximum solar activity the increased polar field reverses polarity. Active belts and bipolar regions in the North and South may be explained by a toroidal field beneath the solar surface. Convective motions in the solar atmosphere create waves of a different kind which dissipate in the solar atmosphere and heat the chromosphere and the corona. There are accelerated and decelerated magnetic sound waves, Alfven's waves, and inner gravitational waves. Alfven's waves are predominant in the chromosphere, especially above the active regions. Acoustic waves are generated with isotropic turbulence and very small Mach numbers. The bremsstrahlung of relativistic electrons generates X and gamma radiation. The cosmic-ray pressure creates bursts and ejections of gases with velocities up to 1500 km/sec. The shock wave propagated in the corona generates plasma waves which are transformed into electromagnetic waves. Relativistic electrons behind the shock wave create magnetic bremsstrahlung. (M.O.W.)

37390 STELLAR EVOLUTION. Proceedings of an International Conference, November 13–15, 1963, Sponsored by the Institute for Space Studies of the Goddard Space Flight Center, NASA. Stein, R. F.; Cameron, A. G. W. (eds.). New York, Plenum Press, 1966. 475p. $19.50. (CONF-631114).

Separate abstracts were prepared for the 40 included papers. (M.O.W.)

For abstracts of individual papers see: 37391–37429 and 37491.

37391 STELLAR EVOLUTION: A SURVEY WITH ANALYTIC MODELS. Stein, Robert F. (Goddard Space Flight Center, New York). pp 3-79 of Stellar Evolution. Stein, R. F.; Cameron, A. G. W. (eds.). New York, Plenum Press, 1966.

The general properties of stellar structure and evolution are discussed, and then analytic models are constructed for the early homogeneous and advanced inhomogeneous stages of evolution. (M.O.W.)

37392 NUCLEAR ENERGY GENERATION IN STARS, AND SOME ASPECTS OF NUCLEOSYNTHESIS. Reeves, Hubert (Univ. of Montreal). pp 83-122 of Stellar Evolution. Stein, R. F.; Cameron, A. G. W. (eds.). New York, Plenum Press, 1966.

Formulas are described for the energy generation rate for each stage of stellar evolution. The uncertainties (uncertainties issuing both from the nuclear physics aspects of the problem and from possible variations in the chemical composition of the reacting material) attached to each formula are discussed. The errors introduced in the analysis of stellar evolution are described when some minor nuclear reactions are neglected. (M.O.W.)

37393 RADIATIVE ABSORPTION AND OPACITY CALCULATIONS. Cox, Arthur N. (Los Alamos Scientific Lab., N. Mex.). pp 123-42 of Stellar Evolution. Stein, R. F.; Cameron, A. G. W. (eds.). New York, Plenum Press, 1966.

An investigation was made for applying absorption coefficients and opacities to stellar atmosphere and interior structure calculations. Methods for calculating the photon absorption and emission by matter are described. Typical data taken from the Aller mixture are presented. (M.O.W.)

37394 ENERGY TRANSPORT BY TURBULENT CONVECTION. Spiegel, Edward A. (New York Univ., New York). pp 143-73 of Stellar Evolution. Stein, R. F.; Cameron, A. G. W. (eds.). New York, Plenum Press, 1966.

An analysis was made to describe the convective heat flux through each layer of a star. Theories are presented for the thermal convection and the dynamics of turbulent convection. (M.O.W.)

37395 NEUTRINOS IN ASTROPHYSICS. Chiu, Hong-Yee (Goddard Space Flight Center, New York). pp 175-90 of Stellar Evolution. Stein, R. F.; Cameron, A. G. W. (eds.). New York, Plenum Press, 1966.

All neutrino processes known to the author are summarized. The combined rates for a wide temperature and density regime are listed. A graph is given of the temperature dependence of the combined rates for a number of densities and also the density dependence for a number of temperatures. (M.O.W.)

37396 CONTRACTING STARS. Hayashi, Chushiro (Kyoto Univ.). pp 193-201 of Stellar Evolution. Stein, R. F.; Cameron, A. G. W. (eds.). New York, Plenum Press, 1966.

Analytical models describing the internal and external properties of expanding stars are described. The depletion of deuterium and lithium during the contraction is discussed. (M.O.W.)

37397 CONTRACTION PHASE OF SOLAR EVOLUTION. Ezer, D.; Cameron, A. G. W. (Goddard Space Flight Center, New York). pp 203-8 of Stellar Evolution. Stein, R. F.; Cameron, A. G. W. (eds.). New York, Plenum Press, 1966.

The Henyey method for calculating stellar evolutionary tracks was used to follow the gravitational contraction of a star of one solar mass. The contraction phase of the evolution of the sun is described. (M.O.W.)

37398 SCHEMATIC PRE-MAIN-SEQUENCE EVOLUTION. von Sengbusch, K. (Max-Planck-Institut, Munich); Temesvary, S. pp 209-13 of Stellar Evolution. Stein, R. F.; Cameron, A. G. W. (eds.). New York, Plenum Press, 1966.

A description is given of the increase in mass inside the photosphere by the accretion formula of Bondi, for a star which is at rest in an interstellar cloud of homogeneous temperature T_a and density P_a. (M.O.W.)

37399 ROLE OF MAGNETIC ACTIVITY DURING STELLAR FORMATION. Schatzmann, E. (Institut d'Astrophysique, Paris). pp 215-18 of Stellar Evolution. Stein, R. F.; Cameron, A. G. W. (eds.). New York, Plenum Press, 1966.

The two problems concerned with the effect of electromagnetic activity during the end phase of stellar formation are discussed. These are the angular momentum of the stars and the problem of surface nuclear reactions. (M.O.W.)

37400 CALCULATIONS OF MAIN-SEQUENCE STELLAR MODELS. Reiz, Anders; Petersen, Joergen Otzen (Univ., Copenhagen). pp 221-9 of Stellar Evolution. Stein, R. F.; Cameron, A. G. W. (eds.). New York, Plenum Press, 1966.

Calculational techniques for the evolution of stars in the main-sequence band are described. Calculations were performed for population I stars of 6, 10, and 15 solar masses and age-zero composition X = 0.70, Y = 0.27, and Z = 0.03. These calculations are presented. (M.O.W.)

37401 EVOLUTION OF STARS NEAR ONE SOLAR MASS. Demarque, Pierre (Univ. of Toronto). pp 231-6 of Stellar Evolution. Stein, R. F.; Cameron, A. G. W. (eds.). New York, Plenum Press, 1966.

Several evolutionary models are described for stars near one solar mass using the general method of computation developed by Henyey. Evolutionary tracks for masses around one solar mass with high and low metal contents are discussed in an attempt to determine the ages of NGC 188 and the globular clusters. (M.O.W.)

37402 EARLY EVOLUTION OF STARS BETWEEN ONE AND THREE SOLAR MASSES. Iben, I. Jr. (Massachusetts Inst. of Tech., Cambridge). pp 237-40 of Stellar Evolution. Stein, R. F.; Cameron, A. G. W. (eds.). New York, Plenum Press, 1966.

The evolution of stars between 1 and 3 $M_\odot$ was investigated, with particular attention given to details of the nuclear reactions and to changes in the chemical composition. An evolutionary sequence of models is begun, for convenience, with the fully convective stage of gravitational contraction. The original composition is taken to be X = 0.64, Y = 0.326, and Z = 0.034. Of the heavy elements, ^{16}O represents 40%, ^{12}C and ^{14}N represent 12.5%. ^3He is taken to be initially zero. The changes in ^1H, ^3He, ^4He, ^{12}C, ^{14}N, and ^{16}O concentrations are followed in detail. Convection zones are calculated with mixing length equal to one-half the density scale height. (M.O.W.)

37403 SOLAR MODELS AND NEUTRINO FLUXES. Sears, R. L. (W. K. Kellogg Radiation Lab., Pasadena, Calif.). pp 245-9 of Stellar Evolution. Stein, R. F.; Cameron, A. G. W. (eds.). New York, Plenum Press, 1966.

Calculations of the expected neutrino flux from the sun, based on models of the solar interior, are presented. The range of neutrino fluxes corresponding to the range of uncertainties in the solar models is described. (M.O.W.)

37404 ADVANCED STAGES OF STELLAR EVOLUTION. Hayashi, Chushiro (Kyoto Univ.). pp 253-62 of Stellar Evolution. Stein, R. F.; Cameron, A. G. W. (eds.). New York, Plenum Press, 1966.

In order to obtain an overall point of view on the advanced stages of stellar evolution, i.e., helium burning and carbon burning, calculations were made for stars of solar mass 15M, 4M, and 0.7M. The basic assumptions used in the calculations are (1) a single star with spherical symmetric distribution of matter, (2) no mixing of chemical composition except in the convective regions, and (3) no mass loss except for possible explosive stages. The essential parameters are the stellar mass and the original chemical composition, which is assumed to be uniform. (M.O.W.)

37405 EVOLUTION OF A STAR OF SEVEN SOLAR MASSES. Hofmeister, E.; Kippenhahn, R.; Weigert, A. (Max-Planck-Institut, Munich). pp 263-77 of Stellar Evolution. Stein, R. F.; Cameron, A. G. W. (eds.). New York, Plenum Press, 1966.

The Henyey method was used to construct a series of evolutionary models for a 7M star. The outer convection zone was calculated using the mixing-length theory with $l/H_p = 1.5$. Four opacity tables were used, one for the outer layers with the original composition and three for the inner layers with three basic compositions. The equation of state included the perfect gas pressure, the radiation pressure, and the degenerate electron pressure for degeneracy parameters larger than −4. For helium-burning, only the $3\alpha \rightarrow {}^{12}C$ reaction was included: the further burning of carbon into oxygen was neglected. The star was taken to have an extreme population I composition. X = 0.602 and Z = 0.044. (M.O.W.)

37406 PRE-SUPERNOVA EVOLUTION (NEUTRINO STARS). Chiu, Hong-Yee (Goddard Space Flight Center, New York). pp 279-89 of Stellar Evolution. Stein, R. F.; Cameron, A. G. W. (eds.). New York, Plenum Press, 1966.

It is shown that the classical homology hypothesis $\rho \sim T^3$ is completely inapplicable to the evolution of stars whose temperatures are over $10^{8\cdot5}$K, where neutrino processes

dominate over photon processes. Instead, neutrino stars evolve with $\rho_c \sim T_c^8$ during gravitational contraction, while during nuclear burning they evolve along the n-v-zero curves which lead any star to a region of very high density. After the exhaustion of nuclear fuel, the central temperature will again increase. The final collapse of all neutrino stars into supernova will probably occur at a density of around 10^{9-10} g/cm^3 and at a temperature around 3 to 4 × 10^{9}°K. (M.O.W.)

37407 MECHANISM OF TYPE II SUPERNOVA EXPLOSIONS. Colgate, Stirling A. (New Mexico Inst. of Mining and Tech., Socorro); White, Richard H. pp 291-301 of Stellar Evolution. Stein, R. F.; Cameron, A. G. W. (eds.). New York, Plenum Press, 1966.

The evolution processes of a pre-supernova star of 10M are discussed. The emission of thermal neutrinos from the high-temperature core shock wave is described. (M.O.W.)

37408 COOLING OF WHITE DWARFS. Savedoff, M. P. (Univ. of Rochester, N. Y.). pp 303-6 of Stellar Evolution. Stein, R. F.; Cameron, A. G. W. (eds.). New York, Plenum Press, 1966.

A brief review is presented of Schwarzschild's calculations for the evolution of white dwarfs. Age calculations were made with respect to Sirius A and Sirius B. (M.O.W.)

37409 FORMATION OF HELIUM IN THE GALAXY. Truran, J. W. (Yale Univ., New Haven); Hansen, C. J.; Cameron, A. G. W. pp 307-16 of Stellar Evolution. Stein, R. F.; Cameron, A. G. W. (eds.). New York, Plenum Press, 1966.

A study was made to determine whether the high helium content of the sun and the O and B stars might result from stellar evolution starting with a pure-hydrogen galaxie. The many uncertainties in the study are pointed out. (M.O.W.)

37410 STELLAR EVOLUTION WITH VARYING G. Dicke, R. H. (Princeton Univ., N. J.). pp 319-29 of Stellar Evolution. Stein, R. F.; Cameron, A. G. W. (eds.). New York, Plenum Press, 1966.

The discrepancies of various theories for determining the age of our galaxy are discussed. The discussion centers on the Hubble red-shift data, the high velocities of population II stars, $^{235}U/^{238}U$ abundance ratio, and the nearly uniform heavy-element abundance in the population I stars. (M.O.W.)

37411 SIMPLIFIED MODELS FOR CEPHEID INSTABILITY. Baker, Norman (Columbia Univ., New York). pp 333-46 of Stellar Evolution. Stein, R. F.; Cameron, A. G. W. (eds.). New York, Plenum Press, 1966.

A general formulation for studying stellar pulsations is described. Discussions are presented on the one-zone model, stability criteria, saturation effect, eigenvalues, depth dependence of the nonadiabatic effects, and the disturbed model. (M.O.W.)

37412 EXCITATION AND GROWTH OF RADIAL PULSATIONS. Cox, J. P. (Joint Inst. for Laboratory Astrophysics, Boulder, Colo.). pp 347-57 of Stellar Evolution. Stein, R. F.; Cameron, A. G. W. (eds.). New York, Plenum Press, 1966.

The physics of the operation of the destabilization mechanism of second helium-ionization was studied using a hydrodynamic code for solving the complete set of nonlinear, nonadiabatic pulsation equations. A stellar model is followed in the course of time, using realistic equations of state and opacities. The basic purpose of these calculations was twofold: (1) to check the linearized calculations that were carried out on stellar pulsations to see if the mechanism of second helium-ionization will really work; and (2) to study certain nonlinear effects such as limiting amplitude, light and velocity curves, etc., of pulsating stars. (M.O.W.)

37413 STELLAR VARIABILITY. Christy, R. F. (California Inst. of Tech., Pasadena). pp 359-69 of Stellar Evolution. Stein, R. F.; Cameron, A. G. W. (eds.). New York, Plenum Press, 1966.

The calculation of the motion of the envelope is performed omitting the core of the star where nuclear-energy generation occurs. The general idea behind these calculations is that the observed pulsation motions of stars arise spontaneously because of the particular physical properties of the envelopes. The relevant physical properties are the equation of state and the opacity. The approach is to integrate numerically the time dependent equations of hydrodynamics and heat flow. Large-amplitude oscillations and their nonlinear effects are studied. (M.O.W.)

37414 T TAURI MASS EJECTION. Kuhi, L. V. (Mt. Wilson and Palomar Observatories, Pasadena, Calif.). pp 373-6 of Stellar Evolution. Stein, R. F.; Cameron, A. G. W. (eds.). New York, Plenum Press, 1966.

The emission spectra from T Tauri stars are briefly discussed. A brief analysis is given for describing the mass loss from the stars. (M.O.W.)

37415 MASS LOSS FROM RED GIANTS. Deutsch, Armin J. (Mt. Wilson and Palomar Observatories, Pasadena, Calif.). pp 377-80 of Stellar Evolution. Stein, R. F.; Cameron, A. G. W. (eds.). New York, Plenum Press, 1966.

Spectroscopic observations of red giants seemed to indicate that a giant M star is surrounded by gas which is seen to rise slowly, and which must then fall back to the star in an observable state of ionization. The amount of mass losses is described with respect to evolutionary requirements. (M.O.W.)

37416 MASS LOSS IN THE PLANETARY NEBULA STAGE. Osterbrock, D. E. (Univ. of Wisconsin, Madison). pp 381-7 of Stellar Evolution. Stein, R. F.; Cameron, A. G. W. (eds.). New York, Plenum Press, 1966.

A summary is given of observational mass loss data from planetary nebulae. The physical picture is that all planetary nebulae are assumed to be objects of the same kind, and in particular it is assumed that the shells all have essentially the same mass. It is further assumed that the shell is expanding or coasting into the vacuum with a constant velocity. (M.O.W.)

37417 AGE DETERMINATION FOR MAIN-SEQUENCE B, A, AND F STARS. Stroemgren, B. G. (Inst. for Advanced Study, Princeton, N. J.). pp 391-4 of Stellar Evolution. Stein, R. F.; Cameron, A. G. W. (eds.). New York, Plenum Press, 1966.

The age of a star can be determined from its precise location in the H-R diagram. The technique for this age determination is briefly outlined. The technique was applied to the Hyades stars in the upper half of the main-sequence band. The results are described. (M.O.W.)

37418 PHOTOMETRY OF B STARS. Crawford, D. L. (Kitt Peak National Observatory, Tucson, Ariz.). pp 395-8 of Stellar Evolution. Stein, R. F.; Cameron, A. G. W. (eds.). New York, Plenum Press, 1966.

One photometric method of locating B-type stars is to measure the Balmer discontinuity and an $H\beta$ index. Diagrams showing measurements of this type are described. (M.O.W.)

37419 ANALYSIS OF FIELD HORIZONTAL-BRANCH AND RR LYRAE STARS. Oke, J. B. (California Inst. of Tech., Pasadena); Greenstein, J. L.; Gunn, J. pp 399-403 of Stellar Evolution. Stein, R. F.; Cameron, A. G. W. (eds.). New York, Plenum Press, 1966.

A discussion is presented on stars which are similar to those found on the horizontal branch of globular clusters. It is confined to stars which are very near or within the variable-star gap. Mass losses, temperatures, and chemical abundances are briefly discussed. (M.O.W.)

37420 ULTRAVIOLET EXCESS IN T TAURI STARS. Walker, Merle F. (Lick Observatory, Mt. Hamilton, Calif.). pp 405-9 of Stellar Evolution. Stein, R. F.; Cameron, A. G. W. (eds.). New York, Plenum Press, 1966.

It is noted that among the group of T Tauri stars contracting toward the main sequence, there are a number which have ultraviolet excess. The spectra from these stars are briefly described. (M.O.W.)

37421 LITHIUM IN MAIN-SEQUENCE STARS. Herbig, G. H. (Lick Observatory, Mt. Hamilton, Calif.). pp 411-15 of Stellar Evolution. Stein, R. F.; Cameron, A. G. W. (eds.). New York, Plenum Press, 1966.

The question as to what happens to the lithium after the T Tauri stars eventually arrive on the main sequence at intermediate masses is discussed. Data are given which suggest that there is a progressive destruction of lithium with time, at least in early G-type stars. (M.O.W.)

37422 RECENT ABUNDANCE DETERMINATIONS. Helfer, H. L. (Univ. of Rochester, N. Y.). pp 417-18 of Stellar Evolution. Stein, R. F.; Cameron, A. G. W. (eds.). New York, Plenum Press, 1966.

A list of abundance determinations is given for 5 groups of stars. The list includes the following ratios: Fe/H, α/Fe, Mg/Ca, Sc/Ca, Mn/Fe, e/Fe, and Ba/Fe (α refers to the elements Mg, Si, S, Ar, K, Ca, and Ti and e refers to the equilibrium-process elements near iron). (M.O.W.)

37423 TRANSPORT OF s-PROCESS ELEMENTS TO THE SURFACES OF STARS. Peterson, Vern L. (National Bureau of Standards, Boulder, Colo.); Wrubel, Marshal H. pp 419-23 of Stellar Evolution. Stein, R. F.; Cameron, A. G. W. (eds.). New York, Plenum Press, 1966.

The s process is a neutron-addition process. A nucleus of atomic number Z absorbs neutrons on a slow time scale, forming isotopes with larger and larger numbers of neutrons until, through a rapid β decay, it becomes an isotope of the element Z + 1. The movement of these nuclei to the surfaces of stars is briefly discussed. (M.O.W.)

37424 CH STARS AND NEUTRON-ADDITION PROCESSES. Wallerstein, G. (Univ. of California, Berkeley); Greenstein, J. L. pp 425-30 of Stellar Evolution. Stein, R. F.; Cameron, A. G. W. (eds.). New York, Plenum Press, 1966.

CH stars were investigated using Palomar spectra at dispersions from 6.7 to 13.5 Å/mm. The spectra of four stars in the yellow region are described. An abundance analysis was made by the curve of growth method using ϵ Virginis, of type G8III, as the standard star. The production of these abundances is discussed. (M.O.W.)

37425 ABUNDANCE DIFFERENCES AMONG POPULATION I STARS. Pagel, B. E. J. (Royal Greenwich Observatory, Herstmonceaux Castle, Eng.). pp 431-6 of Stellar Evolution. Stein, R. F.; Cameron, A. G. W. (eds.). New York, Plenum Press, 1966.

Some abundance features of the late-type stars of population I are discussed. These features confirm earlier conclusions by Wallerstein and by Eggen, Lynden-Bell, and Sandage, from observations of stars of earlier type with ultraviolet excess. The conclusions are: (1) increasing metal deficiency is correlated with increasing dispersion in velocity (W) perpendicular to the galactic plane; in the plane, stars with a large orbital eccentricity are mildly deficient in metals, but the converse does not always hold. (2) Individual abundances of different metals show no correlation with anything, except perhaps luminosity. (M.O.W.)

37426 ELEMENT ABUNDANCES IN THE PECULIAR A STARS. Bidelman, William P. (Univ. of Michigan, Ann Arbor). pp 437-8 of Stellar Evolution. Stein, R. F.; Cameron, A. G. W. (eds.). New York, Plenum Press, 1966.

A discussion is presented on two varieties of stars in which certain elements are definitely very overabundant. Abundance determinations were made for a considerable number of peculiar A stars. Included is a very rough summary of some of the more remarkable results obtained. (M.O.W.)

37427 STELLAR GROUPS AND THE MASS-LUMINOSITY RELATION. Eggen, Olin J. (Royal Greenwich Observatory, Herstmonceaux Castle, Eng.). pp 439-44 of Stellar Evolution. Stein, R. F.; Cameron, A. G. W. (eds.). New York, Plenum Press, 1966.

There are two lines of evidence that point to a separation of the disk stars, within about 200 parsecs of the sun, into two kinds: (a) those which have a chemical composition (H, He, Fe) like that of the Hyades and Pleiades clusters, and which may have beem formed from the same gas cloud within the last few times 10^8 years; and (b) those with only approximately half the helium content of the Hyades stars, and probably formed at distances of greater than 10 kiloparsecs from the galactic center. The kinematic evidence, chemical composition, and solar motion of these stars are described. (M.O.W.)

37428 COMPOSITION DIFFERENCES BETWEEN THE GALAXY AND THE MAGELLANIC CLOUDS. Aller, L. H. (Univ. of California, Los Angeles). pp 445-7 of Stellar Evolution. Stein, R. F.; Cameron, A. G. W. (eds.). New York, Plenum Press, 1966.

The gaseous nebulae were used to determine chemical compositions in the Magellanic Clouds. Abundance analyses were performed for about 40 emission nebulosities in the large cloud and for about 15 or 20 in the small cloud. A brief discussion of the hydrogen and oxygen results is presented. (M.O.W.)

37429 EVOLUTIONARY-SIGNIFICANT GROUP OF ECLIPSING VARIABLES. Sahade, Jorge (Observatorio Astronomico, La Plata, Argentina). pp 449-52 of Stellar Evolution. Stein, R. F.; Cameron, A. G. W. (eds.). New York, Plenum Press, 1966.

The investigation of close binary systems has disclosed the existence of several groups among them that must be significant from the point of view of their evolution. The binaries with a WR or an OF component are discussed. Also systems with underluminous, massive components are discussed. (M.O.W.)

37430 SO(3,R)-HOMOGENEOUS COSMOLOGIES. Shepley, Lawrence Charles. Princeton, N. J., Princeton Univ., 1965. 245p.

Thesis.

Do all cosmological models in general relativity develop singularities? This question is examined for the special case of a model universe invariant under the isometry group SO(3,R). The methods of modern differential geometry employed are presented in some detail. The Cartan structural equations are derived. The Einstein field equations show that each dust-filled universe with the SO(3,R) symmetry develops a singularity. The SO(3,R) symmetry picks out "invariant hypersurfaces" in an SO(3,R)-homogeneous universe. These three-dimensional subsets are submanifolds on which the metric is the same everywhere. A one-parameter family of these subsurfaces fill the manifold. The surfaces are labeled by t; one such invariant subspace is called H(t). The metric of $H(t_0)$ is presumed to be spacelike for an initial time t_0. It is shown that the geometry of H(t) must change from spacelike to lightlike in a finite proper time. It is then shown that the manifold cannot be extended past the time when H(t) becomes lightlike. The proof shows that a lightlike H(t) is inconsistent with a nonzero matter density of dust-like particles. Hence a singularity must appear. The definition of singularity itself and the relationship between non-singularity and completeness are discussed. Two especially important solutions of Einstein's equations are examined, the Gödel universe and T-NUT-M space. The equations of an SO(3,R)-homogeneous dust-filled model universe were cast in a form suitable for numerical integration. Several computed models were found. Some exhibit matter that rotates extremely quickly. Some of these show, in addition, the property that the matter density ρ fluctuates with time. All models exhibit the collapse of the volume of spacelike surfaces which heralds the approach of a singularity. (TCO)

Atomic Physics

Refer also to abstracts 37750, 37777, and 38058.

37431 (INDEC-SR-7, pp 3,76-111) MODELS FOR ELECTRON EMISSION FROM METALS WITH ADSORBED MONOLAYERS. Kaplit, M.; Schrenk, G. L. (Pennsylvania Univ., Philadelphia. Inst. for Direct Energy Conversion).

The ability of a semi-classical model to describe a metal-gas interface was investigated theoretically, and the differences between various macroscopic models is discussed. Using the Thomas-Fermi-Dirac theory, both the microscopic charge distribution and the total electronic energy of the interface were evaluated in such a way that one can distinguish between the classical and quantum mechanical contributions. It was shown that the quantum mechanical corrections are a significant part of the total energy and may may not be neglected. It is concluded that a semi-classical model, using only the concepts of classical atomic physics, is not an adequate representation of the electronic properties of alkali-refractory metal or alkali earth-refractory metal interfaces. Detailed results for both cesium and barium adsorption on (100) and (110) faces of tungsten are presented. (auth)

37432 FORBIDDEN TRANSITIONS IN ATOMIC SYSTEMS, INFLUENCED BY HOMOGENEOUS AND ELECTRIC INTERMOLECULAR FIELDS IN THE PLASMA. Grechikhin, L. I. (Inst. of Physics, Academy of Sciences, BSSR). Dokl. Akad. Nauk BSSR, 10: 232-5(Apr. 1966). (In Russian).

The selection rule of dipole electric radiation which determines the forbidden transitions, is disturbed by several factors. There is a difference between the selection rules of the magnetic dipole and electric quadrupole radiations and those of ordinary dipole radiations; the former are considered as forbidden ones. In the free atom, the forbidden intercombinational transitions, subject to spin-orbital interaction, are observed. If the spin of the nucleus is not zero, the dipole transitions $j \rightarrow j \pm 2$ and $j = 0 \rightarrow j = 0$ take place; they are forbidden by the Δj selection rule. External electric and magnetic fields may be responsible for forbidden transitions in the atomic system. Under the influence of homogeneous and nonhomogeneous fields, various transitions may take place in the plasma. Calculations were carried out for determining the intensity of these interactions for lithium, sodium, copper, and cesium and a generalized formula was derived for determining the probability of transitions under the influence of ions and electrons, using it to calculate the intensity of the forbidden lines of cesium. (TTT)

37433 KIRCHHOFF'S LAW MANIFESTATION IN GAMMA SPECTROSCOPY. Mazurenko, Yu. T. Dokl. Akad. Nauk SSSR, 165: 790-1(Dec. 1, 1965). (In Russian).

According to Kirchhoff's law, the ratio of the spectral radiation coefficient of an equilibrium medium ϵ_γ and the absorption coefficient α is equal to the spectral intensity of the equilibrium radiation at a temperature K_γ of the medium: $\epsilon_\gamma/\alpha_\gamma = K_\gamma$. The problem was considered for the case of a gas consisting of atoms with discrete energy levels, which thus possesses a line spectrum of absorption and emission. It was assumed that the lines are primarily determined by the Doppler broadening caused by the thermal motion of the atoms. Under conditions of thermal equilibrium, the absorption and emission lines may be shifted as the radiation intensity varies with the frequency. When the thermal equilibrium is disturbed, the nonequilibrium emission lines of fluorescence differ. The spectra under such conditions are due only to spontaneous transitions between excited and unexcited states. The large number of excited states present in fluorescent systems cause the difference with respect to thermal emission. An expression was derived that differs from the classic Doppler equation by including a term R, designating the recoil energy of the photon; the expression shows that the emission and absorption lines are spaced at a distance of 2R/h. (TTT)

37434 TRANSITIONAL RADIATION DURING OBLIQUE INCIDENCE ON FILM. Engibaryan, V. A.; Khachatryan, B. V. (Joint Lab. of Radiation, Academy of Sciences, Arm. SSR. Erevan State Univ.). Izv. Akad. Nauk Arm. SSR, Fiz., 1: 11-19(1966). (In Russian).

Transitional radiation occurring during the incidence of charged particles on the film is considered. The radiation intensity formulas for two mutually perpendicular polarizations are derived. Particular cases of the flight of nonrelativistic particles through a thin film as well as through a film of ideal conduction are discussed. (auth)

37435 RELATIVISTIC PARTICLE IONIZATION ENERGY LOSSES. Lorikyan, M. P. (Inst. of Physics, State Atomic Energy Commission, USSR). Izv. Akad. Nauk Arm. SSR, Ser. Fiz. Mat. Nauk, 18: No. 6, 109-11 (1965). (In Russian).

When a relativistic particle enters a medium from a vacuum, the polarization of a thin layer of the medium has no effect on the ionization energy losses. For practical use of this effect it is important to know the optimum thickness of a substance, in which the density of the medium has no substantial effect on the ionization losses. This thickness can be estimated from the relation: $\Delta = d\,\delta$. Here Δ is the increase in ionization energy losses in a thickness a (measured experimentally); δ is the increase in ionization energy losses when the effect of polarization is equal to zero; d is the thickness of the layer where the effect of polarization is not felt. On measuring values of Δ/δ for thickness a from 2×10^{-3} to 10^{-6} cm, the value of d for a polystyrol film is found to be $d = (0.94 \pm 0.66) \times 10^{-4}$ cm. (TTT)

37436 MODIFICATION OF SCHROEDINGER'S EQUATION. Raichev, P. Izv. Fiz. Inst. Aneb, Bulg. Akad. Nauk, 14: 21-6(1966). (In Russian).

Schrödinger's equation is constructed, assuming that the mass term in the equation depends on the binding energy. By the concrete example of Coulomb's potential it is demonstrated that the absolute value of the energy cannot grow in an unlimited manner even when the interaction constant assumes arbitrarily big values. The distance between the particles cannot become arbitrarily small however strong the attraction of the particles may be. The modified equation is written as follows: $\{[\hbar^2/2\mu(E)]\Lambda + U(q)\}\psi(q) = E\psi(q)$, where for the mass function the following model is tested: $\mu(E) = \mu_0\lambda$; $\lambda = (1 + E/\mu_0c^2)^{-1}$. A method is suggested for the experimental check of the validity of the modified equation for a description of the atomic shell: according to the results obtained the energy level with n = 1 should be free from the 96th element onwards. The decay of Br and Cf, therefore, should be accompanied by the rearrangement of the atomic shell. (auth)

37437 GROUP-THEORETICAL CLASSIFICATION OF THE ATOMIC STATES OF g^N CONFIGURATIONS. Wybourne, B. G. (Argonne National Lab., Ill.). J. Chem. Phys., 45: 1100-4(Aug. 15, 1966).

The terms of the g^N configuration of equivalent electrons (or nucleons) are classified in both LS and jj coupling using the methods of group theory. It is suggested that the electronic structure of the g^N configurations, which should be important in an element of atomic number Z = 126, could be most readily calculated in terms of the jj coupling scheme. (auth)

37438 TRANSITION PROBABILITIES FOR H_2, D_2, N_2, N_2^+, AND CO. Fowler, R. G.; Holzberlein, T. M. (Univ. of Oklahoma, Norman). J. Chem. Phys., 45: 1123-5 (Aug. 15, 1966).

The previously observed quenching of the $a\,^3\Sigma_g^+$ state of the hydrogen molecule by neutral collision was confirmed by a study of deuterium. Lifetimes were also measured for what are believed to be the $B\,^2\Sigma_u^+$ state of N_2^+; the $C\,^3\Pi_u$ state of N_2; and the $b\,^3\Sigma$, $d\,^3\Pi$, and $B\,^1\Sigma$ states of CO. (auth)

37439 IONIZATION ENERGIES OF THE NEUTRAL RARE EARTHS. Reader, Joseph; Sugar, Jack (National Bureau of Standards, Washington, D. C.). J. Opt. Soc. Amer., 56: 1189-94(Sept. 1966).

The ionization energies of the neutral rare earths were derived by means of interpolated values for the energy differences between the $4f^N6s^2$, $4f^N6s7s$, and $4f^N6s8s$ configurations and the difference in the effective quantum numbers of the $4f^N6s7s$ and $4f^N6s8s$ configurations. In Ce I the $4f5d^2ns$ series was used. The uncertainty is estimated to be ±0.02 ev in all cases but Ce I for which the estimated uncertainty is ±0.06 ev. Values for La I and Gd I obtained spectroscopically by other workers are also tabulated. The present results are compared with those obtained by means of surface ionization. The calculated result for Tb I was inconclusive because of the lack of sufficient knowledge of the energy-level structure. (auth)

37440 SELF-CONSISTENT PERTURBATION METHOD. I. CALCULATION OF DIPOLE POLARIZABILITY AND SHIELDING FACTOR. Lahiri, J.; Mukherji, A. (Saha Inst. of Nuclear Physica, Calcutta). J. Phys. Soc. Jap., 21: 1178-82(June 1966).

A variation method is described which yields a self-consistent wave function for an atom or molecule subjected to a perturbing field of the type $\Sigma_i h_1(i)$. Through minimization of the second-order energy, completely coupled perturbed orbitals are obtained in the Hartree-Fock scheme. A calculation of the dipole polarizability and shielding factor was done for atoms and ions of He, Li and Be isoelectronic sequences. The results are of much higher accuracy than those hitherto obtained by other methods. (auth)

37441 ABSORPTION AND LUMINESCENCE SPECTRA OF NaI AND NaI(Tl) AT LOW TEMPERATURES. II. Vaidanich, V. I. Opt. Spectros. (USSR) (Engl. Transl.), 20: 250-3(Mar. 1966).

Translated from Opt. Spektros., 20: 459-66(Mar. 1966).

The absorption, excitation, and emission spectra of thallium-activated sodium iodide monocrystals were measured at liquid helium and higher temperatures. New excitation and emission bands were found. The results were compared with earlier published results for KI(Tl). A possible scheme for energy transitions in the thallium ion in NaI(Tl) crystals is discussed. (auth)

37442 HIGH RESOLUTION INVESTIGATION OF THE ENERGY LOSSES OF 30 kev ELECTRONS IN ALUMINUM FOILS OF VARIOUS THICKNESSES. Boersch, H.; Geiger, J.; Imbusch, A.; Niedrig, N. (Technische Univ., Berlin). Phys. Lett., 22: 146-7(Aug. 1, 1966).

The energy loss spectrum of 30-kev electrons in Al foils was investigated with a resolution of 0.07 ev. Corresponding to the dielectric theory the volume plasma excitation loss was observed at 14.99 ev, and the surface energy loss at 6.7 ev. The latter splits up into two peaks for foil thickness less than 300 Å, in agreement with theory. An additional peak was observed at 1.48 ev, which is due to an interband transition. (auth)

37443 MEAN LIVES OF THE 2p AND 3p LEVELS IN ATOMIC HYDROGEN. Bickel, William S.; Goodman, Allan S. (Univ. of Arizona, Tucson). Phys. Rev., 148: 1-4(Aug. 5, 1966).

Radiation from hydrogen atoms in excited states produced by the beam-foil method was studied as a function of time using a vacuum ultraviolet monochromator. Measured values of the mean lives of the 2p and 3p levels in hydrogen are presented and compared with theory. The effects of cascades from levels of higher n were observed and were included in the mean-life calculations. (auth)

37444 SCATTERING OF CHARGED PARTICLES BY NONSPHERICAL ATOMS. Snodgrass, Herschel B. (Univ. of California, Berkeley). Contract AF-AFOSR-130-65. Phys. Rev., 148: 5-10(Aug. 5, 1966).

The problem considered is the calculation of scattering of low-energy charged particles by an atom whose ground-state configuration contains incomplete p or higher l shells. An optical potential is derived which is a matrix in the atomic angular-momentum states and a noncentral operator in the coordinates of the scattered particle; when projected onto the invariant subspaces of total angular momentum for the system, this potential leads to a set of coupled integro-differential equations for the partial-wave scattering amplitudes in which all symmetries are explicit. Various approximations to the optical potential are displayed and related to the permanent and induced charge moments of the atom, and the exchange interaction for electron scattering is derived. Finally, a brief discussion of the determination of the scattering amplitudes is given, including descriptions of low-energy limits, of limits for large total angular momentum, and of the application of the Kohn variational principle. (auth)

37445 RADIATIVE LEVEL SHIFTS. III. HYPERFINE STRUCTURE IN HYDROGENIC ATOMS. Brodsky, Stanley J. (Columbia Univ., New York. Univ. of Minnesota, Minneapolis); Erickson, Glen W. Phys. Rev., 148: 26-46(Aug. 5, 1966).

A comprehensive calculation of the second-order quantum-electrodynamic corrections to the hyperfine splitting of S states is presented. The gauge-invariant reduction of the self-energy expression given by Yennie and Erickson is used to systematically verify previous calculations of orders α, $\alpha(Z\alpha)$, $\alpha(Z\alpha)^2\ln^2(Z\alpha)^{-2}$, and $\alpha(Z\alpha)^2\ln(Z\alpha)^{-2}$ relative to the lowest order Fermi splitting E^F and to obtain a result for the dominant contribution to order $\alpha(Z\alpha)^2$ for the 1S and 2S levels. The new contribution for the 1S state is $(\alpha/\pi)(Z\alpha)^2[18.4 \pm 5]E^F = [2.3 \pm 0.6] \times 10^{-6}E^F$, where α is the fine-structure constant, $Z\alpha$ is the strength of the Coulomb potential, and the error limits are estimates of uncalculated terms. The results for n = 2 provide a substantial check of Zwanziger's calculation of the hyperfine splittings in the 1S and 2S levels. (auth)

37446 ELECTRON TRANSFER IN PROTON–HYDROGEN-ATOM COLLISONS: 2-117 kev. McClure, G. W. (Sandia Lab., Albuquerque, N. Mex.). Phys. Rev., 148: 47-54(Aug. 5, 1966).

The cross section for electron transfer between a proton and a hydrogen atom was measured in the energy range 2 to 117 kev. The apparatus employs a heated target chamber in which hydrogen gas is 79% dissociated. The total density of H atoms in the collision chamber, including both free H atoms and H atoms combined into H_2 molecules, is determined by a differential-Coulomb-scattering measurement, while the density of H_2 molecules is determined by a double-electron-capture measurement. Experimental values of the cross section measured at 19 different energies varied monotonically from 13.3×10^{-16} cm^2 at 1.92 kev to 0.064×10^{-16} cm^2 at 117.5 kev. The results, believed to be accurate to ±5%, are not completely consistent with previous measured values of other investigators. Theoretical calculations of McCarroll and McElroy agree satisfactorily with the measurements at energies lower than 60 kev, but between 60 and 117 kev no theoretical calculation is in satisfactory agreement with the measurements. (auth)

37447 CROSS SECTION FOR ENERGY TRANSFER BETWEEN TWO MOVING PARTICLES. Gerjuoy, E. (Univ. of Pittsburgh). Contract NGR-39-011-35. Phys. Rev., 148: 54-9(Aug. 5, 1966).

The classical cross section $\sigma_{\Delta E}$, for producing a specified energy transfer ΔE in the collision of two particles 1,2 having arbitrary masses and velocities v_1, v_2 in the laboratory system, is derived. The effective average (for fixed speeds v_1,v_2) of $\sigma_{\Delta E}$ over all directions of the particle velocities v_1 and/or v_2 is then computed. These results are required in the classical calculations of atomic-collision cross sections via the procedures recently proposed by Gryzinski. The method will yield the average of any function $F(v,V,\cos\bar{\theta})$ over all directions of the particle velocities, where $v = v_1 - v_2$, V is the velocity of the center of mass, and $\bar{\theta}$ is the angle between v and V. (auth)

37448 ANALYTIC-EXPANSION UNRESTRICTED HARTREE-FOCK WAVE FUNCTION FOR THE ^5D STATE OF Fe. Bagus, P. S.; Liu, B. (Argonne National Lab., Ill.). Phys. Rev., 148: 79-82(Aug. 5, 1966).

An accurate analytic-expansion unrestricted Hartree-Fock wave function is reported for the ^5D state and Fe. The computed values of the magnetic dipole hyperfine-

interaction constants are compared with the experimental values obtained by Childs and Goodman and are in good agreement. (auth)

37449 SINGLE-PARTICLE COUPLING TO COLLECTIVE EXCITATIONS; SOUND IN ^{3}He. Engelsberg, Stanley (Princeton Univ., N. J.); Platzman, P. M. Phys. Rev., 148: 103-8(Aug. 5, 1966).

In order to test the hypothesis that the observed anomalous behavior of the low-temperature specific heat of ^{3}He is due to the interaction of ^{3}He atoms with sound, the coupling of the single particles to the collective excitations must be calculated. Based on an infinite-order perturbation theory, a technique is introduced for finding the effective coupling at long wavelengths. Within this approximation scheme the coupling is found to be of the deformation-potential kind. Vertex corrections make the expression used for the single-particle self-energy exact. A singular vertex function, which is ruled out if perturbation theory is valid but which is required in order to change the coupling from deformation-potential to piezoelectric, leads to an inconsistency. All approximation schemes treated result in a deformation-potential coupling between ^{3}He atoms and sound. Treatments of this coupling have not so far led to results which can explain the observed specific heat. (auth)

37450 ELECTRON EJECTION FROM AN ATOMICALLY CLEAN TUNGSTEN SURFACE BY HELIUM AND NEON METASTABLE ATOMS. MacLennan, D. A. (Univ. of California, Berkeley). Phys. Rev., 148: 218-23(Aug. 5, 1966).

The absolute electron yield γ^m of helium and neon metastable atoms incident on an atomically clean polycrystalline tungsten surface was determined. The value of γ^m for helium excited by 28-volt electrons is 0.306 ± 0.025, where $^1S_0$ and $^3S_1$ yields are equal within an experimental error of 20%; the value of γ^m for neon is 0.215 ± 0.020. The contribution of each of the two neon metastable states to γ^m was not resolved in this determination. These results are consistent with present theory, which predicts that the absolute electron yield of slow rare-gas metastable atoms and ions incident on an atomically clean tungsten surface should be the same. Nitrogen and air contamination of the tungsten surface was observed to reduce the electron yield of helium metastable atoms. This reduction is approximately 45% for nitrogen and 80% for air. Penning cross sections for the ionization of argon by helium and neon metastable atoms were obtained from the yield data to an estimated accuracy of ±30%. They are 9×10^{-16} cm^2 for both $^1S_0$ and $^3S_0$ helium metastable atoms, and 11×10^{-16} cm^2 for an unresolved mixture of $^3P_0$ and $^3P_2$ neon metastable atoms. (auth)

37451 STIMULATED PURE ROTATIONAL RAMAN SCATTERING IN DEUTERIUM. Minck, R. W.; Hagenlocker, E. E.; Rado, W. G. (Ford Motor Co., Dearborn, Mich.). Phys. Rev. Lett., 17: 229-31(Aug. 1, 1966).

Observation of stimulated Raman scattering in deuterium involving transitions between molecular rotational levels is reported. (B.G.D.)

37452 DETACHMENT OF ELECTRONS FROM H^- BY ELECTRON IMPACT. Tisone, G.; Branscomb, L. M. (Joint Inst. for Laboratory Astrophysics, Boulder, Colo.). Phys. Rev. Lett., 17: 236-8(Aug. 1, 1966).

The absolute cross section for the reaction $e + H^- \rightarrow H + 2e$ at electron energy 100 ev and energy dependence from 30 to 500 ev are reported. (B.G.D.)

37453 ELECTRON-IMPACT EXCITATION OF n = 2 STATES IN He. Burke, P. G. (United Kingdom Atomic Energy Authority, Harwell, Eng.); Cooper, J. W.; Ormonde, S. Contract AF 29(601)-6801. Phys. Rev. Lett., 17: 34-58(Aug. 15, 1966).

The results are presented of cross-section calculations for the excitation of the n = 2 states of He by electron impact. It is shown that the structure in these cross sections is due to two previously unreported resonances in the ^2P and ^2D states at 20.2 and 21.0 ev, respectively, in addition to thw well-known 19.3-ev ^2S resonance. The calculation is carried out in the close-coupling approximation including the ground state and all the n = 2 excited states of He. (L.B.S.)

37454 CLASSICAL THEORY OF CHARGE TRANSFER AND IONIZATION OF HYDROGEN ATOMS BY PROTONS. Abrines, R. (Kingston Coll. of Technology, London); Percival, I. C. Proc. Phys. Soc. (London), 88: 861-72 (Aug. 1966).

The theory is presented for obtaining, by a Monte Carlo method, the classical cross sections for charge transfer and ionization of hydrogen atoms by protons, in which the atoms are chosen initially from a microcanonical ensemble. With minor modifications the theory applies to any collisions between three charged particles which do not all have charges of the same sign. Scaling laws and an iterative solution of Kepler's equation are discussed. (auth)

37455 GENERALIZED CORRESPONDENCE PRINCIPLE AND PROTON-HYDROGEN COLLISIONS. Abrines, R. (Kingston Coll. of Technology, London); Percival, I. C. Proc. Phys. Soc. (London), 88: 873-83(Aug. 1966).

The Monte Carlo method is used to obtain total classical cross sections for ionization and charge transfer of hydrogen atoms in any level n by protons in the energy range $38/n^2$ kev to $218/n^2$ kev in the laboratory frame. The cross sections have normal statistical errors of about ±10% for ionization and ±9% or more for charge transfer. For n = 1 the classical ionization cross section agrees with experiment to within about 10 or 15 per cent over the entire range of energies, showing that the agreement between earlier classical theories of ionization and experiment is not simply the result of further dynamical approximations. The classical charge transfer cross section is somewhat higher than experiment. A generalized correspondence principle is derived which states that, for a nonrelativistic quantal system of charged particles, the classically scale-invariant quantities tend to their classical values when the linear dimensions tend to infinity and other quantities are also scaled. The above cross sections are thus correct in the limit $n \rightarrow \infty$. Validity and application of the results are discussed. (auth)

37456 CLASSICAL IMPULSE APPROXIMATION TO IONIZATION OF HYDROGEN ATOMS BY PROTONS. Percival, I. C.; Valentine, N. A. (London Univ.). Proc. Phys. Soc. (London), 88: 885-92(Aug. 1966).

Cross sections for ionization of hydrogen atoms by protons are obtained in the classical impulse (binary encounter) approximation. Cross sections for two velocity distributions of the electron are compared with the Monte Carlo calculations of Abrines and Percival for incident proton energies of 38 kev to 217 kev. They agree to within 10% at 217 kev, but even with the correct velocity distribution the maximum classical impulse cross section at about 38 kev is too large by a factor of 2. A reason is given for the better agreement of the impulse approximation with the total loss (ionization plus charge transfer) cross section. (auth)

37457 MODULATED ABSORPTION OF LIGHT IN AN OPTICAL PUMPING EXPERIMENT ON ^{4}He. Partridge, R. B.; Series, G. W. (Oxford Univ.). Proc. Phys. Soc. (London), 88: 969-82(Aug. 1966).

Optical pumping experiments were performed on helium-4 atoms in the metastable level $2\ ^3S_1$ with the object of studying the modulation of light in absorption in the longitudinal and transverse beams. Magnetic resonance curves were obtained similar to those found in emission in double-resonance experiments. With a particular geometrical arrangement employing circular polarizers, the Bloch magnetic resonance curves were obtained. Modulation at four times the applied frequency was obtained with a linear polarizer in the pumping beam. This modulation is ascribed to the circulation of coherence in the optical pumping cycle. From the behavior of the resonance signals as a function of the frequency and amplitude of the stimulating field, it is inferred that a substantial part of the signal arises from coherence which has survived two complete cycles. The observations are satisfactorily explained by the theory developed previously. (auth)

37458 TRANSFER OF COHERENCE BY COLLISIONS OF ^{3}He ATOMS. Partridge, R. B.; Series, G. W. (Oxford Univ.). Proc. Phys. Soc. (London), 88: 983-93(Aug. 1966).

Magnetic resonance in the ground states of ^{3}He was studied through the interaction with metastable atoms in a gas discharge. Modulation showing the characteristics of the ground-state resonances is observed in a transverse beam of light absorbed by the metastable atoms. This is evidence of the transfer of transverse magnetization (coherence between eigenstates) by collision. A theory is developed which explains the observations in detail. The fact that coherence can be transferred by spin exchange in collision offers the possibility of exploitation in level-crossing or modulation experiments on spectroscopically inaccessible systems. (auth)

37459 HYPERFINE STRUCTURE AND NUCLEAR MOMENTS OF SAMARIUM. Woodgate, G. K. (Oxford Univ.). Proc. Roy. Soc. (London), Ser. A, 293: No. 1432, 117-44(July 5, 1966).

Experimental and theoretical work was carried out on the hyperfine structure of the $4f^6\ ^7F$ ground multiplet of samarium. Hyperfine structure intervals were measured in the levels J = 1, 2, 3, and 4 for both odd isotopes ^{147}Sm and ^{149}Sm by the method of atomic beams. These intervals were fitted to magnetic dipole and electric quadrupole interaction constants. Further measurements at high magnetic field by the method of triple resonance led to the evaluation of the nuclear magnetic dipole moments of the two isotopes. It is shown that a calculation of the breakdown of L–S coupling and of second order corrections, off-diagonal in J, is necessary for an interpretation of the spectrum. The application of these corrections is facilitated by the formulation of an effective Hamiltonian, and the whole problem is treated step by step as a practical example of the use of tensor operator techniques. (J.G.B.)

37460 ENERGY LOSS OF FAST CHARGED PARTICLES IN DIELECTRIC MEDIA. Fowler, G. N.; Hall, A. G. (Univ. of Newcastle upon Tyne, Eng.). pp 976-9 of Proceedings of the Ninth International Conference on Cosmic Rays. Vol. 2. Stickland, A. C. (ed.). London, The Institute of Physics and The Physical Society, 1966.

Various classical and semi-classical calculations of energy loss of relativistic charged particles in dielectric media are compared with mass operator and perturbation theory calculations and with experiment for oxygen. It is argued that classical calculations lead to a misinterpretation of the phenomena. The perturbation method is used to estimate a higher order correction. (auth)

37461 RECOILLESS ABSORPTION OF GAMMA-RADIATION AND ITS APPLICATION TO PROBLEMS OF ELECTRONIC SHIELDING IN RARE EARTHS. Moessbauer, R. L. (Technische Hochschule, Munich). Pure Appl. Chem., 11: 297-309(1965).

The method of recoilless nuclear resonance absorption of gamma radiation as a tool for investigations in nuclear physics, relativity, solid-state physics, chemistry, and biology is discussed. A brief introduction into the basic aspects of this method is presented. The potentialities of the method are illustrated in the second part by describing applications to studies of electronic shielding by closed electron shells in ionic compounds of the rare earths. (auth)

37462 SEMICLASSICAL EVALUATION OF SOME ATOMIC QUANTITIES. Ionescu-Pallas, N. J. (Inst. of Atomic Physics, Bucharest). Rev. Roum. Phys., 11: 359-67(1966).

A semiclassical method for estimating atomic quantities is given for any value of the orbital quantum number. The method is obtained by resorting to a classical picture of the electron motion. The quantities r, r^2, r^3, are evaluated, the results being consistent with estimations through other methods. An expression for $\Psi_s^2(0)$ resembling the well known Fermi-Segrè formula is also obtained. (auth)

37463 HYPERFINE STRUCTURE IN BaII λ 4934 Å AND λ 4554 Å LINES AND NUCLEAR MAGNETIC MOMENTS OF ^{137}Ba AND ^{135}Ba. Comaniciu, N.; Draganescu, V.; Tatu, V. (Inst. of Atomic Physics, Bucharest). Rev. Roum. Phys., 11: 399-408(1966).

By using a Fabry-Pérot recording spectrophotometer and enriched isotope samples the hyperfine structure of the doublet lines in Ba II was examined. The nuclear magnetic moments of the isotopes 135 and 137 were found to be $\mu_I(^{135}\text{Ba}) = (0.843 \pm 0.007)\ \mu_N$ and $\mu_I(^{137}\text{Ba}) = (0.930 \pm 0.007)\ \mu_N$. These values are in good agreement with those given in the literature, obtained through the nuclear incident method. (auth)

37464 MOESSBAUER EFFECT. Nachtigall, Dieter Roentgen Bl., 15: 389-98(Dec. 1962). (In German).

The discovery of this phenomenon, its nature, and applications are reviewed. γ-Quanta transfer recoil impulses to atomic nuclei during emission and absorption. As a result, they experience losses of energy which most frequently prevent nuclear resonance absorption provided the recoil losses of energy are not compensated. Under certain circumstances, the recoil impulses in the case of solid bodies is not transferred to the individual atomic nucleus but to the entire crystal lattice so that the recoil loss of energy is limited and nuclear resonance absorption is able to take place. This process, named the Mössbauer effect after its discoverer, is chiefly applied in nuclear spectroscopy and solid state physics. Particularly impressive is the possibility of using it to trace the red displacement of spectral lines in the field of gravity. Experiments with the Mössbauer effect using ^{57}Fe are outlined. (BBB)

37465 COMPTON SCATTER FROM LOW-ENERGY GAMMA EMITTERS AND ITS SIGNIFICANCE TO COLLIMATION. Stewart, B. M.; Hoedt-Rasmussen, K. (Bispebjerg Hospital, Copenhagen). Scand. J. Clin. Lab. Invest., 17: Suppl. 86, 189(1965).

Precise collimation of low-energy γ radiation, such as that of ^{133}Xe (81 kev) is simple because only thin layers of lead are required to shield from the primary radiation. However, low-energy γ radiation, or bremsstrahlung, has a great tendency to be deflected due to Compton scatter in body tissues. Some deflected rays may therefore originate outside a collimator's view, bouncing into its area of focus. Since many of these deflected rays have almost the same energy as the primary radiation, narrow pulse-height analysis with photopeak counting is a prerequisite for good localization in large tissue masses. Three models were constructed; brain, lung, and kidney, having the ~ density of the living tissue. Each model had a blank inserted without isotope. In all three models measurements with narrow collimation over the central blank area with ^{133}Xe in the outer chamber averaged about 10% of the counting rate over the outer chamber despite use of a narrow window setting over the photopeak on a stable pulse-height analyzer. This figure rose rapidly with slightly larger channel widths to a value of about 25%. The effect was found to be much less pronounced when ^{85}Kr was used. (BBB)

37466 CO, CO_2, AND NO EMISSION SPECTRA EXCITED BY 13-kev ELECTRONS. Koval, A. G.; Koppe, V. T.; Fogel, Ya. M. (Gorkii State Univ., Kharkov). Soviet Astron. AJ (Engl. Transl.), 10: 165-75(July-Aug. 1966).

Translated from Astron. Zh., 43: 209-19(Jan.-Feb. 1966).

Emission spectra were obtained for rarefied CO, CO_2, and NO gases excited by electrons of 13-kev energy. Relative intensities are derived for all the emission bands in each spectrum. A comparison is made with the spectra of CO and CO_2 excited by 37-kev protons, and with the night-sky spectrum of Venus. (auth)

37467 ODD-ODD HYPERFINE INTERACTION AND SPONTANEOUS ORTHO-PARA TRANSITIONS IN HYDROGEN MOLECULES AND MOLECULAR IONS. Yarunin, V. S. Vestn. Leningr. Univ., Ser. Fiz. Khim. (4), No. 1, 16-22(1966). (In Russian).

Spontaneous nuclear ortho-para transitions are shown to be possible in hydrogen molecule and molecular ion as due to hyperfine interaction odd-odd relative to the space

or spin nuclear coordinate permutations. A part of this interaction inversely proportional to the first power of nuclear mass is found for hydrogen molecular ion. (auth)

37468 SPUTTERING OF COPPER BY NOBLE GAS IONS IN THE ENERGY RANGE 100 kev TO 1 Mev AS A FUNCTION OF THE INCIDENT ANGLE. Dupp, Guenter; Scharmann, Arthur (Univ., Giessen, Ger.). Z. Phys., 194: 448-52(1966). (In German).

Using a 1.3-Mev Van de Graaff accelerator, the sputtering ratio S of polycrystalline copper bombarded by Ne^+, Ar^+, Kr^+, and Xe^+ ions was measured as a function of the angle of incidence in the range from 0° to 45°. The ion energy was varied from 100 kev to 1 Mev. The sputtering ratio was found to increase with bombarding angle as $S = S(0°) \cdot (2 - \cos \alpha)/\cos \alpha$ for Ne^+, Ar^+, and Kr^+ ions and as $S = S(0°)/\cos^{\frac{5}{2}} \alpha$ for Xe^+ ions. The increase of the sputtering ratio was found to be independent of the ion energy. (auth)

37469 POLARIZATION OF SLOW ELECTRONS BY SCATTERING ON MERCURY BETWEEN 180 AND 1700 ev. Jost, Klaus; Kessler, Joachim (Technische Hochschule, Karlsruhe, Ger.). Z. Phys., 195: 1-12(1966). (In German).

Angular and energy dependence of the polarization P of slow electrons scattered elastically by a mercury-atom beam were measured. The angular resolution being comparatively high (about ±1°), the results could be compared directly with uncorrected theoretical values and high polarizations (up to $|P| = 0.85 \pm 0.05$) could be observed. The polarization was measured by a Mott detector, the electrons scattered by the mercury atoms having been accelerated to 120 kev. The high yield of this detector made up for the rather low intensity of the observed beam caused by the high angular resolution and resulted in low statistical errors. The experimental results, which cover the angular range from 30 to 150° and energies from 180 to 1700 ev are in good agreement with the theoretical values of Holzwarth and Meister as well as with those of Bunyan and Schonfelder. (auth)

37470 MEASUREMENT OF THE STOPPING POWER OF ^{208}Pb ALPHA RECOIL NUCLEI IN SOLID MATERIAL. Marx, Dieter (Technische Hochschule, Munich). Z. Phys., 195: 26-43(1966). (In German).

The stopping power of C, Ag, and Au for ^{208}Pb atoms recoiling from alpha decay with an energy of 169 kev was obtained by a time-of-flight technique yielding the energy distribution of these recoil atoms after their passage through thin foils. The theory of Biersack (Thomas-Fermi-Firsov potential) and of Lindhard, Scharff and Schiott (Thomas-Fermi-Bohr potential) gives an adequate description of the results including the stopping of heavy particles by heavy target atoms. The values of the stopping power agree with theoretical results within a factor of 1.5 just as the measurements of other authors in the same energy range. However these results for light target atoms are smaller than theory, whereas the measurements are greater by about the same amount. Simplifying assumptions of theory especially concerning the interaction potential may be the reason of these deviations. (auth)

37471 ROTATIONAL ENERGY LEVEL DISTRIBUTION OF MOLECULES EXCITED BY ION IMPACT. Polyakova, G. N.; Tatus', V. I.; Strel'chenko, S. S.; Fogel', Ya. M.; Fridman, V. M. (Physico-Technical Inst., Academy of Sciences, Ukrainian SSR). Zh. Eksp. Teor. Fiz., 50: 1464-71(June 1966). (In Russian).

The experimental arrangement and technique employed for investigating the intensity distribution in the rotational structure of molecular spectra bands are described. The intensity distributions of the rotational lines of the $\lambda = 3914$ and $\lambda = 4278$ Å bands in the spectrum of the first negative system N_2^+ excited by impact of a mixed 30-kev proton and hydrogen atom beam are investigated. The distribution of the rotational line intensity observed was found to deviate from the Boltzmann distribution by an amount which exceeds the experimental errors. (auth)

37472 THEORY OF A BOSE GAS PRODUCED BY BOUND STATES OF FERMI PARTICLES. Popov, V. N. (Steklov Inst. of Mathematic, Leningrad). Zh. Eksp. Teor. Fiz., 50: 1550-8(June 1966). (In Russian).

Temperature Green functions expressed in terms of many-particle scattering amplitudes which are correct in the limit of small densities are found for a system of Fermi particles which can form pair bound states in vacuum. It is shown that the system behaves as a Bose gas, the particles of which (bound states) form a condensate at low temperatures. (auth)

37473 ROTATION OF NORMAL AND SUPERFLUID FERMI SYSTEMS. Kadmenskii, S. G. (Voronizh State Univ., USSR). Zh. Eksp. Teor. Fiz., 50: 1565-72(June 1966). (In Russian).

A self-consistent calculation scheme which takes into account the proper magnetic field of currents arising during the rotation of a Fermi system is developed for the purpose of investigating the rotation of Fermi systems. A generalized Larmor theorem is formulated. The rotation of normal and superfluid systems is investigated in detail in the scheme. It is shown that the moment of inertia of a London superfluid system is zero. The effect of normal and superfluid interactions on the moment of inertia of a Fermi fluid is studied by methods of Fermi fluid theory. It is shown that normal interaction in a normal Fermi system does not affect the moment of inertia. Normal interactions in rotating superfluid Fermi systems are consistently taken into account. Corrections associated with the proper magnetic field are estimated for the case of rotating atomic nuclei. (auth)

37474 THEORY OF ATOMIC ENERGY LEVELS IN A PLASMA. Rostokin, V. I. Zh. Eksp. Teor. Fiz., 50: 1586-91(June 1966). (In Russian).

The energy spectrum of a hydrogen-like atom in a plasma is considered on the basis of the cut-off Coulomb potential model. The analytic solution for bound states is investigated in detail for the case $l = 0$. Approximate expressions are obtained for energies of the S states which define their dependence on the cutoff range. Critical values of the Debye length for which the corresponding S levels disappear are found. (auth)

37475 POLARIZATION OF PHOTOELECTRONS FROM MAGNETIZED NICKEL AND PRODUCTION OF A POLARIZED ELECTRON BEAM. Long, Robert L. Jr. New Haven, Yale Univ., 1965. 200p.

Thesis.

Two possible means of producing a polarized electron beam for use in various experiments were investigated. The first was photoemission from a magnetized nickel crystal. After acceleration of the photoelectrons to 120 kev by an electrostatic accelerator, the polarization was measured by the Mott scattering technique and was found to be zero within the experimental accuracy of 0.02. Possible explanations of this result, including the nature of the electron band structure and depolarizing mechanisms, are discussed. Hence photoemission from ferromagnets does not appear to be a useful source of polarized electrons. The second method investigated was photoionization of an atomic potassium beam polarized by passage through a six-pole magnet. Photoelectrons from the beam were accelerated to 100 or 120 kev and their polarization was measured by the Mott scattering method. A drastic reduction of the electron polarization was found at high oven temperatures and attributed to unpolarized photoelectrons from the diatomic molecule content of the atomic beam. After this was eliminated by thermal dissociation, a polarization of 0.50 ± 0.02, $(89 \pm 4)\%$ of the expected polarization, was obtained with a current of 1.4×10^{-12} amp. The polarization discrepancy was found to be due to photoelectrons from optically excited atoms, and the full expected value was obtained when this contribution was eliminated by optical filters. Hence this method was shown to be successful, and a source of polarized electrons that will provide both larger current and polarization can now be designed. (Dissertation Abstr.)

37476 INTERACTION OF 3 H ATOMS. Wrzesinsky, R. Marburg, Ger., Univ., Marburg, 1964. 127p. $2.00 Gmelin, AED-Diss. 64-1082.

Thesis.

The two lowest terms of the H_3 system are investigated as a function of nuclear coordinates using the valence structure method. Eigenvalues are calculated with an electronic computer. Coupling coefficients for nuclear motion in the two lowest potential surfaces are calculated in the vicinity of the equal-sided triangle constellation. Eigenfunctions are determined by variation methods. (Gmelin Inst.)

37477 ATOMIC COLLISIONS. THE THEORY OF ELECTRON-ATOM COLLISIONS. Academy of Sciences of the Latvian SSR Institute of Physics Transactions XIII. Veldre, V. Ya.; Damburg, R. Ya.; Peterkop, R. K. (eds.). Cambridge, Mass., Massachusetts Institute of Technology Press, 1966. 140p. $7.50.

Translated by M. V. Kurepa.

Detailed discussions are presented for each of the following 17 sections: collisions of slow electrons with atoms, the inclusion of strong coupling in electron collisions with hydrogen atoms, slow electron collisions with hydrogen atoms, the asymptotics of functions which describe partial waves, positron collisions with hydrogen atoms, resonance phenomena in electron scattering by hydrogen atoms, the role of polarization effects in inelastic electron collisions with atoms, radial equations in atomic collision theory, a Coulomb-Born approximation for s-s transitions, use of the Bethe approximation in calculating the excitation cross section of ions by electrons, the behavior of cross sections near the threshold for a new reaction in the case of the attractive Coulombic field, resonance in electron scattering by ions, conservation of particle flux in collisions, ionization cross sections of hydrogen atom using plane wave approximation, ionization of hydrogen atom by slow electrons, ionization of helium atom near the threshold energy, and ionization of the helium atom accompanied by excitation. (M.O.W.)

37478 DISSOCIATION OF A CESIUM FLUORIDE MOLECULE BY IMPACT WITH A FAST ARGON ATOM. Williams, Calvit Herndon Jr. Providence, Brown Univ., 1965. 177p.

Thesis.

A crossed molecular beam apparatus is described in which chemical reactions having activation energies of several electron volts and higher can be studied. One of the beams was formed by charge exchange neutralization of a nearly monoenergetic fast ion beam. The neutrals produced had kinetic energies that could be varied from 7 to 100 ev. A molecular beam effusing from a thermal oven crossed the fast molecular beam at a right angle. A surface ionization detector rotated about the beam intersection in the plane of the two beams. The dissociation of a CsF molecule by impact with a fast Ar atom was studied. For Ar beam energies from 10 to 100 ev, the Cs atom detector current was less than 2×10^{-16} amps at all detector positions within 25° of the Ar beam axis. Therefore, the dissociation cross section was too small to be measured with the presently attained beam intensities. However, a hard sphere analysis of the kinematics of the dissociation was used to calculate values for $\sigma_D(E)$ and $\sigma_D(E,K)$ and to estimate an upper limit to the total dissociation cross section using the experimental results. A program was written for the Brown University computer, an IBM 7070, to calculate the properties of the dissociation of a CsF molecule of random orientation by impact with a fast Ar atom. Cross sections were determined for one set of hard sphere radii and eight values of Ar beam initial kinetic energy. The calculated values of $\sigma_D(E)$ went from 2×10^{-16} cm^2 at an Ar beam energy of 10 ev to about 10×10^{-16} cm^2 at 100 ev. These calculated cross sections can be considered as theoretical upper limits to the true adiabatic dissociation cross sections. The experimental upper limit to the total cross section was estimated by using the present beam intensities and apparatus constants and the calculated hard sphere Cs atom distribution. The experimental upper limits were all greater than the calculated values of $\sigma_D(E)$. (Dissertation Abstr.)

37479 REMARKS ON THE THEORY OF MU-MESIC ATOMS. Ravenhall, D. G. (Univ. of Illinois, Urbana). 12p. (CONF-660209-17). ORAU. Gmelin, AED-CONF-66-023-15.

From Conference on Intermediate Energy Physics, Williamsburg, Va.

A model for calculations on mu-mesic atoms is considered in which the nucleus is represented as a charge distribution and the meson is represented as a Dirac particle that interacts through the Coulomb interactions. Corrections due to nuclear and vacuum polarization are discussed in detail. (D.C.W.)

37480 THEORY OF THE SUB-ATOMIC STRUCTURE OF MATTER. Sporek, K. F. (Owens-Illinois Technical Center, Toledo, Ohio). 15p. (CONF-660611-4). ORAU. Gmelin, AED-CONF-66-172-1.

From Society of Applied Spectroscopy Meeting, Chicago.

A physical model of a universal sub-atomic particle is proposed from which the structures of the electron, proton, neutral radiation and other particles can be derived. It is assumed that the particle has two modes of rotation—axial and precessional—thus resembling, on a smaller scale, atomic particles, e.g., hydrogen atom, which have nuclear magnetic moments. A proton is produced when the axial and precessional rotations of the particle are in the same direction and an electron when the two movements are in opposite directions. In the former case the two magnetic effects combine to produce a magnetically heavy particle in the latter case they cancel each other and result in a light particle. Neutral radiation (light, etc.) is assumed to consist of two identical particles (e.g., electron-electron) bound together by the axial and precessional magnetic fields and thus magnetically neutralized. The energy state of any particle or combination of particles is assumed to depend on the precessional movement. Physical models for a neutron and a hydrogen atom are presented, and the existence of other particles are explained. (M.O.W.)

Cosmic Radiation

See also Elementary Particles and Radiations Nuclear Properties and Reactions

Refer also to abstracts 37102, 37336, 37370, 37372, and 37755.

37481 (COO-818-86) NEUTRINOS UNDERGROUND. Reines, F. (Case Inst. of Tech., Cleveland, Ohio). Apr. 1966. Contract AT(11-1)-818. 15p. (CONF-660411-33). Dep. mn. CFSTI $1.00 cy, $0.50 mn.

From American Physical Society Meeting, Washington, D. C.

An experiment is described in which the interaction of high-energy neutrinos at a distance of 10,492 feet below ground was detected. The description includes the source, detector, background reduction, data recording, data, backgrounds in the ν_μ aperture, expected signal, mass of the W, and future plans. (B.G.D.)

37482 CONTRIBUTION OF THE $K \rightarrow \mu + \nu$ DECAY IN THE μ-MESON BEAM OF COSMIC RAYS 3860 m. ABOVE SEA LEVEL. Gafurov, V. G.; Kashkarov, L. L.; Ivliev, A. I.; Klimenkov, V. M.; Cherdyntsev, V. V. Dokl. Akad. Nauk Tadzh. SSR, 8: No. 6, 7-9(1965). (In Russian).

The contribution of K-meson decay in the μ-meson flux in cosmic rays is determined by measuring the degree of polarization of the μ^+ mesons at 3860 m above sea level by recording the e^+ emitted in the $\mu \rightarrow e$ decay in the forward and backward directions from a Pb target with a thickness of 45 g./sq. cm. The high value for the degree of polarization, $P = 0.49 \pm 0.15$, as compared to earlier data indicates that at higher altitudes the contribution of μ mesons formed from the decay of K mesons in the atmosphere increases, and this contribution was evaluated as $\alpha = 0.22 \pm 0.15$. (TCO)

37483 COSMIC-RAY-PRODUCED NEUTRONS AT GROUND LEVEL: NEUTRON PRODUCTION RATE AND

FLUX DISTRIBUTION. Yamashita, Mikio; Stephens, Lloyd D.; Patterson, H. Wade (Univ. of California, Berkeley). Contract W-7405-eng-48. J. Geophys. Res., 71: 3817-34(Aug. 15, 1966). (UCRL-16042(Rev.)).

The absolute rates of cosmic-ray neutron production and neutron flux distribution on the ground were determined at sea level and mountain altitude at a geomagnetic latitude λ = 44°N in 1964. The thermal neutron flux was measured with a well-calibrated BF_3 counter; a Maxwellian energy distribution with a shifted neutron temperature was assumed. By using two differently moderated BF_3 counters, the fast-neutron flux was determined in the energy range 0.4 ev to 10 Mev. The neutron fluxes were also estimated from the measured production rate, and they are in good agreement with the measured fluxes; possible occurrence of air-ground boundary effects on the neutron flux distribution was considered. Anisotropy of the thermal neutron flux on the ground was experimentally demonstrated, and the angular distribution was well filled by the first two terms of a spherical-harmonics expansion. The air-ground boundary effects are discussed on the basis of experimental results. (auth)

37484 GALACTIC COSMIC-RAY SOURCE AND LOSS PROBLEM. Baker, Paul Jr.; Chasson, R. L.; Kisselbach, V. J. (Univ. of Denver). Nature, 211: 354-5(July 23, 1966).

Substantial direct evidence of a sidereal anisotropy is indicated for the charged galactic cosmic radiation. The results were obtained with a technique of celestial scanning, using a battery of paired narrow-angle muon telescopes, two of which are vertical, and the others with axes tilted at about 38° with respect to zenith and in the north, south, east, and west geographic planes. The results are described. (M.O.W.)

37485 INTERSTELLAR AND INTERGALACTIC ABSORPTION OF COSMIC X RAYS. Felten, James E.; Gould, Robert J. (Univ. of California, San Diego, La Jolla). Phys. Rev. Lett., 17: 401-5(Aug. 15, 1966).

Calculations using improved element abundances and atomic photoelectric cross-section data indicate sizable interstellar x-ray absorption edges at 0.532 and 0.874 kev due to K-shell photoionization of O and Ne, respectively. Results are applied to recent and prospective observations. (auth)

37486 CASE OF TRANSIENT ANISOTROPY DURING THE RECOVERY PHASE OF A FORBUSH DECREASE. Ahluwalia, H. S. (Univ. Mayor de San Andres, La Paz, Bolivia). Planet. Space Sci., 14: 791-805(Aug. 1966).

On July 18, 1959, a short-lived highly anisotropic cosmic ray increase was observed by some of the I.G.Y. network of recording stations during recovery from the third of the series of three closely spaced Forbush decreases. Characteristic features and the solar and terrestrial relationships of this increase are studied. Mechanisms proposed thus far for this increase are critically examined. Arguments are presented to the effect that this could not be solar flare-type increase. It is suggested that this increase was probably produced by galactic cosmic rays which got reflected from receding blast wave and co-rotating shock wave formed during the explosive heating of solar corona following the west limb 3^+ solar flare of July 16, 1959. Corresponding features of associated heliophysical, geophysical and cosmic-ray phenomena were studied. The velocity of the blast wave was determined to be 1700 km/sec and its total thickness about 0.14 a.u. It is believed that this blast wave had considerable fine structure built into it. Evidence indicates that this blast wave probably started to dissolve into background solar wind at a distance of about 1.5 a.u. from sun. (auth)

37487 DESIGN AND THEORY OF MAGNETIC SPECTROMETER FOR MEASUREMENT OF COSMIC-RAY MESONS. Klepikov, N. P.; Nooh, M. G.; El-Mofty, D. O.; Miligui, Z.; Eissa, N. (Ain Shams Univ., Cairo). Proc. Math. Phys. Soc. (U.A.R.), No. 26, 97-111(June 1962).

A magnetic spectrometer was designed for the purpose of measuring the positive excess of cosmic ray mesons in Cairo. The spectrometer can measure the positive and the negative mesons at the same time. Four channels in the apparatus allow particles of different charge to be counted, two for positive particles and the other two for negative particles. For the interpretation of the results, the geometrical cross-sections of different channels for particles having various initial energies and incident upon the instrument at different angles, were calculated. The spectrometer was found to be sensitive in the region between 0.7 and 1.6 Bev. The efficiency of the apparatus was found to be 0.892 ± 0.046. (auth)

37488 INTERPRETATION OF THE ENERGY SPECTRUM OF GALACTIC X RAYS. Hayakawa, Satio (Nagoya Univ., Japan). Progr. Theoret. Phys. (Kyoto), 35: 1162-3(June 1966).

It is pointed out that the thermal emission mechanism giving rise to an exponential spectrum of galactic x rays and the nonthermal mechanism resulting in a power spectrum are not mutually exclusive but stem from a common origin. (L.B.S.)

37489 INVESTIGATION OF THE VAN ALLEN BELT BY MEANS OF SATELLITES ON EQUATORIAL ORBITS. Pizzella, Guido (Univ., Rome). Ric. Sci. Riv., 36: 323-31(May 1966). (In Italian).

A brief review of the earth's radiation belt is given. Attention is called to the fact that detailed knowledge of the properties of trapped radiation is useful for the solution of problems still open in various fields of research, from cosmic rays to plasma physics. A satellite experiment is suggested for studying the problems of diffusion, acceleration and losses of the charged particles in the geomagnetic field. An equatorial orbit is preferred in such an experiment because of the special properties of the geomagnetic equatorial plane. This plane is a symmetry plane for the trapped radiation, and particles having their mirror points in this plane are trapped on particularly simple orbits. Also, the geomagnetic equator is the only plane where all trapped particles pass through. (auth)

37490 ORIGIN OF COSMIC RAYS. Burbidge, Geoffrey. Sci. Amer., 215: No. 2, 32-8(Aug. 1966).

Various possible sources of cosmic rays are considered. In particular the strong radio sources which contain immense fluxes of relativistic particles are discussed as contributors or major sources of cosmic rays. It is pointed out that if this viewpoint is correct then at least some cosmic rays are samples of material from other galaxies. (J.F.P.)

37491 PROBLEM OF DETECTING SOLAR NEUTRINOS. Bahcall, John N. (California Inst. of Tech., Pasadena); Davis, Raymond Jr. pp 241-3 of Stellar Evolution. Stein, R. F.; Cameron, A. G. W. (eds.). New York, Plenum Press, 1966.

The $^{37}Cl(\nu,e^-)^{37}Ar$ reaction is discussed for its usefulness for detecting solar neutrinos. (M.O.W.)

37492 PROCEEDINGS OF THE NINTH INTERNATIONAL CONFERENCE ON COSMIC RAYS, LONDON, SEPTEMBER 1965. VOLUMES 1 and 2. Stickland, A. C. (ed.). London, The Institute of Physics and The Physical Society, 1966. 1135p. 10 Pound, 10s. (CONF-650948(Vols. 1 and 2)).

The conference included 305 papers 20 of which were abstracted previously in NSA as 18: 24348, 19: 20880, 22763, 27116, 37500, 41306, 44970, 44972, 20: 4562, 6022, 7762, 11429 11525, 13604, 17418, 21544, 21545, 21547, 23935, and 23944. Separate abstracts were prepared for 285 papers. (J.F.P.)

For abstracts of individual papers see: 37095–37114, 37368–37380, 37460, 37493–37536, 37536–37719, 37786–37793, 37898–37911, 38110, and 38111.

37493 COSMIC RAYS AND THE INTERPLANETARY FIELD. Quenby, J. J. (Imperial Coll. of Science and Tech., London). pp 3-13 of Proceedings of the Ninth International Conference on Cosmic Rays. Vol. I. Stickland, A. C. (ed.). London, The Institute of Physics and The Physical Society, 1966.

A review is given of recent work, both experimental and theoretical, concerning the propagation of solar protons, the long-term modulation, the Forbush effect and the daily variation of intensity. (auth)

37494 BRIEF OUTLINE OF THE DEVELOPMENT OF COSMIC-RAY MODULATION THEORY. Parker, E. N. (Univ. of Chicago). pp 26-34 of Proceedings of the Ninth International Conference on Cosmic Rays. Vol. I. Stickland, A. C. (ed.). London, The Institute of Physics and The Physical Society, 1966.

The theory of the solar wind predicts that interplanetary space is filled with magnetic lines of force carried out by the wind in a basic spiral pattern from the sun. Small-scale irregularities in the basic pattern are expected. The recent space observations of the solar wind and field confirm this prediction. The effect of the magnetic field is to carry the galactic cosmic rays out of the inner solar system, into which they are diffusing through the small-scale irregularities in the field. Hence the theory of cosmic ray modulation is basically a problem in diffusion and convection. The elementary theory treats the diffusion as isotropic. The more complete treatment, using a tensor diffusion coefficient, was worked out recently. The solar wind and fields are expanding during the time that the individual cosmic ray particles are diffusing through them, with the result that particles are decelerated adiabatically. Solution of some simple examples shows that the typical cosmic ray particle observed at earth has spent a time of the order of days in the solar wind, and may have lost 5–20 per cent of its initial energy. The energy loss gives an intensity reduction which must be added to the cosmic ray density decrease from the outward sweeping fields. A review of the development and the present understanding of the basic theoretical processes involved in cosmic ray modulation by the fields in the solar wind is given. The more difficult task of constructing quantitative models from the observations is not taken up. (auth)

37495 PRELIMINARY RESULTS OF COSMIC-RAY STUDY FROM THE ARTIFICIAL EARTH'S SATELLITE PROTON-1. Grigorov, N. L.; Nesterov, V. E.; Radoport, I. D.; Savenko, I. A.; Skuridin, G. A. (Dept. of Nuclear Physics, Moscow). pp 50-2 of Proceedings of the Ninth International Conference on Cosmic Rays. Vol. I. Stickland, A. C. (ed.). London, The Institute of Physics and The Physical Society, 1966.

Preliminary results of measurements of the energy spectrum of primary cosmic rays and electrons are reported. (auth)

37496 PRIMARY ELECTRONS AND POSITRONS IN THE COSMIC RADIATION. Meyer, P. (Univ. of Chicago). pp 61-7 of Proceedings of the Ninth International Conference on Cosmic Rays. Vol. I. Stickland, A. C. (ed.). London, The Institute of Physics and The Physical Society, 1966.

The present status of investigations on the primary cosmic ray electron-positron component is summarized. The experimental methods which were applied in the study of primary electrons are discussed, and the experimental evidence concerning the energy spectrum, the flux and the charge composition of the electron component, including material available by August 1965 is presented. Finally, the implications of the experimental results on the question of the origin of the primary electrons and their relation to the particles which produce the nonthermal galactic radio emission are considered. (auth)

37497 11-YEAR COSMIC-RAY VARIATIONS. Dorman, I. V.; Dorman, L. I. pp 97-102 of Proceedings of the Ninth International Conference on Cosmic Rays. Vol. I. Stickland, A. C. (ed.). London, The Institute of Physics and The Physical Society, 1966.

Energy characteristics of the 11-year cosmic ray variations are determined from the data of the worldwide network of stations and using the data on the proton and α particle variations in the region of small rigidities. On the basis of the spherically symmetrical dynamic model of the 11-year variation, the electromagnetic conditions in interplanetary space are evaluated and the dimensions of the modulation region are determined. The expected variations in regions of various energies are analyzed for protons, α particles and electrons of galactic cosmic rays. The spectrum of cosmic ray rigidities beyond the modulation region outside the solar system is determined. It is shown that an essential part of the spectrum "bend" is due to the modulation in interplanetary space. Other possible causes of the spectrum "bend" are also discussed. The expected gradient of the cosmic ray intensity in interplanetary space is evaluated from modulation parameters depending on Z and on particle rigidity. The results obtained for the gradient are in agreement with the Mariner II data. Changes in the electromagnetic conditions in interplanetary space with decreasing solar activity are evaluated according to stratospheric measurements obtained in July 1963 and to IMP-I data. (auth)

37498 THEORETICAL COMPOSITION OF COSMIC RAYS OF SUPERNOVA ORIGIN. Colgate, S. A. (New Mexico Inst. of Mining and Tech., Socorro). pp 112-15 of Proceedings of the Ninth International Conference on Cosmic Rays. Vol. I. Stickland, A. C. (ed.). London, The Institute of Physics and The Physical Society, 1966.

The shock acceleration of the outer layers of a supernova star was identified before both with the total energy and energy spectrum of cosmic rays. The nuclear composition of these outer layers should be enriched above cosmic abundance in the elements up to and including the iron group owing to partial mixing with the highly evolved (thermonuclearly synthesized) core. Elements heavier than iron should not be present in a higher abundance than that accreted by the star. The shock acceleration does not allow mixing with the heavy elements produced in the interior of the star (rapid neutron capture, "r process") and furthermore the ion plasma wave dynamic friction in the shock is great enough to accelerate the ions without nuclear destruction. As a consequence a cosmic ray composition enriched up to and including iron is expected since the r process cannot occur in the material immediately behind the shock. The necessary neutron excess occurs, but the time available before expansion is too short to synthesize beyond the first magic number peak. An experiment is undertaken to search for cosmic rays $Z \geq 50$ by identifying their Cherenkov radiation in the plastic backing of photographic film. (auth)

37499 ACCELERATION OF COSMIC-RAY ELECTRONS. Hayakawa, S.; Obayashi, H. (Nagoya Univ., Japan). pp 116-18 of Proceedings of the Ninth International Conference on Cosmic Rays. Vol. I. Stickland, A. C. (ed.). London, The Institute of Physics and The Physical Society, 1966.

The energy spectrum of galactic electrons is discussed as a means of obtaining information about the galactic acceleration, as well as the solar modulation of cosmic rays. Recent observations of cosmic ray electrons cover an energy range of 3 to 3000 Mev, and provide an important clue to the understanding of the acceleration and modulation mechanisms because of the large Z/A value compared with the nuclear components. The knock-on electrons produced in galactic space and the secondary electrons following nuclear interactions caused by cosmic ray protons are considered as well-defined components. The effect of the Fermi acceleration acting on these electrons in interstellar space is estimated for several assumed values of efficiency $a\tau$ with energy loss due to ionization, synchrotron radiation, and finite confinement time. The solar modulation is calculated based on Parker's picture when referring to the recent data on protons and alphas. Taking these modifications into account, a possible upper limit for the galactic acceleration efficiency is found to be $0.5 \lesssim a\tau \lesssim 2$. In order to explain the large flux of low energy electrons some primarily injected electrons seem to be necessary. (auth)

37500 OBSERVATION OF THE ENERGY SPECTRUM OF GALACTIC X RAYS. Hayakawa, S.; Matsuoka, M.; Yamashita, K. (Nagoya Univ., Japan). pp 119-22 of Proceedings of the Ninth International Conference on Cos-

mic Rays. Vol. I. Stickland, A. C. (ed.). London, The Institute of Physics and The Physical Society, 1966.

Observations of galactic x rays in two recent rocket flights are reported. The energy spectrum of isotropic x rays with energies between 5 and 20 kev was obtained with a scintillation counter borne on a Lambda rocket. The energy spectra of Sco X-1, Cyg X-1 and the region near the galactic center in the energy range between 2 and 16 kev were measured with proportional counters borne on a Kappa rocket. The shape of the spectra is interpreted in terms of the thermal radiation at temperatures of $(0.5-1)\times10^{8}$°K, depending on the component. It is suggested that x ray sources are supernova remnants which are active for x-ray emission much longer than for optical and radio emission. The contribution of such sources from all galaxies is able to account for the observed intensity of isotropic x rays. (auth)

37501 GENERAL DYNAMICAL EFFECTS OF COSMIC RAYS IN THE GALAXY. Parker, E. N. (Univ. of Chicago). pp 126-8 of Proceedings of the Ninth International Conference on Cosmic Rays. Vol. I. Stickland, A. C. (ed.). London, The Institute of Physics and The Physical Society, 1966.

Cosmic rays constitute an extremely hot tenuous gas throughout the galaxy whose weight is negligible but whose pressure is considerable. The cosmic ray gas is tied to the ordinary interstellar gas by interstellar magnetic fields of $10^{-6}-10^{-5}$ gauss, forming a composite interstellar "fluid" with dynamical properties differing qualitatively from ordinary gases. There are three modes of hydromagnetic wave propagation. The two slowest modes bear a resemblance to the conventional fast and slow modes. The third is the suprathermal mode with a velocity of propagation which is a significant fraction of the speed of light. The cosmic ray gas appears to be the principal source of stirring to the interstellar medium. It is possible to construct static equilibrium configurations for the thermal interstellar gas and field based on the usual assumption that the interstellar fluid is confined to the disk of the galaxy by the galactic gravitational field. But adding the cosmic ray gas eliminates any true hydrostatic equilibrium. The result is only a quasi-static equilibrium inside the disk with a rapid inflation ($10-100$ km sec^{-1}) of magnetic fields out of both surfaces of the disk. The question then arises as to what extent a galactic halo may be solely a manifestation of the inflation of galactic fields by cosmic rays. (auth)

37502 ORIGIN OF EXTRAGALACTIC COSMIC RAYS. Aizu, K.; Taketani, M.; Fujimoto, Y.; Hasegawa, H.; Kawabata, K. (Tokyo Univ.). pp 129-31 of Proceedings of the Ninth International Conference on Cosmic Rays. Vol. I. Stickland, A. C. (ed.). London, The Institute of Physics and The Physical Society, 1966.

A theory of the explosion and evolution of galaxies, on which the study of the origin of extragalactic cosmic rays has to be based, is developed. For this purpose a new diagram, the (L,L/V) diagram is introduced where L is the radio luminosity and L/V the volume emissivity of galaxies and supernova remnants. Two evolutional sequences of galaxies, the normal sequence and the giant sequence, and one sequence of supernova of type II were found in this diagram. Analysis of these sequences suggested an existence of a similarity relation among the various explosion phenomena. This similarity relation permits an estimation of the contribution of cosmic rays of extragalactic origin. A similar argument was applied to the extragalactic x ray sources. (auth)

37503 EXPANSION OF A RELATIVISTIC GAS INTO INTERGALACTIC SPACE. Gold, T. (Cornell Univ., Ithaca, N. Y.). pp 132-4 of Proceedings of the Ninth International Conference on Cosmic Rays. Vol. I. Stickland, A. C. (ed.). London, The Institute of Physics and The Physical Society, 1966.

Radio sources have shapes in the radio band that suggest that they have resulted from clouds of relativistic gas expanding out into space from an originating galaxy. The energy content of this gas is so great that an origin in a massive galaxy has to be assumed whatever method of production there might be. There is thus the problem of an expansion of such a gas cloud, first through the gas of the parent galaxy, and then through the low density gas of intergalactic space. The modes of expansion and the resulting shapes are discussed. The statistics of the radio source distribution suggest that such clouds have swept over most of the galaxies. The question of the proportion of space filled with cosmic rays is discussed in the light of this information. (auth)

37504 SOLAR AND SIDEREAL DAILY VARIATIONS OF COSMIC-RAY INTENSITY AT A DEPTH OF 60 m.w.e. UNDERGROUND IN LONDON. Thambyahpillai, T.; Dutt, J. C.; Mathews, T.; Romero, F. (Imperial Coll. of Science and Tech., London). pp 138-40 of Proceedings of the Ninth International Conference on Cosmic Rays. Vol. I. Stickland, A. C. (ed.). London, The Institute of Physics and The Physical Society, 1966.

Cosmic ray measurements were made at a depth of 60 Mw(e) in London using two vertical semicubical telescopes from November 1960 onwards and six telescopes from August 1963. The weighted mean values of the data covering three complete years were analyzed for the solar, apparent sidereal and anti-sidereal daily variations whose first harmonics are given. The maximum value for the diurnal variation in stratospheric temperature set by the solar diurnal variation in cosmic ray intensity is about 1.0 degC. Assuming that the anti-sidereal variation arises from amplitude modulation of the solar variation, the true sidereal diurnal variation was estimated to have an amplitude of 0.027% with a time of maximum at 19h 30m local sidereal time. There appear to be systematic differences between the observations of the sidereal daily variation in the northern and southern hemispheres and these are briefly discussed. (auth)

37505 TWO-WAY SIDEREAL ANISOTROPY VERSUS SEASONAL MODULATION. Jacklyn, R. M. (Dept. of External Affairs, Melbourne. Univ. of Tasmania, Hobart). pp 141-3 of Proceedings of the Ninth International Conference on Cosmic Rays. Vol. I. Stickland, A. C. (ed.). London, The Institute of Physics and The Physical Society, 1966.

Some distinctive characteristics of observed daily variations of cosmic ray intensity in sidereal time, as relating to primaries of moderate energy, are reviewed. On the basis of the observations the evidence for a diffuse two-way sidereal anisotropy is briefly discussed, as against an explanation based on seasonal modulation of a daily variation in solar time. In addition to evidence previously reported, results obtained at Hobart with two underground counter telescopes, one scanning a latitude band in a different hemisphere from the other, indicate that the sidereal effect could not possibly be due to a solar daily variation experiencing seasonal modulation connected with the tilt of the earth's axis. On the other hand, the first and second harmonics of best fit to data from underground telescopes scanning widely separated latitude zones are those to be expected from a simple two-way sidereal anisotropy, and lead to a value for the declination. (auth)

37506 POSSIBILITIES OF ISOLATION OF SIDEREAL TIME COSMIC-RAY INTENSITY VARIATIONS. Dorman, L. I.; Inozemtseva, O. I.; Mazaryuk, E. A.; Solov'eva, Z. I. (Izmiran, Moscow). pp 144-6 of Proceedings of the Ninth International Conference on Cosmic Rays. Vol. I. Stickland, A. C. (ed.). London, The Institute of Physics and The Physical Society, 1966.

The possibility of isolating the sidereal-diurnal wave is examined. Methods for taking into account the false effect in analysis of the sidereal-diurnal variations are elaborated on the basis of simultaneous amplitude-phase modulation of the solar-diurnal variations. Data from the network of stations for the neutron and the hard components are analyzed for the period of decreasing and minimum solar activity. (auth)

37507 COSMIC RAY CHANGES DURING A SOLAR CYCLE. Neher, H. V. (California Inst. of Tech.,

Pasadena); Anderson, H. R. pp 153-6 of Proceedings of the Ninth International Conference on Cosmic Rays. Vol. I. Stickland, A. C. (ed.). London, The Institute of Physics and The Physical Society, 1966.

Data from balloon flights covering the past three solar cycles are presented. While the last cycle was covered much more completely, sufficient data exist from the period around the 1937 and 1947 maxima to say something about the behavior of cosmic rays during a typical solar cycle. The hysteresis loop obtained, when cosmic ray intensity at high altitudes and latitudes is plotted against Zurich sunspot number for the large atypical 1958 solar cycle, is not evident in the data for the 1937 and 1947 cycles. It is suggested that Zurich sunspot numbers may not always be a good measure of the effectiveness of the modulating mechanism. The cosmic ray intensity in space, as measured by the ion chamber on Mariner II and IV, increased by 41 per cent from August 1962 to December 1964. This increase can be reconciled with high altitude balloon flights at Thule, Greenland, for the same periods only if one assumes relatively large increases in low energy (<100 Mev for protons) particles in the intervening two years. (auth)

37508 STUDIES OF PRIMARY COSMIC RAYS WITH IONIZATION CHAMBERS. Kane, S. R. (Univ. of Minnesota, Minneapolis); Winckler, J. R.; Arnoldy, R. L. pp 157-60 of Proceedings of the Ninth International Conference on Cosmic Rays. Vol. I. Stickland, A. C. (ed.). London, The Institute of Physics and The Physical Society, 1966.

It is shown that the response ot ion chambers in the atmosphere and in free space is peaked over narrow rigidity intervals; these are 1.5–2.5 Gv, 2.5–3.5 Gv, and 3.0–4.0 Gv for free space, high latitude balloon and Minneapolis balloon chambers, respectively. Using these results and measurements made with the Pioneer V, Mariner II and OGO-A ion chambers, the rigidity dependence of the long term modulation during 1960–1965 is found to be consistent with the form $P^{-\beta}$, where $\beta \simeq 0.8$. The solar cycle effect at 10 g cm^{-2} as measured by balloon flights at Minneapolis and high latitudes is presented. A phase lag of about one year between the total ionization and sunspot numbers exists throughout the cycle. A correlation plot of the high latitude balloon ionization rate and the Deep River neutron monitor for 1958–1965 shows a smooth relation between the two rigidity ranges. The rigidity dependence of the short-term modulation as measured with space ion chambers in several cases is shown to be different from the long-term. The "turn-up" in ionization in the atmosphere at high latitudes observed at solar minimum can be attributed to the presence of low energy S nuclei in the primary radiation at solar minimum. The peak ionization intensity of the present solar minimum appears to have occurred in May 1965. (auth)

37509 SOLAR CYCLE MODULATION OF COSMIC RAYS. Duggal, S. P.; Nagashima, K.; Pomerantz, M. A. (Franklin Inst., Swarthmore, Pa.). pp 161-4 of Proceedings of the Ninth International Conference on Cosmic Rays. Vol. I. Stickland, A. C. (ed.). London, The Institute of Physics and The Physical Society, 1966.

A detailed comparison of observations with the predictions of alternative theories of the long term modulation was carried out. The solar wind and energy modulation models are both consistent with the available data obtained with spacecraft and balloons. Various representations were considered in an attempt to establish the relative superiority of one mechanism over another, and a new criterion is suggested as the most suitable. Calculations of the unmodulated proton and alpha particle spectra indicate that, even at solar minimum, modulation still occurs. (auth)

37510 INVESTIGATION OF THE MODULATION OF THE PRIMARY COSMIC RADIATION USING AN AIRBORNE DETECTOR. Bewick, A.; Hynds, R. J.; Riddle, N. A. (Imperial Coll. of Science and Tech., London). pp 165-9 of Proceedings of the Ninth International Conference on Cosmic Rays. Vol. I. Stickland, A. C. (ed.). London, The Institute of Physics and The Physical Society, 1966.

During the period 1962–65 a number of latitude surveys were made using a scintillator telescope flown at an atmospheric depth of 145 g cm^{-2}. The results of these surveys are reported. By comparison with the results obtained from a detector flown in the satellite Ariel I, a yield function for the above atmospheric depth was constructed and used to relate the results of the surveys to the primary cosmic radiation. During the flights some discrepancies in the Quenby-Wenk rigidity cut-offs were observed. These are discussed and corrections made for them. The observed primary cosmic ray modulation is compared with the predictions of some current theoretical models. (auth)

37511 GALACTIC COSMIC RAYS IN THE SOLAR SYSTEM. Sarabhai, V.; Subramanian, G. (Physical Research Lab., Ahmedabad, India). pp 170-2 of Proceedings of the Ninth International Conference on Cosmic Rays. Vol. I. Stickland, A. C. (ed.). London, The Institute of Physics and The Physical Society, 1966.

In consideration of the zonal distribution of activity on the sun, a new model is proposed for the diffusion of galactic cosmic rays in the solar system. It is suggested that the processes responsible for the 11-year modulation produce conditions such that the density of galactic cosmic rays on both sides of the solar equatorial plane is depressed with respect to the density along the plane. Thus at 1 A.U. there is generally both a radial gradient of intensity as well as a gradient normal to the equatorial plane. Magnetic field irregularities along the spiralling field lines permit the earth to sample the cosmic ray intensity characteristic of interplanetary space at high heliolatitudes. Cosmic ray intensity measured on the earth can then be related to the intensity N_θ due to diffusion along the field lines at each heliolatitude θ and to a factor η_θ which determines, in the neighborhood of the earth, the effectiveness of transverse diffusion from higher heliolatitudes. N_θ is connected with processes occurring at large distances from the sun with a long time constant of the order of months, while η_θ is connected with the distribution of magnetic field irregularities in the interplanetary space in the neighborhood of the earth. The model appears promising for understanding a number of observed cosmic ray effects such as the deficiency of cosmic ray intensity along the garden-hose direction, the day to day changes of the energy spectrum of anisotropy, the 27-day variations and some aspects of the 11-year modulation. (auth)

37512 MODULATION OF COSMIC RAYS BY AN ELECTRIC FIELD. Freier, P. S.; Waddington, C. J. (Univ. of Minnesota, Minneapolis). pp 176-9 of Proceedings of the Ninth International Conference on Cosmic Rays. Vol. I. Stickland, A. C. (ed.). London, The Institute of Physics and The Physical Society, 1966.

A modulation model is discussed which assumes that the decreased intensity of the cosmic radiation is due to the energy loss experienced by particles passing through electric fields in the solar system. The model is mathematically equivalent to a heliocentric electric field. By assuming that the particle source spectra are power laws in total energy per nucleon, the modulation of the differential and integral intensities of protons and helium nuclei is calculated. The predicted modulation observed by sea-level neutron monitors and meson detectors is also calculated and is given as a function of cut-off rigidity. These calculations are compared with the measurements made during the last solar cycle. (auth)

37513 LONG-TERM MODULATION OF THE COSMIC-RAY INTENSITY. Quenby, J. J. (Imperial Coll. of Science and Tech., London). pp 180-3 of Proceedings of the Ninth International Conference on Cosmic Rays. Vol. I. Stickland, A. C. (ed.). London, The Institute of Physics and The Physical Society, 1966.

Axford has recently described the anisotropic diffusion of a nonrelativistic cosmic ray gas in the interplanetary medium in terms of an integral of the Boltzmann equation. This treatment is considered here for the relativistic particles and it is suggested that experimental measurements are consistent with the presence of a boundary to the modulation region lying roughly between 6 A.U and 12 A.U. (auth)

37514 RIGIDITY SPECTRA OF PRIMARY COSMIC RAYS IN THE LAST SOLAR CYCLE. Nerurkar, N. W. (Physical Research Lab., Ahmedabad, India). pp 184-5 of Proceedings of the Ninth International Conference on Cosmic Rays. Vol. I. Stickland, A. C. (ed.). London, The Institute of Physics and The Physical Society, 1966.

Rigidity spectra of primary cosmic radiation, derived from the observations of balloon-borne ion chambers and GM counters at middle and high latitudes during the last cycle of solar activity, are presented. Spectra obtained from the data of the two independent instruments are found to agree well with each other. The exponent of the integral rigidity spectrum of the type $(\text{rigidity})^{-\chi}$ changes systematically between -1.4 ± 0.05 and -1.6 ± 0.05 at 10 Gv during the last solar cycle. The cosmic ray spectrum at the solar minimum of 1964 is quite similar to that of the previous solar minimum of 1954. (auth)

37515 VARIATION OF THE COSMIC-RAY INTENSITY DURING THE ELEVEN-YEAR SOLAR CYCLE. Rose, D. C.; Katzman, J. (National Research Council, Ottawa). pp 186-9 of Proceedings of the Ninth International Conference on Cosmic Rays. Vol. I. Stickland, A. C. (ed.). London, The Institute of Physics and The Physical Society, 1966.

The intensity changes of both the nucleon and meson components of cosmic rays were measured at Ottawa, geomagnetic latitude 56.8°N, since 1954 at Churchill, geomagnetic latitude 68.7°N, and at Resolute, geomagnetic latitude 82.9°N, since 1957. The difference in intensity at Ottawa between solar minimum in 1954 and maximum in 1958 is 25% of the value at solar minimum in the case of the nucleon component and 5% in the case of the meson component. All three stations are north of the latitude effect knee where the geomagnetic rigidity cut-off is well below the cut-off due to the atmospheric absorption. Yet the increase in intensity during decrease in solar activity from 1958 until the end of 1964 is not the same at the three stations. The differences cannot be attributed to any latitude effect and the two components do not behave in the same way. Some form of asymmetry in the dissipation of the modulating mechanism is suggested but no completely acceptable explanation was found. (auth)

37516 RIGIDITY DEPENDENCE OF THE INTENSITY VARIATION DURING THE SOLAR CYCLE. Hatton, C. J.; Marsden, P. L; Schefer, P. V. (Univ. of Leeds, Eng.). pp 193-6 of Proceedings of the Ninth International Conference on Cosmic Rays. Vol. I. Stickland, A. C. (ed.). London, The Institute of Physics and The Physical Society, 1966.

From a comparison of the variation of the intensity ot the nucleonic component recorded at Huancayo and Leeds during the past solar cycle, it is concluded that the intensity of the high rigidity primary particles ($\gtrsim$12 Gv) is not uniquely related to those of low rigidity ($\sim$1 Gv). (auth)

37517 DIFFUSION MECHANISM OF COSMIC-RAY DAILY VARIATION. Krimsky, G. F. (Inst. of Cosmophysical Research and Aeronomy, Academy of Sciences, USSR). pp 197-8 of Proceedings of the Ninth International Conference on Cosmic Rays. Vol. I. Stickland, A. C. (ed.). London, The Institute of Physics and The Physical Society, 1966.

The formation of cosmic ray anisotropy by the solar wind is considered. It is shown that if the magnetic field has a regular component, the anisotropy should have a maximum which is normal to the direction towards the sun and more eastern. The amplitude of anisotropy is calculated as a function of wind velocity and the degree of magnetic field irregularity. The degree of irregularity is characterized by the ratio of the coefficient of cosmic ray diffusion perpendicular to the field to that parallel. If the influence of the induced electric field and the deceleration of cosmic rays by the wind are considered it is found that there will be no anisotropy if the wind is spherically symmetrical even with an irregular isotropic magnetic field. If the wind is restricted to low heliolatitudes, the anisotropy of cosmic rays should be observed on the side of the sun. (auth)

37518 SIMPLE CONTRIBUTION TO THE THEORY OF THE ANISOTROPY OF COSMIC RAYS. Houghton, M. J. (Imperial Coll. of Science and Tech., London). pp 199-200 of Proceedings of the Ninth International Conference on Cosmic Rays. Vol. I. Stickland, A. C. (ed.). London, The Institute of Physics and The Physical Society, 1966.

Simplicity is obtained by assuming that the first invariant is preserved, that the magnetic field is spiral in the ecliptic and the solar wind radial and that $E = -V \times B$. A cosmic ray particle mirroring near the sun has gradient and curvature drifts normal to the ecliptic. The displacement of the guiding center between inward and outward crossings of the earth's orbit is of the order of two gyroradii and is in the opposite direction to the electric field for positive particles. The day to day variations of this drift are not yet fully investigated; an assumption is needed about the gradient of the incoming cosmic rays normal to the ecliptic. Computations of the drift are presented for a typical field. (auth)

37519 SOLAR DIURNAL VARIATION OF THE COSMIC-RAY INTENSITY. Kitamura, M. (Meteorological Research Inst., Tokyo). pp 201-3 of Proceedings of the Ninth International Conference on Cosmic Rays. Vol. I. Stickland, A. C. (ed.). London, The Institute of Physics and The Physical Society, 1966.

In order to investigate the mechanism of the diurnal variation of cosmic rays the world wide data of cosmic neutron intensities obtained by the International Geophysical Year network are analyzed. Subsequently the discussion of the cosmic ray anisotropies in interplanetary space is carried out on the basis of observed facts of daily variation of cosmic ray neutron intensities both at sea level and at mountain altitude and by the application of a quantitative method developed by Nagashima et al., (1961) to study cosmic ray anisotropy. (auth)

37520 CHARACTERISTICS OF ANISOTROPY OF GALACTIC COSMIC RAYS DURING THE SOLAR CYCLE. Sarabhai, V.; Subramanian, G. (Physical Research Lab., Ahmedabad, India). pp 204-7 of Proceedings of the Ninth International Conference on Cosmic Rays. Vol. I. Stickland, A. C. (ed.). London, The Institute of Physics and The Physical Society, 1966.

Applying the method of best fit to the daily variation of cosmic ray intensity observed by neutron monitors at Huancayo, Churchill, Mawson and Mt. Norikura and cubical meson telescopes at Mawson and Churchill, the amplitude, the directions in space of maximum and minimum intensity and the energy spectrum of variation of the anisotropy of galactic cosmic rays are determined for each day from 1958 to 1963. Out of 36 combinations of assumed values for x and E_{min}, in the relations $\delta D(E)/D(E) = aE^{x}$ and $\delta D(E)/D(E) = 0$ for $E \leq E_{min}$, it is found that four combinations account for more than 70 per cent of the total days considered. They are listed. Azimuthal streaming of galactic cosmic rays by itself is insufficient to account for the anisotropy on most days. The direction of maximum of the anisotropy usually lies between 1200 and 1800 hours. The deficiency of the cosmic ray intensity along the direction of the spiralling magnetic field line is observed particularly prominently in type A and B days. With declining solar activity, the frequency of days having a variation spectrum of type D decreases, while the frequency of days of type A increases. It is suggested that this is indicative of a weakening of the strength of the field and/or a reduction of the scale length of magnetic field irregularities in sectors of interplanetary space distinguished by the two types of energy spectrum of anisotropy. (auth)

37521 SEMI-DIURNAL ANISOTROPY OF THE COSMIC RADIATION. Ables, J. G.; McCracken, K. G.; Rao, U. R. (Southwest Center for Advanced Studies, Dallas, Tex.). pp 208-12 of Proceedings of the Ninth International Conference on Cosmic Rays. Vol. I. Stickland, A. C. (ed.). London, The Institute of Physics and The Physical Society, 1966.

Using data from 14 different neutron monitors, the semi-diurnal anisotropy of the cosmic radiation during the period 1953–1965 was investigated. Numerical filter techniques, consisting of numerical heterodyne filtration followed by

phase and amplitude demodulation (complex demodulation) were employed. This process reduces to ordinary harmonic analysis as a special case. The effective filter response function for harmonic analysis is compared with the more desirable response functions employed in this investigation. Phase and amplitude distribution histograms for each station and year were constructed which, when fully corrected for the effects of geomagnetic bending of primary trajectories, indicate a consistent semi-diurnal anisotropy having an amplitude of approximately 0.1% and maxima along a line 60° west of the earth-sun line. A study of the energy dependence of this anisotropy was made which, though not conclusive, indicates that the anisotropy may be energy dependent. (auth)

37522 SURVEY OF THE DIURNAL ANISOTROPY. McCracken, K. G.; Rao, U. R. (Southwest Center for Advanced Studies, Dallas, Tex.). pp 213-18 of Proceedings of the Ninth International Conference on Cosmic Rays. Vol. I. Stickland, A. C. (ed.). London, The Institute of Physics and The Physical Society, 1966.

It is shown that the observed diurnal variation of the cosmic radiation exhibits an impressive agreement with the predictions of the Axford-Parker model of the diurnal anisotropy. The energy dependence, the observed phase, and the dependence upon declination are all in complete agreement with the theory. However, the observed average diurnal variation amplitude is approximately 0.6 of the value predicted by the theory. It is shown that the observed amplitude of the diurnal variation has a broad frequency distribution, and that the characteristics of the variation are consistent with the Axford-Parker theory for all amplitudes less than the theoretical value. It is suggested that the variable amplitude is due to the build-up of a time varying cosmic ray density gradient normal to the ecliptic, the magnitude of the gradient depending upon the extent to which cosmic rays suffer scattering in the interplanetary magnetic fields. It is shown that the diurnal anisotropy was invariant during the period 1957–1965, and that, in particular, it did not change during the sunspot minimum 1963–1965. It is suggested that the normal state of the diurnal anisotropy is summarized by energy independence, variation as the cosine of the declination, a maximum flux, 3.8×10^{-3} times the isotropic flux incident from a direction 90° to the east of the earth-sun line. It is suggested that the 22-year variation in the characteristics of the diurnal variation reported previously can best be regarded as transient deviations from the above situation. The Axford-Parker theory is shown to imply the existence of a semi-annual modulation of the diurnal variation amplitude, and an annual, energy independent variation of the isotropic cosmic ray flux of peak to peak amplitude 0.61 sin ξ_v per cent (where ξ_v is the mean asymptotic co-latitude of viewing of the detector). (auth)

37523 VARIATIONS OF THE LATITUDE DEPENDENCE OF COSMIC-RAY DIURNAL VARIATIONS. Murakami, K.; Kudo, S. (Inst. of Physical and Chemical Research, Tokyo). pp 219-20 of Proceedings of the Ninth International Conference on Cosmic Rays. Vol. I. Stickland, A. C. (ed.). London, The Institute of Physics and The Physical Society, 1966.

The difference of phases and the ratio of amplitudes of diurnal variations between high and low latitude are studied, using the data of the nucleonic component observed at several stations. The correlation of the mean phase difference to the amplitude ratio shows the following: the primary rigidity spectrum of diurnal variations varies, on the average, with the change of the exponent of the spectrum, while the lower limit of rigidity is nearly constant; the mean phase difference is dependent not only on the spectrum but also on the direction of the anisotropy. (auth)

37524 ON THE VARIATION OF THE TIME OF MAXIMUM IN THE DIURNAL VARIATION OF COSMIC-RAY NEUTRON INTENSITY DURING IGY AND IGC. Kanno, T.; Ishida, Y.; Iseki, S. (Fukushima Univ., Japan). pp 221-3 of Proceedings of the Ninth International Conference on Cosmic Rays. Vol. I. Stickland, A. C. (ed.). London, The Institute of Physics and The Physical Society, 1966.

The relation between T_{mn} (the local time of maximum in the diurnal variation of cosmic ray neutron intensity) and the relative sunspot number was discussed for the data obtained during the period after IGC (from January 1959 to December 1961). The results obtained from the data during the period after IGC appeared to be consistent with the following results obtained from the data of IGY, i.e., T_{mn} seems to advance in the low and middle latitudes and to delay in both polar regions and the southern Atlantic Ocean, as the solar phenomena become active, cosmic particles may be modulated within the solar plasma existing relatively near the earth, the lines of force of the geomagnetic field may be assumed to bend westwards in outer space relative to the earth. (auth)

37525 PERIODIC COSMIC-RAY VARIATIONS AND THEIR CHANGE DURING THE CYCLE OF SOLAR ACTIVITY. Kolomeets, E. V.; Sergeeva, G. A.; Nemolochnov, A. N.; Chumbalova, R. A.; Zusmanovich, A. G. (Kirov Kazakh State Univ., Alma-Ata, USSR). pp 224-8 of Proceedings of the Ninth International Conference on Cosmic Rays. Vol. I. Stickland, A. C. (ed.). London, The Institute of Physics and The Physical Society, 1966.

Solar-diurnal and semi-diurnal variations in the neutron component were studied using data obtained from a worldwide network of stations during the period July 1957-June 1965. The amplitude, phase, and energy spectrum of the diurnal variation and their dependence on the cycle of solar activity are investigated. It was concluded that the amplitude of the first harmonic increases as solar activity decreases for stations with cut-off energies from 2 to 2.5 Bev and decreases at middle and low latitudes; the energy spectrum of the solar-diurnal anisotropy can be expressed in the form $\delta D(\epsilon)/D(\bar{\epsilon}) = a\epsilon^{-\gamma}$, where γ is always 0.4–0.5. The coefficient a decreases as solar activity falls. The seasonal effect of solar-diurnal anisotropy with either one or two maxima was detected for different years of solar activity. No dependence of semi-diurnal variation on time (amplitude and phase) was observed. The investigation of the data of μ mesons coming from the south, the north, the east and the west, and falling vertically during the period October 1963 – June 1965 revealed a prominent sidereal-diurnal variation. The amplitude and phase of the variation were determined. Cosmic ray variations for the period of 27 days and the extra flux of particles due to solar activity decrease were analyzed using stratospheric and ground-level data. The amplitudes, energy spectra of 27-day variations and extra flux particles were calculated, their dependence on time being shown. The effects observed were interpreted. (auth)

37526 SOME RESULTS OF STUDIES OF THE SOLAR-DIURNAL VARIATION OF COSMIC RAYS DURING THE IGY PERIOD. Vladimirskii, B. M.; Pankratov, A. K.; Stepanyan, A. A. (Crimean Astrophysical Observatory, USSR). pp 229-30 of Proceedings of the Ninth International Conference on Cosmic Rays. Vol. I. Stickland, A. C. (ed.). London, The Institute of Physics and The Physical Society, 1966.

The parameters of the solar-diurnal variation were found from neutron monitor data for the period of July 1957–December 1958 by the method of construction of the directional intensity. Another region of the relatively stable phases in 02h–06h L.T. was revealed in the phase frequency distribution in addition to the main maximum of the first harmonic. The change of phase occurs sometimes by a jump. Apparently the phase jumps shown by the analysis take place in times of replacement of corpuscular streams. Large amplitudes of the first harmonic of the diurnal variation are connected mainly with sudden commencement (sc) type magnetic storms. It was found that there are two types of sc magnetic storms. For the first type the maximum amplitude occurs before the sc; for the second type it occurs after the sc. The amplitude increases by about 0.35% on average and the duration of this increase is only about one day. The type-IV radio bursts not followed by sc magnetic storms influence the amplitude of the first harmonic of the diurnal variation. It is interesting to note that the ratio of the second mean to the first mean

harmonic for the IGY period according to the data is about three times greater than that according to other studies. It may suggest that the amplitude of the second harmonic is comparable with half of the first in the source of the diurnal variation. (auth)

37527 DIURNAL VARIATION DURING THE PAST SOLAR CYCLE. Faller, A. M.; Marsden, P. L. (Univ. of Leeds, Eng.). pp 231-3 of Proceedings of the Ninth International Conference on Cosmic Rays. Vol. I. Stickland, A. C. (ed.). London, The Institute of Physics and The Physical Society, 1966.

The solar diurnal variation of the nucleonic component of the cosmic radiation from 1957 to 1962 was studied using data from 15 neutron monitor stations. It is concluded that the amplitude and phase of the diurnal wave have not changed significantly during the period considered. (auth)

37528 ASYMMETRIC SOLAR WIND IN CONNECTION WITH THE 27-DAY MODULATION OF THE INTENSITY AND ANISOTROPY OF COSMIC RAYS. Alania, M. V.; Dorman, L. I.; Shatashvili, L. Kh. (Inst. of Geophysics, Academy of Sciences, Georgian SSR. Izmiran, Moscow). pp 235-8 of Proceedings of the Ninth International Conference on Cosmic Rays. Vol. I. Stickland, A. C. (ed.). London, The Institute of Physics and The Physical Society, 1966.

The study of the 27-day modulation of the intensity and anisotropy of cosmic rays gives valuable information on the character of the heliolongitude asymmetry of the radial flux of magnetic inhomogeneities from the sun, and of the asymmetry of distribution of the large scale interplanetary magnetic fields. The 27-day modulation of the solar-diurnal variation of the cosmic neutron component according to observational data from Sulphur Mountain, Climax, Zugspitze, Norikura and Huancayo stations for the period from July 1957 to June 1958 is investigated. The anisotropy modulation is stable during eight revolutions, having a depth of about 40% of the 24-hour harmonic and a complete change of phase of about three hours. It is shown that the end of the solar-diurnal variation vector rotates, the complete revolution taking about 27 days. It is found that at Huancayo station this rotation is clockwise whereas at the rest of the stations it is anticlockwise. The 27-day intensity modulation was investigated using the data of the neutron component observations at Climax and Norikura stations from the period of International Geophysical Year (IGY) onwards. It is shown that the change in the 27-day cosmic intensity variation with solar activity is of helical character if the 27-day wave vectors are plotted on the 27-day dial. In this case the period of the spiral is about 12–18 months and its radius when going from the maximum to the minimum of solar activity decreases significantly from about 1% to almost zero. (auth)

37529 INFLUENCE OF THE CHANGES IN EARTH'S HELIOLATITUDE ON THE COSMIC-RAY INTENSITY IN 1963-1964 AND EVALUATION OF THE COSMIC-RAY INTENSITY GRADIENT PERPENDICULAR TO THE ECLIPTIC PLANE. Dorman, L. I.; Fischer, S. (Moscow State Univ.). pp 239-42 of Proceedings of the Ninth International Conference on Cosmic Rays. Vol. I. Stickland, A. C. (ed.). London, The Institute of Physics and The Physical Society, 1966.

In the presence of the cosmic ray intensity gradient perpendicular to the plane of the solar equator the intensity modulation caused by the inclination of the ecliptic plane to the plane of the solar equator should appear. Various versions of this modulation are compared with observations at eleven stations in 1963–1964. It is shown that during this period two regions of decreased intensity existed near the solar equator, these regions corresponding to the active regions in the northern and southern hemispheres of the sun. (auth)

37530 RIGIDITY DEPENDENCE OF THE COSMIC-RAY DIURNAL VARIATION DURING FORBUSH DECREASE. Ueno, H. (Nagoya Univ., Japan). pp 243-5 of Proceedings of the Ninth International Conference on Cosmic Rays. Vol. I. Stickland, A. C. (ed.). London, The Institute of Physics and The Physical Society, 1966.

The variation of the rigidity dependence of the cosmic ray anisotropy during the development of the cosmic ray storm is discussed. By using spherical harmonics, the latitude dependence of the diurnal variation of the bi-hourly intensity of neutron monitor data observed simultaneously at about 30 stations is obtained for several phases of Forbush decrease. On the other hand, assuming the single anisotropy defined by a rigidity spectrum with three parameters, theoretical latitude dependence curves are calculated using the same method of spherical harmonics. Then the most suitable values of these parameters are determined by comparison of the calculated and observed latitude dependences. (auth)

37531 FIRST AND SECOND SPHERICAL HARMONICS OF THE DAILY VARIATIONS OF COSMIC RAYS. Kuzmin, A. I.; Krimsky, G. F.; Altukhov, A. M.; Krivoshapkin, P. A.; Philippov, V. A.; Skripin, G. V.; Chirkov, N. P. (Inst. of Cosmophysical Research and Aeronomy, Academy of Sciences, USSR). pp 246-8 of Proceedings of the Ninth International Conference on Cosmic Rays. Vol. I. Stickland, A. C. (ed.). London, The Institute of Physics and The Physical Society, 1966.

The first spherical harmonic in the distribution of cosmic rays for different energy intervals was calculated using the data of crossed telescopes located in Yakutsk. A considerable change in the distribution depending on solar cycle was discovered. The contribution of daily oscillations of atmospheric temperature to the observed variations is calculated independently of direct measurements of these oscillations. (auth)

37532 27-DAY AND OTHER CYCLIC VARIATIONS OF COSMIC-RAY INTENSITY. Basilevskaya, G. A. (Lebedev Inst. of Physics, Moscow); Charakhch'yan, T. N. pp 249-50 of Proceedings of the Ninth International Conference on Cosmic Rays. Vol. I. Stickland, A. C. (ed.). London, The Institute of Physics and The Physical Society, 1966.

Using the periodogram method, 27-day variations of cosmic ray intensity in the stratosphere for the period from July 1957 to December 1963 were investigated. Variations were discovered with periods about 27, 22 and 30 days. (auth)

37533 COSMIC-RAY RIGIDITY SPECTRUM DURING A SOLAR ROTATION AND SOLAR WIND VELOCITY. Takahashi, H.; Chiba, T.; Yahagi, N. (Iwate Univ., Morioka, Japan). pp 251-3 of Proceedings of the Ninth International Conference on Cosmic Rays. Vol. I. Stickland, A. C. (ed.). London, The Institute of Physics and The Physical Society, 1966.

An analysis was made of cosmic ray neutron and meson data to study cosmic ray rigidity spectra during solar rotations in the recent period of declining solar activity. The result obtained shows a close correlation between the rigidity spectrum and the associated geomagnetic disturbances. It is concluded from the result that the rigidity spectrum is closely related to solar wind velocity, and the differential rigidity spectrum is steeper the greater the solar wind velocity. The above result is similar to that from a similar analysis of the rigidity spectrum during cosmic ray storms. This suggests that the mechanism of the result is similar to that for cosmic ray storms. (auth)

37534 ANISOTROPY OF FORBUSH-TYPE COSMIC-RAY INTENSITY DECREASE AND ELECTROMAGNETIC CONDITIONS IN INTERPLANETARY SPACE. Fedchenko, K. K. (Polar Geophysical Inst., Academy of Sciences, Apatiti, USSR). pp 254-6 of Proceedings of the Ninth International Conference on Cosmic Rays. Vol. I. Stickland, A. C. (ed.). London, The Institute of Physics and The Physical Society, 1966.

Twenty Forbush decreases with the amplitude greater than 4% in neutron intensity were considered. The data obtained at 53 stations of the worldwide network for the period 1957–1961 were used for the investigation. (auth)

37535 THE FORBUSH DECREASES AND THE 27-DAY RECURRENCE TENDENCY IN THE COSMIC-RAY INTENSITY AT A DEPTH OF 60 m.w.e. UNDERGROUND IN LONDON. Thambyahpillai, T.; Dutt, J. C. (Imperial Coll. of Science and Tech., London). pp 257-60 of Proceedings of the Ninth International Conference on Cosmic Rays. Vol. I. Stickland, A. C. (ed.). London, The Institute of Physics and The Physical Society, 1966.

In order to extend the rigidity dependence analysis of Forbush decreases and the 27-day recurrence tendency to higher rigidities (a few hundred Gv) it is necessary to study these effects in underground meson intensity. Forbush decreases observed by semi-cubical telescopes located at a depth of 60 mwe were investigated in conjunction with those measured by neutron monitors covering a wide range of latitudes. It is found that the fractional change in differential intensity can be represented by a power law in which the exponent varies from 0.8 to 1.1. The underground meson intensity shows a 27-day recurrence tendency similar to that observed at sea level. The amplitude of this effect has decreased continuously over the years from 1961 to 1964. The rigidity dependence of this phenomenon cannot be represented by a simple power law in rigidity. (auth)

37536 COSMIC RAYS AND SOLAR ACTIVITY FROM THE DATA OF MEASUREMENTS IN THE STRATOSPHERE. Charakhch'yan, A. N.; Charakhch'yan, T. N. (Lebedev Inst. of Physics, Moscow. Moscow State Univ.). pp 261-6 of Proceedings of the Ninth International Conference on Cosmic Rays. Vol. I. Stickland, A. C. (ed.). London, The Institute of Physics and The Physical Society, 1966.

Solar cosmic rays. Experimental data testify of constancy of the energy spectrum form of solar cosmic ray protons for the bursts which occur independently and have different amplitude. At proton energies higher than a certain level an abrupt break in the spectrum occurs, this break being connected with limitation of particle acceleration in solar atmosphere. The position of this break in the spectrum is different for different bursts and is not connected with cosmic ray burst amplitude or with a class of chromospheric flare. For solar protons detected near the earth two kinds of differential energy spectra are evident with power exponents γ grouping around values $\gamma_1 \simeq 3.0$ and $\gamma_2 \simeq 6.0$. The first spectrum is due to solar protons propagating diffusely in interplanetary space. The second kind of spectrum, which correlates with the arrival of burst corpuscular streams at the earth, is due to protons trapped by magnetic traps of corpuscular streams from the burst. Time dependence of solar proton intensity near the earth is in good agreement with ideas about diffuse propagation of solar cosmic ray protons in interplanetary space. The proton scattering path for electromagnetically unperturbed interplanetary space increases with proton rigidity P, approximately as $\sqrt{P}$. Kinetic energy of proton flux emitted by the sun during a moderate flare is 10^{29} erg. Cosmic ray intensities near the earth for flares occurring on the visible side of the solar disk are greater by approximately two orders of magnitude as compared with the intensities relating to cosmic ray generation on the remote side of the solar disk. In order to interpret this phenomenon existence of radial magnetic fields of the sun also has to be assumed. Secular variations of galactic cosmic ray intensity. The phenomenon of secular variations of galactic cosmic ray intensity in interplanetary space is almost wholly due to 11-year solar activity which is characterized by the sun-spot group number (or by the spot number). Comparison of experimental data and the data of Parker's theory on cosmic ray modulation (decrease) under the influence of solar wind showed evidence of some spatial and time regularities in cosmic ray modulation in interplanetary space. The radius of the sphere r around the sun, within which galactic cosmic ray modulation occurs under the influence of solar wind, depends upon solar activity η (being the sum of the spot group number for daily data during the month) as $r = \text{const}\ \eta^{\alpha_1}$ where $\alpha_1 \simeq 0.15$. For 1962, the value was about 7 A.U. It was found for the coefficient of galactic cosmic ray diffusion in interplanetary space D that $D = \text{const}.\ E\eta^{-\alpha_2}$ where $\alpha_2 = 0.5$. The total intensity of galactic cosmic rays near the earth ($P \geq 0.5$ Gv) reached at the end of 1964 nearly 90–95% of its initial value corresponding to the primary intensity of cosmic rays beyond the modulation sphere. The corresponding value for the differential intensity ($0.5 \leq P \leq 2.3$ Gv) was 85–90%. Therefore the conclusion should be drawn that for the period of solar minimum there is no significant difference in galactic cosmic ray energy spectra near the earth and beyond the interplanetary space. (auth)

37537 EFFECTS OF COSMIC RAYS ACCORDING TO THE CHROMOSPHERIC FLARES AND FORBUSH EFFECTS DURING SOLAR ACTIVITY MINIMUM. Kolomeets, E. V.; Ivanov, V. Ya.; Lichoded, V. A.; Pivneva, V. T. (Kazakh State Univ., Alma-Ata, USSR). pp 267-70 of Proceedings of the Ninth International Conference on Cosmic Rays. Vol. I. Stickland, A. C. (ed.). London, The Institute of Physics and The Physical Society, 1966.

During the period of the last minimum of solar activity from 1962 to 1965 the following were investigated: The generation of particles in small solar flares and their propagation are considered according to the earth and stratospheric data. Impact zones are analyzed by the increase in the neutron component during "small" solar flares. The dependence of the flare effect on helicoordinates is given. The increase of cosmic ray intensity during rapid disturbances of the geomagnetic field and "small" chromospheric flares are studied. The energetic spectra of the observed increase are estimated. The effects observed are interpreted. The energetic spectra of the Forbush effect during decrease and increase in the intensity of cosmic rays are considered according to the data of the neutron component. The change of cosmic ray intensity during magnetic storms due to the decrease of the rigidity cut-off is studied. The effects observed are interpreted. (auth)

37538 BALLOON STUDIES OF PRIMARY COSMIC RAYS AT SOLAR MINIMUM. Jenkins, R. W.; Wilson, B. G. (Univ. of Alberta, Calgary, Can.). pp 274-6 of Proceedings of the Ninth International Conference on Cosmic Rays. Vol. I. Stickland, A. C. (ed.). London, The Institute of Physics and The Physical Society, 1966.

A Čerenkov-scintillation counter system for the monitoring of cosmic radiation at balloon altitudes was flown at Calgary and Fort Churchill, Canada, on four occasions during late 1964 and 1965. The proton rigidity spectra obtained over the cosmic ray maximum are in good agreement with results obtained near the previous solar minimum by Webber and McDonald. (auth)

37539 CHANGES IN THE COSMIC-RAY INTENSITY CLOSE TO THE ZENITH. Katzman, J. (National Research Council, Ottawa). pp 277-81 of Proceedings of the Ninth International Conference on Cosmic Rays. Vol. I. Stickland, A. C. (ed.). London, The Institute of Physics and The Physical Society, 1966.

The intensity changes of the meson component at Ottawa, Canada, were measured with telescopes containing different masses of absorber and of small solid angle, 5×10^{-4} and 5×10^{-2} sterad. The relative changes shown by these telescopes from November 1958 to January 1962 were 72 and 86% respectively of the total change for the period November 1958 to June 1965, whereas the relative change for both the meson component as determined with an I.G.Y. type cubic telescope and the nucleon component was 41%, and for the nucleon component at Huancayo the relative change was 47%. From the results obtained it is concluded that a single electromagnetic modulation mechanism some 10 to 100 A.U. away from the Earth cannot be the only cause for the variations of the cosmic ray intensity during a cycle of solar activity. (auth)

37540 ANISOTROPY OF COSMIC RAYS IN THE DIRECTION PARALLEL TO THE ROTATION AXIS OF THE EARTH. Kudo, S.; Murakami, K. (Inst. of Physical and Chemical Research, Tokyo). pp 285-7 of Proceedings of the Ninth International Conference on Cosmic Rays. Vol. I. Stickland, A. C. (ed.). London, The Institute of Physics and The Physical Society, 1966.

An anisotropy in the cosmic ray flux perpendicular to the plane of the ecliptic can be detected by comparison of the intensity variations in the northern and southern hemisphere. Three possible examples of this kind of anisotropy have been found in IGY data. They had the following characteristics: The intensity of nucleonic component increased in the northern (or southern) polar region, while no increase was observed in the opposite region. No increase in either neutron or meson intensity was detected elsewhere. No remarkable event occurred on either the sun or the earth at these times. The primary variation spectrum for these increases seems to be little different from that for the diurnal variation. (auth)

37541 FREQUENCY DISTRIBUTION OF SUDDEN CHANGES OF COSMIC-RAY INTENSITY IN CONNECTION WITH SOLAR ACTIVITY. Alania, M. V.; Dorman, L. I.; Koiava, V. K.; Koridze, V. G.; Shatashvili, L. Kh. (Inst. of Geophysics, Academy of Sciences, Georgian SSR. Izmiran, Moscow). pp 288-91 of Proceedings of the Ninth International Conference on Cosmic Rays. Vol. I. Stickland, A. C. (ed.). London, The Institute of Physics and The Physical Society, 1966.

It is shown that the frequency distribution of sudden increases of intensity of the cosmic ray neutron component of type $I_{i+1}-I_i \geq 1\%$ (i is the number of two-hourly time intervals), according to the data of the high mountain stations Climax and Sulphur Mountain, has a maximum about 12 h, local time. The phase of the maximum of such increases depends to some extent on energies of primary particles. Detailed analysis of sudden decreases of intensity of cosmic rays shows that sharp and relatively large decreases also have the tendency to appear at a definite time. But on the basis of observations from 1957 to 1964, the phase of frequency distribution maximum both of increases and decreases does not essentially shift with the change of the solar activity. (auth)

37542 GALACTIC AND SOLAR COSMIC RAYS IN INTERPLANETARY SPACE. Dorman, L. I. (Izmiran, Moscow). pp 292-5 of Proceedings of the Ninth International Conference on Cosmic Rays. Vol. I. Stickland, A. C. (ed.). London, The Institute of Physics and The Physical Society, 1966.

The main information about the character of the modulation effects in the galactic cosmic rays in interplanetary space is given. Detailed consideration is given to the dynamic model connected with the displays of the solar wind of the inhomogeneity flux of the magnetic field from the sun, with the propagation of the shock waves (semi-transparent magnetic "pistons"), with the presence of a large scale spiral like interplanetary magnetic field. Account is taken of the lag of the phenomena in interplanetary space with respect to the events on the sun. Also investigated are the behavior of solar cosmic rays in interplanetary space and their modulation. Comparison is made of the results on the state of interplanetary space obtained from investigations of intensity variations of galactic and solar cosmic rays with the data of direct measurements from satellites and space probes. (auth)

37543 RIGIDITY SPECTRUM OF PRIMARY COSMIC RAYS. Komori, H. (Yamanashi Univ., Kofu, Japan). pp 296-8 of Proceedings of the Ninth International Conference on Cosmic Rays. Vol. I. Stickland, A. C. (ed.). London, The Institute of Physics and The Physical Society, 1966.

The integral rigidity spectrum of primary cosmic rays is analyzed using experimental data. The intensities of each component are plotted as functions of the Mount Washington neutron monitor. The data are split into two groups: one group being for those days when the neutron monitor was counting above its average rate of 2100 and the other group for those, presumably solar active days, when the monitor rate was below average. The solar active days are considered. Assuming that the integral rigidity spectra of the various primary components can be written as $U(R + V)^{-W}$, where R is the rigidity, then U, V, W can be calculated by the method of least squares. The shapes of the heavy particle rigidity spectra thus obtained agree within the 5% significance level with the shape of the proton spectrum. (auth)

37544 APPLICATION OF CONVOLUTION PRODUCT THEORY TO SMOOTHING OF NEUTRON MONITOR DATA. Barouch, E. (Laboratoire de Physique Cosmique, Verriere-le-Buisson, France). pp 299-301 of Proceedings of the Ninth International Conference on Cosmic Rays. Vol. I. Stickland, A. C. (ed.). London, The Institute of Physics and The Physical Society, 1966.

A method of treating neutron monitor records in order to display the daily variation more accurately and objectively is presented. This is done by taking the convolution product of the hourly counts with a function whose Fourier transform is zero outside a closed interval. Results obtained by this method are presented, comparing very favorably with the sliding average technique. The method can easily be extended to the study of other modulation effects. (auth)

37545 MODULATION I. McCracken, K. G. (Southwest Center for Advanced Studies, Dallas). pp 306-8 of Proceedings of the Ninth International Conference on Cosmic Rays. Vol. I. Stickland, A. C. (ed.). London, The Institute of Physics and The Physical Society, 1966.

Cosmic ray modulation during the eleven year solar cycle is reviewed. First order cosmic ray modulation effects, namely, cosmic ray production by the sun, diurnal anisotropy, the eleven-year cycle, and the Forbush decrease effect are considered. Geomagnetic cut-off effects are also discussed. (J.F.P.)

37546 MODULATION II. Sarabhai, V. (Physical Research Lab., Ahmedabad, India). pp 309-11 of Proceedings of the Ninth International Conference on Cosmic Rays. Vol. I. Stickland, A. C. (ed.). London, The Institute of Physics and The Physical Society, 1966.

The modulation of cosmic rays is reviewed. The topics considered include the 11-year solar modulation, energy spectrum of variation, the anisotropy of cosmic rays, and the topology of electromagnetic conditions in interplanetary space. (J.F.P.)

37547 FLUX LIMITS FOR HIGH-ENERGY γ RAYS FROM QUASARS AND OTHER POSSIBLE COSMIC-RAY SOURCES. Long, C. D.; McBreen, B.; Porter, N. A.; Weekes, T. C. (University Coll., Dublin). pp 318-20 of Proceedings of the Ninth International Conference on Cosmic Rays. Vol. I. Stickland, A. C. (ed.). London, The Institute of Physics and The Physical Society, 1966.

A directional night sky Cherenkov telescope was used to look for excess showers coming from the direction of quasars and other possible sources. The threshold detecting energy is 5×10^{12} ev; an excess would indicate a flux of γ rays of this energy. The angular resolution of the system was 3° at the zenith and a counting rate of 40–100 showers/minute was obtained. Both drift scans and ON/OFF comparisons were used and 70,000 showers were observed between January 1964 and April 1965. Of the five quasars observed, all gave a slight excess which approaches statistical significance. Due to atmospheric fluctuations, however, Poisson statistics do not apply. Corrections for systematic errors were applied and tend to increase the positive effect on the quasars. Flux limits are given for all nine sources observed; these do not conflict with current astrophysical theory. The limitations of the technique are discussed and progress on the photography of showers using the optical delay image intensifier system at Dublin is described. (auth)

37548 MEASUREMENTS OF COSMIC-RAY ELECTRON COMPONENT INTENSITY. Rubtsov, V. I. (Lebedev Inst. of Physics, Moscow). pp 324-6 of Proceedings of the Ninth International Conference on Cosmic Rays. Vol. I. Stickland, A. C. (ed.). London, The Institute of Physics and The Physical Society, 1966.

In October 1964 flights of polyethylene balloons were carried out at an altitude of 34 km. An instrument was flown consisting of a telescope made of two scintillation counters with lead plates between them. The coincidences

in the telescope were registered when the pulse height from the counters exceeded that corresponding to the passage of an electron-photon shower produced by an electron with energy above about 3.5 Bev in the lead plates between them. The solid angle of the telescope was overlapped from above by a third scintillation counter. The information about the amount of ionization in the counter permitted us to determine the charge of the particles causing the coincidences. Separation of the proton and electron components was effected using a method of "cutting the beam". This involved covering the telescope during a part of the flight time with a lead absorber. The measured flux of primary electrons proved to be equal to $I = (4 \pm 0.5)$ m^{-2} sec^{-1} sterad^{-1} for electrons of energy $E \geq 3.5$ Bev and $I = (0.9 \pm 0.2)$ m^{-2} sec^{-1} sterad^{-1} for electrons of energy $E \geq 8$ Bev. (auth)

37549 BALLOON OBSERVATION OF HIGH-ENERGY ELECTRONS. **Bleeker, J. A. M.; Burger, J. J.; Scheepmaker, A.; Swanenburg, B. N.; Tanaka, T. (Cosmic Ray Working Group, Academy of Sciences, Delft, Netherlands).** pp 327-30 of **Proceedings of the Ninth International Conference on Cosmic Rays. Vol. I. Stickland, A. C. (ed.). London, The Institute of Physics and The Physical Society, 1966.**

A balloon observation of high energy electrons with a counter system was carried out in the Netherlands. The results obtained at 10 g cm^{-2} of residual atmosphere are presented. The detector has two shower-producing layers, i.e., 5 mm of lead and 10 mm of aluminium, on top of a lead glass Čerenkov total absorption energy spectrometer. By subtracting the number of "Al" events initiated in the aluminium from that of "Pb" events initiated in the lead, most of the nuclear interactions among the "Pb" events are eliminated, thus the contribution of electron initiated showers can be obtained. A hump is observed on the energy spectrum of electrons, being expected as due to the primary electrons above the geomagnetic cut-off energy. The background of atmospheric electrons in this energy range is estimated to be about 20% at 10 g cm^{-2} from the altitude dependence of electrons and photons. The differential energy spectrum of the primary electrons is proportional to $E^{-1.9\pm0.4}$ in the observed energy range from 2 to 15 Bev. This exponent gives a spectral index of the galactic radio emission in agreement with the observed values. On the other hand it appears to small to be explicable in terms of the theory of electron production by interstellar cosmic ray interactions. (auth)

37550 THE FLUX AND EAST-WEST ASYMMETRY OF PRIMARY ELECTRONS AT A GEOMAGNETIC RIGIDITY CUT-OFF OF ABOUT 4.5 GV. **Agrinier, B. (Centre d'Etudes Nucleares, Saclay, Gif-sur-Yvette, France); Koechlin, Y.; Parlier, B.; Vasseur, J.; Bland, C. J.; Boella, G.; Antoni, G. Degli; Dilworth, C.; Scarsi, L.; Sironi, G.** pp 331-4 of **Proceedings of the Ninth International Conference on Cosmic Rays. Vol. I. Stickland, A. C. (ed.). London, The Institute of Physics and The Physical Society, 1966.**

A balloon flight carrying a lead plate spark chamber triggered for shower detection, with magnetometer definition of orientation, was made for the purpose of measuring the flux of primary electrons and their east-west asymmetry at a geomagnetic rigidity cut-off of 4.5 Gv. The balloon reached a ceiling altitude of the order of 3 mb and data were obtained during 9 hours at this altitude. Preliminary results are presented. (auth)

37551 ELECTRONS, HYDROGEN, AND HELIUM NUCLEI OF THE COSMIC RADIATION AS OBSERVED IN 1963 AND 1964. **Waddington, C. J.; Freier, P. S. (Univ. of Minnesota, Minneapolis).** pp 339-41 of **Proceedings of the Ninth International Conference on Cosmic Rays. Vol. I. Stickland, A. C. (ed.). London, The Institute of Physics and The Physical Society, 1966.**

Nuclear emulsions were exposed over Fort Churchill in plate "shufflers" flown in 1963 and 1964. Preliminary data on the low energy hydrogen and helium nuclei observed in 1963 were already reported. These observations are now extended to cover a wider energy range and to include electrons. A similar analysis was made in the shuffler stack flown in 1964 at a time when the counting rate of high latitude sea level neutron monitors had increased by 2.8%. In both stacks the energy spectrum of the hydrogen nuclei was studied over the energy range 80 Mev $\leq E \leq 4$ Bev, which represents a considerable extension over previously available techniques. Similarly the helium nuclei were studied over an energy range of 70 Mev/nucleon $\leq E \leq 1.3$ Bev per nucleon, so that for the first time those two components were studied over a widely overlapping range of rigidities, $0.74 \leq R \leq 4.0$ Gv. Integral and differential intensities for both years are presented, as are those on the small number of electrons observed in each stack. Analysis of these results shows that in this energy range, the modulation cannot be solely velocity dependent and that there exists a clear discrepancy between these results and some of those reported for the IMP-I satellite. (auth)

37552 COSMIC-RAY FLUX VARIATION WITH HEIGHT IN THE STRATOSPHERE. **Chow, B. S.; Wu, K. K.; Simpson, N.; Ames, S.; Hopper, V. D. (Univ. of Melbourne).** pp 342-4 of **Proceedings of the Ninth International Conference on Cosmic Rays. Vol. I. Stickland, A. C. (ed.). London, The Institute of Physics and The Physical Society, 1966.**

A study of the variation of cosmic ray flux with altitude in the stratosphere was carried out at geomagnetic latitude 47°S, longitude 220°E. To avoid errors due to time variations the measurements at different levels in the stratosphere were made either simultaneously or at time separations of the order of a few hours. This was accomplished by either of two methods or a combination of these. One method consisted of suspending equipment some 6 km from a free balloon floating in the stratosphere. The other involved flying up to nine balloons on the one day, each carrying cosmic ray detectors and performing level flights using the valve technique. The flight records obtained by radar tracking and the recording equipment carried by the balloons is described. Constant flight times of the order of 4 hours were required and the height study ranged from 46 g cm^{-2} to 10 g cm^{-2}. Ilford G5 600μ nuclear emulsions were used as detectors and these were area scanned for stars with $N_h \geq 3$ by two scanners independently and corrected for scanning efficiency. A comparison between star counts and Geiger counter measurements made at the same latitude is reported. (auth)

37553 SOLAR MODULATION OF PROTONS AND HELIUM NUCLEI DURING THE PERIOD 1963-1965. **Webber, W. R. (Univ. of Minnesota, Minneapolis).** pp 345-8 of **Proceedings of the Ninth International Conference on Cosmic Rays. Vol. I. Stickland, A. C. (ed.). London, The Institute of Physics and The Physical Society, 1966.**

The low rigidity portions of the primary spectra of protons and helium nuclei were measured on six occasions during 1963–65 using a Čerenkov-scintillation counter carried to altitudes of 2–6 g cm^{-2} by balloons. The range of rigidities over which detailed spectral measurements have been made is 0.4–2 Gv for protons and 0.8–4 Gv for helium nuclei. The measurements cover a period of decreasing solar modulation as evidenced by an increase in Mount Washington neutron monitor rate from a value about 2300 in the summer of 1963 to about 2450 in 1965. The increase in neutron monitor rate was accompanied by much larger increases in the low energy protons and helium nuclei—amounting to a factor of almost two at the lowest rigidities. The energy dependence of the modulation of both protons and helium nuclei is consistent with a $1/\beta$ dependence for $0.45 \leq \beta \leq 0.85$. However, at the same velocity, the modulation for protons is at least twice that for helium nuclei. The modulation thus produces identical changes in the rigidity spectra of the two components. This model is inconsistent with a simple diffusion model for the 11-year variation such as suggested by Parker. However, a model in which diffusion and energy loss occur simultaneously and are of approximately equal importance is explored, and found to be capable of producing the observed modulation. (auth)

37554 MEASUREMENTS OF THE PRIMARY PROTON AND HELIUM SPECTRA AND THEIR MODULATIONS DURING A BALLOON-BORNE CHERENKOV-SCINTILLATION COUNTER. Ormes, J. F.; Webber, W. R. (Univ. of Minnesota, Minneapolis). pp 349-54 of Proceedings of the Ninth International Conference on Cosmic Rays. Vol. I. Stickland, A. C. (ed.). London, The Institute of Physics and The Physical Society, 1966.

During the years 1963–65 the spectra of protons and helium nuclei were studied on eleven flights at seven geomagnetic latitudes using a modified version of the Cherenkov-scintillation counter. The flights attained depths of 2–6 g cm^{-2} which coupled with the detector's large geometry factor (~50 sterad cm^2) enabled details of the helium intensity, and the different contributions, primary and secondary, to the singly charged distribution, to be evaluated as a function of atmospheric depth. These results demonstrate that it is necessary to know in detail the contribution of all nonprimary components, particularly at the lower energies, before a spectrum of primary protons can be determined. The spectra of primary protons and helium nuclei measured on these flights are presented. These spectra cover the range from about 0.6–16 Gv rigidity. The results indicate that the lowest energy protons have increased by more than 50% between 1963 and 1965. The proton spectrum is almost flat down to 0.5 Gv in 1965, but the helium spectrum is falling sharply at the corresponding rigidities. A study of the modulation of these two components during this period reveals that the modulation depends approximately on $1/\beta$ for $0.45 \leq \beta \leq 0.85$ for both components, and at the same velocity, the modulation for protons is at least twice that for helium nuclei. (auth)

37555 FAST NEUTRON INTENSITY ABOVE FORT CHURCHILL, CANADA. Baird, G. A.; Wilson, B. G. (Univ. of Alberta, Calgary, Can.). pp 355-7 of Proceedings of the Ninth International Conference on Cosmic Rays. Vol. I. Stickland, A. C. (ed.). London, The Institute of Physics and The Physical Society, 1966.

Rocket and balloon measurements of neutron intensity above Fort Churchill, Manitoba, were made during 1964 and 1965. The detector consisted of two scintillators, anthracene and plastic, with pulse shape discrimination selection between neutrons, gamma rays and charged particles. Neutrons are detected in the energy range 2–11 Mev. A differential energy spectrum has been obtained with $dN/dE = 0.096(E/3.7)^{-0.85\pm0.30}$ neutrons Mev^{-1} cm^{-2} sec^{-1} for the rocket measurements. The form of the balloon spectrum is given by $e^{-0.0085}\, p\, (E/3.7)^{-1.35\pm0.20}$ neutrons Mev^{-1} cm^{-2} sec^{-1} where p is the pressure. (auth)

37556 THE FLUX OF HELIUM NUCLEI AT HYDERABAD, INDIA ($\lambda = 7.6°N$). Shukla, P. G. (Tata Inst. of Fundamental Research, Bombay). pp 360-1 of Proceedings of the Ninth International Conference on Cosmic Rays. Vol. I. Stickland, A. C. (ed.). London, The Institute of Physics and The Physical Society, 1966.

Using a stack of nuclear emulsions exposed over Hyderabad on 27th March 1962, the flux of helium nuclei at the top of the atmosphere was determined to be 16.3 ± 1.7 particles/m^2 sterad sec. Comparing this value of the flux with similar data obtained at different periods of the solar activity, it is concluded that the flux of helium nuclei at this latitude is independent of the solar activity. Using a flux value for Texas appropriate to the time of this experiment, the exponent of the integral energy spectrum is obtained as $1.31^{+0.15}_{-0.11}$. (auth)

37557 ENERGY SPECTRUM OF PRIMARY HELIUM NUCLEI AT ENERGIES GREATER THAN 6 Gev. Anand, K. C. (Tata Inst. of Fundamental Research, Bombay); Daniel, R. R.; Stephens, S. A.; Bhowmik, B.; Krishna, C. S.; Mathur, P. C.; Aditya, P. K.; Puri, R. K. pp 362-4 of Proceedings of the Ninth International Conference on Cosmic Rays. Vol. I. Stickland, A. C. (ed.). London, The Institute of Physics and The Physical Society, 1966.

A preliminary analysis was made with 528 primary helium nuclei recorded in an emulsion stack flown, oriented in the east-west plane, under 10.2 g cm^{-2} of residual atmosphere over Hyderabad, India. The integral energy spectrum of the primary helium nuclei in the energy region between 6 and 20 Bev/nucleon was obtained by making use of the variation of the geomagnetic cut-off rigidity in the east-west plane. It is found that the integral energy spectrum can be represented by a power law with an exponent $\gamma = 1.84 \pm 0.22$. The vertical intensity of the primary helium nuclei is found to be 16.5 ± 0.8 Peters above an effective cut-off energy of 8.35 Bev/nucleon. (auth)

37558 ENERGY SPECTRUM OF ALPHA PARTICLES BELOW 600 Mev/NUCLEON AT SOLAR MINIMUM. Neelakantan, K. A. (Tata Inst. of Fundamental Research, Bombay). pp 365-7 of Proceedings of the Ninth International Conference on Cosmic Rays. Vol. I. Stickland, A. C. (ed.). London, The Institute of Physics and The Physical Society, 1966.

The differential energy spectrum of helium nuclei of the primary cosmic radiation was determined in the energy interval 82–600 Mev/nucleon. The experiment was performed in a stack of emulsions flown over Fort Churchill, Canada (geomagnetic latitude $\lambda = 71°N$) on 21th June 1964 under 2.7 g cm^{-2} of residual atmosphere. The results indicate that the rigidity spectrum obtained in the present experiment has the same shape as the spectrum measured during 1963, but with increased fluxes, and is different at rigidities R < 1.3 Gv from the alpha spectrum measured in 1954, when the Mount Washington neutron monitor rate was about the same as in the present experiment. In the rigidity interval 1.0–1.3 Gv, the flux of helium nuclei was 18 ± 4 per m^2 sec sterad in 1964 compared with a flux of 31 ± 4 per m^2 sec sterad in 1954. The integral flux of nuclei with $Z \geq 3$ and with energies greater than 150 Mev/nucleon is estimated to be 31 ± 6 per m^2 sec sterad in 1964 compared with 24.5 ± 1.3 per m^2 sec sterad in 1963. (auth)

37559 ON THE ABUNDANCE OF ^{3}He NUCLEI IN THE PRIMARY COSMIC RADIATION. Biswas, S.; Lavakare, P. J.; Ramadurai, S.; Sreenivasan, N. (Tata Inst. of Fundamental Research, Bombay). pp 368-70 of Proceedings of the Ninth International Conference on Cosmic Rays. Vol. I. Stickland, A. C. (ed.). London, The Institute of Physics and The Physical Society, 1966.

The isotopic composition of helium nuclei in the cosmic radiation is determined using a nuclear emulsion stack exposed at 3 g cm^{-2} of atmospheric depth at Fort Churchill, Canada, on 15th June 1963. The method of ionization vs. residual range is used to determine the masses of ^{3}He and ^{4}He nuclei. From a sample of 128 helium nuclei a preliminary value of the ratio $R = {}^3He/({}^3He + {}^4He)$ is obtained as 0.11 ± 0.03 in the kinetic energy interval 115–210 Mev/nucleon. A corresponding value of R = 0.32 ± 0.07 is obtained for the rigidity interval of 0.85–1.12 Gv. The implications of these results are briefly discussed. (auth)

37560 1961-1964 BALLOON OBSERVATIONS OF COSMIC RAYS. Fichtel, C. E.; Durgaprasad, N.; Guss, D. E. (Goddard Space Flight Center, Greenbelt, Md.). pp 371-4 of Proceedings of the Ninth International Conference on Cosmic Rays. Vol. I. Stickland, A. C. (ed.). London, The Institute of Physics and The Physical Society, 1966.

A series of high altitude balloon flights from Fort Churchill carrying nuclear emulsions to study the cosmic radiations was begun in 1961 and repeated each year thereafter. Both the helium nuclei energy spectra and the proton spectra were measured in order to obtain information on particles which had substantially different rigidities for the same velocity. The recent results of this program are combined with other results to obtain a picture of the time variation of the cosmic radiation during the declining phase of solar activity. It was found that the generalized Parker model for cosmic ray modulation is able to explain the data reasonably well for a source spectrum which has either the same rigidity or energy per nucleon spectrum for protons and helium nuclei, but only for certain types of distributions of the sizes of the scat-

tering centers. The derived source spectra for similar energy/nucleon spectra are extremely steep at low energies leading to a very high flux and energy density. The assumption of similar rigidity spectra leads to smaller differential flux values at low energies. (auth)

37561 LOW RIGIDITY END OF THE DIFFERENTIAL SPECTRA OF THE PROTON AND HELIUM COMPONENTS OF THE PRIMARY COSMIC RADIATION. Apparao, M. V. K.; Ramadurai, S. (Tata Inst. of Fundamental Research, Bombay). pp 375-6 of Proceedings of the Ninth International Conference on Cosmic Rays. Vol. I. Stickland, A. C. (ed.). London, The Institute of Physics and The Physical Society, 1966.

The proton and helium differential spectra near the solar system were calculated by starting with power spectra similar in rigidity at the "source" of cosmic rays and taking into account ionization loss and interaction with the interstellar hydrogen. A comparison of the proton and helium spectra so obtained, with the observed spectra at the low rigidity end, suggests that the ratio of the abundance of helium nuclei to protons is higher at low rigidities (<2 Gv) as compared with the ratio at high rigidities at the "source" of cosmic rays. (auth)

37562 MEASUREMENT OF THE PRIMARY COSMIC-RAY HYDROGEN AND HELIUM NUCLEI AT KIRUNA, SWEDEN. Courtier, G. M.; Linney, A. D. (Imperial Coll. of Science and Tech., London). pp 377-9 of Proceedings of the Ninth International Conference on Cosmic Rays. Vol. I. Stickland, A. C. (ed.). London, The Institute of Physics and The Physical Society, 1966.

The results from balloon flights made at geomagnetic latitudes of 50°N and 65°N are presented. Data were obtained on the spectra of primary hydrogen and helium nuclei in 1964 at a time close to solar minimum, using the combined scintillator and scintillator-Čerenkov technique. These data are compared with the results obtained with similar equipment which was flown at the same locations in 1961 and 1962 and also those of other investigators. The implications of these results on the nature of the galactic spectra and the solar modulating mechanism are discussed. (auth)

37563 SOLAR MODULATION OF THE GALACTIC HELIUM SPECTRUM ABOVE 30 Mev PER NUCLEON. Fan, C. Y.; Gloeckler, G.; Simpson, J. A. (Univ. of Chicago). pp 380-2 of Proceedings of the Ninth International Conference on Cosmic Rays. Vol. I. Stickland, A. C. (ed.). London, The Institute of Physics and The Physical Society, 1966.

Time variations in the differential energy spectrum and flux of primary helium nuclei in the energy range 30 to 90 Mev/nucleon were studied over the time period from December 1963 to January 1965. Continuous measurements over most of the one-year period were made using (dE/dx, E) type solid state, charged particle telescopes which were flown on two satellites IMP-I and IMP-II which had highly eccentric orbits. The helium spectra obtained are well represented by a power dependence of the type $\propto E^{+\gamma}$ where E is the particle total kinetic energy. The exponent γ changed from 1.75 to 1.3 in the one-year period while the flux of helium increased by about 75% in the same time interval. Since in addition to this observed modulation, the helium nuclei were continuously present and since the spectrum extends smoothly into the higher energy spectrum measured on balloons, it is believed the low-energy extension of the modulated local galactic helium spectrum is observed. From the measured fractional helium intensity increases with time it can be deduced that the modulation depends predominantly on the particle velocity. (auth)

37564 ABUNDANCES AND ENERGY SPECTRA FOR NUCLEI OF GALACTIC ORIGIN ABOVE 20 Mev PER NUCLEON. Comstock, G. M.; Fan, C. Y.; Simpson, J. A. (Univ. of Chicago). pp 383-6 of Proceedings of the Ninth International Conference on Cosmic Rays. Vol. I. Stickland, A. C. (ed.). London, The Institute of Physics and The Physical Society, 1966.

The individual chemical abundances of nuclei with charge Z extending from Z = 2 to Z = 14 in the energy range 20 to 300 Mev/nucleon were measured in interplanetary space in the OGO-I satellite for approximately 150 hours in October and November 1964. At higher Z, two charge groups were measured, including the Fe group. The energy spectra for C, O and Ne are shown to be remarkably flat and different from the helium spectrum measured simultaneously over the same energy/nucleon range. It is concluded that these spectral differences exist in the cosmic radiation outside the solar system. The relative abundances for $6 \leq Z \leq 14$ display an even-odd Z ratio of approximately 8:1. Li, Be and B, and the Fe group are present with about the same relative abundances as observed at higher energies. It is suggested that the rate of particle acceleration for a wide range of Z competes effectively with the rate of ionization loss at these low energies. The measurements were made with solid state silicon detectors and anticoincidence scintillators arranged to measure energy loss and total energy. (auth)

37565 LOW ENERGY MULTIPLY CHARGED NUCLEI IN THE COSMIC RADIATION. Freier, P. S.; Rno, J. S.; Waddington, C. J. (Univ. of Minnesota, Minneapolis). pp 387-9 of Proceedings of the Ninth International Conference on Cosmic Rays. Vol. I. Stickland, A. C. (ed.). London, The Institute of Physics and The Physical Society, 1966.

Nuclear emulsions mounted in plate "shufflers" were exposed to some 2.5 g cm^{-2} over Fort Churchill in 1963 and 1964. These emulsions were examined for the tracks of multiply charged, $Z \geq 3$, nuclei, with particular emphasis being paid to those particles brought to rest in the emulsions. From these ending particles it appears that during this period near solar minimum the ratio of L to M nuclei with $170 \leq E \leq 360$ Mev per nucleon, corrected to the top of the atmosphere, is 0.55 ± 0.18, which is appreciably greater than the value observed at higher energies. Also given are values for the total integral intensity of all $Z \geq 3$ nuclei in each year, and the differential intensity of M nuclei derived from the ending particles. (auth)

37566 VERY HEAVY LOW-ENERGY COSMIC-RAY NUCLEI. Waddington, C. J.; Freier, P. S. (Univ. of Minnesota, Minneapolis). Contract Nonr 710(60). pp 390-2 of Proceedings of the Ninth International Conference on Cosmic Rays. Vol. I. Stickland, A. C. (ed.). London, The Institute of Physics and The Physical Society, 1966.

A stack of nuclear emulsions having a surface area of 900 cm^2 and mounted in a pressure activated emulsion "camera" was exposed during 1964 at a residual pressure of 2.1 mb over Fort Churchill. These emulsions are being used to measure the intensity of all nuclei having charges of 20 or greater and the differential energy spectrum of these $Z \geq 20$ nuclei between 240 and 650 Mev/nucleon. This range of energies covers the region where nuclei of different charges might be expected to show the greatest spectral changes due to propagation or other causes. Provisional results are reported on the energy spectrum and intensities of these nuclei. These results show that, if acceleration processes are neglected, the mean amount of interstellar or source material traversed by these nuclei does not exceed 2 g cm^{-2}. (auth)

37567 SOLAR COSMIC-RAY HEAVY NUCLEI AND THE 18TH JULY 1961 EVENT. Biswas, S. (Tata Inst. of Fundamental Research, Bombay); Fichtel, C. E.; Guss, D. E. pp 393-5 of Proceedings of the Ninth International Conference on Cosmic Rays. Vol. I. Stickland, A. C. (ed.). London, The Institute of Physics and The Physical Society, 1966.

Energetic heavy nuclei ($Z \geq 3$) were detected in the 18th July 1961 solar particle event. This result brings to four the number of solar cosmic ray bursts in which heavy nuclei were seen. The particles were detected in nuclear emulsions flown on a balloon launched from Fort Churchill shortly after the associated flare appeared on the sun. The average flux of medium nuclei ($6 \leq Z \leq 9$) during that period was 0.13 ± 0.02 particles per m^2 sterad sec Mev/nu-

cleon at approximately 155 Mev/nucleon, or about 40 times the normal galactic cosmic ray medium nuclei flux at that particular time in the solar cycle. This value is consistent with that anticipated on the basis of the relative abundances of hydrogen, helium and medium nuclei in other events. Some large nuclei ($Z \geq 10$) were detected, but light nuclei were so rare that only an upper limit to their abundance could be set ($L/M \leq 0.07$). The unbiased acceleration of multiply charged nuclei in every major solar event now seems more certain and, therefore, it seems to be worth considering this feature in any theory of solar particle acceleration. (auth)

37568 HEAVY NUCLEI IN THE PRIMARY COSMIC RAYS IN JUNE 1963 AT FORT CHURCHILL. Anand, K. C.; Biswas, S.; Lavakare, P. J.; Ramadurai, S.; Sreenivasan, N. (Tate Inst. of Fundamental Research, Bombay). pp 396-9 of Proceedings of the Ninth International Conference on Cosmic Rays. Vol. I. Stickland, A. C. (ed.). London, The Institute of Physics and The Physical Society, 1966.

The composition and energy spectra of heavy nuclei ($Z \geq 3$) in the primary cosmic rays were studied using a nuclear emulsion stack composed of emulsions of different sensitivities, which was exposed at 3.0 g cm^{-2} of residual atmosphere from Fort Churchill, Canada, on 15th June 1963. This preliminary study is based on 335 heavy nuclei analyzed so far. Differential energy spectra of L ($3 \leq Z \leq 5$), M($6 \leq Z \leq 9$) and H($Z \geq 10$) nuclei were obtained in the energy interval of 150–575 Mev/nucleon and integral fluxes for energy greater than 575 Mev/nucleon. The study of the energy dependence of the L/S ratio (S nuclei = $Z \geq 6$) shows that the L/S ratio at the top of the atmosphere was 0.53 ± 0.14, 0.34 ± 0.08, 0.21 ± 0.03 and 0.20 ± 0.03 for nuclei of energies of 150–400, 150–575, greater than 400 and greater than 575 Mev/nucleon respectively. Comparing these results with the known L/S ratio of 0.18 ± 0.04 for nuclei of energy greater than 1.5 Bev/nucleon, it is concluded that the total amount traversed by cosmic rays of energy greater than 400 Mev/nucleon seems to be constant and is equal to 2.5 ± 0.5 g cm^{-2} of hydrogen and this seems to increase to about 7.5 g cm^{-2} for particles of energy 150–400 Mev/nucleon. The ratio of Be/B nuclei at the top of the atmosphere is obtained as 0.30 ± 0.15 and 0.19 ± 0.08 for particles of energy 150–575 and greater than 575 Mev/nucleon respectively and these are discussed in relation to the traversal times of cosmic rays. (auth)

37569 EXPERIMENTAL EXAMINATION OF LOW-ENERGY COSMIC-RAY HEAVY NUCLEI. Fichtel, C. E.; Guss, D. E.; Neelakantan, K. A.; Reames, D. V. (Goddard Space Flight Center, Greenbelt, Md.). pp 400-2 of Proceedings of the Ninth International Conference on Cosmic Rays. Vol. I. Stickland, A. C. (ed.). London, The Institute of Physics and The Physical Society, 1966.

In sounding rocket experiments flown from Fort Churchill in September 1963 and July 1964, finite fluxes of cosmic ray heavy nuclei were detected at energies below the experimental energy cut-off of balloon-borne experiments. The particles were examined by extending large sheets of nuclear emulsions from the sides of the rocket during its period outside the atmosphere. The flux of medium nuclei ($6 \leq Z \leq 9$; Z = nuclear charge) in the energy range from 30 to 150 Mev/nucleon was 0.67 ± 0.13 particles/m^2 sterad sec in September 1963 and 1.17 ± 0.16 particles/m^2 sterad sec in July 1964. The abundances of medium and ($10 \leq Z \leq 19$) nuclei relative to helium nuclei in the same energy intervals were found to be less than the relative abundances previously determined at high energies. This type of change in the relative abundances with energy/nucleon is expected if the nuclei have the same source spectral shape and then pass through a small amount of interstellar matter. Finite fluxes of light nuclei ($3 \leq Z \leq 5$) and very heavy nuclei ($20 \leq Z \leq 28$) were also seen in the 30 to 100 Mev/nucleon and the 60 to 295 Mev/nucleon region respectively. (auth)

37570 SOME IMPLICATIONS OF THE RELATIVE SPECTRA OF THE DIFFERENT CHARGE COMPONENTS IN THE PRIMARY RADIATION. Webber, W. R. (Univ. of Minnesota, Minneapolis). pp 403-6 of Proceedings of the Ninth International Conference on Cosmic Rays. Vol. I. Stickland, A. C. (ed.). London, The Institute of Physics and The Physical Society, 1966.

The differential spectra of the individual charge components–protons through heavy nuclei–measured at different levels of solar modulation from 1963–1965 were presented previously. Utilizing the fact that the solar modulation affects particles of different charge-to-mass ratio in such a way that the ratio of intensities in differential rigidity intervals are not changed, the relative spectra prior to solar modulation can be compared. This comparison suggests the following: The relative spectra of protons and helium nuclei are most reasonably interpreted in terms of identical rigidity spectra at the "source" rather than energy/nucleon spectra. The large increase in P/He (P) ratio at low rigidities may in large part be due to production of secondary protons as well as ionization loss in the interstellar medium. The variation of the P/He, L/M and He/M ratios with energy can be interpreted in terms of ionization loss of the primary radiation moving through an amount of material which monotonically decreases with increasing energy. The spectra of heavy nuclei above 3 Gv systematically become steeper with increasing charge. (auth)

37571 MEASUREMENTS OF THE ENERGY SPECTRUM OF NUCLEI WITH $Z \geq 3$ IN THE PRIMARY RADIATION USING A BALLOON-BORNE CHERENKOV SCINTILLATION COUNTER. Webber, W. R.; Ormes, J. F.; von Rosenvinge, T. (Univ. of Minnesota, Minneapolis). pp 407-11 of Proceedings of the Ninth International Conference on Cosmic Rays. Vol. I. Stickland, A. C. (ed.). London, The Institute of Physics and The Physical Society, 1966.

The spectra of the so called L, M, and H nuclei were measured on eleven balloon flights at seven geomagnetic latitudes during the period 1963–65. The instrument used is a modified version of the Čerenkov scintillation counter. These spectra were measured over the range 1.5 to 16 Gv. The flights attained depths of 2–6 g cm^{-2} which, coupled with the detector's large geometrical factor (~50 sterad cm^2), has enabled details of the absorption of the L, M and H components to be studied in the upper atmosphere. The large geometrical factor has allowed identification of over 10,000 nuclei with $Z \geq 3$, over 2000 being observed on a single flight. A total of about 150 VH nuclei were observed and the spectrum of these nuclei was found to be similar to that of M and LH nuclei above about 2 Gv. The spectrum of the L nuclei is found to be significantly different from that of the M and H nuclei, with the exponent on a power law energy spectrum being 0.3 ± 0.1 larger. The M and LH nuclei spectra are also different from the He nuclei spectra above 3 Gv: the exponent on a power law spectrum being 0.1 ± 0.03 larger with the integral spectrum being given by an average exponent of −1.6 ± 0.03 over the range 3–16 Gv. The solar modulation of these nuclei is found to be similar to that of the He nuclei. (auth)

37572 ^{3}He-^{4}He IN THE PRIMARY COSMIC RADIATION AT FORT CHURCHILL 1963. O'Dell, F. W.; Shapiro, M. M.; Silberberg, R.; Stiller, B. (Naval Research Lab., Washington, D. C.). pp 412-14 of Proceedings of the Ninth International Conference on Cosmic Rays. Vol. I. Stickland, A. C. (ed.). London, The Institute of Physics and The Physical Society, 1966.

The astrophysical significance of the ^{3}He nuclei in the primary cosmic ray helium flux warrants further investigation of the isotopic composition as a function of energy, rigidity and solar modulation. Hitherto, the total fund of data involving isotopic identifications by means of more than one technique of measurement per track has been meager. As an extension of the 1961 flight at magnetic latitude 55°N, data on low energy helium from a balloon flight at Fort Churchill, Canada (73°N), launched on 19th June 1963 were analyzed. The mean pressure altitude for 7.2 hours was 4.0 g cm^{-2}. In the relatively insensitive Ilford K.2 emulsions, both multiple scattering and ionization loss with range were measured employing the Fowler-Perkins method for the latter. About 1000 helium tracks

were followed out, and 317 of these came to rest by ionization loss. For each of 200 of the stopping nuclei, it was possible to make mass measurements by both methods. In this way, reliable isotopic separation was achieved, and the ^{3}He fraction (the ratio ^{3}He/(^{3}He + ^{4}He)) could be measured with significantly higher precision. The following values were obtained for this fraction: 0.10 ± 0.03 in the energy-per-nucleon interval 215–368 Mev/nucleon, and 0.13 ± 0.03 in the rigidity interval 1.03–1.50 Gv. The trend of these results confirms the relatively low values of the ^{3}He fraction reported earlier. (auth)

37573 SEPARATION OF ISOTOPIC NUCLEI OF THE PRIMARY COSMIC RAYS WITH NUCLEAR EMULSIONS. Alvial, G. (Univ., Chile, South America). pp 415-16 of Proceedings of the Ninth International Conference on Cosmic Rays. Vol. I. Stickland, A. C. (ed.). London, The Institute of Physics and The Physical Society, 1966.

Tracks of nuclei of primary cosmic rays which ended in the emulsions themselves were measured in a search for possible separation of isotopes. The energy of the nuclei ranged from 200 to 600 Mev/A and the atomic numbers of the selected tracks were around that of the carbon nucleus. Results of the measurements of the thickness of the tracks are the subject for discussion. Discrimination between protons and deuterons, ^{3}He and ^{4}He, ^{8}Li (hammer track) and ^{7}Li are also discussed. It is along these lines and in strict accordance with these results that isotopic carbon nuclei were found. (auth)

37574 ESTIMATION OF THE RELATIVE ABUNDANCE OF THE CARBON ISOTOPES OF THE PRIMARY COSMIC RAYS. Alvial, G.; Silva, E.; Stantic, S.; Riquelme, J. (Univ., Chile, Santiago). pp 417-18 of Proceedings of the Ninth International Conference on Cosmic Rays. Vol. I. Stickland, A. C. (ed.). London, The Institute of Physics and The Physical Society, 1966.

In an emulsion pack exposed at Minneapolis, Minnesota, at an altitude varying from 6 g cm^{-2} to 3 g cm^{-2}, nuclei whose tracks terminated within the emulsions themselves and whose atomic numbers were from Z = 2 to Z = 8 were well separated by both counting the small δ rays and by measuring the thickness of the tracks. By applying the method of separating the isotopes two groups of carbon isotopes were found. The energy of these nuclei ranged from 200 to 500 Mev/a. The estimation of their relative abundance is the subject of this discussion. (auth)

37575 USE OF SEMICONDUCTOR TELESCOPES IN CHARGE AND ENERGY SPECTROMETRY OF COSMIC PARTICLES. Engelmann, J.; Koch, L.; Meyer, J. P. (Centre d'Etudes Nucleaires, Saclay, Gif-sur-Yvette, France). pp 419-22 of Proceedings of the Ninth International Conference on Cosmic Rays. Vol. I. Stickland, A. C. (ed.). London, The Institute of Physics and The Physical Society, 1966.

Results of a theoretical and experimental study on the capabilities of silicon as a cosmic particle detector are given. The Symon theory on the fluctuations in energy loss, which is valid for a unit charge incident particle is extended to the case of a particle of any charge Z. The most probable energy losses in silicon of protons, electrons and heavy ions were computed and the results compared with values obtained at the Saclay and Orsay accelerators. Landau-Symon fluctuations on these energy losses and corresponding limitations on the Z discrimination were computed for any thickness of silicon. For example, for relativistic particles in the range of the charge of iron, these fluctuations allow a Z discrimination to three units. Data collected on 7th October 1964 by a balloon-borne telescope comprising 2-mm thick silicon detectors at 6.4 g cm^{-2} air residual thickness are given. After correction for secondaries, splash and re-entrant albedo protons, the integral intensities of primary protons and alpha particles at 46°N GM are obtained. The results 680 ± 80 protons/m^2 sterad sec 60 ± 25 alpha particles/m^2 sterad sec are in reasonable agreement with accepted values. (auth)

37576 GAMMA-RAY GENERATION IN THE HIGH ATMOSPHERE. Rocchia, R.; Labeyrie, J.; Ducros, G.; Boclet, D. (Centre d'Etudes Nucleaires, Saclay, Gif-sur-Yvette, France). pp 423-5 of Proceedings of the Ninth International Conference on Cosmic Rays. Vol. I. Stickland, A. C. (ed.). London, The Institute of Physics and The Physical Society, 1966.

The gamma rays produced by the interaction of cosmic rays with the atmosphere create a very important background which counteracts the measurement of other gamma rays of extraterrestrial origin. The flux and spectrum of these atmospheric gamma rays, measured at different atmospheric depths, in the energy range 0.1 to 1.5 Mev are given. A theoretical estimation is given for the respective contribution of the different sources of gamma rays to the production of the measured gamma ray flux. (auth)

37577 HEAVY COSMIC IONS RECORDED IN NUCLEAR EMULSIONS EXPOSED IN A POLAR SATELLITE. Schmitt, R.; Baumann, G.; Kaiser, R.; Annoni, H.; Jung, M.; Cueer, P. (Centre de Recherches Nucleaires, Strasbourg). pp 426 of Proceedings of the Ninth International Conference on Cosmic Rays. Vol. I. Stickland, A. C. (ed.). London, The Institute of Physics and The Physical Society, 1966.

A general research program of the laboratory on the methods of identification of tracks of fragments, hyperfragments and heavy cosmic rays recorded in solid detectors, such as nuclear emulsion, silver monochloride crystal, and nitrocellulose, and mechanisms of their emission from nuclei was undertaken. A spectrum is given of primary cosmic ions of the groups H and VH recorded in Ilford K2 nuclear emulsions exposed in a polar satellite under an absorber, whose mass absorption varied between 4.9 g cm^{-2} and 7.2 g cm^{-2} in the emulsion plane. The exposure time was 74 hours between 208 and 413 km. (auth)

37578 GALACTIC COSMIC RAYS AT SOLAR MINIMUM, 1965. Balasubrahmanyan, V. K.; Hagge, D. E.; Ludwig, G. H.; McDonald, F. B. (Goddard Space Flight Center, Greenbelt, Md.). pp 427-36 of Proceedings of the Ninth International Conference on Cosmic Rays. Vol. I. Stickland, A. C. (ed.). London, The Institute of Physics and The Physical Society, 1966.

A synthesis of preliminary experimental results from cosmic ray experiments flown on OGO-I, IMP-I, II, and III, and high-latitude Skyhook balloon flights provides charge and energy spectra extending from about 20 Mev per nucleon to 1 Bev/nucleon for hydrogen to neon. A multiple Geiger counter cosmic ray monitor flown on these four satellites provided information on the total flux greater than 50 Mev/nucleon. The period from March to June 1965 appears to have minimum solar modulation effects and is operationally defined to be the solar cosmic ray minimum. Energy spectra for particles from H to Ne from 25 to 1 Bev/nucleon are presented. Results on the long-term temporal variation of He nuclei and protons are discussed. The L/M ratio at 100 Mev/nucleon and above 600 Mev/nucleon are found to be 0.29 ± 0.05 and 0.30 ± 0.03. The C/He ratio at 100 Mev/nucleon is found to be 0.021 ± 0.005 whereas above 600 Mev/nucleon the same ratio is found to be 0.036 ± 0.004. The change in this ratio appears to suggest the deceleration of the nuclei of higher Z in the interstellar gas due to ionization. (auth)

37579 MEASUREMENT OF THE ISOTOPIC COMPOSITION OF HELIUM NUCLEI IN THE PRIMARY COSMIC RADIATION IN THE ENERGY INTERVAL 80-150 Mev/NUCLEON. Hofmann, D. J.; Winckler, J. R. (Univ. of Minnesota, Minneapolis). pp 437-9 of Proceedings of the Ninth International Conference on Cosmic Rays. Vol. I. Stickland, A. C. (ed.). London, The Institute of Physics and The Physical Society, 1966.

A dE/dX-E scintillation counter device was flown at absolute solar minimum, in terms of particle influx, on 12th May 1965 from Barrow, Alaska (λ = 69.5°N geomagnetic). 26 hours of data between 3.5 and 4.5 g cm^{-2} atmospheric depth revealed that ^{3}He nuclei were well resolved from ^{4}He nuclei in the energy range 80–150 Mev/nucleon. Energy/nucleon and rigidity spectra were obtained for both nuclear species and the ratio ^{3}He/(^{3}He + ^{4}He) was found to be 0.19 ± 0.05, constant over the interval in terms of

energy/nucleon, and 0.39 ± 0.09 at 0.8 Gv rigidity. The ratio appears to increase toward decreasing rigidities. Since corrections for both solar modulation effects and cosmic ray source effects would tend to lower the observed ratio, the amount of material in interstellar space which this ratio predicts is an upper limit having a value of 6.5 ± 1.5 g cm^{-2}. (auth)

37580 THE ENERGY SPECTRUM OF PRIMARY GALACTIC X RAYS BETWEEN 20 AND 50 kev. Rothenflug, R.; Rocchia, R.; Koch, L. (Centre d'Etudes Nucleaires, Saclay, Gif-sur-Yvette, France). pp 446-8 of Proceedings of the Ninth International Conference on Cosmic Rays. Vol. I. Stickland, A. C. (ed.). London, The Institute of Physics and The Physical Society, 1966.

X rays between 20 and 50 kev were observed in the zenith direction, during the night, with a NaI crystal 50-channel spectrometer, at an atmospheric depth of about 4 g cm^{-2} (37 km) at 43°N latitude. The fluxes observed are: at 20 kev: 0.14 ± 0.05 photon/cm^2 sec sterad kev at 40 kev: 0.03 ± 0.005 photon/cm^2 sec sterad kev. The decrease of the flux J as a function of energy E fits a law of the type $kE^{-\gamma}$ with $\gamma = 2.6 \pm 0.5$. The intensity of the flux observed is in good agreement with the previous results at higher energies (70 kev to 1.5 Mev) and at lower energies (1.5 to 20 kev). (auth)

37581 USE OF A GAS CHERENKOV COUNTER FOR THE STUDY OF THE ISOTOPIC COMPOSITION OF HELIUM NUCLEI IN PRIMARY COSMIC RADIATION. Agrawal, P. C.; Damle, S. V.; Gokhale, G. S.; Joseph, G.; Menon, M. G. K. (Tata Inst. of Fundamental Research, Bombay). pp 453-6 of Proceedings of the Ninth International Conference on Cosmic Rays. Vol. I. Stickland, A. C. (ed.). London, The Institute of Physics and The Physical Society, 1966.

The technique of using a high-pressure gas Čerenkov counter as an energy-threshold device is discussed and a practical counter using sulphur hexafluoride gas as a radiator developed for the study of the isotopic composition of primary helium nuclei at relativistic energies is described. Details about ground calibration are presented. Data obtained from two balloon flights at Hyderabad (λ = 8°N) give $^3He/(^3He + ^4He) = 0.43 \pm 0.23$ above a constant rigidity and $^3He/(^3He + ^4He) = 0.54 \pm 0.26$ above a constant energy per nucleon. Implications of this result are discussed. (auth)

37582 FLUX OF PRIMARY PROTONS AND HELIUM NUCLEI AND EAST-WEST AND NORTH-SOUTH ASYMMETRIES NEAR THE GEOMAGNETIC EQUATOR. Agrawal, P. C.; Damle, S. V.; Gokhale, G. S.; Joseph, G.; Kunte, P. K.; Menon, M. G. K.; Sunderrajan, R. (Tata Inst. of Fundamental Research, Bombay). pp 457-61 of Proceedings of the Ninth International Conference on Cosmic Rays. Vol. I. Stickland, A. C. (ed.). London, The Institute of Physics and The Physical Society, 1966.

Measurements of the vertical intensities of protons and helium nuclei, in flights up to 5 g cm^{-2} depth in the atmosphere over Hyderabad (λ = 8°N) during IQSY (April 1965), with telescopes consisting of two scintillator elements and one Čerenkov element are reported. These are compared with similar measurements during the 1957–1965 period. Within the statistical error there appear to be no solar modulation effects on the proton and helium components above a vertical cut-off rigidity of about 16 Gv. The measurement gives for the vertical proton flux $J_p(0) = 130 \pm 13$ and 102 ± 13 particles/m^2 sec sterad as upper and lower limit respectively; the helium flux $J_{He}(0) = 14.7 \pm 2$ particles/m^2 sec sterad. Preliminary results on the east-west and north-south asymmetries observed in one flight with a similar instrument at 7 g cm^{-2} depth with telescopes inclined at 25° and 40° to the vertical are also reported. The observed asymmetries for singly charged particles are, on average, about two thirds of the expected ones on the basis of proton primaries and an integral spectrum of the form $N(>E) = K(1 + E)^{-1.5}$. (auth)

37583 SPECTRAL COMPOSITION. Waddington, C. J. (Univ. of Minnesota, Minneapolis). pp 462-8 of Proceedings of the Ninth International Conference on Cosmic Rays. Vol. I. Stickland, A. C. (ed.). London, The Institute of Physics and The Physical Society, 1966.

Results on the spectral composition of cosmic radiation are summarized. The aspects of cosmic ray studies covered are x- and γ-ray astronomy, primary cosmic electrons, protons and helium nuclei, cosmic ray isotopic composition, and nuclei above Z = 3. (J.F.P.)

37584 DAILY LATITUDE CURVES OF THE COSMIC-RAY NUCLEONIC COMPONENT OBTAINED IN 1963 BETWEEN 1 AND 6.4 GV. Bachelet, F.; Balata, P.; Dyring, E.; Iucci, N. (Univ., Rome). pp 483-5 of Proceedings of the Ninth International Conference on Cosmic Rays. Vol. I. Stickland, A. C. (ed.). London, The Institute of Physics and The Physical Society, 1966.

A set of daily latitude curves obtained in 1963 by means of the intercalibration of nine European IGY neutron monitors situated near sea level is analyzed to obtain information on the modulation of the primary cosmic ray spectrum at low rigidities. The primary spectral variation is reported for the September Forbush decrease and for the sequence of five 27-day recurrences. (auth)

37585 DAY BY DAY CORRECTION OF THE MESON DIURNAL VARIATION FOR ATMOSPHERIC EFFECTS. Bercovitch, M. (Atomic Energy of Canada Ltd., Chalk River, Ont.). pp 495-7 of Proceedings of the Ninth International Conference on Cosmic Rays. Vol. I. Stickland, A. C. (ed.). London, The Institute of Physics and The Physical Society, 1966.

The correlation between the atmospheric temperature contribution to the diurnal variation observed by a meson monitor at Deep River, and the diurnal variation of two easily and continuously observable atmospheric variables, the ground-level air temperature and the barometric pressure is established. The atmospheric meson diurnal variation vector is taken to be, on a statistical basis, A = M – RN, where M and N represent the observed meson and neutron diurnal variations and R is the factor of proportionality between the meson and neutron monitor responses to the primary anisotropy. It is found that A is proportional in amplitude to T, the ground-level temperature diurnal variation and further, that T and the barometric pressure diurnal variation P are proportional in amplitude. The "best fit" representation of A in terms of T and P is determined by minimizing the mean square deviation between the daily vectors RN and (M – A). Where $A = C_tT + C_pP$ the best fit occurs when $C_t = -0.0052\%/°C$, $C_p = 0.0038\%/mb$, R = 0.47 and the phase of T is shifted by +1.0 hour. These values apply to Deep River where the original hourly meson data was barometer corrected using a coefficient of 0.16%/mb. (auth)

37586 ATMOSPHERIC TEMPERATURE EFFECTS ON THE DIURNAL VARIATION OF COSMIC-RAY INTENSITY. Mori, S.; Ueno, H.; Nagashima, K. (Nagoya Univ., Japan). pp 498-500 of Proceedings of the Ninth International Conference on Cosmic Rays. Vol. I. Stickland, A. C. (ed.). London, The Institute of Physics and The Physical Society, 1966.

Using neutron monitor data during the IGY, Rao et al., and Pomerantz et al., have determined the energy spectrum of the cosmic ray diurnal variation. The energy spectrum is redetermined from neutron monitor data during the IGY by introducing a new parameter of "upper energy cut-off" into the spectrum. Values for the parameters m = 0, P_L = 0 Bev and $P_H = \infty$ are obtained, where m represents the exponent of the energy spectrum, P_L is lower energy cut-off and P_H is upper energy cut-off The atmospheric diurnal variation of the meson intensity is obtained by comparing the diurnal variations expected from this energy spectrum with that observed during the IGY. The temperature effect vector thus obtained has an amplitude of 0.095% and a time of maximum at 7.1 h L.T. (auth)

37587 INVESTIGATION OF COSMIC-RAY DISTRIBUTION USING THE METHOD OF DAILY VARIATIONS. Kuzmin, A. I.; Krimsky, G. F.; Altukhov, A. M.; Krivoshapkin,

P. A.; Philippov, V. A.; Skripin, G. V.; Chirkov, N. P. (Inst. of Cosmophysical Research and Aeronomy, Academy of Sciences, USSR). pp 501-2 of Proceedings of the Ninth International Conference on Cosmic Rays. Vol. I. Stickland, A. C. (ed.). London, The Institute of Physics and The Physical Society, 1966.

Possible effects and methods of investigation of cosmic ray distribution are discussed. The connection between this distribution and daily variations is established. A method is proposed to calculate the influence of the geomagnetic field, the aperture, the orientation of installations and their geographical position on the observed daily variations of cosmic rays. (auth)

37588 ANGULAR DEPENDENCE OF COUPLING COEFFICIENTS OF THE MUON COMPONENT OF COSMIC RAYS. Krimsky, G. F.; Krivoshapkin, P. A.; Skripin, G. V. (Inst. of Cosmophysical Research and Aeronomy, Academy of Sciences, USSR). pp 503-5 of Proceedings of the Ninth International Conference on Cosmic Rays. Vol. I. Stickland, A. C. (ed.). London, The Institute of Physics and The Physical Society, 1966.

Coupling coefficients of the directed muon component are calculated on the earth's surface and at different depths. Pion generation in several successive acts of interaction is calculated, as well as nuclear decay and ionization losses of secondaries. It was established that with the increase of zenith angle coupling coefficients are considerably displaced in the direction of higher energies. (auth)

37589 PROBLEMS OF METHODS OF INVESTIGATION OF COSMIC-RAY VARIATIONS. Dorman, L. I. (Izmiran, Moscow). pp 506-11 of Proceedings of the Ninth International Conference on Cosmic Rays. Vol. I. Stickland, A. C. (ed.). London, The Institute of Physics and The Physical Society, 1966.

Simultaneous amplitude-phase modulation of periodic cosmic ray variations is studied and the properties of satellites of any order are found. General expressions for satellites in the case of the presence of true waves are obtained. The solution of the inverse problem of the determination of the modulation parameters and true waves using the experimentally measured satellites is given. Consideration is also given to the problem of the role of singularities of the solar system geometry in the observed cosmic ray variations (i.e., effects of anticoincidence of the earth's rotation axis and the solar rotation axis with the perpendicular to the ecliptic plane and the asymmetry of distribution of the magnetic inhomogeneity flux from the sun in the meridional plane. (auth)

37590 SOME RESULTS OF THE COMPARISON OF COSMIC-RAY INTENSITY VARIATIONS WITH THE H COMPONENT OF THE EARTH'S GEOMAGNETIC FIELD DURING IGY AND IGC. Chkhetia, A. M.; Dorman, L. I.; Koiava, V. K. (Inst. of Geophysics, Academy of Sciences, Georgian SSR). pp 512-16 of Proceedings of the Ninth International Conference on Cosmic Rays. Vol. I. Stickland, A. C. (ed.). London, The Institute of Physics and The Physical Society, 1966.

The smooth curves of the cosmic ray neutron component intensity variations (according to the data from the mountain stations Sulphur Mountain, Washington, Climax, Zugspitze and Norikura) are compared with the H component of the earth's geomagnetic field (according to the data from the Tbilisi and Tashkent stations) from July 1957 to December 1959. It is shown that this comparison results in a very complicated picture. It is found that although in some cases the correlation is obvious, in other cases the correlation is somewhat distorted. The cases are classified according to the character of the connection of the cosmic ray intensity changes with the changes in the H component of the geomagnetic field of any magnetic storm. Earlier this classification was made either from the point of view of the storm intensity ("weak," "moderate," etc.) or depending on the commencement ("sudden," "gradual"). The comparison of the flattened curves of the cosmic ray neutron component intensity variations and of the H component of the earth's magnetic field has shown that all the events considered can be divided into six types. The results obtained are discussed. (auth)

37591 COSMIC-RAY INTENSITIES IN THE STRATOSPHERE OVER ANTARCTICA AND MURMANSK. Vernov, S. N.; Charakhch'yan, A. N.; Babarykin, V. K.; Bayarevich, V. V.; Stozkov, Yu. I.; Charakhch'yan, T. N. (Moscow State Univ. Lebedev Inst. of Physics, Moscow). pp 517-19 of Proceedings of the Ninth International Conference on Cosmic Rays. Vol. I. Stickland, A. C. (ed.). London, The Institute of Physics and The Physical Society, 1966.

The difference for the yearly cosmic ray intensity in the stratosphere over Mirny and Murmansk is less than 1% in the range of atmospheric pressures 30–200 g cm^{-2}. For pressures below 30 g cm^{-2} there is a 2% excess of cosmic ray intensity at Mirny. This excess cannot be explained by the excess in the number of low energy primary particles only. Comparison of seasonal measurements over Mirny and Murmansk for the summer-winter difference for instance shows that cosmic ray intensity in the maximum does not depend practically on the stratospheric temperature. If a temperature dependence exists at the peak of the cosmic ray intensity curve, then the temperature coefficient is less than $5 \times 10^{-2}\%°K^{-1}$ (auth)

37592 INTENSITY DISTRIBUTIONS OF COSMIC-RAY COMPONENTS AT 307 g cm^{-2} ATMOSPHERIC DEPTH IN THE SOUTH AFRICAN MAGNETIC ANOMALY. van der Walt, A. J.; Stoker, P. H.; Maree, J. P.; Coetzee, W. F. (Potchefstroom Univ., Transvaal, S. Afr.). pp 548-52 of Proceedings of the Ninth International Conference on Cosmic Rays. Vol. I. Stickland, A. C. (ed.). London, The Institute of Physics and The Physical Society, 1966.

Latitude distributions were obtained for nucleonic and neutron components of cosmic radiation at 307 g cm^{-2} atmospheric depth during four aeroplane flights from Cape Town in October 1964. These distributions lie all along the same curve when plotted as a function of vertical threshold rigidities obtained from trajectory integrations, and are compared with distributions obtained in the northern hemisphere at the same pressure altitude. (auth)

37593 LATITUDE SURVEY IN NORTH AMERICA. Carmichael, H. (Atomic Energy of Canada Ltd., Chalk River, Ont.); Bercovitch, M.; Steljes, J. F.; Magidin, M. pp 553-6 of Proceedings of the Ninth International Conference on Cosmic Rays. Vol. I. Stickland, A. C. (ed.). London, The Institute of Physics and The Physical Society, 1966.

During April, May and June 1965, a 23-ton road transport carrying a 3-NM-64 neutron monitor, a 2-MT-64 meson telescope, a digital mercury barometer, and an automatic punched-tape data-logging system travelled from locations in Canada with cut-off rigidities less than 1 Gv, through the United States to the south coast of Mexico where the rigidity cut-off is about 10.5 Gv. For the basic latitude survey, measurements were made at 16 sites where the mean atmospheric pressure was approximately 760 mmHg, but near Mexico City (9.48 Gv), Climax (3.08 Gv) and Mount Washington (1.26 Gv) measurements were made (15 sites) to altitudes of 550, 506, and 603 mmHg, respectively. A preliminary report of the variation of neutron monitor intensity with primary rigidity cut-off and with altitude is given. The accuracy of the trajectory calculation method of determining the cut-off rigidity of a particular location is examined. The barometer coefficient is found to vary with latitude and altitude in the manner reported by Bachelet, Balata, Dyring and Iucci. Eight permanent neutron monitors in Canada, the United States and Mexico were visited and intercalibrated. (auth)

37594 ON THE RELATION OF L-DERIVED CUTOFFS TO THE RESULTS OF NUMERICAL INTEGRATIONS. Ray, E. C. (Goddard Space Flight Center, Greenbelt, Md.). pp 557 of Proceedings of the Ninth International Conference on Cosmic Rays. Vol. I. Stickland, A. C.

(ed.). London, The Institute of Physics and The Physical Society, 1966.

Numerical exploration of the degree of agreement between L derived cosmic ray cut-offs and those obtained by numerically integrating the equations of motion suggests that the former are, in the sense of their definition, accurate to somewhat more than 5%. Since the L derived cut-offs are analogous to Størmer cut-offs, they leave out of account the penumbral effect. (auth)

37595 GEOGRAPHIC DISTRIBUTION OF VERTICAL COSMIC-RAY THRESHOLD RIGIDITIES. Kondo, I. (Univ. of Chicago); Kodama, M. pp 558-63 of Proceedings of the Ninth International Conference on Cosmic Rays. Vol. I. Stickland, A. C. (ed.). London, The Institute of Physics and The Physical Society, 1966.

Threshold rigidities for vertical incident cosmic ray particles were derived using the results of trajectory computations by higher order simulation of the geomagnetic field. Based on the results of such calculations for more than 500 points, a table of vertical threshold rigidities was prepared for a mesh of 5° latitude and 10° longitude intervals. It was found that the interpolation from this table yields threshold rigidities with errors of less than 0.3 Gv at the points where the trajectory calculations were made. Several sources of errors introduced in the threshold rigidity table obtained were examined. There was some evidence that poor representation of the real geomagnetic field by spherical harmonic coefficients at some parts of the earth, possible due to errors in the magnetic charts, may have produced some errors in the threshold rigidities. (auth)

37596 MODULATION OF COSMIC-RAY THRESHOLD RIGIDITY DUE TO GEOMAGNETIC CAVITY FIELD. Makino, T. (Rikkyo Univ., Tokyo); Kondo, I. pp 564-7 of Proceedings of the Ninth International Conference on Cosmic Rays. Vol. I. Stickland, A. C. (ed.). London, The Institute of Physics and The Physical Society, 1966.

The effect of the geomagnetic cavity field on the cosmic ray threshold rigidity was estimated using a recent model of the cavity field. Effective threshold rigidities at four different local times (0, 6, 12 and 18 hours) and several geomagnetic latitudes (0°, 30°, 40°, and 50°) were determined by computing the trajectories of the cosmic ray particles in the distorted geomagnetic field. It was found that the threshold rigidity is increased by the presence of the geomagnetic field cavity. Axial asymmetry of the shape of the cavity was found to produce detectable amplitude in the diurnal variation of the cosmic ray intensity. For example, diurnal variations of 0.2 to 0.3% amplitudes with a maximum at 16–24 hours local time are expected in the nucleonic component intensity at sea level or mountain altitude. Observed evidence which may have connections with these phenomena were discussed. (auth)

37597 INFLUENCE OF THE MAGNETOPAUSE ON COSMIC-RAY PARTICLE TRAJECTORIES. Ahluwalia, H. S. (Univ. Mayor de San Andres, La Paz, Bolivia); McCracken, K. G. pp 568-70 of Proceedings of the Ninth International Conference on Cosmic Rays. Vol. I. Stickland, A. C. (ed.). London, The Institute of Physics and The Physical Society, 1966.

A study of the characteristic effects of the deformed magnetic field on the trajectories and asymptotic directions of arrival of medium energy cosmic rays at three representative stations: Chacaltaya, Deep River and London is presented. For this purpose the spherical harmonic description of the deformed magnetic field given by Mead in 1964 superposed on a Störmer dipole and Finch and Leaton higher degree simulation field configurations was used. It is found that the asymptotic directions of arrival for deformed fields are considerably different from those for undisturbed fields at low rigidities and the mean deviation of each station is larger for the night than for the day hemisphere. There is also evidence of a strong modulation of penumbral bands by the deformed field. There is an indication that a small semidiurnal component, at equatorial stations, results from the deformation of the terrestrial field. The resulting component is, however, an order of magnitude smaller than that observed on many occasions at low latitude stations. (auth)

37598 INFLUENCE OF OUTER SOURCES OF GEOMAGNETIC FIELD UPON THE CUTOFF RIGIDITIES AND POSITION OF IMPACT ZONES. Smirnov, V. S. (Polar Geophysical Inst., Academy of Sciences, USSR). pp 571-2 of Proceedings of the Ninth International Conference on Cosmic Rays. Vol. I. Stickland, A. C. (ed.). London, The Institute of Physics and The Physical Society, 1966.

The effects of the compression and expansion of the magnetosphere on cosmic rays are discussed. It is shown that compression of the magnetosphere results in the cut-off rigidities being increased and the impart zones being displaced westwards. On the contrary, by expansion of the magnetosphere the cut-off rigidities are decreased and the impact zones are displaced eastwards. The combined action of the east current systems flowing along the boundaries of the magnetosphere and being responsible for its compression and the west current systems flowing within the magnetosphere and causing the expansion, results in a weakening of the effect of the external sources on the cosmic rays. In this case the impact zones can be displaced both westwards and eastwards from their location in the undisturbed geomagnetic fields. (auth)

37599 MEASUREMENTS OF NEUTRONS PRODUCED BY THE COSMIC RADIATION. Korff, S. A.; Mendell, R. B.; Holt, S. S. (New York Univ., N. Y.). pp 573-6 of Proceedings of the Ninth International Conference on Cosmic Rays. Vol. I. Stickland, A. C. (ed.). London, The Institute of Physics and The Physical Society, 1966.

Fast neutrons produced by the cosmic radiation in the energy interval from 1 to 10 Mev were measured at several altitudes and latitudes. The measurements were made nearly simultaneously at Palestine, Texas, and at Sioux Falls, South Dakota. The near simultaneity permits normalization for variations in primary intensity. Measurements were also made at Hyderabad, India. The neutrons were measured by employing an organic scintillator in the field of view of a photomultiplier tube. The entire assembly was carried by balloon to about 120,000 feet and remained there for several hours. The neutron energy spectrum was estimated. (auth)

37600 SOME RESULTS OF THE INVESTIGATION OF THE PRIMARY COSMIC-RAY NUCLEI ON THE ARTIFICIAL SATELLITE ELECTRON-2. Fradkin, M. I.; Kurnosova, L. V.; Razorenov, L. A.; Suslov, A. A. (Lebedev Physical Inst., Moscow). pp 577-9 of Proceedings of the Ninth International Conference on Cosmic Rays. Vol. I. Stickland, A. C. (ed.). London, The Institute of Physics and The Physical Society, 1966.

Some results of cosmic ray nucleus investigations are presented. The measurements were conducted by the integral Čerenkov counter. The nuclei with charges $Z \geq 2$, $Z \geq 5$ and $Z \geq 15$ were detected by the device in the energy interval above 600 Mev/nucleon. Preliminary results obtained by the sputnik "Electron 2" are discussed and compared with the data obtained on the second and third Soviet space rockets in 1959, on the Soviet spaceship in 1960 and on the "Mars-1" rocket in 1962. The comparison made shows that one observed an increase of a factor of 1.7–2 in the nuclear fluxes in 1964 relative to the 1959 results. The fluxes of the nuclei with charges $Z \geq 2$, $Z \geq 5$ and $Z \geq 15$ are given. These values are compared with the relative sunspot numbers which characterize the activity of the sun in different years. Some cases of the short-term increases of the fluxes of nuclei with charges $Z \geq 15$ are given. The physical nature of these events is still not clear, but the analysis of some events shows that part of them cannot be explained by statistics. The data of the changes of different nuclear fluxes for long-term intervals are given. (auth)

37601 NEUTRON ALBEDO MEASUREMENTS ON ROCKET FLIGHTS. Lockwood, J. A.; Friling, L.; Wilson,

T. (Univ. of New Hampshire, Durham). pp 580-5 of Proceedings of the Ninth International Conference on Cosmic Rays. Vol. I. Stickland, A. C. (ed.). London, The Institute of Physics and The Physical Society, 1966.

An investigation was made of the neutron intensities above the atmosphere at rocket altitudes utilizing a moderated ^{3}He neutron detector. The ^{3}He proportional counter was encased in a polyethylene moderator, and the moderator and detector were surrounded by a ring of charged particle counters to discriminate against neutrons produced in the detector assembly by primary cosmic rays. Flights were made in 1965 at geomagnetic latitudes of about 0°, 20°, and 50°. The neutron counting rates above the atmosphere at these latitudes, corrected for production, are 0.6 sec^{-1}, 0.75 sec^{-1}, and 2.4 sec^{-1}. These counting rates can be converted to a neutron albedo flux by means of the detector calibration curve and calculated neutron energy spectra. The results are compared with the theoretical calculations of Lingenfelter. Estimates were made of the neutron production in the rocket vehicle and detector assembly. The production in the detector assembly can be compared with experimental measurements. (auth)

37602 VARIATION OF ^{14}C CONTENT IN THE ATMOSPHERE DURING THE PAST TWO THOUSAND YEARS. Kigoshi, K. (Gakushuin Univ., Tokyo); Hasegawa, H.; Yamakoshi, K.; Shibata, S.; Kuroya, H.; Miwa, T.; Mitani, S.; Oshio, T. pp 597-600 of Proceedings of the Ninth International Conference on Cosmic Rays. Vol. I. Stickland, A. C. (ed.). London, The Institute of Physics and The Physical Society, 1966.

In order to study the secular variation of primary cosmic rays the radiocarbon concentration in tree rings of an old cedar tree from Yaku-Island, southern Japan, was measured systematically. About 30 samples were already measured by a 7 liter gas proportional counter. The errors were within 0.3%. A few per cent variation in the radiocarbon concentration in the atmosphere for the past two thousand years was found. The variation is consistent with that expected from the change of the magnetic dipole moment of the earth known from paleomagnetism studies. (auth)

37603 COSMIC RAY PRODUCED LITHIUM AND CALCIUM IN IRON METEORITES. Hintenberger, H.; Voshage, H.; Sarkar, H. (Max-Planck-Institut fuer Chemie, Mainz). pp 602-4 of Proceedings of the Ninth International Conference on Cosmic Rays. Vol. I. Stickland, A. C. (ed.). London, The Institute of Physics and The Physical Society, 1966.

During their flight in interplanetary space meteorites are exposed to cosmic rays and stable as well as radioactive nuclides are formed by the interaction of high energy particles with meteoritic matter. From measurements on these "cosmogenic" nuclides information can be obtained, for example on the duration of the cosmic ray bombardment and the constancy of the cosmic ray intensity. Since the concentrations of all cosmogenic nuclear species are very small in meteorites, low level counting or high sensitivity mass spectrometric techniques must be used for their detection and measurement. So far only a few stable nuclides, mostly rare gases, have been identified as being cosmogenic. In iron meteorites several cosmic ray produced elements with low ionization potential which are ionized with high efficiency by surface ionization were detected. By the measurement of the isotopic constitution of potassium it is possible to determine the cosmic ray exposure ages of iron meteorites. There are peaks in the age distribution curve which indicate that iron meteorites were produced mainly in a few catastrophic collision processes. From the agreement of potassium exposure ages with exposure ages derived from low level counting results on ^{39}Ar, ^{36}Cl and ^{26}Al one can conclude that the cosmic ray intensity has been constant within ±50% during the last 10^9 years. Recently cosmogenic lithium and calcium were detected in the iron meteorite Trenton. For the isotopic ratio ^{7}Li/^{6}Li a value of 1.25 (terrestrial lithium 12.4) was obtained. It is concluded that 1.2 is not too far from the isotopic ratio of pure cosmogenic lithium. For the isotopic ratios ^{44}Ca/^{43}Ca and ^{44}Ca/^{42}Ca in calcium from the meteorite Trenton the values 4.0 and 2.3 respectively were measured which can be compared with the values 14.3 and 3.23 for these ratios in terrestrial calcium. (auth)

37604 HIGHLIGHTS IN AIR SHOWER STUDIES, 1965. Greisen, Kenneth (Cornell Univ., Ithaca, N. Y.). pp 609-15 of Proceedings of the Ninth International Conference on Cosmic Rays. Vol. 2. Stickland, A. C. (ed.). London, The Institute of Physics and The Physical Society, 1966. (NYO-3038-1).

The review of research on extensive air showers focuses its attention on new approaches in those problem areas which seem of major import. First considered are new means of resolving the detailed structure and variability of the showers, properties which reveal indirectly the physics of high energy particle behavior and the composition of primary cosmic rays. Secondly, a brief note is made of the current state of the search for anisotropy in the primary flux. The third topic is the investigation of high-energy primary gamma radiation. Fourthly, attention is called to the recent success in detecting showers by radio methods. Finally, new attacks are described on the extension of knowledge of the primary spectrum to further extremes of energy. Some curious phenomena that may be expected at very high energies are mentioned, and fundamental limitations that may either prevent the particle spectrum from extending much beyond 100 joules, or make the finding of such particles of impressive significance are suggested. (auth)

37605 SOME PROPERTIES OF MUON SHOWERS OBSERVED UNDERGROUND. Barton, J. C. (Northern Polytechnic, London). pp 621-3 of Proceedings of the Ninth International Conference on Cosmic Rays. Vol. 2. Stickland, A. C. (ed.). London, The Institute of Physics and The Physical Society, 1966.

A scintillator stack of area 1.1 m^2 was operated at 60 mwe in coincidence with two other large counters placed at distances up to 6 meters away. The analysis of more than 40,000 coincidence events has shown that the majority of these are due to showers of muons. It is found that muons occurring in showers have a higher probability of interacting in the stack, implying that their mean energy is higher than that of single muons. In about 6% of the events, two or more muons traverse the stack; the multiplicity spectrum of these events is discussed. (auth)

37606 ULTRA-HIGH ENERGY MUONS (>200 Gev) IN EXTENSIVE AIR SHOWERS. Chatterjee, B. K.; Lal, S.; Matano, T.; Murthy, G. T.; Naranan, S.; Sivaprasad, K.; Sreekantan, B. V.; Srinivasa Rao, M. V.; Vishwanath, P. R. (Tata Inst. of Fundamental Research, Bombay). pp 627-31 of Proceedings of the Ninth International Conference on Cosmic Rays. Vol. 2. Stickland, A. C. (ed). London, The Institute of Physics and The Physical Society, 1966.

The absolute number of muons of energy above 220 and above 640 Bev were estimated in showers of size 10^5–10^6 (primary energy 10^{15}–10^{16} ev), using a large air shower array on the surface and muon detectors deep underground in the Kolar Gold Mines, India (11°N, 920 g cm^{-2}). The number of muons may be expressed as $n_\mu(N,>E_\mu) = 1.6 \times 10^5\ (N/10^5)^{0.47\pm0.1}\ E_\mu^{-1.5\pm0.1}$. The implications, in particular the slow increase of n_μ with size, with reference to the multiplicity of pions in nuclear collisions are discussed. The frequency of multiple muons is consistent with a mean production height of 10 km with $\langle p_T \rangle = 0.4-0.6$ Bev/c. The distribution of arrival directions of showers with high energy muons in right ascension shows no deviation from a uniform distribution. (auth)

37607 OBSERVATION OF MUON AIR SHOWERS. Sekido, Y.; Kondo, I.; Murayama, T.; Okuda, H.; Sakakibara, S.; Fujimoto, K. (Nagoya Univ., Japan). pp 632-4 of Proceedings of the Ninth International Conference on Cosmic Rays. Vol. 2. Stickland, A. C. (ed.). London, The Institute of Physics and The Physical Society, 1966.

In order to examine the anisotropy of μ-rich extensive air showers reported by Tokyo Air Shower Group, an observation of muon air showers is being carried out at Nagoya. Parallel beams of cosmic ray particles, i.e., air showers, are detected by large area air Čerenkov detectors. As the zenith angle of the telescope is fixed at 60° and the zenith angle dependence of the electronic component of the air shower is very steep, detected events are mainly due to air showers of high energy muons (>10 Bev). Muon air shower events were selected from observed coincidence events between two tubes of the Čerenkov detector using hodoscopic records of coincidence signals from narrow angle telescopes comprising the detectors. The observed zenith angle dependence at large zenith angle (>45°) is consistent with that computed from the detection probability of muon air showers by this telescope. About a quarter of the observed muon air showers are supposed to be due to primary cosmic rays with energies greater than 10^{16} ev, where the anisotropy was detected by Tokyo Air Shower Group. Preliminary results of the observation are analyzed, but the statistics available are not yet sufficient to obtain any definite conclusion on the anisotropy of muon air showers. (auth)

37608 PROPERTIES OF EXTENSIVE AIR SHOWERS RICH IN MUONS. Chatterjee, B. K.; Murthy, G. T.; Naranan, S.; Sreekantan, B. V.; Srinivasa Rao, M. V.; Tonwar, S. C. (Tata Inst. of Fundamental Research, Bombay). pp 635-6 of Proceedings of the Ninth International Conference on Cosmic Rays. Vol. 2. Stickland, A. C. (ed.). London, The Institute of Physics and The Physical Society, 1966.

The properties of extensive air showers selected by the fourfold coincidence of four muon detectors mutually separated by about 20 m without any restriction on the associated electron component were studied at mountain altitude. It is found that the zenith angle distribution of mu triggered showers is very flat compared with the showers selected by requirements of electron density, particularly at sizes lower than 10^6, indicating that the showers selected by mu trigger are relatively rich in muons. A plot of the arrival direction of showers in celestial coordinates does not reveal anisotropies in either the electron triggered or mu triggered showers in the size range 10^5–10^6. This is also true of higher sizes. A study of the variation of the energy flow in the soft component and in the nuclear active component close to the core reveals that in showers of size less than 10^6 the energy flow in both the components is much lower in mu triggered showers than in electron triggered showers. This difference is more conspicuous in the case of the N component. (auth)

37609 ARRIVAL DIRECTION OF MUON-RICH EXTENSIVE AIR SHOWERS. Matano, T. (Tokyo Univ.); Miura, I.; Nagano, M.; Shibata, S.; Suga, K.; Hasegawa, H. pp 637-8 of Proceedings of the Ninth International Conference on Cosmic Rays. Vol. 2. Stickland, A. C. (ed.). London, The Institute of Physics and The Physical Society, 1966.

In the distribution of arrival directions of muon-rich air showers of size 10^6 the decrease between 15 h and 21 h in right ascension was confirmed by analyzing an increased number of showers. By the study of air showers of size more than 10^7 with an extremely small number of muons the upper limit of the intensity ratio of high energy gamma rays to protons in primary cosmic rays was found to be 5×10^{-3}. (auth)

37610 SOME PROPERTIES OF MU-POOR EAS. Gawin, J. (Univ. of Lodz, Poland); Hibner, J.; Wdowczyk, J.; Zawadzki, A.; Maze, R. pp 639-41 of Proceedings of the Ninth International Conference on Cosmic Rays. Vol. 2. Stickland, A. C. (ed.). London, The Institute of Physics and The Physical Society, 1966.

The number of measurements reported at the Jaipur conference has doubled in the last two years and now the total consists of about 80,000 EAS recordings. The analysis of the results obtained confirms the existence of mu-poor EAS. The distribution of the recorded muon multiplicities in individual showers may be represented quite well in a large interval by a Polya distribution (with a mean of 18 corresponding to the effective area of the detectors of 21 m^2 and to EAS of a mean size of about 10^6). For the lower multiplicities (<5), however, a marked anomaly appears in about 0.7% of showers. It was shown that the observed effect cannot be produced even by a very large fluctuation of the muon number in ordinary EAS, if this fluctuation is continuous. This means that mu-poor EAS constitute a peculiar group. (auth)

37611 NEW DATA ABOUT THE NUCLEAR ACTIVE COMPONENT OF YOUNG ATMOSPHERIC SHOWERS. Babian, Kh. (Inst. of Physics, State Committee on the Utilization of Atomic Energy, Erevan); Grigorov, N. L.; Mamidyanian, E. A.; Shestoperov, V. Ya. pp 646-8 of Proceedings of the Ninth International Conference on Cosmic Rays. Vol. 2. Stickland, A. C. (ed.). London, The Institute of Physics and The Physical Society, 1966.

The energy of the nuclear active component in "young" atmospheric showers was measured with a large ionization calorimeter of area 10 m^2. The results support previous measurements of the nuclear active component energy obtained using an installation with combined filters of graphite and lead. (auth)

37612 DISCUSSION OF ONE MODEL OF THE FORMATION OF EXTENSIVE ATMOSPHERIC SHOWERS. Grigorov, N. L. (Moscow State Univ.); Shestoperov, V. Ya.; Nimmik, R. A.; Babayan, Kh. P.; Boyadzhyan, N. G. pp 649-50 of Proceedings of the Ninth International Conference on Cosmic Rays. Vol. 2. Stickland, A. C. (ed.). London, The Institute of Physics and The Physical Society, 1966.

The spectrum of nuclear active particles of high energy in the cores of extensive atmospheric showers with the number of particles $N \geq 10^5$ was measured with a large ionization calorimeter. It is shown that EAS contain one tenth as many nuclear active particles with $E_\gamma \geq 10^{13}$ ev as would be expected from the model involving a "leading" particle. (auth)

37613 HIGH ENERGY NUCLEAR ACTIVE AND MUONIC COMPONENTS IN EXTENSIVE AIR SHOWERS. Cowsik, R. (Tata Inst. of Fundamental Research, Bombay). pp 656-9 of Proceedings of the Ninth International Conference on Cosmic Rays. Vol. 2. Stickland, A. C. (ed.). London, The Institute of Physics and The Physical Society, 1966.

The high energy ends of the nuclear active and muonic components in air showers are sensitive to the characteristics of very high energy nuclear interactions. Calculations are made on the basis of a "dual" model of high-energy interactions which successfully explains the stationary aspects of cosmic ray propagation through the atmosphere. A special feature of this model is that a large fraction of nonpions produced in high energy nuclear interactions are assumed to be nucleon-antinucleon pairs. The energy spectra and the growth curves of nucleons, pions and muons are presented. The results of the calculation are in general agreement with experimental results. The nuclear active component is dominated by nucleons and its increase at high energy is nearly linear with primary energy. The spectrum of the muon component above about 100 Bev is inconsistent with the experimental values at 220 and 640 Bev obtained at the Kolar Goldmines air shower array by the Tata Institute of Fundamental Research. (auth)

37614 LOW ENERGY NUCLEAR ACTIVE PARTICLES IN EAS. Danilova, T. V. (Lebedev Inst. of Physics, Moscow). pp 660-1 of Proceedings of the Ninth International Conference on Cosmic Rays. Vol. 2. Stickland, A. C. (ed.). London, The Institute of Physics and The Physical Society, 1966.

Measurements of the total number of nuclear active particles in a shower, reported at the Jaipur conference, were compared. The results are in satisfactory agree-

ment without normalization if the transitional effect in the scintillators is taken into account. An interpretation of discontinuities in the dependence of the number of nuclear active particles on shower size is suggested. (auth)

37615 OBSERVATION OF THE CHARACTER OF EAS CORES. Miyake, S.; Hinotani, K.; Ito, N.; Kino, S.; Sasaki, H.; Yoshii, H. (Osaka City Univ.). pp 664-7 of Proceedings of the Ninth International Conference on Cosmic Rays. Vol. 2. Stickland, A. C. (ed.). London, The Institute of Physics and The Physical Society, 1966.

The EAS cores were observed by means of large area scintillation detectors arranged underneath a water tank of various depths up to two meters. The characters of the cores observed were classified into various categories: single, double and multiple cores due to the number of peaks observed in the lateral structure; active and nonactive by further development in the water; sharp and flat depending on their lateral density distribution near the core; and some special cases of very steep structure and complicated cases etc. About 30% of the cores observed have more than two centers of density distribution of charged particles in their core region. The proportion of EAS with multiple cores is independent of shower size and also independent of shower age which is estimated from the lateral distribution of charged particles at distances between 5 and 100 m from the shower axis. These various characters of the cores seem to be caused by the nature of high energy interactions at the nearest effective collision to the observation level. The transverse momentum of particles from these high energy interactions was estimated to range from the order of 1 to a few tens Bev/c. Comparing with the nucleon component observed in EAS, it can be said that the transverse momentum increases slowly with interaction energy. (auth)

37616 STUDIES OF THE CORES OF EXTENSIVE AIR SHOWERS. Bray, A. D.; Crawford, D. F.; Jauncey, D. L.; (and others) (Univ. of Sydney). pp 668-71 of Proceedings of the Ninth International Conference on Cosmic Rays. Vol. 2. Stickland, A. C. (ed.). London, The Institute of Physics and The Physical Society, 1966.

An array of 64 plastic scintillators, about 600 GM counters, 100 tons Pb and three Wilson cloud chambers were used to study the electronic and strongly interacting particles in the cores of air showers. It was shown that up to 2×10^{15} ev total energy the composition of cosmic radiation is much the same as at about 10^{11} ev. Above this energy the galactic component progressively drops out in order of atomic weight. An estimate is given of relative intensity at a given total energy below 2×10^{15} ev of the different types of nuclei. In particular the flux of deuterons is estimated. The elasticity of collision between nucleons and air nuclei is obtained for 22 particular nuclear interactions in the air above the apparatus. The average elasticity and interaction mean free path for 35 cascades throughout the atmosphere is also found. A study of the separation of electromagnetic and strongly interacting cores shows that even at the highest energies the average transverse momentum is approximately 0.4 Bev/c for pions and 1.0 Bev/c for nucleons. (auth)

37617 FINE STRUCTURE OF AIR SHOWER CORES OBSERVED WITH 20 m^2 SPARK CHAMBER. Shibata, S. (Tokyo Univ.); Nagano, M.; Matano, T.; Suga, K.; Hasegawa, H. pp 672-5 of Proceedings of the Ninth International Conference on Cosmic Rays. Vol. 2. Stickland, A. C. (ed.). London, The Institute of Physics and The Physical Society, 1966.

The EAS core is studied with a 20 m^2 spark chamber with fine spatial resolution. Frequencies of several types of cores (double cores, steep cores etc.) are determined and the minimum probability of occurrence of large transverse momentum (≥ 5 Bev/c) at the interaction above 10^{13} ev is found to be 1×10^{-3} which is greater than the usually estimated value 1×10^{-8} using exponential form of p_t distribution at lower energy. A comparison of the response of the spark chamber with that of the plastic scintillation counter just below is made. The result indicates that scintillator studies overestimate both the frequency of double cores and the transverse momentum. (auth)

37618 STUDIES ON HIGH ENERGY CASCADES USING A NEON HODOSCOPE. Samorski, W.; Schnier, C.; Truemper, J. (Univ., Kiel). pp 676-7 of Proceedings of the Ninth International Conference on Cosmic Rays. Vol. 2. Stickland, A. C. (ed.). London, The Institute of Physics and The Physical Society, 1966.

The core approximation of the three-dimensional electromagnetic cascade theory was used to estimate energies and production heights of cascades observed in the neon hodoscope of the air shower experiment at Kiel. Some preliminary results are given. (auth)

37619 EXPERIMENTS ON THE PULSE SPECTRUM OBSERVED FROM SCINTILLATION AND CHERENKOV DETECTORS AT SEA LEVEL. Allan, H. R. (Imperial Coll. of Science and Tech., London); Blake, P. R.; Jones, J. K.; Lillicrap, S. C.; Pidcock, J. K.; Reid, R. J. O.; Turver, K. E. pp 678-80 of Proceedings of the Ninth International Conference on Cosmic Rays. Vol. 2. Stickland, A. C. (ed.). London, The Institute of Physics and The Physical Society, 1966.

Scintillation counters 10-cm thick and water Cherenkov tanks 120-cm deep were used for recording particle densities in air showers. The pulse spectrum from a single detector, of either kind, has a smooth transition region of integral slope about −3 between the pulse heights appropriate to single muons and the larger pulses due to EAS. Evidence indicates that this transition region is probably due to processes occurring within the detector, but more experiments are needed to explain this phenomenon in detail. (auth)

37620 NUCLEAR ACTIVE PARTICLES IN EXTENSIVE AIR SHOWERS NEAR SEA LEVEL. Kameda, T.; Maeda, T.; Oda, H.; Sugihara, T. (Kobe Univ., Japan). pp 681-4 of Proceedings of the Ninth International Conference on Cosmic Rays. Vol. 2. Stickland, A. C. (ed.). London, The Institute of Physics and The Physical Society, 1966.

Nuclear active particles of energy not less than 100 Bev in extensive air showers were studied by the cloud chamber installed in the EAS array of the Institute for Nuclear Study, University of Tokyo. The following results were obtained. The charge to neutral ratio of nuclear active particles indicates that nucleons constitute approximately 30% of nuclear active particles at energy less than 500 Bev, approximately 60% at energies greater than or equal to 500 Bev, and approximately 80% at energies greater than or equal to 1000 Bev. The density of nuclear active particles of energy (E, E + dE) at a distance (r, r + dr) from the axis of a shower of size $N/10^5$ is expressed as $n(E, r, N)dEdr = 0.35\, N^{0.35}\, E^{-1.2} \exp[-(r/r_0)]\, dEdr$ $r_0 = 2.4\, N^{0.32}\, E^{-0.25}$ where E is in units of 100 Bev, and r in meters. An anisotropy of arrival directions of EAS containing nuclear active particles is again found after 1963. In EAS accumulated so far, the dark region is clearly recognized in 15– 23 h right ascension. The anisotropy is more remarkable for EAS of smaller size which are rich in nuclear active particles. (auth)

37621 COMPARATIVE RESPONSE OF CHERENKOV AND SCINTILLATOR DETECTORS TO LARGE AIR SHOWERS. Dufresne, R.; Kellermann, E. W.; Towers, L. (Univ. of Leeds, Eng.). pp 689-90 of Proceedings of the Ninth International Conference on Cosmic Rays. Vol. 2. Stickland, A. C. (ed.). London, The Institute of Physics and The Physical Society, 1966.

The response to air showers of primary energy of the order 10^{17} ev of deep (120 g cm^{-2}) Čerenkov detectors at Haverah Park was compared with scintillation detectors of 8 cm^{-2} thickness at radial distances above 100 m for different inclinations of the shower axis. The results for vertical showers show that the Čerenkov detectors' response indicates an average energy of 100 Mev per incident electron, but that this arises from incident electrons and photons each of energy more nearly 10 Mev,

i.e., from about ten photons for each electron. The data on inclined showers reflect the increasing proportion of muons with increasing zenith angle and are consistent with the view that showers are purely muonic after the traversal of 2000 g cm^{-2} of atmosphere. (auth)

37622 LATERAL DISTRIBUTION, ENERGY SPECTRUM AND FLUCTUATIONS OF THE MUON COMPONENT IN ELECTROMAGNETIC CASCADES. Wdowczyk, J. (Univ. of Lodz, Poland). pp 691-3 of Proceedings of the Ninth International Conference on Cosmic Rays. Vol. 2. Stickland, A. C. (ed.). London, The Institute of Physics and The Physical Society, 1966.

The functions describing the lateral distribution and energy spectrum of muons in electromagnetic cascades in air initiated by primary photons were found. Calculations were made on the assumption that the muon component in an electromagnetic cascade is wholly determined by a cascade of nuclear active particles deriving from the photo-production process. Further, the fluctuations of the muon number in electromagnetic cascades of a given size at the observation level were found after taking into account the fluctuations in the number of muons in showers of a given (primary) energy and the fluctuations in the energy of primary photons producing cascades of constant size. The fluctuations are caused mainly by the changes in the number of high-energy photo-production interactions and by the fluctuations in the energy transferred to the cascade of nuclear active particles during such interactions. Due to the lack of "pilot" particles of clearly higher energy in electromagnetic cascades, the fluctuations are determined mainly by changes in the depth of their origin. All the calculations mentioned were carried out twice: on the assumption of the power law energy spectrum of primary photons and a flat energy spectrum of these photons deriving from the Hayakawa hypothesis. Since there is a marked difference between the two spectra, there are also substantial differences in the results obtained. (auth)

37623 ATTENUATION OF THE MU COMPONENT OF EAS DETERMINED BY THE BAROMETRIC EFFECT. Firkowski, R.; Wdowczyk, J.; Zawadzki, A. (Univ. of Lodz, Poland). pp 694-5 of Proceedings of the Ninth International Conference on Cosmic Rays. Vol. 2. Stickland, A. C. (ed.). London, The Institute of Physics and The Physical Society, 1966.

The barometric effect and the exponent γ of the density spectrum of the penetrating component of EAS were measured in a series of about 65,000 recordings. The barometric effect obtained amounts to $(5.4 \pm 1.2)\%$ per cmHg. The mean attenuation path of the EAS muons of energy above 0.6 Bev is equal to about 640 g cm^{-2}. The exponent γ of the density spectrum of these muons was found to be 2.1 ± 0.1. The interpretation of the data obtained points out the difference between the muon attenuation evaluated on the basis of the barometric effect and on the basis of a two-level measurement. (auth)

37624 SEMI-EMPIRICAL DETERMINATION OF THE FLUCTUATION OF THE EAS MU COMPONENT. Firkowski, R. (Univ. of Lodz, Poland); Gawin, J.; Hibner, J.; Wdowczyk, J.; Zawadzki, A.; Maze, R. pp 696-7 of Proceedings of the Ninth International Conference on Cosmic Rays. Vol. 2. Stickland, A. C. (ed.). London, The Institute of Physics and The Physical Society, 1966.

The fluctuations of the mu component of EAS are divided into two parts; the first consists of all the fluctuations linked with the reception of EAS ("reception" fluctuations); the second represents the fluctuations in the product and the development of EAS ("development" fluctuations). The recording of the EAS mu component by means of a large set of hodoscoped detectors indicates with quite good precision the superposition of both these types of fluctuations ("total" fluctuations). The sole "development" fluctuations can be found, however, on the basis of the calculated "reception" fluctuations and the "total" observed fluctuations. The "reception" fluctuations can be represented by a distribution with standard deviation of 0.34. Since the "total" seem to be satisfactorily represented by a Γ distribution with a standard deviation of 0.48, it follows that the distribution corresponding to the "development" has a standard deviation equal to or less than 0.31. This value is related to muons of a threshold energy amounting to 0.6 Bev. (auth)

37625 THEORETICAL CONSIDERATIONS OF THE RADIOFREQUENCY EMISSION FROM EXTENSIVE AIR SHOWERS. Jelley, J. V. (Atomic Energy Research Establishment, Harwell, Eng.). pp 698-700 of Proceedings of the Ninth International Conference on Cosmic Rays, Vol. 2. Stickland, A. C. (ed.). London, The Institute of Physics and The Physical Society, 1966.

A brief review of the history of attempts to detect radio emissions from extensive air showers is followed by a discussion of various possible mechanisms by which such radiation may occur. These include normal Čerenkov radiation, at mm wavelengths, enhanced Čerenkov radiation due to mutual coherence from the charge excess, synchrotron radiation (magneto-bremsstrahlung), dipole Čerenkov radiation due to charge separation in the earth's field, nuclear bremsstrahlung, transition radiation, direct induction effects, and the possibilities of line emissions. Also mentioned are pulse radar and continuous wave radar with Doppler shifts. An account is then given of the generalized treatment due to Kahn and Lerche, which embraces most of the features of the various processes occurring at meter wavelengths. Special attention is focused on the important problems of mutual coherence, diffraction, Fresnel zones etc., which are imposed by geometrical considerations and the physical dimensions of large air showers. (auth)

37626 DETECTION OF RADIO PULSES OF WAVELENGTH 6.8 m, IN COINCIDENCE WITH EXTENSIVE AIR SHOWERS, IN THE ENERGY REGION 10^{16}–10^{17} ev. Smith, F. G. (Nuffield Radio Astronomy Labs., Jodrell Bank, Eng.); Porter, N. A.; Jelley, J. V. pp 701-5 of Proceedings of the Ninth International Conference on Cosmic Rays, Vol. 2. Stickland, A. C. (ed.). London, The Institute of Physics and The Physical Society, 1966.

A brief description is first given of the original experiment carried out at Jodrell Bank. This was executed on the basis of the Askaryan hypothesis that a negative charge excess in showers should give rise to a considerable enhancement of the normal Čerenkov radiation, due to effects of mutual coherence. The results obtained so far are consistent with this hypothesis, though very preliminary results obtained in a polarization experiment tend to support alternative radiation mechanisms, namely those which arise from charge separation in the earth's field, as indicated by the generalized treatment of Kahn and Lerche. There follows a description of extensions to this work in progress at Jodrell Bank, namely studies of the radio spectrum, attempts to obtain radio pulses in coincidence with Čerenkov light pulses, and plans to commence an analysis of various types of pulse interference, using mobile equipment. In conclusion, there follows a discussion on the future possibilities in this field, looking ahead to the hope that giant showers may be detectable by wholly radio methods. (auth)

37627 STUDIES OF PRIMARY COSMIC RAYS IN THE ENERGY REGION 10^{14} ev TO 10^{17} ev (BOLIVIAN AIR SHOWER JOINT EXPERIMENT). Toyoda, Y. (Kobe Univ, Japan); Suga, K.; Murakami, K.; (and others). pp 708-11 of Proceedings of the Ninth International Conference on Cosmic Rays. Vol. 2. Stickland, A. C. (ed.). London, The Institute of Physics and The Physical Society, 1966.

The accumulation of extensive air showers with extremely few penetrating particles was continued. The distribution in the right ascension of the arrival directions of low mu showers of energy 10^{14} to 10^{16} ev shows a peak between 200° and 220°. Low mu showers of energy 10^{16} to 10^{17} ev may be produced by high energy gamma rays arising from the collisions of cosmic ray protons and thermal photons in intergalactic space. No shower with extremely few penetrating particles among about 10,000 ordinary showers in this energy region was ob-

served. From this result it is concluded that the intensity of extragalactic cosmic ray protons above 2×10^{17} ev is less than 6.5×10^{-2} of the intensity of the cosmic rays observed on the earth when 0.1 ev cm^{-3} of thermal photon density in the intergalactic space is assumed. Above 10^{17} ev, the distribution of the amount of muons in each shower is very narrow and consistent with the Gaussian distribution. This suggests that the main part of the primary cosmic rays above 10^{17} ev consists of protons. (auth)

37628 COMPOSITION OF PHOTON INITIATED SHOWERS AT HIGH ENERGIES. Braun, O.; Sitte, K. (Max-Planck-Institut fuer Kernphysik, Heidelberg). pp 712-14 of Proceedings of the Ninth International Conference on Cosmic Rays. Vol. 2. Stickland, A. C. (ed.). London, The Institute of Physics and The Physical Society, 1966.

The existence of an energetic photon component with a rather low spectral index of the order of 1.3 was predicted in discussions on radioastronomical data and on the origin of cosmic radiation. Various arguments indicate that this component may extend to extremely high energies, so that the giant EAS observed in the Volcano Range experiment might be photon-initiated. In order to investigate this possible interpretation, new calculations were carried out on the production of a nucleonic and a muon component in photonuclear interactions, and on its propagation in an EAS originated by a high energy photon. The calculations are based on a phenomenological model in which two assumptions are made: the photon-nucleon interaction is completely inelastic, and the result of the collision can be described by a one-fireball model with parameters equal to those valid for nucleon-nucleon interactions. The results of preliminary calculations show that up to photon energies around 10^{19} ev the ratio N_μ/N_{el} does not change radically, and that photon-initiated showers remain "muon-poor" up to still higher primary energies. They are also "pion-poor"; the ratio N_π/N_μ is of the order 10^{-2} to 10^{-3}. At 10^{15} ev the relative abundance of muons increases by a factor of the order of 5 between 500 g cm^{-2} and sea level. (auth)

37629 BASJE ANGLE CORRELATION. Barker, P.; Hazen, W.; Hendel, A. (Univ. of Michigan, Ann Arbor). pp 718-19 of Proceedings of the Ninth International Conference on Cosmic Rays. Vol. 2. Stickland, A. C. (ed.). London, The Institute of Physics and The Physical Society, 1966.

Shower arrival directions determined with the BASJE fast-timing method were compared with directions measured in corresponding cloud chamber pictures. The comparison was made for December 1963 and for December 1964. An automatic fast-timing apparatus was installed in September 1964. The standard deviation of the fast-timing arrival direction measurements was 6° in December 1963 and only 2.5° in December 1964. The cloud chamber method has a standard deviation 0.7° parallel to the front of the cloud chamber and 4.3° perpendicular to it. (auth)

37630 DENSITY SPECTRUM OF EXTENSIVE AIR SHOWERS AT 2285 m. McCaughan, J. B. T. (Univ. of Sydney); McCusker, C. B. A.; Seet, S. H.; Wand, R. H.; O'Donnell, B.; Prescott, J. R.; Wilson, B. G. pp 720 of Proceedings of the Ninth International Conference on Cosmic Rays. Vol. 2. Stickland, A. C. (ed.). London, The Institute of Physics and The Physical Society, 1966.

Final results are presented for cloud chamber measurements of the extensive air shower density spectrum at Sulphur Mountain (2285 m). The spectrum becomes progressively steeper in the region above about 4000 particles/m^2. (auth)

37631 ALTITUDE VARIATION OF THE EXTENSIVE AIR SHOWER DENSITY SPECTRUM. Swinson, D. B.; Prescott, J. R. (Univ. of Alberta, Calgary). pp 721-3 of Proceedings of the Ninth International Conference on Cosmic Rays. Vol. 2. Stickland, A. C. (ed.). London, The Institute of Physics and The Physical Society, 1966.

The density spectrum of extensive air showers was measured with proportional counters at altitudes of 2285 m and 3260 m. Both spectra show a pronounced steepening of the spectrum at high densities, similar to that observed in other experiments at sea level. The region in which the steepening occurs moves to higher densities with increasing altitude, the densities at which this occurs being in the proportions 1 : 7.5 : 22 for sea level, 2285 and 3260 m. The results are interpreted in terms of a cut-off in the primary energy/nucleon spectrum. (auth)

37632 SHOWER FRONT STRUCTURE AND THE PROPERTIES OF EXTENSIVE AIR SHOWERS. Baxter, A. J.; Watson, A. A.; Wilson, J. G. (Univ. of Leeds, Eng.). pp 724-6 of Proceedings of the Ninth International Conference on Cosmic Rays. Vol. 2. Stickland, A. C. (ed.). London, The Institute of Physics and The Physical Society, 1966.

The pulse forms recorded from four 34 m^2 water Cherenkov detectors, spaced 500 m apart and operated in an array sensitive to EAS of not less than 2×10^7 particles, were used to examine differences of energy transfer normal to the shower front, for distances 200—900m from the shower axis and as function of zenith angle. These observations are compared with the single particle distributions determined by Linsley and Scarsi. (auth)

37633 ARRIVAL TIME DISTRIBUTIONS OF HEAVY PARTICLES IN AIR SHOWERS. Pal, Y.; Tandon, S. N. (Tata Inst. of Fundamental Research, Bombay). pp 727-30 of Proceedings of the Ninth International Conference on Cosmic Rays. Vol. 2. Stickland, A. C. (ed.). London, The Institute of Physics and The Physical Society, 1966.

The arrival time distributions of nucleons and hypothetical heavy particles of various energies in air showers were calculated taking into account fluctuations in the positions of various interactions. Production and propagation of these particles are characterized by some parameters and their fluxes for different time delays are obtained as functions of these parameters. Specifically it is found that a significant fraction of nucleons and antinucleons of energy about 10 Bev arrive with time delays greater than 100 nsec. (auth)

37634 INSTALLATION FOR STUDY OF EAS AND NUCLEAR INTERACTIONS OF COSMIC RAY PARTICLES WITH ENERGIES 10^{12} TO 10^{16} ev. Erlykin, A. D.; Nesterova, N. M.; Nikolskii, S. I.; Sokolovskii, V. I.; Tukish, E. I.; Yudin, E. P.; Yakovlev, V. I. (Lebedev Inst. of Physics, Moscow). pp 731-3 of Proceedings of the Ninth International Conference on Cosmic Rays. Vol. 2. Stickland, A. C. (ed.). London, The Institute of Physics and The Physical Society, 1966.

Experimental data on the properties and composition of EAS with primary energies in the range 10^{13}-10^{15} ev, on the energy spectrum of nuclear active particles in the range 10^{12}-10^{14} ev, and on the size of showers accompanying them suggested a change in the main characteristics of nuclear interactions in the energy region given. It is very probable that the energy threshold of these changes for proton atmospheric nucleus collisions is $3 \times 10^{13} - 4 \times 10^{13}$ ev. The Lebedev Physical Institute of the Academy of Sciences U.S.S.R. is creating a new installation consisting of two ionization calorimeters, a large number of scintillators, and Čerenkov detectors at an altitude of 3340 m above sea level (Tien-Shan) to study EAS and muons in detail. (auth)

37635 CORRELATIONS BETWEEN THE ELECTRON, MUON AND N COMPONENTS IN EXTENSIVE AIR SHOWERS. Chatterjee, B. K.; Murthy, G. T.; Naranan, S.; Sreekantan, B. V.; Srinivasa Rao, M. V.; Tonwar, S. C.; Vatcha, R. H. (Tata Inst. of Fundamental Research, Bombay). pp 734-7 of Proceedings of the Ninth International Conference on Cosmic Rays. Vol. 2. Stickland, A. C. (ed.). London, The Institute of Physics and The Physical Society, 1966.

With the air shower array at Ootacamund (altitude 2.2 km) the energy spectrum of high energy N particles above 50 Bev was determined for showers of size ranging from a few times 10^4 to 10^7 particles and classified according to

shower size and steepness of the electron lateral distribution. It is found that the number of high energy N particles within 10 m is significantly less in showers which have a flat electron lateral distribution than steep showers of the same size (strong correlations in the lateral distributions of N particles, muons and electrons were reported earlier). It is also found that the variation of total number of N particles with size may be expressed as $N_n \propto N^m$ where m has a value of about 0.7. The low energy N component and muon component also have a similar dependence on shower size. (auth)

37636 EXTENSIVE AIR SHOWER EXPERIMENT AT KIEL. Bagge, E.; Boehm, E.; Fritze, R.; (and others) (Univ., Kiel). pp 738-41 of Proceedings of the Ninth International Conference on Cosmic Rays. Vol. 2. Stickland, A. C. (ed.). London, The Institute of Physics and The Physical Society, 1966.

A description of the air shower experiment at Kiel is given. In its present state the main objective is to study the electromagnetic core structure of showers. For this purpose a neon hodoscope of 32 m^2 area comprising about 180,000 neon tubes is used. The saturation density level of this detector can be varied in the range of 10,000 to 100,000 particles/m^2 by a suitable delay of the trigger pulse. The particle distribution at larger distances from the core is measured by 16 scintillation counters each of 1 m^2 area which also give information about the arrival direction by a fast timing method. The particle and fast timing data obtained by the scintillation counters are recorded by a digital system. (auth)

37637 AIR SHOWERS AT HIGH ALTITUDE. Kamata, K.; Murakami, K.; Kawasaki, S. (Inst. of Physical and Chemical Research, Tokyo). pp 742-3 of Proceedings of the Ninth International Conference on Cosmic Rays. Vol. 2. Stickland, A. C. (ed.). London, The Institute of Physics and The Physical Society, 1966.

Observations of air showers were made at altitudes of 7 km, 9 km, and 11 km above sea level by an air-borne apparatus, which is composed of scintillation counters and spark chambers. The number and the energy flow of shower particles, and the incident zenith angle of each shower are observed at each altitude. The results obtained are as follows: From the zenith angle distribution, it can be deduced that the frequency maximum of showers is at the atmospheric depth of about 400−500 g cm^{-2} for showers of size 10^5 particles. The energy flow of the electronic component near the core increases very slowly with altitude from sea level up to about 11 km, but there is an indication that it rapidly increases from 9 km up to 11 km above sea level for showers with size of the order of 10^5. (auth)

37638 EXTENSIVE AIR SHOWERS OBSERVED IN THE EMULSION CHAMBER. Akashi, M. (Hirosaki Univ., Japan); Watanabe, Z.; Nishimura, J.; (and others). pp 744-50 of Proceedings of the Ninth International Conference on Cosmic Rays. Vol. 2. Stickland, A. C. (ed.). London, The Institute of Physics and The Physical Society, 1966.

Large emulsion chambers (about 10 m^2 area) exposed at mountain altitudes (5200 m and 2800 m) provide us with means of observing the highest energy part of EAS cores. Lateral distribution of high energy γ rays in a cascade, successive interactions in the atmosphere, and the detailed core structure are discussed using the data observed in the chamber. (auth)

37639 VARIATION OF THE CHARACTERISTICS OF EAS WITH ATMOSPHERIC DEPTH. Suri, A. N. (Univ. of Leeds, Eng.). pp 751-3 of Proceedings of the Ninth International Conference on Cosmic Rays. Vol. 2. Stickland, A. C. (ed.). London, The Institute of Physics and The Physical Society, 1966.

A comparative study of extensive air showers produced by primaries of energy greater than or equal to 10^{17} ev was carried out as a function of zenith angle. Results are given on the variation with atmospheric depth of the lateral structure function, of shower front curvature and also of the absorption length. The form of the lateral distribution function and absorption properties of very inclined showers ($\theta > 60°$) suggests that they consist entirely of muons. (auth)

37640 THEORETICAL STUDIES OF THE MUON COMPONENT OF EAS. Holyoak, B.; Thompson, M. G.; Wdowczyk, J. (Univ. of Durham, Eng.). pp 754-7 of Proceedings of the Ninth International Conference on Cosmic Rays. Vol. 2. Stickland, A. C. (ed.). London, The Institute of Physics and The Physical Society, 1966.

Results are presented of calculations concerning the muon component of vertical and inclined showers. Using a simple model of high energy interactions and nuclear active particle cascades the muon energy spectrum, the lateral distribution of muons at sea level and the relation between mean height of origin and sea-level energy were determined. The energy spectra are in acceptable agreement with the Bennett et al. spectra considering the approximations of the model, but the lateral structure of the muon component differs greatly from that experimentally determined. Preliminary results of calculations using a more elaborate model of high energy interactions and a more accurate treatment of cascade processes are given and the role of fluctuations is examined. It is shown that fluctuations in the total number of muons in showers of a given size are due mainly to the fluctuations in the electron component. Even with the more elaborate model the agreement between the lateral structure of showers presented by Bennett et al. and the present results is poor. The spectra of muons in a heavy particle initiated shower are shown to be slightly less steep than the same sized proton-initiated shower. Calculations on horizontal showers (84° to zenith) show that the muon component is ≈2% of that in vertical showers and that the mean muon distance from the axis is at least 8 times that in vertical showers. (auth)

37641 CALCULATIONS ON THE PROPAGATION OF MESONS IN EXTENSIVE AIR SHOWERS. Hillas, A. M. (Univ. of Leeds, Eng.). pp 758-61 of Proceedings of the Ninth International Conference on Cosmic Rays. Vol. 2. Stickland, A. C. (ed.). London, The Institute of Physics and The Physical Society, 1966.

Preliminary results are presented of numerical calculations giving the lateral distribution, energy spectrum and heights of origin of muons in 10^{17} ev air showers, based on an assumed energy spectrum and angular distribution of secondaries from pion-nucleus collisions. Beyond 100 m good agreement with much of the experimental data is obtained, although there are indications that muons really originate higher than predicted by this model. The effect of Coulomb scattering on the lateral distribution is found to be small. The earth's magnetic field should not alter the overall distribution much, but should make densities of positive and negative muons very different in inclined showers. Further work should help to elucidate the part played by pions in ultra-high energy collisions. K mesons are here neglected. (auth)

37642 DIRECT MEASUREMENT OF ATTENUATION LENGTH OF EXTENSIVE AIR SHOWERS. Miyake, S.; Hinotani, K.; Ito, N.; Sasaki, H.; Yoshii, H.; Kino, S. (Osaka City Univ.). pp 762-4 of Proceedings of the Ninth International Conference on Cosmic Rays. Vol. 2. Stickland, A. C. (ed.). London, The Institute of Physics and The Physical Society, 1966.

Attenuation of EAS size by water layers (1.5 m and 2 m) was measured at mountain altitude. As far as the development of cascade and nuclear interactions are concerned, the water layer can be considered to be almost the same medium as the atmosphere, so the attenuation length of each EAS can be easily obtained by comparing the size in air with that underwater. The attenuation length obtained shows large fluctuations from shower to shower, though the mean value is not so inconsistent with the one so far obtained from the absorption rate in the atmosphere. Such a wide spread in observed values of the attenuation length can be explained by the core activity, for the further development and the activity of the core has a close correlation with lateral structure. The attenuation length of EAS is rather

short in general and the active EAS makes the average value longer though the number of events is small. (auth)

37643 DIFFERENTIAL MOMENTUM SPECTRUM AND CHARGE RATIO OF MUONS IN EXTENSIVE AIR SHOWERS. Rochester, G. D.; Somogyi, A. J.; Turver, K. E.; Walton, A. B. (Univ. of Durham, Eng.). pp 765-8 of Proceedings of the Ninth International Conference on Cosmic Rays. Vol. 2. Stickland, A. C. (ed.). London, The Institute of Physics and The Physical Society, 1966.

A solid iron magnet spectrograph was used in conjunction with the Haverah Park EAS arrays to measure the differential momentum spectrum and charge ratio of muons in EAS. The shape of the spectra was determined for muons in showers of different sizes which fell at various lateral distances from the spectrograph. The differential spectra can be represented by power laws of the form $s(p)dp \propto (p/p_0)^{-\gamma i-1} dp$ i = 1 for $p \leq p_0$, i = 2 for $p \geq p_0$ where $p_0 = 6.7$ Bev/c and the values of exponent are tabulated. The charge ratio was found to be not significantly different from unity for the ranges of energy investigated. (auth)

37644 STUDY OF THE EXTENSIVE AIR SHOWERS WITH FIXED MU MESON NUMBER AND WITH FIXED ELECTRON NUMBER. Vernov, S. N.; Khristiansen, G. B.; Abrosimov, A. T.; (and others) (Moscow State Univ.). pp 769-71 of Proceedings of the Ninth International Conference on Cosmic Rays. Vol. 2. Stickland, A. C. (ed.). London, The Institute of Physics and The Physical Society, 1966.

A new method for the study of extensive air showers with fixed mu meson number was examined. Data are presented about mean values and fluctuations of various characteristics of EAS with a fixed number of mu mesons N_μ and electrons N_e. Special attention was paid to the data on correlation between parameter S and other EAS characteristics. It was shown that at fixed values of N_e there is a fairly strong correlation between S and energy fluxes of nuclear active and electron-photon components. At fixed values of N_μ correlation exists between S and N_e as well as between S and the energy fluxes of nuclear active and electron-photon components. (auth)

37645 MUON COMPONENT OF AIR SHOWERS. Allan, H. R.; Blake, P. R.; Pidcock, J. K. (Imperial Coll. of Science and Tech., London). pp 772-3 of Proceedings of the Ninth International Conference on Cosmic Rays. Vol. 2. Stickland, A. C. (ed.). London, The Institute of Physics and The Physical Society, 1966.

Measurements were made on the muon component of air showers in the size range 5×10^6 to 10^8 particles. The lateral distribution function for muons of energy greater than 250 Mev (absorber thickness 20 cm lead) is of the form $\rho_\mu \propto r^{-2.2}$ for r between 300 m and 1000 m, independent of shower size. The total number of muons in a shower N_μ is found to vary with shower size N according to the relation $N_\mu \propto N^{0.5\pm0.1}$. The implications of this result are discussed. (auth)

37646 COMPARISON OF VARIOUS MODELS OF EAS DEVELOPMENT WITH EXPERIMENTAL DATA AND THE PROSPECTS OF COSMOLOGICAL AND NUCLEAR ASPECTS OF EAS INVESTIGATION. Khristiansen, G. B.; Atrashkevich, V. B.; Kalmykov, N. N.; Fomin, Yu. A. (Moscow State Univ.). pp 774-8 of Proceedings of the Ninth International Conference on Cosmic Rays. Vol. 2. Stickland, A. C. (ed.). London, The Institute of Physics and The Physical Society, 1966.

Results of calculations of EAS characteristics at sea and mountain level and in the stratosphere made on different assumptions about the elementary interaction are given. Comparison with the experimental data on fluctuations in EAS at sea level and on the altitude dependence of EAS intensity shows that it is still impossible to choose a unique model of EAS development. However, an increase of one order of magnitude in the experimental statistics on fluctuations may make a choice possible. The prospects of further EAS investigations are considered; particularly the new method of investigation of chemical composition of the primary radiation based on the simultaneous registration of Čerenkov light and muon flux which permits a check of the correctness of the usual assumption that EAS from a nucleus of atomic number A and energy E_0 is the superposition of A showers from primary protons of energies E_0/A. (auth)

37647 MONTE CARLO STUDIES ON EXTENSIVE AIR SHOWER DEVELOPMENT. Thielheim, K. O.; Karius, S. (Univ., Kiel). pp 779-82 of Proceedings of the Ninth International Conference on Cosmic Rays. Vol. 2. Stickland, A. C. (ed.). London, The Institute of Physics and The Physical Society, 1966.

Monte Carlo calculations on extensive air shower development were performed. Frequencies of nuclear active and electromagnetic multicore events are discussed in terms of primary particle atomic number and of excitation of surviving primary baryons. The following results were obtained: Multicore events (as typically observed in scintillator arrays), which could possibly reflect primary composition, are expected mainly in the energy range $10^{14}-10^{16}$ ev; the number of nuclear active subcores, caused by surviving primary baryons, will generally not equal the primary atomic number; the high energy tail of the production spectrum (as caused by excitation of surviving baryons for example) has a strong influence on the frequencies of multicore events; and primary composition could be inferred from the frequencies of multicore events, if the high energy tail of the production spectrum were known. (auth)

37648 MEAN SQUARE ANGULAR AND LATERAL SPREADS OF ELECTRONS AND PHOTONS IN A CASCADE SHOWER. Misaki, A. (Kohnan Univ., Kobe, Japan). pp 783-6 of Proceedings of the Ninth International Conference on Cosmic Rays. Vol. 2. Stickland, A. C. (ed.). London, The Institute of Physics and The Physical Society, 1966.

Mean square angular and lateral spreads of electrons and photons in a cascade shower initiated by a photon are calculated over wide ranges of energies and observation depths under the approximation A and the Landau approximation according to the theory of Nishimura and Kamata. Corresponding quantities as a function of the energy of the shower particle are also obtained. The results are compared with those of the Monte Carlo calculations given by Adachi et al. and the agreement is good. The results are also compared with those of Chartres and Messel, and their results for lateral spreads disagree with those given here. (auth)

37649 MEASUREMENT OF THE TIME VARIATIONS OF SMALL AIR SHOWERS. Jones, J. K. (Imperial Coll. of Science and Tech., London). pp 787-8 of Proceedings of the Ninth International Conference on Cosmic Rays. Vol. 2. Stickland, A. C. (ed.). London, The Institute of Physics and The Physical Society, 1966.

An array of water Čerenkov detectors was set up to measure the solar and sidereal time variations of cosmic radiation ranging from single particles to air showers of size up to $N = 10^6$ particles. The method of stabilization is discussed and results of four months' running of one detector are presented, giving the barometric coefficients of 1–50 equivalent particles in one Čerenkov detector. (auth)

37650 INVERSE PROBLEM IN THE CASCADE THEORY OF SHOWERS. Astafiev, V. A.; Ivanenko, I. P. (Moscow State Univ.). pp 789-91 of Proceedings of the Ninth International Conference on Cosmic Rays. Vol. 2. Stickland, A. C. (ed.). London, The Institute of Physics and The Physical Society, 1966.

It is shown that some characteristics of the interaction of elementary particles with matter may be determined if the energy distributions of the particles in air showers are known at various depths in the atmosphere. These characteristics include the probabilities of interaction, the multiplicities, and the mean energies of the particles in multiple production events. Mathematically the problem is reduced to the solution of some integral equations. A solution for a simple cascade was obtained. (auth)

37651 ENERGY SPECTRUM, POSSIBLE CHEMICAL COMPOSITION, AND ANISOTROPY OF THE ULTRA-HIGH ENERGY PRIMARY COSMIC RADIATION. Khristiansen, G. B.; Abrosimov, A. T.; Atrashkevich, V. B.; Kulikov, G. V.; Solov'eva, V. I.; Fomin, Yu. A. (Moscow State Univ.). pp 799-801 of Proceedings of the Ninth International Conference on Cosmic Rays. Vol. 2. Stickland, A. C. (ed.). London, The Institute of Physics and The Physical Society, 1966.

Data on the energy spectrum of high energy cosmic radiation ($10^{15}-10^{17}$ ev), based on the experimental electron size N_e spectrum and the experimental muon size N_μ spectrum of EAS, are presented. It is shown that the primary energy spectrum undergoes a double variation of its slope. The possible chemical composition of the primary cosmic radiation is analyzed in terms of data on the electron size distribution of EAS with a fixed muon size, and the anisotropy of EAS with a fixed muon size N_μ was investigated. The whole experimental data are treated using the diffusion theory of cosmic ray propagation in the galaxy and metagalaxy on the assumption of a dependence of the diffusion coefficient D of cosmic rays in the galaxy upon energy E. (auth)

37652 TIME LAGS OF NUCLEAR INTERACTING PARTICLES IN EXTENSIVE AIR SHOWERS. Chatterjee, B. K.; Murthy, G. T.; Naranan, S.; Sreekantan, B. V.; Srinivasa Rao, M. V.; Tonwar, S. C. (Tata Inst. of Fundamental Research, Bombay). pp 802-4 of Proceedings of the Ninth International Conference on Cosmic Rays. Vol. 2. Stickland, A. C. (ed.). London, The Institute of Physics and The Physical Society, 1966.

An experiment was carried out at 2.2 km altitude to determine the time lags with respect to the shower front of nuclear interacting particles of various energies. For this purpose a total absorption spectrometer of area 1.4 m^2 was operated at the center of an air shower array. Delays of interacting particles of energy not less than 5 Bev were measured up to a maximum delay of about 300 nsec. The results show: that the peak of all nuclear interacting particles of energy above 5 Bev is displaced with respect to the shower front by about 20 nsec, the average delay is a function of the average energy of the particles, and while nearly 30% of the particles of energy above 5 Bev are delayed by more than 50 nsec, only about 0.4% are delayed beyond 100 nsec. The tail extends right up to 250 nsec. These features quite definitely rule out the possibility that nuclear active particles of energy not less than 5 Bev are predominantly pions. They suggest the production of a large number of nucleon-antinucleon pairs in air showers. (auth)

37653 SEARCH FOR HEAVY MASS PARTICLES IN AIR SHOWERS. Chatterjee, B. K.; Murthy, G. T.; Naranan, S.; Sreekantan, B. V.; Srinivasa Rao, M. V.; Tonwar, S. C. (Tata Inst. of Fundamental Research, Bombay). pp 805-7 of Proceedings of the Ninth International Conference on Cosmic Rays. Vol. 2. Stickland, A. C. (ed.). London, The Institute of Physics and The Physical Society, 1966.

Recently there have been theoretical speculations on the production in high energy collisions of particles much heavier than nucleons. Such particles are expected to behave like nuclear interacting particles in air showers with the difference that even at high energies they will be considerably delayed with respect to the shower front and transfer a much smaller fraction of their energy in nuclear collisions. An experimental search was made at Ootacamund (2.2 km altitude) employing a total absorption spectrometer at the center of an air shower array for the presence of delayed high-energy interacting particles in the interval 60–300 nsec. In 449 hours of observation (about 80,000 showers of size 10^4-10^7) there is no evidence for the passage of a heavy mass particle through the total absorption spectrometer of approximate area 1.5 m^2. A heavy mass particle would have been detected if it had a mass of about 5–10 Bev, energy 40–100 Bev, interacted with a mean free path of about 80–100 g cm^{-2}, transferred 5–10% of its energy in nuclear collisions, and was not more than about 20 m away from the core. (auth)

37654 SEARCH FOR HEAVY PARTICLES IN THE COSMIC RADIATION. Damgaard, G. (Univ. of Copenhagen); Grieder, P.; Hansen, K. H.; Iversen, C.; Lohse, E.; Peters, B.; Rengarayan, T.; Klovning, A.; Lillethun, E. pp 808-9 of Proceedings of the Ninth International Conference on Cosmic Rays. Vol. 2. Stickland, A. C. (ed.). London, The Institute of Physics and The Physical Society, 1966.

Experiments designed to search for long-lived or stable particles with rest masses in the region 5–20 Bev/c^2 are described. Such particles may be produced in air showers and some should arrive at sea level slightly delayed with respect to light particles and γ rays. Energetic particles (penetrating a large amount of absorber) preceded within 20–500 nsec by some other associated particle signal were registered. If the energy is high enough, the registered particles have travelled through the atmosphere appreciably slower than a light signal and must therefore have a large rest mass. Only preliminary upper limits on the flux of such particles are available at present. (auth)

37655 EXTENSIVE AIR SHOWERS. McCusker, C. B. A. (Univ. of Sydney). pp 810-14 of Proceedings of the Ninth International Conference on Cosmic Rays. Vol. 2. Stickland, A. C. (ed.). London, The Institute of Physics and The Physical Society, 1966.

Research on cosmic showers is reviewed. Topics covered include a description of EAS, techniques and apparatus, mesons (μ) in EAS, gamma-produced showers, the cosmic ray energy spectrum, core structure of EAS, transverse momentum in collisions with air nuclei, and cosmic ray composition at different energies. Also the density spectrum of EAS, characteristics of high energy nuclear interactions, and future experiments are discussed. (J.F.P.)

37656 TIEN-SHAN HIGH ALTITUDE INSTALLATION FOR STUDYING STRONG INTERACTIONS AT 100 TO 1000 Gev (PRELIMINARY RESULTS). Dobrotin, N. A.; Denisov, E. V.; Dubrovina, S. A.; (and others) (Lebedev Inst. of Physics, Moscow). pp 817-20 of Proceedings of the Ninth International Conference on Cosmic Rays. Vol. 2. Stickland, A. C. (ed.). London, The Institute of Physics and The Physical Society, 1966.

A new experimental installation which was built and put into operation at the Tien-Shan station (3340 m above sea level) is described. The installation consists of a cloud chamber in a magnetic field (the maximum detectable momentum is about 25 Bev) and an ionization calorimeter (500 ionization chambers separated by lead and iron absorbers). A thin LiH plate is used as a target. The installation makes it possible to investigate individual events of interactions of high energy cosmic ray particles as well as electron nuclear cascades in the ionization calorimeter. Preliminary results of the first few months of operation of the installation are presented. (auth)

37657 INVESTIGATION OF THE NUCLEON INTERACTIONS AT ENERGIES ABOVE 10^{13} ev. Smorodin, Yu. A.; Solov'ev, M. V.; Antonov, R. A.; Baradzei, L. T.; Rykov, V. V.; Kanevskaya, E. A.; Apanasenko, A. V.; Tulinova, S. I.; Sorokin, O. W. (Lebedev Inst. of Physics, Moscow. Moscow State Univ.). pp 827-9 of Proceedings of the Ninth International Conference on Cosmic Rays. Vol. 2. Stickland, A. C. (ed.). London, The Institute of Physics and The Physical Society, 1966.

A short description is presented of aircraft-borne equipment intended for investigation of nucleon interactions at energies greater than 10^{13} ev. The main part of the equipment consists of 90 Cherenkov counters and two layers of x ray films and nuclear emulsions. A system of 20 scintillation counters and two spark chambers is used for EAS detection. Examples of detected events are given. (auth)

37658 INVESTIGATION OF THE NUCLEAR-ACTIVE COMPONENT OF COSMIC RAYS. Vardumian, D. T.; Marikian, G. A.; Matevosian, K. A. (Armenian Academy of Sciences, Erevan). pp 830 of Proceedings of the Ninth International Conference on Cosmic Rays. Vol. 2. Stickland, A. C. (ed.). London, The Institute of Physics and The Physical Society, 1966.

The nuclear interaction of cosmic rays and the character of the charged component accompanying them is studied with an arrangement consisting of an ionization calorimeter, Geiger counter hodoscope and two large spark chambers located above the calorimeter. The cross section for nuclear interaction is determined with the help of the spark chambers between which the substance under investigation is placed. The results show that the nuclear active particles with energies above 150 Bev are almost always (≥80%) accompanied by charged particles, with an average density of about 20 particles m^{-2}, such that the determination of the dependence of the nuclear interaction cross section on energy is made difficult. (auth)

37659 FOUR-MOMENTUM TRANSFERRED IN HIGH-ENERGY INTERACTIONS. Erofeeva, I. N.; Mitshenko, L. G.; Murzin, V. S.; Rapoport, I. D.; Rotshin, A. P.; Saricheva, L. I. (Moscow State Univ.). pp 831-2 of Proceedings of the Ninth International Conference on Cosmic Rays. Vol. 2. Stickland, A. C. (ed.). London, The Institute of Physics and The Physical Society, 1966.

The four-momentum transferred in the collisions of nuclear active particles with nuclei of carbon and aluminum is determined on the basis of the fireball interaction model. The angular distribution of secondaries measured by means of a cloud chamber and the knowledge of primary energy obtained from an ionization calorimeter were used. The longitudinal component of four-momentum is equal to 2.38 ± 0.11 and 1.21 ± 0.28 for carbon and aluminum respectively. (auth)

37660 DISTRIBUTION OF THE ENERGY PORTION TRANSFERRED TO π^0 MESONS. Erofeeva, I. N.; Mitshenko, L. G.; Murzin, V. S.; Rapoport, I. D.; Saricheva, L. I. (Moscow State Univ.). pp 833-4 of Proceedings of the Ninth International Conference on Cosmic Rays. Vol. 2. Stickland, A. C. (ed.). London, The Institute of Physics and The Physical Society, 1966.

The data, obtained by means of an ionization calorimeter, on the mean value and on the distribution of the energy fraction transferred to the electron-photon component when nuclear active particles collide with nuclei of carbon, iron and lead are presented. It is indicated that for pions of energy above or equal to 2×10^{11} ev colliding with nuclei, about 70% of the primary pion energy is very often transferred to the electron-photon component. In a case of nucleon-nuclear collisions, photons, as a rule, carry away less than 60% of the primary energy. The mean values of α_γ in carbon and in iron are equal to 0.17 and 0.27 respectively. (auth)

37661 OBSERVATION OF EXTREMELY HIGH ENERGY NUCLEAR EVENTS BY EMULSION CHAMBER. Akashi, M. (Hirosaki Univ., Japan); Watanabe, Z.; Nishimura, J.; (and others). pp 835-9 of Proceedings of the Ninth International Conference on Cosmic Rays. Vol. 2. Stickland, A. C. (ed.). London, The Institute of Physics and The Physical Society, 1966.

An analysis is presented on the nuclear interactions (incident energy ≥100 Tev) observed by the emulsion chamber exposed at Mount Chacaltaya and Mount Norikura. Measurements are made on the transverse momentum and energy spectrum of γ rays (π^0 mesons) and secondary interactions (survival nucleons, charged π mesons etc.). The inelasticity of nucleons and mesons and the transverse momentum of a fireball are derived from the above results. Consistencies between these results and those of others are examined. (auth)

37662 HIGH-ENERGY JETS PRODUCED BY HEAVY PRIMARY NUCLEI OF COSMIC ORIGIN AND THEIR FRAGMENTATION PRODUCTS. Abraham, F. (Univ. of Chicago); Levi Setti, R.; Tsao, C. H.; Gierula, J.; Rybicki, K.; Wolter, W.; Fricken, R. L.; Huggett, R. W. pp 844-8 of Proceedings of the Ninth International Conference on Cosmic Rays. Vol. 2. Stickland, A. C. (ed.). London, The Institute of Physics and The Physical Society, 1966.

In a large 80 l. emulsion stack flown at Brawley, California, six events initiated by heavy primary nuclei with energies above 10^{12} ev per nucleon have been analyzed. The fragmentation of heavy primary nuclei proves to be, in favourable cases, a powerful tool for an unbiased collection of nucleon induced interactions. Information concerning the multiplicity, angular distributions and inelasticity in nucleon induced jets was obtained. The analysis of jets produced by heavy nuclei yields new information about the process of meson production as well as the parameters describing nucleons involved in the collision. (auth)

37663 HIGH-ENERGY COSMIC-RAY JET RESEARCH AT KRAKOW. pp 849-50 of Proceedings of the Ninth International Conference on Cosmic Rays. Vol. 2. Stickland, A. C. (ed.). London, The Institute of Physics and The Physical Society, 1966.

Systematic study of high energy jets in large emulsion stacks is in progress at the Krakow laboratory. All advantages of large stacks are explored in this investigation. More than a hundred secondary interactions were found in a careful scanning along the track. A large fraction of very low multiplicity jets seems to be characteristic for the multiplicity distribution. Preliminary results are presented. (auth)

37664 GENERATION MECHANISM OF HIGH-ENERGY PIONS IN COSMIC RAYS. Grigorov, N. L.; Shestoperov, V. Ya.; Brikker, S. I.; Podgurskaya, A. V.; Poperekova, L. M.; Plekhova, A. I.; Saveleva, A. I.; Sobinyakov, V. A. (Moscow State Univ.). pp 851-3 of Proceedings of the Ninth International Conference on Cosmic Rays. Vol. 2. Stickland, A. C. (ed.). London, The Institute of Physics and The Physical Society, 1966.

The characteristics of the showers generated in carbon by nuclear active particles of energies greater than 2×10^{12} ev were studied using the method of controllable nuclear photoemulsions. A comparison is made between results from emulsion data and cloud chamber data. The results do not indicate that high energy pions are formed due to disintegration of isobars. (auth)

37665 AZIMUTHAL ANGULAR DISTRIBUTIONS OF SECONDARY PARTICLES IN COSMIC JETS. Mishakova, A. P.; Nikolskii, B. A. (Kurchatov Inst. of Atomic Energy, Moscow). pp 854-6 of Proceedings of the Ninth International Conference on Cosmic Rays. Vol. 2. Stickland, A. C. (ed.). London, The Institute of Physics and The Physical Society, 1966.

A study, using the method of pair angular correlations, is made of the azimuthal angular distributions of secondary particles produced in 169 nuclear collisions with energy $10^{10}-10^{14}$ ev. The isotropic azimuthal angular distribution is observed for the primary collisions produced by nucleons and the anisotropic distribution is observed for the secondary interactions produced by π mesons. The experimental data on the pair angular correlation of the secondary shower particles are discussed from the viewpoint of the fireball model. (auth)

37666 ELASTIC AND ELECTROMAGNETIC PROTON INTERACTIONS AT 30 Gev. McCusker, C. B. A.; Peak, L. S.; Woolcott, R. L. S. (Univ. of Sydney). pp 857-9 of Proceedings of the Ninth International Conference on Cosmic Rays. Vol. 2. Stickland, A. C. (ed.). London, The Institute of Physics and The Physical Society, 1966.

The results of a line scan, in nuclear emulsion, of protons of average energy 3 Tev is presented. No elastic scatters were detected in the scanned length of 594 cm. The probability of detecting an elastic scatter in emulsion is considered and hence the proton-nucleon elastic cross section at 3 Tev is estimated as not greater than 8 mbn with 85% probability. Five examples of trident production were found in the above path length. This figure is consistent with the predictions of quantum electrodynamics. (auth)

37667 INTERACTION PATH OF HIGH-ENERGY NUCLEONS (10^{11} TO 10^{13} ev) IN THE ATMOSPHERE. Grigorov, N. L. (Moscow State Univ.); Sobinyakov, V. A.; Tretyakova, Ch. A.; Shestoperov, V. Ya.; Babayan, Kh. P.; Dulyan, G. G. pp 860-2 of Proceedings of the Ninth International Conference on Cosmic Rays. Vol. 2. Stickland, A. C. (ed.). London, The Institute of Physics and The Physical Society, 1966.

The flux of nuclear active particles of energy 10^{12} ev not

accompanied by secondary particles is measured by a large ionization calorimeter. The evaluation of the absorption path of high-energy protons in the atmosphere is obtained by the comparison of this flux with the flux of primary protons. (auth)

37668 INELASTIC NEUTRON CROSS SECTION MEASUREMENTS NEAR 100 Gev. Bolotov, V. N.; Devishev, M. I.; Klimanova, L. F.; Shmeleva, A. P. (Lebedev Inst. of Physics, Moscow. Inst. of Physics, Erevan). pp 863-4 of Proceedings of the Ninth International Conference on Cosmic Rays. Vol. 2. Stickland, A. C. (ed.). London, The Institute of Physics and The Physical Society, 1966.

An experiment to measure the cross section for high energy cosmic ray neutron interactions with Pb and C nuclei was carried out at an altitude of 2000 m. Large spark chambers were used and the detector selected nucleons in the vicinity of 100 Bev. The results are $\sigma_{Pb} = (1.5 \pm 0.4)$ bn and $\delta_c = (0.2 \pm 0.05)$ bn respectively. (auth)

37669 SHOWER PRODUCTION BY PIONS AND PROTONS WITH MOMENTA 0.1 AND 20 Gev/c IN THIN LAYERS OF MATTER. Khrimian, A. V.; Avakian, V. V.; Pleshko, M. P.; Vartanyan, T. G. (Armenian Academy of Sciences, Erevan). pp 865-9 of Proceedings of the Ninth International Conference on Cosmic Rays. Vol. 2. Stickland, A. C. (ed.). London, The Institute of Physics and The Physical Society, 1966.

In experiments devoted to the investigation of the composition of primary cosmic rays (including electrons and γ rays) with the help of earth satellites and rockets, the showers produced by protons form a high background, while in investigations made in the lower layers of the atmosphere the background consists of electron showers. The effect of the passage of pions and protons with momenta 0.1–20 Bev/c through thin layers of polystyrene, copper and lead were studied. Experimental data are obtained on the multiplicities and energies of the secondary particles as a function of the momentum of the primary proton and pion. The main results are the following: shower events are 15% of the total number of events registered by the detector surrounded by 10–50 g cm^{-2} of heavy metal; the higher the particle momentum, the greater the probability of the production of showers with long-range products; in the momentum region 0.1–0.7 Bev/c, for equal particle momenta, the frequency of shower production by pions is 2–4 times greater than that by protons; the search for primary electrons and γ rays by the method of indication of electron showers without identification of the secondary particles presents great difficulties. (auth)

37670 INELASTIC n-p CROSS SECTION AT 60 Gev. Bozoki, G. (Central Research Inst. of Physics, Budapest); Fenyves, E.; Christov, C.; Ahababian, N.; Betev, B.; Kavlakov, S. T. pp 870-1 of Proceedings of the Ninth International Conference on Cosmic Rays. Vol. 2. Stickland, A. C. (ed.). London, The Institute of Physics and The Physical Society, 1966.

The attenuation of penetrating shower-producing cosmic ray neutrons in paraffin and graphite is measured with a counter hodoscope arrangement at mountain altitude. By the CH_2-C subtraction method the value of the inelastic n-p cross section is determined for energies higher than present accelerator energies. From the attenuation of neutrons in both absorbers the collision mean free path in carbon and paraffin is obtained. Preliminary results are given for neutrons having mean energies of about 60 Bev. (auth)

37671 ANALYSIS OF METHODS OF MEASUREMENT OF THE CHARACTERISTICS OF ELEMENTARY INTERACTIONS. Murzin, V. S. (Moscow State Univ.). pp 872-4 of Proceedings of the Ninth International Conference on Cosmic Rays. Vol. 2. Stickland, A. C. (ed.). London, The Institute of Physics and The Physical Society, 1966.

The effect of the steep spectrum of nuclear active particles and of the method of selection of events on the study of the characteristics of elementary interactions is considered. It is shown, taking the example of photo-emulsion investigations, that the significant errors of energy measurement using the Castagnoli method for individual events introduce large errors in determining the coefficients of inelasticity, multiplicity and other mean characteristics of interactions. Threshold effects influence the measurements up to energies which are ten to a hundred times the threshold energy. (auth)

37672 ENERGY SPECTRA OF CASCADES OBSERVED AT BALLOON ALTITUDES AND THE FLUX OF PRIMARY PROTONS. Malholtra, P. K. (Tata Inst. of Fundamental Research, Bombay); Shukla, P. G.; Stephens, S. A.; (and others). pp 875-7 of Proceedings of the Ninth International Conference on Cosmic Rays. Vol. 2. Stickland, A. C. (ed.). London, The Institute of Physics and The Physical Society, 1966.

A composite detector of heavy metal and nuclear emulsion was used to investigate electromagnetic cascades produced by the cosmic radiation. The stack was exposed on a balloon near the top of the atmosphere for 28 hours. Approximately 4000 cascades were observed and these were classified as arising from nuclear interactions in the overlying atmosphere, in the detector itself or in a thin graphite layer surrounding the detector. The energies of the cascades were estimated from their electron track density. The energy spectra of the various types of cascades are presented. The nuclear spectrum is well approximated by a power law $N(>\Sigma E_\gamma) = \text{const.}\ (\Sigma E_\gamma)^{-1.44\pm0.08}$ for $370 \leq \Sigma E_\gamma \lesssim 4 \times 10^4$ Bev, and the spectrum of individual γ rays by a power law $N(>E_\gamma) = \text{const.}\ E_\gamma^{-1.57\pm0.08}$ for $370 \leq E_\gamma \lesssim 2.5 \times 10^3$ Bev. Above 2.5×10^3 Bev the γ ray spectrum is steeper, with an index -3.0 ± 0.8. These results are compared with similar measurements made at greater depths in the atmosphere. The flux of protons at the top of the atmosphere capable of giving rise to cascades of energy greater than 370 Bev is found to be $(2.10 \pm 0.08) \times 10^{-6}$ cm^{-2} sterad^{-1} sec^{-1}. This is compared with other values over the wide range of primary energy from 10^9 to 10^{20} ev. (auth)

37673 NUCLEAR INTERACTIONS PRODUCED IN THE EMULSION CHAMBER. Akashi, M. (Hirosaki Univ., Japan); Watanabe, Z.; Nishimura, J.; (and others). pp 878-82 of Proceedings of the Ninth International Conference on Cosmic Rays. Vol. 2. Stickland, A. C. (ed.). London, The Institute of Physics and The Physical Society, 1966.

A large emulsion chamber area (6 m^2, thickness 29 cm Pb) was exposed on Mount Chacaltaya (5200 m) for about 10 months in a collaboration of the Japanese and Brazilian emulsion groups. Several hundred γ rays incident upon and nuclear events produced in the chamber with energy higher than 2×10^{12} ev were observed and the results are reported. The results of observation at Mount Norikura (2800 m) carried out by the Japanese group are also included. (auth)

37674 SPECTRUM OF THE NUCLEAR-ACTIVE COMPONENT OF COSMIC RAYS. Kellermann, E. W.; Silk, M. G. (Univ. of Leeds, Eng.). pp 883-4 of Proceedings of the Ninth International Conference on Cosmic Rays. Vol. 2. Stickland, A. C. (ed.). London, The Institute of Physics and The Physical Society, 1966.

A small nuclear calorimeter consisting of five proportional counter trays of area 0.73 m^2 in a matrix of lead and steel was employed to measure the spectrum of nuclear active particles at sea level up to energies of about 5×10^{12} ev. The spectrum can be represented by a power law with exponent between –1.8 and –1.9. Incomplete exclusion of muon contributions results in an exponent of –2.1, whereas contamination by the electron-photon component yields a flatter spectrum. The spectrum obtained is in agreement with the proton spectrum established by the Durham group and with that of nucleons of corresponding energies obtained by emulsion measurements. Operated in conjunction with an air shower array very large fluctuations are found in the relation between bursts due to nuclear active particles and the sizes of accompanying showers. (auth)

37675 CERTAIN ASPECTS OF NUCLEON ISOBAR PRODUCTION IN NUCLEON INTERACTIONS AT ENERGIES 10^3 AND 25 Gev. Galstyan, D. A.; Zhdanov, G. B.; Tretyakova, M. I.; Chernavskii, M. M.; Shcherbakova,

M. N. (Lebedev Inst. of Physics, Moscow). pp 885-6 of Proceedings of the Ninth International Conference on Cosmic Rays. Vol. 2. Stickland, A. C. (ed.). London, The Institute of Physics and The Physical Society, 1966.

Examples of nuclear interactions in photoemulsion giving rise to a large energy transfer to several secondary charged particles were investigated. Such interactions are selected by the presence of a sufficiently narrow and pronounced cone of secondary particles (angles of emergence are very much greater than M_n/E_0 where E_0 is an estimate of the primary energy). The analysis of the energy characteristics of these particles was based on the angular characteristics of secondary interactions (Castagnoli and transverse momentum methods) for cosmic ray events and on the magnetic curvature of the tracks for the accelerator energy region. If the energies are referred to the rest system of some symmetrically decaying intermediate body then the energy values are spread around about 0.5 Bev and the secondary nucleon does not essentially differ from mesons. Such a situation is consistent with the conception of a nucleonic isobar excitation process with mean isobar mass 1.45–1.85 Bev/c^2 for E_0 = 24 Bev and n_s = 3 and about twice this value for $E_0 \sim 10^{13}$ ev ($\bar{n}_s$ = 6). The probability estimate in the interval 2–10% for this type of interaction is also obtained. (auth)

37676 EXPERIMENT TO DETERMINE THE PRIMARY INTENSITY AND THE PRIMARY SPECTRUM AT ENERGIES OF 10^{12} TO 10^{13} ev. Sitte, K. (Max-Planck-Institut fuer Kernphysik, Heidelberg). pp 887-9 of Proceedings of the Ninth International Conference on Cosmic Rays. Vol. 2. Stickland, A. C. (ed.). London, The Institute of Physics and The Physical Society, 1966.

All hitherto available information on the primary spectrum above the geomagnetic cut-off derives from indirect methods, that is, from measurements performed on the secondaries of the cosmic ray primaries. It is, consequently, safe only to the extent to which the theories can be relied upon by which the primary energy is deduced. A direct measurement using only observations on the primaries could, therefore, provide not only more secure data on the spectrum but at the same time also a check on the theories of high energy interactions. It is shown that since protons of different energies begin to emit Čerenkov radiation at different altitudes, an experiment measuring the atmospheric Čerenkov light at an altitude around 10 g cm^{-2} could be performed in which primary intensities can be determined from about 4×10^{11} to about 4×10^{12} ev. A preliminary study of its design features is presented. (auth)

37677 SECONDARY SPECTRA FOR TRUNCATED SPECTRA FOR THE PRIMARY COSMIC RAYS. Pal, Y.; Tandon, S. N. (Tata Inst. of Fundamental Research, Bombay). pp 890-2 of Proceedings of the Ninth International Conference on Cosmic Rays. Vol. 2. Stickland, A. C. (ed.). London, The Institute of Physics and The Physical Society, 1966.

A procedure was developed for calculating the energy spectra of nucleons, muons and γ rays for power law primary energy spectra which are truncated at the low or high energy ends. Using this with a specific model of the break in the primary energy spectrum beyond 10^5 Bev, fluxes of high energy muons and of γ rays at various depths in the atmosphere were calculated and compared with experiments. (auth)

37678 MULTIPLICITY OF HIGH-ENERGY INTERACTIONS. Pinkau, K. (Louisiana State Univ., Baton Rouge). pp 895-7 of Proceedings of the Ninth International Conference on Cosmic Rays. Vol. 2. Stickland, A. C. (ed.). London, The Institute of Physics and The Physical Society, 1966.

In air, the amplitude of the maximum of showers is correlated to the primary energy, while the position of the shower maximum depends on the inelasticity and the multiplicity of the interactions. Since the inelasticity can be assumed to be nearly constant, the position of the maximum of extensive air showers may be used to obtain information on the multiplicity of nuclear interactions causing the showers. The results indicate a logarithmic variation of multiplicity with energy. They also allow the interpretation that heavy nuclei are partly responsible for extensive air showers up to energies of about 5×10^5 Bev, while their intensity appears to be drastically reduced above this energy, leaving mainly protons as the source of air showers. (auth)

37679 TWO-FIREBALL AND CKP MODELS OF ULTRAHIGH-ENERGY INTERACTIONS. Huggett, R. W. (Louisiana State Univ., Baton Rouge). pp 898-900 of Proceedings of the Ninth International Conference on Cosmic Rays. Vol. 2. Stickland, A. C. (ed.). London, The Institute of Physics and The Physical Society, 1966.

Predictions of the two-fireball model of ultra-high energy interactions are compared with those of the Cocconi, Koester and Perkins (CKP) model, an essentially one-center model. For both models the angular distributions in the log tan θ coordinate exhibit a double-maximum structure, but the maxima for the CKP model are less pronounced and broader. It is pointed out that both models predict a dependence of p_t on emission angle, and the formulas expressing the predicted dependences are given. Artificial jets corresponding to each model were constructed using a Monte Carlo method. The resulting artificial jets satisfy the energy-momentum conservation laws and have the properties required by each model. These jets were made to correspond to 3000 Bev nucleon-nucleon interactions with the secondaries having $\langle p_t \rangle$ = 0.38 Bev/c, $\langle p_t^* \rangle$ = 2.1 Bev/c, and a multiplicity of 16. The two-fireball jets were required to have the same p_t distribution as that in the CKP model, and $\bar{\gamma}$ was adjusted to give the same $\langle K^* \rangle$ and σ. Distributions of the inelasticity and some observable physical quantities are obtained and compared with respect to each model. It is found that except for the p_t dependence on angle and the high energy tail of the secondaries' energy spectrum in the laboratory system, the two models can be made to give rather similar features. (auth)

37680 NEW KINEMATICAL APPROACH FOR ANALYSES OF HIGH-ENERGY COSMIC-RAY JETS. Hasegawa, S. (Waseda Univ., Tokyo); Kobayashi, T.; Ohsawa, A.; Shibata, T.; Yajima, N. pp 901-4 of Proceedings of the Ninth International Conference on Cosmic Rays. Vol. 2. Stickland, A. C. (ed.). London, The Institute of Physics and The Physical Society, 1966.

New kinematical approaches were developed for the analysis of the angular distribution of high-energy jets on the basis of the assumption of constant and known transverse momentum of secondary pions. The formulas are applied to the practical analysis of experimental data published to date and discuss the characteristic features of phenomenological models of multiple meson production. (auth)

37681 INVESTIGATION OF HIGH-ENERGY NUCLEAR INTERACTIONS USING A QUARTILE ENERGY ESTIMATOR. Peak, L. S.; Woolcott, R. L. S. (Univ. of Sydney). pp 905-8 of Proceedings of the Ninth International Conference on Cosmic Rays. Vol. 2. Stickland, A. C. (ed.). London, The Institute of Physics and The Physical Society, 1966.

A method of energy estimation for nuclear interactions ($E \leq 10^{14}$ ev) is devised using the quartile angle of the emitted tracks. The resulting estimate is seen not to be critically dependent upon the extraction of the persisting baryon or on the assignment of the median angle within the large gap between the forward and backward cones. The estimate is, however, model dependent, and the good agreement of its predictions at both machine and jet energies, lends support to the model assumed (receding emission centers). Using this estimator which is fairly reliable for individual events, the fireball mass is estimated, and an examination of inelasticities suggests the production of isobars, in keeping with a peripheral mechanism such as that proposed by S.C. Frautschi. (auth)

37682 ANGULAR DISTRIBUTION OF SECONDARY PARTICLES IN MULTIPLE PRODUCTION AT HIGH ENERGIES. Maximenko, V. M.; Slavatinskii, S. A.; Sokolovskii, V. V.; Zelevinskaya, N. G. (Lebedev Inst. of

Physics, Moscow). pp 911-13 of Proceedings of the Ninth International Conference on Cosmic Rays. Vol. 2. Stickland, A. C. (ed.). London, The Institute of Physics and The Physical Society, 1966.

The expected distribution of the parameters $\alpha = (n_{sf} - n_{sb})/(n_{sf} + n_{sb})$ (n_{sf} and n_{sb} being the numbers of charged secondaries emitted in the center-of-mass system within the angle $\theta < 90°$ and $\theta > 90°$ relative to the direction of the colliding nucleons) was calculated taking into account the conservation of energy, momentum and charge. Comparison of the expected and experimental distributions shows an excess of showers with large α (asymmetrical showers). The effect of asymmetrical showers on the primary energy spectrum was calculated as well as the dependence of the multiplicity and inelasticity on the primary energy as derived from the angular distribution of the secondary particles. (auth)

37683 ONE OF THE FEATURES IN THE JETS GENERATED IN THE HYDRODYNAMICAL LANDAU PROCESS. Gerasimova, N. M. (Moscow State Univ.). pp 914-15 of Proceedings of the Ninth International Conference on Cosmic Rays. Vol. 2. Stickland, A. C. (ed.). London, The Institute of Physics and The Physical Society, 1966.

A new criterion for detection of the central collisions of ultra-high energy particles in the jets on the basis of Landau hydrodynamical theory is proposed. It turns out that in the case when the Landau process takes place a relativistic π meson flies backward in the laboratory system. (auth)

37684 TSKHRA-TSKARO INSTALLATION FOR STUDY OF INTERACTIONS OF HIGH-ENERGY PARTICLES OF COSMIC RAYS WITH MATTER. Andronikashvili, E. L.; Chikovani, G. E.; Mandzhavidze, Z. Sh.; Roinishvili, N. N. (Inst. of Physics, Tbilisi, USSR). pp 916-17 of Proceedings of the Ninth International Conference on Cosmic Rays. Vol. 2. Stickland, A. C. (ed.). London, The Institute of Physics and The Physical Society, 1966.

A large installation consisting of a 1000 ton magnet, two cloud chambers, a track spark chamber, an ionization calorimeter and a spark calorimeter which is being installed at 2500 m above sea level is described. With the apparatus it is intended to investigate the cross section and characteristics of the interactions of particles in the energy range $10^{11} - 5 \times 10^{11}$ ev. (auth)

37685 RELATIONSHIP OF NEUTRAL AND CHARGED PARTICLES AMONG NUCLEAR-ACTIVE PARTICLES WITH ENERGIES ABOVE 100 Gev AT MOUNTAIN ALTITUDE. Grigorov, N. L.; Erofeeva, I. N.; Mitshenko, L. G.; Murzin, V. S.; Rapoport, I. D.; Saricheva, L. I.; Bashindyagian, G. L. (Moscow State Univ.). pp 920-1 of Proceedings of the Ninth International Conference on Cosmic Rays. Vol. 2. Stickland, A. C. (ed.). London, The Institute of Physics and The Physical Society, 1966.

The relation of netural and charged particles generating electron-nuclear showers is studied by means of an ionization calorimeter. If the excess of charged particles is due to pions then their portion in the nuclear component reaches 25%. (auth)

37686 HIGH-ENERGY INTERACTIONS. Peters, B. (Univ. of Copenhagen). pp 922-7 of Proceedings of the Ninth International Conference on Cosmic Rays. Vol. 2. Stickland, A. C. (ed.). London, The Institute of Physics and The Physical Society, 1966.

High-energy interactions in extensive air showers and those of mesons (μ) and neutrinos are reviewed. The topics discussed are experimental techniques, fluxes of high-energy particles in the atmosphere, nucleon-nucleon collisions, elastic collisions, interaction cross sections, quasi-elastic collisions and baryon isobar excitation, inelastic processes, transverse momenta of fireballs, and decay products in fireballs. Also considered are the existence of unidentified particles, multiplicity, and π-N collisions. (J.F.P.)

37687 STUDY OF THE μ MESON CHARGE RATIO AT SEA LEVEL. Rastin, B. C.; Baber, S. R.; Bull, R. M.; Nash, W. F. (Univ. of Nottingham, Eng.). pp 931-4 of Proceedings of the Ninth International Conference on Cosmic Rays. Vol. 2. Stickland, A. C. (ed.). London, The Institute of Physics and The Physical Society, 1966.

Extended measurements on the variation of the μ meson charge ratio with energy at sea level, made using the Nottingham Cosmic Ray Spectrometer, are discussed. These measurements apply to single μ mesons for near vertical incidence within the energy range $2.34 < p < 360$ Bev. The data, based on the analysis of some 20,000 events, were compared with other results as well as the more recent theoretical predictions. Conclusions are drawn concerning the possible mechanism responsible for the production of μ mesons at high energies. (auth)

37688 POSITIVE EXCESS OF COSMIC-RAY MUONS AT SEA LEVEL. Volkova, L. V.; Zatsepin, G. T. (Lebedev Inst. of Physics, Moscow). pp 935-6 of Proceedings of the Ninth International Conference on Cosmic Rays. Vol. 2. Stickland, A. C. (ed.). London, The Institute of Physics and The Physical Society, 1966.

Calculations of the positive excess of muons $N_{\mu+}/N_{\mu-}$ at sea level for energies $10^9 - 10^{14}$ ev were made taking into account the change of ratio of protons to neutrons with atmospheric depth. It was suggested that the ratios π^+/π^- and K^+/K^- obtained from emission in nuclear interactions did not depend on their energy, but were different for generation by protons and by neutrons. The calculations showed the increase of the ratio $N_{\mu+}/N_{\mu-}$ with increase of the energy even if the generation of muons by K mesons was not taken into account. (auth)

37689 CHARGE RATIO OF COSMIC-RAY MUONS AT LARGE ZENITH ANGLES. MacKeown, P. K.; Said, S. S.; Wdowczyk, J.; Wolefendale, A. W. (Univ. of Durham, Eng.). pp 937-40 of Proceedings of the Ninth International Conference on Cosmic Rays. Vol. 2. Stickland, A. C. (ed.). London, The Institute of Physics and The Physical Society, 1966.

Preliminary results are presented of a measurement of the muon charge ratio to muon energies of approximately 1000 Bev at sea level, in the range of zenith angles 82.5°–90°, obtained with a modified version of the Durham Horizontal Spectrograph. Combined with the other results they indicate that the μ^+/μ^- ratio is approximately constant up to muon production energies of about 500 Bev. The ratio predicted from the established characteristics of high-energy interactions is calculated, and, from a comparison with the data, the necessary characteristics to account for it are discussed. It is noted that the production of the $T = \frac{1}{2}$ isobar observed in nucleon-nucleon collisions at machine energies, with a slowly decreasing cross section, will account for the observations. The dependence of the μ^+/μ^- ratio on zenith angle is investigated. (auth)

37690 FURTHER OBSERVATION OF THE POSITIVE EXCESS OF COSMIC-RAY MUONS. Kawaguchi, S.; Sakai, T.; Oda, H.; Ueno, H.; Kamiya, Y. (Nagoya Univ., Japan). pp 941-3 of Proceedings of the Ninth International Conference on Cosmic Rays. Vol. 2. Stickland, A. C. (ed.). London, The Institute of Physics and The Physical Society, 1966.

Further observation of the energy dependence of the cosmic ray positive excess was made by using the Nagoya spectrometer, of which the maximum detectable momentum is about 170 Bev/c. During the period April-November 1964, a total of 8343 particles incident from large zenith angles 78° ± 2° was analyzed, and it is shown that: the average charge ratio (positive/negative) in the momentum range 20-40 Bev/c at the time of production is 1.28 ± 0.04; above 40 Bev/c, the charge ratio decreases with increasing momentum and exhibits a minimum around 80 Bev/c; the charge ratio at higher momenta favours increase with momentum and the mean between 100-200 Bev/c reaches almost the same value as that in the momentum below 40 Bev/c. This measurement, together with the previous one, was compared with the observation obtained at large zenith angles by the Durham group and it was found that the results are in general agreement with each other. In particular, the minimum described was confirmed with a statistical accuracy. (auth)

37691 DERIVATION OF THE PION MULTIPLICITY IN NUCLEAR COLLISIONS FROM SEA-LEVEL POSITIVE EXCESS AND TOTAL MUON SPECTRA. Melkman, A. (Hebrew Univ., Jerusalem); Meroz, I.; Yeivin, Y. pp 944-5 of Proceedings of the Ninth International Conference on Cosmic Rays. Vol. 2. Stickland, A. C. (ed.). London, The Institute of Physics and The Physical Society, 1966.

The integral equations relating the pion multiplicity in nuclear collisions and the sea-level positive and negative muon spectra can be solved numerically for the multiplicity. Thus, from the observed total muon spectrum at sea-level one may derive the average pion multiplicity as a function of the collision energy and, from the positive excess data, an "effective" multiplicity is derived which, in combination with the average multiplicity, might yield information about the multiplicity fluctuations. (auth)

37692 HIGH-ENERGY SINGLE-MESON PRODUCTION. Crossland, A. D.; Fowler, G. N. (Univ. of Newcastle upon Tyne, Eng.). pp 950-1 of Proceedings of the Ninth International Conference on Cosmic Rays. Vol. 2. Stickland, A. C. (ed.). London, The Institute of Physics and The Physical Society, 1966.

Some objections to the one pion exchange single pion production model at high energies proposed by Narayan are discussed, and a peripheral model described involving π exchange taking into account unitarity corrections in a more satisfactory way. The result agrees rather well with that found by Narayan. A model involving K^* exchange is also described. The cross section in this case is smaller by a factor of 4 for mesons produced with 0.2 of the incident energy. (auth)

37693 UNDERGROUND INVESTIGATION OF THE PENETRATING COMPONENT OF HIGH-ENERGY COSMIC RADIATION. Vernov, S. N.; Khristiansen, G. B.; Netchin, Yu. A.; Vedeneev, O. V.; Khirenov, B. A. (Moscow State Univ.). pp 952-5 of Proceedings of the Ninth International Conference on Cosmic Rays. Vol. 2. Stickland, A. C. (ed.). London, The Institute of Physics and The Physical Society, 1966.

The new experimental data on the energy and angular distribution of high energy muons ($3 \times 10^{11} - 3 \times 10^{12}$ ev) are presented. These data have been obtained by means of a detector capable of determining the muon tracks and the values of ionization bursts caused by a muon under a layer of heavy matter. Also presented are the data on a new phenomenon, the so-called structural bursts, which are likely to be caused by particle pairs from the atmosphere. (auth)

37694 STUDY OF PROPERTIES OF μ MESONS BY A SPARK CALORIMETER AT THE DEPTH OF 200 m.w.e. UNDERGROUND. Bibilashvili, M. F.; Barnaveli, T. T.; Grubelashvili, G. A.; Muradova, N. A. (Inst. of Physics, Tbilisi, USSR). pp 956-8 of Proceedings of the Ninth International Conference on Cosmic Rays. Vol. 2. Stickland, A. C. (ed.). London, The Institute of Physics and The Physical Society, 1966.

A spark calorimeter, by means of which μ meson properties are studied in the underground laboratory of the Institute of Physics, Academy of Sciences of the U.S.S.R., is a system consisting of spark chambers with layers of lead filters between them. The calorimeter is operated by a telescope of Geiger counters. μ mesons of high energy pass through the calorimeter and generate electron-positron pairs in the filters over the chambers, and cascades of the pairs create bursts in the chambers. The calorimeter is free of a number of disadvantages inherent in ionization calorimeters: it allows us, with efficiency close to unity, to detect both single particles and groups of particles, to distinguish easily the types of interactions and to determine the angles of slopes both of μ mesons and secondary particles. According to the preliminary data the integral spectrum of bursts measured by this calorimeter during 800 hours of operation can be described by an exponential law with exponent $\gamma = -2.3^{+0.4}_{-0.3}$. (auth)

37695 BURST PRODUCTION BY NEAR HORIZONTAL COSMIC-RAY MUONS AT SEA LEVEL. Ashton, F.; Coats, R. B. (Univ. of Durham, Eng.). pp 959-61 of Proceedings of the Ninth International Conference on Cosmic Rays. Vol. 2. Stickland, A. C. (ed.). London, The Institute of Physics and The Physical Society, 1966.

Bursts produced by high-energy muons undergoing large energy transfers were studied. For energy transfers up to 10 Bev where the μ-e collision process is most important there is no significant divergence from accepted theory. At larger energy transfers (>40 Bev) there is an indication that the theoretical bremsstrahlung cross section is too large. (auth)

37696 ANGULAR DISTRIBUTION AND ENERGY SPECTRUM OF THE COSMIC-PARTICLE SHOWERS AT ENERGIES OF ABOUT 10^{12} ev AT LARGE ZENITH ANGLES. Borog, V. V.; Kirillov-Ugryumov, V. G.; Petrukhin, A. A.; Rosental, I. L.; Shestakov, V. V. (Moscow Physical Engineering Inst.). pp 962-3 of Proceedings of the Ninth International Conference on Cosmic Rays. Vol. 2. Stickland, A. C. (ed.). London, The Institute of Physics and The Physical Society, 1966.

Cascade showers were studied by means of the ionization calorimeter. These showers were produced by high-energy cosmic particles at large zenith angles. The angular distribution of showers is given. These were produced by muons and nuclear particles. An integral energy spectrum was obtained for electron-photon showers, produced by muons at zenith angles $\theta \geq 55°$. This was converted into a spectrum of cosmic muons in the range $3 \times 10^{11} - 3 \times 10^{12}$ ev. (auth)

37697 MOMENTUM SPECTRUM OF COSMIC-RAY MUONS IN THE ZENITH ANGLE RANGE 82.5 TO 90 DEG. MacKeown, P. K.; Said, S. S.; Wdowczyk, J.; Wolfendale, A. W. (Univ. of Durham, Eng.). pp 964-6 of Proceedings of the Ninth International Conference on Cosmic Rays. Vol. 2. Stickland, A. C. (ed.). London, The Institute of Physics and The Physical Society, 1966.

The modified Durham "horizontal spectrograph" was used to measure the momentum spectrum of muons in the zenith angle range 82.5-90° to about 2000 Bev/c. The data are analyzed to give an estimate of the K/π ratio in nucleon-air nucleus interactions for primary energies extending to 10^5 Bev. The results confirm earlier conclusions that the ratio is less than about 0.4 over most of the energy range, but there is some slight evidence for an increase in the ratio of the highest energies. (auth)

37698 INVESTIGATION OF THE ELECTROMAGNETIC CASCADES IN IRON AND LEAD AT AN ENERGY OF 100 Gev. Takbaev, Zh. S.; Lukin, Yu. T.; Emelyanov, Yu. A. (Nuclear Science Inst., Tashkent). pp 967-9 of Proceedings of the Ninth International Conference on Cosmic Rays. Vol. 2. Stickland, A. C. (ed.). London, The Institute of Physics and The Physical Society, 1966.

Electron-photon cascade showers were recorded with an "ionization calorimeter". The influence of the value of the radiation length on the form of the mean cascade curve was studied. The experimental mean cascade curve was compared with the theoretical calculations. The fluctuations of cascade showers were studied at various values of the parameter S. (auth)

37699 STUDY OF THE ELECTROMAGNETIC INTERACTIONS OF HIGH-ENERGY MUONS USING A LARGE SCINTILLATOR STACK. Barton, J. C. (Northern Polytechnic, London); Rogers, I. W.; Thompson, M. G. pp 970-2 of Proceedings of the Ninth International Conference on Cosmic Rays. Vol. 2. Stickland, A. C. (ed.). London, The Institute of Physics and The Physical Society, 1966.

A study was made of the electromagnetic interactions of muons at a depth of 60 mwe using a scintillator stack consisting of six large area liquid scintillation counters interleaved with sheets of lead. The energy of a cascade shower produced as the result of an interaction is deduced from its size at maximum development. The results, when combined with a knowledge of the spectrum of muons, provide a test of the theories of knock-on production and bremsstrahlung over a wide energy range. (auth)

37700 STUDY OF CASCADE SHOWERS IN LEAD. Barton, J. C. (Northern Polytechnic, London). pp 973-5 of Proceedings of the Ninth International Conference on Cosmic Rays. Vol. 2. Stickland, A. C. (ed.). London, The Institute of Physics and The Physical Society, 1966.

The scintillator stack experiment has provided more than 30,000 electromagnetic shower events due to muon interactions in the stack at a depth of 60 Mw(e). These were sorted according to their size at maximum development and the average shower behavior deduced for each size. A new computing technique was developed to enable this to be done even though the exact point of initiation of each shower was unknown. The results for shower energies from 0.3 to 30 Bev are compared with analytical and Monte Carlo theories of the shower process. (auth)

37701 MUON INTERACTIONS FAR UNDERGROUND. Creed, D. R. (Univ. of Durham, Eng.); Pattison, J. B. M.; Wolfendale, A. W.; Achar, C. V.; Narasimham, V. S.; Ramana Murthy, P. V. pp 980-3 of Proceedings of the Ninth International Conference on Cosmic Rays. Vol. 2. Stickland, A. C. (ed.). London, The Institute of Physics and The Physical Society, 1966.

Two units comprising scintillators, Geiger counters and flash tubes were operated underground at depths of 816, 1812 and 4100 mwe. Results are presented on the frequencies of the observed secondary particles and multiple penetrating particles. The probability of a muon being accompanied by electrons or generating them in a lead absorber is found to increase with depth, as would be expected from the increasing average muon energy. The observed frequencies of multiple penetrating particles are explained in terms of the tails of extensive air showers together with pions generated locally by the nuclear interactions of energetic muons. (auth)

37702 PHOTONUCLEAR INTERACTIONS OF μ MESONS. Bull, R. M.; Baber, S. R.; Nash, W. F.; Rastin, B. C. (Univ. of Nottingham, Eng.). pp 984-6 of Proceedings of the Ninth International Conference on Cosmic Rays. Vol. 2. Stickland, A. C. (ed.). London, The Institute of Physics and The Physical Society, 1966.

The multiplicity distribution of secondary particles in μ-N interactions was considered. In particular the effect of the intranuclear cascade was investigated using a simple model of the nucleus. The predictions of this model were compared with experimental data. In general a deficiency of single multiplicity events was observed compared with those expected. In conjunction with the solid iron magnetic spectrograph at Nottingham an experimental investigation of these interactions was initiated and preliminary results are presented. (auth)

37703 DEPTH-INTENSITY CURVE OF NUCLEAR EVENTS INDUCED BY MUONS. Ryazhskaya, O. G.; Zatsepin, G. T. (Lebedev Inst. of Physics, Moscow). pp 987-8 of Proceedings of the Ninth International Conference on Cosmic Rays. Vol. 2. Stickland, A. C. (ed.). London, The Institute of Physics and The Physical Society, 1966.

Different processes leading to nuclear reactions induced by muons were considered. It was found that the main yield was given by photonuclear interactions and that nuclear cascades produced in high energy photonuclear interactions played a significant role. The depth-intensity curve of nuclear events can be approximated by the formula: $I_n(x) = AI_\mu(x)\,\overline{E_\mu(x)}^{0.7}$ where A is a constant dependent on the type of nuclear process, $I_\mu(x)$ is the muon intensity and $\overline{E_\mu(x)}$ is the average energy of muons at the depth x. (auth)

37704 INTENSITY AND ANGULAR DISTRIBUTION OF COSMIC RAYS FAR UNDERGROUND. Achar, C. V. (Tata Inst. of Fundamental Research, Bombay); Narasimham, V. S.; Ramana Murthy, P. V.; Creed, D. R.; Pattison, J. B. M.; Wolfendale, A. W. pp 989-91 of Proceedings of the Ninth International Conference on Cosmic Rays. Vol. 2. Stickland, A. C. (ed.). London, The Institute of Physics and The Physical Society, 1966.

An apparatus incorporating scintillators, Geiger counters and neon flash tubes was operated at three locations underground in the Kolar Gold Mines, India, to measure the vertical intensity and angular distributions of penetrating cosmic ray muons. The intensities at the three depths (816, 1812 and 4100 mwe of rock) are, respectively: $(2.39 \pm 0.15) \times 10^{-6}$, $(2.00 \pm 0.12) \times 10^{-7}$ and $(4.63 \pm 0.57) \times 10^{-9}$ cm^{-2} sec^{-1} $sterad^{-1}$. The angular distributions are well represented by expressions of the form $I_\theta = I_0 \cos^n\theta$, where θ is the zenith angle, and the values of n at the successive depths are 1.93 ± 0.22, 3.03 ± 0.16 and 5.12 ± 0.82. (auth)

37705 SCINTILLATION-COUNTER STUDY OF COSMIC RAYS DEEP UNDERGROUND. Barton, J. C. (Northern Polytechnic, London); Stockel, C. T.; Tanfield, D. A. pp 992-6 of Proceedings of the Ninth International Conference on Cosmic Rays. Vol. 2. Stickland, A. C. (ed.). London, The Institute of Physics and The Physical Society, 1966.

A scintillation counter apparatus of area 0.36 m^2 was used to study the total intensity of cosmic rays at various depths, determined from a gravity survey, down to 2200 mwe. The pulse height in the scintillation counter is converted into digital form and recorded on magnetic tape together with hodoscope data from two layers of Geiger counters. It is shown that the pulse height distributions can be analyzed to provide a direct measure of the energy loss of very high-energy muons. (auth)

37706 DEPTH-INTENSITY CURVE OF MUONS AND THEIR ENERGY SPECTRUM. Mikhalchi, E. D.; Zatsepin, G. T. (Lebedev Inst. of Physics, Moscow). pp 997-8 of Proceedings of the Ninth International Conference on Cosmic Rays. Vol. 2. Stickland, A. C. (ed.). London, The Institute of Physics and The Physical Society, 1966.

A simple relation between the depth-intensity curve and the energy spectrum of muons at sea level is found. Fluctuations in energy losses are taken into account. The results are very sensitive to the value taken for the energy losses, especially to the losses by pair production. Great disagreement in the theoretical estimates of this value is stressed. Some experiments which allow a solution of this problem are considered. (auth)

37707 ENERGY LOSSES OF RELATIVISTIC MUONS IN ELECTROMAGNETIC INTERACTIONS. Erlykin, A. D. (Lebedev Inst. of Physics, Moscow). pp 999-1002 of Proceedings of the Ninth International Conference on Cosmic Rays. Vol. 2. Stickland, A. C. (ed.). London, The Institute of Physics and The Physical Society, 1966.

Values b_{rad} and b_{pair} were calculated for matter with Z = 10, Z = 13 and for water using an electronic computer. The influence of atomic electrons on the muon bremsstrahlung process was examined and the contribution of μ-e interactions into b_{rad} was shown to be considerably greater up to $E_\mu \simeq 10^{12}$ ev than that usually taken into account by the replacement of Z^2 by $Z(Z + \xi^{\mu e}_{rad})$ in the expression for b_{rad}. (auth)

37708 EFFECT OF THE LOGARITHMIC INCREASE OF IONIZATION LOSS ON THE RANGE FLUCTUATION OF HIGH-ENERGY μ MESONS. Nishimura, J. (Tokyo Univ.). pp 1003-5 of Proceedings of the Ninth International Conference on Cosmic Rays. Vol. 2. Stickland, A. C. (ed.). London, The Institute of Physics and The Physical Society, 1966.

The range fluctuation problem of high energy μ mesons, which is important in order to interpret the depth-intensity relation, is calculated including the effect of the logarithmic increase of ionization loss of high energy μ mesons. The effect of the knock-on process on the fluctuation problem is also calculated. (auth)

37709 INTENSITY OF STOPPING PIONS AT SEA LEVEL AND UNDERGROUND. Barton, J. C.; Slade, M. (Northern Polytechnic, London). pp 1006-8 of Proceedings of the Ninth International Conference on Cosmic Rays. Vol. 2. Stickland, A. C. (ed.). London, The Institute of Physics and The Physical Society, 1966.

The rate of stopping positive pions was measured by ob-

serving the decay pulses in a scintillation counter of 11.3 liters volume. The events in which both muon and electron pulses were present could be identified unambiguously. The rate at which muons stopped in the detector at sea level and at 60 Mw(e) were 1.1 ± 0.1 g^{-1}/day and (2.6 ± 0.3) 10^{-2} g^{-1}/day respectively and the rates for positive pions (1.0 ± 0.2) 10^{-2} g^{-1}/day and (2.9 ± 0.4) 10^{-4} g^{-1}/day. (auth)

37710 FAST NEUTRON PRODUCTION BY MUONS UNDERGROUND. Short, A. M. (Coll. of Advanced Tech., Birmingham, Eng.). pp 1009-11 of Proceedings of the Ninth International Conference on Cosmic Rays. Vol. 2. Stickland, A. C. (ed.). London, The Institute of Physics and The Physical Society, 1966.

A stack of nuclear emulsion was exposed at a depth of 58 mwe underground to study fast neutrons. The differential energy spectrum of neutrons with energies from 5 to 15 Mev was obtained from measurements on hydrogen recoils. The measured spectrum together with the data on the more energetic neutrons are consistent with calculations which include only three mechanisms for neutron production, namely: the nuclear absorption of stopped negative muons, (γ,n) reactions, and the interactions of fast muons. The results favor the theory of Heitler for the interactions of fast muons. (auth)

37711 KOLAR GOLD FIELD NEUTRINO EXPERIMENT. Achar, C. V. (Tata Inst. of Fundamental Research, Bombay); Menon, M. G. K.; Narasimham, V. S.; (and others). pp 1012-19 of Proceedings of the Ninth International Conference on Cosmic Rays. Vol. 2. Stickland, A. C. (ed.). London, The Institute of Physics and The Physical Society, 1966.

Two telescopes designed for the detection of muons produced by neutrinos were set up at a depth of 7500 mwe in the Kolar Gold Fields in India. Each telescope consists of two vertical walls of plastic scintillators 2-m long and 3-m high separated by 80 cms. Between the scintillator walls there are three columns of neon flash tubes; 5 cms lead can be introduced in between. Each square meter of scintillator is viewed by two adjacent 5-inch diameter photomultipliers. The fourfold coincidence of any two opposite pairs triggers the voltage on the flash tubes. With the use of visual detectors in the form of flash tubes it is possible to determine the zenith angle of the muon to an accuracy better than 2° and thereby to correct for the contribution due to remanent atmospheric muons which leak through; the latter have a steep angular distribution, arriving mostly vertically, whilst the neutrino-induced muons are much more isotopic. One unit with 5-cm lead and another without any lead are in operation. Results up to the time of the conference are presented. Underground neutrino energy spectra were derived as a function of zenith angle and the expected cross sections for neutrino interactions were calculated from theoretical predictions and accelerator experiments. These data are used to give predicted rates and angular distributions of neutrino-induced muons detected by the telescopes of the Tata Institute-Osaka City-Durham collaboration experiment at a depth of 7500 mwe in the Kolar Gold Fields. The interpretation of the observed events will be given. (auth)

37712 ENERGY SPECTRA OF MUONS AND NEUTRINOS GENERATED BY COSMIC RAYS IN DIFFERENT SUBSTANCES. Volkova, L. V.; Zatsepin, G. T. (Lebedev Inst. of Physics, Moscow). pp 1039-40 of Proceedings of the Ninth International Conference on Cosmic Rays. Vol. 2. Stickland, A. C. (ed.). London, The Institute of Physics and The Physical Society, 1966.

The energy spectra of muons and neutrinos generated in dense objects without an atmosphere were calculated. It is found that their intensities are much less than those which are generated on the earth, especially for high energies. The results have some interest for high energy neutrino astrophysicists. The problems connected with the generation of neutrinos of different types in nebulae (of matter and antimatter) are considered. (auth)

37713 MUON DECAYS FROM NEUTRAL PRIMARIES. Cowan, C.; Ryan, D.; Buckwalter, G. (Catholic Univ. of America, Washington, D. C.). pp 1041-4 of Proceedings of the Ninth International Conference on Cosmic Rays. Vol. 2. Stickland, A. C. (ed.). London, The Institute of Physics and The Physical Society, 1966. (CONF-650948-2).

Work reported informally heretofore on the observation of muon decays arising from a neutral primary in the cosmic rays is continuing utilizing a new detector system. Equivalent to the previous system in mass, but built of scintillating plastic and located near sea level with little overburden, the system began collecting data on 11th May 1965 following extensive testing for the anticoincidence factor, etc. After some six weeks of data collection, several strong peaks stood out from the background when muon burst rates were correlated with sidereal time, but appear only weakly on a solar time plot. The times of these peaks are the same as those reported previously for the older system operated underground. The strongest peak observed at present rises in excess of four standard deviations above the general level of the data and occurs when the galactic plane is on the zenith. The progress in the construction of a system with high angular resolution is reported. (auth)

37714 POSSIBLE NUCLEAR INTERACTION OF A MUON OF ENERGY ABOVE 3×10^{14} ev. Matano, T. (Tokyo Univ.); Nagano, M.; Shibata, S.; Suga, K.; Kameda, T.; Toyoda, Y.; Maeda, T.; Hasegawa, H. pp 1045-7 of Proceedings of the Ninth International Conference on Cosmic Rays. Vol. 2. Stickland, A. C. (ed.). London, The Institute of Physics and The Physical Society, 1966.

An almost horizontal air shower was observed. The size of the shower was 9×10^4 and the zenith angle of the arrival direction was determined to be 86° from spark chamber and cloud chamber photographs. The cloud chamber photograph shows a high energy (probably 30-50 Bev) nuclear interaction by the charged shower particle in a lead plate, which suggests that the air shower is not a pure cascade shower but a nucleonic shower. This interesting event seems to be nuclear interaction of a muon (or neutrino) of energy 3×10^{14} ev. (auth)

37715 MUONS AND NEUTRINOS. Wolfendale, A. W. (Univ. of Durham, Eng.). pp 1055-9 of Proceedings of the Ninth International Conference on Cosmic Rays. Vol. 2. Stickland, A. C. (ed.). London, The Institute of Physics and The Physical Society, 1966.

The study of mesons (μ) of atmospheric origin and neutrinos originating from the atmosphere and from extra-terrestrial sources is described. The discussion of mesons (μ) includes the charge ratio, energy-loss rate, burst production, and an air shower at a very large zenith angle. Meson (μ) and solar neutrinos are also considered as well as the detection of neutrino emission from collapsing stars. (J.F.P.)

37716 LABORATORY TECHNIQUE FOR SIMULATING COSMIC-RAY THRESHOLD EFFECTS. Hedgecock, P. C. (Imperial Coll. of Science and Tech., London). pp 1063-5 of Proceedings of the Ninth International Conference on Cosmic Rays. Vol. 2. Stickland, A. C. (ed.). London, The Institute of Physics and The Physical Society, 1966.

Bland's technique for studying cosmic ray threshold rigidities by using a model of the geomagnetic field was extended and to some extent automated to provide additional information on the dipole penumbra and to permit a study of the threshold perturbations produced by superimposing external magnetic fields on a dipole model. Following a discussion of the scaling factors, the physical arrangement of the model and the experimental difficulties, the results of this study of penumbral and threshold perturbation effects are briefly described. (auth)

37717 POTENTIALITIES OF OPERATING CHERENKOV LIGHT RECEIVERS IN THE MIDDLE ULTRAVIOLET REGIONS OF THE SPECTRUM. Charman, W. N. (Atomic Energy Research Establishment, Harwell, Eng.). pp 1066-9 of Proceedings of the Ninth International Conference on Cosmic Rays. Vol. 2. Stickland, A. C. (ed.). London, The Institute of Physics and The Physical Society, 1966.

The Cherenkov technique for studying extensive cosmic ray air showers (EAS) is severely restricted by periods of moonlight and by environmental lighting. The advent of "solar-blind" photomultipliers has opened up the possibility of extending the Cherenkov technique into the ultra-violet spectral region where there is little stray light of terrestrial origin and the absorbing properties of the atmospheric ozone reduce the undesirable background light from the sky. Atmospheric ozone is mainly concentrated in a layer at an altitude of about 20 km, so that in the spectral region 2000-2800 Å, relatively bright sources outside the atmosphere produce very little response in a ground-based light receiver. Since most of the Cherenkov light detected arises from relatively low altitudes, 1-3 km where the ozone concentration is low, calculations show that reasonable counting rates of showers should be obtainable under conditions of bright moonlight and other stray lighting, although significant low-altitude scattering of the ultra-violet Cherenkov light does occur. Preliminary experiments with ultra-violet Cherenkov light receivers, which are at present being carried out at Harwell are described. (auth)

37718 FEASIBILITY OF DETECTING QUARKS IN COSMIC RAYS. Ashton, F. (Univ. of Durham, Eng.). pp 1108-10 of Proceedings of the Ninth International Conference on Cosmic Rays. Vol. 2. Stickland, A. C. (ed.). London, The Institute of Physics and The Physical Society, 1966.

30 Bev proton accelerators appear to be below the energy threshold for quark production. An estimate is made of the expected flux of quarks in the atmosphere as a function of the quark mass and a suitable experimental technique to search for quarks is proposed. (auth)

37719 POSSIBLE FLUX OF HEAVY TRIPLETS AND SIMILAR PARTICLES IN COSMIC RADIATION AND THEIR DETECTION. Pal, Y.; Tandon, S. N. (Tata Inst. of Fundamental Research, Bombay). pp 1111-13 of Proceedings of the Ninth International Conference on Cosmic Rays. Vol. 2. Stickland, A. C. (ed.). London, The Institute of Physics and The Physical Society, 1966.

The possible flux of hypothetical heavy particles produced in high-energy cosmic ray interactions is calculated, based on reasonable assumptions for their production and interaction parameters. The calculated flux is found to be detectable. Possible experiments are suggested for detection of these particles, if they exist. (auth)

Direct Energy Conversion

Refer also to abstract 37867.

37720 (BMWF-FBK-66-06) DIE DIMENSIONIERUNG EINES MIT KERNENERGIE BETRIEBENEN THERMIONISCHEN KONVERTERS. TEIL I. (Evaluation on Structural Design of a Nuclear-Fueled Thermionic Converter. Part I). Guenther, R. (Battelle Institut e. V., Frankfurt am Main (West Germany)). Apr. 1966. 60p. Dep. mn.

A thermionic fuel element in-core type, cylindrical geometry, may be feasible eventually with nuclear fuels of today's technology, if the following properties are approximated: 8 w(e)/cm^2 surface area of the emitter; more than 8% efficiency; 0.3 w(e)/g fuel element; 10^{13} cm^{-2} sec^{-1} thermal neutron flux; 1 year operating time. Technical safety may be achieved when improved nuclear fuels are available. Some details are discussed. The properties of the nuclear-fueled heater are evaluated (auth)

37721 (INDEC-SR-7) STATUS REPORT [ON DIRECT ENERGY CONVERSION]. Altman, Manfred (Pennsylvania Univ., Philadelphia. Inst. for Direct Energy Conversion). Apr. 1, 1966. 164p.

Brief summaries of research on the following topics are reported: characteristics of plasma probes in dense plasmas, plasma diagnostics, measurement of plasma transport properties, characteristics of thermionic plasma diodes with gas mixtures, electron emission studies, plasma centrifuge, atomic scale electrode processes, natural convection mass transport in electrolytic systems, fuel-cell porous-electrode models, transport parameters in fuel-cell electrolytes, battery materials, high temperature thermal diffusivity measurements, thermoelectric properties of graphite compounds, development of efficient tunnel cathodes, and general studies. Separate abstracts were prepared for 4 of the papers dealing primarily with plasma-electromagnetic wave interactions. (M.O.W.)

For abstracts of individual sections see: 37431 and 38193–38195.

37722 (N-65-30843) [MATERIALS ENGINEERING, PLASMA RESEARCH, AND ELECTROCHEMICAL STUDIES IN THE DEVELOPMENT OF DIRECT ENERGY CONVERSION METHODS]. Status Report. (Pennsylvania Univ., Philadelphia. Inst. for Direct Energy Conversion). Jan. 4, 1965. 100p. (NASA-CR-64303; INDEC-SR-5). CFSTI $3.00 cy, $0.75 mn.

Progress is reported on the following: partial molar properties of magnesium-base binary thermal energy storage materials; phase diagrams of the systems MgF_2–MgO and MgF_2–CaO; transient measurement of thermal diffusivity of refractory materials at high temperature; emitter surface physics of plasma diodes; emitter sheath polarity in plasma diodes; investigation of Na–K seeded argon plasma; and transient concentration variation in natural convection electrolysis. Among the research discussed was the formation of simple eutectics in the systems MgF_2–MgO and MgF_2–CaO: 0.085 mole fraction MgO at 1220 ± 2°C; 0.075 mole fraction CaO at 1208 ± 2°C; and approximately 4.5 wt % Al_2O_3 at 1250°C in the system MgF_2–Al_2O_3. (STAR)

37723 THERMOELECTRON EMISSION FROM URANIUM DODECABORIDE. Ermakov, S. V.; Tsarev, B. M. At. Energ. (USSR), 20: 439-40(May 1966). (In Russian).

The emission of thermoelectrons from UB_{12} was investigated by monitoring a suspension of powdered UB_{12} in methyl alcohol placed on a tungsten strip. It was found that the deviation from linearity of the thermoelectron yield at temperatures above 1800°K was due to the tungsten's reaction with UB_4 and UB_2 which, at first, decreases the yield and then increases it. (G.O.Y.)

37724 JET COMPRESSION FOR CLOSED-CYCLE MAGNETOPLASMADYNAMIC ELECTRICAL POWER GENERATION. Shih, C. (Martin Marietta Corp., Baltimore). Contract Nonr-4087(00). J. Spacecraft Rockets, 3: 1121-3(July 1966).

The circulation of MPD working media was investigated. An experimental single-stage jet compressor loop was designed and built to investigate the feasibility of various operating conditions and different compressor geometries. Objectives were to prove feasibility and to obtain preliminary data for performance and efficiency analysis. Operation of the loop was satisfactory and both objectives were met. (R.C.K.)

37725 DEVELOPMENT OF A RESERVOIRLESS THERMIONIC ENERGY CONVERTER. Harbaugh, W. E.; Block, F. G.; Basiulis, A. (Radio Corp. of America, Lancaster, Pa.). Contract AT(30-1)-3429. J. Spacecraft Rockets, 3: 1126-8(July 1966).

A thermionic energy converter is described which is capable of producing substantial quantities of electrical power in space because it has a high power-to-weight ratio, no moving parts, potential long life and reliability, and a high temperature of heat rejection, which makes it possible to reduce radiator size and weight. (R.C.K.)

37726 COMPUTER SIMULATION METHODS FOR PLASMA DIODES WITH COLLISIONS. Burger, Peter (Stanford Univ., Calif.). 4p. (CONF-651049–20). ORAU. Gmelin, AED-CONF-65-324-21.

From IEEE Thermionic Conversion Specialist Conference, San Diego, Calif.

An investigation was made on the effects of particle collisions on the operation of plasma devices. Randomizing

collisions were introduced in a computer program for ions and electrons. The main features of the computer program are described along with some preliminary computations that demonstrate also the damping effect of electron-neutral collisions on the oscillatory behavior of the converter. (M.O.W.)

37727 RECENT ADVANCES IN ELECTRO-FLUID DYNAMIC POWER GENERATION. Brandmaier, Harold E.; Kahn, Bernard (Curtiss-Wright Corp., Wood-Ridge, N. J.). 10p. (CONF-660301-4). ORAU. Gmelin, AED-CONF-66-052-3.

From IEEE International Convention, New York.

High-voltage generating devices and their principles of operation are briefly reviewed. Then, more recent advances in direct energy conversion techniques involving electrofluiddynamic power generation are described. Theoretical and experimental results are given for a typical supersonic electrogasdynamic generator. The present state-of-the-art and areas for further study are discussed, as are the long-range ramifications of the development of practical systems. (auth)

37728 MAGNETOHYDRODYNAMIC INTERNAL COMBUSTION ELECTRIC GENERATOR. Spier, Hans G. (to Baldwin-Lima-Hamilton Corp.). U. S. Patent 3,258,618. June 28, 1966. Filed July 18, 1962.

A MHD generator is provided that uses an internal combustion engine to achieve high-temperature, high-velocity gas flow in a magnetic field. The gases from the internal combustion engine are utilized during the combustion period. The internal combustion generator utilizes cylinders and pistons in multiples so that generated electrical impulses when passed through a common transformer will produce alternating current flow of economically useful frequencies. Any power not absorbed in the MHD generator can be utilized to drive conventional electric generators or other means of useful power absorption. (B.L.M.)

37729 MAGNETICALLY CHANNELED PLASMA DIODE HEAT CONVERTER. Fox, Raymond (to U. S. Atomic Energy Commission). U. S. Patent 3,267,307. Aug. 16, 1966.

A thermionic energy converter is described, with minimized thermal radiation losses. It consists of a generally planar carbide adapted to be heated and a generally planar cold anode, disposed in facing relation to each other, with a magnetic field therebetween within an enclosure having a source for supplying cesium vapor therein. A thermionic electrical current permeable channeled heat shield is disposed between the cathode and anode to minimize transfer of thermal radiation between the heated cathode and cooled anode. (AEC)

Elementary Particles and Radiations

See also Field Theory, Scattering Theory, and Symmetries

Refer also to abstracts 36896, 37686, 38011, 38059, 38140, 38166, 38168, and 38186.

37730 (BNL-10459) THE f* MESON PRODUCED IN K^-p INTERACTION 4.6 AND 5.0 Bev/c. Barnes, V. E.; Dornan, P. J.; Guidoni, P.; (and others) (Brookhaven National Lab., Upton, N. Y.). [1965]. Contract AT(30-2)-Gen-16. 10p. (CONF-660808-4). Dep. mn. CFSTI $1.00 cy, $0.50 mn.

For Presentation at 13th International Conference on High Energy Physics, Berkeley, Calif.

A summary is presented on information on the f* meson produced in K^-p interactions at 4.6 and 5.0 Bev/c. (B.G.D.)

37731 (BNL-10460) $\pi\pi$ RESONANCES FROM 6 Gev/c π^-p INTERACTION. Crennel, David J.; Hough, Paul V. C.; Kalbfleisch, George R.; (and others) (Brookhaven National Lab., Upton, N. Y.). [nd]. Contract AT(30-2)-Gen-16. 9p. (CONF-660808-1). Dep. mn. CFSTI $1.00 cy, $0.50 mn.

For Presentation at 13th International Conference on High Energy Physics, Berkeley, Calif.

Evidence is presented for both charged and neutral $\pi\pi$ enhancements in the mass region 1600–1800 Mev from the reactions $\pi^-p \rightarrow \pi\pi N$ at 6 Bev/c. In the $\pi^+\pi^-$ state an enhancement centered at 1700 Mev with a width of the order of 200 Mev was observed. The $\pi^-\pi^0$ system is shown to have a somewhat narrower peak at ~1625 Mev with a width of about 60 Mev. (B.G.D.)

37732 (BNL-10461) RESONANCE PRODUCTION IN THE REACTIONS $\pi^\pm p \rightarrow KKN$ AT 6 Gev/c. Crennell, David J.; Kalbfleisch, George R.; Lai, Kwan Wu; Scarr, J. Michael; Schumann, Thomas G.; Skillicorn, Ian O.; Webster, Medford S. (Brookhaven National Lab., Upton, N. Y.). [1966]. Contract AT(30-2)-Gen-16. 8p. (CONF-660808-2). Dep. mn. CFSTI $1.00 cy, $0.50 mn.

For Presentation at 13th International Conference on High Energy Physics, Berkeley, Calif.

Resonance production in the KKN final states from $\pi^\pm p$ interactions at 6 Bev/c is reported. The data were obtained from exposures of the BNL 80-inch liquid hydrogen bubble chamber. (B.G.D.)

37733 (BNL-10462) SOME PROPERTIES OF K* (1425). Crennell, David J.; Kalbfleisch, George R.; Lai, Kwan Wu; Scarr, J. Michael; Schumann, Thomas G.; Skillicorn, Ian O.; Webster, Medford S. (Brookhaven National Lab., Upton, N. Y.). [1966]. Contract AT(30-2)-Gen-16. 5p. (CONF-660808-3). Dep. mn. CFSTI $1.00 cy, $0.50 mn.

For Presentation at 13th International Conference on High Energy Physics, Berkeley, Calif.

Determinations of the mass, width, and some quantum numbers of the K* (1425) produced in 6 Bev/c π^--hydrogen reactions are reported. The interactions $\pi^-p \rightarrow \Lambda K^+\pi^-$ and $\pi^+p \rightarrow \Lambda K^+\pi^+$ were considered. (B.G.D.)

37734 (COO-818-87) AN EXPERIMENTAL TEST OF THE LAW OF BARYON CONSERVATION. Gurr, Henry S. (Case Inst. of Tech., Cleveland, Ohio). Nov. 1966. Contract AT(11-1)-818. 89p. Dep. mn. CFSTI $3.00 cy, $0.75 mn.

Thesis.

A 162 m^2 steradian scintillation detector located 3200 m below surface was used to look for high energy fragments from baryon nonconserving nucleon decay. A lower limit on the lifetime of the nucleon from 2×10^{28} to 8×10^{29} years, depending on the assumed decay mode, is established. (auth)

37735 (COO-818-96) RESEARCH PROGRAM IN NEUTRINO PHYSICS, COSMIC RAYS AND ELEMENTARY PARTICLES. Technical Report, October 1, 1965–September 30, 1966. Reines, F. (Case Inst. of Tech., Cleveland, Ohio). July 1966. Contract AT(11-1)-818. 33p. Dep. mn. CFSTI $2.00 cy, $0.50 mn.

A modified version of the table top study of $\bar{\nu}_e + p$ which may not require detection of the delayed coincidence between product positron and neutron is discussed. If the study is successful a measurement of significantly greater accuracy will result since only the positron is involved and hence the uncertainties in the neutron detection efficiency will be eliminated. The equipment being readied for a second improved approach to the detection of double beta decay of ^{150}Nd is described. A large (360 Kgm) composite NaI-plastic detector for the detection of the elastic scattering reaction ($\bar{\nu}_e + e^- \rightarrow \bar{\nu}_e + e^-$) was developed. Some preliminary measurements were made of its characteristics and development of the associated electronics is outlined. The equipment for two solar neutrino experiments ($\nu_e + d$ and $\nu_e + {}^7Li$) in the Morton Salt Company mine is also described. Some preliminary tests were made of a Cherenkov D_2O system. A slight modification of the D_2O system promises to give a new test of baryon conservation which makes fewer assumptions than pre-

vious experiments. The latest and most ambitious test to date of the principle of baryon conservation is reported. Assuming modes of decay which violate only baryon and lepton conservation the lifetime is $>2 \times 10^{28}$ or 8×10^{29} years, depending on the specific mode. This represents an improvement in the limit by an order of magnitude. A discussion is also presented on the South African experiment which has continued to produce data on neutrinos and cosmic rays deep underground. A directional Cherenkov detector section was installed to distinguish neutrinos which penetrate the earth from below. A solar neutrino detector designed to detect the sun via the elastic scattering reaction was also installed and is under preliminary tests. (B.G.D.)

37736 (COO–1297-7) STUDY OF THE ELECTRON MOMENTUM DISTRIBUTION IN SILICON AND GERMANIUM BY POSITRON ANNIHILATION. Erskine, James C. Jr. (Western Reserve Univ., Cleveland, Ohio. Dept. of Physics). June 1966. Contract AT(11-1)-1297. 68p. Dep. mn. CFSTI $3.00 cy, $0.75 mn.

Thesis.

A study is presented on the angular distribution of the two-photon annihilation radiation in order to provide information about the momentum distribution of electrons in solids which can participate in the annihilation process. The study was confined to solids in which positronium is not formed. The study was performed on the well known semiconductors silicon and germanium. (B.G.D.)

37737 (COO–1297-8) CORRELATION OF POSITRON LIFETIME WITH THE ANGLE BETWEEN THE ANNIHILATION GAMMA RAYS. Walters, Virginia Fried (Western Reserve Univ., Cleveland, Ohio. Dept. of Physics). Sept. 1965. Contract AT(11-1)-1297. 83p. Dep. mn. CFSTI $3.00 cy, $0.75 mn.

Thesis.

Two types of positron experiments which are used to explore the structure of condensed materials are discussed. One measures the lifetime of the positron, and therefore the availability of electrons for annihilation. The other measures the angular correlation of the annihilation gamma rays, and gives information about the momentum distribution of the annihilating electrons. (B.G.D.)

37738 (IC–66/89) MATRIX ELEMENTS OF OPERATORS OF CLASS 1 REPRESENTATIONS OF SL(n,C). Fronsdal, C.; Ar-Rashid, Harun (International Centre for Theoretical Physics, Trieste (Italy)). July 1966. 18p. Dep. mn.

Let D be an irreducible representation of the group SL(n,C) by operators T_g in a Hilbert space H. A canonical basis of vectors $h \epsilon H$ is introduced and it is shown how to evaluate the D-functions $(h_1, T_g h_2)$. It has been suggested that one such function has the physical interpretation of the electric charge form factor of the pion. This function is evaluated in detail. (auth)

37739 (JINR-E-2726) THE MEASUREMENT OF THE TRIPLE SCATTERING PARAMETER R_{pn} AT 70° AND THE PHASE-SHIFT ANALYSIS AT 630 Mev. Kazarinov, Yu. M.; Legar, F.; Pisarev, A. F.; Yanout, Z. (Joint Inst. for Nuclear Research, Dubna (USSR). Lab. of Nuclear Problems). 1966. 30p. Dep. mn.

The triple scattering parameter R_{pn} and the polarization in the elastic p-n scattering were measured at 70° for 605 Mev protons. The values were found to be: $R_{pn} = 0.09 \pm 0.19$ $P_{pn} = -0.05 \pm 0.18$. The phase-shift analysis was performed at 630 Mev taking these data into account. Experimental quantities were calculated and further experiments determining the parameters D_{pn}, R_{pn}, A_{pn}, C_{nn}^{pq}, and A_{ss}^{pn} were planned. It follows from the planning that for the given experimental possibilities the measurement of the D_{pn} and A_{pn} parameters is the most effective way to discriminate between the two remaining sets of phase shifts. (auth)

37740 (JINR-P-2780) PEREZARYADKA OSTANOVIVSHIKHSYA π-MEZONOV NA LEGKIKH YADRAKH. (Charge of π-Mesons Stopped on Light Nuclei). Petrukhin, V. I.; Prokoshkin, Yu. D.; Filippov, A. I. (Joint Inst. for Nuclear Research, Dubna (USSR). Lab. of Nuclear Problems). 1966. 5p. Dep. mn.

Measurements were made of the charge exchange of π^- mesons stopped on ^{3}He nuclei. The charge exchange of the stopped π^- mesons on ^{10}B, ^{14}N, and ^{35}Cl was depressed by 10^4 folds. (tr-auth)

37741 (JINR–P-2788) ZAKHVAT MYUONOV V SMESYAKH GAZOV. (Muon Capture in Mixed Gases). Budyashov, Yu. G.; Zinov, V. G.; Konin, A. D.; Mukhin, A. I. (Joint Inst. for Nuclear Research, Dubna (USSR). Lab. of Nuclear Problems). 1966. 9p. Dep. mn.

The probability of nuclear capture of muons in mixed single atom (helium and neon) and multi-atom (nitrogen and carbon oxide) gases in relation to argon was measured using $\mu - x$ radiation recordings. The study did not exhibit any systematical relation between the probability of capture and nuclear charge which is another indication of the influence of molecular size on nuclear capture. (tr-auth)

37742 (UCRL-16293) BACKWARD π^-p SCATTERING AS A FURTHER TEST FOR REGGE HIGH-ENERGY BEHAVIOR. Chew, Geoffrey F.; Stack, John D. (Lawrence Radiation Lab., Univ. of California, Berkeley). July 26, 1965. Contract W-7405-eng-48. 10p. Dep. mn. CFSTI $1.00 cy, $0.50 mn.

Backward π^-p scattering measurements are proposed in order to determine Regge shrinkage above 4 Bev. (B.G.D.)

37743 (UCRL–16866) POLARIZATION IN PROTON-PROTON SCATTERING USING A POLARIZED PROTON TARGET. PART I. 0.330 TO 0.740 Gev. PART II. 1.70 TO 6.15 Gev. Betz, F.; Grannis, P.; Chamberlain, O. (and others) (Lawrence Radiation Lab., Univ. of California, Berkeley). Apr. 1966. Contract W-7405-eng-48. 14p. (CONF-660420–2). Dep. mn. CFSTI $1.00 cy, $0.50 mn.

From International Conference on Two-Body Problems at High Energy, Stony Brook, N. Y.

The results of two experiments to measure the polarization parameter in p-p scattering are reported. Both experiments utilize an unpolarized proton beam incident on a polarized proton target. One experiment was performed at the Berkeley 184-inch cyclotron using incident protons of 328, 614, 679, and 736 Mev kinetic energy. The other experiment was performed at the Bevatron and measurements were taken at 1.7, 2.85, 3.5, 4.0, 5.05, and 6.15 Bev kinetic energy. The angular regions measured were from 20 to 100° center of mass; the square of the four-momentum transfer ranged from 0.1 to 0.8 $(Bev/c)^2$. (auth)

37744 (UR-875-151) $\pi^+ - p$ INTERACTIONS AT 900 Mev. Metzger, Wesley James (Rochester Univ., N. Y. Dept. of Physics and Astronomy). 1966. Contract AT(30-1)-875. 136p. Dep. mn. CFSTI $4.00 cy, $1.00 mn.

The BNL 20-inch liquid hydrogen bubble chamber was exposed to a separated beam of π^+ mesons at 1.02 Bev/c. 6000 events were found and measured. Cross sections for the following reactions were measured: $\pi^+p \rightarrow \pi^+p$ (10.7 ± 0.4 mb.), $\pi^+p \rightarrow \pi^+p\pi^0$ (9.2 ± 0.2 mb.), $\pi^+p \rightarrow \pi^+pe^+e^-$ (0.11 ± 0.04 mb.), $\pi^+p \rightarrow \pi^+\pi^+n$ (1.9 ± 0.1 mb.), $\pi^+p \rightarrow 2$ charged particles + 2 or more neutrals (0.74 ± 0.08 mb.), and $\pi^+p \rightarrow$ four charged particles (0.53 ± 0.04 mb.). The differential cross section for elastic scattering was measured. The forward part was compared to the optical model and an exponential in the square of the four-momentum transfer. The reactions yielding $\pi^+p\pi^0$ and $\pi^+\pi^+n$ were found to be dominated by production of the N*(1236) isobar. The invariant mass spectra of $\pi^+p \rightarrow \pi^+p_+\pi^0$ were fit to the hypothesis that it proceeds via the following intermediate states $\pi^+p \rightarrow \pi^0N^{*++}(1236) \rightarrow \pi^+p\pi^0$ ($5.77^{+0.24}_{-0.21}$ mb.), $\pi^+p \rightarrow \pi^+N^{*+}(1236) \rightarrow \pi^+p\pi^0$ ($2.55^{+0.23}_{-0.26}$ mb.), $\pi^+p \rightarrow \pi^+N^{*+}(1518) \rightarrow \pi^+p\pi^0$ ($0.00^{+0.03}_{-0.00}$ mb.), and $\pi^+p \rightarrow p^+p \rightarrow \pi^+p\pi^0$ ($0.40^{+0.38}_{-0.40}$ mb.) with the inclusion of some non-resonant phase space background. A Monte Carlo program is used to generate the mass spectra for each of these intermediate states. A linear combination of these is fit to the experimental mass spectra. This resulted in the partial cross sections indicated above in parentheses. The distribution of the invariant mass of the

$\pi^+ - \pi^0$ was also compared with the Yodh-Olsson isobar model. Agreement with the Yodh-Olsson curve was somewhat better than with the fitted curve. An intensive study of evidence for the existence of the zeta meson was made in this data and in previously published data. The conclusion of this study is that there is no experimental evidence for the existence of the zeta. If the zeta does, however, exist, this experiment places an upper limit on its production cross section of 0.44 ± 0.31 mb. The production mechanism of the N*(1236) was investigated by measuring its decay angular correlations and from them the helicity density matrix elements of the N*. Only 411 events were identified as being the reaction $\pi^+ + p \rightarrow \pi^+\pi^+n$, providing rather limited statistics. Nevertheless, in a manner similar to that for the reaction $\pi^+ + p \rightarrow \pi^+ pe^+e^-$, the mass spectra were fitted with a sum of the $\pi^+N^{*+}(1236)$ intermediate state and nonresonant three body phase space. This resulted in the following cross section $\pi^+p \rightarrow N^{*+}\pi^+ \rightarrow \pi^+n\pi^+$ ($1.05^{+0.37}_{-0.19}$ mb.). The $\pi^+\pi^+$ invariant mass spectrum was also compared to the Yodh-Olsson model prediction. Both this prediction and the fitted curve, though somewhat different, agreed fairly well with the data. (B.G.D.)

37745 (TT-65-50130) MODERN ASPECTS OF PARTICLE PHYSICS. A Collection of Lectures Given at the Third Session of the Spring School of Theoretical and Experimental Physics Held on 3-13 April 1963 at Nor-Amberd. Alikhanyan, A. I. (ed.) Translation of Vop. Fiz. Elem. Chastits, Gos. Kom. Sovet. Min. SSSR Ispol'z. At. Energ., Fiz. Inst., 1963. 523p. (IPST-Cat.-1429). CFSTI $8.20 cy, $2.25 mn.

37746 MEASUREMENT OF THE PAIR PRODUCTION CROSS SECTION FOR 6.13-Mev GAMMA RADIATION. Bak, Hae-Ill; Weinzierl, Peter. Acta Phys. Austr., 22: 60-6(1966). (In German).

The pair-production cross section was measured for the 6.13 Mev gamma ray from ^{16}N for Cu, Ni, and Ag. The cross sections for the elements selected could be determined without the use of theoretical values for the Compton cross section by a combination of transmission measurements and relative measurements of the pair production events. The results agree with the Bethe-Heitler theory within the limit of error of 3 to 7%. (tr-auth)

37747 PROTON-PROTON SCATTERING AT 12 Gev. Sexl-Eggstain, Hannelore (Univ. of Vienna). Acta Phys. Austr., 22: 167-72(1966).

The elastic scattering of protons by protons with a momentum of (12.4 ± 0.39) Bev/c was investigated in emulsions. 980 events with two prongs were found and of these 238 were identified as elastic. The elastic cross section is (10.0 ± 0.9) mbarn. Using water soaked emulsions and a new scanning technique scattering angles were measured as small as 0.7 degrees (CMS). This is the main advantage of our method compared to the evaluation of bubble chamber photographs. This region of nearly forward scattering is of great theoretical interest, since the extrapolation of the differential cross sections to zero scattering angle yields information on the real part of the scattering amplitude. The results lie distinctly above the optical point and show thus that the scattering amplitude is not purely imaginary even at 10 Bev. For larger angles the results agree well with the counter experiments of Diddens and Lindenbaum. Furthermore the use of line-scan technique enabled proton-neutron interactions to be measured. A separation of the elastic events, however, is almost impossible here, because of the lack of a recoil. (auth)

37748 INFLUENCE OF THE DEUTERON MODEL ON THE INELASTIC ELECTRON-DEUTERON CROSS SECTION. Breitenlohner, P.; Hoelzl, K.; Kocevar, P. (Univ., Graz). Acta Phys. Austr., 22: 206-9(1966).

The influence of some deuteron models on the theoretical e-d cross section at the quasielastic peak is investigated, neglecting final state interactions. Calculations are made using different deuteron wave functions and the results are compared with those using the modified Hulthén wave functions. Numerical results are tabulated. (L.B.S.)

37749 REMARKS ON THE DEUTERON FORM FACTORS I. Zingl, Harald F. K. (Univ., Graz). Acta Phys. Austr., 22: 256-8(1966).

The influence of the various terms, i.e., Coulomb interaction, convective term, Pauli term, Darwin term, and spin-orbit, in determining the deuteron form factor from elastic electron-deuteron scattering is considered. (L.B.S.)

37750 MEASUREMENT OF MAGNETIC MOMENTS OF UNSTABLE PARTICLES. Halpern, Otto. Acta Phys. Austr., 22: 265-6(1966).

The determination of the magnetic moments μ of molecular and submolecular particles is usually done through measurement of the μ H wherein H represents the magnitude of the stationary outside magnetic field. The accuracy of this energy measurement depends on the time T available for the measurement, which in turn is determined by rather trivial experimental conditions or also by the lifetime of the particle. A discussion is presented of the case of positronium. (auth)

37751 UNITARY SPIN ANALYSIS OF NEUTRINO REACTIONS. Horn, D. (Tel-Aviv Univ., Israel). Acta Phys. Austr., 22: 297-310(1966).

Different neutrino reaction amplitudes are analyzed according to their T, U, and V-spin properties. This method is used for $\Delta S = 0$ and $\Delta S = \Delta Q$ reactions which include also meson and resonance production. Relations that stem from pure symmetry arguments are established, and their relevance to experiment is discussed. (auth)

37752 PHOTOPRODUCTION OF NEUTRAL PIONS IN THE ENERGY RANGE 400 TO 600 Mev OF THE INCIDENT PHOTON. Bacci, Cesare (Univ., Rome. INFN, Rome); Mencuccini, Corrado; Penso, Gianni; Silvestrini, Vittorio; Spinetti, Mario; Stella, Bruno; Salvini, Socio G. Atti Accad. Naz. Lincei, Rend., Cl. Sci. Fis., Mat. Natur., 39: 452-69(Dec. 1965).

The baryon resonance of mass 1410 Mev produced from gamma reactions with protons is studied by observing the recoil proton from this resonance decay. The $d\sigma/d\Omega$ for this resonance production versus incident gamma energy is plotted and shown. These results are discussed in the light of various experimental effects. (J.F.P.)

37753 AMPUTATED VERTEX FUNCTIONS OF UNSTABLE PARTICLES. Henning, J. J. (Nasionale Navorsingsinstituut vir Wiskundige Wetenskappe, Pretoria). Commun. Math. Phys., 2: 215-22(1966). (In German).

The normalized form of the amputated vertex functions of an unstable particle is derived from the requirement that the general ansatz for the scattering amplitude of two stable particles with a resonance in the energy variable is unitary in the energy interval below the threshold for three particle production. A Klein-Gordon equation for the unstable particle associated with the resonance is derived. The results are applied to the creation of π^+ and π^0 mesons in inelastic scattering processes. (auth)

37754 REPRESENTATION OF MESON FORCE BY A SERIES OF INVERSE POWERS OF DISTANCE IN A RELATIVISTIC CASE. Saliev, A. pp 199-209 of Integrirovanie Nekotorykh Diffentsial'nykh Uravnenii Matematicheskoi Fiziki, Sbornik. Tashkent, Nauka, 1964. (In Russian).

Integrals were obtained for previously derived meson field equations. Meson charge motion in its own and in Coulomb fields are examined, and the electric field strength and Lorentz force are obtained in the form of limited series in inverse powers of distance for this motion. (J.F.P.)

37755 CHARACTERISTICS OF HIGH-ENERGY PARTICLE INTERACTION WITH NUCLEI OF LIGHT ATOMS. Babayan, Kh. P.; Grigorov, N. L.; Mamidzhanyan, E. A.; Shestoperov, V. Ya. (State Atomic Energy Commission, USSR. Moscow State Univ. Erevan State Univ.). Izv. Akad. Nauk Arm. SSR, Fiz., 1: 45-50(1966). (In Russian).

The results of the investigation of the nuclear-active component of "young" air showers by means of an ioniza-

tion calorimeter are set forth. Events with an average coefficient of inelasticity K > 0.85 are realized with a probability of ~15%, while interactions of the nuclear-active particles are at work with an energy >1.4 $(10)^{12}$ ev with the nuclei of air atoms. (auth)

37756 DETERMINATION OF Λ AND Σ HYPERON PARITY. Palev, Ch. Izv. Fiz. Inst. Aneb, Bulg. Akad. Nauk, 14: 45-50(1966). (In Russian).

The parity of the Σ and Λ hyperons was determined on the basis of the one-dimensional dispersion ratios for the elastic $K^{\pm}$-p dispersion. It was found that the parity of Λ with respect to the K meson is relative and that of Σ negative. The conclusions were drawn with the assumption that the total scattering cross section is directed towards a constant value in the case of high energies, and the diffraction one—to 0. The most likely values of the revised constants of the ΣNK and ΛNK interactions were determined. (auth)

37757 STUDY OF ELECTRON-POSITRON ANNIHILATION BY USING BOGOLIUBOV CANONICAL TRANSFORMATION. Khanna, K. M. (Indian Inst. of Tech., Kharagpur). J. Sci. Eng. Res., Indian Inst. Technol., Karagpur, 9: 135-44(Jan. 1965).

The Bogoliubov canonical transformation was used to study the annihilation of a negatron-positron pair surrounded by virtual negatron-positron pairs. Attention was confined to the ground state of the negatron-positron pair and the number of γ rays produced was calculated. Gamma-ray production is considered under the assumption that the average number of γ rays produced is equal to the average number of negatron-positron pairs in the ground state of the hamiltonian describing the collisions of the process. This assumption is valid on the basis of identification of the ground state of the hamiltonian with the physical particle state and a study of the single photon annihilation of the 3_S state in collision or creation. In order that the laws of energy, charge, and spin conservation are maintained, it is necessary to postulate the existence of a particle with no charge, having the same mass as the mass of an electron or positron, and spin equal to 0, 1, or 2. Such a particle is hitherto unknown and it is conjectured that its lifetime may be very large. (BBB)

37758 GENERAL FORMALISM OF SOME SCATTERING PROCESSES INVOLVING PHOTONS. Rasche, G. (Univ., Zurich); Woolcock, W. S. Nucl. Phys., 87: 51-64(1966).

By correctly defining the polarization vectors of photons and the spinors for particles of spin ½ according to the prescription of Jacob and Wick, the partial-wave expansions of the invariant reaction amplitudes for the processes $\gamma + N \rightarrow \pi + N$, $\gamma + N \rightarrow \gamma + N$ and $\gamma + \gamma \rightarrow N + \bar{N}$ are obtained. No specific representation of the Dirac matrices is necessary. (auth)

37759 THE ALGEGRA OF CURRENTS AND THE $|\Delta I| = ½$ RULE FOR K-MESON NONLEPTONIC DECAY. Bouchiat, C.; Meyer, Ph. (Faculte des Sciences, Orsay, France). Phys. Lett., 22: 198-200(Aug. 1, 1966).

The difficulties occurring in a recent derivation of the $|\Delta I| = ½$ rule for the K meson decay into zero energy-momentum pions are removed by a suitable definition of the unphysical amplitude. The selection rule is shown to be valid only in the limit of zero pion mass of in special models. (auth)

37760 GAUGE CONDITION AND THE EQUAL-TIME AXIAL AND VECTOR CURRENT COMMUTATOR. Nauenberg, M. (CERN, Geneva. Stanford Univ., Calif.). Phys. Lett., 22: 201-2(Aug. 1, 1966).

The equal time commutator between the axial and the vector current is related to the longitudinal component of the off mass shell meson production amplitude by a conserved vector field, and an elementary interpretation is given for this result. (auth)

37761 THE PARAMETERS OF THE REGGE POLE MODEL FOR πN CHARGE-EXCHANGE SCATTERING. Hoehler, G.; Baacke, J.; Eisenbeiss, G. (Technische Hochschule, Karlsruhe, Ger.). Phys. Lett., 22: 203-5 (Aug. 1, 1966).

A set of parameters for the ρ-exchange model is proposed and the indications for a correction term at 6 Bev/c are discussed. (auth)

37762 DYNAMICAL DERIVATION OF BARYON MASSES IN THE QUARK MODEL. Federman, P.; Rubinstein, H. R.; Talmi, I. (Weizman Inst. of Science, Rehovoth, Israel). Phys. Lett., 22: 208-9(Aug. 1, 1966).

The baryon (56,1) multiplet mass differences are obtained from two-body effective interactions between quarks. Three mass relations are obtained for any isospin conserving interaction without assuming any group transformation property. Symmetry conserving triplet forces yield the Gell-Mann Okubo relations. (auth)

37763 DYNAMICAL QUARK MODEL FOR HADRONS. Rubinstein, H. R. (Weizmann Inst. of Science, Rehovoth, Israel). Phys. Lett., 22: 210-11(Aug. 1, 1966).

Assuming I-independence for triplet forces, mass formulas are found for 1^-, 2^+ mesons and meson-decuplet. The Gell-Mann Okubo formula is abandoned. A new classification of states is proposed. A simple, unified picture of linear hadron masses is obtained. (auth)

37764 PHASE OF K_L–K_S REGENERATION IN A SIMPLE REGGE POLE MODEL. Cabibbo, N. (CERN, Geneva). Phys. Lett., 22: 212-13(Aug. 1, 1966).

The phase of K_L–K_S regeneration is evaluated in a simple Regge pole model. The result is compared with data on the interference of K_S, $K_L \rightarrow 2\pi$ and found compatible with the Wolfenstein prediction if $M_L > M_S$. (auth)

37765 POSSIBLE METASTABLE BARYONIC STATES WITH EVEN PARITY IN THE QUARK MODEL. Morpurgo, G. (Univ., Genoa). Phys. Lett., 22: 214-16 (Aug. 1, 1966).

It is remarked that in the quark model very restrictive selection rules do exist for mesonic or electromagnetic excitation of baryonic states characterized by orbital angular momentum L = 1 and even parity. If such states exist due account has to be taken of these selection rules in their experimental detection. (auth)

37766 RHO MESON PHOTOPRODUCTION CROSS SECTIONS IN THE STRONG-ABSORPTION MODEL. Eisenberg, Y. (Weizmann Inst. of Science, Rehovoth, Israel); Ronat, E. E.; Brandstetter, A.; Levy, A.; Gotsman, E. Phys. Lett., 22: 217-19(Aug. 1, 1966).

The experimentally observed differential cross sections of photoproduced ρ^0 mesons, in the energy range of 1.5–6.0 Bev, are quantitatively explained by the strong absorption model developed in the helicity representation. The model enables the total ρ^0p cross sections to be estimated. (auth)

37767 DIRECT SEARCH FOR THE C-VIOLATING DECAY $\eta^0 \rightarrow \pi^0 e^+e^-$. Baglin, C. (Ecole Polytechnique, Paris); Bezaguet, A.; Degrange, B.; Jacquet, F.; Musset, P.; Nguyen-Khac, U.; Nihoul-Boutang, G.; Bingham, H. H.; Michael, W. Phys. Lett., 22: 219-23(Aug. 1, 1966).

No examples of this decay were found in a sample of film containing 387 $\eta^0 \rightarrow \pi^0\pi^+\pi^-$ decays with π^0 detected. The film was taken with the Ecole Polytechnique heavy liquid bubble chamber exposed to 950 Mev/c π^- at Saclay. With 90% confidence the branching ratio $\eta^0 \rightarrow \pi^0e^+e^-$ is less less than 0.23% of all η^0 decays. (auth)

37768 DECAY CORRELATIONS OF PHOTO-PRODUCED RHO MESONS IN THE STRONG-ABSORPTION MODEL. Eisenberg, Y. (Weizmann Inst. of Science, Rehovoth, Israel); Ronat, E. E.; Brandstetter, A.; Levy, A.; Gotsman, E. Phys. Lett., 22: 223-5(Aug. 1, 1966).

The ρ^0 decay angular distributions are calculated by the strong absorption model. Good agreement with the experimental data is obtained, for photoproduced ρ^0 mesons in the energy range 1.5–6.0 Bev. (auth)

37769 KINEMATIC ENHANCEMENT OF RESONANCE PRODUCTION IN CERTAIN TWO-BODY REACTIONS. Morrison, D. R. O. (CERN, Geneva). Phys. Lett., 22: 226-9(Aug. 1, 1966).

An explanation is given of the fact that certain quasi two body reactions have a constant cross section with respect to incident momentum. It is supposed that there is a diffraction scatter at one vertex followed by a final state interaction. This mechanism is applied to reactions produced by incident protons, pions, kaons, and gammas. (auth)

37770 PRODUCTION OF STRANGE PARTICLES IN 8-Gev/c π^+-PROTON INTERACTIONS. II. $K\bar{K}$ PRODUCTION AND ΛK AND $K\bar{K}$ CROSS SECTIONS. Brandt, S. (CERN, Geneva); Cocconi, V. T.; Czyzewski, O.; (and others). Phys. Lett., 22: 230-2(Aug. 1, 1966).

Partial and total cross sections were measured for $K\bar{K}$ production in meson (π^+)-proton interactions. The reaction $p\bar{K}^0K^0\pi^+$ for which the largest number of events were observed is discussed in detail. An appreciable production of $N^{*++}(1238)$ isobar and $K^{*+}(890)$ was found, and upper limits on the production cross sections for φ- and f'-mesons were established. The total cross section for all strange particle production was found to be (3.10 ± 30) mb. (L.B.S.)

37771 EVIDENCE FOR THREE NEW CHARGED BOSONS OF MASSES 1929, 2195, AND 2382 Mev AND NARROW WIDTHS. Chikovani, G.; Dubal, L.; Focacci, M. N.; Kienzle, W.; Levrat, B.; Maglic, B. C.; Martin, M.; Nef, C.; Schuebelin, P.; Seguinot, J. (CERN, Geneva). Phys. Lett., 22: 233-6(Aug. 1, 1966).

Three new bosons, referred to as S, T, and U, were observed in the reaction $\pi^- + p \rightarrow p + X^-$ using the missing-mass spectrometer; their masses are 1929, 2195, and 2382 Mev, respectively. Their physical widths are equal to the experimental resolution and compatible with zero-width, with the upper limits: $\Gamma \leq 35$, ≤ 13, and ≤ 30 Mev, respectively. They are produced with the differential cross section $d\sigma/dt$ between 20 and 40 microbarn per $(Bev/c)^2$ at an average $\bar{t} = 0.3\ (Bev/c)^2$. (auth)

37772 EVIDENCE OF A HIGHER SYMMETRY IN NUCLEON-NUCLEON SCATTERING. Brown, C. N.; Thorndike, E. H. (Univ. of Rochester, N. Y.). Phys. Lett., 22: 236-8(Aug. 1, 1966). (UR-875-150).

SU(12)$\supset$ predicts six relations among the nucleon-nucleon scattering amplitudes. Experimentally the relation $ReB_1 = \frac{1}{2} ReG_0$ is satisfied to 5–10% between 95 and 210 Mev, while the other relations yield fair agreement for forward scattering and poor agreement for non-forward scattering. (auth)

37773 A NEW TEST OF SU(3) IN MESON PHOTOPRODUCTION. Elings, V. B.; Osborne, L. S. (Massachusetts Inst. of Tech., Cambridge). Phys. Lett., 22: 239-40 (Aug. 1, 1966). (MIT-2098-250).

A relation between the production amplitudes for the reactions $\gamma p \rightarrow p\pi^+\pi^-$, pK^+K^-, and $\Sigma^+K^+\pi^-$ is derived from SU(3). The relation is consistent with experimental data. (auth)

37774 POSITRON ANNIHILATION IN A DILUTE METAL: Li–NH_3 SOLUTION. Varlashkin, P. G.; Stewart, A. T. (Univ. of North Carolina, Chapel Hill). Phys. Rev., 148: 459-63(Aug. 5, 1966).

The momentum distribution of photons from positrons annihilating in lithium-ammonia solutions of various concentrations was measured. For all except very dilute solutions, the momentum distribution was found to be independent of concentration and unlike the distribution for ammonia or for a metal. At extremely low concentrations, the distributions resemble more that of pure ammonia. No effect due to a magnetic field was observed for the solutions although a small effect was noted for pure liquid ammonia. In addition the momentum distribution for a concentrated solution was observed to change slightly over the temperature range −164°C to 13°C. These data suggest the formation of a positronium state in this dilute metallic solution. (auth)

37775 DIRECT MEASUREMENT OF THE g FACTOR OF THE FREE POSITRON. Rich, A.; Crane, H. R. (Univ. of Michigan, Ann Arbor). Phys. Rev. Lett., 17: 271-5(Aug. 1, 1966).

An experiment is described for a direct measurement of the g factor of the free positron. The experimental technique follows that already described for the measurement of the g factor of the free electron by Wilkinson and Crane (Phys. Rev. 130: 852(1963)) except for the way the polarization and the analysis of the polarization are accomplished. (B.G.D.)

37776 INTERFERENCE BEATS IN PULSE-STIMULATED CYCLOTRON RADIATION. Wachtel, J. M.; Hirshfield, J. L. (Yale Univ., New Haven). Contract AF 19(628)-5104. Phys. Rev. Lett., 17: 348-51(Aug. 15, 1966).

The experimental observation is reported of a beat phenomenon for a free-electron system, which arises from a cyclotron-resonant pulse imposed on a cloud of initially monoenergetic weakly relativistic electrons in a uniform d-c magnetic field. A brief theory is offered for comparison with experiment. (L.B.S.)

37777 ABSOLUTE VALUE OF THE PROTON g FACTOR. Myint, Than; Kleppner, Daniel; Ramsey, Norman F.; Robinson, Hugh G. (Harvard Univ., Cambridge, Mass.). Phys. Rev. Lett., 17: 405-7(Aug. 15, 1966).

A determination was made of the proton moment in atomic hydrogen for which the diamagnetic correction is known to a high precision, thus allowing an absolute determination of the proton g factor. By comparing the result with previous determinations in water, the experimental value of the magnetic shielding constant for protons in water and in H_2 are obtained. (L.B.S.)

37778 SCATTERING OF POSITRONS AND ELECTRONS FROM PROTONS. Anderson, R. L.; Borgia, B.; Cassiday, G. L.; DeWire, J. W.; Ito, A. S.; Loh, E. C. (Cornell Univ., Ithaca, N. Y.). Phys. Rev. Lett., 17: 407-9(Aug. 15, 1966).

An experiment that compares the elastic scattering of 1200-Mev positrons and electrons from protons is described. The results are given as ratios $R = \Delta\delta^+/\Delta\delta^-$, the $\Delta\delta$'s are the partial cross sections for identical increments of solid angles or q^2. A value of $R = 0.996 \pm 0.020$ was obtained after making the radiative correction, from which it is concluded that the scattering cross sections are the same within the experimental error. (L.B.S.)

37779 NEUTRAL-MESON PRODUCTION CROSS SECTIONS AND MIXING ANGLES IN A QUARK MODEL. Alexander, G.; Lipkin, H. J.; Scheck, F. (Weizmann Inst. of Science, Rehovoth, Israel). Phys. Rev. Lett., 17: 412-16(Aug. 15, 1966).

Quark model predictions for neutral-meson production at finite momentum transfer are presented, which may provide a sensitive test of the model and which also give values for the mixing angles in the meson nonets. The predictions and mixing angles are independent of SU(3)-symmetry-breaking effects in the transition amplitudes. Reasonable agreement with experiment was found for those cases where adequate data are available except in one case. (L.B.S.)

37780 SPIN-2^+ MESON DECAYS IN THE QUARK MODEL. Elitzur, M. (Weizmann Inst. of Science, Rehovoth, Israel); Rubinstein, H. R.; Stern, H.; Lipkin, H. J. Phys. Rev. Lett., 17: 420-2(Aug. 15, 1966).

The spin-2 nonet is described by SU(6) $\underline{405}$ wave functions that are eigenstates of the number of strange quarks. The decay branching ratios are obtained by a rearrangement of the quarks and antiquarks into two quark-antiquark pairs without change in quantum numbers, after an appropriate spin recoupling. (auth)

37781 NOTE ON THE THEORY OF INTERMEDIATE VECTOR MESON. Balasubramanian, T. S. (Univ., Naples). Proc. Nat. Inst. Sci. India, Pt. A, 31: 323-6 (July 1965).

The $\pi-\mu$ decay through an intermediate vector meson is considered. Choosing a simple interaction lagrangian, the interaction hamiltonian is found to consist of a term for the decay mediated by the vector meson and a direct decay term. The apparent contradiction with angular momentum conservation is resolved by showing that the S-matrix ele-

ment to lowest order for the mediated decay process vanishes. The pion, then, decays through the direct interaction. (auth)

37782 NUMERICAL EVALUATION OF THE TWO-NUCLEON SCATTERING LENGTH AND EFFECTIVE RANGE WITH TENSOR FORCES. Lovitch, L. (Columbia Univ., New York); Rosati, S. Proc. Phys. Soc. (London), 88: 909-13(Aug. 1966). (NYO-1932-106).

A middle-point matching procedure is described for obtaining the zero energy scattering solution of the two-nucleon system when tensor forces are present. This yields an accurate and rapid calculation of the effective-range parameters, and, as an example, some numerical results so obtained are presented. (auth)

37783 ELASTIC PHOTOPRODUCTION OF π^0 MESONS FROM DEUTERIUM. Mann, B.; Smith, A. M.; Steward, D. T. (Glasgow Univ.). Proc. Phys. Soc. (London), 88: 915-18(Aug. 1966).

Differential cross sections were determined for the elastic neutral pion photoproduction from deuterons at recoil deuteron angles of 25, 30, and 37° (lab.) within the photon energy range $220 < E_\gamma < 280$ Mev. The experiment was carried out by detecting the recoil deuteron with a counter telescope capable of distinguishing deuterons from protons and measuring their energy. These and previous results were compared with an impulse approximation calculation. (auth)

37784 MOTION OF POSITRONS IN SODIUM. Stewart, A. T.; Shand, J. B.; Kim, S. M. (Univ. of North Carolina, Chapel Hill). Proc. Phys. Soc. (London), 88: 1001-10 (Aug. 1966).

The angular correlation of radiation from positrons annihilating in sodium as a function of temperature was measured. As the temperature was increased the angular correlation data changed as though the angular resolution had become worse. The electron motion in sodium is known and is unlikely to cause this phenomenon. This effect is attributed to positron motion. The results can be given a one-parameter characterization by assigning to the positron an effective temperature (1.9 ± 0.4)T or an effective mass (1.9 ± 0.4)m. Possible causes of this effect are discussed. (auth)

37785 PION-NUCLEON SCATTERING AT 35 AND 39 Mev. Donald, R. A. (Univ. of Liverpool). Proc. Phys. Soc. (London), 88: 1047-9(Aug. 1966).

An extensive analysis of negative pion-proton elastic scattering reported previously is presented. It is concluded that the elastic-scattering data are consistent with the analysis of Hamilton and Woolcock. Some further analysis of charge-exchange scattering at low energies is also presented. (auth)

37786 CONSIDERATIONS ABOUT HIGH ENERGY INTERACTIONS. Cocconi, G. (CERN, Geneva). pp 616-18 of Proceedings of the Ninth International Conference on Cosmic Rays. Vol. 2. Stickland, A. C. (ed.). London, The Institute of Physics and The Physical Society, 1966.

A discussion of present trends in the interpretation of nucleon interactions around 10 Tev and the related measurements that could be performed using the cosmic ray beam is presented. (auth)

37787 CASCADE THEORY OF SHOWERS FOR LIGHT AND HEAVY SUBSTANCES TAKING INTO ACCOUNT THE POLARIZATION OF THE MEDIUM. Bakhtadze, A. K.; Ivanenko, I. P.; Samosudov, B. E. (Moscow State Univ.). pp 792-5 of Proceedings of the Ninth International Conference on Cosmic Rays. Vol. 2. Stickland, A. C. (ed.). London, The Institute of Physics and The Physical Society, 1966.

The one-dimensional cascade theory of photon-electron showers is developed, taking into account the effect of the polarization of the medium upon the cross section for electron bremsstrahlung. Solutions were obtained for the equations of the cascade theory with arbitrary boundary conditions and with source functions of an arbitrary kind. It is found that when polarization effects are taken into account the existing divergences in the cascade functions are eliminated. The cascade curves and energy spectra for the particles were obtained for substances with various Z, and allowance was made for scattering. Some angular problems were also considered. (auth)

37788 PROCESSES OF BREMSSTRAHLUNG AND PAIR PRODUCTION AS THEY ARE REGARDED IN THE CASCADE THEORY OF THE SHOWERS. Guzhavin, V. V.; Ivanenko, I. P. (Moscow State Univ.). pp 796-8 of Proceedings of the Ninth International Conference on Cosmic Rays. Vol. 2. Stickland, A. C. (ed.). London, The Institute of Physics and The Physical Society, 1966.

A new method of solving the fundamental equations of the one-dimensional cascade theory is proposed. This method permits one to obtain more accurate solutions for various initial conditions and arbitrary source functions in light and heavy substances. The method is based on the replacement of the integral operator which describes the processes of bremsstrahlung and pair production by a simple approximate differential operator. Such replacement in many cases significantly simplifies the integro-differential equations of the cascade theory, reducing them to linear differential equations. The proposed method of solution is also used for calculating some characteristics of the three-dimensional development of cascade showers. (auth)

37789 NUCLEAR CASCADE PROCESS IN THE IONIZATION CALORIMETER. Denisov, E. V.; Dedenko, L. G.; Dubrovina, S. A.; (and others) (Lebedev Inst. of Physics, Moscow). pp 824-6 of Proceedings of the Ninth International Conference on Cosmic Rays. Vol. 2. Stickland, A. C. (ed.). London, The Institute of Physics and The Physical Society, 1966.

Using an electronic computer, the characteristic features of the nuclear cascade produced in iron by primary cosmic nucleons at hundreds and thousands of Bev were calculated. The calculated dependence is compared with experimental data obtained with the large ionization calorimeter at the Tien-Shan mountain station. (auth)

37790 INTERACTIONS OF NUCLEONS WITH COMPLEX NUCLEI AT HIGH ENERGIES. Guseva, V. V.; Lebedev, A. M.; Sokolovskii, V. V. (Lebedev Inst. of Physics, Moscow). pp 909-10 of Proceedings of the Ninth International Conference on Cosmic Rays. Vol. 2. Stickland, A. C. (ed.). London, The Institute of Physics and The Physical Society, 1966.

Peculiarities of the interactions of nucleons with complex nuclei at hundreds of Bev were considered in terms of a model of plural collisions of a primary nucleon with nucleons of a target nucleus, neglecting secondary pion interactions within the nucleus. The analysis of experimental data suggests that this model is in better accord with experiment than a model taking into consideration the pion-nucleon interactions only. (auth)

37791 AVERAGE CHARGE DISTRIBUTIONS IN SYSTEMS OF NUCLEONS AND PIONS. Frishman, Y. (Hebrew Univ., Jerusalem); Yeivin, Y. pp 946-9 of Proceedings of the Ninth International Conference on Cosmic Rays. Vol. 2. Stickland, A. C. (ed.). London, The Institute of Physics and The Physical Society, 1966.

Closed expressions are derived for the average charge distributions in systems of nucleons and pions with given total isotopic spin and charge. It is also shown that in nucleon-nucleus collisions with multiple pion production, on the average one third of the pions produced are neutral and the difference between the numbers of positive and negative pions tends to $+\frac{1}{2}$ or $-\frac{1}{2}$ for proton- or neutron-nucleus collisions, respectively, as the total number of produced pions tends to infinity. (auth)

37792 SOLAR NEUTRINO INTERACTION WITH ELECTRONS. Domogatskii, G. V.; Zatsepin, G. T. (Lebedev Inst. of Physics, Moscow). pp 1025-7 of Proceedings of the Ninth International Conference on Cosmic Rays. Vol. 2. Stickland, A. C. (ed.). London, The Institute of Physics and The Physical Society, 1966.

Some details of the expected effect of elastic solar neutrino scattering on the electrons of a medium are given. Different experimental possibilities of detecting this process are discussed. (auth)

37793 SOLAR NEUTRINO DETECTION BY THE REGISTRATION OF ELECTRONS IN REACTIONS $\nu + Z \rightarrow (Z+1) + e^-$. Domogatskii, G. V.; Zatsepin, G. T.; Eramzhyan, R. A. (Lebedev Inst. of Physics, Moscow). pp 1028-9 of Proceedings of the Ninth International Conference on Cosmic Rays. Vol. 2. Stickland, A. C. (ed.). London, The Institute of Physics and The Physical Society, 1966.

The light nuclei ^{7}Li, ^{9}Be, ^{11}B and others are considered as possible solar neutrino detectors. The cross sections and angular distributions of electrons are derived. (auth)

37794 C, P, AND T INVARIANCES AND THE BOOTSTRAP HYPOTHESIS. Tokuda, Naoki (Hokkaido Univ., Sapporo). Progr. Theoret. Phys. (Kyoto), 35: 1043-50 (June 1966).

It is investigated whether the charge conjugation, space reflection and time reversal invariances in the strong interactions can be understood in the framework of the bootstrap dynamics, within a limited model of the pion-nucleon system. It is found that not only the above mentioned invariances but also the charge independence can be attributed to the dynamical self-consistency requirements on the pion-nucleon vertex and on the self-energies of the various particles. (auth)

37795 MASS DIFFERENCES AND A DEFORMED OCTET AXIAL-VECTOR CURRENT. Koyama, Hideyuki (Osaka Univ.). Progr. Theoret. Phys. (Kyoto), 35: 1051-60(June 1966).

In order to investigate the mass differences of the octet $\frac{1}{2}^+$ baryons and the 0^- mesons and the weak leptonic interactions in a unified way, an octet axial vector current is introduced, which is deformed in the direction of the hypercharge axis in the SU(3) space and is assumed to be generated from the strong Lagrangian with breakdown of the symmetry. This is an extension of some ideas of Gell-Mann and Lévy, Nambu and Gürsey. In the lowest order perturbation method, the baryon and the meson mass splittings are derived from the Lagrangian in a consistent way within the order of the electromagnetic mass differences, and a plausible value, 2.412, of d/f is obtained. The deformation of the Lagrangian induces the deviation of G_A/G_V from unity observed in beta decay on the basis of a modified Cabibbo scheme with the angle $\theta_A = \theta_V$. The effective Cabibbo angle θ'_A is given by $\theta'_A = \tan^{-1}(0.80 \tan \theta_A)$ and θ_A is determined to be 0.32 from the lepton pair decays of meson. Modified G-T relations are proposed. (auth)

37796 HIGH-ENERGY ELASTIC SCATTERING AT SMALL MOMENTUM TRANSFERS. Ida, Masakuni (Tokyo Univ.). Progr. Theoret. Phys. (Kyoto), 35: 1074-87(June 1966).

Experimental data on high-energy p-p, $\bar{p}$-p, $\pi^{\pm}$-p and $K^{\pm}$-p elastic scatterings for small momentum transfers are analyzed under the assumptions that the spin effect is negligible at high energies and that the imaginary part of the scattering amplitude predominates over the real one for low momentum transfers. Four parameters, all of which have definite physical meanings, are introduced and determined numerically from experimentally available quantities. It is found that protons are more transparent for a pion or a kaon than for a proton. The transparency increases with increasing energy independently of the shrinkage or nonshrinkage of the diffraction peak. It appears that there exists a non-negligible amount of contribution from the real part of the scattering amplitude to the elastic cross section except for $\bar{p}$-p scattering, which is explainable by a simple model with no real amplitude. (auth)

37797 VALUE OF THE ELECTRIC QUADRUPOLE MOMENT OF THE DEUTERON. Narumi, Hajime (Hiroshima Univ.); Watanabe, Tadashi. Progr. Theoret. Phys. (Kyoto), 35: 1154-5(June 1966).

The electric quadrupole moment of the deuteron was evaluated at 2.796 ± 0.005 m6, based on previous experimental results on nuclear quadrupole coupling. (L.B.S.)

37798 SCATTERING ON A COMPOSITE PARTICLE WITH SMALL BINDING ENERGY AND THE IMPULSE APPROXIMATION. Braun, M. A. Vestn. Leningr. Univ., Ser. Fiz. Khim. (4), No. 1, 11-15(1966). (In Russian).

The scattering on a composite particle (deuteron) is considered in the range of small binding energies. It is shown that the scattering amplitude is reduced to a simple expression resembling the well-known impulse approximation. The elastic scattering is restricted to small scattering angles and is negligible in comparison to the inelastic scattering. The argument is essentially based on the assumption of nonelementarity of the deuteron. (auth)

37799 INTERMEDIATE BOSON PRODUCTION IN THE REACTION $e^- + e^+ \rightarrow W^+ + \mu^- + \bar{\nu}_\mu$. Darbinyan, S. M.; Shakhnazaryan, Yu. G. Yadern. Fiz., 3: 1079-82(June 1966). (In Russian).

The creation of a W-meson in colliding e^-e^+ beams in the reaction $e^- + e^+ \rightarrow W^+ + \mu^- + \bar{\nu}_\mu$ is considered. Expressions were obtained for the differential and total cross sections. The dependence of the integral cross section on the total energy of the initial particles is given on a graph, assuming the anomalous magnetic moment of the W-meson equal to $k = -1, 0, 1$. (auth)

37800 ELASTIC SCATTERING OF γ QUANTA ON PROTONS AT ENERGIES ABOVE THE π-MESON PHOTOPRODUCTION THRESHOLD. Baranov, P. S.; Kuznetsova, V. A.; Slovokhotov, L. T.; Sokol, G. A.; Shtarkov, L. N. (Lebedev Inst. of Physics, Moscow). Yadern. Fiz., 3: 1083-92(June 1966). (In Russian).

The elastic scattering γ quanta on hydrogen at energies above the meson photoproduction threshold was investigated experimentally. Angular distributions were obtained for the γ quantum scattering angles in the region 70 to 150° cms for two mean energies of the γ quanta: 214 and 249 Mev. The experimental data at 249 Mev are in good agreement with previous results. The total cross section for the Compton scattering of γ quanta on protons is calculated using the obtained angular distributions. The results are compared with other experimental results. (auth)

37801 INFLUENCE OF $\pi\pi$ INTERACTIONS ON THE ELECTROMAGNETIC STRUCTURE OF THE NUCLEON. Lendel, A. I.; Lendel, V. I.; Meshcheryakov, V. A.; Ernst, B. M. (Uzhgorod State Univ., USSR. Joint Inst. for Nuclear Research, Dubna, USSR). Yadern. Fiz., 3: 1093-1100(June 1966). (In Russian).

A satisfactory description of the s- and p-wave low energy πN-scattering, taking the latest experimental data into account, is obtained in the framework of the dispersion method, based on the separation of partial waves by combining the forward–backward dispersion relations. The nucleon form-factor parameters are determined and give a correct description of the isovector parts of the nucleon form factors. A simple expression for C_1 in terms of the $\pi\pi$- and πN-interaction parameters is obtained. (auth)

37802 π-MESON PRODUCTION IN 655-Mev pp COLLISIONS AND THE DETERMINATION OF ABSORPTION COEFFICIENTS. Vovchenko, V. G. (Ioffe Inst. of Physics and Tech., Leningrad). Yadern. Fiz., 3: 1101-6(June 1966). (In Russian).

The parameters of the π-meson creation resonance model are re-estimated, taking all possible transitions from the initial pp-system, allowed by S- and P-state emission into account. Three independent parameters give a statistically satisfactory description of the results of measuring cross sections, angular distributions and π^+- and π^0-meson spectra in the reactions $pp \rightarrow \pi^+pn$ and $pp \rightarrow \pi^0pp$. An analysis of inelastic pp-scattering by the partial-wave method is performed on the basis of the resonance model assumptions. (auth)

37803 THE TRIANGULAR DIAGRAM AND DETERMINATION OF π-MESON LOW-ENERGY SCATTERING AMPLITUDE. Anisovich, V. V.; Levin, E. M.; Lipatov,

L. N. (Ioffe Inst. of Physics and Tech., Leningrad). Yadern. Fiz., 3: 1107-10(June 1966). (In Russian).

The role of the triangular diagram in the reaction $\pi + N \rightarrow N + \pi + \pi$ is estimated in the framework of the Olsson–Yodha isobar model. At 500 to 600 Mev the triangular diagram explains the behavior of the π-meson spectrum with $a_0 = 1$, $a_2 = 0$ (a_T is the π-meson scattering length with isospin T). The behavior of the π-meson spectrum cannot be completely explained with the help of a triangular diagram in the framework of the Olsson–Yodha model for energies of the order 400 Mev. It is shown that it is necessary to determine the magnitude of the amplitude for isobar production in the P-state, so as to determine the scattering lengths more exactly and ascertain whether the anomaly in the behavior of the π-meson spectrum is only connected with the triangular diagram or not. (auth)

37804 PRODUCTION OF RESONANCES AT HIGH ENERGIES AND SINGULARITIES IN THE COMPLEX j-PLANE. Kaidalov, A. B.; Karnakov, B. M. (Inst. of Theoretical and Experimental Physics, Moscow). Yadern. Fiz., 3: 1119-26(June 1966). (In Russian).

The production of meson resonances with higher spins is considered at high energies and low values of momentum transfer, assuming that the asymptotic of the production amplitude is determined by singularities in the complex j-plane with definite quantum numbers. The angular distributions of the decay products and the behavior of the resonance production differential cross sections are obtained for $t \rightarrow 0$ and various quantum numbers of the dominating singularity. (auth)

37805 SOLUBLE MODEL FOR THE FORWARD SCATTERING AMPLITUDE. Shirkov, D. V. (Inst. of Mathematics and Computer Tech., USSR). Yadern. Fiz., 3: 1149-53(June 1966). (In Russian).

A model is suggested to describe the forward scattering of spinless particles. The unitarity condition in the model ensures a correct description of the low-energy region near to the threshold and also of the high-energy region if the total cross section tends to a constant. For neutral mesons the model allows an exact solution, the comparison of which with the low-energy elastic model, makes it possible to draw a number of important conclusions. In the real case of charged pions the model gives a system of equations that can be solved by numerical methods. (auth)

37806 POSSIBILITY OF OBSERVING MIRROR PARTICLES. Kobzarev, I. Yu.; Okun, L. B.; Pomeranchuk, I. Ya. (Inst. of Experimental and Theoretical Physics, Moscow). Yadern. Fiz., 3: 1154-60(June 1966). (In Russian).

The possible existence of mirror particles (R) in addition to usual particles (L) is considered in connection with the observed violation of CP-invariance in the $K_2^0 \rightarrow 2\pi$ decay. Their introduction restores the left-right equivalency. It is shown that mirror particles cannot interact with usual particles strongly, semi–strongly or electromagnetically. Weak interactions between L and R particles, due to the exchange of neutrinos, are possible. The L and R particles must have a common gravitational interaction. The question of the existence of macroscopical bodies (stars) consisting of R-matter and their possible observation is discussed. (auth)

37807 ω-MESON PHOTOPRODUCTION AT HIGH ENERGIES. Zhizhin, E. D.; Mur, V. D.; Nikitin, Yu. P. Yadern. Fiz., 3: 1161-8(June 1966). (In Russian).

The complex angular momentum method is used to study the asymptotic behavior and spin structure of the amplitudes of the process $\gamma + N \rightarrow \omega + N$. Most attention is given to the case when the process is due to the exchange of a reggeon with the quantum numbers of vacuum. Under this assumption the asymptotic behavior of the ω-meson photoproduction cross section cannot differ much from the asymptotic cross sections of elastic processes. An expression is obtained for the ω-meson density matrix in the region of small creation angles and the angular distribution of the $\omega \rightarrow \pi^0 + \gamma$ decay products is calculated in certain special cases. (auth)

37808 EXACT SOLUTION TO A BOOTSTRAP PROBLEM. Watson, Howard Lee. La Jolla, San Diego, Calif., Univ. of California, 1965. 60p.

Thesis.

An exact bootstrap solution is found for a model of $K\bar{K}$ scattering in which only the S-wave amplitudes are kept in both the direct and crossed channels. Neither charge independence nor charge symmetry is assumed; thus, there are four independent amplitudes to be calculated. The resulting solution is charge independent and has two independent amplitudes, corresponding to I = 0 and I = 1. A search is made for other solutions, but none are found. (Dissertation Abstr.)

37809 STUDY OF REGGE DYNAMICS IN PION-NUCLEON SCATTERING. Stack III, John David. Berkeley, Calif., Univ. of California, 1965. 92p.

Thesis.

A theoretical study is made of the MacDowell symmetry and the properties of fermion Regge poles. A set of Reggeized bootstrap equations for πN scattering is derived and analyzed. A careful discussion of kinematics is given, the inhomogeneous terms in the integral equation are constructed in detail, and the integral equation is transformed to one of standard Fredholm type. (Dissertation Abstr.)

37810 ANNIHILATION OF POSITRONS IN GASES. Falk, Willie Robert. Vancouver, Can., Univ. of British Columbia, 1965. 264p.

Thesis.

The lifetimes of free positrons were investigated at room temperature in the gases N_2, O_2, CO_2, He, A, and Kr by recording the time distributions of the annihilation events. Whereas all the polyatomic gases exhibited pure exponential decay spectra, the annihilation spectra for the noble gases were more complex exhibiting an initial shoulder followed by an exponential decay. The annihilation spectrum in argon (at 10.5 atm) was investigated in detail. At zero electric field the initial portion of the spectrum is characterized by a relatively low nonconstant annihilation rate, and is attributed to annihilation of positrons slowing down in the energy interval between the positronium formation threshold (8.9 ev in argon) and thermal energy. A velocity-dependent annihilation rate over this energy range is suggested to account for this shoulder in the annihilation spectrum. The time-width of this shoulder is found to be 340 nsec atm. The rest of the spectrum exhibits an exponential decay as observed in the polyatomic gases. Further investigations using applied d-c electric fields (in the range between 0 to 122 v cm^{-1} atm^{-1}) revealed an increase in the mean lifetime of the free positrons with increasing electric field. For a field of 790 v/cm and a pressure of 10.5 atm this lifetime was increased by a factor of 2. A diffusion equation governing the behavior of positrons in the noble gases was derived and solved numerically for different cases of the elastic scattering cross section, the direct annihilation cross section, and the positronium formation cross section. A good fit to the experimental data for argon was obtained using values $20(v_0/v)\pi a_0^2$, $2.25 \times 10^{-4}(v_0/v)^{1.5}\pi a_0^2$, and $5.0 \times 10^{-5}\pi a_0^2$ respectively for these cross sections, where v is the velocity of the positron and v_0 its velocity at thermal energies (25°C). Similar experiments in helium revealed only slight evidence for the presence of a shoulder and only a small dependence of the mean lifetime on the applied electric field. Preliminary investigations in krypton indicates a shoulder width about ½ as great as in argon. The annihilation rate of the free positrons (in the exponential region) was found to be directly proportional to the gas density for all the gases investigated except CO_2. (TCO)

37811 ISOBARIC SPIN DEPENDENCE OF THE NUCLEON-NUCLEON INTERACTION. Green, A. E. S.; Sawada, T.; Sharma, R. D. (Univ. of Florida, Gainesville). 6p. (CONF-660306–11). ORAU. Gmelin, AED-CONF-66-048-7.

From American Physical Society, Conference on Isobaric Spin, Tallahassee.

An attempt to fit the nucleon-nucleon phase shifts with a

relativistic meson-theoretic nuclear force is reported. The generalized Yukawa function is used for each meson field. Direct coupling interactions due to pseudoscalar mesons and a synthesis of a scalar and vector meson were selected for detailed study. Three calculational techniques are pursued; the Born approximation, a Schroedinger equation program, and a program for the direct solution of the two-particle Dirac equation. Results are presented of a set of phase shifts for a simple unbroken relativistic model consisting of a 5ω meson and the π meson. (L.B.S.)

37812 ELECTROMAGNETIC FORM FACTOR OF THE PION. Akerlof, C. W.; Ash, W. W.; Berkelman, K.; Lichtenstein, C. A. (Cornell Univ., Ithaca, N. Y.). 16p. (CONF-660411-4). ORAU. Gmelin, AED-CONF-66-060-16.

From American Physical Society Meeting, Washington, D. C.

Theoretical speculations on the charge radius of the pion are briefly discussed, and methods suggested for measuring the pion form factor are considered. The electroproduction reactor $e + p \rightarrow e + n + \pi^+$ is considered, in particular, the contribution of the pion pole diagram, which involves the pion form factors at the photon-pion vertex. The results of a preliminary experiment are presented, which show the feasibility of measuring the pion form factor by the electroproduction method. (L.B.S.)

37813 APPARENT ρ-PRODUCTION ANOMALY IN $\bar{p}$-d CAPTURE REACTIONS. Chand, Ramesh (Wayne State Univ., Detroit). 9p. (CONF-660411-6). ORAU. Gmelin AED-CONF-66-060-31.

From American Physical Society Meeting, Washington, D. C.

In the phenomenological method, the experimental data obtained by Kalogeropoulos on $\bar{p} + d \rightarrow \rho + \pi + \pi + p$ capture reactions at rest is analyzed. It is found that there is no ρ-production anomaly even if the data are in sharp disagreement with the predictions of SU(12) symmetry for the $\bar{p} + n \rightarrow \rho + \pi + \pi$ capture reactions at rest. (auth)

37814 INTERFERENCE IN THE $K_L \rightarrow \pi^+\pi^-$ SYSTEM. Russ, J. S.; Fitch, V. L.; Roth, R. F.; Vernon, W. (Princeton Univ., N. J.). 5p. (CONF-660411-12). ORAU. Gmelin, AED-CONF-66-060-30.

From American Physical Society Meeting, Washington, D. C.

The completion of an analysis of interference effects between the pion amplitudes from K_L decay and coherent regeneration in beryllium is reported. The results are found to be in good agreement with optical model calculations. Strong construction interference was also exhibited from data taken with a liquid hydrogen target in the kaon beam. (L.B.S.)

37815 THE EFFECTIVE MASS OF THE POSITRON IN METALS. Majumdar, Chanchal K. (Carnegie Inst. of Tech., Pittsburgh). 9p. (CONF-650721-8). ORAU. Gmelin, AED-CONF-65-211-2.

From Positron Annihilation Conference, Detroit.

The problem of finding the effective mass of the positron is reduced to a positron interaction with the Fermi distribution of conduction electrons, and the modern many-body techniques are used to compute this effective mass. It was found that the effective mass in sodium is 1.3 times the bare mass. From a comparison with experimental data it is suggested that strong coupling calculations are necessary in order to obtain reasonable agreement. (J.F.P.)

37816 POSITRONIUM FORMATION AND ANNIHILATION IN ARGON-PROPANE MIXTURE. Leung, C. Y.; Paul, D. A. L. (Univ. of Toronto). 22p. (CONF-650721-7). ORAU. Gmelin, AED-CONF-65-211-3.

From Positron Annihilation Conference, Detroit.

Experiments are described on positron annihilations in liquid and gaseous ethane and argon-propane mixtures. Lifetime measurements were made using a 2-quantum correlation technique of positron formation in argon and propane gases. These experiments were performed in an attempt to explain the low value of I_2 (orthopositronium intensity) in pure liquid argon which is less than one third of that in the pure gas. The data obtained are given, and the time spectrum of positron annihilation is shown. (J.F.P.)

37817 POSITRON LIFETIMES IN LOW-TEMPERATURE HELIUM GAS. Roellig, L. O.; Kelly, T. M. (Wayne State Univ., Detroit). 10p. (CONF-650721-13). ORAU. Gmelin, AED-CONF-65-211-13.

From Positron Annihilation Conference, Detroit.

The results of a series of positron lifetime measurements in helium gas at 4.2°K are presented. A shoulder was observed in the lifetime spectrum, which exhibited an exponential decay, followed by a hump, then another exponential decay. The shape of the annihilation spectrum reported is the basis for a re-examination of the decay process of positrons in helium. It is suggested that the annihilation process which yields the third lifetime in low temperature gaseous helium is the same process which produces the intermediate component in liquid helium. (J.F.P.)

37818 MOMENTUM DISTRIBUTION OF PHOTONS FROM POSITRONS ANNIHILATING IN LITHIUM-AMMONIA SOLUTIONS. Varlashkin, P. G.; Stewart, A. T. (Univ. of North Carolina, Chapel Hill). 7p. (CONF-650721-12). ORAU. Gmelin, AED-CONF-65-211-5.

From Positron Annihilation Conference, Detroit.

The momentum distribution of photons from positrons annihilating in lithium-ammonia solutions of varying concentration is investigated. Although the presence of free electrons in the solutions is established almost beyond question, the angular correlation data fail to reveal a momentum distribution dependent upon Fermi energy. It is suggested that this implies that the positron forms a bound state which is independent of the solution concentration over the reported range. (J.F.P.)

37819 POSITRONIUM FORMATION IN CERTAIN METAL OXIDES. Kusmiss, J. H.; Stewart, A. T. (Univ. of North Carolina, Chapel Hill). 7p. (CONF-650721-6). ORAU. Gmelin, AED-CONF-65-211-7.

From Positron Annihilation Conference, Detroit.

Angular correlation experiments on CaO, MgO, and ZnO in an oxygen atmosphere for gamma pairs from positron annihilation are reported. Also measurements were made on polycrystalline Al_2O_3 in vacuum and in O_2 at atmospheric pressure. The curves obtained for ZnO and MgO are shown, the other results are also described. (J.F.P.)

37820 POSITRON ANNIHILATION IN METALS. Stewart, A. T. (Univ. of North Carolina, Chapel Hill). 41p. (CONF-650721-11). ORAU. Gmelin, AED-CONF-65-211-4.

From Positron Annihilation Conference, Detroit.

A review is given of the behavior of positrons in metal. The history of research on positron annihilation in metals is traced from its beginning to recent developments. The more recent results discussed include those for single crystal and Fermi surface studies, the rare earth metals, metal alloys, liquid metals, and the effects of many-body interactions in metals. (J.F.P.)

37821 CALCULATED CORE ANNIHILATION MOMENTUM DISTRIBUTIONS FOR SEVERAL METALS. Rockmore, D. M.; Stewart, A. T. (Univ. of North Carolina, Chapel Hill). 9p. (CONF-650721-9). ORAU. Gmelin, AED-CONF-65-211-6.

From Positron Annihilation Conference, Detroit.

In order to find the core annihilation momentum distributions, potentials were calculated for Al^{3+}, Be^{2+}, Cu^+, K^+, Mg^{2+}, and Na^+ from Hartree-Fock wavefunctions with exchanges taken from previous work taking conduction electrons into account. The ground state positron wavefunction was then determined using these potentials. The positron and core electron wavefunction product are transformed into the momentum representation to find the radial momentum distribution, and a further integration over the x and y momentum components is performed to obtain the z momentum distribution. A typical comparison for the z momentum distributions with experimental data is shown for magnesium. The scale factors required in comparison

to the positions of the metals in the periodic table are also given. (J.F.P.)

37822 COHERENT PRODUCTION OF MULTIPION RESONANCES. Lubatti, H. J.; Bingham, H. H.; Fretter, W. B.; Michael, W.; Moriyasu, K. (Univ. of California, Berkeley). 10p. (CONF-650927-6). ORAU. Gmelin, AED-CONF-65-222-36.

From American Physical Society Meeting, Honolulu, Hawaii.

A study of coherent production of multipion final states (2 to 5 pions) on complex nuclei by 16 Bev/c negative pions was continued in the Ecole Polytechnique HLBC filled with freon. A large enhancement was observed in the three-pion mass spectrum at approximately 1.08 Bev, along with a shoulder at $M_{3\pi} \simeq 1.32$ Bev and approximately a 3 standard deviation bump near $M_{3\pi} \simeq 1.6$ Mev. The momentum transfer distribution indicates that the 3π production occurs coherently from a nuclear target of $A \sim 19$ (fluorine). (L.B.S.)

Field Theory, Scattering Theory, and Symmetries

See also Elementary Particles and Radiations

37823 (BNL-10387) SOME NON COMPACT GROUPS ASSOCIATED WITH THE VERTEX OPERATOR. Guersey, Feza (Brookhaven National Lab., Upton, N. Y. Yale Univ., New Haven, Conn.). June 1966. Contract AT(30-2)-Gen-16. 27p. (CONF-660540-2). Dep. mn. CFSTI $2.00 cy, $0.50 mn.

From Conference on Non-Compact Groups in Particle Physics, Milwaukee.

The phenomenological symmetries of the baryon-antibaryon-meson vertices and the hypothetical symmetries of quark-antiquark-meson vertices are discussed with remarks on meson-meson-meson vertices. No attempt is made to base such symmetries on field theoretical models or saturation properties of current commutators. (B.G.D.)

37824 (CAR-882-19) APPLICATION OF THE BETHE-SALPETER EQUATION TO THE STATIC BOOTSTRAP MODEL. Lin, Keh-Ying (Carnegie Inst. of Tech., Pittsburgh, Pa.). May 1966. Contract AT(30-1)-882. 164p. Dep. mn. CFSTI $5.00 cy, $1.00 mn.

Thesis.

The bootstrap equations derived from the Bethe-Salpeter equations with ladder approximation are applied to the static models of baryons. An approximation similar to the effective range approximation is made in the static model, and a set of algebraic equations which are convenient for numerical calculation are obtained. Among the models considered, one is the well-known π-N-N* static model, for which a unique self-consistent solution is obtained which fits the experimental data quite well by choosing a suitable cutoff. A similar result is obtained if SU(3) symmetry is assumed, and the so-called F-D mixing angle of the coupling constants turns out to be approximately 38°. A static model is considered which includes π, K, N, N*, Y_1^*, Σ, and Λ in which no self-consistent solution is found. The bootstrap equations in this method are similar to those obtained from the N/D method except that the normalization equations are somewhat different. (auth)

37825 (N-65-31239) QUASI LOCAL ELECTRODYNAMICS. Priou, Maurice (Paris Univ., Orsay (France). Laboratoire de Physique Theorique et Hautes Energies). June 1965. 39p. (TH-101). Dep. mn.

A formalism of gauge invariance theories which allows for a non-zero photon mass and is similar to the non-covariant form of the Felden-Matthews theory is studied. (B.G.D.)

37826 (NP-16231) LECTURES ON HIGH ENERGY SCATTERING. Eden, R. J. (Maryland Univ., College Park. Dept. of Physics and Astronomy). Fall Semester 1965-66. 118p.

A series of lectures is presented on high energy scattering. Topics discussed are experimental survey, theoretical background and assumptions, bounds for total cross sections, bounds for nonforward scattering, crossing symmetry and analyticity in energy, dispersion relations, partial wave amplitudes, and relations for cross sections for different processes. (B.G.D.)

37827 (UCRL-14365) RELATIVISTIC TRANSFORMATIONS VERSUS LORENTZ TRANSFORMATIONS. Schulz, William D. (Lawrence Radiation Lab., Univ. of California, Livermore). Aug. 10, 1965. Contract W-7405-eng-48. 10p. Dep. mn. CFSTI $1.00 cy, $0.50 mn.

Special relativity does not require that fields transform linearly, as is usually assumed. A great deal of mathematical freedom results from allowing the fields to transform in an implicit sense. In particular, it is then easy to construct relativistic quantum mechanical field theories with no high momentum divergencies. (auth)

37828 ON THE INTERPRETATION OF THE FOLDY-WOUTHUYSEN TRANSFORMATION. Breitenlohner, P. (Univ., Graz). Acta Phys. Austr., 22: 217-20(1966).

A Foldy-interaction scheme is presented in which the free hamiltonian is transformed to an energy separating form and the interaction hamiltonian will still contain odd components connecting positive and negative energy states. The Foldy-interaction formalism can be applied to strong interactions instead of electromagnetic interactions, and yields an adequate interpretation of the scattering process. (L.B.S.)

37829 DERIVATION OF AN INTEGRODIFFERENTIAL EQUATION FOR THE 2-PARTICLE DENSE MATRIX. Inthoff, W. (Univ., Mainz). Ann. Phys. (7), 17: 270-7 (1966). (In German).

A necessary equation of condition for the two-particle density matrix is derived in the form of an integro-differential equation according to the method of transformation of coordinates. The relation of the equation to the Hartree-Fock approximation and to one of the two-particle methods of Bopp is investigated. The application of the equation is briefly discussed. (tr-auth)

37830 CURRENTS ALGEBRA AND MODELS OF ELEMENTARY PARTICLES. Okubo, Susumu (Univ. of Rochester, N. Y.). Ann. Phys. (N. Y.), 38: 377-91(July 1966). (UR-875-110).

A new sum rule expressing the β-decay axial vector renormalization constant g_A in terms of circularly polarized photon scattering cross sections by polarized nucleons is derived on basis of an equal-time commutation relation between spatially integrated electric currents. Based upon this sum rule, it is possible in principle to check validities of various models of elementary particles. Also, it is pointed out that models assuming fundamental boson fields may be experimentally ruled out. (auth)

37831 MOELLER OPERATORS FOR SCATTERING ON SINGULAR POTENTIALS. Kupsch, J.; Sandhas, W. (Univ., Bonn). Commun. Math. Phys., 2: 147-54(1966).

The existence of Møller operators is proved for singular potentials which decrease more rapidly at infinity than the Coulomb potential. The question of their uniqueness is discussed. (auth)

37832 GELL-MANN FORMULA FOR REPRESENTATIONS OF SEMISIMPLE GROUPS. Hermann, R. (Argonne National Lab., Ill. Northwestern Univ., Evanston, Ill.). Commun. Math. Phys., 2: 155-64(1966).

A method for constructing representations of noncompact semisimple groups from representations of semidirect product groups is presented. Necessary and sufficient algebraic conditions for the method to work are given, and these are applied to cases of possible interest for the classification of elementary particles. (auth)

37833 PARTICLE SINGULARITIES IN RELATIVISTIC QUANTUM FIELD THEORY. Voelkel, A. H. (Univ., Hamburg). Commun. Math. Phys., 2: 176-214(1966). (In German).

By subtraction of products of three-point functions the

four-point functions in relativistic quantum field theory are decomposed into two parts, in one of which there does not occur any mass-shell-singularity in the variables $k_\alpha + k_\beta$ ($\alpha \neq \beta$; $1 \leq \alpha, \beta \leq 4$). All these singularities are given explicitly by the kernels of the products of the three-point functions. Necessary and sufficient conditions for the non-triviality of unitary S-matrices or some of their elements are proved in terms of statements on the occurrence of mass-shell singularities in the vacuum expectation values of field operators. The strongest result gained is: If $\delta[(\sum_{j=2}^{N-2} k_j)^2 - m^2]\,[(\sum_{j=2}^{N-2} k_j)^2 - m^2] \cdot \langle 0| \prod_{j=1}^{N} \tilde{A}(k_j)|0\rangle$ is equal to zero for some $N > 3$, then all transition amplitudes $T_{2\to n}$ vanish for every n. (auth)

37834 MOMENTUM ENERGY FIELD OF ELEMENTARY PARTICLES. Arzhanykh, I. S. pp 30-64 of Integrirovanie Nekotorykh Diffentsial'nykh Uravnenii Matematicheskoi Fiziki, Sbornik. Tashkent, Nauka, 1964. (In Russian).

Theory for a momentum field in analytical mechanics is applied to force field structure for elementary particles such as photons, electrons, gravitons, and mesons, and also for electric and magnetic dipoles. (J.F.P.)

37835 INHOMOGENEOUS SL(6) GROUP WITH AN EXPANDED TRANSLATION SUBGROUP. Kadyshevskii, V. G.; Todorov, I. T. Izv. Fiz. Inst. Aneb, Bulg. Akad. Nauk, 14: 89-108(1966). (In Russian).

The inhomogeneous SL(6) group denoted ISL(6), considered as a relativistic generalization of SU(6), leads to high-order invariant equations (even for scalar and spin $\frac{1}{2}$ particles), the Dirac-type equation being in addition noninvariant under space reflection. One way to eliminate this difficulty, proposed by W. Rühl, consists in a doubling of the 36-dimensional space of translations of ISL(6). The components of the unitary momentum P are defined as third order minors of the matrix of generator of translations in ISL(6). Thus, a larger symmetry group, $\mathcal{P}_{U_\infty}$ is obtained which contains $SL(6)/Z_3$ as a homogeneous part and an invariant subgroup of 400-dimensional translations, transforming under the representation D(20,20) of SL(6). With this definition a second order Casimir operator, depending only on the unitary momentum P, and correspondingly a second order (Klein-Gordon-type) equation for scalar particles, and a system of linear parity conserving Dirac-type equations for the pair of 20-component spinors $D(20,1) + D(1,\overline{20})$ are obtained. These last equations describe particles of spin $\frac{1}{2}$ and $\frac{3}{2}$ with integral charge. A complete set of polynomial invariants (Casimir operators) of the Lie algebra of $\mathcal{P}_U$ is found, and the possibility of obtaining a mass formula in broken $\mathcal{P}_U$ symmetry is discussed. (auth)

37836 COMPLETENESS AND DISPERSION RELATIONS IN THE COMPLEX ANGULAR MOMENTUM PLANE. Lopez, C. A.; Saavedra, I. (IAEA, Trieste). Nucl. Phys., 87: 65-72(1966).

The set of Jost solutions $\{f(\lambda, -k, r)\}$ of the Schroedinger equation in the complex angular momentum plane is considered here as the set of eigenfunctions of a non-Hermitian operator. The completeness of the set $\{f(\lambda, -k, r)/r\}$ is established, and the orthogonality and completeness relations are explicitly given. It is further shown that, in contrast to the corresponding situation in the k-plane, the completeness relation does not imply here a dispersion relation for the scattering matrix. (auth)

37837 ELECTROMAGNETIC FORM FACTORS FROM THE LOCALITY OF CURRENT DENSITIES. Oehme, R. (International Center for Theoretical Physics, Trieste, Italy). Phys. Lett., 22: 206-8(Aug. 1, 1966).

It is shown that the successful results of collinear groups for electromagnetic form factors can be obtained on the basis of the locality of current density commutators and SU(3) invariance, provided only matrix elements of the commutators with $\Delta J_z = 0$ are considered in the saturation. The necessity of leakage in $\Delta J_z \neq 0$ matrix elements is discussed briefly. (auth)

37838 VARIATIONAL GROUND-STATE ENERGY OF A BOSE SYSTEM. II. Sawada, K. (Univ. of California, San Diego, La Jolla). Phys. Rev., 148: 160-2(Aug. 5, 1966).

The variational calculation using a pair-correlation-type trial function is examined for a Bose system interacting through two-body interactions which are sufficiently attractive to give a negative zero-energy scattering length for the two-body scattering. A simple proof is given that in this case the energy-density curve always has a minimum at a certain density with negative energy, and an upper bound on the variation energy is derived. (auth)

37839 CURRENT COMMUTATION RELATIONS, UNIVERSALITY, AND NONLEPTONIC BARYON DECAYS. Biswas, S. N.; Kumar, Aditya; Saxena, R. P. (Univ. of Delhi). Phys. Rev. Lett., 17: 268-71(Aug. 1, 1966).

An extension of Cabibbo's successful phenomenological form of universal weak interaction for leptonic decays to nonleptonic s- and p-wave decays of baryons is presented assuming the validity of the results obtained by Sugawara and Suzuki and Hara, Nambu, and Schechter for the parity-nonconserving and parity-conserving amplitudes, respectively. (B.G.D.)

37840 ELECTRIC-CHARGE FORM FACTOR ACCORDING TO SL(6,C). Cocho, G.; Fronsdal, C.; Ar-Rashid, Harun; White, R. (IAEA, Trieste). Phys. Rev. Lett., 17: 275-9(Aug. 1, 1966).

An evaluation of the electric charge form factor according to SL(6,C) is presented in order to evaluate weak and electromagnetic vertices. (B.G.D.)

37841 PERTURBATION THEORY OF MULTIPHOTON PROCESSES. Wallace, R. (Bristol Univ., Eng.). Phys. Rev. Lett., 17: 397-8(Aug. 15, 1966).

It is pointed out that a simpler formulation of the theory of multiphoton processes can be derived by employing an interaction potential due to Richards and developed by Power and Zienau rather than the perturbation potential given by the nonrelativistic limit of the Dirac equation. The simplifications are shown by resolving the perturbation into component perturbations corresponding to the various Fourier components of the electromagnetic field. The amplitude for two-photon scattering is considered for illustration. (L.B.S.)

37842 MESON-BARYON COUPLING CONSTANTS IN BROKEN SU(3) AND THE ALGEBRA OF CURRENTS. Bose, S. K.; Hara, Y. (International Centre for Theoretical Physics, Trieste, Italy). Phys. Rev. Lett., 17: 409-12(Aug. 15, 1966).

Using the algebra of currents, the renormalization effects on the meson-baryon coupling constants, due to SU(3) breaking are studied. (auth)

37843 ELECTROMAGNETISM OF HADRONS AND HIGHER SYMMETRIES. Rolnick, William B. (Case Inst. of Tech., Cleveland). Phys. Rev. Lett., 17: 416-19 (Aug. 15, 1966).

Any physically meaningful attempt to find a simple Lie group of rank three, containing among its generators a part of the charge which commutes with C_π and containing SU(3) as a subgroup, is shown to imply the existence of fractionally charged particles. Conjugation with C_π is not an automorphism of such a group and its extension by the group made up of C_π and $C_\pi^2 = E$ is shown to be impossible. The combination of the simple rank-three Lie group with C_π does not lead to a finite-dimensional semisimple Lie group in the neighborhood of the identity. (auth)

37844 RELATIVISTIC QUANTUM FIELD THEORY. Schwinger, Julian (Harvard Univ., Cambridge, Mass.). Phys. Today, 19: No. 6, 27-34(June 1966).

The foundations of quantum field theory, which unites Bohr's complementarity principle and Einstein's relativity are reviewed. Mathematical and physical consequences of the union are discussed. (auth)

37845 FIELD THEORY OF ELEMENTARY PARTICLES. Bialynicki-Birula, Iwo (Univ. of Warsaw). Postepy Fiz., 17: 109-14(1966). (In Polish).

An informal discussion is given on the relation between the quantum field theory and the theory of elementary particles. It is pointed out that the particle aspect of the field theory may be appropriate for treating low energy phenomena but there probably exists a field aspect, not fully understood now, which should be used in dealing with high energy phenomena. (auth)

37846 SYSTEMATICS AND PHENOMENOLOGY OF BOSON MASS LEVELS. III. Iizuka, Jugoro; Okada, Kunihiko; Shito, Okiyasu (Kanazawa Univ., Japan). Progr. Theoret. Phys. (Kyoto), 35: 1061-73(June 1966).

The hidden properties of ur-baryon dynamics deduced from the previous analyses I and II meson mass levels and from other work are investigated. The previous results are discussed from the viewpoint of neutral vector theory with a pair suppression hypothesis. These will be re-expressed in terms of the $U_p(3) \otimes U_{\bar{p}}(3)$ symmetry, although it adds no essentially new result. These considerations are extended to the mutual interactions of meson nonets with the $(\bar{t}\,t)$ structure, and a dynamical interpretation of the A selection rule is presented. It will be conjectured that the dominant part of the effective trilinear vertices is of the $Tr(\phi_a\phi_b\phi_c)$ type and not of the $Tr(\phi_a)Tr(\phi_b\phi_c)$ or $Tr(\phi_a)Tr(\phi_b)Tr(\phi_c)$ type, where ϕ_i(i = a, b, c) denotes a relevant meson nonet. The decay properties of the L = 1 meson systems are also studied, taking $Tr(\phi_a\phi_b\phi_c)$ type vertices and a common 1−8 mixing angle for the L = 1 mesons determined from the linear mass difference equations discussed in II. The calculated results as well as comparisons of them with available data are discussed in detail. (auth)

37847 COMPOSITENESS CONDITIONS AND THE INDEFINITE NATURE OF THE SELF-MASS. Yabuki, Haruichi (Tokyo Univ.). Progr. Theoret. Phys. (Kyoto), 35: 1088-98(June 1966).

Compositeness conditions are investigated in the Green's function approach with particular attention to the self-mass. It is shown that there exist two cases in which the conditions $Z_3 = 0$ and $Z_3 \cdot \delta\mu^2 = 0$ hold. One of them defines the compositeness of a particle, and the other gives the limiting process of Gerstein and Deshpande. The latter process does not lead to the composite solution, but to the intermediate one. The self-mass is found to be indefinite when $Z_3 = 0$. (auth)

37848 PARTICLE MIXING AND THE Z = 0 CONDITION. Muta, Taizo (Kyoto Univ.). Progr. Theoret. Phys. (Kyoto), 35: 1099-1110(June 1966).

The compositeness conditions of particles in quantum field theory are investigated in the case where two particles with identical quantum numbers can appear in the intermediate states of a certain scattering process as a consequence of the particle-mixing interaction. It is shown that, if the generalized propagator renormalization constants are used to state the compositeness condition, the situation first suggested by Srivastava and Choudhury is encountered, but, if the generalized wave-function renormalization constants are used it can be verified that the compositeness criteria still hold good in the presence of particle mixing. (auth)

37849 INTENSELY LOCALIZED SOLUTIONS OF THE CLASSICAL DIRAC-MAXWELL FIELD EQUATIONS. Wakano, Masami (Kyoto Univ.). Progr. Theoret. Phys. (Kyoto), 35: 1117-41(June 1966).

Intensely localized and divergence-free solutions of the classical Dirac-Maxwell field equations are obtained numerically under the assumption that the electrostatic potential is dominant. For the assumption that the electromagnetic vector potential is dominant, such solutions do not exist. The masses of the localized states are negative. However, the possibility of getting a positive mass is shown by taking into account the vacuum polarization energy. Introducing this vacuum polarization effect and the electromagnetic self-energy into the classical Dirac equation the differential cross section for Compton scattering is obtained. The energies of the electron without the vacuum polarization effect take slightly different values for different forms of the spinor field in contrast to the well-known degeneracy in the hydrogen atom. (auth)

37850 REMARKS ON THE TRION MODEL WITH AN ADDITIONAL FORCE FIELD. Namiki, Mikio (Waseda Univ., Tokyo). Progr. Theoret. Phys. (Kyoto), 35: 1156-8(June 1966).

The trion model with an additional force field is developed through discussion of a new charge to be introduced by the Nakano-Nishijima-Gell-Man rule, the linear extension of the force field consistent with the nucleon electric form factor, and inner quantum transitions as a possible origin of apparent fractional charges. (L.B.S.)

37851 SOME ASPECTS OF THE DIRECT INTERACTION. Okabayashi, Takao; Yamada, Masao (Tokyo Univ.). Progr. Theoret. Phys. (Kyoto), 35: 1158-60 (June 1966).

A model of the direct interaction of a spinless particle without the crossed channel is considered, and a new point of view on the high energy limit in connection with the vertex functions and bare coupling constants is proposed. (L.B.S.)

37852 APPROXIMATION METHOD FOR POTENTIAL SCATTERING. Shimauchi, Masaaki (Saga Univ., Japan). Progr. Theoret. Phys. (Kyoto), 35: 1160-2(June 1966).

Phase shifts are calculated by means of an approximation method which introduces square well potentials equivalent to a given central potential. It is shown that an approximate formula is obtained in a simple form with good accuracy by applying the method to scattering by a Gaussian potential. The method gives phase shifts for harmonic well, exponential, and Yukawa potentials in an analytical form. (L.B.S.)

37853 ON RARITA-SCHWINGER QUANTUM FIELDS. Raszillier, I. (Inst. of Physics, Bucharest). Rev. Roum. Phys., 11: 443-4(1966).

A simple group theoretical construction is given for the Rarita-Schwinger fields, starting from the one-particle states of the representations of the inhomogeneous Lorentz group. (L.B.S.)

37854 STRUCTURE OF THE S MATRIX FOR THE QUANTUM PROBLEMS SOLVABLE BY THE CONTOUR INTEGRAL METHOD. Demkov, Yu. N. Vestn. Leningr. Univ., Ser. Fiz. Khim. (4), No. 1, 7-10(1966). (In Russian).

If the hamiltonian H consists of time-independent H_0 and of perturbation V, which linearly depends on time and moreover is a projection operator on the state φ, then the nonstationary and corresponding stationary problems can be solved exactly. In this case the S-matrix is triangular and factorable into binary Landau — Zener factors. This solution can be applied to the heavy particle collision problems when the quasi-crossing of a system of parallel potential curves with a single one takes place. (auth)

37855 BROKEN $\tilde{U}(12)$ SYMMETRY AND THE UNITARITY CONDITION FOR THE S MATRIX. Bokov, O. G.; Nguyen Van Hieu; Rerikh, K. V.; Khelashvili, A. A. (Joint Inst. for Nuclear Research, Dubna. USSR). Yadern. Fiz., 3: 1111-18(June 1966). (In Russian).

The consistency of the broken $\tilde{U}(12)$ symmetry with the unitarity condition for the S-matrix is considered. It is shown that if the matrix element of the operator T, obtained in the broken $\tilde{U}(12)$ symmetry, is substituted into the righthand side of the relation $(T - T^+)/i = TT^+$, then new amplitudes, forbidden in the broken $\tilde{U}(12)$ symmetry theory, appear as a result of the summation and integration over intermediate states, even if all so-called irregular amplitudes, containing momenta explicitly, are taken into account. (auth)

37856 CASIMIR OPERATORS FOR THE ORTHOGONAL AND SYMPLECTIC GROUPS. Perelomov, A. M.; Popov, V. S. (Inst. of Theoretical and Experimental Physics,

Moscow). Yadern. Fiz., 3: 1127-34(June 1966). (In Russian).

Explicit expressions are obtained for the eigenvalues of the invariant operators of arbitrary order (the Casimir operators) for the orthogonal and symplectic groups. (auth)

37857 MAGNETIC MOMENTS OF PARTICLES IN THE QUARK MODEL. Levin, E. M.; Frankfurt, L. L. (Ioffe Inst. of Physics and Tech., Leningrad). Yadern. Fiz., 3: 1135-7(June 1966). (In Russian).

The consequences of the breaking of the SU(3)-symmetry on the magnetic moments of particles in a quark model are considered. (auth)

37858 UNITARY REPRESENTATIONS OF THE GROUP P(SU(r)) UNITING THE POINCARE GROUP WITH THE GROUP OF INTRINSIC SYMMETRIES. Novozhilov, Yu. V.; Terent'ev, I. A. (Leningrad State Univ.). Yadern. Fiz., 3: 1138-48(June 1966). (In Russian).

Methods developed by Wigner for the Poincaré group are used to construct the generators of transformations, belonging to unitary representations of the group P(SU(r)) for nonzero masses. The Wigner operator, transforming a standard r^2 component momentum into an arbitrary one, is constructed in detail. (auth)

37859 ELECTROMAGNETIC PROPERTIES OF NEUTRAL PARTICLES WITH NON-CONSERVATION OF CHARGE PARITY. Berestetskii, V. B. (Inst. of Theoretical and Experimental Physics, Moscow). Yadern. Fiz., 3: 1169(June 1966). (In Russian).

A particle-antiparticle pair annihilation is considered for a momentum system with spin-parity 1^-. In reference to particles and antiparticles, this state can be divided into symmetric and anti-symmetric, respectively. If the particles are bosons, in the symmetric case they are called C-parity conserving, and in the anti-symmetric case, C-parity violating. In the case of fermions, the opposite is true; the first are called C-parity violating, the second C-parity conserving. For neutral particles, the C-parity violating state is forbidden by the similarity principle. The law of conservation of C-parity in electrodynamics forbids the single-photon annihilation of CP-conserving states. By the same token, it forbids the single-photon annihilation of neutral particles. If this law is broken, the forbiddenness disappears. In the case of charged particles this occurs when the particle spin $s \geq 1$, and a new type of electromagnetic form factors is required. Simultaneously this shows the possibility of single-photon annihilation of neutral particles with spin $s \geq 1$. The effective cross section of single-photon annihilation of these neutral particles is given. (G.O.Y.)

37860 HYBRID GROUP SYMMETRY AND ITS FOUNDATION. Stech, Berthold (Middle East Technical Univ., Ankara. Univ., Heidelberg). Z. Phys., 195: 63-73(1966).

It is found that the so-called static SU(6) symmetry together with Lorentz invariance leads in a natural way to the restricting symmetry group for collinear processes. Even for high-momentum transfer processes the predictions of this "hybrid group" should be as good as for the low momentum case. Further insight in the nature of the symmetry is obtained from a systematic study of the transformation properties of the single particle states in the limit of complete mass degeneracy. (auth)

37861 CLUSTER STRUCTURE OF THE S MATRIX. Crichton, James Hamilton. Berkeley, Calif., Univ. of California, 1965. 131p.

Thesis.

Conditions imposed on the S matrix by the requirement that interactions between elementary particles be of short range were investigated. In particular, two distinct properties of elementary-particle interactions called cluster properties are considered: (1) that interactions between particles proceed independently of the presence of other particles far away in space and time; (2) that multiparticle scattering processes occur predominantly by means of a free-propagating particle connecting, in a causal way, successive scattering processes that involve fewer particles. These properties are formulated as limiting equations involving plane-wave S-matrix elements. These equations imply a structure in the S matrix called the cluster structure. The independence of the cluster properties from the usually-postulated properties of the S matrix, Lorentz invariance, and unitarity is demonstrated. It is shown that the S operators obtained from the Feyman perturbation theory and from the LSZ formalism satisfy both cluster properties. It is claimed that any realistic theory of elementary-particle interactions must satisfy these properties. (Dissertation Abstr.)

37862 ABSORPTIVE MODIFICATION OF SINGLE PARTICLE EXCHANGE MODELS AT HIGH ENERGIES. Chiu, Yam-Tsi. New Haven, Yale Univ., 1965. 140p.

Thesis.

The effect of competition from open channels in high-energy scattering has been shown to significantly modify the predictions of the single-particle exchange model for high-energy peripheral reactions. In this work, the proper multichannel potential scattering problem is discussed in detail in the WKB approximation and is considered in the light of the absorptive effects generated by other open competing channels on the Born amplitude of the reaction in question. The modified amplitudes for the single-particle exchange model so obtained are then shown to satisfy the requirement of unitarity to first order in the Born term of the reaction. A self-consistent scheme for unitarization of amplitudes for the single-particle exchange model is considered using the multichannel K-matrix formalism. The parameterization of the amplitudes including spin and the construction of modified single-particle exchange reaction matrices are considered in detail. In particular, reaction matrices for scalar meson, pseudoscalar meson, vector meson, hyperon, and isobar productions in meson-baryon and baryon-baryon scattering were constructed for the modified single-particle exchange model. Construction of Regge amplitudes in the presence of spin and the partial wave analysis of Regge amplitudes in the direct channel were studied. Arguments for the inclusion of absorptive effects in the Regge pole exchange model are presented; and the amplitudes for the n-p charge exchange reaction proceeding via a Regge pole ρ-meson exchange are obtained. Comparisons with experiment for several representative reactions are considered in order to delineate the areas of success and failure of the modified single-particle exchange model. (Dissertation Abstr.)

37863 COMPOSITE PARTICLES IN A SEPARABLE POTENTIAL MODEL. Urrechaga-Altuna, Jesus. Baton Rouge, La., Louisiana State Univ., 1965. 83p.

Thesis.

Composite particles (bound states) are investigated in three separable potential models: (1) the model with one kind of static heavy neutral scalar boson interacting with one kind of light neutral scalar boson, (2) the model with one kind of static heavy boson and two (or any number) kinds of light bosons, (3) the model with two (or any number) kinds of static heavy bosons and one kind of light boson. These models are solved exactly, the last one only in the case of equal interaction form factors. The S-matrix elements are calculated both directly and dispersion-theoretically. The allowed physical processes are found to be elastic scatterings only; the composite particles can neither be created, destroyed, nor altered in any way within the framework of the models studied. The S-matrix elements are shown to be independent of whether the scattering target is a number of heavy bosons or any composite particle formed by the same number (and kinds) of heavy bosons. The composite particle states are identified as those eigenstates of the Hamiltonian for which the total number of heavy bosons is nonzero, the number of free heavy bosons is zero, and the total number of light bosons is greater than the number of free light bosons. The energy of such states is less than the rest energy of its components, i.e., the states are bound states. (Dissertation Abstr.)

37864 DYNAMICS OF ZERO-SPIN COLLISIONS. Lui, Yau-Yin. Nashville, Vanderbilt Univ., 1965. 97p.

Thesis.

The theory of one event, a collision of two particles without spin from which collision two particles without spin emerge, is considered. The collision problem is approached in terms of Poisson brackets of initial state with final-state dynamical variables. These brackets are worked out explicitly, being completely determined by the conservation laws except for two unknown translation-invariant scalar functions, G and y. The corresponding quantum-mechanical problem is formulated and partly solved. The functions G and y would, if known, give the effect on the final state of the only non-Lorentz transformation of the initial state encountered, namely, the changing of the impact parameter. A procedure is suggested, but not completed, whereby one may hope to learn the effects of this transformation. The procedure involves a search for one or more translation-invariant scalar functions known to vanish when the impact parameter is infinite and invariant under the transformation that changes the impact parameter. As a test of the classical methods and results of the work, the energy derivative of the scattering angle is compared with the angular-momentum derivative of the time delay. These two derivatives can be shown to be equal in a nonrelativistic process with a potential; it is shown that their equality depends only on Lorentz covariance, at least for the nonquantum zero-spin case. An attempt was made to find a unique point with commuting components that can serve to mark the space-time position of the event, somewhat as the center of mass marks the position of a system. It is found that there is an infinite number of such points, and there is no evident criterion whereby one of the points can be singled out for special status. (Dissertation Abstr.)

Fluid Physics and Thermodynamics

See also Plasma Physics and Thermonuclear Processes

Refer also to abstracts 36828, 36991, 37937, 38403, and 38404.

37865 (PPL-AF-2) PROPAGATION OF CORRELATIONS IN A BOLTZMANN GAS. Frieman, Edward A.; Goldman, Robert (Princeton Univ., N. J. Plasma Physics Lab.). May 1966. Contract AF49(638)-1555. 64p.

New results are obtained on the propagation of correlations in a Boltzmann gas on the scale of the mean free path and the collisional time scale which appears to support a conjecture of M. Green's on this subject. (auth)

37866 TRANSPORT PROPERTIES OF AN ELECTRON GAS IN A MAGNETIC FIELD. I. THE NONOSCILLATORY TRANSPORT COEFFICIENTS. Dworin, Lowell (Columbia Univ., New York). Ann. Phys. (N. Y.), 38: 431-509(July 1966).

The transport equations for an independent electron gas interacting with fixed, but randomly located, scattering centers in the presence of a constant homogeneous external magnetic field were derived using the Luttinger-Ward propagator formalism. The magnetic field strength H is assumed to be either sufficiently weak that an expansion in the ratio of the magnetic energy $\omega = |e| H/m$ ($\hbar = C = 1$) to the chemical potential μ is valid, or sufficiently strong that an expansion in the ratio of n_i, the density of scattering centers, to ω may be used. In the first case the transport equations satisfied by the first and second order, in both n_i and ω/μ, terms of a gauge invariant function $f_k^{(7)}$ were obtained from which the nonoscillatory part of the transport coefficients may be obtained. To the order studied, the usual Wiedemann-Franz relation is obtained. In the strong magnetic field case the results differ in principle from much of the published literature. (auth)

37867 INTERACTION BETWEEN MAGNETIC FIELDS AND CONDUCTING FLUIDS: MAGNETOHYDRODYNAMICS. Urrutia, Jose Luis. Ing. Aeronaut. Astronaut., 17: 9-17(Sept.-Oct. 1965). (In Spanish).

A general discussion is presented of the electromagnetic properties of gases which are nonconducting at low temperatures, but which rapidly become conducting at higher temperatures. MHD equations are developed which take electrical and thermal conductivity, viscosity, permeability, and dielectric constant into account. MHD accelerators and generators are considered. (Int. Aero. Abstr.)

37868 EXPERIMENTAL STUDY OF THE STRUCTURE OF ELECTRICALLY CONDUCTING TURBULENT LIQUID FLOW. Kolovandin, B. A. Inzh.-Fiz. Zh., 10: 567-72 (May 1966). (In Russian).

The results are presented of the study of particular properties of the structure of the turbulent electrically conducting liquid flow in an open channel carried out with the aid of the inductive anemometer. The flow is affected by external magnetic and electric fields. The essential effect of the Lorentz force normal to the channel bottom on the distribution of the average velocity and specific mean fluctuation velocities is revealed. The comparison is made of the properties obtained with experimental data for an ordinary liquid. (auth)

37869 BOUNDARY LAYER IN CROSSED-FIELDS MHD. Sears, W. R. (Cornell Univ., Ithaca, N. Y.). J. Fluid Mech., 25: 229-40(June 1966).

This boundary layer study of steady, incompressible, plane, crossed-fields MHD flow at large Reynolds number Re and magnetic Reynolds number Rm begins with a review of Hartmann's case, where a boundary layer occurs whose thickness is proportional to $(ReRm)^{-\frac{1}{2}}$. Following this clue, it is shown that in general the boundary layer is a "local Hartmann boundary layer". Its profiles are always exponential and it is determined completely by local quantities. The skin friction and the total electric current in the layer are proportional to the square root of the magnetic Prandtl number, i.e., to $(Rm/Re)^{\frac{1}{2}}$. Thus the exterior flow problem, the solution of which precedes a boundary-layer solution, generally involves a current sheet at the fluid–solid interface. This inviscid-flow problem becomes tractable if $(Rm/Re)^{\frac{1}{2}}$ is small enough to permit a linearized solution. The flow field about a flat plate at zero incidence is calculated in this approximation. It is pointed out that the thin-cylinder solutions of Sears and Resler (1959), which pertain to Rm/Re = 0, can immediately be extended to small, non-zero values of this parameter by linear combination with this flat-plate solution. (auth)

37870 ALIGNED-FIELD HYDROMAGNETIC FLOW PAST A SLENDER BODY. Leibovich, S. (Univ. Coll., London); Ludford, G. S. S. J. Fluid Mech., 25: 289-98 (June 1966).

Previous work on the Sears–Resler–Stewartson controversy is continued, in the context of axially symmetric flow. A new approach is presented using boundary-layer arguments, which remove much of the old complexity. For resistive bodies of shape R(x) a similarity is uncovered with plane airfoils of shape $F(x) = R^2(x)$. As before, Stewartson's slug flows develop fore and aft. For bodies of very high conductivity the Sears–Resler (steady-state) solution turns out to be one possibility. It pertains to bodies (of much higher conductivity than the liquid) into which the initial magnetic field has not diffused. (auth)

37871 FLOW OF AN ELASTICO-VISCOUS LIQUID BETWEEN TWO ELECTRICALLY NON-CONDUCTING INFINITE FLAT PLATES UNDER A UNIFORM TRANSVERSE MAGNETIC FIELD. Gulati, S. P. J. Phys. Soc. Jap., 21: 1411-20(July 1966).

Flow of a visco-elastic fluid near an oscillating plate and between two plates oscillating with a phase difference, with the same frequency and different amplitudes, under a transverse magnetic field fixed relative to the fluid and fixed relative to one of the plates was considered employing a well known simple complex variable technique. Expressions for velocity profile, the induced magnetic field, and the shear stresses on the plates in all the situations were calculated exactly, as well as approximately, in the two limiting cases of small and large values of the Reynolds

number. In the case of two oscillating plates, the skin friction on the two plates tended to the same value in the limiting case when the Reynolds number tended to zero. The shearing stress on the lower plate, in the limiting case when the Reynolds number tended to infinity, behaved as if the other plate were absent. These results held whether the magnetic lines of force were fixed relative to the fluid or to one of the plates. (auth)

37872 MAGNETOHYDRODYNAMIC SHOCK POLAR. Urashima, Shin-o; Morioka, Shigeki (Osaka Univ.). J. Phys. Soc. Jap., 21: 1431-9(July 1966).

The steady shock discontinuity in the flow of a perfectly conducting gas with aligned magnetic field is considered by taking, as the parameters, the Mach number, the Alfvén number ahead of the shock, and the shock angle. The jumps across the shock, which satisfy the various conservation laws as well as the entropy and evolutionary conditions, are calculated by making use of an electronic computer. The possible types of MHD shock polar are shown in the speed-deflection plane for various combination of parameters. (auth)

37873 THEORY OF LIQUID HELIUM THREE. Goldstein, Louis (Los Alamos Scientific Lab., N. Mex.). Phys. Rev., 148: 108-24(Aug. 5, 1966). (LA-DC-7750).

A detailed study of two types of heat-capacity anomalies present in liquid ^{3}He is made. One of these is the plateau formation at intermediate pressures, $p \lesssim 10$ atm. The other anomaly consists in the appearance of a flat constant-pressure heat-capacity maximum, followed by a shallow minimum, between the temperatures of 0.15 and 0.30°K, and the pressures of 10 and 30 atm, approximately. At somewhat higher pressures, over a small pressure range, only the heat-capacity maximum becomes observable. These heat-capacity anomalies originate with the competition of the thermal excitations of the spin and nonspin degrees of freedom, within the theoretical approach advanced here. The observation of the predicted low-amplitude heat-capacity extrema in compressed liquid ^{3}He may require heat-capacity measurements of increased accuracy, preferably at higher pressures. The problem of the heat-capacity behavior at low and very low temperatures was also explored under a restrictive hypothesis. It will be assumed that the nature of the thermal excitations which appear in incontrovertible and independent heat-capacity data, available only at saturation and at temperatures above 0.2°K, persists on the spin and nonspin degrees of freedom down to the absolute zero. With the recently established universal character of the nuclear-paramagnetic-susceptibility ratio law of liquid ^{3}He, down to 0.05°K, the stated assumption leads one to predict that the ratio of the total heat capacity to the temperature approaches parabolically in temperature its finite limit at the absolute zero. In the present theory, deviations from this behavior require a new paramagnetic-susceptibility law at the lowest temperatures. (auth)

37874 STABILITY OF CONDUCTING FREE SURFACE FLUID IN THE PRESENCE OF MAGNETIC AND ELECTRIC FIELDS. Kolovandin, B. A. Prikl. Mekh., 1: No. 11, 95-105(1965). (In Russian).

A plane MHD fluid flow at arbitrary angles, in the presence of electric and magnetic fields, was investigated. A method of successive approximations was used for resolving stability equations for large and small wave numbers. (tr-auth)

37875 MAGNETOHYDRODYNAMIC DISTURBANCES DUE TO THE SUDDEN INTRODUCTION OF AN OSCILLATING DIPOLE IN A FLUID OF FINITE CONDUCTIVITY. El Mohandis, M. G. S. (Ain Shams Univ., Cairo). Proc. Math. Phys. Soc. (U.A.R.), No. 26, 113-24(June 1962).

Mathematical solutions for magnetohydrodynamic perturbations are given for the case of an oscillating dipole placed parallel to the exciting field in an inviscid, incompressible fluid of finite electrical conductivity. (auth)

37876 COUETTE-TYPE FLOW OF AN ELASTICO-VISCOUS FLUID THROUGH POROUS WALLS IN THE PRESENCE OF A TRANSVERSE MAGNETIC FIELD. Mishra, Shankar Prasad. (Univ. Coll. of Engineering, Orissa, India). Proc. Nat. Inst. Sci. India, Pt. A, 31: 327-34(July 1965).

The pressure-induced flow of an elastico-viscous electrically conducting incompressible fluid between two relatively moving plane porous walls in the presence of a transverse magnetic field is discussed. The magnetic field helps in delaying separation. The elastic elements in a viscous liquid quicken the tendency to separation. The tendency to separation is delayed with the increase of suction velocity at the plate whereas it is quickened with the increase of injection velocity. (auth)

37877 VARIATIONAL PRINCIPLES IN MAGNETOHYDRODYNAMICS. Ray, M. (Agra Coll., India); Gupta, S. C. Proc. Nat. Inst. Sci. India, Pt. A, 31: 403-12(July 1965).

Three variational principles for the hydromagnetic flow equations are given. Two of them are restricted principles and one of a general character. The restricted principles cannot be derived as special cases of the general principle. (auth)

37878 MAGNETOHYDRODYNAMIC JET-VORTEX IN A VISCOUS CONDUCTING FLUID. Pao, H. P.; Long, R. R. (Johns Hopkins Univ., Baltimore). Quart J. Mech. Appl. Math., 19: 1-26(Feb. 1966).

A three-dimensional magnetohydrodynamic flow, with jet and vortex nature in a viscous, incompressible, conducting fluid is considered. A general theory is developed that leads to a reduction of the steady-state equations of motion and the equations of magnetic induction to five ordinary, nonlinear differential equations. The asymptotic behavior is analyzed and some particular cases are considered. The problem can be simplified considerably by making two kinds of boundary layer approximations. When the jet motion is so strong that $J/K^2 \gg 1$ and $J/v^2 \gg 1$ the boundary layer approximation of the first kind is in order. The simplified equations are integrated and the analytical solution is obtained, when the conductivity becomes infinite or infinitesimal. When the vortex motion is so strong that $K^2/v^2 \gg 1$, the boundary layer approximation of the second kind is in order. The simplified equations are integrated numerically for a considerable range of the governing parameters. (auth)

37879 MOTION OF AN ELECTRICALLY CONDUCTING LIQUID LOCATED WITHIN TWO COAXIAL CYLINDERS UNDER THE INFLUENCE OF A TRANSVERSE MAGNETIC FIELD. Marcov, N. (Univ. of Bucharest). Studii Cercet. Mat., 18: 161-79(1966). (In Rumanian).

The motion of a viscous, homogeneous, incompressible, electrically conducting liquid, placed inside the two infinite coaxial cylinders is investigated under the action of a transverse magnetic field. It is assumed that the cylinders rotate with angular velocities of ω_1 and ω_2 and that the motion takes place within a plane. The current function of the velocity field and the force function of the magnetic field satisfy a nonlinear differential equation system. The solution is arrived at on the basis of increasing magnetic Reynolds number values, reducing the system to one with quasilinear parabolic characteristics. In the case of permanent motion, this may be simplified to a system of differential equations for which solutions may be found. As a special application of the solution arrived at, as a first approximation, the expressions obtained by P. Smith for the rotation of a conducting liquid in a uniform, transverse magnetic field in the case of a single cylinder are verified. (TTT)

37880 TEMPERATURE AND CONCENTRATION OF CHARGED PARTICLES BEHIND THE FRONT OF A STRONG SHOCK WAVE IN AIR. Petrukhin, A. I.; Proskuryakov, V. A. (Inst. of Geophysics, Academy of Sciences, USSR). Zh. Eksp. Teor. Fiz., 50: 1481-90(June 1966). (In Russian).

The electron temperatures and concentrations of charged particles behind the front of a strong shock wave in air are measured. The shock wave was produced by an electric discharge in a tube at initial pressures of 0.1, 0.2, and 0.5

mm Hg. The temperatures were measured on basis of the relative and absolute spectral line intensities; the charge particle concentrations were measured on basis of Stark broadening of the H_β line. The measured temperature and concentration values are in good agreement with the equilibrium values of the quantities calculated from the shock wave velocity. The maximal values of the electron temperatures are $(60-70) \times 10^3$ °K for charged particle concentrations of the order of $(6-7) \times 10^{16}$ cm^{-3} and of threshold wave front velocities of the order of 45–50 km/sec. The oscillator strengths were measured for two nitrogen lines. For the N II line with a wavelength $\lambda = 4026.09$ Å the measured value is gf = 0.90 and for the N III line with a wavelength $\lambda = 4510.92$ Å the measured value gf = 1.36 with an accuracy to 10–15%. (auth)

37881 EFFECT OF LINE RADIATION ON PRECURSOR IONIZATION. Murty, S. S. R. (Univ. of Florida, Gainesville). 56p. (CONF-660217-5). ORAU. Gmelin, AED-CONF-66-013-9.

From Symposium on Interdisciplinary Aspects of Radiative Energy Transfer, Philadelphia.

Singly ionized monatomic gas with three levels, namely, ground state, excited state, and ionization is considered. The hydrogenic approximation is used to calculate the required cross sections. The conservation equations for the individual species of the partially ionized gas are formulated considering the elastic and inelastic collisions between the species. The electrons are allowed to have a temperature different from that of the heavy particles. These equations are valid for all optical thicknesses. The effect of line radiation on precursor ionization is considered. The equations governing the population of excited atoms by diffusion of resonance radiation usually lead to an integral equation. A simple method of iteration is developed here where the first approximation gives essentially the same results as the more sophisticated methods. Using the present method, the number density of excited atoms is calculated. Now ionization proceeds from ground and excited levels, and it is found that the ionization from excited level becomes the dominant source of electrons away from shock front. (auth)

37882 MAGNETOHYDRODYNAMIC EXPERIMENTS IN AN ELECTROMAGNETIC SHOCK TUBE. Driver, Harry Stephen Thackwray., Vancouver, Can., Univ. of British Columbia, 1964. 122p.

Thesis.

The flow conditions in a low-attenuation electromagnetic shock tube are discussed and compared with those in pressure driven shock tubes and conventional electromagnetic shock tubes. The low-attenuation electromagnetic shock tube differs from the conventional electromagnetic shock tube in that it incorporates a diaphragm separating the high-pressure driver section from the low-pressure expansion section. It was shown that the shock tube gives a plane shock front and a region of shock-heated gas separated from the driver gas by a non-plane contact surface. The electrical conductivity of shock-heated argon was measured for shock speeds of from Mach 8 to Mach 35, and downstream pressures of from 0.01 to 2.0 mm Hg, and was found to agree with theory at the higher downstream pressures but to fall below the theoretical values at the low pressures. The low values of conductivity were attributed to a nonattainment of equilibrium behind the shock front due to the greater relative importance of electron diffusion at low densities. The shock-heated gas was used as the working fluid in two magnetohydrodynamic power generators. In the first the internal resistance of the generator was measured as a function of electrode area and generator current. It was concluded that at high currents a cathode spot was formed, and the measured resistances were related to a theory of cathode spot conduction. In the second generator some effects of the non-scalar conductivity of the plasma at high magnetic fields were investigated. It was shown that the values of Hall voltages in a magnetohydrodynamic generator agree with theory, and can be used to obtain an estimate of the electron density in the plasma. The reduction of the generator current by Hall currents was measured. (Dissertation Abstr.)

37883 HYDROMAGNETIC WAVE VELOCITIES IN A RELATIVISTIC FLUID. Giere, Albert C. University Park, Pa., Pennsylvania State Univ., 1965. 85p.

Thesis.

The velocities of relativistic hydromagnetic waves in a compressible, perfect fluid of infinite conductivity are calculated in the framework of general relativity. The velocities are first obtained in terms of the four-vector magnetic field, i.e., in arbitrary coordinates, and then in terms of the ordinary three-dimensional magnetic field. Several limiting cases are considered, in particular, the incompressible fluid and the fluid in which the magnetic field vanishes. In the former case the result is the relativistic Alfven velocity and in the latter case the result is the relativistic speed of sound. It is found that these velocities reduce to their nonrelativistic values if the fluid pressure, the internal energy, and the applied magnetic energy are small compared to the rest mass energy. The wave velocities are then calculated taking into account the so-called interaction tensor. This tensor was arbitrarily added to the electromagnetic energy tensor in order to make it symmetric, since a symmetric tensor is required by the Einstein field equations. It is found that for a fluid of infinite conductivity, the effect of the interaction tensor on the wave velocities is very small. (Dissertation Abstr.)

37884 ELECTROMAGNETODYNAMICS OF FLUIDS. Hughes, W. F.; Young, F. J. New York, John Wiley and Sons, Inc., 1966. 657p. $17.50.

An introduction to magnetohydrodynamics emphasizing electrodynamic fundamentals and engineering applications is presented. The fields of electrodynamics, thermodynamics, and fluid mechanics are integrated to a unified treatment of fundamental magnetofluid mechanics. Information is included on special relativity, induced electromotive force, and energy. Discussions are also provided on transients, wave motion, and flow development. (J.H.M.)

Geophysics

Refer also to abstracts 37143, 37590, 37597, 37598, 38298, and 38309.

37885 DETERMINATION OF THE DENSITY OF PROTONS AT THE LEVEL OF A SATELLITE BY EXACT NUMERICAL ANALYSIS OF PROTON WHISTLERS. Beghin, Christian; Gendrin, Roger; Siredey, Claude; Vigneron, Jacques (Groupe de Recherches Ionospheriques, Saint-Maur-des-Fosses, France). Ann. Geophys., 110-12(1966). (In French).

First experimental determinations were made using sonagrams; improvement in precision was achieved with a variable-frequency oscillator. The arithmetic product of two functions of time (the experimental wave form, and a theoretical approximation) is taken and the half-width of the Laplace transform of this measured. The frequency resolution of experimental data is better than 0.1 cps; variation of t_0 permits maximizing of the convolution product. By obtaining such experimental points the function $t = t(F_B(s) - f)^{1/4}$ may be constructed for various F_B; only one of these is a straight line, and the error is slightly greater than 0.1 cps for $t_0 > 2$. F_B is thus found to be 327.5 ± 0.1 cps, and $\alpha = 3.25 \pm 0.15$ s$^{1/4}$. Proton density may be calculated from such data as well. Reconstruction of the sonagram and max values of the correlation coefficient for the determination of the function are illustrated. (BBB)

37886 RELATION BETWEEN PROTON FLARES AND THE CORONA IN THE 11-YEAR CYCLE. Gnevyshev, M. N.; Krivsky, L. (Glavnoi Astronomicheskoi Observatorii, Academy of Sciences, USSR). Astron. Zh., 43: 385-9(Mar.-Apr. 1966). (In Russian).

The distribution of the number of proton flares and chromospheric flares has two maxima in the 11-yr cycle. The intensity of the corona, the number of prominences, sunspot areas, and solar radio emission intensity also indicate two maxima. Proton flares appear in regions of enhanced coronal brightness. The second max is characterized by a predominant appearance of especially

strong phenomena, for example, cosmic flares. A catalog of proton flares compiled for the years 1954-1964 is given, with several earlier flares between 1942 and 1954. Max values per year occur in 1957 (0 cosmic flares, 15 subcosmic flares) and 1960 (5 cosmic, 13 subcosmic). A graphical comparison of the 5303 Å coronal line intensity with flare data is given; proton flares occur at similar times and solar latitudes as maxima in coronal intensity. The number of chromospheric flares per single observation also has two maxima in this period: 1957 (0.379 flares/observation) and 1960 (0.223 flares/observation). (BBB)

37887 SEVERAL EXAMPLES OF THE RELATIONSHIP BETWEEN POLAR LIGHTS, SOLAR AND GEOMAGNETIC PHENOMENA. Schroeder, Wilfried (Geophysikalische Station, Bremen-Roennebeck, Ger.). Beitr. Geophys., 74: 7-9(1965). (In German).

Solar and geomagnetic phenomena are correlated with several striking auroral displays. The displays may be connected with the more important flares (class >2). Data for displays, geomagnetic and solar flare data are tabulated; the polar lights of 13 Sept. 1957, 11 Feb. and 8 July 1958, 15 July 1959, and 31 Mar., 1 Apr., and 12 Nov. 1960 are related to such solar flares; it is also noted that these days were particularly disturbed. In two cases correlation was not obtained; the displays of 4 Sept. 1959 are related to the disturbance of 4-5 Sept. 1959, which occur later than the solar flares of 30-31 Aug. 1959, through these were of particularly long duration. The disturbance and displays of 6 Oct. 1960 are matched by peripheral solar flares of 1 Oct. and 4 Oct. and two other flares of class 1 on 5 Oct. Possibly a correlation with M regions may be assumed in both of these cases. (BBB)

37888 OCCURRENCE OF POLAR LIGHTS DURING SLIGHT MAGNETIC DISTURBANCES AND THEIR RELATION TO SOLAR ACTIVITY. Schroeder, Wilfried (Geophysikalische Station, Bremen-Roennebeck, Ger.). Beitr. Geophys., 74: 195-8(1965). (In German).

Accompanying conditions at the occurrence of weak auroral displays are outlined. Closer consideration of 28 visually observed displays indicates that only in a few cases is unobjectionable correlation to solar flares of less than 40 hours duration possible. From geomagnetic observations, Sc was determined on the days surrounding several displays. It follows that after a magnetic storm the deformation of the magnetic field is maintained for a period of time; so it is possible that the weaker solar particle streams which follow may enter this region. These streams have their origin in weaker flares or in M regions. Nine cases are not completely satisfactorily explained by this correlation, although in a few cases activity was observed several days previously; speculative correlation with M regions is suggested in these cases. (BBB)

37889 SOLIDIFICATION OF NAPHTHALENE AND NATURAL ELECTROMAGNETIC FIELDS. Costa, Mariagrazia; Papeschi, Giorgio (Univ., Florence). Geofis. Meteorol. (Genoa), 13: 67-8(1964). (In Italian).

A new test was developed to detect fluctuations in an electromagnetic field. It is based on a phase change in a pure substance, that is, the solidification of molten naphthalene. This test is compared with other chemical, physical, and biological tests used to follow fluctuations with time of field intensity. To conduct the tests, tubes containing naphthalene are maintained at 90°C by a constant temperature water bath, and crystallization of the naphthalene is observed. Daily records for 1963-64 were made of the results, which were compared with other indices of geomagnetic activity. A correlation coefficient of −0.76 was found when the results from the naphthalene tests were compared with readings of geomagnetic activity obtained at the Observatorio Magnetico of Aquila. (BBB)

37890 BEHAVIOR OF T PERCENT IN THE NAPHTHALENE TEST DURING A MAGNETIC STORM. Papeschi, Giorgio; Costa, Mariagrazia (Univ., Florence). Geofis. Meteorol. (Genoa), 13: 69-70(1964). (In Italian).

The napththalene test, which, as previously reported, reacts to natural electromagnetic fields, is affected by magnetic storms to a marked extent. Increased crystallization of naphthalene under a copper shield was observed on the day preceding the start of magnetic storms. Results of the test are explained via mechanisms of magnetic storms; the findings in the test seem to be influenced by secondary electromagnetic radiations, which are produced immediately after a solar event, instead of the geomagnetic disturbances which take place 24 to 36 hours after the event. Data showing the fluctuations in results of the naphthalene crystallization test as correlated with sunspot activity are presented covering the period 1961 to 1964. (BBB)

37891 FIRST RESULTS ON THE RELATIONS BETWEEN THE NAPHTHALENE TEST AND THE LUNAR PHASES. Papeschi, Giorgio; Costa, Mariagrazia (Univ. Florence). Geofis. Meteorol. (Genoa), 13: 79-82(1964).

The use of the naphthalene test to follow changes in electromagnetic activity in correlation with lunar cycles is described. The phase change in naphthalene, from liquid to solid state, under the electromagnetic field is the basis of the test. The naphthalene test has been carried on daily (at 12 AM local time) for two years at Florence. The test is conducted by a statistical evaluation of the solidification of melted naphthalene contained in 20 sealed vials. Ten vials undergo the change of phase under a copper shield and 10 vials are unshielded. The number of test vials solidifying under copper sooner than the vials kept outside is designated T%. T% may range from 0% to 100%. When the result is T% = 50, the copper screen has not influenced the system; when T% > 50, the tested material crystallized more rapidly under the copper screen; when T% < 50, crystallization is higher in the open air. Results of the naphthalene test can be correlated both with the local geomagnetic index and the geomagnetic planetary index, and that it shows a characteristic behavior during geomagnetic storms. A further analysis of the data shows a lunar effect on the crystallization of naphthalene; that is, T% values were lowest at the time of the new moon and highest at full moon. (BBB)

37892 PRE-SC INCREASES OF HF FIELD INTENSITY ON POLAR PATHS AND OF f_0F_2 IN HIGH LATITUDES. Ondoh, Tadanori; Obu, Koji. J. Radio Res. Lab., 12: 275-99(Sept. 1965).

Analysis of data on the pre-SC field intensity and receivable time of the WWV 20-Mc signal at Hiraiso, Japan, and at various Canadian stations, was made for 50 geomagnetic storms. The purpose of the analysis was explanation of the pre-SC increases noted at Hiraiso, which are found to be associated with f_0F_2 increases at approximate apexes along the Washington-Hiraiso path. These increases, like the field-strength increases in the 20- and 25-Mc WWV signals, were found to occur as much as 18 hr before SC. The WWV increase is seen to be due to a deviative-absorption decrease associated with the f_0F_2 increase, which is in turn considered to be caused by low-energy (1 to 2 kev) electrons which enter the polar ionosphere from interplanetary space through the neutral point (or arc) on the magnetospheric boundary. (Int. Aero. Abstr.)

37893 SPATIAL EXTENT OF ENHANCED IONIZATIONS PRODUCED IN ASSOCIATION WITH THE ELEMENTARY GEOMAGNETIC POLAR DISTURBANCES. Hakura, Yukio (Ministry of Posts and Telecommunications, Tokyo); Nagai, Masao. J. Radio Res. Lab., 12: 301-10(Sept. 1965).

A worldwide analysis of ionospheric vertical sounding data during typical elementary geomagnetic disturbances revealed a "lip-shaped" pattern of the enhanced ionization area formed along the midnight auroral zone. Dipole-field type currents originate in this abnormally ionized area. The pattern suggests the spatial extent of the auroral particle precipitation onto the ionosphere. The result is noted in connection with IMP-1 satellite observations of the energetic electrons in the neutral sheet situated in the nightside of the geomagnetosphere. (auth)

37894 ORIGIN OF HIGH-ENERGY ELECTRONS BEYOND THE MAGNETOSPHERE. Shen, C. S. (Purdue

Univ., Lafayette, Ind.); Chang, C. C. Nature, 211: 275-7 (July 16, 1966).

It is suggested that, because of the characteristic geometry and distorted structure of the interplanetary magnetic field near the magnetopause in the transition region, these electrons are locally accelerated by means of a Parker-Wentzel version of the Fermi mechanism. Parker considered the acceleration of charged particles trapped between two shocks which cross each other. Wentzel considered the case that charged particles trapped ahead of a single shock wave which moves into a stronger magnetic field. Calculations related to this hypothesis are described. (M.O.W.)

37895 NEUTRAL POINT IN THE GEOMAGNETIC FIELD. Grad, Harold; Hu, Pung Nien (Space Sciences, Inc., Waltham, Mass.). Contract AF 49-(638)-1666. Phys. Fluids, 9: 1610-11(Aug. 1966).

The neutral point on the boundary of the geomagnetic cavity in the solar wind is discussed. From the equilibrium and stability conditions it is shown that the correct geometry of the neutral point is a cusp. (auth)

37896 PARTICLE HEATING EFFECTS IN THE UPPER F REGION. Nathan, K. V. S. K. (University Coll., London). Planet. Space Sci., 14: 717-30(Aug. 1966).

Nighttime electron temperatures in the upper F region obtained from the satellite Ariel I indicate an energy input to the ionosphere that is corpuscular in origin. Willmore infers an energy flux of order 10 ergs/cm^{-2} per sec by electrons of a few kev. But estimates of energy flux based on observations on the intensity of the spectral bands of nitrogen, and neglecting all effects due to the magnetic field, suggest an energy flux smaller by a least two to three orders of magnitude. A part of the discrepancy is removed on allowing for electron heating by secondary electrons produced in ionizing collisions. A Fokker-Planck type diffusion equation is used to investigate the steady state flux densities built up in the upper atmosphere by a constant source of electrons subject to scattering and energy degradation processes. It is found that, when magnetic field effects are allowed for, the heating effects are consistent with a precipitated flux of order 10^{-3} ergs cm^{-2} sec^{-1}. The discrepancy with the optical evidence is thus entirely removed. (auth)

37897 DIFFERENT GEOMAGNETIC VARIATIONS ASSOCIATED WITH CORPUSCULAR PRECIPITATIONS ON DAY AND NIGHT SIDE OF THE AURORAL ZONE. Morozumi, Henry M. (Lockheed Palo Alto Research Lab., Palo Alto, Calif.). Planet. Space Sci., 14: 807-8(Aug. 1966).

Comparisons were made of different geomagnetic variations associated with corpuscular precipitation at the South pole during the period of October 30 through November 3, 1963. The ionosphere was illuminated at about the same angle for day and night side. A conspicuous day-night effect was found. Magnetic variations were very small during the day and the reverse was true for the night. This difference was attributed to different magnetospheric conditions rather than the change in physical properties of the local ionosphere due to the sunlight. The diurnal variation of the ratio of the change in the horizontal component of the magnetic field to the total energy precipitated is plotted. Also included is the change in the horizontal component of the geomagnetic field as a function of electron energy in the loss cone above the South Pole. (J.H.M.)

37898 MEASUREMENTS OF THE MAGNETIC FIELDS IN INTERPLANETARY SPACE AND THE MAGNETOSPHERE. Ness, N. F. (Goddard Space Flight Center, Greenbelt, Md.). pp 14-25 of Proceedings of the Ninth International Conference on Cosmic Rays. Vol. I. Stickland, A. C. (ed.). London, The Institute of Physics and The Physical Society, 1966.

Direct measurements of magnetic fields in space were performed by satellites and space probes since 1958. The results of these experiments reveal the continual confinement of the geomagnetic field by the "solar wind," forming the magnetosphere and the earth's magnetic tail. At 3-6 R_E permanent effects due to "ring currents" were detected. Enclosing the magnetosphere is a turbulent boundary layer separated from the interplanetary medium by a collisionless magnetohydrodynamic shock wave. At the subsolar point the distance to the termination of the regular geomagnetic field is approximately 10 R_E and to the shock wave 13.4 R_E. The geomagnetic tail is observed out to a distance of 40 R_E trailing away from the sun much in the fashion of cometary tails. The magnetized solar plasma contains a field of approximately 5 gammas which is directed along the classical Archimedean spiral predicted by Parker. The interplanetary field, deduced conclusively to be of solar origin, is structured into four sectors which are readily identifiable during the quiet years of the solar cycle (1963-64). The experiments and their results with respect to our knowledge of fields in space are summarized. (auth)

37899 EARTH'S RADIATION BELT. Vernov, S. N.; Gortchakov, E. V.; Kuznetsov, S. N.; Logatchev, Yu. I.; Sosnovets, E. N.; Tverskoi, B. A.; Chudakov, A. E. (Moscow State Univ.). pp 40-9 of Proceedings of the Ninth International Conference on Cosmic Rays. Vol. I. Stickland, A. C. (ed.). London, The Institute of Physics and The Physical Society, 1966.

Some results of the earth's radiation belt investigation during solar minimum are reviewed. The results obtained from the "electron" series of artificial earth's satellites during 1964 comprise the main experimental material reported here. Individual typical regions such as the inner and outer radiation belts are examined. A general picture of the belts which is typical for the epoch of the solar minimum is given. When analyzing the time variations in the outer belt and outside its boundary the satellite data are compared with the data of ground geophysical stations. The development of the radiation belt theory is briefly reviewed. (auth)

37900 ACCELERATION OF PARTICLES IN THE EARTH'S SHOCK TRANSITION REGION AND BEYOND. Fan, C. Y.; Gloeckler, G.; Simpson, J. A. (Univ. of Chicago). pp 105-8 of Proceedings of the Ninth International Conference on Cosmic Rays. Vol. I. Stickland, A. C. (ed.). London, The Institute of Physics and The Physical Society, 1966.

Pulses of high-energy electrons were observed in the vicinity of the bow shock of the terrestrial magnetosphere with both the Au–Si surface barrier solid state detector (the front detector of the cosmic ray telescope of the University of Chicago) and the GM counter (University of California) on board the IMP-I satellite. These particle pulses were also detected inside the shock transition region with GM counters in earlier satellites. There is experimental evidence that these electrons are accelerated in the shock transition region. By comparing the counting rates of the solid state detector and that of the GM counter on board IMP-I, the energy spectrum of the electrons may be estimated. If the integral spectrum is expressed as $F = F_0E^{-\gamma}$, the value of γ varies from +2.5 to +4.5. Beyond the shock transition region up to the apogee of the IMP-I satellite (200,000 km), pulses of high-energy particles were also observed with the Au–Si solid state detector prior to the arrival of the 27-day recurrent solar plasma of enhanced velocity. It is suggested that these are particles accelerated in space by multiple shock waves associated with the co-rotating shock front. (auth)

37901 ACCELERATION OF PARTICLES IN THE NEUTRAL SHEET OF THE GEOMAGNETIC TAIL. Speiser, T. W. (Goddard Space Flight Center, Greenbelt, Md.). pp 147-50 of Proceedings of the Ninth International Conference on Cosmic Rays. Vol. I. Stickland, A. C. (ed.). London, The Institute of Physics and The Physical Society, 1966.

An analytical study is made of particle trajectories about a neutral sheet. Such a magnetically neutral sheet was observed in the earth's magnetic tail by Ness. A simple model is constructed where the magnetic field varies linearly, reversing across the neutral sheet, and the electric field is everywhere homogeneous, perpendicular to

the magnetic field and parallel to the neutral sheet. The important results in this case are that neither protons nor electrons come out of the neutral sheet, and their energies go to infinity. Another model is constructed by adding a small component of the magnetic field perpendicular to the neutral sheet. This component provides some curvature to the lines of force, and implies that field lines cross the sheet at some rate and are not dragged back to infinity. The addition of this perpendicular component not only serves to bring particles out of the neutral sheet, but turns both electrons and protons in toward the earth. If the perpendicular magnetic field component is small, the particle energy gain will be large and the pitch angles of the particles ejected from the neutral sheet will be small. These results imply that the geomagnetic tail may be the source of auroral particles, the particles originally coming from the solar wind, and the results may also be important in situations such as solar flares, the day-side neutral sheet, and neutral sheets occurring in interplanetary space. (auth)

37902 CORPUSCULAR IONIZING RADIATION IN SPACE IN THE IMMEDIATE VICINITY OF THE EARTH. Vernov, S. N.; Gortchakov, E. V.; Maduev, V. L.; Kchudyakov, A. V. (Moscow State Univ.). pp 303-5 of Proceedings of the Ninth International Conference on Cosmic Rays. Vol. I. Stickland, A. C. (ed.). London, The Institute of Physics and The Physical Society, 1966.

Nomograms for numerical evaluation of the geomagnetically trapped proton fluxes in the energy range 0.5 kev to 100 Mev and electron fluxes in the energy range 0.2–6000 kev at a given point in space in the immediate vicinity of the earth are presented. (auth)

37903 ENERGETIC ELECTRON SPIKES IN AND BEYOND THE TRANSITION REGION. Anderson, K. A. (Univ. of California, Berkeley). pp 520-7 of Proceedings of the Ninth International Conference on Cosmic Rays. Vol. I. Stickland, A. C. (ed.). London, The Institute of Physics and The Physical Society, 1966.

IMP satellite measurements show that the energetic radiation around the earth may be divided into the Van Allen trapping zone, in which charged particles drift completely around the earth, and the distant radiation zone, in which there is no complete azimuthal drift around the earth due to distortions of the geomagnetic field. The distant radiation zone exhibits several distinct features. Among these are the transition spikes. It is shown here that their appearance is very sensitive to geomagnetic disturbance indexes. It is also shown that on many occasions the frequency and size of these energetic electron spikes increase systematically from the magnetopause to the bow shock. Beyond the shock, spikes still appear but with lower frequency and smaller size. (auth)

37904 LOW-ENERGY PARTICLE FLUXES INSIDE THE MAGNETOSPHERE FROM THE DATA OF THE ELECTROSTATIC ANALYZERS OF THE ELECTRON-2 SATELLITE. Vernov, S. N.; Melnikov, V. V.; Savenko, I. A.; Savin, B. I. (Moscow State Univ.). pp 529-31 of Proceedings of the Ninth International Conference on Cosmic Rays. Vol. I. Stickland, A. C. (ed.). London, The Institute of Physics and The Physical Society, 1966.

The spherical electrostatic analyzers of the "Electron-2" satellite could detect particles with energies E_0 = 0.1, 0.2, 0.5, 1, 2.5, 5 and 10 kev in the interval $\Delta E/E_0 \sim 30\%$. At geocentric distances of $4-8$ R_E and at southern geomagnetic latitudes above 40° a long existing region of increased electron intensity was discovered. Electron fluxes in the region reached 10^8-10^9 electron cm^{-2} sec^{-1} kev^{-1}. The extent of the region and the electron fluxes in it undergo considerable changes and correlate positively with geomagnetic activity. Comparison of the results obtained from "Electron-2" with measurements of low energy electrons from "Lunik-2", "Explorer XII" and "Injun-3" permitted a plot to be made of a conjectural spatial form of the region filled with soft electrons and enveloping the earth from the night side. At sunrise and sunset longitudes this region does not intersect the equatorial plane. At distances of 9–11.7 R_E sporadic electron fluxes with energies below about 1 kev and intensities in excess of 10^9 electron cm^{-2} sec^{-1} kev^{-1} were detected on some passes. Ion fluxes with energies from 0.1 to 10 kev did not exceed about 5×10^7 ion cm^{-2} sec^{-1} as a rule. (auth)

37905 INVESTIGATION OF THE OUTER PROTON BELT. Vernov, S. N.; Savenko, I. A.; Tel'tsov, M. V.; Shavrin, P. I. (Moscow State Univ.). pp 532-3 of Proceedings of the Ninth International Conference on Cosmic Rays. Vol. I. Stickland, A. C. (ed.). London, The Institute of Physics and The Physical Society, 1966.

The results of measurements of low energy protons and electrons of the outer radiation belt carried out with radiometric equipment installed on board the "Cosmos-41" satellite are presented. (auth)

37906 COULOMB INTERACTION OF ELECTRONS WITH ENERGY OF 1 Mev IN THE REGION OF A MAGNETIC ANOMALY. Gortchakov, E. V.; Gurevich, A. V.; Timofeev, G. A. (Moscow State Univ.). pp 534-5 of Proceedings of the Ninth International Conference on Cosmic Rays. Vol. I. Stickland, A. C. (ed.). London, The Institute of Physics and The Physical Society, 1966.

The results of a calculation of the longitude dependence of the density of electrons with an energy of 1 Mev at low altitudes are given for a fixed value of the MacIlwain parameter (L = 1.5). A solution of the kinetic equation which takes into account the scattering and deceleration of electrons in the atmosphere was found. It was determined that, during the longitude drift, substantial changes take place in the electron density for altitudes h_{min} less than 200 km. (auth)

37907 PENETRATION OF THE OUTER RADIATION BELT PARTICLES INTO LOW ALTITUDES OF ATMOSPHERE. Charakhch'yan, A. N.; Golenkov, A. E.; Charakhch'yan, T. N. (Lebedev Physical Inst., Moscow. Moscow State Univ.). pp 536-7 of Proceedings of the Ninth International Conference on Cosmic Rays. Vol. I. Stickland, A. C. (ed.). London, The Institute of Physics and The Physical Society, 1966.

Increases of general ionizing radiation in the stratosphere were recorded over Murmansk on 1st and 3rd January, 5th, 12th and 24th March, 28th April and 25th June 1964. In some cases the radiation penetrates to relatively low altitudes (about 15 km). These cases of increased radiation correlate with recurrent magnetic storms, ionospheric perturbations in the auroral zones and galactic radio noise absorption. These cases possibly are due to electrons arriving from the earth's outer radiation belt. (auth)

37908 NEUTRON FLUX IN THE UPPER ATMOSPHERE DURING THE 1964 SOLAR MINIMUM. Greenhill, J. G. (Univ. of Tasmania, Australia); Phillips, J.; Fenton, K. B.; Fenton, A. G.; Bowthorpe, M. pp 538-41 of Proceedings of the Ninth International Conference on Cosmic Rays. Vol. I. Stickland, A. C. (ed.). London, The Institute of Physics and The Physical Society, 1966.

The atmospheric neutron flux was measured in a series of balloon flights in August-October 1964, using a polyethylene moderated BF_3 counter. These flights were made from five different sites ranging from Antarctica to equatorial regions and extend to within 10-15 g cm^{-2} of the top of the atmosphere. The latitude variation of the counting rate increases with altitude to the highest levels reached. The variation at 245 g cm^{-2} is in good agreement with the 1962 observations of Gauger after correcting for the higher solar activity at the time of Gauger's measurements. The latitude variation of the neutron flux at 15 g cm^{-2} is estimated. Assuming this distribution to be similar to the leakage flux distribution, the results are shown to be in good agreement with the 1963 calculations of Lingenfelter. The slow neutron density distribution is evaluated by normalizing the latitude distribution curves to the 1961 data of Miles. The distribution obtained differs significantly from that predicted by Lingenfelter in 1963. The global average carbon-14 production rate is estimated to be 1.85 ± 0.5 cm^{-2} sec^{-1} at the time of the measurements. (auth)

37909 HYPOTHESIS OF ORIGIN AND FORMATION OF RADIATION BELTS AS A RESULT OF PARTICLE DRIFT INTO THE DEPTH OF THE MAGNETOSPHERE. Ershkovich, A. I.; Shabanskii, V. P.; Antonova, A. E. (Moscow State Univ.). pp 543-5 of Proceedings of the Ninth International Conference on Cosmic Rays. Vol. I. Stickland, A. C. (ed.). London, The Institute of Physics and The Physical Society, 1966.

Consideration is given to the hypothetical mechanism of the earthward radial drift of charged particles. The velocity of the drift of the particles is assumed to be proportional to their momenta. It was shown that β decay of albedo neutrons can serve as a sufficiently powerful source in the formation of the belt of relativistic electrons. The proton belt may be formed due to the earthward drift of protons with mean energy $E_p \sim 10-15$ kev filling the region between the magnetospheric boundary and the front of a standing shock wave. (auth)

37910 ON THE EARTH'S RADIATION BELT THEORY. Tverskoi, B. A. (Moscow State Univ.). pp 546-7 of Proceedings of the Ninth International Conference on Cosmic Rays. Vol. I. Stickland, A. C. (ed.). London, The Institute of Physics and The Physical Society, 1966.

The results of investigation of stability of the earth's radiation belts taking into account wave absorption in the ionosphere are set forth. The method of investigation of stability in an inhomogeneous field is described. It is shown that proton fluxes in the outer belt are close to the critical value and therefore the generation of Alfvén waves is sometimes possible. This effect is likely to result in development of Pc-type oscillation. Evaluation of critical electron fluxes depending upon L is given. (auth)

37911 MAGNETOSPHERIC PHENOMENA. Roederer, J. G. (Facultad de Ciencias Exactas y Naturales, Buenos Aires. Goddard Space Flight Center, Greenbelt, Md.). pp 586-94 of Proceedings of the Ninth International Conference on Cosmic Rays. Vol. I. Stickland, A. C. (ed.). London, The Institute of Physics and The Physical Society, 1966.

Research on the physics of the magnetosphere is reviewed. Topics considered are magnetospheric shape and structure, charged particle motion in the magnetosphere, and geomagnetically trapped radiation. (J.F.P.)

37912 STRUCTURE OF THE SOLAR CHROMOSPHERE. Suemoto, Z. (Tokyo Astronomical Observatory). Scientia (Milan), 100: 199-203(Sept.-Oct. 1965).

The nature of sunspots, and particularly of the regions of the sun not occupied by sunspots, is discussed. Anomalies appearing on the sun's surface are not limited to the relatively small areas occupied by sunspots, but are distributed around sunspots for some distance. These regions around sunspot areas are characterized by a great many of bright patches, faculae, which are also closely associated with the stronger magnetic field. Above the faculae the corona is also disturbed in such a way that it is denser and hotter than elsewhere. These regions, coronal condensations, are the source of extremely strong radio waves and x rays from the sun, which fluctuate rapidly. Most the energy comes from that portion of the sun where there are no such activities. In addition to a discussion of the motions and structures of the quiet part of the sun, how the solar atmosphere is stratified from the depths towards the surface is explained. Heat generated in the core of the sun is transferred outwards by radiation up to a depth of one tenth of the radius. Then the thermal propert, of the gas changes and the convection transfer becomes more important as compared with the radiative transfer. This is due to the change in the ionization of hydrogen atoms, primary constituent of the gas. The convection motion becomes greater up to a depth of one thousandth of the radius. At this depth the hydrogen atoms become neutral, the convective motion subsides, and again the heat is transferred by radiation to the surface. This last layer, the photosphere, acts as a barrier against the upward propagation of the convective motion beneath. Existence of the convective layer can be visualized by magnified photographs of the sun taken from a balloon in white light. Such pictures show many of grain-like structures, of average size one-thousandth of the solar radius, called granules. Measurement of velocities of the gas motions in the chromosphere from eclipse observations is also described. (BBB)

37913 CHARGED DUST PARTICLES IN INTERPLANETARY SPACE. Divari, N. B. (Odessa Polytechnic Inst.). Soviet Astron. AJ (Engl. Transl.), 10: 151-5(July-Aug. 1966).

Translated from Astron. Zh., 43: 192-7(Jan.-Feb. 1966).

Implications of the assumption that the dust particles in interplanetary space bear an electric charge are discussed. Several effects observed in the zodiacal light, the Gegenschein, the twilight glow, and noctilucent clouds can then be explained naturally. The earth and moon may have dust tails. Submicron particles are captured by the geomagnetic field, forming the most stable component of the earth's dust cloud. Interplanetary space may be replenished by submicron dust blown from near the moon by the solar wind. (auth)

37914 MAGNETOCONJUGATE PHENOMENA. Wescott, Eugene M. (Univ. of Alaska, College). Space Sci. Rev., 5: 507-61(June 1966).

A review is presented of knowledge accumulated, some theoretical speculation, and some recommendations for future work on geophysical phenomena at magnetically conjugate points on the earth. Discussions are included on cosmic noise absorption, conjugacy of visual auroras, conjugate balloon observations of auroral zone x rays, magnetic variations, micropulsations of the geomagnetic field, and vlf phenomena. (J.H.M.)

37915 RESULTS OF SPACE RESEARCH: SOLAR PROTONS. TRW Space Log, 5: 46-9(Winter 1965-66).

Observations of solar protons are reviewed in relation to understanding of the physics of the sun, and the fact that these solar protons constitute virtually the only potential source of radiation danger for man in space. Satellite observations of solar protons, starting in 1958 with Explorer 4, are surveyed. The flux-time histories obtained have permitted insight into the mode of propagation of the particles from the sun. As demonstrated by the experimental data, the protons showed the general characteristics predicted by the model for isotropic diffusion from a point source. About 60 solar events have resulted in the arrival of high-energy protons in the vicinity of the earth the last decade, and it was possible to correlate such proton fluxes with specific solar flares and to demonstrate that only a few flares give rise to protons which reach the earth. The rise time from optical onset of sun spot activity to flux max at the earth is ~3 hr. The time for decay to half value is 10 to 20 hr. A model flare can be described with reasonable accuracy for predicting proton fluxes from this source. The total flux at the earth from this model event is about 6×10^9 protons/cm^2 with energy E > 30 Mev, and the integral energy flux can be represented by $n(>E) = kE^{-4}$, with k varying inversely with the cube of time and variable from flare to flare. Only one event in recent years was observed with a greater total flux. The closest events in magnitude are listed in a table. The table also shows the radiation dose within the Apollo spacecraft and space suit that would have resulted from the five largest events in the last period of solar activity. The max skin dose received during the February 1956 event would have been 220 rad, as compared to the 500-rad dose set by the National Academy of Sciences as the max permissible in an emergency. The dose to blood-forming organs would have been 20 rad, compared with a level of 100 rad set by the academy as the max permissible. (BBB)

37916 INTRODUCTION TO SOLAR TERRESTRIAL RELATIONS. Proceedings of the Summer School in Space Physics Held in Alpbach, Austria, July 15–August 10, 1963. Ortner, J.; Maseland, H. (eds.). Astrophysics and Space Science Library. Dordrecht, Holland, D. Reidel Publishing Company, 1965. 514p. $19.50.

An introduction to solar terrestrial relationships which

form a part of the field of space physics is presented. Topics covered include: physics of the sun, phenomena occurring in the interplanetary medium, effects produced in the ionosphere, space instrumentation, solar cosmic rays, and ionosphere and planetary atmosphere. (J.H.M.)

37917 MEASUREMENTS OF MAGNETIC FIELDS IN THE VICINITY OF THE MAGNETOSPHERE AND IN INTERPLANETARY SPACE: PRELIMINARY RESULTS FROM MARINER 4. **Coleman, P. J. Jr. (Univ. of California, Los Angeles); Smith, E. J.; Davis, Leverett Jr.; Jones, D. E. 49p. (CONF-650961-6). ORAU. Gmelin, AED-CONF-65-224-13.**

From American Geophysical Union, 5th Western National Meeting, Dallas.

Various preliminary results of an analysis of data from the magnetometer on board Mariner 4 are described. The measurements discussed were obtained between November 28, 1964 and April 1965. During the first day of the flight the spacecraft traversed the magnetosphere and the interaction region between the magnetosphere and interplanetary space. Very abrupt changes in the stability of the field were produced at the position of the earth's bow shock. There were at least seven traversals of the shock between 36.6 and 38.6 R_e in a region approximately 105°, on the dawn side, from the earth-sun line. The gross properties of the interplanetary field are summarized by means of distributions, over 27-day periods, of values of the various parameters pertaining to the field. On the average, the field tends to lie along the expected spiral direction, but the distribution of polarities along this direction is found to change. The tendency, observed previously with the Mariner 2 and IMP magnetometers, for the interplanetary field to have a southward (positive θ component) component persists. Very rough estimates of the power spectra of the variations in the field are presented. (auth)

Gravitation, Quantum Mechanics, and Relativity Theory

Refer also to abstract 38121.

37918 QUADRATIC LAGRANGIANS IN GENERAL RELATIVITY. **Pechlaner, E.; Sexl, R. (Univ. of Vienna). Commun. Math. Phys., 2: 165-75(1966).**

Theories of gravitation similar to general relativity but with an additional R^2 term in the Lagrangian are explored. The Schwarzschild metric is not the exterior solution that can be continued to the interior of the body to give a positive definite mass distribution. The experimental consequences of R^2 terms are investigated. Furthermore, it is shown that a theory with an R^2 term only possesses an interesting singular dependence on the coupling constant. (auth)

37919 VARIATIONAL CALCULATION FOR BOUND STATES IN AN ELECTRIC-DIPOLE FIELD. **Fox, Kenneth (Univ. of Tennessee, Knoxville); Turner, J. E. Contract W-7405-eng-26. J. Chem. Phys., 45: 1142-4 (Aug. 15, 1966). (ORNL-P-1914).**

The quantum-mechanical problem of an electron moving in the field of a permanent electric dipole was investigated in an attempt to determine whether negative energy eigenvalues, i.e., bound states, exist for small dipole moments. When the expectation value of the Hamiltonian is minimized in a variational calculation and then set equal to zero, the solution of the resulting equation gives a value of the dipole moment which is sufficient to assure the existence of a bound state. Use of the trial wavefunction $\psi = \exp(-\alpha r^t)\ (C_0Y_{00} + C_1Y_{10})$ shows that 1.65×10^{-18} esu · cm is sufficient. (auth)

37920 RIGOROUS SOLUTION OF DIRAC'S EQUATION. **Kronig, R.; Visser, J. Koninkl. Ned. Akad. Wetensch., Proc., Ser. B, 69: 332-5(1966).**

A rigorous solution is presented of Dirac's equation for an electron, subject to no other forces than those exerted by a general plane electromagnetic wave. (L.B.S.)

37921 NULL COORDINATES FOR SPHERICALLY SYMMETRIC GRAVITATIONAL COLLAPSE. **de la Cruz, V. (Univ. of Alberta, Edmonton, Can.). Phys. Lett., 22: 152-4 (Aug. 1, 1966).**

The interior and exterior line elements for a collapsing cloud of dust are expressed in terms of null coordinates of Kruskal's type. This gives a singularity-free description of the complete manifold right down to the singular event of maximum implosion. (auth)

37922 DEVELOPMENT OF THE SPACE-TIME VIEW OF QUANTUM ELECTRODYNAMICS. **Feynman, Richard P. (California Inst. of Tech., Pasadena). Phys. Today, 19: No. 8, 31-44(Aug. 1966).**

In efforts to rid quantum electrodynamics of its infinities, there were many false starts. But many ways of formulating the theory, especially with path integrals of actions, were found. A new point of view is developed, one of examining an interaction over all space and time rather than its detailed behavior as a function of time. The reformulation succeeded eight years after its beginning. (auth)

37923 ON THE GRAVITATIONAL SIGNIFICANCE OF DEVIATIONS FROM THE MINKOWSKIAN METRIC. **Sharan, Raghubir (Banaras Hindu Univ., India). Proc. Nat. Inst. Sci. India, Pt. A, 31: 311-22(July 1965).**

Gravitational situations arising out of the introduction of two functions A and B in the flat metric were investigated. Several cases are discussed. In one case, the empty space-time field is characterized by the presence of gravitational radiation. In another case, the empty space-time field equations with cosmological constant provide two differential equations which are integrable in terms of elliptic functions. The Einstein-Maxwell field equations lead to uniform electromagnetic field in one case, and to uniform null electromagnetic field in the other. (auth)

37924 SPINOR APPROACH TO QUATERNION METHODS IN RELATIVITY. **Ellis, J. R. (Bedford Coll., London). Proc. Roy. Irish Acad., Sect. A, 64: 127-42(Mar. 1966).**

A scheme for rewriting the quaternion methods of C. W. Kilmister in terms of spinor theory is proposed. Certain theorems in tensor theory which were deduced by the use of quaternions are proved independently with spinors and augmented by other theorems of a similar type. (auth)

37925 COVARIANT QUANTIZATION OF THE ELECTROMAGNETIC FIELD IN THE LANDAU GAUGE. **Nakanishi, Noboru (Brookhaven National Lab., Upton, N. Y.). Progr. Theoret. Phys. (Kyoto), 35: 1111-16 (June 1966). (BNL-9900).**

A new covariant quantization of the free electromagnetic field is proposed corresponding to the fact that a massless vector bound state in the Bethe-Salpeter formalism is accompanied by a dipole ghost. The Lorentz condition is formulated as an operator identity. (auth)

37926 MODEL OF THE DISPERSIVE NONLINEAR EQUATION. **Yajima, Nobuo; Outi, Akizi; Taniuti, Tosiya (Nagoya Univ., Japan). Progr. Theoret. Phys. (Kyoto), 35: 1142-53(June 1966).**

A model of the dispersive nonlinear equation is considered, which is derived from the Schrödinger equation by means of a nonlinear transformation. The derivation is closely analogous to deriving the Burgers model from the diffusion equation. A solution is then obtained resulting from an initial discontinuity, which corresponds to that of Riemann's problem in the Burgers model. In the solution so obtained, the limit that the Planck constant vanishes is discussed in comparison with the dissipative limit in the Burgers model, which is realized by letting the dissipation constant tend to zero. It is explicitly shown that although in these limits the equations in the two models are the same, nevertheless their solutions are entirely different; for example, as is well known, in the Burgers model one discontinuity develops from the initial discontinuity while in our model two discontinuities develop, across each of which the so-called generalized Rankine-Hougoniot relations are not valid. (auth)

37927 QUANTUM STATISTICAL THEORY OF OPTICAL ROTATION. **Ando, Toshihiko; Nakano, Huzio**

(Nagoya Univ., Japan). Progr. Theoret. Phys. (Kyoto), 35: 1163-5(June 1966).

It is shown that a quantum theory of linear response can be applied to the theory of optical activity for systems of molecules in a solution, segments in ordered and disordered polymers, or ions in certain kinds of crystals. (L.B.S.)

37928 FLUCTUATIONS IN GRAVITATING SYSTEMS. Genkin, I. L. (Astrophysics Inst., Academy of Sciences, Kazkh SSR). Soviet Astron. AJ (Engl. Transl.), 10: 75-7 (July-Aug. 1966).

Translated from Astron. Zh., 43: 96-8(Jan.-Feb. 1966).

Ya. P. Terletskii's results on the influence of gravitation on the formation of fluctuations are generalized to the case of expanding systems. It is shown that in sufficiently large gravitating systems, the magnitude of the fluctuations increases with increasing dimensions of the system. Under certain conditions these fluctuations can become protogalaxies, protoclusters of galaxies, etc. (auth)

37929 WAVEGUIDE ANALOG OF TUNNELING THROUGH QUANTUM POTENTIAL BARRIERS. Campi, Morris (American Univ., Washington, D. C.). 34p. (CONF-651213-14). ORAU. Gmelin, AED-CONF-65-400-30.

Thesis. From American Physical Society, Winter Meeting in the West, Los Angeles.

The electromagnetic expressions for guided waves, which are analogous to the quantum mechanical equations representing barrier tunneling, are derived. This analogy is achieved by comparing the propagation constant of the Schroedinger time independent wave equation with that of the electromagnetic wave equation in waveguide, and by comparing the de Broglie wavelength of a particle to the wavelength of the propagated energy. This results in an expression relating the form of an arbitrary one dimensional energy barrier to the physical dimensions of a section of waveguide. The analogy is tested by the propagation of energy in the TE_{10} mode at both the 3 and 6 cm. bands for the two particular cases of the rectangular and hyperbolic barriers. Although evanescent modes are present at the discontinuous regions, the analog for the rectangular barrier, which is considered to be the worse case, is verified when an effective barrier length l_{eff}, of the order (1.2)l, is used. This experimental verification demonstrates the possibility of waveguide simulation of quantum mechanical energy barriers, the practicality of utilizing an electromagnetic analog for demonstrating the tunneling phenomena, and for measurements of the transmission coefficient through an arbitrarily shaped barrier. (auth)

37930 WIGNER DISTRIBUTION FUNCTIONS IN RELATIVISTIC QUANTUM MECHANICS. VOLUMES I AND II. Irving, Jack Howard. Princeton, N. J., Princeton Univ., 1965. 490p.

Thesis.

In 1932 Wigner suggested that the state of a non-relativistic quantum mechanical system could be represented by a real (though not everywhere positive) distribution function in phase space, which in many respects behaves like the classical distribution function of Gibbs. One remarkable property of the Wigner distribution function is that when multiplied by any classical dynamical variable (function of positions and momenta) and integrated over phase space, it yields the expectation value of the quantum operator corresponding (via the Weyl correspondence) to that classical observable. These concepts are extended to the realm of single-particle relativistic wave mechanics. The non-relativistic theory is reviewed and extended to include a charged particle in an external electromagnetic field. A gauge invariant generalization of the Weyl correspondence is suggested, and from the requirement that the described integral over phase space yield the expectation value, a gauge invariant generalization of the Wigner distribution function is derived. Distribution functions for both the Klein-Gordon (spin zero) and Dirac (spin $\frac{1}{2}$) massive particles are then defined and studied. (TCO)

37931 REGULARITY CONDITIONS IN RELATIVISTIC WAVE MECHANICS. Sanders, Steven Gill. Columbia, S. C., Univ. of South Carolina, 1965. 63p.

Thesis.

Solutions of the Dirac and Sakata-Taketani equations for spherically symmetric potentials are examined in the vicinity of the origin. It is shown that the requirement that a solution be finite at all points of space is too restrictive to be useful as a regularity condition. The consequence of requiring only that the solutions be integrable is examined. In problems with sufficiently singular potentials this condition leads to more than one solution being acceptable at the origin. The presence of too many acceptable solutions at the origin leads to a non-unique energy spectrum. A new condition, obtained from the requirement that the momentum operator $-i\vec{\nabla}$ must be self-adjoint, is then introduced. Because this condition leads to the Dirac condition for the Schrödinger theory, it is called the extended Dirac condition. The application of this condition to the relativistic wave equations for particles possessing the electron's charge e, in a Coulomb field due to a source charge –Ze (where Z is an integer), avoids the ambiguity difficulties associated with the integrability requirement. It does this by rejecting all the solutions obtained for $Z\alpha \geq s + \frac{1}{2}$ (where α is the fine structure constant and s is the spin of the particle, 0, $\frac{1}{2}$, or 1). The difference between these results and those obtained by K. M. Case is discussed and it is concluded that the solutions for high Z accepted by Case must be rejected. In addition, it is noted that the mathematical similarity of the relativistic Coulomb problem and the non-relativistic $1/r^2$ problem is not complete since the Dirac condition is not strong enough to eliminate the ambiguity difficulties for the $1/r^2$ equation even though the extended Dirac condition is strong enough to take care of the ambiguity difficulties for the relativistic Coulomb problem. (Dissertation Abstr.)

37932 SOURCE DYNAMICS FOR ASYMPTOTICALLY FLAT SPACE SOLUTIONS OF GENERAL RELATIVITY. Unti, Theodore Wayne Joseph. Pittsburgh, Univ. of Pittsburgh, 1964. 92p.

Thesis.

Two problems are considered: the behavior of the metric tensor and Weyl tensor for asymptotically flat outgoing radiation solutions to the empty space Einstein field equations, and appropriate definitions of the multipole moments of the source in terms of the physical components of the Weyl tensor. The strong analogy between gravitational theory and Maxwell theory was found useful in introducing these problems and outlining the approach. In the first of these problems, the basis for the calculations is the spinor-tetrad formalism developed by Newman and Penrose, in which the techniques of spinor calculus were used to derive a compact and useful set of equations fully equivalent to the empty space Einstein field equations. After choosing a coordinate system and tetrad, the field equations of Newman and Penrose are solved, subject to the boundary condition that the space-time approach flatness at infinity. This boundary condition, imposed on a physical component of the Weyl tensor, corresponds to the exclusion of incoming radiation of infinite duration. The boundary condition is specialized slightly, however, to allow outgoing quadrupole radiation as well as other properties. The asymptotic solutions, consisting of the metric, the time propagation equations, which show how the Weyl tensor varies from one null hypersurface to the next, and the remaining coordinate freedom is displayed and discussed. In the second problem, definitions for the multipole moments of the source as proposed in Janis and Newman are contrasted with definitions suggested by other authors. The definitions of Janis and Newman, which involve integrations of the Weyl tensor components over the sphere at infinity, were obtained by analogy with the results of linearized theory. The multipole moments so defined, while retaining the essential features of those given by other authors, have the added advantage that they can be measured in principle by the methods of geodesic deviation. A study is made of the source dynamics, using this concept of multipole structure, and some transformation properties of the multipoles are investigated. (Dissertation Abstr.)

37933 QUANTUM MECHANICS. Davydov, A. S. Addison-Wesley Series in Advanced Physics. Reading, Mass., Addison-Wesley Publishing Company, Inc., 1965. 691p. $14.75.

Translation from Kvantovaya Mekhanika by D. ter Haar.

The physical ideas and the mathematical formalism of the quantum theory of the nonrelativistic and quasi-relativistic (up to terms of order v^2/c^2) motion of a single particle in an external field are treated. In particular, the inapplicability of the concept of an essentially relativistic motion of a single particle is shown. Emphasis is placed upon representation theory, the theory of canonical transformations, scattering theory and quantum transition. A relatively detailed exposition is given of the theory of systems consisting of identical bosons and fermions. Several sections are devoted to the theory of molecules, the theory of chemical binding, and solid state theory. The theory of second quantization is used as a method to study systems consisting of a large number of identical particles. In particular, the basic ideas are given of the methods for quantizing the meson field, the electromagnetic field (without charges) and the electron-positron field, neglecting divergencies and renormalization. (L.B.S.)

Low Temperature Physics

Refer also to abstracts 37267, 37268, and 37473.

37934 (BNL–10380) HIGH FIELD SUPERCONDUCTING MAGNETS. Sampson, W. B. (Brookhaven National Lab., Upton, N. Y.). June 20, 1966. Contract AT(30-2)-Gen-16. 18p. (CONF-660436-1). Dep. mn. CFSTI $1.00 hy, $0.50 mn.

From Intermag Conference, Stuttgart, Germany.

Recently a better understanding of the effects of magnetic and thermal transients has led to techniques of superconducting magnet construction with large solenoids which are not subject to current degradation. These techniques are discussed with particular reference to very high-field solenoids (greater than 100 kG) and the possibilities presented by currently available superconductors are indicated. Applications to high-energy physics are considered and existing problems are reviewed. (W.D.M.)

37935 (CEA-R-2906) ETUDE DES SUPRACONDUCTEURS DU SYSTEME ALUMINIUM–MAGNESIUM. (Study of Superconductors in the Aluminium–Magnesium System). Bonnin, Bernard (Commissariat a l'Energie Atomique, Grenoble (France). Centre d'Etudes Nucleaires). 1966. 65p. Dep. mn.

Thesis. Submitted to Univ., Grenoble, France.

An apparatus for the measurement of the magnetization of superconducting alloys by the classical method of extraction was designed and built. Its originality is due to the employment of a cryostat having two helium baths. The lowest temperature reached by pumping on the innermost helium bath using a primary pump combined with a Booster pump was 0.75°K. Temperatures were determined with an aid of Hartshorn bridge. With this apparatus, it was possible to study the influence of extended defects on the irreversible behavior of the magnetization of aluminum–magnesium alloys. It was shown that the effect of these defects is important chiefly in the superconductor alloys of the second kind. The introduction of the extended defects was controlled by electron microscopy and by the measure of the residual resistivities. The critical fields H_c, H_{c1}, H_{c2}, the transition temperatures T_c, and the coefficients of the electronic specific heat γ were measured for these alloys. (auth)

37936 (CLM-R-60) THE PARAMAGNETIC LIMIT IN TYPE II SUPERCONDUCTORS. Hancox, R. (Culham Lab., United Kingdom Atomic Energy Authority, Abingdon (England)). May 1966. 10p. Dep. mn. BIS $0.30. HMSO 2s. 9d.

The critical field of a type II superconductor is reduced by the paramagnetic susceptibility of the normal phase. Theory and experiment are compared and it is shown that for high field superconductors the paramagnetic limit is 30 to 40% higher than is generally assumed. The temperature variation of the critical field is calculated, and used to estimate the critical field of the superconducting compound V_3Ga. (auth)

37937 MICROSCOPIC THEORY OF A NORMAL FERMI LIQUID AT ZERO TEMPERATURE. Tuttle, E. R. (Univ. of Denver); Mohling, F. Ann. Phys. (N. Y.), 38: 510-51 (July 1966).

The microscopic theory of a Fermi liquid formulated by Mohling and based upon the work of Lee and Yang is used to develop a quasi-particle theory of a Fermi liquid at zero temperature. The energy per particle, the particle momentum distribution, and the transformation function $\Delta(k)$ introduced by the Λ transformation are expanded through third order in the "two-quasi-particle reaction matrix" $g_1(k_1k_2 \mid k_3k_4)$. It is shown that the explicit expressions for the three quantities above satisfy the equations basic to Landau's phenomenological theory of a Fermi liquid term by term, provided $\Delta(k)$ is identified as the quasi-particle interaction energy. From this fact, it is concluded that the Λ transformation introduced by Mohling is actually a transformation from a particle representation to a quasi-particle representation of the system. This approach differs from previous efforts in the fact that the series being generated here is not a perturbation series. In fact, the explicit series obtained in this work bears a striking resemblance to that employed by Brueckner. This similarity is investigated in some detail. An extension of the Landau theory to encompass generalized interaction functions is made. This generalization, in conjunction with the explicit expression for the energy per particle, is then used to examine the "many-quasi-particle" potentials which appear in the Λ-transformed equations. (auth)

37938 STABILITY OF A SUPERCONDUCTING FILM. Arutyunyan, R. M. (Baikov Inst. of Metallurgy, Moscow. Central Physico-Technological Lab., Academy of Sciences, Armenian SSR). Izv. Akad. Nauk Arm. SSR, Ser. Fiz. Mat. Nauk, 18: No. 6, 71-9(1965). (In Russian).

The stability of the superconducting state in an ideal film without edges with a thickness of $2d \ll \delta_0(T)$, where $\delta_0(T)$ is the London penetration depth, is considered with a current and with a current in the presence of a magnetic field. The thermodynamic potential ϕ_s of a thin film in the superconducting state is found, and it is shown that the film is in a metastable state in the presence of a current near the transition from a superconducting state to a normal state. (TTT)

37939 HIGH-VOLTAGE PULSE CHARACTERISTICS OF SUPERCONDUCTING TRANSMISSION LINES. Cummings, A. J.; Wilson, A. R. (Edgerton, Germeshausen and Grier, Inc., Las Vegas, Nev.). J. Appl. Phys., 37: 3297-3300(July 1966). (EGG–1183-1164).

Results of high-voltage pulse tests on subminiature, superconducting coaxial delay lines are described. The results show these cables are capable of transmitting 15-kv, 4.0-μsec-long pulses of nanosecond risetimes. The cables were fabricated from both pure and alloyed metals. (auth)

37940 THERMAL CONDUCTIVITY OF SECOND-KIND SUPERCONDUCTOR In–Pb ALLOYS. Mamiya, Takayoshi (Tohoku Univ., Sendai). J. Phys. Soc. Jap., 21: 1032-6 (June 1966).

The thermal conductivity of three specimens of indium–lead alloys, which belong to the second kind of superconductors, was measured as a function of temperature in magnetic fields, in which the specimens go through the mixed state at intermediate temperatures. In the mixed state there appears a minimum value of the thermal conductivity in the temperature variation as well as in the field variation. The measured thermal conductivity is in good agreement with that calculated from the magnetization by using an average energy gap model proposed by Dubeck et al.. (auth)

37941 NUCLEAR SPIN-LATTICE RELAXATION IN SUPERCONDUCTING NIOBIUM. Asayama, Kunisuke

(Osaka Univ.); Masuda, Yoshika. J. Phys. Soc. Jap., 21: 1459-60(July 1966).

Measurements of the nuclear spin-lattice relaxation time T_1 in niobium metal as a function of applied magnetic field in the temperature range of 1.40 to 1.26°K are reported. T_1 was measured by a pulse method using 90–180° pulse sequence of a constant frequency of 3 Mc/sec. The quadrupole effects which are caused by the crystal imperfections, dislocations, or adsorption of the oxygen atoms spread the resonance line over about 3000 gauss. Susceptibility measurements showed that all the samples used were in the superconducting state up to 10 kgauss at 1.4°K. (W.D.M.)

37942 FLUX FLOW IN TYPE-II SUPERCONDUCTORS WITH DIFFERENT FIELD ORIENTATIONS. Staas, F. A.; Druyvesteyn, W. F. Philips Res. Rep., 21: 153-62(June 1966).

Experiments are reported on current-carrying type-II superconductors in the form of a sheet in a magnetic field H. Longitudinal voltages, transverse voltages and critical currents were measured while the orientation of the magnetic field with respect to the sheet and the current was varied. The resistivity in the mixed state is found to be anisotropic for a range of field orientations, whereas the resistivity in the normal state is isotropic. This anisotropic behavior in the mixed state is a direct consequence of the motion of the flux lines. For some special orientations of H it is found that the electric transverse to the current is larger than the electric field in the direction of the current. The calculated ratio of these electric fields is in agreement with the experiments. The dependence of the critical current on the orientation of H does not obey a "Lorentz-force" concept, i.e., $J \times H$ = constant. (auth)

37943 HEIGHT DEPENDENCE AND FINE STRUCTURE OF HELIUM FILM TRANSFER RATES. Allen, J. F.; Armitage, J. G. M. (St. Andrews Univ., Scotland). Phys. Lett., 22: 121-2(Aug. 1, 1966).

The film transfer rate of a glass beaker under conditions of strict cleanliness and minimization of vibration can be described by $\sigma(H,T) = 6.5(\rho s/\rho)H^{-\frac{1}{2}}\ 10^{-5}\ cm^2/sec$, where H is the height of the beaker rim above the beaker level. (auth)

37944 LIFETIME OF VORTEX PAIRS IN SUPERCONDUCTORS. Clem, J. R. (Univ. of Maryland, College Park). Phys. Lett., 22: 125-6(Aug. 1, 1966).

The motion of a vortex pair in a superconductor is examined and the lifetime of the pair calculated. (auth)

37945 THE RESISTIVE BEHAVIOR OF A TYPE-II SUPERCONDUCTOR ON REVERSING THE CURRENT. Druyvesteyn, W. F.; Niessen, A. K.; Staas, F. A. (Philips Gloeilampenfabrieken, Eindhoven, Netherlands). Phys. Lett., 22: 127-8(Aug. 1, 1966).

The resistivity of a sheet of type II superconductor, which is made asymmetric by plating one surface with a normal metal is found to depend on the polarity of the current or the magnetic field. (auth)

37946 THEORY OF DILUTE MIXTURES OF ^{3}He IN LIQUID ^{4}He AT LOW TEMPERATURES. Emery, V. J. (Brookhaven National Lab., Upton, N. Y.). Phys. Rev., 148: 138-45(Aug. 5, 1966). (BNL-10060).

Dilute mixtures of ^{3}He in liquid ^{4}He are regarded as a set of ^{3}He atoms interacting with elementary excitations of the ^{4}He. The coupling between the ^{3}He and the ^{4}He is chosen phenomenologically and it is not weak but, for low temperatures, its main effects may be eliminated by means of two canonical transformations. The equations which determine the transformations describe the motion of a ^{4}He excitation in the presence of one or two ^{3}He atoms and, in the latter case, they resemble Faddeev's equations in the three-body problem. At low temperatures, there are few ^{4}He excitations and many of the properties of the mixture are determined by the effective ^{3}He hamiltonian produced by the transformation. In this respect, the system behaves like a Fermi liquid. The ^{3}He–^{3}He potential is essentially momentum-independent and consists of the Van der Waals interaction together with an effectively repulsive potential induced by the ^{4}He. It is suggested that a Fermi-liquid analysis is the best way of obtaining information about this potential, and the possible existence of a fermion superfluid phase transition is discussed from that point of view. (auth)

37947 BEHAVIOR OF IONS AND QUANTIZED VORTEX RINGS OF LOW ENERGY IN HELIUM II AROUND 0.3 DEG K. Meyer, Lothar (Univ. of Chicago). Phys. Rev., 148: 145-50(Aug. 5, 1966).

Quantized vortex rings of low energy down to 0.1 ev were produced in specially purified liquid helium at 0.3°K and the deflection of rings of 0.15- to 0.5-ev energy in a transverse magnetic field measured. In the same apparatus the Hall mobility of positive ions was measured at 0.3°K, yielding after extrapolation to zero electric field a value $\mu = 3.0 \times 10^4\ cm^2\ V^{-1}\ sec^{-1}$. The drift velocity of ions can reach 40 m sec^{-1} before vortex rings are produced, also at 0.3°K. (auth)

37948 ATTENUATION OF LONGITUDINAL ACOUSTIC WAVES IN TYPE-II SUPERCONDUCTORS. Cooper, L. N.; Houghton, A.; Lee, H. J. (Brown Univ., Providence). Phys. Rev., 148: 198-211(Aug. 5, 1966).

The attenuation of longitudinal sound waves in a superconductor with a spatially dependent energy gap is studied by a Green's-function method. In order that explicit expressions for the ultrasonic loss may be derived, the calculation is restricted to temperatures $T \sim T_c$, the transition temperature. The results of the calculation are used to study ultrasonic attenuation in a type-II superconductor near T_c, which contains a low density of flux lines, $H \sim H_{c1}$. It is assumed that under these conditions the flux tubes in the material are fixed, are well separated, and form a periodic array. It is then shown that not only is the attenuation anisotropic, but anomalous absorption or transmission takes place whenever the sound wavelength matches the distance between vortices. Although the above theory is only for $T \sim T_c$ and $H \sim H_{c1}$, it is expected that this effect will exist over wider ranges of temperature and magnetic field, and, if accessible to experiment, will yield a direct measure of the spacing of flux lines in type-II superconductors. (auth)

37949 CRITICAL MAGNETIC FIELD AND TRANSITION TEMPERATURE OF SYNTHETIC HIGH-FIELD SUPERCONDUCTORS. Watson, J. H. P. (Corning Glass Works, N. Y.). Phys. Rev., 148: 223-30(Aug. 5, 1966).

Measurements of the critical field $\hat{H}$ and transition temperature $\hat{T}$ of superconducting indium in porous glass were made using a low-frequency mutual-inductance technique. The pore sizes of the glasses are well characterized, so that 96% of the pore volume is within ±10% of the mean pore diameter d. Pore diameters from 65 to 250 Å were used. Below $t\ (\equiv T/\hat{T}) = 0.5$, $\hat{H}$ can be represented approximately by $\hat{H} = (3415 \pm 40)\ (1 - t^2)/d^{(1.00 \pm 0.14)}$, where $\hat{H}$ is in kilo-oersteds and d is in Angstrom units. This is in agreement with the predictions of de Gennes and Maki of H_{c2} for type II superconductors in the dirty limit, assuming that the electronic mean free path is proportional to d. Above t = 0.6, there are deviations from de Gennes's prediction for the d dependence and the t dependence of $\hat{H}$. For the small pore sizes the temperature dependence of $\hat{H}$ is qualitatively similar to the Abrikosov prediction of H_{c2} for type II superconductors; however, near t = 1 for the largest pore size the temperature dependence of $\hat{H}$ is similar to that for a type I superconductor. The superconducting transition temperature $\hat{T}$ shows a strong dependence upon d, so that $\hat{T}$ (65 Å) is 4.23°K compared with 3.4°K for the bulk indium. The dependence of $\hat{T}$ on d is conveniently represented by $\hat{T} - T_{bulk} = 1 - 0.0028\ d$, where d is in Angstrom units. The change in $\hat{T}$ may be due to strain, mean-free-path, or surface effects. The samples are similar to inhomogeneous type II superconductors in their magnetic properties, showing hysteresis and flux jumping. (auth)

37950 Nb-25Zr IN STRONG MAGNETIC FIELDS: MAGNETIC, RESISTIVE, ULTRASONIC, AND THERMAL BEHAVIOR. Neuringer, L. J.; Shapira, Y. (Massachusetts Inst. of Tech., Cambridge). Phys. Rev., 148: 231-46(Aug. 5, 1966).

Measurements of the magnetization, electric resistance, ultrasonic attenuation and velocity, and the temperature variation resulting from flux jumps were carried out on Nb–25% Zr in d-c magnetic fields up to 100 kG. The values of the upper critical field H_{c2} obtained from magnetization, resistance, and ultrasonic measurements are compared with each other. The temperature variation of H_{c2} over the interval $1.5°K \leq T \leq T_c$, where $T_c = 10.8°K$, was determined from resistance measurements and the data are compared with the predictions of Maki's theory. It is found that the effects of the Pauli spin paramagnetism on the magnitude and temperature variation of the bulk upper critical field are smaller than those calculated from the theory of Maki. The effects of a magnetic field on the ultrasonic velocity and attenuation in the mixed and normal states of Nb–25% Zr are explained on the basis of the phenomenological theory of Alpher and Rubin. This theory accounts quantitatively for: the attenuation edge of shear and longitudinal waves at H_{c2}, the abrupt change in the velocity of shear waves at H_{c2}, and the effect of a magnetic field on the attenuation of longitudinal and shear waves in the normal state. The Alpher–Rubin theory, although originally derived for impure metals in the normal state, also gives a good description of the behavior of ultrasonic waves in the megacycle range propagating in the mixed state if the electric conductivity is taken to be infinite. At higher ultrasonic frequencies, however, deviations from the theory appear in the mixed state. If these deviations are to be explained within the framework of the Alpher–Rubin theory, one must postulate the existence of a finite effective a-c resistance, in the mixed state, which is operative at these high frequencies. The data suggest that this a-c resistance arises from viscous motion of the flux lines and that it is closely akin to the d-c flow resistance. Observations of heating spikes and abrupt changes in the ultrasonic attenuation, which occur in one-to-one correspondence with flux jumps, are reported. Two of the salient features of the observed flux jumps, and the concomitant heating spikes, are their repetitive occurrence at fixed intervals of the magnetic field and the decrease in their relative spacing when the temperature of the sample is lowered. These features are discussed in light of the recent theory of Swartz and Bean for magnetic instabilities in the mixed state of high-field superconductors. (auth)

37951 PAULI SPIN AND SPIN-ORBIT EFFECTS IN THE MAGNETIZATION OF A SUPERCONDUCTING Ti–Mo ALLOY. Cape, J. A. (North American Aviation Science Center, Thousand Oaks, Calif.). Phys. Rev., 148: 257-63(Aug. 5, 1966).

Results are given for some detailed measurements on the upper critical field H_{c2}, and on the relative slope of the magnetization curve $\chi_s \equiv [(\partial M - M_s)/\partial H]_{H_{c2}}$ for the high-field ($\kappa_G \approx 65$) superconductor Ti–16 at. % Mo. The data on the temperature dependence of H_{c2} and χ_s are shown to be in excellent agreement with recent theories in which Pauli spin paramagnetism and spin-orbit scattering were included in Gor'kov's equations. It is observed that the H_{c2} values at $T \ll T_{c0}$ are smaller than expected for the spin-independent case (no paramagnetic effects) and larger than expected if spin paramagnetism is allowed for but spin-orbit scattering is not. The parameter $\kappa_2 \propto \chi_s^{-\frac{1}{2}}$ is found to decrease with decreasing temperature, in contrast to the case of non-"paramagnetically-limited" type-II superconductors, where κ is observed to increase with decreasing T. When one uses the calculated (from resistivity and specific-heat data) value of 1.75 for the Pauli spin parameter ($\alpha = 3\hbar/2mlv_F$), the experimental points and the theoretical curves for $H_{c2}(T)$ are brought into excellent agreement by the proper choice of a single parameter, τ_{so}, the phenomenological spin-orbit scattering time. For the same value of τ_{so}, the agreement for κ_2 is not so good. The critical-field curve cannot be fitted unless spin-orbit coupling is taken into account. (auth)

37952 STRONG-COUPLING SUPERCONDUCTIVITY. I. Scalapino, D. J.; Schrieffer, J. R.; Wilkins, J. W. (Univ. of Pennsylvania, Philadelphia). Phys. Rev., 148: 263-79(Aug. 5, 1966).

The pairing theory of superconductivity is extended to treat systems having strong electron-phonon coupling. In this regime the Landau quasiparticle approximation is invalid. In the theory phonon and Coulomb interactions are treated on the same basis and the analysis is carried out using the nonzero-temperature Green's functions of the Nambu formalism. The generalized energy-gap equation thus obtained is solved (at T = 0°K) for a model which closely represents lead and the complex energy-gap parameter $\Delta(\omega)$ is plotted as a function of energy for several choices of phonon and Coulomb interaction strengths. An expression for the single-particle tunneling density of states is derived, which, when combined with $\Delta(\omega)$, gives excellent agreement with experiment, if the phonon interaction strength is chosen to give the observed energy gap Δ_0 at zero temperature. The tunneling experiments therefore give a detailed justification of the phonon mechanism of superconductivity and of the validity of the strong-coupling theory. In addition, by combining theory and the tunneling experiments, much can be learned about the electron-phonon interaction and the phonon density of states. The theory is accurate to terms of order the square root of the electron-ion mass ratio, $\sim 10^{-2}$–10^{-3}. (auth)

37953 MAGNETIZATION AND CRITICAL FIELDS OF SUPERCONDUCTING $SrTiO_3$. Ambler, E.; Colwell, J. H.; Hosler, W. R.; Schooley, J. F. (National Bureau of Standards, Washington, D. C.). Phys. Rev., 148: 280-6(Aug. 5, 1966).

Magnetization curves from T = 0.15°K to T_c were measured for two specimens of semiconducting $SrTiO_3$ of electron density about 10^{20} cm^{-3}. Magnetic hysteresis was observed in each case. The temperature dependences of the first and second critical fields were measured and compared with the derivations of Maki. The heat capacity was measured down to 0.3°K for one specimen, yielding γ, the coefficient of the linear term, and an independent value of T_c at the upper part of the specific-heat anomaly. The Ginzburg-Landau κ is shown to vary inversely with the electronic mobility. (auth)

37954 FLUX TRAPPING OF rf FIELDS IN SUPERCONDUCTORS. Haden, C. R.; Hartwig, W. H. (Univ. of Texas, Austin). Contract DA-36-039-AMC-00036(E). Phys. Rev., 148: 313-17(Aug. 5, 1966).

Measurements on superconductive resonant circuits in the frequency range of 10–1000 Mc indicate that flux trapping of the r-f magnetic fields is responsible for a residual loss, not predicted by surface-resistance theories. A simple model, based on flux trapping at local sites, predicts such a loss for both type I and type II materials. The surface resistance due to flux trapping is shown to be proportional to frequency, the density of trapping centers, the penetration depth, and a "threshold" function of the r-f magnetic field. Experimental data are given for several materials, verifying the salient features of the model. It is also concluded that the flux-trapping centers are of a common nature. (auth)

37955 EFFECT OF TRANSITION-METAL IMPURITIES ON THE CRITICAL TEMPERATURE OF SUPERCONDUCTING Al, Zn, In, AND Sn. Boato, G.; Gallinaro, G.; Rizzuto, C. (Univ., Genoa). Phys. Rev., 148: 353-61(Aug. 5, 1966).

The depression in critical temperature T_c of several dilute solid solutions of transition elements in Al, Zn, In, and Sn was measured as a function of residual resistivity and concentration. In Zn–Mn and Zn–Cr, localized moments are present and T_c decreases linearly with concentration with a slope $-dT_c/dc$ of 315 and 170°K/at. %, respectively. By comparing these numbers with theory, a value of about 1.4 ev was found for the s-d exchange integral. In all other alloys, the critical temperature is still depressed but much less than in Zn–Mn and Zn–Cr, and the depression becomes less rapid with increasing concentration of impurities. However, no saturation is found up to the maximum concentrations reached. The effect here found is different from that taking place in dilute al-

loys containing nontransition metals in that the depression of T_c is larger, giving rise to suppression of superconductivity at sufficiently high impurity concentration. An analysis of the data for Al–Mn, Al–Cr, Al–Fe, Zn–Fe, Zn–Co, and Zn–Ni shows that in these systems the observed decrease of T_c is satisfactorily accounted for by the smoothing out of the gap anisotropy and by the formation of localized virtual states, whose effect on the superconducting properties was studied theoretically by Zuckermann. In–Mn and Sn–Mn do not fit the foregoing picture; however, the results obtained rule out the presence of magnetic moments in these two systems in bulk form. The apparent contrast with the results obtained in thin films is discussed. Some results on ternary alloys are also reported. It is shown that no effect on the critical temperature of In–Mn dilute solutions is produced by the addition of Pb. (auth)

37956 EFFECT OF PAULI PARAMAGNETISM ON MAGNETIC PROPERTIES OF HIGH-FIELD SUPERCONDUCTORS. Maki, Kazumi (Univ. of California, San Diego, La Jolla). Phys. Rev., 148: 362-9(Aug. 5, 1966).

The magnetic properties of type-II superconductivity having a large Pauli term are studied. Firstly restriction is made to the case where the spin-orbit scattering is absent. In this case the transition changes at low temperatures from second to first order for $\alpha = 3\mu/\tau_{tr}v^2e \geq 1$, where μ, τ_{tr}, and v are the Bohr magneton, the transport collision time, and the Fermi velocity, respectively. This involves a revised calculation of the parameter $\kappa_2(t)$, which appears in the expression for the magnetization. The calculation of $\kappa_2(t)$ in earlier work was incorrect, as was recently pointed out by de Gennes and co-workers. Secondly, the theory is extended to include the effect of spin-orbit scattering, which may be important in the materials usually considered. In particular, expressions for the parameters $\kappa_1(t)$ and $\kappa_2(t)$ are obtained explicitly in the limit of short spin-orbital mean free path, where $\kappa_1(t) = H_{c2}(t)/\sqrt{2}H_c(t)$, and $H_{c2}(t)$, $H_c(t)$ are the upper critical field and the thermodynamical critical field, respectively. It is shown that in this limit the transition is always second order, independent of temperature. (auth)

37957 TRANSVERSE ULTRASONIC ATTENUATION IN GAPLESS SUPERCONDUCTORS. Maki, Kazumi (Univ. of California, San Diego, La Jolla). Phys. Rev., 148: 370-5(Aug. 5, 1966).

The calculation of the ultrasonic attenuation coefficient of the transverse waves in the gapless superconductors, such as type-II superconductors in a high magnetic field is presented. Particular attention is paid to the electromagnetic absorption term, which is important in the case considered, and the result obtained is a simple generalization of that due to Kadanoff and Falko. Ultrasonic attenuation in type-II superconductors as well as in a superconducting surface sheath in a field above H_{c2} is discussed. (auth)

37958 EFFECTS OF NONMAGNETIC IMPURITIES UPON ANISOTROPY OF THE SUPERCONDUCTING ENERGY GAP. Clem, John R. (Univ. of Illinois, Urbana). Contract DA-31-124-ARO(D)-114; AF 735-65. Phys. Rev., 148: 392-401(Aug. 5, 1966).

The influence of the presence of nonmagnetic impurities upon the anisotropy of the superconducting energy-gap parameter is considered. Using a factorable BCS-like model for the effective electron-electron matrix element, $V_{pp'} = (1 + a_p)\, V(1 + a'_p)$, within the context of an earlier theory by Markowitz and Kadanoff, it is shown that when impurities are present the wave-vector-dependent gap parameter Δ_p is replaced by a complex, wave-vector- and energy-dependent gap parameter $\Delta(p,\omega) = \Delta_1(\omega) + a_p\Delta_a(\omega)$. The behavior of $\Delta_1(\omega)$ and $\Delta_a(\omega)$ is extensively examined as a function of impurity concentration; it is found, for example, that the magnitude of the anisotropic part $\Delta_a(\omega)$ of the gap parameter tends to zero in the limit of large impurity concentration. A model calculation, assuming a rectangular shape for the anisotropy distribution function P(a), illustrates the behavior for small and moderate impurity concentrations. The behavior for large impurity concentrations is found to depend, to lowest order, only upon the mean-squared anisotropy $\langle a^2 \rangle$. The behavior of the effective density of states is also examined; it is shown to become isotropic as the impurity concentration increases. The precise shape of the effective density of states for energies near the gap is obtained for the large-impurity-concentration limit. Experimental manifestations of the reduction of the anisotropy by impurity scattering are briefly discussed. (auth)

37959 ISOTOPE EFFECT IN SUPERCONDUCTING ZINC. Fassnacht, R. E.; Dillinger, J. R. (Univ. of Wisconsin, Madison). Phys. Rev. Lett., 17: 255-7(Aug. 1, 1966). (COO–1098-14).

Results of measurements on isotope effects in superconducting zinc are reported, which indicate a marked reduction in the value of z in $T_c \alpha M^{-z}$, where T_c is the zero-field transition temperature and M is the isotopic mass from the BCS value. (B.G.D.)

37960 PRESSURE DEPENDENCE OF THE RADIUS OF THE NEGATIVE ION IN HELIUM II. Springett, B. E.; Donnelly, R. J. (Univ. of Chicago). Phys. Rev. Lett., 17: 364-7(Aug. 15, 1966).

The pressure dependence of the radius of the negative ion in helium II is derived from measurements of trapping cross section in quantized vortex lines. (auth)

37961 THERMAL AND MAGNETIC PROPERTIES OF DILUTE SOLUTIONS OF ^{3}He IN ^{4}He AT LOW TEMPERATURES. Anderson, A. C.; Edwards, D. O.; Roach, W. R.; Sarwinski, R. E.; Wheatley, J. C. (Univ. of Illinois, Urbana). Contract AT(11-1)-1198. Phys. Rev. Lett., 17: 367-72(Aug. 15, 1966). (COO–1198-371).

Results are presented of measurements of the heat capacity, spin-diffusion coefficient, and nuclear susceptibility of two dilute solutions of ^{3}He in ^{4}He. It is shown that the ^{3}He in dilute solutions have several of the properties associated with a normal Fermi fluid. The measurements also form a quantitative basis for theories of the quasiparticle interactions and for predictions of a low-temperature cooperative state. (L.B.S.)

37962 INTERACTIONS BETWEEN ^{3}He ATOMS IN DILUTE SOLUTIONS OF ^{3}He IN SUPERFLUID ^{4}He. Bardeen, J.; Baym, G.; Pines, D. (Univ. of Illinois, Urbana). Contract ARPA SD-131. Phys. Rev. Lett., 17: 372-5 (Aug. 15, 1966).

The magnitude, sign, and momentum dependence of the effective interaction between ^{3}He atoms in superfluid ^{4}He are derived from the experimental data. Calculations of the Fermi-liquid parameters for the normal state of ^{3}He in solution yield results in agreement with experiment; the temperature for a superfluid transition associated with the ^{3}He is estimated to be $\sim 2 \times 10^{-6}$°K. (auth)

37963 SUPERCONDUCTING MIXED-STATE-STRUCTURE DETERMINATION IN VANADIUM BY NUCLEAR MAGNETIC RESONANCE AND RELAXATION. Fite II, Warner; Redfield, Alfred G. (Columbia Univ., New York). Phys. Rev. Lett., 17: 381-3(Aug. 15, 1966).

Line-shape measurements, which strongly suggest that the vortex structure in the mixed state of vanadium is triangular, and relaxation time measurements for nuclei both near and far from vortex lines are reported. Except near H_{c2} and T_c, the relaxation data are consistent with the assumption that far from vortex lines spins relax at the rate predicted for type-I superconductors by the BCS theory; and spins within a coherence distance of a vortex relax at roughly the same rate as the normal metal. (L.B.S.)

37964 EXPERIMENTAL EVIDENCE FOR A NEW NUCLEAR SPIN-LATTICE RELAXATION PROCESS IN TYPE-II SUPERCONDUCTORS AT LOW TEMPERATURES. Silbernagel, B. G. (Univ. of California, San Diego, La Jolla); Weger, M.; Wernick, J. E. Phys. Rev. Lett., 17: 384-6(Aug. 15, 1966).

The spin-lattice relaxation time (T_1) of the ^{51}V nuclei in the type-II superconductor V_3Si was measured. It was found that at temperatures far below the superconducting transition temperature, T_1 is appreciably shorter than expected

on the basis of the BCS theory of super conductivity. It is believed that the short T_1 observed is due to a spin-diffusion process, of the type proposed by Caroli and Matricon, from the quickly relaxing nuclei to be found in the fluxoid cores of such a type-II superconductor. (L.B.S.)

37965 EFFECT OF RARE-EARTH ADDITIONS ON THE PRESSURE DEPENDENCE OF THE SUPERCONDUCTING TRANSITION TEMPERATURE OF LANTHANUM. Smith, T. F. (Univ. of California, San Diego, La Jolla). Phys. Rev. Lett., 17: 386-90(Aug. 15, 1966).

The superconducting transition temperature for solid solutions of Gd, Pr, Yb, and Ce in lanthanum was measured as a function of pressure up to 10 kbar. The transition temperatures for La–Gd, La–Yb, and La–Pr, while depressed from that of pure lanthanum, exhibit positive pressure dependences. For the La–Pr alloys, $\delta T_c/\delta P$ is enhanced, the increment in slope being proportional to the Gd concentration. This enhancement is consistent with the Abrikosov-Gor'kov theory. The positive pressure dependence of La rapidly decreased with small percentage additions of cerium, resulting in a strong negative pressure dependence of T_c for alloys containing more than 1 at.% Ce. This behavior is attributed to the instability of the 4f electron of Ce. (L.B.S.)

37966 COMMENTS ON "DIRECT EVIDENCE OF FLUX MOTION." Meincke, P. P. M. (Bell Telephone Labs., Murray Hill, N. J.). Phys. Rev. Lett., 17: 390-2(Aug. 15, 1966).

An analysis is made of a two-dimensional analog of an experiment suggested by Pearl to demonstrate that potential differences in superconductors are due to moving vortices. A series of experiments were performed on lead, a lead–indium alloy, and magnetoresistive bismuth to check the validity of the analysis. The results showed an induced voltage in bismuth which was approximately the same as that observed in superconductors and that the voltage can be observed in fields up to several times the critical field. It is concluded that Pearl's experiment does not provide any more direct evidence of the emf produced by flux motion than the usual resistive-state experiment. (L.B.S.)

37967 SOME REMARKS ON THE THEORY OF SUPERCONDUCTIVITY. Bloch, Felix (Stanford Univ., Calif.). Phys. Today, 19: No. 5, 27-29; 32-3; 35-6(May 1966).

Superconductivity theory is discussed in an attempt to interpret some of the characteristic features in terms of general principles. This approach to the problem is compared with the theory of Bardeen, Cooper, and Schreiffer and the degenerate ideal Bose gas. (W.D.M.)

37968 THEORY OF THE SPECIFIC HEAT OF LIQUID ^{4}He ABOVE THE LAMBDA POINT. de Coen, J. L. (Univ. of Libre, Brussels); Tompa, H. Physica, 32: 995-1000 (May 1966).

The constant volume specific heat C_v of liquid helium-4 in random phase approximation above the λ point is calculated. Good qualitative agreement with the experimental curve is obtained both near the λ point and in the region where C_v has a minimum. (auth)

37969 CALCULATION OF a-c LOSSES IN A TYPE-II SUPERCONDUCTOR. Hancox, R. (United Kingdom Atomic Energy Authority, Abingdon, Eng.). Proc. Inst. Elec. Eng. (London), 113: 1221-8(July 1966).

A method of calculating a-c losses in a type II superconductor is discussed, which is applicable to a variety of simple problems. Equations are derived which should be useful in calculating the losses in electrical machines with superconducting windings. These equations show the dependence of the loss on the magnitude and direction of the magnetic field and on the magnitude and phase angle of the transport current. The mathematical assumptions and models involved are considered in detail, and a comparison is made of calculations using the London and Kim approximations to the relationship between critical current density and magnetic field. Finally, the calculated losses are compared with published experimental measurements. (auth)

37970 ALTERNATING CURRENT LOSSES AND MAGNETIC FIELD ABERRATIONS ASSOCIATED WITH USE OF HIGH FIELD SUPERCONDUCTING WIRE IN ADIABATIC DEMAGNETIZATION APPARATUS. Anderson, A. C.; Roach, W. R.; Sarwinski, R. E. (Univ. of Illinois, Urbana). Contract AT(11-1)-1198. Rev. Sci. Instrum., 37: 1024-9 (Aug. 1966). (COO-1198-331).

Experiments were conducted to determine a-c losses, principally near 10^5 cps, in coils and leads fabricated from high-field superconducting wires. The samples were placed in an environment similar to what might be experienced in actual use in a low-temperature experiment utilizing adiabatic demagnetization. The measurements showed that losses associated with the use of high-field superconducting wire could be less than for electric grade copper wire. Further experiments were then carried out to determine what aberrations of magnetic fields would be caused by the presence of high-field superconducting material. (auth)

37971 OPTIMUM CURRENT DISTRIBUTION IN SUPERCONDUCTING COILS. Williams, J. E. C. (Massachusetts Inst. of Tech., Cambridge). Rev. Sci. Instrum., 37: 1030-1(Aug. 1966).

A superconducting winding, sectioned and supplied with currents corresponding to the local field conditions, gives an increased field contribution over that of a single winding. The increased field contribution is derived in terms of the number of sections and the characteristics of the superconducting material. (auth)

37972 NUCLEAR MAGNETIC RESONANCE PROBE FOR CALIBRATING SUPERCONDUCTING SOLENOIDS. Rupp, L. W. Jr. (Bell Telephone Labs., Inc., Murray Hill, N. J.). Rev. Sci. Instrum., 37: 1039-41(Aug. 1966).

A cesium metal NMR probe, which can be used directly with a Varian fluxmeter at liquid helium temperatures, was developed. Such a device is generally useful in accurately calibrating magnetic fields to better than 1 G in the range 7600 to 60,000 G typical of currently available superconducting solenoids. (auth)

37973 SYSTEM FOR OBSERVING SMALL NONLINEARITIES IN TUNNEL JUNCTIONS. Adler, J. G.; Jackson, J. E. (Western Reserve Univ., Cleveland). Rev. Sci. Instrum., 37: 1049-54(Aug. 1966).

A system using a combination of harmonic detection and bridge techniques for the measurement of dV/dI and d^2V/dI^2 of superconducting tunnel junctions having resistances ranging from a few ohms to several thousand ohms is described. These quantities are of fundamental interest in the study of the density of electron states and phonon spectra of superconductors. This system is capable of determining $\sigma = (dV/dI)_n/(dV/dI)_s$, the relative dynamic conductance, where dV/dI is the dynamic resistance of the junction in the normal (n) and superconducting (s) state to within a few parts in 10^5. This high resolution is achieved using very small modulation levels of 60 μv rms (kT at 1°K = 86 μv rms) or less. Finally, circuitry for obtaining dI/dV in the region near the energy gap using extremely low modulation levels (5 to 10 μv rms) and capable of resolving the negative resistance region is also presented. Typical data obtained with this system are shown. (auth)

37974 NEW RESEARCH ON PROPERTIES OF LIQUID HELIUM. Pitaevskii, L. P. (Inst. of Physics Problems, Academy of Sciences, USSR). Usp. Fiz. Nauk, 88: 409-18 (Mar. 1966). (In Russian).

A review is presented of theoretical and experimental research carried out on liquid helium and superfluidity and by various workers in 1964-1965. The review does not claim to be exhaustive, and is limited to the papers which in the author's opinion are of greatest interest. The topics discussed are the energy spectrum of superfluid helium and its effect on superfluidity, vortex filaments and rings in liquid ^{4}He, the interaction between the vortices in the helium with ions, capture of ions by straight line vortex filaments, centripetal compression effects in liquid helium, density measurements, the question of superfluidity of ^{3}He at low temperatures, and the properties of liquid ^{3}He at temperatures that lie definitely outside the superfluidity range. (auth)

37975 JOSEPHSON TUNNELING EFFECT IN SUPERCONDUCTORS. Zharkov, G. F. (Lebedev Inst. of Physics, Moscow). Usp. Fiz. Nauk, 88: 419-38(Mar. 1966). (In Russian).

A review is presented on the tunneling of coupled electron pairs from the ground state (Fermi surface) of one superconductor to the Fermi surface of another through a thin insulating layer, first reported by B. Josephson. The treatment is restricted to bulk superconductors. Subjects treated are the general nature of the Josephson effect, a phenomenological description of the effect and the role played by the wave function of the superconductor in this description, derivation of the equations for the relation between the Josephson current and the binding energy, the influence of the presence of magnetic and electric fields, the influence of the transverse dimensions of the barrier, the Josephson current in barriers connected in parallel and other interference effects, and the nonstationary Josephson effect. In addition to reviewing briefly the contents of many published and unpublished papers dealing with the foregoing topics, mentions are made of papers dealing with other aspects such as the interpretation of the Josephson effect from the point of view of the Ginzburg-Landau theory, of the quasi-spin approach or of paramagnetic impurities in the superconductor, and some possible practical applications of the effect. (auth)

37976 NEW EXPERIMENTAL DATA ON THIN SUPERCONDUCTING FILMS. Maksimov, E. G. Usp. Fiz. Nauk, 88: 587-88(Mar. 1966). (In Russian).

A brief review was made of recent work reported in the Western literature on the superconductivity of thin films, and its dependence on various factors such as film thickness, oxidation of the surface, and others. The main feature considered is the increase in the critical temperature of a thin-film superconductor, compared with the bulk metal, brought about either by the reduction of thickness itself or by formation of a surface oxide coating over the film. Reference to Soviet papers is limited to consideration of the effect of surface superconductivity, and to mention of an alternate derivation of an expression for the critical temperature of a clean superconductor film. (auth)

37977 INVESTIGATION OF THE PROCESSES IN SUPERCONDUCTING FLUX PUMPS. Voigt, Hans (Siemens-Schuckertwerke AG, Erlangen, Ger.). Z. Naturforsch., 21a: 510-14(May 1966). (In German).

An essential process in the operation of a superconducting flux pump is the migration of a normal conducting region with a magnetic flux over a current-penetrable superconducting plate. The connected phenomena, especially voltage and current variation, were analyzed and led to a saturation current, a previously unknown contribution to the losses of a flux pump. The results are compared with experiments. (tr-auth)

37978 A METHOD FOR OBTAINING LOW TEMPERATURES BASED ON DISSOLUTION OF ^{3}He IN ^{4}He. Neganov, B.; Borisov, N.; Liburg, M. (Joint Inst. for Nuclear Research Dubna, USSR). Zh. Eksp. Teor. Fiz., 50: 1445-57 (June 1966). (In Russian).

A method for obtaining low temperature steady state is described which is based on continuous dissolution of liquid ^{3}He in liquid ^{4}He and subsequent continuous separation of the isotopes at an higher temperature. At a ^{3}He circulation rate of about 1.84×10^{-4} mole/sec a témperature of 0.1°K can be maintained at a heat supply of 1800 erg/sec. In the absence of a heat flow the solution temperature can be maintained at 0.055°K. Under fixed external conditions the temperature variations do not exceed 0.001°K. (auth)

37979 MOTION OF ABRIKOSOV LINES UNDER THE ACTION OF AN ELECTRIC FIELD AND THE MECHANISM OF ENERGY DISSIPATION IN HOMOGENEOUS SUPERCONDUCTORS. Kulik, I. O. (Inst. of Physics and Tech. of Low Temperatures, Academy of Sciences, Ukrainian SSR). Zh. Eksp. Teor. Fiz., 50: 1617-30(June 1966). (In Russian).

A theory of "resistive" effects in superconductors of the second kind near the upper critical field H_{c2} is developed. The analysis is based on an application of the time-dependent Ginzburg-Landau equations. A phenomenological deduction of similar equations is presented. If the normal (nonsuperconducting) current is not taken into account the equations permit the existence of quasiequilibrium superconducting states in crossed electric and magnetic fields; these states correspond to motion of Abrikosov lines in a direction perpendicular to E and H. The upper critical field H_{c2} is a function of the electric field strength; however, for superconducting metals or alloys the effect of variation of H_{c2} with E is very small. It is shown that the resistive effects in superconductors should be accompanied by high frequency energy emission (due to the motion of the periodic line structure). Irradiation of a superconductor in the mixed state by an external high frequency field should change the shape of the volt-ampere curve when $H < H_{c2}$. (auth)

37980 SUPERCONDUCTING TRANSITION TEMPERATURE OF A THIN FILM. Kresin, V. Z.; Tavger, B. A. (Moscow State Correspondence Pedagogical Inst.). Zh. Eksp. Teor. Fiz., 50: 1689-98(June 1966). (In Russian).

It is shown that the usual electron-phonon interaction leads to a growth of the critical temperature with decrease of the film thickness L. This is due to the special nature of electron pairing. The growth of T_k is especially great for $L \sim 10^{-6}$ cm; with further decrease of L ($L \approx 10^{-7}$cm) the dependence becomes exponential. The results describe the experimental data. The correctness of this interpretation can be confirmed by measurements of the isotopic effect. The possibility of an electron mechanism due to the presence of different electron groups in the film is also considered. (auth)

37981 NEGATIVE IONS IN LIQUID HELIUM II. Burdick, Boyce. New Haven, Yale Univ., 1965. 64p.

Thesis.

Two models have been proposed for the negative ion in liquid helium II: the free electron model and the self-trapped electron or bubble model. The free electron model was investigated in order to compare it to the bubble model discussed by other investigators. To investigate the properties of a free electron moving in liquid helium, the model of an electron propagating in a periodic lattice is used for calculation from first principles. The wave equation is written for the scattering of a particle of energy k^2 by a lattice of pseudopotentials representing the electron-helium interaction. Only the S-wave, low-energy term of the pseudopotential is retained. The ground state wave function of the electron is Fourier-analyzed using as a basis vectors reciprocal to the space lattice vectors. An integral representation for the Fourier coefficients is introduced and an Ewald transformation is performed yielding sums which are rapidly convergent. The application of the boundary condition at the surfaces of the hard cores yields an algebraic equation for k^2. If the wave function is generalized to a Bloch wave function with nonzero wave vector, the same analysis is performed and the reciprocal mass tensor is calculated. Expressions are obtained for both Bravais lattices and lattices with a basis. The energy of the free electron is found to be larger than that of the bubble and is used to justify the formation of an electron bubble in liquid helium. It is concluded that negative ions in liquid helium II are self-trapped electrons. (Dissertation Abstr.)

37982 HEAT CAPACITY OF ADSORBED HELIUM. Goodstein, David Louis. Seattle, Univ. of Washington, 1965. 132p.

Thesis.

Measurements were made of the heat capacity of submonolayer quantities of ^{3}He and ^{4}He adsorbed on an argon-coated copper sponge in the temperature range 0.25° to 4°K. The results show a qualitative change of behavior at a coverage of about 0.5 layers. Above 0.5 layers the heat capacities are proportional to T^2 with coefficients proportional to the mass of the isotope, results consistent with a picture of a two-dimensional Debye medium. Below 0.5 layers the molar heat capacity is larger in magnitude and

more complicated in behavior, a result that may be interpreted as representing a condition of equilibrium between a condensed and an expanded phase. (Dissertation Abstr.)

37983 THERMAL TRANSPORT IN HELIUM CRYSTALS. Berman, Bernard Theodore. Durham, N. C., Duke Univ., 1965. 185p.

Thesis.

The thermal conductivity of solid helium was measured at molar volumes of 19.5 cc/mole and 20.2 cc/mole from 0.5°K to the melting temperatures. These measurements were made on pure ^4He and ^3He, and mixtures of each in the other of approximately 1%, 4%, 10%, and 50%. The blocked capillary technique was used allowing measurements to be made as a function of temperature at constant volume. The hcp phase pure samples showed the characteristic thermal conductivity maximum just below 1°K. Below the peak the conductivity is characteristic of boundary scattering with a T^3 dependence and a relaxation time related to the geometry of the sample. The conductivity above the peak varies exponentially with 1/T over about three orders of magnitude; this is characteristic of Umklapp scattering. The bcc phase of ^3He shows a double exponential variation with 1/T. Measurements were also made on the bcc phase of ^4He. In the mixtures, small concentrations of isotopic impurity depress the conductivity about a factor of fifty below 1°K. The conductivity is not found to be proportional to c(1-c), where c is the isotope concentration, indicating normal processes must play a significant role. The data are analyzed using the phenomenological theory of Callaway, which takes the effect of normal processes into account. (Dissertation Abstr.)

37984 TRANSPORT PROPERTIES OF DEGENERATE FERMION SYSTEMS. Rothwarf, Allen. Philadelphia, Univ. of Pennsylvania, 1964. 157p.

Thesis.

In Part I the transport phenomena in degenerate Fermion systems at finite temperatures are considered. Starting from formal expressions for the transport coefficients in terms of the correlation functions of the currents involved (Kubo's equations), the expressions are transformed to a form involving the two-particle Green's function. The two-particle Green's function is then expanded in terms of the one-particle Green's function and the vertex part. For a pure system with no interactions other than the particle-particle interaction, the expected results that the static electrical conductivity be infinite while the thermal conductivity remains finite are demonstrated by solving the integral equation for the vertex part. For an interacting system with impurities present it is shown that the particle-particle decay rate does not occur in the expression for the electrical conductivity while it does occur in the thermal conductivity. The Wiedemann-Franz law is thus not true for the interacting system. By going beyond the very low-temperature approximations the results can be applied to the transport properties of ^3He. In Part 2 the decay rate of an electron injected into a superconductor is calculated for the process in which the electron emits a phonon and forms a Cooper pair with one of the already present electrons. The transition probability consists of a normal term in which the lattice plays no essential role and an Umklapp term in which the lattice as a whole can take up some crystal momentum. It was found that the Umklapp process dominates the decay rate. At a temperature of 1.44°K the lifetime of the injected electron was calculated as 1.67×10^{-8} sec. (TCO)

37985 SUPERCONDUCTIVITY OF LANTHANUM AND SOME GOLD-RICH INTERMETALLIC COMPOUNDS. Hamilton, David Carpenter. La Jolla, San Diego, Calif., Univ. of California, 1965. 83p.

Thesis.

The superconductivity of La is discussed, and it is pointed out that one reason for rewriting the periodic table so that Sc, Y, and Lu are in the same column and La is classed with the rare earths is that La is superconductive and Sc, Y, and Lu are not. Some new superconducting compounds are described. These compounds, with transition temperatures in degrees Kelvin, are the following: $AlAu_4$, 0.4–0.7°; Al_2La, 3.2°; Al_2Pt, 0.55–0.48°; Au_5Ca, 0.34–0.38°; AuGa, 1.2°; AuIn, 0.6–0.4°; Au_2Pb, 1.18°; Au_5Sn, 1.1–0.7°; AuSn, 1.25°; $IrSn_2$, 0.65–0.78°; PtSn, 0.37°. The measurements were made by standard techniques. Some remarks on the possibility that Au might be superconducting are included. In an appendix, the superconductivity of a high-pressure form of Zr is discussed. (TCO)

37986 INSTRUMENTATION USING QUANTUM INTERFERENCE IN SUPERCONDUCTORS. Zimmerman, J. E. (Ford Motor Co., Dearborn, Mich.). 24p. (CONF-650813-2). ORAU. Gmelin, AED-CONF-65-216-7.

From 6th Biennial Gas Dynamics Symposium, Evanston, Ill.

Recent investigations of quantum effects in weakly coupled superconductors have established the concept of a superconductor as a system of conduction electrons whose wave function is phase-coherent over large distances. The supercurrent density flowing between two coupled superconductors is a function of the quantum-mechanical phase shift across the coupling. Since the phase shift itself is a line integral of the canonical momentum $2(mv + eA)$, integration over the coupling area leads to interesting periodic relationships between the critical supercurrent and the parameters which determine the momentum, such as magnetic field, velocity, and electrostatic and gravitational potentials. At least three experimental techniques of weak coupling were developed, namely the insulating barrier or Josephson junction, the thin-film bridge, and the point contact between bulk superconductors. These techniques, and the observed interference effects, provide the basis of a number of useful laboratory instruments. Applications to magnetometry, rotation sensing, and parametric amplification were experimentally investigated. In the magnetometer application an ultimate sensitivity at least comparable to the best of existing methods is indicated. (auth)

37987 ROTATIONAL CHARACTER OF LIQUID HELIUM. Borst, Lyle B. 5p. (CONF-660411-5). ORAU. Gmelin, AED-CONF-66-060-22.

From American Physical Society Meeting, Washington, D. C.

Due to the discrepancies in experimental and theoretical research on the rotational properties of liquid helium II, a theoretical discussion of the thermodynamics of liquid II is presented. (M.O.W.)

Neutron Physics

See also REACTOR TECHNOLOGY — Criticality Studies

Refer also to abstracts 37076 and 38352.

37988 (WAPD-TM-572) MATRICES FOR COMPUTING GREULING-GOERTZEL SLOWING-DOWN PARAMETERS AND LEGENDRE POLYNOMIAL COEFFICIENTS FOR SCATTERING IN THE LABORATORY COORDINATE SYSTEM FROM LEGENDRE POLYNOMIAL COEFFICIENTS IN THE CENTER-OF-MOMENTUM SYSTEM. Harris, D. R.; Noll, C. B. (Bettis Atomic Power Lab., West Mifflin, Pa.). Feb. 1966. Contract AT(11-1)-Gen-14. 239p. ORAU.

Nonrelativistic transformation matrices ($T^n_{LL'}$) are used in computations of Greuling-Goertzel slowing down parameters and Legendre polynomial coefficients for scattering in the laboratory coordinate system from Legendre polynomial coefficients in the center-of-momentum system. The elements, $T^n_{LL'}$, of these matrices were computed by a recursive method and are tabulated for n = 0, 1.2; L = 0, 1, 2, 3; L′ = 0, 1, 2, . . . , 10, and for most elements and nuclides of interest in nuclear applications. While the tabulated transformation matrices are formally appropriate for elastic scattering, the tabulated quantities are applicable to nonelastic interactions as well. (auth)

37989 (WAPD-TM-573) TRANS: A FORTRAN-IV PROGRAM FOR CONVERSION OF FORM OF NEUTRON ELASTIC SCATTERING DATA STORED IN THE ROC NUCLEAR DATA LIBRARY. Harris, D. R.; Noll, C. B. (Bettis Atomic Power Lab., Pittsburgh, Pa.). May 1966. Contract AT(11-1)-Gen-14. 20p. Dep. mn. CFSTI $1.00 cy, $0.50 mn.

TRANS is a FORTRAN-IV program for conversion of the form of neutron elastic scattering data stored in the ROC nuclear data library. The data are converted from any form found in the library into the form recommended for retrieval by neutron transport programs, viz., the form consisting of coefficients of Legendre polynomials in the center of momentum coordinate system. Optionally, data are converted to various forms required for comparison with measured and evaluated data. (auth)

37990 MEASUREMENT OF ABSORPTION CROSS SECTIONS FOR FAST NEUTRONS BY RESONANCE DETECTOR IN WATER. Koroleva, V. P.; Stavisskii, Yu. Ya. At. Energ. (USSR), 20: 431-2(May 1966). (In Russian).

An InCl resonance absorber in water used to measure the absorption cross section of fast neutrons. A spherical geometry was used. When a 60 g/l In concentration was irradiated for 15 min, the statistical order of accuracy was ~0.1% for a photoneutron source with a flux of $\sim 3 \times 10^8$ neutrons sec^{-1}. The results were compared with similar results obtained for an Sb–Be source using the same method. (G.O.Y.)

37991 CROSS-SECTION AVERAGING IN THERMAL REGION FOR MEDIA CONTAINING ZIRCONIUM HYDRIDE. Gorbunov, L. M.; Mitenkov, F. M.; Samoilov, O. B.; Farmakovskii, V. V. At. Energ. (USSR), 20: 438-9(May 1966). (In Russian).

The average values in the thermal region were calculated as a function of temperature and of absorption per single H nucleus, using the results obtained by averaging the spectra for infinite homogeneous media poisoned by the absorber. It was found that the averaged absorption cross sections follow a χ^{-1} law and do not exceed 20 barns in the interval from 293 to 773°K. (G.O.Y.)

37992 MEAN VALUE OF THE COLLISIONS IN THE SLOWING-DOWN PROCESS OF NEUTRONS. Mogyorodi, Jozsef. Magyar Tud. Akad. Mat. Kut. Int. Kozlem., 9: 733-41(1964). (In Hungarian).

Let $\sigma_s(x)$ and $\sigma_a(x)$ denote the cross-section of scattering and absorption respectively. These quantities generally depend on the lethargy x of the neutron. The formula $\rho(x) = \sigma_s(x)/[\sigma_s(x) + \sigma_a(x)]$ is the conditional probability that the neutron will be scattered under the condition that it collides with a nucleus at the lethargy level x. If W(x) denotes the distribution function of the lethargy increment gained at a scattering, $\rho(x)$ and W(x) can give the conditional probability that the number of scatterings in the lethargy interval (0,x) will be n, under the condition that the neutron will not be absorbed in this interval. Also, the mean value and the dispersion of the number of scatterings may be given. In the simple case, when $\rho(x)$ does not depend on the lethargy ρ, it is proved that the conditional mean value of the number of collisions in the lethargy interval (0,x), under the condition that the neutron will not be absorbed in this interval, is asymptotically a linear function of the lethargy x. Also the conditional dispersion is given and it is found that this is asymptotically a linear function of $\sqrt{x}$. (auth)

37993 EIGENVALUE PROBLEM OF NEUTRON AGE THEORY. Heyn, Eugen (Institut fuer Reine Mathematik, Berlin-Adlershof, Ger.). Math. Nachr., 31: 179-93(1966). (In German).

The problem of calculation of a critical size for a region of space V filled with a fissionable substance is considered. Several lemmas are given concerning the existence of differentiable functions in the domain, the existence of positive (or zero) functions belonging to the closure of D according to the Friedrichs expansion metric, properties of the Friedrichs expansion operator for points within the domain, and compactness and positive value of an integral operator. For positive a, b, c, l, Θ_T, a system λ, ρ_T, $q(\Theta)$ exists such that: $\rho_T \epsilon L^2(V)$, $q(\Theta) \epsilon L^2(V)$ for each Θ so that $0 \leqq \Theta \leqq \Theta_T$, $\int |q(\Theta) - q(\Theta')|^2 dV \to 0$ for $\Theta \to \Theta'(0 \leq \Theta, \Theta' \leqq \Theta_T)$; $\rho_T \geqq 0$, $q \geq 0$, with the solution normalized; the equation $\rho_T(\underline{r}) = \lambda/4\pi \int_V (\exp(-\underline{r} - \underline{r}'/1))(a\rho_T(\underline{r}') + bq(\underline{r}', \Theta_T))dV_{r'}/(\underline{r} - \underline{r}')^2$ holds; for each function ψ of D_{Δ_0}, the definition domain of the operator Δ_0, the derivative of $(q(\Theta),\psi)$ with respect to θ exists and equals $(q,\Delta_0\psi)$ for each ψ such that $0 \leqq \Theta \leqq \Theta_T$; and $q(\underline{r},0) = c\rho_T(\underline{r})$. Further, only one system exists which fulfills these eigenvalue conditions. The eigenvalues are dependent on the region. (BBB)

37994 RATIO OF INDUCED FISSION VS. SPONTANEOUS FISSION AND THE TRACE ELEMENT ANALYSIS IN PITCHBLENDE. Kenna, B. T.; Attrep, M. Jr. (Univ. of Arkansas, Fayetteville). J. Inorg. Nucl. Chem., 28: 1491-1500(Aug. 1966).

The percentage abundance of 17 elements in pitchblende was determined. From these results and the activity measurements of nuclides such as ^{35}Cl and ^{99}Tc, the ratio, R, of induced fission vs spontaneous fission was estimated to be on the order of 25%. In addition, the thermal neutron flux present in the ore was approximated. The flux contribution from (α,n) reactions on light elements is shown to be quite significant. (auth)

37995 PROTON-INDUCED FISSION OF ^{238}U. Choppin, G. R.; Meyer, E. F. Jr. (Florida State Univ., Tallahassee). J. Inorg. Nucl. Chem., 28: 1509-18(Aug. 1966).

Fission product cross sections for ^{238}U bombarded by protons of 7.1, 9.4, and 12.0 Mev energy are presented. All results were obtained by standard radiochemical techniques. Cumulative fission yields were obtained for approximately twenty-five nuclides in order to analyze the mass distribution as a function of energy. Using Ford's analysis, the mass yields were found to be consistent with the two-mode-of-fission hypothesis with a confidence level of 69%. In addition, primary fission yields were obtained for six shielded or quasi-shielded nuclei to study the distribution of nuclear charge. The data are in better agreement with the postulate of equal charge distribution. (auth)

37996 HELIUM-ION-INDUCED FISSION OF ^{207}Pb FROM 41.1 Mev TO 26.3 Mev. Neuzil, E. F. (Western Washington State Coll., Bellingham). J. Inorg. Nucl. Chem., 28: 1519-26(Aug. 1966).

Helium ion-induced fission of ^{207}Pb at energies from 41.1 to 26.3 Mev indicated that the characteristics of fission of different isotopes of the same element are a function of the even-odd character of the nuclide. The value of the width at half maximum $W_{\frac{1}{2}}$ for the symmetric gaussian fission fragment distribution curve is approximately constant with a value of 17 ± 1 amu for ^{207}Pb. The excitation function for ^{207}Pb appears to be somewhat more steep than that of the even A species of the helium ion-induced fission of ^{206}Pb. The values of the helium ion-induced cross sections for ^{207}Pb at excitation energies of 33.5, 29.9, 25.6, 23.9, 21.3, and 18.7 Mev are 3.08×10^3, 4.83×10^2, 2.72 ± 10^1, 1.61, 6.65×10^{-1}, and 2.87×10^{-1} μbarn, respectively. (auth)

37997 FISSION RECOIL SEPARATION IN MIXTURES WITH URANIUM DIOXIDE POWDERS AS A SIMPLE METHOD OF RANGE DETERMINATION OF FISSION PRODUCTS. Naumann, D.; Burk, W.; Heyne, W.; Guenther, K. (Zentralinstitut fuer Kernforschung, Berlin. Bereich Werkstoffe und Festkoerper und Bereich Theoretische Physik, Rossendorf, Ger.). J. Inorg. Nucl. Chem., 28: 1609-15(Aug. 1966). (In German).

The portion of light and heavy fission products separable by fission recoil in a mixture of UO_2 powder and NaCl in relation to the volume fraction of UO_2 was determined experimentally. The recoil ranges for Sr and Ba in NaCl obtained from the data were in good agreement with calculated values. Under the chosen limits the method is suitable for use in determination of recoil ranges. (tr-auth)

37998 DOSE DEPENDENCE OF F-CENTER PRODUCTION BY FAST NEUTRONS IN MAGNESIUM OXIDE. Henderson, B.; King, R. D. (Atomic Energy Research Establishment, Harwell, Eng.). Phil. Mag. (8), 13: 1149-56(June 1966).

Parallel electron spin resonance and optical absorption studies of magnesium oxide irradiated to six different doses in the range 10^{17} to 10^{19} nvt >1 Mev made possible a detailed correlation of the F-center with the optical band centered at 2500 Å. Thermal bleaching experiments at 320°C for periods between 5 min and two days confirmed this correlation in addition to the less detailed experiments of Wertz et al. (1964). The results were consistent with an oscillator strength of 0.8 for the F-band in magnesium oxide. In samples irradiated to high dose a maximum F-center concentration of 6×10^{18} F/cm^3 was observed at 5×10^{19} nvt. This effect may be associated with the clustering of defects caused by irradiation-induced diffusion at the ambient pile temperature of 150°C. (auth)

37999 SLOW-NEUTRON SCATTERING BY LIQUIDS: HINDERED-TRANSLATOR MODEL. Ardente, V. (EURATOM, Ispra, Italy); Nardelli, G. F.; Reatto, L. Contract 140-63-4 ISP-I; 196-65-4 ISP-I. Phys. Rev., 148: 124-38(Aug. 5, 1966).

A hindered-translator model including damping is constructed with the aim of accounting for the one-particle motions in a liquid, in connection with slow-neutron scattering. Liquids which exhibit the Arrhenius law for self-diffusion are considered and the activation energy U_0 is assumed to represent the energy barrier against translations for a single particle. In the absence of dissipation and for energies below the barrier, the hindered translator is allowed to carry out harmonic oscillations with frequency ω_0 given by the mean field of force experienced by the particle in the liquid. Dissipation is taken into account using methods of nonequilibrium statistical mechanics. Dissipation is considered, first, on the weak-collision hypothesis, and it is assumed that no transitions between vibrational and translational states occur during the time the dynamic correlation persists. By looking into the phase space of the hindered translator at thermal equilibrium, its velocity autocorrelation function is shown to be a weighted superposition of the autocorrelation functions for vibrations and translations, respectively. Explicit expressions are found for their correlation times τ_I and τ_{II}, in terms of the interatomic potential $\varphi(r)$, the radial distribution function $g(r)$, the activation energy U_0, and the self-diffusion coefficient D. Next, the effect that hard collisions have on dissipation is included by simply superimposing hard on weak collisions; terms which contribute to Gaussian and non-Gaussian parts of Van Hove's $G_s(r,t)$ are considered. Finally, the expression for Van Hove's scattering function $S_s(\kappa,\epsilon)$ is given in terms of the physical quantities entering the model. The numerical computation concerns quantities related to the Gaussian part of $G_s(r,t)$. The width of the quasi-elastic peak at different scattering angles, the mean-square displacement versus time, the velocity autocorrelation function, and the Egelstaff $p(\beta)$ are compared with the experimental data for water at 25°C and 75°C and for liquid argon. Fairly good agreement is obtained without using any adjustable parameter. A significant role is played by ω_0 and U_0 in accounting for the different behavior that liquids with similar self-diffusion coefficient may exhibit with respect to slow-neutron scattering. (auth)

38000 INTRAMOLECULAR COHERENT SCATTERING OF NEUTRONS BY CD_4 GAS. West, R. E.; Brugger, R. M.; Griffing, G. W. (Phillips Petroleum Co., Idaho Falls, Idaho). Phys. Rev., 148: 163-9(Aug. 5, 1966).

Measurements on the scattering of neutrons by gaseous CD_4 at a temperature of 306°K were taken on the Materials Testing Reactor (MTR) phased chopper velocity selector for a range of energy transfers between 0 and 156 Mev and momentum transfers between 1.0 and 14 Å^{-1}. Comparison of the data with theoretical calculations shows excellent quantitative agreement. The influence of intramolecular coherent scattering is most evident at small energy transfers. However, the intramolecular coherent scattering is also quite prominent when the energy transfer becomes comparable in magnitude to the energy of a vibrational state. At a temperature of 306°K, approximately 3% of the molecules are in excited vibrational states. In spite of the small percentage of vibrationally excited molecules in the gas, it is found that the contribution to the scattering by the vibrationally excited molecules becomes significant at an energy transfer of about 72 Mev and dominates the scattering at larger energy transfers. (auth)

38001 INELASTIC SCATTERING OF SLOW NEUTRONS IN PENTANE. Ripeanu, S. (Inst. of Atomic Physics, Bucharest). Rev. Roum. Phys., 11: 265-72 (1966).

The energy analyzed angular distributions for pentane at room temperature were measured on the Bucharest triple-axis crystal spectrometer for neutrons of wave lengths 1.2 Å and 1.8 Å. The wave-length resolution was 6% and 4%, respectively. The inelastic scattering component was approximated on the basis of the gas model (M = 1) and subtracted from the corresponding energy distributions experimentally obtained. The line widths and the diffusion parameters were determined from the quasi-elastic peaks. The line widths of the quasi-elastic peaks plotted versus the scattering angle have showed a good agreement with the jump diffusion model proposed by Singwi-Sjölander. (auth)

38002 SCATTERING OF SLOW NEUTRONS BY LINEAR MOLECULES. Kovalchuk, V. G. (Kiev Inst. of Physics). Ukr. Fiz. Zh., 11: 581-9(1966). (In Ukrainian).

The differential scattering cross section of slow neutrons is calculated. Under the assumption that the thermal motion mean energy considerably exceeds the lower boundary of the rotational spectrum of the molecule, but is less than the corresponding boundary of the vibration spectrum, and that the initial energy of the neutrons is less than the first excited vibrational level, an expression is obtained, the basic term of which is similar to the known formula of Krieger and Nelkin. The limits of applicability of this formula are established, depending on the pulse transmitted by the neutron. In the case of small transmission of pulses, when this formula can not be applied, another formula is derived, by means of which the spectral representation of the pulse-correlation function is found. The calculation was carried out with allowance made for the quantum nature of the rotational states of the molecules. (auth)

38003 EXACT SOLUTIONS OF MILNE'S PROBLEM FOR 2 HALF SPACES WITH DIFFERENT MEDIA AND OF THE PROBLEM OF AN INFINITELY EXTENDED PLATE USING SPHERICAL HARMONICS. Korn, A. Karlsruhe, Ger., Technische Hochschule, 1965. 64p. $2.00 Gmelin, AED-Diss. 65-302.

Thesis.

Some mathematical methods for the solution of the Boltzmann equation for two half spaces with different materials are given. Solutions for an extended plate in a homogeneous medium are obtained by the use of spherical harmonics. The results are compared with experimental data. (Gmelin)

38004 EFFECT OF NUCLEAR SPIN CORRELATIONS ON THE SCATTERING OF NEUTRONS BY MOLECULES. Sinha, S. K.; Venkataraman, G. (Atomic Energy Establishment, Trombay, India). 13p. (CONF-650932-10). ORAU. Gmelin, AED-CONF-65-292-10.

From Symposium on the Inelastic Scattering of Neutrons by Condensed Systems, Upton, N. Y.

The scattering of slow neutrons by molecules is usually discussed without considering the restrictions imposed on the molecular wavefunctions by the presence of identical nuclei in the molecule. The theory of neutron scattering, is presented, starting with the work of Zemach and Glauber, taking into account such effects, with special reference to the spherical top molecule. Matrix elements for the scattering between different symmetrized states are evaluated using group theoretical methods. It is shown that coherent scattering can cause only those transitions which leave the symmetry of the total molecular wavefunction unchanged while incoherent scattering can cause transitions between states of different symmetry. The formulas derived for the cross section are different from those obtained in a recent treatment of the same problem. Calculations for methane

have been made and are compared with the case where the effects of nuclear spin correlation are ignored. (auth)

38005 INELASTIC NEUTRON SCATTERING BY SOLID AND LIQUID CYCLOHEXANE. de Graaf, L. A. 12p. (CONF-650932-7). ORAU. Gmelin, AED-CONF-65-292-3.

From Symposium on the Inelastic Scattering of Neutrons by Condensed Systems, Upton, N. Y.

The diffusive motions in liquid and solid cyclohexane have been investigated using a rotating-crystal spectrometer. Scattering spectra of the solid at 165°K and 195°K and the liquid at 295°K and 330°K were measured at 6 different scattering angles between 18° and 80°. The experimental results are compared with the diffusion model of Singwi and Sjölander. Above the phase-transition point (186°K) the measured self-diffusion coefficients do not vary appreciably from the value $D = 5.5 \times 10^{-5}$ cm^2/s determined at 295°K. This indicates that the motion of the protons within a molecule is more important than the motion of the molecule as a whole. (auth)

38006 SLOW NEUTRON SCATTERING BY LIQUIDS: A HINDERED-TRANSLATOR MODEL. Ardente, V. (C.C.R. Euratom, Ispra, Italy); Nardelli, G. F.; Reatto, L. 31p. (CONF-660204-17). ORAU. Gmelin, AED-CONF-66-017-17.

From American Nuclear Society Meeting, San Diego, Calif.

Slow neutron scattering by liquids with very small energy transfer is dominated by the intermolecular motion. A hindered-translator model including damping is constructed with the aim of accounting for the one-particle (center of mass) motions in a liquid, in order to evaluate the incoherent differential cross section. Liquids which exhibit the Arrhenius law for lf-diffusion are considered, and the activation energy U_0 is assumed to represent the energy barrier against translations for a single particle. In the absence of dissipation and for energies below the barrier the hindered-translator is allowed to carry out harmonic oscillations with frequency ω_0 given by the mean field of force experienced by the particle in the liquid. Dissipation is taken into account using methods of nonequilibrium statistical mechanics. Dissipation is considered, first, in the weak collision hypothesis, and it is assumed that no transitions between vibrational and translational states occur during the time the dynamic correlation persists. By looking into the phase space of the hindered-translator at thermal equilibrium, its velocity auto-correlation function is shown to be a weighted superposition of the auto-correlation functions for vibrations and translations, respectively. Explicit expressions are found for their correlation times τ_I and τ_{II}, in terms of the interatomic potential φ (r), the radial distribution function g(r), the activation energy U_0, and the self-diffusion coefficient D. Next, the effect that hard collisions have on dissipation is included by simply superimposing hard on weak collisions; terms which contribute to Gaussian and non-Gaussian parts of Van Hove's self-correlation function, $G_s(r,t)$, are considered. Finally, the expression for Van Hove's scattering function $S_s(\underline{\kappa},\epsilon)$ is given in terms of the physical quantities involved in our model. The numerical computation concerns quantities related to the Gaussian part of $G_s(r,t)$. The width of the quasi-elastic peak at different scattering angles, the mean square displacement of particles $\langle r^2 \rangle = \sigma\gamma(t)$ vs time, the velocity auto-correlation function, and the Egelstaff $p(\beta)$ are compared with the experimental data for water at 25°C and 75°C and for liquid argon. Fairly good agreement is obtained without using any adjustable parameter. A significant role is played by ω_0 and U_0 in accounting for the different behavior that liquids with similar self diffusion coefficient may exhibit with respect to slow neutron scattering. (auth)

38007 FAST NEUTRON SCATTERING FROM SMALL CYLINDERS OF STEEL, ALUMINUM, AND GRAPHITE. Courtney, John C. Washington, D. C., Catholic Univ. of America, 1965. 110p.

Thesis.

Time-of-flight methods were used to measure the spectra of fast neutrons scattered at angles of 20, 45, 70, 110, and 160 deg from the incident beam by small (2-in.-diam, 2.5-in. high) cylinders of steel, aluminum, and graphite. The measurements were made at the General Atomic electron linear accelerator (LINAC), where a pulsed source of bremsstrahlung-produced neutrons was obtained by irradiating a lead target with 14-nsec bursts of 34-Mev electrons. The energy spectrum of the neutrons approximated a fission spectrum. Some of the neutrons struck the scattering sample, which was placed 13 in. from the source, passed through a system of collimators, down a drift tube, and into a liquid scintillator fast-neutron detector. Pulse-shape discrimination circuitry was used to eliminate pulses due to any gamma-ray background. Measured source spectra were used as input for Monte Carlo calculations of the scattered neutrons, and the results were compared with measured scattered spectral intensities. The calculations and experiments, integrated over energy, agreed within 16%. Since the spectral shape was satisfactorily reproduced, it is believed that the uncertainty in the measurement of the integrated fast-neutron flux by foil activation accounts for any discrepancies. These comparisons indicate that the ORNL cross-section library for these elements is adequate to handle neutron scattering calculations. (Dissertation Abstr.)

Nuclear Properties and Reactions

Refer also to abstracts 37126, 37332, 37479, 37790, and 38414.

38008 (AECL–2595) PHYSICS DIVISION PROGRESS REPORT, JULY 1–SEPTEMBER 30, 1965. (Atomic Energy of Canada Ltd., Chalk River (Ontario)). 60p. (PR-P-67). Dep. mn. AECL $1.50.

A report is presented on the developments in nuclear physics research, solid state technology and computer technology. The recoil method for measuring nuclear lifetimes was improved and now uses a 25 cm^3 Li drifted Ge γ-ray detector. Using this technique with the reactions $T(^{12}C, p\gamma)^{14}C$, $T(^{12}C, n\gamma)^{14}N$, and $T(^{16}O, n\gamma)^{18}F$, the lifetimes of five excited states in ^{14}N, ^{14}C, and ^{18}F were measured. The angular correlation technique involving the high resolution magnetic particle spectrometer and four NaI(Tl) γ-ray detectors was used to extend measurements on the reaction $^{12}C(^{16}O, \alpha\gamma)^{24}Mg$. In addition to four levels reported last quarter the decay modes, spins and parities were determined for levels in ^{24}Mg at excitations of 8.12, 8.44 (doubled), 8.65, 9.52 (doubled), 10.1 and 13.2 Mev. A magnetic β-ray spectrometer with pole pieces shaped like the sections of an orange and separated to provide seven gaps was set up at the tandem accelerator for use in studying the internal conversion electrons from γ-ray transitions produced in nuclear reactions. Accurate energy measurements were carried out on the first four transitions of the ground state rotational bands in the nuclei ^{158} Dy, ^{164}Er, ^{168}Yb and ^{174}Hf using (p, 2n) reactions in thin metal targets of ^{159}Tb, ^{165}Ho, ^{169}Tm and ^{175}Lu respectively. The results show that the nuclear moments of inertia increase regularly with increasing spin implying a nuclear softness not evident in earlier less accurate work on these nuclei. The inelastic scattering of neutrons from cobalt oxide was studied with the triple axis crystal spectrometer at the C5 beam facility of NRU. The low lying frequency vs wave-vector dispersion curves for lattice vibrations propagating along the c axis of α quartz at 296°K was measured using the triple axis neutron spectrometer. A CDC-3100 computer with an interface for connecting it electronically to the G-20 computer was installed and executive programs for the two-computer system are being tested and compiled and G-20 input-output subroutines were modified to allow use of the peripheral units of the 3100 directly by the G-20. A number of programs were written for use on the G-20 computer. These include ones for the calculation of the effects of space and image charges in a bunched beam of charged particles, the efficient evaluation of integrals of varying functions, the automatic drawing of arrow diagrams of the results from Program Evaluation and Review Technique (PERT), the study of methods of

analyzing neutron cross section data containing many resonances, the calculation of the efficiency of a hydrocarbon scintillator for the detection of neutrons, and the analysis of γ-γ angular correlation data. (B.G.D.)

38009 (BNL-10420) TESTS OF UNITARITY SYMMETRY IN NUCLEI BY NUCLEUS-HYPERNUCLEUS REACTIONS. Kisslinger, L. S. (Brookhaven National Lab., Upton, N. Y.). July 1966. Contract AT(30-2)-Gen-16. 6p. (CONF-660913-1). Dep. mn. CFSTI $1.00 cy, $0.50 mn.

For Presentation at International Conference on Nuclear Physics, Berkeley, Calif.

A study is presented on meson-nucleus reactions in order to estimate the cross sections for the various processes and to determine which of these, if any, are suitable for an experimental test of the existence of new analog states as approximate eigenstates. (B.G.D.)

38010 (BNL-10438) ELASTIC SCATTERING OF 1 Bev PROTONS FROM HELIUM AND OXYGEN. Igo, G. J.; Friedes, J. L.; Palevsky, H.; Sutter, R. J.; Bennett, G. W.; Corley, D. M.; Simpson, W. D. (Brookhaven National Lab., Upton, N. Y.). July 1966. Contract AT(30-2)-Gen-16. 9p. (CONF-660906-7). Dep. mn. CFSTI $1.00 cy, $0.50 mn.

For Presentation at International Conference on Nuclear Physics, Gatlinburg, Tenn.

An experiment is described on elastic scattering of 1-Bev protons from helium and oxygen in the laboratory angular range 3–42° and 3–22° respectively. Data obtained from the experiment are presented. (B.G.D.)

38011 (JINR-P-2805) IZUCHENIE ZAKHVATA PIONOV GELIEM-3. II. REAKTSII S RAZVALOM YADRA. (Capture of Pions by ^{3}He. II. Nuclear Decay Reactions). Zaimidoroga, O. A.; Kulyukin, M. M.; Sulyaev, R. M.; Falomkin, I. V.; Filippov, A. I.; Tsupko-Sitnikov, V. M.; Shcherbakov, Yu. A. (Joint Inst. for Nuclear Research, Dubna (USSR). Lab. of Nuclear Problems). 1966. 15p. Dep. mn.

A high pressure diffusion chamber was used in the investigation of π meson capture by ^{3}He leading to the processes of nuclear decay. Relative probabilities of these processes and the pulse spectra of the secondary charged particles were measured. (B.G.D.)

38012 (JINR-P-2806) DVOINAYA PEREZARYADKA π^--MEZONOV S ENERGIEI 50-176 Mev V FOTOEMUL'SII. (Double Charge Exchange of 50- to 176-Mev π^- Mesons in Photo Emulsion). Batusov, Yu. A.; Bunyatov, S. A.; Ionitse, G.; Loznyanu, E.; Mikhul, V.; Sidorov, V. M.; Yarba, V. A. (Joint Inst. for Nuclear Research, Dubna (USSR). Lab. of Nuclear Problems). 1966. 5p. Dep. mn.

Total cross section measurements were made for double charge exchange of 50 to 176 Mev π^- mesons in photo emulsions. (tr-auth)

38013 ENERGY WIDTH OF VIRTUAL RESONANCE LEVELS IN ATOMIC NUCLEI. Hohloch, E.; Wildermuth, K. (Univ., Tuebingen, Ger.). Acta Phys. Austr., 22: 251-5(1966).

An explanation is given for the change in level width of excited states of a nucleus with increasing excitation energy in terms of a change in the cluster structure of the nucleus. It is pointed out that the explanation given by Pearlsten, Tang, and Wildermuth (Phys. Rev. 120: 224(1960)) is incorrect. Calculations are made of the t-d and α-n optical potentials, which show that the effective interaction between the triton and deuteron cluster is much stronger than that between the neutron and alpha cluster. Illustrations are given for excited states of ^{5}He and ^{8}Be. (L.B.S.)

38014 LITHIUM-INDUCED REACTIONS AND THE STRUCTURE OF LIGHT NUCLEI. Rotter, I. Ann. Phys. (7), 17: 247-57(1966).

It is shown that the preponderant reaction mechanism in reactions of the type (^{6}Li,α), (^{6}Li,d), (^{7}Li,t), (^{7}Li,α) is the stripping-like mechanism. Effects of nuclear structure are seen to play an important role in the angular distributions and in the spectra of the deuterons, alphas, and tritons, respectively. (auth)

38015 TWO-NUCLEON CORRELATION FUNCTION AND FINAL-STATE INTERACTIONS. Yu, David U. L. (Stanford Univ., Calif.). Contract AF 49(638)-1389. Ann. Phys. (N. Y.), 38: 392-430(July 1966).

A triple coincidence experiment in which an inelastically scattered projectile sends off two closely correlated, high-momentum nucleons from a nucleus is proposed as a direct means of measuring the short range nuclear pair correlation function. An analysis based on potential theory shows that the Fourier transform of the correlation function is amenable to the relative momentum spectrum of the ejected nucleon pair. Final state interactions modify the low momentum components of this spectrum. However, marked characteristics of the short range effects that are not present in a pure independent particle model are expected to persist. These characteristics manifest themselves in the high Fourier components of the relative momentum spectrum. (auth)

38016 THE (e,e'p) REACTION IN THE ^{32}S NUCLEUS. Amaldi, Ugo Jr.; Venuti, Gloria Campos; Cortellessa, Giorgio; Fronterotta, Gabriele; Reale, Armando; Salvadori, Paolo (Istituto Superiore di Sanita, Rome). Atti Accad. Naz. Lincei, Rend., Cl. Sci. Fis., Mat. Natur. (8), 39: 470-4(Dec. 1965).

The (e,e'p) reaction with ^{32}S was investigated to determine the binding energy of inner protons in intermediate nuclei. The binding energies of the various states, according to a shell-model attribution, were found by using a maxwellian fit to the experimental data. The results confirm the high values of the binding energy previously found for ^{27}Al. (L.B.S.)

38017 DIRECT MEASUREMENTS OF THE HALF-LIVES OF SOME SHORT-LIVED XENON AND CESIUM ISOTOPES. Archer, N. P.; Keech, G. L. (McMaster Univ., Hamilton, Ont.). Can. J. Phys., 44: 1823-45(Aug. 1966).

Experimental techniques that are useful in the production and study of the fission product rare gases have been developed. The experimental developments reported in this work include a new radiation-resistant fission-gas-emanating compound, a fast technique for the separation of trace quantities of xenon or krypton from a fission gas mixture, and a "charged-wire chamber" used in the continuous removal of decay products from radioactive gas sources. These methods have been applied in the determination, by direct counting techniques, of the half lives of ^{138}Cs (32.3 ± 0.1 min), ^{139}Cs (9.0 ± 0.15 min), ^{140}Cs (63.8 ± 1.2 sec), ^{137}Xe (3.80 ± 0.05 min), ^{138}Xe (14.1 ± 0.8 min), ^{139}Xe (41.2 ± 0.15 sec), and ^{140}Xe (13.7 ± 0.15). These results compare favorably with the most recently published measurements of these half lives. (auth)

38018 FARADAY-CUP MEASUREMENT OF PROTON TOTAL REACTION CROSS SECTIONS AT 100 Mev. Kirkby, P.; Link, W. T. (McGill Univ., Montreal). Can. J. Phys., 44: 1847-62(Aug. 1966).

The proton total reaction cross sections of 41 elements have been measured at 99 Mev, using a double Faraday cup to measure the proton-beam attenuation. The results are consistent with the semiclassical form of the absorption cross section with a nuclear radius parameter of 1.47 fm (1 fm = 10^{-13} cm) and a mean free path for 99-Mev protons in nuclear matter of 5.7 fm. (auth)

38019 THEORY OF THE PROCESSES OCCURRING IN NUCLEAR QUADRUPOLE RESONANCE. Kessel', A. R.; Korchemkin, M. A. (Kazanskii Fiziko-Tekhnicheskii Institut, Kazan). Fiz. Tverd. Tela, 8: 387-96(Feb. 1966). (In Russian).

The method of kinetic equations was used to calculate the signals of free precession and the spin echo for quadrupole resonance of a nucleus with spin $^3/_2$ in solid models. No correlation of the asymmetry factor η of the crystal field and the orientation of the external variable field was superposed. The calculation of relaxation parameters included terms for local magnetic and electric fields

diagonal to the energy representation of part of the magnetic dipole interactions of the nuclei and spin network relaxation. When $\eta \neq 0$ an additional echo arises of moment $t = 3\tau/2$ and $t = 3\tau$ (where τ is the interval between impulses) dependent on local magnetic fields. The forms of the signals obtained are discussed; the theory explains the experimentally observed form of the echo (approximately exp (-const.t^2)). The parameter η may be determined from the amplitude of the main and the additional echo. (BBB)

38020 THEORY OF ARTIFICIAL TRANSMUTATION OF NUCLEI. Kar, K. C.; Bhattacharyya, A. K. (Inst. of Theoretical Physics, Calcutta). Indian J. Theor. Phys., 13: 1-20(1965).

A theory of the artificial disintegration of the nuclei is presented assuming Yukawa type of extra-nuclear short-range field as in the theory of the alpha disintegration. Physically both the problems are alike, involving the passage of the particle through the different regions of the nuclear field. The only difference is that in the natural disintegration the particle comes from inside the nucleus to the field-free region whereas in the present case the path is reversed. A more or less complete agreement was obtained in both the resonance and non-resonance types of disintegration. (auth)

38021 GAMMA-GAMMA ANGULAR CORRELATION IN ^{131}Cs NUCLEI. Vartapetyan, G. A.; Khudaverdyan, A. G. (Inst. of Physics, Erevan). Izv. Akad. Nauk Arm. SSR, Ser. Fiz. Mat. Nauk, 18: No. 4, 94-100(1965). (In Russian).

The angular correlation of the 495-124 kev cascade in ^{131}Cs was measured on a fast-slow coincidence circuit which contained two NaI detectors 30 × 30 mm. The number of true coincidences was proportional to an experimentally measured correlation function $W'(\theta)$. A correction was applied for the finite, angular resolution of the detectors. The anisotropy $A = [W(180°) - W(90°)]/W(90°)$ was found to be 0.01 ± 0.0045. The existence of an angular correlation of the 495-124 kev cascade excluded a spin of $\frac{1}{2}$ for the 124-kev level. The 124-kev transition has the form M1 (96.9 ± 0.5) + E2 (3.1 ± 0.5)%. (TTT)

38022 EXCITATION STATE OF AXIALLY ODD ATOMIC NUCLEI. Sharipov, Sh. (Inst. of Nuclear Physics, Academy of Sciences, Uzbek SSR). Izv. Akad. Nauk Uz. SSR, Ser. Fiz.-Mat. Nauk, No. 5, 71-9(1965). (In Russian).

The succession of spins and the energy ratios of the excited states of odd nuclei are calculated without separating the excitations into single-particle and collective excitations on the assumption that the angular moment j of the external nucleon is conserved. The nuclear model is assumed to consist of an ellipsoid of rotation, and one external nucleon. The surface of the nucleus can complete small β- and γ-oscillations with respect to the equilibrium values of $\beta_0 \neq 0$ and $\gamma_0 = 0$. The succession of spins and energy ratios of excited rotational-single particle and gamma oscillation states are expressed by two parameters. The theoretical and experimental values of the spins and energy levels of the odd nuclei ^{131}Xe, ^{159}Tb, and ^{195}Au are compared. The agreement indicates that the axial theory can satisfactorily explain the data by taking into account small γ oscillations of the surface of the nucleus on the assumption that j is a good quantum number and that it is possible to separate the β-oscillations from the γ oscillations and the rotational-single particle states. (TTT)

38023 THEORY OF DIRECT NUCLEAR REACTIONS. Bushev, M. Izv. Fiz. Inst. Aneb, Bulg. Akad. Nauk, 14: 73-83(1966). (In Russian).

An attempt is made, based on Butler's theory of deuteron stripping, to take into account a larger number of nuclear interactions in the reactions of stripping. A shell model is used and the first Born approximation is applied to determine the scattering amplitude. The exchange effects, or heavy-particle stripping, is taken into consideration as well. The expression of the scattering amplitude, obtained with the aid of certain approximations, make it possible to determine the angular distribution curves for scattering by some light- and medium-weight nuclei. The comparison of these curves with the experimental ones will show to what degree it is necessary to consider a larger number of nuclear interactions in reactions of this type. (auth)

38024 HIGH-ENERGY PHOTOPROTONS OF THE REACTION ^{40}Ca(γ,p)^{39}K AT 28 AND 60 Mev. Dragnev, T.; Delchev, M. Izv. Fiz. Inst. Aneb, Bulg. Akad. Nauk, 14: 159-66(1966). (In Russian).

The energy and angular distributions of high-energy protons (with energy above 7 Mev) from the reaction ^{40}Ca(γ,p)^{39}K were investigated at $E_{\gamma max} = 28$ and 60 Mev. The method of nuclear emulsion was used. For protons with energy above 15 Mev a larger number of photoplates and a considerably larger surface of the photoplates were examined. The angular distributions of protons with energy above 15 Mev at double $E_{\gamma max}$ differ markedly. A fine structure was observed in the energy distributions of the protons with energy above 15 Mev. (auth)

38025 SHELL-MODEL DESCRIPTION OF NUCLEAR ANALOG STATES. Fallieros, S. (Franklin Inst., Swarthmore, Pa.). J. Franklin Inst., 281: 179-83(Mar. 1966).

A definite value of the isotopic-spin quantum number can be assigned to characterize the ground state of a nucleus even in cases where a nonvanishing neutron excess is present. This is implied by assumptions regarding the shell structure of the nucleus and the fact that the Pauli principle forbids the transformation of a proton from the occupied shells into an equivalent neutron. This situation is the same when an additional proton is allowed to be present in a subshell already occupied by the excess neutrons, but is different when the last proton is promoted into a level previously unoccupied by any other neutron. Then the isotopic spin of the extra proton can couple with that of the remaining nuclear core in two distinct ways, and the two resulting states have significantly different energies, thus leading to a characteristic fragmentation of the original single-proton orbital. This problem is examined within a simplified shell-model framework. The treatment provides a detailed description of the wave functions of the states considered, including the possibility of their decay by particle emission and is consistent with the intermediate-resonance interpretation of their formation in proton-initiated resonant nuclear reactions. This shell-model provides for the splitting of single-proton levels into components with definite isotopic spin in the presence of a neutron-rich nuclear core. Explicit expressions for the renormalized energies, wave functions, and particle-escape widths of the resulting states are obtained. The resonant mechanism is considered as follows. The incident proton interacting with the nucleon target is transformed temporarily into a bound neutron, transferring its energy and charge into the excitation of the analog state of the target. The inverse of this occurs during the re-emission of the proton back into the incident channel. Since no angular momentum transfer is needed for the analog excitation, only one partial wave will resonate in this process, namely, the one with angular momentum identical to that of the bound neutron. (BBB)

38026 QUADRUPOLE MOMENT OF ^{51}V. Murakawa, Kiyoshi (Tokyo Univ.). J. Phys. Soc. Jap., 21: 1466 (July 1966).

In previous work by the author, J. Phys. Soc. Japan 11: 422(1956), the hyperfine structure of VI λ 4851.5 was studied by use of a liquid-air cooled hollow cathode and a Fabry-Perot etalon and the quadrupole moment of ^{51}V was deduced to be $0.2_8 \pm 0.15$ barn. Due to an increase in the resolving power of the etalon the hfs was re-examined. The improved hfs is given and a value of $Q(^{51}V) = -0.04$ barn is calculated. (W.D.M.)

38027 AN 8^- ISOMERIC STATE IN THE 106-NEUTRON NUCLEI: ^{180}W, ^{182}Os, and ^{184}Pt. Burde, J.; Diamond, R. M.; Stephens, F. S. (Univ. of California, Berkeley). Nucl. Phys Phys., 85: 481-503(1966).

The decay of a two-neutron, 8^-, isomeric state was observed in three nuclei having 106 neutrons. The half lives

of these isomers are in the region of 1 msec. In each of the isotones ^{160m}W, ^{162m}Os, and ^{164m}Pt there were observed five prominent transitions. Four of these are the E2 transitions of the 8 → 6 → 4 → 2 → 0 cascade in the ground-state band. The fifth transition is a very hindered E1 that de-excites an 8⁻ 8 isomeric level and populates the 8⁺ 0 level of the ground-state band. Despite the appreciable difference between the properties of these nuclei, as can be seen by comparing the well-developed rotational spectrum of ^{160}W with that of the poor rotor ^{164}Pt, the isomeric transitions seem to exhibit a striking similarity. In ^{164m}Pt, the isomeric decay also populates other levels. Among them were tentatively identified two members of the β-vibrational band. Their position relative to the ground-state band in this transitional-region nucleus is of special interest. (auth)

38028 PRECISION MEASUREMENT OF REACTION THRESHOLDS. **Parks, P. B.; Beard, P. M.; Bilpuch, E. G.; Newson, H. W. (Duke Univ., Durham, N. C.). Nucl. Phys., 85: 504-12(1966).**

The total yield of the ^{39}Ar(p,n)^{39}K reaction was measured in the energy region from E_p = 2.336 to 2.464 Mev. A very thin target produced in a special window-less gas target chamber allowed a proton energy spread less than 140 ev. With this very good resolution, at least 69 clearly resolved resonances are found. A technique for measuring precise neutron energies by neutron transmissions through suitable samples is discussed. Using this system the ground state Q-value was found to be −2.287 ± 0.001 Mev. In the same way, the ^{37}Cl(p,n)^{37}Ar reaction was found to have a Q-value of −1.597 ± 0.001 Mev, which is in excellent agreement with prior investigations. The technique should be accurate to less than ½ kev if a suitable absolute energy standard can be established. (auth)

38029 THE DECAY OF ^{140}Ba. **Moss, G. A.; McDaniels, D. K. (Univ. of Oregon, Eugene). Nucl. Phys., 85: 513-18(1966). (RLO-1921-8).**

A Ge(Li) solid-state detector was used to investigate the gamma spectrum of the odd nucleus ^{140}La resulting from the decay of 12.8-day ^{140}Ba. Gamma rays of the following energies and relative intensities were observed in ^{140}La: 30.45 (30), 118.99(0.1), 132.69(3), 163.10(100), 304.82(94), 423.69 (56), 437.55(33) and 537.38(430) kev. A very weak (relative intensity ≤0.01) gamma ray at 44 kev was found and is included in the decay scheme. (auth)

38030 HALF LIVES OF LEVELS AT 405 kev IN ^{211}Bi AND 377 kev IN ^{53}Mn. **Gorodetzky, S.; Schulz, N.; Bozek, E.; Knipper, A. (Institut de Recherches Nucleaires, Strasbourg). Nucl. Phys., 85: 519-28(1966). (In French).**

The half lives of levels at 405 kev in ^{211}Bi and 377 kev in ^{53}Mn were measured by the delayed coincidence technique using a time-to-height converter. The respective values are $3.18 \pm 0.14 \times 10^{-10}$ and $1.17 \pm 0.06 \times 10^{-10}$ sec. These half lives indicate retardation factors of 1600 and 350 for the M1 component of these transitions. (auth)

38031 APPLICATION OF THE DELAYED COINCIDENCE TECHNIQUE TO MEASUREMENT OF THE SHORT MEAN LIVES IN ^{131}Xe AND ^{143}Pr. **Gorodetzky, S.; Schulz, N.; Bozek, E.; Knipper, A. C. (Institut de Recherches Nucleaires, Strasbourg). Nucl. Phys., 85: 529-36(1966). (In French).**

The half lives of excited states were determined from the simultaneous measurement of the two delayed coincidence curves from the self-comparison method. The results were checked with measurements in the standard comparison method, including a new determination $T_{1/2}$ = $2.5 \pm 0.5 \times 10^{-11}$ sec for the half life of the 412-kev state in ^{198}Hg. The combined results yield the following half lives: $4.7 \pm 0.5 \times 10^{-11}$ sec for the 364-kev state in ^{131}Xe and $4.9 \pm 0.7 \times 10^{-11}$ sec for the second excited state in ^{143}Pr. (auth)

38032 ANGULAR CORRELATIONS FOR E2 AND E3 TRANSITIONS IN COULOMB EXCITATION. **Keddy, R. J. (Univ. of Witwatersrand, Johannesburg); Yoshizawa, Y. Nucl. Phys., 85: 537-44(1966).**

A first-order perturbation theory calculation is made of the particle-gamma angular correlation coefficients used in Coulomb excitation. Both the E2 and E3 cases are treated and are separately compared to the results obtained from the sudden approximation theory for $t_{1/2}/t_{A0} = 0$. (auth)

38033 ONE-PARAMETER FAMILY OF UNITARY ENSEMBLES. **Gaudin, M. (Centre d'Etudes Nucleaires, Saclay, Gif-sur-Yvette, France). Nucl. Phys., 85: 545-75(1966). (In French).**

A one-parameter family of unitary matrix ensembles is studied. The ensemble $E_2(z)$ of unitary random matrices, whose eigenvalues are $\epsilon_j = \exp 2\pi i\varphi_j$, is defined by the following joint probability density. $P(\epsilon_1\epsilon_2 \ldots \epsilon_n)d\varphi_1 d\varphi_2 \ldots d\varphi_n \propto \prod_{i<j} |(\epsilon_i - \epsilon_j)/(\epsilon_i - z\epsilon_j)|^2 d\varphi_1 d\varphi_2 \ldots d\varphi_n$. It realizes a continuous interpolation between the distribution of the eigenvalues in the Dyson unitary ensemble E_2 for $z = 0$ and the uniform distribution of n random points on the unit circle for $z = 1$. The thermodynamic analogy with a circular or linear classical repulsive gas at temperature $\beta^{-1} = 1/2$ is developed. The isotherm $\beta = 2$ and the corresponding virial series are exactly calculated. All the correlation functions are given in the limit of an infinite linear gas or of an infinite series of levels. This model shows the short-range repulsion effect between eigenvalues but no long-range crystalline order, which is a strong characteristic of all ensembles so far studied. (auth)

38034 ANGULAR DISTRIBUTION, ANGULAR CORRELATIONS, AND PLANE POLARIZATION OF GAMMA RAYS OF THE REACTION ^{53}Cr(p,n)^{53}Mn. **Gorodetzky, S.; Beck, F. A.; Bertini, R.; Bozek, E.; Knipper, A. (Institut de Recherches Nucleaires, Strasbourg). Nucl. Phys., 85: 576-92(1966). (In French).**

Levels in the nucleus ^{53}Mn were studied from the observation of gamma rays emitted in the reaction ^{53}Cr(p,n)^{53}Mn. Measurements of their angular distribution, plane polarization, and gamma-gamma angular correlations with oriented initial level allowed the following spin and parity assignments: $J_1^\pi = 5/2^-$ for the first excited state at 380 kev and $J_2^\pi = 3/2^-$ for the second excited state at 1290 kev. Mixing ratios δ_2 for the gamma rays of 380, 910, and 1290 kev were determined. (auth)

38035 THE REACTIONS ^{63,65}Cu(t,p)^{65,67}Cu. **Bjerregaard, J. H.; (Univ. of Copenhagen); Nathan, O.; Hinds, S.; Middleton, R. Nucl. Phys., 85: 593-605(1966).**

Angular distributions of the Cu(t,p) reactions leading to states of ^{65}Cu and ^{67}Cu were measured at an incident energy of 12 Mev. For ^{65}Cu, 27 excited states were observed up to an excitation energy of 3.8 Mev; and for ^{67}Cu, 17 excited states were observed up to 4.3 Mev. The shapes of the angular distributions of the stronger proton groups are similar to known L = 0, L = 2, and L = 3 (t,p) distributions in other medium-weight nuclei. The data for ^{65}Cu are compared with the ^{64}Ni(^{3}He,d) results of Blair, and it is concluded that below 2.2 Mev the same levels are excited in the two experiments. The empirical L assignments for ^{65}Cu are in the majority of the cases consistent with the spin and parity assignments of Blair. The (t,p) data for ^{67}Cu show many similarities with the ^{65}Cu data, and this fact is used for tentative assignments of some levels in ^{67}Cu. (auth)

38036 ALPHA EMISSION FROM HEAVY NUCLEI INDUCED BY NEUTRONS OF 12 TO 23 Mev. **Rubbino, A.; Zubke, D. (Goethe-Univ., Frankfurt am Main). Nucl. Phys., 85: 606-30(1966).**

The α emission from neutron-induced reactions in heavy nuclei was experimentally investigated by means of several small reaction chambers. The irradiated elements were ^{107}Ag, ^{181}Ta, Ir, ^{197}Au, ^{209}Bi, ^{28}Si, and ^{29}Si. Energy spectra, angular distributions, and cross sections were analyzed for the neutron energy region E_n = (12−23) Mev. The results are discussed in a picture including all the known data on this subject and in terms of the contributions due to direct interaction and to evaporation. The α evaporation from neutron-induced reactions is found to be in satisfactory agreement with the statistical predictions. Some considerations for the direct interaction are made. (auth)

38037 SPECTRA OF PHOTO-ALPHA PARTICLES FROM NUCLEI IN THE REGION Z = 12 TO 30. Hoffmann. H.; Prowe. B.; Ullrich. H. (Technische Hochschule. Karlsruhe, Ger.). Nucl. Phys.. 85: 631-40(1966).

Alpha particles produced in Mg, Al. S, Ni. Cu. and Zn by 31-Mev bremsstrahlung were measured at 130° with a solid-state detector telescope. Each of the observed spectra essentially consists of one broad peak. the position of which is shifted from about 3 Mev to 7 Mev as Z increases. By use of suitable values for the level density parameter. the shape of the spectra can be brought to an agreement with the statistical model. (auth)

38038 ESTIMATION OF NUCLEAR STRENGTH FUNCTIONS. Slavinskas, D. D.; Kennett, T. J. (McMaster Univ., Hamilton, Ont.). Nucl. Phys., 85: 641-52(1966).

A method is presented for obtaining unbias estimates of nuclear strength functions from experimental data. The model is based on the assumption that observed reduced neutron widths have a Porter-Thomas distribution and that the level spacings are distributed according to Wigner's surmise. Detailed attention is paid to estimate accuracies and a simple technique for calculating 68% confidence limits is provided. Numerical results are given for ^{75}As. ^{69}Ga, ^{71}Ga, ^{92}Mo, ^{94}Mo, ^{96}Mo, ^{90}Zr, ^{92}Zr, ^{94}Zr, and ^{96}Zr. (auth)

38039 E2 SURFACE RESONANCES IN SPHERICAL NUCLEI. Faessler, Amand (Univ. of Freiburg i. B.). Nucl. Phys., 85: 653-69(1966). (In German).

Quadrupole surface vibrations are considered for the protons and the neutrons separately in medium and heavy even-mass spherical nuclei. The two kinds of oscillations are strongly coupled by the symmetry term in the mass formula. The coupling constant between the proton and the neutron oscillations is calculated with the help of the symmetry energy. With the strong coupling, one gets vibrations of the protons and the neutrons in phase and in anti-phase. The former are the well-known low-energy quadrupole vibrations. The vibrations in anti-phase lie between 5 and 50 Mev in the case where one considers no interaction between the oscillations in phase and in anti-phase. If they do not lie immediately near closed shells, the anti-phase resonances (E2 surface resonances) lie between 15 and 20 Mev. The γ absorption cross section and the inelastic electron scattering cross section are considered for the detection of the E2 surface resonances. It is shown that the γ absorption cross section is negligible compared to the cross section of the E1 giant resonance. The inelastic electron scattering cross section is of the same order as for the giant resonance. Thus it is proposed to search for the E2 surface resonance by comparing the shape of the γ absorption and the electron scattering cross section in the excitation region between 10 and 25 Mev. (auth)

38040 THE E1 $\Delta K = 0$ TRANSITIONS IN DEFORMED ODD-MASS NUCLEI. Faessler, Amand; Udagawa, Takeshi. R. K. (Florida State Univ., Tallahassee). Nucl. Phys.. 85: 670-8(1966).

The transition probabilities calculated for E1 $\Delta K = 0$ transitions using a pair reduction factor are smaller than experiment by factors up to 10^3. The expected mixing of the appropriate states with octupole vibrational bands due to vibration-particle interaction is computed. Whereas the mixing enhances E1 $\Delta K = 0$ transitions as desired. it does not effect E1 $\Delta K = 1$ transitions which were already in good agreement with experiment. This results because the E1 $\Delta K = 1$ octupole bands occur at higher energies and the E3 and E1 strengths are expected to be weaker for transitions into the $\Delta K = 1$ band. This calculation gives good agreement for the transition probabilities in the Eu isotopes where all parameters are available from the previous studies of ^{152}Sm. (auth)

38041 THE INFLUENCE OF THE PAIRING CORRELATIONS AND THE CORIOLIS FORCE ON THE E2 $\Delta K = 1$ TRANSITIONS IN DEFORMED ODD-MASS NUCLEI. Faessler, Amand (Univ. of California, Los Angeles). Nucl. Phys., 85: 679-88(1966).

The influence of the pairing correlations, of the Coriolis mixing, and of corrections to the Coriolis force mainly due to the rotation-vibration interaction on the E2 $\Delta K = 1$ transitions are studied. Because the rotational transitions are as strong as 200 single-particle units and the Nilsson transitions lie between 10^{-2} and 10^{-5} units. a small mixing can enhance the transition probability by several orders of magnitude. The pairing correlations affect the single-particle and the collective part of the transition probability in different ways. Because the single-particle part of the Coriolis force is negative under time reversal. the Coriolis mixing is not reduced by the pairing force. However. the single-particle transition probability can be diminished by more than a factor 100 due to the pair correlations. The agreement of the collective values with the experimental results is good, while the Nilsson transition probabilities with pair correlations are up to several orders of magnitude too small. (auth)

38042 THE ^{13}C(p,n)^{13}N REACTION NEAR THRESHOLD. Dietzsch, O. (Univ., Sao Paulo, Brazil). Nucl. Phys., 85: 689-96(1966).

The ^{13}C(p,n)^{13}N(g.s.) reaction was investigated in an energy range close to threshold using a long counter for detecting the neutrons. An excitation curve at 0° was measured from threshold (3.237 Mev) to 3.85 Mev. Angular distributions were obtained at ten proton bombarding energies from 3.30 to 3.75 Mev. The angular distributions are almost isotropic for energies below 3.35 Mev; the cross section decreases smoothly by ≈25% from 0 to 150°. As the energy is increased, the angular distributions become more anisotropic with peaks in both the forward and backward directions and a minimum that moves from ≈100° at E_p = 3.40 to ≈70° at 3.75 Mev. The results are compared with the conflicting data previously published. (auth)

38043 STRUCTURE EFFECTS IN THE CHARGE RADIUS OF SPHERICAL NUCLEI. Uher, Richard A.; Sorensen, Raymond A. (Carnegie Inst. of Tech., Pittsburgh). Nucl. Phys., 86: 1-46(1966).

Isotope and isomer shifts of the nuclear charge radius are calculated using the pairing plus quadrupole model. To accomplish this, the nuclear system is divided into a core plus a few valence particles. Monopole polarization of the core by the particle is taken into account in a phenomenological manner by assuming that the particles interact independently with the core. Quadrupole polarization of the core by the particles is estimated with the help of an effective quadrupole charge determined by fitting B(E2) transition rates of even-mass nuclei. The independent particle configuration of the valence nucleons is admixed by the pairing plus quadrupole interaction and the resulting wave functions are used to calculate isotope and isomer shifts of the charge radius. The results of even-mass to even-mass isotope shifts show good agreement with experiment, while the odd-even staggering effects observed in the isotope shift can not be obtained. Good agreement is obtained for the few isomer shifts which have been measured. (auth)

38044 PRECISE DETERMINATION OF THE SHAPE OF THE TWICE-FORBIDDEN BETA SPECTRUM OF ^{137}Cs. Hsue, S. T.; Langer, L. M.; Tang, S. M. (Indiana Univ., Bloomington). Nucl. Phys., 86: 47-55(1966).

The shape of the twice-forbidden beta spectrum in the decay of ^{137}Cs was measured in a magnetic spectrometer. By employing an energy-sensitive semiconductor detector at the focus, it was possible to demand that the recorded particles have the correct energy signature corresponding to the momentum setting of the magnetic field. An extremely high degree of discrimination was thus provided against detection of scattered electrons from the intense, low-energy inner group and the internal conversation lines. The shape of the outer group could be fitted with $S \propto q^2 + \lambda^2 p^2$ with $\lambda^2 = 0.004 \pm 0.002$ or with $S = L_0 q^2 + 9\lambda^2 L_1$ with $\lambda^2 = 0.005 + 0.002$. The end-point and intensity of the outer group are 1.176 ± 0.001 Mev and 6.0 ± 0.5%. The end-point and intensity of the inner group are 0.514 ± 0.001 Mev and 94.0 ± 0.5%. The K-internal conversion coefficient is α_K = 0.101 ± 0.007. (auth)

38045 ABOUT THE RESONANCE BEHAVIOR OF ISOSPIN FORBIDDEN NUCLEAR REACTIONS. Mueller, Kh. (Central Inst. for Nuclear Research, Rossendorf, Ger.). Nucl. Phys., 86: 56-64(1966).

The coherence width $\bar{\Gamma}$ for fluctuations in nuclear reactions around 20-Mev excitation energy of the compound nucleus increases drastically with decreasing mass numbers. From this it can be shown that there should exist a region of mass numbers where the violation of isospin selection rules is caused by only a few resonances. For this resonance region, a two-resonance formula for isospin-forbidden reactions is derived. (auth)

380 FURTHER MEASUREMENTS AND ZERO-RANGE DWBA CALCULATIONS FOR THE $^{52}Cr(d,p)^{53}Cr$ REACTION. Alty, J. L.; Green, L. L.; Jones, G. D.; Sharpey-Schafer, J. F. (Univ. of Liverpool). Nucl. Phys., 86: 65-88(1966).

An analysis of angular distributions in the $^{52}Cr(d,p)^{53}Cr$ reaction is made with zero-range DWBA calculations without spin-orbit terms. The variation of the predicted spectroscopic factors with the incident deuteron energy, the set of deuteron optical parameters used, the cut-off, and the neutron wave function is examined. (auth)

38047 FINITE-RANGE DISTORTED WAVE CALCULATIONS FOR THE $^{52}Cr(d,p)^{53}Cr$ REACTION. Mines, J. R. (Univ. of Liverpool). Nucl. Phys., 86: 89-101(1966).

The importance of finite-range and nonlocality corrections in distorted-wave calculations for the $^{52}Cr(d,p)^{53}Cr$ reaction is investigated. (auth)

38048 DECAY OF ^{131}Ce. Norris, A. E.; Friedlander, G.; Franz, E. M. (Brookhaven National Lab., Upton, N. Y.). Nucl. Phys., 86: 102-12(1966). (BNL-10050).

The nuclide ^{131}Ce was produced by (^4He,3n) and (^3He,2n) reactions on barium enriched in ^{130}Ba. A 10-min activity in chemically separated cerium was identified as ^{131}Ce by timed separations of its ^{131}La and ^{131}Ba descendants. The 10-min ^{131}Ce was found to decay principally by electron capture, with 11^{+7}_{-4}% decaying by β^+ emission. The K/β^+ ratio was shown to be ≈ 7, a value that is about an order of magnitude too high for the decay energy involved. This anomaly is unexplained. The energies and intensities of eight γ rays were measured. A 5-min isomer of ^{131}Ce was also found, but its decay mode could not be established unambiguously. Some information on the γ rays of 59-min ^{131}La is also presented. (auth)

38049 POLARIZATION IN THE ELASTIC SCATTERING OF 49-Mev PROTONS BY Ca, ^{58}Ni, ^{60}Ni, AND ^{208}Pb. Craig, R. M.; Dore, J. C.; Lowe, J.; Watson, D. L. (Univ. of Birmingham, Eng.). Nucl. Phys., 86: 113-18(1966).

Angular distributions are presented of the polarization produced in the elastic scattering of 49-Mev protons in the angular range 20–120° (lab). Results for Ca, ^{58}Ni, ^{60}Ni, and ^{208}Pb show the characteristic oscillations well known at lower energies, but exhibit higher maximum polarizations in general. The technique used involved the single scattering of a 49-Mev polarized beam. (auth)

38050 CROSS SECTIONS AS A FUNCTION OF ENERGY FOR THE SCATTERING OF PROTONS FROM ^{12}C. Swint, J. B.; Barnard, A. C. L.; Clegg, T. B.; Weil, J. L. (Rice Univ., Houston, Tex.). Nucl. Phys., 86: 119-29 (1966). (TID-22348).

The scattering of protons from carbon in the range of incident energies 4.7 to 12.8 Mev was investigated using a tandem Van de Graaff accelerator and a differentially pumped gas scattering chamber. Absolute differential cross sections for elastic scattering and for the inelastic scattering reactions $^{12}C(p,p')^{12}C^*$ ($Q = -4.43$ Mev) and $^{12}C(p,p'')^{12}C^*$ ($Q = -7.66$ Mev) were measured at laboratory angles of 25.54, 85.22, 105.23, 121.16, 137.52 and 159.45 as a function of energy in steps of 2.5 to 20 kev. Of particular interest is the splitting of the known resonance at 9.14 Mev, indicating a previously unknown level. (auth)

38051 CROSS SECTIONS AS A FUNCTION OF ANGLE AND COMPLEX PHASE SHIFTS FOR THE SCATTERING OF PROTONS FROM ^{12}C. Barnard, A. C. L.; Swint, J. B.; Clegg, T. B. (Rice Univ., Houston, Tex.). Nucl. Phys., 86: 130-44(1966). (TID-22346).

Absolute differential cross sections as a function of angle for the elastic scattering of protons by ^{12}C, and for the reactions which occur, were measured at incident proton energies $E_p = 2.39, 2.97, 3.97, 4.99, 5.66, 6.18, 6.65, 6.77, 8.07, 8.39, 8.96, 9.39, 9.81$ and 11.60 Mev. Complex phase shifts were obtained to represent the elastic scattering cross sections, the total inelastic cross sections and certain polarization data. The phase-shift values at the above discrete energies were used to estimate a continuous energy dependence for the phase shifts in the range $5.0 \leq E_p \leq 9.5$ Mev, omitting the rapid energy variation due to narrow levels. The estimates were varied slightly to obtain a good fit (except over the narrow levels) to the previously reported cross sections as a continuous function of energy. Finally the narrow levels were included in a calculation of the differential elastic scattering cross section and the polarization at $\theta_{lab} = 50°$, all as a continuous function of energy. The calculation adequately reproduced the experimental data through most of the energy range. Only one of the states close to $E_p = 9.14$ Mev was included in the calculations, so that the results differed significantly from the experimental values above $E_p = 8.5$ Mev. (auth)

38052 REACTION (t,p) WITH THE EVEN ISOTOPES OF Sm. Bjerregaard, J. H. (Univ., Copenhagen); Hansen, Ole; Nathan, O.; Hinds, S. Nucl. Phys., 86: 145-66(1966).

The (t,p) reactions on the even isotopes of Sm were investigated at a bombarding energy of 12 Mev with the purpose of exploring the transition from spherical to deformed nuclei. The reaction protons were detected in the Aldermaston multi-angle spectrograph, the overall energy resolution being about 20 kev full width at half maximum. Levels in ^{146}Sm, ^{150}Sm, ^{152}Sm, ^{154}Sm, and ^{156}Sm were established below 2–3 Mev excitation energy. A number of 0^+ and 2^+ states were identified from the proton angular distribution data. The 0^+ energies (±10 kev) and maximum differential cross sections in mb/sr (±25%) were: ^{146}Sm g.s. (0.29), 2.611 Mev (0.09); ^{150}Sm g.s. (0.57), 0.745 Mev (0.14); ^{152}Sm g.s. (0.19), 0.685 Mev (0.14), 1.091 Mev (0.13); ^{154}Sm g.s. (0.30), 1.117 Mev (0.03), 1.218 Mev (0.10), ^{156}Sm g.s. (0.30), 1.068 Mev (0.02). (auth)

38053 MEASUREMENT OF (p,n) THRESHOLDS AT TANDEM ENERGIES. Rickards, G.; Bonner, B. E.; Phillips, G. C. (Rice Univ., Houston, Tex.). Nucl. Phys., 86: 167-86(1966). (TID-22818).

The "counter ratio" technique of Bonner for measuring neutron thresholds was extended to bombarding energies greater than 6 Mev. Neutron background problems had previously precluded neutron threshold measurements with this technique at these energies. A system was developed which allowed the beam to be stopped 9.14 m from the thin foil target in a heavily shielded cave. No slits were used other than those of the analyzing magnet, and they were shielded from the experimental area. A remotely rectractable plunger permitted accurate alignment of the beam by minimizing the beam current on a Ta disk with a 4.7 mm aperture. The slow counter consisted of 2 BF_3 tubes imbedded in paraffin through which the beam passed. Improvement in background by a factor of 5 or better over stopping the beam in a ^{58}Ni slug at the target was achieved. Thresholds were measured for various (p,n) reactions, and the results are given as follows according to the reaction (level in residual nucleus) threshold energy in Mev: $^{13}C(p,n)^{13}N(0)$ 3.235, (2)6.965; $^{27}Al(p,n)^{27}Si(0)5.800$, (1) 6.611, (2) 6.793, (3) 8.046, (4) 8.549; $^{52}Cr(p,n)^{52}Mn$ (1) 5.975, (2) 6.149; $^{58}Ni(p,n)^{58}Cu$ (0) 9.509; $^{60}Ni(p,n)^{60}Cu$ (0) 7.025, (1) 7.092, (2) 7.325; $^{63}Ni(p,n)^{63}Cu$ (0) 4.812, (1) 4.852, (2) 5.109. Many resonances were observed in the various compound nuclei. (auth)

38054 ABSOLUTE ENERGY CALIBRATION OF NEUTRON THRESHOLDS. Bonner, B. E.; Rickards, G.; Bernard, D. L.; Phillips, G. C. (Rice Univ., Houston, Tex.). Nucl. Phys., 86: 187-92(1966). (TID-22778).

A recently developed low-background system for mea-

suring neutron threshold energies above 5 Mev was used in conjunction with a 180° annular magnetic spectrometer to perform absolute measurements of four neutron threshold energies covering the energy range from 3 to 9.5 Mev. The reactions and the corresponding threshold energy are as follows: $^{13}C(p,n)^{13}N$, 3.2354 ± 0.0024 Mev; $^{27}Al(p,n)^{27}Si$, 5.7943 ± 0.0047 Mev; $^{60}Ni(p,n)^{60}Cu$, 7.0236 ± 0.0071 Mev; $^{58}Ni(p,n)^{58}Cu$, 9.5160 ± 0.0078 Mev. A comprehensive tabulation of the absolute measurements performed in this laboratory during the past several years is given. (auth)

38055 PHOTON SCATTERING BY ORIENTED NUCLEI. **Arenhoevel, Hartmuth; Greiner, Walter (Univ., Frankfurt am Main). Nucl. Phys., 86: 193-207(1966).**

The general formalism of photon scattering by oriented nuclei is developed for electric dipole and electric quadrupole radiation. The differential scattering cross section can be expanded in terms of the orientation parameters f_ν, the coefficients of which contain the interference of the different polarizabilities. Explicit formulas are given for dipole radiation. The photon scattering by aligned ^{165}Ho nuclei is discussed in detail in the framework of the dynamic collective model showing the importance of the scalar-tensor polarizability interference for direct observation of the optical anisotropy of nuclei. (auth)

38056 EFFECT OF A SHORT-RANGE NEUTRON-PROTON INTERACTION ON THE PAIRING MODEL. **Hamamoto, Ikuko (Tokyo Univ.). Nucl. Phys., 86: 208-24(1966).**

The effect of a short-range, neutron-proton interaction on the pairing model is investigated. The change of the single-particle energy levels due to the neutron-proton interaction is estimated. The calculated energies of one-quasi-particle states are compared with the observed energy spectra of odd-mass nuclei. Then, calculation by the Tamm-Dancoff approximation is carried out and the wave functions thus obtained are discussed. Especially, the low-lying level scheme in antimony and iodine isotopes is explained by the neutron-proton interaction. (auth)

38057 COULOMB FORM FACTORS OF ^{10}B AND ^{11}B. **Stovall, T.; Goldemberg, J.; Isabelle, D. B. (Ecole Normale Superieure, Orsay, France). Nucl. Phys., 86: 225-40(1966).**

The electron scattering cross section of ^{10}B and ^{11}B was measured at incident energies of 198.5, 333 and 400 Mev for various scattering angles. The data were analyzed so as to yield values of the mean square charge radius and the nuclear quadrupole moment. Several nuclear models are considered. (auth)

38058 MEASUREMENT AND ANALYSIS OF MUONIC X-RAY SPECTRA IN SPHERICAL NUCLEI. **Acker, H. L. (Univ., Freiburg i. B.); Backenstoss, G.; Daum, C.; Sens, J. C.; De Wit, S. A. Nucl. Phys., 87: 1-50(1966).**

Muonic x-ray spectra for 18 elements with spherical nuclei between Cl and Bi and a sample of ^{206}Pb were investigated. The x-ray transition energies were measured with a Ge Li-drifted detector. The $2p \rightarrow 1s$ transitions were observed for all elements. $3d \rightarrow 2p$- and $4f \rightarrow 3d$-transitions for all elements with $Z \geq 50$, $5g \rightarrow 4f$ transitions for elements with $Z \leq 57$, and for some of the heaviest elements ($Z \geq 79$) higher transitions up to $7i \rightarrow 6h$ were measured. The charge distribution of the nucleus can be determined by the energy of the $2p \rightarrow 1s$ and the $3d \rightarrow 2p$ transitions. The data were analyzed in terms of a two-parametric charge distribution of the Fermi type by solving the Dirac equation numerically. Vacuum polarization effects are included and are checked by comparison with the data on higher transitions. In heavy elements the radial parameter c and the surface thickness t are determined, whereas light and medium Z elements only one parameter can be measured with sufficient accuracy. In Au, Pb and Bi the values for c are slightly higher, for t lower than the results of electron scattering experiments. In Ca and Sb, the $2p \rightarrow 1s$ transitions yield good agreement with electron scattering data. The systematic features of the x-ray data show consistency with a model of constant t 2.21 fm and constant nucleon density ρ_n 0.158 fm $^{-3}$, slightly lower than those obtained from electron scattering by Elton. Relative intensities in the $2p \rightarrow 1s$ spectra and in the $3d \rightarrow 2p$ spectra show deviations from a statistical population of the states for the high-Z elements and for some of the medium-Z nuclei. Hyperfine structure and isotope effects cause observable broadening of the line in the spectra of I, Nd, Au and Bi. Nuclear polarization effects were estimated to be smaller than the experimental error. A number of capture γ-rays was observed, the measurement of which yields an improved energy determination of the levels in ^{120}Sn, ^{122}Sn and ^{138}Ba. In the course of the calibration of the system, values for some γ lines in ^{66}Ga were determined. (auth)

38059 EXCHANGE CURRENT AND DEUTERON PHOTODISINTEGRATION AT THRESHOLD. **Kaschluhn, F.; Lewin, K. (Humboldt Univ., Berlin, Deutsche Akademie der Wissenschaften, Berlin). Nucl. Phys., 87: 73-82 (1966).**

The contribution from the meson exchange current to the deuteron photodisintegration amplitude at threshold is calculated by taking into account the next nearby singularities beyond the nucleon exchange poles in the crossed channels. The procedure is based on potential theory. Starting with the corresponding fourth-order Feynman amplitude with the deuteron-nucleon vertex on the mass shell, a local "exchange potential" is derived. Its contribution to the amplitude is calculated by using the Hulthén function for the initial deuteron state (thus including the off-mass shell properties of the deuteron-nucleon vertex) and the effective range approximation for the final scattering state. The result is combined with the direct γ-nucleon contribution calculated by Austern and Rost and agrees with experiment within the limits of error. (auth)

38060 STATISTICAL ANALYSIS OF THE INTERACTION OF 17 Gev MESONS WITH PHOTOEMULSION HEAVY NUCLEI. **Artykov, I. Z.; Barashenkov, V. S.; Eliseev, S. M. (Joint Inst. for Nuclear Research, Dubna, USSR). Nucl. Phys., 87: 83-7(1966).**

The Monte-Carlo method was used to calculate several hundred internuclear cascades initiated in the Ag and Br nuclei by 17-Bev mesons (π^-). The results of the calculations agree well with some experimental data. (auth)

38061 ON THE RIGIDITY PARAMETERS OF THE OCTUPOLE VIBRATIONS IN ^{19}F. **Zaikin, D. A. (Lebedev Physical Inst., Moscow). Phys. Lett., 22: 158-9(Aug. 1, 1966).**

The ratio of the rigidity parameters for the axial and nonaxial vibrations in ^{19}F is calculated using experimental data on the inelastic scattering of high-energy protons. (auth)

38062 THE 1505 kev RESONANCE IN $^{27}Si(p,\gamma)^{28}P$ AND PROPERTIES OF ^{28}P LEVELS. **Harris, G. I.; Hyder, A. K. Jr. (Aerospace Research Labs., Wright-Patterson AFB, Ohio). Phys. Lett., 22: 159-61(Aug. 1, 1966).**

Angular-correlation and polarization measurements at the E_p = 1505-kev resonance in $^{27}Si(p,\gamma)^{28}P$ yield the ^{28}P level assignments 0.71 (1$^+$), 1.45 (2$^+$), 1.97 (3$^+$), 2.54 (3$^+$), 4.23 (4$^+$), 4.63 (3$^+$), 4.93 (3$^+$), and 7.04 (4$^+$). The 4$^+$ resonance is probably a $(2s_{1/2}, 1f_{7/2})$, T = 1 analog state. (auth)

38063 THE (t,p) AND (t,α) REACTIONS ON ^{48}Ca AND ^{50}Ti. **Williams, D. C.; Knight, J. D.; Leland, W. T. (Los Alamos Scientific Lab., N. Mex.). Phys. Lett., 22: 162-4 (Aug. 1, 1966). (LA-DC-7991)**

Ground-state masses and low-lying excited states are reported for ^{50}Ca, ^{52}Ti, ^{47}K, and ^{46}Sc, as observed in the reaction of 7.5-Mev tritons and alpha particles with ^{48}Ca and ^{50}Ti. (auth)

38064 RADIATIVE PION ABSORPTION IN COMPLEX NUCLEI. **Anderson, D. K.; Eisenberg, J. M. (Univ. of Virginia, Charlottesville). Phys. Lett., 22: 164-6(Aug. 1, 1966). (ORO-2915-60).**

It is shown that radiative absorption of pions may be used to study spin-isospin modes of excitation in nuclei. (auth)

38065 SPIN MEASUREMENT AND ISOSPIN IMPURITY OF THE ^{61}Ga GROUND STATE. **Deutsch, J. P.; Grenacs,**

L. (Louvain Univ., Belg.). Phys. Lett., 22: 166-8(Aug. 1, 1966).

Beta-gamma circular polarization correlation measurements performed on the beta decay of ^{64}Ga yield an asymmetry of A = −0.94 ± 0.14, establishing J = 0 for the ^{64}Ga ground state. The matrix element mixing the analog of the ^{64}Zn ground state into the ^{64}Ga ground state is found to be $\langle|H_C|\rangle$ = 40.0 kev. (auth)

38066 THE REACTION MATRIX AND EFFECTIVE SHELL-MODEL INTERACTIONS FOR THE Ni ISOTOPES. Lawson, R. D. (Argonne National Lab., Ill.); MacFarlane, M. H.; Kuo, T. T. S. Phys. Lett., 22: 168-72(Aug. 1, 1966).

Shell-model calculations were performed for the nickel isotopes with an approximate reaction matrix, corrected in various ways for core polarization, as interaction. The resulting energy levels were compared with experiment and with the predictions of phenomenological shell-model interactions. (auth)

38067 EXCITATION OF SINGLE-PARTICLE STATES IN ^{8}Be BY THE ^{9}Be(p,d)^{8}Be REACTION. Marion, J. B. (California Inst. of Tech., Pasadena); Ludemann, C. A.; Roos, P. G. Phys. Lett., 22: 172-4(Aug. 1, 1966).

The ^{9}Be(p,d)^{8}Be reaction was studied at a bombarding energy of 40.8 Mev. It was found that the 16.93-Mev level of ^{8}Be is strongly excited whereas the 16.63-Mev level is not, in accordance with the prediction of the single-particle model for these isobaric-spin-mixed states. (auth)

38068 ISOBARIC ANALOG STATE POLARIZATION MEASUREMENTS TO DETERMINE THE SPIN OF ^{145}Sm. Fiarman, S.; Ludwig, E. J.; Michelman, L.; Robbins, A. B. (Rutgers State Univ., New Brunswick, N. J.). Phys. Lett., 22: 175-6(Aug. 1, 1966).

Measurements were made on the polarization of protons elastically scattered from ^{144}Sm at energies (10.0 to 10.4 Mev) which scanned an isobaric analog state in ^{145}Eu. A determination of the spin of this state was used to make an assignment of $^{5}/_{2}^{-}$ to the isobaric multiplet which includes the 0.90-Mev state in ^{145}Sm. (auth)

38069 THE THRESHOLD FOR THE REACTION ^{10}B(p,n)^{10}C AND THE ft VALUE OF THE SUPERALLOWED FERMI TRANSITION ^{10}C(β^{+})^{10}B. Freeman, J. M.; Jenkin, J. G.; Murray, G. (Atomic Energy Research Establishment, Harwell, Eng.). Phys. Lett., 22: 177-80(Aug. 1, 1966).

The threshold for the transition ^{10}B(p,n)^{10}C was measured as 4880.0 ± 2.0 kev. In addition, preliminary results are reported for the branching ratios in the position decay of ^{10}C to excited states of ^{10}B and for accurate measurements of the excitation energies of these states. These results together enable the ft value of the pure Fermi transition to ^{10}B** to the calculated with much greater accuracy than has been attained previously. (auth)

38070 REACTIONS ($\pi^{\pm}$,NN) AND TWO-PARTICLE EXCITATION OF LIGHT NUCLEI. Kopaleishvili, T. I.; Machabeli, I. Z.; Goksadze, G. Sh.; Krupennikova, N. B. (Tbilissi State Univ., USSR). Phys. Lett., 22: 181-2(Aug. 1, 1966).

The results of some calculations of the probabilities of the excitation of ^{10}B, ^{12}C, and ^{14}N energy levels in meson ($\pi^{\pm}$,2N) reactions with ^{12}C, ^{14}N, and ^{16}O are presented. (D.C.W.)

38071 SPIN AND PARITY OF THE 3.16-Mev AND 7.54-Mev LEVELS IN ^{35}Cl. Watson, D. D. (Aerospace Research Labs., Wright-Patterson Air Force Base, Ohio). Phys. Lett., 22: 183-5(Aug. 1, 1966).

The E_p = 1214 kev resonance in ^{34}S(p,γ)^{35}Cl produces a dominant 7.54 → 3.16 → 0 cascade. Angular correlation and polarization measurements have led to the assignments (J^{π},T) = ($^{7}/_{2}^{-}$,$^{3}/_{2}$) and ($^{7}/_{2}^{-}$,$^{1}/_{2}$) for the 7.54 and 3.16-Mev levels. The 3.16 → 0 transition is mixed M2/E3. (auth)

38072 ALPHA DECAY FROM EXCITED STATES OF SAMARIUM ISOTOPES. Kvitek, J.; Popov, Yu. P. (Joint Inst. for Nuclear Research, Dubna, USSR). Phys. Lett., 22: 186-8(Aug. 1, 1966).

The (n,α) reactions on ^{147}Sm and ^{149}Sm were investigated at neutron energies up to 200 ev. The lifetimes with respect to alpha decay were obtained for thirteen excited states of ^{148}Sm and ^{150}Sm with $J^{\pi} = 4^{-}$ and 3^{-}. Calculations, made according to the statistical theory, of the probabilities of $4^{-} \rightarrow 2^{+}$ transitions in ^{150}Sm are in good agreement with the experiments. The lifetimes of nine ^{148}Sm states are in the region of 0.2 to 4 ns. The lifetimes of the 3^{-} and 4^{-} levels differ by an order of magnitude. (auth)

38073 (^{3}He,d) REACTIONS ON THE EVEN Sn ISOTOPES. Bassani, G.; Conjeaud, M.; Gastebois, J.; Harar, S.; Laget, J. M.; Picard, J. (Centre d'Etudes Nucleaires, Saclay, France). Phys. Lett., 22: 189-90 (Aug. 1, 1966).

Proton states in the odd Sb isotopes were observed by means of the (^{3}He,d) reaction on the even Sn isotopes at 18 Mev. The assignment of spins and parities to levels up to one Mev energy and preliminary results relative to the spectroscopic factors are presented. (auth)

38074 THE D(d,n)^{3}He AND D(d,p)^{3}H REACTIONS WITH POLARIZED DEUTERONS AT 460 kev. Paetz gen Schieck, H.; Petitjean, C.; Striebel, H. R.; Huber, P. (Univ., Basel). Phys. Lett., 22: 191-3(Aug. 1, 1966).

With the improved Basel source of polarized deuterons, the four components of the analyzing power $P^{a}(\theta)$, $P_{33}{}^{a}(\theta)$, $P_{11}{}^{a}(\theta) - P_{22}{}^{a}(\theta)$ and $P_{13}{}^{a}(\theta)$ of the two (dd)-reactions for polarized deuterons were measured at a mean deuteron energy of 460 kev and were compared with the theory of Rook and Goldfarb. (auth)

38075 LIFETIMES OF THE 5.10- AND 5.83-Mev LEVELS IN ^{14}N. Allen, K. W.; Alexander, T. K.; Healey, D. C. (Chalk River Nuclear Labs., Ont., Can.). Phys. Lett., 22: 193-5(Aug. 1, 1966).

The mean lifetimes of the 5.10 and 5.83-Mev levels of ^{14}N are 12.4 ± 1.4 ps and 18 ± 2 ps, respectively, as determined by a recoil-distance method. Absolute strengths are given for the dipole, quadrupole, and octupole transitions for the γ decay of these levels. (auth)

38076 STUDY OF LOW-LYING ISOBARIC ANALOG STATES OF ^{89}Sr. Cosman, E. R.; Enge, H. A.; Sperduto, A. (Massachusetts Inst. of Tech., Cambridge). Contract AT(30-1)-2098. Phys. Lett., 22: 195-7(Aug. 1, 1966).

Isobaric analog states in ^{89}Sr were studied via the (p,p) and (p,p') reactions on ^{88}Sr at 4.9 to 7.5 Mev and were compared with the results of a (d,p) reaction on ^{88}Sr. The (p,p) data were analyzed with Breit-Wigner theory as well as with coupled-channel calculations. The (p,p') data obtained with the bombarding energy on analog resonances display asymmetries about 90°. (auth)

38077 NEUTRONS FROM DEUTERON BREAKUP ON ^{3}He. Kerr, R. G. (Univ. of Wisconsin, Madison). Phys. Rev., 148: 998-1002(Aug. 19, 1966). (COO-7-395).

Neutron spectra produced by bombarding ^{3}He with deuterons have been measured for bombarding energies from 7 to 12 Mev and neutron emission angles from 0 to 70 deg. The observed spectra exhibit no structure attributable to a state in ^{4}Li. An upper limit for the cross section for forming such a state is deduced. (auth)

38078 EIGENFUNCTIONS FOR A SPHERICAL AND A DEFORMED SAXON-WOODS POTENTIAL. Faessler, Amand; Sheline, Raymond K. (Florida State Univ., Tallahassee). Contract AT(40-1)-2434. Phys. Rev., 148: 1003-20(Aug. 19, 1966).

The eigenfunctions for spherical and deformed Saxon-Woods potentials with a Thomas-type spin-orbit coupling are calculated for mass number A = 185. The expansion coefficients into oscillator functions and the energies are tabulated for the spherical Saxon-Woods functions for N = 4 and 5 proton shells and for N = 5 and 6 neutron shells. For states with a binding energy >2 Mev the first six coef-

ficients contain more than 99% of the Saxon-Woods function. The overlap integral for these states with the corresponding oscillator functions is always greater than 0.92. The basis for the spheroidal nuclei is confined to a single N shell. The deformed potential reproduces the experimental level sequence in the rare-earth nuclei using the optical-model parameters. The well depth, however, is fitted using the binding energy of the last particle. The differences between the quadrupole matrix elements in the Saxon-Woods and oscillator potentials are as large as 60% for states with a binding energy greater than 2 Mev. The γ-ray transitions between states of small binding energy and more than one node are enhanced by several oscillator units. The quadrupole matrix elements and the mixing coefficients for the rare-earth nuclei are tabulated and the expressions for the transition probabilities are given in the (jlK) representation. (auth)

38079 g FACTORS OF EXCITED NUCLEAR STATES BY RESONANT SCATTERING. **Goebel, C. J.; McVoy, K. W. (Univ. of Wisconsin, Madison). Phys. Rev., 148: 1021-4(Aug. 19, 1966).**

If a resonant nuclear state is excited during a scattering process in the presence of a known magnetic field, the state, and so the angular distribution of its decay products, will process through an angle δ which can be used to measure the g value of the state if its lifetime $\tau = \hbar/\Gamma$ is known. The influence of the bandwidth Δ of the incident wave packet on the angle is investigated, and it is found that it varies smoothly from $\delta = \Omega\tau$ (Ω = Larmor precession frequency) for $\Delta \gg \Gamma$ to $\delta = 2\Omega\tau$ for $\Delta \ll \Gamma$. (auth)

38080 OBSERVATION OF THE 4.12-Mev $^{14}O \rightarrow {}^{14}N$ POSITRON SPECTRUM SHAPE. Sidhu, Gurnam S.; Gerhart, J. B. (Univ. of Washington, Seattle). Phys. Rev., 148: 1024-30(Aug. 19, 1966). (RLO-1388-1).

The spectrum shape for the 4.12-Mev $^{14}O \rightarrow {}^{14}N$ allowed positron transition has been measured in the positron energy range greater than 2 Mev. The observed shape deviates markedly from the statistical shape (slope about −11% per Mev at 3 Mev). The $\int\alpha \times r$ forbidden matrix element is extracted from the data and used to calculate the mean life of ^{14}N. For the latter, the value obtained is $(3.3 \pm 0.3) \times 10^{-14}$ sec. The sign of the allowed matrix element $\int\sigma$ is found to be positive. The ft value obtained for the 4.12-Mev transition is $(2.14 \pm 0.03) \times 10^7$ sec and the branching fraction is found to be (0.61 ± 0.01)%. (auth)

38081 PROTON-PROTON SCATTERING: REVISION AND ANALYSIS OF EXPERIMENTAL MEASUREMENTS FROM 1.4 TO 3.0 Mev. **Knecht, David J. (Air Force Cambridge Research Labs., Bedford, Mass.); Dahl, Per F.; Messelt, S. Phys. Rev., 148: 1031-44(Aug. 19, 1966).**

Revised experimental values are given for the differential cross section for proton-proton scattering at energies of 1.397, 1.855, 2.425, and 3.037 Mev. These result from the consolidation and re-evaluation of all published and unpublished data obtained in an experiment reported earlier by Knecht et al. Phase-shift analyses have been made. The preferred solutions determine the S-wave phase shift K_0 and the central-force ("effective") part γ of the P-wave phase shifts, under the assumption that the noncentral-force parts and all higher angular-momentum phase shifts are known with sufficient accuracy from one-pion-exchange theory; the values of γ derived in this way are small, with zero not excluded. Other solutions in which noncentral forces range from zero to very large values are given for comparison. The uncertainty in each of the derived phase shifts is calculated and discussed in detail; uncertainties obtained by the usual statistical method are shown to be too small. The polarization implied by each phase-shift solution has been calculated, and it is shown that reported measurements are in disagreement not only with the present data and theoretical predictions but with any combination of central, tensor, and spin-orbit forces. (auth)

38082 TWO-NUCLEON DISTORTED-WAVE BORN APPROXIMATION ANALYSIS OF $^{19}F(d,\alpha)^{17}O$ DATA. Wesolowski, Jerome J.; Hansen, Luisa F.; Vidal, Jose G.; Stelts, Marion L. (Univ. of California, Livermore). Phys. Rev., 148: 1063-71(Aug. 19, 1966). (UCRL-14731).

The $^{19}F(d,\alpha)^{17}O$ absolute differential cross sections have been measured at bombarding energies of 5.5, 6.5, 7.5, 8.5, 9.5, and 11.5 Mev for the ground and first four excited states of ^{17}O. Attempts were made to fit the ground- and first-excited-state relative differential cross sections, using the two-nucleon DWBA theory of Glendenning. Reasonable fits were obtained only for the ground-state distributions at higher bombarding energies. (auth)

38083 PROPERTIES OF THE 7.03-Mev EXCITED STATE OF ^{14}N. **Swann, C. P. (Franklin Inst., Swarthmore, Pa.). Contract Nonr-3777(00). Phys. Rev., 148: 1119-22(Aug. 19, 1966).**

The 7.03-Mev state in ^{14}N has been excited by resonance scattering of the Doppler-broadened 7.115-Mev radiation from the $^{19}F(p,\alpha\gamma)^{16}O$ reaction. The measurement of the resonance effect as a function of the angle between the proton beam and the γ rays incident on the scatterer gives a cutoff angle which corresponds to a level energy of 7.029 ± 0.006 Mev. The angular distribution of the scattered radiation is consistent with a spin of 2, a fit being obtained for a quadrupole-dipole amplitude ratio of −0.60 ± 0.15. Assuming all the decays of this level are to the ground state, the mean life of this level becomes $(5.4 \pm 0.5) \times 10^{-15}$ sec. (auth)

38084 ENERGETICS OF THE $^{27}Al(^{11}B,p3n)^{34m}Cl$ REACTION FROM RECOIL STUDIES. Kaplan, Morton; Ewart, Alan (Yale Univ., New Haven). Phys. Rev., 148: 1123-32 (Aug. 19, 1966).

The $^{27}Al(^{11}B,p3n)^{34m}Cl$ reaction at bombarding energies from 30 to 115 Mev was studied in detail. Measurements of cross sections, average recoil ranges, and angular distributions of the reaction product ^{34m}Cl, the high-spin member of an isomeric pair, are presented. The excitation function behavior is unusual, exhibiting a relatively slow decrease in cross section at higher energies. The peak cross section is about 16 mb, and at 65 Mev above the excitation-function peak, the cross section is approximately 2% of its maximum value. Recoil range results provide strong evidence that the reaction proceeds by compound-nucleus formation at all energies investigated. At the highest bombarding energy, approximately 66 Mev must be dissipated as particle kinetic energies and photons in the compound nucleus de-excitation. The analysis of angular-distribution experiments indicates that most of this energy appears as kinetic energy of emitted particles. The total particle kinetic energy increases approximately linearly with available energy. Relatively little de-excitation energy is released in the form of gamma radiation, of the order of 7 Mev or less. The trend of total gamma-ray emission energy with increasing available energy is roughly constant, but seems to show a slight decrease. There is no direct evidence that the formation of ^{34m}Cl involves preferential selection of compound nuclei with greater than average angular momentum. On the contrary, if the presence of gamma-ray competition with particle evaporation is taken as a criterion of high angular momentum, then these results may imply a strong discrimination against high-angular-momentum events. The range-energy data for ^{34m}Cl in Al are compared with the predictions of stopping theory. The high velocities encountered in these experiments provide a test of the theoretical formulation relating to electronic stopping. Although general agreement is good, there are systematic deviations which may indicate the approximate character of the theoretical assumptions. (auth)

38085 LIFETIME OF THE 1.52-Mev LEVEL IN ^{42}Ca. **Metzger, F. R.; Tandon, G. K. (Franklin Inst., Swarthmore, Pa.). Phys. Rev., 148: 1133-6(Aug. 19, 1966). (NYO-3525-7).**

Nuclear resonance fluorescence from the first excited state of ^{42}Ca has been observed. The ^{42}K beta decay provided the recoil needed to restore the resonance condition. To fully utilize this recoil, a gaseous source of ^{42}K iodide was used. The measured cross section for resonance scattering corresponds to a width $\Gamma = (4.8 \pm 1.1) \times 10^{-4}$ ev for the 1.52-Mev 2^+ level in ^{42}Ca, or a mean life of 1.4×10^{-12} sec. In arriving at this result, the coefficient λ in the beta-neutrino angular correlation function $W(\theta) = 1 + \lambda(v/c)\cos\theta$

was assumed to have the value $\frac{1}{3}$. The error quoted above for the width Γ takes into account the possibility that λ may range from $-\frac{1}{3}$ to +1. The reduced E2 transition probability corresponding to the measured width, $B(E2, 2 \rightarrow 0) = 74e^2F^4$, is eight times larger than the Weisskopf estimate, and more than 20 times larger than the prediction of a recent calculation by Bertsch. (auth)

38086 $^{28}Si(d,p\gamma)^{29}Si$ ANGULAR CORRELATIONS FROM 4 TO 6 Mev. Hausman, H. J.; David, W. E.; Phillips, C. V.; Sullivan, R. P.; Unrine, G. R. (Ohio State Univ., Columbus). Phys. Rev., 148: 1136-47(Aug. 19, 1966).

A study of the $(d,p\gamma)$ angular correlations involving the 1.28- and 2.03-Mev states in ^{29}Si populated by the $^{28}Si(d,p)^{29}Si$ reaction has been carried out at five deuteron bombarding energies between 4 and 6 Mev. Angular-correlation measurements were carried out in the reaction plane and in that plane perpendicular to the reaction plane which contains the incident-beam direction. The data were analyzed by means of the distorted-wave stripping formalism. Statistical tensors, describing the orientation of the intermediate excited nuclear states, were calculated at each energy. Since the reaction-plane measurements on the 2.03-Mev state alone were sufficient for determining the statistical tensors describing the correlation over the sphere, comparison has been made between the measured perpendicular-plane correlations and the correlations predicted from these statistical tensors. In addition, a combined set of statistical tensors has been calculated utilizing data from the reaction-plane and perpendicular-plane correlations. The magnitudes of the proton polarizations have also been calculated for the 2.03-Mev excited-state reaction using the combined set of statistical tensors. The observed correlations are in agreement with the predictions of a distorted-wave theory and not with those of the plane-wave theory. (auth)

38087 CONVERSION COEFFICIENT OF THE 12.4-kev TRANSITION IN ^{45}Sc. Jones, K. W.; Schwarzschild, A. (Brookhaven National Lab., Upton, N. Y.). Phys. Rev.. 148: 1148-50(Aug. 19, 1966). (BNL-10178).

The K-conversion coefficient α_K of the 0.44-sec, 12.4-kev state of ^{45}Sc was measured by comparison of the intensity of γ rays and x rays emitted by the isomer. A proportional counter was used to observe the radiations. A value of $\alpha_K = 413 \pm 37$ was obtained. The value is in agreement with the theoretical M2 conversion coefficient. (auth)

38088 ENERGY LEVELS OF ^{56}Fe. Dolan, K. W.; McDaniels, D. K.; Wells, D. O. (Univ. of Oregon, Eugene). Phys. Rev., 148: 1151-6(Aug. 19, 1966). (RLO-1921-7).

The energies and relative intensities of the gamma radiations following the decay of ^{56}Co to ^{56}Fe have been measured using a 3-mm depletion-depth lithium-drifted germanium detector. Gamma rays of the following energies were observed (relative intensities in parentheses): 846.5(100.0), 1038.1(12.4), 1238.6(71.2), 1359.9(3.8), 1770.8(15.6), 2015.6 (3.8), 2034.7(7.8), 2598.9(16.0), 3009.5(1.9), 3202.3(2.9), 3254.0(5.8), 3273.6(1.2), 3452.6(0.7), and 3548.3(0.2) kev. A decay scheme was constructed with levels at 846.5(2^+), 2085.1(4^+), 3123.2(4^+), 3445.2(3^+), 3856.0(3^+), 4048.8, 4100.6, 4120.0, 4299.1, and 4394.8 kev. No evidence was found for doublet energy levels at 3123.2 and 3445.2 kev as indicated in recent particle-scattering experiments, thus supporting spin assignments of 1^+ for the unobserved members. The energies of several new gamma-ray standards were established. Energies and relative intensities of gamma-ray transitions following the decay of ^{58}Co to ^{58}Fe were also measured and found to be 810.2(100.0), 863.8(0.64), and 1674.9(0.46) kev. (auth)

38089 NUCLEAR SPIN AND MOMENTS OF ^{45}Ti. Cornwell, R. G.; McCullen, J. D. (Princeton Univ., N. J.). Phys. Rev., 148: 1157-61(Aug. 19, 1966).

The nuclear spin and moments of the radioactive isotope ^{45}Ti have been measured by the atomic-beam magnetic-resonance method. These measurements were performed in the J = 3 fine-structure state. The spin was measured to be $I = \frac{7}{2}$ and the hyperfine interaction constants were determined to be: $|A| = 4.59 \pm 0.07$ Mc/sec and $|B| = 1.5 \pm 1.5$ Mc/sec, with $B/A > 0$. From the known hyperfine interaction constants and nuclear moments of ^{47}Ti and ^{49}Ti the nuclear magnetic dipole and electric quadrupole moments were calculated. The results are (with no diamagnetic or Sternheimer corrections): $|\mu_I| = 0.095 \pm 0.002$ nm and $|Q| = 0.015 \pm 0.015$ b, with $\mu_I/Q > 0$. These results are interpreted from the point of view of certain shell-model calculations. (auth)

38090 EFFECT OF CHEMICAL STATE ON THE DECAY CONSTANT OF ^{235m}U. Mazaki, Hiromasa; Shimizu, Sakae (Kyoto Univ.) Phys. Rev., 148: 1161-7(Aug. 19, 1966).

An experimental investigation of the influence of chemical forms on the decay constant of ^{235m}U was performed. The ^{235m}U atoms from a very thin ^{239}Pu source were collected by the recoil method on platinum, carbon, and silicon plates in a pure argon atmosphere. Applying the differential method with two identical, specially designed 12-stage secondary electron multipliers, emission rates of the internal-conversion electrons of very weak energy from the isomer in different chemical states were compared. The stability and sensitivity of the whole measuring system were checked using ^{14}C and metallic ^{235m}U sources. Metallic uranium (U) and uranium atoms slightly diffused into carbon (UC) or silicon (USi) base were used for the different chemical states. The half-life of ^{235m}U was determined to be $T_{\frac{1}{2}} = 26.05 \pm 0.05$ min by using a low-background 2π gas-flow counter. Furthermore, diffusion of the isomer into the base materials, carbon and silicon, was investigated in some detail. (auth)

38091 PROPERTIES OF SOME LOW EXCITED STATES IN ^{101}Ru FROM THE DECAY OF 3-Y ^{101}Rh. Chilosi, G. (Instituut voor Kernphysisch Onderzoek, Amsterdam); Loebner, K. E. G.; Moro, R.; Speranza, P. R.; Vingiani, G. B. Phys. Rev., 148: 1168-73(Aug. 19, 1966).

Some properties of low-lying excited states and corresponding transitions in ^{101}Ru were established by studying the decay of $^{101}Rh(T_{\frac{1}{2}} = 3.0$ yr) using scintillation spectroscopy. The three gamma rays associated with this decay with energies in kev (intensities) are 128 ± 3 (89 ± 4), 197 ± 3 (100), 320 ± 10 (24 ± 1). They de-excite levels at 128 and 325 kev. A half life of 0.55 ± 0.03 nsec was determined for the 128-kev level and a limit of $\leq$0.3 nsec was set for the 325-kev level using the delayed-coincidence method. The angular correlation between the 128- and 197-kev gamma rays was measured, and the results were fitted to the formula $W(\theta) = 1 + (0.183 \pm 0.025)P_2(\cos\theta)$ or to $W(\theta) = 1 + (0.181 \pm 0.025)P_2(\cos\theta) + (0.020 \pm 0.034)P_4(\cos\theta)$. When these results are combined with Coulomb-excitation data, they yield an assignment of $\frac{5}{2}^+$ for the 128-kev level with a mixing ratio δ of 0.17 ± 0.05 for the corresponding transition. Although a definitive spin assignment can not be inferred for the 325-kev level, a spin $\frac{1}{2}^+$ seems the more probable, with $\delta = -(0.15^{-\infty}_{+0.8}; {}^{+1.9}_{+0.12})$ for the 197-kev mixed transition. (auth)

38092 NUCLEAR-REACTION STUDIES WITH 65-Mev ALPHA PARTICLES ON ZIRCONIUM. Bingham, C. R.; Halbert, M. L.; Bassel, R. H. (Oak Ridge National Lab., Tenn.). Phys. Rev.. 148: 1174-91(Aug. 19, 1966). (ORNL-P-2092).

Differential cross sections for elastic and inelastic scattering and $(\alpha,{}^3He)$ reactions were measured for 65-Mev alpha particles on ^{90}Zr, ^{91}Zr, and ^{92}Zr. Excellent optical-model fits to the elastic data were obtained with four-parameter Woods-Saxon potentials having a real depth of about 35 Mev. A continuum of fits almost as good was found for a class of deeper wells. Distorted-wave predictions for all the inelastic groups studied were made with the collective model. The results were insensitive to the ambiguity in the potentials, and were quite successful for most of the groups. Where comparisons can be made, the values of the deformation parameter β_l are in agreement with results from Coulomb excitation and nuclear scattering of other particles. Exploratory calculations were made for single-particle excitation for the first 2^+ and 4^+ levels of ^{92}Zr. The $(\alpha,{}^3He)$ cross sections were compared with zero-range distorted-wave predictions. Good fits to the

angular distributions were obtained by selection among potentials which provide fits for elastic scattering in the entrance and exit channels. Normalization of the predictions to the data yielded spectroscopic factors in generally good agreement with results from (d,p) and (p,d) measurements for s and d states. In making this comparison, an empirical adjustment by a factor of 17.8 was included. The predictions for $g_{\frac{9}{2}}$ states were generally too small. Spin-orbit and nonlocal corrections do not improve the agreement. Some of the discrepancy may be due to the presence of small portions of the $h_{\frac{11}{2}}$ strength in the low-lying states. (auth)

38093 NUCLEAR DECAY PROPERTIES OF HEAVY NUCLIDES PRODUCED IN THERMONUCLEAR EXPLOSIONS: PAR AND BARBEL EVENTS. Phys. Rev., 148: 1192-8(Aug. 19, 1966). (UCRL-14500).

The nuclear decay properties of heavy nuclides ($A \leq 257$) produced in two low-yield thermonuclear explosions, the Par and Barbel events, were studied with the following results. The α-decay branching of ^{253}Cf was observed, $E_\alpha = 5.978 \pm 0.005$ Mev, $\alpha/(\alpha + \beta^-) = 0.31 \pm 0.04\%$. The α-decay branching of ^{255}Es was observed, $E_\alpha = 6.300 \pm 0.003$ Mev, $\alpha/(\alpha + \beta^-) = 8.5 \pm 0.3\%$. The spontaneous fission half life of ^{250}Cm was remeasured and was found to be $1.74 \pm 0.24 \times 10^4$ years. Upper limits for the half lives of ^{252}Cm and ^{251}Bk were set at 2 and 3 days, respectively. The existence of 80-day ^{257}Fm was confirmed; a sample of ^{257}Fm from the Par event decayed with a half life of 94 ± 10 days. Attempts to produce and detect ^{258}Fm by irradiating Par ^{257}Fm in a reactor neutron flux were unsuccessful. Upper limits for the half life of ^{258}Fm were determined. (auth)

38094 PHOTONEUTRON CROSS SECTIONS OF ^{141}Pr AND ^{127}I FROM THRESHOLD TO 33 Mev. Bramblett, R. L.; Caldwell, J. T.; Berman, B. L.; Harvey, R. R.; Fultz, S. C. (Univ. of California, Livermore). Phys. Rev., 148: 1198-1205(Aug. 19, 1966). (UCRL-7701; UCRL-7701 (Rev.1)).

The photoneutron cross sections for ^{127}I and ^{141}Pr were measured with about 170- and 320-kev photon energy resolution, using monoenergetic photons obtained from annihilation in flight of positrons. The (γ,n), $(\gamma,2n)$, and $(\gamma,3n)$ cross sections were determined experimentally by a neutron-counting technique; hence, the nuclear photon-absorption cross sections were obtained without calculated multiplicity corrections. The photon-absorption cross section obtained for ^{141}Pr is a single-peaked, giant dipole resonance, well described by a Lorentz-shaped curve with a maximum of 320 mb at 15.2 Mev and a width of 4.5 Mev. The ^{127}I giant resonance is broadened slightly by its vibrational deformation. Although a single Lorentz curve is in fair agreement with the data, better agreement is obtained by the sum of two Lorentz curves, when adjusted to fit the data with the restrictions implied by the hydrodynamic model. The parameters of the two curves are: resonance energies, 15.2 and 15.8 Mev; peak cross sections, 180 and 50 mb; and widths, 4.1 and 8 Mev. The integrated nuclear photon-absorption cross sections of ^{127}I and ^{141}Pr, obtained from the areas under the Lorentz curves which fit the data, are 1.8 ± 0.2 and 2.3 ± 0.2 Mev-b, respectively. These integrated cross sections are in good agreement with the dipole sum rule uncorrected for exchange effects, which predicts 1.9 and 2.1 Mev-b. The ^{141}Pr$(\gamma,3n)$ threshold, which was measured to be 28 ± 1 Mev, determines the mass of ^{138}Pr. (auth)

38095 X RAYS AND ELECTRONS EMITTED IN COINCIDENCE WITH THE FISSION OF ^{252}Cf. Atneosen, R. A. (Princeton Univ., N. J.); Thomas, T. D.; Gibson, Walter M.; Perlman, Morris L. Phys. Rev., 148: 1206-20(Aug. 19, 1966). (BNL-9996).

The emission times of K x rays and the yield and spectra of conversion electrons produced in coincidence with the spontaneous fission of ^{252}Cf were measured. The measurements of x-ray yield as a function of time since fission can be analyzed into components with half lives of 2.4, 0.4, 0.05, and <0.01 nsec with relative numbers of nuclei 45, 25, 10, and 20, respectively. The yield of conversion electrons falls almost exponentially from 30 kev, the lowest energy measured, to about 500 kev; this falloff can be accounted for by the energy dependence of internal conversion coefficients. The yield of conversion electrons as a function of mass reaches a maximum at about mass 108, a minimum at mass 130, and a pronounced maximum at about mass 153. There is a sharp decrease in yield beyond this second maximum. The combination of x-ray half-lives and energies observed is consistent with low multipolarity transitions, mostly M1-E2 mixtures with some E2 and perhaps some E1. The gross features of the yield as a function of mass can be understood in terms of the stable nuclear deformations beyond mass 150, of postulated deformations for the neutron-rich nuclides near mass 108, and of the closed-shell properties of nuclides near mass 132. Various explanations for the sharp drop in yield beyond 153 are explored. It is suggested that the amount of spin acquired by a fragment at scission may depend critically on the partner fragment; spherical fragments are less effective at imparting spin to their partners than are deformed ones. This suggestion provides an explanation for the drop in electron yield at mass 153 and for some of the differences between the yield and spectrum of K x rays for ^{252}Cf and these quantities for ^{236}U. (auth)

38096 ^{90}Zr(d,p)^{91}Zr REACTION AT ENERGIES BELOW 4 Mev. Brient, Charles E. (Univ. of Texas, Austin); Hudspeth, Emmett L.; Bernstein, E. M.; Smith, William R. Phys. Rev., 148: 1221-6(Aug. 19, 1966). (ORNL-P-1203).

Angular distributions of the ground-state protons from the ^{90}Zr(d,p)^{91}Zr reaction were measured at five bombarding energies in the region $2.7 < E_d < 3.6$ Mev. Distorted-wave Born approximation calculations for the reaction are in essential agreement with the observations and with predictions based on higher-energy data for proton and deuteron elastic scattering and for deuteron stripping. It is concluded that it should be possible to employ stripping theory to determine nuclear spins, parities, and spectroscopic factors at low bombarding energies, just as the theory has been previously employed at higher energies. (auth)

38097 DECAY OF 25-MIN ^{246}Am AND 1.8-DAY ^{246}Bk. Orth, C. J. (Los Alamos Scientific Lab., N. Mex.). Phys. Rev., 148: 1226-34(Aug. 19, 1966). (LA-DC-7836).

The radiations associated with the β decay of 25-min ^{246}Am and the electron-capture decay of 1.8-day ^{246}Bk were studied with γ-scintillation spectrometers, Ge(Li) detectors, and an Au-surface-barrier electron detector. Conversion-electron lines of the more intense ^{246}Cm transitions were observed, and tentative multipole orders were assigned. A decay scheme is presented on the basis of gamma energy and intensity data, γ-γ coincidence studies, and conversion-electron measurements. The ^{246}Cm level diagram includes excited states at 43, 142, 843, 878, 1078, 1106 1126 (doublet), 1318, 1352, 1369, 1483, 1531, 1598, 1643, ≥1668, and ≥1739 kev. The levels at 843, 878, 1078, 1106, and 1126 (doublet) kev are all directly populated by both 25-min ^{246}Am and 1.8-day ^{246}Bk. The 1126-kev doublet level consists of the $I = 3$ rotational member of a $K^\pi = 1^-$ band based at 1078 kev and a 2^+ state that de-excites by essentially pure E2 transitions to the 0^+ and 2^+ members of the ground-state band. Consideration of the electron-capture decay information and available Nilsson orbitals leads to a spin and parity assignment of 2^- for 1.8-day ^{246}Bk. The present work is in agreement with the previous 2^+ assignment for 25-min ^{246}Am. (auth)

38098 YIELDS OF PRODUCTS WITH A = 100 TO 117 IN THE INTERACTION OF 3- AND 28-Gev PROTONS WITH URANIUM AND LEAD. Porile, Norbert T. (Purdue Univ., Lafayette, Ind. Brookhaven National Lab., Upton, N. Y.). Phys. Rev., 148: 1235-40(Aug. 19, 1966). (BNL-10014)

Cross sections for the formation of 14 isotopes of palladium, cadmium, and indium were measured for lead and uranium targets bombarded by 3- and 28-Bev protons. The isobaric cross section at A = 109 was determined as 32.2 ± 3.8 mb and 27.2 ± 3.5 mb for uranium at 3 and 28 Bev, respectively, and as 5.8 ± 0.6 mb and 6.9 ± 0.7 mb for lead at the corresponding energies. It is found that the yields of neutron-deficient products increase with energy for both

targets by as much as 60–90%. On the other hand, the yields of neutron-excessive products from uranium decrease by 10–30% with increasing energy whereas those from lead show no energy dependence. The yields of neutron-excessive products from uranium are two orders of magnitude larger than those from lead, whereas the neutron-deficient products are formed with slightly larger yields from lead. (auth)

38099 STUDY OF (d,p) AND (d,t) REACTION ON THE ^{136}Xe ISOTOPE. Schneid, Edward J.; Rosner, Baruch (Univ. of Pittsburgh). Phys. Rev., 148: 1241-6(Aug. 19, 1966).

Eight levels of ^{137}Xe and seven of ^{135}Xe were observed in the ^{136}Xe(d,p) and ^{136}Xe(d,t) reactions at 15 Mev. The angular distributions of the proton and triton groups were analyzed using zero-range distorted-wave Born-approximation calculations to extract spectroscopic information. Spin and parity assignments for most of the observed states were attempted. Comparison with (d,p) and (d,t) reaction on ^{138}Ba, ^{120}Ce, and ^{142}Nd reveals that the multiplicity of the hole states in the N = 81 isotones is much lower than that of the particle states in the N = 83 isotones. (auth)

38100 SYSTEMATICS OF 3$^-$ AND 5$^-$ STATES IN ^{40,42,44,48}Ca AND ^{50}Ti FROM INELASTIC ALPHA SCATTERING. Bernstein, A. M.; Lippincott, E. P. Massachusetts Inst. of Tech., Cambridge). Contract AT(30-1)-2098. Phys. Rev. Lett., 17: 321-4(Aug. 8, 1966).

The existence of three 3$^-$ states in ^{40}Ca and ^{48}Ca, six 3$^-$ states in ^{42}Ca and ^{44}Ca, and a 5$^-$ state in ^{40}Ca, ^{42}Ca, and ^{48}Ca (two in ^{44}Ca) was established using the inelastic scattering of 31-Mev alpha particles. The fractionation of the 3$^-$ strength and the rapid and similar drop of 3$^-$ and 5$^-$ strength in going from A = 40 to A = 50 appear to be in disagreement with current ideas about the nature of these states. (D.C.W.)

38101 ANOMALOUS ISOTOPE SHIFT OF THE NUCLEAR CHARGE RADIUS. Perey, F. G. (Oak Ridge National Lab., Tenn.); Schiffer, J. P. Phys. Rev. Lett., 17: 324-8(Aug. 8, 1966).

It is shown that the isospin dependence of the shell-model potential gives rise to the experimentally observed "anomalous" isotopic shift of nuclear charge radii. The charge radii calculated from a Woods-Saxon potential are in qualitative agreement with experimental determinations from electron scattering and from muonic x rays. (auth)

38102 3$^-$ CONTINUUM STATES OF ^{16}O IN THE EIGENCHANNEL REACTION THEORY. Wahsweiler, H. G.; Danos, M.; Greiner, W. (Univ., Frankfurt am Main). Phys. Rev. Lett., 17: 395-7(Aug. 15, 1966).

The complete 3$^-$ part of the S matrix for ^{16}O was computed in the one-particle, one-hole approximation. In the continuum states the isospin invariance is totally broken; analogous partial cross sections for protons and neutrons show large differences. (auth)

38103 TWO NEUTRON SCIENCES. Goldstein, Herbert (Columbia Univ., New York); Goldman, David T. Phys. Today, 19: No. 6, 53-8(June 1966).

Improvements in sources, detectors, models, and data analysis for neutron cross-section studies are discussed. The increasing separation of the work of cross section measurers and designers of neutron devices is discussed, and the role of evaluators and compilers of cross section data is pointed out. (L.B.S.)

38104 DECAY SCHEME OF 5.0-d ^{183}Ta. Bashandy, E.; El-Nesr, M. S.; El-Farrash, A. H. (Atomic Energy Establishment, Cairo). Physica, 32: 837-57(May 1966).

The gamma rays of ^{183}W excited through beta decay of ^{183}Ta have been studied principally by internal conversion spectroscopy using an iron-yoke double-focusing spectrometer at a momentum resolution of about 0.3%. In addition to gamma rays previously reported five new gamma rays were observed with energies of 105.44 ± 0.07, 111.90 ± 0.04, 123.31 ± 0.06, 210.3 ± 0.1, and 394.21 ± 0.30 kev. The 210.3-kev gamma ray is probably due to the depopulation of an 11/2 + (K = 9/2) isomeric state at 309.5 kev, where the 102.49 kev is de-excited. The four other transitions found are not accommodated by the known levels. The multipolarity assignment for each transition was obtained by comparing the observed internal conversion coefficient or conversion line intensity ratios with the theoretical values calculated by Sliv and Band. New information about E2/M1 mixing ratios for some of the gamma transitions have been deduced from measurement of the K/L or L-subshell conversion line intensity ratio. The determined conversion coefficients generally support previous spin assignments. The possible existence of three new levels at 341.18 kev, 394.21 kev, and 517.52 kev is proposed with spin and parity $5/2^-$, $7/2^-$, and $9/2^-$, respectively. A decay scheme for ^{183}Ta is given which satisfactorily accounts for all the results of this investigation. (auth)

38105 HIGH-RESOLUTION INVESTIGATION OF THE ^{30}Si(p,p)^{30}Si REACTION. Walinga, J.; van Rinsvelt, H. A.; Endt, P. M. (Rijksuniversiteit, Utrecht). Physica, 32: 954-65(May 1966).

The differential cross section for elastic scattering of protons on ^{30}Si was measured with surface barrier counters at four angles. Thirty-six ^{30}Si(p,γ)^{31}P resonances are known in the E_p = 1–2 Mev region. Fifteen of these were also observed in the ^{30}Si(p,p)^{30}Si reaction, with natural widths varying from 10 kev down to 13 ev. For all fifteen resonances the proton orbital momenta, and thus the parities, could be determined unambiguously; the spins are known already from the (p,γ) work. Partial widths for proton and γ-ray emission are computed from the widths and the (p,γ) yields. Upper limits are given for the widths of unobserved resonances. (auth)

38106 AN ISOMER OF ^{98}Rh. Aten, A. H. W. Jr.; Kapteyn, Johanna C. (Instituut voor Kernphysisch, Amsterdam). Physica, 32: 989-90(May 1966).

^{98}Rh is formed by irradiating Ru with protons at 17 and 50 Mev and with deuterons at 17 and 25 Mev. In the interval from 10 to roughly 30 minutes after irradiation NaI scintillograms are taken. The complex decay curve is explained by the following assumptions. Two isomers of ^{98}Rh are formed in comparable quantities. One isomer has a half life of 8.7 min and the other one a half life of 3 ± 1 min. The metastable isomer decays mainly by isomeric transition whereas positrons and γ rays are emitted mainly by the ground state. From the shape of the decay curve it cannot be determined which period corresponds to the ^{98m}Rh isomer and which period to ^{98g}Rh. Under these circumstances the question of relative stability of these isomers has not been definitely settled. (S.F.L.)

38107 SPECIFIC GAMMA EMISSION OF NATURAL POTASSIUM AND LANTHANUM. De Ruyter, A. W.; Aten, A. H. W. Jr.; van Dulmen, A.; Krol-Koning, C.; Zuidema, E. (Instituut voor Kernphysisch, Amsterdam). Physica, 32: 991-4(May 1966).

New measurements are reported for the specific gamma activities of natural K and La. Both measurements were made using a heavily shielded, low-background, well-type NaI crystal detector. K was used in aqueous solution to reduce the level of bremsstrahlung. The average of 20 measurements gave a specific gamma emission of K as 3.25 (±0.06)γ/sec/g. Values obtained for natural La at 0.81 and 1.43 Mev were 0.301(±0.005) and 0.513(±0.006)γ/sec/g, respectively. The influence of the value of gamma emission obtained for K on the values of potassium–argon ages is discussed. (S.F.L.)

38108 VARIATIONAL APPROACH TO THE NUCLEAR COLLECTIVE MOTION. da Providencia, J. (Univ., Coimbra, Portugal). Port. Phys., 4: 171-82(1965).

A method for obtaining a classical collective hamiltonian is presented. The starting point is the many-body hamiltonian, and the derivation is based on the variational principle of quantum mechanics. The force and mass parameters are determined without ambiguity by the single-particle energies and by some matrix elements of the two-body interaction. The theory is applied to the dipole state of ^{16}O. The results, which have been obtained by a simple calculation,

compare favorably with results obtained by the diagonalization of the random-phase-approximation matrix, but the present method is valid even when the ground state of the nucleus can not be represented by a single Slater determinant. (auth)

38109 NUCLEAR REACTIONS. Strzalkowski, Adam (Jagellonian Univ., Krakow). Postepy Fiz., 17: 115-28 (1966). (In Polish).

A general review of the principal problems in investigations of nuclear reactions is presented and illustrated with the results obtained in the Polish physical laboratories. (auth)

38110 STUDY OF HIGH-ENERGY INTERACTIONS IN GRAPHITE. Malholtra, P. K. (Tata Inst. of Fundamental Research, Bombay); Shukla, P. G.; Stephens, S. A.; (and others). pp 840-3 of Proceedings of the Ninth International Conference on Cosmic Rays. Vol. 2. Stickland, A. C. (ed.). London, The Institute of Physics and The Physical Society, 1966.

An analysis is given of 46 nuclear interactions in graphite, in each of which at least 1300 Bev was radiated as γ rays. In each event the energies and relative angles of all γ rays within certain fiducial limits were measured. Data are presented concerning the multiplicity of γ rays and their transverse momentum distributions. The mean transverse momentum of all the γ rays, corrected for scanning loss, is 258 ± 12 Mev/c. The mean multiplicity of pions in nucleon-carbon interactions at 1.4×10^4 Bev primary energy is computed to be 33 ± 5. (auth)

38111 CROSS SECTION OF THE REACTION $\nu + {}^{37}Cl \rightarrow {}^{37}Ar + e^-$. Domogatskii, G. V. (Lebedev Inst. of Physics, Moscow); Gavrin, V. N.; Eramzhyan, R. A. pp 1034-6 of Proceedings of the Ninth International Conference on Cosmic Rays. Vol. 2. Stickland, A. C. (ed.). London, The Institute of Physics and The Physical Society, 1966.

It is necessary to know the exact value of the cross section of this process for the determination of the neutrino activity of the sun. The structure of nuclei with A = 37 and A = 38 is considered in terms of the intermediate coupling shell model. The dependence of the energy level position and the probabilities of β transitions from model parameters is investigated. It is shown that the contribution of the $1d_{\frac{3}{2}}$ shell is not important. Some attention is given to the importance of the reaction $^{37}Cl(p,n)^{37}Ar$ for the determination of the energy position of the level with $J = \frac{3}{2}$, $T = \frac{3}{2}$ in ^{37}Ar. The lowest limit and the most probable value of the cross section of the reaction $\nu + {}^{37}Cl \rightarrow {}^{37}Ar + e^-$ are given. (auth)

38112 FINITE-RANGE DISTORTED-WAVE CALCULATIONS ON REACTIONS $^{13}C(p,n)^{13}N$, $^{11}B(p,n)^{11}C$, AND $^{27}Al(n,p)^{27}Mg$. Une, Tsutomu; Yamaji, Shuhei; Yosida, Hiroshi (Osaka Univ.). Progr. Theoret. Phys. (Kyoto), 35: 1010-25 (June 1966).

Finite-range distorted-wave Born approximation calculations are performed on the reactions $^{13}C(p,n)^{13}N$, $^{11}B(p,n)^{11}C$, and $^{27}Al(n,p)^{27}Mg$. The simple shell model with the harmonic oscillator potential is assumed on nuclei for the former two reactions. On the other hand, for the reaction $^{27}Al(n,p)^{27}Mg$, the Nilsson model which describes the deformed nucleus is adopted. A Gaussian form which includes Wigner and Majorana exchange forces is taken for the direct interaction between two nucleons. In the analysis, it is found that the Majorana exchange force plays an important role in reproducing the angular distributions of the experimental data. Good agreement with experiment is obtained for the reactions considered. (auth)

38113 NUCLEAR FORCE AND ENERGY GAP IN FINITE NUCLEI. Bando, Hiroharu; Nagata, Sinobu (Kyoto Univ.). Progr. Theoret. Phys. (Kyoto), 35: 1026-42 (June 1966).

The energy gap in infinite nuclei is shown to vanish at the normal density. The mechanism which produces an energy gap of a reasonable value in finite nuclei is clarified. By using the reaction matrix as the effective interaction, it is stressed that the localization of the wave function in finite nuclei plays an essential role. In order to confirm the results of the qualitative discussion, a calculation of the energy gap is made directly from the free nucleon-nucleon interaction without using the reaction matrix formalism. Three-range Gaussian potentials including a repulsive soft core are adopted as the free nucleon-nucleon interaction; these do not give an energy gap in the case of infinite nuclear matter. A gap equation similar to the usual one is derived by overcoming some difficulties and complications which occur when both the discrete and the continuum states are treated. The calculated results show that the reasonable value of a few Mev for the energy gap is certainly obtained in the case of finite nuclei. (auth)

38114 THE LIFETIME OF THE NEGATIVE MUON IN ^{239}Pu. Cojocaru, V. (Inst. of Atomic Physics, Bucharest); Marinescu, L.; Mihai, I.; Petrascu, M.; Voiculescu, Gh.; Ignatenco, I.; Omelianenco, M. Rev. Roum. Phys., 11: 207-12(1966).

The time distribution of fission due to the nuclear capture of negative muons in plutonium was measured and the value 76 ± 9 ns for the muon lifetime was obtained. There is a good agreement, within the experimental errors, between the experimental value and that calculated with the theoretical formula given by Primacoff. (auth)

38115 LEVEL DENSITY PARAMETER DETERMINATION FROM (α,n) REACTIONS ON ^{27}Al, ^{55}Mn, ^{56}Fe AND Ag. Magda, M. T.; Alevra, A.; Dumitrescu, R.; Lukas, Ingrid R.; Martalogu, N.; Plostinaru, D.; Trutia, Elena; Vilcov, Isabela; Vilcov, N. (Inst. of Atomic Physics, Bucharest). Rev. Roum. Phys., 11: 241-8(1966).

The level density parameter was determined from the energy distribution of the evaporation neutrons emitted at $\theta_{lab} = 90°$ in the (α,n) reactions at $E_\alpha = 17$ Mev. The analysis was performed in the frame of the statistical theory of nuclear reactions. The obtained values present a monotonic variation with the mass number, being in agreement with the predictions of the Fermi gas model. (auth,

38116 SUPERFLUID MODEL WITH FIXED-PARTICLE NUMBER TREATMENT OF ^3H AND ^3He EMISSION. Brandus, I.; Sandulescu, A. (Inst. of Atomic Physics, Bucharest). Rev. Roum. Phys., 11: 273-9(1966).

On the basis of the superfluid model with projected Bardeen-Cooper-Schrieffer wave functions, explicit expressions of the reduced widths for ^3H and ^3He transitions to the rotational bands of intrinsic nuclear states are obtained. (auth)

38117 INTENSIFIED TUNNEL EFFECT FOR ALPHA PARTICLES. Ixaru, Liviu (Inst. of Atomic Physics, Bucharest). Rev. Roum. Phys., 11: 385-98(1966).

By considering the structure of the alpha particle and employing a procedure similar to that given by Zakhariev and Sokolov, a correction is introduced in the expression of the barrier penetrability. (auth)

38118 NUCLEAR MODELS. Juliano, Jose O. Sci. Rev. (Manila), 6: No. 3-4, 7-14(Mar.-Apr. 1965).

A brief and semitechnical review is presented for the present state of knowledge about the nucleus. Topics discussed include composition of nuclei, liquid-drop model, nuclear fission, scattering studies, magic numbers, activation studies, collective motions, energy levels, rotational states, the unified model of Bohr and Mottelson, and the cluster model. (S.F.L.)

38119 POLARIZATION OF PROTONS FROM THE $^{12}C(d,p)^{13}C$ AND $^{40}Ca(d,p)^{41}Ca$ GROUND-STATE REACTIONS. Chiang, Cheng-lieh; Yu, Pan-shui; Hsieh, Tzu; Mao, Chen-lin; Chen, Yeh-hao; Liang, Wen-hsueh; Wang, Chen-hsia; Cheng, Wan-hui; Chao, Chung-yao. Wu Li Hsueh Pao, 22: 554-68(May 1966). (In Chinese).

The polarization of protons emitted at six angles from the $^{12}C(d,p)^{13}C$ and $^{40}Ca(d,p)^{41}Ca$ ground-state reactions was measured. For the ^{12}C reaction, the data at small angles are very close to the results of previous works and are in agreement with the semiclassical sign rule $j_n = l_n \pm \frac{1}{2}$, P = (±). The value at $\theta = 115°$ has not been measured before; P = 0.529 ± 0.068 was obtained at this angle. For

the ^{40}Ca reaction, the sign of polarization which was found in the region of small angles is also in agreement with the semiclassical sign rule and is the same as those found in the work of Nemetz and of Boschitz, but is opposite to those obtained by Takeda and Bercaw. This difference may be due to the difference in the deuteron energy used since, in these experiments, the three with higher deuteron energies all gave the same positive sign of polarization while the three with lower deuteron energies all gave the same negative sign. After a survey of the polarization data now available, it was found that the semiclassical sign rule is still true to a certain degree and that it may be possible to find out a modified sign rule for the use in the nuclear spectroscopy. In some cases, it was found that the pattern of the polarization angular distribution is shifted towards small angles as the deuteron energy is increased, and this may be a characteristic of direct reactions. For the correspondence between the cross-section angular distribution and polarization angular distribution, it was found that the position of a minimum in the cross-section curve may correspond to the position of a change in sign or of a maximum absolute value in the polarization curve and that the position of a maximum in the cross-section curve may also correspond to the position of a change in sign in the polarization curve. These phenomena are discussed using the distorted-wave theory. (auth)

38120 STUDY OF TWO-NUCLEON POTENTIAL IN NUCLEI BY MEANS OF INELASTIC SCATTERING. Liu, Bing-tung; Ho, Kuo-chu. Wu Li Hsueh Pao, 22: 569-79 (May 1966). (In Chinese).

It is proposed that the effective two-nucleon potential in nuclei may be investigated through the direct-reaction process in high-energy nucleon inelastic scattering. Both DWBA and Glauber's many-body high-energy approximations are used in treating the inelastic scattering problem. The effective potential between nucleons within the nucleus is assumed to have various exchange properties and the spin-orbit term in the derivation. The differential cross sections and polarization angular distribution for the inelastic scattering of 185-Mev nucleons by ^{12}C with excitation energies of 9.6 and 22.3 Mev are calculated. Particle-hole model wave functions are used for the nuclear states. All these experimental curves of the differential cross section and polarization can be fitted very well with a reasonable set of potential parameters. (auth)

38121 CONVERGENCE OF A MANY-BODY PERTURBATION SERIES FOR AN ATTRACTIVE FERMI SYSTEM. Tour, Yung. Wu Li Hsueh Pao, 22: 580-8(May 1966). (In Chinese).

The problem of the convergence for Wigner and Schroedinger perturbation series is discussed by means of the functional analysis method. It is found that the convergent radii of two typical perturbation series are equivalent, but the rates of the convergence or divergence are not equivalent. A useful test is given. (auth)

38122 INTRANUCLEAR CASCADES AT ULTRA-HIGH ENERGIES. Artykov, I. Z.; Barashenkov, V. S.; Eliseev, S. M. (Joint Inst. for Nuclear Research, Dubna, USSR). Yadern. Fiz., 3: 978-9(May 1966). (In Russian).

The available experimental data on inelastic particle interaction with nuclei agree with an internuclear cascade model which is considered as a series of independent, two-particle interactions. The results obtained on calculating the total intranuclear cascade at high energies are presented. It is assumed that a leading particle carrying about 70% of the incident particle energy is present. The results show a sharp difference between experiment and theory. With inelastic NN and πN collisions the number of generated particles predicted by theory is a factor of 2 to 4 greater than the number of shower particles observed experimentally. Thus, at present there is no theory that satisfactorily describes the experimental data on nucleon-nuclei interactions at ultrahigh energies of $T \gg 10$ Bev. The internuclear cascade model is unsatisfactory at these high energies. (TTT)

38123 CROSS SECTION OF NUCLEAR FISSION OF TIN IRRADIATED BY OXYGEN IONS. Perfilov, N. A.; Obukhov, A. I.; Shigaev, O. E. Yadern. Fiz., 3: 979-80 (May 1966). (In Russian).

A tin target with a thickness of 3.54 mg/cm^2 was placed in the center of an aluminum ring at an angle of 45° with respect to a beam of 118-Mev oxygen ions. Small glass detectors were arranged on the inside of the aluminum ring. By comparison with gold which has a known cross section it was found that the fission cross section of tin was $\sigma_f = 1.2 \times 10^{-27}$ cm^2. With 109-Mev oxygen ions the fission cross section σ_f was found to be 1.0×10^{-28} cm^2. The error of the determination was estimated at 30 to 40%. A 3×10^{-5}% impurity of U or Th was found on irradiating the tin target with neutrons from a Po-Be source. (TTT)

38124 INVESTIGATION OF THE ^{139}Cs AND ^{140}Cs DECAY. Zherebin, E. A.; Krylov, A. I.; Polikarpov, V. I. Yadern. Fiz., 3: 981-92(June 1966). (In Russian).

The methods and results of the investigation of the decay of ^{139}Cs ($T_{1/2}$ = 9.5 min) and ^{140}Cs ($T_{1/2}$ = 66 sec) fission products on scintillation β and γ spectrometers are given. A fast-slow coincidence circuit is used to study $\beta\gamma$ and $\gamma\gamma$ correlations. The obtained values of the energy and relative γ-quantum intensity, number of γ quanta per β decay, and upper limit of the β-decay energy are given. Decay schemes for ^{139}Cs and ^{140}Cs are suggested on the basis of an analysis of the results obtained. (auth)

38125 TWO NEW SHORT-LIVED ISOMERS OF ^{131m}La AND ^{136m}La. Gritsyna, V. T.; Klyucharev, A. P.; Remaev, V. V. Yadern. Fiz., 3: 993-7(June 1966). (In Russian).

Previously unreported ^{131m}La and ^{136m}La isomers were obtained when isotopic barium targets were irradiated by 20-Mev protons. The isomeric state of the neutron-deficient ^{131}La nucleus with a half-life of 158 ± 5 μsec and transition energy E_γ = 170 ± 5 kev was obtained in the reaction $^{132}Ba(p,2n)^{131m}La$. The isomer ^{136m}La with $T_{1/2}$ = 110 ± 5 msec was produced in the $^{136}Ba(p,n)^{136m}La$ and $^{137}Ba(p,2n)^{136m}La$ reactions. The 170-kev isomeric state of the ^{136}La nucleus decays to the ground state through the 100 ± 5 kev level. (auth)

38126 NEUTRON STATES IN A DEFORMED OPTICAL POTENTIAL. Nemirovskii, P. E.; Chepurnov, V. A. Yadern. Fiz., 3: 998-1010(June 1966). (In Russian).

The energies and functions of neutron states (Ω,π) are calculated in a deformed optical potential. Interactions between neighboring shells of equal parity are taken into account. The results are compared with Nilsson's calculations and with experiments. The order in which the states are occupied and the binding energies are in good agreement with experiments. (auth)

38127 ELECTRIC QUADRUPOLE TRANSITIONS IN DEFORMABLE EVEN-EVEN NUCLEI. Davydov, A. S.; Ovcharenko, V. I. (Inst. of Physics, Academy of Sciences, Ukrainian SSR). Yadern. Fiz., 3: 1011-21(June 1966). (In Russian).

The influence of the deformation of even-even atomic nuclei going over into excited states on the probability of E2 transitions between collective quadrupole-type excited states and on the mean values of the quadrupole electric moment in excited states is investigated. The results of calculations are given as analytical formulas (for $\mu < 0.4$) and tables (for $\mu \leq 1$). The theory is compared with experiments for the ^{154}Gd nucleus. (auth)

38128 DIFFERENTIAL CROSS SECTIONS OF ELASTICALLY SCATTERED 13.6-Mev DEUTERONS. Nemets, O. F.; Sokolov, L. S.; Tokarevskii, V. V.; Chernov, I. P. Yadern. Fiz., 3: 1048-52(June 1966). (In Russian).

Absolute differential cross sections for deuteron elastic scattering by ^{63}Cu, ^{65}Cu, ^{58}Ni, ^{60}Ni, ^{62}Ni, and ^{64}Ni at 13.6 Mev are tabulated. (D.C.W.)

38129 INVESTIGATION OF THE REACTION $^3He(p,d)2p$. Timashev, S. F. (Inst. of Theoretical and Experimental Physics, Moscow). Yadern. Fiz., 3: 1053-9(June 1966). (In Russian).

Angular correlations are shown the measurement of which makes it possible to obtain direct information on the form factor of the virtual disintegration of the ^3He nucleus into three nucleons. This form factor figures in

the amplitude of direct two-nucleon stripping and pick-up reactions. (auth)

38130 DIFFERENTIAL CROSS SECTION OF THE REACTION D(t,α)n IN THE REGION 115 TO 1650 kev. Kobzev, A. P.; Salatskii, V. I.; Telezhnikov, S. A. (Joint Inst. of Nuclear Research, Dubna, USSR). Yadern. Fiz., 3: 1060-3(June 1966). (In Russian).

The differential cross section of the reaction D(t,α)n at 90° in the laboratory system was measured in the energy region 115–1650 kev. The cross sections previously obtained elsewhere for the regions 115–300 kev and 1450–1650 kev were confirmed. The cross sections in the energy region 300–1450 kev differ (up to 10%) from the previous data. (auth)

38131 INVESTIGATION OF THE REACTION ^{3}He + ^{3}He. Wang, Nen-min; Novatskii, V. N.; Osetinskii, G. M.; Tsen, Nai-Gun; Chepurchenko, I. A. (Joint Inst. of Nuclear Research, Dubna, USSR). Yadern. Fiz., 3: 1064-9(June 1966). (In Russian).

The differential cross sections of the reaction ^{3}He + ^{3}He at 90° in the energy region 500–1700 kev were measured using a thin gaseous target. The angular distributions at 882, 1152, 1250, and 1452 kev were also measured. The total cross sections were calculated from the angular distributions in the energy region 500–1450 kev. (auth)

38132 FISSION OF ^{226}Ra BY 12-Mev DEUTERONS AND THE SHAPE OF THE DISTRIBUTION OF THE FRAGMENT KINETIC ENERGY. Nemilov, Yu. A.; Selitski, Yu. A.; Solov'ev, S. M.; Eismont, V. P. Yadern. Fiz., 3: 1070-5(June 1966). (In Russian).

The kinetic energies of pair fragments in the deuteron fission of radium were measured using semiconductor detectors. An asymmetry in the shape of the kinetic energy distributions of fragments with given mass is noted. Various possible explanations of this asymmetry are discussed. (auth)

38133 POSITRON DECAY OF ^{145}Eu. Zhelev, Zh.; Muziol, G. (Joint Inst. for Nuclear Research, Dubna, USSR). Yadern. Fiz., 4: 3-8(July 1966). (In Russian).

It was shown by measuring triple coincidences between 511–511 kev γ-quanta and quanta of the whole γ-spectrum on a scintillation γ-spectrometer and by measuring the positron spectrum on a triple-focusing β-spectrometer that the positron spectrum in the decay of ^{145}Eu has two components. The boundary energies are 1740 ± 40 and 800 ± 40 kev. These two components populate the ground level and the 893.3-kev level with the intensities 1% and 0.35% per decay, respectively. The energy of the decay ^{145}Eu → ^{145}Sm is 2760 ± 40 kev. The data obtained together with data from other papers were used to analyze the intensities of γ transitions in the decay scheme ^{145}Eu → ^{145}Sm. (auth)

38134 DECAY OF ^{182}Ta. Grigorev, E. P.; Zolotavin, A. V.; Sergeev, V. O.; Bekrenev, V. S. (Leningrad State Univ.). Yadern. Fiz., 4: 9-21(July 1966). (In Russian).

The ^{182}Ta internal conversion electron spectrum above 5 kev was investigated. The ratios of the γ-transition probabilities are compared with predictions following from the unified nuclear model. The magnetic moment of the 1289.5-kev level in ^{182}W is determined to be $\mu_1 = 1.27 \pm 0.15\ \mu_{nuc}$ ($\mu_2 = 0.07 \pm 0.15\ \mu_{nuc}$). (auth)

38135 LOW ENERGY LEVELS OF ^{108}Ag. Estulin, I. V. (Moscow State Univ.). Yadern. Fiz., 4: 22-6(July 1966). (In Russian).

A scheme is suggested for the low-lying energy levels and transitions in the odd-odd ^{108}Ag nucleus. Possible states of the nonpaired nucleons are discussed. (auth)

38136 SPINS OF THREE-PARTICLE ISOMERIC STATES IN SPHERICAL NUCLEI WITH ODD MASS NUMBERS. Peker, L. K. (Leningrad State Univ.). Yadern. Fiz., 4: 27-9(July 1966). (In Russian).

Methods of determining the spins of three-particle isomeric states in spherical nuclei with odd mass numbers are suggested. (auth)

38137 REACTION (π^-,nn) AND MODELS OF THE ^{6}Li NUCLEUS. Kopaleishvili, T. I.; Machabeli, I. Z. (Tbilissi State Univ., USSR). Yadern. Fiz., 4: 37-41(July 1966). (In Russian).

The reaction (π^-,nn) with the ^{6}Li nucleus is investigated theoretically. Three different models of this nucleus are used: the shell model, α-deuteron model, and three-particle model. The distribution of the emitted nucleons with respect to the square of the total momenta has been obtained for all three models, and the angular correlations of the emitted nucleons for the shell model and α-deuteron model. The results are compared with the existing experimental data. This comparison leads to the conclusion that the α-deuteron model gives the best description of the experimental data. (auth)

38138 IDENTIFICATION OF ENERGY LEVELS IN LIGHT NUCLEI ACCORDING TO DISINTEGRATION CROSS SECTIONS. Dzhibuti, R. I.; Mamasakhlisov, V. I.; Macharadze, T. S. (Inst. of Physics, Academy of Sciences, Georgian SSR). Yadern. Fiz., 4: 52-6(July 1966). (In Russian).

The photonuclear reaction ^{7}Li(γ,^{3}H)^{4}He is investigated taking into account the interaction of the final state products. It is shown that the large value of the ^{7}Li photodisintegration cross section in the region before and after the maximum on the cross section curve, corresponding to the 4.63-Mev state, is due to direct transitions into the continuous spectrum. (auth)

38139 ELASTIC SCATTERING OF FAST ELECTRONS ON NUCLEI WITH A FERMI DISTRIBUTION OF CHARGE DENSITY. Petkov, I. Zh.; Lukyanov, V. K.; Pol, Yu. S. (Joint Inst. for Nuclear Research, Dubna, USSR). Yadern. Fiz., 4: 57-65(July 1966). (In Russian).

An approximate analytical expression for the differential cross section of the elastic scattering of fast electrons on medium and heavy nuclei has been obtained assuming a Fermi distribution of the charge density. The distortion of the wave function phase for the scattered electron is taken into account in the high energy approximation. The main contribution to the amplitude is given by the poles in the Fermi density. The limit $b \to 0$ (b is the parameter of the density spread) gives an amplitude with a sharp cut-off of the charge density. The results obtained are in good agreement with exact phase-shift analysis calculations. (auth)

38140 ROLE OF UNPHYSICAL PARTIAL-WAVE AMPLITUDE SINGULARITIES IN THE DEUTERON PHOTODISINTEGRATION. Kaminskii, V. A.; Orlov, Yu. V. (Moscow State Univ.). Yadern. Fiz., 4: 118-22(July 1966). (In Russian).

The role of partial reaction amplitude singularities due to non-physical singularities of scattering amplitudes in the energy-variable E plane taking final-state interactions into account is investigated by the example of the M1 deuteron photodisintegration. An explicit expression for the reaction amplitude is obtained. It is shown that terms corresponding to left non-physical singularities give a small contribution to the amplitude. It follows that the main part of the reaction amplitude can be expressed in terms of the Born approximation matrix element and the scattering phase shifts in the physical region of E values. (auth)

38141 NEUTRON-CAPTURE GAMMA-RAY INVESTIGATION OF ^{88}Sr LEVEL STRUCTURE. Schmidt, H.; Michaelis, W.; Weitkamp, C.; Markus, G. (Institut fuer Angewandte Kernphysik, Karlsruhe, Ger.). Z. Phys., 194: 373-94(1966).

The level structure of ^{88}Sr was investigated at the Karlsruhe research reactor FR2 using thermal neutron capture in ^{87}Sr. A pure thermal neutron beam was obtained by Bragg reflection from a lead single crystal. The target was natural strontium which gives a cross section contribution of about 87% for the reaction ^{87}Sr(n,γ)^{88}Sr. High-resolution measurements of the capture gamma spectrum were performed by means of a 4 cm² × 0.5 cm lithium-drifted germanium diode. There were 146 gamma lines observed. Cascade relations were studied by a double and triple coincidence apparatus containing 4'' Ø × 5'' NaI(Tl) crystals

and XP-1040 photomultipliers. In several cases coincident background was subtracted utilizing the double-window technique. By application of the triple sum coincidence method capture gammas from isotopes other than the investigated ^{88}Sr nucleus could be eliminated. Several new levels were established. A transition scheme is proposed and discussed. The neutron binding energy of ^{88}Sr is determined to be 11 111 ± 4 kev. (auth)

38142 INELASTIC DIFFRACTION SCATTERING. Inopin, E. V. (Inst. of Physics and Tech., Academy of Sciences, Ukrainian SSR). Zh. Eksp. Teor. Fiz., 50: 1592-1602(June 1966). (In Russian).

A method is proposed for solving the problem of inelastic scattering of particles by nuclei with the excitation of collective states. The method is based on the possibility of separating the variables in a central field when the scattering involves large angular momenta. It is shown that as a result the inelastic scattering cross section can be expressed in terms of the elastic scattering phase shifts. The results obtained by Austern and Blair in this direction are extended to the case of a nucleus with an arbitrary spin and any approximation with respect to the nonsphericity parameter. (auth)

38143 CONTRIBUTION TO THE THEORY OF DIFFRACTION SCATTERING OF PARTICLES BY NUCLEI BASED ON THE METHOD OF COMPLEX ANGULAR MOMENTA. Tishchenko, B. I.; Shebeko, A. V. (Inst. of Physics and Tech., Academy of Sciences, Ukrainian SSR). Zh. Eksp. Teor. Fiz., 50: 1674-81(June 1966). (In Russian).

Expressions for the elastic and inelastic diffraction scattering of particles by nuclei involving the excitation of collective states are derived by the technique of complex angular momenta. It is assumed that the modulus as well as the phase shift of the S matrix may possess poles in the complex angular momentum plane. It is shown that the presence of poles in the S-matrix phase shift near the poles of its modulus and Coulomb interaction permit one to explain a number of interesting features of the behavior of the differential scattering cross sections, such as the decrease of the oscillation amplitudes of the cross sections with the growth of the nuclear charge, the possibility of inelastic scattering cross-section oscillations in the case when the oscillations are absent in elastic scattering, and the decrease of the oscillation amplitude with the growth of the scattering angle. It is shown that competition between the Coulomb and nuclear phases can explain the cross-section drop (presence of one or two cross section minima which are much lower than the neighboring ones). In this connection it is mentioned that the quantity $\delta(l_0)$ (l_0 is the boundary nuclear angular momentum) can readily be estimated. (auth)

38144 ANGULAR DISTRIBUTIONS AND EXCITATION FUNCTIONS OF GROUND-STATE NEUTRONS RESULTING FROM THE ^{14}N(d,n)^{15}O REACTION. Johnston, Richard Walfred. Austin, Tex., Univ. of Texas, 1965. 121p.

Thesis.

The angular distribution of the ground-state neutrons resulting from the ^{14}N(d,n)^{15}O reaction was measured for deuteron energies of 1.173, 1.797, and 2.098 Mev. The angular range covered was from 0° to 125° in 5° increments. The neutrons were detected by a sphere-type scintillation detector biased so that only the ground-state neutron group was detected. The energy sensitivity of the counter was determined by measuring the yield from the d-d reaction, the cross section for which is well known. The excitation function for the ^{14}N(d,n)^{15}O reaction (ground-state neutrons only) was measured at 0° and at 90° for deuteron energies ranging from 0.533 to 2.413 Mev. Each of the angular distributions peaked at low angles (10° or 15°). No resonance peaks were observed in either excitation function. The value of the differential cross section per unit solid angle ranged from a minimum of 0.265 mb/sterad at a bombarding energy of 0.533 Mev and a laboratory angle of 90° to a maximum of 12.2 mb/sterad at a deuteron energy of 2.413 Mev and an angle of observation of 0°. (Dissertation Abstr.)

38145 NUCLEAR TWO-BODY INTERACTION AND SHELL MODEL STUDIES OF SELECTED LIGHT- AND MEDIUM-WEIGHT NUCLEI. Hughes, Thomas Aloysius. Nashville, Vanderbilt Univ., 1965. 111p.

Thesis.

A study of the potential parameters needed in shell-model calculations was performed by investigating the low-lying energy levels of ^{18}O, ^{18}F, ^{14}N, ^{42}Ca, ^{42}Sc, ^{90}Zr, ^{86}Sr, and ^{90}Y. The two-body interaction was taken to have a central and tensor term with gaussian radial dependence. Harmonic oscillator radial functions were used and configuration mixing was included. Because of the complexity of the matrix elements involved and the large number of configurations employed, a special program was designed. A least-squares fit to the known experimental levels was made, and the potential parameters were thus obtained. No single shell-model potential was found that could duplicate the energy spectra of all the nuclei considered. The calculation on ^{18}O and ^{18}F was sufficiently successful to predict the spins and parities of a number of levels but the T = 1 potential parameters for these two nuclei were not compatible. The mass-40 region does not appear to be explainable within the shell model and collective effects are suspected. The mass-90 calculations assumed a ^{88}Sr core, with the spectrum being determined by two extra-core particles or, in the case of ^{86}Sr, neutron holes. These calculations indicated that the potential parameters needed to fit the experimental data differed from the low-energy nucleon-nucleon scattering data and varied for all three nuclei. Hopefully, the inclusion of core-excited configurations would make these nuclei more amenable to the shell-model approach. (Dissertation Abstr.)

38146 POLARIZATION OF PHOTOPROTONS FROM BERYLLIUM. Hilberg, Robert Henry. New Haven, Yale Univ., 1965. 93p.

Thesis.

The measurement of the polarization of protons produced in the reaction ^{9}Be(γ,p)^{8}Li is described. A magnetic quadrupole lens selected the approximate proton energy range of 11–16 Mev. The polarization was measured by observing the left-right asymmetry in the scattering of the protons from ^{4}He at an angle 55°–80° in the laboratory. A triple coincidence method, one detector before the scattering and two after on each side, was required because of the high background. A value of P = 7.4 ± 5.7% was observed. (Dissertation Abstr.)

38147 COMPARISON OF REACTIONS OF ^{63}Cu COMPOUND NUCLEI FORMED BY ALPHA-PARTICLE, PROTON, AND CARBON-ION BOMBARDMENTS. Stearns, Carole Michels. New York, Columbia Univ., 1963. 86p.

Thesis.

A radiochemical investigation of the reactions of alpha particles with ^{59}Co, protons with ^{62}Ni, and carbon ions with ^{51}V was performed to determine the extent to which de-excitation of the ^{63}Cu reaction intermediate is independent of its mode of formation. Excitation functions were measured for the (α,αn), (p,αn), (^{12}C,αn), (α,α2n), (p,α2n), (^{12}C,α2n), (α,2p), (p,2p), (^{12}C,2p), (α,2n), and (p,2n) reactions at alpha-particle and proton excitation energies of 20 to 50 Mev and carbon-ion energies up to 120 Mev. Higher probabilities for alpha-particle emission were observed in reactions initiated by alpha particles, and, similarly, incident protons enhanced the proton emission events. It was assumed that all the other measured nuclear reactions were the result of evaporation from a ^{63}Cu compound nucleus. The non-compound contributions to the (α,αn), (α,α2n), and (p,2p) yields were calculated after applying a correction to the ^{63}Cu excitation energy to compensate for the different average angular momenta introduced by the protons, alpha particles, and carbon ions. The ^{57}Co, ^{58}Co, and ^{61}Co products were each found to have non-compound components comparable in magnitude and energy dependence to the compound-nucleus portion of the excitation function. (Dissertation Abstr.)

38148 NUCLEAR REACTIONS OF 10- TO 20-Mev DEUTERONS WITH ^{61}Ni. Moorhead, Elizabeth Grace. New York, Columbia Univ., 1964. 88p.

Thesis.

The excitation functions for the (d,2p), (d,2n), (d,αn), and (d,α2n) reactions of ^{61}Ni were measured for 10 to 20 Mev deuterons using radiochemical methods. The deuteron excitation functions were compared with previously measured excitation functions for alpha- and proton-induced reactions leading to the same ^{63}Cu compound nucleus. This comparison showed that the deuteron reactions follow mainly compound-nucleus mechanisms. The deuteron excitation functions were reproduced reasonably well by a calculation based on compound-nucleus theory, which further suggests compound-nucleus behavior. Only the (d,2p) reaction at low energies showed any real deviation from compound-nucleus behavior, and an investigation of this by a stripping-followed-by-evaporation calculation was inconclusive as to the contribution of deuteron stripping to this reaction. (Dissertation Abstr.)

38149 POLARIZATION OF ^{3}He NUCLEI. Axen, David Arnold. Vancouver, Can., Univ. of British Columbia, 1965. 229p.

Thesis.

An atomic-beam type of apparatus designed to produce a polarized ^{3}He beam with an intensity of approximately one microampere and 90% polarization is described. An intense, supersonic neutral beam can be produced with a miniature Laval nozzle cooled to liquid ^{4}He temperatures. The velocity distribution of the particles in the Laval beam and the trajectories of these particles in a radially symmetric hexapole magnet were computed. Sufficient separation of the two beams, consisting of particles in the two possible nuclear spin states, is achieved with a magnet in which the diameter of the gap between the pole pieces increases from 3 mm at the entrance to 6 mm in 15 cm and is then constant for 35 cm. The low-temperature atomic beam source was tested at liquid nitrogen temperature with a ^{4}He beam. The measured beam intensity of 9×10^{13} particles/cm^2/sec at the magnet exit, 76 cm from the nozzle, agrees favorably with the calculated intensity of 1.2×10^{14} atoms/cm^2/sec under these operating conditions. The measured field gradient of 70,000 gauss/cm near the pole tips of the hexapole splitting magnet is more than required for separating the atoms in the two nuclear spin states. A pulsed nuclear magnetic resonance method for measuring the nuclear polarization of the neutral ^{3}He beam prior to ionization is described. The angular distribution and polarization of the protons produced by the D(^{3}He,p)^{4}He reaction with an incident, polarized ^{3}He beam of 150 kev bombarding energy was calculated. This angular distribution is isotropic. In the plane of the reaction, the proton polarization, which may be measured by a second scattering experiment, is $-\frac{2}{3}$ the incident ^{3}He polarization. The angular distribution and polarization of the protons from this reaction were calculated for the case of polarized and unpolarized ^{3}He beams incident on a polarized deuteron target. (TCO)

38150 REACTIONS ^{14}N(n,d)^{13}C, ^{14}N(n,t)^{12}C, ^{15}N(n,d)^{14}C, ^{32}S(n,d)^{31}P AND ^{34}S(n,d)^{33}P INDUCED BY 14-Mev NEUTRONS. Fessenden, Peter. Providence, Brown Univ., 1965. 130p.

Thesis.

A triple coincidence counter telescope consisting of two thin silicon surface barrier dE/dx detectors (114 microns total thickness) and a CsI E detector was used with a pulse multiplier particle discrimination system to detect the charged particles emanating from nuclear reactions induced by 14.1- or 14.8-Mev neutrons. Angular distributions of the outgoing charged particles from the ground state transitions of ^{14}N(n,d)^{13}C and ^{14}N(n,t)^{12}C were measured out to a center-of-mass angle of 100 degrees for 14.1-Mev incident neutrons. The (n,d) distribution was fitted with two l = 1 theoretical curves calculated from the Butler stripping and DWBA theories. The (n,t) results were fitted by two l = 2 curves calculated from the double stripping theory of Newns and the diffraction theory of Dar, and were compared to previous results obtained for ^{12}C(^{3}He,p)^{14}N. The excited state transitions for ^{14}N(n,d)^{13}C (E_x = 3.68 Mev) and ^{14}N(n,t)^{12}C (E_x = 4.43 Mev) were recorded for a few forward angles, but the results were inconclusive. Angular distributions for the ^{15}N(n,d)^{14}C (E_x = 0) reaction were measured out to 60 degrees for E_n = 14.1 and 14.8 Mev. The 14.8-Mev data were fitted with Butler and DWBA curves for l = 1, but the 14.1-Mev data were inconsistent with a pure direct reaction process. The results agree with previous measurements on the inverse ^{14}C(d,n)^{15}N reaction, and indicate that a compound nucleus mechanism contributes strongly near 14.9 Mev of excitation in the compound ^{16}N nucleus. An energy distribution at 0 degrees was obtained for 14.1-Mev neutrons incident on a thin natural sulfur target. The results show a low-lying first excited state of ^{31}P at 0.78 ± 0.12 Mev, which is 50% as intense as the ground state. Preliminary measurements on the ^{34}S(n,d)^{33}P reaction at 0 degrees indicate a large cross section for this transition. (Dissertation Abstr.)

38151 NUCLEAR SPIN RELAXATION IN GASEOUS H_2, HD, AND D_2. Hardy, Walter Newbold. Vancouver, Can., Univ. of British Columbia, 1965. 146p.

Thesis.

The longitudinal and transverse nuclear relaxation times, T_1 and T_2 were measured in normal H_2 gas at 77.5°K in the pressure range 0.05 to 2 atmospheres. In this region T_1 goes through a minimum, and T_2 deviates significantly from a linear dependence on the density. Comparison of the experimental data with existing theory establishes the following results for the J = 1 state of orthohydrogen: autocorrelation functions of the molecular angular momentum operators are exponential or nearly so; the ratio of the correlation times τ_1, τ_2, which are associated with operators of the form J_+, and J_+^2 respectively, lies within the limits $0.6 \leq \tau_1/\tau_2 \lesssim 1$; the splitting of the molecular Zeeman levels cannot be neglected as in the original Schwinger theory. T_1 for the proton and deuteron in HD gas and for the deuterons in normal D_2 gas was measured as a function of temperature and pressure in the range 20 to 373°K and 0 to 8 atmospheres. To within experimental error the dependence of T_1 on the density ρ is linear. In HD below 65°K, when only the J = 0 and J = 1 states of the molecule are appreciably populated, the temperature dependence of T_1/ρ is identical for both proton and deuteron, leading to a value of $\tau_1/\tau_2 = 1.07 \pm 15\%$ for the J = 1 state of HD. Above 100°K, T_1/ρ for the proton is inversely proportional to the temperature, whereas for the deuteron T_1/ρ is almost temperature-independent. The experimental results are interpreted as evidence that in HD gas the process of molecular reorientation is dominated by the anisotropic intermolecular force arising from the separation of the centers of mass and charge of the molecule. In D_2 gas two relaxation times were found, one associated with the S = 1 spin state of paradeuterium and the other associated with the S = 2 spin state of orthodeuterium. At 40°K $(T_1/\rho)_{s=2}$ appears to go through a minimum; the analogous quantity in H_2 measured by previous workers also goes through a minimum, but at 80°K. This is consistent with interpreting the minimum as a quantum mechanical diffraction effect. The J = 2 component of $(T_1/\rho)_{s=2}$, however, does not go through a minimum, which suggests that the intermolecular interactions are significantly different for the J = 1 and J = 2 states of the molecule. (Dissertation Abstr.)

38152 DECAY OF THE Zn^{64*} COMPOUND NUCLEUS FORMED BY NUCLEAR REACTIONS OF P, ^{3}He, ^{4}He, AND ^{12}C WITH ^{63}Cu, ^{61}Ni, ^{60}Ni, AND ^{52}Cr, RESPECTIVELY. Smith, Charles Francis Jr. Berkeley, Calif., Univ. of California, 1965. 118p.

Thesis.

An experimental, radiochemical determination of the excitation functions for reactions involving the [^{64}Zn]* compound nucleus was performed. The reactant pairs are p + ^{63}Cu, ^{3}He + ^{61}Ni, ^{4}He + ^{60}Ni, and ^{12}C + ^{52}Cr, and the observed products for each such pair are ^{63}Zn, ^{62}Zn, and ^{62}Cu. Total reaction cross sections are calculated from the optical model. The ratio of the cross section for a given reaction to the total reaction cross section is compared on an excitation energy abscissa for each product. The shape and magnitude of these ratio curves are essentially constant in each such comparison, suggesting a compound nuclear reaction mechanism. Range measurements for ^{62}Zn recoils are made and compared to calculated ranges based on the theory of Lindhard, Scharff, and Schiøtt for a compound

nuclear reaction. Good agreement is found. The shapes of these curves are compared to a theoretical estimate obtained from evaporation theory and are shown to be similar to the calculated shapes. A displacement of the experimental curves relative to one another along the excitation energy axis is noted and ascribed to angular momentum effects. Using the position of the ^{64}Zn photoexcitation curves of Sagane as reference points, and spin averaged angular momenta of the compound system, the reduced moment of inertia is calculated for the four systems. At least two distinct values are found, indicating a difference between orbital- and spin-angular momenta, the latter causing the greater energy shift in the excitation functions. This observation is shown to be of value in understanding similar energy discrepancies in excitation function comparisons. Because of the observed relation between the mode of formation and the mode of decay of the compound nucleus, it is concluded that the independence postulate is not strictly applicable to this system as a whole. (Dissertation Abstr.)

38153 REACTION ^{37}Cl(d,p)^{38}Cl AND NUCLEAR STRUCTURE OF ^{38}Cl. Sevcik, Frank Jr. Ann Arbor, Mich., Univ. of Michigan, 1963. 95p.

Thesis.

The character and the amount of configuration mixing in the low-lying levels of ^{38}Cl were studied through the ^{37}Cl(d,p)^{38}Cl reaction using deuterons of energy 7.74 Mev and targets of AgCl containing both the natural and an enriched isotopic proportion of ^{37}Cl. The proton groups, analyzed in energy with a double-focusing magnetic spectrometer at sixteen angles from 0° to 90° with respect to the direction of the deuteron beam, were detected in nuclear emulsions. Twenty-one levels of ^{38}Cl were identified below an excitation energy of 4.5 Mev. The absolute differential cross section of the level at 1.986 Mev was determined as 12.8 ± 1.3 mb sterad^{-1} at 15° in the center-of-mass system. The present data are in agreement with earlier results except that the level at 1.658 Mev appears to belong to ^{36}Cl. Distorted-wave-Born-approximation analysis of sixteen angular distributions led to assignments of $l_n = 1$ and $l_n = 3$ only, and provided the values of $(2J_f + 1)S_l$ for the levels. Of the five $l_n = 3$ transitions observed, three contain an admixture of $l_n = 1$. Based on the ratios of values of $(2J_f + 1)S_l$ the following spin assignments for levels at 0.000, 0.671, 0.762, 1.310 Mev and at 1.621, 1.694, 1.748, 1.986 Mev are suggested: J = 2, 5, 3, 4 and J = 2, 1, 0, 3, respectively. A shell model calculation with a two-body residual interaction led to the following conclusions. First, the four lowest-lying levels in ^{38}Cl are well represented by levels of the configuration $\{[\pi|d_{\frac{3}{2}}] \times [\nu|f_{\frac{7}{2}}]\}_J$ and the calculated $l_n = 1$ admixtures for the levels at 0.000 and 0.762 Mev, of 1 percent and 15 percent, agree reasonably well with the experimental determinations of 2 percent and 9 percent, respectively. Second, the seven configurations used are not sufficient for an accurate calculation of the levels between 1.6 and 2.0 Mev. (Dissertation Abstr.)

38154 RADIOACTIVE DECAY OF ^{140}La. Shinners, Carl William. Baton Rouge, La., Louisiana State Univ., 1965. 81p.

Thesis.

The decay of ^{140}La and the energy level scheme of ^{140}Ce were investigated with a beta-ray scintillation spectrometer, a gamma-ray coincidence spectrometer, and a gamma-ray coincidence sum spectrometer. A time-to-amplitude converter was used to measure the mean life of two transitions in ^{140}Ce. Analysis of the beta-ray spectra indicated the presence of eight beta-ray groups of end point energies (in kev) and relative intensities as follows: 2220 ± 50 (8%), 1730 ± 40 (13%), 1410 ± 40 (26%), 1270 ± 20 (18%), 1120 ± 30 (11%), 930 ± 30 (9%), 670 ± 20 (11%), 400 ± 20 (4%). It was also observed that the 1270-kev beta ray is in coincidence with the 923-kev gamma ray. An analysis of the gamma-ray coincidence data produced the following results and conclusions: (1) the energy (in kev) and relative intensity (quanta per 100 disintegrations) of the gamma rays observed were 329 (18), 432 (3), 486 (39), 752 (3), 815 (26), 868 (4), 923 (13), 1597 (96); (2) the 1597-kev gamma-ray transition from the first excited state of ^{140}Ce is in coincidence with all gamma rays observed with energies less than 1600 kev; (3) the 752-, 815-, and 923-kev gamma rays were observed to be only in coincidence with the 1597-kev gamma ray; (4) the 329-, the 432-, and the 868-kev gamma rays are advanced with respect to the 2080-kev level and the 486- and 1597-kev gamma rays are in cascade from the 2080-kev level to the ground state; (5) evidence of a 655-kev transition was observed and concluded to be advanced relative to the 2080-kev level. Analysis of the mean-life measurements showed the mean life of the 2080-kev level and the 815-kev transition to be $(4.99 \pm 0.05) \times 10^{-9}$ sec and $\leq 5 \times 10^{-11}$ sec, respectively. A decay scheme is proposed, which is consistent with the beta-ray spectra and the observed coincidences and with the high-energy gamma rays observed by other investigators. (Dissertation Abstr.)

38155 EXPERIMENTAL STUDIES OF THICK-TARGET BREMSSTRAHLUNG IN THE DIRECTION OF 0 DEG FOR ELECTRON ENERGIES 0.2, 0.4, 0.6, AND 0.8 Mev. Hashmi, R. A. Berlin, Free Univ., 1965. 49p. $2.00 Gmelin, AED-Diss. 65-300.

Thesis.

Spectral distributions of thick-target bremsstrahlung were measured using a scintillation spectrometer. Spectra were calculated from pulse-height distributions by means of a semi-empirical method. The results are in agreement with theoretical data for Z = 29 and 47, but disagree for Z = 4. (Gmelin)

38156 THEORY OF ROTATION-VIBRATION INTERACTION IN DEFORMED EVEN-EVEN NUCLEI. Acker, H.-L. Freiburg i. B., Univ., Freiburg i. B., 1965. 69p. $2.00 Gmelin, AED-Diss. 65-346.

Thesis.

Some assumptions and extensions of the Greiner and Faessler nuclear model for interaction between vibrations and rotations are studied. The results indicate that the description of collective low-energy nuclear states is limited by quadrupole oscillations of the nuclear surface. (Gmelin)

38157 ENERGY AND SPIN DEPENDENCE OF THE ^{56}Fe LEVEL DENSITY FOR EXCITATION ENERGIES 0 TO 20 Mev. Vonach, H. Munich, Technische Hochschule, 1965. 92p. $2.00 Gmelin, AED-Diss. 65-324.

Thesis.

Some methods for the determination of level densities are described. Absolute values for ^{56}Fe between 2 and 20 Mev are given. The spin distribution parameter as a function of excitation energy was determined. The data are in qualitative agreement with theoretical results from a Fermi gas model. (Gmelin)

38158 MEASUREMENTS WITH A HIGH-APERTURE γ SPECTROMETER WITH PLASTICALLY CURVED LiF CRYSTAL. Moll, W. Munich, Technische Hochschule, 1964. 61p. $2.00 Gmelin, AED-Diss. 64-1084.

Thesis.

A γ spectrometer of the DuMont type with a focal length of 50 cm and a curved LiF crystal is described. The transmission is 3×10^{-5} at 25 kev and 0.8×10^{-5} at 100 kev with a resolution of 1 and 5%, respectively. The testing and curving of LiF crystals are described. The low-energy γ spectrum of ^{182}Ta was studied. The energy and intensity of a 31.75-kev transition were determined. (Gmelin Inst.)

38159 SPECTROSCOPY OF FAST NEUTRONS AND REACTION MECHANISM OF THE (d,n) REACTION. Wagner, G. Heidelberg, Univ., Heidelberg, 1964. 31p. $2.00 Gmelin, AED-Diss. 64-1083.

Thesis.

The design and construction of two types of neutron spectrometers, a coincidence spectrometer and a scintillation counter telescope using plastic and CsI(Tl) scintillators, are described. Energy resolution of the telescope was 7%. Reactions (d,n) with Y, Zr, and Nb are studied. Angular distributions of spectra indicate that most processes are compound nucleus reactions. Cross sections are given and reaction mechanisms discussed. (Gmelin Inst.)

38160 EFFECTIVE HAMILTONIAN FOR NUCLEAR MATTER. Stack, Stephen James. Edmonton, Alta., Univ. of Alberta, 1964. 79p.

Thesis.

A method for the calculation of the reaction matrix of the Brueckner theory is described. The two-nucleon interaction is separated into two parts. The separation distance is so defined that the energy is the eigenvalue of the effective Hamiltonian which consists of the long-range part of the interaction and the kinetic energy. The short-range interaction is treated as a perturbation which modifies the wave function. If the outer potential is weak, a plane-wave approximation is used for the unperturbed wave function and the diagonal elements of the reaction matrix are given to first order by the first Born approximation of the long-range potential. The separation distance is calculated self-consistently, the iteration being simplified by the use of the "reference-spectrum" approximation. The singularities in the integral equations of the Brueckner theory and the divergence of the expansion of the reaction matrix are discussed. Attempts to modify the theory to eliminate these difficulties are described. (auth)

38161 NUCLEAR REACTION STUDIES OF ^{12}B AND ^{17}O. Alexander, Thomas Kennedy. Edmonton, Alta., Univ. of Alberta, 1964. 140p.

Thesis.

The first two excited states of ^{12}B were studied using the $^{11}B(d,p)^{12}B$ reaction and particle-gamma coincidence techniques. The gamma branching ratio of the 1.67-Mev state to the 0.95-Mev state was found to be 6 ± 3% of the ground-state transition. An upper limit on the lifetime of the 0.95-Mev state was obtained by direct timing ($\tau < 3 \times 10^{-10}$ sec). The angular correlation of the 0.95-Mev gamma ray measured in time coincidence with protons observed at 90° is isotropic at a bombarding energy of 1.5 Mev. The combined data are not sufficient to determine the spin of the 0.95-Mev state. The proton-gamma angular correlation of the 1.67-Mev state is isotropic for the same experimental conditions. The 3.06- and 3.85-Mev levels of ^{17}O were investigated using the $^{14}C(\alpha,n)^{17}O$ reaction and neutron-gamma coincidence techniques. Doppler-shift measurements of the 3.85- and 2.19-Mev gamma rays yielded $\tau \leq 0.25 \times 10^{-13}$ sec and $\tau = 1.2 \times 10^{-13}$ sec for the lifetimes of the 3.85- and 3.06-Mev states, respectively. The measurements of the neutron-gamma angular correlations, combined with the lifetime estimates, give the spin assignment $5/2^-$ for the 3.85-Mev state and confirm the $1/2^-$ spin assignment for the 3.06-Mev state. A fast timing system was developed for use with solid-state particle detectors. The observation of the time relation between the protons and gamma rays detected in a plastic scintillator was used to demonstrate the performance for p-γ delayed coincidence measurements. For the $^{16}O(d,p)^{17}O$ reaction to the first excited state, the timing resolution obtained was approximately 1.3 nanoseconds. This indicates that lifetimes greater than ~0.5 nanoseconds can be measured directly from the slope of the delayed edge of the resolution curve. (auth)

38162 ALPHA-PARTICLE BREAKUP OF THE 12.71 AND THE 11.83 Mev LEVELS IN ^{12}C. Olsen, William Charles. Edmonton, Alta., Univ. of Alberta, 1964. 147p.

Thesis.

The alpha decay of states in ^{12}C, with special emphasis on those at 11.83- and 12.71-Mev excitation, has been studied using the $^{11}B(d,n)^{12}C$ reaction. Neutron time-of-flight spectra and solid-state detector charged-particle spectra were analyzed by a two-parameter pulse-height analyzer. Angular distributions and spectrum shapes of the alpha particles from the 12.71- and 11.83-Mev states indicate that these states decay sequentially through ^8Be. The 1^+ spin-parity assignment for the 12.71-Mev state is supported by the fact that no transitions to the ground state of ^8Be were observed. Approximately 90% of the transitions from the 11.83-Mev state proceed via $^8Be(2.9)$ while the remaining 10% feed the ground state. There is some evidence to indicate that the 10.84-Mev state of ^{12}C decays exclusively to $^8Be(0)$. The 3^- assignment for the 9.64-Mev state in ^{12}C is favored over 1^- on the basis of the angular distribution of the alpha particles from this state to the ^8Be ground state. The spectrum shape for this group confirms this well-established transition. This work, together with other work reported in the literature, justifies the representation of ^{12}C as a ^8Be-α two-body cluster from the alpha-particle threshold to 16-Mev excitation. Such a representation is in accordance with the Two-Body Cluster Model of Phillips and Tombrello. A frequency-modulated proton magnetic resonance system for the measurement and control of magnetic fields from 1 to 12 kilogauss is described. This system was designed for use with the combined broad range spectrograph and spectrometer facility of the University of Alberta Nuclear Research Center. (auth)

38163 NEUTRON POLARIMETER AND ITS USE FOR THE REACTION $^{11}B(d,n)^{12}C$. Mason, Grenville Robert. Edmonton, Alta., Univ. of Alberta, 1964. 142p.

Thesis.

A neutron polarimeter that can be used to measure the polarization of incident neutrons with energy from 3 Mev to 20 Mev is described. The polarimeter consists basically of an array of nine helium-filled proportional counters. Groups of three counters are separated by collimating vanes which permit He^{2+} recoils to pass from a central group to left- or right-side groups of counters. Sum-coincidence techniques yield the left-right scattering asymmetry from which the polarization may be determined for neutron groups groups well separated in energy. Angular distributions of neutron polarizations were measured for the reactions $D(d,n)^3He$, $T(d,n)^4He$, $^{11}B(d,n)^{12}C_{g.s.}$, and $^{11}B(d,n)^{12}C_{4.43}$ using a 2-Mev Van de Graaff accelerator. Measurements for the first two reactions served primarily as checks on the operation of the polarimeter and yielded values in agreement with those of previous workers. Polarizations for both neutron groups from $^{11}B(d,n)^{12}C$ were found generally to be positive (using the Basel convention) and small (less than thirty %). Angular distributions of the products of polarization values and differential cross sections were fitted with associated Legendre functions, a reasonable fit being obtained with a linear combination of the first, second, and third functions. (auth)

38164 SEARCH FOR A 5.6 Mev LEVEL IN ^7Li. Reedyk, Arie. Edmonton, Alta., Univ. of Alberta, 1963. 46p.

Thesis.

A review of the rotational model of a nucleus is given. The application of this model to ^7Li is shown to lead to the prediction of a level at 5.6-Mev excitation in that nucleus. An experimental search was made for this predicted level by observation of the charged reaction products resulting from deuteron bombardment of ^6Li. No proton group corresponding to a ^7Li level in the vicinity of 5.6-Mev excitation was observed. From the charged-particle spectra resulting from 1.90-Mev bombarding deuterons, an upper limit of .05 mb/sterad is assigned to the backward angle differential cross section for the $^6Li(d,p)^7Li$ reaction going to any possible narrow level around 5.6-Mev excitation in ^7Li. (auth)

38165 SEARCH FOR A PROPOSED NEW LEVEL OF ^7Be. Goble, David Franklin. Edmonton, Alta., Univ. of Alberta, 1963. 57p.

Thesis.

Chesterfield and Spicer applied the rotational model to ^7Li and obtained quantitative agreement with experiment. The validity of the application of this model rests upon the existence of a $3/2^-$ state predicted at an excitation energy of 5.62 Mev. A search was made for the mirror analog of this level in ^7Be. The yield of gamma rays from the reaction $^6Li(p,\gamma)^7Be$ was investigated, but no evidence of a resonance could be found in the region E_p = 200 to 450 kev. Spectra taken at E_p = 800 kev and E_p = 400 kev are in agreement with the results of Warren for the gamma de-excitation of the broad 6.35-Mev level, but a spectrum taken at E_p = 300 kev would seem to indicate that some other process is being observed. (auth)

38166 MUON CAPTURE IN 2s-1d NUCLEI. Silbar, Richard Robert. Ann Arbor, Mich., Univ. of Michigan, 1963. 180p.

Thesis.

A theoretical study of the capture interaction $\mu^- + p \rightarrow n + \nu$ in the 2s-1d nuclei is presented. In Chapter I, the nature of the capture interaction is briefly reviewed. The relevance of the 2s-1d nuclei is discussed. Chapter II develops the effective Hamiltonian for the process from the Lorentz invariant matrix element and applies this to capture rate calculations with a free proton. The expressions for the total average capture rate and for the difference in the rates from the two hyperfine levels are extended to the nuclear case in Chapter III. Here the closure approximation is applied to obtain the nuclear matrix elements in terms of one involving only the initial nuclear wave function. The reasons for the choice of the Nilsson nuclear model are given in Chapter IV. The nuclear matrix elements are broken into the various shell contributions in Chapter V. Chapter VI discusses the closed shell matrix elements and evaluates the radial integrals, using the Wills-Ford muon wave functions. Expressions for the open shell matrix elements are found in Chapter VII. Chapters VIII and IX discuss the choice of the average neutrino momentum and the relevant 2s-1d nuclei for calculation, together with their nuclear parameters. The computer programs and numerical results for the matrix elements occurring in the expressions for the average total capture rate are described and presented in Chapter X. Chapter XI compares the total rates for the nuclei ^{19}F, ^{20}Ne, ^{28}Si, ^{35}Cl, and ^{37}Cl with the experimental values to see what can be said regarding the coupling constants of the interaction on the basis of these calculations. The universal Fermi interaction theory compares favorably with the experimental values at the best choices of the nuclear parameters. The results are not good enough to exclude the absence of the weak magnetism terms, the possibility of a large pseudoscalar term, $g_P = 16\, g_A$, or the absence of the Fermi terms altogether. (Dissertation Abstr.)

38167 THEORY OF INELASTIC ELECTRON-DEUTERON SCATTERING. McGee, Ian James. New Haven, Yale Univ., 1965. 131p.

Thesis.

The formal theory of the electrodisintegration of the deuteron is examined in detail. The restrictions imposed by Lorentz invariance, parity conservation, and time reversal are shown to restrict the number of independent transition amplitudes of the two-nucleon system to eighteen. The structure of these amplitudes and, in particular, the connection between the relativistic and non-relativistic theories is examined using the techniques of dispersion relations. This reveals the proper connection between the n-p-d vertex function, and the non-relativistic deuteron wavefunction. With this completely covariant treatment as a basis, the analysis then changes to an approximate, semi-relativistic approach to permit practical calculations of effects of final state interactions on the cross sections. Correct relativistic kinematics are used throughout, but the interaction is correct only to terms through order m^{-2}, m = nucleon mass. In this approximation, the number of independent amplitudes is reduced to ten and those that remain are amenable to numerical calculation including the effects of final state interactions. (Dissertation Abstr.)

38168 STUDIES OF HIGH-ENERGY NUCLEAR INTERACTIONS WITH NUCLEAR EMULSIONS. Roehrs, H. Kiel, Univ., Kiel, 1964. 184p. $2.00 Gmelin, AED-Diss. 64-1076.

Thesis.

Data from the ICEF 80-liter emulsion stack exposed at high altitude are analyzed. For energy determination of high-energy interactions, Castagnoli's formula is used. Interactions are described by means of the peripheral collision model for nucleons and pions. Inelasticity depends only on the masses of colliding particles. Product particles are emitted from 1 or 2 centers with various multiplicities. The multiplicity distribution can be described by an exponential function. Interaction cross sections for high energies are nearly constant and correspond approximately to the geometrical cross section. (Gmelin)

38169 DECAY OF ^{134}Cs. Nagpal, Tarlok Singh. Vancouver, Can., Univ. of British Columbia, 1964. 105p.

Thesis.

The tests of performance of the modified thin-lens magnetic spectrometer using ring-detection were extended using improved mechanical controls of detector position. It is concluded that the limit of performance with the thin lens magnet has been reached. The decay of $_{55}Cs^{134}_{78}$ was investigated using the modified thin-lens spectrometer, a scintillation spectrometer, and beta-gamma, conversion-electron gamma coincidence techniques. The results support the simpler decay scheme proposed by Van Wijngaarden and Connor. The beta decay has three components with end-point energies and intensities of 659 ± 3 kev(67.3%), 411 kev (2.5%), and 89 kev (30.3%), estimated from the energy level intensity balances in ^{134}Ba. These intensity balances show discrepancies of less than 3% of the total decay intensity. The conversion coefficients, calculated from the conversion electron and gamma-ray intensities lead to the following multipolarity identifications for the transitions in ^{134}Ba; 473 kev (M1 or E2), 563-569 kev (M1 or E2), 605 kev (E2), 797-803 kev (E2), 1036 kev (M1 or E2), 1168 kev (E2), and 1366 kev (E2). The M1 or E2 character of the 473-kev and 1036-kev transitions makes it possible to assign a spin of 3+ or 4+ to the 1641-kev level, which was uncertain before. An unsuccessful search for evidence of a 960-kev gamma ray reported by others puts an upper limit of 0.2% on its intensity. (Dissertation Abstr.)

38170 "BREATHING MODE" COLLECTIVE NUCLEAR VIBRATIONS AND APPLICATION TO ^4He EXCITED STATES. Werntz, Carl; Ueberall, H. (Catholic Univ. of America, Washington, D. C.). 9p. (CONF-660411-13). ORAU. Gmelin, AED-CONF-66-060-4.

From American Physical Society Meeting, Washington, D. C.

A simple collective model of the nuclear "breathing mode" is developed assuming a vibration of the ground-state matter density distribution according to a coordinate scale factor. A quantization of this oscillation leads to an expression for the vibrational amplitude in terms of the empirical energy of the "breathing" excited state, and gives the electromagnetic form factor for the ground-state transition as a derivative of the ground-state form factor with respect to momentum transfer q. Using this model, evidence is presented that the 0^+, T = 0 excited state in ^4He at 20.4 Mev is an example of a breathing mode state; reasonable agreement with the experimental (R. Frosch, Phys. Letters, 19:155(1965)) form factor is obtained both for the magnitude and the q dependence. The second excited state is also treated as a collective dipole state to show that a 2^-, T = 0 assignment is consistent with the experimental electron scattering data. (S.F.L.)

38171 ANALYSIS OF 14 Mev ELASTIC NEUTRON SCATTERING FROM K. Cassola, R. L.; Kushal, R. D. (Ohio Univ., Athens). 6p. (CONF-660430-4). ORAU. Gmelin, AED-CONF-66-149-1.

From Ohio Academy of Science, 75th Annual Meeting, Columbus, Ohio.

An attempt to obtain an improved optical-model fit to the angular distribution of neutrons elastically scattered from potassium at 14 Mev is summarized. It is concluded that the data considered can be explained more adequately in terms of an optical model that uses a derivative surface absorption. (D.C.W.)

38172 ANGULAR DISTRIBUTIONS OF PROTONS AND DEUTERONS FROM $^6Li + ^6Li$ AS A FUNCTION OF ENERGY. Kibler, K. G. (Univ. of Iowa, [Iowa City]). 11p. (CONF-660411-9). ORAU. Gmelin, AED-CONF-66-060-9.

From American Physical Society Meeting, Washington, D. C.

The mechanism of $^6Li + ^6Li$ reactions was investigated by observing deuteron and proton angular distributions from reactions at energies from 2.4 to 9.0 Mev. Energies in the region of the Coulomb barrier were emphasized. The total cross section for the (Li-6,p) reaction tends toward a (2J +

1) dependence as the energy of the incident particle increases. The total cross sections for the three lowest deuteron groups from ^{10}B rise sharply from 2.4 to 4.0 Mev and then increase slowly through the Coulomb-barrier region. Qualitatively, the shape of the angular distributions to the three lowest states of ^{10}B can be explained by an α-tunneling mechanism with varying degrees of virtual Coulomb excitation. (D.C.W.)

38173 FLUCTUATIONS IN NEUTRON TOTAL CROSS SECTIONS IN THE Mev ENERGY REGION. Carlson, A. D. (Univ. of Wisconsin, Madison). 10p. (CONF-660107–52). ORAU. Gmelin, AED-CONF-66-003-114.

From American Physical Society Meeting, New York.

The effects of various types of structure were investigated by measuring the energy dependence of the neutron total cross sections of Al, Sb, Bi, Co, Fe, Pb, ^{206}Pb, Mg, Nb, Pr, Si, S, Ta, Ti, Y, Zn, and Zr. (D.C.W.)

38174 ISOBARIC MASS FORMULA AND COULOMB ENERGIES IN THE 1p-SHELL. Wilkinson, D. H. (Oxford Univ.). 22p. (CONF-660306–12). ORAU. Gmelin, AED-CONF-66-048-8.

From American Physical Society, Conference on Isobaric Spin, Tallahassee.

Some historical comments are made about the quadratic formula relating the masses of members of isobaric multiplets. It is remarked that the formula is still true even if the nuclear forces themselves are charge-dependent provided that the departure from charge-independence is of a two-body character and, like the Coulomb effect, may be treated as a perturbation. This means that charge-independence may be tested through the mass formula only by agreement of the coefficients of the mass formula with computations of the Coulomb energy differences. Computations of Coulomb energy differences in the 1p-shell are presented based on wavefunctions deriving from a study of electron scattering and (p,2p) reactions. Good agreement between the computed Coulomb energy differences and the binding energy differences is found but the need for improvements in the computations is stressed. Weak evidence that the n-p interaction may be some 2% stronger than the n-n or p-p interaction is presented. The critical role played by the binding energy of the "last proton" in calculations of Coulomb energy differences and the related importance of the parentage spectrum are emphasized. (auth)

38175 POLARIZATION EFFECTS IN PHOTONUCLEAR REACTIONS. Raphael, R.; Ueberall, H. (Catholic Univ. of America, Washington, D. C.). 18p. (CONF-660411–11). ORAU. Gmelin, AED-CONF-66-060-3.

From American Physical Society Meeting, Washington, D. C.

Explicit formulas are derived for the angular asymmetries and longitudinal and transverse polarizations of nucleons emitted from nuclei in the (γ,N) reaction, corresponding to linearly or circularly polarized as well as unpolarized incident photons. The reaction is assumed to proceed in two stages: photo-excitation of a single nuclear level and its subsequent decay via nucleon emission. The expressions are given in terms of the nuclear transverse multipole form factors for the excitation and of the reduced matrix elements corresponding to the decay. The results are illustrated by obtaining nucleon angular distributions and transverse polarizations following photo-excitation of the giant dipole resonance in ^{16}O, using Gillet's model and R-matrix theory. The comparison of these results with experiment is satisfactory. (auth)

38176 ON-LINE REDUCTION OF NUCLEAR PHYSICS DATA WITH THE PDP-7. Bevington, Philip R. (Stanford Univ., Calif.). 13p. (CONF-660327–2). ORAU. Gmelin, AED-CONF-66-050-9.

From American Physical Society Meeting, Durham, N. C.

The advantages inherent in a computer system are illustrated with specific ways in which the Stanford Computer for the Analysis of Nuclear Structure (SCANS) is used to reduce, point-by-point, on-line data from nuclear physics experiments, as well as to analyze such data with real-time control. Programs are presented to identify and sort charged particles with thick (E) and thin (dE/dx) solid-state detectors, to stabilize the scale of pulse-height spectra, and to control the acquisition of two-parameter data. The dead time contributed by these programs is shown to be negligible. Also discussed is the ability to control the subsequent analysis of this data in real-time reference to the methods adopted by SCANS to accept, record, and display the data. (auth)

38177 NEUTRON-PROTON CORRELATION EFFECTS IN SPHERICAL EVEN NUCLEI. Chen, H. T.; Goswami, A. (Western Reserve Univ., Cleveland). 15p. (CONF-660107–56). ORAU. Gmelin, AED-CONF-66-003-132.

From American Physical Society Meeting, New York.

The role of neutron-proton pairing correlations in the description of collective quadrupole states of even spherical nuclei with $40 < A < 70$ is studied. It is concluded that neutron-proton pairing correlations are significant in this region and with their inclusion one may be able to extend the region of applicability of the simple pairing plus quadrupole force model to all even spherical nuclei with $A > 40$. (auth)

38178 GAMMA-RAY ANGULAR DISTRIBUTIONS IN INELASTIC NUCLEON SCATTERING VIA COMPOUND NUCLEUS MECHANISM. Van Patter, Douglas M. (Bartol Research Foundation, Swarthmore, Pa.). 42p. (CONF-651118–13). ORAU. Gmelin, AED-CONF-65-329-10.

From American Physical Society Meeting, Gatlinburg, Tenn.

The characteristics of energy-averaged angular distributions of γ rays following inelastic scattering via compound nucleus formation are discussed. The large spin sensitivity of such distributions for ground-state transitions in even-even nuclei has provided the basis for many reliable spin assignments. Examination of the predicted behavior of $(n,n'\gamma)$ distributions near threshold has disclosed features deserving of further study. The influence of multipole mixing is emphasized, particularly for 3(D,Q)2 transitions, whose distributions are especially sensitive to this parameter. A detailed example of the effects of cascades from higher levels is presented. (auth)

38179 PARTICLE ANGULAR CORRELATIONS FOLLOWING NUCLEAR REACTIONS. Kuehner, J. A. (Chalk River Nuclear Labs., Ont.). 22p. (CONF-651118–8). ORAU. Gmelin, AED-CONF-65-329-12.

From American Physical Society Meeting, Gatlinburg, Tenn.

Two separate but related techniques for spin or parity determinations following nuclear reactions which involve a minimum of model-dependent assumptions are described. The first is a method of determining parity in terms of spin, and the second is an angular correlation method capable of yielding unambiguous spin assignments. The results from various reactions performed using these techniques are described. Calculations on the $^{12}C(6\text{-}12,\alpha)^{20}Ne$ at a bombarding energy of 27.2 Mev show that high spin levels are preferentially fed. Experimental results for this reaction are also described. (J.F.P.)

38180 ELECTRIC MONOPOLE NUCLEAR STRENGTH PARAMETERS AND THE IDENTIFICATION OF BETA BANDS IN EVEN NUCLEI. Davidson, J. P. (Rensselaer Polytechnic Inst., Troy, N. Y.). 7p. (CONF-651118–7). ORAU. Gmelin, AED-CONF-65-329-5.

From American Physical Society Meeting, Gatlinburg, Tenn.

The nuclear monopole strength parameter is calculated including beta vibrations exactly and assuming the nucleus rigid against gamma vibrations. The dimensionless ratio for $0_\beta \rightarrow 0_{gnd}$ transitions is plotted as a function of the stretching parameter for deformed but symmetric nuclei. Also included are the experimental points for rare earth and actinide nuclei. (J.F.P.)

38181 SPINS OF ^{58}Ni LEVELS FROM INELASTIC PROTON SCATTERING. Swenson, L. W.; Mohindra, R. K. (Franklin Inst., Swarthmore, Pa.). 8p. (CONF-651118–12). ORAU. Gmelin, AED-CONF-65-329-7.

From American Physical Society Meeting, Gatlinburg, Tenn.

Angular distributions for the $^{58}Ni(p,p')$ reaction leading to various levels were measured at proton energies from 9.10 to 9.55 Mev. These angular distributions were compared with predictions of the Hauser-Feshbach theory in order to find the spins of the levels. The angular distributions and spins obtained are given. (J.F.P.)

38182 N-SUBSHELL RATIOS AND VERY LOW-LYING STATES. Bhalla, C. P. (Univ. of Alabama, Huntsville). 6p. (CONF-651118–14). ORAU. Gmelin, AED-CONF-65-329-16.

From American Physical Society Meeting, Gatlinburg, Tenn.

Internal conversion coefficients for N subshells are calculated for M1 and E2 in the case of the first rotational state of ^{239}Pu. The importance of new calculations and the experimental data are discussed, and a brief description of the calculation is given. The numerical results for the 7.85-kev transition of ^{239}Pu are presented. Also the E2 admixture is calculated to be approximately 0.28 ± 0.07%, and the value of the magnetic decoupling parameter is found to be 0.46 ± 0.09. (J.F.P.)

38183 NEUTRON CROSS SECTIONS OF Ca FROM 2.0 TO 6.5 Mev. Reber, J. D.; Brandenberger, J. D.; Gabbard, F.; Young, T. (Univ. of Kentucky, Lexington). 13p. (CONF-660107–58). ORAU. Gmelin, AED-CONF-66-003-129.

From American Physical Society Meeting, New York.

The differential cross sections for elastic scattering of neutrons by calcium have been measured for neutron energies of 2.15, 3.34, 5.45, 6.00, and 6.53 Mev. The angular distributions were measured with relative errors of less than 5 per cent and absolute errors of about 10 per cent. The total neutron cross section for calcium was measured for neutron energies between 2.2 and 5.3 Mev in 25-kev steps with errors of about 10 per cent. The total neutron cross section for calcium was measured for neutron energies between 2.2 and 5.3 Mev in 25-kev steps with errors of less than 4 per cent. The differential cross sections were measured using time-of-flight techniques and a liquid scintillator equipped with γ-ray discrimination. The total cross section data were taken using a plastic scintillator and time-of-flight techniques. The total cross section is compared to the results of Glasgow and Foster (Report BNL-325), and Stiwer et al. (Nuclear Phys. 62: 165(1965)). (auth)

38184 GAMMA-RAY ANGULAR CORRELATIONS FOLLOWING NUCLEAR REACTIONS. Broude, C. (Chalk River Nuclear Labs., Ont.). 15p. (CONF-651118–6). ORAU. Gmelin, AED-CONF-65-329-2.

From American Physical Society Meeting, Gatlinburg, Tenn.

New developments in the techniques of measuring gamma angular correlations following capture reactions are considered. The methods discussed for preparing discrete gamma-emitting states in an axially symmetric way for analysis of measured gamma correlations are via an intermediate unobserved radiation, e.g., discrete states in which the proton is not observed are axially symmetric, and via an emitted particle which is detected in an axially symmetric way with respect to the incident beam direction. The use of a gamma detector array and a Ge(Li) detector for these measurements is described. (J.F.P.)

38185 $^{36}S(p,\gamma)^{37}Cl$ REACTION FOR PROTON ENERGIES IN THE 800-1800 kev REGION. Hyder, A. K. Jr. (Aerospace Research Labs., Wright-Patterson AFB, Ohio); Harris, Gale I.; Kendziorski, F. R.; Perrizo, J. J. 20p. (CONF-660107-53). ORAU. Gmelin, AED-CONF-66-003-120.

From American Physical Society Meeting, New York.

The lower-lying levels of ^{37}Cl were investigated using the $^{36}S(p,\gamma)^{37}Cl$ reaction, by exposing ^{36}S-enriched CdS targets to a proton beam. Approximately 90 resonances were observed, the majority of which could be attributed to the $^{36}S(p,\gamma)^{37}Cl$ reaction. Singles spectra and angular distributions at several of these resonances were measured. (D.C.W.)

38186 PRODUCTION OF CHARGED PIONS BY 600 Mev PROTONS ON VARIOUS NUCLEI. Heer, E.; Hirt, W.; Martin, M.; Michaelis, E. G.; Serre, C.; Skarek, P.; Wright, B. T. (European Organization for Nuclear Research, Geneva). 20p. (CONF-660209–15). ORAU. Gmelin, AED-CONF-66-023-18.

From Conference on Intermediate Energy Physics, Williamsburg, Va.

The method and analysis of measurements of charged pion production on various nuclei by 600-Mev protons from the CERN synchrocyclotron are discussed in detail. Production cross sections were measured for CH_2, CD_2, Be, C, Al, Cu, Ag, and Pb at pion energies between 100 and 350 Mev and for production angles of 0.8 and 21.5°; the results are presented. Hydrogen cross sections obtained by CH_2-C subtraction, and neutron cross sections evaluated by CD_2-CH_2 subtraction are also presented. The results are in agreement with other data. (L.B.S.)

38187 PROTON GAMMA ANGULAR CORRELATION MEASUREMENTS IN THE REACTION $^{26}Mg(d,p\,\gamma)^{27}Mg$. Eswaran, M. A. (Atomic Energy Establishment, Trombay, India). 10p. (CONF-660411-35). ORAU. Gmelin, AED-CONF-66-060-117.

From American Physical Society Meeting, Washington, D. C.

The first two excited states of ^{27}Mg at 0.98 and 1.69 Mev were investigated by γ-p angular correlation measurements on the reaction $^{26}Mg(d,p\gamma)^{27}Mg$. Spin assignments were made for the first two excited states of ^{27}Mg. (D.C.W.)

38188 STUDY OF NUCLEAR ENERGY LEVELS IN ^{121}Sb, ^{123}Sb, ^{125}Sb, AND ^{127}I USING β- AND γ-ray SPECTROSCOPY. Auble, Ronald L. (Michigan State Univ., East Lansing). 116p. (CONF-660107-51). ORAU. Gmelin, AED-CONF-66-003-121.

Thesis. From American Physical Society Meeting, New York.

The decay schemes of several odd-A tellurium (A = 121, 127) and tin (A = 123, 125) isotopes have been examined in an effort to gain information about the nuclear level structure of adjacent antimony and iodine isotopes. Beta- and gamma-ray single and coincidence spectroscopy were used to determine the ordering of the gamma transitions and, therefore, the energies of the nuclear levels. Several levels which had not been observed in earlier studies were located in each of the four isotopes. Angular correlation measurements on the prominent gamma-gamma cascades in ^{121}Sb, ^{125}Sb, and ^{127}I were made to study the spins of the nuclear states and the mixing ratios of the gamma transitions. The spectrum shape of the beta particles feeding one of the excited states in ^{123}Sb was studied and was found to yield an essentially linear Fermi-Kurie plot. This result, in conjunction with the corresponding log ft value, suggests a nonunique, first-forbidden assignment for this beta transition and limits the possible spin assignments for the ^{123}Sb state. Comparisons are made of the existing experimental data with the predictions of several nuclear models. In the low-energy regions of ^{121}Sb and ^{127}I, sufficient data on mixing ratios and lifetimes are available to make quantitative comparisons with predictions of the single particle model and with the pairing-plus-quadrupole residual interaction calculations of Kisslinger and Sorensen. Partial agreement is found between the experimental data and the latter predictions. At higher excitations, only qualitative comparisons can be made due to the lack of gamma lifetime and mixing-ratio measurements. A model which is found to predict level structure similar to that observed experimentally is one in which the low-lying particle states are coupled to excitations of the nuclear core. However, several high-energy states in ^{125}Sb are found to deviate from the predictions of this model. Thus, other types of excitation must also be assumed to exist. The nature of these states can only be determined after additional experimental data become available. (auth)

Plasma Physics and Thermonuclear Processes

See also Fluid Physics and Thermodynamics

Refer also to abstracts 37063, 37119, 37334, 37387, and 38400.

38189 (AD–636095) MAGNETIC FIELD DESIGN WITH AN ELECTROLYTIC TANK ANALOG. Combes, Lewis S.; Gallagher, Charles C.; Levine, Morton (Air Force Cambridge Research Labs., L. G. Hanscom Field, Mass.). May 1966. 17p. (AFCRL–66-328). CFSTI $1.00 cy, $0.50 mn.

A simplified electrolytic tank was constructed that serves as a relatively easy and reasonably accurate analog method of designing a magnetic field configuration to be used in a plasma containment device. The current density in the electrolyte is directly proportional to the magnetic flux density in the coils and equations were derived from this relation by which flux density, magnetomotive force, inductance, total flux, and energy in the coils can be found from tank measurements. The detailed analysis of a specific magnetic field problem is given. (auth)

38190 (AD–637513) THEORY OF SPHERICAL PROBES IN MONOENERGETIC PLASMAS. Guderley, Karl G.; Valentine, Emma M. (Aerospace Research Labs., Wright-Patterson AFB, Ohio). Feb. 1966. 151p. (ARL–66-0024). CFSTI $5.00 cy, $1.00 mn.

A survey was made of the behavior of a plasma probe in a monoenergetic isotropic homogeneous plasma. (Monoenergetic means that all electrons have the same energy, the energies of the electrons and ions may be different.) The analysis is carried out in the Vlasov approximation. The derivation and a discussion of the equation for the potential in the field around the probe for general distribution functions are first presented. Later the distribution functions are specialized to delta functions. The governing equation is a nonlinear differential equation containing parameters which are ultimately defined by the solution which one wants to find. This solution is found iteratively. In order to obtain the p^{th} approximation a linearization for the vicinity of the $(p-1)^{th}$ approximation is used. A special technique is used in order to obtain a formulation which is numerically stable. On this basis probe characteristics (probe current versus probe potential) were computed for a considerable number of cases, so that a fairly complete survey of the behavior of a probe is obtained. Originally this problem was approached by different methods. They are still valuable for the intuitive insight which they provide. An account of these approaches, and also of their deficiencies is given in the appendix. (auth)

38191 (CLM-R–61) HEAT TRANSMISSION THROUGH A LANGMUIR SHEATH IN THE PRESENCE OF ELECTRON EMISSION. Hobbs, G. D.; Wesson, J. A. (Culham Lab., United Kingdom Atomic Energy Authority, Abingdon (England)). June 1966. 16p. Dep. mn. BIS $0.30. HMSO 1s. 9d.

The steady-state electrostatic sheath which forms between a plasma and a wall in order to prevent a net current flow also acts as a thermal insulator between the hot electrons and the wall. The transmitted heat flux can be written in the form $Q = \frac{1}{4}n\bar{v}_e \cdot 2kT \cdot F$, where $F = (\pi\mu/8)^{\frac{1}{2}}[5 - \ln 2\pi\mu]$ and $\mu = m_e/m_i$. If the wall emits cold electrons due to any cause (e.g. electron, ion or photon impact) the voltage across the sheath is reduced and the thermal insulation impaired, i.e., F is increased. The maximum extent to which this occurs is limited by a saturation of the emission current due to space charge effects. In these circumstances the ratio of emission to primary electron current never exceeds $1 - 8.3\sqrt{\mu}$, the sheath voltage falls to its minimum value of 1 kT and F attains its maximum value given by $F = 0.33 + 2.2\sqrt{\mu}$. (auth)

38192 (COO–1233-32) EQUIPOTENTIAL SURFACES OF A PLASMA MOVING IN A TOROIDAL OCTUPOLE MAGNETIC FIELD. Filimonov, A. B.; Sprott, J. C.; Lenoioni, D. E.; Willig, R. L. (Wisconsin Univ., Madison. Dept. of Physics). June 1966. Contract AT(11-1-)-1233. 18p. (CONF-660633–1). Dep. mn. CFSTI $1.00 cy, $0.50 mn.

From American Physical Society, Division of Plasma Physics, Minneapolis, Minn.

Measurements of the floating potential resulting from a 100-ev hydrogen plasma moving in a toroidal octupole magnetic field of a few kilogauss revealed a definite structure and time evolution of the equipotentials. It was found that in areas of relatively high density (10^{10} cm^{-3}), i.e., in the central region of the toroid, the magnetic field lines were equipotential surfaces. These surfaces (and consequently the $\vec{E} \times \vec{B}/B^2$ drift) agreed qualitatively with solutions found by J. W. Poukey for describing the drift in a uniform magnetic field, i.e., plasma separated into two sections which circulated in such a manner that the cloud propagated perpendicular to the magnetic field. (auth)

38193 (INDEC-SR–7, pp 3,5-13) ELECTRON DENSITY AND COLLISION FREQUENCY IN A RADIALLY INHOMOGENEOUS PLASMA COLUMN. Zelby, Leon W.; Kalagher, R. J. (Pennsylvania Univ., Philadelphia. Inst. for Direct Energy Conversion).

Included is a derivation of the dispersion relation and the attenuation relation for a cylindrical plasma column surrounded by a sheath helix. In particular, the plasma with a varying electron density and collision frequency is considered. These parameters are assumed to be inhomogeneous in the radial direction only and the plasma drift velocity is zero. (M.O.W.)

38194 (INDEC-SR–7, pp 3,22-59) ELECTROMAGNETIC WAVE INTERACTION IN AN INHOMOGENEOUS DRIFTING PLASMA. Zelby, Leon W.; Mehuron, W. O. (Pennsylvania Univ., Philadelphia. Inst. for Direct Energy Conversion).

A theoretical model is developed for the case of an inhomogeneous drifting plasma column where the inhomogeneity of the plasma is represented by radial variations in the electron density and electron drift velocity. The solutions obtained from the model were used to obtain dispersion relations for the column in free-space, the plasma column bounded by a thin dielectric tube, and for the case of a bounded plasma column surrounded by a helix. (M.O.W.)

38195 (INDEC-SR–7, pp 3,60-73) MEASUREMENT OF PLASMA TRANSPORT PROPERTIES IN A Na–K SEEDED ARGON PLASMA. Gottschlich, Chad F.; Chu, T. K. (Pennsylvania Univ., Philadelphia. Inst. for Direct Energy Conversion).

An investigation was made to measure the non-equilibrium ionization produced by an externally applied electric field in a Na–K seeded Ar plasma. The experimental techniques are outlined. The preliminary results are described. (M.O.W.)

38196 (JINR–P-2783-2) O KOLEBANIYAKH OGRANICHENNOI (TSILINDRICHESKOI) PLAZMY S GORYACHIM ELEKTRONNYM TOKOM. (Oscillations of Confined (Cylindrical) Plasma With a Hot Electron Current). Makhan'kov, V. G. (Joint Inst. for Nuclear Research, Dubna (USSR). Lab. of High Energy). 1966. 10p. Dep. mn.

A dispersion equation is obtained for a confined cylindrical plasma with a hot current in the case in which the Debye electron expansion is larger than the transverse dimensions of the system. The excitation and increment of various oscillation modes are analyzed assuming the presence of mirror reflections. (tr-auth)

38197 (LA-3553) PROPOSED STRAIGHT Θ-PINCH DEVICES ENERGIZED BY THE ENERGY STORAGE SUPPLY OF THE TOROIDAL Θ-PINCH (SCYLLAC). Dike, R. S.; Kemp, E. L.; Quinn, W. E. (Los Alamos Scientific Lab., Univ. of California, N. Mex.). Apr. 1966. Contract W-7405-eng-36. 29p. Dep. mn. CFSTI $2.00 cy, $0.50 mn.

The design of the toroidal Scyllac device is extended to include the capability for also energizing straight θ-pinch systems with lengths of up to 22 meters. The linear devices are to be energized by the energy storage supply of and in the same building as the toroidal device. A design

is presented for both a straight "parallel" device, in which the energy supply is connected in parallel to drive a single-turn compression coil, and a straight "series" apparatus in which each half of the energy supply is connected in series with the compression coil. (auth)

38198 (LA-DC-8099) ELECTRON DISTRIBUTION FUNCTION IN A PLASMA WITH EXCITATION COLLISIONS. Mjolsness, R. C.; Petschek, A. G. (Los Alamos Scientific Lab., Univ. of California, N. Mex.). [1963]. Contract W-7405-eng-36. 26p. (CONF-660714-1). Dep. mn. CFSTI $2.00 cy, $0.50 mn.

From Institute for Defense Analysis Meeting, Santa Barbara, Calif.

The equilibration of electron and ion temperatures in a plasma may be hindered by inelastic collisions of electrons with heavy particles. The effect of excitation collisions is examined, assuming that all excitation energy is reradiated from the plasma and that multiple excitations and ionizations may be ignored. The plasma is assumed to be spatially homogeneous and to consist of a fixed number of electrons, heavy neutral particles, and ions. No distinction was made between the various excited states of the ions and neutral particles. The existence of a single, energy-dependent collision frequency was assumed for the excitation collisions of the electrons. Steady-state solutions for the electron distribution function were found. (M.O.W.)

38199 (MATT-400) CUMULATIVE LISTING OF PLASMA PHYSICS LABORATORY REPORTS AND PUBLICATIONS (5TH EDITION). (Princeton Univ., N. J. Plasma Physics Lab.). July 1966. Contract AT(30-1)-1238. 90p. Dep. mn. CFSTI $3.00 cy, $0.75 mn.

A cumulative listing is presented of reports and publications issued by the Princeton University Plasma Physics Laboratory from its inception in July 1951 (under the name Project Matterhorn) to date. (M.O.W.)

38200 (NP-16206) K TEORII FLUKTUATSII V MAGNITOAKTIVNOI PLAZME. (Theory of Fluctuations in Magnetically Active Plasma). Kirochkin, Yu. A. (Khar'kovskii Gosudarstvennyi Universitet (USSR)). 1964. 78p. Dep. mn.

Thesis.

The dissertation is devoted to the theoretical study of the electrodynamic properties of a uniform magnetoactive plasma and investigates, on the basis of kinetic theory, the propagation of waves, the excitation of waves by external currents, the fluctuation in various physical quantities, and the scattering of waves with their mutual transformation on plasma fluctuations. The basic results presented here were published earlier in 5 papers and in contributions to 4 conferences and seminars during the 1959-1963 period. (JPRS)

38201 (NP-16210) COLLECTIVE FLUCTUATIONS IN A LABORATORY MAGNETO-PLASMA PERTURBED BY AN ELECTRON BEAM. Report No. 29. Leheny, Robert F. (Columbia Univ., New York. Plasma Lab.). 1966. 180p.

A study of the interaction between transverse electromagnetic waves and magnetoplasma to determine the state of the electron component of the plasma is described. The induced emission of radiation by collective fluctuations in the electron component of the plasma, resulting from scattering of transverse waves, is investigated in a quiescent laboratory magnetoplasma perturbed by an electron beam. This combination scattering provides information on the intensity and spectra of the longitudinal waves propagating in the gas. By means of a resonance in the scattering, which occurs when the incident or scattered transverse wave is in resonance with the plasma electrons, extremely small amplitude fluctuations have been detected. The deviation from equilibrium resulting from weak perturbations in the form of an electron beam was studied using this technique. Measurements of magnetobremsstrahlung in the absence of perturbations compares well with the level for emission from an equilibrium plasma, and establishes the equilibrium state of the electrons. Magnetobremsstrahlung measurements in the presence of beam perturbations indicate that the weak beam excitation is limited by ohmic dissipation of fluctuation energy. Under suitable conditions, this mechanism is found to thermalize almost the entire directed energy of the beam. Low frequency fluctuations, detected by Langmuir probes, were also observed to be excited by electron beams. These fluctuations are identified as drift wave instabilities, and are shown to accompany anomalous diffusion of plasma across the confining magnetic field lines. (auth)

38202 (NP-16236) COMBINATION SCATTERING OF ELECTRO-MAGNETIC WAVES FROM DRIVEN SPACE CHARGE WAVES IN A LABORATORY MAGNETOPLASMA. Report No. 30. Chen, Yung-Gann (Columbia Univ., New York. Plasma Lab.). 1966. 135p.

Experimental results of combination scattering of microwaves from driven space charge waves in a laboratory magnetoplasma and an analysis are presented. The plasma is generated in the Columbia Q machine. A simple model is also presented to show a better physical picture of scattering which turns out to be in good agreement with the already existing theory when modified to take into account the laboratory conditions. According to theory, by varying the confining magnetic field, the combination scattered signal should show strong enhancement at the cyclotron resonances of the transmitter and the receiver frequencies. Experimental results show these peaks and the line shape as predicted. Measurement of the scattered signal intensity shows that the electron-ion collision effect is approximately as predicted in the theories. Existence of space charge waves in the Q-device plasma was confirmed and its dispersion relation studied by the uhf techniques. Measurement of the frequency-power spectrum of the scattered signal shows good agreement with the theoretical prediction that large scattering should occur when the system becomes resonant to the space charge waves. By scattering from the driven plasma line, the calculated plasma electron number density is in good agreement with those obtained from other methods. Scattering from the hybrid mode of the space charge wave is as predicted. The experimental results demonstrate the usefulness of the combination scattering technique for plasma diagnostics with microwaves. (auth)

38203 (NP-16237) DRIFT WAVE EXCITED ANOMALOUS DIFFUSION IN A FULLY IONIZED MAGNETO-PLASMA. Report No. 28. Eastlund, B. J.; Josephy, K.; Leheny, R. F.; Marshall, T. C. (Columbia Univ., New York. Plasma Lab.). [1966]. 38p.

The transverse diffusion coefficient, $D_\perp$, of a fully ionized plasma in a "Q-machine" was observed to depend on the frequency and amplitude of drift waves. These waves, observed with a floating Langmuir probe and spectrum analyzer, could be impressed on the plasma by (1) a weak electron beam injected along the plasma axis (2) by applying an a-c signal of appropriate frequency to a plate at one end of the plasma (3) drawing d-c current through the plasma or (4) were found to occur naturally. $D_\perp$ was determined from the radial profile of potassium plasma pulses. In all cases, $D_\perp$ was strongly influenced by the amplitude of the low frequency components of the spectrum, and was observed to be proportional to the r.m.s. power of the fluctuations. The impedance of the plasma as a function of the impressed a-c signal showed minima at frequencies close to that of the "drift instability," where the value of $D_\perp$ exhibited strong maxima. (auth)

38204 (NP-16240) BIBLIOGRAPHY ON THE HIGH TEMPERATURE CHEMISTRY AND PHYSICS OF GASES AND PLASMAS. No. 19. Brewer, L. (comp.) (California Univ., Berkeley). June 30, 1966. 16p. National Bureau of Standards Free.

Included is a list of 91 spectroscopy articles of interest in high temperature chemistry, and 51 articles on reactions between gases and condensed phases. (M.O.W.)

38205 (NYO-3565-4) PLASMA INSTABILITIES AND WAVES EXCITED BY AN ANISOTROPIC VELOCITY DISTRIBUTION PRODUCED BY ELECTRON CYCLOTRON RESONANCE. Fourth Quarterly Progress Report, March 1,

1966–May 31, 1966. Shohet, J. L. (Johns Hopkins Univ., Baltimore, Md. Dept. of Electrical Engineering). June 1966. Contract AT(30-1)-3565. 19p. Dep. mn. CFSTI $1.00 cy, $0.75 mn.

A study was made to investigate the ability of a short burst of electron cyclotron resonance radiation to produce an anisotropic velocity distribution, and the waves and instabilities produced from this anisotropy. During this period several plasma diagnostic devices were incorporated into the experimental apparatus and preliminary measurements and analysis of data took place. The results show that a measurement of plasma anisotropy should be possible. (M.O.W.)

38206 (ORNL-P-1539) MOVING STRIATIONS PRODUCED BY A SIMPLE THERMAL INSTABILITY. Alexeff, Igor (Oak Ridge National Lab., Tenn.). [1964]. Contract W-7405-eng-26. 16p. Dep. mn. CFSTI $1.00 cy, $0.50 mn.

A simple thermal instability is investigated as a possible cause of moving striations in discharge tubes. The mathematical treatment predicts which gases should and which should not exhibit the instability. The frequency of oscillation of a cylindrical discharge, due to the instability, also predicted. Not discussed is the velocity with which the instability appears to propagate longitudinally down the discharge. The theoretical predictions are compared with the experimental striation data of several authors, and reasonable agreement is found. (auth)

38207 (PPL-AF-1) THE PRESENT STATE OF PLASMA KINETIC THEORY. Frieman, Edward A. (Princeton Univ., N. J. Plasma Physics Lab.). May 1966. Contract AF49(638)-1555. 23p.

Problem areas in the kinetic theory of plasma are described with respect to the following: the B-B-G-K-Y hierarchy, the ϵ expansions, nonequilibrium processes, and the kinetic equations for an unstable plasma. (M.O.W.)

38208 (PPL-AF-4) SECOND-ORDER MAGNETIC MOMENT OF A CHARGED PARTICLE IN AN AXIALLY-SYMMETRIC STATIC MAGNETIC FIELD. Gardner, C. S. (Princeton Univ., N. J. Plasma Physics Lab.). May 1966. Contract AF49(638)-1555. 14p.

As defined by Kruskal, the magnetic moment of a charged particle of small mass moving in a magnetic field is a series (in general not convergent) $\mu = \mu_0 + \epsilon\mu_1 + \epsilon^2\mu_2 + \ldots$ where $\mu_0 = v_\perp^2/B$, $\epsilon = m/e$, and where μ_1 and μ_2 are functions of the spacial coordinates and velocity components of the particle. The series μ has the property that its time derivative is formally zero. The formula for the first-order correction μ_1 was given by Kruskal for a general field. The formula is given for the second-order correction μ_2, for the special case of a static magnetic field with axial symmetry. (auth)

38209 (PPL-AF-5) DERIVATIONS OF HIERARCHIES FOR N PARTICLE SYSTEMS AND VLASOV SYSTEMS BY MEANS OF THE FUNCTIONAL CALCULUS. Nakayama, Toshio; Dawson, John M. (Princeton Univ., N. J. Plasma Physics Lab.). May 1966. Contract AF49(638)-1555. 29p.

The methods of the functional calculus are applied to the Klimontovich equation and to the Vlasov equations. The equation for the generating functional is derived for both cases. By taking moments of these equations the B-B-G-K-Y hierarchy is obtained for the case of the Klimontovich equation and a similar hierarchy is obtained for the case of the Vlasov equation. The two hierarchies are identical, except for some terms involving individual particle interactions. Methods of solving the Vlasov hierarchy are discussed and it is shown how quasilinear theory can be obtained. (auth)

38210 (UCRL-12455(Rev.1)) PLASMA CONFINEMENT PROPERTIES OF RELATIVISTIC ELECTRON COILS. Christofilos, N. (Lawrence Radiation Lab., Univ. of California, Livermore). Aug. 6, 1965. Contract W-7405-eng-48. 12p. Dep. mn. CFSTI $1.00 cy, $0.50 mn.

The value of the loading factor (ξ) of the Astron E layer required to provide plasma stability is examined. The practical aspect of this discussion is that if an E layer of much smaller loading factor is required for stability than was initially anticipated, one can seek other geometries which can accomplish all three requirements with a much weaker E layer. (M.O.W.)

38211 (AEC-tr-6782) PRODUCTION OF HOT-ELECTRON PLASMA IN MAGNETIC MIRROR TRAPS. Akshanov, B. S.; Volkolupov, Yu. Ya.; Marinin, V. G.; Sinel'nikev, K. D.; Smirnov, A. M. Translated from Paper CN-21/249 Presented at the IAEA Conference on Plasma Physics and Controlled Fusion Research, Culham, England, September 6–10, 1965. 41p. Dep. mn. CFSTI $2.00 cy, $0.50 mn. JCL $4.60 fs, $1.43 mf.

The results are presented of an investigation of a plasma produced by the injection of an electron beam through a magnet system with opposed fields into a magnetic mirror trap. The efficiency of the production method is described. Various plasma properties are described in detail. (M.O.W.)

38212 CONSIDERATION OF SHORT-RANGE FORCES IN THE STATISTICAL MECHANICS OF THE NONEQUILIBRIUM HEAVILY IONIZED PLASMA AND ELECTROLYTE. Kremp, D. (Univ., Rostock, Ger.). Ann. Phys. (7), 17: 278-89(1966). (In German).

Starting from the stochastic Liouville equation for the distribution function of charged particles, the expanded generalized equation of Prigogine and Resibois is first given by means of a collision operator that describes the collision of charged particles and neutral particles. The equations are further simplified on the basis of assumptions concerning the relaxation times of the systems and approximations relative to the concentrations. From the hydrodynamic approximation, equations are obtained for the correlation function in phase space, from which transport coefficients up to the order $\kappa^2 c^2$ can be calculated under consideration of short-range forces. (tr-auth)

38213 THE VELOCITY DISTRIBUTION OF ELECTRONS IN THE POSITIVE COLUMN OF A CONSTRICTED LOW-PRESSURE DISCHARGE. Paulus, I.; Schott, L. (Univ., Kiel). Ann. Phys. (7), 17: 290-300(1966). (In German).

Probe measurements in a nitrogen low-pressure discharge, whose positive column is constricted by a diaphragm, yields a variation of the velocity distribution of electrons of a simple Maxwell distribution type. The observed velocity distribution can be explained as a superposition of two Maxwellian electron groups with different temperatures and intensities. Furthermore as a result of the constriction of the plasma column a stronger axial supporting density gradient and longitudinal electric field strength opposite to the discharge current results, which can be qualitatively explained on the basis of a model. (tr-auth)

38214 UHF PLASMA OSCILLATIONS IN A Hg LOW-PRESSURE DISCHARGE. I. OSCILLATION EXCITATION BY MONOENERGETIC PRIMARY ELECTRONS. Behlke, H.; Drost, H.; Schulz, G.; Pupke, H. (Deutsche Akademie der Wissenschaften, Berlin). Ann. Phys. (7), 17: 305-15 (1966). (In German).

The excitation of uhf-plasma oscillations in a low-pressure Hg discharge by additional primary electron interactions in a plasma was investigated in a long and wide discharge tube. The oscillations were detected by means of a probe in the primary beam with a coaxial line coupled to the probe and a uhf receiver as an indicator. The oscillation region was restricted to a space up to 200 mm from the cathode, which allows a strong dependence on the discharge and electron-beam parameters to be determined relative to position and intensity. The highest oscillation amplitude appeared at low arc currents (2 amp at electron density of 2×10^{10} cm^{-3}), at high primary currents (up to 130 mamp) and at primary velocities of 25 V. The resulting dependency of the maximum uhf amplitude on the neutral gas pressure showed significant oscillation intensities up to 1×10^{-2} torr. Thereby the maximum uhf amplitudes at any given time corresponds to the Langmuir frequency calculated at the

corresponding electron density. The results obtained are discussed along with results of other works. 33 references. (tr-auth)

38215 UHF PLASMA OSCILLATIONS IN A Hg LOW-PRESSURE DISCHARGE. II. ANOMALOUS SCATTERING OF PRIMARY ELECTRONS IN THE UHF PROFILE OF THE CATHODE. **Behlke, H.; Drost, H.; Schulz, G.; Pupke, H. (Deutsche Akademie der Wissenschaften, Berlin). Ann. Phys. (7), 17: 316-21(1966). (In German).**

On the basis of conditions previously obtained for the excitation of uhf-plasma oscillations by monoenergetic primary electrons the mechanism of anomalous electron scattering and the position of the uhf-oscillation profile from the cathode was investigated. The "over-velocity" of the scattered incident electrons determined from probe characteristics was used as a measurement of the anomalous scattering, i.e., the difference between the potential of the electron gun and the negative probe potential, by which the "over-velocity" was actually detected by the probe. The investigation yields information of the local coincidence of the scattering region (scattering zone and regions of constant over-velocity) and uhf-oscillation profiles; no changes in the over-velocity of the primary electrons appeared in front of as well as behind the oscillation profile. Further indications for the velocity modulation process could not be found in the sense of Merrill and Webb. The significance of the results is postulated on the basis of an interaction process of the primary electrons with the plasma, whereby the electron scattering and the excitation of the uhf-plasma oscillation occur simultaneously, but independently from one another. The influence of the cathode-near probe on this process is considered. (tr-auth)

38216 UHF PLASMA OSCILLATIONS IN A Hg LOW-PRESSURE DISCHARGE. III. UHF PROFILE AND FOCUSING LENGTH OF THE PRIMARY ELECTRONS IN THE PLASMA. **Behlke, H.; Drost, H.; Schulz, G.; Pupke, H. (Deutsche Akademie der Wissenschaften, Berlin). Ann. Phys. (7), 17: 322-8(1966). (In German).**

In order to resolve the question of whether the uhf oscillations excited by monoenergetic primary electrons have an influence on the focusing of these electrons in Maxwellian-equilibrium plasma electrons, the focusing length and the oscillation profile were compared for a set of parameters. The distance from the cathode was considered as the focusing length, at which the Langmuir probe characteristic yielded only a single electron group, where an i_{pr}/i_s relation to e^{-8} is the basic criterium. The measurement showed that, in general, the focusing lengths exhibited values 10-20 times as large as the uhf-profile lengths determined under the same conditions. Also a comparison of the focusing lengths with the maximum amplitudes in dependence of arc current, primary current, and neutral gas pressure gave no indication of a mutual dependence of both quantities; the largest focusing lengths were obtained actually under the conditions under which the smallest uhf amplitudes were excited. The results were considered as further evidence of the assumption that not only the scattering of the primary electrons from the cathode but also their focusing in equilibrium of the plasma electrons resulted independently from the excitation of uhf oscillations. (tr-auth)

38217 STATISTICAL THEORY OF RADIATIVE PROCESSES IN PLASMAS. **Mallozzi, Philip J.; Margenau, Henry (Yale Univ., New Haven). Contract Nonr-609(51). Ann. Phys. (N. Y.), 38: 177-237(June 27, 1966).**

The plasma physics work of Prigogine and Balescu is extended, which allows inclusion of radiation as well as particles. The treatment ignores the Coulomb interaction between the electrons, focusing attention cheifly upon the behavior of photons and electrons in the presence of ions and neutral molecules. However, it allows for a transverse index of refraction, which results from an indirect interaction between electrons via the radiation field. The results are applicable to slightly ionized plasmas. Homogeneous plasmas are considered. The treatment is carried out systematically to the fourth order of the Liouville perturbation operator. Conservation principles are derived and an overall H-theorem is proved for the radiating plasma. Concrete results of applications are presented, which show how the general theory entails formulas for the scattering, absorption, and conductivity of microwaves, electron-atom and electron-ion bremsstrahlung, both spontaneous and stimulated, and other effects. (L.B.S.)

38218 KINETIC TEMPERATURE AND IONIZATION LEVEL OF INTERGALACTIC HYDROGEN IN A STEADY-STATE UNIVERSE. **Rees, M. J.; Sciama, D. W. (Univ. of Cambridge, Eng.). Astrophys. J., 145: 6-20(July 1966).**

The ionization equilibrium of intergalactic hydrogen in a steady-state universe is calculated, taking into account collisional ionization, photoionization, and the state of the created material. The results are used to determine the kinetic temperature of the gas as a function of its density, if the density of neutral hydrogen has the very low value of 10^{-11} cm^{-3} deduced by Gunn and Peterson from the spectrum of 3C9. It is found that if the hydrogen is created ionized a kinetic temperature of 3×10^5 °K is required when the total particle density is 10^{-5} cm^{-3}. This is consistent with a previous estimate based on indirect arguments. However, if the hydrogen is created neutral, it is not possible to account for the observed density of neutral gas unless the total gas density is itself very low ($\ll 10^{-7}$ cm^{-3}). It is also shown that the spectra of objects with redshift $z > 1$ imply that carbon and nitrogen are unlikely to be present with their "cosmical" abundances in the intergalactic medium of a steady-state universe. Other implications of this work are also briefly discussed. (auth)

38219 HELICAL MINIMUM $\bar{B}$ MAGNETIC CONFIGURATIONS. **Zueva, I. M.; Solov'ev, L. S. At. Energ. (USSR), 20: 396-401(May 1966). (In Russian).**

Several helical symmetry minimum-$\bar{B}$ magnetic configurations were studied, and analytical expressions were obtained for the specific volume in the vicinity of the helical-magnetic axis. Precise formulas for the specific volume and for the mean power-line twist angle are expressed in a single integral. Graphs for the specific volume, the mean twist angle, and the limiting curves of the magnetic surface were constructed by a numerical evaluation of this integral. (G.O.Y.)

38220 PARAMAGNETIC HIGH-FREQUENCY EFFECT AND ELECTRON PARAMAGNETIC RESONANCE IN PLASMA. **Glagolev, V. M.; Khromkov, I. N.; Cheverev, N. S. At. Energ. (USSR), 20: 401-7(May 1966). (In Russian).**

The interactions of h-f fields in volume resonators with a plasma (density of 10^{13} to 10^{14} cm^{-3}) were studied using constant magnetic field. It was observed that a paramagnetic current developed in the plasma under h-f pressure. The increased static magnetic-field effect inside the plasma agreed with the calculated function of the electron paramagnetic resonance. (G.O.Y.)

38221 PHOTOEXCITATION AND PHOTOIONIZATION OF ENERGETIC HYDROGEN ATOMS. **Grechukhin, D. P.; Karpushkina, E. I.; Sokolov, Yu. L. At. Energ. (USSR), 20: 407-12(May 1966). (In Russian).**

Two methods for improving the injection efficiency of fast hydrogen atoms into magnetic traps are proposed. The first suggests an increase of the population at the upper levels ($n \approx 10$) of the fast H-atom beam by irradiating it using quanta with resonance according to the selected $n_1l_1 \rightarrow n_2l_2$ transition. The population of the n_2-l_2 level is calculated as a function of the radiation density and the time-of-flight of the atom in the light field. The necessary light source power was calculated from the data obtained. The second method suggests the direct photoionization of H atoms in the active trap zone. The light-source power necessary for the efficient photoionization of atoms is evaluated on the basis of the cross section for ionization of the H atom as a function of the radiation wavelength. (G.O.Y.)

38222 THERMODYNAMIC CONSIDERATIONS ON THE SAHA EQUATION. **Diana, Massimo (Univ., Naples. CNR, Rome). Atti Accad. Naz. Lincei, Rend., Cl. Sci. Fis., Mat. Natur., 39: 482-7(Dec. 1965). (In Italian).**

Interactions between particles in a thermal plasma cause reductions in the ionization energy. Lowering of ionization energy was evaluated by expressing the Saha equation in terms of fugacities of ionized gases on the basis of the thermodynamic principles of solutions. (auth)

38223 STUDY OF THE FORMATION OF NEGATIVE IONS IN A FLAME BY MEASUREMENT OF THE HALL EFFECT. Klein, Siegfried; Benattar, Rene (Institut National des Sciences et Techniques Nucleaires, Gif-sur-Yvette, France). Compt. Rend., Ser. B, 262: 1664-7 (June 27, 1966). (In French).

Certain phenomena in flames have previously been explained by the hypothesis of the massive formation, within the flame, of negative ions. The measurement of the Hall effect in a flame has made it possible to show by mobility studies the probability of this hypothesis, in the presence of chlorine, an electronegative gas. (tr-auth)

38224 OBSERVATION OF A CYCLOTRON RESONANCE HARMONIC IN THE HYDROGEN PLASMA OF AN ION SOURCE WITH HIGH FREQUENCY ELECTROMAGNETIC EXCITATION EXPOSED TO THE ACTION OF A WEAK MAGNETIC FIELD. Collet, Luc-Henry; Grolleau, Bernard (Faculte des Sciences, Nantes, France). Compt. Rend., Ser. B, 262: 1668-71(June 27, 1966). (In French).

A phenomenon of electron cyclotron resonance on the second harmonic in the hydrogen plasma of a h-f source in inductive coupling was observed. The B field was transverse. This resonance appears only in a well-defined pressure interval. (tr-auth)

38225 ULTRAHIGH-FREQUENCY DIAGNOSTICS OF ISOTROPIC PLANE-LAYER PLASMA. Vlasov, R. A. (Inst. of Physics, Academy of Sciences, BSSR). Dokl. Akad. Nauk BSSR, 10: 156-8(Mar. 1966). (In Russian).

In the case of the normal incidence of a plane electromagnetic wave on a layer of nonabsorbing plasma, the electric field E follows an equation which becomes more complicated if the angle of incidence changes because the angle and the index of refraction must also be taken into consideration. The goal of diagnostics is to determine the type function related to the electron concentration and the index of refraction, which is the inverse Sturm-Liouville calculation of the operator of a differential equation. A quantitative treatment based on a simplified approximation algorithm was developed. The reflection coefficients were determined on the basis of the optical laws of reflection of plane waves on plane layers. Computational difficulties were solved by adopting a gradual approximation method. By using a multifrequency probing and setting the incidence angle, a more complex parametric analysis may be carried out. (TTT)

38226 ELECTROMAGNETIC FIELDS IN ANISOTROPIC PLASMAGUIDES CONSIDERING THE EFFECT OF ELECTRON COLLISION. Ohkubo, M. (Gunma Univ., Maebashi, Japan). Elec. Eng. Japan, 85: 79-84(1965).

The electron collision effects in the following two specific cases are considered: (1) a cylindrical plasmaguide with an applied axial magnetic field supporting a slow wave, in which the so-called quasistatic approximation is valid; (2) a parallel plane guide with a d-c magnetic field in the direction normal to the axis, in which field components have no variation in the direction of the magnetic field. This analysis showed that in a circular waveguide, the slow surface wave cannot propagate if the collision frequency is much greater than the plasma frequency, irrespective of the strength of the d-c magnetic field. The effect of the collision increases as the ratio of the cyclotron frequency decreases. The TEM wave in the parallel plane guide propagates with phase velocity roughly equal to the speed of light even when the collision frequency is much greater than the plasma frequency irrespective of the d-c magnetic-field strength. When the cyclotron frequency is much higher than that of the plasma, the wave propagates with practically no attenuation with the speed of light, independent of the collision frequency. For this case, the so-called slow wave is practically nonexistent as in the case of circular guides at high collision frequency. When cyclotron frequency is low in comparison with plasma frequency, in both cases, the propagation characteristics are quite different from the $\nu = 0$ case. Due to the continuous variation of the phase characteristics, backward waves exist in some regions. (BBB)

38227 EQUATIONS FOR WAVE PROPAGATION IN AN INHOMOGENEOUS COMPRESSIBLE PLASMA. Burman, R. (Victoria Univ., Wellington, N. Z.). Electron. Lett., 2: 219-20(June 1966).

The propagation of coupled electromagnetic and electroacoustic waves in a planar-stratified compressible electron plasma was considered previously. Some first- and second-order coupled-wave equations were obtained. Some alternative first-order equations are presented. (auth)

38228 BEHAVIOR OF SEPARATION CONSTANTS FOR FINITE GYROMAGNETIC PLASMAS. Bevc, Vladislav (Aerospace Corp., El Segundo, Calif.). IEEE (Inst. Elec. Electron. Engrs.) Trans. Antennas Propagation, AP-13: 918-26(Nov. 1965).

Previous reports are reviewed that are concerned with the propagation of electromagnetic waves through waveguides filled with anisotropic or gyrotropic plasma columns. In most the ions are assumed to be stationary and the collision and thermal effects are neglected. They are confined either to the quasi-static approximation or to a discussion of the problem in general terms with tabulations of auxiliary functions and an outline of the general method of approach for obtaining the solution in the form of dispersion curves without a systematic and comprehensive quantitative presentation and classification of numerous types of ω-β diagrams and field solutions. Even when the motion of ions, collisions, and the thermal effects are neglected, the number of combinations that can arise for reasonable steps in which parameters can be varied is considerable. The parameters to be varied are: (1) the plasma density manifested as the plasma frequency ω_p, assumed uniform throughout the cross section of the waveguide, (2) the intensity of the collimating uniform axial magnetic field B_0 or the corresponding cyclotron frequency ω_H, (3) the size of the column or the radius of the circular waveguide, $\underline{a}$, appearing in the convenient normalizing frequency $\omega_0 = \underline{c}/\underline{a}$ related to the lowest empty waveguide cutoff frequency. For quantitative work which alone can be suited for evaluation of experimental results, it is desirable to establish a system of classification of modes of propagation and to prepare a catalog of solutions. It is shown that the type of the functions appearing in the expressions for electromagnetic fields in finite magnetoplasmas depends only on the properties of the medium manifested in separation constants. The ω-β plane of the Brillouin diagram is partitioned into a definite number of zones characterized by the type of possible field solutions. The general behavior of the separation constants in the ω-β plane including the complex region based on calculations covering a wide variation of the determining parameter is described. Effects of ion motions are discussed, and the generality of the presented approach is pointed out. (BBB)

38229 RADIATION FROM A VERTICAL DIPOLE IN A WARM PLASMA. PART I. Langelier, R. M. (Radiation Inc., Melbourne, Fla.); Schultz, F. V. IEEE (Inst. Elec. Electron. Eng.), Trans. Antennas Propagation, AP-14: 207-12(Mar. 1966).

The radiation characteristics of bound electromagnetic sources, which are situated in or near an ionized gaseous medium, have application to problems associated with plasma diagnostics, plasma circuit devices, and communication with space vehicles passing through the ionosphere and other regions of interplanetary space. The problem considered is that of a vertical electric dipole in a homogeneous warm plasma above a conducting plane. There is no steady applied magnetic field. Transverse and longitudinal waves can exist in the medium and are coupled only through the presence of a source or a boundary. When the effect of ion and neutral particle motions is negligible

compared to electron motion, the plasma is usually represented by a one-fluid model. If, however, ion motion is considered to be important, a two-fluid model is essential. Academically, the problem is of interest, due to the simultaneous existence of acoustic and electromagnetic waves which are excited by the antenna and which, upon reflection from the plane, generate a complex boundary wave. The problem is of practical interest in that it can be considered as a first step in the analysis of sources in or near plasma-covered objects of finite extent. The problem is formulated in terms of two vector potential functions, one of which is used to represent the electromagnetic mode, while the other is used to represent the acoustical mode. The potentials are expressed in terms of their Fourier integral representations, and the formal solution is found by the use of signal-flow graphs. (BBB)

38230 RADIATION FROM A VERTICAL DIPOLE IN A WARM PLASMA. PART II. Langelier, R. M. (Radiation Inc., Melbourne, Fla.); Schultz, F. V. IEEE (Inst. Elec. Electron. Eng.), Trans. Antennas Propagation, AP-14: 213-19 (Mar. 1966).

A numerical evaluation is given of the integrals that constitute the formal solution of the problem of a vertical dipole, which is situated in a homogeneous, warm plasma half-space above a perfectly conducting plane. An asymptotic series expansion is obtained for these integrals by the double saddle point method of integration. The dominant terms of the solution in the far field are shown to consist of a surface wave, which arises from the residue of a pole, and a space wave, which is the leading term of the saddle point contribution. The space wave is identified as the geometrical ray approximation to the solution. It is demonstrated that the surface wave can propagate when the source frequency is either above or below the plasma frequency. The transfer of power from an incident acoustical (p) mode to a boundary-generated electromagnetic (e) mode, and from an incident e mode to a boundary-generated p mode, is investigated at a plasma-conductor interface. It is evident in both situations that only a small percentage of the incident power is transformed into the boundary-generated mode. In the case of a vertical dipole, however, it is shown that, at source frequencies which are near to the plasma frequency, the power in the incident p mode is much larger than that in the e mode. Thus, the boundary-generated e mode, which is due to the incident p mode, is as large as the reflected e mode due to an incident e mode. As a result of this effect, it is pointed out that one can represent the reflected e mode by two image sources. (BBB)

38231 PERMANENTLY MAGNETIZED FERRITE ANTENNA WINDOWS FOR IMPROVING ELECTROMAGNETIC WAVE TRANSMISSION THROUGH A PLASMA. Kofoid, Melvin J. (Boeing Scientific Research Labs., Seattle, Wash.). IEEE (Inst. Elec. Electron. Eng.) Trans. Antennas Propagation, AP-14: 251-2 (Mar. 1966).

A longitudinal magnetic field (B_Z) can be employed to increase the transmission through a plasma of a righthand polarized electromagnetic (EM) wave at below the natural plasma frequency. The B_Z field can be produced by permanently magnetized ferrite material in the form of a thick sheet placed as a window in front of the radiator and directly adjacent to the plasma. It was shown by tests that high-frequency EM waves can be transmitted with only reasonable attenuation through a thick sheet of ferrite which is producing a $B_Z > 1500$ G longitudinal field at the sheet surface. Further, due to its rotational field-displacement properties, the possibility exists that the magnetized ferrite sheet serving as the antenna window may be so constructed to serve simultaneously as an isolator and thereby reduce the changes in load impedance seen by the radiator with varying plasma sheath conditions. A right-cylinder barium ferrite magnet 12.5 cm in dia and 8.0 cm long produced an axially-directed magnetic field at its end surface of $B_Z \cong$ 2000 G intensity and passed 9.0 Gc/sec electromagnetic waves in its axial direction with a transmission loss of 6 db. (This B_Z is insufficient to be used for plasma propagation at a frequency as high as 9.0 Gc/sec, which was simply a convenient test frequency.) The extent to which the microwave transmission properties of ferrite permanent magnet materials may be further improved is, as yet, unknown. However, since the results reported were obtained with a ferrite manufactured without any consideration at all for its possible transmission properties, the possibility of considerable improvement may exist. The results of these first tests on commercially available material are sufficiently good that further research on the use of a permanently magnetized ferrite antenna window for the alleviation of radio re-entry blackout can definitely be recommended. (BBB)

38232 RADIATION FROM A SPHERICAL APERTURE ANTENNA IMMERSED IN A COMPRESSIBLE PLASMA. Wait, James R. (Inst. for Telecommunication Sciences and Aeronomy, Boulder). IEEE (Inst. Elec. Electron. Eng.) Trans. Antennas Propagation, AP-14: 360-8 (May 1966).

An antenna located within the ionosphere will excite electroacoustic waves in addition to the usual electromagnetic waves. One proposed mechanism for the coupling of electromagnetic to electroacoustic energy is assumed to take place within the medium rather than at the antenna itself. A theory is presented for the conversion process which does not invoke an ad hoc coupling mechanism in the medium. The exterior boundary-value problem for a sphere immersed in a compressible plasma medium is solved. The model is a perfectly conducting sphere excited by an aperture, in its surface, which has a specified distribution of the tangential electric field. The configuration is such that Maxwell's equations, when combined with the continuum theory of fluid dynamics, are separable. The sheath at the interface with the plasma is characterized by an absorptive boundary condition which assumes a linear relation between the pressure and the mean velocity of the electrons. It is shown that the TM (transverse magnetic) waves are coupled with the electroacoustic waves, while the TE (transverse electric) waves are decoupled. Some numerical results are presented which show, in quantitative manner, the relative fraction of the total power which is irradiated in the form of electroacoustic waves. (BBB)

38233 PLANE WAVE TRANSMISSION AND REFLECTION COEFFICIENTS FOR LOSSY INHOMOGENEOUS PLASMAS. Bein, G. P. (Cornell Aeronautical Lab., Inc., Buffalo). IEEE (Inst. Elec. Electron. Eng.) Trans. Antennas Propagation, AP-14: 511-13 (July 1966).

Propagation of a plane wave through an inhomogeneous plasma, whose properties vary in the direction of propagation, was treated by a matrix technique which appears to be simpler and faster than previous methods. Propagation is treated by considering the plasma to be divided into several, adjacent, homogeneous slabs which approximate the true variation in the plasma characteristics. Each slab is represented by an equivalent transmission line for the purposes of analysis. The A, B, C, D (or transmission) matrix, which relates the input voltage (amplitude of the transverse electric field) and current (amplitude of the transverse magnetic field) to the output voltage and current, is utilized to determine the overall transmission and reflection coefficients for the plasma. The degree of accuracy of the computed complex transmission and reflection coefficients depends upon the number of slabs chosen to approximate the actual electron density and collision frequency distributions. Results are presented which compare solutions obtained by this technique with an earlier numerical computation of the boundary layer transmission coefficients. The results indicate good agreement between the two methods. (BBB)

38234 CONTROL OF PLASMA COLLISION FREQUENCY FOR ALLEVIATION OF SIGNAL DEGRADATION. Hoffman, Jerome (MITRE Corp., Bedford, Mass.). IEEE (Inst. Elec. Electron. Engrs.) Trans. Commun. Technol., COM-14: 318-23 (June 1966).

When an electromagnetic wave interacts with a plasma, the major effects are reflection, attenuation, and phase shift. The three basic parameters which affect this interaction are the signal frequency, the plasma frequency, and the electron collision frequency. To obtain a functional de-

pendence of the interaction upon these three parameters, Maxwell's equations are solved, through use of the plasma conductivity. The results established a basis from which a collision-frequency-oriented plasma control effort can proceed in appropriate depth. The mechanism investigated is the use of positively charged particles to effect an increase in the collision frequency. The initial results indicate that this technique is a possible control mechanism, contingent upon: (1) the feasibility of producing highly charged particles, (2) the behavior of plasmas perturbed by highly charged particles, and (3) the feasibility of charged particle seeding of plasmas. These contingencies are being theoretically and experimentally investigated. The addition of seed material to rocket exhausts either would have a negligible effect upon, or would result in a slight increase in the specific impulse because of the similarities betwee this technique and ionic propulsion (in particular, the colloidal-particle electrostatic engine). The possibility of using positively charged particles to lower the plasma frequency, and to raise the collision frequency simultaneously, should enable a further saving in required seeding material. (M.O.W.)

38235 EXPERIMENTAL X-BAND ELECTRON-CYCLOTRON-RESONANCE PLASMA ACCELERATOR. Miller, David B. (General Electric Co., King of Prussia, Pa.). IEEE (Inst. Elec. Electron. Engrs.) Trans. Microwave Theory Tech., MTT-14: 162-4(Mar. 1964).

In the experimental x-band accelerator described, rf power (8350 Mcps) from a cw klystron (VA-823J) is delivered from a circular polarizer into the accelerator. The guide cross section through the polarizer and the accelerator is circular, propagating a TE_{11} circular waveguide mode field. The rf power is then guided through a 0.286-in. thick beryllium oxide microwave window into the evacuated region. A continuous flow of gas is introduced on the vacuum side of the window. The magnetic field from the surrounding coils is adjusted to the cyclotron resonance value (2970) in this region, where the injected gas is ionized and the electrons are accelerated in transverse cyclotron orbits by the microwave field. Electron trajectories are converted from transverse to longitudinal by grad B and diffusion processes, and ions are accelerated by the charge-separation field as the gas stream flows down the accelerator duct and out into the vacuum tank. Efficiency of the accelerator exhibits a broad max as a function of flow rate. A magnetic field of ~3350 G (average) maximizes the efficiency. Relatively long operating times (up to 139 sec at 3290 w rf) were achieved at appreciable power levels. During the longer tests, engine temperatures were observed to reach an essentially steady level. The max r-f to plasma stream power conversion efficiency for this accelerator is ~0.25. (BBB)

38236 POSITIVE COLUMN BETWEEN COAXIAL CYLINDERS. Resikyan, A. M. (Inst. of Radiophysics and Electronics, Academy of Sciences, Arm. SSR). Izv. Akad. Nauk Arm. SSR, Fiz., 1: 31-8(1966). (In Russian).

It was shown that as the maximum of the density of charged particles is arranged closer to the inner cylinder, the less its radius with that of the outward cylinder is. It was also shown that this has resulted in a greater distortion of plasmas by the Langmuir sound isolator than by the sound itself. (auth)

38237 REFLECTION AND TRANSMISSION OF ELECTROMAGNETIC WAVES BY A MOVING PLASMA MEDIUM. Yeh, C. (Univ. of Southern California, Los Angeles). J. Appl. Phys., 37: 3079-82(July 1966).

The reflection and transmission of electromagnetic waves by a moving dispersive dielectric half-space or slab are investigated theoretically. The dispersive dielectric medium is assumed to be a cold plasma medium. Two cases of the movement are considered: (a) The plasma medium moves parallel to the interface. (b) The plasma medium moves perpendicular to the interface. It is interesting to note that, for case (a), the reflected and transmitted fields for an incident plane E wave are independent to the movement of the plasma medium. For case (b), the reflected wave and the transmitted wave are functions of the velocity of the moving plasma medium. Detailed results on the reflection and transmission coefficients for case (b) are given and discussed. The electric vector of the incident wave is assumed to be polarized in a direction that is normal to the plane of incidence. (auth)

38238 VELOCITY-PROFILE MEASUREMENT IN PLASMA FLOWS USING TRACERS PRODUCED BY A LASER BEAM. Chen, Che Jen (California Inst. of Tech., Pasadena). J. Appl. Phys., 37: 3092-5(July 1966).

A giant pulse laser is focused in a gas flow by a lens. The plasma drop produced by the gas breakdown is used as a tracer for the flow velocity measurement. The motion of the plasma drop is detected by both electrostatic probe and drum-camera techniques. The estimated experimental error in the present setup is about 3%. The new features of this method are very high spatial resolution, minimum disturbance in the flow due to the instrumentation, and applicability both to un-ionized and ionized flows. (auth)

38239 POWER FLOW IN PLASMA-FILLED WAVEGUIDES. Bevc, Vladislav (Aerospace Corp., El Segundo, Calif.). J. Appl. Phys., 37: 3128-37(July 1966).

The power flow of two types of cyclotron modes propagating in a waveguide filled with a cold collisionless axially magnetized plasma is studied as a function of the location of the point of operation on the Brillouin ($\omega-\beta$) diagram. Dynamic analysis is used throughout. Partition of the total power flow corresponding to E, H, and EH power is examined and compared with results obtained by the quasi-static approximation in the domain of its presumed validity. The inadequacy of the quasistatic approximation for the analysis of the power flow, and hence the field patterns, is shown. New properties of cyclotron and plasmaguide modes obtained from the analysis are presented. A possible explanation is offered for the lack of published experimental observation of cyclotron modes in the superluminous phase velocity region. (auth)

38240 MALKUS THEORY APPLIED TO MAGNETOHYDRODYNAMIC TURBULENT CHANNEL FLOW. Nihoul, Jacques C. J. (Univ., Liege). J. Fluid Mech., 25: 1-16(May 1966).

The turbulent flow of a weakly conducting liquid between parallel plates in the presence of a transverse magnetic field was investigated. The form of the mean velocity profile was determined by a series of constraints resulting from the boundary conditions and the Navier-Stokes equations and by the Malkus postulates on the spectrum of the mean vorticity gradient. The width of the transition regions near the walls was derived in terms of the governing dimensionless numbers and this expression was checked, in the asymptotic laminar case, against the well-known Hartmann result. A graphical method, exploiting the relation between the boundary region thickness and the smallest scale of motion defined by the Malkus theory is proposed to determine the scale of the velocity profile, i.e., the flow rate in terms of the pressure gradient and the magnetic field strength. (auth)

38241 METHOD OF CHARACTERISTICS FOR THE THREE-DIMENSIONAL UNSTEADY MAGNETOFLUID DYNAMICS OF A MULTI-COMPONENT MEDIUM. Sauerwein, Harry (Aerospace Corp., San Bernardino, Calif.). J. Fluid Mech., 25: 17-41(May 1966).

A general numerical method of characteristics applicable to problems in magnetofluid dynamics as well as ordinary fluid dynamics is described. The method can be applied to unsteady three-dimensional flows of chemically reacting, non-equilibrium, multi-component media. Dissipative phenomena must be neglected in order to make the governing equations of change hyperbolic, because the method can be applied only to quasi-linear, hyperbolic, partial differential equations. Practical restrictions on computation time usually require unsteady problems to be limited to cases with short transient times although theoretically the method applies to all unsteady flows. In steady flow the local velocity must be greater than the largest local wave speed. The

characteristic and compatibility equations are derived for the most general case of magnetofluid dynamics. A new finite-difference network and its corresponding equations are developed similarly. Specialization of the general method to consider simpler problems is outlined. Preliminary numerical results of calculations using the method are presented. The practicality and feasibility of utilizing the general numerical method of characteristics on presently available, electronic digital computers are evaluated in the light of recent experience in calculating multidimensional flows with the method. (auth)

38242 MAGNETOGASDYNAMIC FLOW OVER A WEDGE. Pack, D. C.; Swan, G. W. (Univ. of Strathclyde, Glasgow). J. Fluid Mech., 25: 165-78(May 1966).

The solution for the flow of a fully ionized gas over a wedge of finite angle is known for the case when the applied magnetic field is aligned with the incident stream. In this flow there are current sheets on the surfaces of the wedge. When the magnetic field is allowed to deviate slightly from the stream, the current sheets may move into the gas and become shock waves. The magnetic fields adjacent to the wedge above and below it have to be matched. A perturbation method is introduced by means of which expressions for the unknown quantities in the different regions may be determined when there are four shocks attached to the wedge. The results give insight into the manner in which the shock-wave pattern develops as the obliquity of the magnetic field to the stream increases. The question of the stability of the shock waves is also examined. (auth)

38243 A NEGATIVE V'' STELLARATOR. Johnson, J. L.; Christensen, U. R.; Frieman, E. A.; Mosher, D. (Princeton Univ., N. J.). J. Nucl. Energy: Pt. C, 8: 361-72(July-Aug. 1966). (MATT-380).

Analytical and numerical studies of a stellarator configuration indicate that a negative $V''(\psi)$ configuration can be achieved with $\Delta V'/V' \approx 0.01$. Critical pressures such that $\beta_c \sim 0.15$ for ballooning instabilities in the absence of resistivity are obtained. (auth)

38244 HYDROMAGNETIC EQUATIONS WITH VISCOSITY FOR A COLLISIONLESS PLASMA. Simon, A.; Thompson, W. B. (General Atomic Div., General Dynamics Corp., San Diego, Calif.). J. Nucl. Energy: Pt. C, 8: 373-6(July-Aug. 1966).

Starting with Vlasov equation in the drift frame, one may solve for the distribution function in a power series in e, the ratio of the Larmor radius to the characteristic length in the plasma. A closed set of macroscopic equations is obtained by neglecting heat flow along the magnetic field lines. By this procedure, one obtains the magnetic "viscosity" terms. The results expressed in terms of u, the averaged velocity, take a mostly familiar form, but there are some additional terms due to variation of the magnetic field in space and time. Expressed in terms of V, the results are much more complicated except for the special case of the "flute approximation" in which case they resemble the u-frame results but with a reversed sign. This agrees with previous calculations in the finite Larmor radius limit. (auth)

38245 ANALYTICAL DETERMINATION OF THE EIGENFREQUENCIES OF A BOUNDED, ONE-DIMENSIONAL ELECTRON PLASMA. Ehrman, J. B. (Naval Research Lab., Washington, D. C.). J. Nucl. Energy: Pt. C, 8: 377-97(July-Aug. 1966).

The eigenfrequencies of all modes of oscillation of a water-bag distribution of electrons confined in an external parabolic electrostatic potential are determined by analytical methods for all values of a parameter η, which measures the ratio of the electron density to the strength of the external electric field. Two approximations are studied, one for $\eta \ll 1$ (low electron space charge) and the other for $(1-\eta) \ll 1$ (high electron space charge). All eigenfrequencies turn out to be real, but "damping" results from the fact that for $\eta \neq 0$ and $\eta \neq 1$, the frequencies $\omega_n(\eta)$ of the various modes n are not simply related. If the wavelength of the perturbation is much less than a Debye length $\{n \gg (2/\pi) \log [12(2-\sqrt{3})/(1-\eta)]\}$, $[\omega_n(\eta)/n]$ is not strongly dependent on n, while if the wavelength is much greater than a Debye length $\{n \ll (2/\pi) \log [12(2-\sqrt{3})/(1-\eta)]\}$, $\omega_n(\eta)$ is near the plasma frequency ω_p, as expected for a cold plasma, or for the long wavelength limit of an infinite plasma at finite temperature. The focusing effect of the parabolic electrostatic potential in an electron rest frame is similar to that of a periodic alternating magnetic field, such as is used in the NRL Sozotron, in a laboratory frame. It is also similar to the sum of external and ion-produced potentials in which the trapped electrons in an ion-rich plasma diode find themselves. The eigenfunctions of the perturbation current are also obtained, so that the development in time of a given initial perturbation current can be determined. (auth)

38246 STOCHASTIC MOTION OF PARTICLES IN A NON-ADIABATIC MAGNETIC TRAP. Dunnett, D. A.; Laing, E. W. (Glasgow Univ.). J. Nucl. Energy: Pt. C, 8: 399-411(July-Aug. 1966).

The properties of a mirror machine with a spatially modulated central field are investigated. The modulation is simulated by a square oscillation and leads to non-conservation of magnetic moment. Equations are set up which describe, in various degrees of approximation, the equilibrium state of an ensemble of particles interacting only with the magnetic field, given a constant input of particles and taking mirror loss into account. The magnetic mirrors are approximated by reflection of particles without change of magnetic moment but with random Larmor phase. An integral equation is obtained involving transmission and reflection operators for the non-adiabatic central region. In successive approximations, an ergodic hypothesis of Larmor phase in the central region and a Fokker–Planck expansion lead, respectively, to a set of coupled integral equations and their Fokker–Planck counterpart, a set of diffusion equations. Results from the diffusion equations are compared with a numerical study of this magnetic trap reported recently by Dunnett et al. (auth)

38247 ELECTRICAL BREAKDOWN IN BEAMS OF CONDENSED HYDROGEN AND CONDENSED NITROGEN IN HIGH VACUUM. Becker, E. W.; Klingelhoefer, R. (Kernforschungszentrum, Karlsruhe, Ger. Technische Hochschule, Karlsruhe, Ger.). J. Nucl. Energy: Pt. C, 8: 413-17(July-Aug. 1966).

Beams of hydrogen and nitrogen clusters are produced by expanding hydrogen or nitrogen gas out of a Laval-nozzle cooled by liquid hydrogen or liquid nitrogen respectively. The beams are passed through a pair of parallel annular electrodes with a spacing of 22 cm. The electrodes are connected to a 0.1 μF capacitor which is charged to voltages between 10 and 20 kv. Electrical breakdown in these beams is achieved by injection of electrons. The behavior of the resulting plasma column was studied by magnetic probe and image converter measurements. (auth)

38248 INVESTIGATION OF THE POSSIBILITY OF INCREASING THE PLASMA DENSITY IN OGRA-I. Bogdanov, G. F.; Golovin, I. N.; Evlanov, E. N.; (and others) (Kurchatov Inst. of Atomic Energy, Moscow). J. Nucl. Energy: Pt. C, 8: 419-31(July-Aug. 1966).

The conditions are formulated which must be satisfied by the vacuum system of a magnetic mirror trap when a dense plasma is built up using the fast ion injection method. In the previous experiments on Ogra-I and in experiments on the V-3 machine in which 40-kev H_2^+ ions are injected and dissociated by the residual gas and by the lithium arc and in experiments using targets, it was established that bombardment of the titanium-covered cold adsorbing surfaces by fast atoms or ions produces an intense desorption. Taking these results into account it is proposed that all surfaces in the vacuum chamber of Ogra-I which are subjected to bombardment by fast particles should be kept hot during build-up of the plasma, and that adsorption on cold titanium should only be employed in those parts which are inaccessible to fast particle bombardment. It is shown that in order to obtain a dense plasma it is expedient to discontinue using the external injector and to locate the ion source in one of the magnetic mirrors. It is discussed how

the development of cyclotron instability may facilitate the capture of ions in the trap and the build-up of a dense plasma. It is noted that in Ogra-I the adiabatic containment time for protons in the trap exceeds 200 msec, and for a density of hot plasma up to 1×10^8 cm^{-3}, if losses ascribable to instabilities are present, the proton lifetime in the trap determined by these losses is greater than 70 msec. (auth)

38249 MECHANISM OF CAPTURE OF A MOVING PLASMA BY A TRANSVERSE MAGNETIC FIELD. Demidenko, I. I.; Lomino, N. S.; Padalka, V. G.; Safronov, B. G.; Sinel'nikov, K. D. (Inst. of Physics and Tech., Kharkov). J. Nucl. Energy: Pt. C, 8: 433-45(July-Aug. 1966).

When plasma is injected perpendicular to magnetic lines of force, part of the plasma blob is captured and spread along the lines of force. The results obtained make it possible to identify the mechanism which brings about the escape of plasma along the magnetic field. In the range of densities of the moving plasma ($3 \times 10^{11} - 2 \times 10^{14}$ cm^{-3}) and magnetic field strengths (0–2 kG) considered here, this mechanism is the electrostatic repulsion of the polarization space charge formed by the interaction of the plasma with the transverse magnetic field. The optimum values of the injected plasma density and the transverse magnetic field strength are established for which maximum capture occurs; this is of some practical interest in the filling of closed magnetic traps by the external-injection method. (auth)

38250 EXCITATION AND IONIZATION RATES OF NEON IONS IN A STELLARATOR DISCHARGE. Hinnov, Einar (Princeton Univ., N. J.). J. Opt. Soc. Amer., 56: 1179-88(Sept. 1966). (MATT-434).

The intensities of various resonance multiplets of neon ions, from Ne II to Ne VIII, emitted by an ohmically heated hydrogen discharge of the C stellarator, with about 3% neon added, were measured with a calibrated grazing-incidence monochromator. The electron densities ($N_e \sim 10^{13}$ cm^{-3}) were determined by means of 4-mm microwave interferometers, and the electron temperature ($T_e \sim 10-50$ ev) from the electric conductivity of the plasma. The neon-ion concentrations at the different states of ionization were calculated from the light intensities by means of an assumed energy dependence for the excitation cross sections, the magnitude of the cross sections being adjusted to make the sum of the calculated ion concentrations agree with the known total neon concentration. Atomic oscillator strengths deduced from the excitation-rate coefficients thus obtained, were found to be in reasonable agreement with various calculations. Ionization-rate coefficients were deduced from the time behavior of the ion concentrations and the known particle-confinement time in the discharge. As compared with expected values, the measured rate coefficients appear to be increasingly too large with successive states of ionization. The most likely reason for the discrepancies is a possible deviation from Maxwellian electron-energy distribution in the discharge, to which these rate coefficients would be particularly sensitive. (auth)

38251 NEW APPROACH TO THE THEORY OF RELAXATION IN PLASMAS. II. NON-MARKOVIAN PROCESSES. Honda, Naobumi (Tokyo Univ.). J. Phys. Soc. Jap., 21: 1189-1203(June 1966).

As a basis of various discussions on rapidly varying phenomena in the plasma the velocity distribution function of a plasma immersed in a h-f perturbation field is investigated using an approach originally developed by Kubo. The results, which were derived taking into account both the binary and collective interactions, include: an expression for the linear response in velocity distribution function and its asymptotic form for weak interactions and long wavelengths, a connection formula which yields exact values for any transport quantity, a derivation of Kihara's connection formula together with its range of validity, and some account of the absorption of electromagnetic waves in plasmas. (auth)

38252 HARMONIC GENERATION OF ION CYCLOTRON FREQUENCY IN LONGITUDINALLY MAGNETIZED PLASMAS. Yatsui, Kiyoshi; Inuishi, Yoshio (Osaka Univ.). J. Phys. Soc. Jap., 21: 1225-6(June 1966).

Observations of the generation of higher harmonics of ion cyclotron frequency in longitudinally magnetized argon plasma is reported. A typical trace of the frequency spectrum of oscillations corresponding to the higher harmonics of ion cyclotron frequency and the frequency of oscillations as a function of the magnetic field are shown. It was found that the observed maximum order of oscillation harmonics increases with decreasing pressure and that the frequencies of oscillations are not affected by the pressure. (J.F.P.)

38253 COLLISION-INDUCED INSTABILITY IN A MAGNETOACTIVE PLASMA. Shimomura, Noboru; Mitani, Kenji; Tanaka, Shigetoshi (Kyoto Univ. Univ. of Nagoya, Japan). J. Phys. Soc. Jap., 21: 1372-80(July 1966).

The dispersion relations for the waves propagating in a magnetoactive plasma were obtained from the Boltzmann equation with a collision term of the electrons. Two cases in which the wave vector parallel and perpendicular to the uniform magnetic field were studied. Under the assumption that the unperturbed distribution is a spherical shell in velocity space in each case, and two dispersion relations to the zeroth approximation in k were obtained as follows: (A) $\omega(\omega + i\nu)^2 = \omega_p^2[\omega + i\nu - i(V/3)(d\nu/dV)]$ and (B) $\omega(\omega \pm \omega_c + i\nu)^2 = \omega_p^2[\omega \pm \omega_c + i\nu - i(V/3)(d\nu/dV)]$ where ω_c and ω_p are the cyclotron and the plasma frequencies respectively, and ν is the collision frequency with the neutral particles. After some calculations under an assumption $\nu(v) = \text{const} \times v^h$ it was found that initial perturbations grow exponentially for $h > 3$ in (B) and the growth rate is the largest in the magnetic field-free case. (auth)

38254 ELECTRON DENSITY MEASUREMENT BY MICROWAVE SCATTERING FROM UNDERDENSE CYLINDRICAL PLASMAS. Shiobara, Shinji (Inst. of Physical and Chemical Research, Tokyo). J. Phys. Soc. Jap., 21: 1380-7(July 1966).

From Midzuno's scattering theory in the Born approximation, formulas were derived for the phase shift of coherent microwaves caused by cylindrical plasmas. Experiments were made on helium plasmas of 17 to 96 mm diameter at 34GC and on a 45 mm diameter plasma at 9GC with standard type microwave interferometers to examine the applicability of the formulas. Agreement between the values of phase shift predicted by theory and those obtained by experiment was remarkably good when judged from the calibration by Langmuir probe. By the use of the derived formulas, a new method of analysis is proposed for measuring the electron density of underdense cylindrical plasmas for which the phase-shift analysis based on the plane slab approximation may not simply be applied. It was found that the effect of glass wall of the discharge tube on the phase shift is only to shift the point of balance of the interferometer bridge. (auth)

38255 MOMENTS OF THE VELOCITY CHANGE OF A CHARGED PARTICLE IN A MAGNETOPLASMA. Itikawa, Yukikazu (Tokyo Univ.). J. Phys. Soc. Jap., 21: 1387-97(July 1966).

The moments of the velocity change, $\langle \Delta v \rangle / \Delta t$, $\langle \Delta v \Delta v \rangle / \Delta t$, $\cdots$, of a particle in a magnetoplasma were calculated in the wave theory. Here Δv is the change in velocity of the particle during a small time interval Δt and $\langle\ \rangle$ means an average over all the interactions between the particle and the other plasma particles. With use of these moments a kinetic equation for a magnetoplasma was derived. (auth)

38256 PLASMA END LOSS IN A SLOW THETA PINCH. Shiina, Shoichi; Ohnishi, Haruyuki; Yoshimura, Hisamitsu (Nihon Univ., Tokyo). J. Phys. Soc. Jap., 21: 1455-6(July 1966).

The end-loss mechanisms of the plasma were investigated by using the improved mirror coil in which the plasma did not drift to the chamber wall. The experiments were carried out in the same conditions as described previously (J. Phys.

Soc. Japan, 19: 2242(1964)), except for the coil which is 80 cm long and 17 cm I. D. and has a magnetic mirror ratio 1.5. (W.D.M.)

38257 DERIVATION OF THE DISPERSION EQUATION FOR A CYLINDRICAL PLASMA WITH FINITE ELECTRICAL CONDUCTIVITY UNDER THE INFLUENCE OF ITS OWN GRAVITATIONAL FIELD AND AN APPLIED MAGNETIC FIELD. Vasiu, Mircea. Mathematica, 6: 335-50 (1964). (In French).

The derivation of the dispersion equation of an infinitely long, homogeneous, incompressible, and nonviscous cylindrical plasma is presented. The plasma is assumed to have a finite, but sufficiently large, electric conductivity. The plasma is subjected to the action of an applied magnetic field of a particular form, and simultaneously to the action of its own gravitational field. The plasma column has a finite diameter and is surrounded by empty space of indefinite extent. The method employed is the well-known one of "normal oscillations." (Int. Aero. Abstr.)

38258 EXPERIMENTS ON ION CYCLOTRON HEATING OF PLASMA IN THE HELIOTRON-B DEVICE. Hayashi, Shigenori; Mohri, Akihiro (Kyoto Univ.). Mem. Fac. Eng., Kyoto Univ., 27: 443-74(Oct. 1965).

An experimental investigation was made of single-particle ion cyclotron resonance and ion cyclotron heating of plasma generated by Joule heating in the Heliotron-B. The Heliotron magnetic field provides many gradients suitable for causing a phase mixing of ion cyclotron waves propagating along the magnetic lines of force. An r-f coil of the picket-fence type feeds r-f power into the plasma and excites ion cyclotron waves of 12 cm axial wavelength. Power absorption curves were obtained as a function of r-f frequency. It is shown that there are two kinds of loading peaks; one is due to the excitation of ion cyclotron waves, and the other is due to the cyclotron resonance of individual ions. The exciting efficiency of the ion cyclotron waves was above 75%. Doppler shifts of particle cyclotron resonance from the cyclotron frequency were also observed under Joule heating, suggesting that ion beams flow in plasma under Joule heating. The electron temperature was insensitive to this heating. (Int. Aero. Abstr.)

38259 CO-OPERATIVE SCATTERING OF LASER LIGHT BY A THETATRON PLASMA. Evans, D. E.; Forrest, M. J.; Katzenstein, J. (Atomic Energy Research Establishment, Abingdon, Eng.). Nature, 211: 23-4(July 2, 1966).

Measurements are reported of the distribution of light scattered into the electron feature in circumstances when the ratio of the scale length for scattering to the plasma Debye length varied between 1.2 and 1.5. A Kerr cell Q-switched ruby laser and amplifier provided 70-Mw pulses within a divergence angle of 6.7 milliradians and these were used to illuminate the plasma produced by a 45 kJ theta pinch machine, MAGGI II. The experimental arrangement is shown and spectral distributions of scattered light obtained under various machine operating conditions are presented. (W.D.M.)

38260 PINCHED LIGHTNING DISCHARGES. Bruce, C. E. R. (Electrical Research Association, Leatherhead, Eng.). Nature, 211: 62-3(July 2, 1966).

An oscillogram of the largest lightning current obtained by Berger and Vogelsanger (Bull. Schweiz. Elektr. Ver., 56: 2(1965)) in an investigation of lightning striking a mast is compared to the light curve of Nova Herculis 1934. Points of similarity are discussed. (W.D.M.)

38261 LANGMUIR PROBE MEASUREMENTS IN A HYPERSONIC PLASMA FLOW. Kamimoto, Goro; Nishida, Michio. Nippon Koku Gakkaishi, 14: 1-7(Jan. 1966). (In Japanese).

Langmuir probe measurements were performed in order to evaluate the properties of the flow in the working section of a plasma jet wind tunnel. A single plane Langmuir probe was used for conditions when the probe collecting surface is parallel to the flow and the diameter of it is of the same order as the mean free path of a neutral atom. Electron temperature and plasma density are calculated from Langmuir probe characteristics. A typical electron temperature is 3×10^{3}°K and a typical plasma density is 10^{13} particles/cm^3. (auth)

38262 STABILITY OF FLUTE OSCILLATIONS WITH WAVE-PLASMA RESONANCES. Timofeev, A. V. (Kurchatov Inst. of Atomic Energy, Moscow). Nucl. Fusion, 6: 93-100(June 1966). (In Russian).

The flute oscillations of a hot-ion plasma in a nonuniform magnetic field are discussed. It is shown that resonances, at which the phase velocity of the waves is the same as the velocity of the ion Larmor drift, can have a stabilizing effect. In particular, with careful selection of the resonance characteristics, one can control the most dangerous "mode 1" of the flute oscillations. Also examined are resonances of the second type, which appear only in an electric field; at them the phase velocity of the wave is the same as the velocity of the plasma electric drift. In the presence of such resonances, the natural frequencies of the flute oscillations become complex of necessity and, accordingly, the oscillations themselves either grow or are damped. (auth)

38263 OSCILLATIONS OF A BEAM PLASMA IN A HIGH-FREQUENCY ELECTRIC FIELD. Gorbunov, L. M.; Silin, V. P. (Lebedev Inst. of Physics, Moscow). Nucl. Fusion, 6: 118-21(June 1966). (In Russian).

Potential oscillations are considered in a system consisting of a neutral and completely ionized plasma and a neutral beam of charged particles in a high-frequency electric field. Under certain conditions, the uniform external high-frequency field leads to a broadening of the instability region and to an increase of the growth rate. (auth)

38264 DIFFUSION PERPENDICULAR TO THE MAGNETIC FIELD IN THE UNIVERSAL INSTABILITY. Buchelnikova, N. S. (Inst. of Nuclear Physics, Novosibirsk, USSR). Nucl. Fusion, 6: 122-9(June 1966). (In Russian).

Diffusion perpendicular to the magnetic field is investigated in a potassium plasma of nonuniform density in which the "universal" instability is excited. A qualitative picture of such diffusion is obtained by studying the relationship between the radial distribution of plasma density and the magnetic field, and by comparing the experimental densities with calculated ones on the assumption of classical diffusion. For densities of $10^{9}-10^{10}$ cm^{-3}, the radial distribution and the peak density do not depend on the magnetic field. At higher densities, however, the half-width of the distribution becomes smaller and the peak diminishes as the field increases. At densities of $7 \times 10^{10}-5 \times 10^{11}$ cm^{-3} the curves for the radial distribution agree well with the calculations. (auth)

38265 PLASMA DIAGNOSTICS BASED ON THE SELF-REVERSED CONTOURS OF SPECTRAL LINES EMITTED BY INHOMOGENEOUS LAYERS. Ilin, G. G.; Fishman, I. S. Opt. Spectros. (USSR) (Engl. Transl.), 20: 214-17 (Mar. 1966).

Translated from Opt. Spektros., 20: 387-93(Mar. 1966).

A calculation of the self-absorbed contours of spectral lines is carried out for the generalized Voigt contour. New and better schemes of plasma diagnostics are proposed on the basis of these self-reversed contours. (auth)

38266 PLASMA FLUCTUATIONS AND THE CONTROL OF PUMPOUT. Fowler, T. K. (General Atomic Div., General Dynamics Corp., San Diego, Calif.). Phys. Fluids, 9: 1437-41(Aug. 1966). (GA-6946).

Means of preventing low-frequency plasma instabilities possibly causing "pumpout" losses are discussed. The result is a prescription for determining experimentally a scaling law for stable confinement in toroidal magnetic wells. Based on measurement of fluctuations rather than instability thresholds, the method can be applied to existing unstable systems to help decide how best to modify them. Given an unstable steilarator or similar system, one measures $\langle E_k^2 \rangle$, the radial power spectrum of the electric field fluctuations averaged over other coordinates. Asymptotic behavior like $\langle E_k^2 \rangle \propto k^{-3}$, confirmed in certain experi-

ments, indicates instabilities susceptible to magnetic well stabilization and verifies applicability of the method. If applicable, magnetic well parameters sufficient for stability are given in terms of a measured quantity $\propto \int dk^2 \langle E_k^2 \rangle$. Preliminary application to the Model C stellarator indicates that an average well depth of only a few per cent would stabilize it if the length of locally unstable regions could be much reduced. Initial unsuccessful efforts to reduce pumpout by modifying the stellarator field did not achieve these goals, but the stable regime is perhaps not out of reach. (auth)

38267 BALLOONING INTERCHANGE INSTABILITIES OF MAGNETIZED PLASMAS UNDER GRAVITATIONAL FIELDS. Yoshikawa, S. (Princeton Univ., N. J.). Phys. Fluids, 9: 1442-6(Aug. 1966).

The relation between the resistive ballooning mode and the "universal" type instability with gravitational field (simulating the magnetic field curvature) is discussed. It is shown that under appropriate assumptions, the instability of the "universal" type is an extension of the resistive ballooning mode if the collision frequency is replaced in the resistive ballooning mode by the effective kinetic collision frequency $k_z v_e$. The relative importance of these ballooning instabilities to toroidal plasmas is discussed. (auth)

38268 EQUILIBRIUM OF A TOROIDAL PLASMA IN THE MODEL C STELLARATOR. Young, K. M.; Yoshikawa, S.; Sinclair, R. M. (Princeton Univ., N. J.). Phys. Fluids, 9: 1447-53(Aug. 1966).

The equilibrium of a toroidal magnetically-confined plasma was investigated using a circular aperture limiter consisting of four conducting segments. The force acting on the limiter to counteract the expanding forces of the plasma is proportional to the current flowing between the top and bottom limiter segments. With no external rotational transform applied, this current varies with the plasma parameters in close accordance with theory. The application of external rotational transform provides equilibrium at high Ohmic heating current densities (>10 A/cm^2), whereas it does not at lower currents. This experimental result is consistent with the hypothesis that the dominant cause of plasma loss at low Ohmic heating currents is just this lack of equilibrium. (auth)

38269 ION OSCILLATIONS IN A WEAKLY TURBULENT PLASMA. Ichikawa, Yoshi H. (Univ. of Illinois, Urbana). Phys. Fluids, 9: 1454-63(Aug. 1966).

Ion oscillations in a high-temperature electron-ion plasma with high-frequency turbulent fluctuations were investigated by generalizing the quasi-linear theory to a spatially inhomogeneous system. It was found that the feedback effect of the high-frequency fluctuation on the low-frequency oscillation in the system gave rise to a parametric growth of the ion acoustic mode even if the system had a stable velocity distribution with respect to the ion acoustic mode. (auth)

38270 STABILIZING EFFECT OF RADIAL PLASMA DENSITY DISTRIBUTION ON HELICAL INSTABILITY. Adati, K.; Iida, Y.; Sekiguchi, T.; Yamada, N. (Tokyo Univ.). Phys. Fluids, 9: 1464-75(Aug. 1966).

Stabilization of magnetoplasmas against the helical instability was experimentally demonstrated in plasma columns (~4.5 m long) placed in the d-c magnetic field below 0.7 Wb/m^2 by means of the external control of the radial plasma density distribution. It was observed that the value of the critical magnetic field was raised above that for the usual Bessel distribution by a factor of five or higher. It was also observed that the stabilized and the turbulent region could stably coexist in a single plasma column. In the extended magnetic field region of stabilization, the particle diffusion was confirmed to be of the order of the classical one in cases of neon and argon and to be at least greatly reduced in helium as compared with that in the usual fully developed turbulent state. The possible physical mechanisms for the observed phenomenon are also discussed. (auth)

38271 HIGHER-ORDER CORRECTIONS TO THE CHEW-GOLDBERGER-LOW THEORY. Frieman, Edward; Davidson, Ronald; Langdon, Bruce (Princeton Univ., N. J.). Phys. Fluids, 9: 1475-82(Aug. 1966).

A complete higher-order set of equations of the Chew-Goldberger-Low theory was derived. A slight modification of these equations produces the finite Larmor-radius hydromagnetic theory of Kennel and Greene. Some comments on the properties of these equations are given. (auth)

38272 COLLISIONLESS DAMPING OF HYDROMAGNETIC WAVES. Barnes, Aaron (Univ. of Chicago). Phys. Fluids, 9: 1483-95(Aug. 1966).

Numerical solutions were obtained for the dispersion relation for hydromagnetic waves in an infinite, uniform, collisionless plasma. Except for the Alfvén (shear) mode, all hydromagnetic waves are strongly damped in plasmas of moderate or high β (fluid pressure/magnetic pressure). For β greater than about $\frac{1}{2}$, the damping factor $W = -\mathrm{Im}(\omega)/|\mathrm{Re}(\omega)|$ is a few percent greater for the fast mode (except for special directions of propagation) and of order $\frac{1}{2}$ for the slow mode. The least damped (fast) magnetosonic mode exhibits two maxima in a plot of W versus the angle θ between the wave vector k and the static magnetic field: the first maximum occurs for θ between 20° and 40° and is associated with ion heating; the second occurs between 85° and 89° and is associated with electron heating. In addition, the modes associated with the "hose" and "mirror" plasma instabilities are considered in some detail. (auth)

38273 INTERACTION MODELS, NEGATIVE ENERGY WAVES, AND ELECTROSTATIC INSTABILITIES. Hall, Laurence S.; Heckrotte, Warren (Univ. of California, Livermore). Phys. Fluids, 9: 1496-7(Aug. 1966). (UCRL-14468).

It has been possible to introduce certain physical interpretations for the various contributions which a given species may make to the total dispersion relation for electrostatic instabilities of an anisotropic magnetized plasma. These interpretations are helpful in developing one's physical intuition regarding such instabilities. One appropriate specialization is the use of a physical model of the interaction of a distribution of particles with an imposed wave for the case in which the wave is set up primarily by a species other than that which drives the instability. Conversely, when the cooperative nature of the driver species is dominant, it is natural to describe its properties in terms of negative energy waves. The discussion shows the connection between these viewpoints as special cases of the more general description. (auth)

38274 OBSERVATIONS OF INSTABILITIES IN ELECTRON-CYCLOTRON PLASMAS. Ard, W. B. (Oak Ridge National Lab., Tenn.); Dandl, R. A.; Stetson, R. F. Phys. Fluids, 9: 1498-1503(Aug. 1966). (ORNL-P-1763).

Two types of instabilities were studied in an electron-cyclotron plasma confined by magnetic mirrors and heated by continuous wave microwave power at 10.6 Gc. One type of instability resulted in the loss of energetic electrons (E_e > 100 kev) across magnetic field lines, accompanied by oscillations in the 3-30 Mc range. Suppression of this instability was accomplished by increased background pressure. The second type was characterized by loss of fast electrons along field lines through the magnetic mirrors and accompanied by radio-frequency oscillations at 5.3 Gc ($=\frac{1}{2}\omega_{ce}$). The loss was also characterized by a threshold in magnetic field corresponding to locating the heating zones in the mirror throats. The first type of instability appeared to be flute-like and driven by ∇B drifts. The second type may be initiated by the mirror instability in the plasma. (auth)

38275 FIRST CORRECTION TO THE SECOND ADIABATIC INVARIANT OF CHARGED-PARTICLE MOTION. Northrop, T. G. (Univ. of California, Berkeley); Liu, C. S.; Kruskal, M. D. Phys. Fluids, 9: 1503-13(Aug. 1966). (UCRL-16610).

The second term was obtained in the asymptotic series for the second (longitudinal) adiabatic invariant of charged-particle motion in a static magnetic field. This correction to the lowest-order invariant had two sources: the cor-

rection to the lowest-order magnetic moment and the integrated effect of the guiding-center drift across the field lines. The second term was found to vanish at the mirror points; therefore, during its motion between mirror reflections, the guiding center deviated from the surface on which the lowest-order invariant was constant and intersected this surface at reflection. (auth)

38276 TRANSMISSION AND REFLECTION OF ELECTROMAGNETIC WAVES NORMALLY INCIDENT ON A WARM PLASMA. Comstock, Craig (Pennsylvania State Univ., University Park). Phys. Fluids, 9: 1514-21(Aug. 1966).

The solution for an electric field normally incident onto a warm, semi-infinite plasma was obtained by means of a modified Wiener-Hopf technique. The warm plasma was taken into account by means of the relativistic Vlasov equation. It was found that the previously obtained solution of Taylor gave the correct term for the wavenumber in the plasma, but not the correct answer for the field. It was shown that the method of considering an "equivalent" fully infinite plasma corresponds to a physically unrealistic matching of the plasma to the vacuum. The field inside the plasma was found. The field just inside the plasma is discussed. The nonuniform limit from warm to cold plasma found by Taylor was not found. (auth)

38277 HIGH-ENERGY NEUTRAL INJECTION INTO A MIRROR-QUADRUPOLE CUSP MAGNETIC WELL. Hinrichs, C. K.; Osher, J. E. (Aerojet-General Nucleonics, San Ramon, Calif.). Phys. Fluids, 9: 1522-30 (Aug. 1966).

An analytical study of high-energy neutral injection into a mirror-quadrupole cusp magnetic field is described. This magnetic geometry is shown to be particularly well suited to Lorentz ionization of neutral atoms if the injection trajectory describes an oblique angle to the axis of the system and lies in a plane midway between the current carrying bars which produce the cusp field. Along such a trajectory the effective ionizing electric field $v \times B$ can vary from nearly zero to the full value vB. A relative trapping efficiency is defined as the variation in the component of magnetic field perpendicular to the injection path over which ionized particles will be contained. For the particular magnetic field studied, the trapping efficiency for the optimum trajectory is approximately 70 times that for conventional injection perpendicular to the axis. An analog computer was used to trace initial particle orbits to determine which orbits are contained. A somewhat higher trapping efficiency for oblique injection into a six-bar mirror-cusp field is also indicated. (auth)

38278 ELECTROSTATIC PROBE IN A COLLISIONLESS PLASMA. Kiel, R. E.; Gustafson, W. A. (Purdue Univ., Lafayette, Ind.). Phys. Fluids, 9: 1531-9(Aug. 1966).

The theory developed differs from classical Langmuir theory in that the potential at the sheath's edge need not be the ambient potential and the velocity distribution function for each species is determined for all points in space, rather than at the probe surface only. The range of validity of the classical theory is discussed quantitatively by presentation of several solutions for the spatial distributions of potential. Examination of an earlier result given for a moderately negative probe and monoenergetic ions reveals an inconsistent formulation; an exact result is presented. A solution for the infinite collisionless field of arbitrary potential distribution is derived, and an approximate form of this solution is compared with numerical results. (auth)

38279 SPECTROSCOPIC MEASUREMENT OF TEMPERATURES IN AN ARGON PLASMA ARC. Bott, J. F. (Harvard Univ., Cambridge, Mass.). Phys. Fluids, 9: 1540-7(Aug. 1966).

Temperature profiles across the Poiseuille plasma arc were calculated from measured radiation intensities from the atmospheric argon plasma at arc currents from 1 to 400 A. The transition probabilities for several neutral argon lines were calculated from the measurements. The investigation showed the central core of the arc to be in local thermodynamic equilibrium but the sides of the arc to deviate from local thermodynamic equilibrium. The extent of this deviation was found to increase with decreasing current. (auth)

38280 TRAVELING-WAVE INDUCED ELECTROCONVECTION. Melcher, James R. (Massachusetts Inst. of Tech., Cambridge). Phys. Fluids, 9: 1548-55(Aug. 1966).

An electrohydrodynamic traveling-wave induction interaction is shown to pump slightly conducting liquids [electrical conductivities 10^{-6} to 10^{-15} $(\Omega \cdot m)^{-1}$] without electrical contact with the flow. A gradient in fluid conductivity perpendicular to the direction of flow is required. Here, this is provided by a liquid interface, which is exposed to a traveling potential wave imposed by means of a segmented electrode parallel to the interface. Induced charges relax through the liquid to form a traveling wave of surface charge on the interface which lags the wave of image surface charges on the electrode. Hence, a time-average electrical surface traction is produced tending to make the fluid move with the traveling wave. Expressions for the fields, the time-average electric traction, and the fluid velocity (in plane flow) are derived and discussed. Experiments illustrate the validity of these equations and tend to support the model used for the interfacial conduction process. (auth)

38281 HARTMANN FLOW BETWEEN PARALLEL PLANES. Todd, L. (Massachusetts Inst. of Tech., Cambridge). Phys. Fluids, 9: 1602-3(Aug. 1966).

Precise conditions were found which distinguished between the electromagnetic pump, electromagnetic brake, magnetohydrodynamic generator, and the magnetohydrodynamic flow accelerator, whatever the value of the Hartmann number. (auth)

38282 PLASMA TURBULENCE AND QUASI-LINEAR APPROXIMATION. Imamura, Tsutomu (Kwansei Gakuin Univ., Nishinomiya, Japan); Taniuti, Tosiya. Phys. Fluids, 9: 1603-4(Aug. 1966).

A quasi-linear approximation for a turbulent plasma was obtained using the Wiener-Hermite functional expansion for an electric field and a distribution function. Gaussian distributions were obtained with such an approximation. (auth)

38283 PROPAGATION AND DAMPING OF ION WAVES IN A PLASMA WITH NEGATIVE IONS. D'Angelo, N.; Goeler, S. v.; Ohe, T. (Princeton Univ., N. J.). Contract AT(30-1)-1238. Phys. Fluids, 9: 1605-6(Aug. 1966). (MATT-433).

The ion waves split up into two modes of propagation; if the fraction of negative ions is large, the collisionless damping of the faster mode is weak. (auth)

38284 PLASMA WAVE PROPAGATION IN HOT INHOMOGENEOUS MEDIA. Berk, H. L.; Rosenbluth, M. N.; Sudan, R. N. (International Centre for Theoretical Physics, Trieste, Italy). Phys. Fluids, 9: 1606-8(Aug. 1966).

The WKB solution for plasma wave propagation is obtained for the one-dimensional Vlasov equation. In principle, a solution can be obtained to all orders in the smallness parameter. (auth)

38285 ENERGY DENSITY IN A PLASMA OSCILLATION. Ingard, Uno; Manheimer, Wallace M. (Massachusetts Inst. of Tech., Cambridge). Contracts Nonr-1841(42); DA36-039-AMC-03200(E). Phys. Fluids, 9: 1608-10(Aug. 1966).

The frequency dependence of the electrostatic energy density in an undamped (or weakly damped) longitudinal plasma oscillation and the explicit interrelationship between kinetic, electrostatic, and thermal (compressional) energy density are discussed. (auth)

38286 EFFECTIVE INTERACTION IN A QUANTUM VLASOV PLASMA. Braun, E. (Univ. Autonoma de Puebla, Mex. Comision Nacional de Energia Nuclear, Mexico City). Phys. Fluids, 9: 1611-13(Aug. 1966).

The average stationary effective interaction between particles in a quantum Vlasov plasma is obtained for a particle model. The shielding distance is shown to be lar-

ger than the corresponding classical Debye radius. A law of corresponding states is formulated. (auth)

38287 SCHLIEREN PHOTOGRAPHY OF RAIL-TUBE PLASMAS. MacLelland, J. R.; MacKenzie, A. S. V.; Irving, J. (Univ. of Strathclyde, Glasgow). Phys. Fluids, 9: 1613-15(Aug. 1966).

Schlieren photographs of discharges in a parallel plate rail-tube were taken using a pulsed ruby laser as a light source. The photographs show more detail than previously observed and reveal some new facts about the structure of the discharge. (auth)

38288 THEORETICAL OPTIMUM SEED CONCENTRATIONS IN SLIGHTLY IONIZED NONEQUILIBRIUM PLASMAS. Smith, J. Marlin (General Electric Co., Philadelphia); Shair, F. H. Contract NAS 3-6260. Phys. Fluids, 9: 1615-17(Aug. 1966).

Optimum concentration of an alkali metal seed in a noble gas for maximum electrical conductivity is derived for a nonequilibrium plasma in which the nonequilibrium is caused by an applied or induced electric field. (auth)

38289 AXIAL PRESSURE ASYMMETRY PRODUCED BY HALL CURRENTS IN A LINEAR PINCH DISCHARGE. Measures, R. M. (Imperial Coll. of Science and Technology, London). Phys. Fluids, 9: 1617-18(Aug. 1966).

Axial pressure measurements in a z-pinch discharge, modified by the magnetic field of a thin coil, indicated that the radial components of the magnetic field induced a Hall dominated azimuthal current in the plasma over certain regions of the discharge. (auth)

38290 LIMITING GROWTH RATES FOR GENERALIZED HARRIS INSTABILITIES. Brambilla, M.; Schmidt, G. (CEN, Saclay, Gif-sur-Ivette, France). Phys. Lett., 22: 155-7(Aug. 1, 1966).

Loss cone distribution functions of the form $f_0 = \delta(v_\parallel)F(v_\perp)$ are investigated in the limit of vanishing magnetic field, in search of fast growing modes in the presence of B_0. It is found that if $F(v_\perp)$ is single humped (but $\int F dv_\perp$ double humped), all such distribution functions are electrostatically stable. (auth)

38291 CYCLOTRON EXCITATION OF ELECTROMAGNETIC WAVES BY A GYRATING ELECTRON BEAM. Neufeld, Jacob; Wiginton, C. L. (Oak Ridge National Lab., Tenn.). Phys. Rev., 148: 97-103(Aug. 5, 1966). (ORNL-P-2066).

When a tenuous electron stream gyrates around the field lines of a static magnetic field in the presence of a stationary plasma, electromagnetic waves are excited which propagate perpendicular to the magnetic field. Previous theoretical studies involved the assumption that these excited waves are almost longitudinal (quasistatic approximation). Such an assumption is not made in this analysis. It is shown that the excited waves have the electron cyclotron frequency or some multiple thereof. The electric intensity vector rotates in a plane perpendicular to the magnetic field; the phase velocities are of the order of, or exceed, the velocity of light, and for certain plasma-beam systems lower harmonics of the electron cyclotron frequency cannot be excited. Expressions are given for the rate of growth of the waves as a function of the plasma-beam parameters and the harmonic number. (auth)

38292 INTERACTION OF ELECTROMAGNETIC WAVES WITH QUANTUM AND A CLASSICAL PLASMAS. CORRELATION EFFECTS. Nguyen Quang Dong (EURATOM-CEA, Fontenay-aux-Roses, France). Phys. Rev., 148: 151-9(Aug. 5, 1966).

A quantum statistical approach is used to study the interaction of electromagnetic (EM) waves with a hot plasma. The quantum calculation takes into account the correlation effects. The Coulomb interaction between the charged particles is renormalized so as to take care of the collective effects. This renormalization also reduces the number of diagrams to be considered to obtain any desired accuracy. The results for a classical plasma are obtained by passing to the limit $\hbar \to 0$. Some applications are considered for a classical hot plasma. In the damping of EM waves, the contributions of correlations are most important, at the limits of high and low frequencies, than the Landau contribution, which prevails at plasma resonances. Also, the appearance of the ion Doppler spread, instead of the electron Doppler spread, in the data for the scattering of EM waves observed in the ionosphere backscattering experiments, is explained in terms of correlation effects. (auth)

38293 RESISTANCE OF A PLASMA SLAB BETWEEN JUXTAPOSED DISK ELECTRODES. Laporte, O. (Univ. of Michigan, Ann Arbor); Fowler, R. G. Phys. Rev., 148: 170-5(Aug. 5, 1966).

The classical solution of the important (to plasma physics) problem of two opposite electrodes on an infinitely extensive slab of conductor is in principle seriously incorrect. An exact solution of the problem in two dimensions is given. The solution of the three-dimensional problem is presented in the form of a one-dimensional integral equation by a new method. Rapidly converging series solutions are then obtained. The method used has implications of usefulness which go well beyond the present problem. (auth)

38294 OBSERVATION OF ION PLASMA WAVES AT FREQUENCIES HIGHER THAN THE ION PLASMA FREQUENCY. Sessler, G. M. (Bell Telephone Labs., Murray Hill, N. J.). Phys. Rev. Lett., 17: 243-5(Aug. 1, 1966).

Ion plasma waves which are the extension of ion acoustic waves to frequencies larger than the ion plasma frequency were generated in weakly ionized gases. The phase velocity and damping of these waves were measured. (B.G.D.)

38295 HIGH ION β PITCH-ANGLE INSTABILITY. Kennel, Charles F.; Wong, H. Vernon (IAEA, Trieste). Phys. Rev. Lett., 17: 245-6(Aug. 1, 1966).

A high-β plasma instability due to small ion-temperature anisotropies of either sign is derived. (B.G.D.)

38296 DRIFT INSTABILITY DUE TO IMPURITY IONS. Coppi, B.; Furth, H. P.; Rosenbluth, M. N.; Sagdeev, R. Z. (International Centre for Theoretical Physics, Trieste, Italy). Phys. Rev. Lett., 17: 377-9(Aug. 15, 1966).

It is shown that the presence of impurity ions in a hydrogen plasma, especially if their density gradient is different from the plasma gradient, can generate a new instability which is difficult to stabilize and which leads to an outward diffusion of plasma ions and an inward diffusion of impurity ions. (L.B.S.)

38297 NOTE ON THE CALCULATION OF THE DIELECTRIC FUNCTION FOR A HOMOGENEOUS PLASMA. Das Gupta, B.; Das Gupta, P. (Saha Inst. of Nuclear Physics, Calcutta). Physica, 32: 878-84(May 1966).

A method of calculating the dielectric function for a homogeneous plasma using the fluctuation-dissipation theorem is discussed. This method dispenses with the use of any kinetic equation in contrast to the usual methods. Calculations using firstly the "noninteracting dressed" particle picture, and secondly, the expression for the density correlation function obtained by Balescu, are shown to lead to the same dielectric function as obtained usually from the Vlasov equation. (auth)

38298 COMMENT ON " THE NEUTRAL HYDROGEN FLUX IN THE SOLAR PLASMA FLOW" BY S.-I. AKASOFU. Cloutier, Paul A. (Rice Univ., Houston, Tex.). Planet. Space Sci., 14: 809-12(Aug. 1966).

Ionization by electron impact is shown to be a more significant ionization mechanism than photoionization. It is believed that the flux of neutral hydrogen is less than 10^{-5} of the total solar wind flux at 1 a.u. It is suggested that explanations of physical processes in terms of a large concentration of neutral hydrogen in the solar plasma flow should be re-examined. (J.H.M.)

38299 ELECTRICAL PROPERTIES OF A SPHERICAL PLASMA PROBE NEAR THE PLASMA FREQUENCY. Davies, P. G. (Radio and Space Research Station, Ditton Park, Slough, Eng.). Proc. Phys. Soc. (London), 88: 1019-32(Aug. 1966).

An experimental investigation was made to find out how a conductor in a plasma behaves when an alternating potential is applied to it with a frequency in the neighborhood of the plasma frequency. Attention was paid to the way in which the mean current to the probe (the rectified current) depended upon the frequency, particularly when it approached the plasma frequency and when the current became abnormally large (resonance rectification). The probe-to-plasma admittance was also investigated as a function of frequency. The experimental results on rectified current and admittance are compared with values derived from the theory of Buckley for a spherical plasma probe. This theory gives a detailed description of the way in which these quantities depend on the electron-neutral collision frequency and on the frequency of the applied alternating potential. In many respects previous theories are unrealistic because separate sheath, radio-frequency penetration and unperturbed plasma regions, each having different physical characteristics, have been considered. Buckley, using values of sheath potential computed by Bernstein and Rabinowitz from Poisson's equation for spherical symmetry, has shown that it is not necessary to separate the various regions. The effect of collisions between electrons and neutrals is also taken into account in a realistic way by including a collision term in the Boltzmann equation. The experimental data on rectified current and probe-to-plasma admittance are found to agree with the theoretical data which refer to particular values of the ratio of the electron-neutral collision frequency to angular plasma frequency. (auth)

38300 EXTREME ULTRAVIOLET SPECTRA FROM LASER-PRODUCED PLASMAS. Fawcett, B. C.; Gabriel, A. H.; Irons, F. E.; Peacock, N. J.; Saunders, P. A. H. (United Kingdom Atomic Energy Authority, Culham, Abingdon, Eng.). Proc. Phys. Soc. (London), 88: 1051-3 (Aug. 1966).

Plasmas produced by focusing a 400-Mw ruby laser beam onto surfaces of C, Ti, Mn, Fe, Ni, Cu, and Zn, and into argon gas, were observed in the extreme ultraviolet region. Line and continuum radiation were recorded down to 25 Å, including new spectra of Fe XV and Fe XVI and Ni XVII and Ni XVIII. The value of such plasmas for line classification work is demonstrated. (auth)

38301 QUASI-OSCILLATIONS OF COLD, SHARPLY BOUNDED PLASMAS. Leavens, William M. (Inst. for Telecummunication Sciences and Aeronomy, ESSA, Boulder, Colo.); Leavens, Ileana B. Radio Sci., 1: 789-98(July 1966).

The oscillatory modes of a sharply bounded plasma which involve surface charge were studied by a method which includes the behavior of the surface charge. This was accomplished by a generalization of Dawson's method of studying nonlinear oscillations in cold plasmas. The arguments presented are as follows: Surface charge modes are essentially nonlinear, e.g., if the electron cloud is displaced slightly outside the ion cloud the relative perturbation of the electron density is infinite. By solving an equation of motion which includes the motion within the surface charge, it was found that nonlinear phenomena appear quickly, independent of the magnitude of the motion. It was further shown that the surface charge modes have no linearizable analogs in the cold plasma if the density gradient is made finite. The oscillations which can be excited in a real (warm, continuously nonuniform) gaseous plasma clearly do have a linearizable limit. This is an indication for care in identifying observed resonances of gaseous plasmas with the surface charge modes. The nonlinearity of the surface modes is not apparent in previous treatments. It has seemed possible to ignore the motion of the surface charge, because the total amount of surface charge both determines, and is determined by, the motion of all the electrons outside the surface charge. But, this is only true for a short time—the nonoscillatory behavior of the electrons in the surface charge soon causes multistreaming which spreads into the rest of the plasma, invalidating the cold-plasma equations. Detailed calculations are made for a cold plasma slab. The cylinder modes are considered, and the linearized modes of a diffuse boundary are studied. Some simple aspects of the propagation of multistreaming are described. (BBB)

38302 POTENTIALS FOR CYLINDRICAL WARM PLASMAS. Sancer, Maurice I. (Polytechnic Inst. of Brooklyn, Farmingdale, N. Y.). Radio Sci., 1: 799-813 (July 1966).

Existing analysis of electromagnetic fields in anisotropic media involving cylindrical geometry has used two linear combinations of field components as potentials. These combinations are potentials in the sense that they satisfy scalar Helmholtz equations and all of the fields can readily be determined from these combinations. A natural extension of this analysis is presented for the anisotropic warm plasma, the anisotropy being restricted to correspond to an axial external magnetic field. It was shown that this analysis reduced to a standard analysis for the isotropic one-fluid description of the plasma. For the linearized anisotropic n-fluid description of the plasma, it was shown that 2 + n potentials can be introduced, provided a 2 + n by 2 + n matrix has a diagonal Jordan canonical form, which must be found. These potentials are then solutions to Hemholtz equations, and all the dependent variables can readily be calculated from them. The conceptually difficult problem of analyzing cylindrical plasma was thus reduced to the algebraically complex problem of diagonalizing a matrix. (M.O.W.)

38303 WAVE PROPAGATION IN PLASMAS WITH VERY STRONG MAGNETIC FIELD. Lee, S. W.; Liang, C.; Lo, Y. T. (Univ. of Illinois, Urbana). Radio Sci., 1: 815-24(July 1966).

A mathematical model of a low-temperature plasma with low density, weak collision, and strong magnetic field is described by employing the first three moment equations and the Chew, Goldberger, and Low (CGL) approximation. This provided an improvement over two previous models, since on one hand, the perturbing effect of the acoustic waves is included, while on the other hand, it is not necessary to assume that the pressure is isotropic or to use the equation of state (which is true only for high-density and collision-dominated plasma). The propagation of plane waves in such a medium is also studied. In the model described, to the first order, the pressure tensor becomes uniaxial. For propagation along the magnetic field, the wave does not experience the anisotropic effect of the pressure tensor. There exists a plasma mode whose phase velocity is independent of the magnetic field, an ordinary optical mode which propagates slightly faster than light, and an extraordinary optical mode which propagates slightly slower than light. For propagation perpendicular to the magnetic field, at most two optical modes can propagate, one of which propagates only when $\Omega > 1$, and the other always propagates with a velocity faster than that of light when $\Omega < 1$ and propagates slower than light when $\Omega > 1$. For propagation at any other angle, the dispersion relation becomes very complicated. A simple result was obtained when the magnetic field was extremely strong. In this analysis, the results are, in general, not the same as those reached by using a simple cold-plasma model or a warm-plasma model. However, it is believed that the model employed here gives a better description of low-density, weak-collision, and low-temperature plasma with a very strong static magnetic field. (BBB)

38304 RECENT CONCEPTS ON PLASMA OPTIMAL CONTROLLABILITY. I. Krzywoblocki, M. Z. V. (Michigan State Univ., East Lansing). Rev. Roum. Sci. Tech., Ser. Mec., 10: 1345-64(1965).

A brief discussion is presented of the existing variational principles and stability criteria in the classical viscous and inviscid fluid dynamics, stability here being defined as the ability of flow patterns to sustain themselves against small perturbations. The stability criteria of an ionized medium are then discussed, followed by a different definition of the stability of an ionized medium, i.e., all kinds of thermal, kinetic, or stored energy reservoirs are mutually coupled through the motion and distribution of plasma particles. Such a coupling gives rise to an oscillatory or

a unidirectional exchange of energy between these reservoirs. This main concept is called the plasma optimal controllability. (Int. Aero. Abstr.)

38305 TRANSVERSE MICROWAVE CAVITY TECHNIQUE FOR SENSITIVE MEASUREMENT OF TRANSIENT ELECTRON DENSITY DISTRIBUTIONS. Lubin, M. J. (Univ. of Rochester, N. Y.). Rev. Sci. Instrum., 37: 1034-8(Aug. 1966).

A high-resolution transverse microwave probing technique is described utilizing radiating slots cut in an oversize waveguide containing the plasma. General expressions for the transmission coefficient of the doubly infinite cavity are derived and applied to the measurement of precursor electron density distributions in an electromagnetic shock tube. The results compared favorably with the results of other independent measurements. (auth)

38306 SCYLLACITA: COMPACT HIGH-VOLTAGE THETA PINCH MACHINE. Kemp, E. L.; Dolnick, E. M.; Dike, R. S.; Sawyer, G. A.; Tuck, J. L. (Los Alamos Scientific Lab., N. Mex.). Rev. Sci. Instrum., 37: 1065-8 (Aug. 1966). (LA-DC-7467).

A high-voltage theta pinch (Scyllacita) was developed especially for application to experiments with explosively compressed theta pinches. The system is relatively ecnomical, simple, and compact. Twenty-four 14 μF, 20 kv, low inductance capacitors (60 kJ) are divided into two banks. Each capacitor has a 3-element spark gap (trigatron) mounted directly on it. Twelve low inductance cables from each capacitor spark gap combination are connected to a mix header which puts the two banks of capacitors in series when the gaps fire. One-hundred low inductance cables connect the mix header to a collector plate and thus to the 8-cm diam, 24-cm long load coil. The source inductance (coil terminals shorted) is 17 nH. Both mirror coils and straight bore coils were used. With the straight bore coil, the full period of oscillation is 11.7 μsec and the efficiency of energy transfer to the coil is 59%. In second half-cycle operation at 100 mtorr filling pressure with the banks charged to 18 kv, over 10^7 neutrons per discharge are produced in either mirror or straight coil. (auth)

38307 MICROWAVE CAVITY Q SAMPLER FOR PLASMA DIAGNOSTICS. Ferendeci, Altan M. (Case Inst. of Tech., Cleveland). Rev. Sci. Instrum., 37: 1089-91(Aug. 1966).

A microwave cavity resonant frequency sampling technique is described by which the electron density and recombination and diffusion or attachment time of the decaying plasma can be recorded directly on a single oscilloscope photograph. The data appear as displaced lines on which the shift in resonant frequency of the cavity is superimposed. The collision frequency is measured at a single frequency without the sampling unit. Measurements of the change in phase produced by a decaying plasma in a transmitted or reflected microwave signal, plasma heating studies, and microwave-induced ionization in plasma are also performed using this method. (J.F.P.)

38308 MODIFICATION OF PENNING DISCHARGE USEFUL IN PLASMA PHYSICS EXPERIMENTS. Roth, J. Reece (Lewis Research Center, Cleveland). Rev. Sci. Instrum., 37: 1100-1(Aug. 1966).

A modification of the conventional Penning discharge which is useful in generating large-volume steady-state plasmas is described. The discharge can be operated in the high-power mode at much lower neutral background gas pressures, and in strong magnetic fields up to 20 kG. Also ion trapping and higher ion densities in the magnetic bottle are achieved. The discharge is easy to set up, repeatable in operation, and can be used to create plasma in a magnetic bottle or minimum B magnetic field geometry. (J.F.P.)

38309 SOME PROBLEMS IN USE OF LANGMUIR PROBE ON IONOSPHERIC SOUNDING ROCKETS. Ichimiya, Torao; Dote, Toshihiko; Takayama, Kazuo (Inst. of Physical and Chemical Research, Tokyo). Rika Gaku Kenkyusho Hokoku, 40: 75-86(1964). (In Japanese).

Some problems associated with direct measurements in the ionosphere using rocket-borne Langmuir probes are described. After a brief description of them, some new problems which affect measurements by the Langmuir probe method are discussed. These are, for example, existence of negative ions in the plasma, effects of relative motion of the probe to the plasma, deviation of characteristics of the probe from that of the single probe, and the influence of the geomagnetic field on the probe characteristic. Corrections for the existence of negative ions are calculated from Boyd's theory of sheath criterion; they need not be considered in the lower parts of the E and D ionospheric layers. The velocity of rocket may be comparable with or occasionally exceed by several times the mean kinetic velocity of positive ions in ionosphere and it is necessary to take into account the effect of relative velocity when the positive ion density is calculated from the probe data. On the basis of two reasonable assumptions, the probe characteristics in the drifting plasma are deduced theoretically, and the theory was verified experimentally in the multiple collisions range using a low density supersonic wind tunnel. The fact that the potential of the system or rocket and probe interacts with the ionospheric plasma is emphasized. When the potential of the probe is raised with respect to that of the rocket body, the latter may be shifted with respect to the plasma potential. By theoretical considerations of an unsymmetrical floating double probe, the electron current flowing into the probe is calculated and a criteria of how much the characteristics of the probe deviate from that of the single probe are derived. It is concluded that the ratio of the area of the probe to that of the rocket body must be chosen to be less than 1/2000 to 1/3000, if the error of electron current is to be limited to within 10%. In the ionosphere the geomagnetic field is very small (~0.3 G), hence the cyclotron frequency of electrons ω_{ce} is also small. On the other hand, the mean collision time of electrons τ_e is not small because of the rarity of the atmosphere. Then the product $\omega_{ce} \cdot \tau_e$ cannot be neglected compared with unity, and the geomagnetic field affects the probe measurement through influences on the space-charge conduction in the sheath and the value of the saturated electron current. From calculations, the former effect is found to be small and negligible, but the latter cannot be ignored. As the magnetic field increases, the saturation current decreases. At present, the relation between saturation current and magnetic field has not yet been solved. (BBB)

38310 COMPUTER EXPERIMENTS IN PLASMA PHYSICS. Buneman, Oscar; Dunn, Donald (Stanford Univ., Calif.). Sci. J., 2: No. 7, 34-40(July 1966).

Some applications and advantages in using modern computers in understanding the behavior of plasmas are discussed. Experiments show that the equations of motion of many interacting particles can be solved simultaneously, using computers; and, given the initial conditions, the subsequent behavior of all the particles can be calculated. Surveys indicate that computer experiments will grow in number and importance, not only because of their intrinsic value and success, but also because developing computer technology will allow more complex simulations to be made. (J.H.M.)

38311 STABILITY OF A COMPRESSIBLE GRAVITATING CYLINDER OF UNIFORM DENSITY IN A LONGITUDINAL MAGNETIC FIELD. Vandakurov, Yu. V.; Kolesnikova, E. N. (Ioffe Inst. of Physics and Tech., Leningrad). Soviet Astron. AJ (Engl. Transl.), 10: 78-82 (July-Aug. 1966).

Translated from Astron. Zh., 43: 99-104(Jan.-Feb. 1966).

The stability of a perfectly conducting compressible cylinder situated in a longitudinal magnetic field relative to perturbations which are independent of the position along the cylinder is discussed. In the case of a cylinder with a uniform density distribution, an exact solution was obtained for a rotating medium with a parabolic distribution of magnetic and gas pressures. Unstable oscillations (similar to the known instabilities of a compressible gravitating sphere with a uniform density distribution) were found. The most favorable conditions (in the sense of a slow develop-

ment of the instability) are those where the pressure inside the cylinder situated in a magnetic field exceeds the magnetic pressure on the axis by an amount of the order of γp_0, where γ is the ratio of specific heats and p_0 is the pressure at the center. The instability criterion for a cylinder with a uniform density distribution (when the medium is not rotating) is derived. (auth)

38312 INTRODUCTION TO THE INTRINSIC STUDY OF THE CLASS OF STEADY-STATE MOTIONS OF A PERFECT PLASMA IN A STATIONARY MAGNETIC FIELD. Ionescu-Bujor, Claudiu. Stud. Cercet. Mecan. Apl., No. 3, 537-57(1963). (In Rumanian).

In the study of the class of steady-state rotational and three-dimensional motions of a perfect plasma, in a stationary magnetic field, an exact mathematical method explained previously is expounded. With this in mind, the classic system of equations characterizing this class of fluid motions is substituted by an equivalent system where the unknown vector fields (of the velocity $\vec{v}$ of the conducting fluid and of the magnetic flux density $\vec{B}$) are replaced by pairs of parameters defining the lines of force of these vector fields; it is demonstrated that the new system—called "reduced system" of equations for the class of fluid motions in question—is equivalent to the classic system. The "principal system" of equations for this class of fluid motions, the role of which is made precise, is then defined. Two particular cases are considered. (auth)

38313 REMARKS CONCERNING PARTICLE MOTION IN INFINITE d-c MAGNETIC FIELD. Toktarov, K. Vestn. Akad. Nauk Kaz. SSR, No. 1, 85-6(Jan. 1966). (In Russian).

It was suggested that the limits of the drift of particles composing a quasi-plasma may be decreased by reflecting them from a magnetic mirror created by spiral-shaped currents at the surface of a toroidal chamber. Applicability of such a mirror for a magnetic trap depends on the nature of the motion of the particles, especially of deuterons, of the quasi-plasma. This requires estimation of the reflectivity of the magnetic mirror for particles to be participating in fusion reactions. Therefore, the motion of 50-kev deuterons in the magnetic field of an infinite, straight-line current was examined, in order to estimate the magnetic-mirror current required to reflect them. Formulas were derived for determining the drift of the particles. It was found that for $\rho^* = 0.1$, the current required is 9.603×10^4 amp. Such currents are within the realizable limits of plasma research. (TTT)

38314 CHEMICAL PROCESSES IN LOW-TEMPERATURE PLASMA. Polak, L. S. (Topchiev Inst. for Petrochemical Synthesis, Academy of Sciences, USSR). Vestn. Akad. Nauk SSSR, 36: No. 6, 52-6(June 1966). (In Russian).

Plasmochemical processes take place under participation of ions of very active atoms, excited radicals, and molecular fragments and particles with "strange" valences that normally exist only at high temperatures. It is possible to bind final and intermediate compounds in nonequilibrium concentrations by means of such processes. Low-temperature plasma and plasma jets may be used for experiments at flow velocities of 0.2 to 0.8 times the velocity of the sound. Argon, hydrogen, nitrogen + oxygen, methane, and others may be employed as carrier gases, at energies from 10 to 5000 kw, to carry out economically significant chemical processes at temperatures of about 2×10^3 to 6×10^4°K. Because of the strong nonequilibrium character and the relaxation properties of the systems, the rules of ordinary chemistry do not apply. With increasing temperature, the importance of the entropy factor also increases, resulting in stronger dissociation, disintegration, and decomposition. The theory of equilibrium activation leads to the Arrhenius equation but if the system deviates from the Maxwell–Boltzmann distribution, the Arrhenius equation is not applicable. Monte Carlo techniques may be used for calculating the Maxwellization of a mixture containing a hot and a cold gas. Sudden quenching of the reaction products, at rates of 10^{6}°C/sec, as by means of the Laval nozzle, present the chief problem of plasmochemistry. (TTT)

38315 STABILITY OF TRANSVERSE OSCILLATIONS OF A FOCUSED CHARGED BEAM IN AN ABSORBING MEDIUM. Balbekov, V. L.; Kolomenskii, A. A. Zh. Eksp. Teor. Fiz., 50: 1529-36(June 1966). (In Russian).

Transverse stability of a focused beam of charged particles moving through an absorbing medium is considered. The various modes of coherent oscillations (center of mass, size, shape), are determined and their frequencies and increments are found. The possibility of stabilizing the beam by exploiting the energy spread and nonlinearity of the betatron oscillations is studied. The effect of the plasma produced as a result of ionization of the gas is estimated. These problems are of interest in designing accelerators and storage rings of the high beam intensity. (auth)

38316 PLASMA INSTABILITIES AND ANOMALOUS TRANSPORT. Proceedings of a Conference with a Collection of Reprints. Pardo, William B.; Robertson, Harry S. (eds.). Coral Gables, Fla., University of Miami Press, 1966. 301p. $4.00. (CONF-660536).

Separate abstracts were prepared for 16 of the included 31 articles. The remaining 16 articles appeared previously in NSA as 16: 18584, 17: 13656, 18: 28795, 28799, 40677, 19: 10428, 14702, 19295, 23916, 43417, 20: 12235, 17885, 22247, 22249, 24554, and 32579. (M.O.W.)

For abstracts of individual papers see: 38317–38331.

38317 PLASMA STABILITY RESEARCH PROGRAM AT THE UNIVERSITY OF MIAMI. Robertson, Harry S. (Univ. of Miami, Coral Gables, Fla.). pp 7-15 of Plasma Instabilities and Anomalous Transport. Pardo, William B.; Robertson, Harry S. (eds.). Coral Gables, Fla., University of Miami Press, 1966.

Experimental facilities are described for the study of helical instabilities in cesium arc plasmas in axial, Ioffe, and other magnetic field configurations. The development of the plasma loss mechanism is traced as B increases from classical diffusion to various modes of the helical instability with convective transport, and then to turbulent diffusion. A brief description is given of oscillations generated by ion emission from the anode surface. Finally, there is a brief account of a theory of the helical instability in r-f excited electrodeless discharges. The theory predicts that for uniform excitation in a uniform axial magnetic field, at sufficiently high pressure to ensure that the plasma is neutral-collision dominated, the value of the Kadomtsev parameter $y = \mu_+\mu_- B^2$ at onset should be independent of both pressure and tube radius. (auth)

38318 SOME CORRELATED EXPERIMENTAL AND THEORETICAL ASPECTS OF THE FINITE AMPLITUDE HELICAL INSTABILITY. Johnson, Roy R. (Boeing Co., Seattle). pp 19-33 of Plasma Instabilities and Anomalous Transport. Pardo, William B.; Robertson, Harry S. (eds.). Coral Gables, Fla., University of Miami Press, 1966.

The helical instability of the positive column was previously observed experimentally with the use of electrostatic probes, photomultipliers, streak photographs, and framing cameras. It was found that the use of magnetic pickup coils to measure the internal magnetic field provides an accurate means of observing the helical instability at the positive column in a longitudinal magnetic field. New measurements were made of the above mentioned types. The results are described for each. (M.O.W.)

38319 LOW-FREQUENCY INSTABILITY IN CESIUM DISCHARGE AND THERMAL PLASMAS. Decker, John A. Jr. (Sperry Rand Corp., Sudbury, Mass.). pp 49-60 of Plasma Instabilities and Anomalous Transport. Pardo, William B.; Robertson, Harry S. (eds.). Coral Gables, Fla., University of Miami Press, 1966.

The results are presented of two separate, but related, experimental programs which involve instabilities and anomalous plasma loss processes in cesium plasmas. The first experiments used a series of small cesium-discharge tubes, approximately 1 m long by 5 cm diameter, incorporating externally heated thermionic cathodes and designed for operation at pressures from 10^{-2} to 10^{-5} torr at d-c currents up to 1 amp and at axial magnetic

fields up to 5 kG. The low-frequency oscillations from various experiments with this device are described. The second experiments concerned spontaneously generated low-frequency oscillations and anomalously high plasma loss rates observed in the thermal plasma of the TOPSY Q-device. The results from these measurements are described. (M.O.W.)

38320 ANOMALOUS PLASMA LOSS PROCESSES. Ingraham, J. Charles (Massachusetts Inst. of Tech., Cambridge). pp 79-88 of Plasma Instabilities and Anomalous Transport. Pardo, William B.; Robertson, Harry S. (eds.). Coral Gables, Fla., University of Miami Press, 1966.

Brief descriptions are presented of research on the following four topics: anomalous diffusion losses in the afterglow of a pulse discharge in helium, low-frequency oscillations in a steady-state microwave electron cyclotron-resonance discharge, the effect of neutral gas turbulence on the ambipolar diffusion coefficient, and generation of low-frequency waves in a hollow-cathode arc plasma. (M.O.W.)

38321 ENHANCED DIFFUSION STUDIES AT STANFORD. Thomassen, K. I. (Stanford Univ., Calif.). pp 89-90 of Plasma Instabilities and Anomalous Transport. Pardo, William B.; Robertson, Harry S. (eds.). Coral Gables, Fla., University of Miami Press, 1966.

A brief review is presented of plasma research at Stanford. The research includes several linear Penning-type reflex discharges with hot and cold plasmas, a toroidal discharge using the Penning-type source, and a beam-generated plasma experiment. The plasma instabilities associated with experiment are briefly described. (M.O.W.)

38322 CORRELATION OF DENSITY FLUCTUATIONS AND DIFFUSION IN A PLASMA. Tsukishima, T.; McLane, C. K. (Inst. for Telecommunication Sciences and Aeronomy, Boulder, Colo.). pp 94-6 of Plasma Instabilities and Anomalous Transport. Pardo, William B.; Robertson, Harry S. (eds.). Coral Gables, Fla., University of Miami Press, 1966.

An independent approach for the measurement of the plasma diffusion coefficient, based on the theoretically established relationship between the correlation coefficient for density fluctuations and the diffusion coefficient, is developed. This approach introduces its own characteristic difficulties, such as extreme sensitivity to extraneous sources of noise, and to waves, oscillations, and in general, non-thermal noise in the plasma. (M.O.W.)

38323 INVESTIGATION OF FLUTE INSTABILITY WITH AN ALKALI-METAL PLASMA. Chang, T. Y. (Univ. of California, Berkeley). pp 111-18 of Plasma Instabilities and Anomalous Transport. Pardo, William B.; Robertson, Harry S. (eds.). Coral Gables, Fla., University of Miami Press, 1966.

Existing theories for mirror-confined plasmas were made more realistic by assuming the particles to drift under external forces which are proportional to the parallel and perpendicular components of the kinetic energy rather than the mass. The derivation starts from an equivalent Vlasov equation for guiding centers. The characteristic frequencies and the stability boundaries were calculated for several examples. The experimental and theoretical techniques are outlined. (M.O.W.)

38324 DIFFUSION AND INSTABILITIES IN "Q" MACHINE PLASMAS. Rogers, K. C.; Wolf, N. S.; Courville, C.; Motz, R. (Stevens Inst. of Tech., Hoboken, N. J.). pp 119-29 of Plasma Instabilities and Anomalous Transport. Pardo, William B.; Robertson, Harry S. (ed.). Coral Gables, Fla., University of Miami Press, 1966.

An investigation was directed toward an understanding of the detailed relationships between micro-instabilities and cross-field plasma diffusion in low β, highly ionized magnetoplasmas. The research technique was as follows: (1) start with a simple well-defined magnetic field geometry, i.e. uniform field independent of time, (2) establish in this field a fully ionized "quiescent" stable, collision-dominated, isothermal plasma of dimensions large compared to Larmor radii, (3) measure diffusion coefficients (D), (4) cause the plasma to become microscopically unstable either by self or external means of excitation, (5) measure D in the presence of fluctuations and establish detailed parametric dependences of D on the modes and mode amplitudes excited in the plasma, (6) explore the dependence of the self-excited mode spectra on magnetic field configuration in somewhat more complicated field shapes by adding mirrors, Ioffe bars, and possible shear via an axial current, and (7) study D in these fields. Results of measurements for a barium plasma are described. (M.O.W.)

38325 QUIESCENT-PLASMA RESEARCH PROGRAM AT THE UNIVERSITY OF MARYLAND. Lashinsky, H. (Univ. of Maryland, College Park). pp 145-8 of Plasma Instabilities and Anomalous Transport. Pardo, William B.; Robertson, Harry S. (eds.). Coral Gables, Fla., University of Miami Press, 1966.

A basic element of this program is the design and construction of an improved version of a thermal plasma device or "Q machine," in which the instabilities will be studied experimentally. Some of the design objectives and proposed features of this new machine are discussed. (M.O.W.)

38326 FIELD CURVATURE EFFECTS ON ALKALI-METAL-PLASMA CONTAINMENT. Hartman, Charles W.; Munger, Richard H. (Univ. of California, Livermore). pp 149-60 of Plasma Instabilities and Anomalous Transport. Pardo, William B.; Robertson, Harry S. (eds.). Coral Gables, Fla., University of Miami Press, 1966.

Plasma stability in magnetic fields possessing compensating curvature is investigated with a device similar to the Princeton "Q" machine. Alkali-metal plasma is generated by ionization of an annular atomic beam incident on a hot end-plate, 2 inches in diameter. The hot plates are located symmetrically near the ends of the magnetic-field solenoid and are oriented perpendicular to the magnetic axis, so as to maintain azimuthal symmetry in $\int dl/B$. The radial dependence of $\int dl/B$ is continuously variable from radially decreasing (with uniform current in the field windings, so that B is weaker near the end plates than at the midplane) to radially increasing (with B at the midplane reduced, so as to introduce a local region of negative curvature). Using a single hot plate of tungsten and uniform field-current, potassium plasmas of $10^{10}-10^{11}/cm^3$ density are found to exhibit characteristic low-frequency oscillations at 5–20 kc, (B = 1 to 2 kg) with a dependence on plate temperature, atomic-beam intensity, and B similar to that described earlier. In passing from radially decreasing to radially increasing $\int dl/B$, an intensification of the amplitude of oscillation is observed. (auth)

38327 PLASMA DIFFUSION STUDIES IN E-TYPE RF DISCHARGES. Powers, E. J. (Univ. of Texas, Austin). pp 161-4 of Plasma Instabilities and Anomalous Transport. Pardo, William B.; Robertson, Harry S. (eds.). Coral Gables, Fla., University of Miami Press, 1966.

An investigation was made of plasma diffusion across static magnetic fields in an electrodeless E-type r-f discharge. Brief discussions are presented on (1) a comparison of the experimental measurements of the r-f electric field required to sustain a constant-current discharge with that predicted by classical diffusion theory, (2) some preliminary results of correlation measurements, and (3) a comparison of the critical field data for hydrogen with the theoretical work of Timofeev. (M.O.W.)

38328 COMPUTER SIMULATION OF ANOMALOUS DIFFUSION. Hockney, R. W. pp 171-93 of Plasma Instabilities and Anomalous Transport. Pardo, William B.; Robertson, Harry S. (eds.). Coral Gables, Fla., University of Miami Press, 1966.

A computer simulation was made for the anomalous diffusion of plasma confined in the interior of an infinitely long cylinder by a longitudinal magnetic field. Various discussions are presented on scaling laws, the display, quasi-steady state, growth of plasma instabilities, fairly steady diffusion, wall effects, effects of coarse graining, and making the motion-picture film. (M.O.W.)

38329 ANOMALOUS TRANSPORT PHENOMENA IN A RING DISCHARGE. Lindman, Erick; Schlueter, Hans; Ransom, C. J. pp 195-202 of Plasma Instabilities and Anomalous Transport. Pardo, William B.; Robertson, Harry S. (eds.). Coral Gables, Fla., University of Miami Press, 1966.

A quartz tube of diameter 6 cm and length 50 cm is placed in a single-turn coil of the tank circuit of a 3-kw, 30-Mc r-f oscillator. A static magnetic field resembling a mirror field is generated by two d-c coils surrounding the tube on either side of the r-f coil. The "discharge properties" are described. (M.O.W.)

38330 SHALL WE HAVE TO LIVE WITH ANOMALOUS DIFFUSION? Buneman, O. pp 203-6 of Plasma Instabilities and Anomalous Transport. Pardo, William B.; Robertson, Harry S. (eds.). Coral Gables, Fla., University of Miami Press, 1966.

Previous work on anomalous diffusion is briefly reviewed. A brief outline for future research is described. (M.O.W.)

38331 ONSET OF TURBULENCE IN THE POSITIVE COLUMN. Hoh, F. C. (Boeing Co., Seattle). pp 207-17 of Plasma Instabilities and Anomalous Transport. Pardo, William B.; Robertson, Harry S. (eds.). Coral Gables, Fla., University of Miami Press, 1966.

An investigation was made of a physical stabilization mechanism of the helical instability of the positive column in a longitudinal magnetic field due to quasi-linear effects. The quasi-linear steady state, consisting of a density helix rotating around the axis, is then perturbed and a chain of linearized differential equations results. When this state next becomes unstable, a coupled set of helical modes with the same growth rate are excited simultaneously, thus leading to the onset of turbulent behavior. Finally, the boundary condition and the corresponding expansion of the eigenfunction of the linearized problem, which was arbitrarily chosen previously, is reconsidered. (M.O.W.)

38332 COUPLING OF DEGENERATE MODES OF A MICROWAVE CAVITY DUE TO THE PRESENCE OF A MAGNETIZED PLASMA. Crownfield, Frederic R. Jr.; Holt, David; Vacha, Terrance (William and Mary Coll., Williamsburg, Va.). 11p. (CONF-651126-2). ORAU. Gmelin, AED-CONF-65-353-1.

From American Physical Society Meeting, 7th Annual Meeting of the Division of Plasma Physics, San Francisco.

The degenerate, plane polarized, orthogonal TE_{111} modes of a circular cylindrical cavity are coupled and perturbed by the presence of a magnetoactive medium, such as a plasma in a magnetic field. In continuing an earlier investigation, the agreement between theory and experiment was unsatisfactory. It was found that a more exact theory predicts a dependence on plasma electron density which did not occur in the earlier, simplified theory. Results of the newer theory are presented and compared with the older one. Possible application to plasma diagnostics is briefly discussed. (auth)

38333 PROPAGATION OF HYDROMAGNETIC WAVES THROUGH AN ANISOTROPIC PLASMA. Abraham, Barbara (Ames Research Center, Moffett Field, Calif.). 45p. (CONF-650927-28). ORAU. Gmelin, AED-CONF-65-222-59.

From American Physical Society Meeting, Honolulu, Hawaii.

The propagation of small amplitude hydromagnetic waves of a collisionless, anisotropic plasma in a strong magnetic field is treated using the Chew-Goldberger-Low (CGL) fluid equations. The Alfven, fast and slow magneto-acoustic, and entropy modes are analyzed by phase speed and wave front diagrams and compared to their counterparts in magneto-hydrodynamics (MHD) where collisions isotropize the pressure. Two main classes of CGL waves are identified, pseudo-MHD and reverse-MHD where the latter has the slow wave speed greater than the Alfvén wave speed. Significant differences of the CGL hydromagnetic waves as compared to MHD waves are found which have special relevance for a study of infinitesimal and finite discontinuities in space plasmas. (auth)

38334 EXCHANGE AND CORRELATION EFFECTS IN AN INHOMOGENEOUS ELECTRON GAS. Sham, L. J. 27p. (CONF-650927-8). ORAU. Gmelin, AED-CONF-65-222-30.

From American Physical Society Meeting, Honolulu, Hawaii.

The electrostatic instability of a cold, unbounded, uniform, relativistic, neutralized beam of electrons penetrating a temperate, isothermal, unbounded, inhomogeneous, field-free plasma is studied. The plasma and beam ions form a stationary, neutralizing background, and only the electrons are mobile. The effect of the steady magnetic field of the tenuous beam on the stability of the beam-plasma system is neglected. The plasma density inhomogeneity is so mild that all quantities second order or higher in its density gradients are negligible. The plasma equivalent of the equations of hydrodynamics, obtained by taking velocity moments of the collisionless Boltzmann equation and neglecting the heat flow term, and Maxwell's equations determine the behavior of the system completely. The differential equation governing the stability of the system is obtained. For simplicity, this equation is specialized to the one-dimensional case when the electron velocity, density gradient, electric field vector and the propagation vector are all in the z direction. The resulting fourth-order differential equation is shown to yield the well-known dispersion equation for uniform plasmas. In a cold plasma, a second-order differential equation obtained previously is recovered. The stability of the system is studied for various physically interesting inhomogeneous plasma densities. (auth)

38335 VACUUM ULTRA-VIOLET RADIATION FROM PLASMAS. Elton, R. C. (Naval Research Lab., Washington, D. C.). 25p. (CONF-660217-4). ORAU. Gmelin, AED-CONF-66-013-8.

From Symposium on Interdisciplinary Aspects of Radiative Energy Transfer, Philadelphia.

A T-type electromagnetic shock tube operating at ~20,000°K was developed to generate a uniform high density atmosphere into which tracer gases are added in controlled amounts, producing variable degrees of opacity in the vicinity of broadened spectral lines of known shape, such as the Lyman series of hydrogen. Also, two θ-pinch devices operating at temperatures in the million-degree range, suitable for simulating corona equilibrium conditions and solar spectra as well as producing resonance lines of variable optical depth, are described. Experimental complexities peculiar to various regions of the extreme ultraviolet from 10 to 2000 Å are outlined, as is a discussion of absolute intensity determinations. (M.O.W.)

38336 EXPERIMENTS ON SCATTERING LASER LIGHT BY THERMAL DENSITY FLUCTUATIONS IN A PLASMA. Kronast, B. (Institut fuer Plasmaphysik, GmbH, Garching, Ger.). 13p. (CONF-660438-3). ORAU. Gmelin, AED-CONF-66-078-8.

Fron International Quantum Electronics Conference, Phoenix, Ariz.

The results of theoretical investigations on this subject are briefly summarized. By variation of a single parameter the theory successfully describes the entire range from classical Thomson scattering to a type of scattering where collective phenomena are increasingly evident. On the basis of this classification an account is given of measurements of classical Thomson scattering in plasmas and experiments to investigate collective phenomena in the scattering spectrum of plasma. (auth)

38337 PROCESS FOR THE GENERATION, COMPRESSION, AND CONCENTRATION OF A PLASMA. Linhart, Jiri George German Patent 1,216,447. May 12, 1966. Priority date Dec. 3, 1959, Belgium.

A process is described for producing energy by nuclear fusion using a cylindrical reactor, in which a high degree of vacuum has previously been set up, and introducing into it a gas or a mixture of gases through orifices situated in the curved wall of the reactor. The gas or mixture of gases, which takes the form of a cylindrical layer, is then sub-

jected to an electrical discharge across the ends of the reactor in a direction parallel to its axis. (Gmelin Inst.)

38338 MICROWAVE PLASMA DENSITY MEASUREMENT SYSTEM. Heald, M. A. (to U. S. Atomic Energy Commission). U. S. Patent 3,265,967. Aug. 9, 1966.

This patent relates to a microwave system for producing a continuous output signal directly corresponding to the density of a plasma when the plasma is transparent to the microwaves and indicating unambiguously when the plasma is opaque to the microwave. A frequency modulated signal source having a highly frequency sensitive microwave bridge with crystal detectors are employed for generating a carrier frequency which is phase modulated by the time varying plasma sample in one arm of the bridge and connected to the detectors seriatim in a chain is a frequency modulation receiver, comprising a differential amplifier, a limiter, a discriminator and a video amplifier, and an electronic integrator. (AEC)

38339 APPARATUS FOR PRODUCING AND PURIFYING PLASMA. Baker, William R.; Halbach, K. (to U. S. Atomic Energy Commission). U. S. Patent 3,265,583. Aug. 9, 1966.

This patent relates to a magnetohydrodynamic apparatus producing more pure plasma. A short center electrode, uniquely shaped to minimize plasma impingement thereon, extends into one end of an evacuated cylinder. Gas injected through the electrode forms plasma which is directed towards a magnetic containment field at the opposite end of the cylinder by a mirror field. Cylinder diameter near the electrode is fixed, in relation to the electric and magnetic fields, so that the orbits of heavy impurity particles intercept the cylinder while lighter plasma particles clear the wall and progress to the containment field. The electric field is removed before plasma leaves the electrode region and a pulsed magnetic gate blocks remaining impurities which follow the plasma towards the containment region. (AEC)

38340 HIGH DENSITY PLASMA GENERATOR. Swartz, George A. (to Radio Corp. of America). U. S. Patent 3,258,633. June 28, 1966. Filed Sept. 6, 1963.

An apparatus for producing a confined plasma having an ion density greater than 10^{14} ions/cm^3 and an ionization greater than 10% includes a hollow anode, thermionic cathodes facing each end of the anode, and a gas-tight envelope enclosing the anode and cathodes. An alkali metal vapor, preferably Cs, is produced in the envelope, and the pressure of the vapor is adjusted to such a value that the neutral Cs density in the anode is at least 10^{15} neutrals/cm^3. At least portions of the inner surface of the anode have an electron work function higher than the ionization potential of the vapor, and the temperature of the anode surface is maintained at a temperature sufficient to ionize the vapor by contact with the surface portion. An axial magnetic field is established in the region between the cathodes. The anode and both the cathodes have external terminals for applying potentials. (B.L.M.)

38341 FUSION-RESEARCH APPARATUS. Kerst, Donald W. (to General Dynamics Corp.). U. S. Patent 3,258,401. June 28, 1966. Filed July 23, 1962.

A fusion research device includes a toroidal discharge or containment vessel made of a high temperature material, such as ceramic, and provided with a radially extending conduit which is connected to suitable means for filling the discharge tube with a gaseous material and for maintaining the tube at the desired pressure. Disposed sequentially about the discharge tube are a number of generally tubular segments or members of a conductive material, such as Cu. Each tubular member is grounded by one of a number of return transmission plates, which are connected to corresponding ends of the tubular members. The other end of each tubular member is connected to one of a number of supply transmission plates, each of which includes a number of spaced, conductive strips extending from the supply connection to the tubular member associated with that transmission plate with the conductive strips being connected to the periphery of the tubular members. The conductive strips are sized and spaced so that each strip forms an inductance that distributes the current to the associated member in accordance with the current requirements of the separate areas to minimize transverse fields at the gaps between the tubular members. (B.L.M.)

38342 EFFECTS OF THE SHEATH ON PLASMA RESONANCE. Leavens, William Manson Jr. La Jolla, San Diego, Calif., Univ. of California, 1965. 55p.

Thesis.

Plasma resonance spectra were calculated for a realistic model in the absence of a magnetic field by the conductivity kernel method. The results give a reasonably clear picture of the nature of plasma resonance. The plasma is nonuniform and bounded by a sheath, and has diameter a small compared to $2\pi/k$, the free space wavelength. The scattering resonances at the lower frequencies, e.g., the main resonance, are produced by charge density perturbations concentrated at relatively large radii in the plasma. To zeroth order in ka only dipole oscillations are excited by incident plane waves. The problem actually solved is that of the steady, driven, oscillations of a thin one-dimensional slab of Maxwellian plasma, with a wall at $x = 0$, which emits electrons and absorbs all electrons that return to $x = 0$, and an insulated wall at $x = x_w$, which also absorbs electrons. The unperturbed electric field, everywhere in the positive x-direction, is uniform in the plasma, $0 \leq x \leq s$, and joins smoothly to a harmonic oscillator field in the sheath, $s \leq x \leq x_w$. The plasma is excited into steady oscillations by a uniform driving field. The ions are stationary and distributed so as to satisfy Poisson's equation. Collisions are neglected. Each electron traverses the plasma (from zero to its turning point and back) only once. The conductivity kernel equation is obtained by using the linearized Vlasov equation to express the source terms in Maxwell's equations. A computer program that forms the conductivity kernel efficiently was developed. The results show that the sheath has a dominant effect on plasma resonance. Not only is much of the Landau damping that determines the line shapes concentrated near the sheath, but also the resonance frequencies are determined by the properties of the sheath and the neighboring regions of the plasma. (TCO)

38343 APPROACH TO EQUILIBRIUM OF A HOMOGENEOUS PLASMA IN A UNIFORM MAGNETIC FIELD. Haggerty, Michael John. Vancouver, Can., Univ. of British Columbia, 1964. 171p.

Thesis.

The theory of Prigogine and Balescu was applied to a homogeneous single-species plasma in a static uniform magnetic field. A kinetic equation was obtained for the one-particle velocity distribution, which is assumed initially isotropic in directions perpendicular to the field. The only stationary solutions of the kinetic equation are the Maxwellian equilibrium distributions, and an H- theorem was established. The neglect of collisions of the order of duration of one cyclotron period or less (a strong magnetic field approximation) modifies the kinetic equation so that it no longer predicts any relaxation of the velocity components parallel to the magnetic field. An equation for the binary correlation function was obtained in terms of the one-particle velocity distribution, which is in turn determined by the kinetic equation. Equations for the binary spatial correlation function and the binary correlation function for the guiding centers were also obtained. It is demonstrated that the binary spatial correlation function represents the well-known Debye-screened equilibrium correlations when the one-particle velocity distribution is the equilibrium distribution. The assumptions and approximations of the theory are clearly stated, and are discussed in some detail. (Dissertation Abstr.)

38344 EXPERIMENTAL INVESTIGATIONS OF PLASMAS IN ELECTROMAGNETIC SHOCK TUBES. Simpkinson, William Vaughan. Vancouver, Can., Univ. of British Columbia, 1964. 80p.

Thesis.

Attempts to produce shock-heated plasmas in electromagnetic shock tubes are described. Various electrode configurations were tried but no improvement was ob-

served. Some measure of success was attained with an electrodeless driver on the shock tube. Kerr cell photographs showed that with argon in the tube a shock wave appeared to be formed ahead of the discharge plasma. The shock speed was much slower than the speed of the advancing luminous front in the tubes with electrodes. No shock wave could be observed with helium. With argon in the electrodeless tube radiation could be observed from the gas ahead of the shock wave. Time-resolved spectroscopic measurements on this radiation allowed rough determination of electron density and of the population of excited states of argon atoms and ions ahead of the shock front. The values of electron density and temperature expected behind the shock front were calculated from shock theory, taking into account the preheating of the gas. The expected values agreed well with the electron density and temperature determined from spectroscopic measurements on the shock plasma. The study of the precursor radiation was continued in a shock tube with electrodes. In this tube the driving discharge was more luminous and the excitation and ionization of helium and argon ahead of the luminous front could be more readily observed than in the electrodeless tube. The number densities of helium atoms in various excited states were determined from the time-resolved line intensities before and after the passage of the luminous front. The calculation indicates that ahead of the luminous front there is not sufficient time to attain equilibrium. For the high electron density found behind the luminous front, the equilibrium distribution is expected to be reached in times shorter than the observation times, in disagreement with the behavior observed. (TCO)

38345 PLASMA FLOW MODES IN ELECTRIC SHOCK TUBES. Vermillion, Robert Everett. Nashville, Vanderbilt Univ., 1965. 81p.

Thesis.

An electric shock tube was constructed, which employs an exploding wire discharge plasma source, in which three distinct flow modes are observed. These flow modes are investigated experimentally and shown to be compatible with (a) diffusion flow into a vacuum below 10^{-2} torr, (b) discharge plasma flow with no separated shock wave, and (c) discharge plasma flow with a separated shock wave. It is postulated that the existence of the last two modes is determined by whether or not the contact surface exhibits Taylor instability. The Taylor criterion is adapted to apply to the contact surface in a shock tube, and the results are shown to be in general agreement with the observations made. The evidence indicates that the flow consists of a shock wave detached from the discharge plasma if the contact surface is Taylor stable. If the contact surface is Taylor unstable, the discharge plasma is mixed forward into the shock wave and no contact surface exists. The mixed flow differs from conventional shock-tube flow not through the absence of a shock, but through the absence of a contact surface. The strong deceleration in an electric shock tube is found to be due to the flow behaving as a blast wave. Calculations from the assumed Taylor criterion indicate the mass of the material scoured from the electrodes is an important factor in determining the type of flow. The density of the discharge plasma should be low in a strongly attenuating type of flow to assure early stability of the contact surface. It is suggested that the higher Mach number tubes may tend to have a higher density of discharge plasma. Such a mechanism would account for no shock-driver flow in many high Mach number electric shock tubes (Dissertation Abstr.)

38346 ION BEAM-PLASMA INTERACTIONS. Dunnill, William Arthur. Gainesville, Fla., Univ. of Florida, 1965. 114p.

Thesis.

Bohm and Gross have shown that a constant-velocity homogeneous beam of charged particles moving through a homogeneous plasma is unstable. Attempts are made to study the radio frequency noise associated with some of these ion-beam-enhanced instabilities. The work concerning possible oscillatory systems is divided into three phases. The first phase is an investigation of high-energy beam-plasma combinations in which the beam is a hydrogen ion beam in the energy range from 10 to 20 kev with plasmas formed by ionizing air, argon, helium, and hydrogen. The second phase concerns a low-energy ion beam in the range of several hundred volts. Finally, a discharge of a reflex type is studied as a beam-plasma interaction system. For this system both an ion beam or stream and an electron beam are present at low energies with relatively large current densities. It is found that the ion beam alone in a plasma appears to be relatively stable as long as there are electrons present of low thermal energy, which have no special restrictions along the ion beam path. It is also found that diffusion-limited, rather than space-charge-limited, steady ion beams can be extracted from an arc without the use of any external accelerating electrodes. The diffusion current of this low-energy beam is directly coupled to strong oscillations in the arc column. Finally, the oscillations observed in the reflex discharge are found to be adjustable by varying the magnetic field, the discharge length, and the discharge diameter. (Dissertation Abstr.)

38347 SOME ASPECTS OF HIGH β PLASMA CONFINEMENT. Morse, Richard Lee. La Jolla, San Diego, Calif., Univ. of California, 1965. 87p.

Thesis.

The formation of the electromagnetic sheath separating a field-free Maxwellian plasma from a confining field is treated by an adiabatic approximation. It is found that the condition imposed by the approximation is not severe. Solutions are shown for several values of the ion-electron temperature ratio. The problem is done in plane symmetry and with the collisionless approximation. The question of stability is not considered. A cylindrical pinch is treated in the approximation that plasma and field are separated by a thin surface. The external B field is taken to be completely longitudinal as in linear θ-pinches. Particles move in straight lines inside of the surface and bounce off of it specularly. Anisotropies in the velocity distribution are shown to result in instabilities of the mirror and fire hose types as well as flute instabilities of a type that has no analog in small larmor radius theory. Growth rates are obtained and a region of positive stability is found for a particular class of unperturbed distribution functions. The effect of a small net angular momentum is considered. (Dissertation Abstr.)

38348 PARTICLE KINETICS OF PLASMAS. Shkarofsky, I. P.; Johnston, T. W.; Bachynski, M. P. Reading, Mass., Addison-Wesley Publishing Company, 1966. 526p. $17.50.

The 10 included chapters describe in some detail the following: particle kinetics of plasmas, Boltzmann equation, expansion of the electron distribution function, applications of the Boltzmann equation to electron-atom interactions, elastic collisions and scattering cross sections, bremsstrahlung and h-f electric conductivity, Coulomb collisions and the Fokker-Planck equation, transport properties of plasmas, foundations of magnetohydrodynamics, and collisionless plasmas in strong magnetic fields. (M.O.W.)

Shielding

38349 (AD-636788) MONTE CARLO CALCULATION OF SELF-SHIELDING BY ENCAPSULATED GAMMA-RAY SOURCES. Nuclear Radiation Shielding Studies Report No. 3. Preiss, K. (Illinois Univ., Urbana). Aug. 1966. Contract OCD-OS-63-66. 50p. CFSTI $2.00 cy, $0.50 mn.

The dimensions of many encapsulated gamma ray sources used in experiments are not small compared with the mean-free-path-length of the radiation within them. For this reason, the emitted radiation will not be at the source energies only, but will be distributed in a continuous spectrum. Furthermore, if the source is cylindrical, the emitted radiation will not be isotropically distributed about the source. A calculation by the Monte Carlo method to find the energy and angular distributions of photons emitted

from a cylindrical or spherical encapsulated source is described. Computed results are compared with experimental observations of energy and angular distribution, and show good agreement. Calculated spectra for typical cylindrical sources of ^{60}Co encapsulated in iron are given. (auth)

38350 (ORNL-P-2310) SURVEY OF THE U. S. SHIELDING CALCULATIONAL METHODS AND PROGRAMS. Penny, S. K. (Oak Ridge National Lab., Tenn.). [1966]. Contract W-7405-eng-26. 16p. (CONF-660442-1). Dep. mn. CFSTI $1.00 cy, $0.50 mn.

From European Nuclear Energy Agency Seminar-Workshop on Computer Programs for Shielding Calculations, Ispra, Italy.

Changes in the field of shielding calculations and computer techniques are reviewed. The evaluation of different coding systems is discussed and the future of shielding calculational techniques is considered. (J.H.M.)

38351 DISTRIBUTION OF FAST FISSION NEUTRONS ALONG STRAIGHT CYLINDRICAL CHANNELS IN WATER. Mashkovich, V. P.; Nikolaev, A. N.; Sakharov, V. K.; Sinitsyn, B. I.; Tsypin, S. G. At. Energ. (USSR), 20: 416-18(May 1966). (In Russian).

The fission-neutron distribution in water along straight cylindrical channels of 144 to 190 mm in diameter was investigated using neutron threshold detectors containing Al and S. The data for the distribution of fast fission neutrons were taken along the axis of a right-cylindrical channel as well as around its circular contour, and an infinite plane monoenergetic fission-neutron source was used. The data presented can be used for experiments on neutron distributions from sources along step-like channels. (G.O.Y.)

38352 DETERMINATION OF FAST NEUTRON PENETRATION IN CONCRETE BY MEASUREMENT OF THE SCATTERED FIELD OF A COLLIMATED NEUTRON BEAM. Bindewald, H. Hanover, Technische Hochschule, 1965. 56p. $2.00 Gmelin, AED-Diss. 65-317.

Thesis.

The scattered field of a neutron beam was measured using proton-recoil proportional counters. Using a solution of the Boltzmann equation, a formula is given which describes the experimental data if 2 parameters are chosen suitably. From these parameters the transport mean free path, diffusion length, and other material constants of concrete are determined. (Gmelin)

Solid State Physics

See also CHEMISTRY — Inorganic and Physical Chemistry
METALS, CERAMICS, AND OTHER MATERIALS — Properties and Structure

Refer also to abstracts 37736 and 37819–37821.

38353 (BNWL-SA-247) DERIVATION OF AN EXPRESSION FOR RADIATION-INDUCED ELECTRICAL CONDUCTIVITY IN IONIC INSULATORS. Dau, Gary J. (Battelle-Northwest, Richland, Wash. Pacific Northwest Lab.); Davis, Monte V. (Arizona Univ., Tucson). July 16, 1965. Contract AT(45-1)-1830. 20p. Dep. mn. CFSTI $1.00 cy, $0.50 mn.

In the derivation of the conductivity expression, a general theoretical development for the production of conduction band electrons by gamma photons is presented. When charge carrier mobility is considered, the development was limited to crystals having ionic bonding. Due to difficulty in evaluating constants in the developed expression, all constants were combined into one constant, which was considered to be independent of temperature and radiation. This constant was evaluated experimentally. A model was developed for predicting the conductivity of ionic insulators as a function of temperature and radiation dose rate. The model is $\sigma(T,P) = \sigma(T) + PG \exp(-W/kT)(T)^{\frac{1}{2}}$, where the first term on the right represents the ionic conductivity of the material without a radiation field present and the second term describes the radiation-induced conductivity. The term P represents the gamma photon dose rate in R hr^{-1}, G is an experimentally determined constant, and W represents the energy necessary to raise trapped electrons into the conduction band. The temperature dependence of the mobility is represented by $(T)^{\frac{1}{2}}$. Evaluation of experimental data for alumina gave W = 0.086 ± 0.014 ev and $G = 7.4 \times 10^{-21}$ $(ohm^{-1}cm^{-1}K^{\frac{1}{2}}R^{-1}$ hr). (auth)

38354 (FTI-244/T-027) O VZAIMODEISTVII PLAZMENNYKH I SPINOVYKH V FERROMAGNITNYKH POLUPROVODNIKAKH I METALLAKH. (Interaction of Plasma Oscillations and Spin Waves in Ferromagnetic Semiconductors and Metals). Bar'yakhtar, V. G.; Savchenko, M. A.; Stepanov, K. N. (Akademiya Nauk Ukrainskoi SSR, Kharkov. Fiziko-Tekhnicheskii Institut). 1965. 18p. Dep. mn.

The coupled spin, plasma, and electromagnetic waves in ferromagnetic semiconductors and metals were discussed for arbitrary directions of wave propagation. Following a brief historical introduction, theoretical expressions are developed for waves in spatially nondispersive media, in ferromagnetics with "easy axis" magnetic anisotropy, and in ferromagnetics with "easy plane" magnetic anisotropy. The coupled electrostatic and spin oscillations and the interaction between spin and cyclotron waves, expressions for indices of reflection, and the transparency regions are described in detail. The behavior of oscillation frequencies as functions of the wave vector is also given. (JPRS)

38355 (ITEF-355) NEUPRUGOE RASSEYANIE NEITRONOV GEMATITOM. (Inelastic Scattering of Neutrons by Hematite). Alikhanov, R. A. (Gosudarstvennyi Komitet po Ispol'zovaniyu Atomnoi Energii SSSR, Moscow. Institut Teoreticheskoi i Eksperimental'noi Fiziki). 1965. 20p. Dep. mn.

The spectrum of hematite spin waves (in α Fe_2O_3 from the Ural Shabry mines) was investigated using a three-crystal spectrometer described earlier. The experiment was carried out in the range up to 0.64 A^{0-1} and 5.3×10^{-3} ev of transferred momentum and magnon energy, respectively, and it yielded two branches with energy gaps caused by magnetic anisotropy. The widths of the gaps on the two branches were $(1.3 \pm 0.7) \cdot 10^{-3}$ and $(0.4 \pm 0.15) \cdot 10^{-3}$ ev while the respective spin wave velocities were found to be $(1.3 \pm 0.07) \cdot 10^{6}$ cm/sec and $(4.6 \pm 0.5) \cdot 10^{5}$ cm/sec. The article concludes with a comprehensive discussion of the results and a comparison with data gathered by other, mostly Western authors. Discrepancies may be due to different magnetic properties of samples originating in different mines and due to differences in methods of selecting the magnon wave vectors. (JPRS)

38356 (LA-3510) DYNAMICS OF DISORDERED HARMONIC LATTICES. Payton III, Daniel N. (Los Alamos Scientific Lab., Univ. of California, N. Mex.). May 1966. Contract W-7405-eng-36. 166p. Dep. mn. CFSTI $5.00 cy, $1.00 mn.

Thesis. Submitted to Univ. of Missouri, Columbia.

Extensive numerical and analytic studies of vibrational spectra, normal modes, thermodynamic properties, and dynamical properties of harmonic systems with varying degrees of substitutional disorder were made. The effects on observable properties of random mixtures of two or more species of atoms with differing masses and differing couplings to nearest- and next-nearest-neighbors were investigated. Using the IBM-7030 digital computer, spectra for linear chains of 100,000 atoms were obtained. Calculations in two and three dimensions were limited to arrays of approximately 1000 atoms. Varying composition, mass ratio, and order affect the spectra in two and three dimensions in ways analogous to those effected in the linear chain. A physical interpretation of the complex nature of the disordered spectrum is given. The effects of disorder

on the dynamics of binary disordered harmonic chains were studied and found to be quite pronounced. (auth)

38357 MAGNETIC STRUCTURE OF Er_2O_3. Bertaut, Erwin-Felix; Chevalier, Raymond (CEN, Grenoble, France. Laboratoire d'Electrostatique et de Physique du Metal, Grenoble, France). Compt. Rend., Ser. B, 262: 1707-10(June 27, 1966). (In French).

The non-collinear magnetic structure of Er_2O_3 agrees with the predictions of the theory of groups and corresponds to the identity representation of the I a 3 group The spins on the 8b and 24d sites are respectively according to the symmetry axes $\bar{3}$ and 2. (tr-auth)

38358 DAMPING OF SPIN WAVES IN A COLLECTIVE MODEL. Shi, Yan (Central Scientific-Research Inst., Academy of Sciences, Arm. SSR). Izv. Akad. Nauk Arm. SSR, Fiz., 1: 20-4(1966). (In Russian).

The damping of a spin wave in a collective model by means of disintegrating into two separate excitations with opposite spins is investigated. It was found that the damping depends exponentially upon the temperature and the quasi-impulse of the spin wave. An analogy with Landau damping of classical plasma oscillations is observed. The damping is sensitive to the crystal structure. (auth)

38359 SOME PROPERTIES OF YTTRIUM BORIDES. Meerson, G. A.; Zhuravlev, N. N.; Manelis, R. M.; Runov, A. D.; Stepanova, A. A.; Grishina, L. P.; Gramm, N. V. (Moscow State Univ.). Izv. Akad. Nauk SSSR, Neorg. Mater., 2: 608-16(Apr. 1966). (In Russian).

The thermionic and crystallographic constants of the borides YB_4, YB_6, and YB_{12} were measured, and the behavior of these materials in a vacuum at elevated temperatures was studied. The borides were prepared by the vacuum thermal method by reducing Y_2O_3 with B. YB_4 is indexed in a tetragonal lattice with constants a = 7.12, c = 4.04 ± 0.05 Å. YB_6 and YB_{12} are indexed in a cubic lattice with constant a = 4.102 and 7.506 ± 0.002 Å, respectively. It was shown that only YB_4 is stable during high-temperature treatment (up to 2750°K); YB_6 and YB_{12} decompose to form YB_4. The microhardness and strength of the borides decrease in the series $YB_4 \rightarrow YB_6 \rightarrow YB_{12}$ Measurements of the thermionic emission showed that the highest density of the emission current was that of YB_4 (0.284 amp/cm^2 at 1890°K). Currents of 9.68×10^{-4} to 2.01×10^{-5} amp/cm^2 can be obtained from YB_6 and YB_{12} on Ta substrates at maximum operating temperatures of 1790 and 1730°K, respectively. The work function (φ_0) increases from 3.2 to 5.31 to 5.36 in the series $YB_4 \rightarrow YB_6 \rightarrow YB_{12}$. The emissive properties depend substantially on the phase composition of the material. In their emissive properties, the yttrium borides studied are inferior to LaB_6. (auth)

38360 SNOEK ATMOSPHERE DISLOCATION PINNING IN TANTALUM. Baker, G. S. (Aerojet-General Corp., Sacramento, Calif.). J. Appl. Phys., 37: 2983-4(July 1966).

Snoek pinning of dislocations due to oxygen in tantalum was investigated using internal friction and simultaneous deformation techniques. The magnitudes of the pinning in the two oxygen concentrations used (5 ppm and 100 ppm) were found to be approximately 20 kg/cm^2 and 150 kg/cm^2, respectively. This shows that Snoek pinning can contribute a significant fraction of the yield stress in material with high concentrations of dissolved interstitials. (auth)

38361 VACANCY AND INTERSTITIAL CLUSTER PRODUCTION IN NEUTRON-IRRADIATED α IRON. Beeler, J. R. Jr. (General Electric Co., Cincinnati). Contract AT(40-1)-2847. J. Appl. Phys., 37: 3000-9(July 1966).

Vacancy cluster and interstitial cluster production in α iron was computed by simulating atomic collision cascades on a computer. Each collision was determined by the Erginsoy-Vineyard interatomic potential for α iron. The computed densities of displacement spikes produced by primary knock-on atoms with energies above 3 kev correlated qualitatively with the degrees of irradiation hardening observed by Harries et al. in ferritic steel specimens for five different neutron energy spectra. The computed total displaced atom densities did not correlate with the degrees of irradiation hardening observed by Harries et al. Annealing simulations indicated that displacement spikes produced by primary knock-on atoms with energies below 2.5 kev should not contribute importantly to irradiation hardening in specimens irradiated at the temperature (~60°C) adopted by Harries et al. The volume of collided atoms involved in a collision cascade usually exhibited a marked orientation along ⟨110⟩ directions as did the associated displacement spike. Spikes are therefore oriented in the primary slip planes of α iron and each could serve in toto as a barrier to dislocation motion. (auth)

38362 MOESSBAUER STUDY OF THE STRUCTURE AND DECOMPOSITION OF WUSTITE. Shechter, Hanan (Weizmann Inst. of Science, Rehovoth, Israel); Hillman, Peter; Ron, Moshe. J. Appl. Phys., 37: 3043-7(July 1966).

A series of Mössbauer, x-ray, and magnetic measurements was made on wustite ($Fe_{1-x}O$). The main new results are: The dependence of the Mössbauer, quadrupole splitting on heat treatment is very similar to that of the atomic constant, confirming Hoffman's conclusions on the variation of x. The Zeeman Mössbauer lines of untreated wustite below the Curie temperature are completely smeared out; for a sample treated so as to give minimum quadrupole splitting (minimum x) these lines appear. In a heat-treated sample a Zeeman splitting in the Mössbauer spectrum is observed well above the bulk wustite Curie temperature. This is interpreted as the imposition by the magnetic decomposition products of a magnetic ordering on the otherwise paramagnetic residual wustite with which they are in intimate contact. (auth)

38363 LOW-ENERGY-ION-BOMBARDMENT DAMAGE IN GERMANIUM. MacDonald, R. J.; Haneman, D. (Univ. of New South Wales, Sydney). J. Appl. Phys., 37: 3048-56 (July 1966).

The depth of damage induced in Ge films by ions of energies of 200 to 1000 ev was measured for He, Ne, Ar, and Kr bombardment, the depth decreasing from heavier ions. The effects exhibit saturation at critical ion dosages. From the results the damaged layer is deduced to consist of two main regions. The one nearer the surface consists mainly of lattice disorder plus trapped gas, which extends to a depth of approximately 10 atomic layers at 1000-ev ion energy. The second, lower region consists mainly of gas atoms trapped in the relatively ordered lattice, the depth of this region increasing with decreasing ion mass. It is concluded that focused atom emission observed in diamond-type lattices is due to the undisturbed surface region structure and focusing is weakened by the damage induced by ion bombardment. (auth)

38364 RECOMBINATION AND TRAPPING IN ^{60}Co GAMMA-IRRADIATED n-TYPE GERMANIUM. Streetman, B. G. (Oak Ridge National Lab., Tenn.). J. Appl. Phys., 37: 3145-52(July 1966). (ORNL-P-2019).

Measurements of carrier lifetime from 110° to 330°K were made on samples of Sb- and As-doped Ge after irradiation at 77°K and subsequent isochronal annealing. A recombination level near the center of the bank gap and a trapping level were introduced by the irradiation, and a new trap was created by the anneal in each case. The recombination centers constituted a small fraction of the total defect density. Energy-level positions and capture cross sections are presented for the observed levels. It is found that the trapping levels exhibit a multiple negative charge at low temperatures, and one of the traps is tentatively associated with the Sb-divacancy complex. The annealing stages are compared with those observed in the investigation of other properties, and several stages are found to resemble those resulting from the formation and breakup of composite defects containing oxygen. (auth)

38365 PRODUCTION AND ANNEALING OF DEFECTS IN 6- TO 88-Mev ELECTRON-IRRADIATED n-TYPE GERMANIUM. Fischer, J. E.; Corelli, J. C. (Rensselaer Polytechnic Inst., Troy, N. Y.). J. Appl. Phys., 37: 3287-97(July 1966).

Two classes of defect acceptor levels, three classes of minority hole traps, and recombination centers are introduced by 48-Mev-electron bombardment of As- and Sb-doped (n-type) germanium at 85°K. The recovery of traps and acceptors occurs together in five stages, suggesting that the traps and acceptors are due to the same defects. The stages are centered at 150, 200, 360, 460, and about 540°K. The dominant acceptor energy levels are at or below the middle of the forbidden gap, and the dominant trapping energy levels are within 0.16 ev of the valance band. Less than 15% of the removed electrons are trapped by a level 0.20 ev below the conduction band. The recombination centers recover completely below 200°K. After 300°K irradiation with 6-, 47-, and 88-Mev electrons, only one trapping level, located at 0.10 ± 0.01 ev above the valence band in all samples (As- or Sb-doped), is observed. The introduction rate and recovery behavior of this trapping level are independent of As and Sb concentration up to 2×10^{15} donors/cm^3. The decay of excess carriers is analyzed in terms of the large-injection model due to Baicker. The applicability of this model is criticized in light of the present results. The effect of arsenic and antimony on the nature and recovery of the various defects is investigated. The results are compared with those obtained in low-energy-electron (≲1 Mev) and ^{60}Co gamma irradiation. (auth)

38366 X-RADIATION ALIGNMENT OF QUARTZ CRYSTALS FOR IMPROVED HYPERSONIC PROPAGATION. Young, John D. (General Electric Co., Syracuse, N. Y.); Newkirk, John B. J. Appl. Phys., 37: 3304-12 (July 1966).

The generation and detection of a large number of reverberating acoustic echoes in crystalline quartz at liquid-helium temperatures and at frequencies above 1 Gc require an end-face parallelism alignment less than 0.4 sec of arc for 3-mm-diam rods. Parallelism angles of this magnitude are beyond the present commercial capability of optical companies to process quartz rods. An x-radiation technique which induces a permanent bend in quartz crystals and, when applied in a specific azimuth direction, makes the end faces more nearly parallel is described. The acoustic response of quartz crystals at 10 Gc and 4.2°K is used as an indicator of end-face parallelism. The experimental acoustic results show the effects of thermal annealing of quartz crystals the effects of x radiation applied to the specimens in various directions, the effects of increasing dosage of x irradiation, and the effects of rotating the crystal while irradiating it with x rays. The 10-Gc acoustic response of quartz rods was improved from 3 to 7 times by the x-ray correction of the end-face parallelism. (auth)

38367 VACANCY AND INTERSTITIAL CLUSTERS IN NEUTRON-IRRADIATED NICKEL. Brimhall, J. L.; Kissinger, H. E.; Mastel, B. (Battelle-Northwest, Richland, Wash.). J. Appl. Phys., 37: 3317-18(July 1966).

Preliminary observations on neutron-irradiated nickel are reported. These experiments show that both vacancy- and interstitial-type defects are produced in nickel irradiated with neutrons at 40°C. A displacement spike mechanism is used to explain the short-range mobility and subsequent clustering of vacancies. Annealing causes breakup of the vacancy clusters into free vacancies, annihilation of the interstitial clusters and loops, and growth of vacancy loops. Photographs of defect clusters in nickel irradiated with neutrons are shown. (J.F.P.)

38368 POINT DEFECT GENERATION IN LiF BY PLASTIC DEFORMATION AND X IRRADIATION AT LOW TEMPERATURE. Wiegand, D. A.; Turner, R. C.; Smoluchowski, R. (Carnegie Inst. of Tech., Pittsburgh). J. Phys. Chem. Solids, 27: 1251-6(Aug. 1966).

LiF crystals were plastically deformed in compression while at liquid nitrogen temperature and were subjected to x irradiation without intermediate warming. The rates of formation of F and self-trapped hole centers were enhanced in the deformed samples in the early stages of irradiation, but were not influenced at longer irradiation times. These results can be simply interpreted in terms of the generation of negative ion vacancies during plastic deformation and the subsequent trapping of electrons at these vacancies to form F centers during irradiation. The rate of formation of self-trapped holes is enhanced because the rate of electron trapping is enhanced. The saturated enhancement of the self-trapped hole band is proportional to the saturated enhancement of the F band. Since enhancement of the F band was not observed as a result of plastic deformation at room temperature, these results suggest that negative ion vacancies produced during deformation at room temperature are sufficiently mobile to cluster, annihilate or otherwise become unavailable for F center formation during irradiation. The results at low temperature at longer times of irradiation indicate that the rate of generation of new negative ion vacancies during irradiation is insensitive to dislocation density as reported previously for room temperature irradiation. The saturated enhancements of the F and self-trapped hole bands at low temperature as a function of plastic deformation indicate a threshold for vacancy generation at approximately 1% compression for the conditions of this experiment. (auth)

38369 MAGNETIC AND CRYSTALLOGRAPHIC STUDIES ON RARE EARTH GERMANIDES. Sekizawa, Kazuko (Nihon Univ., Tokyo). J. Phys. Soc. Jap., 21: 1137-42(June 1966).

Crystallographic and magnetic studies were made on germanides of rare earth metals Nd, Pr, Sm, Gd, Tb, Dy, Ho, and Er in the composition range near 1:2. The compound RGe_2(R = Gd, Tb, Dy) has an orthorhombic crystal structure, of which the atomic arrangement is unknown. Through the crystallographic survey, four nonstoichiometric phases were found; $DyGe_{1.62}$ with the C32 type of structure (the low-temperature phase), $DyGe_{1.62}$ with the C_c type of structure (the high-temperature one), and $GdGe_{1.67}$ and $DyGe_{1.67}$ with the C_c type of structure. Compounds RGe_2 (R = Gd, Tb, Dy, Ho), $RGe_{1.67}$ (R = Gd, Dy), and $DyGe_{1.62}$, become antiferromagnetic at low temperatures. Compounds $NdGe_2$ and $PrGe_2$ are ferromagnetic as reported previously. Compounds $SmGe_2$ and $ErGe_2$ are paramagnetic above 4.2°K. The Néel temperature of $TbGe_2$ is 42°K, which is the highest among those of heavy rare earth germanides. (auth)

38370 MAGNETIC AND ELECTRIC PROPERTIES OF GdP, TbP AND DyP. Yaguchi, Koichi (Totsuka Works Hitachi Ltd., Yokohama, Japan). J. Phys. Soc. Jap., 21: 1226(June 1966).

The magnetic susceptibility of GdP, TbP, and DyP was measured between liquid nitrogen temperatures and 500°K, and the electric resistivity was measured between liquid nitrogen temperatures and 320°K. The crystal structure and lattice constants were also found. (J.F.P.)

38371 ATTENUATION OF THERMAL NEUTRONS BY PHONONS IN A SINGLE CRYSTAL. I. Kashiwase, Yasuji (Univ. of Nagoya, Japan). J. Phys. Soc. Jap., 21: 1263-72(July 1966).

The effect of thermal vibration on the transmission or reflection of neutrons in a single crystal was investigated theoretically. The formula of imaginary potential which is used to get the absorption coefficient was obtained as a result of thermal inelastic scattering of neutrons. It was made clear that the surface integral taken over the scattering surface is necessary to obtain the imaginary potential of a single crystal for one-phonon inelastic scattering of slow neutrons. (auth)

38372 EFFECTS OF PROTON BOMBARDMENT ON CaF_2 CRYSTALS. Kubo, Kazuko (Japan Atomic Energy Research Inst., Tokyo). J. Phys. Soc. Jap., 21: 1300-3 (July 1966).

New features were observed in synthetic CaF_2 crystals which were colloidally colored by intense proton bombardment. There were (1) a surface of discontinuity at the end of the proton range, (2) a colloidally colored thin layer between the bombarded plane and the range end, and (3) the presence of a plane where the dislocations were most dec-

orated. These phenomena result from the inhomogeneous ionization and heat release during the proton penetration, and the atomic displacements and hydrogen introduction upon stopping of the protons in the crystal. (auth)

38373 STUDY OF THE ENHANCEMENT OF X-RAY COLORATION OF NaCl BY DIVALENT IMPURITIES. Ikeya, Motoji; Itoh, Noriaki; Okada, Touichi; Suita, Tokuo (Osaka Univ.). J. Phys. Soc. Jap., 21: 1304-9(July 1966).

The growth of F centers and the change of d-c conductivity by X irradiation were measured around room temperature in NaCl grown in chlorine atmosphere both pure and doped with Ca^{++}, Cd^{++}, Sr^{++}, and Mn^{++}. The enhancement of coloration by divalent impurities at room temperature was found to be proportional to the square root of the concentration of each impurity. It was also found that the ionic conductivity in doped NaCl was decreased by X irradiation in such a way that the decrease in the concentration of the positive ion vacancies was nearly equal to the increase in the F center concentration. From these results it was concluded that the isolated positive ion vacancies are the source of the F centers at the early stage of coloration. The temperature dependence of the formation rate of F centers in doped NaCl was measured and the activation energy 0.08 ± 0.01 ev was obtained. (auth)

38374 NMR MEASUREMENT OF INTERNAL FIELD AND ELECTRIC QUADRUPOLE INTERACTION IN FERROMAGNETIC Dy METAL. Kobayashi, Shun-ichi; Sano, Naokatsu; Itoh, Junkichi (Osaka Univ.). J. Phys. Soc. Jap., 21: 1456(July 1966).

Nuclear magnetic resonance signals of ^{161}Dy and ^{163}Dy were observed in Dy metal in the ferromagnetic state. Dysprosium is ferromagnetic below 85°K, the direction of the magnetization being in the c-plane. The sample was in the form of a powder of a few microns diameter with purity of 99.9%. The measurement was done at 1.4°K by the spin echo method. Nine resonance lines were observed in the frequency range of 200 Mc/sec to 2000 Mc/sec. (W.D.M.)

38375 MOESSBAUER EFFECT OF ^{119}Sn IN TELLURIUM. Baijal, J.; Baijal, Usha (Univ. of Roorkee, India). J. Phys. Soc. Jap., 21: 1457-8(July 1966).

It has been shown that the mean square displacement (X_2) of the radioactive impurity atoms in a host lattice at low temperatures ($T \to 0$) is given by: $(X_2)_{Imp}/(X_2)_{Host} = (M_{Host}/M_{Imp})^{1/2}$. ($X_2$) was calculated for the host material tellurium by using a linear lattice dynamical model which has also been used to explain the low-temperature behavior of the specific heat of tellurium. It is shown that within the experimental uncertainties one can conclude that $(X_2)_{Imp}$ in Te can be adequately described by considering only a mass change as in the above equation. (W.D.M.)

38376 EXAMINATION OF SURFACES BY SCANNING WITH CHARGED PARTICLES. Pierce, T. B.; Peck, P. F.; Cuff, D. R. A. (Atomic Energy Research Establishment, Harwell, Eng.). Nature, 211: 66-7(July 2, 1966).

The feasibility of examining surfaces by charged-particle scanning is discussed, and results obtained from scanning several test specimens are given. A beam of 1.80-Mev protons (0.008 μamp) collimated by an aperture 0.66 mm in diameter in a tantalum stop was used to scan target sheets of aluminum sandwiched between copper. Gamma rays emitted by the target during irradiation were detected by a 3 × 3 in. NaI(Tl) scintillator, and the output was fed to a 100-channel pulse-height analyzer. (W.D.M.)

38377 INTERSTITIAL DISLOCATION LOOPS IN BERYLLIUM OXIDE IRRADIATED AT HIGH TEMPERATURES. Rau, Robert C. (General Electric Co., Cincinnati). Nature, 211: 71-2(July 2, 1966).

Tilting experiments on chips from two specimens of beryllium oxide irradiated to 3.0 and 5.3 × 10^{20} nvt ($E_n \geq$ 1 Mev) at 1000°C and one irradiated to 3.5 × 10^{20} nvt ($E_n \geq$ 1 Mev) at 1200°C were carried out to determine the nature of the basal and prism plane loops. These specimens contained low enough basal loop concentrations (~10^{15}-10^{16}/cm^3) to allow the investigation of individual loop images. The results established that both the basal and prism plane loops are interstitial in nature, and are both of pure edge character with Burgers vectors perpendicular to their habit planes. Observations of stacking fault contrast within the basal loops for certain g vectors indicated that they are composed of an extra layer inserted into the C stacking positions in the normal ABAB hexagonal stacking sequence. (P.C.H.)

38378 THERMAL ANNEALING OF HEAVY ION DAMAGE IN COPPER. Hesketh, R. V.; Rickards, G. K. (Central Electricity Generating Board, Berkeley, Eng.). Phil. Mag. (8), 13: 1105-11(June 1966).

Dislocation loops and three-dimensional vacancy clusters are created by 150-kev Zn^+ bombardment. The number of vacancies in the clusters after successive isochronal anneals is measured by electron microscopy. At 200°C annealing is thought to take place by interstitial absorption. Thereafter, dislocation loops anneal with an activation energy close to that of self-diffusion, and clusters with an energy of about 1.3 ev. (auth)

38379 TEMPERATURE DEPENDENCE OF THE ABSORPTION OF FAST ELECTRONS IN COPPER. Goringe, M. J. (Cambridge Univ., Eng.). Phil. Mag. (8), 14: 93-7 (July 1966).

Measurements are reported of the temperature dependence of the absorption of 100 kev electrons in copper. The values of μ_0 and $\Delta\mu_g$ deduced from electron microscope images of thickness fringes are compared with the temperature variation predicted by Hall and Hirsch (Proc. roy. Soc. A: 158, 286(1965), and Phil. Mag., 12: 539(1965)). (auth)

38380 THERMAL ANNEALING OF LATTICE PARAMETER CHANGE IN LOW-TEMPERATURE NEUTRON-IRRADIATED ALUMINIUM. Sepp, A. (Technische Hochschule, Darmstadt, Ger.); Himmler, U.; Peisl, H.; Wenzl, H.; Waidelich, W. Phil. Mag. (8), 14: 131-3(July 1966).

Pure aluminium foils were irradiated by neutrons at 4.6°K. The defects created led to a change of the lattice parameter a. The relative change obtained with a dose of 2 × 10^{18} nvt was $\Delta a/a = (4.4_7 \pm 0.4) \times 10^{-4}$. Thermal annealing of the defects was observed in the form of three distinct annealing stages of the lattice parameter change. (auth)

38381 THE EFFECT OF WEAK BRAGG REFLECTED BEAMS ON THE ABSORPTION OF ELECTRONS. II. Hall, C. R. (Cambridge Univ., Eng.). Phil. Mag. (8), 14: 155-64(July 1966).

The apparent absorption of high energy electrons in crystals due to elastic scattering has been considered by a number of authors, and a numerical estimate of the magnitude of this effect by Hall and Hirsch (Phil. Mag., 12: 539(1965), based upon an approximate theory, suggests that this process makes a negligible contribution to the total. The approximation made in that treatment of considering the scattering kinematically is discussed and its effect upon the predictions of the simple theory investigated by performing some numerical calculations based upon the dynamical theory of diffraction. It appears that the mean apparent absorption due to this cause is overestimated by the simple theory, but that in special cases the apparent absorption can be much larger than the mean value. (auth)

38382 FIELD-ION MICROSCOPE STUDY OF NEUTRON IRRADIATED IRIDIUM. Fortes, M. A.; Ralph, B. (Cambridge Univ., Eng.). Phil. Mag. (8), 14: 189-94 (July 1966).

The structure of large clusters in neutron irradiated iridium as seen by field-ion microscope examination is described. Three distinct types of clusters were found. The first containing up to about 200 single vacancies appeared in a compact nearly spherical form while larger clusters collapsed to give dislocation loops. The third type consisted of a dispersion of single vacancies in a small volume such that about 30-40% of the lattice sites in this volume were unoccupied. (auth)

38383 ANTIFERROMAGNETIC RESONANCE IN UO_2. Daniel, M. R. (Univ. of Essex, Eng.). Phys. Lett., 22: 131-2(Aug. 1, 1966).

Resonant absorption of far infrared radiation in UO_2 was observed, which supports an existing theory of the first order magnetic phase change occurring at 30°K. (auth)

38384 HALL EFFECT IN 75 At. PERCENT Bi–25 At. PERCENT Sn ALLOY QUENCHED FILMS BELOW 47 DEG K. Bulow, H.; Schiller, C. K. (Wayne State Univ., Detroit). Phys. Lett., 22: 136-7(Aug. 1, 1966).

Hall effect measurements in quenched 75 at. % Bi–25 at. % Sn alloy films in the temperature range from 5.5°K to 47°K are presented and compared with earlier measurements in pure Bi films and results obtained from electron diffraction patterns of quenched 75 at. %, Bi–25 at. % Sn-films. (auth)

38385 HYPERFINE INTERACTIONS AND THE MAGNETIC FIELDS DUE TO CORE POLARIZATION IN ^{57}Fe. Childs, W. J.; Goodman, L. S. (Argonne National Lab., Ill.). Phys. Rev., 148: 74-8(Aug. 5, 1966).

Magnetic-dipole hyperfine-interaction constants were measured for the $^5D_{4,3,2,1}$ states of the ground term of ^{57}Fe in an atomic-beam magnetic-resonance experiment. The values are a_J = 38.0795(10), 26.351(2), 18.762(2), and 14.077(5) Mc/sec for J = 4, 3, 2, and 1, respectively. The deviations of the ratios of these a factors from theoretical predictions are ascribed to core polarization, and the implications of this assumption are discussed. (auth)

38386 QUADRUPOLE INTERACTION IN ^{121}Sb BY MOESSBAUER TECHNIQUES. Ruby, S. L. (Argonne National Lab., Ill.); Kalvius, G. M.; Snyder, R. E.; Beard, G. B. Phys. Rev., 148: 176-80(Aug. 5, 1966).

Mössbauer techniques were used to study the quadrupole resonance of ^{121}Sb in cubic Sb_2O_3 (senarmontite). The interaction constant was measured to be $e^2qQ = +557 \pm 20$ MHz; except for the sign, this had earlier been determined more accurately by electric-quadrupole-resonance measurements. The sign, which implies a negative electric field gradient, is consistent with a partially covalent bonding of the 5p electrons to the three nearly coplanar oxygen atoms surrounding each antimony atom. The previously unknown quadrupole moment of the first excited $^7/_2^+$ state is found by measuring $R = Q(^7/_2^+)/Q(^5/_2^+)$; its value is found to be 1.38 ± 0.02. Then, using $Q(^5/_2^+) = -(0.54 \pm 0.07)$ b from optical spectroscopy, $Q(^7/_2^+) = -(0.75 \pm 0.09)$ b. (auth)

38387 ANOMALOUS PARTICLE PENETRATION IN PERFECT CRYSTALS. De Wames, R. E.; Hall, W. F.; Lehman, G. W. (North American Aviation Science Center, Thousand Oaks, Calif.). Phys. Rev., 148: 181-5 (Aug. 5, 1966).

A quantum-mechanical calculation of the potential dependence of anomalous transmission of particles through crystals is made, showing that the anomalous effect can always be obtained at sufficiently high particle energy. Both the normal and the anomalous attenuation are found to depart markedly from that calculated from the free-particle cross section when the potential is broad compared to the atomic mean-square displacement. Two experiments to observe the predicted potential dependence are suggested. (auth)

38388 MOESSBAUER HYPERFINE SPECTRA OF Fe^{3+} IN CORUNDUM: MAGNETIC- AND CRYSTAL-FIELD EFFECTS. Wickman, H. H.; Wertheim, G. K. (Bell Telephone Labs., Murray Hill, N. J.). Phys. Rev., 148: 211-17(Aug. 5, 1966).

The Mössbauer technique was employed to study the paramagnetic hfs of ^{57}Fe-doped corundum ($\alpha-Al_2O_3$) in the presence of an external magnetic field. Experiments were performed with an oriented single crystal and with external field strengths to 41 kOe parallel to the trigonal axis of the crystal field at the iron site. The results showed noticeable field-dependent features. Several of these effects were analyzed by detailed calculations of theoretical hfs from the ground-term electronic levels of Fe^{3+}. Effects of small local fields and of mixing of electronic states by crystal-field terms and by the hyperfine interaction are shown to produce gross changes in the Mössbauer spectra. Some of these features were observed; others which require a more homogeneous magnetic field were not observed because major changes in the Mössbauer spectra occur over relatively small ranges of external field strengths. (auth)

38389 ENERGY LEVELS OF TRIVALENT GADOLINIUM AND IONIC CONTRIBUTIONS TO THE GROUND-STATE SPLITTING. Wybourne, B. G. (Argonne National Lab., Ill.). Phys. Rev., 148: 317-27(Aug. 5, 1966).

An attempt is made to estimate the ionic contributions to the ground-state splitting of the trivalent gadolinium ion in a lanthanum ethyl sulfate lattice. The energy levels of the $4f^7$ configuration are calculated and compared with those observed experimentally. The calculated ground-state g factor is found to deviate significantly from its measured value. An attempt was made to estimate the contributions to the ground-state splitting for eight different mechanisms: a fourth-order mechanism that is linear in the crystal-field strength and cubic in the spin-orbit interaction; fourth-order mechanisms that are quadratic in both the crystal-field strength and the spin-orbit interaction; a third-order spin-spin mechanism acting within the $4f^7$ configuration; Pryce's second-order spin-spin configuration mixing mechanism; a second-order relativistic mechanism; mechanisms involving configuration mixing by the crystal field; mechanisms involving nonlinear electrostatically correlated crystal-field interactions; fifth-order configuration interaction mechanisms. The total contribution due to these mechanisms is found to be twice the magnitude of the observed splitting and of opposite sign. It is suggested that no purely ionic model can account for the observed splitting and that the correct explanation must involve the detailed interaction of the gadolinium ion with its ligands. A semi-qualitative explanation of some of the intensity features of the crystal and solution spectra of trivalent gadolinium is attempted. (auth)

38390 MEASURED NUCLEAR MAGNETIC RESONANCE FREE-INDUCTION-DECAY SHAPES AND MOMENTS FOR ^{19}F IN CaF_2. Barnaal, D. E.; Lowe, I. J. (Univ. of Pittsburgh, Pa.). Phys. Rev., 148: 328-31 (Aug. 5, 1966).

The results of NMR free-induction-decay–shape measurements for ^{19}F in single crystals of CaF_2 and polycrystalline CaF_2 are reported. The second and fourth moments of the corresponding absorption line are derived by empirical fits of the decay shapes. The probable errors for the results are smaller than those reported earlier, and the results agree more closely with theoretical predictions for spins in a rigid lattice. (auth)

38391 ELECTRON SPIN RESONANCE OF RARE-EARTH IONS IN CeO_2:Yb^{3+} AND Er^{3+}. Abraham, M. M.; Weeks, R. A.; Clark, G. W.; Finch, C. B. (Oak Ridge National Lab., Tenn.). Phys. Rev., 148: 350-2(Aug. 5, 1966). (ORNL-P-1947).

The paramagnetic resonance spectrum of Yb^{3+} and Er^{3+} in single crystals of CeO_2 was measured at 10 Gc and 4°K. In sites of cubic symmetry, the ground states in both cases are found to be isotropic Γ_7 doublets with $g = 3.424 \pm 0.001$ for Yb^{3+} and $g = 6.747 \pm 0.006$ for Er^{3+}. Hyperfine structures for the odd isotopes were resolved with $A(^{171}Yb) = (877.1 \pm 1.0) \times 10^{-4}$ cm^{-1}, $A(^{173}Yb) = (242.0 \pm 0.3) \times 10^{-4}$ cm^{-1}, and $A(^{167}Er) = (232.1 \pm 0.3) \times 10^{-4}$ cm^{-1}. Nearby charge compensation produces sites of axial symmetry. For Yb^{3+}, one set of axes is along the four ⟨111⟩ crystal directions with $g_{||} = 4.733 \pm 0.004$ and $g_\perp = 2.744 \pm 0.002$. For Er^{3+} two different axial spectra were measured, also with trigonal symmetry about the ⟨111⟩ directions. For one set $g_{||} = 10.25 \pm 0.05$ and $g_\perp = 4.847 \pm 0.005$, and for the other set $g_{||} = 4.539 \pm 0.005$ and $g_\perp = 7.399 \pm 0.007$. In most crystals the linewidths were 20 Oe; however, in some crystals in which no cubic sites were found, the axial linewidths were greater than 50 Oe. Comparisons of the axial g-tensor traces with the cubic g tensor and the magnitude and sign of $\Delta g = g_{||} - g_\perp$ are the basis for a discussion of the possible nature of the charge compensation producing the axial symmetry. (auth)

38392 NUCLEAR QUADRUPOLE RELAXATION AND CHEMICAL SHIFT OF ^{131}Xe IN LIQUID AND SOLID XENON.

Warren, William W. Jr.; Norberg, R. E. (Washington Univ., St. Louis). Phys. Rev., 148: 402-12(Aug. 5, 1966).

The spin-lattice relaxation time and temperature-dependent chemical shift of ^{131}Xe in liquid and solid xenon were measured between 9 and 250°K. A calculation of the transition probabilities for quadrupolar relaxation of ^{131}Xe in solid xenon via the Raman process is described. The calculation is based on the theory of Van Kranendonk, modified for the case of a face-centered cubic lattice with electric-field gradients arising from exchange and van der Waals interactions. The data are shown to verify the predicted temperature dependence of T_1 in the solid above 9°K and the absolute magnitude of T_1 at 100°K. It is demonstrated that the temperature dependence of the data is consistent with the temperature variation of the Debye temperature Θ obtained by Packard and Swenson from specific-heat measurements. Quadrupolar relaxation via diffusing impurities was observed at temperatures near the melting point in solid xenon samples containing roughly 1% air. The quadrupolar relaxation time of ^{131}Xe in liquid xenon was found to vary exponentially with temperature with an "activation energy" $E_A = 640 \pm 30$ cal/mole. This "activation energy" is approximately one-half as large as values previously obtained for the activation energy of self-diffusion in liquid xenon. Measurements of the chemical shift of ^{131}Xe indicate that the local field increases linearly with density in liquid and solid xenon. Least-squares fits to the data yield the change ΔH of the external resonant field with density: $-(1/H_0)\,[\partial(\Delta H)/\partial\rho] = (5.1 \pm 0.5) \times 10^{-7}$ (amagat)$^{-1}$ in liquid xenon and $-(1/H_0)\,[\partial(\Delta H)/\partial\rho] = (18.2 \pm 1.1) \times 10^{-7}$ (amagat)$^{-1}$ in solid xenon. These data support the previous ^{129}Xe shift data of Yen and Norberg but disagree with more recent measurements by Brinkmann and Carr of the density dependence of the ^{129}Xe shift in solid xenon. (auth)

38393 CHARACTERISTIC X-RAY PRODUCTION IN SINGLE CRYSTALS (Al,Cu) BY PROTON BOMBARDMENT. I. PROTONS OF 70 TO 100 kev. Khan, J. M. (Univ. of California, Livermore); Potter, D. L.; Worley, R. D.; Smith, Harold P. Jr. Phys. Rev., 148: 413-19(Aug. 5, 1966). (UCRL-14695).

Characteristic x rays were observed from single crystals of aluminum (K shell) and copper (L shell) during bombardment by 70- to 100-kev protons. The thick-target yield was found to be sensitive to the orientation of the crystals. Studies were performed in the region of the [011] direction (at 45° to the crystal surface normal) and across the (100) plane at 30° to the normal. A yield contour at the [011] direction is presented over an angular region of 20° × 20° and is compared with a polycrystalline value. A single-crystal yield exceeded the polycrystalline value by as much as 30% at one point. For copper the largest observed maximum-to-minimum yield ratio in the vicinity of the [011] direction was 15 to 1. The effect of surface contamination was measured for selected sweeps. Also included is a calculation of a proton-crystal potential and comparison with a planar-averaged Nielsen potential. (auth)

38394 STACKING-FAULT ENERGY AND MANY-BODY FORCE EFFECTS IN SOLID ARGON. Bullough, R. (Atomic Energy Research Establishment, Harwell, Eng.); Glyde, H. R.; Venables, J. A. Phys. Rev. Lett., 17: 249-50(Aug. 1, 1966).

The stacking-fault energy of argon was calculated for the case when the crystal atoms interact through a two-body Lennard-Jones (6,12) potential, $V(R) = \epsilon[(r_0/R)^{12} - 2(r_0/R)^6]$, with $\epsilon = 164.3 \times 10^{-16}$ erg and $r_0 = 3.818$ Å. (B.G.D.)

38395 INTERACTION OF 25-kev ELECTRONS WITH LATTICE VIBRATIONS IN LiF. EXPERIMENTAL EVIDENCE FOR SURFACE MODES OF LATTICE VIBRATION. Boersch, H.; Geiger, J.; Stickel, W. (Technische Univ., Berlin). Phys. Rev. Lett., 17: 379-81(Aug. 15, 1966).

Energy gains and energy losses of 25-kev electrons in LiF were measured for different foil thicknesses. The results are explained by generalizing the dielectric theory of surface plasma oscillations in metal foils given by Ritchie and applying the dielectric formalism to the excitation of surface-lattice vibrations by inelastic electron scattering. The observed energy-loss spectra with maxima between 0.042 and 0.050 ev is interpreted as tangential surface-lattice vibrations, and the thickness dependence of the position of the maximum is attributed to the dispersion of this surface mode. (L.B.S.)

38396 COLOR CENTERS IN X-IRRADIATED NaCl:Ag AND NaCl:(Ag + Ca) CRYSTALS. Topa, V.; Haragea, S. (Inst. of Physics, Bucharest). Phys. Status Solidi, 16: 137-45(July 1, 1966).

A study was made of color centers induced by x irradiation at room temperature in NaCl : Ag and NaCl : (Ag + Ca). It is shown that the induced bands in NaCl : Ag are strongly dependent on the concentration of Ag as well as on the irradiation time and also that the B-, C-, and D bands have a complex structure. Three components of the B-band, four of the C-band, and two of the D band are found at liquid nitrogen temperature. Optical bleaching in the F light shows that only a component of the B-, C-, and D bands is definitely electronic. It is also noted that only the optical bleaching of the F-band in NaCl : Ag results in a simple B band much like that obtained by electrolytic coloring. The incorporation of both Ca and Ag in NaCl and subsequent x irradiation lead to very intensive B- and D bands which are shifted to shorter wavelengths compared with those bands in crystals containing only Ag. The optical bleaching experiments on these crystals suggest that color centers containing both Ca and Ag are probably formed, as in the case of similar crystals electrolytically colored. (auth)

38397 MEASUREMENTS OF THE FREQUENCIES OF THE NORMAL MODES OF MAGNESIUM. Squires, G. L. (Cambridge Univ., Eng.). Proc. Phys. Soc. (London), 88: 919-28(Aug. 1966).

The normal modes of magnesium were investigated by means of the inelastic scattering of slow neutrons. The frequencies of about 1000 phonons were measured with a time-of-flight apparatus, and the values along symmetry directions obtained by an interpolation method. It was found previously that results could be fitted by force models extending to fourth-nearest neighbors or less. It is shown that the measurements cannot be fitted by any tensor force model extending only to fourth-nearest neighbors. The motions of the atoms for a simple force model are discussed. (auth)

38398 PARAMAGNETIC CENTERS FORMED BY IRRADIATION OF THE OXYGENATED COMPOUNDS OF SELENIUM. II. ESR SPECTRA OF POLYCRYSTALLINE IRRADIATED $SeO_4(NH_4)_2$. Constantinescu, M.; Constantinescu, O.; Pascaru, I.; Gird, E. (Inst. of Atomic Physics, Bucharest). Rev. Roum. Phys., 11: 249-59 (1966).

Gamma- and neutron-irradiated polycrystalline $SeO_4(NH_4)_2$ was studied by ESR and radiochemical methods. From the ESR spectra and from the behavior on heating NH_3^+ and O_2^- radicals as well as radicals from selenium which can be of SeO_4^-, SeO_3^- or SeO_2^- type were put into evidence. A mechanism of formation of these species is suggested. The dependence of paramagnetic centers concentration as a function of the integral dose was also examined. (auth)

38399 INVESTIGATIONS OF RADIATION DEFECTS IN GaP BY MEANS OF ELECTRON RESONANCE. Kimmel, H. (Siemens-Schuckertwerke AG, Erlangen, Ger.). Z. Naturforsch., 21a: 526-8(May 1966). (In German).

From the hyperfine structure of the electron resonance spectra of electron- and proton-irradiated GaP, it is shown that defects occur in which unpaired electrons arise in interaction with two Ga atoms or with two P atoms. The observed defects must be treated as the defects corresponding to the Si A centers of this compound crystallizing in the sphalerite lattice. (tr-auth)

38400 NATURE OF PLASMA LOSSES AT 3.6 ev IN THIN SILVER FOILS. Daniels, J. (Univ., Hamburg). Z. Naturforsch., 21a: 652-3(May 1966). (In German).

The hypothesis that the plasma loss at 3.6 ev is composed of a surface loss and a volume loss was tested on silver

foils between 300 and 7°K using a monochromator developed by Hartl. It was established that in variation of the temperature from 300 to 78°K, the volume loss is displaced about 50 mv but the site of the surface loss remains constant. Variation of the silver foil thickness between 400 and 800 Å showed that with increasing thickness the ratio of the intensity of volume and surface losses increase, but the ratio of the intensity of the surface loss to that of the 0-volt loss remains constant. Angular measurements showed that the intensity of the volume loss decreases much slower than that of the surface loss. (J.S.R.)

38401 DEFECT LUMINESCENCE IN CsI. Rehmann, W.; Scharmann, A. (Univ., Giessen, Ger.). Z. Naturforsch., 21a: 666-7(May 1966). (In German).

The defect luminescence of CsI, induced by protons at 1 Mev, was studied as a function of the proton dose. The results showed that after irradiation an emission band appears at about 460 nm, which is displaced up to 500 nm with increasing radiation dose. Its greatest intensity occurs after irradiation with 5×10^{15} protons/cm^2. The defect bands were compared with the emission bands occurring in unirradiated CsI or CsI(Tl) crystals. The effect of the variation of temperature and the Tl concentration under excitation with 1-Mev protons was determined. The results are graphed. The Tl-activated crystal emits a band at 550 nm, which is coupled with the introduction of Tl ions into the CsI lattice. In undoped crystals there is a blue emission band at 430 nm, whose luminescent center is described as an association of a cation vacancy with a divalent positive ion. At low temperatures the undoped crystal emits a band in the ultraviolet spectral range. (J.S.R.)

38402 SOLID-STATE EFFECT IN IRRADIATED ALKALI HALIDE CRYSTALS. O'Brien, Robert Francis. St. Louis, St. Louis Univ., 1965. 172p.

Thesis.

A theoretical and experimental report is presented on the dynamic polarization of nuclei in solids by means of the solid state effect. Nuclear and electron spin resonances were induced simultaneously in a variety of alkali halide crystals irradiated with 50-kv x rays at liquid nitrogen temperature (T = 77°K). The electron spin resonances induced are associated with X_2^- centers produced by the irradiation in concentrations up to 10^{17} centers cm^{-3}. The nuclei were dynamically polarized by means of the forbidden electronic transitions to which they were coupled, and the nuclear magnetic resonance signals were thereby substantially amplified both positively and negatively. The nuclear magnetic resonance signal enhancements of ±45 for ^{23}Na in Ag-doped NaCl and ±20 for ^{7}Li in LiF are the largest yet observed in solids in this temperature range. The theoretical foundations and background of the solid state effect, the X_2^- center and its EPR spectrum, nuclear magnetic relaxation processes in alkali halide crystals are reviewed. A phenomenological theory is developed and experimental results are analyzed both by this and other theories. Experimental data are presented on the power dependence, concentration dependence, and relaxation-time-dependence of the nuclear signal enhancements. Such data are discussed in the light of both previously reported results and this new phenomenological theory, and quantitative results are presented. A detailed description of the instrumentation required for double resonance experiments is presented. The report is concluded with a comprehensive bibliography of pertinent theoretical and experimental developments. (Dissertation Abstr.)

38403 NORMAL FERMI LIQUID THEORY FOR ELECTRONS IN SOLIDS. Jones, Billy Lorraine. Eugene, Ore., Univ. of Oregon, 1965. 80p.

Thesis.

The Fermi liquid theory for interacting electrons moving in a fixed periodic potential is derived. Two methods are used: the Green's function method and the perturbation approach. In the first part the work of Kadanoff and Baym, who derived a kinetic equation for the single-particle Green's function in a system of interacting fermions and then used the quasi-particle concept to derive the Fermi liquid theory for translationally invariant systems is followed. Their formalism is adapted to inhomogeneous systems by rewriting it in operator form. A kinetic equation for an energy-dependent, single-particle density matrix is then derived. The quasi-particle concept is introduced and a formal solution of the kinetic equation is given and discussed. These developments are then specialized to the periodic potential by using a Bloch function representation. A transport equation of the Landau-Boltzmann type is derived for quasi-particles moving within a single energy band. Expressions for the density and current density are then identified from a continuity equation. In the last part it is shown that the Fermi liquid theory can be obtained for the solid from the many-body perturbation theory methods. The perturbation treatment largely follows the work of Luttinger and Nozières, who used similar techniques to derive Landau's results for systems without a lattice potential. The perturbation theory calculation shows that the results obtained from the Green's function approach are exact in the case of slowly varying external fields. The perturbation theory also shows that when the periodic potential is present the change in quasi-particle energy can be expressed in terms of the variation of the quasi-particle distribution function. (TCO)

38404 NUCLEAR MAGNETIC RESONANCE OF ^{131}Xe IN LIQUID AND SOLID XENON. Warren, William Willard Jr. St. Louis, Washington Univ., 1965. 225p.

Thesis.

Extensive NMR studies of ^{131}Xe ($I = 3/2$) in liquid and solid xenon were carried out over a temperature range from 4.2° to 250°K with a coherent pulsed NMR spectrometer operating at 3.0 Mc. Calculations are described, which predict the effects of dipolar and quadrupolar interactions on free precession signals in the xenon rigid lattice. Data are presented that verify the essential predictions of the theory and provide measurements of the strengths of nuclear dipole-dipole interactions and of the magnitudes of static electric field gradients in polycrystalline xenon at 4.2°K. The effects of atomic diffusion in dipolar and quadrupolar interactions are considered, and experimental results are described that support the theory and the earlier studies of self-diffusion in xenon. The theory of quadrupolar spin lattice relaxation in solids via two-phonon (Raman) processes is developed and applied to a calculation of the relaxation time of ^{131}Xe in solid xenon. Data are presented that verify theoretical predictions of the magnitude and temperature dependence of the relaxation time and indicate that the overlap model provides a realistic description of the internal electric field gradients in solid xenon. It is shown that the temperature dependence of the data can be completely accounted for by the introduction of the temperature-dependent Debye temperature obtained from experimental determinations of the entropy of solid xenon. The effects of diffusing impurities are considered. The results of measurements of the temperature-dependent chemical shift in liquid and solid xenon are discussed and compared with earlier ^{129}Xe results. The contribution of exchange interactions to the shift of the local field in the rigid solid is calculated and compared with experiment. The behavior of the shift at the melting point and in the liquid is shown to support a quasi-crystalline model of liquid xenon. (TCO)

38405 CHANGES IN THE CONDUCTIVE PROPERTIES OF CdS INDUCED BY THERMAL NEUTRONS. Oswald, Robert B. Jr. (Harry Diamond Labs., Washington, D. C.); Kikuchi, Chihiro. 22p. (CONF-650707-22). ORAU. Gmelin, AED-CONF-65-152-24.

From IEEE Annual Conference on Nuclear and Space Radiation Effects, Ann Arbor, Mich.

The results of an experimental investigation of thermal neutron irradiation effects on the conductive properties of cadmium sulfide are presented. The production of Frenkel defects by thermal neutrons in CdS results from the recoil of an energetic ^{114}Cd nucleus. The recoil energy is produced by the radiative capture of a thermal neutron by ^{113}Cd and the prompt emission of 9 Mev of gamma energy through the nuclear reaction: $^{113}\mathrm{Cd} + n_{th} \rightarrow (^{114}\mathrm{Cd})^* \rightarrow {}^{114}\mathrm{Cd} + \gamma$.

Since the recoiling nucleus is stable, this mechanism produces defects in the host crystal without the complication of nuclear doping by transmutation. Experimental results show that thermal neutron induced defects completely alter the conductive properties of the CdS host crystals. The conductivity of both initially conducting and insulating single crystals of the dendritic type has changed many orders of magnitude. Thermal neutron induced defects increased the photosensitivity and extend their spectral response into the infrared, indicating the creation of a state about 0.7 ev above the valence band. In addition, the transient response of initially insulating platelet crystals is altered by the production of electron traps. (auth)

38406 BAND GAP IN BERYLLIUM. Shand, J. B.; Stewart, A. T. (Univ. of North Carolina, Chapel Hill). 9p. (CONF-650721–10). ORAU. Gmelin, AED-CONF-65-211-8.

From Positron Annihilation Conference, Detroit.

The energy gap is found at one of the zone boundaries in beryllium. Calculations were made of one of the angular correlations, referring to the known Fermi surface and assuming various values of the relevant energy gap. By fitting the theoretical curves to experimental data obtained, a value was found for the energy gap at the (0,0,2) zone boundary of beryllium which is E = 0.34 ± 0.16 Ryd. (J.F.P.)

38407 TRANSMUTED CENTER FERMI LEVEL SPECTROSCOPY (TCFLS) AS AN ANALYTICAL TOOL FOR CHARACTERIZING SEMICONDUCTOR MATERIALS. Lindeberg, George K. (Minnesota Mining and Manufacturing Co., St. Paul). 17p. (CONF-651015–13). ORAU. Gmelin, AED-CONF-65-312-30.

From American Physical Society Meeting, Chicago.

An idea of Cleland and Crawford for studying semiconductor properties as a function of transmutation doping by decay of a single radioactive species was developed. The theory may be developed with reference to four general conditions necessary for "simple" TCFLS. The possibility in principle of verifying the self-consistency of such cases of simple TCFLS through experimental study of the fractional transmutation as a function of temperature and Fermi level sensitive transport coefficients is demonstrated. The numerical analysis of such simple cases of TCFLS may be interpreted in terms of forbidden band energy level spectra and transport coefficients. "Complex" cases of TCFLS result when one or more of the four conditions fail due to uncontrolled sample structure variation, electron system nonequilibrium, proximity of the Fermi level to the transmutation introduced centers, significant scattering by the latter, and significant impurity level transport. Inherent characteristics of TCFLS are compared with those of resonance spectroscopy. (auth)

38408 QUANTUM-MECHANICAL FLUCTUATIONS AND TUNNELING EFFECTS IN ^{154}Sm. Kumar, Krishna (Michigan State Univ., East Lansing). 7p. (CONF-660411–10). ORAU. Gmelin, AED-CONF-66-060-7.

From American Physical Society Meeting, Washington, D. C.

An investigation was made on the effects of dynamics or quantum mechanics on rotational nuclei such as ^{154}Sm. The energy levels and B(E2) values of ^{154}Sm were calculated. Quantum mechanical fluctuations and root mean square values for β and γ levels are described. It is concluded that in the case of well-deformed nuclei as ^{154}Sm, the effects of dynamics are small, but not negligible. (M.O.W.)

REACTOR TECHNOLOGY

General

Refer also to abstracts 37022 and 38492.

38409 (AECL–2586) SWIFT DRYOUT DATA FOR A 19-ROD, 3.25 IN. DIAMETER BUNDLE COOLED BY STEAM/WATER FOG AT 515 PSIA. Moeck, E. O.; Garg, S. C.; Wikhammer, G. A.; Stern, F.; Dempster, R. T. (Atomic Energy of Canada Ltd., Chalk River (Ontario)). May 1966. 22p. Dep. mn. AECL $1.00.

Dryout occurs in boiling and fog cooled reactors when the thin liquid film on the fuel element evaporates completely and the heat transfer coefficient decreases. Dryout heat fluxes were measured for electrically heated bundles similar to the CANDU warted fuel design in the Steam Water Industrial Fog Test (SWIFT) loop. The geometrical parameters typical of short bundles were simulated, and stripping rings were mounted on the bundle to strip the liquid film flowing along the pressure tube wall. The bundle power at dryout compared to aligned bundles having no stripping rings and no axial gaps decreased by up to 20% with angular misalignment between bundles, increased by up to 150% when the liquid film was stripped off the pressure tube wall, remained unchanged for combined misalignment and stripping rings, was the same for CANDU end-plate and flat-end geometries, and was unaffected by an axial gap between the bundles. (H.D.R.)

38410 (AEEW-M–474) CUSH: A COMPUTER PROGRAMME FOR THE STEADY-STATE HYDRAULIC ANALYSIS OF STEAM-GENERATING REACTOR SYSTEMS. Cushing, W. R.; Ingram, M. C. (Atomic Energy Establishment, Winfrith (England)). Oct. 1965. 52p. Dep. BIS $1.40. HMSO 7s.

The CUSH program is written in FORTRAN and versions exist for the IBM 7090, IBM 7030 and EEC KDF-9 Computers. The Program requires a three dimensional specification of the core power distribution and calculates the distribution of flow and coolant density within the core and primary circuit. (auth)

38411 (BNWL–186) TIME OPTIMAL XENON SHUTDOWN ON THE XENON BOUNDARY. Lewins, Jeffery; Benham, R. D. (Battelle-Northwest, Richland, Wash. Pacific Northwest Lab.). May 1966. Contract AT(45-1)-1830. 39p. Dep. mn. CFSTI $2.00 cy, $0.50 mn.

The time optimal flux program to shutdown a reactor without losing restart capability through Xe poisoning is reviewed. A more rigorous proof of the optimal nature of operating along the Xe boundary is offered, together with a discussion of situations which might not be optimal. It is concluded that for practical purposes operation along the boundary will be optimal. Part of the proof consists of analog computations, and a discussion is given of the suitability of the optimum Xe study to analog techniques. (auth)

38412 (ITEF–406) K TEORII REGULYATORA V GETEROGENNOM REAKTORE. (The Regulation Theory for Heterogeneous Reactors). Galanin, A. D. (Gosudarstvennyi Komitet po Ispol'zovaniyu Atomnoi Energii SSSR, Moscow. Institut Teoreticheskoi i Eksperimental'noi Fiziki). 1965. 20p. Dep. mn.

Starting from a reactor lattice consisting of cylindrical blocks having radii which are small compared with the intralattice distance and an auxiliary block which absorbs only thermal neutrons p times better than the lattice source blocks, the theory of the internal regulation for heterogeneous reactors is developed. Expressions for regulation efficiency P in heterogeneous reactors and for its heterogeneous correction ΔP are presented. In the case of a sufficiently weak block effect the analysis is carried out to the end. The new theory is illustrated for the case of a regulator at the center of a cell with an a = 2L step. Conventional calculations yield $P_0 = 3.65$, while the new approach results in a $\Delta P/P_0 = -0.15$, i.e., the heterogeneous calculation indicates a regulation efficiency increase of 15%. (JPRS)

38413 CALCULATION METHOD OF A TRANSIENT IN A PROMPT CRITICAL FAST REACTOR. Motta, M. (CNEN, Bologna). Energ. Nucl. (Milan), 13: 359-70(July 1966). (In Italian).

A calculation method of a transient in a prompt critical fast reactor is described. A comparison is made between telegraph equation and Stokes-Navier equation of fluid dynamics, in order to explain the shock-wave treatment and the hydrodynamic-thermodynamic portion of calculations, introduced in a code for digital computers. (auth)

38414 REACTIVITY RESPONSE OF A REACTOR AND THE POSSIBILITIES FOR MEASURING EFFECTIVE ABSORPTION CROSS SECTIONS IN REACTORS HAVING A FAST NEUTRON SPECTRUM. Khristov, V. Izv. Fiz. Inst. Aneb, Bulg. Akad. Nauk, 14: 27-37(1966). (In Russian).

The reactivity sensitivity of the reactor IRT is defined and its dependence on the configuration of the active area (fuel core) is calculated. The coordinate correlation of the importance of neutrons for absorbers of small dimensions was measured. The possibility of measuring effective cross sections of absorption by the static method of reactivity and by the global oscillatory method in the IRT reactor, characterized by a fast neutron spectrum, has been studied. For this purpose the neutron spectrum was decreased with the aid of an internal thermal column. The effective absorption cross sections of cobalt, chlorine, manganese, and copper were measured with satisfactory accuracy. (auth)

38415 INVESTIGATIONS OF BOILING OF LIQUID METALS IN FORCED CONVECTION. Grass, G.; Kottowski, H.; Milliot, B. (EURATOM-Forschungszentrum, Ispra, Italy). Nukleonik, 8: 273-82(June 1966). (In German).

An initial investigation on safety problems in fast reactors is described. A forced convection boiling K loop was used. A new measuring method taking advantage of direct joule heating and simultaneous analysis of the voltage changes has been used to study flow patterns in boiling liquid metal loops. For the conditions of the tests, steady state boiling occurred only rarely. Boiling was abrupt, leading to the sudden periodical emptying of the test section producing pressure shocks followed vapor condensation. A by-pass was introduced to simulate parallel channel flow and led to marked differences in the boiling behavior. The boiling and condensation phenomena have been interpreted with the use of the new measuring technique. Further studies are required to establish mechanisms and correlation. (auth)

38416 ECONOMIC SIGNIFICANCE OF NUCLEAR FUEL MANAGEMENT. Warren, Frederick H.; McLeod, N. Barrie (Nuclear Utility Services, Inc., Washington, D. C.). 13p. (CONF-651132–5). ORAU. Gmelin, AED-CONF-65-337-21.

From Atomic Industrial Forum, 12th Annual Conference, Washington, D. C.

A review of the essential considerations of nuclear fuel management is presented. Nuclear fuel management is defined and the functions of fuel management are discussed along with fuel cost sensitivity. (J.R.D.)

Auxiliaries and Components

38417 DEVELOPMENT OF REDUNDANCY TECHNIQUES FOR THE ACHIEVEMENT OF HIGHLY RELIABLE AUTOCONTROL FOR NUCLEAR REACTORS. Lawrence, L. A. J. (United Kingdom Atomic Energy Authority,

Winfrith, Eng.). Chartered Mech. Eng., 12: 603 (Nov. 1965). (AEEW-R-396).

Undesirable transients, brought about by autocontrol failure in plant, may be avoided by arranging the component instruments, controllers, actuators etc. in subsystems to provide a redundant control complex. By careful attention to subsystem saturation levels, such a complex may be given inherent fault-absorbing characteristics so that autocontrol may continue without interruption in spite of a subsystem failure. However, if control must be continuous, significant reliability improvements, over a nonredundant system, can only be achieved if subsystem failures are short, compared with the mean time interval between them. To ensure this, all subsystems must be monitored, which can be done most effectively by deliberately introducing a fault into each subsystem in turn and inspecting the response. Some gain in autocontrol performance can be derived from rejecting a faulty subsystem by converting its output manually into a zero signal fault condition, i.e., one in which no subsystem action is possible. A redundant autocontrol for a research reactor is considered. The subsystems control electric motors through error signals derived from nucleonic instruments, the shaft outputs from the motors being combined by a differential gear for positioning the control rods. Variations in transducer outputs may be time and/or space-dependent. Such variations can lead to problems of design particularly in the fault detecting circuits. (BBB)

Criticality Studies

Refer also to abstracts 38490, 38491, 38493–38495, 38497, and 38498.

38418 (ANL–7120, pp 413-20) RECENT INVESTIGATIONS OF FAST REACTOR REACTIVITY COEFFICIENTS. Hummel, H. H.; Hwang, R. N.; Phillips, K. (Argonne National Lab., Ill.).

Investigation of the equivalence relation between homogeneous and heterogeneous resonance integrals indicated that equivalence theory is satisfactory for ^{238}U resonances in the energy range 1.0 to 1.3 kev. The effect of variations in the fission cross section of ^{239}Pu and the capture cross section of ^{238}U and the effect of the presence of ^{241}Pu on the Na void effect were considered. The results are tabulated. Nonlinearity in spectral component as a function of Na content was studied. It was found that nonlinearity is due primarily to variations in the energy dependence of the adjoint function and hardly at all to variation of effective Na cross section or flux except for events occurring in the vicinity of the 2.85-kev Na resonance. (A.G.W.)

38419 (ANL–7120, pp 421-2) COMMENT ON THE COMPARISON OF SOME SODIUM VOID COEFFICIENTS WITH EXPERIMENTAL DATA. Travelli, A. (Argonne National Lab., Ill.).

Three different sets of cross sections were used in calculations of sodium void coefficients for fast reactors. The three sets were the Argonne Set 224, the Argonne Set 232, and the Argonne Set 224 modified to include the White cross sections for ^{239}Pu and for ^{235}U. The parameter calculated with each set of cross sections and compared with experimental data was the value of the central Na worth. The experimental results fell between the results calculated with the Argonne Sets 224 and 232; calculations with all three cross-section sets were almost within the experimental error. (A.G.W.)

38420 (ANL–7120, pp 423-33) INFLUENCE OF SOME IMPORTANT GROUP CONSTANTS ON INTEGRAL FAST REACTOR QUANTITIES. Kuesters, H.; Metzenroth, M. (Kernforschungszentrum, Karlsruhe (West Germany). Institut fuer Neutronenphysik und Reaktortechnik).

Uncertainties in the group constants used in multigroup calculations for large fast reactors are considered. The effect of resonance self-shielding on multiplication factors for some reactors is shown. The influence of different weighting spectra used in various sets of group constants on the Doppler coefficient, sodium coefficient, and breeding ratios was investigated. The characteristics and preparation of the first Karlsruhe group-constant set KFK 26-10 are briefly described. Effects of uncertainties in microscopic data on reactor calculations are demonstrated. Results of calculations using different group-constant sets are compared with measured data for ZPR III/39. (A.G.W.)

38421 (ANL–7120, pp 440-8) RESULTS OF DOPPLER COEFFICIENT CALCULATIONS FOR FAST REACTORS AND COMPARISON OF DIFFERENT METHODS. PARTS I AND II. Froelich, R.; Ott, K. (Kernforschungszentrum, Karlsruhe (West Germany). Institut fuer Neutronenphysik und Reaktortechnik); Shaviv, G.; Yiftah, S. (Technion–Israel Inst. of Tech., Haifa).

In Part I the results of Doppler coefficient calculations of three different origins are compared and analyzed. The temperature dependence of the Doppler coefficient is investigated. The three different ways commonly used for calculation of Doppler coefficients are discussed and compared. It is concluded that the influence of the use of different resonance data on calculated Doppler reactivity seems fairly small; the influence of the neutron spectrum used is very strong. In Part II the Doppler effect in fast Pu breeder reactors with core volumes of 800, 1500, and 2500 liters was studied. The results of calculations of the change in neutron multiplication factor due to Doppler effect obtained in different ways are compared. (A.G.W.)

38422 (ANL–7120, pp 449-61) EFFECT OF THE FLUCTUATIONS IN COLLISION DENSITY ON FAST-REACTOR DOPPLER EFFECT CALCULATIONS. Hwang, R. N. (Argonne National Lab., Ill.).

An investigation of fluctuations in neutron collision density and their influence on Doppler calculations is restricted to the case of an infinite homogeneous medium with composition typical of a dilute fast reactor. Three special topics concerning the Doppler theory are considered: effect of Placzek oscillations on the reaction rate of individual resonances, effect of incomplete recovery in neutron collision density between resonances on the group reaction rates and the effective cross section of a single resonant material in the mixture of heavy scatterers, and a more general approach to the problem of resonance overlap between two different nuclides. Investigations were carried out both analytically and numerically. It was found that the errors introduced by the fluctuation in the collision density are generally small when the total Doppler effect of the system is considered. (A.G.W.)

38423 (ANL–7120, pp 462-77) COMPARISON OF MONTE CARLO AND RESONANCE INTEGRAL METHODS IN THE DETERMINATION OF DOPPLER EFFECTS IN FAST REACTORS. Olhoeft, J. E.; Krug, H. E. (Westinghouse Electric Corp., Pittsburgh, Pa. Atomic Power Div.); Hwang, R. N. (Argonne National Lab., Ill.).

A comparison of calculations of Doppler effect in fast reactors by the Monte Carlo method and resonance integral techniques is based on a common set of ground rules selected to minimize the effect of uncertainties in nonfuel cross sections. The physical model studied is an infinite array of semi-infinite cylindrical fuel rods in a hexagonal lattice cooled by Na. The Monte Carlo calculations were performed with the REPETITIOUS 3 code, which is described in an appendix. The resonance integral technique is coupled with multigroup analysis. Generally good agreement was obtained in reaction rates calculated by the two methods, but, because of the small changes in reaction rates with temperature, the small discrepancies in reaction rates produce large differences in Doppler effect. It is concluded that uncertainties in the Doppler effect are large enough to justify further sophistication in methods. (A.G.W.)

38424 (ANL–7120, pp 497-503) FAST REACTOR SAFETY CONSIDERATIONS RELATED TO FUEL MACROSTRUCTURE. Peterson, R. E.; Goldsmith, S. (Battelle-Northwest, Richland, Wash. Pacific Northwest Lab.).

Properties of ceramic and cermet fuels for fast reactors are examined in relation to the assumption that a negative

Doppler effect and a negative reactivity coefficient of thermal expansion provide instantaneous negative reactivity feedback in proportion to the energy generated in the event of a prompt burst accident. Transient heat transfer in inhomogeneous fuels and thermal expansion kinetics are considered. The energy release under assumed accidental conditions is estimated, and the ratio of the energy release at the peak of the burst to that obtained if the feedback were instantaneous is evaluated for two different fuel types. (A.G.W.)

38425 (ANL–7120, pp 585-97) ACCURACY OF POWER REACTOR VOID COEFFICIENTS EXTRAPOLATED FROM MEASUREMENTS IN CRITICAL ASSEMBLIES. Engelder, T. C.; Snidow, N. L.; Katman, T. S. (Babcock and Wilcox Co., Lynchburg, Va.).

The effects of four variables on the void coefficient and on the correction required for its extrapolation from that measured in a critical assembly to the value for a reference power reactor are evaluated. The reference reactor is the MARK-XV design for a 1000-Mw(e) supercritical, steam-cooled, fast breeder reactor. The critical assembly is a 5/1 slab operated at room temperature and fueled with 5% ^{240}Pu. It is concluded that the size of the assembly can be reduced substantially without introducing errors larger than those from other sources. The correction for temperature is highly dependent on accurate Doppler measurements. The largest correction is that for Pu isotopic composition; it represents the principal limitation on the accuracy of the measurements. Heterogeneity corrections can be avoided by using the reference reactor fuel forms. (A.G.W.)

38426 (ANL–7120, pp 598-602) SODIUM-VOID COEFFICIENTS. Kato, W. Y.; Rusch, G. K.; Helm, F. H. (Argonne National Lab., Ill.).

Results of sodium-void coefficient measurements on two large carbide assemblies constructed on ZPR-6 are summarized. The first assembly was a 610-liter UC core having a length-to-diameter ratio of approximately unity. The second was a flat pancake-type core having a volume of about 950 liters and a length-to-diameter ratio of ~1:3. The sodium-void coefficient as a function of location was mapped for each assembly. In studies of the heterogeneity effect, measurements were made with different materials placed next to the Na, different widths of Na columns, partial voids in a 1-in.-wide Na column, and discontinuous or staggered voids in the normal drawer loading. Different material arrangements produced large variations in the Na coefficient. In order to obtain reasonable agreement with experimental results, it would appear to be necessary to use two-dimensional transport calculations that take into account the material arrangement. (A.G.W.)

38427 (ANL–7120, pp 603-9) MEASUREMENT AND ANALYSIS OF DOPPLER EFFECT IN PLUTONIUM-FUELED FAST REACTOR ASSEMBLIES. Fischer, G. J.; Meneley, D. A.; Hwang, R. N.; Groh, E. F.; Till, C. E. (Argonne National Lab., Ill.).

Measurements made with the ZPR-3 fast critical assembly are described. Zone-loading procedures were used to produce a mockup of a large fast power breeder using ^{239}Pu, ^{238}U monocarbide fuel, Na coolant, and stainless steel clad and structure. In another assembly 40% of the Na cans were replaced by graphite. The measurements indicated that the positive Doppler reactivity contribution of ^{239}Pu in the fuel and in the neutron-energy spectrum of a large power breeder reactor is small in magnitude compared to the strong negative Doppler effect of ^{238}U. Experimental results are compared with theoretical calculations; experimental and theoretical uncertainties are discussed. It is concluded that much more work must be done with the fissile isotopes in varying fast reactor spectra. (A.G.W.)

38428 (ANL–7120, pp 610-13) RECENT DOPPLER MEASUREMENTS WITH ZPR-6. Till, C. E.; Lewis, R. A.; Groh, E. F. (Argonne National Lab., Ill.).

Improved data-gathering techniques, consisting largely of providing a servo-controlled regulating rod for the reactivity measurement fully automated with the oscillator system, improved the precision of Doppler measurements in the ZPR-6 by better than an order of magnitude. The improved techniques were used to study expansion effects and the temperature dependence of the Doppler effect. Data are summarized on the effects of environment of the sample in the reactor on the measurements, the ^{238}U Doppler effect as a function of temperature, reactivity changes for ^{235}U oxide with freely expanding and axially constrained samples as a function of temperature, reactivity changes for various isotopic ratios of ^{235}U to ^{238}U as a function of temperature, and reactivity effect of expansion of U metal. (A.G.W.)

38429 (ANL–7120, pp 614-15) RECENT RESULTS OF DOPPLER MEASUREMENTS IN FAST-NEUTRON SPECTRA. Carpenter, S. G.; Mountford, L. A.; Springer, T. H.; Tuttle, R. J. (Atomics International, Canoga Park, Calif.).

Doppler measurements in fast-neutron spectra were made using small samples in a multiregion reactor. The variation of reactivity of ^{235}U metal due to temperature and expansion and the derived Doppler reactivity for different calculated median fission energies are shown. It is concluded that the Doppler effect in fast cores is positive for ^{235}U, though it does go negative in the low-kev region. The change in reactivity of ^{238}U metal with temperature is shown. (A.G.W.)

38430 (ANL–7120, pp 616-24) DOPPLER EFFECT IN ^{238}U CAPTURE AND ^{235}U FISSION IN A FAST-NEUTRON SPECTRUM. Pflasterer, G. R. Jr.; Sher, R.; Mayer, W. A.; Warzek, F. G. (General Electric Co., Pleasanton, Calif. Vallecitos Atomic Lab.).

The equipment and method used for activation measurements of the Doppler effect in the fast-neutron spectrum of the Mixed Spectrum Critical Assembly are described. Measurements were made on natural and enriched U metal foils. Results indicate a significant underprediction of the Doppler effect. This discrepancy is believed to be at least partly due to the calculated neutron spectrum being substantially too hard. Random and systematic errors in the measurements are discussed. The technique requires careful control of foil position and counting procedure, but reproducible measurements can be performed to approximately 10% of the magnitude of the observable Doppler effect. (A.G.W.)

38431 (ANL–7120, pp 625-31) TRANSIENT FLUX DISTRIBUTIONS BY DISCONTINUOUS MODEL SYNTHESIS. Godts, J. E. (Westinghouse Electric Corp., Pittsburgh, Pa. Atomic Power Div.); Weinstein, A. S. (Carnegie Inst. of Tech., Pittsburgh, Pa.).

The $1\frac{1}{2}$-group kinetics model considered for a systems study of the Westinghouse Fast Breeder Reactor is presented. The slow-flux group is averaged over the core and represented as a point, while the modal synthesis is used to describe the spatial behavior for the fast-neutron group. Attention is focused on the modal analysis problem, with a brief description of the averaging process proposed for two-dimensional analysis. The strong points of the process for analog computer complexes having repetitive compressed time units are shown. Elements of the analog analyses necessary to implement the transform solution are discussed, and an example of application via digital procedures is briefly described. (A.G.W.)

38432 (ANL–7120, pp 632-5) CRITERIA FOR THE DENSITY OF MONITORING POINTS IN LARGE REACTORS. Gast, Paul F. (Argonne National Lab., Ill.).

The maintaining of a balanced power distribution in large reactors of nonmodular design requires a monitoring system that can be used to estimate the local power at all points in the reactor. Two criteria are proposed for establishing monitoring locations: the expected deviations in the local properties of the reactor medium away from their normal values and the maximum tolerable increases in power above expected levels. An illustrative description is given of the application of these criteria to a situation involving both radial and angular variations in the local $\underline{k}$.

A general theory of reactor monitoring applicable to problems of this type is outlined. (A.G.W.)

38433 (ANL–7120, pp 641-53) CRITICAL REVIEW OF THE PROPERTIES OF MATERIALS AT THE HIGH TEMPERATURES AND PRESSURES SIGNIFICANT FOR FAST REACTOR SAFETY. Miller, David (Argonne National Lab., Ill.).

Techniques for estimating the critical properties of reactor materials at the high temperatures and pressures expected in the course of a hypothetical fast reactor excursion are reviewed. Applications of the law of corresponding states and empirical relations fit to reactor excursion data are discussed. Work on vapor pressures of reactor fuel materials, equations of state, and shock equations of state is summarized. (48 references.) (A.G.W.)

38434 (ANL–7120, pp 654-70) THEORETICAL STUDIES ON THE FAST REACTOR MAXIMUM ACCIDENT. Hicks, E. P.; Menzies, D. C. (Reactor Group, United Kingdom Atomic Energy Authority, Dounreay (Scotland)).

Various aspects of the course of events during and following a hypothetical meltdown accident in a large, fast power reactor were studied theoretically. A major part of the work was concerned with estimates of the size and consequences of the energy release. Most calculations were based on a modified form of the Bethe-Tait model. The current computer code includes a Doppler reactivity feedback effect, and uses a more realistic equation of state than the usual energy-threshold type of equation. The energy release is considerably reduced by the Doppler effect alone; the two effects together typically reduce the peak pressure to values that can hardly be regarded as explosive at all. Most calculations of energy release were based on a homogeneous, spherical core model, but a modified version of the ASTRA reactor explosion code was used for calculations on a finite, cylindrical, two-zone core to investigate the autocatalytic effect of the inwards motion at the zonal boundary; in typical cases the effect was found to be quite negligible. The calculations of energy release led to the conclusion that the useful work done by the adiabatic expansion of the fuel is likely to be small in a typical fast power reactor. A substantial amount of energy generally remains as heat in the fuel at temperatures around 3,000°C, and the possibility that some of this residual energy might be converted into work by secondary processes was studied. The most likely mechanism appears to be the boiling of Na coolant. The damage-producing characteristics of a nuclear energy release were compared with those of a chemical explosive such as TNT. The comparison indicates that the mechanical effects during the early stages of the nuclear incident, up to times of order a few seconds, can usefully be considered in terms of an equivalent charge of TNT, but that the two courses of events diverge substantially at later times. (auth)

38435 (ANL–7120, pp 686-91) A MODIFIED EQUATION OF STATE FOR HYDRODYNAMIC CALCULATIONS IN AX1 NUMERICAL PROGRAM. Jankus, V. Z. (Argonne National Lab., Ill.).

The equation of state presently used in the AX1 program for calculation of energy yield in fast reactor excursions is examined. Numerical inconsistencies that occur when the equation is used in some cases are pointed out. It is suggested that two analytical formulations are needed to calculate both large and small excursions. For large pressures, the equation of state is assumed to be in generalized Bethe-Tait form. For lower pressures, utilization of the equation of state for saturated vapor seems necessary. The absolute temperature is not used in the hydrodynamic calculations, but can be expressed separately as a function of internal energy and specific volume. (A.G.W.)

38436 (ANL–7120, pp 776-88) TRANSIENT RESPONSE OF COUPLED FAST REACTOR CORES. Gunson, W. E.; Heck, F. M.; Daleas, R. S. (Westinghouse Electric Corp., Pittsburgh, Pa. Atomic Power Div.).

Analytical results with regard to the ability of neutronic coupling to enhance the safety characteristics of a modular reactor are presented. The analysis was based on the kinetics model of Avery. A two-module reactor system was selected. The cross-coupling reactivity and cross-coupling lifetime were varied by an order of magnitude for a large and a small finite ramp and sine wave reactivity insertions into one core. It was shown that in a two-core system with only a few tenths per cent coupling coefficient a reactivity insertion into the driver core will result in a significant split of the resultant rise in power between the driver and passive cores. The power rise in the driver core is considerably less than the level that would be attained in an isolated core subjected to the same amount of reactivity insertion. A multimodular reactor thus inherently possesses a promptly acting safety mechanism through the neutronic coupling effect. (A.G.W.)

38437 (ANL–7120, pp 789-93) ENHANCED SAFETY CHARACTERISTICS OF A SODIUM-COOLED COUPLED REACTOR. Eggen, D.; Gibson, A.; Sevy, R.; Silberberg, M. (Atomics International, Canoga Park, Calif.).

The reference design reactor was optimized to obtain a very strong negative Doppler effect and a negative Na void reactivity effect. The design includes a hexagonal array of ten modular fast regions surrounded by low-enriched flux-trap blankets. The kinetic behavior of the reactor was studied in a series of hypothetical accident situations. It was found that the strong Doppler effect on this design is sufficient to control a reactivity insertion of $1 without rapid scram. With normal action of the protective system, a reactivity insertion of $1.65 can be tolerated. The compromise made in economics by emphasizing the Na void reactivity effects was studied. It was concluded that in general increased safety results in increased cost. (A.G.W.)

38438 (ANL–7120, pp 815-25) SURVEY PARAMETER STUDY OF LARGE STEAM-COOLED FAST POWER REACTORS. Kiefhaber, E.; Ott, K. (Kernforschungszentrum, Karlsruhe (West Germany)).

The influence of the following parameters on the reactivity behavior of large fast steam-cooled reactors is discussed: choice of coolant (H_2O or D_2O), isotopic composition of Pu, addition of small amounts of poisons, and accumulation of fission products. Results were analyzed for reasonable values of the geometric buckling, the coolant volume fraction, and the mean steam density under normal operating conditions. Safety criteria for the reactor are listed. Calculations were done for the homogeneous case only. Zero-dimensional and one-dimensional results are presented. (A.G.W.)

38439 (ANL–7120, pp 826-36) FLOOD SAFETY OF STEAM- AND GAS-COOLED FAST REACTORS. Hallam, J. W.; Haling, R. K.; Kilian, P.; Peterson, G. T. (General Electric Co., Pleasanton, Calif. Vallecitos Atomic Lab.).

The Mixed Spectrum Critical Assembly was used for experimental and theoretical studies of the incorporation of resonance poisons into a ^{235}U-fueled fast core as a means of ensuring flooding safety. Poisons used in the experiments were boron carbide clad in stainless steel, EuO_2 similarly clad, and Hf in metal wire form. It was found that Hf has the greatest flooding reactivity hold-down power, but the required volume is large. Economically B_4C seems most favorable. It was generally concluded that it is feasible to achieve flood safety through incorporation of selected resonance poisons into small ^{235}U-fueled steam-cooled fast reactors. Good agreement between calculated and experimental data confirms the validity of the multigroup-diffusion-theory approach. (A.G.W.)

38440 (ANL–7120, pp 881-9) DEVELOPMENT AND GROWTH OF IN-CORE VOIDS DUE TO BOILING DURING FAST REACTOR TRANSIENTS. Noyes, R. C.; Lurie, H.; Jarrett, A. A. (Atomics International, Canoga Park, Calif.).

Selected results of experiments and studies with two digital codes on transient boiling in fast reactors are presented. Significant findings include the following: (1) voiding in a reactor channel starts near the upper boundary of the core and grows axially along the fuel channel, (2) vapor produc-

tion is so rapid that transient self pressurization of the fuel channel occurs, and (3) the resulting two-phase flow is strongly unstable hydrodynamically. (A.G.W.)

38441 (BAW-3492-1(Suppl.1)) ANALYSIS OF LUMPED BURNABLE POISON CRITICAL EXPERIMENTS. Jones, H. M.; Alcorn, F. M.; Paulson, A. E. (Babcock and Wilcox Co., Lynchburg, Va. Atomic Energy Div.). Apr. 1966. Contract AT(30-1)-3492. 29p. (TRG-66-22). Dep. mn. CFSTI $2.00 cy, $0.50 mn.

The developmental work on nuclear analytical methods for distributed control pins is summarized. All the calculations utilized a nuclear code package that was selected after a comparative study of available codes. Four critical experiments have been selected as typical of the B poison pins used in the experiments; B concentration, pin size, and pin distribution were considered. The reported error of the calculated multiplication constant indicates the adequacy of the analytical model. Further work required in some areas is discussed. (auth)

38442 (BNWL-283) NEUTRONICS CHARACTERISTICS OF SELECTED COMPACT FAST REACTORS. Little, W. W. Jr.; Hardie, R. W. (Battelle-Northwest, Richland, Wash. Pacific Northwest Lab.). July 1966. Contract AT(45-1)-1830. 25p. Dep. mn. CFSTI $2.00 cy, $0.50 mn.

The neutronics characteristics of $^{235}UO_2$–W, $^{233}UO_2$–W, and ^{239}PuN–W fueled fast compact reactors are described. The principal items studied are reactor criticality and fuel burnup. For the fuel compositions and void fractions considered, ^{233}U and ^{239}Pu fueled reactors require considerably less fuel than corresponding ^{235}U fueled reactors. All reactors considered are rather insensitive to changes in the refractory metal inventory. (auth)

38443 (GEAP-5148) PLUTONIUM SUBCRITICAL EXPERIMENT PROGRAM. Seventh Quarterly Report, January 1–March 31, 1966. Carver, J. G. (General Electric Co., Pleasanton, Calif. Vallecitos Atomic Lab.). Apr. 1966. Contract AT(04-3)-189. 18p. (EURAEC-1658). Dep. mn. CFSTI $1.00 cy, $0.50 mn.

Work Performed under United States–Euratom Joint Research and Development Program.

The main pressure vessel of the pressurized water system, the core support structure, and the grid plates were received, assembled, and partially tested. A fission converter plate borrowed from ORNL was installed inside a new mounting designed to meet available space requirements. Work was started to reduce the perturbations introduced by beads in the fuel rods and previous lattice calculations were reviewed. Licensing and procurement of critical schedule items are discussed. (H.D.R.)

38444 (JINR-P-2699) PRIMENENIE METODA LOZHNYKH ISTOCHNIKOV K RASCHETAM GETEROGENNOGO YADRA V TSILINDRICHESKOI GEOMETRII. (Application of False Source Method to Heterogeneous Nucleus Calculations in Cylindrical Geometry). Lelek, V. (Joint Inst. for Nuclear Research, Dubna (USSR). Lab. of Theoretical Physics). 1966. 8p. Dep. mn.

Using Feinberg–Galanin's method the calculation of a heterogeneous kernel is made for a line source asymmetrically placed in a moderator of a cylindrical form. It is placed in vacuum or in another medium. These calculations show how the problem of critical size of a reactor with cooled rods is reduced to that of reactor consisting only of a moderator and line rod. Effective values η_{eff} and γ_{eff} (thermal constant) are introduced. (auth)

38445 (RT-FI-(66)1) LE FLUTTUAZIONI DEL LIVELLO DI POTENZA DI UN REATTORE IN CONDIZIONI STAZIONARIE. (Power Level Fluctuations of a Steady-State Operating Reactor). Pacilio, N. (Comitato Nazionale per l'Energia Nucleare, Rome (Italy)). 1966. 46p. Dep. mn.

The correlated relative variance of the number of prompt and delayed neutrons detected is calculated and its dependence on reactivity and counting time is analyzed. Several types of experimental conditions are considered and discussed. (auth)

38446 (TRG-Report-1138) AXIAL STABILITY CALCULATIONS FOR A.G.R. SYSTEMS. Wilson, B.; Enselmoz, J. R.; Hartley, A. J. (Reactor Group, United Kingdom Atomic Energy Authority, Risley (England)). Dec. 13, 1965. 64p. (JNPC-RKWP-P344). Dep. BIS $1.70. HMSO 8s. 6d.

Three methods of calculation of axial stability modes are described. In the modal analysis, criteria for an asymmetric flux, flattened flux and sinusoidal flux have been derived with both one-term and three-term expansions for the harmonic. The steady-state method using the FLIRT program yields a criterion for temperature instability which can accommodate any flux distribution and more accurate harmonic representation. A performance criterion based on the transient performance of the harmonic has been proposed and studied using the analogue method. Stability thresholds and the relation between the performance criterion and stability margins have been obtained. (auth)

38447 (WCAP-2867) EXPERIMENTAL PROGRAM TO INVESTIGATE STABILITY, COMPATIBILITY AND CORROSION OF POISON SOLUTIONS AND STRUCTURAL MATERIALS. TASK 3B. FEASIBILITY OF A CHEMICAL POISON LOOP SYSTEM. Summary Report. Fultonberg, D. N.; Taylor, G. R. (Westinghouse Electric Corp., Pittsburgh, Pa. Atomic Power Div.). July 1966. Contract NAS3-5215. 108p. (NASA-CR-54995).

The experimental programs and the associated facilities designed to investigate the compatibility of various combinations of nuclear poison solutions and structural materials are described. The discussion of the test results and the conclusions drawn are aimed at allowing an assessment of the feasibility of utilizing a Chemical Poison Loop System (CPLS) for the reactivity control of a Tungsten-Water Moderated Rocket Reactor. Reference poison solutions containing cadmium sulfate and preference structural materials of 316 stainless steel and Zircaloy-2 were subjected to low temperature and pressure beaker tests, high temperature and pressure autoclave tests and high temperature and pressure circulating loop tests. (auth)

38448 GENERALIZED POTENTIAL THEORY FOR STATIONARY AND KINETIC CONTROL ROD ANALYSIS OF A THERMAL REACTOR. Ihamuotila, J. (Inst. of Technology, Otaniemi, Finland). Ann. Acad. Sci. Fenn., Ser. A VI, No. 203, 1-18(1966).

A study is made of the application of the integral equation methods of generalized potential theory to the solution of two-group diffusion equations in a cylindrical thermal reactor with a movable central control rod. An iterative method is given for calculating the criticality condition and the flux shapes depending on the insertion depth of the rod. The Laplace-transform is used to solve the kinetic phenomenon caused by a step-wise movement of the rod. Finally the calculation of the flux distribution due to an arbitrary movement of the rod is briefly considered. (auth)

38449 KINETIC BEHAVIOR OF A CIRCULATING-WATER REACTOR FOLLOWING LARGE REACTIVITY CHANGES. Palmer, John A.; Bridgman, C. J.; Verrelli, D. M. (Air Force Inst. of Tech., Wright-Patterson AFB, Ohio). Nucl. Appl., 2: 81-8(Apr. 1966).

A method is described for predicting the kinetic response of circulating-water-cooled and -moderated reactors to large changes in reactivity. This response is displayed in the form of time histories of power, peak fuel plate temperature, energy, reactivity, and period. The validity of the method is verified by the agreement of calculated and experimental data when it is applied directly to the SPERT-IV reactor. The general applicability and usefulness of the method are illustrated by the analysis of the Air Force Nuclear Engineering Test Reactor. A comparison with SPERT-IV, a parametric study, and an accident evaluation are shown as sample results. (auth)

38450 NONITERATIVE METHOD OF COMPUTING NEUTRON FLUX DISTRIBUTIONS AND COOLANT DEN-

SITY PROFILE IN A LIGHT-WATER MODERATED REACTOR. Sha, William T. Nucl. Sci. Eng., 25: 413-21 (1966).

A one-dimensional noniterative method for calculating the fast and thermal neutron flux distribution, effective neutron multiplication factor, power density, enthalpy profile, water density distribution and steam void map of a light-water moderated reactor core is presented and programed as a computer code–ANDREA. In this method, the spatial dependence of the neutron spectrum is accounted for explicitly. The method outlined can be used as one of the design tools for pressurized water reactor (PWR) cores as well as for boiling water reactors (BWR). The novelty of this method lies in its noniterative mathematical formulation which takes into account the nuclear-thermal interaction in a reactor channel. Fission density is directly related to heat generation and heat generation causes density changes in the coolant with subsequent formation of steam voids. The method described here is based on the fact that the above relations are interdependent. As a result, a significant amount of computer time is saved. The method presented is primarily intended for the analysis of large power reactors. (auth)

38451 MULTIGROUP CROSS SECTIONS OF RESONANCE ABSORBERS. Keane, A. (Wollongong Univ. Coll., N. S. W.); Pollard, J. P. Nucl. Sci. Eng., 25: 439-40(1966).

The preparation of multigroup data, typically 18 groups, for input to codes such as CRAM and DSN for systems in which the low-energy resonances dominate is considered. (J.F.P.)

38452 FLUX DISTRIBUTION IN A HIGH-POWER SLAB REACTOR. Smets, Henri B. (OECD, Paris). Nukleonik, 8: 283-7(June 1966).

The flux distribution is computed by a geometric integration in a slab reflected or unreflected system where the buckling is flux dependent. (auth)

38453 INTERPRETATION OF PULSED-SOURCE EXPERIMENTS IN A REFLECTED REACTOR. Waltar, Alan E.; Ruby, Lawrence (Univ. of California, Berkeley). Nukleonik, 8: 287-90(June 1966).

An explanation of the departure of the pulsed-source response curve from a simple exponential for a two-region system is presented. In addition, a new method is proposed for calculating the reactivity based on the two-region model of Cohn. It is shown that the reactivity, which is defined somewhat differently from the choice made by Cohn, can be computed from either core or reflector data. Preliminary experimental results from the AGN-201 Reactor are cited in support of the theory. (auth)

38454 THE KINETIC BEHAVIOR OF A REACTOR COMPOSED OF TWO LOOSELY COUPLED CORES WITH TIME-DEPENDENT COUPLING COEFFICIENTS. Belleni-Morante, A. (Univ., Florence). Nukleonik, 8: 291-6(June 1966).

The behavior of a reactor composed of two loosely coupled cores was studied using a matrix functional equation. Both the multiplication factor matrix K(t) and the coupling matrix $\alpha(t)$ were considered assigned functions of time. Some numerical results were found for the particular case of the UTR-10 Reactor. (auth)

38455 APPLICATION OF A PHENOMENOLOGICAL THERMALIZATION MODEL TO IRRADIATED HEAVY WATER LATTICES. Kind, A.; Rossi, G. (CCR Euratom, Ispra, Italy). 12p. (CONF-660204-19). ORAU. Gmelin, AED-CONF-66-017-14.

From American Nuclear Society Meeting, San Diego, Calif.

A simple thermalization model of phenomenological type previously established for unirradiated heavy water lattices is generalized to take into account resonance absorption in the thermal region. An application of the model to the ECO ^{239}Pu bearing synthetic fuel elements and a detailed comparison with the transport code THERMOS are presented. (auth)

Design and Feasibility

Refer also to abstracts 38439, 38496, and 38497–38499.

38456 (ANL-7120, pp 205-29) CONCEPTUAL DESIGN AND PRELIMINARY ACCIDENT ANALYSIS OF A SODIUM-COOLED, CARBIDE-FUELED, LARGE MODULAR FAST REACTOR. Wright, J. H.; Gunson, W. E.; Heck, F. M.; Daleas, R. S. (Westinghouse Electric Corp., Pittsburgh, Pa. Atomic Power Div.).

The reactor design consists generally of seven modules separated by a graphite reflecting region and coupled by the neutron flux. The core region of each module is surrounded by fertile axial and radial blankets. The fuel is pellets of 90% dense stabilized Pu–U carbide Na-bonded to stainless steel cladding. The Na outlet temperature is 1100°F. The electrical output is expected to be 1375 Mw(e). The plant design includes three heat transfer loops arranged to permit temporary operation at two-thirds capacity with one component out of service. Safety features of the plant design are pointed out and potential accidents to the reactor are reviewed. The response of the reactor to five selected events or chains of events was determined by means of digital power-excursion computer programs. Analysis of these results indicates that the behavior of the reactor should not imperil the public or the operating staff, nor even result in economically severe damage to the plant. (A.G.W.)

38457 (ANL-7120, pp 261-85) DISCUSSION OF PAPERS AMONG PANEL. (Argonne National Lab., Ill.).

Points discussed by the panel included the following: cost of containment relative to overall costs, reactivity increase on loss of Na, reliability of control systems and possible backup safeguards, consequences of failure to scram, feasibility of underground reactors, credibility of pressure vessel failure, attitude of utility companies toward fast reactors with regard to safety and maintenance, advisability of designing reactors for 1000-Mw(e) capacity and the major problems involved, advantages and disadvantages of various coolants, uncertainties in calculations, areas requiring further study, and the experimental facilities needed. (A.G.W.)

38458 (ANL-7120, pp 692-719) MODEL INVESTIGATION OF EXPLOSION CONTAINMENT IN SINGLE TANK FAST REACTORS. Rees, N. J. M. (Atomic Weapons Research Establishment, Foulness Outstation (England)).

Experiments were performed with chemical explosives to simulate on a model scale the rapid release of energy in the core of a fast reactor under maximum accident conditions. The model reactor tank was an overstrong cylindrical vessel of 24-in. diameter and 24 in. deep, closed by a loosely fitting core-access plug of 7¾-in. diameter in the center of the roof. The shock pressure loading on the core plug, walls, and roof were measured by means of 12 piezoelectric pressure gauges. Water was used to simulate the coolant in the reactor tank; levels of 1.1, 4.0, and 8.3 in. below the roof were used. The explosive charges used were 2 oz RDX/TNT 60/40 (Comp. B); in some experiments the charge was placed in a model of a typical core and breeder support structure within the main tank; in others it was used bare. The pressure loadings on the walls of the main tank clearly showed the direct shock wave, the reflected shock from the base of the tank, and the reflected rarefaction from the water surface. The pressure loading on the roof was due to the impact of water thrown upwards when the direct shock was reflected at the surface. The impact pressure loading on the roof appears to be reflected, and a pulse was propagated back down through the contents of the vessel. The loose core-access plug was ejected from the thick-walled vessels at velocities varying from 40 to 74 ft sec^{-1}. The lower velocities were observed when premature failure of a vessel occurred and the highest when the vessel was full of water. These velocities correspond to 0.6 and 2.1% of the charge blast energy being imparted to the plug. For a 1.1-in. air gap between the water sur-

face and the roof, the presence of the model reactor structure surrounding the charge seemed to have little effect on the plug ejection velocity, which was 61 ft sec^{-1}. (auth)

38459 (ANL–7120, pp 720-33) COMPARISON OF PRESSURE LOADING PRODUCED BY CONTAINED EXPLOSIONS IN WATER AND SODIUM. Drevon, G. A. V. (Commissariat a l'Energie Atomique, Saclay (France). Centre d'Etudes Nucleaires); Falgayrettes, M. F. G. (Commissariat a l'Energie Atomique, Cadarache (France). Centre d'Etudes Nucleaires); Walford, F. J. (Atomic Weapons Research Establishment, Foulness Outstation (England)).

Joint experiments by the CEA-Euratom and the UKAEA were carried out at Cadarache, France, using water and hot Na coolant in a small-scale model representative of current fast reactor design. The single stainless-steel coolant tank was about 9.5 in. in diameter and 16.5 in. deep and contained a model breeder and reflector. The coolant in the reactor vessel was heated by a radiant muffle heater surrounding the lower part of the reactor vessel, the whole of which was contained in a strong steel vessel with a removable lid. This lid represented the core-access plug and was attached to the strong vessel by bolts on which were mounted strain gauges to measure the hold-down forces. Pressure gauges mounted in this lid measured the coolant-impact pressure loading produced under the various experimental conditions. The accident energy release in the core of the vessel was simulated by the detonation of 15-, 30-, or 60-g charges of Hexogene in a reentrant cavity at the base of the reactor vessel. All experiments were performed with the coolant level 5 cm below the lid. The Na temperatures were varied between 150 and 550°C; in the experiments with water, temperatures of 20 and 90°C were used. The peak impact pressures measured in the Na experiments were greater than those obtained in the water experiments. The impulse in the measured pressure loadings was also greater in the Na experiments, as were the lid-hold-down loads measured on the strain-gauge bolts. It is clear that for a given explosive release of energy in a fixed geometry the blast effects will be greater in Na than in water. (auth)

38460 (ANL–7120, pp 766-75) FARET CORE-I REFERENCE DESIGN. Persiani, P. J.; Bump, T. R.; Kann, W. J. (Argonne National Lab., Ill.).

The fuel-irradiation program and the reference core planned for the first experiment in the Fast Reactor Test Facility (FARET) are described. It is planned to study simultaneously the performance of several different designs of ceramic and metal fuel assemblies over a range of operating conditions in a small (70-liter) core. An enrichment technique will be used in which ^{235}U will be substituted for ^{238}U. Preliminary results are summarized for a series of FARET critical experiments in ZPR-3 intended to firm up the physics analysis of multifueled nonuniform core loadings. (A.G.W.)

38461 (CONF-651110–29) STEADY-STATE-COUPLED FLUID FLOW AND HEAT CONDUCTION ANALYSIS OF A HEAT-GENERATING SOLID, AS APPLIED TO REACTOR DESIGN. Lee, A. Y. (Westinghouse Electric Corp., Pittsburgh, Pa. Astronuclear Lab.). Nov. 1965. Contract SNP-1. 25p. Dep. mn. CFSTI $1.00 cy, $0.50 mn.

From American Society of Mechanical Engineers, Annual Winter Meeting, Chicago.

A method of solution of the steady-state-coupled fluid flow and heat conduction analysis of a heat-generating solid body that is cooled by a fluid flow along parallel channels is described. The major objectives of the analysis are the determination of flow distribution, axial temperature rise and pressure drop of the coolant as well as the spatial temperature distribution of the solid material. The solution is applicable to any solid body of arbitrary geometry having axially and transversely varying heat generation rates. Calculation example for a long rectangular bar internally cooled along 12 parallel channels which are arranged in a square array is given. Results from this coupled analysis and that obtained from an isolated channel analysis are compared. The effects of plugged channels on the material temperature of this sample solid body are also discussed. (auth)

38462 (GEAP–4929) NINE-ROD CRITICAL HEAT FLUX INVESTIGATION AT 1000 PSIA. Hench, J. E.; Boehm, R. F. (General Electric Co., San Jose, Calif. Atomic Power Equipment Dept.). Jan. 1966. Contract AT(04-3)-189. 33p. Dep. mn. CFSTI $2.00 cy, $0.50 mn.

An experimental study is in progress to determine the critical heat flux variation in water at high pressure. The completed tests have utilized a nine-rod test section with unobstructed geometry (i.e., negligible spacer effect). Seventy-five data points are presented for the mass velocity range of 0.3 to 1.25 Mlb/hr-ft^2 at 1000 psia. (auth)

38463 (IITRI–578P22-15) STUDIES OF REACTOR CONTAINMENT STRUCTURES. Final Report. Salmon, M. A. (IIT Research Inst., Chicago, Ill.). June 1966. Contract AT(11-1)-578. 113p. Dep. mn. CFSTI $4.00 cy, $0.75 mn.

The extent to which openings reduce the strength of containment vessels and the design of reinforcements are studied. Methods for the analysis of the response of spherical shell segments with rigidly reinforced openings are developed and limit analysis solutions are given for finding the strength of reinforcements. Results of tests on thin-walled cylinders and on flat plates with reinforced circular openings are compared with theory to determine the validity of the analytical methods developed. (H.D.R.)

Fuels

Refer also to abstracts 37211, 38494, and 38495.

38464 (AERE–M–1607) THE EFFECT OF NEUTRON FLUX ON THE FISSION PRODUCT GAS EMISSION FROM UO_2 AT HIGH TEMPERATURES. Jackson, G.; Davies, D.; Waterman, M. J. (Atomic Energy Research Establishment, Harwell (England)). July 1965. 10p. Dep. mn.

The emission of gaseous fission products from UO_2 (density 10.5 $g.cm^{-3}$) was studied at 800 to 1600°C in a thermal neutron flux of 2×10^{13} $n.cm^{-2}$ sec^{-1}, (a rating of 6 Mw/t). Comparison with previous results at a lower flux showed that the relation between fractional release and decay constant is dependent on the flux. The apparent diffusion coefficient for ^{133}I is seven times greater than that of ^{133}Xe at 1000°C. (auth)

38465 (ANL–7120, pp 289-300) METAL FUELS FOR FAST REACTORS. Macherey, R. E.; Kelman, L. R.; Kittel, J. H. (Argonne National Lab., Ill.).

Details of irradiation performance, alloy development and compatibility, and jacket corrosion resistance for U–Pu fuel alloy and jacket systems are discussed. Fuel systems of importance are U–Pu-fissium fuel with a V alloy jacket, U–Pu–Ti fuel with a V alloy jacket, and U–Pu–Zr fuel with stainless steel and V alloy jackets. A burnup level of 8.7 at. % was achieved with a U–15 wt % Pu–10 wt % fissium alloy jacketed in Nb–1 wt % Zr at a maximum jacket temperature of 545°C. Ti and Zr additions to U–Pu alloys were found to raise the solidus temperature some 300°C. The higher U–Pu–Zr alloys were found to be compatible with Type 304 stainless steel and form no molten reaction products to temperatures above 800°C. It is concluded that the prospects that metallic fuel specimens now in preparation will exceed burnups of 10 at. % are very good. (A.G.W.)

38466 (ANL–7120, pp 301-13) COMPATIBILITY OF MODIFIED CARBIDE FUELS WITH STAINLESS STEEL. Jordan, K. R.; Herbst, R. J.; Palm, R. G. (Westinghouse Electric Corp., Pittsburgh, Pa. Atomic Power Div.).

The possibility that the compatibility of liquid-metal-bonded nonstoichiometric mixed monocarbide (U,Pu)C fast breeder reactor fuels with stainless steel might be improved by additions of Fe, Cr, UFe_2, or $Cr_{23}C_6$ was studied. The polyphase compositions resulting from heat

treatment included no low-melting eutectic formers or unstable higher carbides. Modified compositions were successfully pelletized by cold pressing and sintering. Improved compatibility was experimentally demonstrated in Ar and liquid metal environments between contact-bonded, iron-modified, initially hypostoichiometric UC and 316 stainless steel. Experiments with gas- and Na-bonded $Cr_{23}C_6$-modified compositions are in progress. (A.G.W.)

38467 (ANL-7120, pp 314-27) MIXED-CARBIDE FUELS FOR FAST REACTORS. Neimark, L. A.; Ayer, J. E.; Kruger, O. L.; Latimer, T. W.; Walter, C. M. (Argonne National Lab., Ill.).

The synthesis, fabrication, compatibility, and irradiation of slightly hyperstoichiometric mixed carbides with a U–Pu ratio of 4:1 were studied. Arc melting and fusion of the elements with a W-tipped electrode were successfully used for synthesis on a laboratory scale. Techniques were demonstrated for producing high-quality pressed and sintered pellets and vibratorily compacted fuel columns. Tests showed stainless steel to be an acceptable jacket material from a compatibility standpoint, but there is still a need for making nonstoichiometric fuel more compatible with the jacket and for finding stronger jacket materials. Promising irradiation results on vibratorily compacted carbide indicate that this system is worthy of consideration for future reactors. (A.G.W.)

38468 (ANL-7120, pp 389-91) COMMENT [ON PHASE-EQUILIBRIA DATA ON Pu–O AND U–O SYSTEMS]. Skavdahl, R. E. (Battelle-Northwest, Richland, Wash. Pacific Northwest Lab.).

Several plutonium oxide samples varying in O: Pu atomic ratio from 1.92 to about 1.6 were examined by differential thermal analysis and found to exhibit during cooling a broad exothermic peak at about 250°C. A small, extremely sharp exothermic reaction on heating was observed at about 875°C for a sample that, before heating, had an O: Pu ratio of 1.55 and, after cooling, an O: Pu ratio of 1.62. Additional melting-point data confirmed previous work on the location of the substoichiometric liquidus line in the U–O system. A capsule containing uranium oxide with O: U between 1.93 and 1.98 was irradiated for one cycle in the MTR. The material exhibited melting to about 20% of the radius and columnar grain growth to about 70%. (A.G.W.)

38469 (ANL-7120, pp 400-9) MICROANALYTICAL STUDIES OF MICRO- AND MACRO-SEGREGATION IN OXIDE FUELS. Bauer, A. A.; Beisswenger, H.; Giacchetti, G.; Patrassi, E.; Schumacher, G.; Theisen, R. (Kernforschungszentrum, Karlsruhe (West Germany). Institut fuer Angewandte Reaktorphysik).

The segregation of CeO_2 in UO_2 annealed in a temperature gradient was investigated. Electron-microprobe techniques were used for the study; shielding of the apparatus was provided for microanalysis of irradiated materials. Pellets of UO_2–CeO_2 were submitted to thermal diffusion for up to 600 hr and temperature gradients ranging up to 5000°C/cm. Two significant mechanisms for the migration of CeO_2 in UO_2 were identified: thermal diffusion and vapor transport. Thermal diffusion in the direction of increasing temperature predominates at lower temperatures; above about 1900°C preferential evaporation of CeO_2 from the high-temperature end of the specimen and vapor transport leading to a segregation on a microscale predominates. (A.G.W.)

38470 (ANL-7120, pp 478-85) TRANSIENT TEMPERATURE DISTRIBUTIONS IN FAST REACTOR FUELS WITH WIDELY VARYING THERMAL DIFFUSIVITY. Sanathanan, C. K.; Carter, J. C.; Brittan, R. O. (Argonne National Lab., Ill.).

A study is described in which new calculational methods for determining transient temperature distributions in UO_2 were devised and transient thermal characteristics of UO_2 were analyzed. The calculational methods take into account the variation with temperature of the thermal conductivity and the heat capacity. The effect of internal radiation on the steady-state and transient thermal response of UO_2 is discussed. (A.G.W.)

38471 (ANL-7120, pp 486-93) TRANSIENT TEMPERATURE DISTRIBUTION IN FUEL ELEMENTS. Godts, J. E.; Restelli, E. F. Jr. (Westinghouse Electric Corp., Pittsburgh, Pa. Atomic Power Div.).

A transform solution for temperature distributions within a cladded fuel rod is described. Discontinuous kernels and mixed geometry are used with finality and completeness preserved in the transformation. By considering the problem in mixed geometries, there is considerable simplification of the transcendental equation that yields the eigenvalues of the transformation. Also included are quantitative checks with nodal method solutions and an analysis of several TREAT experiments in which the fast periods considered are typical of those that may be expected in a fast reactor. (A.G.W.)

38472 (ANL-7120, pp 514-23) THE APPLICATION OF EXPERIMENTAL DATA FROM TREAT MELTDOWN STUDIES TO REACTOR ACCIDENT ANALYSIS. Stachura, S. J.; Silberberg, M. (Atomics International, Canoga Park, Calif.).

Results of recent TREAT meltdown studies of ceramic fuel in Na are presented, and the significance of these results with respect to large core meltdown is indicated. The course of fuel motion in a large core was estimated for a simplified case, and the associated reactivity effects were determined. These reactivity effects were then incorporated into the AIREK reactor kinetics code in order to estimate core behavior subsequent to gross fuel melting in central regions of the core. A discussion of those parameters that can influence meltdown behavior is also presented. (auth)

38473 (ANL-7120, pp 524-33) MIXED OXIDE FUEL MOVEMENT AT VARIOUS POWER LEVELS AND IN TRANSIENTS. Rabin, S. A.; Baily, W. E.; Hanson, J. E.; Knight, F. W. (General Electric Co., San Jose, Calif. Advanced Products Operation).

Experimental observations on the movements of mixed oxide fuel within the cladding in various fuel-temperature regimes are summarized. Radial movement occurs but introduces no objectionable fuel-cladding interactions. Differential fuel-cladding thermal expansion can be accommodated under representative FCR conditions. No evidence of significant axial redistribution exists in mixed oxide operated below center melting. Both upward and downward movement of fuel are noted as a result of transient melting. Molten expansion in an overpower condition can be accommodated in short fuel segments provided sufficient void volume is available. (A.G.W.)

38474 (ANL-7120, pp 534-9) STATUS OF RECENT MELTDOWN STUDIES. Dickerman, C. E.; Robinson, L. E.; Willis, F. L.; Stephany, W.; August, C. (Argonne National Lab., Ill.).

The current status of meltdown studies at Argonne National Laboratory is reviewed. Experimental expansion of fuel is compared with calculated data. Evidence from TREAT studies of cladding failure due to dissolution by molten fuel and to thermal expansion is presented. Work on fuel movement following failure is discussed briefly. (A.G.W.)

38475 (ANL-7120, pp 540-8) SAFETY AND ECONOMIC ASPECTS OF VENTED FUEL IN SODIUM-COOLED REACTORS. O'Neill, G. L.; Knight, F. W.; Leitz, F. J.; Sherer, D. B. (General Electric Co., San Jose, Calif. Advanced Products Operation).

Various methods of accommodating fission gases from high-burnup, high-power-density FCR fuel are reviewed. Results of a preliminary demonstration test of vented-to-coolant fuel are summarized. A large reactor plant using vented-to-coolant fuel was compared with one using vented-to-plenum fuel from standpoints of economics and safety. Vented-to-coolant designs showed no significant increase in costs and possibly a small net reduction. Safety disadvantages stem from lowered internal pressure. Problems involved in release of fission-product gases and detection of failed fuel elements are considered. (A.G.W.)

38476 (ANL-7120, pp 751-8) MIXED FUEL-CYCLE FAST BREEDER REACTORS: NUCLEAR, SAFETY, AND

MATERIALS CONSIDERATIONS. Loewenstein, W. B.; Blumenthal, B. (Argonne National Lab., Ill.).

The core of the proposed reactor will be constituted of two types of fuel subassemblies: one will be the standard type containing Pu–^{238}U fuel elements with axial segments of fertile material, the other will consist of a central region of ^{233}U–Th fuel with axial core extremities of Pu–^{238}U fuel. The core is reflected by a blanket of natural or depleted U with the necessary engineering compromises. Calculations for various configurations indicate that the magnitude of the positive Na reactivity can be significantly lowered by introducing a central core of ^{233}U–Th fuel. Pertinent properties of metals, carbides, and oxides are reviewed and various combinations of these materials are considered for use in fuel elements. (A.G.W.)

38477 (ANL–7120, pp 855-61) FISSION PRODUCT RETENTION IN SODIUM AND APPLICATIONS TO VENTED FUEL ELEMENT DESIGN. Kunkel, W.; Berger, S. (Atomics International, Canoga Park, Calif.).

Safety problems associated with vented-fuel-element design arise generally from increased radioactivity levels in the Na coolant and in the cover gas. Data from several experiments on fission-product retention in Na are tabulated. Radioactivity levels in Na samples from the Sodium Reactor Experiment following a partial fuel melting are shown. Work on cold-trapping of fission products and on transport delay time of Xe and Kr isotopes from formation in the fuel to appearance in the cover gas is discussed briefly. Results of an analytical study to determine the activity in the high-bay area and in the reactor cover gas during normal operation of a vented-fuel power reactor are summarized. It is concluded that the noble gases and their daughters probably constitute the primary radioactivity concern as far as routine operation and maintenance are concerned. Some evidence suggests that a suitably designed Na-cleanup system employing a cold trap or some form of C may be an effective means of removing fission products from the primary coolant. (A.G.W.)

38478 (ANL–7120, pp 862-7) FUEL-FAILURE DETECTION IN SODIUM-COOLED REACTORS. Porges, K. G. (Argonne National Lab., Ill.).

The EBR-II cladding-failure monitor is described briefly. It consists essentially of a fast delayed-neutron monitor installed on a loop that samples the coolant at the heat exchanger and a wire precipitator that monitors the gas blanket. Possible future additions to the EBR-II detection-failure facilities include a charge-collection fission product detector located on the sampling loop and a monitor installed on the charging machine for identifying subassemblies containing failed fuel elements during reactor unloading. Suggestions are made for improvements in detection efficiency and for sampling systems capable of locating the cladding failure in future reactors. A scheme for coding EBR-II type fuel elements with different gases or solids is presented briefly. (A.G.W.)

38479 (BNWL–264) PRELIMINARY HYDRAULIC ANALYSIS OF THE CONCEPTUAL FFTF CERMET DRIVER FUEL ELEMENT DESIGN. Crandall, G. J. (Battelle-Northwest, Richland, Wash. Pacific Northwest Lab.). July 1966. Contract AT(45-1)-1830. 68p. Dep. mn. CFSTI $3.00 cy, $0.75 mn.

The fuel element consists of a fuel rod bundle surrounded by a stainless steel liner. Fuel rod bundle and liner slip as a unit into the fuel element process tube. Spiral ribs are attached to the fuel element liner and they create a spiral channel annulus between the fuel element liner and process tube. A hexagonal honeycomb grid fuel rod spacer design is illustrated. Pressure loss due to fuel rod spacers is calculated by three techniques. Sodium flow rate through the annulus is determined as a function of annulus hydraulic parameters. Sodium leakage between annulus spiral channels and the strength of fuel rod spacer strips to withstand the fluid forces are analyzed. (H.D.R.)

38480 (EUR–2522.f) ELEMENTS COMBUSTIBLES ESSOR. Rapport Final 20.1.1962–20.11.1962. (ESSOR Fuel Elements. Final Report, January 20, 1962–November 11, 1962). Depoitier, J.; Timmermans, W.; Huberlant, M.; Mathieu, F.; Marchal, F.; Detavernier, W.; Michiels, H. (Centre d'Etude de l'Energie Nucleaire, Mol (Belgium)). June 1966. 94p. Dep. mn.

The ESSOR fuel element with a base of 26% U–Al may be compared to the BR2 element, several fabrication parameters of which have already been determined. Fabrication of a composite fuel plate for the ESSOR reactor has therefore been carried out by extrapolating these parameters. It has, however, been necessary, in order to limit the intermetallic compounds, to add to the fuel alloy an element stabilizing the UAl_3 phase, as a result of which the fuel alloy is still able to be laminated. Unfortunately this element hampers chemical analysis. However, promising results have been obtained by substituting gamma counting for such analysis. Bevelling of the tips of the meat has made it possible to reduce to within the scheduled limits the dog-boning customary after lamination. A 60° bevel appears in first approximation to be the most appropriate for the bevelled zone to be kept within the authorized limits after lamination. Finally, the triplex-element assembly has been carried out under vacuum, as this technique makes it possible to obtain composite plates with a minimum of blisters. (auth)

38481 HIGH-TEMPERATURE GAS LOOP AND EXPERIMENTS OF FINNED FUEL ELEMENTS. Okamoto, Yoshizo; Negoya, Shinichi (Japan Atomic Energy Research Inst., Tokyo). Bull. JSME (Jap. Soc. Mech. Eng.), 9: 166-74(1966).

In an attempt to solve some problems arising in the heat removal from gas-cooled nuclear reactors, thermal tests with an out-of-pile mock-up loop capable of giving the same conditions as in-pile operation conditions were conducted. In using finned rods and clusters on fuel elements of gas-cooled reactors, thermal performance of the fuels was obtained by the use of this loop. The loop experiments were devoted to heat-transfer and fluid-dynamic tests of fuel elements and structures of interest in the advanced gas-cooled reactor program of Japan. Data concerning various design specifications, safety systems, functional tests, and modifications of a high temperature pressurized gas are given. The unique feature of the loop is a mechanically sealed blower. Considerable modification and maintenance has been required with the mechanical sealing mechanism during high-temperature operation. The use of double water-lubricated seals necessitates a cold trap-system to separate drained water and gas. Detailed information which can be obtained by functional tests includes the flow rate of sealing gas and the water content in the loop. This loop design was used for thermal tests of polygonal finned fuel specimens. Heat removal tests of the polygonal spiral fins with splitters were made by the use of this loop. Based upon these experiments, a new correlation of heat transfer and fluid dynamics for its fuel assemblies is introduced. (BBB)

38482 ENGINEERING FOR THE FISSION GAS IN UO_2 FUEL. Lewis, W. Bennett (Atomic Energy of Canada Ltd., Chalk River, Ont.). Nucl. Appl., 2: 171-81(Apr. 1966).

Fuel may be designed for fission gas containment within the fuel clad or for venting, also to survive possible ruptures of the clad. Fission gas behavior varies widely with the UO_2 starting material and, with its irradiation history of time and temperature. Below 1000°C, most gas remains trapped; between 1000 and 1800°C, most gas becomes trapped at some time in small closed pores. Expansion of the pores causes swelling. Escape from the pores is by cracking or by radiation-induced reabsorption. Fuel rods are commonly designed with a plenum to collect gas, but the high density of pores and plasticity of the oxide delays or prevents much of the gas from reaching the plenum. For irradiations up to 12,000 Mwd/t, satisfactory designs were achieved without a plenum. Above 1800°C, most gas escapes, but the process of escape is not well established and requires consideration in each case by the design engineer. Available knowledge most relevant to design is briefly reviewed and illustrated in photographs and graphs. (auth)

38483 NUCLEAR INDUSTRY PREPARES TO USE COMMERCIAL PLUTONIUM FUELS. Power Eng., 70: 66-8(May 1966).

Present and future aspects of the development of Pu as a nuclear fuel are assessed. Extensive research on Pu use in water reactors is being supported. Economics and potential for Pu utilization are being evaluated in the program's first phase. Plutonium fueling of boiling water reactors and pressurized water reactors is being studied. Large prototype fast reactors probably will be operating before mid-1970. Technical uncertainty for these reactors should be no greater than it was for the Dresden-Yankee-Indian Point reactor generation. When fast reactors reach a stage of operating on self-generating Pu, they should be insensitive to U ore costs. Up to insertion of fuel elements in a reactor, Pu technology developed for thermal and fast reactors should be mostly interchangeable. Enriched-U fueled reactors being built today produce significant amounts of Pu, and at high-exposure levels, nearly half of the power generated by a fuel element nearing the end of its useful burnup comes from fissioning of its contained Pu. Thus, much of this inbred Pu is burned before discharge from the reactor. Only 0.5 to 1.0% of power reactor spent fuel content is Pu. It is recoverable by reprocessing. (BBB)

38484 HEAT TRANSFER LIMITATIONS ON NUCLEAR REACTOR FUEL ELEMENTS. Rogers, J. T. (Canadian General Electric, Peterborough, Ont.). 64p. (CONF-651019-5). ORAU. Gmelin, AED-CONF-65-294-8.

From 15th Canadian Chemical Engineering Conference, Quebec City.

Limitations on the rates of external heat transfer on fuel elements for Canadian heavy-water-moderated, organic-cooled reactors (OCDR), and boiling-light-water-cooled (BLW) reactors are examined. With organic coolants in simple flow geometries, heat fluxes are limited by departure from nucleate boiling, (DNB). Experiments with simulated partial fuel bundles have shown that the failure mechanism can be either DNB, occurring locally, or coke-out, the formation and deposition of coolant decomposition products on heated surfaces and the rapid growth of the deposited layers. In BLW reactors, critical heat fluxes (CHF) are caused by DNB at low qualities and by dry-out at higher qualities. Parameters governing these phenomena in tubes and annuli are fairly well established and some analytical models are being developed. Data for fuel bundles, including reactor application effects, are becoming available. Increases of critical heat flux by swirl flow and by roughened flow tubes are possible. Heat-transfer-optimized fuel bundles, and new fuel designs with higher heat flux limitations are being developed. A rational method of minimizing the margin of safety on critical heat fluxes is being developed. (auth)

38485 FLEXIBLE CLAD NUCLEAR FUEL ELEMENT. Zebroski, Edwin L. (to General Electric Co.). U. S. Patent 3,262,860. July 26, 1966. Filed Dec. 26, 1962.

A cylindrical fuel element is described with a flexible cladding which is capable of adjusting to dimensional changes of the fuel with temperature and irradiation. The cladding tube contains a number of uniformly spaced, U-shaped longitudinal folds which deflect radially to maintain direct contact with the fuel material under variable operating conditions. (H.D.R.)

Power and Power-Breeder Reactors

Refer also to abstracts 38419, 38439, 38456, 38457, and 38477.

38486 (ACNP-66551) ELK RIVER REACTOR OPERATIONS ANALYSIS PROGRAM. SPENT FUEL SHIPPING CASK CRITICALITY ANALYSIS: TASK 617. Kendrick, E. D. Jr. (Allis-Chalmers Mfg. Co., Bethesda, Md. Atomic Energy Div.). July 1966. Contract AT(11-1)-1357. 22p. Dep. mn. CFSTI $2.00 cy, $0.50 mn.

Results are presented of criticality calculations for the Elk River Reactor 28-element spent fuel shipping cask. The addition of one weight percent of Cd to the Al used in fabrication of the 28-element fuel basket is determined to be sufficient to preclude criticality. Assumptions used in the study are conservative and the results show that the requirements of 10 CFR 71 will be met for any combination of fuel elements now available or presently contemplated for use in the ERR core. (auth)

38487 (AECL-2584) THE FUTURE OF NUCLEAR ENERGY. Lewis, W. B. (Atomic Energy of Canada Ltd., Chalk River (Ontario)). Mar. 1966. 19p. (DL-69). Dep. mn. AECL $0.50.

The main prospect for large-scale use of nuclear power lies with fission in thermal neutron reactors and perhaps in fast reactors, but nuclear spallation and fusion may be brought into use. Radioactivity is important for small power sources. A prospective demand even as large as 3×10^{10} kw(e) could be met from U and Th without breeder reactors. The unit cost of power will be lower the larger the demand, so in the future controlled power may be applied to air conditioning cities, winterizing traffic routes, desalting water, commuter travel, production of chemical fuels and possibly changing a local climate. Great engineering effort is required. There are technical problems due to damage of metals by fast neutrons that limit the performance of reactors. Economic performance of fast breeder reactors is in doubt because of such damage since it is believed necessary to reach high doses of several times 10^{23} fast neutrons per square centimeter. Phenomena of creep under irradiation are taken into account but little understood. A plea is repeated for larger programs and removal of secrecy that would allow freer international exchange of information on the behavior of materials under irradiation at high temperatures. (auth)

38488 (AERE-R-5031) OVERALL THERMAL EFFICIENCIES OF COMBINED GAS-STEAM CYCLES IN AN M.H.D.-REACTOR SYSTEM. Parsons, M. J.; Rice, G. (Atomic Energy Research Establishment, Harwell (England)). June 1966. 39p. Dep. BIS $1.10. HMSO 5s. 6d.

The efficiency of a combined reactor–MHD–steam plant was established for various values of reactor outlet temperature, MHD duct inlet and outlet temperatures and steam generator inlet and outlet temperatures. The system considered used Ar or He as the working fluid for the reactor and MHD duct. K seeding was added for the MHD duct and nonthermal ionization was assumed to occur. A range of steam conditions was considered up to 3500 psi and 1050°F superheat and reheat. The sizes of the major components were also compared for a suitable range of gas pressures. The study of efficiencies showed that the gas topper cycle and the steam cycle must always be considered together because of their interdependence in the heat exchanger. Not to do this leads to serious over-estimates of the gains possible with a topping cycle. For example it was found that a steam cycle thermal efficiency of 52% could be improved to only 56% when all thermodynamic considerations were taken into account, whereas ignoring these would have led to a figure of 63% under the same conditions. A steam cycle efficiency of 52% corresponds to an overall station efficiency of about 45% for a nuclear plant and 40% for a conventional plant, compared with the 42% and 37% expected in practice in 1970. (auth)

38489 (ANL-7120) PROCEEDINGS OF THE CONFERENCE ON SAFETY, FUELS, AND CORE DESIGN IN LARGE FAST POWER REACTORS, ARGONNE NATIONAL LABORATORY, ILLINOIS, OCTOBER 11-14, 1965. (Argonne National Lab., Ill.). Contract W-31-109-eng-38. 925p. (CONF-651009). Dep. mn. CFSTI $9.25 cy, $3.75 mn.

Separate abstracts were prepared for fifty-three of the seventy-nine papers included. The remaining twenty-six papers were previously abstracted for NSA. For abstract numbers of papers previously abstracted, see CONF-651009 in the report number index. (A.G.W.)

For abstracts of individual papers see: 38418–38440, 38456–38460, 38465–38478, and 38490–48500.

38490 (ANL–7120, pp 3-23) SUMMARY OF INTERCOMPARISON CALCULATIONS PERFORMED IN CONJUNCTION WITH CONFERENCE ON SAFETY, FUELS, AND CORE DESIGN IN LARGE FAST POWER REACTORS. Okrent, D. (Argonne National Lab., Ill.).

In order to compare reactor calculations made by various groups, a group of representative single-region bare cores, blanketed cores in spherical geometry, and one reactor of a flat cylindrical shape were specified. Various institutions were asked to compute several parameters of potential interest in connection with each reactor core. Information requested included buckling to go critical, Doppler effect, coolant void effects, reactor spectrum, critical masses, and breeding ratios. Brief discussions of computing methods used by each participant are included. Results for each reactor core are presented in tables and graphs. Possible reasons for differences noted are considered briefly. (A.G.W.)

38491 (ANL–7120, pp 24-32) CALCULATED PHYSICS PARAMETERS AND THEIR UNCERTAINTIES IN A 1000-Mw(e) FAST CERAMIC REACTOR. Greebler, P.; Cowan, C. L.; Fies, C. L.; Gyorey, G. L.; Sueoka, J. R. (General Electric Co., San Jose, Calif. Advanced Products Operation).

Physics parameters calculated for a 1000-Mw(e) fast ceramic oxide reactor in a recent design study are presented. An extensive survey was carried out to identify those uncertainties in nuclear data and calculation methods expected to have a significant effect on the calculated parameters. The effects of these uncertainties on safety and economic physics parameters were calculated using a simplified model of the reactor. The results show that physics performance of large fast reactors cannot now be reliably predicted. Favorable or unfavorable combinations of the uncertainties strongly influence the core design and make large differences in the safety and economics parameters. (auth)

38492 (ANL–7120, pp 54-66) PROGRAM PROPOSED FOR SAFETY STUDIES OF THE FAST NEUTRON PROJECT OF THE EURATOM–CEA ASSOCIATION. Denielou, G.; Falgayrettes, M.; Fournier, J.; Robin, M. G. (Commissariat a l'Energie Atomique, Cadarache (France). Centre d'Etudes Nucleaires).

The proposed program of safety studies concerns large fast-neutron reactors with Na cooling and mixed UO_2-PuO_2 oxide fuel. The program includes studies of the origin, evolution, and effects of different types of accidents. Three examples are given: propagation of a fuel-pin explosion, meltdown propagation in a fuel subassembly, and after-heat cooling of a molten core. Other areas in which research is suggested include Na boiling, physical data for ceramic fuel in liquid and gaseous phases, containment shells, behavior of fission products in case of an accident, and Na–water or NaK–water reactions. (A.G.W.)

38493 (ANL–7120, pp 85-93) A LARGE METAL-FUELED FAST REACTOR STUDY. PART I. NEUTRONICS CALCULATIONS FOR A 1,000-Mwe PLUTONIUM–URANIUM, METAL-FUELED: FAST BREEDER REACTOR. Butler, D. K.; Loewenstein, W. B.; Meneghetti, D.; Phillips, K. E. (Argonne National Lab., Ill.).

The general design of the reactor studied was that of a ring of six cylindrical core modules separated by and surrounded by a fertile blanket. Results of some neutronics calculations for single-enriched and zone-enriched modules are described. The effects of radial Be-containing regions at the core-blanket and/or blanket-reflector interfaces upon critical enrichment, breeding and core conversion ratio, Na void effects, and Doppler effects of isolated modules are listed. The neutronics effects of use of fissium alloy fuel and low-capture alloy fuels, such as Ti or Zr alloys, were studied. The maximum reactivity coupling of a module to the ring of modules was estimated. Two properties of the 1000-Mw(e) system connected with long-term operation were studied: the equilibrium fuel composition and the change in reactivity to be expected between refuelings. Calculations were made of the dynamic behavior of a single module for two kinds of transient conditions: ramp insertions of reactivity and loss of coolant flow. (A.G.W.)

38494 (ANL–7120, pp 94-103) A LARGE METAL-FUELED FAST REACTOR STUDY. PART II. CORE DESIGN AND FUEL CYCLE. Link, L. E.; Ayer, J. E.; Hub, K. A.; Mecham, W. J.; Trice, V. G. Jr.; Weills, J. T. (Argonne National Lab., Ill.).

The general core design is that of a ring of six cylindrical core modules separated by and surrounded by a fertile blanket. The inner and outer radial peripheries of the fertile blankets are surrounded by Be regions. These are surrounded by steel inner and outer radial reflectors. The outer 24 subassemblies of the core are at higher enrichment to improve power flattening. A U–Pu–Ti alloy clad with a Ti–V alloy is used as fuel. A proposed fuel cycle consists of three basic components: breakdown of the fuel subassembly, pyrochemical refining of the spent fuel, and fabrication of the fuel subassembly. The pyrochemical process employs liquid-phase reactions at temperatures of 1200 to 2300°F to effect adequate removal of fission products and the reconstruction of the fuel. A cost analysis of the fuel cycle is included. (A.G.W.)

38495 (ANL–7120, pp 104-23) SELECTED OPTIMIZATION STUDIES IN THE USE OF CARBIDE FUEL IN LARGE FAST BREEDER REACTORS. Sofer, G. A.; Kazi, A. H.; Teer, B. R.; Cherry, B. H. (United Nuclear Corp., White Plains, N. Y. Development Div.).

The results of a number of selected optimization studies on the use of (UPu)C fuel in 1000-Mw(e) fast breeder reactors are summarized. A 3-module core was selected as a reference conceptual design, which features a breeding ratio of 1.65, a negative reactivity effect for voiding the core regions, and sufficient blanket between the modules to effect neutronic isolation. Use is made of recent physical-property and irradiation-test data for (UPu)C, and present best estimates of fuel-cycle cost factors including the effects of private fuel ownership. It is concluded that (UPu)C continues to be a very attractive fast breeder fuel, with potential fuel-cycle costs in the range from 0.20 to 0.40 mill/kwh(e). (auth)

38496 (ANL–7120, pp 136-40) STEAM COOLING FOR FAST REACTORS. Webb, R. A.; Schluderberg, D. C. (Babcock and Wilcox Co., Lynchburg, Va. Atomic Energy Div.).

The possibilities of cooling a direct-cycle fast reactor with steam at 1200 psi were investigated. It was found that the required breeding ratio for a doubling time under 10 yr and a net power output of 1000 Mw(e) could be obtained with an equilibrium Pu cycle based on a pancake geometry and partial surface roughening. An integral arrangement of the Loeffler cycle is proposed, in which the desuperheating and steam-separating equipment, the bypass coolant flow, and circulators are located inside the reactor pressure vessel. A reheat cycle is included in the system to improve plant efficiency. Calculations of capital, fuel, and operation costs lead to a total of 2.50 mill/kwhr. (A.G.W.)

38497 (ANL–7120, pp 157-61) CONTRIBUTION TO SAFETY PROBLEMS RELATED TO A 1000-Mwe FAST POWER REACTOR PROJECT. Denielou, G.; Abdon, R.; Fournier, J.; Ladet, J.; Puig, I.; Robin, M.; Zaleski, C. P. (Commissariat a l'Energie Atomique, Cadarache (France). Centre d'Etudes Nucleaires).

Design data, temperature coefficients of reactivity, power coefficients, and reactivity due to Na loss for a 1000-Mw(e) reference reactor are shown in tables and graphs. Integrated negative Doppler reactivity and total reactivity requirements for operation are discussed briefly. Possible accidents are considered in three groups: those that positively can be avoided by design, those that cannot be positively avoided but whose consequences can be limited by design, and other accidents such as generalized and total loss of flow and complete plugging of a subassembly. (A.G.W.)

38498 (ANL–7120, pp 185-204) SAFETY AND ECONOMIC CHARACTERISTICS OF A 1000-Mwe FAST SO-

DIUM-COOLED REACTOR DESIGN. Cohen, K. P.; O'Neill, G. L. (General Electric Co., San Jose, Calif. Advanced Products Operation).

A design for a 1000-Mw(e) fast, sodium-cooled, mixed-oxide-fueled reactor is presented, based on an updated set of safety and design criteria. Primary emphasis was placed on safety and assurance of technical feasibility. The criteria developed have implications on the areas of reactivity coefficients, core and fuel design, and primary-system design. The economic performance of the reactor represents a distinctly conservative projection of the capability of this present concept. Only a limited amount of optimization was carried out. Accident analyses were performed in sufficient detail to determine the characteristic behavior of the plant in common accident situations and to demonstrate that the design satisfies the safety criteria. Fuel costs were calculated. Calculations of capital and operating costs were not performed, except insofar as previous estimates for similar designs may be applicable. Some consideration was given to the effects of uncertainties in the physics data and fuel performance on economics. (auth)

38499 (ANL-7120, pp 839-47) EXPERIMENTAL STUDIES OF THE HIGH-TEMPERATURE INTERACTION OF FUEL AND CLADDING MATERIALS WITH LIQUID SODIUM. Swift, David L.; Baker, Louis Jr. (Argonne National Lab., Ill.).

In order to simulate the contact of coolant with reactor materials in a meltdown accident, small samples of reactor material were heated to temperatures as high as 2400°C and dropped into a pool of liquid Na. The quenched sample of reactor material was removed from the Na, cleaned with alcohol, and examined for evidence of interaction. When solid specimens of potential cladding materials were dropped into molten Na, there was a brief period of bubbling, but the recovered sample showed no sign of chemical reaction. Molten materials fragmented upon contact with liquid Na. Cladding materials tested included Nb, V, V-20% Ti, Nb-1% Zr, Ti, Zr, steels, Ni, and Al. The most violent fragmentation occurred with stainless steel. Fuel materials studied were U metal and UO_2 pellets. Uranium metal fragmented forming a fragile filamentary network. The UO_2 pellets cracked and Na was absorbed into the cracks. There was no evidence of chemical reaction. It is suggested that the fragmentation process occurs as a molten material cools through the region of boiling where there is violent growth and collapse of vapor bubbles. (A.G.W.)

38500 (ANL-7120, pp 868-72) PRELIMINARY EVALUATION OF A TECHNIQUE TO STUDY EXPULSION OF SODIUM INTO AIR. Charak, I.; Smith, F. A. (Argonne National Lab., Ill.).

In the technique developed, 1- to 2-g quantities of Na were heated to about 1200°F in an Ar atmosphere and ejected into an air chamber at velocities of about 100 ft/sec. To eject the Na a 0.38-caliber shell was used to fire a Teflon pellet against the spring-steel diaphragm on which the capsule containing the Na rested. Equipment was provided for measuring Na velocity and air cell pressure and for photographing at high speed the sequence of Na-air reactions. Preliminary experiments were conducted in which water was ejected into air and Na was ejected into Ar. It was observed in the first Na-air expulsion that all the Na did not react instantaneously with the air. Further experiments are being planned. (A.G.W.)

38501 (APDA-301) DESIGN AND OPERATING EXPERIENCE WITH THE CONTROL AND SAFETY ROD DRIVE MECHANISMS FOR THE ENRICO FERMI FAST BREEDER REACTOR. Hess, J. W. (Atomic Power Development Associates, Inc., Detroit, Mich.). June 1, 1966. Contract AT(11-1)-865. 221p. Dep. mn. CFSTI $6.00 cy, $1.25 mn.

The design of the regulating, shim, and safety rod drives for the Enrico Fermi Fast Breeder Reactor is described. The history and evolution of the design, and the design philosophy, from the early concept stages, to the development of the prototype drives and the final design of the present Fermi plant units are discussed. Noteworthy problems encountered are discussed in some depth, and a detailed description of the present machines is given. Included also is a summary of the testing and operating experience with the equipment, and an evaluation of the present design, based on that experience. Suggestions for improvements in present or future equipment are made where pertinent. In general, discussion is limited to the mechanical design; electrical, instrumentation, or nuclear aspects are treated only when they are particularly relevant. (auth)

38502 (EURAEC-1662) THE STEADY-STATE AND DYNAMIC BEHAVIOR OF A BOILING WATER REACTOR. Quarterly Progress Report No. 19, July 1-October 1, 1965. (Technische Hogeschool, Eindhoven (Netherlands)). Oct. 1965. Contract 069-64-1TEEN. 26p. (EUR-2854; WW-016-R93). Dep. mn. CFSTI $2.00 cy, $0.50 mn.

Work Performed under United States-Euratom Joint Research and Development Program.

Experiments were prepared to be carried out in the pressurized boiling loops under steady-state and nonsteady-state conditions at saturation temperatures and subcoolings. Difficulties encountered in preparation are discussed. Programming of a linearized model to describe the hydraulics of a boiling channel was completed and the results obtained indicate agreement with experiments. (H.D.R.)

38503 (EURAEC-1663) HEAT TRANSFER AND FLUID FLOW CHARACTERISTICS IN A PRESSURIZED WATER REACTOR. Quarterly Progress Report No. 7, July 1-September 1, 1965. (Technische Hogeschool, Eindhoven (Netherlands)). Oct. 1965. Contract 011-64-1TEEN. 29p. (EUR-2855; WW-015-R95). Dep. mn. CFSTI $2.00 cy, $0.50 mn.

Work Performed under United States-Euratom Joint Research and Development Program.

Experiments were carried out on a single rod square annulus geometry for determining the influence of a cold wall and mixing between the fuel channel and a surrounding channel on the burnout power. The tests were interrupted during 6 weeks because of a failure of a transductor. During this time corrosion tests were done for the Reactor Center Netherlands. Calibrations were done in an air-water loop and experiments were done in the 140 atmospheres pressurized loop on a two channel geometry by making mass and heat balances in two adjacent channels. The theoretical study on the hydraulic coupling of parallel channels is being continued. (auth)

38504 (EURAEC-1664) HEAT TRANSFER AND FLUID FLOW CHARACTERISTICS IN A PRESSURIZED WATER REACTOR. Quarterly Progress Report No. 8, October 1, 1965-January 1, 1966. (Technische Hogeschool, Eindhoven (Netherlands)). Contract 011-64-1-Teen(R.D.). 28p. (EUR-2856; WWO-15-R96). Dep. mn. CFSTI $2.00 cy, $0.50 mn.

Work Performed under United States-Euratom Joint Research and Development Program.

Experiments were finished on a single rod square annulus geometry for determining the influence of a cold wall and mixing between the fuel channel and a surrounding channel on the burnout power. Experiments were carried out in an air-water loop on a two channel geometry by making mass and heat balances in two adjacent channels. Measurements were made on void fraction in the air-water loop during non-symmetric injections of air at different levels. The test section on the two channel geometry in the 140 atmospheres pressurized loop was fabricated. The theoretical study on the hydraulic coupling of parallel channels was continued. (auth)

38505 (EURAEC-1672) HEAT TRANSFER AND FLUID FLOW CHARACTERISTICS IN A PRESSURIZED WATER REACTOR. Quarterly Progress Report No. 9, January 1-April 1, 1966. (Technische Hogeschool, Eindhoven (Netherlands)). May 1966. Contract 011-64-1-Teen(R.D.). 23p. (EUR-2864; WWO-15-R100). Dep. mn. CFSTI $1.00 cy, $0.50 mn.

Work Performed under United States–Euratom Joint Research and Development Program.

Experiments were carried out on a seven-rod cluster element to determine the influence of the shroud distance and mixing between the fuel channel and surrounding channels on the burnout power. Technological tests were done with the mixing test section in the pressurized loop among which performance tests on the newly installed void meters was a main item. Continued are the calibrations in an air water loop and a theoretical study on the hydraulic coupling of parallel channels. (auth)

38506 (NDA–2143-7) MCR PROGRAM SHIELD STUDY IN THE ORNL LID TANK. Schamberger, R. D. (General Motors Corp., Detroit, Mich.). Apr. 21, 1961. Contract AT(30-1)-2303. 48p. Dep. mn. CFSTI $2.00 cy, $0.50 mn.

For Nuclear Development Corp. of America, White Plains, N. Y.

A series of lid tank experiments was performed at ORNL to assist in the design of the MCR shield. Neutron and gamma ray measurements were taken behind configurations containing LiH, Fe and LiH, borated Fe and LiH, and Pb and LiH. These experiments were primarily concerned with determining the nature of the secondary gamma production and the influence of boration, reflector thickness, and core composition on the secondary gamma production. The experimental data and descriptions of the configurations are presented. (auth)

38507 (NDA-Memo–2143-11) MILITARY COMPACT REACTOR PROGRAM SHIELD STUDY IN THE ORNL LID TANK: SUPPLEMENT. Kam, F.; Schamberger, R. (General Motors Corp., Detroit, Mich.). June 6, 1961. Contract AT(30-1)-2303. 24p. Dep. mn. CFSTI $1.00 cy, $0.50 mn.

For Nuclear Development Corp. of America, White Plains, N. Y.

Point kernel calculational methods were applied to analyze gamma and fast neutron dose rates of lid tank measurements. The effective removal cross section for a thick piece of steel backed by LiH and H_2O was measured. The effective energies of the secondary radiation produced in lead and steel were determined. (auth)

38508 (NYO–2764-2) FEASIBILITY STUDY OF A UNIFIED DIGITAL INSTRUMENTATION AND CONTROL SYSTEM FOR NUCLEAR POWER PLANTS. Final Report, April 1961–June 1965. Gertz, D.; Levine, J. (Ford Instrument Co., Long Island City, N. Y.). June 30, 1965. Contract AT(30-1)-2764. 369p. Dep. mn. CFSTI $7.00 cy, $1.75 mn.

A program to develop basic techniques which, applied to nuclear power plant instrumentation and control systems, would greatly enhance long term operational reliability is described. The methods used to accomplish this goal include analysis, experimental investigation, development of laboratory models, evaluation of experimental prototypes, and study of system applications. The results of this program are presented in three major ways, including significant aspects of development effort, operating demonstrations of several engineering models, and application of developed techniques to power plant systems. With knowledge and appreciation of the difficulties experienced with state-of-the-art power plant instrumentation, stringent design goals were established as a basis for the development of improved equipment. These goals could best be met through the development of all-digital instrumentation and control systems utilizing techniques and hardware not then available in existing technology. The development effort is described in terms of the major problems encountered, and the various techniques investigated for their solution. The features of each of these approaches are discussed as a result of actual test results of evaluation models and their eventual application to power plant systems. The merits as well as the limitations of the equipment are reviewed, including recommendations where further development work is advisable. (auth)

38509 (ORNL-TM–1449) EFFECT OF TWO-PASS FLOW IN THE BONUS SUPERHEATER ASSEMBLIES. Sanders, J. P. (Oak Ridge National Lab., Tenn.). Apr. 22, 1966. Contract W-7405-eng-26. 5p. Dep. mn. CFSTI $1.00 cy, $0.50 mn.

A brief study was made of the effect of redesigning the BONUS superheater assemblies for two-pass flow rather than four-pass flow. Based on the design criteria and assumed uniform distribution of flow, it was estimated that the heat transfer coefficient in the superheater would be reduced from 598 to 343 $Btu/hr \cdot ft^2 \cdot °F$. This reduction would result in cladding temperatures approaching 1500°F at the point of maximum heat flux; these temperatures are above the allowable limit for the Inconel cladding. (auth)

38510 (ORO–649) BOILING NUCLEAR SUPERHEATER (BONUS) POWER STATION: PUNTA HIGUERA SITE NEAR RINCON, PUERTO RICO. Project Completion Report. (Oak Ridge Operations Office (AEC), Tenn.). June 1966. 160p. Dep. mn. CFSTI $5.00 cy, $1.00 mn.

The BONUS Power Station project is described from the time of authorization to project completion. Design, cost, and performance data are summarized with attention to the various factors which affected the original schedule and cost estimates. Research and development work performed by the Atomic Energy Commission and the construction of the generating facilities by the Puerto Rico Water Resources Authority are described. Estimated final costs are summarized. (H.D.R.)

38511 POTENTIAL CONTRIBUTION TO ELECTRICITY GENERATION OF HYDROELECTRIC POWER AND NUCLEAR ENERGY. Hinton, Christopher Advance. Sci., 22: 326-33(Sept. 1965).

Comparative economic and technical data for fossil-fuel, hydroelectric, and nuclear-energy power plants are examined. Nuclear generation costs are independent of fuel transport, and, as the capital cost of nuclear power stations falls to a level which gives cheap nuclear power (which will happen in the 1970's), these must be built near the points of consumption. British nuclear power development is discussed. It has achieved a marked downward trend in cost both by achieving higher top temperatures and larger unit sizes in reactors, and by the development of the integral reactor with a prestressed reinforced concrete shell. Reactors using fuel elements of the Calder Hall type now being built are estimated to have a capital cost of about £100 per kw and a unit cost of about 0.67d, which is still well above the cost of about 0.5d/unit at which power can be generated in fossil-fuel fired stations. Nuclear generation tends to be more competitive in the larger unit sizes and when operated on base load. It may therefore be difficult to justify in the small supply systems. Development of hydro resources, when these are available, is likely to be more attractive to the less developed countries as long as their resources of technical manpower are limited and their demands for electricity relatively small. Added to this, nuclear development probably requires more foreign currency and may have the political drawback of dependence for fuel supplies on a foreign power. Elsewhere, competition from nuclear generation is certain to become increasingly strong. The long life of hydro plants gives them some advantage but nuclear power offers a system in which the trend of capital and operating costs will be downwards. (BBB)

38512 ECONOMIC ASPECTS FOR STIMULATING NUCLEAR POWER. Batov, V. V.; Koryakin, Yu. I. At. Energ. (USSR), 20: 379-84(May 1966). (In Russian).

A review of the budget and of the plans for developing nuclear power in the Soviet Union is presented. Fuel costs, wages, production norms, and the economics of various reactors are considered. (G.O.Y.)

38513 EFFECTS OF CERTAIN CYCLE PARAMETERS ON EFFICIENCY OF GAS-TURBINE NUCLEAR PLANTS. Ratnikov, E. F.; Shustov, M. V. At. Energ. (USSR), 20: 412-15(May 1966). (In Russian).

The effects of increased pressure, of degeneration of the initial gas pressure, of fuel cladding, temperature, and gas loop pneumatic resistance on the nuclear gas turbine internal efficiency were analyzed taking into consideration the

characteristics of the reactor active zone. Data are given on a nuclear gas turbine with intermediate cooling and gas heating. The design of a nuclear gas turbine with one intermediate heating unit and a triple gas cooling unit is discussed. (G.O.Y.)

38514 ADVANCED GAS-COOLED REACTOR POWER STATIONS. Dent, K. H. (United Kingdom Atomic Energy Authority, Windscale, Eng.). Elec. Export Rev., 4: 113-15(Oct.-Dec. 1965).

This review points out that the advanced gas-cooled reactor (AGR) is a high-efficiency, high-availability plant; it is a very safe system and it allows remarkable freedom in siting. So far the only AGR that has been built is the small prototype plant at Windscale which has now been in operation for two and a half years. The purpose of this plant has been to provide operating experience, and to prove the fuel, the moderator and other components in large-scale operation. A series of AGR power stations has been designed for export. These range from a station of 1 × 300 Mw output up to one of 2 × 1200 Mw output. The reactor units are of integral design. That is, each reactor and the whole of its primary circuit including the boiler is placed within a single prestressed concrete pressure vessel. The vessel can be of spherical or cylindrical shape and different arrangements of the internal components can be used. The fuel of an AGR is high-melting-point ceramic uranium dioxide, manufactured into pellets which are canned in stainless steel to form fuel pins; in a typical design, thirty-six of these pins are assembled as a cluster within a graphite sleeve. These assemblies are put together at a station on a central steel tie rod to make up a fuel stringer, the graphite sleeves forming a continuous channel for the coolant gas from bottom to top of the core. The whole of this gas circuit is made such that entry for routine inspection or maintenance is unnecessary. It has no moving parts other than the circulators and the control rods, each of which is removable for maintenance. The pre-stressed concrete pressure vessel is constructed in situ. It is provided with a mild steel gastight liner, insulated on the gas side with stainless steel foil insulation and cooled on the outside to an acceptable temperature for the concrete by a water cooling system. Economics of the AGR installation are also discussed. (BBB)

38515 DEVELOPMENT IN FRANCE OF NATURAL URANIUM-GRAPHITE-GAS REACTORS. Saltcevsky, Boris; Tanguy, Pierre-Yves. Ind. At., 10: No. 5-6, 49-59(1966). (In French).

The development of improved EDF-4 and Inca type reactors is studied. After reviewing the prototypes which permitted the EDF and the CEA to shift from the first reactors in Marcoule to the Saint-Laurent-1 (EDF-4) reactor, the following constructions of the EDF-4 technical level are presented: Saint-Laurent-2, Fessenheim-1, for which the economic prospects are most encouraging and broadly competitive. A list is given of the chief characteristics of the Inca technique, using an annular metallic fuel, which enables significantly greater performance, while retaining the advantages of a natural cycle. The construction of the first unit of this type, Bugey-1, began in 1966, and the prospects are most promising, especially for central stations of 1,000 and 1,200 Mw(e) power. (auth)

38516 THE GROWTH OF THE BRITISH NUCLEAR POWER PROGRAM. Hill, John M. (United Kingdom Atomic Energy Authority, London). Ind. At., 10: No. 5-6, 60-6(1966).

Progress in the British nuclear power program is reviewed along with changes in the types of reactors from Berkeley through Wylfa. Future stages of the program are mentioned briefly. (M.H.R.)

38517 HEAVY WATER POWER REACTORS. Bailly du Bois, Bernard. Ind. At., 10: No. 5-6, 67-74(1966). (In French).

The present status of heavy water reactors throughout the world is reviewed, and it is shown that certain advantages accruing from an excellent fuel-cycle economy should enable this type of reactor to compete with the more proven thermal reactors and to afford a satisfactory solution to U supply problems. The French program includes the construction of the prototype EL-4 in Brittany and a number of development tasks, in particular on fuel elements in cans with low neutron losses. The engineering studies have to do with a reference reactor of 600 Mw(e), and envisage several variants in the mechanical design of the reactor bloc, for subsequent constructions. (auth)

38518 ORGEL PROJECT. Leny, Jean-Claude (Orgel Project, Ispra, Italy). Ind. At., 10: No. 5-6, 75-82 (1966). (In French).

The Orgel project is intended to test a variant of moderate-power, heavy-water reactors cooled by an organic liquid (mixture of polyphenyls). In 1960 its construction was allocated to Euratom. Some details on the Orgel as it is conceived are given, and helpful comparisons with other variants of heavy-water reactors are made. (M.H.R.)

38519 CHOICE OF AN AVERAGE HEAT FLUX AT THE FUEL ELEMENT SURFACE OF PRESSURIZED WATER REACTORS. Ulfskii, G. V. Inzh.-Fiz. Zh., 10: 613-19(May 1966). (In Russian).

A method is given for determining maximum permissible average heat flux on the fuel element surface of the pressurized water reactor in the case of cosinusoidal distribution of heat transfer along the fuel element height and with subcooling to boiling at the channel outlet where the temperature is ≥10°C. (tr-auth)

38520 NUCLEAR POWER BECOMES COMPETITIVE. Petrol. Press Serv., 32: 249-51(July 1965).

The long term implications for the coal and oil industries of the promise of competitive nuclear-base electricity are discussed. The fall in the capital cost of nuclear stations is traced and compared with current coal-fired stations. Dungeness B is expected to cost £67/kw and to have low operating costs. If nuclear plants can generate current at 10% below coal-fired plant costs, a level of coal consumption of 80 million tons in 1970 could hardly be justified. Oil is considered to be less vulnerable. (auth)

38521 STEAM TURBINES FOR NUCLEAR POWER PLANTS. Sinton, Walter (Westinghouse Electric Corp., Philadelphia). Westinghouse Eng., 24: 110-13(July 1966).

Present reactor systems supply steam to the turbine at low pressure and temperature when compared to large fossil-fired plants. The design approach for nuclear steam turbines must offset two basic limitations. Because of the relatively low energy content per pound of steam, the turbine inlet and exhaust must pass large volumetric flows, and moisture separation, reheat, or both must be used to prevent excessive blade erosion and reduced thermal efficiency. These limitations are examined in detail. Specifications are tabulated for twelve Westinghouse nuclear turbines of 100 Mw rating and above, and nuclear turbine performance records are examined. (H.D.R.)

38522 CONTAINMENT STRUCTURES: REACTOR CONTAINMENT STRUCTURES ABROAD. Gluckmann, Alexis L. (Gibbs and Hill, Inc., New York). 35p. (CONF-650829-2). ORAU. Gmelin, AED-CONF-65-238-1.

From American Society of Corrosion Engineers, Power Division Specialty Conference, Denver.

Some containment structures designed for pressurized water reactors in Belgium, Spain, Japan, Italy, and Switzerland are described. (auth)

38523 ESADA DEVELOPMENT PROGRAM HIGH TEMPERATURE GAS-COOLED REACTOR. Le Clair, Titus G. (General Atomic Div., General Dynamics Corp., San Diego, Calif.). 24p. (CONF-651071-1). ORAU. Gmelin, AED-CONF-65-356-2.

From American Nuclear Society, New York State Intersectional Meeting, Buffalo.

The Empire States Atomic Development Associates development program on the High Temperature Gas-Cooled Reactor (HTGR) concept is summarized. Brief descriptions are given of the Peach Bottom Power Reactor, fuel and fuel

cycle development, prestressed concrete reactor vessel testing, and a 330 Mw power plant proposed by the Public Service Company of Colorado. Potential engineering and economic benefits of the HTGR concept are discussed. (H.D.R.)

Process Heat Reactors

38524 LARGE-SCALE NUCLEAR DESALTING PLANTS. Galstaun, Lionel S. (Bechtel Corp., San Francisco). 12p. (CONF-651132–6). ORAU. Gmelin, AED-CONF-65-337-3.

From Atomic Industrial Forum, 12th Annual Conference, Washington, D. C.

A comparison is made of the costs of desalting water in 150 million gallon per day multi-stage desalting plants. Both dual purpose nuclear power-water and water-only plants are considered. The basis for the dual purpose units has been the commercially available light water reactors, whereas the single purpose unit used the Deep Pool Reactor Concept. All estimates of cost, including capital, fixed annual, operating costs, and fuel cycle costs were related to the basis used in the report for the Metropolitan Water District of Southern California. The results show that the costs in every case are lower when electricity and power are produced. One major reason is the higher cost for energy in the single purpose plant. (auth)

Propulsion and Space

See also ENGINEERING — Space Propulsion

Refer also to abstract 37034.

38525 (NUS–208) ENVIRONMENTAL SAFETY ASPECTS OF NUCLEAR ROCKET FLIGHT OPERATIONS. Semi-Annual Progress Report, May–October 1964. (Nuclear Utility Services, Inc., Washington, D. C.). Dec. 1964. Contracts AT(11-1)-651; SNPC-6. 64p. Dep. mn. CFSTI $3.00 cy, $0.75 mn.

The work conducted during this period is divided into two major categories: Ground Safety Program Activities and Flight Safety Program Activities and Flight Safety Program Activities. The Ground Safety activities include: NRDS effluent work; modification and application of the NURSE-1 computer program to the NRDS situation; NRDS Safety Advisory Panel activities; and a preliminary study of effluent decontamination. The Flight Safety activities include: those generated by assignment under the Radiological Effects Working Group; the examination and development of models for the description of particle velocities created by destruct action; and work on nuclear transient codes. (auth)

38526 COMMENTS ON NUCLEAR-POWERED SURFACE EFFECT SHIP DESIGN PROBLEMS. Petroff, Alex N. (Univ. of Michigan, Ann Arbor). J. Aircraft, 3: 78 (Jan.-Feb. 1966).

Some comparisons are made of the specifications and operating characteristics of lighter than air vehicles (such as a He–filled airship) and surface effect ships with respect to nuclear-powered propulsion. Pertinent characteristics and performance are given for a proposed He–filled airship to carry 200 passengers a distance of 3500 miles. A measure of efficiency with respect to the load carrying capacity, aerodynamics, and propulsion is given. In the light of recent improvements in structural materials and turbofan engines and with application of boundary-layer control, the case of the airship becomes even more promising than indicated by this data. If nuclear power is contemplated, considering the length of an airship of ~1000 ft, the weight of shielding material could be considerably reduced in comparison with shorter machines. This implies that large rigid airships as a means of economic mass transportation at speeds of 100 mph or higher warrant careful consideration and future studies. (BBB)

38527 SNAP-8 REACTOR AND SHIELD DESIGNS AND OPERATING EXPERIENCE. Johnson, C. E.; Mason, D. G. (Atomics International, Canoga Park, Calif.). Contract AT-(11-1)-GEN-8. J. Spacecraft Rockets, 3: 1099-1105 (July 1966).

The SNAP 8 reactor is a heat source suitable for long-endurance 10- to 50-kw space electric power supplies. Two tests have demonstrated its feasibility: the SNAP 8 Experimental Reactor (S8ER) and the SNAP 8 Developmental Reactor Mockup (S8DRM-1). The S8ER demonstrated stable long-term operation of the reactor core and reflector. During 500 days of nuclear operation, it operated one year in the power range 400 to 600 kw(t) with a 1300°F coolant outlet temperature and continuously for over 5000 hr. Post-test examination revealed cracks in ~80% of the cladding tubes, the cause of which is being investigated. Automatic control system performance and structural capabilities of the reactor design were verified in non-nuclear testing of the S8DRM-1. The reactor and shield design is summarized for manned and unmanned space applications. Curves are provided, allowing spacecraft designers to estimate shield weight for both applications rapidly as a function of payload diameter, payload separation distance, dose rate for manned applications, and total dose for unmanned applications. The design approach to high reliability is described. (auth)

38528 NOZZLE TUBE-WALL TEMPERATURE MEASUREMENT BY RADIOMETRIC TECHNIQUES. Geery, E. L. (Aerojet-General Corp., Sacramento, Calif.); Thompson, W. R.; Beveridge, J. H.; Helm, W. J. J. Spacecraft Rockets, 3: 1144-6 (July 1966).

A radiometer mounted on the outside of a rocket nozzle window is described for viewing the cooled side of the heated wall through the coolant (LH_2) flow without disturbing the hot gases or coolant. The radiometric device measures at more than two wavelengths, employs a single detector, operates in the near-infrared region, and is capable of continuous measurement. (J.R.D.)

38529 NUCLEAR REACTOR OPERATION IN SPACE. Sayers, J.; Walker, J. (Univ. of Birmingham, Eng.). Nature, 211: 60 (July 2, 1966).

It was estimated that the gamma radiation from a 1-Mw nuclear reactor operated in space could produce about 5×10^{12} electrons/sec by Compton scattering in the spherical shell of a large heat radiator placed around the reactor. This would result in a positive potential on the shell of some 0.8 Mv. In the present note it is concluded that the ambient plasma at 1000 km will provide a powerful mechanism for neutralizing the charge of any body within it. It is further pointed out that a modest positive ion source or a 10% leakage of fast neutrons could be used to prevent buildup of charge in regions of space where the ambient plasma is negligible. (W.D.M.)

Research and Test Reactors

Refer also to abstracts 38471, 38472, and 38474.

38530 (GA–6078) HAZARDS SUMMARY FOR THE ACCELERATOR PULSED FAST ASSEMBLY. Crosbie, K. L.; Russell, J. L. Jr. (General Dynamics Corp., San Diego, Calif. General Atomic Div.). Feb. 25, 1965. 71p. (DOCKET–50-235). Dep. mn. CFSTI $3.00 cy, $0.75 mn.

Descriptions are given of the GA linear accelerator facility, the Accelerator Pulsed Fast Assembly (APFA), and instrumentation and controls. The operating procedures for the assembly are outlined. A detailed hazards analysis was made with respect to normal conditions, accident conditions, flooding, power failure, manual assembly, falling objects, "fat-man" hazard, moderation, release of radioactive material, fire, earthquakes, and tuning accidents. (M.O.W.)

38531 (GEAP–5133) A DESCRIPTION OF FUEL AND OTHER CORE MATERIALS PROCURED FOR SEFOR CRITICAL EXPERIMENTS IN ZPR-III. Johnson, M. L. (General Electric Co., San Jose, Calif. Advanced Products). Dec. 1965. Contract AT(04-3)-540. 32p. Dep. mn. CFSTI $2.00 cy, $0.50 mn.

Critical Experiments for the Southwest Experimental Fast Oxide Reactor (SEFOR) are being conducted in the Zero Power Reactor-III (ZPR-III) fast-flux critical assembly at the National Reactor Testing Station, Idaho. In the ZPR-III, core materials in the form of small blocks are loaded into the compartmented core structure. Stainless steel cans containing metal alloy (19.5 wt % Pu-78.0 wt % U-2.5 wt % Mo) and cans containing Na_2CO_3 were developed and procured to simulate the oxide fuel and Na in SEFOR. Sintered BeO blocks coated with Kel-F were also procured. Ni blocks were provided for reflector material, and Kel-F-coated Boral blocks simulated the B_4C radial shield annulus. Quantities, weights, and design features of these materials are described. (auth)

38532 (NASA-TN-D-3555) CRITICAL MASS STUDIES WITH THE NASA ZERO POWER REACTOR II. II. HETEROGENEOUS ARRAYS OF CYLINDRICAL VOIDS. Fox, Thomas A.; Mueller, Robert A.; Ford, C. Hubbard (National Aeronautics and Space Administration, Cleveland, Ohio. Lewis Research Center). Aug. 1966. 24p. CFSTI $1.00 cy, $0.50 mn.

The ZPR-II was used to determine several critical cylindrical configurations of aqueous fuel solutions that contain heterogeneous arrays of voids. These voids are cylindrical, symmetrically arranged parallel to the axis of the reactor, and extend the height of the core. A wide range of highly enriched aqueous uranyl fluoride fuel concentrations are studied. Data are also presented on the thermal neutron flux distributions in the central radial plane and on the variation of void reactivity importance with radial position. (H.D.R.)

38533 (NP-16168(Pt.A)) AQUEOUS HOMOGENEOUS SUSPENSION REACTOR PROJECT. PART A. RESEARCH AND DEVELOPMENT. Annual Report, 1965. (Keuring van Electrotechnische Materialen, N. V., Arnhem (Netherlands)). 36p. Dep. mn.

A research and development report is presented on irradiation of fuel in capsules and on the applicability of a fine fuel for a suspension reactor. (B.G.D.)

38534 (NP-16168(Pt.B)) AQUEOUS HOMOGENEOUS SUSPENSION REACTOR PROJECT. PART B. KSTR: DESIGN AND CONSTRUCTION. Annual Report, 1965. (Keuring van Electrotechnische Materialen, N. V., Arnhem (Netherlands)). 27p. Dep. mn.

A report is presented on the development of the Kema Suspension Test Reactor. Included are designs of reactor systems and components, instrumentation, and construction. (B.G.D.)

38535 RADIOACTIVE POLLUTION IN THE AREA OF THE NUCLEAR REACTOR IRT-1000. Mishev, I.; Radicheva, M. Izv. Fiz. Inst. Aneb, Bulg. Akad. Nauk, 14: 57-65(1966). (In Russian).

Results are presented of two-year long measurements of the activity of soils, plants, aerosols and sewer waters and waters of the second circle of the reactor, in the area of the IRT-1000 nuclear reactor, Sofia. The samples were periodically taken from fixed points around the reactor and their specific β-activity was measured after preliminary processing. The results show, with the methods applied, that no pollution was discovered in the area around the IRT-1000 reactor during the period mentioned. The considerable increased activity of some samples at certain time is due to the fall out which is constantly precipitated on the ground and which carries the products of nuclear explosions in the atmosphere. (auth)

38536 THE EFFECTIVENESS OF RESONANCE NEUTRONS FOR THE VVR-S REACTOR CHAIN REACTION. Stefanescu, Al. (Inst. of Atomic Physics, Bucharest). Rev. Roum. Phys., 11: 261-4(1966).

The measurement of the effectiveness of resonance neutrons carried out by the combination of foil activation and danger coefficient techniques is presented. The result obtained is $F_r = 1.05 \pm 0.12$ for the center of the active core of VVR-S reactor. (auth)

WASTE DISPOSAL AND PROCESSING

See also BIOLOGY AND MEDICINE — Ecology
CHEMISTRY — Radiochemistry
CHEMISTRY — Separation Processes and Procedures
HEALTH AND SAFETY

Refer also to abstract 37041.

38537 BEHAVIOR OF RADIOACTIVE STRONTIUM, CESIUM, AND COBALT IN MARINE WATER. Ojima, Tsutomu; Toratani, Hirokazu; Fujimoto, Hiroshi. Ann. Rep. Radiat. Center Osaka Prefect., 6: 93-7 (1965).

The physicochemical behavior of ^{89}Sr, ^{90}Sr, ^{137}Cs, and ^{60}Co ions was studied in relation to pH of marine water, trace elements dissolved in it, fragments of marine organisms living in it, and sea sediments. (auth)

38538 WASTE DISPOSAL. Fineman, P. Reactor Fuel Process., 9: 110-20 (Spring, 1966).

Treatment of low- and intermediate-level-activity wastes by ion exchange and incorporation in asphalt, conversion of high-level-activity wastes to solids, final disposal, and fission-product recovery are discussed. (M.C.G.)

38539 CONTAINMENT OF RADIOACTIVE WASTES. Nelson, Murrell D. Jr. (to Mobil Oil Corp.). U. S. Patent 3,262,274. July 26, 1966. Filed Sept. 27, 1962.

A method is described which provides complete containment of radioactive waste in a desired subsurface storage area. The waste composition consists of nuclide-containing materials such as aqueous solutions, nonaqueous solutions, other fluids, and cement having oil as a continuous phase. Advantages of this method are that the earth needs only to blanket the hazardous radioactive emission; surrounding formations are warmed by heat released in decay which makes any stored petroleum more mobile; and the heat generated may be recovered by heat exchangers. (F.S.)

GENERAL AND MISCELLANEOUS

38540 (PAEC(A)IN-652) CARBON-14. A Literature Search. (Philippine Atomic Energy Commission, Manila). Jan. 1965. 140p. Dep. mn.

Eight hundred and forty references on ^{14}C are listed under the following subject headings: general and miscellaneous, biology and medicine, chemistry, engineering, geology and mineralogy, health and safety, instrumentation, mathematics and computers, and physics and reactor technology. The references cited were abstracted in Nuclear Science Abstracts from Jan. 1947 to April 1963. The entries are arranged alphabetically by title under the subject headings. Personal author and corporate author indexes are provided. (M.C.G.)

38541 EUROPEAN ASSESSMENT OF NUCLEAR AND CONVENTIONAL FUEL COSTS. Von Geldern, Eduard R. 18p. (CONF-651132-4). ORAU. Gmelin, AED-CONF-65-337-22.

From Atomic Industrial Forum, 12th Annual Conference, Washington, D. C.

Results of an economic study of fuels carried out by EURATOM countries are presented. Data and information from the study are presented on coal, fuel oil, natural gas, natural U, enriched U, and Pu. (J.R.D.)

CORPORATE AUTHOR INDEX

This index contains entries for this period for all report literature and, in addition, for certain published literature items for which it is felt that a corporate approach is especially desirable, e.g., symposia, conference proceedings, and meetings.

Each entry under a corporate author is a shortened version of the title of the publication, followed by the *NSA* volume and abstract number. Report numbers are given in parentheses.

The phrase "Progress report" is abbreviated as "Prog. rpt.," permitting a more rapid and complete alphabetical arrangement of the titles without changing the location of the progress report titles in relation to the other titles.

A

AEROSPACE RESEARCH LABS., WRIGHT-PATTERSON AFB, OHIO.
Theory of spherical probes in monoenergetic plasmas, 20: 38190 (AD-637513)

AIR FORCE CAMBRIDGE RESEARCH LABS., L. G. HANSCOM FIELD, MASS.
Magnetic field design with an electrolytic tank analog, 20: 38189 (AD-636095)

AKADEMIYA NAUK SSSR, NOVOSIBIRSK. INSTITUT YADERNOI FIZIKI.
Status of operation at the positron-electron accumulator VEPP-2, 20: 37321 (NP-16205)

AKADEMIYA NAUK UKRAINSKOI SSR, KHARKOV. FIZIKO-TEKHNICHESKII INSTITUT.
Interaction of plasma oscillations and spin waves in ferromagnetic semiconductors and metals, 20: 38354 (FTI-244/T-027)

ALLIS-CHALMERS MFG. CO., BETHESDA, MD. ATOMIC ENERGY DIV.
Elk River Reactor spent fuel shipping cask criticality analysis, 20: 38486 (ACNP-66551)

AMES LAB., IOWA STATE UNIV. OF SCIENCE AND TECH.
Bibliography on mass spectroscopy, 20: 36712 (IS-1335)

ARGONNE NATIONAL LAB., ILL.
Accuracy of power reactor void coefficients extrapolated from measurements in critical assemblies, 20: 38425 (ANL-7120, pp 585-97)
Application of experimental data from TREAT meltdown studies to reactor accident analysis, 20: 38472 (ANL-7120, pp 514-23)
Calculated physics parameters and their uncertainties in a 1000-Mw(e) fast ceramic reactor, 20: 38491 (ANL-7120, pp 24-32)
Comment on phase-equilibria data on Pu–O and U–O systems, 20: 38468 (ANL-7120, pp 389-91)
Comment on the comparison of some sodium void coefficients with experimental data, 20: 38419 (ANL-7120, pp 421-2)
Comparison of Monte Carlo and resonance integral methods in determination of Doppler effects in fast reactors, 20: 38423 (ANL-7120, pp 462-77)
Comparison of pressure loading produced by contained explosions in water and sodium, 20: 38459 (ANL-7120, pp 720-33)
Compatibility of modified carbide fuels with stainless steel, 20: 38466 (ANL-7120, pp 301-13)
Conceptual design and preliminary accident analysis of a Na-cooled, carbide-fueled, large modular fast reactor, 20: 38456 (ANL-7120, pp 205-29)
Conference on safety, fuels, and core design in large fast power reactors, Argonne Nat'l. Lab., 10/65, 20: 38489 (ANL-7120)
Contribution to safety problems related to 1000-Mwe fast power reactor project, 20: 38497 (ANL-7120, pp 157-61)
Cost estimate for remote refabrication of metallic fuels, 20: 37195 (ANL-6950)
Criteria for the density of monitoring points in large reactors, 20: 38432 (ANL-7120, pp 632-5)
Critical review of the properties of materials at the high temperatures and pressures significant for fast reactor safety, 20: 38433 (ANL-7120, pp 641-53)
Development and growth of in-core voids due to boiling during fast reactor transients, 20: 38440 (ANL-7120, pp 881-9)
Discussion of papers among panel, 20: 38457 (ANL-7120, pp 261-85)
Doppler effect in ^{238}U and ^{235}U fission in a fast-neutron spectrum, 20: 38430 (ANL-7120, pp 616-24)
Effect of fluctuations in collision density on fast-reactor Doppler effect calculations, 20: 38422 (ANL-7120, pp 449-61)
Enhanced safety characteristics of a sodium-cooled coupled reactor, 20: 38437 (ANL-7120, pp 789-93)
Experimental studies of the high-temperature interaction of fuel and cladding materials with liquid sodium, 20: 38499 (ANL-7120, pp 839-47)
Faret Core-I reference design, 20: 38460 (ANL-7120, pp 766-75)
Fast reactor safety considerations related to fuel macrostructure, 20: 38424 (ANL-7120, pp 497-503)
Fission product retention in sodium and applications to vented fuel element design, 20: 38477 (ANL-7120, pp 855-61)
Flood safety of steam- and gas-cooled fast reactors, 20: 38439 (ANL-7120, pp 826-36)
Fuel-failure detection in sodium-cooled reactors, 20: 38478 (ANL-7120, pp 862-7)
Influence of some important group constants on integral fast reactor quantities, 20: 38420 (ANL-7120, pp 423-33)
Large metal-fueled fast reactor study. I., 20: 38493 (ANL-7120, pp 85-93)
Large metal-fueled fast reactor study. II., 20: 38494 (ANL-7120, pp 94-103)
Measurement and analysis of Doppler effect in Pu-fueled fast reactor assemblies, 20: 38427 (ANL-7120, pp 603-9)
Metal fuels for fast reactors, 20: 38465 (ANL-7120, pp 289-300)
Microanalytical studies of micro- and macro-segregation in oxide fuels, 20: 38469 (ANL-7120, pp 400-9)
Mixed-carbide fuels for fast reactors, 20: 38467 (ANL-7120, pp 314-27)
Mixed fuel-cycle fast breeder reactors: nuclear, safety, and materials considerations, 20: 38476 (ANL-7120, pp 751-8)
Mixed oxide fuel movement at various power levels and in transients, 20: 38473 (ANL-7120, pp 524-33)
Model investigation of explosion containment in single tank fast reactors, 20: 38458 (ANL-7120, pp 692-719)
Modified equation of state for hydrodynamic calculations in AX1 numerical program, 20: 38435 (ANL-7120, pp 686-91)
Preliminary evaluation of a technique to study expulsion of sodium into air, 20: 38500 (ANL-7120, pp 868-72)
Program proposed for safety studies of fast neutron project of EURATOM-CEA association, 20: 38492 (ANL-7120, pp 54-66)
Recent Doppler measurements with ZPR-6, 20: 38428 (ANL-7120, pp 610-13)
Recent investigations of fast reactor reactivity coefficients, 20: 38418 (ANL-7120, pp 413-20)
Recent results of Doppler measurements in fast-neutron spectra, 20: 38429 (ANL-7120, pp 614-15)
Results of Doppler coefficient calculations for fast reactors and comparison of different methods, 20: 38421 (ANL-7120, pp 440-8)
Safety and economic aspects of vented fuel in sodium-cooled reactors, 20: 38475 (ANL-7120, pp 540-8)
Safety and economic characteristics of 1000-Mwe fast Na-cooled reactor design, 20: 38498 (ANL-7120, pp 185-204)
Selected optimization studies in the use of carbide fuel in large fast breeder reactors, 20: 38495 (ANL-7120, pp 104-23)

Sodium-void coefficients, 20: 38426 (ANL-7120, pp 598-602)
Status of recent meltdown studies, 20: 38474 (ANL-7120, pp 534-9)
Steam cooling for fast reactors, 20: 38496 (ANL-7120, pp 136-40)
Summary of intercomparison calculations performed in conjunction with conference, 20: 38490 (ANL-7120, pp 3-23)
Survey parameter study of large steam-cooled fast power reactors, 20: 38438 (ANL-7120, pp 815-25)
Theoretical studies on the fast reactor maximum accident, 20: 38434 (ANL-7120, pp 654-70)
Transient flux distributions by discontinuous model synthesis, 20: 38431 (ANL-7120, pp 625-31)
Transient response of coupled fast reactor cores, 20: 38436 (ANL-7120, pp 776-88)
Transient temperature distributions in fast reactor fuels with widely varying thermal diffusivity, 20: 38470 (ANL-7120, pp 478-85)
Transient temperature distribution in fuel elements, 20: 38471 (ANL-7120, pp 486-93)

ARIZONA UNIV., TUCSON.
Derivation of an expression for radiation-induced electrical conductivity in ionic insulators, 20: 38353 (BNWL-SA-247)

ARMY ENGINEER NUCLEAR CRATERING GROUP, LIVERMORE, CALIF.
Cloud development studies, Project Pre-Schooner II., 20: 36958 (PNE-511)

ATOMIC ENERGY ESTABLISHMENT, WINFRITH (ENGLAND).
CUSH: program for steady-state hydraulic analysis of steam-generating reactor systems, 20: 38410 (AEEW-M-474)

ATOMIC ENERGY OF CANADA LTD., CHALK RIVER (ONTARIO).
Future of nuclear energy, 20: 38487 (AECL-2584)
Ion chamber d-c amplifier, A-10,080, 20: 37066 (AECL-2536)
Prog. rpt. on physics, 7-9/65, 20: 38008 (AECL-2595)
SWIFT dryout data for 19-rod bundle cooled by steam/water fog, 20: 38409 (AECL-2586)
Time of flight encoder using integrated circuits, 20: 37067 (AECL-2578)

ATOMIC ENERGY RESEARCH ESTABLISHMENT, HARWELL (ENGLAND).
Effect of neutron flux on fission product gas emission from UO_2, 20: 38464 (AERE-M-1607)
Overall thermal efficiencies of combined gas-steam cycles in an MHD-reactor system, 20: 38488 (AERE-R-5031)

ATOMIC POWER DEVELOPMENT ASSOCIATES, INC., DETROIT, MICH.
Design and operating experience with control and safety rod drive mechanisms for Enrico Fermi Fast Breeder Reactor, 20: 38501 (APDA-301)

ATOMIC WEAPONS RESEARCH ESTABLISHMENT, FOULNESS OUTSTATION (ENGLAND).
Comparison of pressure loading produced by contained explosions in water and sodium, 20: 38459 (ANL-7120, pp 720-33)
Model investigation of explosion containment in single tank fast reactors, 20: 38458 (ANL-7120, pp 692-719)

ATOMICS INTERNATIONAL, CANOGA PARK, CALIF.
Application of experimental data from TREAT meltdown studies to reactor accident analysis, 20: 38472 (ANL-7120, pp 514-23)
Development and growth of in-core voids due to boiling during fast reactor transients, 20: 38440 (ANL-7120, pp 881-9)
Digital computer study of the dynamics of the combined rotating unit shaft-bearing system, 20: 36977 (NAA-SR-11944)
Effects of contaminants on Hg pool boiling heat transfer, 20: 36987 (NAA-SR-11949)
Enhanced safety characteristics of a sodium-cooled coupled reactor, 20: 38437 (ANL-7120, pp 789-93)
Errors in measurements of building leakage due to dynamic temperature effects, 20: 36978 (NAA-SR-12001)
Fission product retention in sodium and applications to vented fuel element design, 20: 38477 (ANL-7120, pp 855-61)
Recent results of Doppler measurements in fast-neutron spectra, 20: 38429 (ANL-7120, pp 614-15)

B

BABCOCK AND WILCOX CO., LYNCHBURG, VA.
Accuracy of power reactor void coefficients extrapolated from measurements in critical assemblies, 20: 38425 (ANL-7120, pp 585-97)

BABCOCK AND WILCOX CO., LYNCHBURG, VA. ATOMIC ENERGY DIV.
Analysis of lumped burnable poison critical experiments, 20: 38441 (BAW-3492-1(Suppl.1))
Steam cooling for fast reactors, 20: 38496 (ANL-7120, pp 136-40)

BATTELLE INSTITUT E. V., FRANKFURT AM MAIN (WEST GERMANY).
Structural design of nuclear-fueled thermionic converter. I., 20: 37720 (BMWF-FBK-66-06)

BATTELLE MEMORIAL INST., COLUMBUS, OHIO.
Prog. rpt. on civilian applications, 4/66, 20: 37168 (BMI-1771)
Prog. rpt. on civilian applications, 5/66, 20: 37169 (BMI-1774)

BATTELLE-NORTHWEST, RICHLAND, WASH. PACIFIC NORTHWEST LAB.
Comment on phase-equilibria data on Pu–O and U–O systems, 20: 38468 (ANL-7120, pp 389-91)
Derivation of an expression for radiation-induced electrical conductivity in ionic insulators, 20: 38353 (BNWL-SA-247)
Fast reactor safety considerations related to fuel macrostructure, 20: 38424 (ANL-7120, pp 497-503)
Neutronics characteristics of selected compact fast reactors, 20: 38442 (BNWL-283)
Personnel neutron dosimeter developments, 20: 37070 (BNWL-SA-537)
Precision long counter for measuring fast neutron flux density, 20: 37069 (BNWL-260)
Preliminary hydraulic analysis of conceptual FFTF cermet driver fuel element design, 20: 38479 (BNWL-264)
Time optimal xenon shutdown on the xenon boundary, 20: 38411 (BNWL-186)

BETTIS ATOMIC POWER LAB., PITTSBURGH, PA.
Air–water mixing tests, 20: 36989 (WAPD-TM-492)
TRANS: a FORTRAN-IV program for conversion of form of neutron elastic scattering data stored in ROC nuclear data library, 20: 37989 (WAPD-TM-573)

BETTIS ATOMIC POWER LAB., WEST MIFFLIN, PA.
Environmental radioactivity at Shippingport Atomic Power Station, 20: 37026 (PNRO-SMD-137)
Matrices for computing Greuling-Goertzel slowing-down parameters and Legendre polynomial coefficients for scattering, 20: 37988 (WAPD-TM-572)

BONN UNIV. (WEST GERMANY).
Radiochemical cyclomerization, 20: 36860 (NP-16150)

BROOKHAVEN NATIONAL LAB., UPTON, N. Y.
Combination of cylindrical current sheets to cancel external field, 20: 37313 (BNL-10143)
Elastic scattering of 1 Bev protons from He and O, 20: 38010 (BNL-10438)
Elliptical current sheets to produce constant-gradient field, 20: 37317 (BNL-10341)
f^* meson produced in K⁻p interaction 4.6 and 5.0 Bev/c, 20: 37730 (BNL-10459)
Fields produced by cylindrical current arrays, 20: 37314 (BNL-10148)
Fields produced by elliptical current sheets, 20: 37318 (BNL-10436)
Forces on currents in two-dimensional magnetic fields, 20: 37316 (BNL-10324)
High field superconducting magnets, 20: 37934 (BNL-10380)
Mixed radiation Rem responding rate meter, 20: 37068 (BNL-10321)
Noncompact groups associated with vertex operator, 20: 37823 (BNL-10387)
$\pi\pi$ resonances from 6 Bev/c π^-p interaction, 20: 37731 (BNL-10460)
Properties of K* (1425), 20: 37733 (BNL-10462)
Resonance production in the reactions $\pi^\pm p \rightarrow$ KKN at 6 Bev/c, 20: 37732 (BNL-10461)
Space-independent model of two-phase flow and its application to experiment, 20: 36984 (BNL-963)
Stored energy and inductance in two-dimensional fields, 20: 37315 (BNL-10323)
Tests of unitarity symmetry in nuclei by nucleus-hypernucleus reactions, 20: 38009 (BNL-10420)

BUNDESFORSCHUNGSANSTALT FUER LEBENSMITTELFRISCHHALTUNG, KARLSRUHE (WEST GERMANY).
Bibliography on food irradiation, No. 05, 6/66, 20: 37138 (AED-C-05-05)

C

CALIFORNIA UNIV., BERKELEY.
Bibliography on the high-temperature chemistry and physics of gases and plasmas, 20: 38204 (NP-16240)

CALIFORNIA UNIV., LOS ANGELES.
Synchrocyclotron conversion, 20: 37320 (CONF-660510-19)

CALIFORNIA UNIV., RIVERSIDE.
Possible roles for emulsion as a detector in experiments with future high-energy accelerators, 20: 37077 (UCR-34P107-34)

CARNEGIE INST. OF TECH., PITTSBURGH, PA.
Transient flux distributions by discontinuous model synthesis, 20: 38431 (ANL-7120, pp 625-31)

CARNEGIE INST. OF TECH., PITTSBURGH, PA. DEPT. OF PHYSICS.
Application of Bethe-Salpeter equation to static bootstrap model, 20: 37824 (CAR-882-19)

CASE INST. OF TECH., CLEVELAND, OHIO.
Experimental test of the law of baryon conservation, 20: 37734 (COO-818-87)
Neutrinos underground, 20: 37481 (COO-818-86)
Prog. rpt. on neutrino physics, cosmic rays, and elementary particles, 10/65-9/66, 20: 37735 (COO-818-96)

CENTRE D'ETUDE DE L'ENERGIE NUCLEAIRE, MOL (BELGIUM).
Prog. rpt. on ESSOR fuel elements, final, 1–11/62, 20: 38480 (EUR-

2522.f)

CENTRO INFORMAZIONI STUDI ESPERIENZE, MILAN (ITALY).
Liquid volume fraction in adiabatic two-phase vertical upflow-round conduit, 20: 36985 (EURAEC-1088)

COLORADO STATE UNIV., FORT COLLINS. DEPT. OF POULTRY SCIENCE.
Prog. rpt. on x irradiation of the developing avian embryo as a factor of aging, 1/62-12/65, 20: 36605 (COO-1119-5)

COLUMBIA UNIV., NEW YORK. PLASMA LAB.
Combination scattering of electromagnetic waves from driven space charge waves in a laboratory magnetoplasma, 20: 38202 (NP-16236)
Drift wave excited anomalous diffusion in a fully ionized magnetoplasma, 20: 38203 (NP-16237)
Fluctuations in magnetoplasma perturbed by electron beam, 20: 38201 (NP-16210)

COMITATO NAZIONALE PER L'ENERGIA NUCLEARE, ROME (ITALY).
Power level fluctuations of steady-state operating reactor, 20: 38445 (RT-FI-(66)1)

COMMISSARIAT A L'ENERGIE ATOMIQUE, CADARACHE (FRANCE). CENTRE D'ETUDES NUCLEAIRES.
Comparison of pressure loading produced by contained explosions in water and sodium, 20: 38459 (ANL-7120, pp 720-33)
Contribution to safety problems related to 1000-Mwe fast power reactor project, 20: 38497 (ANL-7120, pp 157-61)
Program proposed for safety studies of fast neutron project of EURATOM-CEA association, 20: 38492 (ANL-7120, pp 54-66)

COMMISSARIAT A L'ENERGIE ATOMIQUE, GRENOBLE (FRANCE). CENTRE D'ETUDES NUCLEAIRES.
Study of superconductors in the Al–Mg system, 20: 37935 (CEA-R-2906)

COMMISSARIAT A L'ENERGIE ATOMIQUE, SACLAY (FRANCE). CENTRE D'ETUDES NUCLEAIRES.
Comparison of pressure loading produced by contained explosions in water and sodium, 20: 38459 (ANL-7120, pp 720-33)
Frequency modulation of uhf signals in electron linear accelerator, 20: 37319 (CEA-R-2976)

CULHAM LAB., UNITED KINGDOM ATOMIC ENERGY AUTHORITY, ABINGDON (ENGLAND).
Heat transmission through Langmuir sheath in presence of electron emission, 20: 38191 (CLM-R-61)
Paramagnetic limit in type II superconductors, 20: 37936 (CLM-R-60)

D

DENVER RESEARCH INST., UNIV. OF DENVER, COLO.
Axisymmetric thermoelastic problems in bispherical coordinates, 20: 36957 (DRI-2327)

DIKEWOOD CORP., ALBUQUERQUE, N. MEX.
Firestorm start-criteria, 20: 36995 (AD-636794)

DU PONT DE NEMOURS (E. I.) & CO., AIKEN, S. C. SAVANNAH RIVER LAB.
High-temperature carbon for iodine adsorption, 20: 36976 (DP-MS-66-45)
Performance of sieve trays under GS heavy water process conditions. I., 20: 37160 (DP-1025)
Portable multipurpose radiation monitor, 20: 37071 (DP-993)

E

EUROPEAN ATOMIC ENERGY COMMUNITY.
Prog. rpt. on ESSOR fuel elements, final, 1–11/62, 20: 38480 (EUR-2522.f)

EUROPEAN ORGANIZATION FOR NUCLEAR RESEARCH, GENEVA (SWITZERLAND).
Prog. rpt., annual, 1965, 20: 37308 (NP-16226)

F

FORD INSTRUMENT CO., LONG ISLAND CITY, N. Y.
Unified digital instrumentation and control system for nuclear power plants, final, 4/61–6/65, 20: 38508 (NYO-2764-2)

FRANKLIN INST. RESEARCH LABS., PHILADELPHIA, PA.
Determination of gas bearing stability by response to a step-jump, 20: 36980 (TID-23270)

G

GENERAL DYNAMICS CORP., SAN DIEGO, CALIF. GENERAL ATOMIC DIV.
Hazards summary for the accelerator pulsed fast assembly, 20: 38530 (GA-6078)

GENERAL ELECTRIC CO., PLEASANTON, CALIF. VALLECITOS ATOMIC LAB.
Doppler effect in ^{238}U and ^{235}U fission in a fast-neutron spectrum, 20: 38430 (ANL-7120, pp 616-24)
Flood safety of steam- and gas-cooled fast reactors, 20: 38439 (ANL-7120, pp 826-36)
Prog. rpt. on Pu subcritical experiment program, 1–3/66, 20: 38443 (GEAP-5148)

GENERAL ELECTRIC CO., RICHLAND, WASH. HANFORD ATOMIC PRODUCTS OPERATION.
Recovery of aluminum nitrate nonahydrate from redox acid waste, 20: 36925 (HW-82771(Pt.3))

GENERAL ELECTRIC CO., SAN JOSE, CALIF. ADVANCED PRODUCTS OPERATION.
Calculated physics parameters and their uncertainties in a 1000-Mw(e) fast ceramic reactor, 20: 38491 (ANL-7120, pp 24-32)
Fuel and macore materials for SEFOR, 20: 38531 (GEAP-5133)
Mixed oxide fuel movement at various power levels and in transients, 20: 38473 (ANL-7120, pp 524-33)
Safety and economic aspects of vented fuel in sodium-cooled reactors, 20: 38475 (ANL-7120, pp 540-8)
Safety and economic characteristics of 1000-Mwe fast Na-cooled reactor design, 20: 38498 (ANL-7120, pp 185-204)

GENERAL ELECTRIC CO., SAN JOSE, CALIF. ATOMIC POWER EQUIPMENT DEPT.
Multirod, forced flow, transition and film boiling measurements, 20: 36986 (GEAP-5073)
Nine-rod critical heat flux investigation at 1000 psia, 20: 38462 (GEAP-4929)

GENERAL MOTORS CORP., DETROIT, MICH.
Military Compact Reactor program shield study, 20: 38506 (NDA-2143-7)
Military Compact Reactor program shield study, Suppl., 20: 38507 (NDA-Memo-2143-11)

GOSUDARSTVENNYI KOMITET PO ISPOL'ZOVANIYU ATOMNOI ENERGII SSSR, MOSCOW. INSTITUT TEORETICHESKOI I EKSPERIMENTAL'NOI FIZIKI.
Inelastic scattering of neutrons by hematite, 20: 38355 (ITEF-355)
Regulation theory for heterogeneous reactors, 20: 38412 (ITEF-406)

GOSUDARSTVENNYI KOMITET PO ISPOL'ZOVANIYU ATOMNOI ENERGII SSSR, MOSCOW. SOYUZNYI NAUCHNO-ISSLEDOVATEL'SKII INSTITUT PRIBOROSTROENIYA.
Application of the similarity method to radiation fields during adjustment of neutron radiation meters, 20: 37074 (NP-16202)
Calibration of thermal-neutron radiation meters in diffuse flow, 20: 37073 (NP-16201)
Problem of utilizing nuclear D(d,n)^{3}He and T(d,n)^{4}He reactions for calibration of fast-neutron radiation meters, 20: 37075 (NP-16204)

GOSUDARSTVENNYI KOMITET PO ISPOL'ZOVANIYU ATOMNOI ENERGII SSSR, OBNINSK. FIZIKO-TEKHNICHESKII INSTITUT.
Application of the similarity method to radiation fields during adjustment of neutron radiation meters, 20: 37074 (NP-16202)
Problem of utilizing nuclear D(d,n)^{3}He and T(d,n)^{4}He reactions for calibration of fast-neutron radiation meters, 20: 37075 (NP-16204)

GRENOBLE UNIV. (FRANCE).
Study of superconductors in the Al–Mg system, 20: 37935 (CEA-R-2906)

I

IIT RESEARCH INST., CHICAGO, ILL.
Design and applications of β-excited x-ray sources, 20: 36915 (N-66-17678)
Reactor containment structures, 20: 38463 (IITRI-578P22-15)

ILLINOIS UNIV., URBANA.
Self shielding by encapsulated gamma sources, 20: 38349 (AD-636788)

INSTITUTUL DE FIZICA ATOMICA, ACADEMIA R. P. R., BUCHAREST (ROMANIA).
Radiolytic behavior of iron ions in acetylene aqueous solution, 20: 36858 (IFA-CR-73)

INTERNATIONAL ATOMIC ENERGY AGENCY, VIENNA (AUSTRIA).
Symposium on radioisotope instruments in industry and geophysics, Warsaw, 10/65. II., 20: 37133 (STI-PUB-112(Vol.2))
Symposium on radioisotope instruments in industry and geophysics, Warsaw, 10/65. I., 20: 37139 (STI-PUB-112(Vol.1))

INTERNATIONAL CENTRE FOR THEORETICAL PHYSICS, TRIESTE (ITALY).
Matrix elements of operators of class 1 representations of SL(n,C), 20: 37738 (IC-66/89)

J

JET PROPULSION LAB., CALIF. INST. OF TECH., PASADENA.
Observations with University of Iowa equipment on Mariner IV., 20: 37341 (N-66-17354)

JOHN COLLINS WARREN LABS., MASSACHUSETTS GENERAL HOSPITAL, BOSTON.
Prog. rpt. on mechanisms and regulations of nucleic acid and protein syn-

thesis, and their possible relationship to radiation damage, 9/65-8/66, 20: 36555 (NYO-2643-22)

JOHNS HOPKINS UNIV., BALTIMORE, MD. DEPT. OF ELECTRICAL ENGINEERING.
Prog. rpt. on plasma waves and instabilities, 3–5/66, 20: 38205 (NYO-3565-4)

JOHNS-MANVILLE RESEARCH AND ENGINEERING CENTER, MANVILLE, N. J.
Prog. rpt. on 1800-400F fibrous-type insulation for radioisotope power systems, 3-6/66, 20: 36983 (ALO-3633-1)

JOINT INST. FOR NUCLEAR RESEARCH, DUBNA (USSR). LAB OF HIGH ENERGY.
Oscillations of confined (cylindrical) plasma with a hot electron current, 20: 38196 (JINR-P-2783-2)

JOINT INST. FOR NUCLEAR RESEARCH, DUBNA (USSR). LAB OF NUCLEAR PROBLEMS.
Capture of pions by ^{3}He. II., 20: 38011 (JINR-P-2805)
Charge of π mesons stopped on light nuclei, 20: 37740 (JINR-P-2780)
Double charge exchange of 50- to 176-Mev π^- mesons in photo emulsion, 20: 38012 (JINR-P-2806)
Measurement of the triple scattering parameter R_{pn} at 70° and the phase-shift analysis at 630 Mev, 20: 37739 (JINR-E-2726)
Muon capture in mixed gases, 20: 37741 (JINR-P-2788)

JOINT INST. FOR NUCLEAR RESEARCH, DUBNA (USSR). LAB OF THEORETICAL PHYSICS.
Application of false source method to heterogeneous nucleus calculations in cylindrical geometry, 20: 38444 (JINR-P-2699)

K

KERNFORSCHUNGSZENTRUM, KARLSRUHE (WEST GERMANY).
Survey parameter study of large steam-cooled fast power reactors, 20: 38438 (ANL-7120, pp 815-25)

KERNFORSCHUNGSZENTRUM, KARLSRUHE (WEST GERMANY). INSTITUT FUER ANGEWANDTE KERNPHYSIK.
Application of germanium diodes in gamma ray spectroscopy, 20: 37072 (KFK-429)

KERNFORSCHUNGSZENTRUM, KARLSRUHE (WEST GERMANY). INSTITUT FUER ANGEWANDTE REAKTORPHYSIK.
Microanalytical studies of micro- and macro-segregation in oxide fuels, 20: 38469 (ANL-7120, pp 400-9)

KERNFORSCHUNGSZENTRUM, KARLSRUHE (WEST GERMANY). INSTITUT FUER NEUTRONENPHYSIK UND REAKTORTECHNIK.
Influence of some important group constants on integral fast reactor quantities, 20: 38420 (ANL-7120, pp 423-33)
Results of Doppler coefficient calculations for fast reactors and comparison of different methods, 20: 38421 (ANL-7120, pp 440-8)

KEURING VAN ELECTROTECHNISCHE MATERIALEN, N. V., ARNHEM (NETHERLANDS).
Prog. rpt. on aqueous homogeneous suspension reactor project, annual, 1965, 20: 38533 (NP-16168(Pt.A))
Prog. rpt. on aqueous homogeneous suspension reactor project, annual, 1965, 20: 38534 (NP-16168(Pt.B))

KHAR'KOVSKII GOSUDARSTVENNYI UNIVERSITET (USSR).
Theory of fluctuations in magnetoactive plasma, 20: 38200 (NP-16206)

L

LAWRENCE RADIATION LAB., UNIV. OF CALIFORNIA, BERKELEY.
Backward π^- p scattering as a further test for Regge high-energy behavior, 20: 37742 (UCRL-16293)
Polarization in proton-proton scattering using polarized proton target. Pt. I and Pt. II., 20: 37743 (UCRL-16866)

LAWRENCE RADIATION LAB., UNIV. OF CALIFORNIA, LIVERMORE.
Cloud development studies, Project Pre-Schooner II., 20: 36958 (PNE-511)
Effects of underground nuclear explosions on natural gas well performance, 20: 36961 (UCRL-12229)
Flange design using Al foil for ultrahigh-vacuum application, 20: 37000 (UCID-4548(Rev.4))
Plasma confinement properties of relativistic electron coils, 20: 38210 (UCRL-12455(Rev.1))
Relativistic transformations versus Lorentz transformations, 20: 37827 (UCRL-14365)
Surface motion measurements, 20: 36959 (PNE-603F)

LOS ALAMOS SCIENTIFIC LAB., UNIV. OF CALIFORNIA, N. MEX.
Characteristics of the aerosol produced from burning plutonium, 20: 37022 (LA-DC-6942)
Dynamics of disordered harmonic lattices, 20: 38356 (LA-3510)
Electron distribution function in a plasma with excitation collisions, 20: 38198 (LA-DC-8099)
Potentiometric titration of cerium and manganese following separation from plutonium and cobalt, 20: 36713 (LA-3402)
Retention of ^{54}Mn by four mammalian species, 20: 36554 (LA-DC-7305)
Straight θ-pinch devices energized by energy storage supply of Scyllac, 20: 38197 (LA-3553)
Study of some of the parameters affecting Knudsen effusion, 20: 37307 (LA-3509)

M

MARYLAND UNIV., COLLEGE PARK. DEPT. OF PHYSICS AND ASTRONOMY.
Lectures on high energy scattering, fall semester, 1965-66, 20: 37826 (NP-16231)

MASSACHUSETTS INST. OF TECH., CAMBRIDGE. DIV. OF SPONSORED RESEARCH.
Some hydrodynamic characteristics of bubbly mixtures flowing vertically upward in tubes, 20: 36988 (TID-23261)

MISSOURI UNIV., COLUMBIA.
Dynamics of disordered harmonic lattices, 20: 38356 (LA-3510)

N

NATIONAL AERONAUTICS AND SPACE ADMINISTRATION, CLEVELAND, OHIO. LEWIS RESEARCH CENTER.
Critical mass studies with NASA Zero Power Reactor II, 20: 38532 (NASA-TN-D-3555)

NATIONAL AERONAUTICS AND SPACE ADMINISTRATION, LANGLEY STATION, VA. LANGLEY RESEARCH CENTER.
Cross-linking of polyvinylidene fluoride by gamma radiation, 20: 36859 (N-66-13497)
Polyimidazopyrrolones: new class of radiation-resistant polymers, 20: 36846 (N-66-13499)

NATIONAL LEAD CO. OF OHIO, CINCINNATI.
Report of fire resistance tests fuel core shipping container No. 1, 20: 37024 (NLCO-899)

NAVAL CIVIL ENGINEERING LAB., PORT HUENEME, CALIF.
Simulation of waves generated by underwater nuclear explosions, 20: 37306 (AD-636408)

NAVAL SCHOOL OF AVIATION MEDICINE, PENSACOLA, FLA.
Tissue dosages from alpha particles and heavy nuclei in solar particle beams in space, 20: 37023 (N-65-33865)

NEW MEXICO UNIV., ALBUQUERQUE.
Study of some of the parameters affecting Knudsen effusion, 20: 37307 (LA-3509)

NORTHWESTERN UNIV., EVANSTON, ILL.
Ultraviolet spectroscopy of irradiated polyethylene. II., 20: 36857 (COO-1088-21)

NUCLEAR DEVELOPMENT CORP. OF AMERICA, WHITE PLAINS, N. Y.
Military Compact Reactor program shield study, 20: 38506 (NDA-2143-7)
Military Compact Reactor program shield study, Suppl., 20: 38507 (NDA-Memo-2143-11)

NUCLEAR UTILITY SERVICES, INC., WASHINGTON, D. C.
Prog. rpt. on environmental safety aspects of nuclear rocket flight operations, 5–10/64, 20: 38525 (NUS-208)

O

OAK RIDGE GASEOUS DIFFUSION PLANT, TENN.
Fluid-bed volatility component, engineering feasibility, and scale-up studies at the Oak Ridge Gaseous Diffusion Plant, 20: 36926 (K-L-6091)
Tables of 10-10 uranium unit cost components, 20: 37161 (K-OA-1313)

OAK RIDGE NATIONAL LAB., TENN.
Effects of two-pass flow in the bonus superheater assemblies, 20: 38509 (ORNL-TM-1449)
Investigation of denitration of high-nitrate plutonia sols by baking, 20: 36786 (ORNL-TM-1558)
Moving striations produced by a simple thermal instability, 20: 38206 (ORNL-P-1539)
Removal of protactinum from molten fluoride breeder blanket mixtures, 20: 36927 (ORNL-TM-1543)
Repair of DNA, 20: 36578 (ORNL-P-2240)
Solubilities of HF and DF in molten fluorides, 20: 36785 (ORNL-P-2202)
Survey of U. S. shielding calculational methods and programs, 20: 38350 (ORNL-P-2310)
Table of the ratio B_0B_{max} for magnet coils with rectangular cross section and uniform current density, 20: 36979 (ORNL-3972)

OAK RIDGE OPERATIONS OFFICE (AEC), TENN.
Boiling Nuclear Superheater (BONUS) Power Station, 20: 38510 (ORO-649)

OHIO AGRICULTURAL EXPERIMENT STATION, WOOSTER. DEPT. OF BOTANY AND PLANT PATHOLOGY.

Radiological investigations at Neotoma, 20: 36548 (TID-23036)

OHIO STATE UNIV., COLUMBUS.
Radiological investigations at Neotoma, 20: 36548 (TID-23036)

P

PARIS UNIV., ORSAY (FRANCE). LABORATOIRE DE PHYSIQUE THEORIQUE ET HAUTES ENERGIES.
Quasi local electrodynamics, 20: 37825 (N-65-31239)

PENNSYLVANIA STATE UNIV., UNIVERSITY PARK. MATERIALS RESEARCH LAB.
Prog. rpt. on crystal chemistry studies, 2/14-5/13/66, 20: 36784 (AD-636054)

PENNSYLVANIA UNIV., PHILADELPHIA. INST. FOR DIRECT ENERGY CONVERSION.
Electromagnetic wave interaction in an inhomogeneous drifting plasma, 20: 38194 (INDEC-SR-7, pp 3.22-59)
Electron density and collision frequency in a radially inhomogeneous plasma column, 20: 38193 (INDEC-SR-7, pp 3.5-13)
Measurement of plasma transport properties in a Na–K seeded Ar plasma, 20: 38195 (INDEC-SR-7, pp 3.60-73)
Models for electron emission from metals with adsorbed monolayers, 20: 37431 (INDEC-SR-7, pp 3.76-111)
Prog. rpt. on direct energy conversion, 4/66, 20: 37721 (INDEC-SR-7)
Prog. rpt. on materials engineering, plasma research, and electrochemical studies in direct energy conversion methods, 1/65, 20: 37722 (N-65-30843)

PHILADELPHIA GENERAL HOSPITAL, PA.
Prog. rpt. on effect of x-ray irradiation on phospholipid metabolism, 10/65-5/66, 20: 36606 (NYO-1864-23)

PHILIPPINE ATOMIC ENERGY COMMISSION, MANILA.
Bibliography on ^{14}C, 20: 38540 (PAEC(A)IN-652)

PHILLIPS PETROLEUM CO. IDAHO FALLS, IDAHO., ATOMIC ENERGY DIV.
RSAC: Radiological safety analysis computer program, 20: 37167 (IDO-17151)

PRINCETON UNIV., N. J. PLASMA PHYSICS LAB.
Cumulative listing of reports and publications, 20: 38199 (MATT-400)
Derivations of hierarchies for N particle systems and Vlasov systems, 20: 38209 (PPL-AF-5)
Present state of plasma kinetic theory, 20: 38207 (PPL-AF-1)
Propagation of correlations in a Boltzmann gas, 20: 37865 (PPL-AF-2)
Second-order magnetic moment of a charged particle in an axially-symmetric static magnetic field, 20: 38208 (PPL-AF-4)

PRODUCTION GROUP, UNITED KINGDOM ATOMIC ENERGY AUTHORITY, ANNON (SCOTLAND).
Prog. rpt. on health and safety at Chapelcross, annual, 1965, 20: 37025 (PG-Report-705)

R

RADIOPTICS, INC., PLAINVIEW, N. Y.
Nuclear radiation processing of optical maser materials, 20: 37280 (NYO-3330-11)

REACTOR GROUP, UNITED KINGDOM ATOMIC ENERGY AUTHORITY, DOUNREAY (SCOTLAND).
Theoretical studies on the fast reactor maximum accident, 20: 38434 (ANL-7120, pp 654-70)

REACTOR GROUP, UNITED KINGDOM ATOMIC ENERGY AUTHORITY, RISLEY (ENGLAND).
Axial stability calculations for A.G.R. systems, 20: 38446 (TRG-Report-1138)

REYNOLDS ELECTRICAL AND ENGINEERING CO., INC., MERCURY, NEV.
On-site radiological safety for Project SULKY, 20: 36960 (PNE-717F)

ROCHESTER UNIV., N. Y. DEPT. OF PHYSICS AND ASTRONOMY.
Interactions (π-p) at 900 Mev, 20: 37744 (UR-875-151)

S

SANDIA CORP., ALBUQUERQUE, N. MEX.
Axisymmetric thermoelastic problems in bispherical coordinates, 20: 36957 (DRI-2327)
Computation of neutron flux from foil activation data: SPECTRA code, 20: 37076 (SC-DC-66-1512)
Prog. rpt. on booster rocket altitude abort program, 1-4/66, 20: 36996 (SC-CR-66-2045)
Transient annealing in semiconductor devices following pulsed neutron irradiation, 20: 37129 (SC-DC-66-1820)

STATE UNIV. OF IOWA, IOWA CITY. DEPT. OF PHYSICS AND ASTRONOMY.
Observations with University of Iowa equipment on Mariner IV., 20: 37341 (N-66-17354)

T

TECHNION–ISRAEL INST. OF TECH., HAIFA.
Results of Doppler coefficient calculations for fast reactors and comparison of different methods, 20: 38421 (ANL-7120, pp 440-8)

TECHNISCHE HOGESCHOOL, EINDHOVEN (NETHERLANDS).
Prog. rpt. on heat transfer and fluid flow characteristics in a PWR, 7–9/65, 20: 38503 (EURAEC-1663)
Prog. rpt. on heat transfer and fluid flow characteristics in PWR, 10/65–1/66, 20: 38504 (EURAEC-1664)
Prog. rpt. on heat transfer and fluid flow characteristics in PWR, 1–4/66, 20: 38505 (EURAEC-1672)
Prog. rpt. on steady-state and dynamic behavior of a BWR, 7–10/65, 20: 38502 (EURAEC-1662)

TELEDYNE INDUSTRIES, INC., ALEXANDRIA, VA. EARTH SCIENCES DIV.
Seismic measurements of PALANQUIN, 20: 37010 (AD-631340)

TENNESSEE UNIV., KNOXVILLE. DEPT. OF ZOOLOGY AND ENTOMOLOGY.
Prog. rpt. on effects of radiation on host-parasite relationships, 6/54-6/66, 20: 36607 (TID-23114)

TRW SYSTEMS, REDONDO BEACH, CALIF.
Prog. rpt. on booster rocket altitude abort program, 1-4/66, 20: 36996 (SC-CR-66-2045)

U

UNION CARBIDE CORP., OAK RIDGE, TENN. Y-12 PLANT.
High-pressure gas mixing facility, 20: 36981 (Y-1546)

UNITED NUCLEAR CORP., WHITE PLAINS, N. Y. DEVELOPMENT DIV.
Selected optimization studies in the use of carbide fuel in large fast breeder reactors, 20: 38495 (ANL-7120, pp 104-23)

UNITED STATES–EURATOM JOINT RESEARCH AND DEVELOPMENT PROGRAM.
Liquid volume fraction in adiabatic two-phase vertical upflow-round conduit, 20: 36985 (EURAEC-1088)
Multirod, forced flow, transition and film boiling measurements, 20: 36986 (GEAP-5073)
Prog. rpt. on heat transfer and fluid flow characteristics in a PWR, 7–9/65, 20: 38503 (EURAEC-1663)
Prog. rpt. on heat transfer and fluid flow characteristics in PWR, 10/65–1/66, 20: 38504 (EURAEC-1664)
Prog. rpt. on heat transfer and fluid flow characteristics in PWR, 1–4/66, 20: 38505 (EURAEC-1672)
Prog. rpt. on Pu subcritical experiment program, 1–3/66, 20: 38443 (GEAP-5148)
Prog. rpt. on steady-state and dynamic behavior of a BWR, 7–10/65, 20: 38502 (EURAEC-1662)

USTAV JADERNEHO VYZKUMU, CESKOSLOVENSKA AKADEMIE VED, REZ.
Hydrogen formation in the radiolysis of liquid methanol, 20: 36861 (UJV-1553)

V

VIRGINIA POLYTECHNIC INST., BLACKSBURG. DEPT. OF CHEMISTRY.
Solubilities of HF and DF in molten fluorides, 20: 36785 (ORNL-P-2202)

W

WESTERN RESERVE UNIV., CLEVELAND, OHIO. DEPT. OF PHYSICS.
Correlation of positron lifetime with the angle between the annihilation gamma rays, 20: 37737 (COO-1297-8)
Electron momentum distribution in Si and Ge by positron annihilation, 20: 37736 (COO-1297-7)

WESTINGHOUSE ELECTRIC CORP., PITTSBURGH, PA. ASTRO-NUCLEAR LAB.
Steady-state-coupled fluid flow and heat condition analysis of heat-generating solid, as applied to reactor design, 20: 38461 (CONF-651110-29)

WESTINGHOUSE ELECTRIC CORP., PITTSBURGH, PA. ATOMIC POWER DIV.
Comparison of Monte Carlo and resonance integral methods in determination of Doppler effects in fast reactors, 20: 38423 (ANL-7120, pp 462-77)
Compatibility of modified carbide fuels with stainless steel, 20: 38466 (ANL-7120, pp 301-13)
Conceptual design and preliminary accident analysis of a Na-cooled, carbide-fueled, large modular fast reactor, 20: 38456 (ANL-7120, pp 205-29)

Stability, compatibility and corrosion of poison solutions and structural materials, 20: 38447 (WCAP-2867)
Transient flux distributions by discontinuous model synthesis, 20: 38431 (ANL-7120, pp 625-31)
Transient response of coupled fast reactor cores, 20: 38436 (ANL-7120, pp 776-88)
Transient temperature distribution in fuel elements, 20: 38471 (ANL-7120, pp 486-93)
WISCONSIN UNIV., MADISON. DEPT. OF PHYSICS.
Equipotential surfaces of a plasma moving in a toroidal octupole magnetic field, 20: 38192 (COO-1233-32)

Y

YALE UNIV., NEW HAVEN, CONN.
Noncompact groups associated with vertex operator, 20: 37823 (BNL-10387)
YALE UNIV., NEW HAVEN, CONN. HAMMOND LAB.
Binary phase diagrams of halide salts, 20: 36787 (YALE-2723(Vol.1))
Binary phase diagrams of halide salts, 20: 36788 (YALE-2723(Vol.2))

PERSONAL AUTHOR INDEX

Each entry after an author's name is a shortened version of the title of the report or article, followed by the *NSA* volume and abstract number. Report numbers are given in parentheses.

The phrase "Progress report" is abbreviated as "Prog. rpt.," permitting a more rapid and complete alphabetical arrangement of the titles without changing the location of the progress report titles in relation to the other titles.

Because of problems involving the mechanical preparation of this index, all accent marks are omitted. The following changes in spelling have been introduced to reduce some of the confusion which might result from omitting the accents:

ä	becomes	ae
ö		oe
ø		oe
ü		ue (except in transliterated Chinese names)

A

ABAROV, U., Radioactivation method for determining potassium in rocks using magnetic β separator, 20: 36752

ABDON, R., Contribution to safety problems related to 1000-Mwe fast power reactor project, 20: 38497 (ANL-7120, pp 157-61)

ABE, Shigeki, Activation analysis of titanium in iron by photonuclear reactions, 20: 36760

ABLES, J. G., Semi-diurnal anisotropy of the cosmic radiation, 20: 37521

ABRAHAM, Barbara, Propagation of hydromagnetic waves through an anisotropic plasma, 20: 38333

ABRAHAM, F., High-energy jets produced by heavy primary nuclei of cosmic origin and their fragmentation products, 20: 37662

ABRAHAM, M. M., Electron spin resonance of rare-earth ions in CeO_2 : Yb^{3+} and Er^{3+}, 20: 38391

ABRAMS, I. A., Measurements of large γ-radiation doses and fluxes by means of photoactivation of isomeric nuclear states, 20: 37079

ABRAMYAN, E. A., Transformer-type high-current accelerator, 20: 37322

ABRINES, R., Classical theory of charge transfer and ionization of hydrogen atoms by protons, 20: 37454

ABRINES, R., Generalized correspondence principle and proton-hydrogen collisions, 20: 37455

ABROSIMOV, A. T., Energy spectrum, possible chemical composition, and anisotropy of ultrahigh-energy primary cosmic radiation, 20: 37651

ABROSIMOV, A. T., Study of the extensive air showers with fixed μ meson number and with fixed electron number, 20: 37644

ACHAR, C. V., Intensity and angular distribution of cosmic rays far underground, 20: 37704

ACHAR, C. V., Kolar Gold Field neutrino experiment, 20: 37711

ACHAR, C. V., Muon interactions far underground, 20: 37701

ACKER, H. L., Measurement and analysis of muonic x-ray spectra in spherical nuclei, 20: 38058

ACKER, H. L., Theory of rotation-vibration interaction in deformed even-even nuclei, 20: 38156

ADATI, K., Stabilizing effect of radial plasma density distribution on helical instability, 20: 38270

ADDA, Y., Diffusion of iron and silver in beryllium, 20: 37250

ADDA, Y., Self-diffusion of beryllium, 20: 37249

ADITYA, P. K., Energy spectrum of primary He nuclei at energies greater than 6 Bev, 20: 37557

ADLER, J. G., System for observing small nonlinearities in tunnel junctions, 20: 37973

AGRAWAL, P. C., Flux of primary protons and helium nuclei and east-west and north-south asymmetries near the geomagnetic equator, 20: 37582

AGRAWAL, P. C., Use of a gas Cherenkov counter for the study of the isotopic composition of He nuclei in primary cosmic radiation, 20: 37581

AGRINIER, B., Flux and east-west asymmetry of primary electrons at a geomagnetic rigidity cut-off of about 4.5 GV, 20: 37550

AHABABIAN, N., Inelastic n-p cross section at 60 Bev, 20: 37670

AHLUWALIA, H. C., Influence of the magnetopause on cosmic-ray particle trajectories, 20: 37597

AHLUWALIA, H. S., Case of transient anisotropy during the recovery phase of a Forbush decrease, 20: 37486

AHLUWALIA, H. S., Solar daily variation recorded at a low-latitude station by east and west pointing telescopes during periods of maximum and minimum solar activity, 20: 37373

AIZU, K., Origin of extragalactic cosmic rays, 20: 37502

AKASHI, M., Extensive air showers observed in the emulsion chamber, 20: 37638

AKASHI, M., Nuclear interactions produced in the emulsion chamber, 20: 37673

AKASHI, M., Observation of extremely high-energy nuclear events by emulsion chamber, 20: 37661

AKERLOF, C. W., Electromagnetic form factor of the pion, 20: 37812

AKHUND-ZADE, A. I., Cytogenetic analysis of the mutagenic effect of ionizing radiation and alkylating compounds in peas, 20: 36621

AKSHANOV, B. S., Production of hot-electron plasma in magnetic mirror traps, 20: 38211 (AEC-tr-6782)

ALANIA, M. V., Asymmetric solar wind in connection with the 27-day modulation of the intensity and anisotropy of cosmic rays, 20: 37528

ALANIA, M. V., Frequency distribution of sudden changes of cosmic-ray intensity in connection with solar activity, 20: 37541

ALBERT, Philippe, Determination of O in Al and Zr by irradiation with ^3He ions, 20: 36741

ALBITSKAYA, E. F., Effect of ultraviolet irradiation on the functional condition of basic cerebral nervous processes in man, 20: 36626

ALBOM, M. J., Coatings for extreme temperature environments, 20: 37192

ALCORN, F. M., Analysis of lumped burnable poison critical experiments, 20: 38441 (BAW-3492-1(Suppl. 1))

ALEKSANDROVA, V. N., Effects of γ radiation on the scale formation process, 20: 37182

ALEKSEEV, A. G., 68.5-cm Sector-focused cyclotron, 20: 37324

ALEKSEEV, F. A., Pulsed neutron generator for boreholes and its use in nuclear geophysics, 20: 37017

ALEVRA, A., Level density parameter determination from (α,n) reactions on ^{27}Al, ^{55}Mn, ^{56}Fe, and Ag, 20: 38115

ALEXANDER, G., Neutral-meson production cross sections and mixing angles in a quark model, 20: 37779

ALEXANDER, T. K., Lifetimes of the 5.10- and 5.83-Mev levels in ^{14}N, 20: 38075

ALEXANDER, Thomas Kennedy, Nuclear reaction studies of ^{12}B and ^{17}O, 20: 38161

ALEXEFF, Igor, Moving striations produced by a simple thermal instability, 20: 38206 (ORNL-P-1539)

ALIA, P., Liquid volume fraction in adiabatic two-phase vertical upflow-round conduit, 20: 36985 (EURAEC-1088)

ALIKHANOV, R. A., Inelastic scattering of neutrons by hematite, 20: 38355 (ITEF-355)

ALIKHANYAN, A. I., Modern aspects of particle physics, 20: 37745 (TT-65-50130)

ALLAN, H. R., Experiments on the pulse spectrum observed from scintillation and Cherenkov detectors at sea level, 20: 37619

ALLAN, H. R., Muon component of air showers, 20: 37645

ALLEN, J. F., Height dependence and fine structure of helium film transfer rates, 20: 37943

ALLEN, K. W., Lifetimes of the 5.10- and 5.83-Mev levels in ^{14}N,

20: 38075
ALLER, L. H., Composition differences between the galaxy and the Magellanic clouds, 20: 37428
ALLIO, R. J., Multiaxial strain fatigue in Zircaloy-4, 20: 37235
AL'SHEVSKII, L. E., Effect of ultrasound on the ductility of high-boron stainless steels, 20: 37221
ALTMAN, Manfred, Prog. rpt. on direct energy conversion, 4/66, 20: 37721 (INDEC-SR-7)
ALTSTETTER, C. J., Effect of zirconium on the thermodynamic and mechanical properties of niobium–nitrogen alloys, 20: 37274
ALTUKHOV, A. M., First and second spherical harmonics of the daily variations of cosmic rays, 20: 37531
ALTUKHOV, A. M., Investigation of cosmic-ray distribution using the method of daily variations, 20: 37587
ALTY, J. L., Further measurements and zero-range DWBA calculations for the $^{52}Cr(d,p)^{53}Cr$ reaction, 20: 38046
ALVAREZ, M. R., Quantitative cytophotometric studies of nuclear protein in Vicia faba following acute irradiation, 20: 36588
ALVIAL, G., Estimation of the relative abundance of the carbon isotopes of the primary cosmic rays, 20: 37574
ALVIAL, G., Separation of isotopic nuclei of the primary cosmic rays with nuclear emulsions, 20: 37573
AMALDI, Ugo Jr., (e,e'p) reaction in the ^{32}S nucleus, 20: 38016
AMANTOVA, I. A., Spectrophotometric studies of ascorbic complexes. IV., 20: 36833
AMANTOVA, I. A., Spectrophotometric study of ascorbic complexes. V., 20: 36852
AMBLER, E., Magnetization and critical fields of superconducting $SrTiO_3$, 20: 37953
AMES, S., Cosmic-ray flux variation with height in the stratosphere, 20: 37552
AMONENKO, V. M., Purification of cerium by electric transport combined with zone melting, 20: 36936
ANAND, K. C., Energy spectrum of primary He nuclei at energies greater than 6 Bev, 20: 37557
ANAND, K. C., Heavy nuclei in the primary cosmic rays in June 1963 at Fort Churchill, 20: 37568
ANDA, R., Solar daily variation recorded at a low-latitude station by east and west pointing telescopes during periods of maximum and minimum solar activity, 20: 37373
ANDERSEN, H. A., Ionization chamber, 20: 37124
ANDERSON, A. C., Alternating current losses and magnetic field aberrations associated with use of high-field superconducting wire in adiabatic demagnetization apparatus, 20: 37970
ANDERSON, A. C., Thermal and magnetic properties of dilute solutions of ^3He in ^4He at low temperatures, 20: 37961
ANDERSON, D. K., Radiative pion absorption in complex nuclei, 20: 38064
ANDERSON, H. R., Cosmic ray changes during a solar cycle, 20: 37507
ANDERSON, K. A., Energetic electron spikes in and beyond the transition region, 20: 37903
ANDERSON, R. L., Scattering of positrons and electrons from protons, 20: 37778
ANDERSON, W. A., Permeability relationships using Darcy permeability, vacuum decay, pressure decay, and pore size distribution methods on graphitic materials, 20: 37225
ANDO, Toshihiko, Quantum statistical theory of optical rotation, 20: 37927
ANDRE, B., Behavior of MOS structures in the case of an induced ionization, 20: 37130
ANDREEVA, A. B., Chemistry of Ce in systems of Al_2O_3, Cr_2O_3, and Ga_2O_3 with Ce_2O_3, 20: 36808
ANDREEVA, A. B., Reactions of La and Nd oxides with oxides of elements of groups III and IV, 20: 36840
ANDRONIKASHVILI, E. L., Tskhra-Tskaro installation for study of interactions of high-energy particles of cosmic rays with matter, 20: 37684
ANDRZEJAK, Ryszard, Calibration pulse generator with nanosecond pulses, 20: 37049
ANGINO, Ernest E., Thermoluminescence of some carbonates, ThO_2, and $BaTiO_3$, 20: 36913
ANISOVICH, V. V., Triangular diagram of π-meson low-energy scattering, 20: 37803
ANNONI, H., Heavy cosmic ions recorded in nuclear emulsions exposed in a polar satellite, 20: 37577
ANOKHIN, V. L., Extraction of fission products from water by foaming, 20: 36934
ANTHONY, Anne-Marie, Preparation of monocrystals of hafnium oxide by the method of fused salts, 20: 37197
ANTONI, G. Delgli, Flux and east-west asymmetry of primary electrons at a geomagnetic rigidity cut-off of about 4.5 GV, 20: 37550
ANTONOV, R. A., Investigation of the nucleon interactions at energies above 10^{13} ev, 20: 37657
ANTONOVA, A. E., Hypothesis of origin and formation of radiation belts as a result of particle drift into the depth of the magnetosphere, 20: 37909
ANTONOVSKAYA, E. I., Passivity of molybdenum, 20: 37184
APANASENKO, A. V., Investigation of the nucleon interactions at energies above 10^{13} ev, 20: 37657
APATEANU, V., Current status of the use of bone marrow transplants in therapeutics, 20: 36667
APATEANU, V., Viability of preserved bone marrow cells, 20: 36546
APPARAO, M. V. K., Fast neutrons of solar origin, 20: 37375
APPARAO, M. V. K., Low rigidity end of the differential spectra of the proton and helium components of the primary cosmic radiation, 20: 37561
AQUA, E. N., Faulting in cold-worked Ta-10 at.% Re and W-20 at.% Re, 20: 37217
ARAFA, S., Photochemical reaction induced in borate glasses containing arsenic and manganese, 20: 36887
ARAKI, Chiroru, Effect of gamma radiation on Ni, Zn, and Ag chelates of tetraphenylporphine, 20: 36889
ARCHAMBEAU, C. B., Detection, analysis, and interpretation of teleseismic signals. I., 20: 36968
ARCHER, D. W., Emf studies of electrolytic dissociation. IX., 20: 36830
ARCHER, N. P., Direct measurements of the half-lives of some short-lived xenon and cesium isotopes, 20: 38017
ARD, W. B., Observations of instabilities in electron-cyclotron plasmas, 20: 38274
ARDENTE, V., Slow-neutron scattering by liquids: hindered-translator model, 20: 37999
ARDENTE, V., Slow-neutron scattering by liquids: a hindered-translator model, 20: 38006
ARECCHI, F. T., Measurement of the time evolution of a radiation field by joint photocount distributions, 20: 37311
ARENHOEVEL, Hartmuth, Photon scattering by oriented nuclei, 20: 38055
ARIPOV, G., Spectral analysis with γ rays from (n,γ) reactions, 20: 36750
ARLETT, C. F., Radiation sensitivity of a cytoplasmic mutant of Aspergillus nidulans, 20: 36629
ARMITAGE, J. G. M., Height dependence and fine structure of helium film transfer rates, 20: 37943
ARNHEIM, Norman Jr., Age dependence of locations of x-ray-induced somatic crossing-over in Drosophila, 20: 36619
ARNOLDY, R. L., Studies of primary cosmic rays with ionization chambers, 20: 37508
AR-RASHID, Harun, Electric-charge form factor according to SL(6,C), 20: 37840
AR-RASHID, Harun, Matrix elements of operators of class 1 representations of SL(n,C), 20: 37738 (IC-66/89)
ARTYKOV, I. Z., Intranuclear cascades at ultra-high energies, 20: 38122
ARTYKOV, I. Z., Statistical analysis of the interaction of 17 Bev mesons with photoemulsion heavy nuclei, 20: 38060
ARUTYUNYAN, R. M., Stability of a superconducting film, 20: 37938
ARZHANYKH, I. S., Momentum-energy field of elementary particles, 20: 37834
ASADA, Tsunesaburo, Radiation damage in luminescence intensity of anthracene, 20: 37131
ASAI, Takuo, Neutron activation analysis of human blood and hair, 20: 36728
ASATIANI, T. L., Ionization measurement in a streamer chamber, 20: 37110
ASAYAMA, Kunisuke, Nuclear spin-lattice relaxation in superconducting niobium, 20: 37941
ASH, W. W., Electromagnetic form factor of the pion, 20: 37812
ASHTON, F., Burst production by near horizontal cosmic-ray muons at sea level, 20: 37695
ASHTON, F., Feasibility of detecting quarks in cosmic rays, 20: 37718
ASHTON, F., Liquid scintillation counters, 20: 37107
ASKILL, J., Diffusion of ^{182}Ta in bcc Ti, 20: 37175
ASTAFIEV, V. A., Inverse problem in the cascade theory of showers, 20: 37650
ATEN, A. H. W. Jr., Isomer of ^{98}Rh, 20: 38106
ATEN, A. H. W. Jr., Specific gamma emission of natural K and La, 20: 38107
ATNEOSEN, R. A., X rays and electrons emitted in coincidence with the fission of ^{252}Cf, 20: 38095
ATRASHKEVICH, V. B., Comparison of various models of EAS development with experimental data and the prospects of cosmological and nuclear aspects of EAS investigation, 20: 37646
ATRASHKEVICH, V. B., Energy spectrum, possible chemical composition, and anisotropy of ultrahigh-energy primary cosmic radiation, 20: 37651
ATTREP, M. Jr., Ratio of induced fission vs. spontaneous fission and the trace element analysis in pitchblende, 20: 37994
ATTWENGER, W., Digital methods in thickness gaging, 20: 37058
AUBLE, Ronald L., Study of nuclear energy levels in ^{121}Sb, ^{123}Sb, ^{125}Sb, and ^{127}I using β- and γ-ray spectroscopy, 20: 38188
AUERBACH, Philip B., Nuclear radiation sensitive switch, 20: 37062
AUGUST, C., Status of recent meltdown studies, 20: 38474 (ANL-7120, pp 534-9)
AUNGST, R. C., Additional crack propagation tests on Zircaloy-2 reactor pressure tubes, 20: 37172

AURAND, Karl, Question of endangering the environment by the application of radioactive materials in medicine, 20: 36678
AUSLENDER, V. L., Status of operation at the positron-electron accumulator VEPP-2, 20: 37321 (NP-16205)
AVAKIAN, V. V., Shower production by pions and protons with momenta 0.1 and 20 Bev/c in thin layers of matter, 20: 37669
AVAKYAN, Ts. M., Link between luminescence of rhodopsin and the visibility of x rays, 20: 36587
AVGUSTINIK, A. I., Structure of the alloys of the Zr–C–Ta system, 20: 37270
AXEN, David Arnold, Polarization of ^{3}He nuclei, 20: 38149
AXFORD, W. I., Effect of cosmic-ray friction on the solar wind, 20: 37372
AYER, J. E., Cost estimate for remote refabrication of metallic fuels, 20: 37195 (ANL-6950)
AYER, J. E., Large metal-fueled fast reactor study. II., 20: 38494 (ANL-7120, pp 94-103)
AYER, J. E., Mixed-carbide fuels for fast reactors, 20: 38467 (ANL-7120, pp 314-27)
AZUMA, Kunio, Estimation of equilibrium separation factor in isotopic separation by chromatography, 20: 37162
AZUMA, Toshio, Neutron activation analysis of human blood and hair, 20: 36728

B

BAACKE, J., Parameters of the Regge pole model for πN charge-exchange scattering, 20: 37761
BABARYKIN, V. K., Cosmic-ray intensities in the stratosphere over Antarctica and Murmansk, 20: 37591
BABAYAN, Kh. P., Characteristics of high-energy particle interaction with nuclei of light atoms, 20: 37755
BABAYAN, Kh. P., Discussion of one model of the formation of extensive atmospheric showers, 20: 37612
BABAYAN, Kh. P., Interaction path of high-energy nucleons (10^{11} to 10^{13} ev) in the atmosphere, 20: 37667
BABER, S. R., Photonuclear interactions of μ mesons, 20: 37702
BABER, S. R., Study of the μ meson charge ratio at sea level, 20: 37687
BABIAN, Kh., New data about the nuclear-active component of young atmospheric showers, 20: 37611
BACCI, Cesare, Photoproduction of neutral pions in the energy range 400 600 Mev of the incident photon, 20: 37752
BACHELET, F., Daily latitude curves of cosmic-ray nucleonic component obtained in 1963 between 1 and 6.4 Gv, 20: 37584
BACHELET, F., Some properties of radiation recorded by IGY neutron monitors in lower atmosphere, 20: 37099
BACHYNSKI, M. P., Particle kinetics of plasmas, 20: 38348
BACKENSTOSS, G., Measurement and analysis of muonic x-ray spectra in spherical nuclei, 20: 38058
BACKOFEN, W. A., Mechanical properties of cold-worked and neutron-irradiated iron, 20: 37304
BACON, D. F., Current splitting in divided-electrode spark chambers, 20: 37109
BACON, D. F., Theoretical analysis of the performance of high-resolution magnetic hodoscopes, 20: 37106
BACON, T. C., Large Wilson cloud chamber and its application to ionization calorimetry work, 20: 37108
BACQ, Z. M., Influence of cystamine administered by mouth to mice irradiated with gamma rays at a low dose-rate, 20: 36666
BAGDASAROV, K. N., Electrolytic separation of lead from microquantities of thorium and uranium and their photometric determination, 20: 36773
BAGGE, E., Extensive air shower experiment at Kiel, 20: 37636
BAGLIN, C., Direct search for the C-violating decay $\eta^0 \to \pi^0 e^+ e^-$, 20: 37767
BAGUS, P. S., Analytic-expansion unrestricted Hartree-Fock wave function for the ^{5}D state of Fe, 20: 37448
BAHCALL, John N., Problem of detecting solar neutrinos, 20: 37491
BAHCALL, John N., Solar neutrinos, 20: 37366
BAIJAL, J., Moessbauer effect of ^{119}Sn in Te, 20: 38375
BAIJAL, Usha, Moessbauer effect of ^{119}Sn in Te, 20: 38375
BAILLY DU BOIS, Bernard, Heavy water power reactors, 20: 38517
BAILY, W. E., Mixed oxide fuel movement at various power levels and in transients, 20: 38473 (ANL-7120, pp 524-33)
BAIRD, G. A., Fast neutron intensity above Fort Churchill, Canada, 20: 37555
BAK, Hee-Ill, Pair production cross section for 6.13-Mev gamma radiation, 20: 37746
BAKER, G. S., Snoek atmosphere dislocation pinning in Ta, 20: 38360
BAKER, Louis Jr., Experimental studies of the high-temperature interaction of fuel and cladding materials with liquid sodium, 20: 38499 (ANL-7120, pp 839-47)
BAKER, Norman, Simplified models for Cepheid instability, 20: 37411
BAKER, P. Jr., Results from the new Denver multidirectional meson telescope, 20: 37095
BAKER, P. S., Chemistry of electromagnetically separated stable isotopes, 20: 37163
BAKER, P. S., Isotopes and Radiation Technology. Vol. 3, Number 3, 20: 37136
BAKER, Paul Jr., Galactic cosmic-ray source and loss problem, 20: 37484
BAKER, William R., Apparatus for producing and purifying plasma, 20: 38339
BAKHTADZE, A. K., Cascade theory of showers for light and heavy substances taking into account the polarization of the medium, 20: 37787
BALASUBRAHMANYAN, V. K., Galactic cosmic rays at solar minimum, 1965, 20: 37578
BALASUBRAMANIAN, T. S., Note on the theory of intermediate vector meson, 20: 37781
BALATA, P., Daily latitude curves of cosmic-ray nucleonic component obtained in 1963 between 1 and 6.4 Gv, 20: 37584
BALATA, P., Some properties of radiation recorded by IGY neutron monitors in lower atmosphere, 20: 37099
BALBEKOV, V. I., Stability of transverse oscillations of a focused charged beam in an absorbing medium, 20: 38315
BALLA, G. A., Increased radioisotope uptake by malignant cells in a high oxygen environment resulting from H_2O_2 breakdown, 20: 36576
BANDO, Hiroharu, Nuclear force and energy gap in finite nuclei, 20: 38113
BANKS, E., Moessbauer effect in $MnFeO_3$, 20: 36817
BANKS, E. E., Basic features of the isothermal promonotectoid transformation in a Zr–2.5Nb alloy, 20: 37234
BAQUE, Pierre, Oxidation mechanism of Zr–Cu alloys in CO, 20: 37183
BARADZEI, L. T., Investigation of the nucleon interactions at energies above 10^{13} ev, 20: 37657
BARAN, V., Extraction of alkalized solutions of uranyl salts with tributyl phosphate, 20: 36932
BARANOV, P. S., Elastic scattering of γ quanta on protons above π-meson photoproduction threshold, 20: 37800
BARASHENKOV, V. S., Intranuclear cascades at ultra-high energies, 20: 38122
BARASHENKOV, V. S., Statistical analysis of the interaction of 17 Bev mesons with photoemulsion heavy nuclei, 20: 38060
BARBOUR, J. P., Electron accelerator with a peak beam power of 10^{10} watts, 20: 37339
BARBUR, I., Thermal annealing of paramagnetic defects induced by γ irradiation in $(NH_4)_2SO_4$ and $(ND_4)_2SO_4$ single crystals, 20: 36874
BARDEEN, J., Interactions between ^{3}He atoms in dilute solutions of ^{3}He in superfluid ^{4}He, 20: 37962
BARGHUSEN, J. J., Production of uranium oxides, 20: 37205
BARGHUSEN, J. J., Safety in chemical processing, 20: 36954
BARGHUSEN, J. J., Volatility processes, 20: 36950
BARKAS, Walter H., Possible roles for emulsion as a detector in experiments with future high-energy accelerators, 20: 37077 (UCR-34P107-34)
BARKER, P., BASJE angle correlation, 20: 37629
BARKOVSKII, V. N., 68.5-cm Sector-focused cyclotron, 20: 37324
BARNAAL, D. E., Measured nuclear magnetic resonance free-induction-decay shapes and moments for ^{19}F in CaF_2, 20: 38390
BARNARD, A. C. L., Cross sections as a function of energy for the scattering of protons from ^{12}C, 20: 38050
BARNARD, A. C. L., Cross sections as a function of angle and complex phase shifts for the scattering of protons from ^{12}C, 20: 38051
BARNAVELI, T. T., Properties of μ mesons at 200 m.w.e. underground, 20: 37694
BARNES, Aaron, Collisionless damping of hydromagnetic waves, 20: 38272
BARNES, R. S., Theories of swelling and gas retention in reactor materials, 20: 37299
BARNES, V. E., f* meson produced in K–p interaction 4.6 and 5.0 Bev/c, 20: 37730 (BNL-10459)
BAROUCH, E., Application of convolution product theory to smoothing of neutron monitor data, 20: 37544
BARR, R. E., Flame-temperature measurement by thermal neutron probe, 20: 37310
BARTLETT, E. S., Effect of oxidation-protection coatings on the tensile behavior of refractory metal alloys at low temperature, 20: 37276
BARTLETT, E. S., Niobium alloys containing beryllium, 20: 37245
BARTLETT, R. W., Kinetics of Ta_5Si_3 and Cb_5Si_3 growth in disilicide coatings on Ta and Cb, 20: 37190
BARTON, C. J., Removal of protactinium from molten fluoride breeder blanket mixtures, 20: 36927 (ORNL-TM-1543)
BARTON, J. C., Development of scintillation counters based on medicinal paraffin, 20: 37112
BARTON, J. C., Intensity of stopping pions at sea level and underground, 20: 37709
BARTON, J. C., Scintillation-counter study of cosmic rays deep underground, 20: 37705
BARTON, J. C., Some properties of muon showers observed underground, 20: 37605

BARTON, J. C., Study of the electromagnetic interactions of high-energy muons using a large scintillator stack, 20: 37699
BARTON, J. C., Study of cascade showers in lead, 20: 37700
BARTON, J. C., Use of pulse shape discrimination with scintillation counters for cosmic-ray studies, 20: 37111
BAR'YAKHTAR, V. G., Interaction of plasma oscillations and spin waves in ferromagnetic semiconductors and metals, 20: 38354 (FTI-244/T-027)
BASARGIN, Yu. G., 68.5-cm Sector-focused cyclotron, 20: 37324
BASHANDY, E., Decay scheme of 5.0-d ^{183}Ta, 20: 38104
BASHINDYAGIAN, G. L., Relationship of neutral and charged particles among nuclear-active particles with energies above 100 Bev at mountain altitude, 20: 37685
BASILEVSKAYA, G. A., 27-day and other cyclic variations of cosmic-ray intensity, 20: 37532
BASIULIS, A., Development of a reservoirless thermionic energy converter, 20: 37725
BASSANI, G., Reactions (^{3}He,d) on even Sn isotopes, 20: 38073
BASSEL, R. H., Nuclear-reaction studies with 65-Mev α particles on Zr, 20: 38092
BATES, J. Lambert, Melting points of hypostoichiometric uranium dioxide, 20: 37220
BATOV, V. V., Economic aspects for stimulating nuclear power, 20: 38512
BATUSOV, Yu. A., Double charge exchange of 50- to 176-Mev π^- mesons in photo emulsion, 20: 38012 (JINR-P-2806)
BATYAEV, I. M., Electron absorption spectra of Ce(III) salts in water–TBP mixtures and in pure TBP, 20: 36831
BATZER, T. H., Flange design using Al foil for ultrahigh-vacuum application, 20: 37000 (UCID-4548(Rev.4))
BAUER, A. A., Microanalytical studies of micro- and macro-segregation in oxide fuels, 20: 38469 (ANL-7120, pp 400-9)
BAUM, John W., Mixed radiation Rem responding rate meter, 20: 37068 (BNL-10321)
BAUMANN, G., Heavy cosmic ions recorded in nuclear emulsions exposed in a polar satellite, 20: 37577
BAUMGARTNER, W. V., Personnel neutron dosimeter developments, 20: 37070 (BNWL-SA-537)
BAXTER, A. J., Shower front structure and the properties of extensive air showers, 20: 37632
BAYAREVICH, V. V., Cosmic-ray intensities in the stratosphere over Antarctica and Murmansk, 20: 37591
BAYER, Ryszard, Coincidence circuit for x-ray spectrometry, 20: 37093
BAYER, Ryszard, 10-MHz linear window amplifier, 20: 37048
BAYM, G., Interactions between ^{3}He atoms in dilute solutions of ^{3}He in superfluid ^{4}He, 20: 37962
BEARD, G. B., Quadrupole interaction in ^{121}Sb by Mœssbauer techniques, 20: 38386
BEARD, P. M., Precision measurement of reaction thresholds, 20: 38028
BECK, F. A., Angular distribution, angular correlations, and plane polarization of gamma rays of the reaction ^{53}Cr(p,n)^{53}Mn, 20: 38034
BECK, Hans R., Possibilities of legal control of radiation protection of patients from the viewpoint of the x radiologist, 20: 36679
BECKER, E. W., Electrical breakdown in beams of condensed hydrogen and condensed nitrogen in high vacuum, 20: 38247
BECKER, Josef, Forty-third meeting of German X-Ray Society, Cologne, 5/62, 20: 36691
BECKERLEY, James, Nuclear radiation processing of optical maser materials, 20: 37280 (NYO-3330-11)
BEELER, J. R. Jr., Vacancy and interstitial cluster production in neutron-irradiated α iron, 20: 38361
BEGHIN, Christian, Determination of the density of protons at the level of a satellite by exact numerical analysis of proton whistlers, 20: 37885
BEHLKE, H., Uhf plasma oscillations in Hg low-pressure discharge. I., 20: 38214
BEHLKE, H., Uhf plasma oscillations in Hg low-pressure discharge. II., 20: 38215
BEHLKE, H., Uhf plasma oscillations in a Hg low-pressure discharge. III., 20: 38216
BEIN, G. P., Plane wave transmission and reflection coefficients for lossy inhomogeneous plasmas, 20: 38233
BEISING, K., Bibliography on food irradiation, No. 05, 6/66, 20: 37138 (AED-C-05-05)
BEISSWENGER, H., Microanalytical studies of micro- and macro-segregation in oxide fuels, 20: 38469 (ANL-7120, pp 400-9)
BEKRENEV, V. S., Decay of ^{182}Ta, 20: 38134
BELL, Vernon L., Polyimidazopyrrolones: new class of radiation-resistant polymers, 20: 36846 (N-66-13499)
BELLACK, Stephen, Protective action of Bacillus subtilis on x-irradiated mice, 20: 36673
BELLENI-MORANTE, A., Kinetic behavior of reactor composed of two loosely coupled cores, 20: 38454
BENASSI, Enrico, Effect of ionizing radiation on delayed hypersensitivity, 20: 36655
BENATTAR, Rene, Formation of negative ions in a flame by measurement of the Hall effect, 20: 38223
BENHAM, R. D., Time optimal xenon shutdown on the xenon boundary, 20: 38411 (BNWL-186)
BENJAMIN, Benny Moses, Recombination of hydrogen and oxygen in the presence of water vapor under the influence of radiation, 20: 36910
BENNETT, G. A., Compact pyrochemical processes, 20: 36952
BENNETT, G. W., Elastic scattering of 1 Bev protons from He and O, 20: 38010 (BNL-10438)
BENNETT, Willard H., Electron beams from a duoplasmatron using a hollow cathode arc as electron source, 20: 37045
BENSON, R. H., Measurement of beta radioactivity in gas samples using a plastic scintillator cell, 20: 37086
BENSON, Royal H., Limitations of tritium measurements by liquid scintillation counting of emulsions, 20: 36720
BERCOVITCH, M., Day by day correction of the meson diurnal variation for atmospheric effects, 20: 37585
BERCOVITCH, M., Introduction of meteorological corrections into meson monitor data, 20: 37101
BERCOVITCH, M., Latitude survey in North America, 20: 37593
BERCOVITCH, M., Meteorological factors affecting the counting rate of neutron monitors, 20: 37100
BERESTETSKII, V. B., Electromagnetic properties of neutral particles, 20: 37859
BEREZKIN, V. G., Kinetics of radiation polymerization of acrylonitrile from the gas phase on a mineral substrate, 20: 36882
BERG, R. E., Measurement of high-energy γ-rays with Ge(Li) detectors, 20: 37126
BERGER, S., Fission product retention in sodium and applications to vented fuel element design, 20: 38477 (ANL-7120, pp 855-61)
BERGERE, Roland, Frequency modulation of uhf signals in electron linear accelerator, 20: 37319 (CEA-R-2976)
BERGESON, H. E., University of Utah neutrino detector, 20: 37104
BERGNER, Per-Erik E., Tracer theory: a review, 20: 36544
BERGSNOV-HANSEN, Bjorn, Low-pressure study of heterogeneous H–deuterium exchange at steady state, 20: 36818
BERK, H. L., Plasma wave propagation in hot inhomogeneous media, 20: 38284
BERKELMAN, K., Electromagnetic form factor of the pion, 20: 37812
BERMAN, B. L., Photoneutron cross sections of ^{141}Pr and ^{127}I from threshold to 33 Mev, 20: 38094
BERMAN, David A., Effect of Ca, Sr, and Mg on positive inotropic action of fluoride, 20: 36567
BERNAL, G. E., Ion emission from laser irradiated tungsten, 20: 37298
BERNARD, D. L., Absolute energy calibration of neutron thresholds, 20: 38054
BERNDT, A. F., Gamma-phase in the Pu–Hg system, 20: 37244
BERNE, A., Measurement of the time evolution of a radiation field by joint photocount distributions, 20: 37311
BERNHARD, H., Chelate exchanger on basis of 8-hydroxyquinoline, 20: 36754
BERNSTEIN, A. M., Systematics of 3$^-$ and 5$^-$ states in ^{40,42,44,48}Ca and ^{50}Ti from inelastic alpha scattering, 20: 38100
BERNSTEIN, E. M., Reaction ^{90}Zr(d,p)^{91}Zr at energies below 4 Mev, 20: 38096
BERRY, R. J., Perturbations in x-ray dose response in vitro with time after plating, 20: 36664
BERRY, R. Stephen, Ionization of molecules at low energies, 20: 36819
BERTAUT, Erwin-Felix, Magnetic structure of Er_2O_3, 20: 38357
BERTAZZONI, U., Effect of x irradiation on nicotinamide adenine dinucleotides content of rat thymocytes, 20: 36590
BERTI, F., Regulation of lipid transport and radiation-induced hyperlipemia, 20: 36580
BERTINI, R., Angular distribution, angular correlations, and plane polarization of gamma rays of the reaction ^{53}Cr(p,n)^{53}Mn, 20: 38034
BERTMAN, Bernard Theodore, Thermal transport in He crystals, 20: 37983
BESPALOV, D. F., Pulsed neutron generator for boreholes and its use in nuclear geophysics, 20: 37017
BETEV, B., Inelastic n-p cross section at 60 Bev, 20: 37670
BETH, R. A., Combination of cylindrical current sheets to cancel external field, 20: 37313 (BNL-10143)
BETH, Richard A., Elliptical current sheets to produce constant-gradient field, 20: 37317 (BNL-10341)
BETH, Richard A., Fields produced by cylindrical current arrays, 20: 37314 (BNL-10148)
BETH, Richard A., Fields produced by elliptical current sheets, 20: 37318 (BNL-10436)
BETH, Richard A., Forces on currents in two-dimensional magnetic fields, 20: 37316 (BNL-10324)
BETH, Richard A., Stored energy and inductance in two-dimensional fields, 20: 37315 (BNL-10323)
BETZ, F., Polarization in proton-proton scattering using polarized proton target. Pt. I and Pt. II., 20: 37743 (UCRL-16866)
BEVAN, J. S., Voltage calibration of a 400-kv Van de Graaff machine,

20: 37331
BEVC, Vladislav, Behavior of separation constants for finite gyromagnetic plasmas, 20: 38228
BEVC, Vladislav, Power flow in plasma-filled wave-guides, 20: 38239
BEVERIDGE, J. H., Nozzle tube-wall temperature measurement by radiometric techniques, 20: 38528
BEVINGTON, Philip R., On-line reduction of nuclear physics data with the PDP-7, 20: 38176
BEWICK, A., Investigation of the modulation of the primary cosmic radiation using an airborne detector, 20: 37510
BEZAGUET, A., Direct search for the C-violating decay $\eta^0 \to \pi^0 e^+ e^-$, 20: 37767
BHALLA, C. P., N-subshell ratios and very low-lying states, 20: 38182
BHATT, V. L., Fast neutrons of solar origin, 20: 37375
BHATTACHARYYA, A. K., Theory of artificial transmutation of nuclei, 20: 38020
BHOWMIK, B., Energy spectrum of primary He nuclei at energies greater than 6 Bev, 20: 37557
BIALYNICKI-BIRULA, Iwo, Relativistic quantum field theory, 20: 37845
BIBILASHVILI, M. F., Properties of μ mesons at 200 m.w.e. underground, 20: 37694
BICKEL, William S., Mean lives of the 2p and 3p levels in atomic hydrogen, 20: 37443
BIDELMAN, William P., Element abundances in the peculiar A stars, 20: 37426
BIERSACK, Jochen, Theory of stochastic acceleration. I., 20: 37335
BIERSACK, Jochen, Theory of stochastic acceleration. II., 20: 37336
BILINSKI, Halka, Precipitation and hydrolysis of metallic ions. II., 20: 36789
BILPUCH, E. G., Precision measurement of reaction thresholds, 20: 38028
BINDEWALD, H., Determination of fast neutron penetration in concrete by measurement of the scattered field of a collimated neutron beam, 20: 38352
BINGHAM, C. R., Nuclear-reaction studies with 65-Mev α particles on Zr, 20: 38092
BINGHAM, H. H., Coherent production of multipion resonances, 20: 37822
BINGHAM, H. H., Direct search for the C-violating decay $\eta^0 \to \pi^0 e^+ e^-$, 20: 37767
BIR, R., Plutonium and uranium mass spectrometry measurements on irradiated fuels, 20: 36783
BISHAY, A., Photochemical reaction induced in borate glasses containing arsenic and manganese, 20: 36887
BISHOP, Vernon S., Hemodynamic parameters in heart failure, produced by embolization and radiation, 20: 36660
BISNOVATYI-KOGAN, G. S., Critical mass of a hot isothermal white dwarf with general relativistic effects taken into account, 20: 37383
BISWAS, S., Abundance of ^{3}He nuclei in the primary cosmic radiation, 20: 37559
BISWAS, S., Heavy nuclei in the primary cosmic rays in June 1963 at Fort Churchill, 20: 37568
BISWAS, S., Solar cosmic-ray heavy nuclei and the 18th July 1961 event, 20: 37567
BISWAS, S. N., Current commutation relations, universality, and nonleptonic baryon decays, 20: 37839
BITTER, Francis, Megagauss magnets using capacitor discharges, 20: 36982
BIZZOZERO, O. Joseph Jr., Radiation-related leukemia in Hiroshima and Nagasaki, 1946–1964. I., 20: 36645
BJERREGAARD, J. H., Reactions ^{63,65}Cu(t,p)^{65,67}Cu, 20: 38035
BJERREGAARD, J. H., Reaction (t,p) with even isotopes of Sm, 20: 38052
BLACKBURN, D., Synthesis of 2,4,7-triamino-6-phenylpteridine (triamterene) labeled with tritium or ^{14}C, 20: 36922
BLACKBURN, R., Linear energy transfer effect in radiolysis of cyclohexane, 20: 36888
BLAKE, P. R., Experiments on the pulse spectrum observed from scintillation and Cherenkov detectors at sea level, 20: 37619
BLAKE, P. R., Muon component of air showers, 20: 37645
BLAND, C. J., Flux and east-west asymmetry of primary electrons at a geomagnetic rigidity cut-off of about 4.5 GV, 20: 37550
BLAUTH, Erich W., Dynamic mass spectrometers, 20: 36777
BLAVOUX, B., Potassium in sections of 5 borings made in Evian quaternary formations, 20: 37012
BLEEKER, J. A. M., Balloon observation of high-energy electrons, 20: 37549
BLINOV, G. A., Status of operation at the positron-electron accumulator VEPP-2, 20: 37321 (NP-16205)
BLOCH, Felix, Theory of superconductivity, 20: 37967
BLOCK, F. G., Development of a reservoirless thermionic energy converter, 20: 37725
BLUMENTHAL, B., Mixed fuel-cycle fast breeder reactors: nuclear, safety, and materials considerations, 20: 38476 (ANL-7120, pp 751-8)
BLYUMENTSEV, A. M., Neutron radiative capture gamma spectrometry as a method of determining the composition of iron-bearing rocks and ores, 20: 37019
BOARDMAN, C., Post-explosion environment resulting from the Salmon event, 20: 36970
BOATO, G., Effect of transition-metal impurities on the critical temperature of superconducting Al, Zn, In, and Sn, 20: 37955
BOCLET, D., Gamma-ray generation in the high atmosphere, 20: 37576
BODNHAR, R., The structure of $YbSb_2$, a $ZrSi_2$ isotope, 20: 37238
BOEDEKER, R. R., Flame-temperature measurement by thermal neutron probe, 20: 37310
BOEHM, E., Extensive air shower experiment at Kiel, 20: 37636
BOEHM, G. G. A., Ultraviolet spectroscopy of irradiated polyethylene. II., 20: 36857 (COO-1088-21)
BOEHM, R. F., Nine-rod critical heat flux investigation at 1000 psia, 20: 38462 (GEAP-4929)
BOELLA, G., Flux and east-west asymmetry of primary electrons at a geomagnetic rigidity cut-off of about 4.5 GV, 20: 37550
BOERSCH, H., High resolution investigation of the energy losses of 30 kev electrons in aluminum foils of various thicknesses, 20: 37442
BOERSCH, H., Interaction of 25-kev electrons with lattice vibrations in LiF, 20: 38395
BOGDANOV, G. F., Increasing plasma density in Ogra-I, 20: 38248
BOGOMOLOV, K. S., Anomalous positive effects of preliminary irradiation. I., 20: 36895
BOKOV, O. G., Broken Ü(12) symmetry and unitarity condition for the S matrix, 20: 37855
BOLING, M. E., Resistance of Micrococcus radiodurans to uv radiation. III., 20: 36610
BOLOTOV, V. N., Inelastic neutron cross section measurements near 100 Bev, 20: 37668
BOLT, Wilhelm, Investigations with a tritium-labeled N-mustard gas derivative in carcinoma treatment, 20: 36705
BONNER, B. E., Absolute energy calibration of neutron thresholds, 20: 38054
BONNER, B. E., Measurement of (p,n) thresholds at tandem energies, 20: 38053
BONNIN, Bernard, Study of superconductors in the Al–Mg system, 20: 37935 (CEA-R-2906)
BONZEL, H. P., Influence of surface structure and purity of Cu samples and of α irradiation on the diffusion of ^{63}Ni in Cu, 20: 37300
BOREMSKAYA, S. F., Analysis of mixtures of oxides of rare earths and alkaline earths, 20: 36776
BORESKOV, G. K., Homomolecular and isotopic exchange of oxygen on gadolinium oxide, 20: 36826
BORGIA, B., Scattering of positrons and electrons from protons, 20: 37778
BORISOV, N., Method for obtaining low temperatures based on dissolution of ^{3}He in ^{4}He, 20: 37978
BOROG, V. V., Angular distribution and energy spectrum of cosmic-particle showers at 10^{12} ev, 20: 37696
BORST, Lyle B., Rotational character of liquid He, 20: 37987
BOSE, S. K., Meson-baryon coupling constants in broken SU(3) and the algebra of currents, 20: 37842
BOSTANDZHYAN, N. H., Spark chamber operation at high voltage pulse delay, 20: 37088
BOTT, J. F., Spectroscopic measurement of temperatures in an argon plasma arc, 20: 38279
BOTTOMS, Eva, Effect of ultraviolet irradiation on skin collagen, 20: 36595
BOUAZIZ, Roger, Preparation of monocrystals of hafnium oxide by the method of fused salts, 20: 37197
BOUCHIAT, C., Albebra of currents and the $|\Delta| = \frac{1}{2}$ rule for K-meson nonleptonic decay, 20: 37759
BOUDNITSKAYA, E. V., Changes in the content of unsaturated higher fatty acids in the free lipid fraction of irradiated leaves, 20: 36598
BOWTHORPE, M., Neutron flux in the upper atmosphere during the 1964 solar minimum, 20: 37908
BOYADZHYAN, N. G., Discussion of one model of the formation of extensive atmospheric showers, 20: 37612
BOYD, George E., Radiolytic decomposition of crystalline alkali metal and alkaline earth bromates, 20: 36899
BOZEK, E., Angular distribution, angular correlations, and plane polarization of gamma rays of the reaction ^{53}Cr(p,n)^{53}Mn, 20: 38034
BOZEK, E., Application of the delayed coincidence technique to measurement of the short mean lives in ^{131}Xe and ^{143}Pr, 20: 38031
BOZEK, E., Half lives of levels at 405 kev in ^{211}Bi and 377 kev in ^{53}Mn, 20: 38030
BOZOKI, G., Inelastic n-p cross section at 60 Bev, 20: 37670
BRABEC, Vlastislav, Measurements of nondestructive fuel burnup by means of γ spectroscopy of fission products, 20: 37287
BRACKENBUSH, L. W., Personnel neutron dosimeter developments, 20: 37070 (BNWL-SA-537)
BRADATSCH, H., Computer experiments on radiation annealing of Frenkel defects, 20: 37294
BRADLEY, E. F., Niobium alloys containing beryllium, 20: 37245

BRAILEY, R. H. E., Prog. rpt. on 1800–400F fibrous-type insulation for radioisotope power systems, 3–6/66, 20: 36983 (ALO-3633-1)
BRAMBILLA, M., Limiting growth rates for generalized Harris instabilities, 20: 38290
BRAMBLETT, R. L., Photoneutron cross sections of ^{141}Pr and ^{127}I from threshold to 33 Mev, 20: 38094
BRANDENBERGER, J. D., Neutron cross sections of Ca from 2.0 to 6.5 Mev, 20: 38183
BRANDMAIER, Harold E., Recent advances in electrofluiddynamic power generation, 20: 37727
BRANDSTETTER, A., Decay correlations of photo-produced rho mesons in the strong-absorption model, 20: 37768
BRANDSTETTER, A., Rho meson photoproduction cross sections in the strong-absorption model, 20: 37766
BRANDT, S., Production of strange particles in 8-Bev/c π^+-proton interactions. II., 20: 37770
BRANDUS, I., Superfluid model with fixed-particle number treatment of ^3H and ^3He emission, 20: 38116
BRANICA, Marko, Precipitation and hydrolysis of metallic ions. II., 20: 36789
BRANSCOMB, L. M., Detachment of electrons from H^- by electron impact, 20: 37452
BRATER, D. C., Fluid-bed volatility component, engineering feasibility, and scale-up studies at the Oak Ridge Gaseous Diffusion Plant, 20: 36926 (K-L-6091)
BRAUN, E., Effective interaction in a quantum Vlasov plasma, 20: 38286
BRAUN, M. A., Scattering on a composite particle with small binding energy and the impulse approximation, 20: 37798
BRAUN, O., Composition of photon-initiated showers at high energies, 20: 37628
BRAY, A. D., Studies of the cores of extensive air showers, 20: 37616
BREITENLOHNER, P., Influence of the deuteron model on the inelastic electron-deuteron cross section, 20: 37748
BREITENLOHNER, P., Interpretation of Foldy-Wouthuysen transformation, 20: 37828
BREITLING, Gerhard, Question of the subtle adaptation of the irradiation field in fast electrons, 20: 36700
BRENAN, C., Ion exchange method of estimating ^{90}Sr and other radionuclides in rainwater, 20: 36759
BRESADOLA, S., Intralymphatic isotope therapy with a new radioactive phosphate compound (^{32}P) in fat soluble radiopaque contrast media, 20: 36684
BREWER, L., Bibliography on the high-temperature chemistry and physics of gases and plasmas, 20: 38204 (NP-16240)
BRICARD, J., Action of radioactivity and of pollution upon parameters of atmospheric electricity, 20: 37003
BRIDGMAN, C. J., Kinetic behavior of a circulating-water reactor following large reactivity changes, 20: 38449
BRIENT, Charles E., Reaction $^{90}Zr(d,p)^{91}Zr$ at energies below 4 Mev, 20: 38096
BRIGGS, D. A., Particle counting in locally produced showers using vidicon television techniques, 20: 37114
BRIKKER, S. I., Generation mechanism of high-energy pions in cosmic rays, 20: 37664
BRINHALL, J. L., Vacancy and interstitial clusters in neutron-irradiated nickel, 20: 38367
BRINKMAN, J. A., Control of swelling by nucleation, 20: 37302
BRINKMANN, F., Time decay of scintillations of anthracene and p-terphenyl single crystals with α particles as a function of the direction of incidence, 20: 37305
BRITTAN, R. O., Transient temperature distributions in fast reactor fuels with widely varying thermal diffusivity, 20: 38470 (ANL-7120, pp 478-85)
BRODSKY, Stanley J., Radiative level shifts. III., 20: 37445
BROQUET, Daniele, Distribution of chromium in marine organisms, 20: 36552
BROUDE, C., Gamma-ray angular correlations following nuclear reactions, 20: 38184
BROWN, Bernard, Anticoincidence shielded gamma-ray spectrometer for nuclear reaction studies, 20: 37115
BROWN, C. N., Evidence of a higher symmetry in nucleon-nucleon scattering, 20: 37772
BROWN, P. E., Potassium–argon ages of some Dalradian, Moine, and related Scottish rocks, 20: 37016
BROWN, W. Lynn, Set formation to nonrewarded cues by normal and previously irradiated rhesus monkeys, 20: 36638
BROWN, W. Lynn, Social distractibility of previously irradiated female rhesus monkeys, 20: 36639
BROWN, William A., Photoelectric recording of the profile of H on a microsecond time scale, 20: 37063
BRUCE, C. E. R., Pinched lightning discharges, 20: 38260
BRUECHER, Erno, Investigation of the mechanism of the NH_4-lactate elution separation of trace lanthanides, 20: 36939
BRUEGGEMANN, J., Equipment of Radiochemical and Radiobiological Section in Inst. of Animal Physiology and Nutrition of University of Munich, 20: 37040
BRUGGER, R. M., Intramolecular coherent scattering of neutrons by CD_4 gas, 20: 38000
BRUSSE, M. J., Effects of moisture content on irradiated seeds of Lupinus angustifolius L., 20: 36646
BRYAN, R. G., Potentiometric titration of cerium and manganese following separation from plutonium and cobalt, 20: 36713 (LA-3402)
BUBEN, N. Ya., Formation of radicals during radiolysis of organic solids. III., 20: 36883
BUCHELNIKOVA, N. S., Diffusion perpendicular to the magnetic field in the universal instability, 20: 38264
BUCKMAN, R. W. Jr., Apparatus for determining creep behavior under conditions of ultrahigh vacuum, 20: 37263
BUCKWALTER, G., Muon decays from neutral primaries, 20: 37713
BUCZWINSKI, T. A., Cost estimate for remote refabrication of metallic fuels, 20: 37195 (ANL-6950)
BUDDEMEYER, E. U., Radiation dose to the rat thyroid from several radioiodine nuclides, 20: 36561
BUDKER, G. I., Status of operation at the positron-electron accumulator VEPP-2, 20: 37321 (NP-16205)
BUDNIKOV, P. P., Growing BeO single crystals, 20: 36814
BUDYASHOV, Yu. G., Muon capture in mixed gases, 20: 37741 (JINR-P-2788)
BULL, R. M., Photonuclear interactions of μ mesons, 20: 37702
BULL, R. M., Study of the μ meson charge ratio at sea level, 20: 37687
BULLOUGH, R., Stacking-fault energy and many-body force effects in solid argon, 20: 38394
BULOW, H., Hall effect in 75 at.% Bi–25 at.% Sn alloy quenched films below 47°K, 20: 38384
BUMP, T. R., Faret Core-I reference design, 20: 38460 (ANL-7120, pp 766-75)
BUNEMAN, O., Shall we have to live with anomalous diffusion?, 20: 38330
BUNEMAN, O., Stability of crossed-field electron beams, 20: 37329
BUNEMAN, Oscar, Computer experiments in plasma physics, 20: 38310
BUNYATOV, S. A., Double charge exchange of 50- to 176-Mev π^- mesons in photo emulsion, 20: 38012 (JINR-P-2806)
BURBIDGE, E. M., Quasi-stellar objects, radiogalaxies, and the origin of cosmic rays, 20: 37370
BURBIDGE, G. R., Quasi-stellar objects, radiogalaxies, and the origin of cosmic rays, 20: 37370
BURBIDGE, Geoffrey, Origin of cosmic rays, 20: 37490
BURDE, J., Isomeric state (8$^-$) in ^{180}W, ^{182}Os, and ^{184}Pt, 20: 38027
BURDICK, Boyce, Negative ions in liquid He II, 20: 37981
BURGER, J. J., Balloon observation of high-energy electrons, 20: 37549
BURGER, K., Study of back coordination in iron chelates by the Moessbauer method, 20: 36823
BURGER, Peter, Computer simulation methods for plasma diodes with collisions, 20: 37726
BURGESS, Mitchell P., Performance of sieve trays under GS heavy water process conditions. I., 20: 37160 (DP-1025)
BURGHARD, G., Synthesis of 2,4,7-triamino-6-phenylpteridine (triamterene) labeled with tritium or ^{14}C, 20: 36922
BURK, W., Fission recoil separation in mixtures with uranium dioxide powders as a simple method of range determination of fission products, 20: 37997
BURKE, P. G., Electron-impact excitation of n = 2 states in He, 20: 37453
BURKE, T. P., Examination of the overpressure and underpressure methods of operating a photoelectric nucleus counter, 20: 37094
BURMAN, R., Equations for wave propagation in an inhomogeneous compressible plasma, 20: 38227
BURNS, H. M., Report of fire resistance tests fuel core shipping container No. 1, 20: 37024 (NLCO-899)
BURR, A. A., Effect of certain rare-earth solutes upon the f.c.c./b.c.c. transformation temperature of Th, 20: 37242
BURRIS, L., Compact pyrochemical processes, 20: 36952
BUSCHOW, K. H. J., Crystal structures of the rare-earth compounds of the form R_2Ni_{17}, R_2Co_{17} and R_2Fe_{17}, 20: 37243
BUSEY, H., Characteristics of the aerosol produced from burning plutonium, 20: 37022 (LA-DC-6942)
BUSH, Elizabeth T., Relative efficiency of a new liquid scintillation fluor, p-bis-(p-methylstyryl)benzene, 20: 36863
BUSHEV, M., Theory of direct nuclear reactions, 20: 38023
BUTLER, D. K., Large metal-fueled fast reactor study. I., 20: 38493 (ANL-7120, pp 85-93)
BUTLER, T. A., Production of ^{33}P from ^{36}Cl and ^{33}S by fast-neutron irradiation, 20: 37166
BUTRA, F. P., Growing BeO single crystals, 20: 36814

C

CABIBBO, N., Phase of K_L-K_S regeneration in a simple Regge pole model, 20: 37764

CAILLAT, Roger, Oxidation mechanism of Zr–Cu alloys in CO, 20: 37183

CAKRT, E., Extraction of alkalized solutions of uranyl salts with tributyl phosphate, 20: 36932

CALDWELL, J. T., Photoneutron cross sections of ^{141}Pr and ^{127}I from threshold to 33 Mev, 20: 38094

CALDWELL, Richard L., Geological prospecting comprising directional irradiation and detection, 20: 37021

CALKINS, John Cloud, Lethal effects of x rays and uv light on ciliate protozoans, 20: 36661

CALUSARU, A., Thermal annealing of paramagnetic defects induced by γ irradiation in $(NH_4)_2SO_4$ and $(ND_4)_2SO_4$ single crystals, 20: 36874

CAMERON, A. G. W., Conference on stellar evolution, New York, 11/63, 20: 37390

CAMERON, A. G. W., Contraction phase of solar evolution, 20: 37397

CAMERON, A. G. W., Cooling and detectability of neutron stars, 20: 37355

CAMERON, A. G. W., Formation of helium in the galaxy, 20: 37409

CAMERON, A. G. W., Rotation of neutron stars, 20: 37363

CAMERON, A. G. W., Some effects of nuclear forces on neutron-star models, 20: 37356

CAMERON, J. F., Review of the design and application of radioisotope instruments in industry, 20: 37148

CAMERON, J. F., Simple radioisotope x-ray transmission gage for measuring suspended sediment concentrations in rivers, 20: 37057

CAMPAGNARI, F., Effect of x irradiation on nicotinamide adenine dinucleotides content of rat thymocytes, 20: 36590

CAMPBELL, Charles J., Clinical studies in laser photocoagulation, 20: 36682

CAMPBELL, Charles J., Prophylactic photocoagulation of recurrent toxoplasmic retinochoroiditis, 20: 36683

CAMPBELL, D. J., Ion chamber d-c amplifier, A-10,080, 20: 37066 (AECL-2536)

CAMPI, Morris, Waveguide analog of tunneling through quantum potential barriers, 20: 37929

CANFIELD, J., X-ray photoconductivity of anthracene, 20: 36873

CANTERFORD, J. H., Reactivity of transition metal fluorides. III., 20: 36804

CAPE, J. A., Pauli spin and spin-orbit effects in the magnetization of a superconducting Ti–Mo alloy, 20: 37951

CAPELLEN, J., Bibliography on mass spectroscopy, 20: 36712 (IS-1335)

CAPPELAERE, P., Effect of ionizing radiations on the HeLa cell. II., 20: 36616

CARDEN, Joan E., Isotopes and Radiation Technology. Vol. 3, Number 3, 20: 37136

CARDEN, Joan E., Preparation, properties, and uses of kryptonates in chemical analysis, 20: 36749

CARLSON, A. D., Fluctuations in neutron total cross sections in the Mev energy region, 20: 38173

CARLSON, Lorne Edwin, Nanosecond beam burst production, 20: 37337

CARMICHAEL, H., Introduction of meteorological corrections into meson monitor data, 20: 37101

CARMICHAEL, H., Latitude survey in North America, 20: 37593

CARON, C., Use of a surface hygrometer for checking resin injections in salvaging the temples of Abu Simbel, 20: 37134

CARPENTER, S. G., Recent results of Doppler measurements in fast-neutron spectra, 20: 38429 (ANL-7120, pp 614-15)

CARRIKER, A. Wendell, Polymer degradation dosimeter of polyisobutylene heptane, 20: 37117

CARROLL, R. M., Fission-gas release during fissioning in UO_2, 20: 37291

CARSTEN, Arland, Early and late effects of x irradiation on the cerebral cortex of the monkey, 20: 36656

CARTER, J. C., Transient temperature distributions in fast reactor fuels with widely varying thermal diffusivity, 20: 38470 (ANL-7120, pp 478-85)

CARVER, J. G., Prog. rpt. on Pu subcritical experiment program, 1–3/66, 20: 38443 (GEAP-5148)

CASSIDAY, G. L., Scattering of positrons and electrons from protons, 20: 37778

CASSOLA, R. L., Analysis of 14 Mev elastic neutron scattering from K, 20: 38171

CATER, C. W., Effect of ultraviolet irradiation on skin collagen, 20: 36595

CAVAILLES, J., Continuous measurement of galvanization coatings by means of x-ray fluorescence, 20: 37151

CAVENESS, William F., Early and late effects of x irradiation on the cerebral cortex of the monkey, 20: 36656

CEROVIC, Danica, Grain growth in alpha-uranium, 20: 37222

CHAMBERLAIN, O., Polarization in proton-proton scattering using polarized target. Pt. I and Pt. II., 20: 37743 (UCRL-16866)

CHAND, Ramesh, Apparent ρ-production anomaly in p-d capture reactions, 20: 37813

CHANDRA, Girish, Lifetimes of positronium in polymers irradiated by gamma rays, 20: 36896

CHANG, C. C., Origin of high-energy electrons beyond the magnetosphere, 20: 37894

CHANG, C. C., Viscous model of the solar wind, 20: 37350

CHANG, T. Y., Investigation of flute instability with an alkali-metal plasma, 20: 38323

CHANG, W. H., Prevention of molybdenum alloy ingot cracking by capping, 20: 37219

CHAO, Chung-yao, Polarization of protons from the ^{12}C(d,p)^{13}C and ^{40}Ca(d,p)^{41}Ca ground-state reactions, 20: 38119

CHAPIRO, Adolphe, Radiochemical polymerization of lauryl methacrylate in liquid and solid phases, 20: 36875

CHAPLIN, R. L., Apparatus for electron irradiation studies at low temperatures, 20: 37054

CHAPMAN, B. B., Protein electrophoretic changes following total-body irradiation of normal and tumor-bearing rats, 20: 36582

CHARAK, I., Preliminary evaluation of a technique to study expulsion of sodium into air, 20: 38500 (ANL-7120, pp 868-72)

CHARAKHCH'YAN, A. N., Cosmic rays and solar activity from the data of measurements in the stratosphere, 20: 37536

CHARAKHCH'YAN, A. N., Cosmic-ray intensities in the stratosphere over Antarctica and Murmansk, 20: 37591

CHARAKHCH'YAN, A. N., Penetration of the outer radiation belt particles into low altitudes of atmosphere, 20: 37907

CHARAKHCH'YAN, T. N., Cosmic rays and solar activity from the data of measurements in the stratosphere, 20: 37536

CHARAKHCH'YAN, T. N., Cosmic-ray intensities in the stratosphere over Antarctica and Murmansk, 20: 37591

CHARAKHCH'YAN, T. N., Penetration of the outer radiation belt particles into low altitudes of atmosphere, 20: 37907

CHARAKHCH'YAN, T. N., 27-day and other cyclic variations of cosmic-ray intensity, 20: 37532

CHARBONNIER, F. M., Electron accelerator with a peak beam power of 10^{10} watts, 20: 37339

CHARLESBY, A., Linear energy transfer effect in radiolysis of cyclohexane, 20: 36888

CHARMAN, W. N., Potentialities of operating Cherenkov light receivers in the middle ultraviolet regions of spectrum, 20: 37717

CHASE, John W., Radiolytic decomposition of crystalline alkali metal and alkaline earth bromates, 20: 36899

CHASSON, R. L., Barometric correction anomaly and nucleonic component time variations during IQSY, 20: 37096

CHASSON, R. L., Galactic cosmic-ray source and loss problem, 20: 37484

CHASSON, R. L., Results from the new Denver multidirectional meson telescope, 20: 37095

CHATTERJEE, B. K., Correlations between the electron, muon, and N components in extensive air showers, 20: 37635

CHATTERJEE, B. K., Properties of extensive air showers rich in muons, 20: 37608

CHATTERJEE, B. K., Search for heavy mass particles in air showers, 20: 37653

CHATTERJEE, B. K., Time lags of nuclear-interacting particles in extensive air showers, 20: 37652

CHATTERJEE, B. K., Ultra-high energy muons (>200 Bev) in extensive air showers, 20: 37606

CHAUDAKOV, A. E., Earth's radiation belt, 20: 37899

CHEADLE, B. A., Effect of heat treatment on texture of fabricated Zr-rich alloys, 20: 37198

CHEN, Che Jen, Velocity-profile measurement in plasma flows using tracers produced by a laser beam, 20: 38238

CHEN, H. F., Simplified 180° focusing β-ray spectrometer, 20: 37120

CHEN, H. T., Neutron-proton correlation effects in spherical even nuclei, 20: 38177

CHEN, J. F., Simplified 180° focusing β-ray spectrometer, 20: 37120

CHEN, P. C., Two-phase flow through apertures, 20: 36990

CHEN, Yeh-hao, Polarization of protons from the ^{12}C(d,p)^{13}C and ^{40}Ca(d,p)^{41}Ca ground-state reactions, 20: 38119

CHEN, Yung-Gann, Combination scattering of electromagnetic waves from driven space charge waves in a laboratory magnetoplasma, 20: 38202 (NP-16236)

CHENG, Wan-hui, Polarization of protons from the ^{12}C(d,p)^{13}C and ^{40}Ca(d,p)^{41}Ca ground-state reactions, 20: 38119

CHENOUARD, J., Plutonium and uranium mass spectrometry measurements on irradiated fuels, 20: 36783

CHEPURCHENKO, I. A., Reaction ^{3}He + ^{3}He, 20: 38131

CHEPURNOV, V. A., Neutron states in a deformed optical potential, 20: 38126

CHERDYNTSEV, V. V., Decay $K \rightarrow \mu + \nu$ in μ-meson beam of cosmic rays 3860 m. above sea level, 20: 37482

CHERNAVSKII, M. M., Certain aspects of nucleon isobar production in nucleons interactions at energies 10^3 and 25 Bev, 20: 37675

CHERNOV, I. P., Cross sections of elastically scattered 13.6-Mev deuterons, 20: 38128

CHERNOVA, A. I., Products formed by radiolysis of benzene in aqueous solutions of sodium nitrate, 20: 36881

CHERNYAK, A. S., Extraction of metals from aqueous solutions of hydrohalic acids by means of dialkylalkylphosphinates, 20: 36941
CHERNYSHEV, E. A., Formation of radicals during radiolysis of organic solids. III., 20: 36883
CHERRY, B. H., Selected optimization studies in the use of carbide fuel in large fast breeder reactors, 20: 38495 (ANL-7120, pp 104-23)
CHERTOPRUD, V. E., Some properties of the phase of solar activity, 20: 37385
CHERTOPRUD, V. E., Statistical properties of the optical variability of the quasistellar radio source 3C 273, 20: 37382
CHESSELET, Roger, Experimental study of dispersion of fallout nuclear debris in sea water, 20: 37037
CHEVALIER, Raymond, Magnetic structure of Er_2O_3, 20: 38357
CHEVEREV, N. S., Paramagnetic high-frequency effect and electron paramagnetic resonance in plasma, 20: 38220
CHEW, Geoffrey F., Backward π^- p scattering as a further test for Regge high-energy behavior, 20: 37742 (UCRL-16293)
CHIANG, Cheng-lieh, Polarization of protons from the $^{12}C(d,p)^{13}C$ and $^{40}Ca(d,p)^{41}Ca$ ground-state reactions, 20: 38119
CHIBA, T., Cosmic-ray rigidity spectrum during a solar rotation and solar rotation and solar wind velocity, 20: 37533
CHIKOVANI, G., Evidence for three new charged bosons of masses 1929, 2195, and 2382 Mev and narrow widths, 20: 37771
CHIKOVANI, G. E., Tskhra-Tskaro installation for study of interactions of high-energy particles of cosmic rays with matter, 20: 37684
CHILDS, W. J., Hyperfine interactions and the magnetic fields due to core polarization in ^{57}Fe, 20: 38385
CHILOSI, G., Properties of some low excited states in ^{101}Ru from the decay of 3-y ^{101}Rh, 20: 38091
CHIRKOV, N. P., First and second spherical harmonics of the daily variations of cosmic rays, 20: 37531
CHIRKOV, N. P., Investigation of cosmic-ray distribution using the method of daily variations, 20: 37587
CHIU, Hong-Yee, Neutrinos in astrophysics, 20: 37395
CHIU, Hong-Yee, Pre-supernova evolution (neutrino stars), 20: 37406
CHIU, Yam-Tsi, Absorptive modification of single particle exchange models at high energies, 20: 37862
CHIZHEVSKII, A. L., Physicochemical reactions as indicators of cosmic phenomena, 20: 37002
CHKHEIDZE, I. I., Formation of radicals during radiolysis of organic solids. III., 20: 36883
CHKHETIA, A. M., Some results of comparison of cosmic-ray intensity variations with the H component of the earth's geomagnetic field during IGY and IGC, 20: 37590
CHONE, Bruno, In vivo investigations with ^{3}H-thymidine for the study of tumor cell kinetics in punctates, 20: 36704
CHOPPIN, G. R., Proton-induced fission of ^{238}U, 20: 37995
CHOUROULINKOV, I., Thymus origin of lymphomatoses in mice after irradiation by x rays, 20: 36613
CHOW, B. S., Cosmic-ray flux variation with height in the stratosphere, 20: 37552
CHRENKA, A., Microwave detector using plasma, 20: 37119
CHRISTENSEN, A. Noerlund, Hydrothermal preparation of some rare earth oxide hydroxides, 20: 36791
CHRISTENSEN, U. R., Negative V'' stellarator, 20: 38243
CHRISTOFILOS, N., Plasma confinement properties of relativistic electron coils, 20: 38210 (UCRL-12455(Rev.1))
CHRISTOV, C., Inelastic n-p cross section at 60 Bev, 20: 37670
CHRISTY, R. F., Stellar variability, 20: 37413
CHU, Florence C. H., Clinical evaluation of the treatment of advanced head and neck cancers with high-energy electron beams, 20: 36685
CHU, T. K., Measurement of plasma transport properties in a Na–K seeded Ar plasma, 20: 38195 (INDEC-SR-7, pp 3.60-73)
CHU, T. Y., Determination of gas bearing stability by response to a step-jump, 20: 36980 (TID-23270)
CHUBB, T. A., Observations of hard x-ray emission from solar flares, 20: 37360
CHUMBALOVA, R. A., Periodic cosmic-ray variations and their change during the cycle of solar activity, 20: 37525
CHUPRUNOV, D. L., Utilization of fast charged particle inelastic scattering for analysis of composition of materials, 20: 36732
CHYSKY, J., Investigation of occupational exposures to ionizing radiation in the Czechoslovak Socialist Republic, 20: 37035
CIOCCO, Antonio, Radiation-related leukemia in Hiroshima and Nagasaki, 1946–1964. I., 20: 36645
CLARK, Don H., Travel times and amplitudes from the Salmon explosion, 20: 36967
CLARK, G. W., Electron spin resonance of rare-earth ions in CeO_2 : Yb^{3+} and Er^{3+}, 20: 38391
CLARK, J. W. G., Continuous automatic analysis of dry powders and aqueous suspensions using radioisotope techniques, 20: 37152
CLAUDEL, Bernard, Physicochemical properties of thorium formates with different degrees of hydration, 20: 36795
CLAYTON, C. G., Coal-ash monitor with low dependence on ash composition, 20: 37153
CLAYTON, C. G., Review of the design and application of radioisotope instruments in industry, 20: 37148
CLAYTON, Robert N., Oxygen-18/oxygen-16 ratios of minerals from the iron formations of Quebec, 20: 37013
CLEGG, T. B., Cross sections as a function of energy for the scattering of protons from ^{12}C, 20: 38050
CLEGG, T. B., Cross sections as a function of angle and complex phase shifts for the scattering of protons from ^{12}C, 20: 38051
CLEM, J. R., Lifetime of vortex pairs in superconductors, 20: 37944
CLEM, John R., Effects of nonmagnetic impurities upon anisotropy of the superconducting energy gap, 20: 37958
CLOOS, O., Dosimetry of ionizing radiation, 20: 37081
CLOUGH, W. R., Tensile fracture of Zr and Zr-rare earth solid-solution alloys, 20: 37231
CLOUTIER, Paul A., Comment on "the neutral hydrogen flux in the solar plasma flow" by S.-I. Akasofu, 20: 38298
COATES, R. L., RSAC: Radiological safety analysis computer program, 20: 37167 (IDO-17151)
COATS, R. B., Burst production by near horizontal cosmic-ray muons at sea level, 20: 37695
COATS, R. B., Liquid scintillation counters, 20: 37107
COBB, R., Evidence for a source of primary gamma rays, 20: 37365
COCCHI, Umberto, Irradiation of brain tumors, 20: 36694
COCCONI, G., Considerations about high-energy interactions, 20: 37786
COCCONI, V. T., Production of strange particles in 8-Bev/c π^+-proton interactions. II., 20: 37770
COCHO, G., Electric-charge form factor according to SL(6,C), 20: 37840
COETZEE, W. F., Intensity distributions of cosmic-ray components at 307 g cm^{-2} atmospheric depth in the South African magnetic anomaly, 20: 37592
COHEN, K. P., Safety and economic characteristics of 1000-Mwe fast Na-cooled reactor design, 20: 38498 (ANL-7120, pp 185-204)
COJOCARU, V., Lifetime of the μ^- in ^{239}Pu, 20: 38114
COLBURN, D. S., Discontinuities in the solar wind, 20: 37387
COLEMAN, C. E., Hydrogen embrittlement of α–Zr: a review, 20: 37187
COLEMAN, P. J. Jr., Measurements of magnetic fields in vicinity of magnetosphere and in interplanetary space, 20: 37917
COLGATE, S. A., Theoretical composition of cosmic rays of supernova origin, 20: 37498
COLGATE, Stirling A., Mechanism of type II supernova explosions, 20: 37407
COLLET, Luc-Henry, Observation of a cyclotron resonance harmonic in hydrogen plasma, 20: 38224
COLLING, D. A., High-field superconductivity of Ta–Ti alloys, 20: 37268
COLLINS, J. O., Prog. rpt. on 1800–400F fibrous type insulation for radioisotope power systems, 3–6/66, 20: 36983 (ALO-3633-1)
COLOMBINI, C., Intralymphatic isotope therapy with a new radioactive phosphate compound (^{32}P) in fat soluble radiopaque contrast media, 20: 36684
COLVER, C. Phillip, Nucleate and film boiling heat transfer to nitrogen and methane at elevated pressures and large temperature differences, 20: 36993
COLWELL, J. H., Magnetization and critical fields of superconducting $SrTiO_3$, 20: 37953
COMANICIU, N., Nuclear magnetic moments of ^{137}Ba and ^{135}Ba, 20: 37463
COMBES, Lewis S., Magnetic field design with an electrolytic tank analog, 20: 38189 (AD-636095)
COMSTOCK, Craig, Transmission and reflection of electromagnetic waves normally incident on a warm plasma, 20: 38276
COMSTOCK, G. M., Abundances and energy spectra for nuclei of galactic origin above 20 Mev per nucleon, 20: 37564
CONJEAUD, M., Reactions (^{3}He,d) on even Sn isotopes, 20: 38073
CONSTANTINESCU, M., Paramagnetic centers formed by irradiation of oxygenated compounds of Se. II., 20: 38398
CONSTANTINESCU, O., Paramagnetic centers formed by irradiation of oxygenated compounds of Se. II., 20: 38398
COOPER, J. W., Electron-impact excitation of n = 2 states in He, 20: 37453
COOPER, L. N., Attenuation of longitudinal acoustic waves in type-II superconductors, 20: 37948
COPPI, B., Drift instability due to impurity ions, 20: 38296
CORELLI, J. C., Production and annealing of defects in 6- to 80-Mev electron-irradiated n-type Ge, 20: 38365
CORLEY, D. M., Elastic scattering of 1 Bev protons from He and O, 20: 38010 (BNL-10438)
CORNISH, S. D., Gemini carbon dioxide sensor, 20: 37064
CORNMAN, W. R., Advantages of ^{60}Co for heat and radiation sources, 20: 37165
CORNWELL, R. G., Nuclear spin and moments of ^{45}Ti, 20: 38089
CORRY, P. M., Simple magnetic tape recording system for medical scintiscanners, 20: 37083

CORTELLESSA, Giorgio, (e,e'p) reaction in the ^{32}S nucleus, 20: 38016
COSMAN, E. R., Low-lying isobaric analog states of ^{89}Sr, 20: 38076
COSTA, Mariagrazia, Behavior of T% in the naphthalene test during a magnetic storm, 20: 37890
COSTA, Mariagrazia, First results on the relations between the naphthalene test and the lunar phases, 20: 37891
COSTA, Mariagrazia, Solidification of naphthalene and natural electromagnetic fields, 20: 37889
COUCHAT, P., Grain moisture measurements with neutrons: application to the problems of conditioning and storage, 20: 37154
COURTIER, G. M., Measurement of the primary cosmic-ray H and He nuclei at Kiruna, Sweden, 20: 37562
COURTNEY, John C., Fast neutron scattering from small cylinders of steel, Al, and graphite, 20: 38007
COURVILLE, C., Diffusion and instabilities in "Q" machine plasmas, 20: 38324
COWAN, C., Muon decays from neutral primaries, 20: 37713
COWAN, C. L., Calculated physics parameters and their uncertainties in a 1000-Mw(e) fast ceramic reactor, 20: 38491 (ANL-7120, pp 24-32)
COWAN, E. W., Stereoscopic viewer for measuring positions and angles in three dimensions, 20: 37052
COWDEN, R. R., Quantitative cytophotometric studies of nuclear protein in Vicia faba following acute irradiation, 20: 36588
COWLEY, J. M., Irradiation effects in beryllia and zinc oxide, 20: 37281
COWSIK, R., High-energy nuclear-active and muonic components in extensive air showers, 20: 37613
COX, Arthur N., Radiative absorption and opacity calculations, 20: 37393
COX, J. P., Excitation and growth of radial pulsations, 20: 37412
COX, James L. Jr., Electron beams from a duoplasmatron using a hollow cathode arc as electron source, 20: 37045
CRAGLE, R. G., Effect of feeding thiocyanate to dairy cows on absorption and clearance of intramammary iodine, 20: 36563
CRAIG, Douglas K., Investigation of the interactions that occur between I_2 radionuclides and an iron oxide aerosol in the respirable size range, 20: 36918
CRAIG, G. B., Etching dislocations in zirconium, 20: 37227
CRAIG, G. B., Redistribution of oxygen and iron during zone refining of zirconium, 20: 37177
CRAIG, R. M., Polarization in the elastic scattering of 49-Mev protons by Ca, ^{58}Ni, ^{60}Ni, and ^{208}Pb, 20: 38049
CRANDALL, G. J., Preliminary hydraulic analysis of conceptual FFTF cermet driver fuel element design, 20: 38479 (BNWL-264)
CRANE, H. R., Direct measurement of the g factor of the free positron, 20: 37775
CRAVAROLO, L., Liquid volume fraction in adiabatic two-phase vertical upflow-round conduit, 20: 36985 (EURAEC-1088)
CRAWFORD, D. F., Studies of the cores of extensive air showers, 20: 37616
CRAWFORD, D. L., Photometry of B stars, 20: 37418
CREED, D. R., Intensity and angular distribution of cosmic rays far underground, 20: 37704
CREED, D. R., Muon interactions far underground, 20: 37701
CRENNELL, David J., $\pi\pi$ resonances from 6 Bev/c π^-p interaction, 20: 37731 (BNL-10460)
CRENNELL, David J., Properties of K* (1425), 20: 37733 (BNL-10462)
CRENNELL, David J., Resonance production in the reactions $\pi^\pm p \rightarrow KKN$ at 6 Bev/c, 20: 37732 (BNL-10461)
CRICHTON, James Hamilton, Cluster structure of the S matrix, 20: 37861
CRISPIN, A., Development of scintillation counters based on medicinal paraffin, 20: 37112
CROOKS, R. N., Radium, radon, and daughter products in drinking waters in Great Britain, 20: 37031
CROSBIE, K. L., Hazards summary for the accelerator pulsed fast assembly, 20: 38530 (GA-6078)
CROSSLAND, A. D., High-energy single-meson production, 20: 37692
CROWNFIELD, Frederic R. Jr., Coupling of degenerate modes of a microwave cavity due to the presence of a magnetized plasma, 20: 38332
CUEER, P., Heavy cosmic ions recorded in nuclear emulsions exposed in a polar satellite, 20: 37577
CUFF, D. R. A., Examination of surfaces by scanning with charged particles, 20: 38376
CUMMINGS, A. J., High-voltage pulse characteristics of superconducting transmission lines, 20: 37939
CUPAK, Miloslav, Application of propene as basic counting gas in proportional counters, 20: 37092
CURTICE, Vondo, Clinical studies in laser photocoagulation, 20: 36682
CURTIS, S. B., Hazard from highly ionizing radiation in space, 20: 36627
CUSHING, W. R., CUSH: program for steady-state hydraulic analysis of steam-generating reactor systems, 20: 38410 (AEEW-M-474)
CZERNECKI, A., Ionization gas analyzer, 20: 36768
CZERWIK, Z., Temperature effects in x-ray radiolysis of frozen Fricke solutions, 20: 36867
CZYZEWSKI, O., Production of strange particles in 8-Bev/c π^+-proton interactions. II., 20: 37770

D

DAGLISH, J. C., Coal-ash monitor with low dependence on ash composition, 20: 37153
DAHL, Per F., Proton-proton scattering: revision and analysis of experimental measurements from 1.4 to 3.0 Mev, 20: 38081
DAHLBERG, E. P., Some effects of prestrain at 77°K on the mechanical properties of Zr at room temperature, 20: 37228
DALEAS, R. S., Conceptual design and preliminary accident analysis of a Na-cooled, carbide-fueled, large modular fast reactor, 20: 38456 (ANL-7120, pp 205-29)
DALEAS, R. S., Transient response of coupled fast reactor cores, 20: 38436 (ANL-7120, pp 776-88)
DALEBROUX, Marc Augustin, Genetic variability induced by ionizing radiations in quantitative traits of Habrobracon, 20: 36659
DAMBURG, R. Ya., Atomic collisions, 20: 37477
DAMGAARD, G., Search for heavy particles in the cosmic radiation, 20: 37654
DAMLE, S. V., Flux of primary protons and helium nuclei and east-west and north-south asymmetries near the geomagnetic equator, 20: 37582
DAMLE, S. V., Use of a gas Cherenkov counter for the study of the isotopic composition of He nuclei in primary cosmic radiation, 20: 37581
DAMM, J. Z., Dichroism in R-bands induced in γ-irradiated potassium chloride crystals, 20: 36905
DANDL, R. A., Observations of instabilities in electron-cyclotron plasmas, 20: 38274
D'ANGELO, N., Propagation and damping of ion waves in a plasma with negative ions, 20: 38283
DANIEL, M. R., Antiferromagnetic resonance in UO_2, 20: 38383
DANIEL, R. R., Energy spectrum of primary He nuclei at energies greater than 6 Bev, 20: 37557
DANIEL, R. R., Fast neutrons of solar origin, 20: 37375
DANIELS, J., Nature of plasma losses at 3.6 ev in thin silver foils, 20: 38400
DANILOV, V. I., Increasing the internal beam current of the JINR synchrocyclotron by additional electrostatic focusing, 20: 37328
DANILOVA, T. V., Low energy nuclear active particles in EAS, 20: 37614
DANOS, M., 3^- continuum states of ^{16}O in the eigenchannel reaction theory, 20: 38102
DA PROVIDENCIA, J., Variational approach to the nuclear collective motion, 20: 38108
DARBINYAN, S. M., Intermediate boson production in reaction $e^- + e^+ \rightarrow W^+ + \mu^- + \bar{\nu}_\mu^\mu$, 20: 37799
DA ROCHA, A. F. G., Study of the distribution of dose in radiotherapy with the aid of electronic computers, 20: 36686
DARRAS, Raymond, Oxidation mechanism of Zr–Cu alloys in CO, 20: 37183
DARUSCHY, P., Studies about the analysis of tritium-containing steam in air, 20: 37028
DAS GUPTA, B., Note on the calculation of the dielectric function for a homogeneous plasma, 20: 38297
DAS GUPTA, P., Note on the calculation of the dielectric function for a homogeneous plasma, 20: 38297
DAUJAT, Pierre, Frequency modulation of uhf signals in electron linear accelerator, 20: 37319 (CEA-R-2976)
DAUM, C., Measurement and analysis of muonic x-ray spectra in spherical nuclei, 20: 38058
DAUTREPPE, D., Interpretation of stage I in Ni irradiated by electrons, 20: 37297
DAVID, W. E., Angular correlations of $^{28}Si(d,p\gamma)^{29}Si$ from 4 to 6 Mev, 20: 38086
DAVIDENKO, N. K., Stability of cationic complexes of rare earth elements with tartaric and trihydroxyglutaric acids, 20: 36838
DAVIDSON, J. P., Electric monopole nuclear strength parameters and the identification of beta bands in even nuclei, 20: 38180
DAVIDSON, Ronald, Higher-order corrections to the Chew-Goldberger-Low theory, 20: 38271
DAVIES, D., Effect of neutron flux on fission product gas emission from UO_2, 20: 38464 (AERE-M-1607)
DAVIES, P. G., Electrical properties of a spherical plasma probe near the plasma frequency, 20: 38299
DAVIES, R. D., Magnetic fields in the galaxy as deduced from radio measurements, 20: 37368
DAVIS, Burtron Hamilton, Preparation and adsorptive properties of thorium oxide, 20: 36843
DAVIS, E. J., Prog. rpt. on 1800–400F fibrous-type insulation for radioisotope power systems, 3–6/66, 20: 36983 (ALO-3633-1)
DAVIS, Leverett Jr., Measurements of magnetic fields in vicinity of magnetosphere and in interplanetary space, 20: 37917
DAVIS, Monte V., Derivation of an expression for radiation-induced electrical conductivity in ionic insulators, 20: 38353 (BNWL-SA-247)
DAVIS, Raymond Jr., Problem of detecting solar neutrinos, 20: 37491

DAVTYAN, I. A., Effect of europium oxide admixtures on the polymorphism of zirconium dioxide, 20: 36815
DAVYDOV, A. S., Electric quadrupole transitions in deformable even-even nuclei, 20: 38127
DAVYDOV, A. S., Quantum mechanics, 20: 37933
DAWSON, John M., Derivations of hierarchies for N particle systems and Vlasov systems, 20: 38209 (PPL-AF-5)
DAWSON, K. B., Isotope dilution method for determining amounts and activities of proline and hydroxyproline in tissues, 20: 36562
DAWSON, R. K., Report of fire resistance tests fuel core shipping container No. 1, 20: 37024 (NLCO-899)
DAY, Walter C., Cloud development studies, Project Pre-Schooner II, 20: 36958 (PNE-511)
DEAN, R. Y., Recovery of aluminum nitrate nonahydrate from redox acid waste, 20: 36925 (HW-82771(Pt.3))
de Carvalho, R. Guedes
see Guedes de Carvalho, R.
DECKER, John A. Jr., Low-frequency instability in cesium discharge and thermal plasmas, 20: 38319
DE COEN, J. L., Theory of the specific heat of liquid ^{4}He above the λ point, 20: 37968
DEDENKO, L. G., Nuclear cascade process in the ionization calorimeter, 20: 37789
DE GRAAF, L. A., Inelastic neutron scattering by solid and liquid cyclohexane, 20: 38005
DEGRANGE, B., Direct search for the C-violating decay $\eta^0 \rightarrow \pi^0 e^+ e^-$, 20: 37767
DE LA CRUZ, V., Null coordinates for spherically symmetric gravitational collapse, 20: 37921
DE LAMOTTE, E., Effect of zirconium on the thermodynamic and mechanical properties of niobium–nitrogen alloys, 20: 37274
DELANEY, R. M., Flame-temperature measurement by thermal neutron probe, 20: 37310
DELCHEV, M., Double-pulse ionization chamber for correlation measurements of the energy, angle, and mass distributions in the fission of heavy nuclei, 20: 37089
DELCHEV, M., High-energy photoprotons of the reaction ^{40}Ca(γ,p)^{39}K at 28 and 60 Mev, 20: 38024
DELLWEG, H., Enzymatic degradation of uv-irradiated DNA, 20: 36596
DEMAILLE, A., Effect of ionizing radiations on the HeLa cell. II., 20: 36616
DEMARQUE, Pierre, Evolution of stars near one solar mass, 20: 37401
DEMIDENKO, I. I., Mechanism of capture of a moving plasma by a transverse magnetic field, 20: 38249
DEMIDOVICH, V. N., Ionization-mechanical detector for ionizing particles, 20: 37080
DEMKOV, Yu. N., Structure of S matrix for quantum problems, 20: 37854
DEMPSTER, R. T., SWIFT dryout data for 19-rod bundle cooled by steam/water fog, 20: 38409
DENIELOU, G., Contribution to safety problems related to 1000-Mwe fast power reactor project, 20: 38497 (ANL-7120, pp 157-61)
DENIELOU, G., Program proposed for safety studies of fast neutron project of EURATOM-CEA association, 20: 38492 (ANL-7120, pp 54-66)
DENISOV, E. V., Nuclear cascade process in the ionization calorimeter, 20: 37789
DENISOV, E. V., Tein-Shan high-altitude installations for studying strong interactions at 100 to 1000 Bev (preliminary results), 20: 37656
DENISOV, Yu. V., Structure of glasses of the Na_2O–B_2O_3 system activated with rare earths. Europium, 20: 36813
DENT, K. H., Advanced gas-cooled reactor power stations, 20: 38514
DE PANGHER, J., Precision long counter for measuring fast neutron flux density, 20: 37069 (BNWL-260)
DEPOITIER, J., Prog. rpt. on ESSOR fuel elements, final, 1–11/62, 20: 38480 (EUR-2522.f)
DE PROOST, M., Radiation sensitizers in the preservation for sterilization of food, drugs, and medical supplies, 20: 37144
DERIBON, V. F., Stability of cationic complexes of rare earth elements with tartaric and trihydroxyglutaric acids, 20: 36838
DERMENDZHIEV, E., Double-pulse ionization chamber for correlation measurements of the energy, angle, and mass distributions in the fission of heavy nuclei, 20: 37089
DE RUYTER, A. W., Specific gamma emission of natural K and La, 20: 38107
DESPAIN, L. G., Ionization chamber, 20: 37124
DETAVERNIER, W., Prog. rpt. on ESSOR fuel elements, final, 1–11/62, 20: 38480 (EUR-2522.f)
DEUTSCH, Armin J., Mass loss from red giants, 20: 37415
DEUTSCH, J. P., Spin measurement and isospin impurity of the ^{64}Ga ground state, 20: 38065
DEVISHEV, M. I., Inelastic neutron cross section measurements near 100 Bev, 20: 37668
DEVOE, J. R., Moessbauer spectrometer for the structural analysis of materials, 20: 37056
DE WAMES, R. E., Anomalous particle penetration in perfect crystals, 20: 38387
DE WIRE, J. W., Scattering of positrons and electrons from protons, 20: 37778
DE WIT, S. A., Measurement and analysis of muonic x-ray spectra in spherical nuclei, 20: 38058
DEXTER, A. H., Advantages of ^{60}Co for heat and radiation sources, 20: 37165
DEYNEGA, N., Device for estimating nuclear-explosion yield, 20: 37061
DEYRIS, Michele, Determination of O in Al and Zr by irradiation with ^{3}He ions, 20: 36741
DEZSI, Zoltan, Determination of isodose curves, 20: 36688
DIAMOND, R. M., Isomeric state (8–) in ^{180}W, ^{182}Os, and ^{184}Pt, 20: 38027
DIANA, Massimo, Thermodynamic considerations on the Saha equation, 20: 38222
DIAZ NOGUEIRA, E., Distribution coefficients of Pu(IV) during extraction with TBP, 20: 36928
DICKE, R. H., Stellar evolution with varying G, 20: 37410
DICKERMAN, C. E., Status of recent meltdown studies, 20: 38474 (ANL-7120, pp 534-9)
DIETL, H., Scattering of gamma rays and neutrons to investigate underground aquifers, 20: 37135
DIETZSCH, O., Reaction ^{13}C(p,n)^{13}N near threshold, 20: 38042
DIKE, R. S., Scyllacita: compact high-voltage theta pinch machine, 20: 38306
DIKE, R. S., Straight θ-pinch devices energized by energy storage supply of Scyllac, 20: 38197 (LA-3553)
DILLINGER, J. R., Isotope effect in superconducting zinc, 20: 37959
DILWORTH, C., Flux and east-west asymmetry of primary electrons at a geomagnetic rigidity cut-off of about 4.5 GV, 20: 37550
DISS, Carol, Effect of irradiated medium on the growth of L5178Y lymphoma cells, 20: 36633
DIVARI, N. B., Charged dust particles in interplanetary space, 20: 37913
DOBROTIN, N. A., Tein-Shan high-altitude installations for studying strong interactions at 100 to 1000 Bev (preliminary results), 20: 37656
DOBROVOLSKII, A. G., Slip casting of zirconium boride, 20: 37201
DOBROVOLSKII, G. G., Slip casting of zirconium boride, 20: 37201
DODSON, Helen W., Related flares, 20: 37347
DOERING, Paul, Results of ^{131}I-triiodothyronine test with ion exchange resin, 20: 36573
DOHERTY, P. D., Flame-temperature measurement by thermal neutron probe, 20: 37310
DOKUKINA, N. V., Heat resistance of alloys on base of W and Nb silicides, 20: 37262
DOLAN, K. W., Energy levels of ^{56}Fe, 20: 38088
DOLE, Malcolm, Ultraviolet spectroscopy of irradiated polyethylene. II., 20: 36857 (COO-1088-21)
DOLMATOV, S. A., Kinetics of radiation-induced allyl polymerization. II., 20: 36880
DOLNICK, E. M., Scyllacita: compact high-voltage theta pinch machine, 20: 38306
DOMOGATSKII, G. V., Cross section of the reaction $\nu + {}^{37}Cl \rightarrow {}^{37}Ar + e^-$, 20: 38111
DOMOGATSKII, G. V., Experimental possibilities of the observation of neutrinos from collapsing stars, 20: 37379
DOMOGATSKII, G. V., Solar neutrino interaction with electrons, 20: 37792
DOMOGATSKII, G. V., Solar neutrino detection by the registration of electrons in reactions $\nu + Z \rightarrow (Z+1) + e^-$, 20: 37793
DONALD, R. A., Pion-nucleon scattering at 35 and 39 Mev, 20: 37785
DONNELLY, R. J., Pressure dependence of the radius of the negative ion in He II, 20: 37960
DORE, J. C., Polarization in the elastic scattering of 49-Mev protons by Ca, ^{58}Ni, ^{60}Ni, and ^{208}Pb, 20: 38049
DORMAN, I. V., 11-year cosmic-ray variations, 20: 37497
DORMAN, L. I., Asymmetric solar wind in connection with the 27-day modulation of the intensity and anisotropy of cosmic rays, 20: 37528
DORMAN, L. I., Frequency distribution of sudden changes of cosmic-ray intensity in connection with solar activity, 20: 37541
DORMAN, L. I., Galactic and solar cosmic rays in interplanetary space, 20: 37542
DORMAN, L. I., Influence of the changes in Earth's heliolatitude on the cosmic-ray intensity in 1963-1964, 20: 37529
DORMAN, L. I., Possibilities of isolation of sidereal time cosmic-ray intensity variations, 20: 37506
DORMAN, L. I., Problems of methods of investigation of cosmic-ray variations, 20: 37589
DORMAN, L. I., Some results of comparison of cosmic-ray intensity variations with the H component of the earth's geomagnetic field during IGY and IGC, 20: 37590
DORMAN, L. I., 11-year cosmic-ray variations, 20: 37497
DORNAN, P. J., f* meson produced in K⁻p interaction 4.6 and 5.0 Bev/c, 20: 37730 (BNL-10459)

DOROFEEV, G. A., Application of the similarity method to radiation fields during adjustment of neutron radiation meters, 20: 37074 (NP-16202)
DOROFEEV, G. A., Calibration of thermal-neutron radiation meters in diffuse flow, 20: 37073 (NP-16201)
DOROFEEV, G. A., Problem of utilizing nuclear D(d,n)^{3}He and T(d,n)^{4}He reactions for calibration of fast-neutron radiation meters, 20: 37075 (NP-16204)
DOROSHKEVICH, A. G., Variation of the moment of inertia of a star during accretion, 20: 37384
DOSDAT, Jean, Inhibition of growth of recrystallization grain and hardening of Mg–Zr alloys. I., 20: 37252
DOTE, Toshihiko, Some problems in use of Langmuir probe on ionospheric sounding rockets, 20: 38309
DRAGANESCU, V., Nuclear magnetic moments of ^{137}Ba and ^{135}Ba, 20: 37463
DRAGNEV, T., Double-pulse ionization chamber for correlation measurements of the energy, angle, and mass distributions in the fission of heavy nuclei, 20: 37089
DRAGNEV, T., High-energy photoprotons of the reaction ^{40}Ca(γ,p)^{39}K at 28 and 60 Mev, 20: 38024
DRAGOUN, Otakar, Measurements of nondestructive fuel burnup by means of γ spectroscopy of fission products, 20: 37287
DRAKE, G. A., Retention of ^{54}Mn by four mammalian species, 20: 36554 (LA-DC-7305)
DRAKE, John W., Ultraviolet mutagenesis in bacteriophage T4. II., 20: 36636
DREVON, G. A. V., Comparison of pressure loading produced by contained explosions in water and sodium, 20: 38459 (ANL-7120, pp 720-33)
DREYER, Howard S., Emanation of xenon and krypton from oxide fuels during reactor operation, 20: 37303
DRIESSENS, J., Effect of ionizing radiations on the HeLa cell. II., 20: 36616
DRIVER, Harry Stephen Thackwray, Magnetohydrodynamic experiments in an electromagnetic shock tube, 20: 37882
DROST, H., Uhf plasma oscillations in Hg low-pressure discharge. I., 20: 38214
DROST, H., Uhf plasma oscillations in Hg low-pressure discharge. II., 20: 38215
DROST, H., Uhf plasma oscillations in Hg low-pressure discharge. III., 20: 38216
DRUYVESTEYN, W. F., Flux flow in type-II superconductors with different field orientations, 20: 37942
DRUYVESTEYN, W. F., Resistive behavior of a type-II superconductor on reversing the current, 20: 37945
DUBAL, L., Evidence for three new charged bosons of masses 1929, 2195, and 2382 Mev and narrow widths, 20: 37771
DUBROVINA, S. A., Nuclear cascade process in the ionization calorimeter, 20: 37789
DUBROVINA, S. A., Tein-Shan high-altitude installations for studying strong interactions at 100 to 1000 Bev (preliminary results), 20: 37656
DUCROS, G., Gamma-ray generation in the high atmosphere, 20: 37576
DUDNIK, E. M., Production and properties of W–LaB_6, 20: 37258
DUFRESNE, R., Comparative response of Cherenkov and scintillator detectors to large air showers, 20: 37621
DUFTSCHMID, K. E., Digital methods in thickness gaging, 20: 37058
DUGGAL, S. P., Solar cycle modulation of cosmic rays, 20: 37509
DULYAN, G. G., Interaction path of high-energy nucleons (10^{11} to 10^{13} ev) in the atmosphere, 20: 37667
DUMITRESCU, R., Level density parameter determination from (α,n) reactions on ^{27}Al, ^{55}Mn, ^{56}Fe, and Ag, 20: 38115
DUNJIC, A., Current intensity and flux of x rays, 20: 37091
DUNN, Donald, Computer experiments in plasma physics, 20: 38310
DUNNETT, D. A., Stochastic motion of particles in a non-adiabatic magnetic trap, 20: 38246
DUNNILL, William Arthur, Ion beam-plasma interactions, 20: 38346
DUPONT, A., Effect of ionizing radiations on the HeLa cell. II., 20: 36616
DUPOUY, J.-M., Diffusion of iron and silver in beryllium, 20: 37250
DUPOUY, J.-M., Self-diffusion of beryllium, 20: 37249
DUPP, Guenter, Sputtering of Cu by noble gas ions in the energy range 100 kev to 1 Mev as a function of the incident angle, 20: 37468
DURGAPRASAD, N., Balloon observations of cosmic rays, 1961–1964, 20: 37560
DUTHIE, J. G., Evidence for a source of primary gamma rays, 20: 37365
DUTREIX, A., Secondary standards in dosimetry, 20: 37090
DUTREIX, J., Secondary standards in dosimetry, 20: 37090
DUTT, J. C., Forbush decreases and the 27-day recurrence tendency in the cosmic-ray intensity at a depth of 60 m.w.e. underground in London, 20: 37535
DUTT, J. C., Solar and sidereal daily variations of cosmic-ray intensity at a depth of 60 m.w.e. underground in London, 20: 37504
DVORINA, L. A., Preparation of rare earth silicides, 20: 37176
DWORIN, Lowell, Transport properties of an electron gas in a magnetic field. I., 20: 37866
DYE, D. L., Hazard from highly ionizing radiation in space, 20: 36627
DYKE, W. P., Electron accelerator with a peak beam power of 10^{10} watts, 20: 37339
DYRING, E., Daily latitude curves of cosmic-ray nucleonic component obtained in 1963 between 1 and 6.4 Gv, 20: 37584
DYRING, E., Multiplicity effect in an IGY neutron monitor, 20: 37098
DZHIBUTI, R. I., Identification of energy levels in light nuclei according to disintegration cross sections, 20: 38138
DZHURINSKII, B. F., Structure of glasses of the Na_2O–B_2O_3 system activated with rare earths. Europium, 20: 36813

E

EASTLUND, B. J., Drift wave excited anomalous diffusion in a fully ionized magnetoplasma, 20: 38203 (NP-16237)
EASTON, J. F., Gas scintillation, 20: 37127
EBERT, D. D., Cost estimate for remote refabrication of metallic fuels, 20: 37195 (ANL-6950)
EDEN, R. J., Lectures on high energy scattering, fall semester, 1965-66, 20: 37826 (NP-16231)
EDGECUMBE, J., CaI as a high-gain secondary emission material, 20: 37046
EDISON, G. E., Mechanical properties of cold-worked and neutron-irradiated iron, 20: 37304
EDWARDS, D. O., Thermal and magnetic properties of dilute solutions of ^{3}He in ^{4}He at low temperatures, 20: 37961
EFIMOV, V. A., Critical water boiling in a rod-bundle model, 20: 36992
EFRYUSHINA, N. P., Complexes of Nd, Ho, and Er with pyrogallosulfonic acid, 20: 36837
EGGEN, D., Enhanced safety characteristics of a sodium-cooled coupled reactor, 20: 38437 (ANL-7120, pp 789-93)
EGGEN, Olin J., Stellar groups and the mass-luminosity relation, 20: 37427
EHRENBERG, L., Effects of diethyl pyrocarbonate on barley seeds, 20: 36589
EHRENBERG, L., Synthesis of some tritium-labeled mutagenic alkyl alkanesulfonates, 20: 36916
EHRMAN, J. B., Analytical determination of the eigenfrequencies of a bounded, one-dimensional electron plasma, 20: 38245
EICHHORN, Hans-Juergen, Frequency of radiofibroses in sound lung tissue after intensive radiotherapy of bronchial carcinomas, 20: 36703
EIFE, K., Use of neutron-induced gamma-radiation spectrometry to investigate the elemental composition of rocks in boreholes, 20: 37018
EISENBEISS, G., Parameters of the Regge pole model for πN charge-exchange scattering, 20: 37761
EISENBERG, E., Israel food irradiation program and progress during 1964–1966, 20: 37155
EISENBERG, J. M., Radiative pion absorption in complex nuclei, 20: 38064
EISENBERG, Y. Decay correlations of photo-produced rho mesons in the strong-absorption model, 20: 37768
EISENBERG, Y., Rho meson photoproduction cross sections in the strong-absorption model, 20: 37766
EISMONT, V. P., Fission of ^{226}Ra by 12-Mev deuterons, 20: 38132
EISSA, N., Design and theory of magnetic spectrometer for measurement of cosmic-ray mesons, 20: 37487
EL-FARRASH, A. H., Decay scheme of 5.0-d ^{183}Ta, 20: 38104
ELINGS, V. B., New test of SU(3) in meson photoproduction, 20: 37773
ELISEEV, S. M., Intranuclear cascades at ultra-high energies, 20: 38122
ELISEEV, S. M., Statistical analysis of the interaction of 17 Bev mesons with photoemulsion heavy nuclei, 20: 38060
ELITZUR, M., Spin-2^{+} meson decays in the quark model, 20: 37780
ELLIS, J. R., Spinor approach to quaternion methods in relativity, 20: 37924
ELLS, C. E., Effect of heat treatment on texture of fabricated Zr-rich alloys, 20: 37198
EL-MOFTY, D. O., Design and theory of magnetic spectrometer for measurement of cosmic-ray mesons, 20: 37487
EL MOHANDIS, M. G. S., Magnetohydrodynamic disturbances due to the sudden introduction of an oscillating dipole in a fluid of finite conductivity, 20: 37875
EL-NESR, M. S., Decay scheme of 5.0-d ^{183}Ta, 20: 38104
ELROD, H. G. Jr., Determination of gas bearing stability by response to a step-jump, 20: 36980 (TID-23270)
EL'SHUNI, K. A., Influence of partial reparation of the damaging effect of irradiation on the frequency of chlorophyll mutations in barley, 20: 36622
EL'SHUNI, K. A., Mutations in spring wheat Lutescens 62 treated with fast neutrons and gamma rays, 20: 36620
ELTON, R. C., Vacuum ultraviolet radiation from plasmas, 20: 38335
EMELYANOV, Yu. A., Electromagnetic cascades in iron and lead at 100 Bev, 20: 37698

EMERY, V. J., Theory of dilute mixtures of ^{3}He in liquid ^{4}He at low temperatures, 20: 37946
ENCHEVICH, I. B., Increasing the internal beam current of the JINR synchrocyclotron by additional electrostatic focusing, 20: 37328
ENDRES, G. W. R., Personnel neutron dosimeter developments, 20: 37070 (BNWL-SA-537)
ENDT, P. M., High-resolution investigation of the $^{30}Si(p,p)^{30}Si$ reaction, 20: 38105
ENGE, H. A., Low-lying isobaric analog states of ^{89}Sr, 20: 38076
ENGELBRECHT, C. A., Parameters governing the response of the nuclear soil density gage, 20: 37020
ENGELDER, T. C., Accuracy of power reactor void coefficients extrapolated from measurements in critical assemblies, 20: 38425 (ANL-7120, pp 585-97)
ENGELMANN, R. J., Snow and rain washout coefficients for process plant radioiodine vapor, 20: 37033
ENGELSBURG, Stanley, Single-particle coupling to collective excitations; sound in ^{3}He, 20: 37449
ENGIBARYAN, V. A., Transitional radiation during oblique incidence on film, 20: 37434
ENGLEMANN, J., Use of semiconductor telescopes in charge and energy spectrometry of cosmic particles, 20: 37575
ENOMOTO, S., X-ray spectroanalysis using a ^{147}Pm beta source, 20: 36765
ENSELMOZ, J. R., Axial stability calculations for A.G.R. systems, 20: 38446 (TRG-Report-1138)
EPSTEIN, John H., Affinity of melanin for chloroquine, 20: 36564
ERAMZHYAN, R. A., Cross section of the reaction $\nu + {}^{37}Cl \rightarrow {}^{37}Ar + e^-$, 20: 38111
ERAMZHYAN, R. A., Solar neutrino detection by the registration of electrons in reactions $\nu + Z \rightarrow (Z+1) + e^-$, 20: 37793
ERICKSON, Glen W., Radiative level shifts. III., 20: 37445
ERLYKIN, A. D., Energy losses of relativistic muons in electromagnetic interactions, 20: 37707
ERLYKIN, A. D., Installation for study of EAS and nuclear interactions of cosmic-ray particles with energies 10^{12} to 10^{16} ev, 20: 37634
ERMAKOV, S. V., Thermoelectron emission from uranium dodecaboride, 20: 37723
ERNST, B. M., Influence of $\pi\pi$ interactions on structure of the nucleon, 20: 37801
EROFEEVA, I. N., Distribution of the energy portion transferred to π^0 mesons, 20: 37660
EROFEEVA, I. N., Four-momentum transferred in high-energy interactions, 20: 37659
EROFEEVA, I. N., Relationship of neutral and charged particles among nuclear-active particles with energies above 100 Bev at mountain altitude, 20: 37685
EROSOV, Yu. I., Production and properties of W–LaB_6, 20: 37258
ERSHKOVICH, A. I., Hypothesis of origin and formation of radiation belts as a result of particle drift into the depth of the magnetosphere, 20: 37909
ERSKINE, James C. Jr., Electron momentum distribution in Si and Ge by positron annihilation, 20: 37736 (COO-1297-7)
ESCOBAR, V. I., Solar daily variation recorded at a low-latitude station by east and west pointing telescopes during periods of maximum and minimum solar activity, 20: 37373
ESTEVE, D., Behavior of MOS structures in the case of an induced ionization, 20: 37130
ESTRADA, J., Distribution coefficients of Pu(IV) during extraction with TBP, 20: 36928
ESTULIN, I. V., Low energy levels of ^{108}Ag, 20: 38135
ESWARAN, M. A., Proton gamma angular correlation measurements in the reaction $^{26}Mg(d,p\gamma)^{27}Mg$, 20: 38187
ETTINGER, H. J., Characteristics of the aerosol produced from burning plutonium, 20: 37022 (LA-DC-6942)
EUBANKS, A. G., Electron densitometer for irradiation studies in electron microscope, 20: 37116
EUTHYMIOU, P. C., Effect of neutron and γ irradiation carrier lifetime and detectivity of InSb, 20: 37295
EVANS, Albert E., Anticoincidence shielded gamma-ray spectrometer for nuclear reaction studies, 20: 37115
EVANS, D. E., Co-operative scattering of laser light by a thetatron plasma, 20: 38259
EVANS, H. J., Perturbations in x-ray dose response in vitro with time after plating, 20: 36664
EVLANOV, E. N., Increasing plasma density in Ogra-I, 20: 38248
EWART, Alan, Energetics of the $^{27}Al(^{11}B,p3n)^{34m}Cl$ reaction from recoil studies, 20: 38084
EZER, D., Contraction phase of solar evolution, 20: 37397
EZOP, J. J., Design and applications of β-excited x-ray sources, 20: 36915 (N-66-17678)

F

FAESSLER, Amand, Eigenfunctions for a spherical and a deformed Saxon-Woods potential, 20: 38078
FAESSLER, Amand, E1 $\Delta K = 0$ transitions in deformed odd-mass nuclei, 20: 38040
FAESSLER, Amand, E2 surface resonances in spherical nuclei, 20: 38039
FAESSLER, Amand, Influence of pairing correlations and Coriolis force on transitions in deformed odd-mass nuclei, 20: 38041
FALGAYRETTES, M., Program proposed for safety studies of fast neutron project of EURATOM-CEA association, 20: 38492 (ANL-7120, pp 54-66)
FALGAYRETTES, M. F. G., Comparison of pressure loading produced by contained explosions in water and sodium, 20: 38459 (ANL-7120, pp 720-33)
FALK, Willie Robert, Annihilation of positrons in gases, 20: 37810
FALLER, A. M., Diurnal variation during the past solar cycle, 20: 37527
FALLIEROS, S., Shell-model description of nuclear analog states, 20: 38025
FALOMKIN, I. V., Capture of pions by ^{3}He. II., 20: 38011 (JINR-P-2805)
FAN, C. Y., Abundances and energy spectra for nuclei of galactic origin above 20 Mev per nucleon, 20: 37564
FAN, C. Y., Acceleration of particles in the Earth's shock transition region and beyond, 20: 37900
FAN, C. Y., Protons and He nuclei within interplanetary magnetic regions which co-rotate with the Sun, 20: 37371
FAN, C. Y., Solar modulation of the galactic He spectrum above 30 Mev per nucleon, 20: 37563
FARMAKOVSKII, V. V., Cross-section averaging in thermal region for media containing zirconium hydride, 20: 37991
FARR, Richard S., Interaction with ^{131}I-labeled antigens as approach to detecting tuberculosis, 20: 36681
FARRAR, E., Potassium–argon ages of some Dalradian, Moine, and related Scottish rocks, 20: 37016
FARRELL, John Joseph, Magnetic properties of $CeFe_2$, $LuNi_5$, and some 1:2 intermetallic compounds of lanthanide metals with Ni and Co, 20: 37279
FASSNACHT, R. E., Isotope effect in superconducting zinc, 20: 37959
FAWCETT, B. C., Extreme ultraviolet spectra from laser-produced plasmas, 20: 38300
FEDCHENKO, K. K., Anisotropy of Forbush-type cosmic-ray intensity decrease and electromagnetic conditions in interplanetary space, 20: 37534
FEDERMAN, P., Dynamical derivation of baryon masses in the quark model, 20: 37762
FEDORCSAK, I., Effects of diethyl pyrocarbonate on barley seeds, 20: 36589
FEDOROV, B. A., Theory of low-angle scattering of x rays by RNA molecules in solution, 20: 36586
FEDOROVA, G. V., Anisotropy of the Hall effect in Gd, 20: 37178
FEKHRETDINOV, F. A., Thermodiffusive interaction of tantalum and boron carbide powder in a vacuum, 20: 36809
FEL'DMAN, I. I., Neutron radiative capture gamma spectrometry as a method of determining the composition of iron-bearing rocks and ores, 20: 37019
FELTEN, James E., Interstellar and intergalactic absorption of cosmic x rays, 20: 37485
FENG, J., Simplified 180° focusing β-ray spectrometer, 20: 37120
FENTON, A. G., Neutron flux in the upper atmosphere during the 1964 solar minimum, 20: 37908
FENTON, K. B., Neutron flux in the upper atmosphere during the 1964 solar minimum, 20: 37908
FENYVES, E., Inelastic n-p cross section at 60 Bev, 20: 37670
FERENDECI, Altan M., Microwave cavity Q sampler for plasma diagnostics, 20: 38307
FERREIRA DE MIRANDA, Carlos, Preparation of $PaCl_5$ and absorption spectra, 20: 36798
FERRILL, Mitchell D., Root extension in a longleaf pine plantation, 20: 36560
FESSENDEN, Peter, Reactions $^{14}N(n,d)^{13}C$, $^{14}N(n,t)^{12}C$, $^{15}N(n,d)^{14}C$, $^{32}S(n,d)^{31}P$, and $^{34}S(n,d)^{33}P$ induced by 14-Mev neutrons, 20: 38150
FEYNMAN, Richard P., Development of the space-time view of quantum electrodynamics, 20: 37922
FIARMAN, S., Isobaric analog state polarization measurements to determine the spin of ^{145}Sm, 20: 38068
FICHTEL, C. E., Balloon observations of cosmic rays, 1961–1964, 20: 37560
FICHTEL, C. E., Experimental examination of low-energy cosmic-ray heavy nuclei, 20: 37569
FICHTEL, C. E., Solar cosmic-ray heavy nuclei and the 18th July 1961 event, 20: 37567
FIELD, E. O., Aggregated ^{99m}Tc-labeled albumin for lung, 20: 36919
FIELD, E. O., Isotope dilution method for determining amounts and activities of proline and hydroxyproline in tissues, 20: 36562
FIELD, George B., Density of intergalactic hydrogen molecules, 20: 37353
FIELD, Paul E., Solubilities of HF and DF in molten fluorides, 20: 36785

(ORNL-P-2202)
FIES, C. L., Calculated physics parameters and their uncertainties in a 1000-Mw(e) fast ceramic reactor, 20: 38491 (ANL-7120, pp 24-32)
FILIMONOV, A. B., Equipotential surfaces of a plasma moving in a toroidal octupole magnetic field, 20: 38192 (COO-1233-32)
FILIPPOV, A. I., Capture of pions by ^{3}He. II., 20: 38011 (JINR-P-2805)
FILIPPOV, A. I., Charge of π mesons stopped on light nuclei, 20: 37740 (JINR-P-2780)
FINCH, C. B., Electron spin resonance of rare-earth ions in CeO_2 : Yb^{3+} and Er^{3+}, 20: 38391
FINDEIS, A. F., Liquid scintillation determination of ^{45}Ca and ^{89}Sr in unicellular algae, 20: 36747
FINEMAN, P., Waste disposal, 20: 38538
FINNEY, J. W., Increased radioisotope uptake by malignant cells in a high oxygen environment resulting from H_2O_2 breakdown, 20: 36576
FIRKOWSKI, R., Attenuation of the μ component of EAS determined by the barometric effect, 20: 37623
FIRKOWSKI, R., Semi-empirical determination of the fluctuation of the EAS μ component, 20: 37624
FISCHER, G. J., Measurement and analysis of Doppler effect in Pu-fueled fast reactor assemblies, 20: 38427 (ANL-7120, pp 603-9)
FISCHER, J. E., Production and annealing of defects in 6- to 80-Mev electron-irradiated n-type Ge, 20: 38365
FISCHER, S., Influence of the changes in Earth's heliolatitude on the cosmic-ray intensity in 1963–1964, 20: 37529
FISHMAN, I. S., Plasma diagnostics based on the self-reversed contours of spectral lines emitted by inhomogeneous layers, 20: 38265
FITCH, V. L., Interference in the $K_L \to \pi^+\pi^-$ system, 20: 37814
FITE II, Warner, Superconducting mixed-state-structure determination in vanadium by nuclear magnetic resonance and relaxation, 20: 37963
FITI, Mario, Radiolytic behavior of iron ions in acetylene aqueous solution, 20: 36858 (IFA-CR-73)
FITTING, Wilfried, Effect of iodine-containing x-ray contrast media on serum iodide concentration iodide uptake, 20: 36572
FLEISHER, Martin, Effects of γ irradiation on the structure of ribonuclease, 20: 36584
FLINN, E. A., Detection, analysis, and interpretation of teleseismic signals. I., 20: 36968
FLORKOWSKI, T., Simple radioisotope x-ray transmission gage for measuring suspended sediment concentrations in rivers, 20: 37057
FLOWERS, J. W., Hollow gas arc discharge device utilizing an off-center cathode, 20: 37065
FOA, E., Economic aspects of the food irradiation program in Israel, 20: 37157
FOCACCI, M. N., Evidence for three new charged bosons of masses 1929, 2195, and 2382 Mev and narrow widths, 20: 37771
FOGEL, Yu. M., CO, CO, and NO emission spectra excited by 13-kev electrons, 20: 37466
FOGEL', Yu. M., Rotational energy level distribution of molecules excited by ion impact, 20: 37471
FOMENKO, V. S., Production and properties of W–LaB_6, 20: 37258
FOMIN, Yu. A., Comparison of various models of EAS development with experimental data and the prospects of cosmological and nuclear aspects of EAS investigation, 20: 37646
FOMIN, Yu. A., Energy spectrum, possible chemical composition, and anisotropy of ultrahigh-energy primary cosmic radiation, 20: 37651
FORBES, W. F., Effect of radiation on collagen. I., 20: 36585
FORD, C. Hubbard, Critical mass studies with NASA Zero Power Reactor II, 20: 38532 (NASA-TN-D-3555)
FORREST, M. J., Co-operative scattering of laser light by a thetatron plasma, 20: 38259
FORTES, M. A., Field-ion microscope study of neutron irradiated iridium, 20: 38382
FOURNIER, J., Contribution to safety problems related to 1000-Mwe fast power reactor project, 20: 38497 (ANL-7120, pp 157-61)
FOURNIER, J., Program proposed for safety studies of fast neutron project of EURATOM-CEA association, 20: 38492 (ANL-7120, pp 54-66)
FOWLER, E. E., New developments and trends in the isotope industry, 20: 37142
FOWLER, G. N., Energy loss of fast charged particles in dielectric media, 20: 37460
FOWLER, G. N., High-energy single-meson production, 20: 37692
FOWLER, R. G., Resistance of a plasma slab between juxtaposed disk electrodes, 20: 38293
FOWLER, R. G., Transition probabilities for H_2, D_2, N_2, N_2^+, and CO, 20: 37438
FOWLER, T. K., Plasma fluctuations and the control of pumpout, 20: 38266
FOX, Kenneth, Variational calculation for bound states in an electric-dipole field, 20: 37919
FOX, Raymond, Magnetically channeled plasma diode heat converter, 20: 37729
FOX, Thomas A., Critical mass studies with NASA Zero Power Reactor II, 20: 38532 (NASA-TN-D-3555)
FRADKIN, M. I., Some results of the investigation of the primary cosmic-ray nuclei on the artificial satellite Electron-2, 20: 37600
FRANK, L. A., Observations with University of Iowa equipment on Mariner IV, 20: 37341 (N-66-17354)
FRANKE, Herbert, Autoradiographic studies with a radiation protection material, 20: 36670
FRANKFURT, L. L., Magnetic moments of particles in the quark model, 20: 37857
FRANZ, E. M., Decay of ^{131}Ce, 20: 38048
FREEMAN, J. M., Threshold for the reaction ^{10}B(p,n)^{10}C and the ft value of the superallowed Fermi transition ^{10}C(β^+)^{10}B, 20: 38069
FREIER, P. S., Electrons, H, and He nuclei of cosmic radiation observed in 1963 and 1964, 20: 37551
FREIER, P. S., Low energy multiply charged nuclei in the cosmic radiation, 20: 37565
FREIER, P. S., Modulation of cosmic rays by an electric field, 20: 37512
FREIER, P. S., Very heavy low-energy cosmic-ray nuclei, 20: 37566
FRENZEL, D., Influence of α radiation on the self-diffusion in Pb, 20: 37272
FRETTER, W. B., Coherent production of multipion resonances, 20: 37822
FRICKEN, R. L., High-energy jets produced by heavy primary nuclei of cosmic origin and their fragmentation products, 20: 37662
FRIDMAN, V. M., Rotational energy level distribution of molecules excited by ion impact, 20: 37471
FRIEDES, J. L., Elastic scattering of 1 Bev protons from He and O, 20: 38010 (BNL-10438)
FRIEDLANDER, G., Decay of ^{131}Ce, 20: 38048
FRIEDMAN, H., Observations of hard x-ray emission from solar flares, 20: 37360
FRIEDMANN, Gerhard, Experience in the radiotreatment of 242 brain tumors, 20: 36693
FRIEMAN, E. A., Negative V'' stellarator, 20: 38243
FRIEMAN, Edward, Higher-order corrections to the Chew-Goldberger-Low theory, 20: 38271
FRIEMAN, Edward A., Present state of plasma kinetic theory, 20: 38207 (PPL-AF-1)
FRIEMAN, Edward A., Propagation of correlations in a Boltzmann gas, 20: 37865 (PPL-AF-2)
FRILING, L., Neutron albedo measurements on rocket flights, 20: 37601
FRISCHBIER, Hans-Joachim, In vivo investigations with ^{3}H-thymidine for the study of tumor cell kinetics in punctates, 20: 36704
FRISCHKORN, Rolf, Determination and localization problems in the radio-therapy of carcinoma of the cervix uterus, 20: 36699
FRISHMAN, Y., Average charge distributions in systems of nucleons and pions, 20: 37791
FRITZE, R., Extensive air shower experiment at Kiel, 20: 37636
FRITZ-NIGGLI, Hedi, Radioinduced back mutations in dependence on the chromosome activity and the milieu, 20: 36653
FROELICH, R., Results of Doppler coefficient calculations for fast reactors and comparison of different methods. I and II., 20: 38421 (ANL-7120, pp 440-8)
FROMM, Eckehard, p-T-c-representation of the Nb–O and Ta–O systems, 20: 36836
FRONSDAL, C., Electric-charge form factor according to SL(6,C), 20: 37840
FRONSDAL, C., Matrix elements of operators of class 1 representations of SL(n,C), 20: 37738 (IC-66/89)
FRONTEROTTA, Gabriele, (e,e'p) reaction in the ^{32}S nucleus, 20: 38016
FUCCILLO, D. A., Isotopes and Radiation Technology. Vol. 3, Number 3, 20: 37136
FUCCILLO, D. A. Jr., Radioisotope instruments in industry and geophysics, 20: 37143
FUHRMAN, Z. A., Technique for preparing samples of small fragile particles for electron microscope examination by means of replicas, 20: 37173
FUJII, Toro, Development of mutated cells in wheat embryo, 20: 36650
FUJII, Toro, Radiosensitivity in plants. VII., 20: 36648
FUJIMOTO, Hiroshi, Behavior of radioactive Sr, Cs, and Co in marine water, 20: 38537
FUJIMOTO, K., Observation of muon air showers, 20: 37607
FUJIMOTO, Y., Origin of extragalactic cosmic rays, 20: 37502
FUKAI, Rinnosuke, Chemical composition of shallow-water sediments in the Bay of Roquebrune, 20: 36553
FUKAI, Rinnosuke, Distribution of chromium in marine organisms, 20: 36552
FUKUI, Tokinori, ESR of γ-irradiated sodium polyphosphate. I., 20: 36870
FULTONBERG, D. N., Stability, compatibility and corrosion of poison solutions and structural materials, 20: 38447 (WCAP-2867)
FULTZ, S. C., Photoneutron cross sections of ^{141}Pr and ^{127}I from threshold to 33 Mev, 20: 38094
FURCHNER, J. E., Retention of ^{54}Mn by four mammalian species, 20: 36554 (LA-DC-7305)

FURSOV, V. N., Mutations of cotton plant Gossypium barbadense, 20: 36623
FURTH, H. P., Drift instability due to impurity ions, 20: 38296
FURUTA, Junichiro, Radiography using ^{192}Ir, 20: 36954

G

GABBARD, F., Neutron cross sections of Ca from 2.0 to 6.5 Mev, 20: 38183
GABBIANI, G., Action of histamine liberators on calcification produced by various metals, 20: 36557
GABRIEL, A. H., Extreme ultraviolet spectra from laser-produced plasmas, 20: 38300
GAEBEL, Eva, Experience in the radiotreatment of 242 brain tumors, 20: 36693
GAFUROV, V. G., Decay $K \rightarrow \mu + \nu$ in μ-meson beam of cosmic rays 3860 m. above sea level, 20: 37482
GALANIN, A. D., Regulation theory for heterogeneous reactors, 20: 38412 (ITEF-406)
GALIANO, J. A., Activation analysis of impurities in U. I., 20: 36714
GALIANO, J. A., Activation analysis of impurities in U. II., 20: 36715
GALLAGHER, Charles C., Magnetic field design with an electrolytic tank analog, 20: 38189 (AD-636095)
GALLINARO, G., Effect of transition-metal impurities on the critical temperature of superconducting Al, Zn, In, and Sn, 20: 37955
GALSTAUN, Lionel S., Large-scale nuclear desalting plants, 20: 38524
GALSTYAN, D. A., Certain aspects of nucleon isobar production in nucleons interactions at energies 10^3 and 25 Bev, 20: 37675
GAPONOV, V. A., Transformer-type high-current accelerator, 20: 37322
GARDELLA, Joseph W., Prog. rpt. on mechanisms and regulations of nucleic acid and protein synthesis, and their possible relationship to radiation damage, 9/65–8/66, 20: 36555 (NYO-2643-23)
GARDNER, C. S., Second-order magnetic moment of a charged particle in an axially-symmetric static magnetic field, 20: 38208 (PPL-AF-4)
GARG, S. C., SWIFT dryout data for 19-rod bundle cooled by steam/water fog, 20: 38409 (AECL-2586)
GARLAND, W., High-pressure gas mixing facility, 20: 36981 (Y-1546)
GARMIRE, G., Intergalactic photon density, 20: 37374
GARNETT, J. E., Advances in the gamma-absorptiometric determination of uranium and plutonium in solution, 20: 36767
GARRETT, M. W., Table of the ratio B_0/B_{max} for magnet coils with rectangular cross section and uniform current density, 20: 36979 (ORNL-3972)
GARTON, W. R. S., Auto-ionization-broadened Rydberg series in the spectrum of La I, 20: 37351
GARVIN, Robert G., Performance of sieve trays under GS heavy water process conditions. I., 20: 37160 (DP-1025)
GARWIN, E. L., CsI as a high-gain secondary emission material, 20: 37048
GARZON, Oro Lucy, Nondestructive determination of nitrogen in diamond by photoactivation, 20: 36746
GAST, Paul F., Criteria for the density of monitoring points in large reactors, 20: 38432 (ANL-7120, pp 632-5)
GASTEBOIS, J., Reactions (^{3}He,d) on even Sn isotopes, 20: 38073
GAUDIN, M., One-parameter family of unitary ensembles, 20: 38033
GAVRIN, V. N., Cross section of the reaction $\nu + {}^{37}Cl \rightarrow {}^{37}Ar + e^-$, 20: 38111
GAWIN, J., Semi-empirical determination of the fluctuation of the EAS μ component, 20: 37624
GAWIN, J., Some properties of μ-poor EAS, 20: 37610
GAZARYAN, K. A., Ionization measurement in a streamer chamber, 20: 37110
GEBALSKI, Stanislaw, Diffusion siliconizing and aluminizing of molybdenum in powders, 20: 37204
GEBELT, Robert E., Preparation and thermodynamics of europium dicarbide, 20: 36844
GEERY, E. L., Nozzle tube-wall temperature measurement by radiometric techniques, 20: 38528
GEHLEN, Kurt V., Sulfur isotopes and the formation of ore strata, 20: 37011
GEIGER, J., High resolution investigation of the energy losses of 30 kev electrons in aluminum foils of various thicknesses, 20: 37442
GEIGER, J., Interaction of 25-kev electrons with lattice vibrations in LiF, 20: 38395
GEISLER, M., New method for the reduction of Compton continua in γ scintillation spectra, 20: 37123
GENDRIN, Roger, Determination of the density of protons at the level of a satellite by exact numerical analysis of proton whistlers, 20: 37885
GENKIN, I. L., Fluctuations in gravitating systems, 20: 37928
gen Schieck, H. Paetz
see Paetz gen. Schieck, H.
GERASIMOV, V. V., Effects of γ radiation on the scale formation process, 20: 37182
GERASIMOVA, N. M., One of the features in the jets generated in the hydrodynamical Landau process, 20: 37683
GERHART, J. B., Observation of the 4.12-Mev $^{14}O \rightarrow {}^{14}N$ positron spectrum shape, 20: 38080
GERJUOY, E., Cross section for energy transfer between two moving particles, 20: 37447
GERRARD, Martha, Isotopes and Radiation Technology. Vol. 3, Number 3, 20: 37136
GERTZ, D., Unified digital instrumentation and control system for nuclear power plants, final, 4/61–6/65, 20: 38508 (NYO-2764-2)
GHALLA, M., X-ray photoconductivity of anthracene, 20: 36873
GIACCHETTI, G., Microanalytical studies of micro- and macro-segregation in oxide fuels, 20: 38469 (ANL-7120, pp 400-9)
GIAUX, G., Effect of ionizing radiations on the HeLa cell. II., 20: 36616
GIBALA, R., Clustering of O in solid solution in Nb. I., 20: 37213
GIBALA, R., Clustering of O in solid solution in Nb. II., 20: 37214
GIBSON, A., Enhanced safety characteristics of a sodium-cooled coupled reactor, 20: 38437 (ANL-7120, pp 789-93)
GIBSON, Walter M., X rays and electrons emitted in coincidence with the fission of ^{252}Cf, 20: 38095
GIERE, Albert C., Hydromagnetic wave velocities in a relativistic fluid, 20: 37883
GIERULA, J., High-energy jets produced by heavy primary nuclei of cosmic origin and their fragmentation products, 20: 37662
GILBERT, David I., Magnetic-gradient particle accelerator, 20: 37340
GILBERT, Gareth E., Radiological investigations at Neotoma, 20: 36548 (TID-23036)
GINZBURG, V. L., Origin of cosmic rays, 20: 37388
GIRALT, G., Behavior of MOS structures in the case of an induced ionization, 20: 37130
GIRARDI, F., Use of an automated system including a radiochemical step in activation analysis, 20: 36782
GIRD, E., Paramagnetic centers formed by irradiation of oxygenated compounds of Se. II., 20: 38398
GISEKE, H., Study on the extraction of rare earths with tributyl phosphate. II., 20: 36938
GLAGOLEV, V. M., Paramagnetic high-frequency effect and electron paramagnetic resonance in plasma, 20: 38220
GLAUNER, Rolf, Responsibility of the doctor in the radiation detection of patients, 20: 36709
GLICKSMAN, A. S., Isotope dilution method for determining amounts and activities of proline and hydroxyproline in tissues, 20: 36562
GLICKSMAN, Arvin S., Clinical evaluation of the treatment of advanced head and neck cancers with high-energy electron beams, 20: 36685
GLOECKLER, G., Acceleration of particles in the Earth's shock transition region and beyond, 20: 37900
GLOECKLER, G., Protons and He nuclei within interplanetary magnetic regions which co-rotate with the Sun, 20: 37371
GLOECKLER, G., Solar modulation of the galactic He spectrum above 30 Mev per nucleon, 20: 37563
GLUCKMANN, Alexis L., Containment structures, 20: 38522
GLUKHOVA, L. P., Determination of microquantities of U in soils, rocks, and minerals by means of arsenazo III, 20: 36774
GLUSHKOVA, V. B., Effect of europium oxide admixtures on the polymorphism of zirconium dioxide, 20: 36815
GLYDE, H. R., Stacking-fault energy and many-body force effects in solid argon, 20: 38394
GNEVYSHEV, M. N., Relation between proton flares and the corona in the 11-year cycle, 20: 37886
GOBLE, David Franklin, Search for a proposed new level of ^{7}Be, 20: 38165
GODFREY, W. L., Recovery of aluminum nitrate nonahydrate from redox acid waste, 20: 36925 (HW-82771(Pt.3))
GODTS, J. E., Transient flux distributions by discontinuous model synthesis, 20: 38431 (ANL-7120, pp 625-31)
GODTS, J. E., Transient temperature distribution in fuel elements, 20: 38471 (ANL-7120, pp 486-93)
GOEBEL, C. J., Factors of excited nuclear states by resonant scattering, 20: 38079
GOEDDEL, W. V., Pilot-scale extrusion of graphite fuel elements for HTGRs, 20: 37196
GOELER, S. v., Propagation and damping of ion waves in a plasma with negative ions, 20: 38283
GOKHALE, G. S., Flux of primary protons and helium nuclei and east-west and north-south asymmetries near the geomagnetic equator, 20: 37582
GOKHALE, G. S., Use of a gas Cherenkov counter for the study of the isotopic composition of He nuclei in primary cosmic radiation, 20: 37581
GOKSADZE, G. Sh., Reactions ($\pi^\pm$,NN) and two-particle excitation of light nuclei, 20: 38070
GOLD, T., Expansion of a relativistic gas into intergalactic space, 20: 37503
GOLD, V., Kinetics of H isotope exchange reactions. XIV., 20: 36849
GOLDBERG, G. N., Oxidation of Nb–Zr and Nb–Zr–Re alloys in oxygen at 1000°C, 20: 37193
GOLDEMBERG, J., Coulomb form factors of ^{10}B and ^{11}B, 20: 38057

GOLDMAN, David T., Two neutron sciences, 20: 38103
GOLDMAN, Morton I., Safety aspects of ground testing for large nuclear rockets, 20: 37034
GOLDMAN, Robert, Propagation of correlations in a Boltzmann gas, 20: 37865 (PPL-AF-2)
GOLDSMITH, S., Fast reactor safety considerations related to fuel macrostructure, 20: 38424 (ANL-7120, pp 497-503)
GOLDSTEIN, Herbert, Two neutron sciences, 20: 38103
GOLDSTEIN, Louis, Theory of liquid helium three, 20: 37873
GOLENKOV, A. E., Penetration of the outer radiation belt particles into low altitudes of atmosphere, 20: 37907
GOLOVIN, I. N., Increasing plasma density in Ogra-I, 20: 38248
GOLUBTSOV, I. V., Evaporation of W, Mo, and Ta in vacuum, 20: 36834
GONCHARUK, A. B., Germanides of lanthanum, 20: 37259
GONGWER, L. E., ^{14}C-labeled polyoxyethylene (20) sorbitan monolaurate and metabolic fate in rats, 20: 36921
GOODMAN, Allen S., Mean lives of the 2p and 3p levels in atomic hydrogen, 20: 37443
GOODMAN, L. S., Hyperfine interactions and the magnetic fields due to core polarization in ^{57}Fe, 20: 38385
GOODSTEIN, David Louis, Heat capacity of adsorbed He, 20: 37982
GOODWIN, J. G., Effects of oxygen on the mechanical and corrosion properties of hafnium, 20: 37170
GOPALAKRISHNAN, Sarada, Estimates of biospheric contamination and radiation dose from fallout for all the pre-treaty tests of nuclear weapons, 20: 37004
GORBUNOV, G. V., Pulsed neutron generator for boreholes and its use in nuclear geophysics, 20: 37017
GORBUNOV, L. M., Cross-section averaging in thermal region for media containing zirconium hydride, 20: 37991
GORBUNOV, L. M., Oscillations of a beam plasma in a high-frequency electric field, 20: 38263
GORINGE, M. J., Temperature dependence of the absorption of fast electrons in copper, 20: 38379
GORKIN, Z. D., Effect of ultraviolet irradiation on the functional condition of basic cerebral nervous processes in man, 20: 36626
GORODETZKY, S., Angular distribution, angular correlations, and plane polarization of gamma rays of the reaction $^{53}Cr(p,n)^{53}Mn$, 20: 38034
GORODETZKY, S., Application of the delayed coincidence technique to measurement of the short mean lives in ^{131}Xe and ^{143}Pr, 20: 38031
GORODETZKY, S., Half lives of levels at 405 kev in ^{211}Bi and 377 kev in ^{53}Mn, 20: 38030
GORTCHAKOV, E. V., Corpuscular ionizing radiation in space in the immediate vicinity of the Earth, 20: 37902
GORTCHAKOV, E. V., Coulomb interaction of electrons with energy of 1 Mev in the region of a magnetic anomaly, 20: 37906
GORTCHAKOV, E. V., Earth's radiation belt, 20: 37899
GOSWAMI, A., Neutron-proton correlation effects in spherical even nuclei, 20: 38177
GOTSMAN, E., Decay correlations of photo-produced rho mesons in the strong-absorption, 20: 37768
GOTSMAN, E., Rho meson photoproduction cross sections in the strong-absorption model, 20: 37766
GOTTSCHLICH, Chad F., Measurement of plasma transport properties in a Na–K seeded Ar plasma, 20: 38195 (INDEC-SR-7, pp 3.60-73)
GOUD, Paulus Arie, Study of electron beams and their formation in electrostatic electron guns, 20: 37312
GOULD, Robert J., Interstellar and intergalactic absorption of cosmic x rays, 20: 37485
GOUVEIA, M. A., Formation constants of lanthanide lactate complexes, 20: 36824
GRAD, Harold, Neutral point in the geomagnetic field, 20: 37895
GRAMM, N. V., Properties of yttrium borides, 20: 38359
GRANNIS, P., Polarization in proton-proton scattering using polarized proton target. Pt. I and Pt. II., 20: 37743 (UCRL-16866)
GRANOVSKII, Yu. V., Solid solution region in system Sc_2O_3–Fe_2O_3–MnO_x, 20: 36839
GRANZOW, A., Radiation-chemical production and optical absorption spectra of organic S radicals in organic glasses at −196°C, 20: 36894
GRASS, F., Chelate exchanger on basis of 8-hydroxyquinoline, 20: 36754
GRASS, G., Investigations of boiling of liquid metals in forced convection, 20: 38415
GRECHIKHIN, L. I., Forbidden transitions in atomic systems, 20: 37432
GRECHUKHIN, D. P., Photoexcitation and photoionization of energetic hydrogen atoms, 20: 38221
GREEBLER, P., Calculated physics parameters and their uncertainties in a 1000-Mw(e) fast ceramic reactor, 20: 38491 (ANL-7120, pp 24-32)
GREEN, A. E. S., Isobaric spin dependence of the nucleon-nucleon interaction, 20: 37811
GREEN, G., Advances in the gamma-absorptiometric determination of uranium and plutonium in solution, 20: 36767
GREEN, L. L., Further measurements and zero-range DWBA calculations for the $^{52}Cr(d,p)^{53}Cr$ reaction, 20: 38046
GREEN, W. V., Stress dependence of the creep rate of a uranium-loaded graphite, 20: 37224
GREENE, R. E., Chemistry of electromagnetically separated stable isotopes, 20: 37163
GREENE, R. E., Isotopes and Radiation Technology. Vol. 3, Number 3, 20: 37136
GREENFIELD, M. A., Errors in measurements of building leakage due to dynamic temperature effects, 20: 36978 (NAA-SR-12001)
GREENHILL, J. G., Neutron flux in the upper atmosphere during the 1964 solar minimum, 20: 37908
GREENSPAN, J., Twin-particle interaction in beryllium, 20: 37216
GREENSTEIN, J. L., Analysis of field horizontal-branch and RR Lyrae stars, 20: 37419
GREENSTEIN, J. L., CH stars and neutron-addition processes, 20: 37424
GREER, C. L., Computation of neutron flux from foil activation data: SPECTRA code, 20: 37076 (SC-DC-66-1512)
GREGORY, B. L., Transient annealing in semiconductor devices following pulsed neutron irradiation, 20: 37129 (SC-DC-66-1820)
GREHIER, J., Energy released at high temperature by irradiated graphite, 20: 37283
GREINER, W., 3^- continuum states of ^{16}O in the eigenchannel reaction theory, 20: 38102
GREINER, Walter, Photon scattering by oriented nuclei, 20: 38055
GREISEN, Kenneth, Highlights in air shower studies, 1965, 20: 37604
GRENACS, L., Spin measurement and isospin impurity of the ^{64}Ga ground state, 20: 38065
GRIEDER, P., Search for heavy particles in the cosmic radiation, 20: 37654
GRIFFIN, E. E. Jr., Transient radiation effects on insulated gate field effect transistors, 20: 37132
GRIFFING, G. W., Intramolecular coherent scattering of neutrons by CD_4 gas, 20: 38000
GRIFFITH, Peter, Some hydrodynamic characteristics of bubbly mixtures flowing vertically upward in tubes, 20: 36988 (TID-23261)
GRIFFITHS, David John, Optical Faraday rotation studies in Pr ethylsulfate, 20: 36855
GRIFFITHS, W. K., Studies of the barometric coefficients of IGY and NM-64 neutron monitors, 20: 37097
GRIGOREV, E. P., Decay of ^{182}Ta, 20: 38134
GRIGORIU, G., Current status of the use of bone marrow transplants in therapeutics, 20: 36667
GRIGORIU, G., Viability of preserved bone marrow cells, 20: 36546
GRIGOROV, N. L., Characteristics of high-energy particle interaction with nuclei of light atoms, 20: 37755
GRIGOROV, N. L., Discussion of one model of the formation of extensive atmospheric showers, 20: 37612
GRIGOROV, N. L., Generation mechanism of high-energy pions in cosmic rays, 20: 37664
GRIGOROV, N. L., Interaction path of high-energy nucleons (10^{11} to 10^{13} ev) in the atmosphere, 20: 37667
GRIGOROV, N. L., New data about the nuclear-active component of young atmospheric showers, 20: 37611
GRIGOROV, N. L., Preliminary results of cosmic-ray study from the artificial Earth's satellite Proton-1, 20: 37495
GRIGOROV, N. L., Relationship of neutral and charged particles among nuclear-active particles with energies above 100 Bev at mountain altitude, 20: 37685
GRIGOROVA, I. K., Anisotropy of the Hall effect in Gd, 20: 37178
GRISHINA, L. P., Properties of yttrium borides, 20: 38359
GRITSYNA, V. T., Isomers of ^{131m}La and ^{136m}La, 20: 38125
GRITZNER, G., Polarographic studies on uranium compounds in dimethylformamide and dimethylsulfoxide, 20: 36745
GROH, E. F., Measurement and analysis of Doppler effect in Pu-fueled fast reactor assemblies, 20: 38427 (ANL-7120, pp 603-9)
GROH, E. F., Recent Doppler measurements with ZPR-6, 20: 38428 (ANL-7120, pp 610-13)
GROLLEAU, Bernard, Observation of a cyclotron resonance harmonic in hydrogen plasma, 20: 38224
GRUBELASHVILI, G. A., Properties of μ mesons at 200 m.w.e. underground, 20: 37694
GRUEN, L. C., Kinetics of H isotope exchange reactions. XIV., 20: 36849
GRUENEWALD, Th., Dose distribution during irradiation with a pulsed scanning electron beam, 20: 36672
GRUNDHAUSER, F. J., Electron accelerator with a peak beam power of 10^{10} watts, 20: 37339
GRUNE, Werner N., Natural radioactivity in ground water supplies in Maine and New Hampshire, 20: 37006
GRUZ, E. A., Anomalous positive effects of preliminary irradiation. I., 20: 36895
GUALANDI, Dante, Powder metallurgy of SAP composites for nuclear applications, 20: 37210
GUDERLEY, Karl G., Theory of spherical probes in monoenergetic plasmas, 20: 38190 (AD-637513)

GUDZENKO, L. I., Some properties of the phase of solar activity, 20: 37385
GUEDES DE CARVALHO, R., Formation constants of lanthanide lactate complexes, 20: 36824
GUENTHER, K., Fission recoil separation in mixtures with uranium dioxide powders as a simple method of range determination of fission products, 20: 37997
GUENTHER, R., Structural design of nuclear-fueled thermionic converter. I., 20: 37720 (BMWF-FBK-66-06)
GUERIN, M., Thymus origin of lymphomatoses in mice after irradiation by x rays, 20: 36613
GUERSEY, Feza, Noncompact groups associated with vertex operator, 20: 37823 (BNL-10387)
GUIDONI, P., f^0 meson produced in K-p interaction 4.6 and 5.0 Bev/c, 20: 37730 (BNL-10459)
GUILBOT, A., Effect of gamma-rays on potato starch in relation to its water content, 20: 36599
GULATI, S. P., Flow of an elastico-viscous liquid between two electrically non-conducting infinite flat plates under a uniform transverse magnetic field, 20: 37871
GUNN, J., Analysis of field horizontal-branch and RR Lyrae stars, 20: 37419
GUNSON, W. E., Conceptual design and preliminary accident analysis of a Na-cooled, carbide-fueled, large modular fast reactor, 20: 38456 (ANL-7120, pp 205-29)
GUNSON, W. E., Transient response of coupled fast reactor cores, 20: 38436 (ANL-7120, pp 776-88)
GUPTA, Gopi N., Combustion method for assay of ^{3}H, ^{14}C, and ^{35}S in biological, biochemical, and organic materials, 20: 36721
GUPTA, S. C., Variational principles in magnetohydrodynamics, 20: 37877
GUREVICH, A. V., Coulomb interaction of electrons with energy of 1 Mev in the region of a magnetic anomaly, 20: 37906
GURR, Henry S., Experimental test of the law of baryon conservation, 20: 37734 (COO-818-87)
GUSEVA, L. N., Intermediate phases in the Cr–Nb system, 20: 37239
GUSEVA, V. V., Interactions of nucleons with complex nuclei at high energies, 20: 37790
GUSS, D. E., Balloon observations of cosmic rays, 1961–1964, 20: 37560
GUSS, D. E., Experimental examination of low-energy cosmic-ray heavy nuclei, 20: 37569
GUSS, D. E., Solar cosmic-ray heavy nuclei and the 18th July 1961 event, 20: 37567
GUSTAFSON, W. A., Electrostatic probe in a collisionless plasma, 20: 38278
GUTMANN, V., Polarographic studies on uranium compounds in dimethylformamide and dimethylsulfoxide, 20: 36745
GUZHAVIN, V. V., Processes of bremsstrahlung and pair production as they are regarded in the cascade theory of the showers, 20: 37788
GUZZI, G., Use of an automated system including a radiochemical step in activation analysis, 20: 36782
GWYTHER, Myfanwy M., Aggregated ^{99m}Tc-labeled albumin for lung scintiscanning, 20: 36919
GYOREY, G. L., Calculated physics parameters and their uncertainties in a 1000-Mw(e) fast ceramic reactor, 20: 38491 (ANL-7120, pp 24-32)

H

HABERSBERGEROVA, A., Hydrogen formation in the radiolysis of liquid methanol, 20: 36861 (UJV-1553)
HADEN, C. R., Flux trapping of r-f fields in superconductors, 20: 37954
HAGEMANN, Gerd, Flux density distribution of fast electrons and use in radiation therapy, 20: 36689
HAGENBRUCH, R., Structure investigations on lanthanide oxalates. I., 20: 36835
HAGENLOCKER, E. E., Stimulated pure rotational Raman scattering in deuterium, 20: 37451
HAGGE, D. E., Galactic cosmic rays at solar minimum, 1965, 20: 37578
HAGGERTY, Michael John, Approach to equilibrium of a homogeneous plasma in a uniform magnetic field, 20: 38343
HAKURA, Yukio, Spatial extent of enhanced ionizations produced in association with the elementary geomagnetic polar disturbances, 20: 37893
HALBACH, K., Apparatus for producing and purifying plasma, 20: 38339
HALBERT, M. L., Nuclear-reaction studies with 65-Mev α particles on Zr, 20: 38092
HALING, R. K., Flood safety of steam- and gas-cooled fast reactors, 20: 38439 (ANL-7120, pp 826-36)
HALL, A. G., Energy loss of fast charged particles in dielectric media, 20: 37460
HALL, C. R., Effect of weak Bragg reflected beams on the absorption of electrons. II., 20: 38381
HALL, J. D., On-line nuclear analysis system, 20: 36769
HALL, Laurence S., Interaction models, negative energy waves, and electrostatic instabilities, 20: 38273
HALL, W. F., Anomalous particle penetration in perfect crystals, 20: 38387
HALLAM, J. W., Flood safety of steam- and gas-cooled fast reactors, 20: 38439 (ANL-7120, pp 826-36)
HALLET, R. W. Jr., Nuclear propulsion and manned interplanetary flight, 20: 36999
HALPERN, Otto, Measurement of magnetic moments of unstable particles, 20: 37750
HAMADA, Kunihiko, Renal clearance. III., 20: 36608
HAMAMOTO, Ikuko, Effect of a short-range neutron-proton interaction on the pairing model, 20: 38056
HAMILTON, David Carpenter, Superconductivity of lanthanum and some gold-rich intermetallic compounds, 20: 37985
HAMPTON, Marlene, ESR of x-irradiated single crystal of KH_2AsO_4, 20: 36884
HAMRIN, C. E. Jr., Thermal conductivity of H up to 660 atm and 74.6°C, 20: 36991
HANCOX, R., Calculation of a-c losses in a type-II superconductor, 20: 37969
HANCOX, R., Paramagnetic limit in type II superconductors, 20: 37936 (CLM-R-60)
HANEMAN, D., Low-energy-ion-bombardment damage in germanium, 20: 38363
HANKIEWICZ, E., Radiation-induced isotope exchange in some C_6-hydrocarbons, 20: 36866
HANSEN, C. J., Formation of helium in the galaxy, 20: 37409
HANSEN, K. H., Search for heavy particles in the cosmic radiation, 20: 37654
HANSEN, Luisa F., Two-nucleon distorted-wave Born approximation analysis of $^{19}F(d,\alpha)^{17}O$ data, 20: 38082
HANSEN, Ole, Reaction (t,p) with even isotopes of Sm, 20: 38052
HANSEN, Sponsz M., Nuclear blasting for mining and leaching, 20: 36975
HANSEN, Sponsz M., Rock breaking takes a giant step into the space age, 20: 36974
HANSON, J. E., Mixed oxide fuel movement at various power levels and in transients, 20: 38473 (ANL-7120, pp 524-33)
HARA, Y., Meson-baryon coupling constants in broken SU(3) and the algebra of currents, 20: 37842
HARAGEA, S., Color centers in x-irradiated NaCl : Ag and NaCl : (Ag + Ca) crystals, 20: 38396
HARAR, S., Reactions (^{3}He,d) on even Sn isotopes, 20: 38073
HARBAUGH, W. E., Development of a reservoirless thermionic energy converter, 20: 37725
HARDIE, D., Hydrogen embrittlement of α–Zr: a review, 20: 37187
HARDIE, R. W., Neutronics characteristics of selected compact fast reactors, 20: 38442 (BNWL-283)
HARDY, Walter Newbold, Nuclear spin relaxation in gaseous H_2, HD, and D_2, 20: 38151
HARMAN, C. V., Studies of the barometric coefficients of IGY and NM-64 neutron monitors, 20: 37097
HARRIS, D. R., Matrices for computing Greuling-Goertzel slowing-down parameters and Legendre polynomial coefficients for scattering, 20: 37988 (WAPD-TM-572)
HARRIS, D. R., TRANS: a FORTRAN-IV program for conversion of form of neutron elastic scattering data stored in ROC nuclear data library, 20: 37989 (WAPD-TM-573)
HARRIS, G. I., 1505 kev resonance in $^{29}Si(p,\gamma)^{30}P$ and properties of ^{30}P levels, 20: 38062
HARRIS, Gale I., Sulfur-36 $(p,\gamma)^{37}Cl$ reaction for proton energies in the 800-1800 kev region, 20: 38185
HARTLEY, A. J., Axial stability calculations for A.G.R. systems, 20: 38446 (TRG-Report-1138)
HARTMAN, Charles W., Field curvature effects on alkali-metal-plasma containment, 20: 38326
HARTWIG, W. H., Flux trapping of r-f fields in superconductors, 20: 37954
HARVEY, R. R., Photoneutron cross sections of ^{141}Pr and ^{127}I from threshold to 33 Mev, 20: 38094
HASEGAWA, Akinori, ESR of γ-irradiated sodium polyphosphate. I., 20: 36870
HASEGAWA, H., Arrival direction of muon-rich extensive air showers, 20: 37609
HASEGAWA, H., Fine structure of air shower cores observed with 20 m^2 spark chamber, 20: 37617
HASEGAWA, H., Origin of extragalactic cosmic rays, 20: 37502
HASEGAWA, H., Possible nuclear interaction of a muon of energy above 3×10^{14} ev, 20: 37714
HASEGAWA, H., Variation of ^{14}C content in the atmosphere during the past two thousand years, 20: 37602
HASEGAWA, S., New kinematical approach for analyses of high-energy cosmic-ray jets, 20: 37680
HASHMI, M. H., Colorimetric determination of Au, Pt, and Ce, 20: 36725
HASHMI, R. A., Experimental studies of thick-target bremsstrahlung in the direction 0° for electron energies 0.2, 0.4, 0.6, and 0.8 Mev, 20: 38155
HASSID, A., Liquid volume fraction in adiabatic two-phase vertical upflow-

round conduit, 20: 36985 (EURAEC-1088)
HATCH, L. P., Pyrolytic carbon decladding, 20: 36956
HATCH, Richard Calder, Gamma radiolysis of aqueous stannous chloride–hydrochloric acid solutions, 20: 36911
HATTON, C. J., Rigidity dependence of the intensity variation during the solar cycle, 20: 37516
HATTON, C. J., Studies of the barometric coefficients of IGY and NM-64 neutron monitors, 20: 37097
HAUSMAN, H. J., Angular correlations of $^{28}Si(d,p\gamma)^{29}Si$ from 4 to 6 Mev, 20: 38086
HAYAKAWA, S., Acceleration of cosmic-ray electrons, 20: 37499
HAYAKAWA, S., Observation of the energy spectrum of galactic x rays, 20: 37500
HAYAKAWA, Satio, Interpretation of the energy spectrum of galactic x rays, 20: 37488
HAYASHI, Chushiro, Advanced stages of stellar evolution, 20: 37404
HAYASHI, Chushiro, Contracting stars, 20: 37396
HAYASHI, Shigenori, Experiments on ion cyclotron heating of plasma in the Heliotron-B device, 20: 38258
HAZEN, W., BASJE angle correlation, 20: 37629
HEALD, M. A., Microwave plasma density measurement system, 20: 38338
HEALEY, D. C., Lifetimes of the 5.10- and 5.83-Mev levels in ^{14}N, 20: 38075
HEALY, J. H., Crustal seismic measurements in Southern Mississippi, 20: 36965
HEATHERLY, J. L., High-pressure gas mixing facility, 20: 36981 (Y-1546)
HECK, F. M., Conceptual design and preliminary accident analysis of a Na-cooled, carbide-fueled, large modular fast reactor, 20: 38456 (ANL-7120, pp 205-29)
HECK, F. M., Transient response of coupled fast reactor cores, 20: 38436 (ANL-7120, pp 776-88)
HECKROTTE, Warren, Interaction models, negative energy waves, and electrostatic instabilities, 20: 38273
HEDEMAN, E. Ruth, Related flares, 20: 37347
HEDGECOCK, P. C., Laboratory technique for simulating cosmic-ray threshold effects, 20: 37716
HEER, E., Production of charged pions by 600 Mev protons on various nuclei, 20: 38186
HEIDERSDORF, Sidney D., Alaska radiological health activities, 20: 37042
HEILIG, Walter, Treatment of cancerous metastases with small doses, 20: 36698
HEINZ, W. F., Parameters governing the response of the nuclear soil density gage, 20: 37020
HELD, Kalman, Nuclear radiation processing of optical maser materials, 20: 37280 (NYO-3330-11)
HELFER, H. L., Recent abundance determinations, 20: 37422
HELM, F. H., Sodium-void coefficients, 20: 38426 (ANL-7120, pp 598-602)
HELM, W. J., Nozzle tube-wall temperature measurement by radiometric techniques, 20: 38528
HELTERBRAN, Wayne, Travel times and amplitudes from the Salmon explosion, 20: 36967
HENCH, J. E., Nine-rod critical heat flux investigation at 1000 psia, 20: 38462 (GEAP-4929)
HENDEL, A., BASJE angle correlation, 20: 37629
HENDERSON, B., Dose dependence of F-center production by fast neutrons in Mg oxide, 20: 37998
HENDRICKSON, A. A., Strength of tantalum columbium alloy single crystals, 20: 37215
HENGLEIN, A., Radiation-chemical production and optical absorption spectra of organic S radicals in organic glasses at −196°C, 20: 36894
HENNELLY, E. J., Advantages of ^{60}Co for heat and radiation sources, 20: 37165
HENNEY, J., Phases in the Zr–C–O system, 20: 37264
HENNING, J. J., Amputated vertex functions of unstable particles, 20: 37753
HENTZ, Forrest C. Jr., Equilibrium ultracentrifugation of hydrolyzed Th(IV) solutions, 20: 36802
HERBER, Rolfe H., Moessbauer-effect studies of weak nuclear quadrupole interactions in ^{119}Sn, 20: 36816
HERBIG, G. H., Lithium in main-sequence stars, 20: 37421
HERBST, R. J., Compatibility of modified carbide fuels with stainless steel, 20: 38466 (ANL-7120, pp 301-13)
HERMANN, R., Gell-Mann formula for representations of semisimple groups, 20: 37832
HERRIN, Eugene, Epicenter determination for the Salmon event, 20: 36969
HERRING, F. G., ESR of x-irradiated single crystal of KH_2AsO_4, 20: 36884
HESKETH, R. V., Thermal annealing of heavy ion damage in copper, 20: 38378
HESS, J. W., Design and operating experience with control and safety rod drive mechanisms for Enrico Fermi Fast Breeder Reactor, 20: 38501 (APDA-301)
HETENYI, G. Jr., Glucose production rates in dogs determined by two different tracers and tracer methods, 20: 36565
HETHERINGTON, J. S., Apparatus for determining creep behavior under conditions of ultrahigh vacuum, 20: 37263
HEYN, Eugen, Eigenvalue problem of neutron age theory, 20: 37993
HEYNE, W., Fission recoil separation in mixtures with uranium dioxide powders as a simple method of range determination of fission products, 20: 37997
HIBNER, J., Semi-empirical determination of the fluctuation of the EAS μ component, 20: 37624
HIBNER, J., Some properties of μ-poor EAS, 20: 37610
HICKS, E. P., Theoretical studies on the fast reactor maximum accident, 20: 38434 (ANL-7120, pp 654-70)
HIGGINS, Frederick B. Jr., Natural radioactivity in ground water supplies in Maine and New Hampshire, 20: 37006
HIGGINS, G. T., Basic features of the isothermal promonotectoid transformation in a Zr–2.5Nb alloy, 20: 37234
HILBERG, Robert Henry, Polarization of photoprotons from beryllium, 20: 38146
HILL, John M., Growth of the British nuclear power program, 20: 38516
HILLAS, A. M., Calculations on the propagation of mesons in extensive air showers, 20: 37641
HILLMAN, Peter, Moessbauer study of the structure and decomposition of Wustite, 20: 38362
HILLS, H. K., Observations with University of Iowa equipment on Mariner IV, 20: 37341 (N-66-17354)
HILTON, D. A., Determination of ^{137}Cs in irradiated U and Th, 20: 36758
HILTON, D. A., Separation of ^{90}Sr and ^{137}Cs from fission-product solutions by anion exchange paper chromatography, 20: 36748
HILTON, L. K., University of Utah neutrino detector, 20: 37104
HIMMLER, U., Thermal annealing of lattice parameter change in low-temperature neutron-irradiated aluminium, 20: 38380
HINDS, S., Reactions $^{63,65}Cu(t,p)^{65,67}Cu$, 20: 38035
HINDS, S., Reaction (t,p) with even isotopes of Sm, 20: 38052
HINNOV, Elmar, Excitation and ionization rates of neon ions in a stellarator discharge, 20: 38250
HINOTANI, K., Direct measurement of attenuation length of extensive air showers, 20: 37642
HINOTANI, K., Observation of the character of EAS cores, 20: 37615
HINRICHS, C. K., High-energy neutral injection into a mirror-quadrupole cusp magnetic well, 20: 38277
HINTENBERGER, H., Cosmic ray produced lithium and calcium in iron meteorites, 20: 37603
HINTERBERGER, H., Efficient light coupler for threshold Cherenkov counters, 20: 37118
HINTON, Christopher, Potential contribution to electricity generation of hydroelectric power and nuclear energy, 20: 38511
HIRAI, Toshio, Thorium–ThC phase diagram, 20: 37265
HIRANO, Hiroshi, Texture and microstructure of thin-walled Zircaloy-2 tubes, 20: 37237
HIRAOKA, Eiichi, Radiography using ^{192}Ir, 20: 36994
HIRSHFIELD, J. L., Interference beats in pulse-stimulated cyclotron radiation, 20: 37776
HIRT, W., Production of charged pions by 600 Mev protons on various nuclei, 20: 38186
HISSONG, D. E., Protein electrophoretic changes following total-body irradiation of normal and tumor-bearing rats, 20: 36582
HO, Kuo-chu, Study of two-nucleon potential in nuclei by means of inelastic scattering, 20: 38120
HOBBS, G. D., Heat transmission through Langmuir sheath in presence of electron emission, 20: 38191 (CLM-R-61)
HOCKNEY, R. W., Computer simulation of anomalous diffusion, 20: 38328
HODGINS, J. W., Irradiated wood-polymer combinations, 20: 37145
HODSON, A. L., Large Wilson cloud chamber and its application to ionization calorimetry work, 20: 37108
HODSON, A. L., Particle counting in locally produced showers using vidicon television techniques, 20: 37114
HOEDT-RASMUSSEN, K., Compton scatter from low-energy gamma emitters and its significance to collimation, 20: 37465
HOEGDAHL, Ove. T., Determination of copper in hydrogenated fats by neutron activation analysis, 20: 36724
HOEHLER, G., Parameters of the Regge pole model for πN charge-exchange scattering, 20: 37761
HOELZL, K., Influence of the deuteron model on the inelastic electron-deuteron cross section, 20: 37748
HOFFMAN, Jerome, Control of plasma collision frequency for alleviation of signal degradation, 20: 38234
HOFFMANN, H., Spectra of photo-alpha particles from nuclei in the region $Z = 12$ to 30, 20: 38037
HOFMANN, D. J., Measurement of the isotopic composition of He nuclei in the primary cosmic radiation in the energy interval 80–150 Mev/nucleon, 20: 37579
HOFMEISTER, E., Evolution of a star of seven solar masses, 20: 37405
HOH, F. C., Onset of turbulence in the positive column, 20: 38331

HOHENSTEIN, Jack, Precision technique for measuring asymmetric distortions in optical lenses, 20: 37053
HOHLOCH, E., Energy width of virtual resonance levels in atomic nuclei, 20: 38013
HOLT, David, Coupling of degenerate modes of a microwave cavity due to the presence of a magnetized plasma, 20: 38332
HOLT, S. S., Measurements of neutrons produced by the cosmic radiation, 20: 37599
HOLYOAK, B., Theoretical studies of the muon component of EAS, 20: 37640
HOLZAPFEL, H., Study on the extraction of rare earths with tributyl phosphate. II., 20: 36938
HOLZBERLEIN, T. M., Transition probabilities for H_2, D_2, N_2, N_2^+, and CO, 20: 37438
HONDA, Naobumi, New approach to theory of relaxation in plasmas. II., 20: 38251
HONMA, Toshio, Thorium–ThC phase diagram, 20: 37265
HOPKINS, Ted E., Atomic parameters in the lanthanum trifluoride structure, 20: 36805
HOPPER, V. D., Cosmic-ray flux variation with height in the stratosphere, 20: 37552
HORN, D., Unitary spin analysis of neutrino reactions, 20: 37751
HORROCKS, D. L., Low-level alpha-disintegration rate determinations with a one-multiplier phototube liquid scintillation spectrometer, 20: 37082
HORTON, H. R., RSAC: Radiological safety analysis computer program, 20: 37167 (IDO-17151)
HOSAKA, Yoshinobu, Effects of process variables on the telomerization of ethylene with C tetrachloride induced by gamma radiation, 20: 36890
HOSAKA, Yoshinobu, Telomerization of ethylene with C tetrachloride induced by γ radiation under constant ethylene pressure, 20: 36891
HOSLER, W. R., Magnetization and critical fields of superconducting $SrTiO_3$, 20: 37953
HOUGH, Paul V. C., $\pi\pi$ resonances from 6 Bev/c π^-p interaction, 20: 37731 (BNL-10460)
HOUGHTON, A., Attenuation of longitudinal acoustic waves in type-II superconductors, 20: 37948
HOUGHTON, M. J., Simple contribution to the theory of the anisotropy of cosmic rays, 20: 37518
HOUTERMANS, F. G., Thermoluminescence of meteorites, 20: 37359
HOWARD, J. M., Digital computer study of the dynamics of the combined rotating unit shaft-bearing system, 20: 36977 (NAA-SR-11944)
HOWARD, N., New remotely controlled unit for treatment of uterine carcinoma, 20: 36687
HOWELL, M. Gertrude, Formula index to NMR literature data. Vol. 2, 20: 36842
HSIEH, Tze, Polarization of protons from the $^{12}C(d,p)^{13}C$ and $^{40}Ca(d,p)^{41}Ca$ ground-state reactions, 20: 38119
HSUE, S. T., Precise determination of the shape of the twice-forbidden beta spectrum of ^{137}Cs, 20: 38044
HU, Pang Nien, Neutral point in the geomagnetic field, 20: 37895
HUANG, Suei-rong, Radiation-induced decomposition of some inorganic sulfates, 20: 36903
HUANG, Y. C., Effect of zirconium on the thermodynamic and mechanical properties of niobium–nitrogen alloys, 20: 37274
HUB, K. A., Large metal-fueled fast reactor study. II., 20: 38494 (ANL-7120, pp 94-103)
HUBER, P., Reactions $D(d,n)^3He$ and $D(d,p)^3H$ with polarized deuterons at 460 kev, 20: 38074
HUBERLANT, M., Prog. rpt. on ESSOR fuel elements, final, 1–11/62, 20: 38480 (EUR-2522.f)
HUDSPETH, Emmett L., Reaction $^{90}Zr(d,p)^{91}Zr$ at energies below 4 Mev, 20: 38096
HUGGETT, R. W., Balloon experiment using spark chambers and an ionization spectrometer, 20: 37103
HUGGETT, R. W., High-energy jets produced by heavy primary nuclei of cosmic origin and their fragmentation products, 20: 37662
HUGGETT, R. W., Two-fireball and the CKP models of ultrahigh-energy interactions, 20: 37679
HUGHES, Thomas Aloysius, Nuclear two-body interaction and shell model studies of selected light- and medium-weight nuclei, 20: 38145
HUGHES, W. F., Electromagnetodynamics of fluids, 20: 37884
HULSE, E. V., Gastric emptying in rats after part-body irradiation, 20: 36628
HUMMEL, H. H., Recent investigations of fast reactor reactivity coefficients, 20: 38418 (ANL-7120, pp 413-20)
HUSMANN, Otto K., Critical temperatures for surface ionization and work functions of W–Re alloys, W, Re, and Ir, 20: 37277
HUTCHINSON, F. B., Radiation sterilization of sugar cane leafhoppers, 20: 37146
HUTCHISON, Dorris J., Chromosomal mapping by means of mutational induction in synchronous populations of Streptococcus faecalis, 20: 36635
HWANG, R. N., Comparison of Monte Carlo and resonance integral methods in determination of Doppler effects in fast reactors, 20: 38423 (ANL-7120, pp 462-77)
HWANG, R. N., Effect of fluctuations in collision density on fast-reactor Doppler effect calculations, 20: 38422 (ANL-7120, pp 449-61)
HWANG, R. N., Measurement and analysis of Doppler effect in Pu-fueled fast reactor assemblies, 20: 38427 (ANL-7120, pp 603-9)
HWANG, R. N., Recent investigations of fast reactor reactivity coefficients, 20: 38418 (ANL-7120, pp 413-20)
HYDE, K. R., Preparation of uranium nitride and carbonitrides from uranium oxide in a fluidized bed, 20: 36850
HYDER, A. K. Jr., Sulfur-36 $(p,\gamma)^{137}Cl$ reaction for proton energies in the 800-1800 kev region, 20: 38185
HYDER, A. K. Jr., 1505 kev resonance in $^{29}Si(p,\gamma)^{30}P$ and properties of ^{30}P levels, 20: 38062
HYNDS, R. J., Investigation of the modulation of the primary cosmic radiation using an airborne detector, 20: 37510

I

IBEN, I. Jr., Early evolution of stars between one and three solar masses, 20: 37402
ICHIBA, Katsuya, Functional test of a decontamination apparatus for radio-contaminated rainwater, 20: 37029
ICHIKAWA, Yoshi H., Ion oscillations in a weakly turbulent plasma, 20: 38269
ICHIMIYA, Tomo, Some problems in use of Langmuir probe on ionospheric sounding rockets, 20: 38309
IDA, Masakuni, High-energy elastic scattering at small momentum transfer, 20: 37796
IGNATENCO, I., Lifetime of the μ^- in ^{239}Pu, 20: 38114
IGO, G. J., Elastic scattering of 1 Bev protons from He and O, 20: 38010 (BNL-10438)
IHAMUOTILA, J., Generalized potential theory for stationary and kinetic control rod analysis of a thermal reactor, 20: 38448
IIDA, Y., Stabilizing effect of radial plasma density distribution on helical instability, 20: 38270
IIZUKA, Jugoro, Systematics and phenomenology of boson mass levels. III., 20: 37846
IKEYA, Motoji, Study of the enhancement of x-ray coloration of NaCl by divalent impurities, 20: 38373
ILIN, G. G., Plasma diagnostics based on the self-reversed contours of spectral lines emitted by inhomogeneous layers, 20: 38265
IMAMURA, Tsutomu, Plasma turbulence and quasi-linear approximation, 20: 38282
IMBUSCH, A., High resolution investigation of the energy losses of 30 kev electrons in aluminum foils of various thicknesses, 20: 37442
INGRAM, A. G., Effect of oxidation-protection coatings on the tensile behavior of refractory metal alloys at low temperature, 20: 37276
IMOTO, Minoru, Plastic scintillators. II., 20: 36847
IMOTO, Minoru, Plastic scintillators. III., 20: 36848
INGARD, Uno, Energy density in a plasma oscillation, 20: 38285
INGRAHAM, J. Charles, Anomalous plasma loss processes, 20: 38320
INGRAM, M. C., CUSH: program for steady-state hydraulic analysis of steam-generating reactor systems, 20: 38410 (AEEW-M-474)
INOPIN, E. V., Inelastic diffraction scattering, 20: 38142
INOZEMTSEVA, O. I., Possibilities of isolation of sidereal time cosmic-ray intensity variations, 20: 37506
INTERLENGHI, A. M., Recent developments of gas detectors visualizing tracks of charged particles, 20: 37043
INTHOFF, W., Derivation of an integrodifferential equation for the 2-particle density matrix, 20: 37829
INUISHI, Yoshio, Harmonic generation of ion cyclotron frequency in longitudinally magnetized plasmas, 20: 38252
IOFFE, Z. M., Comets in the solar wind, 20: 37386
IONA, M., Results from the new Denver multidirectional meson telescope, 20: 37095
IONESCU-BUJOR, Claudiu, Steady-state motions of perfect plasma in stationary magnetic field, 20: 38312
IONESCU-PALLAS, N. J., Semiclassical evaluation of some atomic quantities, 20: 37462
IONITSE, G., Double charge exchange of 50- to 176-Mev π^- mesons in photo emulsion, 20: 38012 (JINR-P-2806)
IRELAND, D. R., Multiaxial plastic flow of Zircaloy-2 determined from hardness data, 20: 37230
IRONS, F. E., Extreme ultraviolet spectra from laser-produced plasmas, 20: 38300
IRVING, J., Schlieren photography of rail-tube plasmas, 20: 38287
IRVING, Jack Howard, Wigner distribution functions in relativistic quantum mechanics. I and II., 20: 37930
ISABELLE, D. B., Coulomb form factors of ^{10}B and ^{11}B, 20: 38057
ISBIN, H. S., Two-phase flow through apertures, 20: 36990
ISEKI, S., Variation of the time of maximum in the diurnal variation of

cosmic-ray neutron intensity during IGY and IGC, 20: 37524
ISHIDA, Y., Variation of the time of maximum in the diurnal variation of cosmic-ray neutron intensity during IGY and IGC, 20: 37524
ISHIYAMA, Toshio, Decontamination of radioactive Ru. III., 20: 36929
ISHIYAMA, Toshio, Decontamination property of coal humic acid column, 20: 36930
ITIKAWA, Yukikazu, Moments of the velocity change of a charged particle in a magnetoplasma, 20: 38255
ITO, A. S., Scattering of positrons and electrons from protons, 20: 37778
ITO, N., Direct measurement of attenuation length of extensive air showers, 20: 37642
ITO, N., Observation of the character of EAS cores, 20: 37615
ITO, Tatuo, Studies in offspring of Wistar rats treated with anticancer drugs or x irradiation. III., 20: 36643
ITOH, Junkichi, NMR measurement of internal field and electric quadrupole interaction in ferromagnetic Dy metal, 20: 38374
ITOH, Noriaki, Study of the enhancement of x-ray coloration of NaCl by divalent impurities, 20: 38373
IUCCI, N., Daily latitude curves of cosmic-ray nucleonic component obtained in 1963 between 1 and 6.4 Gv, 20: 37584
IUCCI, N., Some properties of radiation recorded by IGY neutron monitors in lower atmosphere, 20: 37099
IVANENKO, I. P., Cascade theory of showers for light and heavy substances taking into account the polarization of the medium, 20: 37787
IVANENKO, I. P., Inverse problem in the cascade theory of showers, 20: 37650
IVANENKO, I. P., Processes of bremsstrahlung and pair production as they are regarded in the cascade theory of the showers, 20: 37788
IVANOV, E., Switching circuit for photomultiplier tubes, 20: 37051
IVANOV, V. Yu., Effects of cosmic rays according to the chromospheric flares and Forbush effects during solar activity minimum, 20: 37537
IVERSEN, C., Search for heavy particles in the cosmic radiation, 20: 37654
IVERSON, Richard L., Photosynthesis and uptake of ^{85}Sr in freshwater plankton, 20: 36568
IVLIEV, A. I., Decay $K \rightarrow \mu + \nu$ in μ-meson beam of cosmic rays 3860 m. above sea level, 20: 37482
IWAI, Mineko, Neutron activation analysis of human blood and hair, 20: 36728
IWASHITA, Fumio, Method for reprocessing an irradiated nuclear fuel, 20: 36943
IXARU, Liviu, Intensified tunnel effect for alpha particles, 20: 38117

J

JACKLYN, R. M., Two-way sidereal anisotropy versus seasonal modulation, 20: 37505
JACKSON, G., Effect of neutron flux on fission product gas emission from UO_2, 20: 38464 (AERE-M-1607)
JACKSON, J. E., System for observing small nonlinearities in tunnel junctions, 20: 37973
JACKSON, Wayne H., Crustal seismic measurements in Southern Mississippi, 20: 36965
JACQUET, F., Direct search for the C-violating decay $\eta^0 \rightarrow \pi^0 e^+ e^-$, 20: 37767
JAKES, D., Effect of some preparation conditions on the surface area and structure of ammonium polyuranate, 20: 36801
JANIK, B., Contribution to the study of DNA from irradiated tissues, 20: 36591
JANKUS, V. Z., Modified equation of state for hydrodynamic calculations in AX1 numerical program, 20: 38435 (ANL-7120, pp 686-91)
JARRETT, A. A., Development and growth of in-core voids due to boiling during fast reactor transients, 20: 38440 (ANL-7120, pp 881-9)
JAUNCEY, D. L., Studies of the cores of extensive air showers, 20: 37616
JEAN, P., Action of histamine liberators on calcification produced by various metals, 20: 36557
JEFFERIES, J. T., Loop prominences and coronal condensations. III., 20: 37348
JEFFERY, R. A., Deformation twinning in rhenium single crystals, 20: 37257
JEHENSON, Pierre, Powder metallurgy of SAP composites for nuclear applications, 20: 37210
JELLEY, J. V., Detection of radio pulses of wavelength 6.8 m, in coincidence with extensive air showers, in the energy region 10^{16}–10^{17} ev, 20: 37626
JELLEY, J. V., Theoretical considerations of the radiofrequency emission from extensive air showers, 20: 37625
JELLUM, Egil, Role of cystamine–nucleic acid interactions in protection against x-ray-induced damage of DNA, 20: 36665
JENDRYCHOWSKA-BONAMOUR, Anne-Marie, Radiochemical copolymerization of mixtures of styrene with acrylonitrile. I., 20: 36876
JENDRYCHOWSKA-BONAMOUR, Anne-Marie, Radiochemical copolymerization of mixtures of styrene with acrylonitrile. II., 20: 36877
JENDRYCHOWSKA-BONAMOUR, Anne-Marie, Radiochemical copolymerization of mixtures of styrene with acrylonitrile. III., 20: 36878
JENKIN, J. G., Threshold for the reaction $^{10}B(p,n)^{10}C$ and the ft value of the superallowed Fermi transition $^{10}C(\beta^+)^{10}B$, 20: 38069
JENKINS, G. M., Temperature dependence of the irradiation-induced creep of graphite, 20: 37223
JENKINS, R. W., Balloon studies of primary cosmic rays at solar minimum, 20: 37538
JENSEN, Eberhart, Opacity properties of sunspots, 20: 37354
JERVIS, R. E., Hair individualization studies, 20: 36781
JIGGINS, A. H., Voltage calibration of a 400-kv Van de Graaff machine, 20: 37331
JOERGENSEN, Chr. Klixbuell, Orbital energy differences and chemical bonding in rare earths, 20: 36845
JOHNSEN, K., Intersecting storage rings. Description of the project itself, 20: 37326
JOHNSON, A. J., Spectrographic determination of fluoride in plutonium nitrate solutions, 20: 36730
JOHNSON, C. E., SNAP-8 reactor and shield designs and operating experience, 20: 38527
JOHNSON, Everett R., Radiation-induced decomposition of some inorganic sulfates, 20: 36903
JOHNSON, Gerald W., Excavation with nuclear explosives. Promise and problems, 20: 36972
JOHNSON, J. L., Negative V'' stellarator, 20: 38243
JOHNSON, James E., Deposition of fallout ^{137}Cs on forage and transfer to milk, 20: 37036
JOHNSON, James E., Transfer of fallout ^{137}Cs from soil to dairy cattle feeds, 20: 37038
JOHNSON, James S., Equilibrium ultracentrifugation of hydrolyzed Th(IV) solutions, 20: 36802
JOHNSON, Kenneth G., Radiation-related leukemia in Hiroshima and Nagasaki, 1946–1964. I., 20: 36645
JOHNSON, M. L., Fuel and core materials for SEFOR, 20: 38531 (GEAP-5133)
JOHNSON, Roy R., Some correlated experimental and theoretical aspects of the finite amplitude helical instability, 20: 38318
JOHNSTON, Richard Walfred, Angular distributions and excitation functions of ground-state from $^{14}N(d,n)^{15}O$ reaction, 20: 38144
JOHNSTON, T. W., Particle kinetics of plasmas, 20: 38348
JOHNSTON, W. V., Control of swelling by nucleation, 20: 37302
JONES, Arthur W., Prog. rpt. on effects of radiation on host-parasite relationships, 6/54–6/66, 20: 36607 (TID-23114)
JONES, Billy Lorraine, Normal Fermi liquid theory for electrons in solids, 20: 38403
JONES, D. A., Cost estimate for remote refabrication of metallic fuels, 20: 37195 (ANL-6950)
JONES, D. E., Measurements of magnetic fields in vicinity of magnetosphere and in interplanetary space, 20: 37917
JONES, Dave C., Longevity in neutron-exposed guinea pigs, 20: 36640
JONES, G. D., Further measurements and zero-range DWBA calculations for the $^{52}Cr(d,p)^{53}Cr$ reaction, 20: 38046
JONES, H. M., Analysis of lumped burnable poison critical experiments, 20: 38441 (BAW-3492-1(Suppl.1))
JONES, J. K., Experiments on the pulse spectrum observed from scintillation and Cherenkov detectors at sea level, 20: 37619
JONES, J. K., Measurement of the time variations of small air showers, 20: 37649
JONES, J. W. S., Phases in the Zr–C–O system, 20: 37264
JONES, K. W., Conversion coefficient of the 12.4-kev transition in ^{45}Sc, 20: 38087
JONKE, A. A., Commercial aspects of fuel processing, 20: 36945
JONKE, A. A., Safety in chemical processing, 20: 36954
JORDAAN, J. M. Jr., Simulation of waves generated by underwater nuclear explosions, 20: 37306 (AD-636408)
JORDAN, James N., Travel times and amplitudes from the Salmon explosion, 20: 36967
JORDAN, K. R., Compatibility of modified carbide fuels with stainless steel, 20: 38466 (ANL-7120, pp 301-13)
JORDAN, P., Compensation of fluorescence extinguishing in scintillation counting, 20: 36743
JOSEPH, G., Flux of primary protons and helium nuclei and east-west and north-south asymmetries near the geomagnetic equator, 20: 37582
JOSEPH, G., Use of a gas Cherenkov counter for the study of the isotopic composition of He nuclei in primary cosmic radiation, 20: 37581
JOSEPHY, K., Drift wave excited anomalous diffusion in a fully ionized magnetoplasma, 20: 38203 (NP-16237)
JOSLIN, C. A. F., New remotely controlled unit for treatment of uterine carcinoma, 20: 36687
JOSSOUD, M., Grain moisture measurements with neutrons: application to the problems of conditioning and storage, 20: 37154
JOST, Klaus, Polarization of slow electrons by scattering on mercury between 180 and 1700 ev, 20: 37469
JULIANO, Jose O., Nuclear models, 20: 38118

JUNG, M., Heavy cosmic ions recorded in nuclear emulsions exposed in a polar satellite, 20: 37577
JUNG, Till, Consequences of irradiation to the face, especially to the dentures, 20: 36708

K

KACZMAR, U., Compensation of fluorescence extinguishing in scintillation counting, 20: 36743
KADMENSKII, S. G., Rotation of normal and superfluid Fermi systems, 20: 37473
KADYSHEVSKII, V. G., Inhomogeneous SL(6) group with an expanded translation subgroup, 20: 37835
KAHAN, R. S., Economic aspects of the food irradiation program in Israel, 20: 37157
KAHAN, R. S., Israel food irradiation program and progress during 1964–1966, 20: 37155
KAHN, Bernard, Recent advances in electrofluiddynamic power generation, 20: 37727
KAI, T., Study on the plasma proteins of patients who survived the A bomb, 20: 36581
KAIDALOV, A. B., Production of resonances at high energies and singularities in the complex j-plane, 20: 37804
KAINDL, K., International project on the irradiation of fruits and fruit juices, 20: 37156
KAINZ, Gerold, Instrument compensation of the quenching effects in determination of ^{14}C and ^{35}S, 20: 36771
KAISER, R., Heavy cosmic ions recorded in nuclear emulsions exposed in a polar satellite, 20: 37577
KALAGHER, R. J., Electron density and collision frequency in a radially inhomogeneous plasma column, 20: 38193 (INDEC-SR-7, pp 3.5-13)
KALBFLEISCH, George R., $\pi\pi$ resonances from 6 Bev/c π^-p interaction, 20: 37731 (BNL-10460)
KALBFLEISCH, George R., Properties of K* (1425), 20: 37733 (BNL-10462)
KALBFLEISCH, George R., Resonance production in the reactions $\pi^\pm$p → KKN at 6 Bev/c, 20: 37732 (BNL-10461)
KALINKOV, M., New scintillation hypothesis for the superstars and their connection with the galaxies, 20: 37358
KALMYKOV, N. N., Comparison of various models of EAS development with experimental data and the prospects of cosmological and nuclear aspects of EAS investigation, 20: 37646
KALOUSOVA, Vilma, Patho-anatomical findings in pigs whole-body irradiated with gamma rays, 20: 36657
KALVIUS, G. M., Quadrupole interaction in ^{121}Sb by Moessbauer techniques, 20: 38386
KAM, F., Military Compact Reactor program shield study, Suppl., 20: 38507 (NDA-Memo-2143-11)
KAMATA, K., Air showers at high altitude, 20: 37637
KAMEDA, T., Nuclear-active particles in extensive air showers near sea level, 20: 37620
KAMEDA, T., Possible nuclear interaction of a muon of energy above 3×10^{14} ev, 20: 37714
KAMEMOTO, Yuichiro, Behavior of polonium evaporated from fused salt, 20: 36736
KAMIMOTO, Goro, Langmuir probe measurements in a hypersonic plasma flow, 20: 38261
KAMINSKII, V. A., Role of unphysical partial-wave amplitude singularities in the deuteron photodisintegration, 20: 38140
KAMIYA, Y., Further observation of the positive excess of cosmic-ray muons, 20: 37690
KANAYA, K., Electrical optical properties of three-electrode electron lenses, 20: 37330
KANE, S. R., Studies of primary cosmic rays with ionization chambers, 20: 37508
KANEVSKAYA, E. A., Investigation of the nucleon interactions at energies above 10^{13} ev, 20: 37657
KANN, W. J., Faret Core-I reference design, 20: 38460 (ANL-7120, pp 766-75)
KANNO, T., Variation of the time of maximum in the diurnal variation of cosmic-ray neutron intensity during IGY and IGC, 20: 37524
KAPLAN, Morton, Energetics of the $^{27}Al(^{11}B,p3n)^{34m}Cl$ reaction from recoil studies, 20: 38084
KAPLIT, M., Models for electron emission from metals with adsorbed monolayers, 20: 37431 (INDEC-SR-7, pp 3.76-111)
KAPTEYN, Johanna C., Isomer of ^{98}Rh, 20: 38106
KAR, K. C., Theory of artificial transmutation of nuclei, 20: 38020
KARIMOV, A. L., Role of gamma treatment of oocytes in the realization of radiation injury of Drosophila sperm cells, 20: 36625
KARIUS, S., Monte Carlo studies on extensive air shower development, 20: 37647
KARKLIT, A. K., Thermodynamics of vaporization of refractory oxides at high temperatures, 20: 36841
KARNAKOV, B. M., Production of resonances at high energies and singularities in the complex j-plane, 20: 37804
KARPOV, V. N., Phase diagram of the system WO_3–Nd_2O_3, 20: 37240
KARPOV, V. N., Phase diagram of the system $Nd_2(WO_4)_3$–Na_2WO_4, 20: 37241
KARPUSHKINA, E. I., Photoexcitation and photoionization of energetic hydrogen atoms, 20: 38221
KARTASHOV, N. P., Rapid analysis of RaA aerosol concentration and of latent energy in the air, 20: 36733
KARTUSHIN, V. P., Effect of gamma radiation on flotation properties of anionic collector agents, 20: 36893
KARTUZHANSKII, A. L., Correlations of hidden image parameters in optical and nuclear photoemulsions, 20: 37121
KASCHLUHN, F., Exchange current and deuteron photodisintegration at threshold, 20: 38059
KASHCHEEV, N. F., Extraction of thorium with diisoamyl methylphosphonate from nitric acid solutions, 20: 36942
KASHIDA, Yoshihiko, Determination of ^{14}C and ^{3}H by liquid scintillation spectrometer. VI., 20: 36764
KASHIWASE, Yasuji, Attenuation of thermal neutrons by phonons in a single crystal. I., 20: 38371
KASHKAROV, L. L., Decay $K \to \mu + \nu$ in μ-meson beam of cosmic rays 3860 m. above sea level, 20: 37482
KASHY, E., Measurement of high-energy γ-rays with Ge(Li) detectors, 20: 37126
KASS, I. E., Underwater beacon, 20: 37158
KASSAL, Thomas Theodore, Reactions of deuterium atoms with olefins at 90°K, 20: 36856
KATAOKA, Takeshi, Ion exchange equilibria in the system of uranyl sulfate ion–Cl^- and NO_3^-, 20: 36931
KATMAN, T. S., Accuracy of power reactor void coefficients extrapolated from measurements in critical assemblies, 20: 38425 (ANL-7120, pp 585-97)
KATO, W. Y., Sodium-void coefficients, 20: 38426 (ANL-7120, pp 598-602)
KATYAL, M., Thorium–melanoxetin complex: a spectrophotometric study, 20: 36742
KATZ, Edward, Biosynthesis of highly labeled actinomycins, 20: 36545
KATZ, H. M., Fissile fuel recovery process, 20: 36955
KATZ, R. N., Twin-particle interaction in beryllium, 20: 37216
KATZENSTEIN, J., Co-operative scattering of laser light by a thetatron plasma, 20: 38259
KATZMAN, J., Changes in the cosmic-ray intensity close to the Zenith, 20: 37539
KATZMAN, J., Variation of the cosmic-ray intensity during the eleven-year solar cycle, 20: 37515
KAVLAKOV, S. T., Inelastic n-p cross section at 60 Bev, 20: 37670
KAWABATA, K., Origin of extragalactic cosmic rays, 20: 37502
KAWABATA, Keisuke, Luminescence of fused quartz excited with pulsed electrons, 20: 36864
KAWAGUCHI, S., Further observation of the positive excess of cosmic-ray muons, 20: 37690
KAWAKATSU, H., Electrical optical properties of three-electrode electron lenses, 20: 37330
KAWANISHI, Masaharu, Radiation damage in luminescence intensity of anthracene, 20: 37131
KAWASAKI, S., Air showers at high altitude, 20: 37637
KAWASHIMA, Toshihiko, Effects of additional elements on discontinuous precipitation in Cu–Be alloys, 20: 37253
KAZARINOV, Yu. M., Measurement of the triple scattering parameter R_{pn} at 70° and the phase-shift analysis at 630 Mev, 20: 37739 (JINR-E-2726)
KAZI, A. H., Selected optimization studies in the use of carbide fuel in large fast breeder reactors, 20: 38495 (ANL-7120, pp 104-23)
KCHUDYAKOV, A. V., Corpuscular ionizing radiation in space in the immediate vicinity of the Earth, 20: 37902
KEANE, A., Multigroup cross sections of resonance absorbers, 20: 38451
KECK, Gertrud, Measurements of radioactive fallout in the years 1963 and 1964, 20: 37008
KEDDY, R. J., Angular correlations for E2 and E3 transitions in Coulomb excitation, 20: 38032
KEECH, G. L., Direct measurements of the half-lives of some short-lived xenon and cesium isotopes, 20: 38017
KEHRER, R., Scattering of gamma rays and neutrons to investigate underground aquifers, 20: 37135
KEIL, R., Strontium-90 in Mecklenburg hay, 20: 36671
KELER, E. K., Chemistry of Ce in systems of $Al_2O_3CrO_3$, and Ga_2O_3 with Ce_2O_3, 20: 36808
KELER, E. K., Effect of europium oxide admixtures on the polymorphism of zirconium dioxide, 20: 36815
KELER, E. K., Reactions of La and Nd oxides with oxides of elements of groups III and IV, 20: 36840
KELLER, Donald L., Prog. rpt. on civilian applications, 4/66, 20: 37168 (BMI-1771)
KELLER, Donald L., Prog. rpt. on civilian applications, 5/66, 20: 37169

(BMI-1774)
KELLERMANN, E. W., Comparative response of Cherenkov and scintillator detectors to large air showers, 20: 37621
KELLERMANN, E. W., Spectrum of the nuclear-active component of cosmic rays, 20: 37674
KELLY, T. M., Positron lifetimes in low-temperature helium gas, 20: 37817
KELMAN, L. R., Metal fuels for fast reactors, · 20: 38465 (ANL-7120, pp 289-300)
KEMP, E. L., Scyllacita: compact high-voltage theta pinch machine, 20: 38306
KEMP, E. L., Straight θ-pinch devices energized by energy storage supply of Scyllac, 20: 38197 (LA-3553)
KENDE, Andrew S., Formula index to NMR literature data. Vol. 2, 20: 36842
KENDRICK, E. D. Jr., Elk River Reactor spent fuel shipping cask criticality analysis, 20: 38486 (ACNP-66551)
KENDZIORSKI, F. R., Sulfur-36 (p,γ)^{137}Cl reaction for proton energies in the 800-1800 kev region, 20: 38185
KENNA, B. T., Ratio of induced fission vs. spontaneous fission and the trace element analysis in pitchblende, 20: 37994
KENNALLY, James R., Oxygen-tube combustion method for liquid scintillation assay of ^{14}C and tritium, 20: 36723
KENNEL, Charles F., High ion β pitch-angle instability, 20: 38295
KENNETT, T. J., Estimation of nuclear strength functions, 20: 38038
KENNY, A. W., Radium, radon, and daughter products in drinking waters in Great Britain, 20: 37031
KEPAK, F., Sorption of ^{131}I on hydrated Fe_2O_3, 20: 36800
KERR, J. R. W., Radium, radon, and daughter products in drinking waters in Great Britain, 20: 37031
KERR, R. G., Neutrons from deuteron breakup on ^{3}He, 20: 38077
KERST, Donald W., Fusion-research apparatus, 20: 38341
KESSEL', A. R., Theory of the processes occurring in nuclear quadrupole resonance, 20: 38019
KESSLER, Joachim, Polarization of slow electrons by scattering on mercury between 180 and 1700 ev, · 20: 37469
KEUFFEL, J. W., University of Utah neutrino detector, 20: 37104
KEVAN, Larry, Paramagnetic relaxation of trapped electrons in irradiated alkaline ices, 20: 36871
KHACHATRYAN, B. V., Transitional radiation during oblique incidence on film, · 20: 37434
KHAN, J. M., Characteristic x-ray production in single crystals (Al,Cu) by proton bombardment. I., · 20: 38393
KHANNA, K. M., Electron-positron annihilation by Bogoliubov canonical transformation, 20: 37757
KHAPAEV, M. M., Focusing of beams of fast charged particles in stellerator type fields, 20: 37334
KHELASHVILI, A. A., Broken Ū(12) symmetry and unitarity condition for the S matrix, 20: 37855
KHIRENOV, B. A., Underground investigation of the penetrating component of high-energy cosmic radiation, 20: 37693
KHOPKAR, S. M., Cation exchange studies of Tl(I) on Dowex 50W-X8: separation from mixtures, 20: 36935
KHRIMIAN, A. V., Shower production by pions and protons with momenta 0.1 and 20 Bev/c in thin layers of matter, 20: 37669
KHRISTIANSEN, G. B., Comparison of various models of EAS development with experimental data and the prospects of cosmological and nuclear aspects of EAS investigation, 20: 37646
KHRISTIANSEN, G. B., Energy spectrum, possible chemical composition, and anisotropy of ultrahigh-energy primary cosmic radiation, 20: 37651
KHRISTIANSEN, G. B., Study of the extensive air showers with fixed μ meson number and with fixed electron number, 20: 37644
KHRISTIANSEN, G. B., Underground investigation of the penetrating component of high-energy cosmic radiation, 20: 37693
KHRISTOV, V., Reactivity response and effective absorption cross sections in reactors, · 20: 38414
KHROMKOV, I. N., Paramagnetic high-frequency effect and electron paramagnetic resonance in plasma, 20: 38220
KHUDAVERDYAN, A. G., Gamma-gamma angular correlation in ^{131}Cs nuclei, 20: 38021
KHUSNUTDINOV, R. I., Determination of Ir in Cu and Ni slugs and Pt concentrates by neutron activation analysis, 20: 36751
KHUSNUTDINOV, R. I., Preparation of Ir and Rh standard solutions by electrolytic dissolution, 20: 36775
KHVOSTOVA, V. V., Cytogenetic analysis of the mutagenic effect of ionizing radiation and alkylating compounds in peas, 20: 36621
KHVOSTOVA, V. V., Influence of partial reparation of the damaging effect of irradiation on the frequency of chlorophyll mutations in barley, 20: 36622
KHVOSTOVA, V. V., Mutations in spring wheat Lutescens 62 treated with fast neutrons and gamma rays, 20: 36620
KIBLER, K. G., Angular distributions of protons and deuterons from ^{6}Li + ^{6}Li as a function of energy, 20: 38172
KICK, H., Calibration-curve-obtained emission spectrographic ^{15}N determination with the Q24-Zeiss spectrograph, 20: 36772
KIDO, Yasumasa, Functional test of a decontamination apparatus for radiocontaminated rainwater, 20: 37029
KIEFHABER, E., Survey parameter study of large steam-cooled fast power reactors, · 20: 38438 (ANL-7120, pp 815-25)
KIEL, R. E., Electrostatic probe in a collisionless plasma, 20: 38278
KIENZLE, W., Evidence for three new charged bosons of masses 1929, 2195, and 2382 Mev and narrow widths, 20: 37771
KIGOSHI, K., Variation of ^{14}C content in the atmosphere during the past two thousand years, 20: 37602
KIKUCHI, Chihiro, Changes in the conductive properties of CdS induced by thermal neutrons, · 20: 38405
KILIAN, P., Flood safety of steam- and gas-cooled fast reactors, · 20: 38439 (ANL-7120, pp 826-36)
KIM, L., Homotransplantation studies in dogs following selective radioisotopic lymphatic ablation, 20: 36641
KIM, S. M., Motion of positrons in sodium, 20: 37784
KIMELDORF, Donald J., Longevity in neutron-exposed guinea pigs, 20: 36640
KIMMEL, H., Investigations of radiation defects in GaP by means of electron resonance, · 20: 38399
KIND, A., Application of a phenomenological thermalization model to irradiated heavy water lattices, · 20: 38455
KING, R. D., Dose dependence of F-center production by fast neutrons in Mg oxide, 20: 37998
KINNEBERG, Bruce I., Spectrofluorometric analysis of rare earth chelates of thenoyltrifluoroacetone, benzoylacetone, and dibenzoylmethane by computer spectrum stripping techniques, 20: 36722
KINO, S., Direct measurement of attenuation length of extensive air showers, 20: 37642
KINO, S., Observation of the character of EAS cores, 20: 37615
KIPPENHAHN, R., Evolution of a star of seven solar masses, · 20: 37405
KIRILLOV-UGRYUMOV, V. G., Angular distribution and energy spectrum of cosmic-particle showers at 10^{12} ev, 20: 37696
KIRKBRIGHT, G. F., Determination of trace amounts of copper in niobium and tantalum by atomic-absorption spectroscopy, 20: 36726
KIRKBY, P., Faraday-cup measurement of proton total reaction cross sections at 100 Mev, 20: 38018
KIRKPATRICK, M. E., Investigation of porous tungsten formed from spherical tungsten powders, 20: 37199
KIROCHKIN, Yu. A., Theory of fluctuations in magnetoactive plasma, 20: 38200 (NP-16206)
KIRSCHMAN, J. C., ^{14}C-labeled polyoxyethylene (20) sorbitan monolaurate and metabolic fate in rats, 20: 36921
KISLYI, P. S., Conversion of ZrB_{12} into ZrB_2, 20: 36810
KISO, Yoshiyuki, Preliminary study of the determination of hydrogen content in heavy water by means of neutron transmission, 20: 36740
KISSELBACH, V. J., Barometric correction anomaly and nucleonic component time variations during IQSY, 20: 37096
KISSELBACH, V. J., Galactic cosmic-ray source and loss problem, 20: 37484
KISSELBACH, V. J., Results from the new Denver multidirectional meson telescope, 20: 37095
KISSINGER, H. E., Vacancy and interstitial clusters in neutron-irradiated nickel, · 20: 38367
KISSLINGER, L. S., Tests of unitarity symmetry in nuclei by nucleus-hypernucleus reactions, 20: 38009 (BNL-10420)
KITAGAWA, Michiharu, Conduction carriers in neutron-irradiated ZnS single crystals, 20: 36865
KITAGAWA, Toshio, Clinical evaluation of the treatment of advanced head and neck cancers with high-energy electron beams, 20: 36685
KITAMURA, M., Solar diurnal variation of the cosmic-ray intensity, 20: 37519
KITTEL, J. H., Metal fuels for fast reactors, · 20: 38465 (ANL-7120, pp 289-300)
KIZEL, V. A., Structure of glasses of the Na_2O–B_2O_3 system activated with rare earths. Europium, 20: 36813
KLEIN, Siegfried, Formation of negative ions in a flame by measurement of the Hall effect, 20: 38223
KLEPIKOV, N. P., Design and theory of magnetic spectrometer for measurement of cosmic-ray mesons, · 20: 37487
KLEPPNER, Daniel, Absolute value of the proton g factor, 20: 3777
KLIMANOVA, L. F., Inelastic neutron cross section measurements near 100 Bev, 20: 37668
KLIMENKOV, V. M., Decay $K \rightarrow \mu + \nu$ in μ-meson beam of cosmic rays 3860 m. above sea level, · 20: 37482
KLINGELHOEFER, R., Electrical breakdown in beams of condensed hydrogen and condensed nitrogen in high vacuum, 20: 38247
KLOVNING, A., Search for heavy particles in the cosmic radiation, 20: 37654
KLYUCHAREV, A. P., Isomers of ^{131m}La and ^{136m}La, 20: 38125
KLYUEVA, E. D., Effect of γ radiation on flotation properties of anionic

collector agents, 20: 36893
KNECHT, David J., Proton-proton scattering: revision and analysis of experimental measurements from 1.4 to 3.0 Mev, 20: 38081
KNEZEVIC, Zvonko, Polonium-210 amount in tobacco. Determination of Po in the environment, 20: 37030
KNIGHT, F. W., Mixed oxide fuel movement at various power levels and in transients, 20: 38473 (ANL-7120, pp 524-33)
KNIGHT, F. W., Safety and economic aspects of vented fuel in sodium-cooled reactors, 20: 38475 (ANL-7120, pp 540-8)
KNIGHT, J. D., Reactions (t,p) and (t,α) on ^{48}Ca and ^{50}Ti, 20: 38063
KNIPPER, A., Angular distribution, angular correlations, and plane polarization of gamma rays of the reaction ^{53}Cr(p,n)^{53}Mn, 20: 38034
KNIPPER, A., Half lives of levels at 405 kev in ^{211}Bi and 377 kev in ^{53}Mn, 20: 38030
KNIPPER, A. C., Application of the delayed coincidence technique to measurement of the short mean lives in ^{131}Xe and ^{143}Pr, 20: 38031
KO, W. H., Sodium distribution in thermal oxide on silicon by radiochemical and MOS analysis, 20: 36744
KOBA, Teresa, 10-MHz linear window amplifier, 20: 37048
KOBAYASHI, Shun-ichi, NMR measurement of internal field and electric quadrupole interaction in ferromagnetic Dy metal, 20: 38374
KOBAYASHI, T., New kinematical approach for analyses of high-energy cosmic-ray jets, 20: 37680
KOBAYASHI, Yutaka, p-Bis-(o-methylstyryl)benzene, useful secondary fluor for liquid scintillation counting, 20: 36862
KOBZAREV, I. Yu., Possibility of observing mirror parsticles, 20: 37806
KOBZEV, A. P., Cross section of D(t,α)n in the energy region at 115 to 1650 kev, 20: 38130
KOCEVAR, P., Influence of the deuteron model on the inelastic electron-deuteron cross section, 20: 37748
KOCH, H., Neutron activation analysis of luminophorescent zinc compounds. I., 20: 36755
KOCH, H., Neutron activation analysis of luminophorescent Zn compounds. II., 20: 36756
KOCH, H., Neutron activation analysis of luminophorescent Zn compounds. III., 20: 36757
KOCH, L., Energy spectrum of primary galactic x rays between 20 and 50 kev, 20: 37580
KOCH, L., Use of semiconductor telescopes in charge and energy spectrometry of cosmic particles, 20: 37575
KOCHAROV, G. E., Solar neutrinos, 20: 37377
KOCHER, L. F., Personnel neutron dosimeter developments, 20: 37070 (BNWL-SA-537)
KODAMA, M., Geographic distribution of vertical cosmic-ray threshold rigidities, 20: 37595
KOECHLIN, Y., Flux and east-west asymmetry of primary electrons at a geomagnetic rigidity cut-off of about 4.5 GV, 20: 37550
KOESTER, Charles J., Clinical studies in laser photocoagulation, 20: 36682
KOESTER, Charles J., Prophylactic photocoagulation of recurrent toxoplasmic retinochoroiditis, 20: 36683
KOFOID, Melvin J., Permanently magnetized ferrite antenna windows for improving electromagnetic wave transmission through a plasma, 20: 38231
KOIAVA, V. K., Frequency distribution of sudden changes of cosmic-ray intensity in connection with solar activity, 20: 37541
KOIAVA, V. K., Some results of comparison of cosmic-ray intensity variations with the H component of the earth's geomagnetic field during IGY and IGC, 20: 37590
KOLBANOVSKII, Yu. A., Kinetics of radiation polymerization of acrylonitrile from the gas phase on a mineral substrate, 20: 36882
KOLESNIKOVA, E. N., Stability of a compressible gravitating cylinder of uniform density in a longitudinal magnetic field, 20: 38311
KOLOMEETS, E. V., Effects of cosmic rays according to the chromospheric flares and Forbush effects during solar activity minimum, 20: 37537
KOLOMEETS, E. V., Periodic cosmic-ray variations and their change during the cycle of solar activity, 20: 37525
KOLOMENSKII, A. A., Stability of transverse oscillations of a focused charged beam in an absorbing medium, 20: 38315
KOLOVANDIN, B. A., Experimental study of the structure of electrically conducting turbulent liquid flow, 20: 37868
KOLOVANDIN, B. A., Stability of conducting free surface fluid in the presence of magnetic and electric fields, 20: 37874
KOMAROV, V. N., Calculation method for azeotropic steam fractionation, applied to the TBP–CCl_4 system, 20: 36731
KOMISSAROVA, L. N., Solid solution region in system Sc_2O_3–Fe_2O_3–MnO_x, 20: 36839
KOMORI, H., Rigidity spectrum of primary cosmic rays, 20: 37543
KONDO, I., Geographic distribution of vertical cosmic-ray threshold rigidities, 20: 37595
KONDO, I., Modulation of cosmic-ray threshold rigidity due to geomagnetic cavity field, 20: 37596
KONDO, I., Observation of muon air showers, 20: 37607
KONDROR, V. I., Hypophyseal-adrenal system in development of symptoms of radiation-induced pathology, 20: 36668
KONIN, A. D., Muon capture in mixed gases, 20: 37741 (JINR-P-2788)
KONOPLYA, S. P., Mutations of cotton plant Gossypium barbadense, 20: 36623
KONYAEVA, M. P., Effect of irradiation on aminotransferase of central nervous system and muscle, 20: 36601
KOOI, E., Influence of heat treatments and ionizing irradiations on the charge distributions and the number of surface states in the Si–SiO_2 system, 20: 37285
KOONTZ, R. L., Errors in measurements of building leakage due to dynamic temperature effects, 20: 36978 (NAA-SR-12001)
KOPAL, Zdenek, Advances in astronomy and astrophysics. Vol. 4, 20: 37342
KOPALEISHVILI, T. I., Reactions (π^z,NN) and two-particle excitation of light nuclei, 20: 38070
KOPALEISHVILI, T. I., Reaction (π^-,nn) and models of the ^{6}Li nucleus, 20: 38137
KOPEIKIN, V. A., Thermodiffusive interaction of tantalum and boron carbide powder in a vacuum, 20: 36809
KOPPE, V. T., CO, CO_2, and NO emission spectra excited by 13-kev electrons, 20: 37466
KORCHEMKIN, M. A., Theory of the processes occurring in nuclear quadrupole resonance, 20: 38019
KORECZ, L., Study of back coordination in iron chelates by the Moessbauer method, 20: 36823
KORFF, S. A., Measurements of neutrons produced by the cosmic radiation, 20: 37599
KORIDZE, V. G., Frequency distribution of sudden changes of cosmic-ray intensity in connection with solar activity, 20: 37541
KORKHAUS, Gustav, Consequences of irradiation to the face, especially to the dentures, 20: 36708
KORN, A., Exact solutions of Milne's problem for 2 half spaces with different media, 20: 38003
KOROCHKINA, L. M., Effect of ultrasound on the ductility of high-boron stainless steels, 20: 37221
KOROGODIN, V. I., Kinetic regularities in the postradiation recuperation of cells, 20: 36642
KOROLEVA, V. P., Measurement of absorption cross sections for fast neutrons by resonance detector in water, 20: 37990
KORYAKIN, Yu. I., Economic aspects for stimulating nuclear power, 20: 38512
KOSIANCIC, Eugene J., Investigation of denitration of high-nitrate plutonia sols by baking, 20: 36786 (ORNL-TM-1558)
KOSTINER, E., Moessbauer effect in $MnFeO_3$, 20: 36817
KOTTOWSKI, H., Investigations of boiling of liquid metals in forced convection, 20: 38415
KOVAL, A. G., CO, CO_2, and NO emission spectra excited by 13-kev electrons, 20: 37466
KOVALCHUK, V. G., Scattering of slow neutrons, 20: 38002
KOVALENKO, P. N., Electrolytic separation of lead from microquantities of thorium and uranium and their photometric determination, 20: 36773
KOYAMA, Hideyuki, Mass differences and a deformed octet axial-vector current, 20: 37795
KOZHEVNIKOV, D. A., Theoretical investigations in nuclear geophysics in the USSR, 20: 37001
KOZHINA, I. I., Some properties of U_2O_5, 20: 36832
KRAMER, G., X-ray photoconductivity of anthracene, 20: 36873
KREBS, Adolph T., Radiation-induced premature aging in leaves and autumnal events in nature, 20: 36609
KREMP, D., Short-range forces in statistical mechanics of plasma and electrolyte, 20: 38212
KREPLIN, R. W., Observations of hard x-ray emission from solar flares, 20: 37360
KRESIN, V. Z., Superconducting transition temperature of a thin film, 20: 37980
KRIMIGIS, S. M., Observations with University of Iowa equipment on Mariner IV, 20: 37341 (N-66-17354)
KRIMSKY, G. F., Angular dependence of coupling coefficients of the muon component of cosmic rays, 20: 37588
KRIMSKY, G. F., Diffusion mechanism of cosmic-ray daily variation, 20: 37517
KRIMSKY, G. F., First and second spherical harmonics of the daily variations of cosmic rays, 20: 37531
KRIMSKY, G. F., Investigation of cosmic-ray distribution using the method of daily variations, 20: 37587
KRISHNA, C. S., Energy spectrum of primary He nuclei at energies greater than 6 Bev, 20: 37557
KRIVOSHAPKIN, P. A., Angular dependence of coupling coefficients of the muon component of cosmic rays, 20: 37588
KRIVOSHAPKIN, P. A., First and second spherical harmonics of the daily variations of cosmic rays, 20: 37531
KRIVOSHAPKIN, P. A., Investigation of cosmic-ray distribution using the

method of daily variations, 20: 37587
KRIVSKY, L., Relation between proton flares and the corona in the 11-year cycle, 20: 37886
KROCK, R. H., Fiber-reinforced and continuous-skeleton W–Cu composite materials, 20: 37246
KROH, J., Radiation-induced isotope exchange in some C_6-hydrocarbons, 20: 36866
KROH, J., Radiation-induced H-T exchange in aromatic hydrocarbons saturated with tritiated water, 20: 36868
KROH, J., Temperature effects in x-ray radiolysis of frozen Fricke solutions, 20: 36867
KROL-KONING, C., Specific gamma emission of natural K and La, 20: 38107
KRONAST, B., Experiments on scattering laser light by thermal density fluctuations in a plasma, 20: 38336
KRONIG, R., Rigorous solution of Dirac' equation, 20: 37920
KRUEGER, A. F., Transient radiation effects on insulated gate field effect transistors, 20: 37132
KRUG, H. E., Comparison of Monte Carlo and resonance integral methods in determination of Doppler effects in fast reactors, · 20: 38423 (ANL-7120, pp 462-77)
KRUGER, O. L., Mixed-carbide fuels for fast reactors, · 20: 38467 (ANL-7120, pp 314-27)
KRUGLYKH, A. A., Purification of cerium by electric transport combined with zone melting, 20: 36936
KRUPENNIKOVA, N. B., Reactions ($\pi^{\pm}$,NN) and two-particle excitation of light nuclei, 20: 38070
KRUSKAL, M. D., First correction to the second adiabatic invariant of charged-particle motion, 20: 38275
KRYLOV, A. I., Decay of ^{139}Cs and ^{140}Cs, 20: 38124
KRZYWOBLOCKI, M. Z. V., Recent concepts on plasma optimal controllability. I., 20: 38304
KUBO, Kazuko, Effects of proton bombardment on CaF_2 crystals, 20: 38372
KUDO, S., Anisotropy of cosmic rays in the direction parallel to the rotation axis of the Earth, 20: 37540
KUDO, S., Variations of the latitude dependence of cosmic-ray diurnal variations, · 20: 37523
KUEHN, W., Continuous gas analyses by means of x-ray fluorescence, 20: 36766
KUEHNER, J. A., Particle angular correlations following nuclear reactions, 20: 38179
KUESTERS, H., Influence of some important group constants on integral fast reactor quantities, · 20: 38420 (ANL-7120, pp 423-33)
KUHI, L. V., T Tauri mass ejection, · 20: 37414
KUKS, I. M., Device for estimating AgBr microcrystal energy threshold sensitivity to charged particles, 20: 37122
KULIK, I. O., Motion of Abrikosov lines and energy dissipation in homogeneous superconductors, 20: 37979
KULIKOV, G. V., Energy spectrum, possible chemical composition, and anisotropy of ultrahigh-energy primary cosmic radiation, 20: 37651
KULKARNI, V. G., Lifetimes of positronium in polymers irradiated by gamma rays, 20: 36896
KULYUKIN, M. M., Capture of pions by ^{3}He. II., 20: 38011 (JINR-P-2805)
KUMAR, Aditya, Current commutation relations, universality, and nonleptonic baryon decays, 20: 37839
KUMAR, Krishna, Quantum-mechanical fluctuations and tunneling effects in ^{154}Sm, · 20: 38408
KUNIMOTO, Nobuo, Texture and microstructure of thin-walled Zircaloy-2 tubes, 20: 37237
KUNKEL, W., Fission product retention in sodium and applications to vented fuel element design, · 20: 38477 (ANL-7120, pp 855-61)
KUNSEMILLER, D. F., Multirod, forced flow, transition and film boiling measurements, 20: 36986 (GEAP-5073)
KUNTE, P. K., Flux of primary protons and helium nuclei and east-west and north-south asymmetries near the geomagnetic equator, 20: 37582
KUO, T. T. S., Reaction matrix and effective shell-model interactions for the Ni isotopes, 20: 38066
KUPER, A. B., Sodium distribution in thermal oxide on silicon by radiochemical and MOS analysis, 20: 36744
KUPSCH, J., Moeller operators for scattering on singular potentials, 20: 37831
KURNOSOVA, L. V., Some results of the investigation of the primary cosmic-ray nuclei on the artificial satellite Electron-2, 20: 37600
KUROYA, H., Variation of ^{14}C content in the atmosphere during the past two thousand years, 20: 37602
KUSHAKOVSKII, V. I., Growing BeO single crystals, 20: 36814
KUSHAL, R. D., Analysis of 14 Mev elastic neutron scattering from K, 20: 38171
KUSMISS, J. H., Positronium formation in certain metal oxides, 20: 37819
KUTZIM, Heinrich, Physiology and clinical course of iodine metabolism, 20: 36570
KUZENKOVA, M. A., Conversion of ZrB_{12} into ZrB_2, 20: 36810
KUZMA, Yu. B., X-ray investigation of Nb–W–B, 20: 37261
KUZ'MICHEV, Yu. S., Effect of ultrasound on the ductility of high-boron stainless steels, 20: 37221
KUZMIN, A. I., First and second spherical harmonics of the daily variations of cosmic rays, 20: 37531
KUZMIN, A. I., Investigation of cosmic-ray distribution using the method of daily variations, 20: 37587
KUZMIN, V. A., Neutrino spectroscopy of the Sun, · 20: 37378
KUZMIN, V. A., Thermometry of the solar interior by neutrino experiments, 20: 37380
KUZNETSOV, S. N., Earth's radiation belt, 20: 37899
KUZNETSOVA, V. A., Elastic scattering of γ quanta on protons above π-meson photoproduction threshold, 20: 37800
KVITEK, J., Alpha decay from excited states of Sm isotopes, 20: 38072
KYAZIMOV, E. A., Kinetics of radiation polymerization of acrylonitrile from the gas phase on a mineral substrate, 20: 36882

L

LABEYRIE, J., Gamma-ray generation in the high atmosphere, 20: 37576
LADET, J., Contribution to safety problems related to 1000-Mwe fast power reactor project, 20: 38497 (ANL-7120, pp 157-61)
LAFFERTY, Robert H. Jr., Isotopes and Radiation Technology. Vol. 3, Number 3, 20: 37136
LAGET, J. M., Reactions (^{3}He,d) on even Sn isotopes, 20: 38073
LAGU, R. G., Lifetimes of positronium in polymers irradiated by gamma rays, 20: 36896
LAHIRI, J., Self-consistent perturbation method. I., · 20: 37440
LAI, Kwan Wu, Properties of K* (1425), 20: 37733 (BNL-10462)
LAI, Kwan Wu, Resonance production in the reactions $\pi^{\pm}p \to KKN$ at 6 Bev/c, 20: 37732 (BNL-10461)
LAING, E. W., Stochastic motion of particles in a non-adiabatic magnetic trap, 20: 38246
LAJTHA, L. G., Cytokinetics and regulation of progenitor cells, 20: 36594
LAKH, V. I., X-ray investigation of Nb–W–B, 20: 37261
LAKNER, John F., High pressure consolidation of submicron tungsten, 20: 37200
LAKOSI, L., High-accuracy fluid-density gage, 20: 37059
LAL, D., Some aspects of astrophysical studies based on observations of isotopic changes, · 20: 37369
LAL, S., Ultra-high energy muons (>200 Bev) in extensive air showers, 20: 37606
LALOU, Claude, Experimental study of dispersion of fallout nuclear debris in sea water, 20: 37037
LAMBERT, D. G., Detection, analysis, and interpretation of teleseismic signals. I., 20: 36968
LANDSMAN, D. A., Preparation of uranium nitride and carbonitrides from uranium oxide in a fluidized bed, 20: 36850
LANDSPERSKY, H., Effect of some preparation conditions on the surface area and structure of ammonium polyuranate, 20: 36801
LANDSPERSKY, Hanus, Activated sintering of UO_2, 20: 37202
LANGDON, Bruce, Higher-order corrections to the Chew-Goldberger-Low theory, 20: 38271
LANGELIER, R. M., Radiation from a vertical dipole in a warm plasma. I., 20: 38229
LANGELIER, R. M., Radiation from a vertical dipole in a warm plasma. II., 20: 38230
LANGENDORFF, Hanns, Effects of small irradiation doses and low-dose outputs, 20: 36652
LANGER, L. M., Precise determination of the shape of the twice-forbidden beta spectrum of ^{137}Cs, 20: 38044
LANGEROVA, I., Determination of potassium in biological material by various methods of neutron-activation analysis, 20: 36735
LAPIDOT, M., Economic aspects of the food irradiation program in Israel, 20: 37157
LAPIDOT, M., Israel food irradiation program and progress during 1964–1966, 20: 37155
LAPORTE, O., Resistance of a plasma slab between juxtaposed disk electrodes, 20: 38293
LAPSHOV, Yu. K., Production and properties of W–LaB_6, 20: 37258
L'ARCHEVEQUE, R. V., Time of flight encoder using integrated circuits, 20: 37067 (AECL-2578)
LARSON, L. T., Determination of the basal-pole orientation in zirconium by polarized-light microscopy, 20: 37266
LASHINSKY, H., Quiescent-plasma research program at the University of Maryland, 20: 38325
LASOTA, Jan Piotr, Relativistic astrophysics, · 20: 37367
LATIMER, T. W., Mixed-carbide fuels for fast reactors, · 20: 38467 (ANL-7120, pp 314-27)
LAUFFENBURGER, Ivan, Incorporation of uranyl cations in carbonates during formation, 20: 36796
LAUFFENBURGER, Ivan, Incorporation of uranyl cations in silicates during formation, 20: 36797

LAUGHLIN, Ronald L., Radiological investigations at Neotoma, 20: 36548 (TID-23036)
LAVAKARE, P. J., Abundance of ^{3}He nuclei in the primary cosmic radiation, 20: 37559
LAVAKARE, P. J., Heavy nuclei in the primary cosmic rays in June 1963 at Fort Churchill, 20: 37568
LAWRENCE, J. H., Homotransplantation studies in dogs following selective radioisotopic lymphatic ablation, 20: 36641
LAWRENCE, L. A. J., Development of redundancy techniques for the achievement of highly reliable autocontrol for nuclear reactors, 20: 38417
LAWROSKI, Stephen, Reactor Fuel Processing. Vol. 9. Number 2, 20: 36944
LAWSON, Neel S., Acridine orange and dye exclusion viability tests applied to irradiated Ehrlich tumor cells, 20: 36631
LAWSON, R. D., Reaction matrix and effective shell-model interactions for the Ni isotopes, 20: 38066
LAYZER, David, Significance of the cosmological energy equation, 20: 37352
LAZAREV, E. M., Kinetics and activation energy of oxidation of alloys of the Nb–V–Ti system, 20: 37191
LEAKEY, G. A., Time of flight encoder using integrated circuits, 20: 37067 (AECL-2578)
LEAVENS, Ileana B., Quasi-oscillations of cold, sharply bounded plasmas, 20: 38301
LEAVENS, William M., Quasi-oscillations of cold, sharply bounded plasmas, 20: 38301
LEAVENS, William Manson Jr., Effects of the sheath on plasma resonance, 20: 38342
LEBEDEV, A. M., Interactions of nucleons with complex nuclei at high energies, 20: 37790
LEBEDEV, A. T., Effect of γ radiation on flotation properties of anionic collector agents, 20: 36893
LEBEDEV, V. N., Experimental determination of radiation quality factors in the vicinity of high-energy accelerators, 20: 37323
LE CLAIR, Titus G., ESADA development program high temperature gas-cooled reactor, 20: 38523
LEE, A. Y., Steady-state-coupled fluid flow and heat conduction analysis of heat-generating solid, as applied to reactor design, 20: 38461 (CONF-651110-29)
LEE, H. J., Attenuation of longitudinal acoustic waves in type-II superconductors, 20: 37948
LEE, S. W., Wave propagation in plasmas with very strong magnetic field, 20: 38303
LEE, W. R., Hemopoietic response of guinea pig to gamma irradiation, 20: 36611
LEEDS, D. H., Metallurgical evaluation of various infiltrated tungsten materials in air and nitrogen plasmas, 20: 37188
LEGAR, F., Measurement of the triple scattering parameter R_{pn} at 70° and the phase-shift analysis at 630 Mev, 20: 37739 (JINR-E-2726)
LEHENY, R. F., Drift wave excited anomalous diffusion in a fully ionized magnetoplasma, 20: 38203 (NP-16237)
LEHENY, Robert F., Fluctuations in magnetoplasma perturbed by electron beam, 20: 38201 (NP-16210)
LEHMAN, G. W., Anomalous particle penetration in perfect crystals, 20: 38387
LEHNERT, S. M., Effect of irradiation on DNA synthesis in the regenerating livers of rats, 20: 36593
LEHR, P., Observation of Zr foil specimens under the electron transmission microscope. Study of plastic deformation, 20: 37248
LEIBOVICH, S., Aligned-field hydromagnetic flow past a slender body, 20: 37870
LEITZ, F. J., Safety and economic aspects of vented fuel in sodium-cooled reactors, 20: 38475 (ANL-7120, pp 540-8)
LELAND, W. T., Reactions (t,p) and (t,α) on ^{48}Ca and ^{50}Ti, 20: 38063
LELEK, V., Application of false source method to heterogeneous nucleus calculations in cylindrical geometry, 20: 38444 (JINR-P-2699)
LENCIONI, D. E., Equipotential surfaces of a plasma moving in a toroidal octupole magnetic field, 20: 38192 (COO-1233-32)
LENDEL, A. I., Influence of $\pi\pi$ interactions on structure of the nucleon, 20: 37801
LENDEL, V. I., Influence of $\pi\pi$ interactions on structure of the nucleon, 20: 37801
LENY, Jean-Claude, ORGEL project, 20: 38518
LEONOV, A. I., Chemistry of Ce in systems of Al_2O_3, Cr_2O_3, and Ga_2O_3 with Ce_2O_3, 20: 36808
LEONOV, V. A., Natural radioactivity of skeletons, 20: 36559
LERCHE, I., Non-relativistic equations of bulk motion of a relativistic gas, 20: 37344
LESIGANG-BUCHTELA, Margrit, Thin-layer chromatography of inorganic ions, 20: 36753
LEUNG, C. Y., Positronium formation and annihilation in argon-propane mixture, 20: 37816
LEUNG, P. S., Motions of water molecules in K ferrocyanide trihydrate, water, and ice, 20: 36821
LEVIN, E. M., Magnetic moments of particles in the quark model, 20: 37857
LEVIN, E. M., Triangular diagram of π-meson low-energy scattering, 20: 37803
LEVINE, J., Unified digital instrumentation and control system for nuclear power plants, final, 4/61–6/65, 20: 38508 (NYO-2764-2)
LEVINE, L. P., Ion emission from laser irradiated tungsten, 20: 37298
LEVINE, Morton, Magnetic field design with an electrolytic tank analog, 20: 38189 (AD-636095)
LEVI SETTI, R., High-energy jets produced by heavy primary nuclei of cosmic origin and their fragmentation products, 20: 37662
LEVRAT, B., Evidence for three new charged bosons of masses 1929, 2195, and 2382 Mev and narrow widths, 20: 37771
LEVY, A., Decay correlations of photo-produced rho mesons in the strong-absorption model, 20: 37768
LEVY, A., Rho meson photoproduction cross sections in the strong-absorption model, 20: 37766
LEVY, R. H., Stability of crossed-field electron beams, 20: 37329
LEWIN, K., Exchange current and deuteron photodisintegration at threshold, 20: 38059
LEWINS, Jeffery, Time optimal xenon shutdown on the xenon boundary, 20: 38411 (BNWL-186)
LEWIS, E. E., Generalization of the Dirac chord method to include charged-particle phenomena, 20: 37309
LEWIS, R. A., Recent Doppler measurements with ZPR-6, 20: 38428 (ANL-7120, pp 610-13)
LEWIS, R. E., Production of ^{33}P from ^{36}Cl and ^{33}S by fast-neutron irradiation, 20: 37166
LEWIS, W. B., Future of nuclear energy, 20: 38487 (AECL-2584)
LEWIS, W. Bennett, Engineering for the fission gas in UO_2 fuel, 20: 38482
LIANG, C., Wave propagation in plasmas with very strong magnetic field, 20: 38303
LIANG, Wen-hsueh, Polarization of protons from the $^{12}C(d,p)^{13}C$ and $^{40}Ca(d,p)^{41}Ca$ ground-state reactions, 20: 38119
LIBURG, M., Method for obtaining low temperatures based on dissolution of ^{3}He in ^{4}He, 20: 37978
LICHODED, V. A., Effects of cosmic rays according to the chromospheric flares and Forbush effects during solar activity minimum, 20: 37537
LICHTENSTEIN, C. A., Electromagnetic form factor of the pion, 20: 37812
LIENER, A., Thermoluminescence of meteorites, 20: 37359
LILLETHUN, E., Search for heavy particles in the cosmic radiation, 20: 37654
LILLICRAP, S. C., Experiments on the pulse spectrum observed from scintillation and Cherenkov detectors at sea level, 20: 37619
LIN, Keh-Ying, Application of Bethe-Salpeter equation to static bootstrap model, 20: 37824 (CAR-882-19)
LIN, W. C., ESR of x-irradiated single crystal of KH_2AsO_4, 20: 36884
LINDEBERG, George K., Transmuted center Fermi level spectroscopy as an analytical tool for characterizing semiconductor materials, 20: 38407
LINDEN, Wolfried, Biological dose equivalent of ^{60}Co γ and 200-kv x radiation, 20: 36654
LINDMAN, Erick, Anomalous transport phenomena in a ring discharge, 20: 38329
LINDSAY, Willard L., Transfer of fallout ^{137}Cs from soil to dairy cattle feeds, 20: 37038
LINHART, Jiri George, Process for the generation, compression, and concentration of a plasma, 20: 38337
LINK, L. E., Large metal-fueled fast reactor study. II., 20: 38494 (ANL-7120, pp 94-103)
LINK, W. T., Faraday-cup measurement of proton total reaction cross sections at 100 Mev, 20: 38018
LINNEY, A. D., Measurement of the primary cosmic-ray H and He nuclei at Kiruna, Sweden, 20: 37562
LINSON, L. M., Stability of crossed-field electron beams, 20: 37329
LIPATOV, L. N., Triangular diagram of π-meson low-energy scattering, 20: 37803
LIPKIN, H. J., Neutral-meson production cross sections and mixing angles in a quark model, 20: 37779
LIPKIN, H. J., Spin-2$^+$ meson decays in the quark model, 20: 37780
LIPPINCOTT, E. P., Systematics of 3$^-$ and 5$^-$ states in $^{40,42,44,48}Ca$ and ^{50}Ti from inelastic alpha scattering, 20: 38100
LITTLE, W. W. Jr., Neutronics characteristics of selected compact fast reactors, 20: 38442 (BNWL-283)
LITUNOVSKII, R. N., 68.5-cm Sector-focused cyclotron, 20: 37324
LIU, B., Analytic-expansion unrestricted Hartree-Fock wave function for the ^{5}D state of Fe, 20: 37448
LIU, Bing-tung, Study of two-nucleon potential in nuclei by means of inelastic scattering, 20: 38120
LIU, C. K., Viscous model of the solar wind, 20: 37350
LIU, C. S., First correction to the second adiabatic invariant of charged-particle motion, 20: 38275
LIVERSAGE, W. E., New remotely controlled unit for treatment of uterine

carcinoma, 20: 36687
LLOYD, M. H., Investigation of denitration of high-nitrate plutonia sols by baking, 20: 36786 (ORNL-TM-1558)
LO, Y. T., Wave propagation in plasmas with very strong magnetic field, 20: 38303
LOBANOV, E. M., Determination of Ir in Cu and Ni slugs and Pt concentrates by neutron activation analysis, 20: 36751
LOBANOV, E. M., Preparation of Ir and Rh standard solutions by electrolytic dissolution, 20: 36775
LOBANOV, E. M., Radioactivation method for determining potassium in rocks using magnetic β separator, 20: 36752
LOBANOV, E. M., Spectral analysis with γ rays from (n,γ) reactions, 20: 36750
LOC, Vutien, Preparation of monocrystals of hafnium oxide by the method of fused salts, 20: 37197
LOCKWOOD, J. A., Neutron albedo measurements on rocket flights, 20: 37601
LOEBNER, K. E. G., Properties of some low excited states in ^{101}Ru from the decay of 3-γ ^{101}Rh, 20: 38091
LOEWENSTEIN, W. B., Large metal-fueled fast reactor study. I., 20: 38493 (ANL-7120, pp 85-93)
LOEWENSTEIN, W. B., Mixed fuel-cycle fast breeder reactors: nuclear, safety, and materials considerations, 20: 38476 (ANL-7120, pp 751-8)
LOGAN, D. M., Dehydration of uv-irradiated uridine and its derivatives, 20: 36597
LOGATCHEV, Yu. I., Earth's radiation belt, 20: 37899
LOH, E. C., Scattering of positrons and electrons from protons, 20: 37778
LOHSE, E., Search for heavy particles in the cosmic radiation, 20: 37654
LOMINO, N. S., Mechanism of capture of a moving plasma by a transverse magnetic field, 20: 38249
LOMMASSON, T. E., Firestorm start-criteria, 20: 36995 (AD-636794)
LONG, C. D., Flux limits for high-energy γ rays from quasars and other possible cosmic-ray sources, 20: 37547
LONG, C. D., Radio system for the detection of air showers, 20: 37102
LONG, R. R., Magnetohydrodynamic jet-vortex in a viscous conducting fluid, 20: 37878
LONG, Robert L. Jr., Polarization of photoelectrons from magnetized nickel and production of a polarized electron beam, 20: 37475
LONTZ, Robert J., Electron spin resonance analysis of a γ-irradiated single crystal of pentafluoropropionamide, 20: 36872
LOPATO, L. M., Phase transformations of certain rare earth chromites, 20: 36812
LOPEX, C. A., Completeness and dispersion relations in the complex angular momentum plane, 20: 37836
LOPEZ PEREZ, B., Distribution coefficients of Pu(IV) during extraction with TBP, 20: 36928
LORIERS, Henri, Oxidation mechanism of Zr–Cu alloys in CO, 20: 37183
LORIKYAN, M. P., Relativistic particle ionization energy losses, 20: 37435
LOUGHMAN, W. D., Homotransplantation studies in dogs following selective radioisotopic lymphatic ablation, 20: 36641
LOVATT, J. H., Ion exchange method of estimating ^{90}Sr and other radionuclides in rainwater, 20: 36759
LOVITCH, L., Numerical evaluation of the two-nucleon scattering length and effective range with tensor forces, 20: 37782
LOWE, I. J., Measured nuclear magnetic resonance free-induction-decay shapes and moments for ^{19}F in CaF_2, 20: 38390
LOWE, J., Polarization in the elastic scattering of 49-Mev protons by Ca, ^{58}Ni, ^{60}Ni, and ^{208}Pb, 20: 38049
LOZNYANU, E., Double charge exchange of 50- to 176-Mev π^- mesons in photo emulsion, 20: 38012 (JINR-P-2806)
LUBATTI, H. J., Coherent production of multipion resonances, 20: 37822
LUBIN, M. J., Transverse microwave cavity technique for sensitive measurement of transient electron density distributions, 20: 38305
LUCAS, D. R., Effect of x rays on the metabolism of the retina, 20: 36630
LUCAS, M., Plutonium and uranium mass spectrometry measurements on irradiated fuels, 20: 36783
LUDEMANN, C. A., Excitation of single-particle states in ^{8}Be by the ^{9}Be(p,d)^{8}Be reaction, 20: 38067
LUDFORD, G. S. S., Aligned-field hydromagnetic flow past a slender body, 20: 37870
LUDWIG, E. J., Isobaric analog state polarization measurements to determine the spin of ^{145}Sm, 20: 38068
LUDWIG, G. H., Galactic cosmic rays at solar minimum, 1965, 20: 37578
LUECK, G., Computer experiments on radiation annealing of Frenkel defects, 20: 37294
LUI, Yau-Yin, Dynamics of zero-spin collisions, 20: 37864
LUKAS, Ingrid R., Level density parameter determination from (α,n) reactions on ^{27}Al, ^{55}Mn, ^{56}Fe, and Ag, 20: 38115
LUKIN, Yu. T., Electromagnetic cascades in iron and lead at 100 Bev, 20: 37698
LUKYANOV, V. K., Elastic scattering of fast electrons on nuclei with a Fermi distribution of charge density, 20: 38139
LUPAKOV, I. S., Effect of ultrasound on the ductility of high-boron stainless steels, 20: 37221
LURIE, H., Development and growth of in-core voids due to boiling during fast reactor transients, 20: 38440 (ANL-7120, pp 881-9)
LYNCH, C. T., Dislocation etch pits and phase relationships in dimolybdenum carbide single crystals, 20: 37247
LYNCH, C. T., Preparation of alkoxides of some transition and rare-earth metals, 20: 36851
LYUDVINSKAYA, T. A., Slip casting of zirconium boride, 20: 37201
LYUTAYA, M. D., Germanides of lanthanum, 20: 37259

M

MABUCHI, Tomoo, Differences in effects of γ rays and fast neutrons from Po–Be source on paddy rice, 20: 36649
MAC DONALD, R. J., Low-energy-ion-bombardment damage in germanium, 20: 38363
MAC EWAN, J. R., Effect of UO_2 density on fission-product gas release and sheath expansion, 20: 37254
MAC EWAN, J. R., Migration of xenon through a UO_2 matrix containing trapping sites, 20: 37293
MAC FARLANE, M. H., Reaction matrix and effective shell-model interactions for the Ni isotopes, 20: 38066
MACHABELI, I. Z., Reaction (π^-,nn) and models of the ^{6}Li nucleus, 20: 38137
MACHABELI, I. Z., Reactions $(\pi^\pm,NN)$ and two-particle excitation of light nuclei, 20: 38070
MACHARADZE, T. S., Identification of energy levels in light nuclei according to disintegration cross sections, 20: 38138
MACHEREY, R. E., Metal fuels for fast reactors, 20: 38465 (ANL-7120, pp 289-300)
MAC INTYRE, R. M., Potassium–argon ages of some Dalradian, Moine, and related Scottish rocks, 20: 37016
MAC KENZIE, A. S. V., Schlieren photography of rail-tube plasmas, 20: 38287
MAC KENZIE, K. R., Synchrocyclotron conversion, 20: 37320 (CONF-660510-19)
MAC KEOWN, P. K., Charge ratio of cosmic-ray muons at large zenith angles, 20: 37689
MAC KEOWN, P. K., Momentum spectrum of cosmic-ray muons in the zenith angle range 82.5 to 90°, 20: 37697
MAC LELLAND, J. R., Schlieren photography of rail-tube plasmas, 20: 38287
MAC LENNAN, D. A., Electron ejection from an atomically clean tungsten surface by helium and neon metastable atoms, 20: 37450
MADUEV, V. L., Corpuscular ionizing radiation in space in the immediate vicinity of the earth, 20: 37902
MAEDA, T., Nuclear-active particles in extensive air showers near sea level, 20: 37620
MAEDA, T., Possible nuclear interaction of a muon of energy above 3×10^{14} ev, 20: 37714
MAG, P., Study of back coordination in iron chelates by the Moessbauer method, 20: 36823
MAGDA, M. T., Level density parameter determination from (α,n) reactions on ^{27}Al, ^{55}Mn, ^{56}Fe, and Ag, 20: 38115
MAGIDIN, M., Latitude survey of North America, 20: 37593
MAGLIC, B. C., Evidence for three new charged bosons of masses 1929, 2195, and 2382 Mev and narrow widths, 20: 37771
MAJUMDAR, Chanchal K., Effective mass of the positron in metals, 20: 37815
MAKARENKO, G. N., Physical properties of certain rare earth dicarbides, 20: 36811
MAKEPEACE, C. E., Threshold centrifuge simultaneous separation and concentration of U compounds, 20: 36933
MAKHAN'KOV, V. G., Oscillations of confined (cylindrical) plasma with a hot electron current, 20: 38196 (JINR-P-2783-2)
MAKI, Kazumi, Effect of Pauli paramagnetism on magnetic properties of high-field superconductors, 20: 37956
MAKI, Kazumi, Transverse ultrasonic attenuation in gapless superconductors, 20: 37957
MAKIDONO, J., Study on the plasma proteins of patients who survived the A bomb, 20: 36581
MAKINO, T., Modulation of cosmic-ray threshold rigidity due to geomagnetic cavity field, 20: 37596
MAKSIMOV, E. G., New experimental data on thin superconducting films, 20: 37976
MALHOLTRA, P. K., Energy spectra of cascades observed at balloon altitudes and the flux of primary protons, 20: 37672
MALHOLTRA, P. K., Study of high-energy interactions in graphite, 20: 38110
MALIK, K. K., Thorium–melanoxetin complex: a spectrophotometric study, 20: 36742
MALINOVSKY, O. V., Role of gamma treatment of oocytes in the realization of radiation injury of Drosophila sperm cells, 20: 36625

MALLAMS, J. T., Increased radioisotope uptake by malignant cells in a high oxygen environment resulting from H_2O_2 breakdown, 20: 36576
MALLOZZI, Philip J., Statistical theory of radiative processes in plasmas, 20: 38217
MALTBY, Per., Opacity properties of sunspots, 20: 37354
MAL'TSEVA, I. I., Effect of γ radiation on flotation properties of anionic collector agents, 20: 36893
MALY, Ludek, Measurements of nondestructive fuel burnup by means of γ spectroscopy of fission products, 20: 37287
MAMASAKHLISOV, V. I., Identification of energy levels in light nuclei according to disintegration cross sections, 20: 38138
MAMIDYANIAN, E. A., New data about the nuclear-active component of young atmospheric showers, 20: 37611
MAMIDZHANYAN, E. A., Characteristics of high-energy particle interaction with nuclei of light atoms, 20: 37755
MAMIYA, Takayoshi, Thermal conductivity of second-kind superconductor In–Pb alloys, 20: 37940
MAMURO, Tetsuo, Decontamination of radioactive Ru. III., 20: 36929
MAMURO, Tetsuo, Decontamination property of coal humic acid column, 20: 36930
MANDZHAVIDZE, Z. Sh., Tskhra-Tskaro installation for study of interactions of high-energy particles of cosmic rays with matter, 20: 37684
MANELIS, R. M., Properties of yttrium borides, 20: 38359
MANHEIMER, Wallace M., Energy density in a plasma oscillation, 20: 38285
MANN, B., Elastic photoproduction of π^0 mesons from deuterium, 20: 37783
MANOLOV, L., Condensation phenomena and decontamination of the ground air layer from radioactive products, 20: 37005
MANSON, D. J., Flame-temperature measurement by thermal neutron probe, 20: 37310
MANUABA, I. B. A., Study of back coordination in iron chelates by the Moessbauer method, 20: 36823
MAO, Chen-lin, Polarization of protons from the $^{12}C(d,p)^{13}C$ and $^{40}Ca(d,p)^{41}Ca$ ground-state reactions, 20: 38119
MARCESSE, J., Grain moisture measurements with neutrons: application to the problems of conditioning and storage, 20: 37154
MARCESSE, J., Use of a surface hygrometer for checking resin injections in salvaging the temples of Abu Simbel, 20: 37134
MARCHAL, F., Prog. rpt. on ESSOR fuel elements, final, 1–11/62, 20: 38480 (EUR-2522.f)
MARCHENKO, B. N., Increasing the internal beam current of the JINR synchrocyclotron by additional electrostatic focusing, 20: 37328
MARCOV, N., Motion of conducting liquid in two coaxial cylinders under influence of magnetic field, 20: 37879
MARCU, Gheorghe, Analysis of sulfuric acid solutions using the method of backscattered β radiations, 20: 36770
MARCU, Gheorghe, Formation of complex combinations of ^{241}Am and ^{246}Cm in citric acid media by electrophoresis on paper, 20: 36829
MARCZEWSKI, Stanislaw, Action of x and γ rays on hydration of protein in blood serum, 20: 36579
MAREE, J. P., Intensity distributions of cosmic-ray components at 307 g cm^{-2} atmospheric depth in the South African magnetic anomaly, 20: 37592
MARGENAU, Henry, Statistical theory of radiative processes in plasmas, 20: 38217
MARGOLINAS, S., Problems in the production and development of a wide range of radioisotope gages, 20: 37149
MARIKIAN, G. A., Investigation of the nuclear-active component of cosmic rays, 20: 37658
MARIKYAN, G. A., Spark chamber operation at high voltage pulse delay, 20: 37088
MARINESCU, L., Lifetime of the μ^- in ^{239}Pu, 20: 38114
MARININ, V. G., Production of hot-electron plasma in magnetic mirror traps, 20: 38211 (AEC-tr-6782)
MARINOV, M., Amplitude spectrum analysis by sections, 20: 37044
MARION, J. B., Excitation of single-particle states in ^8Be by the $^9Be(p,d)^8Be$ reaction, 20: 38067
MARION, Jerry B., Anticoincidence shielded gamma-ray spectrometer for nuclear reaction studies, 20: 37115
MARKUS, G., Neutron-capture gamma-ray investigation of ^{88}Sr level structure, 20: 38141
MARSDEN, P. L., Diurnal variation during the past solar cycle, 20: 37527
MARSDEN, P. L., Rigidity dependence of the intensity variation during the solar cycle, 20: 37516
MARSHALL, T. C., Drift wave excited anomalous diffusion in a fully ionized magnetoplasma, 20: 38203 (NP-16237)
MARTALOGU, N., Level density parameter determination from (α,n) reactions on ^{27}Al, ^{55}Mn, ^{56}Fe, and Ag, 20: 38115
MARTIN, J. H., Prog. rpt. on health and safety at Chapelcross, annual, 1965, 20: 37025 (PG-Report-705)
MARTIN, M., Evidence for three new charged bosons of masses 1929, 2195, and 2382 Mev and narrow widths, 20: 37771
MARTIN, M., Production of charged pions by 600 Mev protons on various nuclei, 20: 38186
MARTIN, T. C., On-line nuclear analysis system, 20: 36769
MARTINCOVA, Z., Random errors in neutron-activation analysis, 20: 36734
MARTINELLI, P., Continuous measurement of galvanization coatings by means of x-ray fluorescence, 20: 37151
MARTIN-MATEO, M. C., Assays with ^{59}Fe in Gallus domesticus, 20: 36569
MARX, Dieter, Measurement of the stopping power of ^{208}Pb alpha recoil nuclei in solid material, 20: 37470
MARX, G., Interstellar vehicle propelled by terrestrial laser beam, 20: 36997
MASELAND, H., Introduction to solar terrestrial relations, 20: 37916
MASHKOVICH, V. P., Distribution of fast fission neutrons along straight cylindrical channels in water, 20: 38351
MASON, D. G., SNAP-8 reactor and shield designs and operating experience, 20: 38527
MASON, Granville Robert, Neutron polarimeter and its use for the reaction $^{11}B(d,n)^{12}C$, 20: 38163
MASSEY, L. M. Jr., Degradation of pectin by γ radiation under various moisture conditions, 20: 36879
MASTEL, B., Vacancy and interstitial clusters in neutron-irradiated nickel, 20: 38367
MASUDA, Yoshiko, Nuclear spin-lattice relaxation in superconducting niobium, 20: 37941
MATANO, T., Arrival direction of muon-rich extensive air showers, 20: 37609
MATANO, T., Fine structure of air shower cores observed with 20 m^2 spark chamber, 20: 37617
MATANO, T., Possible nuclear interaction of a muon of energy above 3×10^{14} ev, 20: 37714
MATANO, T., Ultra-high energy muons (>200 Bev) in extensive air showers, 20: 37606
MATEEV, Frequency of radiofibroses in sound lung tissue after intens[illegible]erapy of bronchial carcinomas, 20: 36703
MATEVOS[illegible], K. A., Investigation of the nuclear-active component of cosmic rays, 20: 37658
MATEVOSYAN, E. M., Ionization measurement in a streamer chamber, 20: [illegible]10
MA[illegible]SYAN, K. A., Spark chamber operation at high voltage pulse delay, 20: 37088
MATHE, Georges, Whole-body irradiation and implantation of allogenic bone marrow in man, 20: 36669
MATHEWS, T., Solar and sidereal daily variations of cosmic-ray intensity at a depth of 60 m.w.e. underground in London, 20: 37504
MATHIE, J., Self-diffusion of beryllium, 20: 37249
MATHIEU, F., Prog. rpt. on ESSOR fuel elements, final, 1–11/62, 20: 38480 (EUR-2522.f)
MATHUR, P. C., Energy spectrum of primary He nuclei at energies greater than 6 Bev, 20: 37557
MATSUI, Masakazu, Coprecipitation behavior of rare earth elements with calcium oxalate upon precipitation from a homogeneous system, 20: 36794
MATSUMURA, Seiji, Differences in effects of γ rays and fast neutrons from Po–Be source on paddy rice, 20: 36649
MATSUMURA, Seiji, Radiosensitivity in plants. VII., 20: 36648
MATSUMURA, Takashi, Decontamination of radioactive Ru. III., 20: 36929
MATSUMURA, Takashi, Decontamination property of coal humic acid column, 20: 36930
MATSUOKA, M., Observation of the energy spectrum of galactic x rays, 20: 37500
MATSUTANI, M., Study on the plasma proteins of patients who survived the A bomb, 20: 36581
MATVEICHUK, V. T., Infrared absorption spectra of chromites of rare earth elements, 20: 36807
MATZKE, Hj., Diffusion in doped UO_2, 20: 37256
MAUGER, Anthony B., Biosynthesis of highly labeled actinomycins, 20: 36545
MAUGEST, J., Problems in the production and development of a wide range of radioisotope gages, 20: 37149
MAURUS, P., Possibilities of surveillance of radioactive contamination of meat and meat products, 20: 37039
MAUTE, R. L., Measurement of beta radioactivity in gas samples using a plastic scintillator cell, 20: 37086
MAXIMENKO, V. M., Angular distribution of secondary particles in multiple production at high energies, 20: 37682
MAYER, W. A., Doppler effect in ^{238}U and ^{235}U fission in a fast-neutron spectrum, 20: 38430 (ANL-7120, pp 616-24)
MAZAKI, Hiromasa, Effect of chemical state on the decay constant of ^{235m}U, 20: 38090
MAZARYUK, E. A., Possibilities of isolation of sidereal time cosmic-ray intensity variations, 20: 37506

MAZDIYASNI, K. S., Preparation of alkoxides of some transition and rare-earth metals, 20: 36851

MAZE, R., Semi-empirical determination of the fluctuation of the EAS μ component, 20: 37624

MAZE, R., Some properties of μ-poor EAS, 20: 37610

MAZURENKO, Yu. T., Kirchhoff's law manifestation in gamma spectroscopy, 20: 37433

MC BREEN, B., Flux limits for high-energy γ rays from quasars and other possible cosmic-ray sources, 20: 37547

MC BREEN, B., Radio system for the detection of air showers, 20: 37102

MC CABE, J. T., Determination of gas bearing stability by response to a step-jump, 20: 36980 (TID-23270)

MC CARTHY, G. J., Prog. rpt. on crystal chemistry studies, 2/14–5/13/66, 20: 36784 (AD-636054)

MC CAUGHAN, J. B. T., Density spectrum of extensive air showers at 2285 m, 20: 37630

MC CLENDON, Leslie, On-site radiological safety for Project SULKY, 20: 36960 (PNE-717F)

MC CLURE, G. W., Electron transfer in proton–H atom collisions at 2 to 117 kev, 20: 37446

MC CORKLE, K. H., Method of preparing high-density, compactible U dioxide particles, 20: 37212

MC CRACKEN, K. G., Celestial source of x rays in the energy range 20 to 58 kev, 20: 37376

MC CRACKEN, K. G., Influence of the magnetopause on cosmic-ray particle trajectories, 20: 37597

MC CRACKEN, K. G., Modulation I, 20: 37545

MC CRACKEN, K. G., Semi-diurnal anisotropy of the cosmic radiation, 20: 37521

MC CRACKEN, K. G., Survey of the diurnal anisotropy, 20: 37522

MC CULLEN, J. D., Nuclear spin and moments of ^{45}Ti, 20: 38089

MC CUSKER, C. B. A., Density spectrum of extensive air showers at 2285 m, 20: 37630

MC CUSKER, C. B. A., Elastic and electromagnetic proton interactions at 30 Bev, 20: 37666

MC CUSKER, C. B. A., Extensive air showers, 20: 37655

MC DANELS, David L., Stress-rupture properties of W wire from 1200 to 2500°F, 20: 37251

MC DANIELS, D. K., Decay of ^{140}Ba, 20: 38029

MC DANIELS, D. K., Energy levels of ^{56}Fe, 20: 38088

MC DONALD, F. B., Galactic cosmic rays at solar minimum, 1965, 20: 37578

MC DOWELL, A. A., Set formation to nonrewarded cues by normal and previously irradiated rhesus monkeys, 20: 36638

MC DOWELL, A. A., Social distractibility of previously irradiated female rhesus monkeys, 20: 36639

MC DOWELL, C. A., ESR of x-irradiated single crystal of KH_2AsO_4, 20: 36884

MC GEE, Ian James, Theory of inelastic electron-deuteron scattering, 20: 38167

MC KINLEY, J. C., Report of fire resistance tests fuel core shipping container No. 1, 20: 37024 (NLCO-899)

MC KINNEY, F. E., Isotopes and Radiation Technology. Vol. 3, Number 3, 20: 37136

MC LANE, C. K., Correlation of density fluctuations and diffusion in a plasma, 20: 38322

MC LEOD, N. Borrie, Economic significance of nuclear fuel management, 20: 38416

MC VOY, K. W., Factors of excited nuclear states by resonant scattering, 20: 38079

MEAD, J. C., Report of fire resistance tests fuel core shipping container No. 1, 20: 37024 (NLCO-899)

MEASURES, R. M., Axial pressure asymmetry produced by Hall currents in a linear pinch discharge, 20: 38289

MECHAM, W. J., Commercial aspects of fuel processing, 20: 36945

MECHAM, W. J., Evaluation of remote systems, 20: 36953

MECHAM, W. J., Large metal-fueled fast reactor study. II., 20: 38494 (ANL-7120, pp 94-103)

MECHAM, W. J., Molten-salt fluoride-volatility processing of aluminum-base alloys, 20: 36951

MEDVEDEV, A. A., Thermodiffusive interaction of tantalum and boron carbide powder in a vacuum, 20: 36809

MEEHAN, John Patrick, Crystal field effects in zirconium oxide, 20: 36854

MEERSON, G. A., Properties of yttrium borides, 20: 38359

MEERSON, G. A., Thermodiffusive interaction of tantalum and boron carbide powder in a vacuum, 20: 36809

MEHURON, W. O., Electromagnetic wave interaction in an inhomogeneous drifting plasma, 20: 38194 (INDEC-SR-7, pp 3.22-59)

MEI, J. Y., Simplified 180° focusing β-ray spectrometer, 20: 37120

MEINCKE, P. P. M., Comments on "direct evidence of flux motion", 20: 37966

MELCHER, James R., Traveling-wave induced electroconvection, 20: 38280

MELKMAN, A., Derivation of the pion multiplicity in nuclear collisions from sea-level positive excess and total muon spectra, 20: 37691

MELLERIO, J., Lasers and ultrasonics, 20: 36612

MELNGAILIS, J., Model for change in elastic modulus of a solid caused by point defects, 20: 37296

MEL'NIKOV, G. P., Electronic digital spectrometers in experimental nuclear physics, 20: 37128

MELNIKOV, V. V., Low-energy particle fluxes inside the magnetosphere from the data of the electrostatic analyzers of the Electron-2 satellite, 20: 37904

MELSOM, Sigurd, Determination of copper in hydrogenated fats by neutron activation analysis, 20: 36724

MENCUCCINI, Corrado, Photoproduction of neutral pions in the energy range 400 to 600 Mev of the incident photon, 20: 36652

MENDELL, R. B., Measurements of neutrons produced by the cosmic radiation, 20: 37599

MENDELSON, R. A., Investigation of porous tungsten formed from spherical tungsten powders, 20: 37199

MENEGHETTI, D., Large metal-fueled fast reactor study. I., 20: 38493 (ANL-7120, pp 85-93)

MENELEY, D. A., Measurement and analysis of Doppler effect in Pu-fueled fast reactor assemblies, 20: 38427 (ANL-7120, pp 603-9)

MENON, M. G. K., Flux of primary protons and helium nuclei and east-west and north-south asymmetries near the geomagnetic equator, 20: 37582

MENON, M. G. K., Kolar Gold Field neutrino experiment, 20: 37711

MENON, M. G. K., Use of a gas Cherenkov counter for the study of the isotopic composition of He nuclei in primary cosmic radiation, 20: 37581

MENTZEN, Bernard, Physicochemical properties of thorium formates with different degrees of hydration, 20: 36795

MENZIES, D. C., Theoretical studies on the fast reactor maximum accident, 20: 38434 (ANL-7120, pp 654-70)

MEREN, Eiichiro, Neutron activation analysis of human blood and hair, 20: 36728

MEROZ, I., Derivation of the pion multiplicity in nuclear collisions from sea-level positive excess and total muon spectra, 20: 37691

MERSOL, S. A., Dislocation etch pits and phase relationships in dimolybdenum carbide single crystals, 20: 37247

MERZ, E., Nuclear recoil and radiation effects on metal phthalocyanines, 20: 36886

MESHCHERYAKOV, V. A., Influence of $\pi\nu$ interactions on structure of the nucleon, 20: 37801

MESSELT, S., Proton-proton scattering: revision and analysis of experimental measurements from 1.4 to 3.0 Mev, 20: 38081

METZENROTH, M., Influence of some important group constants on integral fast reactor quantities, 20: 38420 (ANL-7120, pp 423-33)

METZGER, F. R., Lifetime of the 1.52-Mev level in ^{42}Ca, 20: 38085

METZGER, Wesley James, Interactions Kπ-p) at 900 Mev, 20: 37744 (UR-875-151)

METZNER, Wolfgang, Radiochemical cyclomerization, 20: 36860 (NP-16150)

MEYER, E. F. Jr., Proton-induced fission of ^{238}U, 20: 37995

MEYER, Hans, Forty-third meeting of German X-Ray Society, Cologne, 5/62, 20: 36691

MEYER, J. P., Use of semiconductor telescopes in charge and energy spectrometry of cosmic particles, 20: 37575

MEYER, Lothar, Behavior of ions and quantized vortex rings of low energy in He II around 0.3°K, 20: 37947

MEYER, M. A., Chemically inaggressive liquid scintillators, 20: 37113

MEYER, M. A., Experimental study of some of the basic properties of spark chambers, 20: 37105

MEYER, P., Primary electrons and positrons in the cosmic radiation, 20: 37496

MEYER, Ph., Algebra of currents and the $|\Delta| = \frac{1}{2}$ rule for K-meson nonleptonic decay, 20: 37759

MICHAEL, W., Coherent production of multipion resonances, 20: 37822

MICHAEL, W., Direct search for the C-violating decay $\eta^0 \rightarrow \pi^0 e^+ e^-$, 20: 37767

MICHAELIS, E. G., Production of charged pions by 600 Mev protons on various nuclei, 20: 38186

MICHAELIS, W., Application of germanium diodes in gamma ray spectroscopy, 20: 37072 (KFK-429)

MICHAELIS, W., Neutron-capture gamma-ray investigation of ^{88}Sr level structure, 20: 38141

MICHELMAN, L., Isobaric analog state polarization measurements to determine the spin of ^{148}Sm, 20: 38068

MICHIELS, H., Prog. rpt. on ESSOR fuel elements, final, 1–11/62, 20: 38480 (EUR-2522.f)

MICHLMAYR, M., Polarographic studies on uranium compounds in dimethylformamide and dimethylsulfoxide, 20: 36745

MICKE, A., Influence of modifying factors on the action of ionizing radiation on plant cells, 20: 36658

MICKEY, Wendell V., Travel times and amplitudes from the Salmon explosion, 20: 36967

MIDDLETON, R., Reactions ^{63,65}Cu(t,p)^{65,67}Cu, 20: 38035

MIHAI, I., Lifetime of the μ^- in ^{239}Pu, 20: 38114

MIKHAIL, R. Sh., Activation and sintering behavior of calcium oxide, 20: 36904

MIKHALCHI, E. D., Depth-intensity curve of muons and their energy spectrum, 20: 37706

MIKHALEVA, T. N., Utilization of fast charged particle inelastic scattering for analysis of composition of materials, 20: 36732

MIKHUL, V., Double charge exchange of 50- to 176-Mev π^- mesons in photo emulsion, 20: 38012 (JINR-P-2806)

MILHAM, R. C., High-temperature carbon for iodine adsorption, 20: 36976 (DP-MS-66-45)

MILIGUI, Z., Design and theory of magnetic spectrometer for measurement of cosmic-ray mesons, 20: 37487

MILLER, David, Critical review of the properties of materials at the high temperatures and pressures significant for fast reactor safety, 20: 38433 (ANL-7120, pp 641-53)

MILLER, David B., Experimental x-band electron-cyclotron-resonance plasma accelerator, 20: 38235

MILLER, J. A., Potassium–argon ages of some Dalradian, Moine, and related Scottish rocks, 20: 37016

MILLER, J. K., Effect of feeding thiocyanate to dairy cows on absorption and clearance of intramammary iodine, 20: 36563

MILLIOT, B., Investigations of boiling of liquid metals in forced convection, 20: 38415

MILLS, D., Etching dislocations in zirconium, 20: 37227

MILLS, D., Redistribution of oxygen and iron during zone refining of zirconium, 20: 37177

MILSTEAD, C. E., Cs–graphite sorption isotherms determined by a static method, 20: 36799

MINCK, R. W., Stimulated pure rotational Raman scattering in deuterium, 20: 37451

MINCZEWSKI, J., Spectrographic determination of trace amounts of rare earths. III., 20: 36729

MINER, F. J., Primary analytical standards for Pu, 20: 36727

MINES, J. R., Finite-range distorted wave calculations for the $^{52}Cr(d,p)^{53}Cr$ reaction, 20: 38047

MINIER-CASSAYRE, C., Interpretation of stage I in Ni irradiated by electrons, 20: 37297

MINYAEV, O. A., 68.5-cm Sector-focused cyclotron, 20: 37324

Miranda, Carlos Ferreira de
see Ferreira de Miranda, Carlos

MIRONOV, V. F., Formation of radicals during radiolysis of organic solids. III., 20: 36883

MISAKI, A., Mean square angular and lateral spreads of electrons and photons in a cascade shower, 20: 37648

MISHAKOVA, A. P., Azimuthal angular distributions of secondary particles in cosmic jets, 20: 37665

MISHEV, I., Radioactive pollution in the area of the nuclear reactor IRT-1000, 20: 38535

MISHRA, Shanker Prasad, Couette-type flow of an elasticoviscous fluid through porous walls in the presence of a transverse magnetic field, 20: 37876

MITANI, Kenji, Collision-induced instability in a magnetoactive plasma, 20: 38253

MITANI, S., Variation of ^{14}C content in the atmosphere during the past two thousand years, 20: 37602

MITENKOV, F. M., Cross-section averaging in thermal region for media containing zirconium hydride, 20: 37991

MITSHENKO, L. G., Distribution of the energy portion transferred to π^0 mesons, 20: 37660

MITSHENKO, L. G., Four-momentum transferred in high-energy interactions, 20: 37659

MITSHENKO, L. G., Relationship of neutral and charged particles among nuclear-active particles with energies above 100 Bev at mountain altitude, 20: 37685

MIURA, I., Arrival direction of muon-rich extensive air showers, 20: 37609

MIURA, M., Study on the plasma proteins of patients who survived the A bomb, 20: 36581

MIURA, Masaji, ESR of γ-irradiated sodium polyphosphate. I., 20: 36870

MIWA, T., Variation of ^{14}C content in the atmosphere during the past two thousand years, 20: 37602

MIYAKE, S., Direct measurement of attenuation length of extensive air showers, 20: 37642

MIYAKE, S., Observation of the character of EAS cores, 20: 37615

MIZUHIRA, Binchi, Electron-microscopic autoradiography, 20: 37050

MJOLSNESS, R. C., Electron distribution function in a plasma with excitation collisions, 20: 38198 (LA-DC-8099)

MOECK, E. O., SWIFT dryout data for 19-rod bundle cooled by steam/water fog, 20: 38409 (AECL-2586)

MOECKEL, H., Radiation-chemical production and optical absorption spectra of organic S radicals in organic glasses at −196°C, 20: 36894

MOESSBAUER, R. L., Recoilless absorption of gamma radiation and its application to problems of electronic shielding in rare earths, 20: 37461

MOGYORODI, Jozsef, Mean value of the collisions in the slowing-down process of neutrons, 20: 37992

MOHINDRA, R. K., Spins of ^{58}Ni levels from inelastic proton scattering, 20: 38181

MOHLING, F., Microscopic theory of a normal fermi liquid at zero temperature, 20: 37937

MOHRI, Akihiro, Experiments on ion cyclotron heating of plasma in the Heliotron-B device, 20: 38258

MOISEITSEVA, Z. K., Thermodiffusive interaction of tantalum and boron carbide powder in a vacuum, 20: 36809

MOLE, R. H., Sensitivity of rat oocytes to x rays, 20: 36632

MOLIN, Yu. N., Formation of radicals during radiolysis of organic solids. III., 20: 36883

MOLL, W., Measurements with a high-aperture γ spectrometer with plastically curved LiF crystal, 20: 38158

MOLOCHNIKOVA, N. P., Solvent extraction of protactinium and other elements as phenylarsonates, 20: 36940

MONK, C. B., Emf studies of electrolytic dissociation. IX., 20: 36830

MOORE, D. J., Thermal decomposition of irradiated mercuric oxalate, 20: 36898

MOORE, D. J., Thermal decomposition of gamma-irradiated barium azide, 20: 36900

MOORHEAD, Elizabeth Grace, Nuclear reactions of 10- to 20-Mev deuterons with ^{61}Ni, 20: 38148

MOREHOUSE, Robert Lymon, Electron spin resonance studies of some simple radicals trapped in krypton, 20: 36909

MOREL, P. A., Migration of xenon through a UO_2 matrix containing trapping sites, 20: 37293

MORETON, R., Silicon carbide coatings on molybdenum and tungsten, 20: 37188

MORGAN, I. L., On-line nuclear analysis system, 20: 36769

MORI, S., Atmospheric temperature effects on the diurnal variation of cosmic-ray intensity, 20: 37586

MORIGUCHI, Etsuko, Enzymatic breakdown of uv-irradiated DNA by the extract from Micrococcus lysodeicticus, 20: 36583

MORIOKA, Shigeki, Magnetohydrodynamic shock polar, 20: 37872

MORIYASU, K., Coherent production of multipion resonances, 20: 37822

MORLEY, Morgan J., Magnetic-gradient particle accelerator, 20: 37340

MORO, R., Properties of some low excited states in ^{101}Ru from the decay of 3-γ ^{101}Rh, 20: 38091

MOROZUMI, Henry M., Different geomagnetic variations associated with corpuscular precipitations on day and night side of the auroral zone, 20: 37897

MORPURGO, G., Possible metastable baryonic states with even parity in the quark model, 20: 37765

MORRIS, J. B., Preparation of uranium nitride and carbonitrides from uranium oxide in a fluidized bed, 20: 36850

MORRIS, M., University of Utah neutrino detector, 20: 37104

MORRISON, D. R. O., Kinematic enhancement of resonance production in certain two-body reactions, 20: 37769

MORSE, L. E., Method of preparing high-density, compactible U dioxide particles, 20: 37212

MORSE, Richard Lee, Some aspects of high β plasma confinement, 20: 38347

MORTON, J. R., Electron spin resonance spectra of radiation-damaged inorganic crystals, 20: 36902

MOSER, H., Scattering of gamma rays and neutrons to investigate underground aquifers, 20: 37135

MOSER, P., Interpretation of stage I in Ni irradiated by electrons, 20: 37297

MOSER, P., Study of defects produced by irradiation in Fe, 20: 37288

MOSHER, D., Negative V″ stellarator, 20: 38243

MOSOVA, L. N., Purification of cerium by electric transport combined with zone melting, 20: 36936

MOSS, G. A., Decay of ^{140}Ba, 20: 38029

MOSS, W. D., Characteristics of the aerosol produced from burning plutonium, 20: 37022 (LA-DC-6942)

MOTTA, M., Calculation method of a transient in a prompt critical fast reactor, 20: 38413

MOTZ, R., Diffusion and instabilities in "Q" machine plasmas, 20: 38324

MOUNTFORD, L. A., Recent results of Doppler measurements in fast-neutron spectra, 20: 38429 (ANL-7120, pp 614-15)

MUELLER, Robert A., Critical mass studies with NASA Zero Power Reactor II, 20: 38532 (NASA-TN-D-3555)

MUELLER, Robert F., Oxygen-18/oxygen-16 ratios of minerals from the iron formations of Quebec, 20: 37013

MUKHERJI, A., Self-consistent perturbation method. I., 20: 37440

MUKHIN, A. I., Muon capture in mixed gases, 20: 37741 (JINR-P-2788)

MULLER, B. H., Calculation of the r.m.s. jump distance in liquids from the intermolecular contribution to nuclear spin relaxation, 20: 36828

MULLER, Harry D., Prog. rpt. on x irradiation of the developing avian embryo as a factor of aging, 1/62–12/65, 20: 36605 (COO-1119-5)

MULLER, Kh., About the resonance behavior of isospin forbidden nuclear

reactions, 20: 38045
MULLER, O., Prog. rpt. on crystal chemistry studies, 2/14–5/13/66, 20: 36784 (AD-636054)
MUNGER, Richard H., Field curvature effects on alkali-metal-plasma containment, 20: 38326
MUR, V. D., ω-Meson photoproduction at high energies, 20: 37807
MURADOVA, N. A., Properties of μ mesons at 200 m.w.e. underground, 20: 37694
MURAKAMI, K., Air showers at high altitude, 20: 37637
MURAKAMI, K., Anisotropy of cosmic rays in the direction parallel to the rotation axis of the Earth, 20: 37540
MURAKAMI, K., Studies of primary cosmic rays in the energy region 10^{14} to 10^{17} ev, 20: 37627
MURAKAMI, K., Variations of the latitude dependence of cosmic-ray diurnal variations, 20: 37523
MURAKAMI, Yotaro, Effects of additional elements on discontinuous precipitation in Cu–Be alloys, 20: 37253
MURAKAWA, Kiyoshi, Quadrupole moment of ^{51}V, 20: 38026
MURAMATSU, M., Scintillation counting with plastic phosphor for determining tritium radioactivity at surfaces, 20: 37087
MURAMATSU, Mitsuo, Sheet scintillation counting of tritium in surface films, 20: 36738
MURASE, Takeo, Microchemical detection of cesium using ion-exchange resin particles, 20: 36761
MURAYAMA, T., Observation of muon air showers, 20: 37607
MURGATROYD, R. A., Effect of variations in composition and heat treatment on the properties of Zr–Nb alloys, 20: 37236
MURNAGHAN, D. J. B., Radio system for the detection of air showers, 20: 37102
MURRAY, G., Threshold for the reaction $^{10}B(p,n)^{10}C$ and the ft value of the superallowed Fermi transition $^{10}C(\beta^+)^{10}B$, 20: 38069
MURTHY, G. T., Correlations between the electron, muon, and N components in extensive air showers, 20: 37635
MURTHY, G. T., Properties of extensive air showers rich in muons, 20: 37608
MURTHY, G. T., Search for heavy mass particles in air showers, 20: 37653
MURTHY, G. T., Time lags of nuclear-interacting particles in extensive air showers, 20: 37652
MURTHY, G. T., Ultra-high energy muons (>200 Bev) in extensive air showers, 20: 37606
MURTY, S. S. R., Effect of line radiation on precursor ionization, 20: 37881
MURZIN, V. S., Analysis of methods of measurement of the characteristics of elementary interactions, 20: 37671
MURZIN, V. S., Distribution of the energy portion transferred to π^0 mesons, 20: 37660
MURZIN, V. S., Four-momentum transferred in high-energy interactions, 20: 37659
MURZIN, V. S., Relationship of neutral and charged particles among nuclear-active particles with energies above 100 Bev at mountain altitude, 20: 37685
MUSSET, P., Direct search for the C-violating decay $\eta^0 \rightarrow \pi^0 e^+ e^-$, 20: 37767
MUTA, Taizo, Particle mixing and the $Z = 0$ condition, 20: 37848
MUXART, Roland, Preparation of $PaCl_5$ and absorption spectra, 20: 36798
MUZIOL, G., Positron decay of ^{145}Eu, 20: 38133
MYASOEDOV, B. F., Solvent extraction of protactinium and other elements as phenylarsonates, 20: 36940
MYAZDRIKOV, O. A., Ionization-mechanical detector for ionizing particles, 20: 37080
MYINT, Than, Absolute value of the proton g factor, 20: 37777

N

NACHTIGALL, Dieter, Moessbauer effect, 20: 37464
NAGAI, Masao, Spatial extent of enhanced ionizations produced in association with the elementary geomagnetic polar disturbances, 20: 37893
NAGANO, M., Arrival direction of muon-rich extensive air showers, 20: 37609
NAGANO, M., Fine structure of air shower cores observed with 20 m^2 spark chamber, 20: 37617
NAGANO, M., Possible nuclear interaction of a muon of energy above 3×10^{14} ev, 20: 37714
NAGASAWA, Kakuso, Functional test of a decontamination apparatus for radio-contaminated rainwater, 20: 37029
NAGASHIMA, K., Atmospheric temperature effects on the diurnal variation of cosmic-ray intensity, 20: 37586
NAGASHIMA, K., Solar cycle modulation of cosmic rays, 20: 37509
NAGATA, Sinobu, Nuclear force and energy gap in finite nuclei, 20: 38113
NAGPAL, Turlok Singh, Decay of ^{134}Cs, 20: 38169
NAGY, A. G., Investigation of the chemical forms of carrier-free ^{131}I by paper electrophoresis, 20: 36792
NAHRMANN, Hans, Investigations with a tritium-labeled N-mustard gas derivative in carcinoma treatment, 20: 36705
NAIK, M. C., Diffusion of iron and silver in beryllium, 20: 37250
NAKANISHI, Noboru, Covariant quantization of the electromagnetic field in the Landau gauge, 20: 37925
NAKANO, Huzio, Quantum statistical theory of optical rotation, 20: 37927
NAKAYA, Todoo, Plastic scintillators. II., 20: 36847
NAKAYA, Todoo, Plastic scintillators. III., 20: 36848
NAKAYAMA, Toshio, Derivations of hierarchies for N particle systems and Vlasov systems, 20: 38209 (PPL-AF-5)
NAMIKI, Miko, Trion model with an additional force field, 20: 37850
NARANAN, S., Correlations between the electron, muon, and N components in extensive air showers, 20: 37635
NARANAN, S., Properties of extensive air showers rich in muons, 20: 37608
NARANAN, S., Search for heavy mass particles in air showers, 20: 37653
NARANAN, S., Time lags of nuclear-interacting particles in extensive air showers, 20: 37652
NARANAN, S., Ultra-high energy muons (>200 Bev) in extensive air showers, 20: 37606
NARASIMHAM, V. S., Intensity and angular distribution of cosmic rays far underground, 20: 37704
NARASIMHAM, V. S., Kolar Gold Field neutrino experiment, 20: 37711
NARASIMHAM, V. S., Muon interactions far underground, 20: 37701
NARDELLI, G. F., Slow-neutron scattering by liquids: hindered-translator model, 20: 37999
NARDELLI, G. F., Slow neutron scattering by liquids: a hindered-translator model, 20: 38006
NARUMI, Hojime, Value of the electric quadrupole moment of the deuteron, 20: 37797
NASH, W. F., Current splitting in divided-electrode spark chambers, 20: 37109
NASH, W. F., Photonuclear interactions of μ mesons, 20: 37702
NASH, W. F., Study of the μ meson charge ratio at sea level, 20: 37687
NASH, W. F., Theoretical analysis of the performance of high-resolution magnetic hodoscopes, 20: 37106
NATARAJAN, A. T., Effects of diethyl pyrocarbonate on barley seeds, 20: 36589
NATHAN, K. V. S. K., Particle heating effects in the upper F region, 20: 37896
NATHAN, O., Reaction (t,p) with even isotopes of Sm, 20: 38052
NATHAN, O., Reactions $^{63,65}Cu(t,p)^{65,67}Cu$, 20: 38035
NAUENBERG, M., Gauge condition and the equal-time axial and vector current commutator, 20: 37760
NAUMANN, D., Fission recoil separation in mixtures with uranium dioxide powders as a simple method of range determination of fission products, 20: 37997
NAVTANOVICH, M. L., Extraction of metals from aqueous solutions of hydrohalic acids by means of dialkylalkylphosphinates, 20: 36941
NAZARCHUK, T. N., Analysis of mixtures of oxides of rare earths and alkaline earths, 20: 36776
NAZARYAN, A. A., Ionization measurement in a streamer chamber, 20: 37110
NEDOSTUP, G. A., Neutron radiative capture gamma spectrometry as a method of determining the composition of iron-bearing rocks and ores, 20: 37019
NEDYALKOV, I., New scintillation hypothesis for the superstars and their connection with the galaxies, 20: 37358
NEDYALKOV, I. P., Dynamics of the dense astrophysical shells, 20: 37357
NEELAKANTAN, K. A., Energy spectrum of alpha particles below 600 Mev/nucleon at solar minimum, 20: 37558
NEELAKANTAN, K. A., Experimental examination of low-energy cosmic-ray heavy nuclei, 20: 37569
NEF, C., Evidence for three new charged bosons of masses 1929, 2195, and 2382 Mev and narrow widths, 20: 37771
NEGANOV, B., Method for obtaining low temperatures based on dissolution of ^3He in ^4He, 20: 37978
NEGOYA, Shinichi, High-temperature gas loop and experiments of finned fuel elements, 20: 38481
NEHER, H. V., Cosmic ray changes during a solar cycle, 20: 37507
NEIMARK, L. A., Mixed-carbide fuels for fast reactors, 20: 38467 (ANL-7120, pp 314-27)
NELSON, C. T., Errors in measurements of building leakage due to dynamic temperature effects, 20: 36978 (NAA-SR-12001)
NELSON, M. F., ^{14}C-labeled polyoxyethylene (20) sorbitan monolaurate and metabolic fate in rats, 20: 36921
NELSON, Murrell D. Jr., Containment of radioactive wastes, 20: 38539
NELSON, P. A., Preparation and properties of uranium and plutonium nitrides, 20: 37207
NELSON, R. S., Theories of swelling and gas retention in reactor materials, 20: 37299
NEMENOV, L. M., Low- and medium-energy acceleration of ions and their application in nuclear physics, 20: 37333
NEMETS, O. F., Cross sections of elastically scattered 13.6-Mev deuterons, 20: 38128

NEMILOV, Yu. A., Fission of ^{226}Ra by 12-Mev deuterons, 20: 38132
NEMIROVSKII, P. E., Neutron states in a deformed optical potential, 20: 38126
NEMODRUK, A. A., Determination of microquantities of U in soils, rocks, and minerals by means of arsenazo III, 20: 36774
NEMOLOCHNOV, A. N., Periodic cosmic-ray variations and their change during the cycle of solar activity, 20: 37525
NERURKAR, N. W., Rigidity spectra of primary cosmic rays in the last solar cycle, 20: 37514
NESBITT, Lyle Edwin, Thermogravimetric study of some gas-solid reactions, 20: 36853
NESMEYANOV, An. N., Evaporation of W, Mo, and Ta in vacuum, 20: 36834
NESS, N. F., Measurements of the magnetic fields in interplanetary space and the magnetosphere, 20: 37898
NESTEROV, V. E., Preliminary results of cosmic-ray study from the artificial Earth's satellite Proton-1, 20: 37495
NESTEROVA, N. M., Installation for study of EAS and nuclear interactions of cosmic-ray particles with energies 10^{12} to 10^{16} ev, 20: 37634
NETCHIN, Yu. A., Underground investigation of the penetrating component of high-energy cosmic radiation, 20: 37693
NEUFELD, Jacob, Cyclotron excitation of electromagnetic waves by a gyrating electron beam, 20: 38291
NEUMAIER, F., Scattering of gamma rays and neutrons to investigate underground aquifers, 20: 37135
NEURINGER, L. J., Niobium–25 Zr in strong magnetic fields: magnetic, resistive, ultrasonic, and thermal behavior, 20: 37950
NEUZIL, E. F., Helium-ion-induced fission of ^{207}Pb from 41.1 to 26.3 Mev, 20: 37996
NEWKIRK, John B., X-radiation alignment of quartz crystals for improved hypersonic propagation, 20: 38366
NEWMAN, R. C., Effect of cosmic-ray friction on the solar wind, 20: 37372
NEWSON, H. W., Precision measurement of reaction thresholds, 20: 38028
NEYMARK, V. E., Effect of ultrasound on the ductility of high-boron stainless steels, 20: 37221
NGUYEN-KHAC, U., Direct search for the C-violating decay $\eta^0 \to \pi^0 e^+ e^-$, 20: 37767
NGUYEN QUANG DONG, Interaction of electromagnetic waves with quantum and a classical plasmas. Correlation effects, 20: 38292
NGUYEN VAN HIEU, Broken $\tilde{U}(12)$ symmetry and unitarity condition for the S matrix, 20: 37855
NICHOLS, L. L., Precision long counter for measuring fast neutron flux density, 20: 37069 (BNWL-260)
NICKSON, James J., Clinical evaluation of the treatment of advanced head and neck cancers with high-energy electron beams, 20: 36685
NICOLAU, C. T., Current status of the use of bone marrow transplants in therapeutics, 20: 36667
NICOLAU, C. T., Viability of preserved bone marrow cells, 20: 36546
NIEBUHR, J., Suboxides of niobium, 20: 36825
NIEDRIG, N., High resolution investigation of the energy losses of 30 kev electrons in aluminum foils of various thicknesses, 20: 37442
NIESAR, K. H., Equipment of Radiochemical and Radiobiological Section in Inst. of Animal Physiology and Nutrition of University of Munich, 20: 37040
NIESSEN, A. K., Resistive behavior of a type-II superconductor on reversing the current, 20: 37945
NIHOUL, Jacques C. J., Malkus theory applied to magnetohydrodynamic turbulent channel flow, 20: 38240
NIHOUL-BOUTANG, G., Direct search for the C-violating decay $\eta^0 \to \pi^0 e^+ e^-$, 20: 37767
NIKITIN, Yu. P., ω-Meson photoproduction at high energies, 20: 37807
NIKOLAEV, A. N., Distribution of fast fission neutrons along straight cylindrical channels in water, 20: 38351
NIKOLAEV, V. N., 68.5-cm Sector-focused cyclotron, 20: 37324
NIKOLSKII, B. A., Azimuthal angular distributions of secondary particles in cosmic jets, 20: 37665
NIKOLSKII, S. I., Installation for study of EAS and nuclear interactions of cosmic-ray particles with energies 10^{12} to 10^{16} ev, 20: 37634
NIMNIK, R. A., Discussion of one model of the formation of extensive atmospheric showers, 20: 37612
NINOMIYA, R., Glucose production rates in dogs determined by two different tracers and tracer methods, 20: 36565
NISHIDA, Michio, Langmuir probe measurements in a hypersonic plasma flow, 20: 38261
NISHIMURA, J., Effect of the logarithmic increase of ionization loss on the range fluctuation of high-energy μ mesons, 20: 37708
NISHIMURA, J., Extensive air showers observed in the emulsion chamber, 20: 37638
NISHIMURA, J., Nuclear interactions produced in the emulsion chamber, 20: 37673
NISHIMURA, J., Observation of extremely high-energy nuclear events by emulsion chamber, 20: 37661
NOELLER, Hans-Georg, Mass spectrometer, 20: 36779
NOLL, C. B., Matrices for computing Greuling-Goertzel slowing-down parameters and Legendre polynomial coefficients for scattering, 20: 37988 (WAPD-TM-572)
NOLL, C. B., TRANS: a FORTRAN-IV program for conversion of form of neutron elastic scattering data stored in ROC nuclear data library, 20: 37989 (WAPD-TM-573)
NOOH, M. G., Design and theory of magnetic spectrometer for measurement of cosmic-ray mesons, 20: 37487
NORBERG, R. E., Nuclear quadrupole relaxation and chemical shift of ^{131}Xe in liquid and solid Xe, 20: 38392
NOREM, Walter Endre, Adiabatic calorimeter and use to study order-disorder reactions in Ni–Mo alloys, 20: 37278
NORIN, Rolf, Crystal structure of $Nb_{12}O_{29}$(mon), 20: 36790
NORRIS, A. E., Decay of ^{131}Ce, 20: 38048
NORTHROP, John H., Virus-producing cells and mutants in K12λ cultures exposed to uv light, triethylenemelamine, or H_2O_2, 20: 36617
NORTHROP, T. G., First correction to the second adiabatic invariant of charged-particle motion, 20: 38275
NOTLEY, M. J. F., Effect of UO_2 density on fission-product gas release and sheath expansion, 20: 37254
NOVATSKII, V. N., Reaction $^3He + {}^3He$, 20: 38131
NOVOZHILKOV, Yu. V., Unitary representations of group P(SU(r)), 20: 37858
NOYES, R. C., Development and growth of in-core voids due to boiling during fast reactor transients, 20: 38440 (ANL-7120, pp 881-9)
NOYORI, Kimiharu S., Clinical studies in laser photocoagulation, 20: 36682
NOYORI, Kimiharu S., Prophylactic photocoagulation of recurrent toxoplasmic retinochoroiditis, 20: 36683
NUMBERGER, Josef, Radiation burden through ^{131}I and thyroid function, 20: 36675

O

OBAYASHI, H., Acceleration of cosmic-ray electrons, 20: 37499
O'BRIEN, Robert Francis, Solid-state effect in irradiated alkali halide crystals, 20: 38402
OBU, Koji, Pre-SC increases of hf field intensity on polar paths and of f_0F_2 in high latitudes, 20: 37892
OBUKHOV, A. I., Cross section of nuclear fission of tin irradiated by oxygen ions, 20: 38123
O'CONNELL, D., New remotely controlled unit for treatment of uterine carcinoma, 20: 36687
ODA, H., Further observation of the positive excess of cosmic-ray muons, 20: 37690
ODA, H., Nuclear-active particles in extensive air showers near sea level, 20: 37620
ODDOU, J. L., Interpretation of stage I in Ni irradiated by electrons, 20: 37297
O'DELL, F. W., ^3He-^4He in the primary cosmic radiation at Fort Churchill 1963, 20: 37572
O'DONNELL, B., Density spectrum of extensive air showers at 2285 m, 20: 37630
O'DONNELL, T. A., Reactivity of transition metal fluorides. II., 20: 36803
O'DONNELL, T. A., Reactivity of transition metal fluorides. III., 20: 36804
OEHME, R., Electromagnetic form factors from the locality of current densities, 20: 37837
OESER, Heinz, Functional radiodamage of the brain, 20: 36651
OGDEN, H. R., Effect of oxidation-protection coatings on the tensile behavior of refractory metal alloys at low temperature, 20: 37276
OHE, T., Propagation and damping of ion waves in a plasma with negative ions, 20: 38283
OHKUBO, M., Electromagnetic fields in anisotropic plasmaguides considering the effect of electron collision, 20: 38226
OHNISHI, Hiroyuki, Plasma end loss in a slow theta pinch, 20: 38256
OHNO, Seigo, Sensitive gas chromatography of para-, orthohydrogen, hydrogen deuteride, and deuterium, 20: 36737
OHSAWA, A., New kinematical approach for analyses of high-energy cosmic-ray jets, 20: 37680
OJIMA, Tsutomu, Behavior of radioactive Sr, Cs, and Co in marine water, 20: 38537
OKABAYASHI, Takeo, Some aspects of the direct interaction, 20: 37851
OKABE, Shigeru, Luminescence of fused quartz excited with pulsed electrons, 20: 36864
OKADA, Kunihiko, Systematics and phenomenology of boson mass levels. III., 20: 37846
OKADA, Minoru, T-E_γ charts of short-lived nuclides formed by neutron activation, 20: 36739
OKADA, S., Effect of irradiation on DNA synthesis in the regenerating livers of rats, 20: 36593
OKADA, Takeshi, Texture and microstructure of thin-walled Zircaloy-2 tubes, 20: 37237

OKADA, Tsuichi, Study of the enhancement of x-ray coloration of NaCl by divalent impurities, 20: 38373
OKAMOTO, Yoshizo, High-temperature gas loop and experiments of finned fuel elements, 20: 38481
OKE, J. B., Analysis of field horizontal-branch and RR Lyrae stars, 20: 37419
O'KELLEY, J. C., Liquid scintillation determination of ^{45}Ca and ^{89}Sr in unicellular algae, 20: 36747
OKRENT, D., Summary of intercomparison calculations performed in conjunction with conference, 20: 38490 (ANL-7120, pp 3-23)
OKUBO, Susumu, Currents algebra and models of elementary particles, 20: 37830
OKUDA, H., Observation of muon air showers, 20: 37607
OKUN, L. B., Possibility of observing mirror particles, 20: 37806
OLHOEFT, J. E., Comparison of Monte Carlo and resonance integral methods in determination of Doppler effects in fast reactors, 20: 38423 (ANL-7120, pp 462-77)
OLIVE, Ph., Potassium in sections of 5 borings made in Evian quaternary formations, 20: 37012
OLLENDORFF, W., Structure investigations on lanthanide oxalates. I., 20: 36835
OLSEN, William Charles, Alpha-particle breakup of the 12.71 and the 11.83 Mev levels in ^{12}C, 20: 38162
OMELIANENCO, M., Lifetime of the μ^- in ^{239}Pu, 20: 38114
ONDOH, Tadanori, Pre-SC increases of hf field intensity on polar paths and of f_0F_2 in high latitudes, 20: 37892
O'NEILL, G. L., Safety and economic aspects of vented fuel in sodium-cooled reactors, 20: 38475 (ANL-7120, pp 540-8)
O'NEILL, G. L., Safety and economic characteristics of 1000-Mwe fast Na-cooled reactor design, 20: 38498 (ANL-7120, pp 185-204)
ONNIS, A., Intralymphatic isotope therapy with a new radioactive phosphate compound (^{32}P) in fat soluble radiopaque contrast media, 20: 36684
ONO, Masayoshi, Preliminary study of the determination of hydrogen content in heavy water by means of neutron transmission, 20: 36740
ORDAN'YAN, S. S., Structure of the alloys of the Zr–C–Ta system, 20: 37270
OREKHOV, V. D., Products formed by radiolysis of benzene in aqueous solutions of sodium nitrate, 20: 37881
OREL, M. A., Effect of γ radiation on flotation properties of anionic collector agents, 20: 36893
ORLOV, Yu. V., Role of unphysical partial-wave amplitude singularities in the deuteron photodisintegration, 20: 38140
ORMEROD, M. G., Reaction of OH radicals with nucleic acid bases, 20: 36806
ORMES, J. F., Measurements of the primary proton and He spectra and their modulations using a balloon-borne Cherenkov-scintillation counter, 20: 37554
ORMES, J. F., Measurements of energy spectrum of nuclei with $Z \geq 3$ using a balloon-borne Cherenkov scintillation counter, 20: 37571
ORMONDE, S., Electron-impact excitation of n = 2 states in He, 20: 37453
ORRALL, F. Q., Loop prominences and coronal condensations. III., 20: 37348
ORTH, C. J., Decay of 25-min ^{246}Am and 1.8-day ^{246}Bk, 20: 38097
ORTNER, J., Introduction to solar terrestrial relations, 20: 37916
OSBORN, A. W., Radiation sterilization of sugar cane leafhoppers, 20: 37146
OSBORNE, L. S., New test of Su(3) in meson photoproduction, 20: 37773
OSETINSKII, G. M., Reaction $^3He + {}^3He$, 20: 38131
OSHER, J. E., High-energy neutral injection into a mirror-quadrupole cusp magnetic well, 20: 38277
OSHIO, T., Variation of ^{14}C content in the atmosphere during the past two thousand years, 20: 37602
OSIPOVA, V. V., Some properties of U_2O_5, 20: 36832
OSMOND, D. G., Hemopoietic response of guinea pig to gamma irradiation, 20: 36611
OSTERBROCK, D. E., Mass loss in the planetary nebula stage, 20: 37416
OSTERMAN, Siv, Synthesis of some tritium-labeled mutagenic alkyl alkanesulfonates, 20: 36916
OSWALD, Robert B. Jr., Changes in the conductive properties of CdS induced by thermal neutrons, 20: 38405
OTOUPAL, Pavel, Patho-anatomical findings in pigs whole-body irradiated with gamma rays, 20: 36657
OTT, K., Results of Doppler coefficient calculations for fast reactors and comparison of different methods. I and II., 20: 38421 (ANL-7120, pp 440-8)
OTT, K., Survey parameter study of large steam-cooled fast power reactors, 20: 38438 (ANL-7120, pp 815-25)
OTTINGER, R. S., Prog. rpt. on booster rocket altitude abort program, 1–4/66, 20: 36996 (SC-CR-66-2045)
OUTI, Akizi, Model of the dispersive nonlinear equation, 20: 37926
OVCHARENKO, V. I., Electric quadrupole transitions in deformable even-even nuclei, 20: 38127
OYA, Shinzo, Method of producing improved polycarbonate, 20: 36907
OZERNOI, L. M., Statistical properties of the optical variability of the quasistellar radio source 3C 273, 20: 37382

P

PACILIO, N., Power level fluctuations of steady-state operating reactor, 20: 38445 (RT-FI-(66)1)
PACK, D. C., Magnetogasdynamic flow over a wedge, 20: 38242
PADALKA, V. G., Mechanism of capture of a moving plasma by a transverse magnetic field, 20: 38249
PADERNO, Yu. B., Physical properties of certain rare earth dicarbides, 20: 36811
PAETZGEN SCHIECK, H., Reactions $D(d,n)^3He$ and $D(d,p)^3H$ with polarized deuterons at 460 kev, 20: 38074
PAGEL, B. E. J., Abundance differences among population I stars, 20: 37425
PAIGE, D. M., Plant and equipment design and operation, 20: 36949
PAIX, D., Do-it-yourself external standardization for a liquid scintillation counter, 20: 37085
PAL, Y., Arrival time distributions of heavy particles in air showers, 20: 37633
PAL, Y., Possible flux of heavy triplets and similar particles in cosmic radiation and their detection, 20: 37719
PAL, Y., Secondary spectra for truncated spectra for the primary cosmic rays, 20: 37677
PALCHEVSKII, V. V., Electron absorption spectra of Ce(III) salts in water–TBP mixtures and in pure TBP, 20: 36831
PALEV, Ch., Determination of Λ and Σ hyperon parity, 20: 37756
PALEVSKY, H., Elastic scattering of 1 Bev protons from He and O, 20: 38010 (BNL-10438)
PALM, R. G., Compatibility of modified carbide fuels with stainless steel, 20: 38466 (ANL-7120, pp 301-13)
PALMER, John A., Kinetic behavior of a circulating-water reactor following large reactivity changes, 20: 38449
PALOMARES DELGADO, F., Solvent extraction applied to analysis of U. II., 20: 36717
PALOMARES DELGADO, F., Solvent extraction applied to analysis of U. III., 20: 36718
PALOMARES DELGADO, F., Spectrophotometric determination of U with arsenazo, 20: 36716
PALSHIN, E. S., Solvent extraction of protactinium and other elements as phenylarsonates, 20: 36940
PANKRATOV, A. K., Some results of studies of the solar-diurnal variation of cosmic rays during the IGY period, 20: 37526
PAO, H. P., Magnetohydrodynamic jet-vortex in a viscous conducting fluid, 20: 37878
PAOLETTI, R., Regulation of lipid transport and radiation-induced hyperlipemia, 20: 36580
PAPE, Rudolf, X-ray therapy with small doses with special consideration of the treatment of children, 20: 36707
PAPESCHI, Giorgio, Behavior of T% in the naphthalene test during a magnetic storm, 20: 37890
PAPESCHI, Giorgio, First results on the relations between the naphthalene test and the lunar phases, 20: 37891
PAPESCHI, Giorgio, Solidification of naphthalene and natural electromagnetic fields, 20: 37889
PAPWORTH, D. G., Sensitivity of rat oocytes to x rays, 20: 36632
PARDO, William B., Conference on plasma instabilities and anomalous transport, Coral Gables, 5/66, 20: 38316
PARK, Efton L. Jr., Nucleate and film boiling heat transfer to nitrogen and methane at elevated pressures and large temperature differences, 20: 36993
PARKER, E. N., Brief outline of the development of cosmic-ray modulation theory, 20: 37494
PARKER, E. N., General dynamical effects of cosmic rays in the galaxy, 20: 37501
PARKER, E. N., Non-relativistic equations of bulk motion of a relativistic gas, 20: 37344
PARKER, J. L., University of Utah neutrino detector, 20: 37104
PARKS, P. B., Precision measurement of reaction thresholds, 20: 38028
PARLIER, B., Flux and east-west asymmetry of primary electrons at a geomagnetic rigidity cut-off of about 4.5 GV, 20: 37550
PARSONS, M. J., Overall thermal efficiencies of combined gas–steam cycles in an MHD-reactor system, 20: 38488 (AERE-R-5031)
PARTRIDGE, R. B., Modulated absorption of light in an optical pumping experiment on ^4He, 20: 37457
PARTRIDGE, R. B., Transfer of coherence by collisions of ^3He atoms, 20: 37458
PASCARU, I., Paramagnetic centers formed by irradiation of oxygenated compounds of Se. II., 20: 38398
PASHLEY, J. H., Fluid-bed volatility component, engineering feasibility, and scale-up studies at the Oak Ridge Gaseous Diffusion Plant, 20: 36926 (K-L-6091)

PASTERNAK, R. A., Low-pressure study of heterogeneous H–deuterium exchange at steady state, 20: 36818
PATRASSI, E., Microanalytical studies of micro- and macro-segregation in oxide fuels, · 20: 38469 (ANL-7120, pp 400-9)
PATTEN, Bernard C., Photosynthesis and uptake of ^{85}Sr in freshwater plankton, 20: 36568
PATTERSON, Don W., Nuclear decoupling, full and partial, 20: 36964
PATTERSON, H. Wade, Cosmic-ray-produced neutrons at ground level: neutron production rate and flux distribution, 20: 37483
PATTISON, J. B. M., Intensity and angular distribution of cosmic rays far underground, 20: 37704
PATTISON, J. B. M., Muon interactions far underground, 20: 37701
PATZELT, R., Digital methods in thickness gaging, 20: 37058
PAUL, D. A. L., Positronium formation and annihilation in argon-propane mixture, 20: 37816
PAULSON, A. E., Analysis of lumped burnable poison critical experiments, 20: 38441 (BAW-3492-1(Suppl.1))
PAULUS, I., Velocity distribution of electrons in positive column of discharge, 20: 38213
PAULY, J., Use of an automated system including a radiochemical step in activation analysis, 20: 36782
PAVLIKOV, V. N., Phase transformations of certain rare earth chromites, 20: 36812
PAVLOV, V. S., Purification of cerium by electric transport combined with zone melting, 20: 36936
PAVLOVA, M. P., Natural radioactivity of skeletons, 20: 36559
PAWEL, Otto, Patho-anatomical findings in pigs whole-body irradiated with gamma rays, 20: 36657
PAYTON III, Daniel N., Dynamics of disordered harmonic lattices, 20: 38356 (LA-3510)
PEACOCK, N. J., Extreme ultraviolet spectra from laser-produced plasmas, 20: 38300
PEAK, L. S., Elastic and electromagnetic proton interactions at 30 Bev, 20: 37666
PEAK, L. S., Investigation of high-energy nuclear interactions using a quartile energy estimator, 20: 37681
PECHLANER, E., Quadratic Lagrangians in general relativity, 20: 37918
PECK, P. F., Examination of surfaces by scanning with charged particles, 20: 38376
PEDROCCHI, E., Liquid volume fraction in adiabatic two-phase vertical upflow-round conduit, 20: 36935 (EURAEC-1088)
PEISACH, Max, Analysis of surfaces by scattering of accelerated alpha particles, 20: 36719
PEISL, H., Thermal annealing of lattice parameter change in low-temperature neutron-irradiated aluminium, · 20: 38380
PEKER, L. K., Spins of three-particle isomeric states in spherical nuclei with odd mass numbers, 20: 38136
PELEKIS, L. L., Measurements of large γ-radiation doses and fluxes by means of photoactivation of isomeric nuclear states, 20: 37079
PENNY, S. K., Survey of U. S. shielding calculational methods and programs, 20: 38350 (ORNL-P-2310)
PENSO, Gianni, Photoproduction of neutral pions in the energy range 400 to 600 Mev of the incident photon, 20: 37752
PERCIVAL, I. C., Classical theory of charge transfer and ionization of hydrogen atoms by protons, · 20: 37454
PERCIVAL, I. C., Classical impulse approximation to ionization of hydrogen atoms by protons, · 20: 37456
PERCIVAL, I. C., Generalized correspondence principle and proton-hydrogen collisions, · 20: 37455
PEREC, Liliana, Radiochemical polymerization of lauryl methacrylate in liquid and solid phases, 20: 36875
PERELOMOV, A. M., Casimir operators for the orthogonal and symplectic groups, 20: 37856
PERETTO, P., Interpretation of stage I in Ni irradiated by electrons, 20: 37297
PEREY, F. G., Anomalous isotope shift of the nuclear charge radius, 20: 38101
PEREZ, R. B., Dynamic method for in-pile fission-gas release studies, 20: 37292
PERFILOV, N. A., Cross section of nuclear fission of tin irradiated by oxygen ions, 20: 38123
PERKINS, R. W., Snow and rain washout coefficients for process plant radioiodine vapor, 20: 37033
PERKONS, A. K., Hair individualization studies, 20: 36781
PERKS, A. J., Dimensional changes and radiation creep of graphite at very high neutron doses, 20: 37282
PERLMAN, Morris L., X rays and electrons emitted in coincidence with the fission of ^{252}Cf, 20: 38095
PERRIZO, J. J., Sulfur-36 $(p,\gamma)^{137}Cl$ reaction for proton energies in the 800-1800 kev region, 20: 38185
PERRY, Harold, Clinical evaluation of the treatment of advanced head and neck cancers with high-energy electron beams, 20: 36685
PERSIANI, P. J., Faret Core-I reference design, · 20: 38460 (ANL-7120, pp 766-75)
PETERKOP, R. K., Atomic collisions, · 20: 37477
PETERS, B., High-energy interactions, 20: 37686
PETERS, B., Search for heavy particles in the cosmic radiation, 20: 37654
PETERS, B. C., Strength of tantalum columbium alloy single crystals, 20: 37215
PETERS, M. K., Determination of trace amounts of copper in niobium and tantalum by atomic-absorption spectroscopy, 20: 36726
PETERSEN, Joergen Otzen, Calculations of main-sequence stellar models, 20: 37400
PETERSON, G. T., Flood safety of steam- and gas-cooled fast reactors, 20: 38439 (ANL-7120, pp 826-36)
PETERSON, R. E., Fast reactor safety considerations related to fuel macrostructure, · 20: 38424 (ANL-7120, pp 497-503)
PETERSON, Vern L., Transport of s-process elements to the surfaces of stars, · 20: 37423
PETITJEAN, C., Reactions $D(d,n)^3He$ and $D(d,p)^3H$ with polarized deuterons at 460 kev, 20: 38074
PETKOV, I. Zh., Elastic scattering of fast electrons on nuclei with a Fermi distribution of charge density, 20: 38139
PETRASCU, M., Lifetime of the μ^- in ^{239}Pu, 20: 38114
PETREMENT, J., Solvent extraction applied to analysis of U. II., 20: 36717
PETREMENT, J., Solvent extraction applied to analysis of U. III., 20: 36718
PETREMENT, J., Spectrophotometric determination of U with arsenazo, 20: 36716
PETROFF, Alex N., Comments on nuclear-powered surface effect ship design problems, · 20: 38526
PETROV, V. I., Application of the similarity method to radiation fields during adjustment of neutron radiation meters, 20: 37074 (NP-16202)
PETROV, V. I., Calibration of thermal-neutron radiation meters in diffuse flow, 20: 37073 (NP-16201)
PETROV, V. I., Problem of utilizing nuclear $D(d,n)^3He$ and $T(d,n)^4He$ reactions for calibration of fast-neutron radiation meters, 20: 37075 (NP-16204)
PETRUKHIN, A. A., Angular distribution and energy spectrum of cosmic-particle showers at 10^{12} ev, 20: 37696
PETRUKHIN, A. I., Temperature and concentration of charged particles behind the front of a strong shock wave in air, 20: 37880
PETRUKHIN, V. I., Charge of π mesons stopped on light nuclei, 20: 37740 (JINR-P-2780)
PETSCHEK, A. G., Electron distribution function in a plasma with excitation collisions, 20: 38198 (LA-DC-8099)
PEZDIRTZ, George F., Cross-linking of polyvinylidene fluoride by gamma radiation, 20: 36859 (N-66-13497)
PEZDIRTZ, George F., Polyimidazopyrrolones: new class of radiation-resistant polymers, 20: 36846 (N-66-13499)
PFAFFELHUBER, Josef, Radiation protection in the framework of the atomic law of the German Republic, 20: 36676
PFENNIGWERTH, P. L., Air–water mixing tests, 20: 36989 (WAPD-TM-492)
PFLASTERER, G. R. Jr., Doppler effect in ^{238}U and ^{235}U fission in a fast-neutron spectrum, · 20: 38430 (ANL-7120, pp 616-24)
PFREPPER, G., Neutron activation analysis of luminophorescent zinc compounds. I., 20: 36755
PFREPPER, G., Neutron activation analysis of luminophorescent Zn compounds. II., 20: 36756
PFREPPER, G., Neutron activation analysis of luminophorescent Zn compounds. III., 20: 36757
PHILIPPOV, V. A., First and second spherical harmonics of the daily variations of cosmic rays, · 20: 37531
PHILIPPOV, V. A., Investigation of cosmic-ray distribution using the method of daily variations, 20: 37587
PHILLIPS, C. V., Angular correlations of $^{28}Si(d,p\gamma)^{29}Si$ from 4 to 6 Mev, 20: 38086
PHILLIPS, G. C., Absolute energy calibration of neutron thresholds, 20: 38054
PHILLIPS, G. C., Measurement of (p,n) thresholds at tandem energies, 20: 38053
PHILLIPS, J., Neutron flux in the upper atmosphere during the 1964 solar minimum, 20: 37908
PHILLIPS, K., Recent investigations of fast reactor reactivity coefficients, 20: 38418 (ANL-7120, pp 413-20)
PHILLIPS, K. E., Large metal-fueled fast reactor study. I., · 20: 38493 (ANL-7120, pp 85-93)
PHILLIPS, Richard D., Longevity in neutron-exposed guinea pigs, 20: 36640
PICARD, J., Reactions (^3He,d) on even Sn isotopes, 20: 38073
PICKLESIMER, M. L., Deformation, creep, and fracture in alpha-Zr alloys, 20: 37226
PICKLESIMER, M. L., Determination of the basal-pole orientation in zirconium by polarized-light microscopy, 20: 37266

PICKLESIMER, M. L., Mechanical anisotropy of Zircaloy-2, 20: 37232
PIDCOCK, J. K., Experiments on the pulse spectrum observed from scintillation and Cherenkov detectors at sea level, 20: 37619
PIDCOCK, J. K., Muon component of air showers, 20: 37645
PIEAU, Claude, Effects of x rays on young embryo of the blindworm, 20: 36615
PIERCE, T. B., Examination of surfaces by scanning with charged particles, 20: 38376
PIETRA, R., Use of an automated system including a radiochemical step in activation analysis, 20: 36782
PIKEL'NER, S. B., Dynamics of the solar atmosphere, 20: 37389
PIKULEV, A. T., Effect of irradiation on aminotransferase of central nervous system and muscle, 20: 36601
PIMENOV, M. I., Application of the similarity method to radiation fields during adjustment of neutron radiation meters, 20: 37074 (NP-16202)
PIMENOV, M. I., Calibration of thermal-neutron radiation meters in diffuse flow, 20: 37073 (NP-16201)
PINES, D., Interactions between ^{3}He atoms in dilute solutions of ^{3}He in superfluid ^{4}He, 20: 37962
PINKAS, Leonard Lieber Hirsch, Influence of genotype on rate of strontium absorption by barley, 20: 36575
PINKAU, K., Balloon experiment using spark chambers and an ionization spectrometer, 20: 37103
PINKAU, K., Multiplicity of high-energy interactions, 20: 37678
PISAREV, A. F., Measurement of the triple scattering parameter R_{pn} at 70° and the phase-shift analysis at 630 Mev, 20: 37739 (JINR-E-2726)
PISAREVSKII, A. N., Mechanism of protective effect of S-β-AET, 20: 36663
PISSOT, Anne-Marie, Preparation of $PaCl_5$ and absorption spectra, 20: 36798
PITAEVSKII, L. P., New research on properties of liquid helium, 20: 37974
PIVNEVA, V. T., Effects of cosmic rays according to the chromospheric flares and Forbush effects during solar activity minimum, 20: 37537
PIZZELLA, Guido, Investigation of the Van Allen belt by means of satellites on equatorial orbits, 20: 37489
PLAJNER, Zdenek, Measurements of nondestructive fuel burnup by means of γ spectroscopy of fission products, 20: 37287
PLANAS, J., Assays with ^{59}Fe in Gallus domesticus, 20: 36569
PLATZMAN, P. M., Single-particle coupling to collective excitations; sound in ^{3}He, 20: 37449
PLEISS, Guenther, Autoradiographic studies with a radiation protection material, 20: 36670
PLEKHOVA, A. I., Generation mechanism of high-energy pions in cosmic rays, 20: 37664
PLESHKO, M. P., Shower production by pions and protons with momenta 0.1 and 20 Bev/c in thin layers of matter, 20: 37669
PLONKA, A. M., Radiation-induced H-T exchange in aromatic hydrocarbons saturated with tritiated water, 20: 36868
PLOSTINARU, D., Level density parameter determination from (α,n) reactions on ^{27}Al, ^{55}Mn, ^{56}Fe, and Ag, 20: 38115
PNEUMAN, G. W., Interaction of the solar wind with a large-scale solar magnetic field, 20: 37349
POBELL, F., Studies of Sn and Sn–In alloys in superconductive state using Moessbauer effect, 20: 37271
PODCHERNYAEVA, I. A., Production and properties of W–LaB_6, 20: 37258
PODGURSKAYA, A. V., Generation mechanism of high-energy pions in cosmic rays, 20: 37664
POENARU, D., Switching circuit for photomultiplier tubes, 20: 37051
POHLIT, W., Dosimetry of ionizing radiation, 20: 37081
POKROVSKII, B. I., Solid solution region in system Sc_2O_3–Fe_2O_3–MnO_x, 20: 36839
POL, Yu. S., Elastic scattering of fast electrons on nuclei with a Fermi distribution of charge density, 20: 38139
POLAK, L. S., Chemical processes in low-temperature plasma, 20: 38314
POLAK, L. S., Kinetics of radiation-induced allyl polymerization. II., 20: 36880
POLFEROV, E. A., Increasing the internal beam current of the JINR synchrocyclotron by additional electrostatic focusing, 20: 37328
POLIKARPOV, V. I., Decay of ^{139}Cs and ^{140}Cs, 20: 38124
POLLARD, J., Observation of Zr foil specimens under the electron transmission microscope. Study of plastic deformation, 20: 37248
POLLARD, J. P., Multigroup cross sections of resonance absorbers, 20: 38451
POLLVOGT, U., Balloon experiment using spark chambers and an ionization spectrometer, 20: 37103
POLLYCOVE, M., Homotransplantation studies in dogs, following selective radioisotopic lymphatic ablation, 20: 36641
POLUEKTOV, N. S., Complexes of Nd, Ho, and Er with pyrogallosulfonic acid, 20: 36837
POLYAKOVA, G. N., Rotational energy level distribution of molecules excited by ion impact, 20: 37471
POMERANCHUK, I. Ya., Possibility of observing mirror particles, 20: 37806
POMERANTZ, M. A., Solar cycle modulation of cosmic rays, 20: 37509
POOLE, Darrell O., Analysis of surfaces by scattering of accelerated alpha particles, 20: 36719
POPEREKOVA, L. M., Generation mechanism of high-energy pions in cosmic rays, 20: 37664
POPICHENKO, E. Ya., Slip casting of zirconium boride, 20: 37201
POPOV, V. N., Theory of Bose gas produced by bound states of Fermi particles, 20: 37472
POPOV, V. S., Casimir operators for the orthogonal and symplectic groups, 20: 37856
POPOV, Yu. P., Alpha decay from excited states of Sm isotopes, 20: 38072
POPPER, P., Symposium on special ceramics, Stoke-on-Trent, Eng., 7/64, 20: 37179
PORGES, K. G., Fuel-failure detection in sodium-cooled reactors, 20: 38478 (ANL-7120, pp 862-7)
PORILE, Norbert T., Yields of products with A = 100 to 117 in the interaction of 3- and 28-Bev protons with U and Pb, 20: 38098
PORTER, N. A., Detection of radio pulses of wavelength 6.8 m, in coincidence with extensive air showers, in the energy region 10^{16}–10^{17} ev, 20: 37626
PORTER, N. A., Flux limits for high-energy γ rays from quasars and other possible cosmic-ray sources, 20: 37547
PORTER, N. A., Radio system for the detection of air showers, 20: 37102
POSPISIL, J., Influence of ionizing radiation on the Dische-positive material in urine and blood of irradiated animals, 20: 36604
POTTER, D. L., Characteristic x-ray production in single crystals (Al,Cu) by proton bombardment. I., 20: 38393
POULOS, T. A., ^{14}C-labeled polyoxyethylene (20) sorbitan monolaurate and metabolic fate in rats, 20; 36921
POWELL, B. M., Lattice dynamics of transition metals, 20: 37273
POWERS, E. J., Plasma diffusion studies in E-type r-f discharges, 20: 38327
POWSNER, E. R., Energy absorption in cylinders containing an axial source, 20: 37032
POZDEEVA, A. A., Passivity of molybdenum, 20: 37184
PRAKASH, S., Thorium–melanoxetin complex: a spectrophotometric study, 20: 36742
PREISS, K., Self shielding by encapsulated gamma sources, 20: 38349 (AD-636788)
PRESCOTT, J. R., Altitude variation of the extensive air shower density spectrum, 20: 37631
PRESCOTT, J. R., Density spectrum of extensive air showers at 2285 m, 20: 37630
PRIMENOV, M. I., Problem of utilizing nuclear D(d,n)^{3}He and T(d,n)^{4}He reactions for calibration of fast-neutron radiation meters, 20: 37075 (NP-16204)
PRING, B., Synthesis of some tritium-labeled mutagenic alkyl alkanesulfonates, 20: 36916
PRINGLE, B. H., Protein electrophoretic changes following total-body irradiation of normal and tumor-bearing rats, 20: 36582
PRIOU, Maurice, Quasi local electrodynamics, 20: 37825 (N-65-31239)
PROBST, W. G., Study of the distribution of dose in radiotherapy with the aid of electronic computers, 20: 36686
PROKHOROV, V. M., Computation of radioactive isotope concentration in an enclosed tank during isotope adsorption by the bottom layer, 20: 36711
PROKOSHKIN, D. A., Kinetics and activation energy of oxidation of alloys of the Nb–V–Ti system, 20: 37191
PROKOSHKIN, Yu. D., Charge of π mesons stopped on light nuclei, 20: 37740 (JINR-P-2780)
PROSKURYAKOV, V. A., Temperature and concentration of charged particles behind the front of a strong shock wave in air, 20: 37880
PROUT, E. G., Thermal decomposition of irradiated mercuric oxalate, 20: 36898
PROUT, E. G., Thermal decomposition of gamma-irradiated barium azide, 20: 36900
PROWE, B., Spectra of photo-alpha particles from nuclei in the region Z = 12 to 30, 20: 38037
PUIG, I., Contribution to safety problems related to 1000-Mwe fast power reactor project, 20: 38497 (ANL-7120, pp 157-61)
PUJIC, Zdravko, Polonium-210 amount in tobacco. Determination of Po in the environment, 20: 37030
PULLAN, B. R., Large Wilson cloud chamber and its application to ionization calorimetry work, 20: 37108
PUPKE, H., Uhf plasma oscillations in Hg low-pressure discharge. I., 20: 38214
PUPKE, H., Uhf plasma oscillations in Hg low-pressure discharge. II., 20: 38215
PUPKE, H., Uhf plasma oscillations in a Hg low-pressure discharge. III., 20: 38216
PURI, R. K., Energy spectrum of primary He nuclei at energies greater than 6 Bev, 20: 37557
PUSCH, W. G., Prog. rpt. on 1800–400F fibrous-type insulation for radio-

isotope power systems, 3–6/66, 20: 36983 (ALO-3633-1)
PUSHLENKOV, M. F., Calculation method for azeotropic steam fractionation, applied to the TBP–CCl_4 system, 20: 36731
PUVION, E., Effect of ionizing radiations on the HeLa cell. II., 20: 36616

Q

QUACK, Guenter, Tele-x-ray and telecobalt therapy in metastases, 20: 36697
QUENBY, J. J., Cosmic rays and the interplanetary field, 20: 37493
QUENBY, J. J., Long-term modulation of the cosmic-ray intensity, 20: 37513
QUINN III, James L., Year book of nuclear medicine. Vol. 1, 20: 36690
QUINN, W. E., Straight θ-pinch devices energized by energy storage supply of Scyllac, 20: 38197 (LA-3553)

R

RABIN, S. A., Mixed oxide fuel movement at various power levels and in transients, 20: 38473 (ANL-7120, pp 524-33)
RADICHEVA, M., Radioactive pollution in the area of the nuclear reactor IRT-1000, 20: 38535
RADO, W. G., Stimulated pure rotational Raman scattering in deuterium, 20: 37451
RADOPORT, I. D., Preliminary results of cosmic-ray study from the artificial Earth's satellite Proton-1, 20: 37495
RADWAN, Z., Spectrographic determination of trace amounts of rare earths. III., 20: 36729
RAICHEV, P., Modification of Schroedinger's equation, 20: 37436
RAKOVIC, M., Determination of potassium in biological material by various methods of neutron-activation analysis, 20: 36735
RAKOVIC, M., Random errors in neutron-activation analysis, 20: 36734
RALLS, K. M., High-field superconductivity of Ta–Ti alloys, 20: 37268
RALLS, K. M., Microstructure and superconductivity of a 44.7 at.% Nb(Cb)-54.3 at.% Ti alloy containing O, 20: 37267
RALPH, B., Field-ion microscope study of neutron irradiated iridium, 20: 38382
RAMADURAI, S., Abundance of ^{3}He nuclei in the primary cosmic radiation, 20: 37559
RAMADURAI, S., Heavy nuclei in the primary cosmic rays in June 1963 at Fort Churchill, 20: 37568
RAMADURAI, S., Low rigidity end of the differential spectra of the proton and helium components of the primary cosmic radiation, 20: 37561
RAMANA MURTHY, P. V., Intensity and angular distribution of cosmic rays far underground, 20: 37704
RAMANA MURTHY, P. V., Muon interactions far underground, 20: 37701
RAMSELL, T. G., Hemopoietic response of guinea pig to gamma irradiation, 20: 36611
RAMSEY, N. W., New remotely controlled unit for treatment of uterine carcinoma, 20: 36687
RAMSEY, Norman F., Absolute value of the proton g factor, 20: 3777
RANDOLPH, P., Post-explosion environment resulting from the Salmon event, 20: 36970
RANDOLPH, Philip, Salmon seismic experiment, 20: 36962
RANDOW, F., Strontium-90 in Mecklenburg hay, 20: 36671
RANDOW, F., Strontium-90 in milk, 20: 36674
RANGARAJAN, C., Estimates of biospheric contamination and radiation dose from fallout for all the pre-treaty tests of nuclear weapons, 20: 37004
RANGNEKAR, Asha V., Cation exchange studies of Tl(I) on Dowex 50W-X8: separation from mixtures, 20: 36935
RANNIKKO, Simo, X-ray standardization and comparison of the Finnish and Swedish x-ray standards, 20: 37078
RANSOM, C. J., Anomalous transport phenomena in a ring discharge, 20: 38329
RAO, C. U., Effect of thermal neutron irradiation on mitosis, 20: 36644
RAO, U. R., Semi-diurnal anisotropy of the cosmic radiation, 20: 37521
RAO, U. R., Survey of the diurnal anisotropy, 20: 37522
RAPHAEL, R., Polarization effects in photonuclear reactions, 20: 38175
RAPOPORT, I. D., Distribution of the energy portion transferred to π^0 mesons, 20: 37660
RAPOPORT, I. D., Four-momentum transferred in high-energy interactions, 20: 37659
RAPOPORT, I. D., Relationship of neutral and charged particles among nuclear-active particles with energies above 100 Bev at mountain altitude, 20: 37685
RAPP, Robert A., Oxidation of Nb–Zr and Nb–Zr–Re alloys in oxygen at 1000°C, 20: 37193
RAPPAPORT, Paul, Space power: the next step, 20: 36998
RAPPENEAU, J., Energy released at high temperature by irradiated graphite, 20: 37283
RASCHE, G., General formalism of some scattering processes involving photons, 20: 37758
RASHID, Abdur, Colorimetric determination of Au, Pt, and Ce, 20: 36725
RASTIN, B. C., Photonuclear interactions of μ mesons, 20: 37702
RASTIN, B. C., Study of the μ meson charge ratio at sea level, 20: 37687
RASZILLIER, I., Rarita-Schwinger quantum fields, 20: 37853
RATNIKOV, E. F., Effects of certain cycle parameters on efficiency of gas-turbine nuclear plants, 20: 38513
RAU, Robert C., Interstitial dislocation loops in beryllium oxide irradiated at high temperatures, 20: 38377
RAUERT, W., Scattering of gamma rays and neutrons to investigate underground aquifers, 20: 37135
RAUP, David M., Fractionation of the stable isotopes of C and O in marine calcareous organisms: the Echinoidea. I., 20: 36549
RAUP, David M., Fractionation of the stable isotopes of C and O in marine calcareous organisms: the Echinoidea. II., 20: 36550
RAVENHALL, D. G., Remarks on the theory of μ-mesic atoms, 20: 37479
RAWSON, D., Post-explosion environment resulting from the Salmon event, 20: 36970
RAY, E. C., Relation of L-derived cutoffs to the results of numerical integrations, 20: 37594
RAY, M., Variational principles in magnetohydrodynamics, 20: 37877
RAZORENOV, L. A., Some results of the investigation of the primary cosmic-ray nuclei on the artificial satellite Electron-2, 20: 37600
READER, Joseph, Ionization energies of the neutral rare earths, 20: 37439
READY, J. F., Ion emission from laser irradiated tungsten, 20: 37298
REALE, Armando, (e,e'p) reaction in the ^{32}S nucleus, 20: 38016
REAMES, D. V., Experimental examination of low-energy cosmic-ray heavy nuclei, 20: 37569
REATTO, L., Slow-neutron scattering by liquids: hindered-translator model, 20: 37999
REATTO, L., Slow neutron scattering by liquids: a hindered-translator model, 20: 38006
REBER, J. D., Neutron cross sections of Ca from 2.0 to 6.5 Mev, 20: 38183
REDFIELD, Alfred G., Superconducting mixed-state-structure determination in vanadium by nuclear magnetic resonance and relaxation, 20: 37963
REED, D., Determination of ^{137}Cs in irradiated U and Th, 20: 36758
REED-HILL, R. E., Some effects of prestrain at 77°K on the mechanical properties of Zr at room temperature, 20: 37228
REEDYK, Arie, Search for a 5.6 Mev level in ^{7}Li, 20: 38164
REES, M. J., Kinetic temperature and ionization level of intergalactic hydrogen in a steady-state universe, 20: 38218
REES, N. J. M., Model investigation of explosion containment in single tank fast reactors, 20: 38458 (ANL-7120, pp 692-719)
REEVES, Hubert, Nuclear energy generation in stars, and some aspects of nucleosynthesis, 20: 37392
REHMAN, W., Defect luminescence in CsI, 20: 38401
REID, R. J. O., Experiments on the pulse spectrum observed from scintillation and Cherenkov detectors at sea level, 20: 37619
REILLY, J. J., Pyrolytic carbon decladding, 20: 36956
REINES, F., Prog. rpt. on neutrino physics, cosmic rays, and elementary particles, 10/65–9/66, 20: 37735 (COO-818-96)
REIZ, Anders, Calculations of main-sequence stellar models, 20: 37400
REMAEV, V. V., Isomers of ^{131m}La and ^{136m}La, 20: 38125
RENGARAYAN, T., Search for heavy particles in the cosmic radiation, 20: 37654
RERIKH, K. V., Broken $\bar{U}(12)$ symmetry and unitarity condition for the S matrix, 20: 37855
RESIKYAN, A. M., Positive column between coaxial cylinders, 20: 38236
RESTELLI, E. F. Jr., Transient temperature distribution in fuel elements, 20: 38471 (ANL-7120, pp 486-93)
RETIEF, J. J., Experimental study of some of the basic properties of spark chambers, 20: 37105
REUSCHL, H., Effect of gamma-rays on potato starch in relation to its water content, 20: 36599
REUTER, F. W., Microstructure and superconductivity of a 44.7 at.% Nb(Cb)-54.3 at.% Ti alloy containing O, 20: 37267
REVEL, Gilles, Determination of O in Al and Zr by irradiation with ^{3}He ions, 20: 36741
REYNOLDS, M. B., Radiation effects in some engineering alloys, 20: 37286
RHODES, B. A., Radiation dose to the rat thyroid from several radioiodine nuclides, 20: 36561
RHODES, J. R., Coal-ash monitor with low dependence on ash composition, 20: 37153
RICE, G., Overall thermal efficiencies of combined gas–steam cycles in an MHD-reactor system, 20: 38488 (AERE-R-5031)
RICH, A., Direct measurement of the g factor of the free positron, 20: 37775
RICHARDS, V., Homotransplantation studies in dogs following selective radioisotopic lymphatic ablation, 20: 36641
RICHMOND, C. R., Retention of ^{54}Mn by four mammalian species, 20: 36554 (LA-DC-7305)

RICKARDS, G., Absolute energy calibration of neutron thresholds, 20: 38054
RICKARDS, G., Measurement of (p,n) thresholds at tandem energies, 20: 38053
RICKARDS, G. K., Thermal annealing of heavy ion damage in copper, 20: 38378
RIDDLE, N. A., Investigation of the modulation of the primary cosmic radiation using an airborne detector, 20: 37510
RIEDEL, J., Princeton-Pennsylvania accelerator standard magnet current regulators, 20: 37338
RIEDINGER, A. B., Cs–graphite sorption isotherms determined by a static method, 20: 36799
RILEY, J. S., Gemini carbon dioxide sensor, 20: 37064
RIPEANU, S., Inelastic scattering of slow neutrons in pentane, 20: 38001
RIQUELME, J., Estimation of the relative abundance of the carbon isotopes of the primary cosmic rays, 20: 37574
RITTENHOUSE, P. L., Mechanical anisotropy of Zircaloy-2, 20: 37232
RITTLER, M. Catherine, Clinical studies in laser photocoagulation, 20: 36682
RITTLER, M. Catherine, Prophylactic photocoagulation of recurrent toxoplasmic retinochoroiditis, 20: 36683
RITZL, Friedrich, Investigations with a tritium-labeled N-mustard gas derivative in carcinoma treatment, 20: 36705
RIVIERE, M. R., Thymus origin of lymphomatoses in mice after irradiation by x rays, 20: 36613
RIZZUTO, C., Effect of transition-metal impurities on the critical temperature of superconducting Al, Zn, In, and Sn, 20: 37955
RNO, J. S., Low energy multiply charged nuclei in the cosmic radiation, 20: 37565
ROACH, W. R., Alternating current losses and magnetic field aberrations associated with use of high-field superconducting wire in adiabatic demagnetization apparatus, 20: 37970
ROACH, W. R., Thermal and magnetic properties of dilute solutions of ^{3}He in ^{4}He at low temperatures, 20: 37961
ROBBINS, A. B., Isobaric analog state polarization measurements to determine the spin of ^{145}Sm, 20: 38068
ROBERTS, A. S. Jr., Electron beams from a duoplasmatron using a hollow cathode arc as electron source, 20: 37045
ROBERTSON, B. C., Meteorological factors affecting the counting rate of neutron monitors, 20: 37100
ROBERTSON, Harry S., Conference on plasma instabilities and anomalous transport, Coral Gables, 5/66, 20: 38316
ROBERTSON, Harry S., Plasma stability research program at the University of Miami, 20: 38317
ROBERTSON, John A. L., Nuclear reactor fuel, 20: 37181
ROBERTSON, William D., Binary phase diagrams of halide salts, 20: 36787 (YALE-2723(Vol.1))
ROBERTSON, William D., Binary phase diagrams of halide salts, 20: 36788 (YALE-2723(Vol.2))
ROBIN, M., Contribution to safety problems related to 1000-Mwe fast power reactor project, 20: 38497 (ANL-7120, pp 157-61)
ROBIN, M. G., Program proposed for safety studies of fast neutron project of EURATOM-CEA association, 20: 38492 (ANL-7120, pp 54-66)
ROBINSON, D. M., Perturbations in x-ray dose response in vitro with time after plating, 20: 36664
ROBINSON, Hugh G., Absolute value of the proton g factor, 20: 3777
ROBINSON, L. E., Status of recent meltdown studies, 20: 38474 (ANL-7120, pp 534-9)
ROCCHIA, R., Energy spectrum of primary galactic x rays between 20 and 50 kev, 20: 37580
ROCCHIA, R., Gamma-ray generation in the high atmosphere, 20: 37576
ROCCO, G. G., Nondestructive determination of nitrogen in diamond by photoactivation, 20: 36746
ROCHESTER, G. D., Differential momentum spectrum and charge ratio of muons in extensive air showers, 20: 37643
ROCKMORE, D. M., Calculated core annihilation momentum distributions for several metals, 20: 37821
RODE, E. Ya., Phase diagram of the system WO_3–Nd_2O_3, 20: 37240
RODE, E. Ya., Phase diagram of the system $Nd_2(WO_4)_3$–Na_2WO_4, 20: 37241
RODEAN, Howard C., Effects of underground nuclear explosions on natural gas well performance, 20: 36961 (UCRL-12229)
RODRIGUEZ, Pablo J., Calculation of the efficiency of the ^{85}Kr nuclear battery, 20: 37159
ROEDBERG, Harald, Umbra intensity of a large sunspot, 20: 37364
ROEDERER, J. G., Magnetospheric phenomena, 20: 37911
ROEHRS, H., Studies of high-energy nuclear interactions with nuclear emulsions, 20: 38168
ROELLIG, H. E., Interaction between sintered aluminum and uranium dioxide, 20: 37203
ROELLIG, L. O., Positron lifetimes in low-temperature helium gas, 20: 37817
ROGERS, I. W., Study of the electromagnetic interactions of high-energy muons using a large scintillator stack, 20: 37699
ROGERS, J. T., Heat transfer limitations on nuclear reactor fuel elements, 20: 38484
ROGERS, K. C., Diffusion and instabilities in "Q" machine plasmas, 20: 38324
ROGERS, Leo A., Free-field motion near a nuclear explosion in salt: Project Salmon, 20: 36963
ROHRER, Robert, Cloud development studies, Project Pre-Schooner II, 20: 36958 (PNE-511)
ROINISHVILI, N. N., Tskhra-Tskaro installation for study of interactions of high-energy particles of cosmic rays with matter, 20: 37684
ROIZIN, Leon, Early and late effects of x irradiation on the cerebral cortex of the monkey, 20: 36656
ROLNICK, William B., Electromagnetism of hadrons and higher symmetries, 20: 37843
ROMAGNOLO, A., Intralymphatic isotope therapy with a new radioactive phosphate compound (^{32}P) in fat soluble radiopaque contrast media, 20: 36684
ROMERO, F., Solar and sidereal daily variations of cosmic-ray intensity at a depth of 60 m.w.e. underground in London, 20: 37504
RON, Moshe, Moessbauer study of the structure and decomposition of Wustite, 20: 38362
RONAT, E. E., Decay correlations of photo-produced rho mesons in the strong-absorption model, 20: 37768
RONAT, E. E., Rho meson photoproduction cross sections in the strong-absorption model, 20: 37766
RONDENAY, R., Industrial uses of irradiation, 20: 37140
ROOS, P. G., Excitation of single-particle states in ^{8}Be by the ^{9}Be(p,d)^{8}Be reaction, 20: 38067
ROSATI, S., Numerical evaluation of the two-nucleon scattering length and effective range with tensor forces, 20: 37782
ROSE, D. C., Variation of the cosmic-ray intensity during the eleven-year solar cycle, 20: 37515
ROSE, Sewell C. Jr., Some hydrodynamic characteristics of bubbly mixtures flowing vertically upward in tubes, 20: 36988 (TID-23261)
ROSENBLUTH, M. N., Drift instability due to impurity ions, 20: 38296
ROSENBLUTH, M. N., Plasma wave propagation in hot inhomogeneous media, 20: 38284
ROSENFELD, Judy Vadasz, Effect of gamma radiation on conductivity of electrolyte solutions, 20: 36912
ROSENTAL, I. L., Angular distribution and energy spectrum of cosmic-particle showers at 10^{12} ev, 20: 37696
ROSNER, Baruch, Reaction (d,p) and (d,t) on ^{136}Xe, 20: 38099
ROSS, S. L., Irradiated wood-polymer combinations, 20: 37145
ROSSI, G., Application of a phenomenological thermalization model to irradiated heavy water lattices, 20: 38455
ROSTOKIN, V. I., Theory of atomic energy levels in a plasma, 20: 37474
ROTARIU, G. J., Advances in radioisotope instrumentation development; program of the USAEC, 20: 37150
ROTH, J. Reece, Modification of Penning discharge useful in plasma physics experiments, 20: 38308
ROTH, R. F., Interference in the $K_L \to \pi^+\pi^-$ system, 20: 37814
ROTHENFLUG, R., Energy spectrum of primary galactic x rays between 20 and 50 kev, 20: 37580
ROTHWARF, Allen, Transport properties of degenerate fermion systems, 20: 37984
ROTSHIN, A. P., Four-momentum transferred in high-energy interactions, 20: 37659
ROTTER, I., Lithium-induced reactions and the structure of light nuclei, 20: 38014
ROY, Rustum, Prog. rpt. on crystal chemistry studies, 2/14–5/13/66, 20: 36784 (AD-636054)
ROYCE, B. S. H., Low-temperature annealing processes in alkali halides, 20: 36901
ROYLANCE, P. J., Hemopoietic response of guinea pig to gamma irradiation, 20: 36611
ROZENBERG, Jean, Photochemical separation of isotopes, 20: 37164
ROZEN'FEL'D, S. Sh., Effect of γ radiation on flotation properties of anionic collector agents, 20: 36893
RUBBINO, A., Alpha emission from heavy nuclei induced by neutrons of 12 to 23 Mev, 20: 38036
RUBINSTEIN, H. R., Dynamical derivation of baryon masses in the quark model, 20: 37762
RUBINSTEIN, H. R., Dynamical quark model for hadrons, 20: 37763
RUBINSTEIN, H. R., Spin-2$^+$ meson decays in the quark model, 20: 37780
RUBTSOV, V. I., Measurements of cosmic-ray electron component intensity, 20: 37548
RUBY, Lawrence, Interpretation of pulsed-source experiments in a reflected reactor, 20: 38453
RUBY, S. L., Quadrupole interaction in ^{121}Sb by Moessbauer techniques, 20: 38386
RUD, B. M., Physical properties of certain rare earth dicarbides, 20: 36811
RUEBE, Werner, Functional radiodamage of the brain, 20: 36651

RUEGG, F. C., Moessbauer spectrometer for the structural analysis of materials, 20: 37056
RUNOV, A. D., Properties of yttrium borides, 20: 38359
RUPP, A. F., Isotopes and Radiation Technology. Vol. 3, Number 3, 20: 37136
RUPP, L. W. Jr., Nuclear magnetic resonance probe for calibrating superconducting solenoids, 20: 37972
RUSANOVA, L. N., Intermediate phases in the Cr–Nb system, 20: 37239
RUSCH, G. K., Sodium-void coefficients, 20: 38426 (ANL-7120, pp 598-602)
RUSH, J. J., Motions of water molecules in K ferrocyanide trihydrate, water, and ice, 20: 36821
RUSS, J. S., Interference in the $K_L \to \pi^+\pi^-$ system, 20: 37814
RUSSELL, J. L. Jr., Hazards summary for the accelerator pulsed fast assembly, 20: 38530 (GA-6078)
RYAN, D., Muon decays from neutral primaries, 20: 37713
RYAZHSKAYA, O. G., Depth-intensity curve of nuclear events induced by muons, 20: 37703
RYBICKI, K., High-energy jets produced by heavy primary nuclei of cosmic origin and their fragmentation products, 20: 37662
RYDER, P., Studies of the barometric coefficients of IGY and NM-64 neutron monitors, 20: 37097
RYKOV, V. V., Investigation of the nucleon interactions at energies above 10^{13} ev, 20: 37657
RYSS, Yo. I., Nerve trunk regeneration in acute radiation lesion, 20: 36614
RZEPSKI, Observation of Zr foil specimens under the electron transmission microscope. Study of plastic deformation, 20: 37248

S

SAAVEDRA, I., Completeness and dispersion relations in the complex angular momentum plane, 20: 37836
SADASIVAN, S., Estimates of biospheric contamination and radiation dose from fallout for all the pre-treaty tests of nuclear weapons, 20: 37004
SADOWSKI, Henry, Nuclear radiation processing of optical maser materials, 20: 37280 (NYO-3330-11)
SAFONOV, A. N., Increasing the internal beam current of the JINR synchrocyclotron by additional electrostatic focusing, 20: 37328
SAFRONOV, B. G., Mechanism of capture of a moving plasma by a transverse magnetic field, 20: 38249
SAGDEEV, R. Z., Drift instability due to impurity ions, 20: 38296
SAGE, C. R., Bibliography on mass spectroscopy, 20: 36712 (IS-1335)
SAHADE, Jorge, Evolutionary-significant group of eclipsing variables, 20: 37429
SAID, S. S., Charge ratio of cosmic-ray muons at large zenith angles, 20: 37689
SAID, S. S., Momentum spectrum of cosmic-ray muons in the zenith angle range 82.5 to 90°, 20: 37697
SAITCEVSKY, Boris, Development in France of natural U–graphite–gas reactors, 20: 38515
SAKAGUCHI, Jiro, Method for graftcopolymerizing highly substituted cellulose-maleate, 20: 36906
SAKAI, T., Further observation of the positive excess of cosmic-ray muons, 20: 37690
SAKAKIBARA, S., Observation of muon air showers, 20: 37607
SAKHAROV, V. K., Distribution of fast fission neutrons along straight cylindrical channels in water, 20: 38351
SAKHAROV, V. N., Consequences of uv-microbeam irradiation of the nucleoli of living cells, 20: 36592
SAKUMOTO, Akihiso, Hydrazine formation in the γ radiolysis of an aqueous solution of ammonia, 20: 36869
SALATSKAYA, M. I., Experimental determination of radiation quality factors in the vicinity of high-energy accelerators, 20: 37323
SALATSKII, V. I., Cross section of D(t,α)n in the energy region at 115 to 1650 kev, 20: 38130
SALIEV, A., Representation of meson force by a series of inverse powers of distance in a relativistic case, 20: 37754
SALMON, M. A., Reactor containment structures, 20: 38463 (IITRI-578P22-15)
SALVADORI, Paolo, (e,e'p) reaction in the ^{32}S nucleus, 20: 38016
SALVINI, Socio G., Photoproduction of neutral pions in the energy range 400 to 600 Mev of the incident photon, 20: 37752
SAMOCHOCKA, Krystyna, Formation of complex combinations of ^{241}Am and ^{246}Cm in citric acid media by electrophoresis on paper, 20: 36829
SAMOILOV, O. B., Cross-section averaging in thermal region for media containing zirconium hydride, 20: 37991
SAMORSKI, W., Studies on high-energy cascades using a neon hodoscope, 20: 37618
SAMOSUDOV, B. E., Cascade theory of showers for light and heavy substances taking into account the polarization of the medium, 20: 37787
SAMPSON, W. B., High field superconducting magnets, 20: 37934 (BNL-10380)
SAMS, W. Mitchell Jr., Affinity of melanin for chloroquine, 20: 36564
SAMSAHL, Knut, Anion-exchange method for sorption of trace elements in neutron-irradiated biological material, 20: 36762
SAMSONOV, G. V., Production and properties of W–LaB_6, 20: 37258
SANA, J. V., Cost estimate for remote refabrication of metallic fuels, 20: 37195 (ANL-6950)
SANATHANAN, C. K., Transient temperature distributions in fast reactor fuels with widely varying thermal diffusivity, 20: 38470 (ANL-7120, pp 478-85)
SANCER, Maurice I., Potentials for cylindrical warm plasmas, 20: 38302
SANDER, H. H., Transient annealing in semiconductor devices following pulsed neutron irradiation, 20: 37129 (SC-DC-66-1820)
SANDERS, J. P., Effect of two-pass flow in the bonus superheater assemblies, 20: 38509 (ORNL-TM-1449)
SANDERS, Steven Gill, Regularity concitions in relativistic wave mechanics, 20: 37931
SANDHAS, W., Moeller operators for scattering on singular potentials, 20: 37831
SANDS, George D., Cross-linking of polyvinylidene fluoride by gamma radiation, 20: 36859 (N-66-13497)
SANDULESCU, A., Superfluid model with fixed-particle number treatment of ^3H and ^3He emission, 20: 38116
SANDULOV, D. B., Growing BeO single crystals, 20: 36814
SANKARANARAYANAN, K., Components of genetic loads in irradiated populations of Drosophila melanogaster, 20: 36618
SANNI, A. O., Use of pulse shape discrimination with scintillation counters for cosmic-ray studies, 20: 37111
SANO, Hirotoshi, Moessbauer-effect studies of weak nuclear quadrupole interactions in ^{119}Sn, 20: 36816
SANO, Masakatsu, Catalytic decomposition of H peroxide on the γ-irradiated Ni oxide, 20: 36885
SANO, Naokatsu, NMR measurement of internal field and electric quadrupole interaction in ferromagnetic Dy metal, 20: 38374
SARABHAI, V., Characteristics of anisotropy of galactic cosmic rays during the solar cycle, 20: 37520
SARABHAI, V., Galactic cosmic rays in the solar system, 20: 37511
SARABHAI, V., Modulation II, 20: 37546
SARABHAI, Vikram, Galactic cosmic rays in the solar system, 20: 37345
SARDI, Andras, Activation determination of Si in sputum of silicotic patients, 20: 36542
SARICHEVA, L. I., Distribution of the energy portion transferred to π^0 mesons, 20: 37660
SARICHEVA, L. I., Four-momentum transferred in high-energy interactions, 20: 37659
SARICHEVA, L. I., Relationship of neutral and charged particles among nuclear-active particles with energies above 100 Bev at mountain altitude, 20: 37685
SARKAR, H., Cosmic ray produced lithium and calcium in iron meteorites, 20: 37603
SARWINSKI, R. E., Alternating current losses and magnetic field aberrations associated with use of high-field superconducting wire in adiabatic demagnetization apparatus, 20: 37970
SARWINSKI, R. E., Thermal and magnetic properties of dilute solutions of ^3He in ^4He at low temperatures, 20: 37961
SASAKI, H., Direct measurement of attenuation length of extensive air showers, 20: 37642
SASAKI, H., Observation of the character of EAS cores, 20: 37615
SATO, Yuji, Neutron activation analysis of human blood and hair, 20: 36728
SATOW, Tsuneo, Thorium–ThC phase diagram, 20: 37265
SAUERBECK, D., Procedure for the continuous recording of the isotopic exchange between solution and solid phase, 20: 36793
SAUERWEIN, Harry, Method of characteristics for the three-dimensional unsteady magnetofluid dynamics of a multi-component medium, 20: 38241
SAUNDERS, P. A. H., Extreme ultraviolet spectra from laser-produced plasmas, 20: 38300
SAVAGE, Howard, Isothermal drop calorimeter for alpha-active, pyrophoric materials, 20: 37055
SAVCHENKO, M. A., Interaction of plasma oscillations and spin waves in ferromagnetic semiconductors and metals, 20: 38354 (FTI-244/T-027)
SAVEDOFF, M. P., Cooling of white dwarfs, 20: 37408
SAVELEVA, A. I., Generation mechanism of high-energy pions in cosmic rays, 20: 37664
SAVENKO, I. A., Investigation of the outer proton belt, 20: 37905
SAVENKO, I. A., Low-energy particle fluxes inside the magnetosphere from the data of the electrostatic analyzers of the Electron-2 satellite, 20: 37904
SAVENKO, I. A., Preliminary results of cosmic-ray study from the artificial Earth's satellite Proton-1, 20: 37495
SAVIN, B. I., Low-energy particle fluxes inside the magnetosphere from the data of the electrostatic analyzers of the Electron-2 satellite, 20: 37904
SAVITSKII, P., Use of radioisotope instruments in industry in the USSR, 20: 37147
SAVVIN, S. B., Arsenazo III. Methods of photometric determination, 20: 36778

SAWADA, K., Variational ground-state energy of a Bose system. II., 20: 37838

SAWADA, T., Isobaric spin dependence of the nucleon-nucleon interaction, 20: 37811

SAWYER, G. A., Scyllacita: compact high-voltage theta pinch machine, 20: 38306

SAXENA, R. P., Current commutation relations, universality, and non-leptonic baryon decays, 20: 37839

SAXENA, R. S., Electrometric studies on the compositions of thorium polyvanadates, 20: 36822

SAYERS, J., Nuclear reactor operation in space, 20: 38529

SAZONOV, L. A., Homomolecular and isotopic exchange of oxygen on gadolinium oxide, 20: 36826

SCALAPINO, D. J., Strong-coupling superconductivity. I., 20: 37952

SCARR, J. Michael, Properties of K* (1425), 20: 37733 (BNL-10462)

SCARR, J. Michael, Resonance production in the reactions $\pi^{\pm}p \rightarrow KKN$ at 6 Bev/c, 20: 37732 (BNL-10461)

SCARSI, L., Flux and east-west asymmetry of primary electrons at a geomagnetic rigidity cut-off of about 4.5 GV, 20: 37550

SCHADE, J. P., Early and late effects of x irradiation on the cerebral cortex of the monkey, 20: 36656

SCHAEFER, Hermann J., Tissue dosages from alpha particles and heavy nuclei in solar particle beams in space, 20: 37023 (N-65-33865)

SCHAMBERGER, R., Military Compact Reactor program shield study, Suppl., 20: 38507 (NDA-Memo-2143-11)

SCHAMBERGER, R. D., Military Compact Reactor program shield study, 20: 38506 (NDA-2143-7)

SCHARMANN, A., Defect luminescence in CsI, 20: 38401

SCHARMANN, Arthur, Sputtering of Cu by noble gas ions in the energy range 100 kev to 1 Mev as a function of the incident angle, 20: 37468

SCHATZMANN, E., Role of magnetic activity during stellar formation, 20: 37399

SCHECK, F., Neutral-meson production cross sections and mixing angles in a quark model, 20: 37779

SCHEEPMAKER, A., Balloon observation of high-energy electrons, 20: 37549

SCHEFER, P. V., Rigidity dependence of the intensity variation during the solar cycle, 20: 37516

SCHENK, M., Radiation-induced phase transformations in $BaTiO_3$, 20: 37301

SCHERER, V., Structure investigations on lanthanide oxalates. I., 20: 36835

SCHERMULY, Willi, Evaluation of the growth activity of bone metastases, 20: 36701

Schieck, H. Paetz gen.
see Paetz gen. Schieck, H.

SCHIFFER, J. P., Anomalous isotope shift of the nuclear charge radius, 20: 38101

SCHILLER, C. K., Hall effect in 75 at.% Bi–25 at.% Sn alloy quenched films below 47°K, 20: 38384

SCHILLING, C. E., Method of preparing high-density, compactible U dioxide particles, 20: 37212

SCHINDLER, A., Kinetic studies in ethylene polymerization with Ziegler type catalysts. III., 20: 36827

SCHLUDERBERG, D. C., Steam cooling for fast reactors, 20: 38496 (ANL-7120, pp 136-40)

SCHLUETER, Hans, Anomalous transport phenomena in a ring discharge, 20: 38329

SCHMELE, Rolf, Results of ^{131}I-triiodothyronine test with ion exchange resin, 20: 36573

SCHMIDT, G., Limiting growth rates for generalized Harris instabilities, 20: 38290

SCHMIDT, H., Application of germanium diodes in gamma ray spectroscopy, 20: 37072 (KFK-429)

SCHMIDT, H., Neutron-capture gamma-ray investigation of ^{88}Sr level structure, 20: 38141

SCHMIDT, W., Balloon experiment using spark chambers and an ionization spectrometer, 20: 37103

SCHMITT, R., Heavy cosmic ions recorded in nuclear emulsions exposed in a polar satellite, 20: 37577

SCHNEID, Edward J., Reaction (d,p) and (d,t) on ^{136}Xe, 20: 38099

SCHNEIDER, G., Manufacture of fuel elements for an atomic reactor, 20: 37208

SCHNIER, C., Studies on high-energy cascades using a neon hodoscope, 20: 37618

SCHOEN, Detlev, Undesired co-irradiation of the organism in deep therapy of malignant tumors, 20: 36702

SCHONFELD, E., Improved accuracy in determination of radionuclide concentrations in solutions containing fast-decaying isotopes by least-squares resolution of the gamma-ray spectra, 20: 36780

SCHOOLEY, J. F., Magnetization and critical fields of superconducting $SrTiO_3$, 20: 37953

SCHOTT, L., Velocity distribution of electrons in positive column of discharge, 20: 38213

SCHREIBER, R. E., Multiaxial strain fatigue in Zircaloy-4, 20: 37235

SCHREIER, M., Solar daily variation recorded at a low-latitude station by east and west pointing telescopes during periods of maximum and minimum solar activity, 20: 37373

SCHRENK, G. L., Models for electron emission from metals with adsorbed monolayers, 20: 37431 (INDEC-SR-7, pp 3.76-111)

SCHRIEFFER, J. R., Strong-coupling superconductivity. I., 20: 37952

SCHROEDER, Wilfried, Occurrence of polar lights during slight magnetic disturbances and their relation to solar activity, 20: 37888

SCHROEDER, Wilfried, Several examples of relationship between polar lights, solar and geomagnetic phenomena, 20: 37887

SCHUEBELIN, P., Evidence for three new charged bosons of masses 1929, 2195, and 2382 Mev and narrow widths, 20: 37771

SCHUESSLER, Richard, Origin of the secondary effect of iodated x-ray contrast media on the thyroid, 20: 36571

SCHULTZ, F. V., Radiation from a vertical dipole in a warm plasma. I., 20: 38229

SCHULTZ, F. V., Radiation from a vertical dipole in a warm plasma. II., 20: 38230

SCHULZ, G., Uhf plasma oscillations in Hg low-pressure discharge. I., 20: 38214

SCHULZ, G., Uhf plasma oscillations in Hg low-pressure discharge. II., 20: 38215

SCHULZ, G., Uhf plasma oscillations in a Hg low-pressure discharge. III., 20: 38216

SCHULZ, N., Application of the delayed coincidence technique to measurement of the short mean lives in ^{131}Xe and ^{143}Pr, 20: 38031

SCHULZ, N., Half lives of levels at 405 kev in ^{211}Bi and 377 kev in ^{53}Mn, 20: 38030

SCHULZ, William D., Relativistic transformations versus Lorentz transformations, 20: 37827 (UCRL-14365)

SCHULZE, H.-A., Strontium-90 in Mecklenburg hay, 20: 36671

SCHULZE, H.-A., Strontium-90 in milk, 20: 36674

SCHUMACHER, G., Microanalytical studies of micro- and macro-segregation in oxide fuels, 20: 38469 (ANL-7120, pp 400-9)

SCHUMACHER, Werner, Indication of thyroid therapy by radioiodide localization, 20: 36706

SCHUMANN, Thomas G., Properties of K* (1425), 20: 37733 (BNL-10462)

SCHUMANN, Thomas G., Resonance production in the reactions $\pi^{\pm}p \rightarrow KKN$ at 6 Bev/c, 20: 37732 (BNL-10461)

SCHWARTZ, A. S., Pilot-scale extrusion of graphite fuel elements for HTGRs, 20: 37196

SCHWARZ, Henry P., Prog. rpt. on effect of x-ray irradiation on phospholipid metabolism, 10/65–5/66, 20: 36606 (NYO-1864-23)

SCHWARZSCHILD, A., Conversion coefficient of the 12.4-kev transition in ^{45}Sc, 20: 38087

SCHWEITZER, D. G., Fissile fuel recovery process, 20: 36955

SCHWERDTEL, E., Glass vessels with roughened surface for measurement of low-energy β radiation in liquid scintillators, 20: 37084

SCHWINGER, Julian, Relativistic quantum field theory, 20: 37844

SCIACCA, T. P. Jr., Electron densitometer for irradiation studies in electron microscope, 20: 37116

SCIAMA, D. W., Kinetic temperature and ionization level of intergalactic hydrogen in a steady-state universe, 20: 38218

SCIAMA, D. W., Origin of the microwave background radiation, 20: 37362

SCOTT, Benjamin F., Oxygen-tube combustion method for liquid scintillation assay of ^{14}C and tritium, 20: 36723

SCOTT, J. A., Examination of the overpressure and underpressure methods of operating a photoelectric nucleus counter, 20: 37094

SCOTT, O. C. A., Effect of irradiated medium on the growth of L5178Y lymphoma cells, 20: 36633

SCOTTEN, William C., Performance of sieve trays under GS heavy water process conditions. I., 20: 37160 (DP-1025)

SEARS, R. L., Solar models and neutrino fluxes, 20: 37403

SEARS, W. R., Boundary layer in crossed-fields MHD, 20: 37869

SEBASTIAN, M. F., Assays with ^{59}Fe in Gallus domesticus, 20: 36569

SEDDON, W. E., Preparation of uranium nitride and carbonitrides from uranium oxide in a fluidized bed, 20: 36850

SEDLAKOVA, L., Effect of some preparation conditions on the surface area and structure of ammonium polyuranate, 20: 36801

SEELENTAG, Walter, Present exposure of the population through medical radiation uses and its significance, 20: 36677

SEET, S. H., Density spectrum of extensive air showers at 2285 m, 20: 37630

SEGUINOT, J., Evidence for three new charged bosons of masses 1929, 2195, and 2382 Mev and narrow widths, 20: 37771

SEKIDO, Y., Observation of muon air showers, 20: 37607

SEKIGUCHI, T., Stabilizing effect of radial plasma density distribution on helical instability, 20: 38270

SEKIZAWA, Kazuko, Magnetic and crystallographic studies on rare earth germanides, 20: 38369

SELEZNEV, A. F., Mechanism of protective effect of S-β-AEC, 20: 36663

SELITSKI, Yu. A., Fission of ^{226}Ra by 12-Mev deuterons, 20: 38132
SELYE, H., Action of histamine liberators on calcification produced by various metals, 20: 36557
SEN, S. K., Effect of thermal neutron irradiation on mitosis, 20: 36644
SENS, J. C., Measurement and analysis of muonic x-ray spectra in spherical nuclei, 20: 38058
SEPP, A., Thermal annealing of lattice parameter change in low-temperature neutron-irradiated aluminium, 20: 38380
SERAFIMOV, N., Action of histamine liberators on calcification produced by various metals, 20: 36557
SERGEEV, V. O., Decay of ^{182}Ta, 20: 38134
SERGEEVA, G. A., Periodic cosmic-ray variations and their change during the cycle of solar activity, 20: 37525
SERIES, G. W., Modulates absorption of light in an optical pumping experiment on ^{4}He, 20: 37457
SERIES, G. W., Transfer of coherence by collisions of ^{3}He atoms, 20: 37458
SERRE, C., Production of charged pions by 600 Mev protons on various nuclei, 20: 38186
SESSLER, G. M., Observation of ion plasma waves at frequencies higher than the ion plasma frequency, 20: 38294
SETAELAE, Kai, Decorporation of radiostrontium, 20: 36556
SETLOW, Jane K., Resistance of Micrococcus radiodurans to uv radiation. III., 20: 36610
SETLOW, R. B., Repair of DNA, 20: 36578 (ORNL-P-2240)
SEVCIK, Frank Jr., Reaction ^{37}Cl(d,p)^{38}Cl and nuclear structure of ^{38}Cl, 20: 38153
SEVY, R., Enhanced safety characteristics of a sodium-cooled coupled reactor, 20: 38437 (ANL-7120, pp 789-93)
SEXL, R., Quadratic Lagrangians in general relativity, 20: 37918
SEXL-EGGSTAIN, Hannelore, Proton-proton scattering at 12 Bev, 20: 37747
SEYDEL, H. Gunter, Acridine orange and dye exclusion viability tests applied to irradiated Ehrlich tumor cells, 20: 36631
SHA, William T., Noniterative method of computing neutron flux distributions and coolant density profile in a light-water moderated reactor, 20: 38450
SHABANSKII, V. P., Hypothesis of origin and formation of radiation belts as a result of particle drift into the depth of the magnetosphere, 20: 37909
SHAFFER, James H., Solubilities of HF and DF in molten fluorides, 20: 36785 (ORNL-P-2202)
SHAHINIAN, P., Effect of nitrogen on tensile and creep-rupture properties of niobium, 20: 37218
SHAIR, F. H., Theoretical optimum seed concentrations in slightly ionized nonequilibrium plasmas, 20: 38288
SHAKHNAZARYAN, Yu. G., Intermediate boson production in reaction $e^- + e^+ \to W^+ + \mu^- + \nu^\mu$, 20: 37799
SHAM, L. J., Exchange and correlation effects in an inhomogeneous electron gas, 20: 38334
SHAMRAI, F. I., Heat resistance of alloys on base of W and Nb silicides, 20: 37262
SHAND, J. B., Band gap in beryllium, 20: 38406
SHAND, J. B., Motion of positrons in sodium, 20: 37784
SHAPIRA, Y., Niobium–25 Zr in strong magnetic fields: magnetic, resistive, ultrasonic, and thermal behavior, 20: 37950
SHAPIRO, Gilbert, Polarized accelerator targets, 20: 37332
SHAPIRO, M. M., ^{3}He-^{4}He in the primary cosmic radiation at Fort Churchill 1963, 20: 37572
SHAPLYGIN, I. S., Solid solution region in system Sc_2O_3–Fe_2O_3–MnO_x, 20: 36839
SHARAN, Roghubir, Gravitational significance of deviations from the Minkowskian metric, 20: 37923
SHARIPOV, Sh., Excitation state of axially odd atomic nuclei, 20: 38022
SHARKHATUNYAN, R. O., Ionization measurement in a streamer chamber, 20: 37110
SHARMA, B., Physical and chemical mutagens according to mutations in second generation, 20: 36634
SHARMA, O. P., Electrometric studies on the compositions of thorium polyvanadates, 20: 36822
SHARMA, R. D., Isobaric spin dependence of the nucleon-nucleon interaction, 20: 37811
SHARMA, Taleshwar, Oxygen-18/oxygen-16 ratios of minerals from the iron formations of Quebec, 20: 37013
SHARPEY-SCHAFER, J. F., Further measurements and zero-range DWBA calculations for the ^{52}Cr(d,p)^{53}Cr reaction, 20: 38046
SHATASHVILI, L. Kh., Asymmetric solar wind in connection with the 27-day modulation of the intensity and anisotropy of cosmic rays, 20: 37528
SHATASHVILI, L. Kh., Frequency distribution of sudden changes of cosmic-ray intensity in connection with solar activity, 20: 37541
SHAVIV, G., Results of Doppler coefficient calculations for fast reactors and comparison of different methods. I and II., 20: 38421 (ANL-7120, pp 440-8)
SHAVRIN, P. I., Investigation of the outer proton belt, 20: 37905
SHCHERBAKOV, Yu. A., Capture of pions by ^{3}He. II., 20: 38011 (JINR-P-2805)
SHCHERBAKOVA, M. N., Certain aspects of nucleon isobar production in nucleons interactions at energies 10^3 and 25 Bev, 20: 37675
SHEBEKO, A. V., Theory of diffraction scattering based on method of complex angular momenta, 20: 38143
SHECHTER, Hanan, Moessbauer study of the structure and decomposition of Wustite, 20: 38362
SHELDON, W. R., Hazard from highly ionizing radiation in space, 20: 36627
SHELINE, R. K., E1 $\Delta K = 0$ transitions in deformed odd-mass nuclei, 20: 38040
SHELINE, Raymond K., Eigenfunctions for a spherical and a deformed Saxon-Woods potential, 20: 38078
SHEMET, V. V., Extraction of metals from aqueous solutions of hydrohalic acids by means of dialkylalkylphosphinates, 20: 36941
SHEN, C. S., Origin of high-energy electrons beyond the magnetosphere, 20: 37894
SHEPLEY, Lawrence Charles, SO(3,R)-homogeneous cosmologies, 20: 37430
SHER, R., Doppler effect in ^{238}U and ^{235}U fission in a fast-neutron spectrum, 20: 38430 (ANL-7120, pp 616-24)
SHERER, D. B., Safety and economic aspects of vented fuel in sodium-cooled reactors, 20: 38475 (ANL-7120, pp 540-8)
SHESTAKOV, V. V., Angular distribution and energy spectrum of cosmic-particle showers at 10^{12} ev, 20: 37696
SHESTOPEROV, V. Ya., Characteristics of high-energy particle interaction with nuclei of light atoms, 20: 37755
SHESTOPEROV, V. Ya., Discussion of one model of the formation of extensive atmospheric showers, 20: 37612
SHESTOPEROV, V. Ya., Generation mechanism of high-energy pions in cosmic rays, 20: 37664
SHESTOPEROV, V. Ya., Interaction path of high-energy nucleons (10^{11} to 10^{13} ev) in the atmosphere, 20: 37667
SHESTOPEROV, V. Ya., New data about the nuclear-active component of young atmospheric showers, 20: 37611
SHESTOV, A. V., Increasing the internal beam current of the JINR synchrocyclotron by additional electrostatic focusing, 20: 37328
SHEVCHENKO, A. V., Infrared absorption spectra of chromites of rare earth elements, 20: 36807
SHEVCHENKO, V. F., Application of the similarity method to radiation fields during adjustment of neutron radiation meters, 20: 37074 (NP-16202)
SHEVCHENKO, V. F., Calibration of thermal-neutron radiation meters in diffuse flow, 20: 37073 (NP-16201)
SHEVCHENKO, V. F., Problem of utilizing nuclear D(d,n)^{3}He and T(d,n)^{4}He reactions for calibration of fast-neutron radiation meters, 20: 37075 (NP-16204)
SHI, Yan, Damping of spin waves in a collective model, 20: 38358
SHIBATA, S., Arrival direction of muon-rich extensive air showers, 20: 37609
SHIBATA, S., Fine structure of air shower cores observed with 20 m^2 spark chamber, 20: 37617
SHIBATA, S., Possible nuclear interaction of a muon of energy above 3×10^{14} ev, 20: 37714
SHIBATA, S., Variation of ^{14}C content in the atmosphere during the past two thousand years, 20: 37602
SHIBATA, T., New kinematical approach for analyses of high-energy cosmic-ray jets, 20: 37680
SHIGAEV, O. E., Cross section of nuclear fission of tin irradiated by oxygen ions, 20: 38123
SHIH, C., Jet compression for closed-cycle magnetoplasmadynamic electrical power generation, 20: 37724
SHIINA, Shoichi, Plasma end loss in a slow theta pinch, 20: 38256
SHIMAUCHI, Masaaki, Approximation method for potential scattering, 20: 37852
SHIMAZAKI, T. T., Effects of contaminants on Hg pool boiling heat transfer, 20: 36987 (NAA-SR-11949)
SHIMELEVICH, Yu. S., Pulsed neutron generator for boreholes and its use in nuclear geophysics, 20: 37017
SHIMIZU, Sakae, Effect of chemical state on the decay constant of ^{235m}U, 20: 38090
SHIMOKAWA, Junichi, Estimation of equilibrium separation factor in isotopic separation by chromatography, 20: 37162
SHIMOMURA, Noboru, Collision-induced instability in a magnetoactive plasma, 20: 38253
SHINNERS, Carl William, Radioactive decay of ^{140}La, 20: 38154
SHIOBARA, Shinji, Electron density measurement by microwave scattering from underdense cylindrical plasmas, 20: 38254
SHIPP, E., Radiation sterilization of sugar cane leafhoppers, 20: 37146
SHIRKOV, D. V., Soluble model for the forward scattering amplitude, 20: 37805
SHITO, Okiyasu, Systematics and phenomenology of boson mass levels.

III., 20: 37846
SHKAROFSKY, I. P., Particle kinetics of plasmas, 20: 38348
SHKLOVSKII, I. S., Synchrotron radiation spectrum of the Crab Nebula, 20: 37381
SHMELEVA, A. P., Inelastic neutron cross section measurements near 100 Bev, 20: 37668
SHOMET, J. L., Prog. rpt. on plasma waves and instabilities, 3–5/66, 20: 38205 (NYO-3565-4)
SHONO, Yoshihiko, Conduction carriers in neutron-irradiated ZnS single crystals, 20: 36865
SHORT, A. M., Fast neutron production by muons underground, 20: 37710
SHOTKIN, Louis M., Space-independent model of two-phase flow and its application to experiment, 20: 36984 (BNL-963)
SHTARKOV, L. N., Elastic scattering of γ quanta on protons above π-meson photoproduction threshold, 20: 37800
SHUKLA, P. G., Flux of He nuclei at Hyderabad, India ($\lambda = 7.6°N$), 20: 37556
SHUKLA, P. G., Study of high-energy interactions in graphite, 20: 38110
SHUKLA, P. G., Energy spectra of cascades observed at balloon altitudes and the flux of primary protons, 20: 37672
SHURE, K., Radiation-damage exposure and embrittlement of reactor pressure vessels, 20: 37289
SHUSTER, Sam, Effect of ultraviolet irradiation on skin collagen, 20: 36595
SHUSTOV, M. V., Effects of certain cycle parameters on efficiency of gas-turbine nuclear plants, 20: 38513
SHVAIKO-SHVAIKOVSKII, V. E., Chemistry of Ce in systems of Al_2O_3, Cr_2O_3, and Ga_2O_3 with Ce_2O_3, 20: 36808
SIBATA, S., Electrical optical properties of three-electrode electron lenses, 20: 37330
SIDHU, Gurnam, Observation of the 4.12-Mev $^{14}O \rightarrow {}^{14}N$ positron spectrum shape, 20: 38080
SIDOROV, V. M., Double charge exchange of 50- to 176-Mev π^- mesons in photo emulsion, 20: 38012 (JINR-P-2806)
SIDOROVA, K. K., Chlorophyll mutations as an indication of differences in the mutability of pea varieties, 20: 36624
SIFFERT, Bernard, Incorporation of uranyl cations in silicates during formation, 20: 36797
SIGNORELLI, Robert A., Stress-rupture properties of W wire from 1200 to 2500°F, 20: 37251
SIKOV, M. R., Protein electrophoretic changes following total-body irradiation of normal and tumor-bearing rats, 20: 36582
SILBAR, Richard Robert, Muon capture in 2s-1d nuclei, 20: 38166
SILBERBERG, M., Application of experimental data from TREAT meltdown studies to reactor accident analysis, 20: 38472 (ANL-7120, pp 514-23)
SILBERBERG, M., Enhanced safety characteristics of a sodium-cooled coupled reactor, 20: 38437 (ANL-7120, pp 789-93)
SILBERBERG, R., ^3He-^4He in the primary cosmic radiation at Fort Churchill 1963, 20: 37572
SILBERNAGEL, B. G., New nuclear spin-lattice relaxation process in type-II superconductors, 20: 37964
SILIN, V. P., Oscillations of a beam plasma in a high-frequency electric field, 20: 38263
SILK, M. G., Spectrum of the nuclear-active component of cosmic rays, 20: 37674
SILLEN, Lars Gunnar, Precipitation and hydrolysis of metallic ions. II., 20: 36789
SILVA, E., Estimation of the relative abundance of the carbon isotopes of the primary cosmic rays, 20: 37574
SILVESTRINI, Vittorio, Photoproduction of neutral pions in the energy range 400 to 600 Mev of the incident photon, 20: 37752
SIMIC, Miroslav M., Histologic changes in the locally irradiated spleen related to the immune response, 20: 36637
SIMMONS, J. H. W., Dimensional changes and radiation creep of graphite at very high neutron doses, 20: 37282
SIMON, A., Hydromagnetic equations with viscosity for a collisionless plasma, 20: 38244
SIMONNE, J., Behavior of MOS structures in the case of an induced ionization, 20: 37130
SIMPKINSON, William Vaughan, Experimental investigations of plasmas in electromagnetic shock tubes, 20: 38344
SIMPSON, D. A., Liquid scintillation counters, 20: 37107
SIMPSON, J. A., Abundances and energy spectra for nuclei of galactic origin above 20 Mev per nucleon, 20: 37564
SIMPSON, J. A., Acceleration of particles in the Earth's shock transition region and beyond, 20: 37900
SIMPSON, J. A., Protons and He nuclei within interplanetary magnetic regions which co-rotate with the Sun, 20: 37371
SIMPSON, J. A., Solar modulation of the galactic He spectrum above 30 Mev per nucleon, 20: 37563
SIMPSON, N., Cosmic-ray flux variation with height in the stratosphere, 20: 37552
SIMPSON, W. D., Elastic scattering of 1 Bev protons from He and O, 20: 38010 (BNL-10438)
SINCLAIR, R. M., Equilibrium of a toroidal plasma in the model C stellarator, 20: 38268
SINEL'NIKEV, K. D., Production of hot-electron plasma in magnetic mirror traps, 20: 38211 (AEC-tr-6782)
SINEL'NIKOV, K. D., Mechanism of capture of a moving plasma by a transverse magnetic field, 20: 38249
SINEL'NIKOVA, V. S., Physical properties of aluminides of transition metals, 20: 37260
SINGER, R. M., Fissile fuel recovery process, 20: 36955
SINGH, B. B., Reaction of OH radicals with nucleic acid bases, 20: 36806
SINGH, R. P., Thorium–melanoxetin complex: a spectrophotometric study, 20: 36742
SINHA, S. K., Effect of nuclear spin correlations on the scattering of neutrons by molecules, 20: 38004
SINITSYN, B. I., Distribution of fast fission neutrons along straight cylindrical channels in water, 20: 38351
SINTON, Walter, Steam turbines for nuclear power plants, 20: 38521
SIREDAY, Claude, Determination of the density of protons at the level of a satellite by exact numerical analysis of proton whistlers, 20: 37885
SIRONI, G., Flux and east-west asymmetry of primary electrons at a geomagnetic rigidity cut-off of about 4.5 GV, 20: 37550
SISMAN, O., Fission-gas release during fissioning in UO_2, 20: 37291
SITTE, K., Composition of photon-initiated showers at high energies, 20: 37628
SITTE, K., Experiment to determine the primary intensity and the primary spectrum at energies of 10^{12} to 10^{13} ev, 20: 37676
SIVAN, Y., Economic aspects of the food irradiation program in Israel, 20: 37157
SIVAPRASAD, K., Ultra-high energy muons (>200 Bev) in extensive air showers, 20: 37606
SIZMANN, R., Computer experiments on radiation annealing of Frenkel defects, 20: 37294
SKAREK, P., Production of charged pions by 600 Mev protons on various nuclei, 20: 38186
SKAVDAHL, R. E., Comment on phase-equilibria data on Pu–O and U–O systems, 20: 38468 (ANL-7120, pp 389-91)
SKILLICORN, Ian O., Properties of K* (1425), 20: 37733 (BNL-10462)
SKILLICORN, Ian O., Resonance production in the reactions $\pi^{\pm}p \rightarrow KKN$ at 6 Bev/c, 20: 37732 (BNL-10461)
SKINNER, J., Development of a production method for ThO_2–UO_2 fuel, 20: 37211
SKRIPCHENKO, N. V., Infrared absorption spectra of chromites of rare earth elements, 20: 36807
SKRIPIN, G. V., Angular dependence of coupling coefficients of the muon component of cosmic rays, 20: 37588
SKRIPIN, G. V., First and second spherical harmonics of the daily variations of cosmic rays, 20: 37531
SKRIPIN, G. V., Investigation of cosmic-ray distribution using the method of daily variations, 20: 37587
SKURIDIN, G. A., Preliminary results of cosmic-ray study from the artificial Earth's satellite Proton-1, 20: 37495
SLADE, M., Intensity of stopping pions at sea level and underground, 20: 37709
SLATTERY, G. F., Some aspects of the beta ⇄ alpha transformation in Zr–2.5Nb alloy with variable cooling rate and soak temperature, 20: 37233
SLAVATINSKII, S. A., Angular distribution of secondary particles in multiple production at high energies, 20: 37682
SLAVINSKAS, D. D., Estimation of nuclear strength functions, 20: 38038
SLIEPCEVICH, C. M., Nucleate and film boiling heat transfer to nitrogen and methane at elevated pressures and large temperature differences, 20: 36993
SLOBODIAN, Evelyn, Effects of γ irradiation on the structure of ribonuclease, 20: 36584
SLOVOKHOTOV, L. T., Elastic scattering of γ quanta on protons above π-meson photoproduction threshold, 20: 37800
SMETS, Henri B., Flux distribution in a high-power slab reactor, 20: 38452
SMILEY, S. H., Fluid-bed volatility component, engineering feasibility, and scale-up studies at the Oak Ridge Gaseous Diffusion Plant, 20: 36926 (K-L-6091)
SMIRNOV, A. M., Production of hot-electron plasma in magnetic mirror traps, 20: 38211 (AEC-tr-6782)
SMIRNOV, V. S., Influence of outer sources of geomagnetic field upon the cutoff rigidities and position of impact zones, 20: 37598
SMITH, A. M., Elastic photoproduction of π^0 mesons from deuterium, 20: 37783
SMITH, Benjamin M., Natural radioactivity in ground water supplies in Maine and New Hampshire, 20: 37006
SMITH, Charles Francis Jr., Decay of $^{64*}Zn$ compound nucleus, 20: 38152
SMITH, E., Deformation twinning in rhenium single crystals, 20: 37257
SMITH, E. J., Measurements of magnetic fields in vicinity of magnetosphere and in interplanetary space, 20: 37917

SMITH, F. A., Preliminary evaluation of a technique to study expulsion of sodium into air, 20: 38500 (ANL-7120, pp 868-72)
SMITH, F. G., Detection of radio pulses of wavelength 6.8 m, in coincidence with extensive air showers, in the energy region 10^{16}–10^{17} ev, 20: 37626
SMITH, H., Ion exchange method of estimating ^{90}Sr and other radionuclides in rainwater, 20: 36759
SMITH, Harold P. Jr., Characteristic x-ray production in single crystals (Al,Cu) by proton bombardment. I., 20: 38393
SMITH, J. Merlin, Theoretical optimum seed concentrations in slightly ionized nonequilibrium plasmas, 20: 38288
SMITH, T. F., Effect of rare-earth additions on the pressure dependence of the superconducting transition temperature of lanthanum, 20: 37965
SMITH, William R., Reaction $^{90}Zr(d,p)^{91}Zr$ at energies below 4 Mev, 20: 38096
SMOLUCHOWSKI, R., Point defect generation in LiF by plastic deformation and x irradiation, 20: 88368
SMORODIN, Yu. A., Investigation of the nucleon interactions at energies above 10^{13} ev, 20: 37657
SNIDOW, N. L., Accuracy of power reactor void coefficients extrapolated from measurements in critical assemblies, 20: 38425 (ANL-7120, pp 585-97)
SNODGRASS, Herschel B., Scattering of charged particles by nonspherical atoms, 20: 37444
SNYDER, R. E., Quadrupole interaction in ^{121}Sb by Moessbauer techniques, 20: 38386
SOBINYAKOV, V. A., Generation mechanism of high-energy pions in cosmic rays, 20: 37664
SOBINYAKOV, V. A., Interaction path of high-energy nucleons (10^{11} to 10^{13} ev) in the atmosphere, 20: 37667
SOELDNER, J. Stuart, Critical variables in radioimmunoassay of serum insulin, 20: 36543
SOFER, G. A., Selected optimization studies in the use of carbide fuel in large fast breeder reactors, 20: 38495 (ANL-7120, pp 104-23)
SOKOL, G. A., Elastic scattering of γ quanta on protons above π-meson photoproduction threshold, 20: 37800
SOKOLOV, I. I., Metabolism of phosphoproteins in muscles after irradiation, 20: 36602
SOKOLOV, L. S., Cross sections of elastically scattered 13.6-Mev deuterons, 20: 38128
SOKOLOV, Yu. L., Photoexcitation and photoionization of energetic hydrogen atoms, 20: 38221
SOKOLOVSKII, V. D., Homomolecular and isotopic exchange of oxygen on gadolinium oxide, 20: 36826
SOKOLOVSKII, V. I., Installation for study of EAS and nuclear interactions of cosmic-ray particles with energies 10^{12} to 10^{16} ev, 20: 37634
SOKOLOVSKII, V. V., Angular distribution of secondary particles in multiple production at high energies, 20: 37682
SOKOLOVSKII, V. V., Interactions of nucleons with complex nuclei at high energies, 20: 37790
SOLNTSEV, V. M., Some properties of U_2O_5, 20: 36832
SOLOMON, Philip M., Density of intergalactic hydrogen molecules, 20: 37353
SOLOV'EV, L. S., Helical minimum B magnetic configurations, 20: 38219
SOLOV'EV, M. V., Investigation of the nucleon interactions at energies above 10^{13} ev, 20: 37657
SOLOV'EV, S. M., Fission of ^{226}Ra by 12-Mev deuterons, 20: 38132
SOLOV'EVA, V. I., Energy spectrum, possible chemical composition, and anisotropy of ultrahigh-energy primary cosmic radiation, 20: 37651
SOLOV'EVA, Z. I., Possibilities of isolation of sidereal time cosmic-ray intensity variations, 20: 37506
SOMMER, K., Calibration-curve-obtained emission spectrographic ^{15}N determination with the Q24-Zeiss spectrograph, 20: 36772
SOMOGYI, A. J., Differential momentum spectrum and charge ratio of muons in extensive air showers, 20: 37643
SONA, A., Measurement of the time evolution of a radiation field by joint photocount distributions, 20: 37311
SONETT, C. P., Discontinuities in the solar wind, 20: 37387
SOPER, N. J., Potassium–argon ages of some dalradian, Maine, and related Scottish rocks, 20: 37016
SORENSEN, Raymond A., Structure effects in the charge radius of spherical nuclei, 20: 38043
SOROKIN, O. W., Investigation of the nucleon interactions at energies above 10^{13} ev, 20: 37657
SOSNOVETS, E. N., Earth's radiation belt, 20: 37899
SOULHIER, R., Fission-gas release from UO_2 during irradiation up to 2000°C, 20: 37290
SPALTER, Harold F., Prophylactic photocoagulation of recurrent toxoplasmic retinochoroiditis, 20: 36683
SPEISER, T. W., Acceleration of particles in the neutral sheet of the neutral sheet of the geomagnetic tail, 20: 37901
SPEJEWSKI, E. H., Beta spectrum shape measurements with a 4π semiconductor spectrometer, 20: 37125
SPERANZA, P. R., Properties of some low excited states in ^{101}Ru from the decay of 3-y ^{101}Rh, 20: 38091
SPERDUTO, A., Low-lying isobaric analog states of ^{89}Sr, 20: 38076
SPIEGEL, Edward A., Energy transport by turbulent convection, 20: 37394
SPIER, Hans G., Magnetohydrodynamic internal combustion electric generator, 20: 37728
SPIJKERMAN, J. J., Moessbauer spectrometer for the structural analysis of materials, 20: 37056
SPINETTI, Mario, Photoproduction of neutral pions in the energy range 400 to 600 Mev of the incident photon, 20: 37752
SPLICHAL, William F. Jr., Portable multipurpose radiation monitor, 20: 37071 (DP-993)
SPOREK, K. F., Theory of the sub-atomic structure of matter, 20: 37480
SPORRE, B., Multiplicity effect in an IGY neutron monitor, 20: 37098
SPRINGER, Donald L., Calculation of first-zone P wave amplitudes for Salmon Event and for decoupled sources, 20: 36966
SPRINGER, T. H., Recent results of Doppler measurements in fast-neutron spectra, 20: 38429 (ANL-7120, pp 614-15)
SPRINGETT, B. E., Pressure dependence of the radius of the negative ion in He II, 20: 37960
SPROTT, J. C., Equipotential surfaces of a plasma moving in a toroidal octupole magnetic field, 20: 38192 (COO-1233-32)
SQUIRES, G. L., Measurements of the frequencies of the normal modes of magnesium, 20: 38397
SREBRODOL'SKII, D. M., Pulsed neutron generator for boreholes and its use in nuclear geophysics, 20: 37017
SREEKANTAN, B. V., Correlations between the electron, muon, and N components in extensive air showers, 20: 37635
SREEKANTAN, B. V., Properties of extensive air showers rich in muons, 20: 37608
SREEKANTAN, B. V., Search for heavy mass particles in air showers, 20: 37653
SREEKANTAN, B. V., Time lags of nuclear-interacting particles in extensive air showers, 20: 37652
SREEKANTAN, B. V., Ultra-high energy muons (>200 Bev) in extensive air showers, 20: 37606
SREENIVASAN, N., Abundance of ^{3}He nuclei in the primary cosmic radiation, 20: 37559
SREENIVASAN, N., Heavy nuclei in the primary cosmic rays in June 1963 at Fort Churchill, 20: 37568
SRINIVASA RAO, M. V., Correlations between the electron, muon, and N components in extensive air showers, 20: 37635
SRINIVASA RAO, M. V., Properties of extensive air showers rich in muons, 20: 37608
SRINIVASA RAO, M. V., Search for heavy mass particles in air showers, 20: 37653
SRINIVASA RAO, M. V., Time lags of nuclear-interacting particles in extensive air showers, 20: 37652
SRINIVASA RAO, M. V., Ultra-high energy muons (>200 Bev) in extensive air showers, 20: 37606
STAAS, F. A., Flux flow in type-II superconductors with different field orientations, 20: 37942
STAAS, F. A., Resistive behavior of a type-II superconductor on reversing the current, 20: 37945
STACHURA, S. J., Application of experimental data from TREAT meltdown studies to reactor accident analysis, 20: 38472 (ANL-7120, pp 514-23)
STACK, John D., Backward π^-p scattering as a further test for Regge high-energy behavior, 20: 37742 (UCRL-16293)
STACK III, John David, Study of Regge dynamics in pion-nucleon scattering, 20: 37809
STACK, Stephen James, Effective Hamiltonian for nuclear matter, 20: 38160
STADNYK, B. I., X-ray investigation of Nb–W–B, 20: 37261
STALEY, D. O., Diurnal oscillations of radon and thoron and their decay products, 20: 37007
STANLEY, Elizabeth M., Isotope dilution method for determining amounts and activities of proline and hydroxyproline in tissues, 20: 36562
STANLEY, Elizabeth C., Spectrofluorometric analysis of rare earth chelates of thenoyltrifluoroacetone, benzoylacetone, and dibenzoylmethane by computer spectrum stripping techniques, 20: 36722
STANTIC, S., Estimation of the relative abundance of the carbon isotopes of the primary cosmic rays, 20: 37574
STARCUK, Zenon, Application of propane as basic counting gas in proportional counters, 20: 37092
STARNES, P. E., Continuous automatic analysis of dry powders and aqueous suspensions using radioisotope techniques, 20: 37152
STARODUBSKAYA, A. A., Electrolytic separation of lead from microquantities of thorium and uranium and their photometric determination, 20: 36773
STAVISSKII, Yu. Ya., Measurement of absorption cross sections for fast neutrons by resonance detector in water, 20: 37990
STEARNS, Carole Michels, Comparison of reactions of ^{63}Cu compound nuclei formed by alpha-particle, proton, and C-ion bombardments,

20: 38147
STECH, Berthold, Hybrid group symmetry and its foundation, 20: 37860
STEEN, Hugh F., Project Gasbuggy: nuclear application for increasing production, 20: 36973
STEER, R. W., Air–water mixing tests, 20: 36989 (WAPD-TM-492)
STEFANESCU, Al., Effectiveness of resonance neutrons for VVR-S reactor chain reaction, 20: 38536
STEIDL, J., Digital methods in thickness gaging, 20: 37058
STEIN, R. F., Conference on stellar evolution, New York, 11/63, 20: 37390
STEIN, Robert F., Stellar evolution: a survey with analytic models, 20: 37391
STEINFINK, H., The structure of $YbSb_2$, a $ZrSi_2$ isotype, 20: 37238
STELJES, J. F., Introduction of meteorological corrections into meson monitor data, 20: 37101
STELJES, J. F., Latitude survey in North America, 20: 37593
STELLA, Bruno, Photoproduction of neutral pions in the energy range 400 to 600 Mev of the incident photon, 20: 37752
STELTS, Marion L., Two-nucleon distorted-wave Born approximation analysis of $^{19}F(d,\alpha)^{17}O$ data, 20: 38082
STENERSON, R. O., University of Utah neutrino detector, 20: 37104
STEPANOV, A. V., 68.5-cm Sector-focused cyclotron, 20: 37324
STEPANOV, K. N., Interaction of plasma oscillations and spin waves in ferromagnetic semiconductors and metals, 20: 38354 (FTI-244/T-027)
STEPANOVA, A. A., Properties of yttrium borides, 20: 38359
STEPANYAN, A. A., Some results of studies of the solar-diurnal variation of cosmic rays during the IGY period, 20: 37526
STEPHANY, W., Status of recent meltdown studies, 20: 38474 (ANL-7120, pp 534-9)
STEPHEN, D. R., Temperature dependence of the irradiation-induced creep of graphite, 20: 37223
STEPHENS, F. S., Isomeric state (8⁻) in ^{180}W, ^{182}Os, and ^{184}Pt, 20: 38027
STEPHENS, J. F., Intestinal damage by E. necatrix and absorption of orally administered ^{65}Zn, 20: 36566
STEPHENS, Lloyd D., Cosmic-ray-produced neutrons at ground level: neutron production rate and flux distribution, 20: 37483
STEPHENS, S. A., Energy spectrum of primary He nuclei at energies greater than 6 Bev, 20: 37557
STEPHENS, S. A., Energy spectra of cascades observed at balloon altitudes and the flux of primary protons, 20: 37672
STEPHENS, S. A., Study of high-energy interactions in graphite, 20: 38110
STERN, F., SWIFT dryout data for 19-rod bundle cooled by steam/water fog, 20: 38409 (AECL-2586)
STERN, H., Spin-2⁺ meson decays in the quark model, 20: 37780
STETSON, R. F., Observations of instabilities in electron-cyclotron plasmas, 20: 38274
STEVENSON, C. E., Preparation for fuel processing, 20: 36946
STEVENSON, C. E., Solvent-extraction processes, 20: 36948
STEWART, A. T., Band gap in beryllium, 20: 38406
STEWART, A. T., Calculated core annihilation momentum distributions for several metals, 20: 37821
STEWART, A. T., Momentum distribution of photons from positrons annihilating in lithium-ammonia solutions, 20: 37818
STEWART, A. T., Motion of positrons in sodium, 20: 37784
STEWART, A. T., Positron annihilation in a dilute metal: Li–NH_3 solution, 20: 37774
STEWART, A. T., Positronium formation in certain metal oxides, 20: 37819
STEWART, A. T., Positron annihilation in metals, 20: 37820
STEWART, B. M., Compton scatter from low-energy gamma emitters and its significance to collimation, 20: 37465
STEWART, D. F., Reactivity of transition metal fluorides. II., 20: 36803
STEWART, D. T., Elastic photoproduction of π^0 mesons from deuterium, 20: 37783
STEWART, J., Evidence for a source of primary gamma rays, 20: 37365
STICKEL, W., Interaction of 25-kev electrons with lattice vibrations in LiF, 20: 38395
STICKLAND, A. C., Conference on cosmic rays. Vol. I. London, 9/65, 20: 37492
STICKLAND, A. C., High-energy cosmic-ray jet research at Krakow, 20: 37663
STILLER, B., ^3He-^4He in the primary cosmic radiation at Fort Churchill 1963, 20: 37572
STINCHCOMB, T. G., Design and applications of β-excited x-ray sources, 20: 36915 (N-66-17678)
STOCKEL, C. T., Scintillation-counter study of cosmic rays deep underground, 20: 37705
STOECKLER, Hans A., Moessbauer-effect studies of weak nuclear quadrupole interactions in ^{119}Sn, 20: 36816
STOEPPLER, M., Continuous gas analyses by means of x-ray fluorescence, 20: 36766
STOKER, P. H., Intensity distributions of cosmic-ray components at 307 g cm^{-2} atmospheric depth in the South African magnetic anomaly, 20: 37592
STOLYAROV, K. P., Spectrophotometric studies of ascorbic complexes. IV., 20: 36833
STOLYAROV, K. P., Spectrophotometric study of ascorbic complexes. V., 20: 36852
STONE, D., Critical variables in radioimmunoassay of serum insulin, 20: 36543
STONE, H. H., Removal of protactinium from molten fluoride breeder blanket mixtures, 20: 36927 (ORNL-TM-1543)
STONEHILL, E. H., Chromosomal mapping by means of mutational induction in synchronous populations of Streptococcus faecalis, 20: 36635
STOOP, J., Effect of nitrogen on tensile and creep-rupture properties of niobium, 20: 37218
STOTHERS, R., Quasars as the origin of primordial matter in a steady-state universe, 20: 37361
STOUFFER, J. C., Recovery of aluminum nitrate nonahydrate from redox acid waste, 20: 36925 (HW-82771(Pt.3))
STOVALL, T., Coulomb form factors of ^{10}B and ^{11}B, 20: 38057
STOZKOV, Yu. I., Cosmic-ray intensities in the stratosphere over Antarctica and Murmansk, 20: 37591
STREETMAN, B. G., Recombination and trapping in ^{60}Co gamma-irradiated n-type Ge, 20: 38364
STREL'CHENKO, S. S., Rotational energy level distribution of molecules excited by ion impact, 20: 37471
STRIEBEL, H. R., Reactions D(d,n)^{3}He and D(d,p)^{3}H with polarized deuterons at 460 kev, 20: 38074
STROEMGREN, B. G., Age determination for main-sequence B, A, and F stars, 20: 37417
STRONG, R. G., Kinetic studies in ethylene polymerization with Ziegler type catalysts. III., 20: 36827
STRZALKOWSKI, Adam, Nuclear reactions, 20: 38109
STRZYZEWSKA, B., Spectrographic determination of trace amounts of rare earths. III., 20: 36729
STURROCK, Jean, Effect of irradiated medium on the growth of L5178Y lymphoma cells, 20: 36633
SUAREZ, C., Preparing carrier-free $H_2{}^{35}SO_4$ from reactor irradiated KCl, 20: 36920
SUBRAMANIAN, G., Characteristics of anisotropy of galactic cosmic rays during the solar cycle, 20: 37520
SUBRAMANIAN, G., Galactic cosmic rays in the solar system, 20: 37345
SUBRAMANIAN, G., Galactic cosmic rays in the solar system, 20: 37511
SUDAN, R. N., Plasma wave propagation in hot inhomogeneous media, 20: 38284
SUEMOTO, Z., Structure of the solar chromosphere, 20: 37912
SUEOKA, J. R., Calculated physics parameters and their uncertainties in a 1000-Mw(e) fast ceramic reactor, 20: 38491 (ANL-7120, pp 24-32)
SUGA, K., Arrival direction of muon-rich extensive air showers, 20: 37609
SUGA, K., Fine structure of air shower cores observed with 20 m^2 spark chamber, 20: 37617
SUGA, K., Possible nuclear interaction of a muon of energy above 3×10^{14} ev, 20: 37714
SUGA, K., Studies of primary cosmic rays in the energy region 10^{14} to 10^{17} ev, 20: 37627
SUGAR, Jack, Ionization energies of the neutral rare earths, 20: 37439
SUGIHARA, T., Nuclear-active particles in extensive air showers near sea level, 20: 37620
SUITA, Tokuo, Study of the enhancement of x-ray coloration of NaCl by divalent impurities, 20: 38373
SUKHOTIN, A. M., Passivity of molybdenum, 20: 37184
SULC, J., Effect of some preparation conditions on the surface area and structure of ammonium polyuranate, 20: 36801
SULLIVAN, P. D., Effect of radiation on collagen. I., 20: 36585
SULLIVAN, R. P., Angular correlations of $^{28}Si(d,p\gamma)^{29}Si$ from 4 to 6 Mev, 20: 38086
SULYAEV, R. M., Capture of pions by ^3He. II., 20: 38011 (JINR-P-2805)
SUNDERRAJAN, R., Flux of primary protons and helium nuclei and east-west and north-south asymmetries near the geomagnetic equator, 20: 37582
SURI, A. N., Variation of the characteristics of EAS with atmospheric depth, 20: 37639
SUSLOV, A. A., Some results of the investigation of the primary cosmic-ray nuclei on the artificial satellite Electron-2, 20: 37600
SUSLOV, A. P., Ionization-mechanical detector for ionizing particles, 20: 37080
SUTTER, R. J., Elastic scattering of 1 Bev protons from He and O, 20: 38010 (BNL-10438)
SUZUKI, Hideyo, Adsorption of ^{32}P onto glass wall, 20: 36923
SUZUKI, Kenshi, Enzymatic breakdown of uv-irradiated DNA by the extract from Micrococcus lysodeicticus, 20: 36583
SVEC, H. J., Bibliography on mass spectroscopy, 20: 36712 (IS-1335)
SWAN, G. W., Magnetogasdynamic flow over a wedge, 20: 38242
SWANENBURG, B. N., Balloon observation of high-energy electrons, 20: 37549
SWANN, C. P., Properties of the 7.03-Mev excited state of ^{14}N, 20: 38083
SWANSON, E. W., Effect of feeding thiocyanate to dairy cows on absorption

and clearance of intramammary iodine, 20: 36563
SWARTZ, George A., High density plasma generator, 20: 38340
SWENSON, L. W., Spins of ^{58}Ni levels from inelastic proton scattering, 20: 38181
SWIFT, David L., Experimental studies of the high-temperature interaction of fuel and cladding materials with liquid sodium, 20: 38499 (ANL-7120, pp 839-47)
SWINSON, D. B., Altitude variation of the extensive air shower density spectrum, 20: 37631
SWINT, J. B., Cross sections as a function of energy for the scattering of protons from ^{12}C, 20: 38050
SWINT, J. B., Cross sections as a function of angle and complex phase shifts for the scattering of protons from ^{12}C, 20: 38051
SYROVATSKII, S. I., Origin of cosmic rays, 20: 37388
SZARVAS, Pal, Investigation of the mechanism of the NH_4-lactate elution separation of trace lanthanides, 20: 36939

T

TABOR, P., High-accuracy fluid-density gage, 20: 37059
TAGGART, James, Epicenter determination for the Salmon event, 20: 36969
TAKAHASHI, H., Cosmic-ray rigidity spectrum during a solar rotation and solar wind velocity, 20: 37533
TAKAHASHI, Jun, Method for preparing specimens suitable for liquid scintillation counting from ^{3}H-labeled biological material by means of combustion, 20: 36763
TAKANASHI, S., Study on the plasma proteins of patients who survived the A bomb, 20: 36581
TAKAYAMA, Kazuo, Some problems in use of Langmuir probe on ionospheric sounding rockets, 20: 38309
TAKBAEV, Zh. S., Electromagnetic cascades in iron and lead at 100 Bev, 20: 37698
TAKEHISA, Masaaki, Effects of process variables on the telomerization of ethylene with C tetrachloride induced by γ radiation, 20: 36890
TAKEHISA, Masaaki, Reaction of butene-1 with phosgene induced by γ radiation, 20: 36892
TAKEHISA, Masaaki, Telomerization of ethylene with C tetrachloride induced by γ radiation under constant ethylene pressure, 20: 36891
TAKETANI, M., Origin of extragalactic cosmic rays, 20: 37502
TAKEUCHI, Sakae, Thorium–ThC phase diagram, 20: 37265
TALMI, I., Dynamical derivation of baryon masses in the quark model, 20: 37762
TALPOVA, H., Determination of potassium in biological material by various methods of neutron-activation analysis, 20: 36735
TAN, B. L., Simplified 180° focusing β-ray spectrometer, 20: 37120
TAN, Bian Djoen, X-ray-induced abnormalities and recovery in Hymenolepis microstoma, 20: 36662
TANAKA, Shigetoshi, Collision-induced instability in a magnetoactive plasma, 20: 38253
TANAKA, T., Balloon observation of high-energy electrons, 20: 37549
TANDON, G. K., Lifetime of the 1.52-Mev level in ^{42}Ca, 20: 38085
TANDON, S. N., Arrival time distributions of heavy particles in air showers, 20: 37633
TANDON, S. N., Possible flux of heavy triplets and similar particles in cosmic radiation and their detection, 20: 37719
TANDON, S. N., Secondary spectra for truncated spectra for the primary cosmic rays, 20: 37677
TANEMURA, T., X-ray spectroanalysis using a ^{147}Pm beta source, 20: 36765
TANENBAUM, A. L., Effect of neutron and γ irradiation carrier lifetime and detectivity of InSb, 20: 37295
TANFIELD, D. A., Scintillation-counter study of cosmic rays deep underground, 20: 37705
TANG, S. M., Precise determination of the shape of the twice-forbidden beta spectrum of ^{137}Cs, 20: 38044
TANGUY, Pierre-Yves, Development in France of natural U–graphite–gas reactors, 20: 38515
TANIUTI, Tosiya, Model of the dispersive nonlinear equation, 20: 37926
TANIUTI, Tosiya, Plasma turbulence and quasi-linear approximation, 20: 38282
TASHIRO, Shiegeki, Method for producing polymer of dioxaspiroheptane by ionizing radiation, 20: 36914
TATU, V., Nuclear magnetic moments of ^{137}Ba and ^{135}Ba, 20: 37463
TATUS', V. I., Rotational energy level distribution of molecules excited by ion impact, 20: 37471
TAUPIN, J. L., Energy released at high temperature by irradiated graphite, 20: 37283
TAURE, I. Ya., Measurements of large γ-radiation doses and fluxes by means of photoactivation of isomeric nuclear states, 20: 37079
TAVGER, B. A., Superconducting transition temperature of a thin film, 20: 37980
TAYLOR, F. G. Jr., Predicted seasonal radiosensitivity of southeastern tree species, 20: 36551
TAYLOR, G. R., Stability, compatibility and corrosion of poison solutions and structural materials, 20: 38447 (WCAP-2867)
TAYLOR, T. I., Motions of water molecules in K ferrocyanide trihydrate, water, and ice, 20: 36821
TEDMON, C. S. Jr., High-temperature oxidation of ductile Cr–Re alloys, 20: 37186
TEER, B. R., Selected optimization studies in the use of carbide fuel in large fast breeder reactors, 20: 38495 (ANL-7120, pp 104-23)
TELEZHNIKOV, S. A., Cross section of D(t,α)n in the energy region at 115 to 1650 kev, 20: 38130
TEL'TSOV, M. V., Investigation of the outer proton belt, 20: 37905
TEMESVARY, S., Schematic pre-main-sequence evolution, 20: 37398
TEMPLETON, David H., Atomic parameters in the lanthanum trifluoride structure, 20: 36805
TEOFILOVSKI, Cedomir, Behavior of ^{131}I polymetatelluric acid irradiated in the nuclear reactor, 20: 36917
TEPLY, J., Hydrogen formation in the radiolysis of liquid methanol, 20: 36861 (UJV-1553)
TERENT'EV, I. A., Unitary representations of group P(SU(r)), 20: 37858
TERHUNE, R. W., Surface motion measurements, 20: 36959 (PNE-603F)
TERRILL, James G. Jr., Natural radioactivity in ground water supplies in Maine and New Hampshire, 20: 37006
TEULIN, I. I., Effect of ultrasound on the ductility of high-boron stainless steels, 20: 37221
THAMBYAHPILLAI, T., Forbush decreases and the 27-day recurrence tendency in the cosmic-ray intensity at a depth of 60 m.w.e. underground in London, 20: 37535
THAMBYAHPILLAI, T., Solar and sidereal daily variations of cosmic-ray intensity at a depth of 60 m.w.e. underground in London, 20: 37504
THEISEN, R., Microanalytical studies of micro- and macro-segregation in oxide fuels, 20: 38469 (ANL-7120, pp 400-9)
THIELHEIM, K. O., Monte Carlo studies on extensive air shower development, 20: 37647
THODOS, G., Thermal conductivity of H up to 660 atm and 74.6°C, 20: 36991
THOMAS, T. D., X rays and electrons emitted in coincidence with the fission of ^{252}Cf, 20: 38095
THOMASSEN, K. I., Enhanced diffusion studies at Stanford, 20: 38321
THOMPSON, M. G., Study of the electromagnetic interactions of high-energy muons using a large scintillator stack, 20: 37699
THOMPSON, M. G., Theoretical studies of the muon component of EAS, 20: 37640
THOMPSON, W. B., Hydromagnetic equations with viscosity for a collisionless plasma, 20: 38244
THOMPSON, W. R., Nozzle tube-wall temperature measurement by radiometric techniques, 20: 38528
THORNDIKE, E. H., Evidence of a higher symmetry in nucleon-nucleon scattering, 20: 37772
THOSAR, B. V., Lifetimes of positronium in polymers irradiated by gamma rays, 20: 36896
TILL, C. E., Measurement and analysis of Doppler effect in Pu-fueled fast reactor assemblies, 20: 38427 (ANL-7120, pp 603-9)
TILL, C. E., Recent Doppler measurements with ZPR-6, 20: 38428 (ANL-7120, pp 610-13)
TIMASHEV, S. F., Reaction ^{3}He(p,d)2p, 20: 38129
TIMMERMANS, W., Prog. rpt. on ESSOR fuel elements, final, 1–11/62, 20: 38480 (EUR-2522.f)
TIMOFEEV, A. V., Stability of flute oscillations with wave-plasma resonances, 20: 38262
TIMOFEEV, G. A., Coulomb interaction of electrons with energy of 1 Mev in the region of a magnetic anomaly, 20: 37906
TISHCHENKO, B. I., Theory of diffraction scattering based on method of complex angular momenta, 20: 38143
TISONE, G., Detachment of electrons from H^- by electron impact, 20: 37452
TITTLE, C. W., Applications of radioisotope instruments in geophysics, 20: 37060
TODD, L., Hartmann flow between parallel planes, 20: 38281
TODOROV, I. T., Inhomogeneous SL(6) group with an expanded translation subgroup, 20: 37835
TOENNIS, Wilhelm, Operability limits as indication for radiotherapy in brain tumors, 20: 36692
TOIVOLA, Ahti, X-ray standardization and comparison of the Finnish and Swedish x-ray standards, 20: 37078
TOKAREVSKII, V. V., Cross sections of elastically scattered 13.6-Mev deuterons, 20: 38128
TOKIMOTO, Yoshiko, Functional test of a decontamination apparatus for radio-contaminated rainwater, 20: 37029
TOKTAROV, K., Remarks concerning particle motion in infinite d-c magnetic field, 20: 38313
TOKUDA, Naoki, C, P, and T invarinaces and the bootstrap hypothesis, 20: 37794
TOKUNAGA, Chiho, Effect of gamma radiation on Ni, Zn, and Ag chelates of tetraphenylporphine, 20: 36889

TOKUNAGA, Chiyoko, Age dependence of locations of x-ray-induced somatic crossing-over in Drosophila, 20: 36619
TOKUNAGA, N., Scintillation counting with plastic phosphor for determining tritium radioactivity at surfaces, 20: 37087
TOKUNAGA, Noboru, Sheet scintillation counting of tritium in surface films, 20: 36738
TOLEA, Florian, Analysis of sulfuric acid solutions using the method of backscattered β radiations, 20: 36770
TOLKACHEV, S. S., Some properties of U_2O_5, 20: 36832
TOMAN, John, Rock breaking takes a giant step into the space age, 20: 36974
TOMCSANYI, Attila, Activation determination of Si in sputum of silicotic patients, 20: 36642
TOMOMOTO, Takanori, Plastic scintillators. III., 20: 36848
TOMPA, H., Theory of the specific heat of liquid ^{4}He above the λ point, 20: 37968
TONWAR, S. C., Correlations between the electron, muon, and N components in extensive air showers, 20: 37635
TONWAR, S. C., Properties of extensive air showers rich in muons, 20: 37608
TONWAR, S. C., Search for heavy mass particles in air showers, 20: 37653
TONWAR, S. C., Time lags of nuclear-interacting particles in extensive air showers, 20: 37652
TOPA, V., Color centers in x-irradiated NaCl : Ag and NaCl : (Ag + Ca) crystals, 20: 38396
TORATANI, Hirokazu, Behavior of radioactive Sr, Cs, and Co in marine water, 20: 38537
TOSCH, Reinhard, Indication of thyroid therapy by radioiodide localization, 20: 36706
TOUR, Yung, Convergence of a many-body perturbation series for an attractive Fermi system, 20: 38121
TOWERS, L., Comparative response of Cherenkov and scintillator detectors to large air showers, 20: 37621
TOYODA, Y., Possible nuclear interaction of a muon of energy above 3×10^{14} ev, 20: 37714
TOYODA, Y., Studies of primary cosmic rays in the energy region 10^{14} to 10^{17} ev, 20: 37627
TRAVELLI, A., Comment on the comparison of some sodium void coefficients with experimental data, 20: 38419 (ANL-7120, pp 421-2)
TRAVESI, A., Activation analysis of impurities in U. I., 20: 36714
TRAVESI, A., Activation analysis of impurities in U. II., 20: 36715
TRESVYATSKII, S. G., Phase transformations of certain rare earth chromites, 20: 36812
TRETYAKOVA, Ch. A., Interaction path of high-energy nucleons (10^{11} to 10^{13} ev) in the atmosphere, 20: 37667
TRETYAKOVA, M. I., Certain aspects of nucleon isobar production in nucleons interactions at energies 10^3 and 25 Bev, 20: 37675
TRICE, V. G. Jr., Large metal-fueled fast reactor study. II., 20: 38494 (ANL-7120, pp 94-103)
TRONCOSO, O., Solar daily variation recorded at a low-latitude station by east and west pointing telescopes during periods of maximum and minimum solar activity, 20: 37373
TROUSIL, J., Investigation of occupational exposures to ionizing radiation in the Czechoslovak Socialist Republic, 20: 37035
TROUT, H. E. Jr., Effects of oxygen on the mechanical and corrosion properties of Hafnium, 20: 37170
TRUEMPER, J., Studies on high-energy cascades using a neon hodoscope, 20: 37618
TRURAN, J. W., Formation of helium in the galaxy, 20: 37409
TRUTIA, Elena, Level density parameter determination from (α,n) reactions on ^{27}Al, ^{55}Mn, ^{56}Fe, and Ag, 20: 38115
TSAO, C. H., High-energy jets produced by heavy primary nuclei of cosmic origin and their fragmentation products, 20: 37662
TSAPKOV, N. T., Effect of γ radiation on flotation properties of anionic collector agents, 20: 36893
TSAREV, B. M., Thermoelectron emission from uranium dodecaboride, 20: 37723
TSEN, Nai-Gun, Reaction ^{3}He + ^{3}He, 20: 38131
TSERKASEVICH, K. V., Complexes of Nd, Ho, and Er with pyrogallosulfonic acid, 20: 36837
TSUJII, Yukio, Radiography using ^{192}Ir, 20: 36994
TSUKISHIMA, T., Correlation of density fluctuations and diffusion in a plasma, 20: 38322
TSUPKO-SITNIKOV, V. M., Capture of pions by ^{3}He. II., 20: 38011 (JINR-P-2805)
TSURUFUJI, Susumu, Method for preparing specimens suitable for liquid scintillation counting from ^{3}H-labeled biological material by means of combustion, 20: 36763
TSURUTA, Sachiko, Cooling and detectability of neutron stars, 20: 37355
TSURUTA, Sachiko, Rotation of neutron stars, 20: 37363
TSURUTA, Sachiko, Some effects of nuclear forces on neutron-star models, 20: 37356
TSYPIN, S. G., Distribution of fast fission neutrons along straight cylindrical channels in water, 20: 38351
TUCHSCHEER, Th., Bibliography on food irradiation, No. 05, 6/66, 20: 37138 (AED-C-05-05)
TUCHWEBER, B., Action of histamine liberators on calcification produced by various metals, 20: 36557
TUCK, J. L., Scyllacita: compact high-voltage theta pinch machine, 20: 38306
TUKISH, E. I., Installation for study of EAS and nuclear interactions of cosmic-ray particles with energies 10^{12} to 10^{16} ev, 20: 37634
TULINOVA, S. I., Investigation of the nucleon interactions at energies above 10^{13} ev, 20: 37657
TULLOCH, H. J. C., Preparation of uranium nitride and carbonitrides from uranium oxide in a fluidized bed, 20: 36850
TULLY, G. R. Jr., Pilot-scale extrusion of graphite fuel elements for HTGRs, 20: 37196
TURK, D. E., Intestinal damage by E. necatrix and absorption of orally administered ^{65}Zn, 20: 36566
TURNER, J. E., Variational calculation for bound states in an electric-dipole field, 20: 37919
TURNER, R. C., Point defect generation in LiF by plastic deformation and x irradiation, 20: 88368
TURVER, K. E., Differential momentum spectrum and charge ratio of muons in extensive air showers, 20: 37643
TURVER, K. E., Experiments on the pulse spectrum observed from scintillation and Cherenkov detectors at sea level, 20: 37619
TUTTLE, E. R., Microscopic theory of a normal Fermi liquid at zero temperature, 20: 37937
TUTTLE, R. J., Recent results of Doppler measurements in fast-neutron spectra, 20: 38429 (ANL-7120, pp 614-15)
TVERSKOI, B. A., Earth's radiation belt, 20: 37899
TVERSKOI, B. A., Earth's radiation belt theory, 20: 37910
TYMPL, M., Extraction of alkalized solutions of uranyl salts with tributyl phosphate, 20: 36932

U

UCHURKHANOV, M. M., Effect of γ radiation on flotation properties of anionic collector agents, 20: 36893
UDAGAWA, Takeshi, E1 $\Delta K = 0$ transitions in deformed odd-mass nuclei, 20: 38040
UEBERALL, H., "Breathing mode" collective nuclear vibrations and application to ^{4}He excited states, 20: 38170
UEBERALL, H., Polarization effects in photonuclear reactions, 20: 38175
UEMURA, Kiyoshi, Method for producing graft polymers, 20: 36908
UENO, H., Atmospheric temperature effects on the diurnal variation of cosmic-ray intensity, 20: 37586
UENO, H., Further observation of the positive excess of cosmic-ray muons, 20: 37690
UENO, H., Rigidity dependence of the cosmic-ray diurnal variation during diurnal variation during Forbush decrease, 20: 37530
UHER, Richard A., Structure effects in the charge radius of spherical nuclei, 20: 38043
UKRAINTSEV, E. V., Extraction of thorium with diisoamyl methylphosphonate from nitric acid solutions, 20: 36942
ULFSKII, G. V., Choice of an average heat flux at the fuel element surface of pressurized water reactors, 20: 38519
ULLRICH, H., Spectra of photo-alpha particles from nuclei in the region Z = 12 to 30, 20: 38037
UNE, Tsutomu, Calculations on reactions ^{13}C(p,n)^{13}N, ^{11}B(p,n)^{11}C, and ^{27}Al(n,p)^{27}Mg, 20: 38112
UNRINE, G. R., Angular correlations of ^{28}Si(d,pγ)^{29}Si from 4 to 6 Mev, 20: 38086
UNRUH, C. M., Personnel neutron dosimeter developments, 20: 37070 (BNWL-SA-537)
UNTI, Theodore Wayne Joseph, Source dynamics for asymptotically flat space solutions of general relativity, 20: 37932
URASHIMA, Shin-o, Magnetohydrodynamic shock polar, 20: 37872
URRECHAGA-ALTUNA, Jesus, Composite particles in a separable potential model, 20: 37863
URRUTIA, Jose Luis, Magnetohydrodynamics. Interaction between magnetic fields and conducting fluids, 20: 37867
URSU, I., Thermal annealing of paramagnetic defects induced by γ irradiation in $(NH_4)_2SO_4$ and $(ND_4)_2SO_4$ single crystals, 20: 36874
UY, J. C., Effect of certain rare-earth solutes upon the f.c.c./b.c.c. transformation temperature of Th, 20: 37242

V

VACHA, Terrance, Coupling of degenerate modes of a microwave cavity due to the presence of a magnetized plasma, 20: 38332
VAHLDIEK, F. W., Dislocation etch pits and phase relationships in dimolybdenum carbide single crystals, 20: 37247
VAIDANICH, V. I., Absorption and luminescence spectra of NaI and NaI(Tl)

at low temperatures. II., 20: 37441
VALENTI[illegible], Emma M., Theory of spherical probes in monoenergetic plasmas, 20: 38190 (AD-637513)
VALENTINE, N. A., Classical impulse approximation to ionization of hydrogen atoms by protons, 20: 37456
VAN ALLEN, J. A., Observations with University of Iowa equipment on Mariner IV, 20: 37341 (N-66-17354)
VAN CANEGHEM, P., Current intensity and flux of x rays, 20: 37091
VAN CANEGHEM, P., Influence of cystamine administered by mouth to mice irradiated with gamma rays at a low dose-rate, 20: 36666
VANDAKUROV, Yu. V., Stability of a compressible gravitating cylinder of uniform density in a longitudinal magnetic field, 20: 38311
VANDERSCHMIDT, G. F., Gemini carbon dioxide sensor, 20: 37064
VAN DER WALT, A. J., Intensity distributions of cosmic-ray components at 307 g cm^{-2} atmospheric depth in the South African magnetic anomaly, 20: 37592
VAN DER WALT, W. J., Irradiation of groundnuts, 20: 36647
VAN DER WESTHUIZEN, P. J., Chemically inaggressive liquid scintillators, 20: 37113
VAN DULMEN, A., Specific gamma emission of natural K and La, 20: 38107
VAN NICE, L. J., Prog. rpt. on booster rocket altitude abort program, 1–4/66, 20: 36996 (SC-CR-66-2045)
VANNIER, R., Problems in the production and development of a wide range of radioisotope gages, 20: 37149
VAN PATTER, Douglas M., Gamma-ray angular distributions in inelastic nucleon scattering via compound nucleus mechanism, 20: 38178
VAN RINSVELT, H. A., High-resolution investigation of the $^{30}Si(p,p)^{30}Si$ reaction, 20: 38105
VAN'T VEER, Frans, Gaseous pressure in sunspots, 20: 37343
VAN'T VEER-MINNERET, Claude, Gaseous pressure in sunspots, 20: 37343
VARDUMIAN, D. T., Investigation of the nuclear-active component of cosmic rays, 20: 37658
VARGAS, Louis P., Spectrofluorometric analysis of rare earth chelates of thenoyltrifluoroacetone, benzoylacetone, and dibenzoylmethane by computer spectrum stripping techniques, 20: 36722
VARLASHKIN, P. G., Momentum distribution of photons from positrons annihilating in lithium-ammonia solutions, 20: 37818
VARLASHKIN, P. G., Positron annihilation in a dilute metal: Li–NH_3 solution, 20: 37774
VARTANYAN, T. G., Shower production by pions and protons with momenta 0.1 and 20 Bev/c in thin layers of matter, 20: 37669
VARTAPETYAN, G. A., Gamma-gamma angular correlation in ^{131}Cs nuclei, 20: 38021
VASIL'EV, R. D., Application of the similarity method to radiation fields during adjustment of neutron radiation meters, 20: 37074 (NP-16202)
VASIL'EV, R. D., Calibration of thermal-neutron radiation meters in diffuse flow, 20: 37073 (NP-16201)
VASIL'EV, R. D., Problem of utilizing nuclear $D(d,n)^3He$ and $T(d,n)^4He$ reactions for calibration of fast-neutron radiation meters, 20: 37075 (NP-16204)
VASIL'EV, S. S., Utilization of fast charged particle inelastic scattering for analysis of composition of materials, 20: 36732
VASIL'EV, V. N., 68.5-cm Sector-focused cyclotron, 20: 37324
VASIL'EVA, E. V., Kinetics and activation energy of oxidation of alloys of the Nb–V–Ti system, 20: 37191
VASINA, V. N., Effects of γ radiation on the scale formation process, 20: 37182
VASIU, Mircea, Derivation of the dispersion equation for a cylindrical plasma with finite electrical conductivity under the influence of its own gravitational field and an applied magnetic field, 20: 38257
VASSEUR, J., Flux and east-west asymmetry of primary electrons at a geomagnetic rigidity cut-off of about 4.5 GV, 20: 37550
VATCHA, R. H., Correlations between the electron, muon, and N components in extensive air showers, 20: 37635
VEDENEEV, O. V., Underground investigation of the penetrating component of high-energy cosmic radiation, 20: 37693
VEEH, H. Herbert, Ages of Pleistocene high sea level stand by $^{230}Th/^{238}U$ and $^{234}U/^{238}U$ ratios, 20: 37014
VEJVODA, E., Spectrographic determination of fluoride in plutonium nitrate solutions, 20: 36730
VELDRE, V. Yu., Atomic collisions, 20: 37477
VENABLES, J. A., Stacking-fault energy and many-body force effects in solid argon, 20: 38394
VENARD, J. T., In-reactor stress-rupture properties of a 20Cr–25Ni, Cb-stabilized steel, 20: 37284
VENERUS, Ernest Ronald, Theoretical investigations of fission-product deposition from flowing gas streams, 20: 37041
VENKATARAMAN, G., Effect of nuclear spin correlations on the scattering of neutrons by molecules, 20: 38004
VENNETT, R. M., Tensile fracture of Zr and Zr-rare earth solid-solution alloys, 20: 37231
VENUTI, Gloria Campos, $(e,e'p)$ reaction in the ^{32}S nucleus, 20: 38016
VERA PALOMINO, J., Solvent extraction applied to analysis of U. II., 20: 36717
VERA PALOMINO, J., Solvent extraction applied to analysis of U. III., 20: 36718
VERA PALOMINO, J., Spectrophotometric determination of U with arsenazo, 20: 36716
VERMILLION, Robert Everett, Plasma flow modes in electric shock tubes, 20: 38345
VERNON, W., Interference in the $K_L \to \pi^+\pi^-$ system, 20: 37814
VERNOV, S. N., Corpuscular ionizing radiation in space in the immediate vicinity of the Earth, 20: 37902
VERNOV, S. N., Cosmic-ray intensities in the stratosphere over Antarctica and Murmansk, 20: 37591
VERNOV, S. N., Earth's radiation belt, 20: 37899
VERNOV, S. N., Investigation of the outer proton belt, 20: 37905
VERNOV, S. N., Low-energy particle fluxes inside the magnetosphere from the data of the electrostatic analyzers of the Electron-2 satellite, 20: 37904
VERNOV, S. N., Study of the extensive air showers with fixed μ meson number and with fixed electron number, 20: 37644
VERNOV, S. N., Underground investigation of the penetrating component of high-energy cosmic radiation, 20: 37693
VERRELLI, D. M., Kinetic behavior of a circulating-water reactor following large reactivity changes, 20: 38449
VEYSSIERE, Andre, Frequency modulation of uhf signals in electron linear accelerator, 20: 37319 (CEA-R-2976)
VIDAL, Jose G., Two-nucleon distorted-wave Born approximation analysis of $^{19}F(d,\alpha)^{17}O$ data, 20: 38082
VIGNERON, Jacques, Determination of the density of protons at the level of a satellite by exact numerical analysis of proton whistlers, 20: 37885
VIJAYALAKSHMI, B., Fast neutrons of solar origin, 20: 37375
VILCOV, Isabela, Level density parameter determination from (α,n) reactions on ^{27}Al, ^{55}Mn, ^{56}Fe, and Ag, 20: 38115
VILCOV, N., Level density parameter determination from (α,n) reactions on ^{27}Al, ^{55}Mn, ^{56}Fe, and Ag, 20: 38115
VINGIANI, G. B., Properties of some low excited states in ^{101}Ru from the decay of 3-y ^{101}Rh, 20: 38091
VISHWANATH, P. R., Ultra-high energy muons (>200 Bev) in extensive air showers, 20: 37606
VISSER, J., Rigorous solution of Dirac' equation, 20: 37920
VITALI, R., Technique for preparing samples of small fragile particles for electron microscope examination by means of replicas, 20: 37173
VLADIMIROV, Yu. A., Very faint luminescence in biochemical reactions, 20: 36547
VLADIMIRSKII, B. M., Some results of studies of the solar-diurnal variation of cosmic rays during the IGY period, 20: 37526
VLASOV, R. A., Diagnostics of plasma, 20: 38225
VOELKEL, A. H., Particle singularities in relativistic quantum field theory, 20: 37833
VOEVODSKII, V. V., Formation of radicals during radiolysis of organic solids. III., 20: 36883
VOGEL, Karl-Heinz, Question of the subtle adaptation of the irradiation field in fast electrons, 20: 36700
VOHRA, K. G., Estimates of biospheric contamination and radiation dose from fallout for all the pre-treaty tests of nuclear weapons, 20: 37004
VOICULESCU, Gh., Lifetime of the μ^- in ^{239}Pu, 20: 38114
VOIGT, Hans, Investigation of the processes in superconducting flux pumps, 20: 37977
VOLKENSHTEIN, N. V., Anisotropy of the Hall effect in Gd, 20: 37178
VOLKOLUPOV, Yu. Ya., Production of hot-electron plasma in magnetic mirror traps, 20: 38211 (AEC-tr-6782)
VOLKOVA, L. V., Energy spectra of muons and neutrinos generated by cosmic rays in different substances, 20: 37712
VOLKOVA, L. V., Positive excess of cosmic-ray muons at sea level, 20: 37688
VONACH, H., Energy and spin dependence of the ^{56}Fe level density for excitation energies 0 to 20 Mev, 20: 38157
VON GELDERN, Eduard R., European assessment of nuclear and conventional fuel costs, 20: 38541
VON ROSENVINGE, T., Measurements of energy spectrum of nuclei with $Z \geq 3$ using a balloon-borne Cherenkov scintillation counter, 20: 37571
VON SENGBUSCH, K., Schematic pre-main-sequence evolution, 20: 37398
VOROB'EV, Yu. A., Utilization of fast charged particle inelastic scattering for analysis of composition of materials, 20: 36732
VORONKOVA, L. N., Consequences of uv-microbeam irradiation of the nucleoli of living cells, 20: 36592
VOROSHILOV, Yu. V., X-ray investigation of Nb–W–B, 20: 37261
VOSHAGE, H., Cosmic ray produced lithium and calcium in iron meteorites, 20: 37603
VOVCHENKO, V. G., π-Meson production in 655-Mev pp collisions, 20: 37802

W

WACHBERGER, Eugen, Instrument compensation of the quenching effects in determination of ^{14}C and ^{35}S, 20: 36771

WACHTEL, J. M., Interference beats in pulse-stimulated cyclotron radiation, 20: 37776

WACHTMEISTER, C. A., Synthesis of some tritium-labeled mutagenic alkyl alkanesulfonates, 20: 36916

WACKER, A., Enzymatic degradation of uv-irradiated DNA, 20: 36596

WADDINGTON, C. J., Electrons, H, and He nuclei of cosmic radiation observed in 1963 and 1964, 20: 37551

WADDINGTON, C. J., Low energy multiply charged nuclei in the cosmic radiation, 20: 37565

WADDINGTON, C. J., Modulation of cosmic rays by an electric field, 20: 37512

WADDINGTON, C. J., Spectral composition, 20: 37583

WADDINGTON, C. J., Very heavy low-energy cosmic-ray nuclei, 20: 37566

WADE, Clarence W. R., Deuterium isotope effects in the mutarotations of α-D-glucose and β-D-fructose, 20: 36577

WAGNER, C. N. J., Faulting in cold-worked Ta-10 at.% Re and W-20 at.% Re, 20: 37217

WAGNER, G., Spectroscopy of fast neutrons and reaction mechanism of the (d,n) reaction, 20: 38159

WAGNER, J. I., Fissile fuel recovery process, 20: 36955

WAHBA, I. J., Degradation of pectin by γ radiation under various moisture conditions, 20: 36879

WAHSWEILER, H. G., 3⁻ continuum states of ^{16}O in the eigenchannel reaction theory, 20: 38102

WAIDELICH, W., Thermal annealing of lattice parameter change in low-temperature neutron-irradiated aluminium, 20: 38380

WAIT, James R., Radiation from a spherical aperture antenna immersed in a compressible plasma, 20: 38232

WAKANO, Masami, Intensely localized solutions of the classical Dirac-Maxwell field equations, 20: 37849

WALFORD, F. J., Comparison of pressure loading produced by contained explosions in water and sodium, 20: 38459 (ANL-7120, pp 720-33)

WALINGA, J., High-resolution investigation of the $^{30}Si(p,p)^{30}Si$ reaction, 20: 38105

WALKER, J., Nuclear reactor operation in space, 20: 38529

WALKER, J. V., Computation of neutron flux from foil activation data: SPECTRA code, 20: 37076 (SC-DC-66-1512)

WALKER, Merle F., Ultraviolet excess in T Tauri stars, 20: 37420

WALLACE, R., Perturbation theory of multiphoton processes, 20: 37841

WALLERSTEIN, G., CH stars and neutron-addition processes, 20: 37424

WALSTAM, Rune, Therapeutic short-distance and intracavitary gamma beam techniques, 20: 36680

WALTAR, Alan E., Interpretation of pulsed-source experiments in a reflected reactor, 20: 38453

WALTER, C. M., Mixed-carbide fuels for fast reactors, 20: 38467 (ANL-7120, pp 314-27)

WALTER, Erich, Construction characteristics of cesium telecurie devices, 20: 36710

WALTERS, Virginia Fried, Correlation of positron lifetime with the angle between the annihilation gamma rays, 20: 37737 (COO-1297-8)

WALTON, A. B., Differential momentum spectrum and charge ratio of muons in extensive air showers, 20: 37643

WAMBERSIE, A., Secondary standards in dosimetry, 20: 37090

WAMPLER, E. Joseph, Density of intergalactic hydrogen molecules, 20: 37353

WAND, R. H., Density spectrum of extensive air showers at 2285 m, 20: 37630

WANG, Chen-hsia, Polarization of protons from the $^{12}C(d,p)^{13}C$ and $^{40}Ca(d,p)^{41}Ca$ ground-state reactions, 20: 38119

WANG, Nen-min, Reaction $^3He + {}^3He$, 20: 38131

WANG, R., The structure of $YbSb_2$, a $ZrSi_2$ isotype, 20: 37238

WARD, Gerald M., Deposition of fallout ^{137}Cs on forage and transfer to milk, 20: 37036

WARD, John W., Study of some of the parameters affecting Knudsen effusion, 20: 37307 (LA-3509)

WARREN, David H., Crustal seismic measurements in Southern Mississippi, 20: 36965

WARREN, Frederick H., Economic significance of nuclear fuel management, 20: 38416

WARREN, Goyen, Isotope dating of Antarctic rocks: summary, 20: 37015

WARREN, William W. Jr., Nuclear quadrupole relaxation and chemical shift of ^{131}Xe in liquid and solid Xe, 20: 38392

WARREN, William Willard Jr., Nuclear magnetic resonance of ^{131}Xe in liquid and solid Xe, 20: 38404

WARWICK, Constance S., Sunspot configurations and proton flares, 20: 37346

WARZEK, F. G., Doppler effect in ^{238}U and ^{235}U fission in a fast-neutron spectrum, 20: 38430 (ANL-7120, pp 616-24)

WATANABE, Tadashi, Value of the electric quadrupole moment of the deuteron, 20: 37797

WATANABE, Z., Extensive air showers observed in the emulsion chamber, 20: 37638

WATANABE, Z., Nuclear interactions produced in the emulsion chamber, 20: 37673

WATANABE, Z., Observation of extremely high-energy nuclear events by emulsion chamber, 20: 37661

WATERBURY, G. R., Potentiometric titration of cerium and manganese following separation from plutonium and cobalt, 20: 36713

WATERMAN, M. J., Effect of neutron flux on fission product gas emission from UO_2, 20: 38464 (AERE-M-1607)

WATSON, A. A., Shower front structure and the properties of extensive air showers, 20: 37632

WATSON, D. D., Spin and parity of the 3.16-Mev and 7.54-Mev levels in ^{35}Cl, 20: 38071

WATSON, D. L., Polarization in the elastic scattering of 49-Mev protons by Ca, ^{58}Ni, ^{60}Ni, and ^{208}Pb, 20: 38049

WATSON, Howard Lee, Exact solution to a bootstrap problem, 20: 37808

WATSON, J. H. P., Critical magnetic field and transition temperature of synthetic high-field superconductors, 20: 37949

WDOWCZYK, J., Attentuation of the μ component of EAS determined by the barometric effect, 20: 37623

WDOWCZYK, J., Charge ratio of cosmic-ray muons at large zenith angles, 20: 37689

WDOWCZYK, J., Lateral distribution, energy spectrum, and fluctuations of the muon component in electromagnetic cascades, 20: 37622

WDOWCZYK, J., Momentum spectrum of cosmic-ray muons in the zenith angle range 82.5 to 90°, 20: 37697

WDOWCZYK, J., Semi-empirical determination of the fluctuation of the EAS μ component, 20: 37624

WDOWCZYK, J., Some properties of μ-poor EAS, 20: 37610

WDOWCZYK, J., Theoretical studies of the muon component of EAS, 20: 37640

WEBB, John S., Formula index to NMR literature data. Vol. 2, 20: 36842

WEBB, P. N., Isotope dating of Antarctic rocks: summary, 20: 37015

WEBB, R. A., Steam cooling for fast reactors, 20: 38496 (ANL-7120, pp 136-40)

WEBBER, W. R., Measurements of the primary proton and He spectra and their modulations using a balloon-borne Cherenkov-scintillation counter, 20: 37554

WEBBER, W. R., Measurements of energy spectrum of nuclei with $Z \geq 3$ using a balloon-borne Cherenkov scintillation counter, 20: 37571

WEBBER, W. R., Solar modulation of protons and helium nuclei during the period 1963–1965, 20: 37553

WEBBER, W. R., Some implications of the relative spectra of the different charge components in the primary radiation, 20: 37570

WEBER, A. H., Flame-temperature measurement by thermal neutron probe, 20: 37310

WEBER, Jon B., Fractionation of the stable isotopes of C and O in marine calcareous organisms: the Echinoidea. I., 20: 36549

WEBER, Jon N., Fractionation of the stable isotopes of C and O in marine calcareous organisms: the Echinoidea. II., 20: 36550

WEBSTER, Medford S., Properties of K* (1425), 20: 37733 (BNL-10462)

WEBSTER, Medford S., Resonance production in the reactions $\pi^{\pm}p \rightarrow KK^0$ at 6 Bev/c, 20: 37732 (BNL-10461)

WEEKES, T. C., Flux limits for high-energy γ rays from quasars and other possible cosmic-ray sources, 20: 37547

WEEKS, R. A., Electron spin resonance of rare-earth ions in CeO_2: Yb^{3+} and Er^{3+}, 20: 38391

WEEKS, T. C., Radio system for the detection of air showers, 20: 37102

WEESE, John A., Axisymmetric thermoelastic problems in bispherical coordinates, 20: 36957 (DRI-2327)

WEGER, M., New nuclear spin-lattice relaxation process in type-II superconductors, 20: 37964

WEIGEL, F., Structure investigations on lanthanide oxalates. I., 20: 36835

WEIGERT, A., Evolution of a star of seven solar masses, 20: 37405

WEIL, J. L., Cross sections as a function of energy for the scattering of protons from ^{12}C, 20: 38050

WEILLS, J. T., Large metal-fueled fast reactor study. II., 20: 38494 (ANL-7120, pp 94-103)

WEINSTEIN, A. S., Transient flux distributions by discontinuous model synthesis, 20: 38431 (ANL-7120, pp 625-31)

WEINSTEIN, D., Yield point occurrence in polycrystalline alpha-zirconium, 20: 37229

WEINZIERL, Peter, Pair production cross section for 6.13-Mev gamma radiation, 20: 37746

WEIR, J. R., In-reactor stress-rupture properties of a 20Cr–25Ni, Cb-stabilized steel, 20: 37284

WEISSBACH, Herbert, Biosynthesis of highly labeled actinomycins, 20: 36545

WEITKAMP, C., Neutron-capture gamma-ray investigation of ^{88}Sr level structure, 20: 38141

WELLS, D. O., Energy levels of ^{56}Fe, 20: 38088
WENDE, Sigurd, Detection of cerebral radiation damage with radioactive isotopes, 20: 36696
WENDENBURG, J., Radiation-chemical production and optical absorption spectra of organic S radicals in organic glasses at −196°C, 20: 36894
WENZL, H., Thermal annealing of lattice parameter change in low-temperature neutron-irradiated aluminium, 20: 38380
WERNER, G., Study on the extraction of rare earths with tributyl phosphate. II., 20: 36938
WERNICK, J. E., New nuclear spin-lattice relaxation process in type-II superconductors, 20: 37964
WERNTZ, Carl, "Breathing mode" collective nuclear vibrations and application to ^4He excited states, 20: 38170
WERT, C. A., Clustering of O in solid solution in Nb. I., 20: 37213
WERT, C. A., Clustering of O in solid solution in Nb. II., 20: 37214
WERTH, Glenn, Salmon seismic experiment, 20: 36962
WERTHEIM, G. K., Moessbauer effect in $MnFeO_3$, 20: 36817
WERTHEIM, G. K., Moessbauer hyperfine spectra of Fe^{3+} in corundum: magnetic- and crystal-field effects, 20: 38388
WESCOTT, Eugene M., Magnetoconjugate phenomena, 20: 37914
WESOLOWSKI, Jerome J., Two-nucleon distorted-wave Born approximation analysis of $^{19}F(d,\alpha)^{17}O$ data, 20: 38082
WESSON, J. A., Heat transmission through Langmuir sheath in presence of electron emission, 20: 38191 (CLM-R-61)
WEST, R. E., Intramolecular coherent scattering of neutrons by CD_4 gas, 20: 38000
WEST, T. S., Determination of trace amounts of copper in niobium and tantalum by atomic-absorption spectroscopy, 20: 36726
WESTLAKE, D. G., Stress orientation of zirconium hydride in a single crystal of zirconium, 20: 37269
WEY, Raymond, Incorporation of uranyl cations in carbonates during formation, 20: 36796
WEY, Raymond, Incorporation of uranyl cations in silicates during formation, 20: 36797
WHANG, Y. C., Viscous model of the solar wind, 20: 37350
WHAPHAM, A. D., Electron microscope observation of the fission-gas bubble distribution in UO_2, 20: 37255
WHEATLEY, J. C., Thermal and magnetic properties of dilute solutions of ^3He in ^4He at low temperatures, 20: 37961
WHEELER, R. G., Multiaxial plastic flow of Zircaloy-2 determined from hardness data, 20: 37230
WHEELER, V., Post-explosion environment resulting from the Salmon event, 20: 36970
WHITE, Donald R., Vibrational relaxation in $CO–D_2$ mixtures, 20: 26820
WHITE, J. E., Alloying-element/dispersed-phase interactions in W-base alloys, 20: 37185
WHITE, J. E., Metallurgical evaluation of various infiltrated tungsten materials in air and nitrogen plasmas, 20: 37188
WHITE, R., Electric-charge form factor according to SL(6,C), 20: 37840
WHITE, Richard H., Mechanism of type II supernova explosions, 20: 37407
WHITE, W. B., Prog. rpt. on crystal chemistry studies, 2/14–5/13/66, 20: 36784 (AD-636054)
WHITFIELD, J. F., Effect of x irradiation on nicotinamide adenine dinucleotides content of rat thymocytes, 20: 36590
WHITMORE, G. F., Dehydration of uv-irradiated uridine and its derivatives, 20: 36597
WHITTAKER, A., Advances in the gamma-absorptiometric determination of uranium and plutonium in solution, 20: 36767
WICKMAN, H. H., Moessbauer hyperfine spectra of Fe^{3+} in corundum: magnetic- and crystal-field effects, 20: 38388
WIDMAN, J. C., Energy absorption in cylinders containing an axial source, 20: 37032
WIEGAND, D. A., Point defect generation in LiF by plastic deformation and x irradiation, 20: 88368
WIESER, P., Distribution of natural radioactive aerosol particles, 20: 37027
WIESNER, L., Continuous gas analyses by means of x-ray fluorescence, 20: 36766
WIGINTON, C. L., Cyclotron excitation of electromagnetic waves by a gyrating electron beam, 20: 38291
WIKHAMMER, G. A., SWIFT dryout data for 19-rod bundle cooled by steam/water fog, 20: 38409 (AECL-2586)
WIKLE, K. G., Role of Be as a dilute alloying addition to Group VIII and Group I transition metals, 20: 37275
WILCOX, George E., Nuclear radiation: tool for anticollision guidance, 20: 37141
WILDERMUTH, K., Energy width of virtual resonance levels in atomic nuclei, 20: 38013
WILKINS, J. W., Strong-coupling superconductivity. I., 20: 37952
WILKINSON, D. H., Isobaric mass formula and Coulomb energies in the 1p-shell, 20: 38174
WILLIAMS, Calvit Herndon Jr., Dissociation of a cesium fluoride molecule by impact with a fast argon atom, 20: 37478
WILLIAMS, D. C., Reactions (t,p) and (t,α) on ^{48}Ca and ^{50}Ti, 20: 38063
WILLIAMS, J. E. C., Optimum current distribution in superconducting coils, 20: 37971
WILLIAMS, L. S., Infiltrated oxide cermets, 20: 37209
WILLIG, R. L., Equipotential surfaces of a plasma moving in a toroidal octupole magnetic field, 20: 38192 (COO-1233-32)
WILLIS, F. L., Status of recent meltdown studies, 20: 38474 (ANL-7120, pp 534-9)
WILSON, A. R., High-voltage pulse characteristics of superconducting transmission lines, 20: 37939
WILSON, B., Axial stability calculations for A.G.R. systems, 20: 38446 (TRG-Report-1138)
WILSON, B. G., Balloon studies of primary cosmic rays at solar minimum, 20: 37538
WILSON, B. G., Density spectrum of extensive air showers at 2285 m, 20: 37630
WILSON, B. G., Fast neutron intensity above Fort Churchill, Canada, 20: 37555
WILSON, B. J., Radiochemical manual, 20: 36924
WILSON, Daniel W., Deposition of fallout ^{137}Cs on forage and transfer to milk, 20: 37036
WILSON, Daniel W., Transferof fallout ^{137}Cs from soil to dairy cattle feeds, 20: 37038
WILSON, J. G., Shower front structure and the properties of extensive air showers, 20: 37632
WILSON, M., Auto-ionization-broadened Rydberg series in the spectrum of La I, 20: 37351
WILSON, P., Reactivity of transition metal fluorides. II., 20: 36803
WILSON, T., Neutron albedo measurements on rocket flights, 20: 37601
WINCHELL, H. S., Homotransplantation studies in dogs following selective radioisotopic lymphatic ablation, 20: 36641
WINCKLER, J. R., Measurement of the isotopic composition of He nuclei in the primary cosmic radiation in the energy interval 80–150 Mev/nucleon, 20: 37579
WINCKLER, J. R., Studies of primary cosmic rays with ionization chambers, 20: 37508
WINSTON, R., Efficient light coupler for threshold Cherenkov counters, 20: 37118
WINTON, J., Effect of variations in composition and heat treatment on the properties of Zr–Nb alloys, 20: 37236
WIRSING, E., Pyrolytic carbon decladding, 20: 36956
WOJTOWICZ, Stefan, Calibration pulse generator with nanosecond pulses, 20: 37049
WOLEFENDALE, A. W., Charge ratio of cosmic-ray muons at large zenith angles, 20: 37689
WOLF, N. S., Diffusion and instabilities in "Q" machine plasmas, 20: 38324
WOLFENDALE, A. W., Intensity and angular distribution of cosmic rays far underground, 20: 37704
WOLFENDALE, A. W., Momentum spectrum of cosmic-ray muons in the zenith angle range 82.5 to 90°, 20: 37697
WOLFENDALE, A. W., Muon interactions far underground, 20: 37701
WOLFENDALE, A. W., Muons and neutrinos, 20: 37715
WOLFSON, C. J., University of Utah neutrino detector, 20: 37104
WOLTER, W., High-energy jets produced by heavy primary nuclei of cosmic origin and their fragmentation products, 20: 37662
WONG, H. Vernon, High ion β pitch-angle instability, 20: 38295
WONG, James, Method for the production of zirconium alloys of continuously higher corrosion resistance, 20: 37194
WOODGATE, G. K., Hyperfine structure and nuclear moments of samarium, 20: 37459
WOODS, Frank W., Root extension in a longleaf pine plantation, 20: 36560
WOOLCOCK, W. S., General formalism of some scattering processes involving photons, 20: 37758
WOOLCOTT, R. L. S., Elastic and electromagnetic proton interactions at 30 Bev, 20: 37666
WOOLCOTT, R. L. S., Investigation of high-energy nuclear interactions using a quartile energy estimator, 20: 37681
WORLEY, R. D., Characteristic x-ray production in single crystals (Al,Cu) by proton bombardment. I., 20: 38393
WRENSHALL, G. A., Glucose production rates in dogs determined by two different tracers and tracer methods, 20: 36565
WRIGHT, B. T., Production of charged pions by 600 Mev protons on various nuclei, 20: 38186
WRIGHT, J. H., Conceptual design and preliminary accident analysis of a Na-cooled, carbide-fueled, large modular fast reactor, 20: 38456 (ANL-7120, pp 205-29)
WRUBEL, Marshal H., Transport of s-process elements to the surfaces of stars, 20: 3/423
WRZESINSKY, R., Interaction of 3 H atoms, 20: 37476
WU, K. K., Cosmic-ray flux variation with height in the stratosphere, 20: 37552
WULFF, J., High-field superconductivity of Ta–Ti alloys, 20: 37268

WULFF, J., Microstructure and superconductivity of a 44.7 at.% Nb(Cb)-54.3 at.% Ti alloy containing O, 20: 37267
WYBOURNE, B. G., Energy levels of trivalent gadolinium and ionic contributions to the ground-state splitting, 20: 38389
WYBOURNE, B. G., Group-theoretical classification of the atomic states of g^n configurations, 20: 37437

Y

YABUKI, Hiroichi, Compositeness conditions and the indefinite nature of the self-mass, 20: 37847
YAFTAH, S., Results of Doppler coefficient calculations for fast reactors and comparison of different methods. I and II., 20: 38421 (ANL-7120, pp 440-8)
YAGUCHI, Koichi, Magnetic and electric properties of GdP, TbP, and DyP, 20: 38370
YAHAGI, N., Cosmic-ray rigidity spectrum during a solar rotation and solar wind velocity, 20: 37533
YAJIMA, N., New kinematical approach for analyses of high-energy cosmic-ray jets, 20: 37680
YAJIMA, Nobuo, Model of the dispersive nonlinear equation, 20: 37926
YAKOVLEV, V. I., Installation for study of EAS and nuclear interactions of cosmic-ray particles with energies 10^{12} to 10^{16} ev, 20: 37634
YAKUBSON, K. I., Use of neutron-induced gamma-radiation spectrometry to investigate the elemental composition of rocks in boreholes, 20: 37018
YAMADA, Masao, Some aspects of the direct interaction, 20: 37851
YAMADA, N., Stabilizing effect of radial plasma density distribution on helical instability, 20: 38270
YAMAGISHI, Shigeru, Behavior of polonium evaporated from fused salt, 20: 36736
YAMAJI, Shuhei, Calculations on reactions $^{13}C(p,n)^{13}N$, $^{11}B(p,n)^{11}C$, and $^{27}Al(n,p)^{27}Mg$, 20: 38112
YAMAKOSHI, K., Variation of ^{14}C content in the atmosphere during the past two thousand years, 20: 37602
YAMAMOTO, Kiyoko, Effect of gamma radiation on Ni, Zn, and Ag chelates of tetraphenylporphine, 20: 36889
YAMAMOTO, Satoru, Effects of additional elements on discontinuous precipitation in Cu–Be alloys, 20: 37253
YAMASHINA, Toshiro, Catalytic decomposition of H peroxide on the γ-irradiated Ni oxide, 20: 36885
YAMASHITA, K., Observation of the energy spectrum of galactic x rays, 20: 37500
YAMASHITA, Mikio, Cosmic-ray-produced neutrons at ground level: neutron production rate and flux distribution, 20: 37483
YAMAZAKI, H., Electrical optical properties of three-electrode electron lenses, 20: 37330
YAMAZAKI, Mikio, Determination of ^{14}C and ^{3}H by liquid scintillation spectrometer. VI., 20: 36764
YAMIROV, V. N., Ionization measurement in a streamer chamber, 20: 37110
YANO, Takeo, Ion exchange equilibria in the system of uranyl sulfate ion–Cl^- and NO_3^-, 20: 36931
YANOUT, Z., Measurement of the triple scattering parameter R_{pn} at 70° and the phase-shift analysis at 630 Mev, 20: 37739 (JINR-E-2726)
YARBA, V. A., Double charge exchange of 50- to 176-Mev π^- mesons in photo emulsion, 20: 38012 (JINR-P-2806)
YARBROUGH, J. D., Liquid scintillation determination of ^{45}Ca and ^{89}Sr in unicellular algae, 20: 36747
YARUNIN, V. S., Odd-odd hyperfine interaction and spontaneous ortho-para transitions in H, 20: 37467
YASUMORI, Iwao, Sensitive gas chromatography of para-, orthohydrogen, hydrogen deuteride, and deuterium, 20: 46737
YASUMOTO, Masahiko, Effects of process variables on the telomerization of ethylene with C tetrachloride induced by γ radiation, 20: 36890
YASUMOTO, Masahiko, Reaction of butene-1 with phosgene induced by γ radiation, 20: 36892
YASUMOTO, Masahiko, Telomerization of ethylene with C tetrachloride induced by γ radiation under constant ethylene pressure, 20: 36891
YATSUI, Kiyoshi, Harmonic generation of ion cyclotron frequency in longitudinally magnetized plasmas, 20: 38252
YEH, C., Reflection and transmission of electromagnetic waves by a moving plasma medium, 20: 38237
YEIVIN, Y., Average charge distributions in systems of nucleons and pions, 20: 37791
YEIVIN, Y., Derivation of the pion multiplicity in nuclear collisions from sea-level positive excess and total muon spectra, 20: 37691
YOFFEY, J. M., Hemopoietic response of guinea pig to gamma irradiation, 20: 36611
YON, E., Sodium distribution in thermal oxide on silicon by radiochemical and MOS analysis, 20: 36744
YORK, D., Potassium–argon ages of some Dalradian, Moine, and related Scottish rocks, 20: 37016
YOSHIDA, Hiroyuki, Effects of additional elements on discontinuous precipitation in Cu–Be alloys, 20: 37253
YOSHII, H., Direct measurement of attenuation length of extensive air showers, 20: 37642
YOSHII, H., Observation of the character of EAS cores, 20: 37615
YOSHIKAWA, S., Ballooning interchange instabilities of magnetized plasmas under gravitational fields, 20: 38267
YOSHIKAWA, S., Equilibrium of a toroidal plasma in the model C stellarator, 20: 38268
YOSHIMOTO, K., Study on the plasma proteins of patients who survived the A bomb, 20: 36581
YOSHIMOTO, T., Study on the plasma proteins of patients who survived the A bomb, 20: 36581
YOSHIMURA, Hisamitsu, Plasma end loss in a slow theta pinch, 20: 38256
YOSHIZAWA, Y., Angular correlations for E2 and E3 transitions in Coulomb excitation, 20: 38032
YOSIDA, Hiroshi, Calculations on reactions $^{13}C(p,n)^{13}N$, $^{11}B(p,n)^{11}C$, and $^{27}Al(n,p)^{27}Mg$, 20: 38112
YOUNG, F. J., Electromagnetodynamics of fluids, 20: 37884
YOUNG, John D., X-radiation alignment of quartz crystals for improved hypersonic propagation, 20: 38366
YOUNG, K. M., Equilibrium of a toroidal plasma in the model C stellarator, 20: 38268
YOUNG, R. A., X-ray specimen temperature control with gas streams, 20: 37047
YOUNG, T., Neutron cross sections of Ca from 2.0 to 6.5 Mev, 20: 38183
YU, David U. L., Two-nucleon correlation function and final-state interactions, 20: 38015
YU, Pan-shui, Polarization of protons from the $^{12}C(d,p)^{13}C$ and $^{40}Ca(d,p)^{41}Ca$ ground-state reactions, 20: 38119
YUDIN, B. F., Thermodynamics of vaporization of refractory oxides at high temperatures, 20: 36841
YUDIN, E. P., Installation for study of EAS and nuclear interactions of cosmic-ray particles with energies 10^{12} to 10^{16} ev, 20: 37634
YUPKO, V. L., Physical properties of certain rare earth dicarbides, 20: 36811

Z

ZABLOCKI, C. J., Electrical transients observed during underground nuclear explosions, 20: 36971
ZAIKIN, D. A., Rigidity parameters of the octupole vibrations in ^{19}F, 20: 38061
ZAIMIDOROGA, O. A., Capture of pions by ^{3}He. II., 20: 38011 (JINR-P-2805)
ZALESKI, C. P., Contribution to safety problems related to 1000-Mwe fast power reactor project, 20: 38497 (ANL-7120, pp 157-61)
ZALIKIN, G. A., Strontium-90 excretion from the blood stream into the gastro-intestinal tract in rats, 20: 36558
ZALKIN, Allen, Atomic parameters in the lanthanum trifluoride structure, 20: 36805
ZAMECNIK, Paul C., Prog. rpt. on mechanisms and regulations of nucleic acid and protein synthesis, and their possible relationship to radiation damage, 9/65–8/66, 20: 36555 (NYO-2643-22)
ZANNER, F. J., Tensile fracture of Zr and Zr-rare earth solid-solution alloys, 20: 37231
ZATSEPIN, G. T., Depth-intensity curve of muons and their energy spectrum, 20: 37706
ZATSEPIN, G. T., Depth-intensity curve of nuclear events induced by muons, 20: 37703
ZATSEPIN, G. T., Energy spectra of muons and neutrinos generated by cosmic rays in different substances, 20: 37712
ZATSEPIN, G. T., Experimental possibilities of the observation of neutrinos from collapsing stars, 20: 37379
ZATSEPIN, G. T., Neutrino spectroscopy of the Sun, 20: 37378
ZATSEPIN, G. T., Positive excess of cosmic-ray muons at sea level, 20: 37688
ZATSEPIN, G. T., Solar neutrino interaction with electrons, 20: 37792
ZATSEPIN, G. T., Solar neutrino detection by the registration of electrons in reactions $\nu + Z \rightarrow (Z+1) + e^-$, 20: 37793
ZAWADZKI, A., Attentuation of the μ component of EAS determined by the barometric effect, 20: 37623
ZAWADZKI, A., Semi-empirical determination of the fluctuation of the EAS μ component, 20: 37624
ZAWADZKI, A., Some properties of μ-poor EAS, 20: 37610
ZEBROSKI, Edwin L., Flexible clad nuclear fuel element, 20: 38485
ZELBY, Leon W., Electron density and collision frequency in a radially inhomogeneous plasma column, 20: 38193 (INDEC-SR-7, pp 3.5-13)
ZELBY, Leon W., Electromagnetic wave interaction in an inhomogeneous drifting plasma, 20: 38194 (INDEC-SR-7, pp 3.22-59)
ZEL'CHINSKII, M., Experimental determination of radiation quality factors in the vicinity of high-energy accelerators, 20: 37323
ZELEVINSKAYA, N. G., Angular distribution of secondary particles in multiple production at high energies, 20: 37682
ZELINSKII, V. G., Methylation of guanidinacetic acid in liver sections of

rats subjected to x-ray irradiation, 20: 36603
ZHARKOV, G. F., Josephson tunneling effect in superconductors, 20: 37975
ZHDANOV, G. B., Certain aspects of nucleon isobar production in nucleons interactions at energies 10^3 and 25 Bev, 20: 37675
ZHELEV, Zh., Positron decay of ^{145}Eu, 20: 38133
ZHELEZNOVA, L. P., Electron absorption spectra of Ce(III) salts in water–TBP mixtures and in pure TBP, 20: 36831
ZHELTIKOV, A. N., Neutron radiative capture gamma spectrometry as a method of determining the composition of iron-bearing rocks and ores, 20: 37019
ZHEREBIN, E. A., Decay of ^{139}Cs and ^{140}Cs, 20: 38124
ZHEVERZHEEVA, V. F., Extraction of fission products from water by foaming, 20: 36934
ZHIZHIN, E. D., ω-Meson photoproduction at high energies, 20: 37807
ZHURAVLEV, N. N., Properties of yttrium borides, 20: 38359
ZHURBIN, G. I., Incorporation of 2-^{14}C-acetate in muscle and serum proteins of irradiated rabbits, 20: 36574
ZHURBIN, G. I., Renewal of rabbit muscle and serum proteins in radiation sickness, 20: 36600
ZICHA, B., Influence of ionizing radiation on the Dische-positive material in urine and blood of irradiated animals, 20: 36604
ZIL'BERMAN, B. Ya., Calculation method for azeotropic steam fractionation, applied to the TBP–CCl_4 system, 20: 36731
ZIMA, Gordon E., High pressure consolidation of submicron tungsten, 20: 37200
ZIMBRICK, John, Paramagnetic relaxation of trapped electrons in irradiated alkaline ices, 20: 36871
ZIMMERMAN, J. E., Instrumentation using quantum interference in superconductors, 20: 37986
ZINGL, Harold F. K., Remarks on the deuteron form factors I., 20: 37749
ZINOV, V. G., Nuon capture in mixed gases, 20: 37741 (JINR-P-2788)
ZOLOTAVIN, A. V., Decay of ^{182}Ta, 20: 38134
ZUBIETA, M., Solar daily variation recorded at a low-latitude station by east and west pointing telescopes during periods of maximum and minimum solar activity, 20: 37373
ZUBKE, D., Alpha emission from heavy nuclei induced by neutrons of 12 to 23 Mev, 20: 38036
ZUELCH, Klaus J., Changes in tumors after irradiation and possibility of injuries in normal brain, 20: 36695
ZUEVA, I. M., Helical minimum B magnetic configurations, 20: 38219
ZUIDEMA, E., Specific gamma emission of natural K and La, 20: 38107
ZUMWALT, L. R., Cs–graphite sorption isotherms determined by a static method, 20: 36799
ZUSMANOVICH, A. G., Periodic cosmic-ray variations and their change during the cycle of solar activity, 20: 37525

SUBJECT INDEX

Main entries in this index are generally specific materials, things, and processes. These are followed by modifiers that describe the properties of, and processes applied to, the main entries.

The number preceding the colon is the *NSA* volume number, and the number following is the abstract number. The designation (R) following the abstract number indicates that the abstract is of a progress report; (P) indicates a patent; and (T) indicates a translation. Abstracts for reports other than progress reports carry no letter designation. References to report numbers, where appropriate, are included after the abstract number of the citation. Published literature (journal article or book) is identifiable by the absence of a report number.

The user should bear in mind that the ideas presented in the original literature, rather than key words, have been indexed. The indexers have tried to select what seemed the most probable and logical place to look for typical information. Since it is not possible to anticipate where a user would look for information, numerous cross references are included in cumulative indexes to assist him in his search.

Experience in using an index of this type will be the best guide in obtaining the desired information, and a consideration of synonymous or closely related terms will prove valuable.

Information must be so indexed as to be of the greatest use to the greatest number of users. This requires that a topic be indexed to headings that most specifically describe it and not ordinarily to the headings that describe its ultimate use, nor to the general class headings that include the specific headings. For example, information on the treatment of thyroid disease with I-131 would be indexed under Thyroid Gland and under Iodine Isotopes I-131, but not necessarily under Radiotherapy. A study of the effects of x radiation on hair would be indexed under both X Radiation and Hair. However, the information would not be indexed under the experimental animal, e.g., Rats, unless the report discusses the effects on rat hair as compared with the effect on the hair of other animals.

The broad, general class headings are used only for general information or for comprehensive reports or articles.

Subject Heading Styles

Generally, the direct form of subject entry is used rather than inverted headings, e.g., Amino Acids rather than Acids, Amino; Helium Isotopes He-4 rather than Helium—isotopes He-4 or Helium—He-4 isotopes. Note, however, that in some cases parenthetic modifying terms or inverted headings of the form Neutrons, Fast are used in preference to a direct entry that would result in the scattering of information. Organic compounds are usually entered in the index in the inverted form so that substituted compounds can be listed near the parent compound; e.g., Benzene, Bromo- rather than Bromobenzene. In general, the style of nomenclature used is that of Chemical Abstracts, except that some items listed in that publication as subheadings are elevated to form part of the main heading; e.g., Butyric Acid, Methyl Ester rather than Butyric Acid—methyl ester.

Alphabetization

Main headings are alphabetized word-by-word. A parenthetic qualifier following a main heading is disregarded in alphabetizing unless there are two or more headings identical except for the parenthetic qualifier, in which case the qualifier determines the order. Headings involving Greek letters are arranged as if the names of the letters were spelled out.

Examples:

M-Capture
  see Electron Capture
Magnesium
Magnesium Alloys
Manganese Fluorides
Manganese(II) Fluorides
Mesons
Mesons (π)
Mesons (ρ)
3-Pentanol, 2,4-Dimethyl-
2-Pentanol, 2-Methyl-
2-Pentanol, 4-Methyl-

Nomenclature of Inorganic Compounds

Inorganic compounds are indexed in the direct form, listing cations in the order of increasing valence in the case of polycationic salts of varying valence and in alphabetic order for polycationic salts in which all cations have the same valence; e.g., Sodium Aluminum Silicates and Potassium Sodium Sulfates.

Multicomponent Alloys and Other Systems

Multicomponent alloys, except well-known trade names, are indexed under a main heading in the form "element alloy" for each element in the alloy. The modifier begins with element symbols for each component arranged alphabetically as if the English name for the element were spelled out.

Example: Copper-Gold Alloy is indexed
  Copper Alloys
    Cu-Au...
  Gold Alloys
    Cu-Au...

Well-known alloys such as Zircaloy-2 are indexed directly to the trade name; cross references referring from each component of the alloy to the entry for the trade name appear in cumulative indexes.

Multicomponent systems of non-metallic elements are indexed in a manner similar to alloys except the main heading used contains the word "Systems" in place of "Alloys."

Example: Silicon–Tungsten Systems are indexed
  Silicon Systems
    Si-W...
  Tungsten Systems
    Si-W...

Multicompound systems and mixtures of compounds are indexed under the main heading for each component com-

pound; the modifiers begin with an alphabetical listing of compound formulas.

Example: Lead Titanate–Lead Zirconate is indexed
Lead Titanates
$PbTiO_3$-$PbZrO_3$...
Lead Zirconates
$PbTiO_3$-$PbZrO_3$...

A mixed system of compounds and elements is indexed using a combined form of the above conventions, e.g., a dispersion of copper and alumina would be indexed

Aluminum Oxides
Al_2O_3-Cu...
Copper Systems
Al_2O_3-Cu..

Physical States and Configurations of Materials

Specification of the physical state, if other than normal, or geometric configuration of the material is included in the modifying phrase, i.e., liquid metals would be indexed to the metal with "liquid" in the modifier, and carbon crucibles would be indexed to Carbon with "crucibles" appropriately placed in the modifier and also to Crucibles if appropriate.

Modifying Phrases

The modifiers appearing under a main heading are written specifically to describe the relation of the item being indexed to that main heading. The modifier, therefore, will generally contain more useful information about that relation than will a title or a phrase written to be used under every main heading assigned to the item. Effort is exerted to begin the modifier with the word judged to be of greatest use to the greatest number of users; this, however, does not obviate the need to consider all modifiers under the main heading(s) of interest.

Modifiers are usually intended to form a meaningful phrase when combined with the main heading. Some are intended to be read following the main heading, e.g., the entry Hydrogen—sorption by charcoal is read "hydrogen sorption by charcoal"; however, as a result of placing the important word first, many modifiers must be arranged for smooth reading, e.g., Formaldehyde—yields in radiolysis of ethyl ether, effects of deuterium on is read "effects of deuterium on formaldehyde yields in radiolysis of ethyl ether" and Uranium—crystal structure of, effect of cooling rate on allotropic transformations in is read "effect of cooling rate on allotropic transformations in crystal structure of uranium." Prepositions are sometimes omitted if no ambiguity results.

Special characters are added to modifiers in the field of physics; if the modifier does not establish the experimental or theoretical character of a reference, a symbol (E), (T), or (E/T) is placed immediately after the modifying phrase and before the journal reference number. The value of this identification has been established by the American Institute of Physics.

A

ACCELERATORS
beam acceleration in circular, absorption effects on, (T), 20: 37335
design of transformer-type high-current electron, 20: 37322
design with magnetic gradient, for micrometeorite impact simulation, 20: 37340(P)
radiation quality factors near, (E), 20: 37323
storage rings for, operation of electron-positron VEPP-2, 20: 37321 (NP-16205)
targets for, development of polarized, 20: 37332
theory of stochastic acceleration, 20: 37336

ACCELEROMETERS
use in measurement of surface motion, 20: 36959 (PNE-603F)

ACCIDENTS
mechanisms and types of fast-reactor, 20: 38492 (ANL-7120, pp 54-66)

ACETAMIDE, 2,2'-DITHIOBIS[*N*-ETHYL-
protection against radiation damage in calf-thymus DNA, mechanism of, 20: 36665

ACETAMIDE, IODO-
effects on radiosensitivity of bacteria, spores, and yeasts, 20: 37144
effects on uv radiation effects on pyrimidine dimers in *Micrococcus radiodurans* DNA, 20: 36610

ACETATES
effects on copper determination, 20: 36726

ACETIC ACID
acetic acid–ethylene glycol–$HClO_4$, properties for etching zirconium, 20: 37227

ACETIC ACID, AMYL ESTER
effects on copper determination by absorption spectroscopy, 20: 36726

ACETIC ACID, TRICHLORO-
analytical use for determination of silicon in sputum by activation methods, 20: 36542

ACETONE, THENOYLTRIFLUORO-
complexes with rare earths, spectrofluorometric analysis for rare earths in, 20: 36722

ACETYLENE
radiolysis of aqueous solutions of, in presence of iron ions, 20: 36858 (IFA-CR-73)

ACOUSTIC WAVES
attenuation in type-II superconductors near transition temperature, (T), 20: 37948
interactions with electromagnetic waves in plasma, coupling of, 20: 38232
propagation in quartz crystals at low temperatures and above 1 Bc, x-ray alignment technique for, 20: 38366
propagation in strong magnetoplasma, (T), 20: 38303
propagation in warm plasma, from vertical dipoles, 20: 38229
propagation in warm plasma, from vertical dipoles, 20: 38230
propagation of electro-acoustic waves in compressible inhomogeneous plasma, (T), 20: 38227

ACRIDINES
use of acridine orange for viability tests on irradiated Ehrlich ascites tumor cells, 20: 36631

ACRYLONITRILES
radioinduced graft polymerization of, on INZ-600 brick, kinetics of gamma, 20: 36882
acrylonitrile–styrene, radiochemical grafting of, on polyvinyl chloride at 0 to 50°C, 20: 36877
acrylonitrile–styrene, radioinduced polymerization of, at −78, 0, and 50°C, effects of dimethylformamide and oil on, 20: 36876
acrylonitrile–styrene, radioinduced grafting on polytetrafluoroethylene, effects of monomer diffusion rate on, 20: 36878

ACTINOMYCIN
labeling with tritium, biosynthetic procedure for, 20: 36545

ACTIVATION ANALYSIS
equipment and methods for, use of automation in, 20: 36782
errors in neutron, method for evaluation of random, 20: 36734
interference of fission products in uranium samples in, 20: 36714
method for oxygen in aluminum and zirconium using helium-3 ions, 20: 36741
standard solutions for, preparation of iridium and rhodium, 20: 36775
system for continuous on-line, 20: 36769
use for determination of iron in ores and rocks in boreholes, 20: 37019
use in analysis of rocks in boreholes, 20: 37018
use in geophysics, 20: 37060
use in geophysics, in Soviet Union, 20: 37001
use in hair individualization studies, 20: 36781

ADENINE
reactions with hydroxyl radicals, ESR spectral studies on, 20: 36806

ADENOSINEPHOSPHORIC ACIDS
radiation effects on content of, in rat liver, x, 20: 36603

ADRENAL GLANDS
radiosensitivity effects on animals, review on, 20: 36668

ADRENOCORTICOTROPIC HORMONE
radiosensitivity effects on animals, review on, 20: 36668

AEROSOLS
analysis of air for polonium-218, method of, 20: 36733
distribution of thoron decay products in, measurement of, 20: 37027
interaction of labeled iron oxide, with iodine-131, 20: 36918
properties of, produced in plutonium and sodium fires, 20: 37022 (LA-DC-6942)

AGE
effects of, on somatic crossing over of *D. melanogaster* of x-irradiated, 20: 36619

AGE ESTIMATION
method of, argon–potassium, 20: 37016
method of, using sulfur isotopes, 20: 37011
methods of, for Antarctic rocks, 20: 37015

AGING
radiation effects on chicken, 20: 36605(R) (COO-1119-5)

AIR
analysis for methane using beta sources, instrument for, 20: 37150
analysis for polonium-218, method of, 20: 36733
chemical reactions of subsonic, with infiltrated tungsten materials at high heat fluxes, 20: 37188
mixing with water, tracer study of, 20: 36989 (WAPD-TM-492)
oxidizing effects on chromium–rhenium alloys at high temperatures, mechanisms of, 20: 37186
oxidizing effects on niobium–vanadium–titanium alloys at 900 to 1200°C, kinetics and mechanisms of, 20: 37191
sodium expulsion into, equipment and method for study of, 20: 38500 (ANL-7120, pp 868-72)
air–water, bubbly flow upward in tubes, hydrodynamic characteristics of, 20: 36988 (TID-23261)

AIR FORCE ENGINEERING TEST REACTOR
reactivity changes in, kinetic response to, 20: 38449

AIRCRAFT
guidance systems for, gamma sources for anti-collision, 20: 37141

ALASKA
radiation monitoring program in, 20: 37042

ALBUMINS
effects on iodine-131-labeled triiodothyronine metabolism in human thyroid, 20: 36573
preparation of aggregates of technetium-99-labeled, for use in scinti-scanning of lungs, 20: 36919
uptake of iodine-131-labeled human serum, by tumor tissues in oxygen environment in man and rabbits, 20: 36576

ALFALFA
cesium-137 deposition from fallout on, and transfer to milk, 20: 37036
cesium-137 transfer from soils to, for dairy cattle feed, 20: 37038

ALGAE
analysis for calcium-45 and strontium-89 in cells of, liquid scintillation spectrometric, 20: 36747
chromium distribution in seaweed, 20: 36552

ALKALI METAL HALIDES
effects on radiosensitivity of bacteria, spores, and yeasts, 20: 37144
radiation effects on, electron spin resonance spectra of radicals from, 20: 36902
solid-state effect in irradiated, (E/T), 20: 38402

ALKALI METALS
containment of plasmas of, field curvature effects on, (E/T), 20: 38326

ALKALINE EARTH OXIDES
determination in presence of rare earth oxides using Arsenazo, complexometric, 20: 36776

ALKENES
reactions with deuterium atoms at 77 to 90°K, 20: 36856
yields of, from gamma-induced reactions of 1-butene and phosgene, 20: 36892

ALLOYS
positron annihilation in, review of, 20: 37820

ALLYL ALCOHOL
radioinduced polymerization of, kinetics of, 20: 36880

ALPHA DECAY
tunnel effect in, (T), 20: 38117

ALPHA PARTICLES
detection and measurement of, development of portable monitor for, 20: 37071 (DP-993)
doses to tissues from, in solar particle beams in space, 20: 37023 (N-65-33865)
effects on alkali metal and alkaline earth bromates, 20: 36899
effects on cyclohexane in presence of iodine, 20: 36888
effects on nickel diffusion in copper at 200 to 520°C, 20: 37300
effects on self diffusion in lead, 20: 37272

reactions (α,He-3) with zirconium-90, zirconium-91, and zirconium-92 at 65 Mev, (E/T), 20: 38092
reactions (α,n) with aluminum-27 at 17 Mev, level density parameters from, (E), 20: 38115
reactions (α,n) with manganese-55 at 17 Mev, level density parameters from, (E), 20: 38115
reactions (α,n) with iron-56 at 17 Mev, level density parameters from, (E), 20: 38115
reactions (α,n) with silver at 17 Mev, level density parameters from, (E), 20: 38115
reactions (α,n) with carbon-14, oxygen-17 energy levels from, (E), 20: 38161
reactions with anthracene and terephenyl, decay of scintillations from, 20: 37305
reactions with cobalt-59 at 20 to 50 Mev, copper-63 compound nucleus formation in, (E), 20: 38147
scattering by calcium-40, calcium-42, calcium-44, calcium-48, and titanium-50 at 31 Mev, inelastic, (E), 20: 38100
scattering by zirconium-90, zirconium-91, and zirconium-92 at 65 Mev, elastic and inelastic, (E/T), 20: 38092
scattering of, from surfaces, chemical analysis by, 20: 36719
tunnel effect in nuclei, effect of structure on, (T), 20: 38117

ALPHA SOURCES
decay of, performance of one-multiplier phototube liquid scintillation spectrometer for measuring rate of, 20: 37082
monitoring after Sulky Event, 20: 36960 (PNE-717F)
use for automatic corrections in liquid scintillation counting of carbon-14 and tritium, 20: 36743

ALPS MOUNTAINS (EUROPE)
fallout monitoring at Weissee and Schneiderau 1963 and 1964, 20: 37008

ALTITUDE
effects on fallout content in Austrian Alps, 20: 37008

ALUMINUM
analysis for oxygen by helium-3 activation, 20: 36741
analysis of, using proton inelastic scattering at 6.6 Mev, 20: 36732
cosmic particle reactions in, four-momentum transfer in, (E/T), 20: 37659
deposition on sintered molybdenum powder for oxidation protection, 20: 37204
determination in coal using neutron activation, system for continuous on-line, 20: 36769
effects on determination of chromium in ores by neutron activation analysis, 20: 36750
effects on radioinduced swelling in uranium, 20: 37302
electron reactions at 30 kev in foils of, energy-loss spectrum of, (E/T), 20: 37442
fabrication into Zircaloy-4 tube liners, by explosive welding, 20: 37168(R) (BMI-1771)
fabrication into Zircaloy-4 tube liners, by explosive welding, 20: 37169(R) (BMI-1774)
gamma reactions (γ,α) at 31 Mev, alpha spectra from, (E), 20: 38037
neutron absorption cross section in pitchblende, thermal, 20: 37994
neutron scattering by cylinders of, spectra from fast, (E/T), 20: 38007
neutron total cross sections at high energies, fluctuations in, 20: 38173
positron annihilation with core electrons in, momentum distributions for, (T), 20: 37821
proton reactions at 600 Mev, cross sections for meson ($\pi^{\pm}$) production in, 20: 38186
proton reactions at 70 to 100 kev, x ray emission from, (E), 20: 38393
radiation damage in, annealing of neutron, (E), 20: 38380
reactions of powdered, with urania at 600°C, 20: 37203
reactions with liquid sodium at high temperatures, 20: 38499 (ANL-7120, pp 839-47)
separation from metal mixtures by thin layer chromatography, 20: 36753
separation of, from thallium by ion-exchange chromatography, 20: 36935
surface structure examination of, by proton scattering, (E), 20: 38376
testing of, use of iridium-192 in radiographic, 20: 36994

ALUMINUM ALLOYS
properties of intermetallic compound, for high-temperature coatings, 20: 37192
properties of intermetallic compound, with transition metals, 20: 37260
Al–Au, superconductivity of $AlAu_4$, 20: 37985
Al–Cr, superconducting critical temperature of, transition-metal impurity effects on depression of, (E), 20: 37955
Al–Fe, critical temperature of superconducting, transition-metal impurity effects on depression of, (E), 20: 37955
Al–Hf, properties of intermetallic compound, 20: 37260
Al–La, superconductivity of Al_2La, 20: 37985
Al–Mg, magnetization of superconducting, (E), 20: 37935 (CEA-R-2906)
Al–Mg, thermodynamic properties of, partial molar, 20: 37722(R) (N-65-30843)
Al–Mn, superconducting critical temperature of, transition-metal impurity effects on depression of, (E), 20: 37955
Al–Mo, formation of intermetallic compound, on sintered molybdenum, 20: 37204
Al–Mo, properties of intermetallic compound, 20: 37260
Al–Nb, properties of intermetallic compound, 20: 37260
Al–Pt, superconductivity of Al_2Pt, 20: 37985
Al–Ta, properties of intermetallic compound, 20: 37260
Al–Ti, properties of intermetallic compound, 20: 37260
Al–U, fabrication of ESSOR fuel elements of, 20: 38480(R) (EUR-2522.f)
Al–U, separation of uranium from irradiated, by molten-salt fluoride volatility process, 20: 36951
Al–V, properties of intermetallic compound, 20: 37260
Al–Zr, properties of intermetallic compound, 20: 37260

ALUMINUM BROMIDES
$AlBr_3$–$AlCl_3$, phase diagrams, 20: 36787 (YALE-2723(Vol.1))
$AlBr_3$–$AsBr_3$, phase diagrams, 20: 36787 (YALE-2723(Vol.1))
$AlBr_3$–$BiBr_3$, phase diagrams, 20: 36787 (YALE-2723(Vol.1))
$AlBr_3$–$HgBr_2$, phase diagrams, 20: 36787 (YALE-2723(Vol.1))
$AlBr_3$–$SbBr_3$, phase diagrams, 20: 36787 (YALE-2723(Vol.1))
$AlBr_3$–$SnBr_3$, phase diagrams, 20: 36787 (YALE-2723(Vol.1))

ALUMINUM CHLORIDES
reactions with uranium hexafluoride, 20: 36803
$AlBr_3$–$AlCl_3$, phase diagrams, 20: 36787 (YALE-2723(Vol.1))
$AlCl_3$–CsCl, phase diagrams, 20: 36787 (YALE-2723(Vol.1))
$AlCl_3$–KCl, phase diagrams, 20: 36787 (YALE-2723(Vol.1))
$AlCl_3$–NaCl, phase diagrams, 20: 36787 (YALE-2723(Vol.1))

ALUMINUM CHLORIDES, DIETHYL-
diethyl aluminum chloride–$TiCl_4$, catalytic effects on ethylene polymerization, deuterium and hydrogen exchange reactions during, 20: 36827

ALUMINUM FLUORIDES
AlF_3–KF, phase diagrams, 20: 36787 (YALE-2723(Vol.1))
AlF_3–LiF, phase diagrams, 20: 36787 (YALE-2723(Vol.1))
AlF_3–NaF, phase diagrams, 20: 36787 (YALE-2723(Vol.1))

ALUMINUM IODIDES
AlI_3–AsI_3, phase diagrams, 20: 36787 (YALE-2723(Vol.1))
AlI_3–HgI_2, phase diagrams, 20: 36787 (YALE-2723(Vol.1))
AlI_3–KI, phase diagrams, 20: 36787 (YALE-2723(Vol.1))
AlI_3–SbI_3, phase diagrams, 20: 36787 (YALE-2723(Vol.1))
AlI_3–SnI_4, phase diagrams, 20: 36787 (YALE-2723(Vol.1))

ALUMINUM IONS
effects on copper determination, 20: 36726
effects on formation of single-crystal beryllium oxide, 20: 36814

ALUMINUM ISOTOPES Al-27
alpha reactions (α,n) at 17 Mev, level density parameters from, (E), 20: 38115
boron-11 reactions (B-11,p3n) at 30–115 Mev, cross sections, recoil ranges, and angular distributions of chlorine-34m from, (E), 20: 38084
neutron reactions (n,p) with, calculations using finite-range distorted-wave Born approximation, (T), 20: 38112
proton reactions (p,n) with, thresholds for, (E), 20: 38053
proton reactions (p,n) with, threshold energy for, (E), 20: 38054

ALUMINUM NITRATES
separation of nonahydrate of, from Redox acid waste by crystallization techniques, 20: 36925 (HW-82771(Pt.3))
use as salting-out agent in solvent extraction of uranium, 20: 36717

ALUMINUM OXIDES
analysis of high-purity, symposium on, 20: 37179
effects on rate of polymerization of allyl alcohol, 20: 36880
effects on sintering behavior of urania powders, 20: 37202
iron-57 Mössbauer hyperfine spectra in, crystal and magnetic field effects on, (E), 38388
positronium lifetime in, (E), 20: 37819
reactions of sulfur-bearing, with nickel at high temperatures, 20: 37168(R) (BMI-1771)
reactions of sulfur-bearing, with nickel at high temperatures, 20: 37169(R) (BMI-1774)
reactions with lanthanum and neodymium oxides in solid state, 20: 36840
separation from urania in organic slurries, centrifugal, 20: 36933
vaporization of, thermodynamics of, 20: 36841
Al–Al_2O_3, fabrication by powder metallurgy, 20: 37210
Al_2O_3–Ag, preparation and properties of alumina-base cermets of, 20: 37209
Al_2O_3–Ce_2O_3, phase studies at temperatures to 2600°C, 20: 36808
Al_2O_3–MgF_2, phase studies, 20: 37722(R) (N-65-30843)
Al_2O_3–NaF–Si, properties as coating for D-43 and TZM alloys, 20: 37276
Al_2O_3–Pd–Ag, preparation and properties of alumina-base cermets of, 20: 37209

ALUMINUM SILICATES
content of, in sediments of Bay of Roquebrune, 20: 36553

ALUMINUM SYSTEMS

Al–Al_2O_3, fabrication by powder metallurgy, 20: 37210

ALUMS
flotation of, on gamma-irradiated anionic collector agents, 20: 36893

AMERICIUM
diffusion of, during plutonium vaporization studies, 20: 37307 (LA-3509)
separation from nitric acid by solvent extraction using TBP with bis(2-ethylhexyl) phosphate or octyl phenylphosphate, 20: 36937

AMERICIUM COMPLEXES
with citric acid, formation of, electrophoretic studies of, 20: 36829

AMERICIUM IONS
spectra of, effects of chemical bonding and transitions on, 20: 36845

AMERICIUM ISOTOPES Am-241
uses in carbon dioxide sensor for Gemini spacecraft, 20: 37064

AMERICIUM ISOTOPES Am-246
beta decay, (E), 20: 38097

AMIDES
preparation and properties of lithium phosphamide, symposium on, 20: 37179

AMINES
solvent properties of tertiary, for ruthenium, 20: 36948
solvent properties for plutonium, 20: 36948
uses in fuel element processing, 20: 36948

AMMONIA
radioinduced free radicals of, in krypton, 20: 36909
radiolysis of aqueous solutions of, production of hydrazine in gamma, 20: 36869
NH_3–Li, positron annihilation in solutions of, photon momentum distribution from, (E), 20: 37774
NH_3–Li, positron annihilation in solutions of, photon momentum distribution from, (E), 20: 37818

AMMONIUM CARBONATES
$(NH_4)_2CO_3$–$MgCl_2$–SiO_2–$UO_2(NO_3)_2$, reactions in, silicate formation in, 20: 36797
$(NH_4)_2CO_3$–SiO_2–$UO_2(NO_3)_2$, reactions in, silicate formation in, 20: 36797

AMMONIUM LACTATES
properties for ion exchange separation of trace lanthanides, 20: 36939

AMMONIUM NITRATES
effects on rare earth distribution coefficients between TBP and nitric acid, 20: 36938
use as salting-out agent in solvent extraction of uranium, 20: 36717

AMMONIUM SELENATES
radioinduced paramagnetic centers in, γ- and neutron-, 20: 38398

AMMONIUM SULFATES
radioinduced defects in normal and deuterated, thermal annealing of gamma, 20: 36874

AMMONIUM URANATES
crystal structure and surface area of, effects of preparation conditions on, 20: 36801

AMPLIFIERS
design of d-c, for ionization chamber, 20: 37066 (AECL-2536)
design of 10-MHz linear window, 20: 37048

ANALYSIS
book: *Arsenazo III. Methods of Photometric Determination of Rare Earth and Actinide Elements*, 20: 36778

ANIMAL CELLS
radiation effects on hamster and HeLa, after plating and trypsinization, 20: 36664
radiation effects on nucleoli in tissue cultures of, uv, 20: 36592
radiation effects on HeLa cells, electron microscopy study on, gamma, 20: 36616
radiation effects on viability of Ehrlich ascites tumorous, use of dyes for assaying, x, 20: 36631
radiation effects on DNA in, repair mechanisms for uv and x, 20: 36578 (ORNL-P-2240)

ANIMAL REPRODUCTION
radiation effects on chicken, 20: 36605(R) (COO-1119-5)

ANIMALS
radiation effects on collagen in kangaroo skin, uv, 20: 36595
radiation effects on brain function in, dose effects in, 20: 36651
radiation injuries in, role of adrenal and pituitary glands in, 20: 36668
radioinduced hyperlipemia in, mechanism of, 20: 36580

ANION EXCHANGE MATERIALS
reactions with nitric acid systems in Redox Process, 20: 36954

ANIONS
model for, in liquid helium II, 20: 37981

ANNEALING
effects on energy release from irradiated graphite, 20: 37283

ANTARCTIC OCEAN
rock ages in, argon-40/potassium-40 determination of, 20: 37015

ANTENNAS
electroacoustic and electromagnetic wave propagation from plasma immersed, coupling of, 20: 38232
electromagnetic wave propagation in plasma, ferrite windows for improving, 20: 38231
radiations from, propagation in warm plasma, 20: 38229
radiations from, propagation in warm plasma, 20: 38230

ANTHRACENE
alpha and beta reactions with, decay of scintillations from, 20: 37305
preparation of 15 derivatives of, for use as wavelength shifters in plastic scintillators, 20: 36848
radiation effects on luminescence intensity of, γ and uv, 20: 37131
radiation effects on photoconductivity of, 20: 36873

ANTIBIOTICS
effects of polymyxin and viomycin as histamine liberators on calcification produced by various metals in rats, 20: 36557

ANTIGENS
iodine-131 incorporation in complexes, use as test for tuberculosis, 20: 36681

ANTIMONY
effects of impurities of, on defect recovery in germanium, (E), 20: 38365
effects on determination of iridium in ores by neutron activation analysis, 20: 36751
neutron total cross sections at high energies, fluctuations in, 20: 38173
separation from arsenic and tin by thin layer chromatography, 20: 36753
separation of, from thallium by ion-exchange chromatography, 20: 36935
x-ray spectra from mu-mesic atoms of, (E), 20: 38058

ANTIMONY ALLOYS
Sb–In, radiation effects on carrier lifetime and detectivity of, gamma and neutron, 20: 37295
Sb–Yb, crystal structure of $YbSb_2$ in, 20: 37238

ANTIMONY BROMIDES
$AlBr_3$–$SbBr_3$, phase diagrams, 20: 36787 (YALE-2723(Vol.1))
$SbBr_3$–$AsBr_3$, phase diagrams, 20: 36787 (YALE-2723(Vol.1))
$SbBr_3$–$BiBr_3$, phase diagrams, 20: 36787 (YALE-2723(Vol.1))
$SbBr_3$–$SbCl_3$, phase diagrams, 20: 36788 (YALE-2723(Vol.2))
$SbBr_3$–SbI_3, phase diagrams, 20: 36788 (YALE-2723(Vol.2))
$SbBr_3$–$SnBr_4$, phase diagrams, 20: 36788 (YALE-2723(Vol.2))

ANTIMONY CHLORIDES
reactions with uranium hexafluoride, 20: 36803
$AlCl_3$–$SbCl_3$, phase diagrams, 20: 36787 (YALE-2723(Vol.1))
$SbBr_3$–$SbCl_3$, phase diagrams, 20: 36788 (YALE-2723(Vol.2))
$SbCl_3$–$BiCl_3$, phase diagrams, 20: 36787 (YALE-2723(Vol.1))
$SbCl_3$–KCl, phase diagrams, 20: 36788 (YALE-2723(Vol.2))
$SbCl_3$–SbI_3, phase diagrams, 20: 36788 (YALE-2723(Vol.2))
$SbCl_3$–$SnCl_4$, phase diagrams, 20: 36788 (YALE-2723(Vol.2))

ANTIMONY IODIDES
AlI_3–SbI_3, phase diagrams, 20: 36787 (YALE-2723(Vol.1))
$SbBr_3$–SbI_3, phase diagrams, 20: 36788 (YALE-2723(Vol.2))
$SbCl_3$–SbI_3, phase diagrams, 20: 36788 (YALE-2723(Vol.2))

ANTIMONY ISOTOPES Sb-113
energy levels, (E), 20: 38073

ANTIMONY ISOTOPES Sb-115
energy levels, (E), 20: 38073

ANTIMONY ISOTOPES Sb-117
energy levels, (E), 20: 38073

ANTIMONY ISOTOPES Sb-119
energy levels, (E), 20: 38073

ANTIMONY ISOTOPES Sb-121
energy level structure, (E), 20: 38188
energy levels, (E), 20: 38073
meson (μ^-) capture by, tin-120 energy levels from, (E), 20: 38058
nuclear quadrupole interactions in antimony oxides, Mössbauer study of, (E), 20: 38386

ANTIMONY ISOTOPES Sb-123
energy level structure, (E), 20: 38188
energy levels, (E), 20: 38073
meson (μ^-) capture by tin-122 energy levels from, (E), 20: 38058

ANTIMONY ISOTOPES Sb-125
energy level structure, (E), 20: 38188
energy levels, (E), 20: 38073

ANTIMONY OXIDES
antimony-121 nuclear quadrupole interactions in, Mössbauer study of, (E), 20: 38386

ANTINEUTRINOS
interactions with protons, detection of, 20: 37735(R) (COO-818-96)

ANTIPROTONS
interactions with deuterons, meson (ρ) production in, 20: 37813

ARGON
electric conductivity of shock-heated, 20: 37882
ion cyclotron frequency harmonic generation in longitudinally magnetized plasma of, (E), 20: 38252
ion wave propagation in weakly ionized plasma of, damping and phase velocity of, (E), 20: 38294
ionization effects in sodium–potassium seeded plasma of, nonequilibrium, 20: 37722(R) (N-65-30843)

ionization properties of potassium–sodium seeded plasma of, (E), 20: 38195(R) (INDEC-SR-7, pp 3.60-73)
neutron scattering by liquid, hindered-translator model for one-particle motions in slow, 20: 37999
plasma of, production and properties of shock-heated, 20: 38344
positron annihilation in, (E), 20: 37810
reactions with cesium fluorides, cross sections for, 20: 37478
stability of plasma of, density distribution effect on helical, (E), 20: 38270
stacking-fault energy in fcc solid, determination of, 20: 38394
temperature profiles across plasma arc of, 20: 38279
use as carrier in plasmochemistry, 20: 38314

ARGON IONS
effects on germanium films, depth of damage from, (E), 20: 38363
sputtering on copper at 100 kev to 1 Mev, 20: 37468

ARGON ISOTOPES Ar-40
content in Antarctic rocks, 20: 37015
content in Scottish rocks, 20: 37016
proton reactions (p,n) at 2.336 to 2.464 Mev, resonance structure and ground-state Q value of, (E), 20: 38028

ARGON SYSTEMS
Ar–propane, postronium lifetime in, (E), 20: 37816

ARGONNE ADVANCED RESEARCH REACTOR
fuel plates for, development of, 20: 37168(R) (BMI-1771)
fuel plates for, fabrication of prototype, 20: 37169(R) (BMI-1774)

ARGONNE FAST REACTOR EXPERIMENT TEST
core-I reference design and irradiation program for, 20: 38460 (ANL-7120, pp 766-75)

ARSENAZO III
analytical use for photometric determination of uranium in minerals, rocks, and soils, 20: 36774
book: *Arsenazo III. Methods of Photometric Determination of Rare Earth and Actinide Elements*, 20: 36778

ARSENIC
effects of impurities of, on defect recovery in germanium, (E), 20: 38365
neutron absorption cross section in pitchblende, thermal, 20: 37994
radiation effects on optical absorption of, in alkali borate glass, 20: 36887
separation from antimony and tin by thin layer chromatography, 20: 36753
yields from radiolysis of arsenic phthalocyanine, 20: 36886

ARSENIC BROMIDES
$AlBr_3$–$AsBr_3$, phase diagrams, 20: 36787 (YALE-2723(Vol.1))
$AsBr_3$–$BiBr_3$, phase diagrams, 20: 36787 (YALE-2723(Vol.1))
$AsBr_3$–$SnBr_3$, phase diagrams, 20: 36787 (YALE-2723(Vol.1))
$SbBr_3$–$AsBr_3$, phase diagrams, 20: 36787 (YALE-2723(Vol.1))

ARSENIC CHLORIDES
reactions with uranium hexafluoride, 20: 36803

ARSENIC FLUORIDES
reactions with uranium hexafluoride, 20: 36803
thermodynamic properties, 20: 36950

ARSENIC IODIDES
AlI_3–AsI_3, phase diagrams, 20: 36787 (YALE-2723(Vol.1))

ARSENIC ISOTOPES As-75
neutron strength functions of, calculation of, 20: 38038

ARSINE
radioinduced free radicals of, in krypton, 20: 36909

ASCORBIC ACID
complexes with erbium and holmium, molar extinction coefficients and stability constants for, 20: 36852
complexes with europium, molar extinction coefficients for, (E), 20: 36833

ASTRONAUTS
radiation hazards from highly ionizing radiation, 20: 36627

ASTRONOMY
book: *Advances in Astronomy and Astrophysics*, Vol. IV, 20: 37342

ASTROPHYSICS
book: *Advances in Astronomy and Astrophysics*, Vol. IV, 20: 37342
book: *Introduction to Solar Terrestrial Relations*, 20: 37916
dynamics of dense opaque shells in, 20: 37357
neutrino processes in, 20: 37395
relativistic, survey on, 20: 37367
research in, using isotopic composition of extraterrestrial and terrestrial material, 20: 37369

ATMOSPHERE
cosmic nucleon flux at 10^{11} to 10^{13} ev in, interaction path determination from, (E), 20: 37667
cosmic quark flux in, (T), 20: 37718
cosmic ray interactions in, gamma production from, (E/T), 20: 37576
decontamination of, by hydrometeors, 20: 37005
effects on cosmic meson intensity diurnal variations, corrections for, (T), 20: 37585
effects on cosmic ray diurnal intensity variation, 20: 37586
electric properties of, effects of pollution and radioactivity on, 20: 37003
neutron flux in upper, during 1964 solar minimum, (E), 20: 37908
radioactivity from release of fission products to, computer analysis of, 20: 37167 (IDO-17151)
shock wave propagation in, charged particle density and temperature in front of, 20: 37880
tritium content in water vapor in, method for measuring, 20: 37028

ATOMIC BEAMS
photoionization of potassium, polarized electrons from, (E), 20: 37475

ATOMIC ENERGY, LEGAL ASPECTS
possibilities of, for radiation protection of medical patients, 20: 36679
provisions of German Atomic Law for radiation protection, 20: 36676

ATOMIC EXPLOSIONS
effects on leukemia development in humans in Hiroshima and Nagasaki, 1946 to 1964, 20: 36645
energy yield from, design of device for estimating, 20: 37061
firestorms from, prediction of the effects of, 20: 36995 (AD-636794)
use of underground, to increase productivity of natural gas wells, 20: 36961 (UCRL-12229)

ATOMIC MODELS
for sub-atomic structure of matter, 20: 37480

ATOMIC STRUCTURE
atomic quantities for, semiclassical determination of, 20: 37462

ATOMS
charged-particle scattering by nonspherical, optical potential for, (T), 20: 37444
energy level structure of, modified Schroedinger equation for, 20: 37436
energy levels in plasma, theory of, 20: 37474
energy levels of, forbidden transitions in, 20: 37432
energy levels of, group theory classification of g^N, 20: 37437
hyperfine structure of hydrogenic, second-order quantum electrodynamic corrections for S-state, (T), 20: 37445
interactions with electrons, book on, 20: 37477(T)
reactions with moving unequal-mass particles, energy transfer in, (T), 20: 37447

AURORAL STORMS
data for 1957–1960, 20: 37887
occurrence and properties of magnetoconjugate, 20: 37914
properties of, relation to magnetic disturbances and solar activity, 20: 37887
properties of, relation to magnetic disturbances and solar activity, 20: 37888

AUSTRALIA
radioisotope production and uses in, 20: 37137

AUSTRIA
fallout monitoring in Alps 1963 and 1964, variation with altitude, 20: 37008

AUTORADIOGRAPHY
method of, using electron microscope, photographic emulsions, and developing methods, 20: 37050
use in determining uranium distribution in centrifugal separation processes, 20: 36933

B

BACTERIA
radiation effects on enzymatic breakdown in DNA from *Micrococcus lysodeicticus*, uv, 20: 36583
radiation effects on pyrimidine dimers in *Micrococcus radiodurans* DNA, repair mechanism in uv, 20: 36610
radiation effects on DNA in, repair mechanisms for uv and x, 20: 36578 (ORNL-P-2240)
radioinduced mutations in synchronous populations of *Streptococcus faecalis*, chromosome mapping by, 20: 36635
radiosensitivity of, effects of chemicals on, 20: 37144
use of *Bacillus subtilis* as a radioprotective substance, 20: 36673

BACTERIOPHAGES
radioinduced mutations in T4, uv, 20: 36636

BALANCES
design of thermo-, for thermogravimetry of gas-solid reactions, 20: 36853

BARITES
analysis for components of, by scattering of accelerated alpha particles, 20: 36719

BARIUM
determination of, using Arsenazo III, photometric, 20: 36778
diffusion in magnetic mirror machines, (E/T), 20: 38324
hyperfine structure of λ 4934 and 4554 Å lines in, 20: 37463
neutron absorption cross section in pitchblende, thermal, 20: 37994
ranges of recoil, in sodium chloride–uranium dioxide mixtures, 20: 37997
separation of, from thallium by ion-exchange chromatography, 20: 36935
stability in magnetic mirror machines, (E/T), 20: 38324
x-ray spectra from mu-mesic atoms of, (E), 20: 38058

BARIUM AZIDES

radiation effects on thermal decomposition of, gamma, 20: 36900
radiation effects on electric properties of, gamma, 20: 36900

BARIUM BROMIDES
$BaBr_2$–$BaCl_2$, phase diagrams, 20: 36787 (YALE-2723(Vol.1))
$BaBr_2$–BaF_2, phase diagrams, 20: 36787 (YALE-2723(Vol.1))
$BaBr_2$–BaI_2, phase diagrams, 20: 36787 (YALE-2723(Vol.1))
$BaBr_2$–$CaCl_2$, phase diagrams, 20: 36787 (YALE-2723(Vol.1))
$BaBr_2$–KBr, phase diagrams, 20: 36787 (YALE-2723(Vol.1))
$BaBr_2$–LiBr, phase diagrams, 20: 36787 (YALE-2723(Vol.1))
$BaBr_2$–NaBr, phase diagrams, 20: 36787 (YALE-2723(Vol.1))
$BaBr_2$–$SrBr_2$, phase diagrams, 20: 36787 (YALE-2723(Vol.1))
$BaBr_2$–SrI_2, phase diagrams, 20: 36787 (YALE-2723(Vol.1))

BARIUM CARBONATES
thermoluminescence properties of, for use as radiation dosimeter, 20: 36913

BARIUM CHLORIDES
$BaBr_2$–$BaCl_2$, phase diagrams, 20: 36787 (YALE-2723(Vol.1))
$BaCl_2$–BaF_2, phase diagrams, 20: 36787 (YALE-2723(Vol.1))
$BaCl_2$–$BeCl_2$, phase diagrams, 20: 36787 (YALE-2723(Vol.1))
$BaCl_2$–$CaCl_2$, phase diagrams, 20: 36787 (YALE-2723(Vol.1))
$BaCl_2$–$CdCl_2$, phase diagrams, 20: 36787 (YALE-2723(Vol.1))
$BaCl_2$–KCl, phase diagrams, 20: 36787 (YALE-2723(Vol.1))
$BaCl_2$–LiCl, phase diagrams, 20: 36787 (YALE-2723(Vol.1))
$BaCl_2$–$MgCl_2$, phase diagrams, 20: 36787 (YALE-2723(Vol.1))
$BaCl_2$–NaCl, phase diagrams, 20: 36787 (YALE-2723(Vol.1))
$BaCl_2$–$PbCl_2$, phase diagrams, 20: 36787 (YALE-2723(Vol.1))
$BaCl_2$–RbCl, phase diagrams, 20: 36787 (YALE-2723(Vol.1))
$BaCl_2$–$SrCl_2$, phase diagrams, 20: 36787 (YALE-2723(Vol.1))
$BaCl_2$–TlCl, phase diagrams, 20: 36787 (YALE-2723(Vol.1))
$BaCl_2$–$ZnCl_2$, phase diagrams, 20: 36787 (YALE-2723(Vol.1))

BARIUM FLUORIDES
$BaBr_2$–BaF_2, phase diagrams, 20: 36787 (YALE-2723(Vol.1))
$BaCl_2$–BaF_2, phase diagrams, 20: 36787 (YALE-2723(Vol.1))
BaF_2–BeF_2, phase diagrams, 20: 36787 (YALE-2723(Vol.1))
BaF_2–CaF_2, phase diagrams, 20: 36787 (YALE-2723(Vol.1))
$BaFe_2$–BaI_2, phase diagrams, 20: 36787 (YALE-2723(Vol.1))
BaF_2–KF, phase diagrams, 20: 36787 (YALE-2723(Vol.1))
BaF_2–LiF, phase diagrams, 20: 36787 (YALE-2723(Vol.1))
BaF_2–NaF, phase diagrams, 20: 36787 (YALE-2723(Vol.1))
BaF_2–RbF, phase diagrams, 20: 36787 (YALE-2723(Vol.1))
BaF_2–SrF_2, phase diagrams, 20: 36787 (YALE-2723(Vol.1))

BARIUM IODIDES
$BaBr_2$–BaI_2, phase diagrams, 20: 36787 (YALE-2723(Vol.1))
$BaFe_2$–BeI_2, phase diagrams, 20: 36787 (YALE-2723(Vol.1))
BaI_2–SrI_2, phase diagrams, 20: 36787 (YALE-2723(Vol.1))

BARIUM ISOTOPES
purification of electromagnetically separated, 20: 37163

BARIUM ISOTOPES Ba-132
proton reactions (p,2n) at 20 Mev, production isomeric lanthanum-131 in, (E), 20: 38125

BARIUM ISOTOPES Ba-134
energy levels of, from cesium-134 decay, (E), 20: 38169

BARIUM ISOTOPES Ba-135
nuclear magnetic moment, (E), 20: 37463

BARIUM ISOTOPES Ba-136
proton reactions (p,n) at 20 Mev, production of isomeric lanthanum-136 in, (E), 20: 38125

BARIUM ISOTOPES Ba-137
internal conversion coefficient for, K, (E), 20: 38044
nuclear magnetic moment, (E), 20: 37463
proton reactions (p,2n) at 20 Mev, production of isomeric lanthanum-136 in, (E), 20: 38125
separation from waste solutions using humic acid column, 20: 36930

BARIUM ISOTOPES Ba-138
energy levels, (E), 20: 38058

BARIUM ISOTOPES Ba-139
yields in proton fission of uranium-238 at 7.1, 9.4, and 12.0 Mev, 20: 37995

BARIUM ISOTOPES Ba-140
decay scheme, (E), 20: 38029
yields in proton fission of uranium-238 at 7.1, 9.4, and 12.0 Mev, 20: 37995

BARIUM TITANATES
radioinduced phase transformations in, mechanisms of neutron, 20: 37301
thermoluminescence properties of, for use as radiation dosimeter, 20: 36913

BARLEY
effects of diethyl pyrocarbonate on cells and growth of seeds of, 20: 36589
radiation effects on chromosomes in seed of, effects of diethyl pyrocarbonate on fast neutron and gamma, 20: 36589
radiation effects on chlorophyll mutation frequency in, effects of partial reparation on, 20: 36622
radiosensitivity variations with seed moisture, storage time, and oxygen supply, x, 20: 36658
strontium absorption by, genotype effect on rate of, 20: 36575

BARYONS
decay of, nonleptonic p- and s-wave, 20: 37839
form factors of SL(6,c) symmetry for charge, 20: 37840
interactions with mesons in broken SU(3), renormalization effects on coupling constants for, 20: 37842
interactions with baryons and mesons, matrices for modified single-particle exchange model of, 20: 37862
mass differences in quark model, 20: 37762
mass differences of octet ½⁺, deformed octet axial vector current for, 20: 37795
mass formulas for, dynamic quark model for, 20: 37763
properties of, application of Bethe-Salpeter equation to static bootstrap model for, 20: 37824 (CAR-882-19)

BARYONS, RESONANCE
photoproduction of N* (1410) on protons at 400 to 600 Mev, 20: 37752
production in neutrino interactions, unitary spin analysis of, 20: 37751
production in proton interactions, mechanism of, 20: 37769
production of even-parity metastable, selection rules in quark model for, 20: 37765
production of N* (1236) and N* (1518) in meson (π^+)-proton interactions at 900 Mev, (E), 20: 37744 (UR-875-151)
production of N* (1238) in meson (π^+) interactions with protons at 8 Bev/c, cross sections for, (E), 20: 37770
production of N*, in cosmic nucleon interactions in nuclear emulsions, (T), 20: 37675

BEACONS
design of radioisotope-powered underwater, 20: 37158(P)

BEANS
radiation effects on nuclear proteins in *Vicia faba*, cytophotometric measurements on, 20: 36588
radiation effects on fatty acid content in free lipid fraction in seedling leaves of, x, 20: 36598

BEARINGS
evaluation of, using computers, 20: 36977 (NAA-SR-11944)
stability of gas, determination using step-response method, 20: 36980

BEHAVIOR
radiation effects on response-perseveration learning set for nonrewarded cues in male monkeys, fast-neutron, 20: 36638
radiation effects on social distractibility of female monkeys, γ and neutron, 20: 36639

BELGIAN REACTOR-3
containment structure design, 20: 38522

BENTONITES
use with cellulose for flocculation of ruthenium in waste solutions, 20: 36929

BENZENE
effects on radioinduced polymerization of allyl alcohol, 20: 36880
effects on solvent properties of diisopentyl methylphosphonate for thorium in nitric acid solutions, 20: 36942
nuclear spin relaxation in liquid, intermolecular contribution to, 20: 36828
radiation effects on deuterium exchange with heavy water, 20: 36866
radiolysis of aqueous solutions of, kinetics and yields of gamma, 20: 36881
radiolysis of, in tritiated water, hydrogen–tritium exchange in gamma, 20: 36868
benzene–TBP, solvent properties for uranium, 20: 36718

BENZENE, *p*-BIS(*o*-METHYLSTYRYL)-
properties for use in liquid scintillation counters, 20: 36862
properties for use in liquid scintillation counters, 20: 36863

BENZENE, DISTYRYL-
preparation of derivatives of, for use as wavelength shifters in plastic scintillators, 20: 36847

BENZENE, NITRO-
formation by radiolysis of aqueous benzene, 20: 36881

BENZENEARSONIC ACID, *o*-(1,8-DIHYDROXY-3,6-DISULFO-2-NAPHTHYLAZO)-
analytical use for complexometric determination of alkaline earth and rare earth oxides in mixtures, 20: 36776
complexes with iron, stability of, 20: 36716
complexes with uranyl ions, stability of, 20: 36716
use in spectrophotometric determination of uranium, 20: 36716

BENZENESULFONIC ACID, TRIHYDROXY-
complexes with erbium, helium, and neodymium, formation of, potentiometric and spectrophotometric studies of, 20: 36837

BENZENETHIOL
radioinduced radical formation in, in organic glasses at –196°C, spectra from gamma, 20: 36894

BENZOQUINONE

effects on radioinduced polymerization of allyl alcohol, 20: 36880
radiation effects on cycloisomerization of Diels-Alder adducts of, to 1,3-diene, 20: 36860 (NP-16150)
BENZYL SULFIDE
radioinduced radical formation in, in organic glasses at −196°C, spectra from gamma, 20: 36894
BERKELIUM ISOTOPES Bk-246
electron-capture decay, (E), 20: 38097
BERKELIUM ISOTOPES Bk-251
half life, (E), 20: 38093
BERYLLIUM
diffusion at 565 to 1050°C, self, 20: 37249
diffusion of iron and silver in, tracer studies of, 20: 37250
effects as additive to group I and VIII transition metals, review on, 20: 37275
effects on tensile properties of niobium alloys, 20: 37245
meson (K^0) regeneration in, 20: 37814
polarizability and shielding factor for atomic, dipole, (T), 20: 37440
positron annihilation in, electron band gap at boundary from, (E/T), 20: 38406
positron annihilation with core electrons in, momentum distributions for, (T), 20: 37821
proton reactions at 600 Mev, cross sections for meson ($\pi^{\pm}$) production in, 20: 38186
reactions with carbon nitrogen and oxygen in group VIII transition metal alloys, 20: 37275
recrystallization of, twin precipitation reactions in, 20: 37216
solubility in group VIII transition metals and alloys, 20: 37275
BERYLLIUM ALLOYS
properties and stoichiometry of intermetallic compound, with group VIII transition metals, 20: 37275
properties of intermetallic compound, for high-temperature coatings, 20: 37192
Be–Co–Cu, precipitation in, effects of additive metals in discontinuous, 20: 37253
Be–Cr–Nb, tensile properties of, 20: 37245
Be–Cu, precipitation in, effects of additive metals on discontinuous, 20: 37253
Be–Nb–W, tensile properties of, 20: 37245
BERYLLIUM CHLORIDES
$BaCl_2$–$BeCl_2$, phase diagrams, 20: 36787 (YALE-2723(Vol.1))
$BeCl_2$–BeF_2, phase diagrams, 20: 36787 (YALE-2723(Vol.1))
$BeCl_2$–$CaCl_2$, phase diagrams, 20: 36787 (YALE-2723(Vol.1))
$BeCl_2$–LiCl, phase diagrams, 20: 36787 (YALE-2723(Vol.1))
$BeCl_2$–$MgCl_2$, phase diagrams, 20: 36787 (YALE-2723(Vol.1))
$BeCl_2$–NaCl, phase diagrams, 20: 36787 (YALE-2723(Vol.1))
BERYLLIUM FLUORIDES
BaF_2–BeF_2, phase diagrams, 20: 36787 (YALE-2723(Vol.1))
$BeCl_2$–BeF_2, phase diagrams, 20: 36787 (YALE-2723(Vol.1))
BeF_2–CaF_2, phase diagrams, 20: 36787 (YALE-2723(Vol.1))
BeF_2–CsF, phase diagrams, 20: 36787 (YALE-2723(Vol.1))
BeF_2–KF, phase diagrams, 20: 36787 (YALE-2723(Vol.1))
BeF_2–LiF, chemical properties, 20: 36951
BeF_2–LiF, phase diagrams, 20: 36787 (YALE-2723(Vol.1))
BeF_2–LiF, solvent properties for hydrogen fluoride gas, effects of deuterium on, 20: 36785 (ORNL-P-2202)
BeF_2–LiF–ThF_4, separation of protactinum from molten, 20: 36927 (ORNL-TM-1543)
BeF_2–MgF_2, phase diagrams, 20: 36787 (YALE-2723(Vol.1))
BeF_2–NaF, phase diagrams, 20: 36787 (YALE-2723(Vol.1))
BeF_2–SrF_2, phase diagrams, 20: 36787 (YALE-2723(Vol.1))
BERYLLIUM IONS
polarizability and shielding factor for, dipole, (T), 20: 37440
BERYLLIUM ISOTOPES Be-7
energy levels, (E), 20: 38165
tracer use in beryllium self diffusion, 20: 37249
BERYLLIUM ISOTOPES Be-8
energy level widths in, effects of cluster structure on vitrual-resonance, 20: 38013
energy levels of, excitation of single-particle, (E), 20: 38067
BERYLLIUM ISOTOPES Be-9
gamma reactions (γ,p) with, polarization of protons from, (E), 20: 38146
performance as solar neutrino detector, 20: 37793
proton reactions (p,d) at 40.8 Mev, excitation of single-particle beryllium-8 energy levels in, (E), 20: 38067
BERYLLIUM MODERATED REACTORS
core design and fuel cycle for 1000-Mw(e) fast breeder, 20: 38494 (ANL-7120, pp 94-103)
design, economics, and safety of 1000-Mw(e) sodium-cooled fast, 20: 38498 (ANL-7120, pp 185-204)
neutronics calculations for 1000-Mw(e) fast breeder, 20: 38493 (ANL-7120, pp 85-93)
physics parameters of 1000-Mw(e) fast ceramic, calculation of, 20: 38491 (ANL-7120, pp 24-32)
BERYLLIUM OXIDES
development for SEFOR core materials, 20: 38531 (GEAP-5133)
preparation of single-crystal, from gas-vapor phase at 1400 to 1600°C, effects of ions on, 20: 36814
radiation effects on interstitial dislocation loops in, at high temperature, neutron, 20: 38377
radiation effects on, electron and neutron, 20: 37281
BeO–PuO_2–ThO_2, fabrication for gas-cooled reactor fuels, processes for, 20: 37168(R) (BMI-1771)
BERYLLIUM OXIDES (IMPREGNATED)
krypton and xenon release from, during reactor operations, 20: 37303
BETA PARTICLES
activity in bones in leukemic patients, 20: 36559
detection and measurement of low-energy, performance of surface roughened glass vessels for measuring, 20: 37084
detection and measurement of, design of plastic scintillator cell for, 20: 37086
detection and measurement of tritium, using plastic scintillator, 20: 37087
detection and measurement of, development of portable monitor for, 20: 37071 (DP-993)
detection and measurement of, limitations of liquid scintillation emulsion counting method for, 20: 36720
effects on tissue homografts in dogs by lymphatic ablation, 20: 36641
reactions with anthracene and terephenyl, decay of scintillations from, 20: 37305
BETA SOURCES
use of promethium-147, in x-ray spectroscopic analysis, 20: 36765
BETA SPECTROMETERS
design and performance of 4π semiconductor, 20: 37125
design of 180°, 20: 37120
design of, for use in analysis of rocks for potassium, 20: 36752
performance of modified thin-lens magnetic, 20: 38169
BIBLIOGRAPHIES
on carbon-14, 20: 38540 (PAEC(A)IN-652)
on design and use of radioisotope instruments in industry, 20: 37148
on effects of hypophyseal-adrenal system in development of symptoms of radioinduced pathology, 20: 36668
on food irradiation, 20: 37138 (AED-C-05-05)
on gases and plasma, chemistry and physics of, 20: 38204 (NP-16240)
on mass spectroscopy, 20: 36712 (IS-1335)
on nuclear geophysical techniques in Soviet Union, 20: 37001
on plasma research, 20: 38199 (MATT-400)
on radioinduced hyperlipemia in animals, 20: 36580
on reactor-material properties at high temperatures, 20: 38433 (ANL-7120, pp 641-53)
on solid state effect in crystals, (E/T), 20: 38402
BIOCHEMISTRY
book: *Very Faint Luminescence in Biochemical Reactions*, 20: 36547
BIOLOGICAL MATERIALS
analysis of tritium-labeled, combustion-liquid scintillation, 20: 36763
analysis of, for carbon-14, sulfur-35, and tritium, combustion method for, 20: 36721
analysis of, for potassium by neutron activation methods, 20: 36735
separation of radioactive trace elements from neutron-irradiated, by ion exchange, 20: 36762
BIOLOGICAL STRESS
effects on phosphatide content in blood plasma of man, 20: 36606(R) (NYO-1864-23)
BISMUTH
magnetic flux motion in magnetoresistive, induced voltage from, (E/T), 20: 37966
neutron total cross sections at high energies, fluctuations in, 20: 38173
separation from metal mixtures by thin layer chromatography, 20: 36753
separation of, from thallium by ion-exchange chromatography, 20: 36935
x-ray spectra from mu-mesic atoms of, (E), 20: 38058
BISMUTH ALLOYS
Bi–Sn, Hall effect in quenched films of, below 47°K, 20: 38384
BISMUTH BROMIDES
$AlBr_3$–$BiBr_3$, phase diagrams, 20: 36787 (YALE-2723(Vol.1))
$AsBr_3$–$BiBr_3$, phase diagrams, 20: 36787 (YALE-2723(Vol.1))
$BiBr_3$–$PbBr_2$, phase diagrams, 20: 36787 (YALE-2723(Vol.1))
$BiBr_3$–$SnBr_4$, phase diagrams, 20: 36787 (YALE-2723(Vol.1))
$SbBr_3$–$BiBr_3$, phase diagrams, 20: 36787 (YALE-2723(Vol.1))
BISMUTH CHLORIDES
reactions with vanadium pentafluoride, 20: 36804
$BiCl_3$–CuCl, phase diagrams, 20: 36787 (YALE-2723(Vol.1))
$BiCl_3$–KCl, phase diagrams, 20: 36787 (YALE-2723(Vol.1))
$BiCl_3$–$PbCl_2$, phase diagrams, 20: 36787 (YALE-2723(Vol.1))
$SbCl_3$–$BiCl_3$, phase diagrams, 20: 36787 (YALE-2723(Vol.1))
BISMUTH COMPOUNDS
geochemistry of, effects of solar activity on, (E), 20: 37002
BISMUTH ISOTOPES Bi-209

neutron reactions (n,α) at 12 to 23 Mev, (E), 20: 38036
BISMUTH ISOTOPES Bi-210
content in drinking waters in Great Britain, 20: 37031
BISMUTH ISOTOPES Bi-211
energy level at 405 kev, half life of, (E), 20: 38030
BISMUTH ISOTOPES Bi-212
content in atmosphere, diurnal oscillations of, (T), 20: 37007
BISMUTH ISOTOPES Bi-214
content in atmosphere, diurnal oscillations of, (T), 20: 37007
BLOOD
analysis of human, activation, 20: 36728
analysis of, for carbon-14 and tritium by scintillation counting, combustion method for, 20: 36721
radiation effects on Dische-positive materials in dog, pig, and sheep, gamma, 20: 36604
radiation effects on hematopoietic response in guinea pig, effects of unilateral limb shielding on gamma, 20: 36611
radioinduced hyperlipemia in animal, mechanism of, 20: 36580
strontium-90 transport from rat, into gastrointestinal tract, 20: 36558
BLOOD CELLS
radiation effects on human, protective effects of bone marrow transplants against whole-body, 20: 36669
BLOOD FORMATION
effects of transplanted preserved bone marrow on, 20: 36546
BLOOD PICTURE
radiation and mercaptopurine effects on, in progeny of treated rats, 20: 36643
BLOOD PLASMA
enhancement by, of the oncolytic effect of irradiated tumors, 20: 36582
phosphatide content and composition in, of men and rats, 20: 36606(R) (NYO-1864-23)
radiation effects on proteins in, of Hiroshima bomb survivors, personnel, and cancer patients, 20: 36581
BLOOD SERUM
effects of lyophilization of, on radiation effects on proteins in rats, 20: 36582
effects of radiation sickness on renewal intensity and specific radioactivities of proteins in rabbit, 20: 36600
effects on iodine-131-labeled triiodothyronine metabolism in human thyroid, 20: 36573
radiation effects on uptake of carbon-14-labeled acetate by proteins in rabbit, 20: 36574
radioinduced hydration of proteins in, α and x, 20: 36579
BOILERS
deconditioning of mercury, by contamination, 20: 36987 (NAA-SR-11949)
failure during hydrostatic testing, analysis of, 20: 37180
BOILING
critical heat flux measurements on multirod geometries, 20: 36986 (GEAP-5073)
critical water, in rod bundles, (T), 20: 36992
flow in, space-independent model of two-phase, 20: 36984 (BNL-963)
heat transfer in mercury, effects of surface and system contaminants on pool, 20: 36987 (NAA-SR-11949)
nucleate, in nitrogen and methane, 20: 36993
voids due to transient, in fast reactor cores, 20: 38440 (ANL-7120, pp 881-9)
BOILING REACTORS
development of, steady-state and dynamic behavior analysis, 20: 38502(R) (EURAEC-1662)
heat transfer in, critical heat flux variation at high pressure, 20: 38462 (GEAP-4929)
heat transfer limitations on fuel elements, 20: 38484
BONDING
methods for transition metals using beryllium, 20: 37275
BONE MARROW
clinical uses of transplants of, review of, 20: 36667
effects of transplants of, on radiation sickness in man, 20: 36669
preservation techniques for, 20: 36546
radiation effects on cytokinetics and regulation of progenitor cells in, methods for assaying, 20: 36594
radiation effects on hematopoietic response in guinea pig, effects of unilateral limb shielding on gamma, 20: 36611
radiation effects on homografts of, in dogs by lymphatic ablation, 20: 36641
tests for viability of preserved, 20: 36546
BONE TUMORS
radiodiagnosis of growth activity of metastases, 20: 36701
BONES
analysis of, for carbon-14 and tritium by scintillation counting, combustion method for, 20: 36721
radioactivity of, in leukemic patients, beta and gamma, 20: 36559
BORAL
development for SEFOR core materials, 20: 38531 (GEAP-5133)
BORATE GLASS
crystal structure of rare earth-activated, 20: 36813
radiation effects on optical absorption of, containing arsenic or manganese, 20: 36887
BORIDES
electric and thermal conductivity of metal, symposium on, 20: 37179
BORON
B–stainless steel, ductility of, effects of ultrasound on, 20: 37221
BORON BROMIDES
reactions with uranium hexafluoride, 20: 36803
BORON CARBIDES
development for SEFOR core materials, 20: 38531 (GEAP-5133)
effects on reactivity of gas- and steam-cooled fast reactors during flooding, 20: 38439 (ANL-7120, pp 826-36)
reactions with tantalum at 1200 to 1700°C, 20: 36809
BORON CHLORIDES
reactions with niobium, tantalum, and vanadium pentafluorides, 20: 36804
reactions with uranium hexafluoride, 20: 36803
BORON HYDRIDES
radioinduced free radicals of, in krypton, 20: 36909
BORON IONS
polarizability and shielding factor for, dipole, (T), 20: 37440
BORON ISOTOPES B-10
electron elastic scattering at 198 to 400 Mev, Coulomb form factors from, (E), 20: 38057
energy level excitation in meson ($\pi^{\pm}$) reactions ($\pi^{\pm}$,2N) with carbon-12, (E), 20: 38070
energy level transitions, (E), 20: 38069
mesons (π^{-}) reactions with, charge exchange in, (E), 20: 37740 (JINR-P-2780)
proton reactions (p,n) with, threshold for, (E), 20: 38069
BORON ISOTOPES B-11
deuteron reactions (d,p) with, boron-12 energy levels from, (E), 20: 38161
deuteron reactions (d,n) with, angular distribution of neutron polarization in, (E), 20: 38163
electron elastic scattering at 198 to 400 Mev, Coulomb form factors from, (E), 20: 38057
performance as solar neutrino detector, 20: 37793
proton reactions (p,n) with, calculations using finite-range distorted-wave Born approximation, (T), 20: 38112
reactions (B-11,p3n) with aluminum-27 at 30–115 Mev, cross sections, recoil ranges, and angular distributions of chlorine-34m from, (E), 20: 38084
with, deuteron reactions (d,n) with, alpha decay of carbon-12 energy levels from, (E), 20: 38162
BORON ISOTOPES B-12
energy levels at 0.95 and 1.67 Mev, (E), 20: 38161
BORON OXIDES
B_2O_3–Eu_2O_3–Na_2O, spectra at liquid nitrogen temperature and room temperature, absorption and emission, 20: 36813
BORON SYSTEMS
B–Nb–W, phase studies of, 20: 37261
BOSONS
interactions in system of, variational ground-state energy for two-body, (T), 20: 37838
mass levels of, urbaryon dynamics for, 20: 37846
production from bound states of fermions, (T), 20: 37472
production of (1929), (2195), and (2382) charged, in meson (π^{-}) interactions with protons at 12 Bev/c, (E), 20: 37771
production of intermediate vector, in meson (π) decay, (T), 20: 37781
production of intermediate W, in electron-positron annihilations, (T), 20: 37799
BRAIN
radiation effects on cerebral cortex of monkey, x, 20: 36656
radiation effects on function of animal and human, dose effects in, 20: 36651
radiation injuries during radiotherapy, 20: 36694
radiation injuries to, during radiotherapy, 20: 36695
radiation injuries in, use of gamma encephalography for detecting x, 20: 36696
BRAIN TUMORS
radiotherapy and operability limits of, indications for, 20: 36692
radiotherapy effects on, 20: 36694
radiotherapy of, injuries and morphological changes in, 20: 36695
radiotherapy of, with and without extirpation, 20: 36693
BREEDER REACTORS
fuel elements for, fabrication of nitride, 20: 37168(R) (BMI-1771)
fuel elements for, fabrication of nitride, 20: 37169(R) (BMI-1774)
fuels for, breeding ratios of carbide and nitride, 20: 37168(R) (BMI-1771)
BREMSSTRAHLUNG
energy transfer to, from cosmic meson (π) reactions with nuclei, (E), 20: 37660

reactions (γ,p) with calcium-40 at 28 and 60 Mev, proton angular and energy distributions from, (E), 20: 38024
spectra from electron reactions with thick targets at 0.2 to 0.8 Mev, (E), 20: 38155
theory for, in electromagnetic cascade showers, 20: 37788
BRICKS
radioinduced polymerization of acrylonitrile on INZ-600, at 300°C, 20: 36882
BRITISH REACTORS
environs monitoring of Chapelcross, 20: 37025(R) (PG-Report-705)
BRITTANY POWER REACTOR (EL-4)
development, 20: 38517
BROMINE
meson (π⁻) reactions at 17 Bev in nuclear emulsions, (T), 20: 38060
BROMINE FLUORIDES
reactions with uranium, 20: 36950
BROMINE IONS
yields from radiolysis of bromates, 20: 36899
BROMINE ISOTOPES Br-82
yields of, from proton fission of uranium-238 at 12 Mev, 20: 37995
BROMINE ISOTOPES Br-83
yields in proton fission of uranium-238 at 7.1, 9.4, and 12.0 Mev, 20: 37995
BUBBLES
distribution of fission-gas, in post-irradiation annealed uranium dioxide, 20: 37255
flow of, hydrodynamic characteristics of upward, 20: 36988 (TID-23261)
formation and movement of radioinduced, in fuels and reactor materials, 20: 37299
BUTANE, 1-CHLORO-
yields of, from gamma-induced reactions of 1-butene and phosgene, 20: 36892
BUTANE, 2-CHLORO-
yields of, from gamma-induced reactions of 1-butene and phosgene, 20: 36892
BUTANE, 1,2-DICHLORO-
yields of, from gamma-induced reactions of 1-butene and phosgene, 20: 36892
1,3-BUTANEDIONE, 1-PHENYL- COMPLEXES
with rare earths, spectrofluorometric analysis for rare earths in, 20: 36722
1-BUTANOL
effects on copper determination by absorption spectroscopy, 20: 36726
1-BUTANOL, 3-METHYL-
solvent properties for protactinium in acid solutions, 20: 36940
2-BUTANONE
effects on copper determination by absorption spectroscopy, 20: 36726
2-BUTANONE, 3-METHYL-
effects on copper determination by absorption spectroscopy, 20: 36726
1-BUTENE
radioinduced reactions of, with phosgene at −78 to 35°C, gamma, 20: 36892
BUTYL PHOSPHATE COMPLEXES
with cerium, absorption spectra of, 20: 36831
BUTYL PHOSPHATES
cerium compound absorption spectra in, 20: 36831
effects on solvent properties of diisopentyl methylphosphonate for thorium in nitric acid solutions, 20: 36942
solvent properties of, for plutonium, 20: 36928
solvent properties for rare earths, 20: 36938
uses in fuel element processing, 20: 36948
benzene–TBP, solvent properties for uranium, 20: 36718
bis(2-ethylhexyl)phosphate–TBP, solvent properties for americium, 20: 36937
CCl_4–TBP–H_2O, azeotropic distillation of, 20: 36731
cyclohexane–TBP, solvent properties for uranium, 20: 36714
cyclohexane–TBP, solvent properties for uranium, 20: 36718
ethyl acetate–TBP, solvent properties for uranium, 20: 36717
hexane–TBP, solvent properties for uranium, 20: 36932
octyl phenylphosphonate–TBP, solvent properties for americium, 20: 36937
TBP–H_2O, cerium compound absorption spectra in, 20: 36831
4-methyl-2-pentanone–TBP, solvent properties for uranium, 20: 36716

C

CADMIUM
effects on discontinuous precipitation in beryllium–copper alloys, 20: 37253
separation from metal mixtures by thin layer chromatography, 20: 36753
separation from neutron-irradiated biological materials by ion exchange, 20: 36762
separation of, from thallium by ion-exchange chromatography, 20: 36935
CADMIUM BROMIDES
$CdBr_2$–AgBr, phase diagrams, 20: 36787 (YALE-2723(Vol.1))
$CdBr_2$–$CdCl_2$, phase diagrams, 20: 36787 (YALE-2723(Vol.1))
$CdBr_2$–CdI_2, phase diagrams, 20: 36787 (YALE-2723(Vol.1))
$CdBr_2$–CuBr, phase diagrams, 20: 36787 (YALE-2723(Vol.1))
$CdBr_2$–KBr, phase diagrams, 20: 36787 (YALE-2723(Vol.1))
$CdBr_2$–NaBr, phase diagrams, 20: 36787 (YALE-2723(Vol.1))
$CdBr_2$–$PbBr_2$, phase diagrams, 20: 36787 (YALE-2723(Vol.1))
$CdBr_2$–$ZnBr_2$, phase diagrams, 20: 36787 (YALE-2723(Vol.1))
CADMIUM CARBONATES
formation of, effect of insoluble uranyl ions on, 20: 36796
CADMIUM CHLORIDES
reactions with isopropylamine, thermogravimetric study of, 20: 36853
$CdBr_2$–$CdCl_2$, phase diagrams, 20: 36787 (YALE-2723(Vol.1))
$CdCl_2$–AgCl, phase diagrams, 20: 36787 (YALE-2723(Vol.1))
$CdCl_2$–$CsCl_2$, phase diagrams, 20: 36787 (YALE-2723(Vol.1))
$CdCl_2$–CdF_2, phase diagrams, 20: 36787 (YALE-2723(Vol.1))
$CdCl_2$–CsCl, phase diagrams, 20: 36787 (YALE-2723(Vol.1))
$CdCl_2$–CuCl, phase diagrams, 20: 36787 (YALE-2723(Vol.1))
$CdCl_2$–$InCl_3$, phase diagrams, 20: 36787 (YALE-2723(Vol.1))
$CdCl_2$–KCl, phase diagrams, 20: 36787 (YALE-2723(Vol.1))
$CdCl_2$–LiCl, phase diagrams, 20: 36787 (YALE-2723(Vol.1))
$CdCl_2$–LiF, phase diagrams, 20: 36787 (YALE-2723(Vol.1))
$CdCl_2$–$MgCl_2$, phase diagrams, 20: 36787 (YALE-2723(Vol.1))
$CdCl_2$–NaCl, phase diagrams, 20: 36787 (YALE-2723(Vol.1))
$CdCl_2$–$PbCl_2$, phase diagrams, 20: 36787 (YALE-2723(Vol.1))
$CdCl_2$–RbCl, phase diagrams, 20: 36787 (YALE-2723(Vol.1))
$CdCl_2$–$SnCl_2$, phase diagrams, 20: 36787 (YALE-2723(Vol.1))
$CdCl_2$–$SrCl_2$, phase diagrams, 20: 36787 (YALE-2723(Vol.1))
$CdCl_2$–TlCl, phase diagrams, 20: 36787 (YALE-2723(Vol.1))
$CdCl_2$–$ZnCl_2$, phase diagrams, 20: 36787 (YALE-2723(Vol.1))
CADMIUM FLUORIDES
$CdCl_2$–CdF_2, phase diagrams, 20: 36787 (YALE-2723(Vol.1))
$CdCl_2$–CdI_2, phase diagrams, 20: 36787 (YALE-2723(Vol.1))
$CdCl_2$–NaF, phase diagrams, 20: 36787 (YALE-2723(Vol.1))
CdF_2–CdI_2, phase diagrams, 20: 36788 (YALE-2723(Vol.2))
CADMIUM IODIDES
$CdBr_2$–CdI_2, phase diagrams, 20: 36787 (YALE-2723(Vol.1))
$CdCl_2$–CdI_2, phase diagrams, 20: 36787 (YALE-2723(Vol.1))
CdF_2–CdI_2, phase diagrams, 20: 36788 (YALE-2723(Vol.2))
CdI_2–CuI, phase diagrams, 20: 36788 (YALE-2723(Vol.2))
CdI_2–HgI_2, phase diagrams, 20: 36788 (YALE-2723(Vol.2))
CdI_2–InI_3, phase diagrams, 20: 36788 (YALE-2723(Vol.2))
CdI_2–KI, phase diagrams, 20: 36788 (YALE-2723(Vol.2))
CdI_2–NaI, phase diagrams, 20: 36788 (YALE-2723(Vol.2))
CdI_2–PbI_2, phase diagrams, 20: 36788 (YALE-2723(Vol.2))
CADMIUM ISOTOPES
production in proton reactions with lead and uranium at 3 and 28 Bev, cross sections for, (E), 20: 38098
CADMIUM ISOTOPES Cd-115
yields in proton fission of uranium-238 at 7.1, 9.4, and 12.0 Mev, 20: 37995
CADMIUM SULFATES
compatibility with 316 stainless steel and Zircaloy-2, 20: 38447 (WCAP-2867)
CADMIUM SULFIDES
radiation effects on electric conductivity of, thermal neutron, (E), 20: 38405
CALCIFICATION
effects of various histamine liberators on, relationship to several metal calcergens in rats, 20: 36557
CALCITES
flotation of, on gamma-irradiated anionic collector agents, 20: 36893
CALCIUM
abundance in coronal condensations, (E), 20: 37348
content in African pitchblende, estimation of induced fission vs spontaneous fission from, 20: 37994
determination in blood and hair of man, activation, 20: 36728
effects on inotropic action of fluoride in rat ventricle, 20: 36567
neutron absorption cross section in pitchblende, thermal, 20: 37994
neutron elastic scattering at 2.15 to 6.53 Mev, differential cross sections for, (E), 20: 38183
neutron total cross sections at 2.2 to 5.3 Mev, (E), 20: 38183
positron annihilation with core electrons in, momentum distributions for, (T), 20: 37821
production in iron meteorites by cosmic radiation, isotopic ratios for, (E), 20: 37603
proton elastic scattering at 49 Mev, angular distribution of polarization in, 20: 38049
x-ray spectra from mu-mesic atoms of, (E), 20: 38058
CALCIUM ALLOYS

Ca–Au, superconductivity of Au_5Ca, 20: 37985
CALCIUM BROMATES
radiolysis of, gamma, neutron, and lithium-6 fission product recoil, 20: 36899
CALCIUM BROMIDES
$CaBr_2$–CaF_2, phase diagrams, 20: 36787 (YALE-2723(Vol.1))
$CaBr_2$–KBr, phase diagrams, 20: 36787 (YALE-2723(Vol.1))
$CaBr_2$–LiBr, phase diagrams, 20: 36787 (YALE-2723(Vol.1))
$CaBr_2$–NaBr, phase diagrams, 20: 36787 (YALE-2723(Vol.1))
CALCIUM CARBONATES
content of, in sediments of Bay of Roquebrune, 20: 36553
thermoluminescence properties of, for use as radiation dosimeter, 20: 36913
CALCIUM CHLORIDES
$BaBr_2$–$CaCl_2$, phase diagrams, 20: 36787 (YALE-2723(Vol.1))
$BaCl_2$–$CaCl_2$, phase diagrams, 20: 36787 (YALE-2723(Vol.1))
$BaCl_2$–$CdCl_2$, phase diagrams, 20: 36787 (YALE-2723(Vol.1))
$BeCl_2$–$CaCl_2$, phase diagrams, 20: 36787 (YALE-2723(Vol.1))
$CaCl_2$–AgCl, phase diagrams, 20: 36787 (YALE-2723(Vol.1))
$CaCl_2$–CaF_2, phase diagrams, 20: 36787 (YALE-2723(Vol.1))
$CaCl_2$–CaI_2, phase diagrams, 20: 36787 (YALE-2723(Vol.1))
$CaCl_2$–CsCl, phase diagrams, 20: 36787 (YALE-2723(Vol.1))
$CaCl_2$–CuCl, phase diagrams, 20: 36787 (YALE-2723(Vol.1))
$CaCl_2$–KCl, phase diagrams, 20: 36787 (YALE-2723(Vol.1))
$CaCl_2$–LiCl, phase diagrams, 20: 36787 (YALE-2723(Vol.1))
$CaCl_2$–$MgCl_2$, phase diagrams, 20: 36787 (YALE-2723(Vol.1))
$CaCl_2$–NaCl, phase diagrams, 20: 36787 (YALE-2723(Vol.1))
$CaCl_2$–$PbCl_2$, phase diagrams, 20: 36787 (YALE-2723(Vol.1))
$CaCl_2$–RbCl, phase diagrams, 20: 36787 (YALE-2723(Vol.1))
$CaCl_2$–$SnCl_2$, phase diagrams, 20: 36787 (YALE-2723(Vol.1))
$CaCl_2$–$SrCl_2$, phase diagrams, 20: 36787 (YALE-2723(Vol.1))
$CaCl_2$–TlCl, phase diagrams, 20: 36787 (YALE-2723(Vol.1))
$CaCl_2$–$ZnCl_2$, phase diagrams, 20: 36787 (YALE-2723(Vol.1))
$CdCl_2$–$CaCl_2$, phase diagrams, 20: 36787 (YALE-2723(Vol.1))
CALCIUM FLUORIDES
analysis for components of, by scattering of accelerated alpha particles, 20: 36719
flotation of, on gamma-irradiated anionic collector agents, 20: 36893
fluorine-19 NMR in, free-induction decay shapes and moments for, (E), 20: 38390
radiation effects on crystals of, 15-Mev proton, 20: 38372
BaF_2–CaF_2, phase diagrams, 20: 36787 (YALE-2723(Vol.1))
BeF_2–CaF_2, phase diagrams, 20: 36787 (YALE-2723(Vol.1))
$CaBr_2$–CaF_2, phase diagrams, 20: 36787 (YALE-2723(Vol.1))
$CaCl_2$–CaF_2, phase diagrams, 20: 36787 (YALE-2723(Vol.1))
CaF_2–CaI_2, phase diagrams, 20: 36787 (YALE-2723(Vol.1))
CaF_2–KF, phase diagrams, 20: 36787 (YALE-2723(Vol.1))
CaF_2–LiF, phase diagrams, 20: 36787 (YALE-2723(Vol.1))
CaF_2–MgF_2, phase diagrams, 20: 36787 (YALE-2723(Vol.1))
CaF_2–NaF, phase diagrams, 20: 36787 (YALE-2723(Vol.1))
CaF_2–RbF, phase diagrams, 20: 36787 (YALE-2723(Vol.1))
CaF_2–SrF_2, phase diagrams, 20: 36787 (YALE-2723(Vol.1))
CALCIUM HYDROXIDES
radiation effects on surface area of oxide produced by thermal decomposition of, x, 20: 36904
CALCIUM IODIDES
$CaCl_2$–CaI_2, phase diagrams, 20: 36787 (YALE-2723(Vol.1))
CaF_2–CaI_2, phase diagrams, 20: 36787 (YALE-2723(Vol.1))
CALCIUM IONS
effects on formation of single-crystal beryllium oxide, 20: 36814
CALCIUM ISOTOPES
energy levels of, systematics of 3- and 5-, (E), 20: 38100
CALCIUM ISOTOPES Ca-40
alpha inelastic scattering at 31 Mev, (E), 20: 38100
deuteron reactions (d,p) with, proton angular distribution and polarization in, (E), 20: 38119
energy level systematics, determination using alpha inelastic scattering at 31 Mev, 20: 38100
gamma reactions (γ,p) at 28 and 60 Mev, proton angular and energy distributions from, (E), 20: 38024
CALCIUM ISOTOPES Ca-42
alpha inelastic scattering at 31 Mev, (E), 20: 38100
energy level at 1.52 Mev, lifetime of, (E), 20: 38085
energy level systematics, determination using alpha inelastic scattering at 31 Mev, 20: 38100
energy levels of, shell-model potential parameters for low-lying, (T), 20: 38145
CALCIUM ISOTOPES Ca-44
alpha inelastic scattering at 31 Mev, (E), 20: 38100
energy level systematics, determination using alpha inelastic scattering at 31 Mev, 20: 38100
CALCIUM ISOTOPES Ca-45
determination of, with strontium-89 in whole algae cells, liquid scintillation spectrometric, 20: 36747
CALCIUM ISOTOPES Ca-48
alpha inelastic scattering at 31 Mev, (E), 20: 38100
energy level systematics, determination using alpha inelastic scattering at 31 Mev, 20: 38100
triton reactions (t,α) and (t,p) at 7.5 Mev, calcium-50 and potassium-47 energy levels and masses from, (E), 20: 38063
CALCIUM ISOTOPES Ca-50
energy levels and ground-state mass, (E), 20: 38063
CALCIUM NITRATES
use as salting-out agent in solvent extraction of uranium, 20: 36717
CALCIUM OXALATES
calcium oxalate–Ce, precipitation reactions in, distribution coefficients of, 20: 36794
calcium oxalate–Lu, precipitation reactions in, distribution coefficients of, 20: 36794
calcium oxalate–Y, precipitation reactions in, distribution coefficients of, 20: 36794
calcium oxalate–Eu, precipitation reactions in, distribution coefficients of, 20: 36794
CALCIUM OXIDES
effects on sintering behavior of urania powders, 20: 37202
positronium lifetime in, (E), 20: 37819
radiation effects on surface area of, x, 20: 36904
vaporization of, thermodynamics of, 20: 36841
CaO–MgF_2, phase studies, 20: 37722(R) (N-65-30843)
CALCIUM SYSTEMS
Ca–NaCl–Ag, radioinduced color centers in, x, 20: 38396
CALDER HALL REACTORS
boiler failure at Sizewell, analysis of, 20: 37180
development of, review of, 20: 38516
CALIFORNIUM ISOTOPES Cf-252
fission fragments of, conversion-electron and K x-ray emission by, (E), 20: 38095
CALIFORNIUM ISOTOPES Cf-253
alpha decay of, branching ratio for, (E), 20: 38093
CALORIMETERS
design of adiabatic, for specific heat determination from 250 to 1000°C, 20: 37278
design of isothermal drop, for measuring heat of alpha-active pyrophoric materials, 20: 37055
CAMERAS
lens distortions, design of apparatus for measuring asymmetric, 20: 37053
CARBIDES
electric and thermal conductivity of metal, symposium on, 20: 37179
CARBON
cosmic meson (π) reactions in, energy transfer to photons from, (E), 20: 37660
cosmic neutron attenuation at 60 Bev, collision mean free path and neutron-proton cross section from, (E), 20: 37670
cosmic neutron reactions at 100 Bev, cross sections for, (E), 20: 37668
cosmic particle reactions in, four-momentum transfer in, (E/T), 20: 37659
cosmic particle reactions with, meson (π) production from, (E), 20: 37664
cosmic proton inelastic scattering by, effective cross section for, (E), 20: 37495
decomposition of pyrolytic coating of, on fuel elements, 20: 36955(P)
deposition on thorium dicarbide particles, 20: 37206
effects on reactions of nitrogen with plutonium dioxide and uranium dioxide, 20: 37207
laser beam reactions with, uv spectra from plasma produced from, (E), 20: 38300
meson (K_L^0) and (K_S^0) regeneration in, Regge-pole model for, 20: 37764
proton reactions at 600 Mev, cross sections for meson ($\pi^\pm$) production in, 20: 38166
radiation doses to tissues from, in solar particle beams in space, 20: 37023 (N-65-33865)
reactions with beryllium in group VIII transition metal alloys, 20: 37275
stopping power for lead-208 alpha recoil nuclei, 20: 37470
CARBON (ACTIVATED)
properties of coconut-shell, for use in air filtration systems, 20: 36976 (DP-MS-66-45)
CARBON DIOXIDES
monitoring of, in Gemini spacecraft, radioisotope uses in instrument for, 20: 37064
positron annihilation in, (E), 20: 37810
spectra from 13-kev electron and 37-kev proton excited, emission, 20: 37466(T)
Co_2–propane, properties for proportional detectors, 20: 37092
CARBON IONS
polarizability and shielding factor for, dipole, (T), 20: 37440
CARBON ISOTOPES

abundance in primary cosmic radiation, estimation of relative, (E), 20: 37574
CARBON ISOTOPES C-10
beta decay of, branching ratios and ft values for, (E), 20: 38069
CARBON ISOTOPES C-12
carbon-12 reactions (C-12,α) at 27.2 Mev, neon-20 levels from, (T), 20: 38179
carbon-12 reactions (C-12,αγ) at 15.55 Mev, neon-20 levels from, 20: 38008(R) (AECL-2595)
deuteron reactions (d,p) with, proton angular distribution and polarization in, (E), 20: 38119
energy level excitation in meson ($\pi^{\pm}$) reactions ($\pi^{\pm}$,2N) with nitrogen-14, (E), 20: 38070
energy levels at 11.83 and 12.71 Mev, alpha-particle breakup and spin-parity assignments of, (E), 20: 38162
gamma reactions (γ,N) with, polarization effects in, (T), 20: 38175
meson (π^-) capture by, radiative, (T), 20: 38064
meson ($\pi^{\pm}$) reactions (π^-,2n) and (π^+,2p) with, boron-10 energy level excitation in, (E), 20: 38070
nucleon inelastic scattering at 185 Mev, (T), 20: 38120
oxygen-16 reactions (O-16,α) with, magnesium-24 levels from, 20: 38008(R) (AECL-2595)
proton elastic scattering at 4.7 to 12.8 Mev, excitation functions for, (E), 20: 38050
proton elastic scattering at 2.4 to 11.6 Mev, differential cross sections for, (E), 20: 38051
proton inelastic scattering at 6.0 to 12.8 Mev, excitation, 20: 38050
proton reactions (p,α) at 11.6 Mev, differential cross sections for, (E), 20: 38051
reactions (C-12,nγ) with tritium at 12 and 17.75 Mev, nitrogen-14 level lifetimes from, 20: 38008(R) (AECL-2595)
reactions (C-12,pγ) with tritium at 22 Mev, carbon-14 level lifetimes from, 20: 38008(R) (AECL-2595)
reactions with chromium-52, formation and decay of zinc-64 in, 20: 38152
reactions with vanadium-51 up to 120 Mev, copper-63 compound nucleus formation in, (E), 20: 38147
CARBON ISOTOPES C-13
content in sea urchins, variations in, 20: 36549
content in sea urchins, environmental and genetic factors in variations in, 20: 36550
proton reactions (p,n) at 3.237 to 3.85 Mev, angular distribution and excitation function for, (E), 20: 38042
proton reactions (p,n) with, thresholds for, (E), 20: 38053
proton reactions (p,n) with, threshold energy for, (E), 20: 38054
proton reactions (p,n) with calculations using finite-range distorted-wave Born approximation, (T), 20: 38112
CARBON ISOTOPES C-14
alpha reactions (α,n) with, oxygen-17 energy levels from, (E), 20: 38161
bibliography on, 20: 38540 (PAEC(A)IN-652)
content in tree rings, cosmic ray secular variation determination from, (E), 20: 37602
determination by liquid scintillation counting, use of external alpha or gamma source in automatic corrections in, 20: 36743
determination of, in biological and organic materials, combustion method for, 20: 36721
determination of, in organic compounds, oxygen-tube combustion method for scintillation, 20: 36723
determination of, in plant tissue by liquid scintillation counting, oxygen flask combustion technique for sample preparation for, 20: 36764
determination of, instrumentation effects on quenching of energy spectrum in, 20: 36771
energy level lifetimes from tritium (C-12,pγ) reactions at 22 Mev, 20: 38007(R) (AECL-2595)
incorporation in Tween 20, methods for, 20: 36921
incorporation in 2,4,7-triamino-6-phenylpteridine, method for, 20: 36922
radiation effects on uptake of acetate labeled by, by muscle and serum proteins in rabbits, 20: 36574
tracer use for measuring glucose production in dogs, 20: 36565
use in isotopic dilution studies on metabolism in rat skin collagen, 20: 36562
CARBON MONOXIDES
energy level transition probabilities and lifetimes in, 20: 37438
excitation of, in shock tubes, effects of dueterium and helium on, 20: 36820
reactions with copper–zirconium alloys at high temperatures, mechanisms of, 20: 37183
spectra from 13-kev electron and 37-kev proton excited, emission, 20: 37466(T)
CO–O, vibrational relaxation of, in shock tubes, 20: 36820
CARBON SULFIDES
reactions with vanadium pentafluoride, 20: 36804
CARBON SYSTEMS
C–Mo–Ti–Zr, crack formation in Mo-3 alloy ingots, effects of molybdenum capping on, 20: 37219
C–Nb–W–Zr, tensile properties of D-43, effects of brittle coatings on, 20: 37276
C–O–Zr, phase studies, 20: 37264
C–Ta–Zr, phase studies, 20: 37270
C–Th, phase studies, 20: 37265
CARBON TETRACHLORIDE
effects on reactions of free electrons in organic sulfur radicals in organic glasses, 20: 36894
radioinduced telomerization of ethylene with, under constant ethylene pressure, gamma, 20: 36891
radioinduced telomerization of ethylene with, effect of process variables on gamma, 20: 36890
reactions with uranium hexafluoride, 20: 36803
CCl_4–TBP–H_2O, azeotropic distillation of, 20: 36731
CARBONATES
poly-, radioinduced crosslinking of, 20: 36907(P)
CARCINOMAS
radiotherapy of bronchial, frequency of radiofibroses in lung tissue after, 20: 36703
radiotherapy of head and neck, use of electron beams for, 20: 36685
radiotherapy of mammary, development of metastases in gamma and x, 20: 36697
radiotherapy of uterine, remote control unit for γ, 20: 36687
radiotherapy of uterine cervical, dose distribution in radium, 20: 36699
radiotherapy of, low-dose x, 20: 36698
CASCADE SHOWERS
bremsstrahlung and pair production in theory for electromagnetic, 20: 37788
distribution of electromagnetic, at 100 Bev in lead and iron, (E), 20: 37698
meson (μ) energy spectrum and lateral distribution in electromagnetic air, (T), 20: 37622
production in iron by primary cosmic nucleons at high energies, (T), 20: 37789
theory for photon-electron, with polarization of medium, 20: 37787
theory for, inverse problem in cascade, 20: 37650
CATALYSTS
preparation and sorptive properties of thorium oxide, 20: 36843
CATTLE
iodine-125 and iodine-131 metabolism in, effects of dietary thiocyanate on, 20: 36563
CAVITY RESONATORS
coupling of degenerate modes of circularly cylindrical, by magnetized plasma, (T), 20: 38332
CELLULOSE
carboxymethyl-, use in slip casting of zirconium borides, 20: 37201
use with bentonite for flocculation of ruthenium in waste solutions, 20: 36929
CELLULOSE ACETATES
graft-copolymerization of, with vinyl monomers, 20: 36905(P)
CENTRIFUGES
performance in separation of urania from other oxides in organic slurries, 20: 36933
CHALCOPYRITES
flotation of, on gamma-irradiated anionic collector agents, 20: 36893
CERAMIC MATERIALS
degradation at high temperatures, electric effects on, 20: 37179
properties for use at high temperatures, symposium on, 20: 37179
properties of, for high-temperature coatings on refractory metals, 20: 37192
CERIUM
content in African pitchblende, estimation of induced fission vs spontaneous fission from, 20: 37994
determination in cobalt, manganese, and plutonium alloys by ion exchange separation and potentiometric titration, 20: 36713 (LA-3402)
determination in hydrochloric acid solutions, spectrographic carrier-distillation, 20: 36729
determination in solutions, colorimetric, 20: 36725
effects on crystal structure of cobalt, iron, and nickel intermetallic compounds, 20: 37243
energy levels of, ionization energies from, (T), 20: 37439
liquid, purification by electric transport and zone melting, 20: 36936
neutron absorption cross section in pitchblende, thermal, 20: 37994
separation from radioactive waste solutions, 20: 38538
separation from water by foaming, 20: 36934
separation of, from thallium by ion-exchange chromatography, 20: 36935
separation of, from other lanthanides by ion exchange using ammonium lactate, mechanism of, 20: 36939
x-ray spectra from mu-mesic atoms of, (E), 20: 38058
yields from radiolysis of cerium phthalocyanine, 20: 36886
CERIUM ALLOYS
Ce–Co, crystal structure of intermetallic compounds in, 20: 37243

Ce–Co–Mn–Pu, analysis for cerium and manganese by ion exchange separation and potentiometric titration, 20: 36713 (LA-3402)
Ce–Co–Pu, analysis for cerium by ion exchange separation and potentiometric titration, 20: 36713 (LA-3402)
Ce–Co–Pu, combustion of, properties of aerosols, produced in, 20: 37022 (LA-DC-6942)
Ce–Fe, crystal structure of intermetallic compounds in, 20: 37243
Ce–Fe, magnetic properties of $CeFe_2$, (E), 20: 37279
Ce–La, superconducting transition temperature of, pressure dependence of, (E/T), 20: 37965
Ce–Ni, crystal structure of intermetallic compounds in, 20: 37243
CERIUM CARBIDES
properties at 20 to 1300°C, 20: 36811
CERIUM CHLORIDES
effects as calcergen, relation to histamine liberators in rats, 20: 36557
spectra in tri-*n*-butyl phosphate and tri-*n*-butyl phosphate–water, 20: 36831
CERIUM COMPLEXES
with tartaric acid and trihydroxyglutaric acid, stability constants for, 20: 36838
with TBP, absorption spectra of, 20: 36831
CERIUM FLUORIDES
preparation and properties of, 20: 36950
CERIUM HYDROXIDES
preparation and crystal structure of, 20: 36791
CERIUM ISOTOPES Ce-130
decay, (E), 20: 38048
CERIUM ISOTOPES Ce-131
decay of isomeric, (E), 20: 38048
CERIUM ISOTOPES Ce-134
use in testing converter components, 20: 37725
CERIUM ISOTOPES Ce-140
energy levels of, from lanthanum-140 decay, (E), 20: 38154
CERIUM ISOTOPES Ce-141
dispersion from fallout in seawater, 20: 37037
yields in proton fission of uranium-238 at 7.1, 9.4, and 12.0 Mev, 20: 37995
CERIUM ISOTOPES Ce-143
yields in proton fission of uranium-238 at 7.1, 9.4, and 12.0 Mev, 20: 37995
CERIUM ISOTOPES Ce-144
dispersion from fallout in seawater, 20: 37037
CERIUM NITRATES
spectra in tri-*n*-butyl phosphate and tri-*n*-butyl phosphate–water, 20: 36831
CERIUM OXIDES
reactions with lanthanum and neodymium oxides in solid state, 20: 36840
Al_2O_3–Ce_2O_3, phase studies at temperatures to 2600°C, 20: 36808
Ce_2O_3–Cr_2O_3, phase studies at temperatures to 2600°C, 20: 36803
Ce_2O_3–Ga_2O_3, phase studies at temperatures to 2600°C, 20: 36808
CeO_2–UO_2, radiation effects on clad, 20: 37168(R) (BMI-1771)
CeO_2–UO_2, radiation effects on clad, 20: 37169(R) (BMI-1774)
CeO_2–UO_2, segregation due to temperature gradients in, 20: 38469 (ANL-7120, pp 400-9)
CERIUM SILICIDES
preparation of, method for, 20: 37176
CERIUM SULFATES
spectra in tri-*n*-butyl phosphate and tri-*n*-butyl phosphate–water, 20: 36831
use as oxidant in plutonium separation, 20: 36727
CERIUM SYSTEMS
calcium oxalate–Ce, precipitation reactions in, distribution coefficients of, 20: 36794
CERMETS
crystal structure and properties of thoria-tungsten, effects of metal additions on, 20: 37185
fabrication of Al–Al_2O_3, for nuclear uses, 20: 37210
preparation and properties of silver and silver alloy infiltrated oxide-base, 20: 37209
CESIUM
determination in hydrochloric acid solutions, spectrographic carrier-distillation, 20: 36729
determination of trace amounts of, by ion exchange and colorimetry using potassium bismuth iodide, 20: 36761
effects of, on separation of plutonium from dicesium plutonium hexachloride by slurry–ion exchange methods, 20: 36727
energy levels of ionized, forbidden transitions in, 20: 37432
separation from radioactive waste solutions, 20: 38538
separation from water by foaming, 20: 36934
sorption by graphite at 800 to 1100°C, 20: 36799
stability of discharge and thermal plasmas of, low-frequency, (E), 20: 38319
use in NMR probes used with Varian fluxmeter at low temperatures, 20: 37972
x-ray spectra from mu-mesic atoms of, (E), 20: 38058
CESIUM BROMATES
radiolysis of, gamma, neutron, and lithium-6 fission product recoil, 20: 36899
CESIUM BROMIDES
CsBr–NaBr, phase diagrams, 20: 36788 (YALE-2723(Vol.2))
CESIUM CHLORIDES
$AlCl_3$–CsCl, phase diagrams, 20: 36787 (YALE-2723(Vol.1))
$CaCl_2$–CsCl, phase diagrams, 20: 36787 (YALE-2723(Vol.1))
$CdCl_2$–CsCl, phase diagrams, 20: 36787 (YALE-2723(Vol.1))
CsCl–AgCl, phase diagrams, 20: 36787 (YALE-2723(Vol.1))
CsCl–CuCl, phase diagrams, 20: 36788 (YALE-2723(Vol.2))
CsCl–KCl, phase diagrams, 20: 36788 (YALE-2723(Vol.2))
CsCl–LiCl, phase diagrams, 20: 36788 (YALE-2723(Vol.2))
CsCl–$MgCl_2$, phase diagrams, 20: 36788 (YALE-2723(Vol.2))
CsCl–NaCl, phase diagrams, 20: 36788 (YALE-2723(Vol.2))
CsCl–$PbCl_2$, phase diagrams, 20: 36788 (YALE-2723(Vol.2))
CsCl–RbCl, phase diagrams, 20: 36788 (YALE-2723(Vol.2))
CsCl–$SrCl_2$, phase diagrams, 20: 36788 (YALE-2723(Vol.2))
CsCl–TlCl, phase diagrams, 20: 36788 (YALE-2723(Vol.2))
CESIUM FLUORIDES
dissociation by argon-atom impact, cross sections for, 20: 37478
BeF_2–CsF, phase diagrams, 20: 36787 (YALE-2723(Vol.1))
CsF–LiF, phase diagrams, 20: 36788 (YALE-2723(Vol.2))
CsF–NaF, phase diagrams, 20: 36788 (YALE-2723(Vol.2))
CESIUM IODIDES
performance as high-gain secondary emission material for transmission-type electron multipliers, (E), 20: 37046
radioinduced defect luminescence in, proton, (E), 20: 38401
CESIUM ISOTOPES Cs-131
energy level transitions in, angular correlation for, (E), 20: 38021
CESIUM ISOTOPES Cs-134
decay scheme, (E), 20: 38169
CESIUM ISOTOPES Cs-136
yields of, from proton fission of uranium-238 at 12 Mev, 20: 37995
CESIUM ISOTOPES Cs-137
beta spectrum of, shape of twice-forbidden, (E), 20: 38044
body burden in Eskimos, 20: 37042
content in meat and meat products, 20: 37039
deposition from fallout on forage and transfer to milk, 20: 37036
determination in irradiated thorium and uranium using ion exchange on ring oven, spectrometric, 20: 36758
distribution in sea water, from waste disposal, 20: 38537
separation from strontium-90 in rain water by ion exchange, 20: 36759
separation from waste solutions using humic acid column, 20: 36930
separation of, from fission products in nitric acid solutions, chromatographic, 20: 36748
transfer from soil to dairy cattle feeds, 20: 37038
uses in graphite sorption studies, 20: 36799
CESIUM ISOTOPES Cs-138
half life measurement, 20: 38017
CESIUM ISOTOPES Cs-139
decay scheme, (E/T), 20: 38124
half life measurement, 20: 38017
CESIUM ISOTOPES Cs-140
decay scheme, (E/T), 20: 38124
half life measurement, 20: 38017
CESIUM OXIDES
ion EPR in single crystals of, erbium and ytterbium, (E), 20: 38391
CESIUM PLUTONIUM CHLORIDES
analysis of, for plutonium using slurry–ion exchange methods, effects of cesium on, 20: 36727
CHARGED PARTICLE BEAMS
focusing in helical magnetic fields, (T), 20: 37334
stability of transverse oscillations of focused, in absorbing media, 20: 38315
CHARGED PARTICLES
absorption by nuclei with formation of compound nuclei, (T), 20: 38020
acceleration in circular accelerators, absorption effects on, (T), 20: 37335
acceleration in neutral sheet of geomagnetic tail, models for, 20: 37901
acceleration of, theory of stochastic, 20: 37336
density and temperature in front of shock wave in air, 20: 37880
detection and measurement of, instrument for, 20: 37080
distribution of geomagnetically trapped, in Van Allen belts, 20: 37911
effects on Van Allen belt formation, drift mechanism for, (T), 20: 37909
energy loss in dielectric media at high energies, (T), 20: 37460
flux in stratosphere, increases of, (E), 20: 37907
flux of high-energy pulses of, beyond magnetospheric shock transition region, (E), 20: 37900
interactions in plasma, moments of velocity change for, (T), 20: 38255

interactions in quantum Vlasov plasma, (T), 20: 38286
interactions with films, transitional radiation from oblique, (T), 20: 37434
motion in helical magnetic fields, 20: 37334
motion in magnetic fields, magnetic moment of, (T), 20: 38208 (PPL-AF-4)
motion in magnetosphere, review of, 20: 37911
motion in non-adiabatic magnetic traps, stochastic, 20: 38246
motion in static magnetic fields, correction to second adiabatic invariant of, (T), 20: 38275
origin of auroral, from geomagnetic tail, (T), 20: 37901
scattering by nonspherical atoms, optical potential for, (T), 20: 37444
scattering of, at high energy, analysis of materials using inelastic, 20: 36732

CHEMICAL ANALYSIS
krypton-85 uses in, 20: 36749

CHEMICAL CONTAMINATION
effects on mercury pool boiling heat transfer, 20: 36987 (NAA-SR-11949)

CHEMICAL RADIATION DETECTORS
performance of acrylic glass, for electron flux measurements, 20: 36689
standards for iron sulfate, secondary, 20: 37090

CHERENKOV DETECTORS
design and performance of gas counter, for cosmic helium isotope measurement, 20: 37581
light coupler for threshold, design and performance of, 20: 37118
performance in middle uv regions for EAS detection, 20: 37717
pulse spectra from, for EAS particle densities, 20: 37619
response of deep, to EAS at 10^{17} ev, 20: 37621

CHICKENS
iron-59 distribution in serum protein fractions, 20: 36569
radiation effects on aging of developing embryos of, x, 20: 36605(R) (COO-1119-5)
zinc-65 uptake from infected intestine of, 20: 36566

CHLORAMPHENICOL
effects on uv radiation effects on pyrimidine dimers in *Micrococcus radiodurans* DNA, 20: 36610
protection against mutation induction in Schizosaccharomyces by nitrite, 20: 36653

CHLORIDE IONS
effects on radioinduced defects in potassium bromide, 20: 36901

CHLORIDES
$Cl^- - NO_3^- - UO_2SO_4$, ion exchange equilibria in, 20: 36931

CHLORINE
content in African pitchblende, estimation of induced fission vs spontaneous fission from, 20: 37994
determination in blood and hair of man, activation, 20: 36728
neutron absorption cross sections for, reactivity method for measuring, 20: 38414
neutron absorption cross section in pitchblende, thermal, 20: 37994
x-ray spectra from mu-mesic atoms of, (E), 20: 38058

CHLORINE ISOTOPES
separation by photochemical methods, 20: 37164

CHLORINE ISOTOPES Cl-35
energy levels at 3.16 and 7.54 Mev, spin-parity and transitions of, (E), 20: 38071
meson (μ^-) capture by protons in, rate of, 20: 38166
mesons (π^-) reactions with, charge exchange in, (E), 20: 37740 (JINR-P-2780)
performance as solar neutrino detector, 20: 37793

CHLORINE ISOTOPES Cl-36
neutron reactions (n,α), phosphorus-33 production in, (E), 20: 37166

CHLORINE ISOTOPES Cl-37
deuteron reactions (d,p) at 7.74 Mev, structure of chlorine-38 from, (E), 20: 38153
energy levels from sulfur-36 (p,γ) reaction, (E), 20: 38185
meson (μ^-) capture by protons in, rate of, 20: 38166
neutrino capture rate in, (T), 20: 37366
neutrino reactions with, cross section for, (T), 20: 38111
proton reactions (p,n) at 1.63 to 1.71 Mev, Q value of, (E), 20: 38028

CHLORINE ISOTOPES Cl-38
energy levels of, from chlorine-38 (d,p) reaction, (E), 20: 38153

CHROMATOGRAPHY
isotope separation by, estimation of separation factor in, 20: 37162

CHROMIUM
content of, in sediments of Bay of Roquebrune, 20: 36553
corrosion by boiling hydrofluoric acid–nitric acid solutions, 20: 37169(R) (BMI-1774)
determination of, in uranium, by activation analysis, 20: 36715
determination of, in ores by neutron activation analysis, 20: 36750
distribution of, in marine organisms, 20: 36552
effects on compatibility of mixed carbide reactor fuels with stainless steel, 20: 38466 (ANL-7120, pp 301-13)
effects on crystal field properties of zirconium oxide, 20: 36854
separation from metal mixtures by thin layer chromatography, 20: 36753

CHROMIUM ALLOYS
Al–Cr, superconducting critical temperature of, transition-metal impurity effects on depression of, (E), 20: 37955
Be–Cr–Nb, tensile properties of, 20: 37245
Cr–Co–Fe–Mn–Mo–Ni, corrosion of Vitallium, by boiling hydrofluoric acid–nitric acid solutions, 20: 37169(R) (BMI-1774)
Cr–Co–Fe–Mn–Mo–Ni–Ti, corrosion of Hanford 22, by boiling hydrofluoric acid–nitric acid solutions, 20: 37169(R) (BMI-1774)
Cr–Co–Fe–Mo–Ni, corrosion of Haynes 21, by boiling hydrofluoric acid–nitric acid solutions, 20: 37169(R) (BMI-1774)
Cr–Co–Fe–Mn–Mo–Ni–Ti, corrosion of Hanford 23 and 24, by boiling hydrofluoric acid–nitric acid solutions, 20: 37169(R) (BMI-1774)
Cr–Co–Fe–W, corrosion of Rexalloy 33, by boiling hydrofluoric acid–nitric acid solutions, 20: 37169(R) (BMI-1774)
Cr–Cu–Fe–Mn–Mo–Ni–Ti, corrosion of Hanford 21, by boiling hydrofluoric acid–nitric acid solutions, 20: 37169(R) (BMI-1774)
Cr–Cu–Fe–Mn–Mo–Ni, corrosion of Illium R, by boiling hydrofluoric acid–nitric acid solutions, 20: 37169(R) (BMI-1774)
Cr–Fe–Mn–Mo–Ni–Ti, corrosion of Hanford 20, by boiling hydrofluoric acid–nitric acid solutions, 20: 37169(R) (BMI-1774)
Cr–Fe–Mn–Mo–Ni–Ti, corrosion of Hanford 17, by boiling hydrofluoric acid–nitric acid solutions, 20: 37169(R) (BMI-1774)
Cr–Fe–Mn–Ni, corrosion of corronel 230, by boiling hydrofluoric acid–nitric acid solutions, 20: 37168(R) (BMI-1771)
Cr–Fe–Mn–Ni, corrosion of corronel 230, by boiling hydrofluoric acid–nitric acid solutions, 20: 37169(R) (BMI-1774)
Cr–Nb, phase studies of intermetallic compound, 20: 37239
Cr–Ni, corrosion of Blaw Nox NA 55 and NA 64 by boiling hydrofluoric acid–nitric acid solutions, 20: 37169(R) (BMI-1774)
Cr–Re, oxidation at high temperatures, mechanisms of, 20: 37186
Cr–Y, properties of chromium-base, effects of interstitial nitrogen and oxygen on, 20: 37168(R) (BMI-1771)
Cr–Y, solubility of nitrogen in chromium-base, 20: 37169(R) (BMI-1774)
Cr–Zn, superconducting critical temperature of, transition-metal impurity effects on depression of, (E), 20: 37955

CHROMIUM CARBIDES
effects on compatibility of mixed carbide reactor fuels with stainless steel, 20: 38466 (ANL-7120, pp 301-13)

CHROMIUM CHLORIDES
reactions with isopropylamine, thermogravimetric study of, 20: 36853

CHROMIUM IONS
effects on copper determination, 20: 36726
effects on formation of single-crystal beryllium oxide, 20: 36814

CHROMIUM ISOTOPES Cr-52
carbon-12 reactions with, formation and decay of zinc-64 in, 20: 38152
deuteron reactions (d,p) at 8 to 11 Mev, (E/T), 20: 38046
deuteron reactions (d,p) with finite-range distorted-wave calculations for, (T), 20: 38047
proton reactions (p,n) with, thresholds for, (E), 20: 38053

CHROMIUM ISOTOPES Cr-53
proton reactions (p,n) with, manganese-53 energy levels from, (E), 20: 38034

CHROMIUM NITRATES
radiation effects on electric conductivity of solutions of, gamma, 20: 36912

CHROMIUM OXIDES
formation by oxidation of chromium–rhenium alloys, mechanisms of high-temperature, 20: 37186
reactions with lanthanum and neodymium oxides in solid state, 20: 36840
$Ce_2O_3 - Cr_2O_3$, phase studies at temperatures to 2600°C, 20: 36808

CHROMIUM SULFATES
radiolysis of hydrated, gamma, 20: 36903

CHROMOSOMES
frequency of lethal, following cessation of radiation, 20: 36618
interphase volume estimation, 20: 36551
mapping of, by radioinduced mutations in synchronous populations of *Streptococcus faecalis*, 20: 36635
radiation effects on barley seed, effects of diethyl pyrocarbonate on fast neutron and gamma, 20: 36589
radiation effects on breakages in, thermal neutron, 20: 36644

CITRATES
effects on plutonium-237 excretion in rats, 20: 37025(R) (PG-Report-705)
effects on strontium-90 excretion in rats, 20: 37025(R) (PG-Report-705)

CITRIC ACID
complexes with americium-241 and curium-246, formation of, electrophoretic studies of, 20: 36829

CIVILIAN DEFENSE
protection of population from incendiary attacks, 20: 36995 (AD-636794)

CLOUD CHAMBERS
design of large Wilson, for ionization calorimetry studies, 20: 37108

COAL

analysis for ash content, using backscattering of x radiation, 20: 37153
analysis of, system for continuous on-line activation, 20: 36769
cost of fuel, comparison with nuclear fuels, 20: 38541
electric power from, cost comparison with nuclear-generated, 20: 38520

COATINGS
deposition and performance of silicon carbide, on molybdenum and tungsten, 20: 37189
deposition of aluminum and silicon on sintered molybdenum, process for, 20: 37204
deposition of, processes for refractory metal protection, 20: 37192
effects of brittle, on D-43 and TZM alloys, 20: 37276
for reactor fuel elements, corrosion, inspection, and welding of, 20: 37208
performance at high temperatures, evaluation methods, 20: 37192
performance of carbon, on urania particles in radiation fields, 20: 37168(R) (BMI-1771)
preparation of high-purity rare earth and transition-metal oxide, methods for, 20: 36851
testing of materials for fuel, 20: 37174
thickness measurements on, by scattering of accelerated alpha particles, 20: 36719

COBALT
content of, in sediments of Bay of Roquebrune, 20: 36553
determination in uranium compounds by neutron activation analysis, 20: 36714
determination in zinc sulfate and sulfide, interfering reactions in activation, 20: 36755
determination in zinc sulfate and sulfide using ion exchange chromatography and activation methods, 20: 36757
effects on determination of iridium in ores by neutron activation analysis, 20: 36751
neutron absorption cross sections for, reactivity method for measuring, 20: 38414
neutron absorption cross section in pitchblende, thermal, 20: 37994
neutron total cross sections at high energies, fluctuations in, 20: 38173
separation from metal mixtures by thin layer chromatography, 20: 36753
separation from neutron-irradiated biological materials by ion exchange, 20: 36762
separation of, from thallium by ion-exchange chromatography, 20: 36935

COBALT ALLOYS
effects of beryllium additions on, 20: 37275
Be–Co–Cu, precipitation in, effects of additive metals in discontinuous, 20: 37253
Ce–Co, crystal structure of intermetallic compounds in, 20: 37243
Ce–Co–Mn–Pu, analysis for cerium and manganese by ion exchange separation and potentiometric titration, 20: 36713 (LA-3402)
Ce–Co–Pu, analysis for cerium by ion exchange separation and potentiometric titration, 20: 36713 (LA-3402)
Ce–Co–Pu, combustion of, properties of aerosols produced in, 20: 37022 (LA-DC-6942)
Co–Dy, crystal structure of intermetallic compounds in, 20: 37243
Co–Er, crystal structure of intermetallic compounds in, 20: 37243
Co–Gd, crystal structure of intermetallic compounds in, 20: 37243
Co–Ho, crystal structure of intermetallic compounds in, 20: 37243
Co–La, crystal structure of intermetallic compounds in, 20: 37243
Co–Nd, crystal structure of intermetallic compounds in, 20: 37243
Co–Pr, crystal structure of intermetallic compounds in, 20: 37243
Co–rare earth, crystal structure of intermetallic compounds in, 20: 37243
Co–rare earths, magnetic properties of $LnCo_2$ series, 20: 37279
Co–Sm, crystal structure of intermetallic compounds in, 20: 37243
Co–Tb, crystal structure of intermetallic compounds in, 20: 37243
Co–Y, crystal structure of intermetallic compounds in, 20: 37243
Co–Zn, critical temperature of superconducting, transition-metal impurity effects on depression of, (E), 20: 37955
Cr–Co–Fe–Mn–Mo–Ni, corrosion of Vitallium, by boiling hydrofluoric acid–nitric acid solutions, 20: 37169(R) (BMI-1774)
Cr–Co–Fe–Mn–Mo–Ni–Ti, corrosion of Hanford 22, by boiling hydrofluoric acid–nitric acid solutions, 20: 37169(R) (BMI-1774)
Cr–Co–Fe–Mn–Mo–Ni–Ti, corrosion of Hanford 23 and 24, by boiling hydrofluoric acid–nitric acid solutions, 20: 37169(R) (BMI-1774)
Cr–Co–Fe–Mo–Ni, corrosion of Haynes 21, by boiling hydrofluoric acid–nitric acid solutions, 20: 37169(R) (BMI-1774)
Cr–Co–Fe–W, corrosion of Rexalloy 33, by boiling hydrofluoric acid–nitric acid solutions, 20: 37169(R) (BMI-1774)

COBALT CHLORIDES
reactions with isopropylamine, thermogravimetric study of, 20: 36853

COBALT(II) COMPLEXES
with dimethylglyoxime, magnetic moments for, 20: 36823
with salicylaldehyde and its derivatives, magnetic moments of, 20: 36823

COBALT IONS
effects on copper determination, 20: 36726

COBALT ISOTOPES Co-56
beta decay of, iron-56 energy levels from, (E), 20: 38088

COBALT ISOTOPES Co-59
alpha reactions at 20 to 50 Mev, copper-63 compound nucleus formation in, (E), 20: 38147

COBALT ISOTOPES Co-60
distribution in sea water, from waste disposal, 20: 38537
production and use of, for heat and radiation sources, economics of, 20: 37165
separation from waste solutions using humic acid column, 20: 36930
use in radiotherapy, determination of isodose curves for, 20: 36688
use in remotely controlled unit for uterine cancer radiotherapy, 20: 36687

COBALT SULFATES
radiolysis of hydrated, gamma, 20: 36903

COINCIDENCE CIRCUITS
design and performance of, for x-ray spectrometry, 20: 37093

COINCIDENCE COUNTERS
design and performance of multidirectional meson telescope, 20: 37095
performance of high-resolution magnetic, theoretical analysis for, 20: 37106

COLLAGEN
radiation effects on, in kangaroo and mouse skin, uv, 20: 36595
radioinduced free radicals in, electron spin resonance spectra of, 20: 36585

COLLIMATORS
performance of gamma, Compton scattering effects on, 20: 37465

COMBUSTION
method of oxygen-flask, for determination of tritium and carbon-14 by liquid scintillation, 20: 36764

COMBUSTION ANALYSIS
method for, of tritium-labeled biological material, 20: 36763

COMETS
structure of, solar wind effects on, 20: 37386(T)

COMPACTS
chemical reactions in aluminum–urania, at 600°C, 20: 37203

COMPRESSORS
performance of single-stage jet, 20: 37724

COMPUTER PROGRAMS
AIREK C3, use for reactor core meltdown analysis, 20: 38472 (ANL-7120, pp 514-23)
ANDREA, for coolant density profile and neutron flux distributions in light-water moderated reactors, 20: 38450
AX1, for calculation of fast reactor excursions, equation of state for use in, 20: 38435 (ANL-7120, pp 686-91)
CUSH, for steady-state hydraulic analysis of steam-generating reactor systems, 20: 38410 (AEEW-M-474)
FLIRT, for reactor axial stability analysis, 20: 38446 (TRG-Report-1138)
for calculating axisymmetric thermoelastic problems in bispherical coordinates, 20: 36957 (DRI-2327)
for calculation of argon-cesium fluoride reaction cross sections, 20: 37478
for estimating refabrication costs for metal fuels, 20: 37195 (ANL-6950)
for hydraulic analysis of pressurized boiling reactor loops, 20: 38502(R) (EURAEC-1662)
for reactor containment structure analysis, 20: 38463 (IITRI-578P22-15)
for reactor shutdown by xenon poisoning, 20: 38411 (BNWL-186)
for rocket reactor excursion analysis, 20: 38525(R) (NUS-208)
for rotordynamic analysis of SNAP-2 Combined Rotating Unit-V, 20: 36977 (NAA-SR-11944)
for shielding calculations, 20: 38350 (ORNL-P-2310)
FRENIC, for analysis of beta-decay curves on IBM-709, 20: 37995
NURSE-1, application to rocket reactor effluent transport, 20: 38525(R) (NUS-208)
P1MG, for analysis of distributed reactor control pins, 20: 38441 (BAW-3492-1(Suppl.1))
RSAC, for calculation of radiation doses from release of fission products in atmosphere, symbolic, for IBM 7040, 20: 37167 (IDO-17151)
SPECTRA, for determining neutron flux from foil activation data, 20: 37076 (SC-DC-66-1512)
THERMOS, for analysis of distributed reactor control pins, 20: 38441 (BAW-3492-1(Suppl.1))
TRANS, for conversion of form of neutron elastic scattering data stored in ROC nuclear data library, 20: 37989 (WAPD-TM-573)

COMPUTERS
use for plasma diagnostics, 20: 38310
use for shielding calculations, 20: 38350 (ORNL-P-2310)
use for simulation of plasma anomalous diffusion, 20: 38328
use for simulation of annealing of Frenkel defects in crystal lattices, 20: 37294
use for simulation of electron-ion collisions in plasma diodes, 20: 37726
use for studying dose distribution in radiotherapy, 20: 36686
use of analog, for transient neutron flux distribution analysis, 20: 38431 (ANL-7120, pp 625-31)

use of PDP-7 on-line for data analysis in nuclear physics experiments, 20: 38176

CONCRETES
neutron penetration in, fast, (E), 20: 38352
prestressed, development for reactor pressure vessels, 20: 38523

CONFERENCES
see also introduction to Report Number Index
Radioisotope Instruments in Industry and Geophysics, Symposium on, Warsaw, Poland, Oct. 1965, summary of, 20: 37143
Safety, Fuels, and Core Design in Large Fast Power Reactors, Conference on, Argonne National Lab., Oct. 11–14, 1965, 20: 38489 (ANL-7120)

CONVERSION ELECTRONS
emission by californium-252 fission fragments, (E), 20: 38095

COPPER
content in African pitchblende, estimation of induced fission vs spontaneous fission from, 20: 37994
content of, in sediments of Bay of Roquebrune, 20: 36553
determination in fats, activation, 20: 36724
determination in zinc sulfate and sulfide, interfering reactions in activation, 20: 36755
determination in zinc sulfate using ion exchange and activation methods, 20: 36756
determination of trace amounts of, in niobium and tantalum by absorption spectroscopy, effects of ions on, 20: 36726
determination of, in uranium, by activation analysis, 20: 36715
effects on determination of iridium in ores by neutron activation analysis, 20: 36751
electron absorption at 100 kev in, temperature dependence of, (E), 20: 38379
energy levels of ionized, forbidden transitions in, 20: 37432
gamma reactions (γ,α) at 31 Mev, alpha spectra from, (E), 20: 38037
gamma reactions at 6.13 Mev, pair-production cross sections for, (E), 20: 37746
laser beam reactions with, uv spectra from plasma produced from, (E), 20: 38300
neutron absorption cross sections for, reactivity method for measuring, 20: 38414
neutron absorption cross section in pitchblende, thermal, 20: 37994
plutonium determination on plates of, by alpha counting, 20: 36736
positron annihilation with core electrons in, momentum distributions for, (T), 20: 37821
proton reactions at 600 Mev, cross sections for meson ($\pi^{\pm}$) production in, 20: 38186
proton reactions at 70 to 100 kev, x ray emission from, (E), 20: 38393
radiation damage in, from zinc ion reactions at 150 kev, annealing of, (E), 20: 38378
radiation effects on nickel diffusion in, alpha, 20: 37300
radioinduced defects in, model for change in elastic modulus from, 20: 37296
separation from metal mixtures by thin layer chromatography, 20: 36753
separation from neutron-irradiated biological materials by ion exchange, 20: 36762
separation of, from thallium by ion-exchange chromatography, 20: 36935
sputtering by neon, argon, krypton, and xenon ions at 100 kev to 1 Mev, 20: 37468
thermal capacity at 250 to 930°C, 20: 37278
yields from radiolysis of copper phthalocyanine, 20: 36886

COPPER ALLOYS
effects of beryllium additions on, 20: 37275
Be–Co–Cu, precipitation in, effects of additive metals on discontinuous, 20: 37253
Be–Cu, precipitation in, effects of additive metals on discontinuous, 20: 37253
Cr–Cu–Fe–Mn–Mo–Ni–Ti, corrosion of Hanford 21, by boiling hydrofluoric acid–nitric acid solutions, 20: 37169(R) (BMI-1774)
Cr–Cu–Fe–Mn–Mo–Ni, corrosion of Illium R, by boiling hydrofluoric acid–nitric acid solutions, 20: 37169(R) (BMI-1774)
Cu–W, properties of tungsten-strengthened composite, 20: 37246
Cu–Zr, oxidation by carbon monoxide at high temperatures, mechanisms of, 20: 37183

COPPER BROMIDES
$CdBr_2$–CuBr, phase diagrams, 20: 36787 (YALE-2723(Vol.1))
CuBr–AgBr, phase diagrams, 20: 36787 (YALE-2723(Vol.1))
CuBr–CuI, phase diagrams, 20: 36788 (YALE-2723(Vol.2))
CuBr–KBr, phase diagrams, 20: 36788 (YALE-2723(Vol.2))

COPPER CHLORIDES
reactions with isopropylamine, thermogravimetric study of, 20: 36853
$BiCl_3$–CuCl, phase diagrams, 20: 36787 (YALE-2723(Vol.1))
$CaCl_2$–CuCl, phase diagrams, 20: 36787 (YALE-2723(Vol.1))
$CdCl_2$–CuCl, phase diagrams, 20: 36787 (YALE-2723(Vol.1))
CsCl–CuCl, phase diagrams, 20: 36788 (YALE-2723(Vol.2))
CuBr–CuCl, phase diagrams, 20: 36788 (YALE-2723(Vol.2))
CuCl–AgCl, phase diagrams, 20: 36787 (YALE-2723(Vol.1))
CuCl–CuI, phase diagrams, 20: 36788 (YALE-2723(Vol.2))
CuCl–HgCl, phase diagrams, 20: 36788 (YALE-2723(Vol.2))
CuCl–KCl, phase diagrams, 20: 36788 (YALE-2723(Vol.2))
CuCl–LiCl, phase diagrams, 20: 36788 (YALE-2723(Vol.2))
$CuCl–MgCl_2$, phase diagrams, 20: 36788 (YALE-2723(Vol.2))
$CuCl–PbCl_2$, phase diagrams, 20: 36788 (YALE-2723(Vol.2))
CuCl–RbCl, phase diagrams, 20: 36788 (YALE-2723(Vol.2))
$CuCl–SnCl_2$, phase diagrams, 20: 36788 (YALE-2723(Vol.2))
CuCl–TlCl, phase diagrams, 20: 36788 (YALE-2723(Vol.2))
$CuCl–ZnCl_2$, phase diagrams, 20: 36788 (YALE-2723(Vol.2))

COPPER IODIDES
CdI_2–CuI, phase diagrams, 20: 36788 (YALE-2723(Vol.2))
CuBr–CuI, phase diagrams, 20: 36788 (YALE-2723(Vol.2))
CuCl–CuI, phase diagrams, 20: 36788 (YALE-2723(Vol.2))
CuI–AgI, phase diagrams, 20: 36787 (YALE-2723(Vol.1))

COPPER ISOTOPES Cu-60
energy levels, (E), 20: 38053

COPPER ISOTOPES Cu-61
energy levels, (E), 20: 38053

COPPER ISOTOPES Cu-62
energy levels, (E), 20: 38053

COPPER ISOTOPES Cu-63
compound nucleus formation by alpha, carbon-ion, and proton reactions, (E), 20: 38147
deuteron elastic scattering at 13.6 Mev, differential cross sections for, (E), 20: 38128
energy levels, (E), 20: 38053
proton reactions with, formation and decay of zinc-64 in, 20: 38152
triton reactions (t,p) at 12 Mev, copper-65 energy levels from, (E), 20: 38035

COPPER ISOTOPES Cu-65
deuteron elastic scattering at 13.6 Mev, differential cross sections for, (E), 20: 38128
energy levels from copper-63 (t,p) reactions, (E), 20: 38035
triton reactions (t,p) at 12 Mev, copper-67 energy levels from, (E), 20: 38035

COPPER ISOTOPES Cu-67
energy levels from copper-65 (t,p) reactions, (E), 20: 38035

COPPER MINERALS
flotation of bornite, on gamma-irradiated anionic collector agents, 20: 36893

COPPER NITRATES
radiation effects on electric conductivity of solutions of, gamma, 20: 36912

COPPER PERCHLORATES
radiation effects on electric conductivity of solutions of, gamma, 20: 36912

COPPER SULFATES
radiation effects on electric conductivity of solutions of, gamma, 20: 36912
radiolysis of hydrated, gamma, 20: 36903

CORROSION-RESISTANT ALLOYS
production of zirconium, 20: 37194(P)

CORTISONE
radiosensitivity effects on animals, review on, 20: 36668

COSMIC ALPHA PARTICLES
content in primary cosmic radiation, (E), 20: 37572
content in primary cosmic radiation, (E), 20: 37581
energy and rigidity spectra at 82 to 600 Mev/nucleon, 20: 37558
energy and rigidity spectra in primary cosmic radiation, at 80 to 150 Mev/nucleon, (E), 20: 37579
energy spectra and flux at 30 to 90 Mev/nucleon, time variations of differential, 20: 37563
energy spectra at 70 to 1300 Bev/nucleon, differential and integral, (E), 20: 37551
energy spectra at 0.6 to 16 Bv rigidity, modulation of, (E), 20: 37554
energy spectra at low rigidities, differential, (T), 20: 37561
energy spectra of primary, at 6 to 20 Bev, (E), 20: 37557
energy spectra of primary, mechanisms for, (E), 20: 37562
energy spectra of, time variation during declining solar activity, (E), 20: 37560
flux of primary, above 16 Bv rigidity, 20: 37582
flux of primary, asymmetry effects on, 20: 37582
flux of, dependence on solar activity, (E), 20: 37556
intensities of primary, integral, (E), 20: 37575
intensity during 1963 to 1965, solar modulation of, (E/T), 20: 37553

COSMIC ELECTRONS
asymmetry and flux of primary at 4.5 Bv geomagnetic rigidity cutoff, (E), 20: 37550
distribution of high-energy, in EAS cores, (E), 20: 37638
distributions in photon-initiated cascade showers, mean square angular and lateral, (T), 20: 37648

energy spectra at 2 to 15 Bev, differential, (E), 20: 37549
energy spectra of, galactic acceleration efficiency and solar modulation determination from, (E), 20: 37499
flux at $3(10)^8$ to $2(10)^{10}$ ev, 20: 37495
flux of primary, above 3.5 and 8 Bev, (E), 20: 37548
intensity of, differential and integral, (E), 20: 37551
origin of primary, correlations with nonthermal galactic radio emission, 20: 37496
properties of primary, review of, 20: 37496

COSMIC MESONS
detection and measurement of, design and performance of multidirectional telescope for, 20: 37095
flux of, meteorological corrections for measurements of, 20: 37101
intensity variations during 11-year solar cycle, (E), 20: 37515
intensity variation of, correction for atmospheric effects on diurnal, (T), 20: 37585
measurement of positive excess in Cairo of, spectrometer for, 20: 37487
production in nucleon-air nucleus interactions, K/π ratio for, (E), 20: 37697
production of high-energy single K, model for, 20: 37692

COSMIC MESONS (μ)
angular and energy distribution and structural bursts at 0.3 to 3.0 Tev, underground, (E), 20: 37693
angular distribution and vertical intensity at 816 to 4100 mwe underground, (E), 20: 37704
attenuation in EAS, barometric effect for determining, (E), 20: 37623
burst production by high-energy near-horizontal, at sea level, (E), 20: 37695
charge ratio and differential momentum spectrum in EAS, (E), 20: 37643
charge ratio at 20 to 200 Bev/c, energy dependence of positive excess in, (E), 20: 37690
charge ratio below 1000 Bev at sea level, energy dependence of, (E), 20: 37689
charge ratio of, energy dependence of, (E), 20: 37687
charge ratio of, mechanism for positive excess in, (T), 20: 37692
coupling coefficients of directed, angular dependence of, (T), 20: 37588
distribution and flux in EAS, (E), 20: 37645
distribution in EAS, anisotropy determination from, (E), 20: 37607
energy loss of very high energy, depth dependence above 2200 mwe underground, (E), 20: 37705
energy spectra, (E/T), 20: 37696
energy spectra and production in EAS, model for, 20: 37613
energy spectra and lateral distribution in electromagnetic air showers, (T), 20: 37622
energy spectra at sea level, relation to depth-intensity curve, (T), 20: 37706
energy spectra for truncated primary, (T), 20: 37677
flux at 10^9 to 10^{14} ev at sea level, positive excess in, (T), 20: 37688
flux at 3860 m above sea level, $K + \mu + \gamma$ contribution to, (E), 20: 37482
flux in EAS above 200 and 640 Bev, absolute number in, (E), 20: 37606
flux of, correlations with sidereal time, (E), 20: 37713
intensity fluctuations in EAS, semi-empirical determination of, 20: 37624
intensity of stopping, at sea level and 60 mwe underground, (E), 20: 37709
intensity variations of, periodic, 20: 37525
interactions at 0.1 to 10^3 Bev at 60 mwe underground, electromagnetic, (E), 20: 37699
interactions in lead, intranuclear cascade effects on multiplicity distributions from, (E/T), 20: 37702
interactions with lead at 0.3 to 30 Bev at 60 mwe underground, electromagnetic shower production from, (E), 20: 37700
interactions with lead at 816 to 4100 mwe underground, particle production frequencies from, (E), 20: 37701
momentum spectra below 2000 Bev/c at 82.5 to 90° zenith angle, (E), 20: 37697
nuclear reactions induced by, processes leading to, (T), 20: 37703
propagation in EAS, lateral distribution, energy spectra, and heights of origin for, (E), 20: 37641
properties in EAS, models for, 20: 37640
properties of showers of, at 60 Mw(e) underground, (E), 20: 37605
range fluctuation of high-energy, knock-on and ionization loss effects on, (T), 20: 37708
reactions with nuclear matter and water, energy losses from relativistic, (T), 20: 37707
reactions with nuclei at 58 mwe underground, fast neutron differential energy spectrum from, (E), 20: 37710
reactions with nuclei at $3(10)^{14}$ ev, horizontal air shower production from, (E), 20: 37714
research on, review of, 20: 37715
spectra at 10^{11} to 10^{12} ev at 600 Mw(e) underground, integral burst, (E), 20: 37694

COSMIC MESONS (π)
energy spectra and production in EAS, model for, 20: 37613
intensity of stopping positive, at sea level and 60 mwe underground, (E), 20: 37709
production in cosmic nuclear interactions, multiplicity of, (T), 20: 37691
production in nucleon-air nucleus interactions, K/π ratio for, (E), 20: 37697
production of high-energy single, model for, 20: 37692
reactions in carbon, lead, and iron, energy transfer to photons from, (E), 20: 37660
transmission through thin layers of matter at 0.1 to 20 Bev/c, shower production from, (E), 20: 37669

COSMIC NEUTRINOS
detection of, design of instruments for, 20: 37104
detection of, method for, 20: 37491
detection underground, method for, 20: 37481 (COO-818-86)
emission from neutron stars, properties of, 20: 37355
energy spectra at 7500 mwe underground, zenith angle dependence of, (E), 20: 37711
flux of solar, model calculation of, 20: 37403
flux of, correlations with sidereal time, (E), 20: 37713
fluxes of, for astrophysical studies, 20: 37395
interactions at 7500 mwe underground, cross sections for, (E), 20: 37711
properties in pre-supernova evolution, 20: 37406
reactions with nuclei at $3(10)^{14}$ ev, horizontal air shower production from, (E), 20: 37714
research on, review of, 20: 37715

COSMIC NEUTRONS
attenuation in carbon and paraffin at 60 Bev, collision mean free path and neutron-proton cross section from, (E), 20: 37670
energy spectra of fast, differential, 20: 37555
energy spectra of secondary, at 1 to 10 Mev, (E), 20: 37599
flux of, altitude effects on performance of monitor for measuring, 20: 37099
flux of, barometric pressure effects on monitor for, 20: 37096
flux of, barometric coefficient effects on monitor for, 20: 37097
flux of, meteorological effects on monitor counting rate for measuring, 20: 37100
flux of, multiplicity effects on monitor for measuring, 20: 37098
intensity, (E), 20: 37519
intensity distributions in South African magnetic anomaly, latitude dependence of, (E), 20: 37592
intensity modulation of, asymmetric solar wind correlations with 27-day, (E), 20: 37528
intensity of, albedo flux from, (E), 20: 37601
intensity of, frequency distribution of sudden increases in, (E), 20: 37541
intensity variation of, variation of time of maximum of diurnal, (E), 20: 37524
intensity variations of, periodic, 20: 37525
intensity variation during solar cycle, amplitude and phase of diurnal, (E), 20: 37527
intensity variations in, data smoothing for measurements of, (T), 20: 37544
intensity variations of, correlations with geomagnetic H component, (E), 20: 37590
intensity variations of, correlations with altitude and primary rigidity cutoff, (E), 20: 37593
reactions with carbon and lead at 100 Bev, cross sections for, (E), 20: 37668

COSMIC NUCLEONS
arrival time in air showers, (T), 20: 37633
energy spectra and production in EAS, model for, 20: 37613
energy spectra for truncated primary, (T), 20: 37677
flux in atmosphere at 10^{11} to 10^{13} ev, interaction path determination from, (E), 20: 37667
intensity distributions in South African magnetic anomaly, latitude dependence of, (E), 20: 37592
intensity variations during 11-year solar cycle, (E), 20: 37515
interactions above 10^3 ev, design and performance of equipment for measuring, 20: 37657
interactions at 10 Tev, research on, 20: 37786
interactions in emulsions at 25 and 10^3 Bev, isobar production from, (T), 20: 37675
reactions in iron at high energies, cascade shower production from, (T), 20: 37789

COSMIC PARTICLES
abundance of nuclei ($2 \leq Z \leq 14$), at 20 to 300 Mev/nucleon, (E), 20: 37564
arrival time of heavy, in air showers, (T), 20: 37633
carbon isotope abundance in primary, estimation of relative, (E), 20: 37574
charge and energy measurement of, performance of silicon telescope detectors for, 20: 37575

charge and energy spectra at 0.02 to 1 Bev/nucleon, at solar minimum, (E), 20: 37578
composition and energy spectra of nuclei ($Z \geq 3$), (E), 20: 37568
composition of, (E), 20: 37583
detection and measurement of, design and performance of instrument for, 20: 37103
detection of quarks, technique for, 20: 37718
energy spectra and intensity of nuclei ($Z \geq 20$) at 240 to 650 Mev/nucleon, differential, (E), 20: 37566
energy spectra of nuclei ($3 \leq Z \leq 26$), at 1.5 to 16 Bv, (E), 20: 37571
energy spectra of nuclear-active, in EAS, (E), 20: 37635
flux in EAS cores below $2\ (10)^{15}$ Bev/c, (E), 20: 37616
flux of heavy nuclei at low energies, (E), 20: 37569
flux of heavy, from high-energy interactions, 20: 37719
flux of heavy, upper limit for, (E), 20: 37654
flux of nuclear-active, at low energies in EAS, (E), 20: 37614
flux of nuclei ($Z \geq 3$) in, (E), 20: 37565
flux of nuclei ($2 \leq Z \leq 15$), above 600 Mev/nucleon, (E), 20: 37600
flux of primary nuclei, at 200 to 600 Mev/nucleon, (E), 20: 37573
flux of quarks in atmosphere, (T), 20: 37718
helium isotope content in primary, ratio of, (E), 20: 37581
interactions above 100 Tev, meson and nucleon inelasticity and fireball transverse momentum determinations from, (E), 20: 37661
interactions above 10^{14} ev, fireball mass estimation for, (T), 20: 37681
interactions at high energies, review of, 20: 37686
interactions at high energies, hypothetical heavy particle flux from, (T), 20: 37719
interactions at ultra-high energies in jets, criterion for detection of, 20: 37683
interactions at 100 to 1000 Bev, strong, (E), 20: 37656
interactions in lead and iron at 100 Bev, cascade shower distributions from, (E), 20: 37698
interactions of nuclear-active, (E), 20: 37658
interactions of, methods for determining properties of, (T), 20: 37671
interactions of, meson (π) multiplicity in, (T), 20: 37691
interactions with matter, design of installation for detecting, 20: 37684
production of heavy, in air showers, (E), 20: 37653
properties of charged and neutral nuclear-active, above 100 Bev, (E), 20: 37685
reactions in aluminum and carbon, four-momentum transfer in, (E/T), 20: 37659
reactions in nuclear emulsions, 20: 38168
reactions of nuclear-active, with light nuclei, (E), 20: 37755
reactions with carbon, meson (π) production in showers from, (E), 20: 37664
reactions with graphite at high energies, gamma and meson (π) production from, (E), 20: 38110
spectra of heavy ion, (E), 20: 37577
trajectories of medium-energy, magnetopause effects on, (T), 20: 37597

COSMIC PHOTONS

density of intergalactic starlight, (T), 20: 37374
distribution of high-energy, in EAS cores, (E), 20: 37638
distributions in photon-initiated cascade showers, mean square angular and lateral, (T), 20: 37648
energy spectra and flux of primary x-ray, at 20 to 50 kev, (E), 20: 37580
energy spectra for truncated primary, (T), 20: 37677
energy spectra of isotropic, (E), 20: 37500
flux at 10^8 to $3(10)^9$ ev, 20: 37495
flux from stellar sources, limits for, (E), 20: 37547
intensity in meson (μ)-poor EAS, (E), 20: 37609
measurement of primary gamma, atmospheric gamma production effects on, (E/T), 20: 37576

COSMIC PROTONS

doses from solar-flare, properties of, 20: 37915
emission in solar flares, (T), 20: 37346
energy spectra at 80 to 4000 Bev, differential and integral, (E), 20: 37551
energy spectra at 0.6 to 16 Bv rigidity, modulation of, (E), 20: 37554
energy spectra at low rigidities, differential, (T), 20: 37561
energy spectra of primary, mechanisms for, (E), 20: 37562
energy spectra of, time variation during declining solar activity, (E), 20: 37560
flux of primary cascade-producing, (E), 20: 37672
flux of primary, above 16 Bv rigidity, 20: 37582
flux of primary, asymmetry effects on, 20: 37582
intensities of primary, integral, (E), 20: 37575
intensity during 1963 to 1965, solar modulation of, (E/T), 20: 37553
intensity in meson (μ)-poor EAS, (E), 20: 37609
interactions in emulsion chamber above 2 Tev, energy spectra, flux, and jet from, (E), 20: 37673
interactions with protons, effective cross section for inelastic, (E), 20: 37495
motion of, viscous model of solar wind, (T), 20: 37350
rigidity spectra at solar minimum, (E), 20: 37538
scattering by carbon, effective cross section for inelastic, (E), 20: 37495
scattering by emulsion nuclei at 3 Tev, upper limit for nucleon-proton cross section for elastic, (E), 20: 37666
transmission through thin layers of matter at 0.1 to 20 Bev/c, shower production from, (E), 20: 37669

COSMIC RADIATION

absorption of x, by intergalactic and interstellar matter, 20: 37485
acceleration and intensity modulation of, determination from cosmic electron energy spectra, (T), 20: 37499
calcium and lithium production from, in iron meteorites, (E), 20: 37603
composition and energy spectrum of primary, at 10^{10} to 10^{14} ev, (E), 20: 37495
composition at 0.4 to 30 Bev/nucleon, 20: 37495
composition of, (E), 20: 37583
conference, 20: 37492
cutoff rigidities and impact zones of, magnetospheric effects on, (T), 20: 37598
detection deep underground, 20: 37735(R) (COO-818-96)
detection of, scintillation counter pulse-shape discrimination for, 20: 37111
diffusion in solar system, model for, 20: 37511
diffusion in solar system of galactic, (T), 20: 37345
effects of friction of, on solar wind, (T), 20: 37372
electron–positron component of primary, review of, 20: 37496
energy and intensity during solar cycle, spectrum for anisotropy variation in, 20: 37520
energy and intensity during solar minimum, chromospheric flare and Forbush effects on, (E), 20: 37537
energy of charged, sidereal anisotropy effects on, 20: 37484
energy spectra and intensity at 10^{12} to 10^{13} ev, experiment for determining, 20: 37676
energy spectra of charge components in primary, comparison prior to solar modulation, (E), 20: 37570
energy spectra of primary, stochastic acceleration effects on, (T), 20: 37336
flux of, exploding galaxy contributions to, 20: 37370
flux of, semi-diurnal anisotropy of, 20: 37521
flux parallel to earth rotation axis, anisotropy of, (E), 20: 37540
flux variation in stratosphere, height dependence of, (E), 20: 37552
flux variations of, energy properties of 11-year, 20: 37497
geomagnetic variations of corpuscular, in auroral zone, 20: 37897
helium isotope energy and rigidity spectra in primary, at 80 to 150 Mev/nucleon, (E), 20: 37579
helium-3 and -4 content in primary, ratio of, (E), 20: 37572
helium-3 content in primary, ratio for, (E), 20: 37559
intensity decrease of, interplanetary magnetic field effects on anisotropy of Forbush, (E), 20: 37534
intensity decrease at 60 Mw(e) underground, Forbush and 27-day recurrence in, (E), 20: 37535
intensity distribution of, daily variation method for determining, (T), 20: 37587
intensity during last 10^9 years, determination from cosmic ray-produced nuclei in iron meteorites, (E), 20: 37603
intensity in stratosphere, temperature dependence of, (E), 20: 37591
intensity modulation of, review of, 20: 37493
intensity modulation of, review of theory for, 20: 37494
intensity modulation of primary, rigidity dependence of, (E), 20: 37508
intensity modulation of primary, models for solar cycle, (E/T), 20: 37509
intensity modulation of primary, time differential spectra for, (E), 20: 37510
intensity modulation of, solar system electric field effects on, (T), 20: 37512
intensity modulation of relativistic, long-term, (T), 20: 37513
intensity modulation of, earth heliolatitude effects on, 20: 37529
intensity modulation in interplanetary space, (T), 20: 37542
intensity modulation of, review of 11-year solar cycle effects on, 20: 37545
intensity modulation of, review of mechanisms for, 20: 37546
intensity modulation of, velocity dependence of, (E), 20: 37551
intensity of, anisotropy in, (T), 20: 37518
intensity secular variation of primary, determination from carbon-14 content in tree rings, (E), 20: 37602
intensity variations in, effects of solar corona discharges on, 20: 37486
intensity variations at 60 mwe underground, amplitude of sidereal and solar diurnal, (E), 20: 37504
intensity variations of, two-way sidereal anisotropy of diurnal, (T), 20: 37505
intensity variations of, sidereal time isolation for, (E/T), 20: 37506
intensity variations of, during solar cycle, (E), 20: 37507

intensity variations during 11-year solar cycle, (E), 20: 37515
intensity variations in, diffusion mechanism for diurnal, (T), 20: 37517
intensity variation of, model for solar diurnal, (E/T), 20: 37519
intensity variation of, diurnal anisotropy of, (E), 20: 37522
intensity variations of, variations of latitude dependence of diurnal, (E), 20: 37523
intensity variations of, periodic, 20: 37525
intensity variation of, solar-diurnal, (E), 20: 37526
intensity variation during Forbush decrease, rigidity dependence of diurnal, (T), 20: 37530
intensity variations of, first and second spherical harmonics for diurnal, 20: 37531
intensity variations in stratosphere, cyclic, (E), 20: 37532
intensity variations in stratosphere during solar minimum, secular, (E), 20: 37536
intensity variations near zenith, mechanisms for, (E), 20: 37539
intensity variations of, atmospheric temperature effects on diurnal, (E), 20: 37586
intensity variations of, simultaneous amplitude-phase modulation of, (T), 20: 37589
intensity variation during solar cycle, rigidity dependence of, (E), 20: 37516
interactions in atmosphere, gamma production from, (E/T), 20: 37576
kinetic effects in galaxy, 20: 37501
measurement of solar, Mariner IV instrumentation for, 20: 37341 (N-66-17354)
nuclear reactions in meson (μ)-produced, processes leading to, (T), 20: 37703
nuclear-active component spectra below 5 Tev, correlations with accompanying shower size, (E), 20: 37674
origin of, 20: 37388
origin of extragalactic, (T), 20: 37502
origin of, effects of gas expansion in intergalactic space on, (T), 20: 37503
origin of, in radio galaxies and quasars, 20: 37490
origin of, supernova, (T), 20: 37498
particle interactions at 100 to 1000 Bev in, design and performance of high-altitude installation for detecting strong, 20: 37656
properties at 10^{15} to 10^{17} ev, anisotropy, composition and energy spectrum, (E), 20: 37651
reactions in atmosphere at ground level, neutron production from, 20: 37483
reactions with dense matter, differential energy spectra for meson (μ) and neutrino production from, (T), 20: 37712
research on, using isotopic composition of extraterrestrial and terrestrial material, 20: 37369
rigidity cutoff for, numerical integration correlations with L-derived, 20: 37594
rigidity cutoff of, geomagnetic cavity field modulation of, (T), 20: 37596
rigidity cutoffs for vertical, geographic distribution of, (T), 20: 37595
rigidity spectra during solar rotation, correlations with solar wind velocity, (E), 20: 37533
rigidity spectra of primary, during solar cycle, (E), 20: 37514
rigidity spectra of primary, correlations with solar activity, (E), 20: 37543
rigidity threshold effects in, experimental model for simulating, 20: 37716
spectra of primary, solar modulation at low rigidities, (E), 20: 37584

COSMIC-RAY SPECTROMETERS
design for measurement of positive excess of mesons, 20: 37487

COSMIC SHOWERS
angular distribution of high-energy jet, kinematical analysis for, 20: 37680
angular distribution and energy spectra at 10^{12} ev at large zenith angles, (E), 20: 37696
arrival direction distribution of meson (μ)-rich EAS, anisotropy in, (E), 20: 37609
arrival directions of EAS, anisotropy of, (E), 20: 37620
arrival directions of air, BASJE fast-timing method for determining angle correlations for, 20: 37629
attenuation length of EAS, in water at mountain altitudes, (E), 20: 37642
composition and properties of EAS, installation for study of, 20: 37634
composition of photon-initiated, at high energies, (T), 20: 37628
core properties of EAS, (E), 20: 37638
core structure of EAS, electromagnetic, (E), 20: 37636
cores of EAS, fine structure of various types of, (E), 20: 37617
cores of EAS, properties of, (E), 20: 37615
density spectra of EAS, altitude dependence of, (E), 20: 37631
density spectra of EAS, at 2285 m above sea level, (E), 20: 37630
detection of EAS, performance of Cherenkov light receivers in middle uv regions for, 20: 37717
detection of, using radio system, 20: 37102
development of EAS, models for, 20: 37646
development of EAS, electromagnetic and nuclear-active multicore-event frequency in, (T), 20: 37647
electron and photon mean square angular and lateral spreads in photon-initiated, (T), 20: 37648
electron component energy flow near core in EAS, (E), 20: 37637
energies and production heights of EAS, (E), 20: 37618
energy of nuclear-active component in young air, 20: 37611
energy spectra of electromagnetic primary-proton produced, (E), 20: 37672
gamma to proton intensity ratio in meson (μ)-poor EAS, upper limit for, (E), 20: 37609
intensity variations of small air, time dependence of, (E), 20: 37649
interactions at ultra high energies in, models for, 20: 37679
magnitude of, correlations with cosmic nuclear-active spectra below 5 Tev, (E), 20: 37674
meson (μ) and nuclear active components in high-energy EAS, model for, 20: 37613
meson (μ) attenuation in EAS, barometric effect for determining, (E), 20: 37623
meson (μ) charge ratio and differential momentum spectrum in EAS, (E), 20: 37643
meson (μ) component of EAS, models for, 20: 37640
meson (μ) distribution in EAS, anisotropy determination from, (E), 20: 37607
meson (μ) distribution and flux in EAS, (E), 20: 37645
meson (μ) flux in EAS, above 200 and 640 Bev, absolute numbers in, (E), 20: 37606
meson (μ) intensity fluctuations in EAS, semi-empirical determination of, 20: 37624
meson (μ) propagation in EAS, lateral distribution, energy spectra, and heights of origin for, (T), 20: 37641
meson (π) production at 2 Tev in carbon, (E), 20: 37664
multiplicity distribution in high-energy jets, (E), 20: 37663
multiplicity of high-energy EAS, energy dependence of, (E), 20: 37678
nucleon and heavy particle arrival-time distributions in air, (T), 20: 37633
occurrence frequency of EAS, at 400 to 500 g cm^{-2} atmospheric depth, (E), 20: 37637
particle composition and density above 100 Bev in EAS, (E), 20: 37620
particle composition of EAS, (E), 20: 37621
particle densities in EAS, pulse spectrum from Cherenkov detectors for, (E), 20: 37619
particle distribution in jets at 10^{10} to 10^{14} ev, azimuthal angular distributions of secondary, (E), 20: 37665
particle energy spectra in EAS, nuclear-active, (E), 20: 37635
particle flux at low energies in EAS, lower and upper limits for nuclear-active, (E), 20: 37614
particle flux in cores of EAS, below 2 $(10)^{15}$ Bev/c, (E), 20: 37616
particle interactions at ultra-high energies in jet, criterion for detection of, 20: 37683
particle multiple production at high energies in, angular distribution of secondary, (T), 20: 37682
particle production in air, heavy, (E), 20: 37653
particle spectra at high energy in cores of EAS, nuclear-active, (E), 20: 37612
particle time lags in EAS, nuclear-active, (E), 20: 37652
production of electromagnetic, from meson (μ) interactions in lead at 0.3 to 30 Bev at 60 mwe underground, (E), 20: 37700
production of horizontal air, by mesons (μ) and neutrinos at 3 $(10)^{14}$ ev, 20: 37714
properties of EAS, rich in mesons (μ), 20: 37608
properties of EAS, at 10^{14} to 10^{17} ev, (E), 20: 37627
properties of EAS, with fixed electron and meson (μ) numbers, (E), 20: 37644
properties of EAS, at 10^{15} to 10^{17} ev, (E), 20: 37651
properties of EAS, review of research on, 20: 37655
properties of meson (μ), at 60 Mw(e) underground, (E), 20: 37605
properties of meson (μ)-poor EAS, (E), 20: 37610
properties of primary-produced jets, above 10^{12} ev, (E), 20: 37662
radio emission from EAS, mechanisms for, (T), 20: 37625
radio pulse emission from EAS, at 10^{16} to 10^{17} ev, (E), 20: 37626
reactions of young-air, with light nuclei, (E), 20: 37755
research on EAS, review of, 20: 37604
structure of EAS, (E), 20: 37632
structure of EAS, variation with atmospheric depth of, (E), 20: 37639

COSMOLOGY
energy equation, kinematical significance of, (T), 20: 37352
matter creation in steady state universe, quasar origin of, 20: 37361
models of universe, singularities in SO(3,R) homogeneous, 20: 37430

COTTON
radioinduced mutations in *Gossypium barbadense* species of, gamma and

thermal neutron, 20: 36623
COUMARIN
radiation and photon effects on, 20: 36860 (NP-16150)
CRATERS
production by raw-charges, 20: 36959 (PNE-603F)
production of in hard rock using nuclear explosions, 20: 36960 (PNE-717F)
CREATINE
radiation effects on synthesis of, in rat liver, x, 20: 36603
CREEP
effects of temperature on radioinduced in graphite, 20: 37223
stress dependence of, in uranium-loaded graphite, 20: 37224
CRITICAL ASSEMBLIES
control-rod worths in nonuniform loading of ZPR-III, 20: 38460 (ANL-7120, pp 766-75)
coolant void coefficient measurements in, extrapolation to large fast power reactors, 20: 38425 (ANL-7120, pp 585-97)
design and operation of APFA, 20: 38530 (GA-6078)
hazards analysis of APFA, 20: 38530 (GA-6078)
neutron Doppler effect in plutonium-fueled fast, in ZPR-3, (E/T), 20: 38427 (ANL-7120, pp 603-9)
neutron Doppler effect measurements in ZPR-6, 20: 38428 (ANL-7120, pp 610-13)
reactivity sodium-void coefficient measurements in ZPR-6, 20: 38426 (ANL-7120, pp 598-602)
CRITICALITY STUDIES
neutron age theory for, eigenvalue problem in, 20: 37993
CROSS SECTIONS
effects of variations in, on reactivity coefficient calculations, 20: 38419 (ANL-7120, pp 421-2)
CRUSTACEA
chromium distribution in, 20: 36552
CRYOGENICS
equipment for measuring magnetization of Al–Mg superconductors, 20: 37935 (CEA-R-2906)
CRYSTAL STRUCTURE
defects in recrystallized beryllium, effects on strength, 20: 37216
determination by electron microscopy, replicate methods for, 20: 37173
effects on superconductivity of niobium–oxygen–titanium systems, 20: 37267
models of close-packed hexagonal, in zirconium alloys, 20: 37226
CRYSTALLOGRAPHY
basal-pole orientation in zirconium by polarized-light microscopy, 20: 37266
CRYSTALS
annealing of Frenkel defects in neutron irradiated, computer simulation of, 20: 37294
electron absorption due to elastic scattering at high energies, (T), 20: 38381
kinetics of disordered harmonic, (E/T), 20: 38356 (LA-3510)
nuclear quadrupole resonance in, (T), 20: 38019
particle transmission in perfect, anomalous, (T), 20: 38387
radiation effects at low temperatures, design of sample holder for studying electron, 20: 37054
radiation effects on inorganic, electron spin resonance spectra of radicals from, 20: 36902
spin wave damping in, collective model for, (T), 20: 38358
CULTURE MEDIA
effects of irradiated, on growth of lymphoma cells, 20: 36633
CURIUM
determination of, using Arsenazo III, photometric, 20: 36778
CURIUM COMPLEXES
with citric acid, formation of, electrophoretic studies of, 20: 36829
CURIUM IONS
spectra of, effects of chemical bonding and transitions on, 20: 36845
CURIUM ISOTOPES Cm-246
energy levels, (E), 20: 38097
CURIUM ISOTOPES Cm-250
fission of, half life for spontaneous, (E), 20: 38093
CURIUM ISOTOPES Cm-252
half life, (E), 20: 38093
CURRENT REGULATORS
design for Princeton synchrotron magnet, 20: 37338
CYANIDES
effects on rate of strontium absorption by barley, 20: 36575
CYCLOALKENES
radiation and photon effects on, 20: 36860 (NP-16150)
CYCLOBUTANE
radioinduced formation, 20: 36860 (NP-16150)
CYCLOHEXANE
effects on radioinduced polymerization of allyl alcohol, 20: 36880
neutron scattering by solid and liquid, inelastic, 20: 38005
radiation effects on deuterium exchange with heavy water, 20: 36866
radiolysis of, effects of iodine on alpha and gamma, 20: 36888
cyclohexane–TBP, solvent properties for uranium, 20: 36714
cyclohexane–TBP, solvent properties for uranium, 20: 36718
CYCLOHEXANONE
effects on copper determination by absorption spectroscopy, 20: 36726
CYCLOTRON RADIATION
emission by electrons, interference beats in pulse-stimulated, (E/T), 20: 37776
emission from electron beam interactions with plasma, (T), 20: 38291
CYCLOTRONS
design of 68.5-cm sector-focused, 20: 37324
development and uses of ion, in Soviet Union, 20: 37333
CYLINDERS
photon energy absorption by, with axial source, 20: 37032
stability of compressible gravitating, in longitudinal magnetic fields, 20: 38311(T)
CYTOSINE
reactions with hydroxyl radicals, ESR spectral studies on, 20: 36806

D

DATA RECORDING SYSTEMS
design of magnetic tape, for use with medical scintiscenner, 20: 37083
DATA TABULATIONS
cosmic ray rigidity cutoffs, geographic distribution of vertical, 20: 37595
magnetic field ratios for magnet coils, 20: 36979 (ORNL-3972)
matrices for computing Greulung-Goertzel slowing down parameters and Legendre polynomial coefficients for neutron scattering, 20: 37988 (WAPD-TM-572)
of solar flares for 1954–1964, 20: 37886
uranium unit cost components for gaseous diffusion plant, 10-10, 20: 37161 (K-OA-1313)
DECONTAMINATION
equipment for rainwater, 20: 37029
DEGASIFICATION
equipment and procedures for, 20: 36983(R) (ALO-3633-1)
DENSITOMETERS
use of radiometric, in industry, 20: 37148
DENSITY
measurement of fluid, radiometric instrument for, 20: 37059
measurement of soil, using gamma backscattering, gage response in, 20: 37020
DEUTERIUM
depletion in contracting stars, 20: 37396
determination of, in deuterium hydride and hydrogen mixture, chromatographic, 20: 36737
deuteron reactions (d,n) at 460 Mev, polarization measurements using polarized deuterons, (E), 20: 38074
deuteron reactions (d,p) at 460 Mev, polarization measurements using polarized deuterons, (E), 20: 38074
deuteron reactions (d,n) with, angular distribution of neutron polarization in, (E), 20: 38163
effects on solubility of hydrogen fluoride gas in molten beryllium fluoride–lithium fluoride, 20: 36785 (ORNL-P-2202)
effects on vibrational excitation of carbon monoxide in shock tubes, 20: 36820
energy level transition probabilities and lifetimes in, 20: 37438
exchange and transfer reactions with hydrogen during ethylene polymerization, in catalyst system, 20: 36827
exchange with hydrogen on molybdenum filaments at 25 to 800°C, 20: 36818
helium-3 reactions (He-3,p) with, angular distribution and polarization of protons from, (E), 20: 38149
isotope effects on mutarotations of α-D-glucose and β-D-fructose, 20: 36577
laser beam Raman scattering in, stimulated pure rotational, 20: 37451
nuclear spin relaxation in gaseous, as function of pressure and temperature, (E), 20: 38151
reactions of atoms of, with olefins at 77 to 90°K, 20: 36856
triton reactions (t,α) at 0.115 to 1.650 Mev, differential cross sections for, (E), 20: 38130
DEUTERIUM HYDRIDES
determination of, in deuterium and hydrogen mixture, chromatographic, 20: 36737
nuclear spin relaxation in gaseous, as function of pressure and temperature, (E), 20: 38151
DEUTERIUM SYSTEMS
CO–O, vibrational relaxation of, in shock tubes, 20: 36820
DEUTERONS
electric quadrupole moment of, (E/T), 20: 37797
flux in EAS cores below 2 $(10)^{15}$ Bev/c, (E), 20: 37616
form factor from electron-deuteron interactions, (T), 20: 37749

interactions with electrons, inelastic, (T), 20: 38167
interactions with electrons, effect of deuteron models on cross sections for inelastic, (T), 20: 37748
interactions with electrons, deuteron form factor from, (T), 20: 37749
interactions with photons at 220 to 280 Mev, differential cross sections for meson (π^0) production in, (E), 20: 37783
interactions with elementary particles, amplitude for, (T), 20: 37798
interactions with antiprotons, meson (ρ) production in, 20: 37813
neutron reactions (n,t) at 14 Mev, (E), 20: 38150
photodisintegration at threshold, effect of meson exchange current in, (T), 20: 38059
photodisintegration of, nonphysical partial-wave amplitude singularities in, (T), 20: 38140
reactions (d,α) with fluorine-19 at 5.5 to 11.5 Mev, two-nucleon DWBA analysis of, (E/T), 20: 38082
reactions (d,f) with radium-226 at 12 Mev, energy distribution of fission fragments from, (E), 20: 38132
reactions (d,n) and (d,p) with deuterium at 460 Mev, polarization measurements using polarized deuterons, (E), 20: 38074
reactions (d,n) with helium-3, neutron spectra from, (E), 20: 38077
reactions (d,n) with nitrogen-14 at 1.173, 1.797, and 2.098 Mev, angular distributions and excitation functions for, (E), 20: 38144
reactions (d,n) with niobium, yttrium, and zirconium, cross sections and mechanism of, (E), 20: 38159
reactions (d,n) with boron-11, alpha decay of carbon-12 energy levels from, (E), 20: 38162
reactions (d,n) with boron-11, deuterium, and tritium, angular distribution of neutron polarization in, (E), 20: 38163
reactions (d,pγ) with silicon-28 at 4 to 6 Mev, angular correlations of, 20: 38086
reactions (d,p γ) with magnesium-26 at 1.8 Mev, magnesium-27 energy levels from γ-p angular correlation measurements on, (E), 20: 38187
reactions (d,p) and (d,t) with xenon-136 at 15 Mev, xenon-135 and xenon-137 energy levels from, (E), 20: 38099
reactions (d,p) with chromium-52 at 8 to 11 Mev, (E/T), 20: 38046
reactions (d,p) with chromium-52, finite-range distorted-wave calculations for, (T), 20: 38047
reactions (d,p) with zirconium-90 at 2.7 to 3.6 Mev, proton angular distribution from, (E), 20: 38096
reactions (d,p) with calcium-40 and carbon-12, proton angular distribution and polarization in, (E), 20: 38119
reactions (d,p) with chlorine-37 at 7.74 Mev, structure of chlorine-38 from, (E), 20: 38153
reactions (d,p) with lithium-6, lithium-7 energy levels from, (E), 20: 38164
reactions with nickel-61 at 10 to 20 Mev, excitation functions for, (E), 20: 38148
scattering by copper isotopes and nickel isotopes at 13.6 Mev, differential cross sections for, (E), 20: 38128

DEXTRAN
effect as histamine liberator on calcification produced by various metals in rats, 20: 36557

DIAMONDS
analysis for nitrogen by photoactivation, 20: 36746

DIET
cesium-137 uptake from fallout by cattle, and transfer to milk, 20: 37036
effects of thiocyanate in, on radioiodine metabolism in cows, 20: 36563

DIFFUSION
of xenon in urania, effects of trapping sites on, 20: 37293

DIOXANE
effects on gamma radiolysis of nickel, silver, and zinc chelates of tetraphenylporphine, 20: 36889
radioluminescence of liquid, quenching effects of AET on, 20: 36663(T)
dioxane–H_2O, cerium compound absorption spectra in, 20: 36831

DIOXASPIROHEPTANE
radioinduced polymerization, 20: 36914(P)

DIRECT ENERGY CONVERSION DEVICES
electrofluiddynamic, design and performance of, 20: 37727
research on, 20: 37721(R) (INDEC-SR-7)

DISULFIDES
protection against radiation damage in calf-thymus DNA, mechanism of, 20: 36665

DIURETICS
preparation of carbon-14- or tritium-labeled triamterene, 20: 36922

DOGS
manganese-54 metabolism in, 20: 36554 (LA-DC-7305)
production of glucose in, use of carbon-14 and tritium tracers for 20: 36565
radiation effects on Dische-positive material in blood and urine in, gamma, 20: 36604
radiation effects on tissue homografts in, by lymphatic ablation, 20: 36641
radiation sickness in, nerve trunk regeneration in relation to phase of, 20: 36614
radioinduced heart failure in, hemodynamic parameters in, gamma, 20: 36660

DOSIMETERS
design and performance of polymer degradation, using polyisobutylene in heptane, 20: 37117
design of, for radiation protection measurements, 20: 36680
development of neutron, review of, 20: 37070 (BNWL-SA-537)
standards for, secondary, 20: 37090

DROSOPHILA
radiation effects on, in Israel, 20: 37155
radiation effects on egg-to-adult viability in *D. melanogaster*, x, 20: 36618
radiation effects on sperm cells in succeeding generations of, after oocyte exposure, gamma, 20: 36625
radioinduced somatic crossing over in, effects of age on location of, 20: 36619

DRUGS
radiosterilization of, role of chemicals as sensitizers in, 20: 37144

DUAL-TEMPERATURE PROCESS
sieve tray performance testing for GS heavy water process, 20: 37160 (DP-1025)

DUSTS
gravitational collapse of spherical cloud of, null coordinates for, 20: 37921
properties of interplanetary, with charge, 20: 37913(T)

DYES
use of eosin yellow and nitrosin for viability tests on Ehrlich ascites tumor cells, 20: 36631

DYSPROSIUM
determination in hydrochloric acid solutions, spectrographic carrier-distillation, 20: 36729
effects on crystal structure of cobalt, iron, and nickel intermetallic compounds, 20: 37243
energy levels of, ionization energies from, (T), 20: 37439
neutron absorption cross section in pitchblende, thermal, 20: 37994
nuclear magnetic resonances in ferromagnetic, (E), 20: 38374

DYSPROSIUM ALCOHOLATES
preparation of, and thermal decomposition to oxide coatings and powders, 20: 36851

DYSPROSIUM ALLOYS
Co–Dy, crystal structure of intermetallic compounds in, 20: 37243
Dy–Fe, crystal structure of intermetallic compounds in, 20: 37243
Dy–Ge, crystal structure, (E), 20: 38369
Dy–Ni, crystal structure of intermetallic compounds in, 20: 37243

DYSPROSIUM CHROMITES
spectra of, infrared, 20: 36807

DYSPROSIUM COMPLEXES
with tartaric acid and trihydroxyglutaric acid, stability constants for, 20: 36838

DYSPROSIUM HYDROXIDE OXIDES
preparation and crystal structure of, 20: 36791

DYSPROSIUM HYDROXIDES
preparation and crystal structure of, 20: 36791

DYSPROSIUM IONS
spectra of, effects of chemical bonding and transitions on, 20: 36845

DYSPROSIUM ISOTOPES Dy-158
energy level transitions from terbium-159 (p,2n) reactions, ground state rotational, 20: 38008(R) (AECL-2595)

DYSPROSIUM ISOTOPES Dy-161
nuclear magnetic resonances of, in ferromagnetic dysprosium, (E), 20: 38374

DYSPROSIUM ISOTOPES Dy-163
nuclear magnetic resonances of, in ferromagnetic dysprosium, (E), 20: 38374

DYSPROSIUM LACTATES
formation constant of, potentiometric determination of, 20: 36824

DYSPROSIUM OXIDES
Dy_2O_3–ReO_2, magnetic properties and structure of compounds formed in, 20: 36784(R) (AD-636054)

DYSPROSIUM PHOSPHIDES
crystal structure, 20: 38370
electric conductivity and magnetic susceptibility, 20: 38370

E

ECHINODERMS
chromium distribution in, 20: 36552

ECOLOGY
of plants of Neotoma Valley, Ohio, 20: 36548 (TID-23036)

EINSTEINIUM ISOTOPES E_s-255
alpha decay of, branching ratio for, (E), 20: 38093

ELECTRIC ARCS
design of hollow gas, with off-center cathode, 20: 37065(P)

ELECTRIC CELLS
performance in purification of molten cerium, 20: 36936
ELECTRIC CONDENSERS
design for magnet coil excitation, 20: 36982
ELECTRIC CONDUCTIVITY
radiation effects on, in electrolyte solutions, gamma, 20: 36912
ELECTRIC DISCHARGE
design modification and performance of Penning, 20: 38308
electron velocity distribution in low-pressure nitrogen, (E), 20: 38213
plasma diffusion across magnetic field in r-f, (E), 20: 38327
plasma diffusion in ring r-f, anomalous, (E/T), 20: 38329
plasma oscillations in, 20: 38346
plasma production and properties in, hydrogen, 20: 38247
plasma stability in, research on, (E), 20: 38321
striations in, production analysis of, 20: 38206 (ORNL-P-1539)
ELECTRIC FIELDS
effects of solar-system, on cosmic ray intensity, (T), 20: 37512
effects on positron annihilation in argon, (E), 20: 37810
electron motion in dipole, variational calculation of bound states for, 20: 37919
plasma oscillations in h-f, beam, 20: 38263
production of transient during underground explosions, 20: 36971
ELECTRIC INSULATORS
properties at high temperatures, symposium on, 20: 37179
radioinduced conductivity in, gamma, (T), 20: 38353 (BNWL-SA-247)
ELECTRIC METERS
design and performance of system for measuring small nonlinearities in superconducting tunnel junctions, 20: 37973
ELECTRIC POWER
generation by MPD generators, 20: 37724
generation of, fossil and nuclear energy-source comparisons for, 20: 38520
generation of, using combined MHD and internal combustion generators, 20: 37728(P)
production in space using thermionic energy converter, 20: 37725
ELECTRIC PROBES
design and performance of Faraday-cup, for radial current density distribution measurements of electron beams, 20: 37045
performance for hypersonic plasma flow measurements, 20: 38261
performance of Langmuir, on ionospheric sounding rockets, 20: 38309
properties of spherical, near plasma frequency, (E), 20: 38299
properties of spherical, in monoenergetic plasmas, (T), 20: 38190 (AD-637513)
ELECTRICITY
production of, economics of hydro and nuclear plants, 20: 38511
transmission of high-voltage pulse of, using superconducting coaxial delay lines, (E), 20: 37939
ELECTRODES
design of beam-forming, for electron guns, 20: 37312
plasma slab electric conductivity between juxtaposed disk, 20: 38293
ELECTRODYNAMICS
book: *Electromagnetodynamics of Fluids*, 20: 37884
ELECTROHYDRODYNAMIC CELLS
energy conversion in, review of, 20: 37727
ELECTROHYDRODYNAMICS
pumping of liquids by induced charges, (T/E), 20: 38280
ELECTROLYSIS
transient concentration variation in natural convection, 20: 37722(R) (N-65-30843)
use in fuel element reprocessing, 20: 36952
ELECTROLYTIC CELLS
design for magnetic field analog studies, 20: 38189 (AD-636095)
ELECTROMAGNETIC FIELDS
fluctuation detection by naphthalene test, magnetic storm effects on, 20: 37890
fluctuation detection by solidification of naphthalene, correlation with lunar phases in, 20: 37891
properties in anisotropic plasmaguides, electron collision effects on, 20: 38226
properties in warm cylindrical magnetoplasmas, potentials for, 20: 38302
quantization in Landau gauge, covariant, 20: 37925
theory of, in Minkowskian metric, 20: 37923
ELECTROMAGNETIC SEPARATION
chemistry in, review of, 20: 37163
ELECTROMAGNETIC WAVES
emission in stellar evolutions, effects on, 20: 37399
interactions with inhomogeneous drifting plasma, dispersion relations for, (T), 20: 38194(R) (INDEC-SR-7, pp 3.22-59)
interactions with magnetoplasma, collective fluctuations from, 20: 38201 (NP-16210)
interactions with plasma, diagnostics from, (T), 20: 38225
interactions with electroacoustic waves in plasma, coupling of, 20: 38232
interactions with plasma, electron collision frequency in, 20: 38234
interactions with warm plasma, transmission and reflection during, (T), 20: 38276
interactions with classical and quantum plasma, correlation effects in, (T), 20: 38292
interactions with ferromagnetic plasma, (T), 20: 38354 (FTI-244/T-027)
propagation in compressible inhomogeneous plasma, (T), 20: 38227
propagation in gyrotropic plasma, separation constants for, 20: 38228
propagation in inhomogeneous plasmas, properties of, (T), 20: 38233
propagation in plasma, ferrite antenna windows for improving, 20: 38231
propagation in warm plasma, from vertical dipoles, 20: 38229
propagation in warm plasma, from vertical dipoles, 20: 38230
propagation of electro-acoustic waves in compressible inhomogeneous plasma, (T), 20: 38227
reflection and transmission by moving cold plasma, (T), 20: 38237
ELECTRON BEAMS
alignment for crystal studies at low temperatures, technique for, 20: 37054
current density distributions in, design and performance of Faraday-cup probe for measuring radial, 20: 37045
dose distribution with pulsed scanning, 20: 36672
interactions in inhomogeneous field-free plasma, correlation and exchange effects from, (T), 20: 38334
interactions in low-pressure mercury discharge, excitation of uhf-plasma oscillations by, 20: 38214
interactions with magnetoplasma, collective fluctuations from, 20: 38201 (NP-16210)
interactions with low-pressure mercury discharge, excitation of uhf oscillations by, (E), 20: 38215
interactions with low-pressure mercury discharge, excitation of uhf oscillations by, (E), 20: 38216
interactions with plasma, cyclotron radiation excitation from, (T), 20: 38291
production in electrostatic electron guns, 20: 37312
production of polarized, methods for, (E), 20: 37475
RBE for treatment of advanced head and neck carcinomas, 20: 36685
reactions with aluminum foils at 30 kev, energy-loss spectrum of, (E/T) 20: 37442
scattering by lithium-fluoride foils at 25 kev, excitation of surface-lattice vibrations by, (E/T), 20: 38395
scattering by mercury at 180 to 1700 ev, polarization from elastic, (E), 20: 37469
stability of crossed-field, (T), 20: 37329
uses in refractory material melting, symposium on, 20: 37179
ELECTRON-DIFFRACTION ANALYSIS
use in radiation effects testing of beryllia and zinc oxide, 20: 37281
ELECTRON MICROSCOPES
materials irradiation studies at low energies in, design and performance of electron beam current monitor, 20: 37116
ELECTRON MICROSCOPY
method for autoradiographic, photographic emulsions and developing methods for, 20: 37050
of beryllia and zinc oxide irradiation, 20: 37281
of ceramic fuel particles, replicate sample preparation for, 20: 37173
of zirconium foil deformation, 20: 37248
ELECTRON MULTIPLIER TUBES
gain of transmission-type, using cesium iodide as secondary emission material, 20: 37046
ELECTRON PAIRS
production by gamma reactions with copper, nickel, and silver at 6.13 Mev, cross sections for, (E), 20: 37746
ELECTRON SOURCES
design and performance of high-density, using duoplasmatron with hollow cathode arc, 20: 37045
design and performance of FEBETRON, for 10,000-amp beam current production, 20: 37339
design of electrostatic electron guns, 20: 37312
ELECTRONS
absorption in crystals due to high-energy elastic scattering, (T), 20: 38381
cyclotron radiation from, interference beats in pulse-stimulated, (E/T), 20: 37776
decay rate of, injected into superconductors, 20: 37984
density beyond magnetosphere, origin of, 20: 37894
density in magnetic anomaly region, longitude dependence of, (T), 20: 37906
detection of, silver bromide energy sensitivity threshold in nuclear emulsions for, 20: 37122
Dirac equation for, 20: 37920
distributions in Van Allen belts, spikes in, (E), 20: 37903
dosimetry of, polymer degradation dosimeter for, 20: 37117
dosimetry of, use of probe method in, 20: 37081
effects of pulsed, on luminescence of fused quartz, 20: 36864
effects on beryllia flakes, 20: 37281

effects on electric conductivity and magnetism of nickel, 20: 37297
effects on gallium phosphides, defect determination from hyperfine ESR structure from, (E), 20: 38399
effects on light-sensitivity of film, 20: 36895
effects on n-type germanium at 6 to 88 Mev, annealing of defects from, (E), 20: 38365
effects on polyethylene, 20: 36857 (COO-1088-21)
effects on silicoörganic compounds, EPR studies of free radical yield in, 20: 36883
effects on zinc oxide smokes, 20: 37281
ejection from tungsten by helium and neon atoms, (E), 20: 37450
emission from alkali earth-surrounded metals, models for, (T), 20: 37431(R) (INDEC-SR-7, pp 3.76-111)
emission from uranium dodecaboride, thermionic, (E), 20: 37723
energy and intensity of, in outer Van Allen belt, (E), 20: 37905
energy precipitations in loss cone of auroral zone, geomagnetic variations from, 20: 37897
energy spectra of high-energy pulses of, near magnetospheric bow shock, (E), 20: 37900
flux density distribution measurements of, 20: 36689
flux in magnetosphere at 0 to 10 kev, structure of, (E), 20: 37904
flux in Van Allen belts, effects of critical, (T), 20: 37910
flux of geomagnetically trapped at 0.2 to 6000 kev, near earth, (E), 20: 37902
interactions in solids, Fermi liquid theory for, 20: 38403
interactions with atoms, book on, 20: 37477(T)
interactions with deuterons, inelastic, (T), 20: 38167
interactions with ions in plasma diodes, computer simulation of, 20: 37726
interactions with deuterons, effect of deuteron models on cross sections for inelastic, (T), 20: 37748
interactions with deuterons, deuteron form factor from, (T), 20: 37749
interactions with positrons, Bogoliubov canonical transformation for annihilation, 20: 37757
interactions with protons at 1200 Mev, cross sections for elastic, (E), 20: 37778
interactions with solar neutrinos, methods for detecting, 20: 37792
interactions with positrons, W meson production in, (T), 20: 37799
interactions with protons, meson (π^+) form factors from, (E/T), 20: 37812
LET determination by comparison of energy dose measurements of, 20: 36689
model for, in liquid helium II, 20: 37981
momentum distribution in germanium and silicon, positron annihilation method for determining, 20: 37736 (COO-1297-7)
motion in electric dipole fields, variational calculation of bound states for, 20: 37919
photoproduced from atomic potassium beams, polarization of, (E), 20: 37475
photoproduced on magnetized nickel crystals, polarization of, (E), 20: 37475
reactions (e,e'p) with sulfur-32 at 408 Mev, proton binding energies from, (E), 20: 38016
reactions in copper at 100 kev, temperature dependence of, (E), 20: 38379
reactions with helium, excitation cross sections for n = 2 states from, (T), 20: 37453
reactions with hydrogen ions at 100 ev, cross sections for electron detachment from, (E), 20: 37452
reactions with moving unequal-mass particles, energy transfer in, (T), 20: 37447
reactions with silver foils at 3.6 ev, plasma losses in, (E), 20: 38400
reactions with thick targets at 0.2 to 0.8 Mev, bremsstrahlung spectra from, (E), 20: 38155
relaxation of trapped, in gamma-irradiated alkaline ices, paramagnetic, 20: 36871
scattering by boron-10 and boron-11 at 198 to 400 Mev, Coulomb form factors from elastic, (E), 20: 38057
scattering by nuclei with a Fermi charge distribution, elastic, (T), 20: 38139
scattering in ionosphere, heating effects from, 20: 37896
temperatures in ionospheric F region, 20: 37896
transmission in perfect crystals, anomalous, (T), 20: 38387
transport properties of gas of, in magnetic fields, 20: 37866
tunneling in superconductors, review of Josephson, 20: 37975
use in therapy, material for adaptation of irradiation field for, 20: 36700
velocity distribution in low-pressure nitrogen discharge, (E), 20: 38213

ELECTROSTATIC LENSES
aberrations and focal properties of three-electrode, chromatic and spherical, 20: 37330

ELECTROSTATICS
plasma wave propagation in hot inhomogeneous media, (T), 20: 38284

ELEMENTARY PARTICLES
annihilation of neutral, cross section of single-photon, 20: 37859
compositeness condition and self-mass of, 20: 37847
compositeness condition in quantum field theory for, particle mixing in, 20: 37848
electromagnetic properties of neutral, with C-parity violation, 20: 37859
energy-momentum field for, 20: 37834
existence of mirror, in stars, 20: 37806
field theory of, 20: 37845
flux of quarks in cosmic radiation, (T), 20: 37718
form factors for, locality of current densities and SU(3) invariance for electromagnetic, 20: 37837
interactions at high energies in nuclear emulsions, (E), 20: 38168
interactions of composite, separable potential model for, 20: 37863
interactions of spinless, model for forward amplitude for, 20: 37805
interactions of zero-spin, dynamics of, (T), 20: 37864
interactions of, amputated vertex functions for, 20: 37753
interactions of, cluster structure of S matrix for, (T), 20: 37861
interactions of, high-energy behavior in direct, 20: 37851
interactions of, interpretation of Foldy-Wouthuysen transformation for strong, 20: 37828
interactions with deuterons, amplitudes for, (T), 20: 37798
magnetic moments in quark model, 20: 37857
mass formula in broken P_U symmetry, 20: 37835
properties of, current algebras for tests of models for, 20: 37830
properties of, trion model for, 20: 37850
research program at CERN, 1965, 20: 37308(R) (NP-16226)
scattering by nuclei, with excitation of collective states, inelastic, (T), 20: 38142
scattering by nuclei, with excitation of collective states, diffraction, (T), 20: 38143
scattering of, lectures on high-energy, (T), 20: 37826 (NP-16231)
symmetry group for, expanded translation subgroup in SL(6), 20: 37835
symmetry group for, properties of static SU(6), 20: 37860
symmetry group P(SU(r)) for nonzero-mass, unitary representation of, 20: 37858
symmetry groups for, vertex operator association with noncompact, 20: 37823 (BNL-10387)
symmetry groups for, Gell-Mann formula for representation of semisimple, 20: 37832
symmetry groups for strongly interacting, electromagnetism and higher, 20: 37843
symmetry groups for, Casimir operators for orthogonal and symplectic, 20: 37856
wave equations for, regularity conditions for relativistic, 20: 37931

ELEMENTS
determination in coal using neutron activation, system for continuous on-line, 20: 36769
photoionization by cosmic x rays, in interstellar and intergalactic space, 20: 37485
proton reactions at 100 Mev, total cross sections for, (E), 20: 38018

ELK RIVER POWER REACTOR
spent fuel shipping cask criticality analysis, 20: 38486 (ACNP-66551)

EMBRYOS
radiation effects on blindworm, x, 20: 36615
radiation effects on aging of developing chicken, x, 20: 36605(R) (COO-1119-5)

EMULSIONS
scintillation counting of, limitations in tritium measurements by, 20: 36720

ENDOCRINE GLANDS
book: *Yearbook of Nuclear Medicine*, Vol. I, 1966, 20: 36690

ENDOXAN
effects of tritium-labeled, on inoperable tumors, 20: 36705

ENERGY
release and storage by irradiated graphite, 20: 37283

ENGLAND (DEVON)
radiation monitoring of drinking water supplies in, for radium, radon, and daughter products, 20: 37031

ENZYMES
effects on synthesis of nucleic acids and proteins, 20: 36555(R) (NYO-2643-22)
hydrolysis by, use in detection of uv-damaged DNA, 20: 36596
radiation effects on uptake of carbon-14-labeled acetate by aldolase, 20: 36574
radiation effects on breakdown of *Micrococcus lysodeicticus* DNA, uv, 20: 36583
radiation effects on, in regenerating rat liver DNA, mechanism of x, 20: 36593
radiation effects on renewal intensity of muscle, 20: 36600
radiation effects on aminotransferase activities in central nervous system and skeletal muscle in rats, neutron, 20: 36601

EQUATION OF STATE

for reactor materials at high pressures and temperatures, review, 20: 38433 (ANL-7120, pp 641-53)
for use in calculations on fast reactor excursions, 20: 38435 (ANL-7120, pp 686-91)
EQUIPMENT AND PROCEDURES
development of, for heat transfer studies, 20: 36993
ERBIUM
determination in hydrochloric acid solutions, spectrographic carrier-distillation, 20: 36729
effects on crystal structure of cobalt, iron, and nickel intermetallic compounds, 20: 37243
effects on phase transformation temperature of thorium, 20: 37242
energy levels of, ionization energies from, (T), 20: 37439
neutron absorption cross section in pitchblende, thermal, 20: 37994
ERBIUM ALLOYS
Co–Er, crystal structure of intermetallic compounds in, 20: 37243
Er–Fe, crystal structure of intermetallic compounds in, 20: 37243
Er–Ge, crystal structure, (E), 20: 38369
Er–Ni, crystal structure of intermetallic compounds in, 20: 37243
Er–Th, phase studies of, 20: 37242
ERBIUM CHLORIDES
reactions with isopropylamine, thermogravimetric study of, 20: 36853
ERBIUM CHROMITES
spectra of, infrared, 20: 36807
ERBIUM COMPLEXES
with ascorbic acid, molar extinction coefficients and stability constants for, 20: 36852
with pyrogallosulfonic acid, formation of, potentiometric and spectrophotometric studies of, 20: 36837
with tartaric acid and trihydroxyglutaric acid, stability constants for, 20: 36838
ERBIUM HYDROXIDE OXIDES
preparation and crystal structure of, 20: 36791
ERBIUM HYDROXIDES
preparation and crystal structure of, 20: 36791
ERBIUM IONS
electron paramagnetic resonance in cesium oxide single crystals at 10 Bc, (E), 20: 38391
spectra of, effects of chemical bonding and transitions on, 20: 36845
ERBIUM ISOTOPES Er-164
energy level transitions from holmium-165 (p,2n) reactions, ground state rotational, 20: 38008(R) (AECL-2595)
ERBIUM ISOTOPES Er-167
hyperfine structure in cesium oxide single crystals at 10 Bc, EPR determination of, (E), 20: 38391
ERBIUM LACTATES
formation constant of, potentiometric determination of, 20: 36824
ERBIUM OXIDES
magnetic structure of, 20: 38357
Er_2O_3–ReO_2, magnetic properties and structure of compounds formed in, 20: 36784(R) (AD-636054)
ESCHERICHIA COLI
effects of various mutagens in increasing proportion of virus-producing cells and several mutants of, 20: 36617
ETHANE
nuclear spin relaxation in liquid, intermolecular contribution to, 20: 36828
positronium lifetime in, (E), 20: 37816
ETHANOL
radiolysis of, yields of hydrogen in, 20: 36861 (UJV-1553)
ETHYL ACETATE
solvent properties for copper, 20: 36726
ethyl acetate–TBP, solvent properties for uranium, 20: 36717
ETHYL ETHER
effects on copper determination by absorption spectroscopy, 20: 36726
ETHYL SULFATES
effects on peas, genetic, 20: 36634
ETHYLAMINE, 2,2'-DITHIOBIS-
effects of oral, on gamma radiation effects on mice, 20: 36666
protection against radiation damage in calf-thymus DNA, mechanism of, 20: 36665
ETHYLAMINE, 2,2'-DITHIOBIS[*N,N*-DIMETHYL-
protection against radiation damage in calf-thymus DNA, mechanism of, 20: 36665
ETHYLENE
polymerization of, deuterium exchange and transfer reactions with hydrogen in catalyst system for, 20: 36827
radioinduced telomerization of, with carbon tetrachloride, effect of process variables on gamma, 20: 36890
radioinduced telomerization of, with carbon tetrachloride under constant ethylene pressure, gamma, 20: 36891
ETHYLENE, CHLORO- POLYMERS
radioinduced grafting of acrylonitrile–styrene mixture on, at 0 to 50°C, 20: 36877
ETHYLENE, DIFLUORO- POLYMERS
radiation effects on cross linking in, gamma, 20: 36859 (N-66-13497)
ETHYLENE GLYCOL
acetic acid–ethylene glycol–$HClO_4$, properties for etching zirconium, 20: 37227
ETHYLENE POLYMERS
positronium lifetime in gamma irradiated, dose dependence of slow, (E), 20: 36896
radiation effects on, electron, 20: 36857 (COO-1088-21)
ETHYLENE, TETRAFLUORO- POLYMERS
positron lifetime distribution in Teflon, correlation with angle between annihilation gamma rays, 20: 37737 (COO-1297-8)
positronium lifetime in gamma irradiated, dose dependence of slow, (E), 20: 36896
radioinduced grafting of acrylonitrile–styrene mixture on, 20: 36878
ETHYLENIMINE
effects on chlorophyll mutation frequency, meiosis, and mitosis in peas, 20: 36621
effects on chlorophyll and morphological mutations in pea varieties, 20: 36624
effects on peas, genetic, 20: 36634
EUROPIUM
content in African pitchblende, estimation of induced fission vs spontaneous fission from, 20: 37994
determination in complexes with diketones, spectrofluorometric, 20: 36722
determination in hydrochloric acid solutions, spectrographic carrier-distillation, 20: 36729
energy levels of, ionization energies from, (T), 20: 37439
neutron absorption cross section in pitchblende, thermal, 20: 37994
reactions with graphite, thermodynamics of, 20: 36844
separation of, from other lanthanides by ion exchange using ammonium lactate, mechanism of, 20: 36939
EUROPIUM CARBIDES
preparation and thermodynamic properties of, 20: 36844
EUROPIUM CHROMITES
spectra of, infrared, 20: 36807
EUROPIUM COMPLEXES
with ascorbic acid, molar extinction coefficients for, 20: 36833
with diketones, spectrofluorometric analysis for, 20: 36722
with tartaric acid and trihydroxyglutaric acid, stability constants for, 20: 36838
EUROPIUM IONS
spectra of, effects of chemical bonding and transitions on, 20: 36845
EUROPIUM ISOTOPES Eu-145
beta decay of, gamma-transition intensities in, (E), 20: 38133
beta decay of, positron spectrum from, (E), 20: 38133
EUROPIUM ISOTOPES Eu-156
yields in proton fission of uranium-238 at 7.1, 9.4, and 12.0 Mev, 20: 37995
EUROPIUM ISOTOPES Eu-157
yields in proton fission of uranium-238 at 7.1, 9.4, and 12.0 Mev, 20: 37995
EUROPIUM OXIDES
effects on reactivity of gas- and steam-cooled fast reactors during flooding, 20: 38439 (ANL-7120, pp 826-36)
B_2O_3–Eu_2O_3–Na_2O, spectra at liquid nitrogen temperature and room temperature, absorption and emission, 20: 36813
Eu_2O_3–ZrO_2, phase studies, 20: 36815
EUROPIUM SYSTEMS
calcium oxalate–Eu, precipitation reactions in, distribution coefficients of, 20: 36794
EXHAUST SYSTEMS
filters for iodine adsorption in, properties of coconut-shell activated carbon, 20: 36976 (DP-MS-66-45)
EXPERIMENTAL BREEDER REACTOR-II
fuel reprocessing for, 20: 36952
fuel-element failure detection in, 20: 38478 (ANL-7120, pp 862-7)
EXPLOSION CLOUDS
formation in Pre-Schooner II cratering event, 20: 36958 (PNE-511)
EXPLOSIONS
analysis of rocket-abort, (T), 20: 36996(R) (SC-CR-66-2045)
containment in single-tank fast reactors, model tests of, 20: 38458 (ANL-7120, pp 692-719)
pressure produced by contained, in sodium and water, 20: 38459 (ANL-7120, pp 720-33)
EYES
radiation effects on glycolysis and respiration in guinea pig and rat retina, x, 20: 36630
radioinduced lesions in, laser beam, 20: 36612
radiotherapy of diseases of, use of lasers in retinal photocoagulation, 20: 36682

reaction to receptors in, to light quanta, 20: 36587(T)
toxoplasmic retinochoroiditis in human, use of lasers for radiotherapy of, 20: 36683

F

FALLOUT
cesium-137 deposition from, on forage and transfer to milk, 20: 37036
cesium-137 uptake from, by corn seedlings, 20: 37038
dispersion in seawater, 20: 37037
effects on atmospheric electricity, (T), 20: 37003
in vicinity of Shippingport Atomic Power Station, Penna., 20: 37026 (PNRO-SMD-137)
measurements in environment of IRT-1000 Reactor, 20: 38535
monitoring at Neotoma Valley, Ohio, 1958 through 1964, 20: 36548 (TID-23036)
monitoring in Alaska, program for, 20: 37042
monitoring in Austrian Alps, variations with altitude, 20: 37008
monitoring in Germany, data for 1965, 20: 37009
radiation dose to biosphere from, 1945 through 1962, 20: 37004
FAST FLUX TEST FACILITY
fuel elements for, hydraulic analysis of, 20: 38479 (BNWL-264)
FAST REACTORS
accidents in, energy release and mechanical effects in maximum, (T), 20: 38434 (ANL-7120, pp 654-70)
boiling in core of, voids due to transient, 20: 38440 (ANL-7120, pp 881-9)
calculations concerning, effects of group-constant uncertainties on, 20: 38420 (ANL-7120, pp 423-33)
calculations concerning, comparison of, 20: 38490 (ANL-7120, pp 3-23)
conference on safety, fuels, and core design in large power, 20: 38489 (ANL-7120)
coolant void coefficients for, extrapolation from critical assembly measurements, 20: 38425 (ANL-7120, pp 585-97)
cooling of 1000-Mw(e) breeder, by steam at 1200 psi, 20: 38496 (ANL-7120, pp 136-40)
core design and fuel cycle for 1000-Mw(e) metal-fueled breeder, 20: 38494 (ANL-7120, pp 94-103)
criticality and performance of compact, tungsten-cermet fueled, 20: 38442 (BNWL-283)
design and safety of large power, panel discussion on, 20: 38457 (ANL-7120, pp 261-85)
design and safety of 1000-Mw(e) power breeder, 20: 38497 (ANL-7120, pp 157-61)
design and safety of 1375-Mw(e) sodium-cooled carbide-fuel modular, 20: 38456 (ANL-7120, pp 205-29)
design, economics, and safety of 1000-Mw(e) sodium-cooled, 20: 38498 (ANL-7120, pp 185-204)
economic and safety aspects of vented-fuel sodium-cooled, 20: 38475 (ANL-7120, pp 540-8)
excursions in, equation of state for calculations on, 20: 38435 (ANL-7120, pp 686-91)
explosion containment in single-tank, model tests of, 20: 38458 (ANL-7120, pp 692-719)
explosion containment in, model tests of, 20: 38459 (ANL-7120, pp 720-33)
fission-product retention by sodium in vented-fuel-element, 20: 38477 (ANL-7120, pp 855-61)
fuel development for, evaluation of plutonium, 20: 38483
fuel movement within cladding in, mixed oxide, 20: 38473 (ANL-7120, pp 524-33)
fuel optimization studies for 1000-Mw(e) breeder, plutonium–uranium carbide, 20: 38495 (ANL-7120, pp 104-23)
fuel reprocessing for, 20: 36952
fuels for power breeder, mixed plutonium–uranium-238 and uranium-233–thorium, 20: 38476 (ANL-7120, pp 751-8)
fuels for, development of metallic, 20: 38465 (ANL-7120, pp 289-300)
fuels for, development of carbide, 20: 38466 (ANL-7120, pp 301-13)
fuels for, development of carbide, 20: 38467 (ANL-7120, pp 314-27)
neutron Doppler coefficient calculations for, comparison of methods, 20: 38421 (ANL-7120, pp 440-8)
neutron Doppler effect calculations for, effect of collision density fluctuations on, 20: 38422 (ANL-7120, pp 449-61)
neutron Doppler effect calculations for, comparison of methods, 20: 38423 (ANL-7120, pp 462-77)
neutron Doppler effect in ZPR-3 mockup of, (E/T), 20: 38427 (ANL-7120, pp 603-9)
neutron Doppler effect for uranium-235 in, 20: 38429 (ANL-7120, pp 614-15)
neutron flux distribution in, analysis of transient, 20: 38431 (ANL-7120, pp 625-31)
neutronic coupling in modular, safety effects of, 20: 38436 (ANL-7120, pp 776-88)
neutronics calculations for 1000-Mw(e) metal-fueled breeder, 20: 38493 (ANL-7120, pp 85-93)
physics parameter study of large steam-cooled power, 20: 38438 (ANL-7120, pp 815-25)
physics parameters of 1000-Mw(e) ceramic, calculation of, 20: 38491 (ANL-7120, pp 24-32)
power monitoring in large, selection of points for, 20: 38432 (ANL-7120, pp 632-5)
program for estimating cost of fuel refabrication by remote control for, 20: 37195 (ANL-6950)
reactivity coefficients in sodium-cooled, (T), 20: 38418 (ANL-7120, pp 413-20)
reactivity of prompt critical, calculation method for, 20: 38413
reactivity sodium void coefficients for, comparison of calculated and experimental, 20: 38419 (ANL-7120, pp 421-2)
safety analysis of sodium-cooled, plutonium-fueled, 20: 37022 (LA-DC-6942)
safety characteristics of sodium-cooled coupled, 20: 38437 (ANL-7120, pp 789-93)
safety of gas- and steam-cooled, during flooding, 20: 38439 (ANL-7120, pp 826-36)
safety of, relation of fuel properties to, 20: 38424 (ANL-7120, pp 497-503)
safety research program of EURATOM-CEA on, 20: 38492 (ANL-7120, pp 54-66)
safety studies on, boiling of potassium in forced convection, 20: 38415
temperature distribution in fuels, calculation of transient, 20: 38470 (ANL-7120, pp 478-85)
FATS
analysis for copper in hydrogenated, activation, 20: 36724
FECES
analysis of, for carbon-14 and tritium by scintillation counting, combustion method for, 20: 36721
FERMI FAST BREEDER REACTOR
control and safety rod drive mechanisms for, design and operation of, 20: 38501 (APDA-301)
FERMIONS
perturbation series for interacting many-body systems of, convergence of, 20: 38121
Regge poles for, properties of, (T), 20: 37809
rotation of normal and superfluid, 20: 37473
theory for Bose gas production from bound state, 20: 37472
theory of normal liquid of, at zero temperature, 20: 37937
transport properties of degenerate systems of, at finite temperatures, (T), 20: 37984
FERMIUM ISOTOPES Fm-257
half life, (E), 20: 38093
FERMIUM ISOTOPES Fm-258
production by neutron reactions with fermium-257, (E), 20: 38093
FERRITES
electromagnetic wave propagation in, performance of, 20: 38231
FERROMAGNETIC MATERIALS
plasma oscillations and spin waves in, interaction of, (T), 20: 38354 (FTI-244/T-027)
FIELD THEORY
field equations in, localized solutions of classical Dirac-Maxwell, 20: 37849
gauge invariance in, formulation of, 20: 37825 (N-65-31239)
particle singularities in relativistic quantum, 20: 37833
quantum fields in, group theoretical construction of Rarita-Schwinger, 20: 37853
relativistic quantum, development of, 20: 37844
transformations in quantum, Lorentz and relativistic, 20: 37827 (UCRL-14365)
FILMS
analysis for tritium in surface, by scintillation counting, 20: 36738
charged-particle interactions with, transitional radiation from, (T), 20: 37434
flow transfer rates of helium, height dependence and fine structure of, (E), 20: 37943
superconducting state in ideal, with current, (T), 20: 37938
FINLAND
x-ray standards in, 20: 37078
FIRES
prediction of, in urban areas, 20: 36995 (AD-636794)
FISSION
theory of two-mode, testing of, 20: 37995
FISSION FRAGMENTS
conversion-electron and K x-ray emission by californium-252, (E), 20: 38095
distributions of, use of double-pulse ionization chamber for measuring angular, energy, and mass, 20: 37089
energy distribution from deuteron fission of radium-226 at 12 Mev, (E),

20: 38132
FISSION PRODUCTS
behavior of gaseous, in ceramic fuels, 20: 38482
control of gaseous, in reactor fuel alloys, 20: 37302
deposition from isothermal gas streams, calculation of, 20: 37041
diffusion from clad ceramic fuel elements, 20: 37168(R) (BMI-1771)
diffusion from fuels, determination methods for, 20: 37292
diffusion from urania at 150 to 2000°C, mechanisms of, 20: 37290
diffusion from urania at temperatures below 1500°C, mechanisms of, 20: 37291
diffusion of krypton and xenon from irradiated ceramic fuel elements, mechanisms of, 20: 37303
dispersion in fallout from nuclear tests, 20: 37004
effects of, in neutron activation analysis of uranium samples, 20: 36714
effects on fuels, theories of swelling, 20: 37299
effects on reactivity of large steam-cooled fast power reactors, 20: 38438 (ANL-7120, pp 815-25)
gamma spectra of, measurement for nondestructive fuel burnup determination, 20: 37287
gas bubble distribution in post-irradiation annealed uranium dioxide, electron microscopy studies on, 20: 37255
mass distributions from helium ion-induced fission of lead-207 at 41.1 to 26.3 Mev, 20: 37996
radiation dose from atmospheric release of up to 200, computer analysis of, 20: 37167 (IDO-17151)
ranges of recoil, in sodium chloride–uranium dioxide mixtures, 20: 37997
release from reactor fuel elements, effects of uranium dioxide density on, 20: 37254
release of gaseous, from vented-fuel sodium-cooled fast reactors, 20: 38475 (ANL-7120, pp 540-8)
release of gaseous, from uranium dioxide at 800 to 1600°C, 20: 38464 (AERE-M-1607)
retention by sodium in vented-fuel reactors, 20: 38477 (ANL-7120, pp 855-61)
separation from neptunium and uranium by ion exhcange using 8-quinolinol, 20: 36754
separation from radioactive waste solutions, 20: 38538
separation of cesium-137 and strontium-90 from nitric acid solutions of, chromatographic, 20: 36748
yields distributions from proton fission of uranium-238, charge and mass, 20: 37995
FISSIONABLE MATERIAL
criticality calculations using neutron age theory, eigenvalue problem in, 20: 37993
FISSIUM
fissium–Pu–U, development as fast reactor fuel, 20: 38465 (ANL-7120, pp 289-300)
FLAMES
ion formation in, Hall measurement of, 20: 38223
temperature measurement of oxyhydrogen, by thermal neutron scattering, 20: 37310
FLANGES
design with aluminum foil for use in ultra-high vacuum systems, 20: 37000 (UCID-4548(Rev.4))
FLAVONE, 3′,4′,7,8-TETRAHYDROXY-
complexes with thorium, preparation and properties of, 20: 36742
FLOCCULATION
use of cellulose–bentonite for, of ruthenium in waste solutions, 20: 36929
FLUID FLOW
analysis of two-phase, through tube apertures, 20: 36990
boiling effects on, in fast reactor cores, 20: 38440 (ANL-7120, pp 881-9)
boundary layers in crossed magnetic fields, 20: 37869
electrohydrodynamic, traveling-wave induced, (T/E), 20: 38280
equations for solid bodies with parallel coolant channels, 20: 38461 (CONF-651110-29)
hydromagnetic, past a slender body, 20: 37870
magnetohydrodynamic, Malkus theory of turbulent channel, 20: 38240
magnetohydrodynamic, between parallel planes, Hartmann, (T), 20: 38281
magnetohydrodynamic, between non-conducting plates in magnetic field, visco-elastic, 20: 37871
magnetohydrodynamic, perturbations due to oscillating dipole in, (T), 20: 37875
magnetohydrodynamic, between moving plane porous walls, (T), 20: 37876
magnetohydrodynamic, variational principles for equations of incompressible viscous, 20: 37877
magnetohydrodynamic, equations for jet-vortex, (T), 20: 37878
stability of MHD, (T), 20: 37874
two-phase adiabatic, liquid volume fraction measurements in upward, 20: 36985 (EURAEC-1088)
two-phase bubbly, hydrodynamic characteristics of upward, 20: 36988 (TID-23261)
two-phase, space-independent model of boiling hydraulic channel, 20: 36984 (BNL-963)
FLUID FUEL REACTORS
design and construction of KSTR, 20: 38534(R) (NP-16168(Pt.B))
development and research of KSTR, 20: 38533(R) (NP-16168(Pt.A))
FLUIDIZATION
development for protective coating deposition, 20: 37192
fluid bed production of uranium carbonitrides and uranium nitrides, processes for, 20: 36850
FLUIDS
density measurement using gamma absorption, instrument for, 20: 37059
hydromagnetic wave velocities in relativistic, calculation of, 20: 37883
FLUORIDE IONS
effects on copper determination, 20: 36726
FLUORIDE VOLATILITY PROCESSES
corrosion studies on materials for, 20: 37168(R) (BMI-1771)
corrosion studies on materials for, 20: 37169(R) (BMI-1774)
development of molten-salt, for processing aluminum–uranium fuels, 20: 36951
FLUORIDES
determination in plutonium nitrates using green CaF band spectrum, method for, 20: 36730
effects on rat ventricle contractions, modification by calcium, strontium, and magnesium, 20: 36567
FLUORINE
radiation doses to tissues from, in solar particle beams in space, 20: 37023 (N-65-33865)
FLUORINE IONS
polarizability and shielding factor for, dipole, (T), 20: 37440
FLUORINE ISOTOPES F-18
energy level lifetimes from tritium (O-16,nγ) reactions at 18 Mev, 20: 38008(R) (AECL-2595)
energy levels of, shell-model potential parameters for low-lying, (T), 20: 38145
FLUORINE ISOTOPES F-19
deuteron reactions (d,α) at 5.5 to 11.5 Mev, two-nucleon DWBA analysis of, (E/T), 20: 38082
meson (μ^-) capture by protons in, rate of, 20: 38166
nuclear magnetic resonance in calcium fluorides, free-induction decay shapes and moments for, (E), 20: 38390
nuclear octupole deformations in, rigidity parameters of, (T), 20: 38061
performance as solar neutrino detector, 20: 37793
FLUXMETERS
use with cesium NMR probes for calibrating superconducting solenoids, 20: 37972
FOOD
radiation processing of, bibliography on, 20: 37138 (AED-C-05-05)
radiation processing of, to destroy microorganisms, 20: 37140
radiation processing of, review of trends in, 20: 37142
radiation processing of, in Israel, 20: 37155
radiation processing of, in Israel, economic aspects of, 20: 37157
radiosterilization of, role of chemicals as sensitizers in, 20: 37144
FORENSIC SCIENCE
activation analysis of hair for individualization studies, 20: 36781
analysis of human blood and hair in, activation, 20: 36728
FORMAMIDE, *N,N*-DIMETHYL-
effects on radioinduced polymerization of acrylonitrile–styrene mixture, 20: 36876
use in polarographic studies of uranium salts, 20: 36745
FORMIC ACID
analytical use for determination of silicon in sputum by activation methods, 20: 36542
FORMIC ACID, OXYDI-, DIETHYL ESTER
effects on cells and growth of barley seeds, 20: 36589
FREE RADICALS
electron spin resonance spectra of, in x-irradiated potassium dihydrogen arsenate, 20: 36884
electron spin resonance spectra of, in irradiated crystals, 20: 36902
electron spin resonance spectra of, from gamma-irradiated pentafluoropropionamide, 20: 36872
radioinduced from hydrides in krypton, ESR studies of, 20: 36909
radioinduced in collagen, magnetic resonance of, 20: 36585
yields from electron radiolysis of silicoórganic compounds, EPR study of electron, 20: 36883
FRENCH REACTORS
development of natural uranium–graphite–gas, 20: 38515
FRUCTOSE
mutarotations of β-D-, deuterium isotope effects in, 20: 36577
FRUITS
radiation preservation of, 20: 37156
radiation processing of, in Israel, 20: 37155

radiation processing of, in Israel, economic aspects of, 20: 37157
FUNGI
mutation induction by nitrite in, protective effects of chloramphenicol against, 20: 36653
radioinduced mutations in, environmental effects on, 20: 36653
radiosensitivity of cytoplasmic mutant of *Aspergillus nidulans*, uv, 20: 36629
FURAN, TETRAHYDRO-2-METHYL-
radiation effects on organic sulfur compounds in glasses of, gamma, 20: 36894

G

GADOLINIUM
determination in complexes with diketones, spectrofluorometric, 20: 36722
determination in hydrochloric acid solutions, spectrographic carrier-distillation, 20: 36729
effects on crystal structure of cobalt, iron, and nickel intermetallic compounds, 20: 37243
effects on phase transformation temperature of thorium, 20: 37242
Hall effect in, anisotropy of, 20: 37178
neutron absorption cross section in pitchblende, thermal, 20: 37994
separation from hydrochloric acid solutions by solvent extraction using dialkyl alkylphosphonates, 20: 36941
GADOLINIUM ALLOYS
Co–Gd, crystal structure of intermetallic compounds in, 20: 37243
Gd–Fe, crystal structure of intermetallic compounds in, 20: 37243
Gd–Ge, crystal structure and magnetic properties, 20: 38369
Gd–La, superconducting transition temperature of, pressure dependence of, (E/T), 20: 37965
Gd–Ni, crystal structure of intermetallic compounds in, 20: 37243
Gd–Th, phase studies of, 20: 37242
GADOLINIUM CHROMITES
spectra of, infrared, 20: 36807
GADOLINIUM COMPLEXES
with diketones, spectrofluorometric analysis for, 20: 36722
with tartaric acid and trihydroxyglutaric acid, stability constants for, 20: 36838
GADOLINIUM IONS
energy levels in lanthanum ethyl sulfate, ionic contributions to ground-state splitting of, (T), 20: 38389
spectra of, effects of chemical bonding and transitions on, 20: 36845
GADOLINIUM ISOTOPES Gd-154
energy level transitions in, E2, (T), 20: 38127
nuclear strength parameter correlation with beta bands in, (T), 20: 38180
GADOLINIUM LACTATES
formation constant of, potentiometric determination of, 20: 36824
GADOLINIUM OXIDES
oxygen isotopic exchange on, at −78 to 500°C, 20: 36826
Gd_2O_3–ReO_2, magnetic properties and structure of compounds formed in, 20: 36784(R) (AD-636054)
GADOLINIUM PHOSPHIDES
crystal structure, 20: 38370
electric conductivity and magnetic susceptibility, 20: 38370
GAGES
development of radioisotope-using, 20: 37142
development of radioisotope, for industry, 20: 37149
GALAXIES
age determination of, review of, 20: 37410
cosmic ray acceleration by, cosmic electron energy spectra for determining efficiency of, 20: 37499
cosmic ray kinetic effects in, 20: 37501
cosmic-ray emission from radio, 20: 37490
effects of exploding, on cosmic ray flux, 20: 37370
element abundance in Magellanic Clouds, 20: 37428
evolution of, scintillation model for, 20: 37358
gas motion in, non-relativistic equations of bulk, (T), 20: 37344
helium formation in, 20: 37409
magnetic fields in, distribution and strength of, (E), 20: 37368
radiation background in, origin of microwave, 20: 37362
radio emission from, correlations with primary cosmic electron origin, 20: 37496
x-ray sources in, energy spectra from, 20: 37488
GALENAS
analysis for components of, by scattering of accelerated alpha particles, 20: 36719
GALLIUM
separation from neutron-irradiated biological materials by ion exchange, 20: 36762
yields from radiolysis of gallium phthalocyanine, 20: 36886
GALLIUM ALLOYS
Au–Ga, superconductivity of AuGa, 20: 37985
Ga–V, critical field of superconducting V_3Ga, (T), 20: 37936 (CLM-R-60)
GALLIUM ISOTOPES Ga-64
beta decay of, beta-gamma circular polarization correlation in, (E), 20: 38065
energy levels of, spin and isospin impurity of ground-state, (E), 20: 38065
GALLIUM ISOTOPES Ga-66
energy levels, (E), 20: 38058
GALLIUM ISOTOPES Ga-69
neutron strength functions of, calculation of, 20: 38038
GALLIUM ISOTOPES Ga-71
neutron strength functions of, calculation of, 20: 38038
GALLIUM OXIDES
reactions with lanthanum and neodymium oxides in solid state, 20: 36840
Ce_2O_3–Ga_2O_3, phase studies at temperatures to 2600°C, 20: 36808
GALLIUM PHOSPHIDES
radioinduced defects in, ESR study of electron and proton, 20: 38399
GAMMA-ABSORPTION ANALYSIS
use of, for solutions containing plutonium and uranium, 20: 36767
GAMMA RADIATION
absorption of 23.8 kev, from superconducting tin and tin alloys, 20: 37271
absorption of, recoil nuclear resonance, 20: 37461
activity in bones in leukemic patients, 20: 36559
angular correlations for E2 and E3 transitions in Coulomb excitation, (T), 20: 38032
angular correlations from nuclear reactions, performance of detectors for measuring, 20: 38184
content in herbaceous and woody plants and lichens of Neotoma Valley, Ohio, 1962 and 1964, 20: 36548 (TID-23036)
detection and measurement of, design of Rem responding rate meter for, 20: 37068 (BNL-10321)
detection and measurement of, development of portable monitor for, 20: 37071 (DP-993)
dose calculations for deposited fallout in India, 20: 37004
dosimetry of, polymer degradation dosimeter for, 20: 37117
dosimetry using photoactivation of isomeric nuclear states, 20: 37079
effects in producing mutations in peanuts, 20: 36647
effects on alkali metal and alkaline earth bromates, 20: 36899
effects on alkaline ices, role of trapped electrons in, 20: 36871
effects on anatomy and pathology in pigs, whole-body, 20: 36657
effects on aqueous liquid ammonia solution, production of hydrazine in, 20: 36869
effects on benzene, decomposition products from, 20: 36881
effects on blood serum proteins, chemical, 20: 36579
effects on carrier lifetime and detectivity of antimony–indium semiconductors, 20: 37295
effects on catalytic activity, surface excess oxygen, and electric conductivity of nickel oxide, 20: 36885
effects on chlorophyll mutation frequency, meiosis, and mitosis in peas, 20: 36621
effects on chlorophyll and morphological mutations in pea varieties, 20: 36624
effects on chromosomes in barley seed, effects of diethyl pyrocarbonate on, 20: 36589
effects on color changes and fall of leaves, 20: 36609
effects on conductivity of electrolyte solutions, 20: 36912
effects on corrosion of stainless steel by water, 20: 37182
effects on cross linking in polyvinylidene fluoride, 20: 36859 (N-66-13497)
effects on crystal structure of normal and deuterated ammonium sulfate, 20: 36874
effects on cyclohexane in presence of iodine, 20: 36888
effects on cyclomerization of 4-carbon compounds, 20: 36860 (NP-16150)
effects on decomposition of pectins at various moisture levels, 20: 36879
effects on decomposition of inorganic sulfates, 20: 36903
effects on deuterium–hydrogen exchange in gaseous and liquid deuterium–hydrocarbon systems, 20: 36866
effects on dichroism in R-bands of potassium chloride spectra, 20: 36905
effects on Dische-positive material in dog, pig, and rabbit blood and urine, 20: 36604
effects on Drosophila sperm cells in succeeding generations after oocyte exposure, 20: 36625
effects on electric conductivity in ionic insulators, (T), 20: 38353 (BNWL-SA-247)
effects on flotation properties of anionic collector agents, 20: 36893
effects on genetic variability in Habrobracon, 20: 36659
effects on grafting of acrylonitrile–styrene mixture on polyvinyl chloride, 20: 36877
effects on grafting of acrylonitrile–styrene mixtures on polytetrafluoroethylene, 20: 36878

effects on heart function in dogs, 20: 36660
effects on HeLa cells, electron microscopy study on, 20: 36616
effects on hematopoietic response in guinea pigs, effects of unilateral limb shielding on, 20: 36611
effects on hydrides in krypton, ESR studies of, 20: 36909
effects on insulated-gate FET transistors, gain and drain current from, 20: 37132
effects on luminescence intensity of anthracene, 20: 37131
effects on *Lupinus* seeds, variations with moisture content, 20: 36646
effects on mice, effects of oral cystamine on, 20: 36666
effects on mutation frequency in wheat, 20: 36620
effects on mutation induction in cotton species *Gossypium barbadense*, 20: 36623
effects on mutations in wheat embryos, 20: 36650
effects on n-type germanium, recombination and trapping from, (E), 20: 38364
effects on nickel, silver, and zinc chelates of tetraphenylporphine in dioxane, 20: 36889
effects on optical maser materials, 20: 37280 (NYO-3330-11)
effects on optical absorption of alkali borate glass containing arsenic or manganese, 20: 36887
effects on organic sulfur compounds in organic glass at −196°C, 20: 36894
effects on paramagnetic center formation in ammonium selenates, 20: 38398
effects on peas, genetic, 20: 36634
effects on pentafluoropropionamide monocrystals, ESR studies of, 20: 36872
effects on phthalocyanines, 20: 36886
effects on polyimidazopyrrolones, 20: 36846 (N-66-13499)
effects on polymerization of dodecyl methacrylate, 20: 36875
effects on polymerization of acrylonitrile–styrene mixture, 20: 36876
effects on potassium bromide, 20: 36901
effects on potato starch, effects of water content on, 20: 36599
effects on radioinduced polymerization of acrylonitrile on INZ-600 brick at 300°C, 20: 36882
effects on rats, biological, 20: 36654
effects on reactions of 1-butene and phosgene at −78 to 35°C, 20: 36892
effects on recombination of hydrogen and oxygen, 20: 36910
effects on rice, RBE comparison of fast neutron and, 20: 36649
effects on social distractibility behavior of female monkeys, 20: 36639
effects on sodium polyphosphates, ESR studies of, 20: 36870
effects on southeastern tree species, predicted seasonal, 20: 36551
effects on structure of ribonuclease, 20: 36584
effects on telomerization of ethylene with carbon tetrachloride, 20: 36890
effects on telomerization of ethylene with carbon tetrachloride under constant ethylene pressure, 20: 36891
effects on thermal decomposition of mercury oxalate, 20: 36898
effects on thermal decomposition and electric properties of barium azide, 20: 36900
effects on toluene and benzene saturated with tritiated water, 20: 36868
effects on wheat, effects of polyploidy on, 20: 36648
energy absorption in cylinders with axial source, 20: 37032
interactions with deuterons, nonphysical partial-wave amplitude singularities in disintegration, (T), 20: 38140
interactions with protons at 214 and 249 Mev, angular distributions from elastic, 20: 37800
interactions with protons, kinematic enhancement of resonance production in, 20: 37769
measurement of high-energy, using lithium-drifted germanium detectors, 20: 37126
monitoring after Sulky Event, 20: 36960 (PNE-717F)
monitoring in personnel in Prague, use of film dosimeters for, 20: 37035
production from cosmic ray interactions in atmosphere, (E/T), 20: 37576
reactions (γ,α) with aluminum, copper, magnesium, nickel, sulfur, and zinc at 31 Mev, alpha spectra from, (E), 20: 38037
reactions (γ,He-3) with lithium-7, cross sections for, 20: 38138
reactions (γ,n), (γ,2n), and (γ,3n) with iodine-127 and praseodymium-141, cross sections for, (E), 20: 38094
reactions (γ,n) with nuclei, polarization effects in, (T), 20: 38175
reactions (γ,p) with beryllium-9, polarization of protons from, (E), 20: 38146
reactions with copper, nickel, and silver at 6.13 Mev, pair-production cross sections for, (E), 20: 37746
scattering by nuclei, g factor measurement by resonant, (T), 20: 38079
scattering effects on collimation of, Compton, 20: 37465
scattering of, use in research on underground water supplies, 20: 37135
spectra of, from encapsulated sources, (T), 20: 38349 (AD-636788)

GAMMA SOURCES
collimators for, Compton scattering effects on, 20: 37465
design of cesium telecurie, for radiotherapy, 20: 36710
design of, for radiotherapy, 20: 36680
detection of primary, in direction of Cygnus constellation, 20: 37365
half lives of, chart of energy function of, 20: 36739
production and use of cobalt-60 for, economics of, 20: 37165
shielding by encapsulated, Monte Carlo calculation of self-, (T), 20: 38349 (AD-636788)
use for automatic corrections in liquid scintillation counting of carbon-14 and tritium, 20: 36743
use for detecting radiation injuries in brain, 20: 36696
use in anti-collision guidance systems, 20: 37141
use in geophysics, research program in Soviet Union on, 20: 37001

GAMMA SPECTRA
reduction of Compton continua in scintillation, method for, 20: 37123

GAMMA SPECTROMETERS
design and response of scintillation anticoincidence-shielded, 20: 37115
design of Mössbauer, 20: 37056
design using curved lithium–fluoride crystals, 20: 38158
development using lithium-drifted germanium diodes, 20: 37072 (KFK-429)
efficiency of scintillation-type, reduction of Compton continua for improvement of, 20: 37123
performance in fuel burnup determinations, 20: 37287

GAMMA SPECTROSCOPY
Kirchhoff's law in, 20: 37433
use for determining iron in ores and rocks in boreholes, 20: 37019
use in analysis of rocks in boreholes, 20: 37018
use in nondestructive determination of fuel burnup, 20: 37287

GAS ANALYZERS
description of continuous, using x-ray fluorescence, 20: 36766
design using ionization chamber with beta source, 20: 36768

GAS COOLED REACTORS
design and safety of large fast power, panel discussion on, 20: 38457 (ANL-7120, pp 261-85)
design of British advanced, for power production, 20: 38514
development, 20: 38523
development of natural uranium, graphite-moderated, in France, 20: 38515
fuel element fabrication processes for, 20: 37168(R) (BMI-1771)
fuel elements for, heat transfer and fluid dynamics of, 20: 38481
safety of fast, during flooding, 20: 38439 (ANL-7120, pp 826-36)
stability of AGR systems, analysis of axial, 20: 38446 (TRG-Report-1138)

GAS FLOW
fission product deposition from, calculation of, 20: 37041
magnetohydrodynamic, over a wedge, (T), 20: 38242
magnetohydrodynamic, shock discontinuities in, with aligned magnetic field, (T), 20: 37872

GAS TURBINE ENGINES
ceramics for, symposium on, 20: 37179

GASEOUS DIFFUSION PLANTS
uranium unit cost components, tables of 10-10, 20: 37161 (K-OA-1313)

GASEOUS REACTIONS
radioinduced graft polymerization during, 20: 36908

GASES
analysis using x-ray fluorescence, continuous, 20: 36766
beta activity in, design of plastic scintillator cell for measuring, 20: 37086
bibliography on high-temperature, 20: 38204 (NP-16240)
electric discharges in, striation production from, 20: 38206 (ORNL-P-1539)
electromagnetic properties of, (T), 20: 37867
expansion of relativistic, in intergalactic space, (T), 20: 37503
interactions with magnetic fields, MHD properties of, (T), 20: 37867
ion mobility in, measurement of, using ionization chamber with beta source, 20: 36768
kinetic theory for Boltzmann, propagation of correlations in, 20: 37865 (PPL-AF-2)
mesons (μ) capture in mixed, 20: 37741 (JINR-P-2788)
mixing of, high-pressure facility for, 20: 36981 (Y-1546)
motion of relativistic, bulk, (T), 20: 37344
production of Bose, using bound states of Fermi particles, (T), 20: 37472
shock wave interactions with, effect of line radiation on precursor ionization in, 20: 37881
spectra of high-temperature, bibliography on, 20: 38204 (NP-16240)
spectra of, Kirchhoff's law in absorption and emission, (T), 20: 37433
gas–liquid, two-phase adiabatic flow of, liquid volume fraction measurements in upward, 20: 36985 (EURAEC-1088)

GASKETS
design of aluminum-foil, for use with flange in ultra-high vacuum systems, 20: 37000 (UCID-4548(Rev.4))

GASTROINTESTINAL TRACT
book: *Yearbook of Nuclear Medicine*, Vol. I, 1966, 20: 36690
strontium-90 transport from rat blood stream to, 20: 36558

GATING SYSTEMS
design and performance for photomultiplier tubes, 20: 37051
GENETICS
book: *Very Faint Luminescence in Biochemical Reactions*, 20: 36547
effects on carbon-13 and oxygen-18 isotopic variations in sea urchins, 20: 36550
influence of genotype on barley absorption of strontium, 20: 36575
radiation effects on egg-to-adult viability in *D. melanogaster*, 20: 36618
radiation hazards to, significance of medical, 20: 36677
radiation hazards in, significance of medical, 20: 36709
radioinduced variability in Habrobracon, gamma, 20: 36659
GEOMAGNETIC FIELDS
charged-particle acceleration in neutral sheet in tail of, models for, 20: 37901
conjugate point phenomena, 20: 37914
effects of cavity, on cosmic ray rigidity cutoff, (T), 20: 37596
effects on cosmic ray intensity, 20: 37545
electron and proton fluxes in, near earth, (E), 20: 37902
electron density in anomaly region of, longitude dependence of, (T), 20: 37906
fluctuation detection by solidification of naphthalene, correlation with lunar phases in, 20: 37891
fluctuations of, solidification of naphthalene for detecting, 20: 37889
intensity correlations with cosmic neutron variations, H component, (E), 20: 37590
measurement in magnetosphere and interplanetary space regions, 20: 37917
pulsations in magnetoconjugate micro-, 20: 37914
solar wind neutral point in, geometry of, (T), 20: 37895
structure in magnetosphere, review of measurements, 20: 37898
variations at conjugate points, 20: 37914
variations of, associated with corpuscular precipitation at South Pole, 20: 37897
GEOMAGNETIC STORMS
effects on enhanced ionizations in, spatial extent of, 20: 37893
effects on naphthalene crystallization test, 20: 37890
intensity variations in, pre-SC, 20: 37892
GEOPHYSICAL PROSPECTING
instruments and techniques in, radiometric, 20: 37060
method for, using directional radiation analysis, 20: 37021(P)
neutron source for well logging in gas and oil wells, 20: 37017
use of radiometric instruments and techniques in, conference on, 20: 37133 (STI-PUB-112(Vol.2))
GEOPHYSICS
instruments and techniques in, radiometric, 20: 37060
neutron source for well logging in gas and oil wells, 20: 37017
radioisotope uses in, 20: 37143
research on, using isotopic composition of extraterrestrial and terrestrial material, 20: 37369
use of radiometric instruments and techniques in, conference on, 20: 37133 (STI-PUB-112(Vol.2))
use of radiometric instruments and techniques in Soviet Union, 20: 37001
GERMANIUM
electron momentum distribution in, positron annihilation method for determining, 20: 37736 (COO-1297-7)
performance of detectors of, for measuring gamma angular correlations, 20: 38184
radioinduced damage at 200 to 1000 ev in films of, ion, (E), 20: 38363
radioinduced defects at 6 to 88 Mev in n-type, annealing of electron, 20: 38365
radioinduced recombination and trapping in antimony- and arsenic-doped, gamma, (E), 20: 38364
response linearity of detectors of, (E), 20: 37126
use of lithium-drifted diodes of, in neutron capture gamma spectroscopy, 20: 37072 (KFK-429)
yields from radiolysis of germanium phthalocyanine, 20: 36886
GERMANIUM ALLOYS
Dy–Ge, crystal structure, (E), 20: 38369
Er–Ge, crystal structure, (E), 20: 38369
Gd–Ge, crystal structure and magnetic properties, 20: 38369
Ge–Ho, crystal structure, (E), 20: 38369
Ge–La, preparation and properties of intermetallic compounds, 20: 37259
Ge–Nd, crystal structure and magnetic properties, 20: 38369
Ge–Pr, crystal structure and magnetic properties, 20: 38369
Ge–Sm, crystal structure and magnetic properties, 20: 38369
Ge–Tb, crystal structure and magnetic properties, 20: 38369
GERMANIUM HYDRIDES
radioinduced free radicals of, in krypton, 20: 36909
GERMANIUM ISOTOPES Ge-77
yields from helium ion-induced fission of lead-207 at 41.1 to 26.3 Mev, 20: 37996
GERMANIUM ISOTOPES Ge-78
yields from helium ion-induced fission of lead-207 at 41.1 to 26.3 Mev, 20: 37996
GERMANY
fallout monitoring in, data in annual weather service report, 20: 37009
radiation protection measures at University of Munich, 20: 37040
radioisotope production and uses in, 20: 37137
strontium-90 content in hay in, 1962, 20: 36671
strontium-90 content in milk in, 1962 through 1964, 20: 36674
GLANDS
metabolism of thyroxine and triiodothyronine in lachrymal, in mice, 20: 36570
GLASS
performance of surface roughened, for measuring beta activity in tritium phosphors, 20: 37084
phosphorus-32 adsorbed by, removal of, 20: 36923
radiation effects on optical properties of rare-earth doped, 20: 37280 (NYO-3330-11)
GLOBULIN
iron-59 distribution in, of chicken serum fractions, 20:36569
radiation effects on rat, effects of serum lyophilization and tumors on whole-body x, 20: 36582
GLUCOSE
mutarotations of α-D-, deuterium isotope effects in, 20: 36577
production in dogs, use of carbon-14 and tritium tracers for measuring, 20: 36565
GLUTARIC ACID, TRIHYDROXY-
complexes with rare earths, stability constants for, 20: 36838
GLYCINE, *N*-AMIDINO-
radiation effects on methylation of, in rat liver, x, 20: 36603
GLYCOLYSIS
radiation effects on, in guinea pig and rat retina, x, 20: 36630
GLYOXIME, DIMETHYL-
complexes with iron, Moessbauer spectra of, at +23, −78, and −195°C, 20: 36823
GOLD
determination in solutions, colorimetric, 20: 36725
determination using x-ray fluorescence, instrument for, 20: 37150
effects of beryllium additions on, 20: 37275
effects on determination of iridium in ores by neutron activation analysis, 20: 36751
separation from neutron-irradiated biological materials by ion exchange, 20: 36762
stopping power for lead-208 alpha recoil nuclei, 20: 37470
superconductivity, 20: 37985
vapor pressure of, effusion method for measuring, 20: 37307 (LA-3509)
x-ray spectra from mu-mesic atoms of, (E), 20: 38058
GOLD ALLOYS
Al–Au, superconductivity of $AlAu_4$, 20: 37985
Au–Ga, superconductivity of AuGa, 20: 37985
Au–In, superconductivity of AuIn, 20: 37985
Au–Pb, superconductivity of Au_2Pb, 20: 37985
Au–Sn, superconductivity of Au_5Sn and AuSn, 20: 37985
Ca–Au, superconductivity of Au_5Ca, 20: 37985
GOLD ISOTOPES Au-195
energy levels of, energy ratios and spins of, (E/T), 20: 38022
GOLD ISOTOPES Au-197
neutron reactions (n,α) at 12 to 23 Mev, (E), 20: 38036
GONADS
protection of, during radiotherapy in children, 20: 36707
radiation effects on Drosophila sperm cells in succeeding generations after oocyte exposure, gamma, 20: 36625
GRAIN GROWTH
in magnesium–zirconium alloys, effects of hydration on during recrystallization, 20: 37252
GRAPHITE
coating with hafnia and zirconia by alkoxide decomposition, 20: 36851
cosmic particle reactions at high energies, gamma and meson (π) production from, (E), 20: 38110
energy release and storage by irradiated, 20: 37283
neutron scattering by cylinders of, spectra from fast, (E/T), 20: 38007
permeability of, methods of determining, 20: 37225
properties of dense, effects of fabrication on, 20: 37168(R) (BMI-1771)
properties of dense, effects of fabrication on, 20: 37169(R) (BMI-1774)
radioinduced creep in, effects of temperature on, 20: 37223
radioinduced creep and dimensional changes in, neutron, 20: 37282
radioinduced energy storage, effects of high temperatures on, 20: 37283
reactions with europium, thermodynamics of, 20: 36844
sorptive properties for cesium at 800 to 1100°C, 20: 36799
GRAPHITE (IMPREGNATED)
creep rates of, effects of stress on, 20: 37224
fabrication by extrusion, feasibility of, 20: 37196
GRAPHITE MODERATED REACTORS
development of natural uranium, gas-cooled, in France, 20: 38515

GRAVITATION
collapse of spherical dust cloud, null coordinates for, 20: 37921
effect on plasma ballooning interchange instabilities, (T), 20: 38267
fluctuations in, formation of, 20: 37928(T)
theory in general relativity, quadratic lagrangians in, 20: 37918
theory of, in Minkowskian metric, 20: 37923
GROUND WATERS
radioactivity of Maine and New Hampshire, 20: 37006
GROWTH
radiation effects on lymphoma cell, by exposure of culture medium, 20: 36633
GUANIDINE, 1,1'-(DITHIODIETHYLENE)DI-
protection against radiation damage in calf-thymus DNA, mechanism of, 20: 36665
GUANINE
reactions with hydroxyl radicals, ESR spectral studies on, 20: 36806
GUINEA PIGS
radiation effects on delayed hypersensitivity in, x, 20: 36655
radiation effects on hematopoietic response in, effects of unilateral limb shielding on gamma, 20: 36611
radiation effects on glycolysis and respiration in retina in, x, 20: 36630
radiation effects on longevity of, fast-neutron, 20: 36640
GYROMAGNETIC RATIO
measurement for excited nuclear states by resonant scattering, theoretical basis for, 20: 38079

H

HAFNIUM
corrosion and mechanical properties of, effects of oxygen on, 20: 37170
determination of, using Arsenazo III, photometric, 20: 36778
effects on crystal structure and properties of thoria-tungsten cermets, 20: 37185
effects on reactivity of gas- and steam-cooled fast reactors during flooding, 20: 38439 (ANL-7120, pp 826-36)
HAFNIUM ALCOHOLATES
preparation of, and thermal decomposition to oxide coatings and powders, 20: 36851
HAFNIUM ALLOYS
Al–Hf, properties of intermetallic compound, 20: 37260
HAFNIUM ISOTOPES
purification of electromagnetically separated, 20: 37163
HAFNIUM ISOTOPES Hf-174
energy level transitions from lutetium-175 (p,2n) reactions, ground state rotational, 20: 38008(R) (AECL-2595)
HAFNIUM ISOTOPES Hf-178
nuclear strength parameter correlation with beta bands in, (T), 20: 38180
HAFNIUM OXIDES
deposition on graphite by alkoxide decomposition, 20: 36851
preparation of monocrystals of, using fused salts, 20: 37197
HAIR
analysis of human, activation, 20: 36728
analysis of, for individualization, by neutron activation, 20: 36781
HALIDES
phase diagrams of binary systems of, 20: 36787 (YALE-2723(Vol.1))
HALL EFFECT
measurement in gadolinium, anisotropy of, 20: 37178
use for measuring ion formation in flames, 20: 38223
HALOGENS
effects on quenching of energy spectra in determination of carbon-14, sulfur-35, and tritium, 20: 36771
HAMSTERS
radiation effects on tissue cells of, after plating and trypsinization, 20: 36664
HANDBOOKS AND MANUALS
book: *The Radiochemical Manual*. Second Edition, 20: 36924
HARDNESS
anisotropy of Knoop metallic, relations with plastic flow of polycrystalline metals, 20: 37230
of magnesium–zirconium alloys, effects of hydration on, 20: 37252
HASTELLOY F
corrosion by boiling hydrofluoric acid–nitric acid solutions, 20: 37169(R) (BMI-1774)
HEAD
radiotherapy of carcinomas of, use of electron beams for, 20: 36685
HEALTH PHYSICS
book: *Yearbook of Nuclear Medicine*, Vol. I, 1966, 20: 36690
research program at CERN, 1965, 20: 37308(R) (NP-16226)
HEART
failure produced by embolization in, hemodynamic parameters in, 20: 36660
radioinduced failure of dog, hemodynamic parameters in, gamma, 20: 36660
HEAT
recovery from stored waste, 20: 38539(P)
sources of, economics of production and use of cobalt-60 as, 20: 37165
HEAT EXCHANGERS
efficiency of, in combined MHD-reactor system, 20: 38488 (AERE-R-5031)
HEAT TRANSFER
coefficient measurements in boiling on multirod geometries, 20: 36986 (GEAP-5073)
convective, in nitrogen and methane, 20: 36993
equations for solid bodies with parallel coolant channels, 20: 38461 (CONF-651110-29)
from reactor fuel elements, limitations on rates of external, 20: 38484
in MIN-K type insulations, analysis of, 20: 36983(R) (ALO-3633-1)
HEAVY WATER REACTORS
development for power, 20: 38517
heat transfer limitations on fuel elements, 20: 38484
neutron thermalization in, phenomenological model application, 20: 38455
physics parameter study of large steam-cooled fast power, 20: 38438 (ANL-7120, pp 815-25)
HELIUM
effects on vibrational excitation of carbon monoxide in shock tubes, 20: 36820
electron density measurements in underdense plasma of, 20: 38254
electron reactions with, excitation cross sections for n = 2 states from, (T), 20: 37453
film transfer rates, height dependence and fine structure of, (E), 20: 37943
formation in galaxies, 20: 37409
ion mobility and quantized vortex rings in liquid II, at 3°K, (E), 20: 37947
ion trapping by vortex lines in rotating liquid II, pressure effects on radius of negative, 20: 37960
ions in liquid II, model for negative, 20: 37981
neutron absorption cross section in pitchblende, thermal, 20: 37994
plasma of, production and properties of shock-heated, 20: 38344
polarizability and shielding factor for atomic, dipole, (T), 20: 37440
positron annihilation in, (E), 20: 37810
positron lifetimes in gaseous, at low temperatures, (E), 20: 37817
properties of liquid II, rotational, 20: 37987
proton elastic scattering at 1 Bev, differential cross section for, (E), 20: 38010 (BNL-10438)
radiation doses to tissues from, in solar particle beams in space, 20: 37023 (N-65-33865)
reactions with tungsten, electron ejection from, (E), 20: 37450
stability of plasma of, density distribution effect on helical, (E), 20: 38270
theory for dilute mixtures of helium-3 in liquid helium-4 at low temperatures, 20: 37946
HELIUM IONS
beams of, production and polarization of helium-3, 20: 38149
effects on germanium films, depth of damage from, (E), 20: 38363
energy spectra of solar co-rotating, 20: 37371
reactions with lead-207 at 41.1 to 26.3 Mev, cross sections for fission, 20: 37996
HELIUM ISOTOPES He-3
content in primary cosmic radiation, ratio for, (E), 20: 37559
content in primary cosmic radiation, (E), 20: 37572
content in primary cosmic radiation, (E), 20: 37581
deuteron reactions (d,n) at 7 to 12 Mev, neutron spectra from, (E), 20: 38077
dissolution in liquid helium-4, low temperatures from, 20: 37978
emission in nuclear transitions superfluid model for reduced widths for, 20: 38116
energy and rigidity spectra in primary cosmic radiation, at 80 to 150 Mev/nucleon, (E), 20: 37579
meson (π) reactions with, decay processes from, 20: 38011 (JINR-P-2805)
mesons (π^-) reactions with, charge exchange in, (E), 20: 37740 (JINR-P-2780)
nuclear spin relaxation in liquid, intermolecular contribution to, 20: 36828
particle coupling to collective excitations in atomic, single, (T), 20: 37449
polarization of neutral beams of, (E), 20: 38149
proton reactions (p,d) with, angular correlations in, (E), 20: 38129
reactions (He-3,d) with even tin isotopes at 18 Mev, energy levels of odd antimony isotopes from, (E), 20: 38073
reactions (He-3,n) and (He-3,p) with oxygen in aluminum and zirconium, analytical uses of, 20: 36741
reactions (He-3,p) with deuterium, angular distribution and polarization of protons from, (E), 20: 38149
reactions of atoms of, coherence transfer by spin exchange in, (E), 20: 37458

reactions with helium-3 at 0.5 to 1.7 Mev, cross sections for, (E), 20: 38131
reactions with nickel-61, formation and decay of zinc-64 in, 20: 38152
superfluidity of, review, 20: 37974
thermal capacity of liquid, anomalies in, (T), 20: 37873
thermal capacity of adsorbed, at 0.25 to 4°K, 20: 37982
thermal conductivity of crystals of, from 0.5°K to melting, 20: 37983
transport properties of, (T), 20: 37984
He-3–He-4, magnetic and thermal properties of superfluid, (E), 20: 37961
He-3–He-4, reactions in superfluid, 20: 37962
He-3–He-4, theory for dilute mixtures at low temperatures, 20: 37946
He-3–He-4, thermal conductivity of crystals of, from 0.5°K to melting, 20: 37983

HELIUM ISOTOPES He-4
content in primary cosmic radiation, (E), 20: 37572
content in primary cosmic radiation, (E), 20: 37581
energy and rigidity spectra in primary cosmic radiation, at 80 to 150 Mev/nucleon, (E), 20: 37579
energy levels in breathing-mode collective model, (T), 20: 38170
helium-3 dissolution in, low temperatures from liquid, 20: 37978
optical pumping of atoms of, modulated absorption of light from, 20: 37457
reactions with nickel-60, formation and decay of zinc-64 in, 20: 38152
specific heat of liquid, above lambda point, (T), 20: 37968
superfluidity of, review, 20: 37974
thermal capacity of adsorbed, at 0.25 to 4°K, 20: 37982
thermal conductivity of crystals of, from 0.5°K to melting, 20: 37983
He-3–He-4, magnetic and thermal properties of superfluid, (E), 20: 37961
He-3–He-4, reactions in superfluid, 20: 37962
He-3–He-4, theory for dilute mixtures at low temperatures, 20: 37946
He-3–He-4, thermal conductivity of crystals of, from 0.5°K to melting, 20: 37983

HELIUM ISOTOPES He-5
energy level widths in, effects of cluster structure on virtual-resonance, 20: 38013

HEMATITES
neutron inelastic scattering at 0.0053 ev, spin wave spectra from, (E), 20: 38355 (ITEF-355)

HEMATOPOIETIC SYSTEM
book: *Yearbook of Nuclear Medicine*, Vol. I, 1966, 20: 36690
radiation effects on guinea pig, effects of unilateral limb shielding on gamma, 20: 36611

HEMOLYSIN
radiation effects on, in rat spleen, local x, 20: 36637

HEPTANE
heptane–polyisobutylene, use in polymer degradation dosimeter, 20: 37117

HETEROGENEOUS REACTORS
control of, internal regulation theory, 20: 38412 (ITEF-406)
critical size analysis using false source method, 20: 38444 (JINR-P-2699)

HEXADECANE
analysis of, for tritium, combustion method for, 20: 36721

HEXANE
radiation effects on deuterium exchange with heavy water, 20: 36866
hexane–TBP, solvent properties for uranium, 20: 36932

1-HEXANOL
effects on copper determination by absorption spectroscopy, 20: 36726

HIGH-PRESSURE SYSTEMS
description of, for gas mixing, 20: 36981 (Y-1546)

HIROSHIMA
leukemia development in humans in, 1946 to 1964, 20: 36645
radiation effects on blood plasma proteins in bomb survivors, 20: 36581

HISTAMINE
effects of liberators of, on calcification produced by various metals in rats, 20: 36557

HOLMIUM
determination in hydrochloric acid solutions, spectrographic carrier-distillation, 20: 36729
effects on crystal structure of cobalt, iron, and nickel intermetallic compounds, 20: 37243
effects on phase transformation temperature of thorium, 20: 37242
energy levels of, ionization energies from, (T), 20: 37439
neutron absorption cross section in pitchblende, thermal, 20: 37994

HOLMIUM ALLOYS
Co–Ho, crystal structure of intermetallic compounds in, 20: 37243
Ge–Ho, crystal structure, (E), 20: 38369
Ho–Fe, crystal structure of intermetallic compounds in, 20: 37243
Ho–Ni, crystal structure of intermetallic compounds in, 20: 37243
Ho–Th, phase studies of, 20: 37242
Ho–Zr, fracture at 78, 197, and 373°K, mechanism of, 20: 37231

HOLMIUM CHROMITES
spectra of, infrared, 20: 36807

HOLMIUM COMPLEXES
with ascorbic acid, molar extinction coefficients and stability constants for, 20: 36852
with pyrogallosulfonic acid, formation of, potentiometric and spectrophotometric studies of, 20: 36837
with tartaric acid and trihydroxyglutaric acid, stability constants for, 20: 36838

HOLMIUM HYDROXIDE OXIDES
preparation and crystal structure of, 20: 36791

HOLMIUM HYDROXIDES
preparation and crystal structure of, 20: 36791

HOLMIUM IONS
spectra of, effects of chemical bonding and transitions on, 20: 36845

HOLMIUM ISOTOPES Ho-165
proton reactions (p,2n) with, gamma transitions in ground state rotational bands from, 20: 38008(R) (AECL-2595)

HORNBLENDE
oxygen-16/-18 ratio in, effect of metamorphism on, 20: 37013

HUMIC ACIDS
use for extraction of barium-137, cesium-137, cobalt-60, and strontium-89 from waste solutions, 20: 36930

HUMIDITY
neutron measurement of, in maize, conditioning and storage using, 20: 37154

HYDRAZINE
production of, by gamma radiolysis of liquid ammonia and water, 20: 36869

HYDRAZYL, DIPHENYLPICRYL-
effects on radioinduced polymerization of allyl alcohol, 20: 36880

HYDROCHLORIC ACID
HCl–$SnCl_2$, radiolysis of aqueous solutions of, gamma, 20: 36911

HYDROFLUORIC ACID
solubility in molten beryllium fluoride–lithium fluoride, deuterium effects on, 20: 36785 (ORNL-P-2202)
HF–HNO_3, corrosive effects on corronel 230, 20: 37168(R) (BMI-1771)
HF–HNO_3, effects on corrosion resistant alloys, 20: 37169(R) (BMI-1774)

HYDROGEN
analysis for para- and ortho-, chromatographic, 20: 36737
atomic interactions with electrons, book on, 20: 37477(T)
density of intergalactic molecular, (E), 20: 37353
determination in heavy water, neutron attenuation measurements for, 20: 36740
determination of, in deuterium and deuterium hydride mixture, chromatographic, 20: 36737
effects on embrittlement of alpha-zirconium, review of, 20: 37187
electric discharges in beams of condensed, plasma properties from, 20: 38247
electron cyclotron resonance harmonic in plasma of, 20: 38224
energy level transition probabilities and lifetimes in, 20: 37438
energy level transitions in molecular, ortho-para, (T), 20: 37467
energy levels in mean lives of 2p and 3p, (E), 20: 37443
exchange and transfer reactions with deuterium during ethylene polymerization in catalyst system, 20: 36827
hyperfine structure of, second-order quantum electrodynamic corrections for S-state, (T), 20: 37445
interactions of atomic, coupling coefficients for, 20: 37476
ion wave propagation in weakly ionized plasma of, damping and phase velocity of, (E), 20: 38294
ionization level of intergalactic, (E), 20: 38218
ionization of, effects of Rydberg electron in auto-, 20: 36819
kinetic temperature of intergalactic, (E), 20: 38218
neutron absorption cross section in pitchblende, thermal, 20: 37994
nuclear spin relaxation in gaseous, at 77.5°K, (E), 20: 38151
photon reactions with atoms of, excitation and ionization in, (T), 20: 38221
proton reactions at 2 to 117 kev with atomic, electron transfer in, (E), 20: 37446
proton reactions with atomic, cross sections for charge transfer and ionization in, (T), 20: 37454
proton reactions with atomic, total cross sections for charge transfer and ionization in, (T), 20: 37455
proton reactions with atomic, cross sections for ionization in, (T), 20: 37456
radiation doses to tissues from, in solar particle beams in space, 20: 37023 (N-65-33865)
radioinduced recombination with oxygen in presence of water vapor, gamma, 20: 36910
stability of plasma of, effect of impurity ions on drift, 20: 38296
thermal conductivity of, effects of pressure and temperature on, 20: 36991
use as carrier in plasmochemistry, 20: 38314
yields from gamma radiolysis of hydrochloric acid–stannous chloride

solutions, 20: 36911
yields in radiolysis of ethanol and methanol, 20: 36861 (UJV-1553)
HYDROGEN IONS
electron reactions at 100 ev, cross sections for electron detachment from, (E), 20: 37452
energy level transitions in molecular, ortho-para, (T), 20: 37467
yields from gamma radiolysis of hydrochloric acid–stannous chloride solutions, 20: 36911
HYDROGEN ISOTOPES
separation by photochemical methods, 20: 37164
HYDROGEN PEROXIDES
decomposition of, on gamma-irradiated nickel oxide, 20: 36885
effects on *E. coli* cultures, increased virus-producing cells and other mutants from, 20: 36617
formation by radiolysis of aqueous benzene, 20: 36881
yields from gamma radiolysis of hydrochloric acid–stannous chloride solutions, 20: 36911
HYDROGEN SELENIDES
radioinduced free radicals of, in krypton, 20: 36909
HYDROGEN SULFIDES
radioinduced free radicals of, in krypton, 20: 36909
radioinduced radical formation in, in organic glasses at –196°C, spectra from gamma, 20: 36894
HYDROMAGNETIC WAVES
dispersion relation in collisionless plasma, (E), 20: 38272
interaction with given plasma particle distribution, instabilities in, (T), 20: 38273
propagation in anisotropic plasma, modes for, (T), 20: 38333
velocities in relativistic fluids, calculation of, 20: 37883
HYDROQUINONE
effects on radioinduced polymerization of allyl alcohol, 20: 36880
formation by radiolysis of aqueous benzene, 20: 36881
HYDROXYL IONS
yields from gamma radiolysis of hydrochloric acid–stannous chloride solutions, 20: 36911
HYDROXYL RADICAL
reactions with purines and pyrimidines, ESR spectral studies on, 20: 36806
HYGROMETERS
use of radiometric surface, for control of resin injection into rock, 20: 37134
HYPERONS (Λ)
production in meson (K)-proton interactions, parity determination from, 20: 37756
HYPERONS (Σ)
production in meson (K)-proton interactions, parity determination from, 20: 37756
HYPOXANTHINE
reactions with hydroxyl radicals, ESR spectral studies on, 20: 36806

I

ICE
molecular motion in, neutron scattering studies of, 20: 36821
ILMENITES
flotation of, on gamma-irradiated anionic collector agents, 20: 36893
IMMUNE REACTIONS
effects of radioinduced lymphatic ablation on, in dogs, 20: 36641
immunoassay of insulin using iodine-131, 20: 36543
radiation effects on histology of rat spleen during immune response, local x, 20: 36637
radiation effects on host, to tapeworm infestations, 20: 36607(R) (TID-23114)
use of iodine-131-labeled antigens as test for tuberculosis, 20: 36681
IMMUNITY
radiation effects on guinea pig and rabbit, x, 20: 36655
INDENE
radiation and photon effects on, 20: 36860 (NP-16150)
INDEXES
book: *Formula Index to NMR Literature Data. Vol. 2: 1961–1962 References*, 20: 36842
INDIA
fallout monitoring, 1945 through 1962, 20: 37004
INDIUM
separation from neutron-irradiated biological materials by ion exchange, 20: 36762
superconducting critical field and transition temperature in porous glass, (E), 20: 37949
INDIUM ALLOYS
Au–In, superconductivity of AuIn, 20: 37985
In–Mn, critical temperature of superconducting, transition-metal impurity effects on depression of, (E), 20: 37955
In–Mn–Pb, critical temperature of superconducting, transition-metal-impurity effects on depression of, (E), 20: 37955
In–Pb, magnetic flux motion in superconducting, induced voltage from, (E/T), 20: 37966
In–Pb, superconductivity of, effect of transport-current polarity on, (E), 20: 37945
In–Pb, thermal conductivity of superconducting, temperature dependence of, (E), 20: 37940
In–Sn, gamma spectra from tin-119 in, at 2 to 6°K, 20: 37271
In–Sn, magnetic flux trapping at 10 to 1000 Mc in superconducting, (E/T), 20: 37954
In–Sn, properties of superconducting, 20: 37271
Sb–In, radiation effects on carrier lifetime and detectivity of, gamma and neutron, 20: 37295
INDIUM CHLORIDES
effects as calcergen, relation to histamine liberators in rats, 20: 36557
$CdCl_2$–$InCl_3$, phase diagrams, 20: 36787 (YALE-2723(Vol.1))
$InCl_3$–AgCl, phase diagrams, 20: 36787 (YALE-2723(Vol.1))
$InCl_3$–NaCl, phase diagrams, 20: 36788 (YALE-2723(Vol.2))
$InCl_3$–$PbCl_2$, phase diagrams, 20: 36788 (YALE-2723(Vol.2))
$InCl_3$–$SnCl_2$, phase diagrams, 20: 36788 (YALE-2723(Vol.2))
$InCl_3$–TlCl, phase diagrams, 20: 36788 (YALE-2723(Vol.2))
$InCl_3$–$ZnCl_2$, phase diagrams, 20: 36788 (YALE-2723(Vol.2))
INDIUM IODIDES
CdI_2–InI_3, phase diagrams, 20: 36788 (YALE-2723(Vol.2))
InI_3–PbI_2, phase diagrams, 20: 36788 (YALE-2723(Vol.2))
InI_3–SnI_2, phase diagrams, 20: 36788 (YALE-2723(Vol.2))
INDIUM ISOTOPES
production in proton reactions with lead and uranium at 3 and 28 Bev, cross sections for, (E), 20: 38098
INFECTIONS
effects of *Eimeria necatrix* on zinc-65 uptake from chicken intestine, 20: 36566
INFRARED RADIATION
effects on blood serum proteins, chemical, 20: 36579
INSECTS
radiosterilization of sugar cane leafhoppers, 20: 37146
INSTRUMENTATION
development of, using quantum interference in superconductors, 20: 37986
INSTRUMENTS
development of radioisotope-using, for geophysics and industry, 20: 37143
use of radioisotope, in industry in Soviet Union, 20: 37147
use of radiometric, in geophysics, 20: 37060
use of radiometric, in industry, 20: 37139 (STI-PUB-112(Vol.1))
use of radiometric, in geophysics, 20: 37001
INSULIN
radioimmunoassay using iodine-131 labeling of, 20: 36543
INTERMETALLIC COMPOUNDS
properties of, for high-temperature coatings, 20: 37192
INTERNAL COMBUSTION ENGINES
use with MHD generator for power production, 20: 37728(P)
INTESTINE
zinc-65 uptake from infected chicken, 20: 36566
INVERTEBRATES
radiation effects on response to tapeworm infestations, x, 20: 36607(R) (TID-23114)
IODIDES
effects on iodine-131-labeled triiodothyronine metabolism in human thyroid, 20: 36573
uptake by human thyroid, effects of iodine-containing x-ray contrast media on, 20: 36572
IODINE
effects in x-ray contrast media on thyroid, secondary, 20: 36571
effects on alpha and gamma radiolysis of cyclohexane, 20: 36888
metabolism in mice, autoradiography of, 20: 36570
separation from water by foaming, 20: 36934
sorption on activated carbon filters, 20: 36976 (DP-MS-66-45)
x-ray spectra from mu-mesic atoms of, (E), 20: 38058
IODINE ISOTOPES
use in localization studies for indication of thyroid radiotherapy, 20: 36706
IODINE ISOTOPES I-125
radiation dose to rat thyroid from, 20: 36561
uptake by udder and blood plasma of cows, effects of dietary thiocyanate on, 20: 36563
IODINE ISOTOPES I-127
energy level structure, (E), 20: 38188
gamma reactions (γ,n), (γ,2n), and (γ,3n) from threshold to 33 Mev, cross sections, (E), 20: 38094
IODINE ISOTOPES I-129
radiation dose to rat thyroid from, 20: 36561
IODINE ISOTOPES I-131
chemical properties of carrier-free, paper-electrophoresis studies of, 20: 36792

effects on radiation burden in women, effects of thyroid function on, 20: 36675
incorporation in antigens, use as test for tuberculosis, 20: 36681
incorporation in insulin complexes, use for immunoassay of insulin, 20: 36543
interactions with iron oxide aerosol, 20: 36918
preparation and storage of, in defined chemical form, 20: 36792
production of, by neutron irradiation of polymetatelluric acid, 20: 36917
radiation dose to rat thyroid from, 20: 36561
sorption of, from aqueous solutions on hydrated ferric oxide containing silver, 20: 36800
stack disposal of vapours, rain and snow washout coefficients for, 20: 37033
uptake by tumor tissue in man and rabbits in oxygen environment, 20: 36576
uptake by udder and blood plasma of cows, effects of dietary thiocyanate on, 20: 36563
use as tracer in study of tree root extension, 20: 36560
yields in proton fission of uranium-238 at 7.1, 9.4, and 12.0 Mev, 20: 37995

IODINE ISOTOPES I-132
yields of, from proton fission of uranium-238 at 12 Mev, 20: 37995

IODINE ISOTOPES I-133
release from irradiated uranium dioxide, apparent diffusion coefficient, 20: 38464 (AERE-M-1607)
yields in proton fission of uranium-238 at 7.1, 9.4, and 12.0 Mev, 20: 37995

ION BEAMS
acceleration and uses in nuclear physics, 20: 37333
interactions with plasmas, instabilities associated with, 20: 38346

ION EXCHANGE
equilibria in systems of uranyl, sulfate, chloride, and nitrate ions, 20: 36931

ION EXCHANGE MATERIALS
sorptive properties of Dowex 1–X4 for plutonium, 20: 36947

ION EXCHANGE PROCESSES
development of, for processing of irradiated fuels, 20: 36947

ION EXCHANGERS
design for removal of strontium-90 and yttrium-90 from rainwater, 20: 37029

ION SOURCES
design of nanosecond pulsed, for Van de Graaff accelerators, 20: 37337
ion escape probability from uniform isotropic, Dirac chord method generalization for determining, 20: 37309

IONIZATION CHAMBERS
design and performance for measurements of interplanetary charged particles, 20: 37124
design of d-c amplifier for, 20: 37066 (AECL-2536)
standards for, secondary, 20: 37090
use of argon-filled high-pressure, in fluid-density gage, 20: 37059
use of double-pulse, for fission-fragment correlations from heavy nuclei, 20: 37089
use with beta source for analysis of gases, 20: 36768
uses in x-ray standardization in Finland and Sweden, 20: 37078

IONOSPHERE
electron density beyond magnetosphere, origin of, 20: 37894
electron temperatures in F region of, 20: 37896
geomagnetic storms in polar, pre-SC increases during, 20: 37892
ionization in, geomagnetic storm effects on, 20: 37893
magnetic field measurements in, 20: 37917
plasma diagnostics in, use of Langmuir probes for determining, 20: 38309
proton density in, determination by analysis of proton whistlers, (T), 20: 37885

IONS
emission from laser beam irradiation of tungsten, 20: 37298
escape probability from uniform isotropic source, Dirac chord method generalization for determining, 20: 37309
interactions with electrons in plasma diodes, computer simulation of, 20: 37726
mobility in gases, measurement of, using ionization chamber with beta source, 20: 36768
oscillations in weakly turbulent electron-ion plasma, (T), 20: 38269
production in flames, Hall measurement of, 20: 38223
reactions with molecules, rotational energy level distributions from, 20: 37471
reactions with moving unequal-mass particles, energy transfer in, (T), 20: 37447

IRIDIUM
determination of, in ores by neutron activation analysis, 20: 36751
ionization and work functions of, critical temperatures for, 20: 37277
neutron reactions (n,α) at 12 to 23 Mev, (E), 20: 38036
preparation of standard solutions of, by electrolytic dissolution for activation analysis, 20: 36775
radiation effects in, cluster formations from neutron, (E), 20: 38382
yields from radiolysis of iridium phthalocyanine, 20: 36886

IRIDIUM ALLOYS
Ir–Sn, superconductivity of $IrSn_2$, 20: 37985

IRIDIUM ISOTOPES Ir-192
uses in radiography, 20: 36994

IRON
abundance in coronal condensations, (E), 20: 37348
cosmic meson (π) reactions in, energy transfer to photons from, (E), 20: 37660
cosmic nucleon reactions in, cascade shower production from primary, (T), 20: 37789
cosmic particle interactions at 100 Bev, cascade shower distributions from, (E), 20: 37698
determination in ores and rocks, in boreholes using neutron activation, 20: 37019
determination in zinc sulfate and sulfide, interfering reactions in activation, 20: 36755
determination in zinc sulfate and sulfide using ion exchange chromatography and activation methods, 20: 36757
diffusion in beryllium at 700 to 1076°C, 20: 37250
effects on compatibility of mixed carbide reactor fuels with stainless steel, 20: 38466 (ANL-7120, pp 301-13)
effects on determination of chromium in ores by neutron activation analysis, 20: 36750
effects on determination of iridium in ores by neutron activation analysis, 20: 36751
effects on discontinuous precipitation in beryllium–copper alloys, 20: 37253
effects on radioinduced swelling in uranium, 20: 37302
effects on spectrophotometric determination of uranium using arsenazo, 20: 36716
iron-57 NMR in, magnetic dipole hyperfine-interaction constants from core polarization from, (E), 20: 38385
laser beam reactions with, uv spectra from plasma produced from, (E), 20: 38300
neutron absorption cross section in pitchblende, thermal, 20: 37994
neutron total cross sections at high energies, fluctuations in, 20: 38173
radiation effects on, magnetic coaxing studies of, neutron, 20: 37288
radiation effects on mechanical properties of cold-worked, neutron, 20: 37304
radioinduced interstitial cluster and vacancy production in α, computer determination of neutron, 20: 38361
separation from hydrochloric acid solutions by solvent extraction using dialkyl alkylphosphonates, 20: 36941
separation from iodide zirconium by zone refining, 20: 37177
separation from metal mixtures by thin layer chromatography, 20: 36753
separation from neutron-irradiated biological materials by ion exchange, 20: 36762
separation from protactinium by solvent extraction using isoamyl alcohol, 20: 36940
separation of, from thallium by ion-exchange chromatography, 20: 36935
shielding of encapsulated gamma sources in, (T), 20: 38349 (AD-636788)
wave functions for ^5D state of, unrestricted Hartree-Fock, 20: 37448
x-ray spectra from mu-mesic atoms of, (E), 20: 38058

IRON ALLOYS
effects of beryllium additions on, 20: 37275
Al–Fe, critical temperature of superconducting, transition-metal impurity effects on depression of, (E), 20: 37955
Ce–Fe, crystal structure of intermetallic compounds in, 20: 37243
Ce–Fe, magnetic properties of $CeFe_2$, (E), 20: 37279
Cr–Co–Fe–Mn–Mo–Ni, corrosion of Vitallium, by boiling hydrofluoric acid–nitric acid solutions, 20: 37169(R) (BMI-1774)
Cr–Co–Fe–Mn–Mo–Ni–Ti, corrosion of Hanford 22, by boiling hydrofluoric acid–nitric acid solutions, 20: 37169(R) (BMI-1774)
Cr–Co–Fe–Mo–Ni, corrosion of Haynes 21, by boiling hydrofluoric acid–nitric acid solutions, 20: 37169(R) (BMI-1774)
Cr–Co–Fe–Mn–Mo–Ni–Ti, corrosion of Hanford 23 and 24, by boiling hydrofluoric acid–nitric acid solutions, 20: 37169(R) (BMI-1774)
Cr–Co–Fe–W, corrosion of Rexalloy 33, by boiling hydrofluoric acid–nitric acid solutions, 20: 37169(R) (BMI-1774)
Cr–Cu–Fe–Mn–Mo–Ni–Ti, corrosion of Hanford 21, by boiling hydrofluoric acid–nitric acid solutions, 20: 37169(R) (BMI-1774)
Cr–Cu–Fe–Mn–Mo–Ni, corrosion of Illium R, by boiling hydrofluoric acid solutions, 20: 37169(R) (BMI-1774)
Cr–Fe–Mn–Mo–Ni–Ti, corrosion of Hanford 20, by boiling hydrofluoric acid–nitric acid solutions, 20: 37169(R) (BMI-1774)
Cr–Fe–Mn–Mo–Ni–Ti, corrosion of Hanford 17, by boiling hydrofluoric acid–nitric acid solutions, 20: 37169(R) (BMI-1774)
Cr–Fe–Mn–Ni, corrosion of corronel 230, by boiling hydrofluoric acid–nitric acid solutions, 20: 37168(R) (BMI-1771)

Cr–Fe–Mn–Ni, corrosion of corronel 230, by boiling hydrofluoric acid–nitric acid solutions, 20: 37169(R) (BMI-1774)
Dy–Fe, crystal structure of intermetallic compounds in, 20: 37243
Er–Fe, crystal structure of intermetallic compounds in, 20: 37243
Fe–Nd, crystal structure of intermetallic compounds in, 20: 37243
Fe–Pr, crystal structure of intermetallic compounds in, 20: 37243
Fe–rare earth, crystal structure of intermetallic compounds in, 20: 37243
Fe–Sm, crystal structure of intermetallic compounds in, 20: 37243
Fe–Tb, crystal structure of intermetallic compounds in, 20: 37243
Fe–U, effects on compatibility of mixed carbide reactor fuels with stainless steel, 20: 38466 (ANL-7120, pp 301-13)
Fe–Y, crystal structure of intermetallic compounds in, 20: 37243
Fe–Zn, critical temperature of superconducting, transition-metal impurity effects on depression of, (E), 20: 37955
Gd–Fe, crystal structure of intermetallic compounds in, 20: 37243
Ho–Fe, crystal structure of intermetallic compounds in, 20: 37243

IRON CARBONATES
formation of, effect of insoluble uranyl ions on, 20: 36796

IRON CHLORIDES
reactions with isopropylamine, thermogravimetric study of, 20: 36853

IRON(II) COMPLEXES
with dimethylglyoxime, magnetic moments and back-coordination effects in, Moessbauer studies of, 20: 36823
with salicylaldehyde and its derivatives, magnetic moments and back-coordination effects in, Moessbauer studies of, 20: 36823

IRON(III) COMPLEXES
with dimethylglyoxime, magnetic moments and back-coordination effects in, Moessbauer studies of, 20: 36823

IRON IONS
complexes with arsenazo, stability of, 20: 36716
complexes with phenanthroline, stability of, 20: 36716
effects on copper determination, 20: 36726
effects on formation of single-crystal beryllium oxide, 20: 36814
radiation chemistry of, in aqueous acetylene solutions, 20: 36858 (IFA-CR-73)
yields of trivalent, in radiolysis of iron sulfates at 40 kev, effect of temperature on, 20: 36867

IRON ISOTOPES Fe-56
alpha reactions (α,n) at 17 Mev, level density parameters from, (E), 20: 38115
energy level assignments at 846.5 to 4394.8 kev, (E), 20: 38088
energy level density in, energy and spin dependence of, (E), 20: 38157
gamma spectra, (E), 20: 38088

IRON ISOTOPES Fe-57
Mössbauer hyperfine spectra in aluminum oxide, crystal and magnetic field effects on, (E), 20: 38388
nuclear magnetic resonance in iron, magnetic-dipole hyperfine-interaction constants from core polarization from, (E), 20: 38385

IRON ISOTOPES Fe-59
tracer use for iron diffusion in beryllium, 20: 37250
uptake and distribution among serum protein fractions in chickens, 20: 36569

IRON NITRATES
radiation effects on electric conductivity of solutions of, gamma, 20: 36912

IRON ORES
analysis in boreholes, activation, 20: 37019
genesis of, determination by oxygen-16/18 ratio, 20: 37013
oxygen-16/-18 ratios in, from Quebec, 20: 37013

IRON OXIDES
analysis for titanium by activation methods, 20: 36760
crystal structure and decomposition of wustite, Mössbauer study of, 20: 38362
interactions of aerosols of, with iodine-131, 20: 36918
separation from uranin in organic slurries, centrifugal, 20: 36933

IRON(III) OXIDES
reactions with lanthanum and neodymium oxides in solid state, 20: 36840
sorptive properties of, for iodine-131, effects of silver on, 20: 36800
Fe_2O_3–MnO_x–Sc_2O_3, phase studies of solid solutions in, 20: 36839

IRON SILICATES
content of, in sediments of Bay of Roquebrune, 20: 36553

IRON SULFATES
radiolysis of frozen, effects of temperature on yields of trivalent iron from, 20: 36867

IRON(II) SULFATES
use as dosimeter, secondary standards for, 20: 37090

IRRADIATION FACILITIES
design and economics of portable, for industrial use, 20: 37140

ISONIAZID
analytical use in colorimetric determination of cerium, gold, and platinum, 20: 36725

ISOPROPYL ETHER
effects on copper determination by absorption spectroscopy, 20: 36726

ISOPROPYLAMINE
reactions with solid chlorides, thermogravimetric study of, 20: 36853

ISOTOPE EFFECTS
of deuterium on mutarotations of α-D-glucose and β-D-fructose, 20: 36577
of deuterium on solubility of hydrogen fluoride gas in molten beryllium fluoride–lithium fluoride, 20: 36785 (ORNL-P-2202)
on nuclear charge distribution, (T), 20: 38101

ISOTOPE SEPARATION METHODS
chromatographic, estimation of separation factor in, 20: 37162
efficiency of photochemical, 20: 37164

ISOTOPES
production and uses of, Technical Progress Review on, Spring 1966, 20: 37136

ISOTOPIC EXCHANGE
between solution and solid phase, method for continuous recording of, 20: 36793
deuterium–hydrogen, on molybdenum filaments at 25 to 800°C, 20: 36818
hydrogen–tritium, between *tert*-butyl alcohol and water, effects of perchloric acid on, 20: 36849
of oxygen on gadolinium oxide, 20: 36826
radiation effects on deuterium exchange between heavy water and benzene, cyclohexane, and *n*-hexane, gamma, 20: 36866
radioinduced, in benzene and toluene saturated with tritiated water, 20: 36868

ISRAEL
food irradiation program in, progress of, 1964-66, 20: 37155
radiation processing of agricultural produce in, survey of, July 1965, 20: 37157

J

JAWS
effects of radiotherapy of face on, in children, 20: 36708

K

KIDNEYS
radiation effects on mouse, neutron and x, 20: 36608
radiation effects on homografts of, in dogs by lymphatic ablation, 20: 36641

KRYPTON
positron annihilation in, (E), 20: 37810
radioinduced hydride radicals in, ESR studies of, 20: 36909

KRYPTON IONS
effects on germanium films, depth of damage from, (E), 20: 38363
sputtering on copper at 100 kev to 1 Mev, 20: 37468

KRYPTON ISOTOPES Kr-85
incorporation of, in solids for use in chemical analysis, 20: 36749
performance in nuclear batteries, 20: 37159
uses in chemical analysis, 20: 36749

KRYPTON ISOTOPES Kr-86
diffusion from BeO–UO_2 and UO_2 fuel elements during reactor operation, 20: 37303

KRYPTONATES
preparation, properties, and uses of, in chemical analysis, 20: 36749

L

LABORATORIES
description of radioprotective measures used in radiobiological work at University of Munich, Germany, 20: 37040

LABORATORY EQUIPMENT
current losses and magnetic field aberrations in adiabatic demagnetization apparatus using high-field superconducting wires, 20: 37970
design of sample holder for studies of electron effects on crystals at low temperatures, 20: 37054

LANTHANUM
content in African pitchblende, estimation of induced fission vs spontaneous fission from, 20: 37994
determination in hydrochloric acid solutions, spectrographic carrier-distillation, 20: 36729
determination of, using Arsenazo III, photometric, 20: 36778
gamma activity of natural, specific, (E), 20: 38107
neutron absorption cross section in pitchblende, thermal, 20: 37994
separation from hydrochloric acid solutions by solvent extraction using dialkyl alkylphosphonates, 20: 36941
separation from protactinium by solvent extraction using isoamyl alcohol, 20: 36940

superconductivity, 20: 37985
x-ray spectra from mu-mesic atoms of, (E), 20: 38058

LANTHANUM ALLOYS
Al–La, superconductivity of Al_2La, 20: 37985
Ce–La, superconducting transition temperature of, pressure dependence of, (E/T), 20: 37965
Co–La, crystal structure of intermetallic compounds in, 20: 37243
Gd–La, superconducting transition temperature of, pressure dependence of, (E/T), 20: 37965
Ge–La, preparation and properties of intermetallic compounds, 20: 37259
La–Pr, superconducting transition temperature of, pressure dependence of, 20: 37965
La–Yb, superconducting transition temperature of, pressure dependence of, (E/T), 20: 37965

LANTHANUM BORIDES
LaB_6–W, physical properties and work function of, 20: 37258

LANTHANUM CARBIDES
properties at 20 to 1300°C, 20: 36811

LANTHANUM CHLORIDES
effects as calcergen, relation to histamine liberators in rats, 20: 36557
reactions with isopropylamine, thermogravimetric study of, 20: 36853

LANTHANUM CHROMITES
phase studies, 20: 36812
spectra of, infrared, 20: 36807

LANTHANUM COMPLEXES
with tartaric acid and trihydroxyglutaric acid, stability constants for, 20: 36838

LANTHANUM ETHYL SULFATES
gadolinium trivalent ion level splitting in lattices of, ionic contributions to ground-state, (T), 20: 38389

LANTHANUM FLUORIDES
crystal structure of, atomic parameters in, 20: 36805

LANTHANUM IONS
ionization potential of singley ionized, (E), 20: 37351

LANTHANUM ISOTOPES La-131
decay of, gamma transitions in, (E), 20: 38048
production of isomeric, in proton reactions (p, 2n) with barium-132, (E), 20: 38125

LANTHANUM ISOTOPES La-136
production of isomeric, in proton reactions with barium-136 and barium-137, (E), 20: 38125

LANTHANUM ISOTOPES La-139
meson (μ^-) capture by, barium-138 energy levels from, (E), 20: 38058

LANTHANUM ISOTOPES La-140
decay scheme, (E), 20: 38154
gamma spectra of, energies and relative intensities of, (E), 20: 38029
yields of, from proton fission of uranium-238 at 12 Mev, 20: 37995

LANTHANUM LACTATES
formation constant of, potentiometric determination of, 20: 36824

LANTHANUM OXIDES
effects on diffusion in uranium dioxide, mechanism of, 20: 37256
reactions with oxides of tri- and tetravalent elements in solid state, 20: 36840

LANTHANUM SILICIDES
preparation of, method for, 20: 37176

LEACHING
nuclear explosion uses for, 20: 36975

LEAD
cosmic meson (μ) interactions in, intranuclear cascade effects on multiplicity distributions from, (E/T), 20: 37702
cosmic meson (μ) interactions at 0.3 to 30 Bev at 60 mwe underground, electromagnetic shower production from, 20: 37700
cosmic meson (π) reactions in, energy transfer to photons from, (E), 20: 37660
cosmic mesons (μ) interactions at 816 to 4100 mwe underground, particle production frequencies from, (E), 20: 37701
cosmic neutron reactions at 100 Bev, cross sections for, (E), 20: 37668
cosmic particle interactions at 100 Bev, cascade shower distributions from, (E), 20: 37698
determination in presence of thorium and uranium, electrophotometric, 20: 36773
diffusion in, radiation effects on self, 20: 37272
diffusion in, tracer studies of self, 20: 37272
magnetic flux motion in superconducting, induced voltage from, (E/T), 20: 37966
neutron absorption cross section in pitchblende, thermal, 20: 37994
neutron total cross sections at high energies, fluctuations in, 20: 38173
proton reactions at 3 and 28 Bev, A = 100 product yields in, (E), 20: 38098
proton reactions at 600 Mev, cross sections for meson ($\pi^{\pm}$) production in, 20: 38186
separation from metal mixtures by thin layer chromatography, 20: 36753
separation from thorium and uranium by electrolytic precipitation, 20: 36773
separation of, from thallium by ion-exchange chromatography, 20: 36935
superconductivity of, model for strong electron-phonon coupling in, (T), 20: 37952
x-ray spectra from mu-mesic atoms of, (E), 20: 38058

LEAD ACETATES
effects as calcergen, relation to histamine liberators in rats, 20: 36557

LEAD ALLOYS
Au–Pb, superconductivity of Au_2Pb, 20: 37985
In–Mn–Pb, critical temperature of superconducting, transition-metal-impurity effects on depression of, (E), 20: 37955
In–Pb, magnetic flux motion in superconducting, induced voltage from, (E/T), 20: 37966
In–Pb, superconductivity of, effect of transport-current polarity on, (E), 20: 37945
In–Pb, thermal conductivity of superconducting, temperature dependence of, (E), 20: 37940

LEAD BROMIDES
$BiBr_3$–$PbBr_2$, phase diagrams, 20: 36787 (YALE-2723(Vol.1))
$CdBr_2$–$PbBr_2$, phase diagrams, 20: 36787 (YALE-2723(Vol.1))
$HgBr_2$–$PbBr_2$, phase diagrams, 20: 36788 (YALE-2723(Vol.2))
$PbBr_2$–KBr, phase diagrams, 20: 36788 (YALE-2723(Vol.2))
PbBr–NaBr, phase diagrams, 20: 36788 (YALE-2723(Vol.2))
$PbBr_2$–$PbCl_2$, phase diagrams, 20: 36788 (YALE-2723(Vol.2))
$PbBr_2$–PbI_2, phase diagrams, 20: 36788 (YALE-2723(Vol.2))
$PbBr_2$–TlBr, phase diagrams, 20: 36788 (YALE-2723(Vol.2))

LEAD CHLORIDES
$BaCl_2$–$PbCl_2$, phase diagrams, 20: 36787 (YALE-2723(Vol.1))
$BiCl_3$–$PbCl_2$, phase diagrams, 20: 36787 (YALE-2723(Vol.1))
$CaCl_2$–$PbCl_2$, phase diagrams, 20: 36787 (YALE-2723(Vol.1))
$CdCl_2$–$PbCl_2$, phase diagrams, 20: 36787 (YALE-2723(Vol.1))
$CsCl$–$PbCl_2$, phase diagrams, 20: 36788 (YALE-2723(Vol.2))
$CuCl$–$PbCl_2$, phase diagrams, 20: 36788 (YALE-2723(Vol.2))
$InCl_3$–$PbCl_2$, phase diagrams, 20: 36788 (YALE-2723(Vol.2))
$PbBr_2$–$PbCl_2$, phase diagrams, 20: 36788 (YALE-2723(Vol.2))
$PbCl_2$–AgCl, phase diagrams, 20: 36787 (YALE-2723(Vol.1))
$PbCl_2$–$HgCl_2$, phase diagrams, 20: 36788 (YALE-2723(Vol.2))
$PbCl_2$–KCl, phase diagrams, 20: 36788 (YALE-2723(Vol.2))
$PbCl_2$–LiCl, phase diagrams, 20: 36788 (YALE-2723(Vol.2))
$PbCl_2$–$MgCl_2$, phase diagrams, 20: 36788 (YALE-2723(Vol.2))
$PbCl_2$–PbI_2, phase diagrams, 20: 36788 (YALE-2723(Vol.2))
$PbCl_2$–RbCl, phase diagrams, 20: 36788 (YALE-2723(Vol.2))
$PbCl_2$–$SnCl_2$, phase diagrams, 20: 36788 (YALE-2723(Vol.2))
$PbCl_2$–$SrCl_2$, phase diagrams, 20: 36788 (YALE-2723(Vol.2))
$PbCl_2$–TlCl, phase diagrams, 20: 36788 (YALE-2723(Vol.2))
$PbCl_2$–$ZnCl_2$, phase diagrams, 20: 36788 (YALE-2723(Vol.2))

LEAD FLUORIDES
PbF_2–KF, phase diagrams, 20: 36788 (YALE-2723(Vol.2))
PbF_2–NaF, phase diagrams, 20: 36788 (YALE-2723(Vol.2))

LEAD IODIDES
CdI_2–PbI_2, phase diagrams, 20: 36788 (YALE-2723(Vol.2))
InI_3–PbI_2, phase diagrams, 20: 36788 (YALE-2723(Vol.2))
$PbBr_2$–PbI_2, phase diagrams, 20: 36788 (YALE-2723(Vol.2))
$PbCl_2$–PbI_2, phase diagrams, 20: 36788 (YALE-2723(Vol.2))
PbI_2–AgI, phase diagrams, 20: 36787 (YALE-2723(Vol.1))
PbI_2–NaI, phase diagrams, 20: 36788 (YALE-2723(Vol.2))

LEAD IONS
effects on copper determination, 20: 36726

LEAD ISOTOPES
content ratios in ore deposits in Southern German, 20: 37011
purification of electromagnetically separated, 20: 37163

LEAD ISOTOPES Pb-206
neutron total cross sections at high energies, fluctuations in, 20: 38173
x-ray spectra from mu-mesic atoms of, (E), 20: 38058

LEAD ISOTOPES Pb-207
helium ion fission at 41.1 to 26.3 Mev, cross sections and mass distributions for, 20: 37996

LEAD ISOTOPES Pb-208
proton elastic scattering at 49 Mev, angular distribution of polarization in, (E), 20: 38049
range of alpha recoil nuclei of, in carbon, gold, and silver, (E), 20: 37470

LEAD ISOTOPES Pb-210
content in drinking waters in Great Britain, 20: 37031

LEAD ISOTOPES Pb-212
content in atmosphere, diurnal oscillations of, (T), 20: 37007
use in measurement of self diffusion in lead, 20: 37272

LEAD ISOTOPES Pb-214
content in atmosphere, diurnal oscillations of, (T), 20: 37007

LEAKS
rates of, errors in measurement of, 20: 36978 (NAA-SR-12001)

LEAVES
radiation effects on fatty acid content in free lipid fraction of seedling

bean, x, 20: 36598
radiation effects on color changes and fall of, neutron, γ, and x, 20: 36609
LECTURES
on high-energy scattering, 20: 37826 (NP-16231)
LEUKEMIA
development in humans in Hiroshima and Nagasaki, 1946 to 1964, 20: 36645
effects on natural beta and gamma radioactivity in bones of patients, 20: 36559
radiation effects on incidence of, in mice and rats, review of low-dose, 20: 36652
radioinduced in mice with thymic origin, x, 20: 36613
LEUKOCYTES
radiation effects on nicotinamide adenine dinucleotides content in rat thymocytes, x, 20: 36590
LEVEL INDICATORS
use of radiometric, in industry, 20: 37148
LIFE SPANS
radiation effects on rat and guinea pig, fast-neutron, 20: 36640
radiation effects on mouse and rat, review of low-dose, 20: 36652
LIGHT
absorption in optical pumping of helium-4, modulated, 20: 37457
effects of natural, on thermal decomposition of mercury oxalate, 20: 36898
effects on sensitivity of film, 20: 36895
effects on strontium-85 photosynthesis and uptake in freshwater plankton, 20: 36568
LIGHTNING
pinch effect in, (T), 20: 38260
LINEAR ACCELERATORS
frequency modulation of uhf signals in electron, 20: 37319 (CEA-R-2976)
LINOLEIC ACID
radiation effects on content of, in free lipid fraction in seedling bean leaves, x, 20: 36598
LINOLENIC ACID
radiation effects on content of, in free lipid fraction in seedling bean leaves, x, 20: 36598
LIPIDS
effects of fraction of free, from irradiated seedling bean leaves on wheat seed, toxic, 20: 36598
radiation effects on fatty acid content in fraction of free, in seedling bean leaves, x, 20: 36598
radioinduced hyperlipemia in animals, mechanism of, 20: 36580
radiosensitivity effects on animals, review on, 20: 36668
LIQUID FLOW
structure of electrically conducting turbulent, 20: 37868
LIQUID METAL COOLED REACTORS
accidents in fast, energy release and mechanical effects in maximum, 20: 38434 (ANL-7120, pp 654-70)
calculations concerning, effects of group-constant uncertainties on, 20: 38420 (ANL-7120, pp 423-33)
core design and fuel cycle for 1000-Mw(e) fast breeder, 20: 38494 (ANL-7120, pp 94-103)
design and safety of large fast power, panel discussion on, 20: 38457 (ANL-7120, pp 261-85)
design and safety of 1000-Mw(e) power breeder, 20: 38497 (ANL-7120, pp 157-61)
design and safety of 1375-Mw(e) sodium-cooled carbide-fuel modular, 20: 38456 (ANL-7120, pp 205-29)
design, economics, and safety of 1000-Mw(e) sodium-cooled fast, 20: 38498 (ANL-7120, pp 185-204)
economic and safety aspects of vented-fuel sodium-cooled fast, 20: 38475 (ANL-7120, pp 540-8)
fission-product retention by sodium in vented-fuel-element, 20: 38477 (ANL-7120, pp 855-61)
neutron Doppler effect in ZPR-3 mockup of, (E/T), 20: 38427 (ANL-7120, pp 603-9)
neutron Doppler effect calculations for, comparison of methods, 20: 38423 (ANL-7120, pp 462-77)
neutronics calculations for 1000-Mw(e) fast breeder, 20: 38493 (ANL-7120, pp 85-93)
physics parameters of 1000-Mw(e) fast ceramic, calculation of, 20: 38491 (ANL-7120, pp 24-32)
reactivity coefficients in sodium-cooled fast, (T), 20: 38418 (ANL-7120, pp 413-20)
reactivity sodium void coefficients for, comparison of calculated and experimental, 20: 38419 (ANL-7120, pp 421-2)
safety characteristics of sodium-cooled coupled fast, 20: 38437 (ANL-7120, pp 789-93)
safety research program of EURATOM-CEA in fast, 20: 38492 (ANL-7120, pp 54-66)
LIQUIDS
motion of conducting, in coaxial cylinders in magnetic field, 20: 37879
neutron scattering by, hindered-translator model for, (T), 20: 38006
theory of normal Fermi, at zero temperature, 20: 37937
gas–liquid, two-phase adiabatic flow of, liquid volume fraction measurements in upward, 20: 36985 (EURAEC-1088)
LITHIUM
depletion in contracting stars, 20: 37396
depletion in main sequence stars, 20: 37421
energy levels of ionized, forbidden transitions in, 20: 37432
polarizability and shielding factor for atomic, dipole, (T), 20: 37440
production in iron meteorites by cosmic radiation, isotopic ratios for, (E), 20: 37603
LITHIUM BROMATES
radiolysis of, gamma, neutron, and lithium-6 fission product recoil, 20: 36899
LITHIUM BROMIDES
$BaBr_2$–LiBr, phase diagrams, 20: 36787 (YALE-2723(Vol.1))
$CaBr_2$–LiBr, phase diagrams, 20: 36787 (YALE-2723(Vol.1))
LiBr–AgBr, phase diagrams, 20: 36787 (YALE-2723(Vol.1))
LiBr–KBr, phase diagrams, 20: 36788 (YALE-2723(Vol.2))
LiBr–LiF, phase diagrams, 20: 36788 (YALE-2723(Vol.2))
LiBr–$MgBr_2$, phase diagrams, 20: 36788 (YALE-2723(Vol.2))
LiBr–NaBr, phase diagrams, 20: 36788 (YALE-2723(Vol.2))
LiBr–RbBr, phase diagrams, 20: 36788 (YALE-2723(Vol.2))
LiBr–SiCl, phase diagrams, 20: 36788 (YALE-2723(Vol.2))
LiBr–$SrBr_2$, phase diagrams, 20: 36788 (YALE-2723(Vol.2))
LITHIUM CHLORIDES
$BaCl_2$–LiCl, phase diagrams, 20: 36787 (YALE-2723(Vol.1))
$BeCl_2$–LiCl, phase diagrams, 20: 36787 (YALE-2723(Vol.1))
$CaCl_2$–LiCl, phase diagrams, 20: 36787 (YALE-2723(Vol.1))
$CdCl_2$–LiCl, phase diagrams, 20: 36787 (YALE-2723(Vol.1))
CsCl–LiCl, phase diagrams, 20: 36788 (YALE-2723(Vol.2))
CuCl–LiCl, phase diagrams, 20: 36788 (YALE-2723(Vol.2))
LiBr–SiCl, phase diagrams, 20: 36788 (YALE-2723(Vol.2))
LiCl–AgCl, phase diagrams, 20: 36787 (YALE-2723(Vol.1))
LiCl–$HgCl_2$, phase diagrams, 20: 36788 (YALE-2723(Vol.2))
LiCl–KCl, determination of polonium in, by evaporation and deposition on metal plates, 20: 36736
LiCl–KCl, phase diagrams, 20: 36788 (YALE-2723(Vol.2))
LiCl–LiF, phase diagrams, 20: 36788 (YALE-2723(Vol.2))
LiCl–$MgCl_2$, phase diagrams, 20: 36788 (YALE-2723(Vol.2))
LiCl–NaCl, phase diagrams, 20: 36788 (YALE-2723(Vol.2))
LiCl–RbCl, phase diagrams, 20: 36788 (YALE-2723(Vol.2))
LiCl–$SnCl_2$, phase diagrams, 20: 36788 (YALE-2723(Vol.2))
LiCl–$SrCl_2$, phase diagrams, 20: 36788 (YALE-2723(Vol.2))
LiCl–TlCl, phase diagrams, 20: 36788 (YALE-2723(Vol.2))
$PbCl_2$–LiCl, phase diagrams, 20: 36788 (YALE-2723(Vol.2))
LITHIUM FLUORIDES
electron scattering at 25 kev by foils of, excitation of surface-lattice vibrations by, (E/T), 20: 38395
radiation effects on point defects in plastically deformed, x, 20: 38368
radiation effects on, electron spin resonance spectra of radicals from, 20: 36902
AlF_3–LiF, phase diagrams, 20: 36787 (YALE-2723(Vol.1))
BaF_2LiF, phase diagrams, 20: 36787 (YALE-2723(Vol.1))
BeF_2–LiF, chemical properties, 20: 36951
BeF_2–LiF, phase diagrams, 20: 36787 (YALE-2723(Vol.1))
BeF_2–LiF, solvent properties for hydrogen fluoride gas, effects of deuterium on, 20: 36785 (ORNL-P-2202)
BeF_2–LiF–ThF_4, separation of protactinum from molten, 20: 36927 (ORNL-TM-1543)
CaF_2–LiF, phase diagrams, 20: 36787 (YALE-2723(Vol.1))
$CdCl_2$–LiF, phase diagrams, 20: 36787 (YALE-2723(Vol.1))
CsF–LiF, phase diagrams, 20: 36788 (YALE-2723(Vol.2))
LiBr–LiF, phase diagrams, 20: 36788 (YALE-2723(Vol.2))
LiCl–LiF, phase diagrams, 20: 36788 (YALE-2723(Vol.2))
LiF–KF, phase diagrams, 20: 36788 (YALE-2723(Vol.2))
LiF–MgF_2, phase diagrams, 20: 36788 (YALE-2723(Vol.2))
LiF–NaF, phase diagrams, 20: 36788 (YALE-2723(Vol.2))
LiF–RbF, phase diagrams, 20: 36788 (YALE-2723(Vol.2))
LiF–SrF_2, phase diagrams, 20: 36788 (YALE-2723(Vol.2))
LiF–ThF_4, separation of protactinium from molten, 20: 36927 (ORNL-TM-1543)
LiF–ZnF_2, phase diagrams, 20: 36788 (YALE-2723(Vol.2))
LITHIUM IODIDES
LiI–AgI, phase diagrams, 20: 36787 (YALE-2723(Vol.1))
LITHIUM IONS
polarizability and shielding factor for, dipole, (T), 20: 37440
reactions with light nuclei, structure effects in, (T), 20: 38014
LITHIUM ISOTOPES
separation by photochemical methods, 20: 37164
LITHIUM ISOTOPES Li-4
formation by helium-3 (d,n) reactions, search for, (E), 20: 38077

LITHIUM ISOTOPES Li-6
deuteron reactions (d,p) with, lithium-7 energy levels from, (E), 20: 38164
lithium-6 reactions (Li-6,d) and (Li-6,p) at 2.4 to 9.0 Mev, angular distributions for, (E), 20: 38172
meson reactions (π^-,2n) with, description using various models of the lithium-6 nucleus, (T), 20: 38137
proton reactions (p,γ) with, gamma spectra from, (E), 20: 38165
reactions (Li-6,α) and (Li-6,d) with light nuclei, structure effects in, (T), 20: 38014

LITHIUM ISOTOPES Li-7
energy level at 5.6 Mev, search for, (E), 20: 38164
gamma reactions (γ,He-3) with, cross sections for, 20: 38138
performance as solar neutrino detector, 20: 37793
reactions (Li-7,α) and (Li-7,t) with light nuclei, structure effects in, (T), 20: 38014

LITHIUM SYSTEMS
NH_3–Li, positron annihilation in solutions of, photon momentum distribution from, (E), 20: 37774
NH_3–Li, positron annihilation in solutions of, photon momentum distribution from, (E), 20: 37818

LIVER
analysis of, for carbon-14 and tritium by scintillation counting, combustion method for, 20: 36721
radiation effects on DNA synthesis in regenerating rat, mechanism of x, 20: 36593
radiation effects on methylation of guanidinacetic acid in rat, x, 20: 36603

LUMINESCENCE
book: *Very Faint Luminescence in Biochemical Reactions*, 20: 36547

LUNGS
radiation effects on radiofibroses development in, after therapy of bronchial carcinoma, 20: 36703
scanning of, preparation of technetium-99-labeled albumin aggregates for use in, 20: 36919

LUTETIUM
determination in complexes with diketones, spectrofluorometric, 20: 36722
determination in hydrochloric acid solutions, spectrographic carrier-distillation, 20: 36729
effects on phase transformation temperature of thorium, 20: 37242
neutron absorption cross section in pitchblende, thermal, 20: 37994

LUTETIUM ALLOYS
Lu–Ni, magnetic properties of $LuNi_5$, 20: 37279
Lu–Th, phase studies of, 20: 37242

LUTETIUM COMPLEXES
with diketones, spectrofluorometric analysis for, 20: 36722
with tartaric acid and trihydroxyglutaric acid, stability constants for, 20: 36838

LUTETIUM ISOTOPES Lu-175
proton reactions (p,2n) with, gamma transitions in ground state rotational bands from, 20: 38008(R) (AECL-2595)

LUTETIUM LACTATES
formation constant of, potentiometric determination of, 20: 36824

LUTETIUM SYSTEMS
calcium oxalate–Lu, precipitation reactions in, distribution coefficients of, 20: 36794

LYMPH SYSTEM
radiation effects on growth of lymphoma cells by exposure of culture medium, 20: 36633
radioinduced lymphatic ablation in dog, effects on tissue homografts, 20: 36641

M

MAGNESIUM
determination in blood and hair of man, activation, 20: 36728
effects on discontinuous precipitation in beryllium–copper alloys, 20: 37253
effects on inotropic action of fluoride in rat ventricle, 20: 36567
gamma reactions (γ,α) at 31 Mev, alpha spectra from, (E), 20: 38037
neutron absorption cross section in pitchblende, thermal, 20: 37994
neutron inelastic scattering by, frequency of normal lattice modes from, 20: 38397
neutron total cross sections at high energies, fluctuations in, 20: 38173
positron annihilation with core electrons in, momentum distributions for, (T), 20: 37821

MAGNESIUM ALLOYS
thermodynamic properties of thermal energy-storage binary, partial molar, 20: 37722(R) (N-65-30843)
Al–Mg, magnetization of superconducting, (E), 20: 37935 (CEA-R-2906)
Al–Mg, thermodynamic properties of, partial molar, 20: 37722(R) (N-65-30843)
Mg–Zr, recrystallization grain growth of, effects of hydration on, 20: 37252

MAGNESIUM BROMIDES
LiBr–$MgBr_2$, phase diagrams, 20: 36788 (YALE-2723(Vol.2))
$MgBr_2$–KBr, phase diagrams, 20: 36788 (YALE-2723(Vol.2))
$MgBr_2$–NaBr, phase diagrams, 20: 36788 (YALE-2723(Vol.2))

MAGNESIUM CARBONATES
content of, in sediments of Bay of Roquebrune, 20: 36553
thermoluminescence properties of, for use as radiation dosimeter, 20: 36913

MAGNESIUM CHLORIDES
$BaCl_2$–$MgCl_2$, phase diagrams, 20: 36787 (YALE-2723(Vol.1))
$BeCl_2$–$MgCl_2$, phase diagrams, 20: 36787 (YALE-2723(Vol.1))
$CaCl_2$–$MgCl_2$, phase diagrams, 20: 36787 (YALE-2723(Vol.1))
$CdCl_2$–$MgCl_2$, phase diagrams, 20: 36787 (YALE-2723(Vol.1))
CsCl–$MgCl_2$, phase diagrams, 20: 36788 (YALE-2723(Vol.2))
CuCl–$MgCl_2$, phase diagrams, 20: 36788 (YALE-2723(Vol.2))
LiCl–$MgCl_2$, phase diagrams, 20: 36788 (YALE-2723(Vol.2))
$MgCl_2$–AgCl, phase diagrams, 20: 36787 (YALE-2723(Vol.1))
$MgCl_2$–KCl, phase diagram, 20: 36788 (YALE-2723(Vol.2))
$MgCl_2$–NaCl, phase diagrams, 20: 36788 (YALE-2723(Vol.2))
$MgCl_2$–RbCl, phase diagrams, 20: 36788 (YALE-2723(Vol.2))
$MgCl_2$–$SnCl_2$, phase diagrams, 20: 36788 (YALE-2723(Vol.2))
$MgCl_2$–$SrCl_2$, phase diagrams, 20: 36788 (YALE-2723(Vol.2))
$MgCl_2$–TlCl, phase diagrams, 20: 36788 (YALE-2723(Vol.2))
$MgCl_2$–$ZnCl_2$, phase, 20: 36788 (YALE-2723(Vol.2))
$(NH_4)_2CO_3$–$MgCl_2$–SiO_2–$UO_2(NO_3)_2$, reactions in, silicate formation in, 20: 36797
$PbCl_2$–$MgCl_2$, phase diagrams, 20: 36788 (YALE-2723(Vol.2))

MAGNESIUM FLUORIDES
Al_2O_3–MgF_2, phase studies, 20: 37722(R) (N-65-30843)
BeF_2–MgF_2, phase diagrams, 20: 36787 (YALE-2723(Vol.1))
CaF_2–MgF_2, phase diagrams, 20: 36787 (YALE-2723(Vol.1))
CaO–MgF_2, phase studies, 20: 37722(R) (N-65-30843)
LiF–MgF_2, phase diagrams, 20: 36788 (YALE-2723(Vol.2))
MgF_2–KF, phase diagrams, 20: 36788 (YALE-2723(Vol.2))
MgF_2–MgO, phase studies, 20: 37722(R) (N-65-30843)
MgF_2–NaF, phase diagrams, 20: 36788 (YALE-2723(Vol.2))
MgF_2–RbF, phase diagrams, 20: 36788 (YALE-2723(Vol.2))

MAGNESIUM IODIDES
MgI_2–KI, phase diagrams, 20: 36788 (YALE-2723(Vol.2))
MgI_2–NaI, phase diagrams, 20: 36788 (YALE-2723(Vol.2))

MAGNESIUM IONS
effects on copper determination, 20: 36726
effects on formation of single-crystal beryllium oxide, 20: 36814

MAGNESIUM ISOTOPES Mg-24
energy levels from carbon-12 (O-16,α) reactions, 20: 38008(R) (AECL-2595)

MAGNESIUM ISOTOPES Mg-25
performance as solar neutrino detector, 20: 37793

MAGNESIUM ISOTOPES Mg-26
deuteron reactions (d,pγ) at 1.8 Mev, magnesium-27 energy levels from γ-p angular correlation measurements on, (E), 20: 38187
performance as solar neutrino detector, 20: 37793

MAGNESIUM ISOTOPES Mg-27
energy-level quantum numbers and transitions, (E), 20: 38187

MAGNESIUM OXIDES
effects on sintering behavior of urania powders, 20: 37202
neutron production above 1 Mev of F-centers in, (E), 20: 37998
positronium lifetime in, (E), 20: 37819
thermal diffusivity at high temperatures, transient measurement of, 20: 37722(R) (N-65-30843)
vaporization of, thermodynamics of, 20: 36841
MgF_2–MgO, phase studies, 20: 37722(R) (N-65-30843)
MgO–Pd–Ag, preparation and properties of magnesia-base cermets of, 20: 37209

MAGNESIUM SILICATES
formation of, in silica solution, effect of insoluble uranyl ions on, 20: 36797

MAGNESIUM SULFATES
radiolysis of hydrated, gamma, 20: 36903

MAGNET COILS
current distribution in superconducting, optimum, (T), 20: 37971
design of, B_o/B_{max} ratio tables for, 20: 36979 (ORNL-3972)
design of, electrolytic tank analog for, 20: 38189 (AD-636095)
power supplies for, design of capacitor, 20: 36982
properties of relativistic electron, for plasma containment, 20: 38210 (UCRL-12455(Rev.1))

MAGNETIC FIELDS
analysis of analog, electrolytic tank design for, 20: 38189 (AD-636095)
cancellation of external, use of combination of cylindrical current sheets for, 20: 37313 (BNL-10143)
charged-particle magnetic moment in, second-order, (T), 20: 38208 (PPL-AF-4)

charged-particle beam focusing in helical, 20: 37334
currents in two-dimensional forces on, 20: 37316 (BNL-10324)
distribution and strength of galactic, (E), 20: 37368
effect of h-f, on plasma, paramagnetic, (E), 20: 38220
effects of interplanetary, on cosmic ray Forbush decrease, (E), 20: 37534
effects of strong d-c, on niobium–zirconium superconducting properties, 20: 37950
effects of transverse, on flow of visco-elastic fluid between non-conducting plates, (T), 20: 37871
effects on radioinduced defects in iron, 20: 37288
electron transport properties in, 20: 37866
energy and inductance in two-dimensional, stored, 20: 37315 (BNL-10323)
flow in, Malkus theory of turbulent channel, 20: 38240
fluid flow boundary layers in crossed, 20: 37869
interaction of solar wind with solar, (T), 20: 37349
interactions with conducting fluids, MHD properties of, (T), 20: 37867
particle injection into mirror-cusp, high-energy neutral, (T), 20: 38277
plasma confinement in toroidal, Chew-Goldberger-Low theory at higher order for, 20: 38271
plasma containment in, curvature effects on, (E/T), 20: 38326
plasma diffusion in, properties of, 20: 38249
plasma diffusion in, computer simulation of anomalous, 20: 38328
plasma equilibrium in uniform, homogeneous, (T), 20: 38343
plasma fluctuations and pumpout in toroidal wells, (T), 20: 38266
plasma instability in, collision-induced, (T), 20: 38253
plasma motion in toroidal octupole, equipotential surfaces of, 20: 38192 (COO-1233-32)
production by cylindrical current arrays, 20: 37314 (BNL-10148)
production by elliptical current sheets, 20: 37318 (BNL-10436)
production of constant-gradient, use of elliptical current sheets for, 20: 37317 (BNL-10341)
production of helical minimum-B configuration, (T), 20: 38219
production of large, by capacitive discharges in magnet coils, 20: 36982
structure in interplanetary space, review of, 20: 37898

MAGNETIC MIRROR MACHINES
charged-particle motion in non-adiabatic, stochastic, 20: 38246
design of, 20: 38325
plasma diffusion and instabilities in Q-type, (E/T), 20: 38324
plasma diffusion in Q-type, (T), 20: 38203 (NP-16237)
plasma diffusion in, properties of, 20: 38313
plasma instabilities in, electron-cyclotron, (E), 20: 38274
plasma ion cyclotron heating in Heliotron-B, 20: 38258
plasma production in, hot-electron, 20: 38211(T) (AEC-tr-6782)
plasma stability in, flute, (E/T), 20: 38323

MAGNETIC MIRRORS
charged-particle motion in, correction to second adiabatic invariant of, (T), 20: 38275
particle injection into, high-energy neutral, (T), 20: 38277
plasma end loss in slow theta pinch, (E), 20: 38256

MAGNETIC PROBES
design and performance of cesium NMR, for use with Varian fluxmeter at low temperatures, 20: 37972

MAGNETIC RESONANCE
equipment for double-resonance experiments, 20: 38402
measurement of electron para-, in plasma, (E), 20: 38220
radiation effects on, of collagen solutions, light, uv, and x, 20: 36585

MAGNETITES
oxygen-16/-18 ratios in, from iron formations in Quebec, 20: 37013

MAGNETOHYDRODYNAMIC CELLS
design for plasma production and purification, 20: 38339(P)
electric power generation by, 20: 37724
performance in combination with internal combustion electric generator for production of a-c current, 20: 37728(P)
performance of, using shock-heated argon, 20: 37882
thermal efficiency of gas–steam cycle in reactor-coupled, 20: 38488 (AERE-R-5031)

MAGNETOHYDRODYNAMICS
book: *Electromagnetodynamics of Fluids*, 20: 37884
discontinuities in solar wind, 20: 37387
electric conductivity of nonequilibrium plasma, seeding for, 20: 38288
flow between parallel planes, Hartmann, (T), 20: 38281
flow in viscous conducting fluid, jet-vortex, (T), 20: 37878
flow in, Malkus theory of turbulent channel, 20: 38240
flow in, numerical method of characteristics for, (T), 20: 38241
flow of visco-elastic fluid between non-conducting plates, (T), 20: 37871
flow over wedges in, (T), 20: 38242
fluid flow between moving plane porous walls in, (T), 20: 37876
fluid flow in crossed magnetic fields, 20: 37869
fluid flow in, properties of, (T), 20: 37867
fluid flow in, stability of conducting free surface in, (T), 20: 37874
fluid flow in, variational principles for equations of incompressible viscous, 20: 37877
fluid flow past a slender body, axially symmetric, 20: 37870
liquid flow in, structure of electrically conducting, 20: 37868
liquid motion in coaxial cylinders, 20: 37879
perturbations due to oscillating dipoles, (T), 20: 37875
properties of, (T), 20: 37867
shock discontinuities in perfectly conducting gas flow, (T), 20: 37872

MAGNETOSPHERE
charged-particle acceleration in neutral sheet in tail of, models for, 20: 37901
effects of compression and expansion of, on cosmic ray cutoff rigidities and impact zones, (T), 20: 37598
effects of magnetopause on cosmic particle trajectories, (T), 20: 37597
electron flux at 0 to 10 kev, structure of, (E), 20: 37904
electron high-energy pulses near bow shock of, spectra of, (E), 20: 37900
magnetic field measurements in, 20: 37917
properties of, review of, 20: 37911
solar wind interactions with, discontinuities in, 20: 37387
structure of, review of measurements of, 20: 37898

MAGNETS
design and construction of superconducting, 20: 37934 (BNL-10380)

MAINE
radioactivity in ground water in, 20: 37006

MAIZE
cesium-137 transfer from soils to, for dairy cattle feed, 20: 37038
water content of, determination of, using neutron thermalization, 20: 37154

MALEIC ACID, DERIVATIVES
cellulose, graft-copolymerization of, with vinyl monomers, 20: 36906(P)

MALEIMIDE, *N*-ETHYL-
effects on radiosensitivity of bacteria, spores, and yeasts, 20: 37144

MALONIC ACID, YTTERBIUM SALTS
dissociation constants of, electrolytic, 20: 36830

MAMMALS
radiation effects on response to tapeworm infestations, x, 20: 36607(R) (TID-23114)

MAMMARY GLAND
radiotherapy of carcinomas of, development of metastases in gamma and x, 20: 36697

MAN
analysis of blood and hair of, activation, 20: 36728
effects of biological stress on phosphatide content of blood plasma, 20: 36606(R) (NYO-1864-23)
efficiency of preserved bone marrow transplants in stimulating blood formation in, 20: 36546
leukemia development in, in Hiroshima and Nagasaki, 1946 to 1964, 20: 36645
metabolism of iodine-131-labeled triiodothyronine in thyroid in, factors affecting, 20: 36573
phosphatide content and composition in blood, 20: 36606(R) (NYO-1864-23)
radiation burden from iodine-131 in, effects of thyroid function on, 20: 36675
radiation effects on function of basic cerbral nervous processes in, uv, 20: 36626
radiation effects on brain function in, dose effects in, 20: 36651
radiation effects on thymine metabolism in, 20: 37025(R) (PG-Report-705)
radiation sickness in, protective effects of bone marrow transplants against, 20: 36669
radioactivity of bones in, with leukemia, beta and gamma, 20: 36559
uptake of iodine-131 and mercury-203-labeled compounds by tumors in, in oxygen environment, 20: 36576
^{137}Cs body burden of Eskimos, 20: 37042

MANGANESE
determination in cerium, cobalt, and plutonium alloys by ion exchange separation and potentiometric titration, 20: 36713 (LA-3402)
determination in zinc sulfate and sulfide, interfering reactions in activation, 20: 36755
determination in zinc sulfate and sulfide using ion exchange chromatography and activation methods, 20: 36757
determination of, in uranium, by activation analysis, 20: 36715
laser beam reactions with, uv spectra from plasma produced from, (E), 20: 38300
neutron absorption cross sections for, reactivity method for measuring, 20: 38414
neutron absorption cross section in pitchblende, thermal, 20: 37994
radiation effects on optical absorption of, in alkali borate glass, 20: 36887
separation from metal mixtures by thin layer chromatography, 20: 36753
separation of, from thallium by ion-exchange chromatography, 20: 36935

MANGANESE ALLOYS
Al–Mn, superconducting critical temperature of, transition-metal impurity effects on depression of, (E), 20: 37955
Ce–Co–Mn–Pu, analysis for cerium and manganese by ion exchange

separation and potentiometric titration, 20: 36713 (LA-3402)
Cr–Co–Fe–Mn–Mo–Ni, corrosion of Vitallium, by boiling hydrofluoric acid–nitric acid solutions, 20: 37169(R) (BMI-1774)
Cr–Co–Fe–Mn–Mo–Ni–Ti, corrosion of Hanford 22, by boiling hydrofluoric acid–nitric acid solutions, 20: 37169(R) (BMI-1774)
Cr–Co–Fe–Mn–Mo–Ni–Ti, corrosion of Hanford 23 and 24, by boiling hydrofluoric acid–nitric acid solutions, 20: 37169(R) (BMI-1774)
Cr–Cu–Fe–Mn–Mo–Ni–Ti, corrosion of Hanford 21, by boiling hydrofluoric acid–nitric acid solutions, 20: 37169(R) (BMI-1774)
Cr–Cu–Fe–Mn–Mo–Ni, corrosion of Illium R, by boiling hydrofluoric acid–nitric acid solutions, 20: 37169(R) (BMI-1774)
Cr–Fe–Mn–Mo–Ni–Ti, corrosion of Hanford 20, by boiling hydrofluoric acid–nitric acid solutions, 20: 37169(R) (BMI-1774)
Cr–Fe–Mn–Mo–Ni–Ti, corrosion of Hanford 17, by boiling hydrofluoric acid–nitric acid solutions, 20: 37169(R) (BMI-1774)
Cr–Fe–Mn–Ni, corrosion of corronel 230, by boiling hydrofluoric acid–nitric acid solutions, 20: 37168(R) (BMI-1771)
Cr–Fe–Mn–Ni, corrosion of corronel 230, by boiling hydrofluoric acid–nitric acid solutions, 20: 37169(R) (BMI-1774)
In–Mn, critical temperature of superconducting, transition-metal impurity effects on depression of, (E), 20: 37955
In–Mn–Pb, critical temperature of superconducting, transition-metal impurity effects on depression of, (E), 20: 37955
Mn–Sn, critical temperature of superconducting, transition-metal impurity effects on depression of, (E), 20: 37955
Mn–Zn, superconducting critical temperature of, transition-metal impurity effects on depression of, (E), 20: 37955

MANGANESE FERRATES
Moessbauer spectrum of, at 4.2, 78, and 300°K, 20: 36817

MANGANESE IONS
effects on copper determination, 20: 36726
effects on formation of single-crystal beryllium oxide, 20: 36814

MANGANESE ISOTOPES Mn-52
energy levels, (E), 20: 38053

MANGANESE ISOTOPES Mn-53
energy level at 377 kev, half life of, (E), 20: 38030
energy levels, (E), 20: 38053
energy levels from chromium-53 (p,n) reaction, (E), 20: 38034

MANGANESE ISOTOPES Mn-54
metabolism in dogs, monkeys, mice, and rats, 20: 36554 (LA-DC-7305)

MANGANESE ISOTOPES Mn-55
alpha reactions (α,n) at 17 Mev, level density parameters from, (E), 20: 38115

MANGANESE OXIDES
Fe_2O_3–MnO_x–Sc_2O_3, phase studies of solid solutions in, 20: 36839

MANGANESE STEEL
Mn–Mo, radiation effects on A302B at 450 to 480°F, neutron, 20: 37289

MANGANESE SULFATES
radiolysis of hydrated, gamma, 20: 36903

MASERS (OPTICAL)
beam reactions with argon gas, carbon, and metals, plasma production from, (E), 20: 38300
beam reactions with tungsten, ion emission from, 20: 37298
beam scattering on plasma thermal density fluctuations, review of, 20: 38336
electromagnetic, thermal, and ultrasonic effects on eyes from, 20: 36612
light scattering by plasma from, diagnostic uses of, (E), 20: 38259
materials for, gamma radiation effects on, 20: 37280 (NYO-3330-11)
operation of ruby, 20: 37174
use for plasma-flow velocity profile measurements, 20: 38238
use for propulsion of interstellar vehicles, (T), 20: 36997
use in radiotherapy of eye lesions, 20: 36682
use in radiotherapy of recurrent toxoplasmic retinochoroiditis, 20: 36683

MASS SPECTROGRAPHY
bibliography on, 20: 36712 (IS-1335)

MASS SPECTROMETERS
book: *Dynamic Mass Spectrometers*, 20: 36777(T)
design, 20: 36779(P)

MATTER
creation of primordial, in steady-state universe, 20: 37361
distribution in space of dustlike, cosmological energy equation, (T), 20: 37352

MEATS
cesium-137 content in, importance of monitoring, 20: 37039

MEDICAL SUPPLIES
radiosterilization of, role of chemicals as sensitizers in, 20: 37144

MEDICINE
book: *Yearbook of Nuclear Medicine*, Vol. I, 1966, 20: 36690
diagnosis of tuberculosis by silicon content of sputum, 20: 36542
legal control of radiation protection of patients in, possibilities of, 20: 36679
radiation exposure to populations in, significance of, 20: 36677
radiation monitoring of personnel in, device for, 20: 36680
radiodiagnosis and radiotherapy in, responsibility of doctor in, 20: 36709
research in nuclear, 20: 36691
use of unsealed radioactive materials in, contamination hazards from, 20: 36678

MEIOSIS
effects of ethylenimine and ethylmethanesulfonate on, in peas, 20: 36621
radiation effects on pea, fast neutron and gamma, 20: 36621

MELAMINE, TRIETHYLENE-
effects on *E. coli* cultures, increased virus-producing cells and other mutants from, 20: 36617

MELTING
point measurement for hypostoichiometric urania, 20: 37220

MERCURY
boiling heat transfer, effects of surface and system contaminants on pool, 20: 36987 (NAA-SR-11949)
electric discharges in, electron excitation of uhf oscillations in low-pressure, (E), 20: 38215
electric discharges in, electron excitation of uhf oscillations in low-pressure, (E), 20: 38216
electron elastic scattering at 180 to 1700 ev, polarization from, (E), 20: 37469
neutron absorption cross section in pitchblende, thermal, 20: 37994
oscillations in low-pressure plasma of, electron-beam excitation of uhf, 20: 38214
separation from metal mixtures by thin layer chromatography, 20: 36753
x-ray spectra from mu-mesic atoms of, (E), 20: 38058
Hg–H_3PO_4, reduction of irradiated potassium chloride by, preparation of sulfur-35-labeled sulfuric acid by, 20: 36920

MERCURY ALLOYS
Hg–Pu, crystal structure of intermetallic compound Pu_5Hg_{21} in, 20: 37244

MERCURY BROMIDES
$AlBr_3$–$HgBr_2$, phase diagrams, 20: 36787 (YALE-2723(Vol.1))
$HgBr_2$–$PbBr_2$, phase diagrams, 20: 36788 (YALE-2723(Vol.2))

MERCURY CHLORIDES
CuCl–HgCl, phase diagrams, 20: 36788 (YALE-2723(Vol.2))
$HgCl_2$–KCl, phase diagrams, 20: 36788 (YALE-2723(Vol.2))
$HgCl_2$–NaCl, phase diagrams, 20: 36788 (YALE-2723(Vol.2))
$HgCl_2$–TlCl, phase diagrams, 20: 36788 (YALE-2723(Vol.2))
$HgCl_2$–$ZnCl_2$, phase diagrams, 20: 36788 (YALE-2723(Vol.2))
LiCl–$HgCl_2$, phase diagrams, 20: 36788 (YALE-2723(Vol.2))
$PbCl_2$–$HgCl_2$, phase diagrams, 20: 36788 (YALE-2723(Vol.2))

MERCURY IODIDES
AlI_3–HgI_2, phase diagrams, 20: 36787 (YALE-2723(Vol.1))
CdI_2–HgI_2, phase diagrams, 20: 36788 (YALE-2723(Vol.2))
HgI_2–AgCl, phase diagrams, 20: 36787 (YALE-2723(Vol.1))
HgI_2–KI, phase diagrams, 20: 36788 (YALE-2723(Vol.2))

MERCURY ISOTOPES
separation by photochemical methods, 20: 37164

MERCURY ISOTOPES Hg-198
energy level at 412 kev, half life of, (E), 20: 38031

MERCURY ISOTOPES Hg-203
excretion in rats, effects of BAL on, 20: 37025(R) (PG-Report-705)
uptake by tumor tissue in man and rabbits in oxygen environment, 20: 36576

MERCURY OXALATES
radiation effects on thermal decomposition of, gamma, sunlight, and x, 20: 36898

MESIC ATOMS
theory of mu, 20: 37479
x-ray spectra from (μ), (E), 20: 38058

MESON SHOWERS
calculations for meson (π^-) reactions with emulsion nuclei at 17 Bev, (T), 20: 38060

MESONS
decay of, deformed octet axial vector current for weak leptonic, 20: 37795
decay properties of L = 1, 20: 37846
decays of spin-2^+, in quark model, 20: 37780
interactions of neutral, model for forward amplitude for, 20: 37805
interactions with baryons in broken SU(3), renormalization effects on coupling constants for, 20: 37842
interactions with baryons, matrices for modified single-particle exchange model of, 20: 37862
mass differences of 0^-, deformed octet axial vector current for, 20: 37795
mass formulas for, dynamic quark model for, 20: 37763
motion of, electric field strength and Lorentz force for, (T), 20: 37754
photoproduction on protons, SU(3) amplitudes for, (E/T), 20: 37773
production in neutrino interactions, unitary spin analysis of, 20: 37751
production of charged, gauge condition and equal-time commutator for

electromagnetic, 20: 37760
production of neutral, cross sections and mixing angles in quark model for, (T), 20: 37779
reactions with nuclei, tests of unitary symmetry from, 20: 38009 (BNL-10420)

MESONS, RESONANCE
production at high energies, singularities in complex j-plane for, 20: 37804
production in proton interactions, mechanism of, 20: 37769
production of f*, in meson (K⁻)-proton interactions at 4.6 and 5.0 Bev/c, 20: 37730 (BNL-10459)
production of K* (1425) in meson ($\pi^{\pm}$)-proton interactions at 6 Bev/c, 20: 37733 (BNL-10462)
production of K* (890) in meson (π^+) interactions with protons at 8 Bev/c, (E), 20: 37770
production of multipion, in meson (π^-) reactions with freon at 16 Bev/c, (E), 20: 37822
production of $\pi\pi$, in meson (π^-)-proton interactions at 6 Bev/c, (E), 20: 37731 (BNL-10460)

MESONS (η^0)
decay of, branching ratio for $\pi^0 e^+ e^-$, (E), 20: 37767

MESONS (f)
production in meson (π^+) interactions with protons at 8 Bev/c, cross sections for, (E), 20: 37770

MESONS (K)
decay of, contribution to cosmic meson (μ) flux from, (E), 20: 37482
decay of, current algebra and $|\Delta I| = \frac{1}{2}$ rule for nonleptonic, 20: 37759
interactions with protons, hyperon (Λ) and (Σ) production from, 20: 37756
interactions with protons, kinematic enhancement of resonance production in, 20: 37769
interactions with mesons ($\bar{K}$), exact bootstrap solution for, 20: 37808

MESONS (K^-)
interactions with protons at 4.6 and 5.0 Bev/c, f* production in, 20: 37730 (BNL-10459)
interactions with protons at high energies, elastic, (E/T), 20: 37796

MESONS (K^0)
decay of, existence of mirror particles from CP violation in 2π, 20: 37806
decay of, interference between amplitudes in 2π, 20: 37814
regeneration in beryllium, 20: 37814
regeneration of $K_L - K_S$ in carbon, Regge-pole model for, 20: 37764

MESONS (K^+)
interactions with protons at high energies, elastic, (E/T), 20: 37796

MESONS (μ)
capture in mixed gases, 20: 37741 (JINR-P-2788)
production from cosmic ray reactions with dense matter, differential energy spectra for, (T), 20: 37712

MESONS (μ^-)
capture by plutonium-239, lifetime of, (E), 20: 38114
interactions with protons in 2s-1d nuclei, (T), 20: 38166

MESONS (ω)
decay of, angular distributions in, (T), 20: 37807
photoproduction on nucleons, asymptotic behavior of cross section for, (T), 20: 37807

MESONS (ϕ)
production in meson (π^+) interactions with protons at 8 Bev/c, cross sections for, (E), 20: 37770

MESONS (π)
charge distribution in meson (π)-nucleon systems, (T), 20: 37791
decay through intermediate vector meson, leptonic, (T), 20: 37781
form factors of, electromagnetic, (E/T), 20: 37812
form factors of, SL (n,C) symmetry for determining charge, 20: 37738 (IC-66/89)
interactions with nucleons, Regge-pole model for charge-exchange, 20: 37761
interactions with protons, kinematic enhancement of resonance production in, 20: 37769
interactions with protons at 35 and 39 Mev, charge exchange in, (T), 20: 37785
interactions with nucleons, C, P, and T invariances in bootstrap mechanism for, 20: 37794
interactions with nucleons, electromagnetic form factors from, (T), 20: 37801
interactions with nucleons at 500 to 600 Mev, amplitudes for, 20: 37803
interactions with nucleons, Regge dynamics in, (T), 20: 37809
photoproduction on nucleons, (T), 20: 37758
production from cosmic particle reactions with graphite at high energies, (E), 20: 38110
production in proton-proton interactions at 655 Mev, (E/T), 20: 37802
reactions with freon at 16 Bev/c, coherent production of 3π resonances in, (E), 20: 37822
reactions with helium-3, decay processes from, 20: 38011 (JINR-P-2805)

MESONS (π^-)
capture by complex nuclei, radiative, (T), 20: 38064
interactions of, model for forward amplitude for, 20: 37805
interactions with protons at 6 Bev/c, $\pi\pi$ resonance production in, (E), 20: 37731 (BNL-10460)
interactions with protons at 6 Bev/c, resonance production in, 20: 37732 (BNL-10461)
interactions with protons at 6 Bev/c, K* (1425) production in, (E), 20: 37733 (BNL-10462)
interactions with protons above 4 Bev, Regge shrinkage in, (T), 20: 37742 (UCRL-16293)
interactions with protons at 12 Bev/c, production of charged bosons (1929), (2195), and (2382) in, (E), 20: 37771
interactions with protons at high energies, elastic, (E/T), 20: 37796
production in proton reactions with beryllium at 600 Mev, cross sections for, (E), 20: 38186
production in proton reactions with carbon at 600 Mev, cross sections for, (E), 20: 38186
production in proton reactions with aluminum at 600 Mev, cross sections for, (E), 20: 38186
production in proton reactions with copper at 600 Mev, cross sections for, (E), 20: 38186
production in proton reactions with silver at 600 Mev, cross sections for, (E), 20: 38186
production in proton reactions with lead at 600 Mev, cross sections for, (E), 20: 38186
production in proton interactions with neutrons at 600 Mev, cross sections (E), 20: 38186
reactions (π^-,2n) with carbon-12, nitrogen-14, and oxygen-16, energy level excitation in, (E), 20: 38070
reactions (π^-,2n) with lithium-6, description using various models of the lithium-6 nucleus, (T), 20: 38137
reactions in nuclear emulsions at 50 to 176 Mev, total cross sections for double charge-exchange, (E), 20: 38012 (JINR-P-2806)
reactions with bromine and silver nuclei at 17 Bev, in nuclear emulsions, (T), 20: 38060
reactions with nuclei, charge exchange in, (E), 20: 37740 (JINR-P-2780)

MESONS (π^0)
decay of, 20: 37753
photoproduction of, 20: 37753
photoproduction on deuterons at 220 to 280 Mev, differential cross sections for, (E), 20: 37783

MESONS (π^+)
decay of, 20: 37753
interactions of, model for forward amplitude for, 20: 37805
interactions with protons at 6 Bev/c, resonance production in, 20: 37732 (BNL-10461)
interactions with protons at 6 Bev/c, K* (1425) production in, (E), 20: 37733 (BNL-10462)
interactions with protons at 900 Mev, cross sections for, (E), 20: 37744 (UR-875-151)
interactions with protons at 900 Mev, N* (1236) and N* (1518) production in, (E), 20: 37744 (UR-875-151)
interactions with protons at 8 Bev/c, cross sections for strange particle production in, (E), 20: 37770
interactions with protons at high energies, elastic, (E/T), 20: 37796
photoproduction of, 20: 37753
production in proton reactions with beryllium at 600 Mev, cross sections for, (E), 20: 38186
production in proton reactions with carbon at 600 Mev, cross sections for, (E), 20: 38186
production in proton reactions with aluminum at 600 Mev, cross sections for, (E), 20: 38186
production in proton reactions with copper at 600 Mev, cross sections for, (E), 20: 38186
production in proton reactions with silver at 600 Mev, cross sections for, (E), 20: 38186
production in proton reactions with lead at 600 Mev, cross sections for, (E), 20: 38186
production in proton interactions with protons at 600 Mev, cross sections for, (E), 20: 38186
reactions (π^+,2p) with carbon-12, nitrogen-14, and oxygen-16, energy excitation in, (E), 20: 38070

MESONS (ρ)
production in antiproton interactions with deuterons, 20: 37813

MESONS (ρ^0)
decay angular distributions for photoproduced, strong absorption model for, 20: 37768
photoproduction on protons at 1.5 to 6.0 Bev, cross sections for, (E/T), 20: 37766

METABOLISM
radiation effects on, in guinea pig and rat retina, x, 20: 36630

METAL COATINGS
development for protection of materials at high temperatures, 20: 37192
thickness measurement using x-ray fluorescence, 20: 37151
METAL POWDERS
x-ray absorption analysis of, instrument for automatic continuous, 20: 37152
METALLIC FILMS
thickness measurements on, by scattering of accelerated alpha particles, 20: 36719
METALLOGRAPHY
etching methods for zirconium dislocations, 20: 37227
METALLURGICAL EQUIPMENT
design for hot pressing, symposium on, 20: 37179
METALS
analysis of, using charged-particle inelastic scattering at high energy, 20: 36732
electron emission from alkali earth-surrounded, models for, (T), 20: 37431(R) (INDEC-SR-7, pp 3.76-111)
liquid boiling, under forced convection, 20: 38415
plastic flow of polycrystalline, determination by hardness, 20: 37230
positron annihilation in, review of, 20: 37820
METEORITES
calcium and lithium production in iron, from cosmic radiation, (E), 20: 37603
impact effects of micro-, accelerator for simulating, 20: 37340(P)
thermoluminescent properties, 20: 37359
METEOROLOGY
German Weather Service annual report, 20: 37009
METERS
design for measuring nuclear-explosion yield, 20: 37061
METHACRYLIC ACID, DODECYL ESTER
radioinduced polymerization of liquid and solid, effect of mineral oil on, 20: 36875
METHANE
boiling data for, nucleate and film, 20: 36993
determination in air using beta sources, instrument for, 20: 37150
neutron scattering at 0 to 156 Mev by deuterated, intramolecular coherent, (E), 20: 38000
neutron scattering by gaseous, calculation of, (T), 20: 38004
nuclear spin relaxation in liquid, intermolecular contribution to, 20: 36828
radioinduced free radicals of, in krypton, 20: 36909
use as carrier in plasmochemistry, 20: 38314
METHANE, DIIODO-
properties for oxide particle suspension in centrifuges, 20: 36933
METHANESULFONIC ACID
effects on chlorophyll and morphological mutations in pea varieties, 20: 36624
METHANESULFONIC ACID, ETHYL ESTER
effects on chlorophyll mutation frequency, meiosis, and mitosis in peas, 20: 36621
preparation and properties of tritium-labeled, 20: 36916
METHANESULFONIC ACID, ISOPROPYL ESTER
preparation and properties of tritium-labeled, 20: 36916
METHANESULFONIC ACID, METHYL ESTER
preparation and properties of tritium-labeled, 20: 36916
METHANOL
radiolysis of, yields of hydrogen in, 20: 36861 (UJV-1553)
methanol–NaI, properties for oxide particle suspension in centrifuges, 20: 36933
METHYL SULFOXIDE
use in polarographic studies of uranium salts, 20: 36745
MICE
effects of *Bacillus subtilis* preparations on radiosensitivity of, 20: 36673
effects of radiation-processed fruits on, 20: 37156
efficiency of preserved bone marrow transplants in stimulating blood formation in, 20: 36546
manganese-54 metabolism in, 20: 36554 (LA-DC-7305)
metabolism of iodine, thyroxine, and triiodothyronine in, autoradiography of, 20: 36570
metabolism of strontium-85, -89, and -90 in live, design of radiation detectors for measuring, 20: 36556
radiation effects on, effects of oral cystamine on gamma, 20: 36666
radiation effects on, protective effects of *Bacillus subtilis* preparations against x, 20: 36673
radiation effects on skin pigments, use in studying affinity of melanin for chloroquine, uv, 20: 36564
radiation effects on cytokinetics and regulation of progenitor cells in bone marrow in, methods for assaying, 20: 36594
radiation effects on collagen in skin of, uv, 20: 36595
radiation effects on kidney tissues and renal clearance rates in, neutron and x, 20: 36608
radiation effects in producing lymphomatoses of thymic origin in various strains of, x, 20: 36613
radiation effects on leukemia incidence, life span, and mutation induction in, review on low-dose x, 20: 36652
MICROANALYSIS
use of electron-probe, for segregation studies in oxides, 20: 38469 (ANL-7120, pp 400-9)
MICROORGANISMS
radiation effects on, in fruit juices, 20: 37156
MICROSCOPY
use of polarized-light in measuring basal-pole orientation in zirconium, 20: 37266
MICROWAVE EQUIPMENT
design and performance of, for charged particle track measurement, 20: 37043
design and performance of cavity Q sampler for plasma diagnostics, 20: 38307
design for plasma density measurements, 20: 38338(P)
design of probe for electron-density measurements in shock tubes, 20: 38305
power flow in plasma-filled waveguides, (T), 20: 38239
production in galaxy, origin of, 20: 37362
waveguide analog of tunneling through quantum potential barriers, 20: 37929
MICROWAVES
detection and measurement of, design and performance of plasma device for, 20: 37119
interactions with magnetoplasma space-charge waves, (E), 20: 38202 (NP-16236)
scattering from underdense cylindrical plasma, (E), 20: 38254
MILITARY COMPACT REACTOR
shielding for, design and testing of, 20: 38506 (NDA-2143-7)
shielding for, design and testing of, 20: 38507 (NDA-Memo-2143-11)
MILK
cesium-137 content in, by deposition from fallout on forage, 20: 37036
strontium-90 content of, in Germany, 1962 through 1964, 20: 36674
MINERALS
age determination by potassium–argon content, 20: 37016
analysis for uranium using Arsenazo III, photometric, 20: 36774
x-ray absorption and fluorescence analysis of, instruments for automatic continuous, 20: 37152
MINING
nuclear explosion uses for, 20: 36975
MISSISSIPPI
crustal structure in southern, seismic measurements for determining, 20: 36965
MITOCHONDRIA
luminescence of, from biochemical reactions, 20: 36547
MITOSIS
effects of ethylenimine and ethylmethanesulfonate on, in peas, 20: 36621
luminescence production in, 20: 36547
radiation effects on nucleolus, uv, 20: 36592
radiation effects on pea, fast neutron and gamma, 20: 36621
radiation effects on *Pisum sativum* root tip cell, thermal neutron, 20: 36644
MIXED SPECTRUM CRITICAL ASSEMBLY
activation measurements of Doppler effect in uranium-235 and uranium-238 in, 20: 38430 (ANL-7120, pp 616-24)
reactivity of, effects of flooding and poisons on, 20: 38439 (ANL-7120, pp 826-36)
MOLECULAR BEAMS
reactions of crossed, apparatus for study of, 20: 37478
MOLECULES
diffusion of, parameters affecting Knudsen, 20: 37307 (LA-3509)
ionization of, effects of Rydberg electron in auto-, 20: 36819
magnetic moments of, 20: 37750
neutron scattering by linear, thermal, (T), 20: 38002
neutron scattering by, effects of nuclear spin correlations on, (T), 20: 38004
reactions with moving unequal-mass particles, energy transfer in, (T), 20: 37447
spectra lines from ion excited, rotational structure of, 20: 37471
MOLLUSKS
chromium distribution in, 20: 36552
MOLYBDENUM
coating of sintered, by aluminizing and siliconizing, 20: 37204
content in African pitchblende, estimation of induced fission vs spontaneous fission from, 20: 37994
crystal structure of, determination by phonon dispersion, 20: 37273
deuterium–hydrogen exchange on, at 25 to 800°C, 20: 36818
effects on crystal structure and properties of thoria-tungsten cermets, 20: 37185
effects on radioinduced swelling in uranium, 20: 37303

evaporation in vacuum at 2063 to 3203°K, effects of pressure on, 20: 36834
neutron absorption cross section in pitchblende, thermal, 20: 37994
oxidation by potassium hydroxide and by sulfuric acid, passivation mechanisms in, 20: 37184
properties for capping Mo-3 alloy ingots to prevent cracks, 20: 37219
protection against oxidation, silicon carbide coatings for, 20: 37189
yields from radiolysis of molybdenum phthalocyanine, 20: 36886

MOLYBDENUM ALLOYS
Al–Mo, formation of intermetallic compound, on sintered molybdenum, 20: 37204
Al–Mo, properties of intermetallic compound, 20: 37260
Cr–Co–Fe–Mn–Mo–Ni, corrosion of Vitallium, by boiling hydrofluoric acid–nitric acid solutions, 20: 37169(R) (BMI-1774)
Cr–Co–Fe–Mn–Mo–Ni–Ti, corrosion of Hanford 22, by boiling hydrofluoric acid–nitric acid solutions, 20: 37169(R) (BMI-1774)
Cr–Co–Fe–Mo–Ni, corrosion of Haynes 21, by boiling hydrofluoric acid–nitric acid solutions, 20: 37169(R) (BMI-1774)
Cr–Co–Fe–Mn–Mo–Ni–Ti, corrosion of Hanford 23 and 24, by boiling hydrofluoric acid–nitric acid solutions, 20: 37169(R) (BMI-1774)
Cr–Cu–Fe–Mn–Mo–Ni–Ti, corrosion of Hanford 21, by boiling hydrofluoric acid–nitric acid solutions, 20: 37169(R) (BMI-1774)
Cr–Cu–Fe–Nb–Mo–Ni, corrosion of Illium R, by boiling hydrofluoric acid–nitric acid solutions, 20: 37169(R) (BMI-1774)
Cr–Fe–Mn–Mo–Ni–Ti, corrosion of Hanford 20, by boiling hydrofluoric acid–nitric acid solutions, 20: 37169(R) (BMI-1774)
Cr–Fe–Mn–Mo–Ni–Ti, corrosion of Hanford 17, by boiling hydrofluoric acid–nitric acid solutions, 20: 37169(R) (BMI-1774)
Mn–Mo, radiation effects on A302B at 450 to 480°F, 20: 37289
Mo–Nb, crystal structure of, determination by phonon dispersion, 20: 37273
Mo–Ni, thermal capacity data and order-disorder reactions in, 20: 37278
Mo–Pu–U, development for SEFOR fuels, 20: 38531 (GEAP-5133)
Mo–Ti, critical field and magnetization of superconducting, Pauli spin and spin-orbit effects on, (E), 20: 37951
Mo–Ti–Zr, tensile properties of TZM, effects of brittle coatings on, 20: 37276
Mo–U, radioinduced swelling of Zircaloy-clad, at 500°C, 20: 37302

MOLYBDENUM CARBIDES
dislocations in single-crystal, effects of structure on, 20: 37247

MOLYBDENUM FLUORIDES
reactions with uranium hexafluoride, 20: 36803

MOLYBDENUM IONS
effects on copper determination, 20: 36726

MOLYBDENUM ISOTOPES Mo-92
neutron strength functions of, calculation of, 20: 38038

MOLYBDENUM ISOTOPES Mo-94
neutron strength functions of, calculation of, 20: 38038

MOLYBDENUM ISOTOPES Mo-96
neutron strength functions of, calculation of, 20: 38038

MOLYBDENUM ISOTOPES Mo-99
tracer uses for vaporization of molybdenum in vacuo, 20: 36834
yields from helium ion-induced fission of lead-207 at 41.1 to 26.3 Mev, 20: 37996
yields in proton fission of uranium-238 at 7.1, 9.4, and 12.0 Mev, 20: 37995

MOLYBDENUM OXIDES
effects on sintering behavior of urania powders, 20: 37202

MOLYBDENUM SILICIDES
formation on sintered molybdenum, protective effects of, 20: 37204

MOLYBDENUM SYSTEMS
C–Mo–Ti–Zr, crack formation in Mo-3 alloy ingots, effects of molybdenum capping on, 20: 37219

MONKEYS
manganese-54 metabolism in, 20: 36554 (LA-DC-7305)
radiation effects on cerebral cortex of, x, 20: 36656
radiation effects on response-perseveration learning set for nonrewarded cues in male, fast-neutron, 20: 36638
radiation effects on social distractibility behavior of female, γ and neutron, 20: 36639

MONTE CARLO METHOD
use for neutron Doppler effect calculations for fast reactors, 20: 38423 (ANL-7120, pp 462-77)

MOON
effects on electromagnetic activity correlated with naphthalene test, 20: 37891

MÖSSBAUER EFFECT
measurement of, spectrometer for, 20: 37056
properties of, review, 20: 37464

MULTIPLICATION FACTOR
calculation for fast breeder reactors, comparison of methods, 20: 38421 (ANL-7120, pp 440-8)
changes of, effects on circulating-water reactors, 20: 38449

MUONIUM
hyperfine structure of, second-order quantum electrodynamic corrections for S-state, (T), 20: 37445

MUSCLES
analysis of, for carbon-14 and tritium by scintillation counting, combustion method for, 20: 36721
effects of calcium, strontium, and magnesium on the inotropic action of fluoride in rat ventricle, 20: 36567
effects of radiation sickness on renewal intensity and specific radioactivities of proteins in rabbit, 20: 36600
radiation effects on uptake of carbon-14-labeled acetate by proteins in rabbit, 20: 36574
radiation effects on aminotransferase activities in rat skeletal, neutron, 20: 36601
radiation effects on content and metabolism of phosphoproteins in denerved and intact rabbit, x, 20: 36602

MUTAGENS
effects of uv light, triethylene melamine, and hydrogen peroxide on the proportion of virus-producing cells and other mutants in cultures of *E. coli*, 20: 36617

MUTATIONS
effects of ethylenimine and ethylmethanesulfonate on chlorophyll, in peas, 20: 36621
effects of ethylenimine and methanesulfonate on chlorophyll and morphological, in pea varieties, 20: 36624
effects of various mutagens in increasing proportion of virus-producing cells and other *E. coli*, 20: 36617
induced by chemicals in peas, 20: 36634
radiation effects on peas chlorophyll, fast neutron and gamma, 20: 36621
radiation effects on barley chlorophyll, effects of partial reparation on, 20: 36622
radiation effects on chlorophyll and morphological, in pea varieties, gamma, 20: 36624
radiation effects on embryonic wheat, gamma, 20: 36650
radioinduced in bacteriophage T4, uv, 20: 36636
radioinduced in cotton species *Gossypium barbadense*, gamma and thermal neutron, 20: 36623
radioinduced in mouse and rats, review of, 20: 36652
radioinduced in peas, γ and fast neutron, 20: 36634
radioinduced in peanuts, resistance to virus disease, γ, 20: 36647
radioinduced in synchronous populations of *Streptococcus faecalis*, chromosome mapping by, 20: 36635
radioinduced in wheat, fast neutron and gamma, 20: 36620
radioinduced somatic crossing over in *D. melanogaster*, effects of age on location of, 20: 36619
radiosensitivity of cytoplasmic, *Aspergillus nidulans*, uv, 20: 36629

N

NAGASAKI
leukemia development in humans in, 1946 to 1964, 20: 36645

NAPHTHALENE
crystallization for detecting electromagnetic field activity, 20: 37889
crystallization for detecting electromagnetic field activity, correlation with lunar phases of, 20: 37891
crystallization test for detecting electromagnetic activity, magnetic storm effects on, 20: 37890

NATURAL GAS
cost of fuel, comparison with nuclear fuels, 20: 38541
production of, use of nuclear explosions for increasing, 20: 36973
well productivity, improvement by underground nuclear explosions, 20: 36961 (UCRL-12229)

NEBULAE
mass loss in planetary, 20: 37416
synchrotron radiation spectra from Crab, 20: 37381(T)

NECK
radiotherapy of carcinomas of, use of electron beams for, 20: 36685

NEODYMIUM
content in African pitchblende, estimation of induced fission vs spontaneous fission from, 20: 37994
determination in hydrochloric acid solutions, spectrographic carrier-distillation, 20: 36729
effects on crystal structure of cobalt, iron, and nickel intermetallic compounds, 20: 37243
effects on phase transformation temperature of thorium, 20: 37242
energy levels of, ionization energies from, (T), 20: 37439
neutron absorption cross section in pitchblende, thermal, 20: 37994
separation from hydrochloric acid solutions by solvent extraction using dialkyl alkylphosphonates, 20: 36941
x-ray spectra from mu-mesic atoms of, (E), 20: 38058

NEODYMIUM ALLOYS
Co–Nd, crystal structure of intermetallic compounds in, 20: 37243
Fe–Nd, crystal structure of intermetallic compounds in, 20: 37243

Ge–Nd, crystal structure and magnetic properties, 20: 38369
Nd–Ni, crystal structure of intermetallic compounds in, 20: 37243
Nd–Th, phase studies of, 20: 37242
Nd–Zr, fracture at 78, 197, and 373°K, mechanisms of, 20: 37231

NEODYMIUM CARBIDES
properties at 20 to 1300°C, 20: 36811

NEODYMIUM CHLORIDES
reactions with isopropylamine, thermogravimetric study of, 20: 36853

NEODYMIUM CHROMITES
phase studies, 20: 36812
spectra of, infrared, 20: 36807

NEODYMIUM COMPLEXES
with pyrogallosulfonic acid, formation of, potentiometric and spectrophotometric studies of, 20: 36837
with tartaric acid and trihydroxyglutaric acid, stability constants for, 20: 36838

NEODYMIUM ETHYL SULFATES
electron spin resonance of crystals of, 20: 36855

NEODYMIUM IONS
spectra of, effects of chemical bonding and transitions on, 20: 36845

NEODYMIUM ISOTOPES Nd-147
yields in proton fission of uranium-238 at 7.1, 9.4, and 12.0 Mev, 20: 37995

NEODYMIUM OXALATES
crystal structure of monoclinic decahydrate of, 20: 36835

NEODYMIUM OXIDES
reactions with oxides of tri- and tetravalent elements in solid state, 20: 36840
Nd_2O_3–ReO_2, magnetic properties and structure of compounds formed in, 20: 36784(R) (AD-636054)
Nd_2O_3–WO_3, phase diagrams, 20: 37240

NEODYMIUM TUNGSTATES
formation by high-temperature reactions of neodymium oxides and tungsten oxides, 20: 37240
$Nd_2(WO_4)_3$–Na_2WO_4, phase diagrams, 20: 37241

NEON
photoionization by cosmic x rays, cross sections for interstellar K-shell, 20: 37485
reactions with tungsten, electron ejection from, (E), 20: 37450
stability of plasma of, density distribution effect on helical, (E), 20: 38270

NEON IONS
effects on germanium films, depth of damage from, (E), 20: 38363
excitation and ionization in Stellarator discharges, 20: 38250
polarizability and shielding factor for, dipole, (T), 20: 37440
sputtering on copper at 100 kev to 1 Mev, 20: 37468

NEON ISOTOPES Ne-20
energy levels from carbon-12 (C-12,α) reactions, parities and spins of, (T), 20: 38179
energy levels from carbon-12 (C-12,$\alpha\gamma$) reactions at 15.55 Mev, 20: 38008(R) (AECL-2595)
meson (μ^-) capture by protons in, rate of, 20: 38166

NEPTUNIUM
determination of, using Arsenazo III, photometric, 20: 36778
separation from neutron-irradiated biological materials by ion exchange, 20: 36762
separation from uranium and its fission products by ion exchange using 8-quinolinol, 20: 36754

NEPTUNIUM IONS
spectra of, effects of chemical bonding and transitions on, 20: 36845

NERVES
regeneration in dogs with radiation sickness, 20: 36614

NERVOUS SYSTEM
book: *Yearbook of Nuclear Medicine*, Vol. I, 1966, 20: 36690
radiation effects on aminotransferase activities in rat, neutron, 20: 36601
radiation effects on function of basis processes in human, uv, 20: 36626
radiosensitivity effects on radiation injuries, muscle tissue in rabbits, 20: 36602
radiotherapy of diseases of, use of low doses for, 20: 36707

NEUTRINOS
capture by chlorine-37, rate of, (T), 20: 37366
detection of solar, performance of nuclei for, 20: 37793
emission from collapsing stars, methods for observing, 20: 37379
emission from sun, solar interior temperature determination from, 20: 37380
flux of solar, (T), 20: 37377
interaction amplitudes of, unitary spin analysis of, 20: 37751
interactions of solar, with electrons, methods for detecting, 20: 37792
interactions of, research on, 20: 37735(R) (COO-818-96)
production from cosmic ray reactions with dense matter, differential energy spectra for, (T), 20: 37712
reactions with chlorine-37, cross section for, (T), 20: 38111
research on solar, using isotopic composition of extraterrestrial and terrestrial material, 20: 37369
spectra of solar, use for solar structure parameter determination, 20: 37378

NEUTRON-ABSORPTION ANALYSIS
of rocks in boreholes, 20: 37018

NEUTRON CAPTURE CROSS SECTIONS
calculation of average thermal, for media containing zirconium hydride, (T), 20: 37991
measurement for fast neutrons using indium resonance detector in water, 20: 37990

NEUTRON CROSS SECTIONS
for phosphorus and sulfur isotopes, fast, (E), 20: 37166
measurement of, developments in, 20: 38103

NEUTRON RESONANCE CROSS SECTIONS
calculation of, multigroup data preparation for, (T), 20: 38451

NEUTRON SOURCES
design for cross section measurements, developments in, 20: 38103
design for pulsed neutron-neutron logging in gas and oil wells, 20: 37017
design of thermal, for calibration of radiometers, 20: 37073 (NP-16201)
use in calibration of radiometers, 20: 37074 (NP-16202)
use in calibration of radiometers, 20: 37075 (NP-16204)
use in geophysics, research program in Soviet Union on, 20: 37001

NEUTRON SPECTROMETERS
design and construction for fast neutrons, 20: 38159
design of time-of-flight encoder for, 20: 37067 (AECL-2578)

NEUTRON TOTAL CROSS SECTIONS
fluctuations at high energies, 20: 38173

NEUTRONS
absorption in reactors, multigroup cross sections for resonance, (T), 20: 38451
age theory for criticality calculations, eigenvalue problem in, 20: 37993
capture gamma spectroscopy, use of lithium-drifted germanium diodes in, 20: 37072 (KFK-429)
collision density in fast reactors, effects on Doppler-effect calculations, 20: 38422 (ANL-7120, pp 449-61)
decay of, high energy fragments from baryon nonconserving, 20: 37734 (COO-818-87)
density in reflected reactors, pulsed two-region calculations, 20: 38453
detection and measurement of, construction of gas scintillators for, 20: 37127
detection and measurement of, design of Rem responding rate meter for, 20: 37068 (BNL-10321)
detection and measurement of, development of portable monitor for, 20: 37071 (DP-993)
diffusion in a cylindrical reactor, generalized potential theory, 20: 38448
dosimetry of, use of probe method in, 20: 37081
effects of resonance, on reactivity in WWR-S reactor, 20: 38536
effects on alkali metal and alkaline earth bromates, 20: 36899
effects on α iron, interstitial cluster and vacancy production from, (T), 20: 38361
effects on aminotransferase activities in central nervous system and skeletal muscle in rats, 20: 36601
effects on A302B steel at 450 to 480°F, 20: 37289
effects on beryllia flakes, 20: 37281
effects on carrier lifetime and detectivity of antimony–indium semiconductors, 20: 37295
effects on chromosomes in barley seed, effects of diethyl pyrocarbonate on, 20: 36589
effects on color changes and fall of leaves, 20: 36609
effects on graphite energy storage, relations with annealing, 20: 37283
effects on interstitial dislocation loops in beryllium oxide at high temperatures, 20: 38377
effects on iron at 77°K, magnetic coaxing studies of, 20: 37288
effects on kidney tissues and renal clearance of mice, 20: 36608
effects on mechanical properties of pressure vessel steels and structural steels, 20: 37286
effects on mechanical properties of cold-worked iron, 20: 37304
effects on nickel, interstitial and vacancy clusters from, (E), 20: 38367
effects on niobium-stabilized stainless steel, 20: 37284
effects on optical absorption of alkali borate glass containing arsenic or manganese, 20: 36887
effects on paramagnetic center formation in ammonium selenates, 20: 38398
effects on phthalocyanines, 20: 36886
effects on silicon, transient annealing of, 20: 37129 (SC-DC-66-1820)
effects on social distractibility behavior of female monkeys, 20: 36639
effects on type 347 stainless steel, 20: 37168(R) (BMI-1771)
effects on type 347 stainless steel, 20: 37169(R) (BMI-1774)
effects on zinc oxide smokes, 20: 37281
energy measurement by transmission, technique for, 20: 38028
flux density of, construction and testing of precision long counter for measuring, 20: 37069 (BNWL-260)
flux distribution in fast reactors, analysis of transient, 20: 38431

(ANL-7120, pp 625-31)
flux distribution in high-power slab reactors, 20: 38452
flux distributions in cylindrical fuel solutions, effects of voids, 20: 38532 (NASA-TN-D-3555)
flux from foil activation data, computer program for determining, 20: 37076 (SC-DC-66-1512)
flux in upper atmosphere during 1964 solar minimum, (E), 20: 37908
flux variations in steady-state operating reactors, 20: 38445 (RT-FI-(66)1)
interactions with protons in nuclei, short-range, (T), 20: 38056
interactions with protons at 600 Mev, cross section for meson (π^-) production in, (E), 20: 38186
interactions with protons at 630 Mev, phase shift analysis and triple scattering parameters of, (E), 20: 37739 (JINR-E-2726)
interactions with protons at 12 Bev/c, angular distributions for, (E), 20: 37747
interactions with protons, amplitudes for Regge pole exchange model of, 20: 37862
pairing correlations with protons in spherical even nuclei, 20: 38177
polarization of instrument for measurement of, 20: 38163
production by cosmic-ray reactions in atmosphere at ground level, 20: 37483
reactions (n,α) with bismuth-209, gold-197, iridium, silicon-28, silicon-29, and silver-107 at 12 to 23 Mev, (E), 20: 38036
reactions (n,d) with nitrogen-14, nitrogen-15, sulfur-32, and sulfur-34 at 14 Mev, (E), 20: 38150
reactions (n,p) with aluminum-27, calculations using finite-range distorted-wave Born approximation, (T), 20: 38112
reactions (n,t) with nitrogen-14 at 14 Mev, (E), 20: 38150
reactions in iridium, cluster formation from, (E), 20: 38382
reactions with aluminum at 4.6°K, defect annealing in, (E), 20: 38380
reactions with calcium at 2.2 to 5.3 Mev, total cross section for, (E), 20: 38183
reactions with tellurium to produce iodine-131, 20: 36917
scattering by calcium at 2.15 to 6.53 Mev, differential elastic cross sections for, 20: 38183
scattering by gaseous deuterated methane at 0 to 156 Mev, intramolecular coherent, (E), 20: 38000
scattering by gaseous methane at 0.025 ev, calculation of, (T), 20: 38004
scattering by hematites at 0.0053 ev, spin wave spectra from inelastic, (E), 20: 38355 (ITEF-355)
scattering by liquids, hindered-translator model for, (T), 20: 38006
scattering by magnesium, frequency of normal lattice modes from, 20: 38397
scattering by molecules, effects of nuclear spin correlations on, (T), 20: 38004
scattering by nuclei, slowing down parameters and Legendre polynomial coefficients for, 20: 37988 (WAPD-TM-572)
scattering by potassium at 14 Mev, optical-model analysis of elastic, (T), 20: 38171
scattering by solid and liquid cyclohexane, inelastic, 20: 38005
scattering data in ROC nuclear data library, computer program for conversion of form of elastic, 20: 37989 (WAPD-TM-573)
scattering of, use in research on underground water supplies, 20: 37135
spectra from alpha reactions (α,n) with aluminum-27 at 17 Mev, level density parameters from evaporation, (E), 20: 38115
spectra from alpha reactions (α,n) with manganese-55 at 17 Mev, level density parameters from evaporation, (E), 20: 38115
spectra from alpha reactions (α,n) with iron-56 at 17 Mev, level density parameters from evaporation, (E), 20: 38115
spectra from alpha reactions (α,n) with silver at 17 Mev, level density parameters from evaporation, (E), 20: 38115
thermalization in heavy water lattices, phenomenological model application, 20: 38455
thermalization of, mean number of collisions in, (T), 20: 37992
transmission in perfect crystals, anomalous, (T), 20: 38387
transport theory for, solution of Milne problem for two half-spaces with different media, 20: 38003

NEUTRONS, FAST
absorption cross section for, measurement using indium resonance detector in water, 20: 37990
capture in uranium-235 and uranium-238 matrices, Doppler effect in, 20: 38430 (ANL-7120, pp 616-24)
effects on annealing of Frenkel defects in crystals, computer simulation of, 20: 37294
effects on behavioral responses of male monkeys, 20: 36638
effects on chlorophyll mutation frequency, meiosis, and mitosis in peas, 20: 36621
effects on creep and dimensional changes in graphite, 20: 37282
effects on electric conductivity and Hall effect in zinc sulfide single crystals, 20: 36865
effects on longevity of guinea pigs and rats, 20: 36640
effects on mutation frequency in wheat, 20: 36620
effects on peas, genetic, 20: 36634
effects on phase transformations in barium titanates, 20: 37301
effects on rice, RBE comparison of gamma radiation and, 20: 36649
flux distributions in light-water moderated reactor, computer program for, 20: 38450
flux of solar, at 20 to 160 Mev, (E), 20: 37375
penetration in concrete, (E), 20: 38352
production from cosmic meson (μ) reactions with nuclei at 58 mwe underground, differential energy spectrum from, (E), 20: 37710
reactions (n,α) with chlorine-36, phosphorus-33 production in, (E), 20: 37166
reactions (n,p) with sulfur-33, phosphorus-33 production in, (E), 20: 37166
reactions in magnesium oxide, F-center production, (E), 20: 37998
scattering by aluminum, graphite, and steel cylinders, spectra from, (E/T), 20: 38007

NEUTRONS, FISSION
distribution along straight cylindrical ducts in water, (E), 20: 38351

NEUTRONS, THERMAL
attenuation by phonons in single crystals, (T), 20: 38371
capture cross sections for media containing zirconium hydride, averaging of, (T), 20: 37991
dosimetry in tissues, 20: 37025(R) (PG-Report-705)
effects on cadmium sulfide electric conductivity, (E), 20: 38405
effects on mitosis in *Pisum sativum* root tip cells, 20: 36644
effects on mutation induction in cotton species *Gossypium barbadense*, 20: 36623
flux distribution in pitchblende, 20: 37994
flux distributions in light-water moderated reactor, computer program for, 20: 38450
reactions (n,γ) with strontium-87, strontium-88 neutron binding energy levels from, (E), 20: 38141
scattering by linear molecules, (T), 20: 38002
scattering by liquids, hindered-translator model for one-particle motions in, 20: 37999
scattering from oxyhydrogen flame, temperature measurement by, 20: 37310
scattering in pentane, angular distributions from inelastic, (E), 20: 38001
transmission by light and heavy water, determination of hydrogen content in heavy water by, 20: 36740

NEVADA TEST SITE
nuclear rocket tests at, safety aspects of, 20: 37034

NEW HAMPSHIRE
radioactivity in ground water in, 20: 37006

NICHROME
corrosion by boiling hydrofluoric acid–nitric acid solutions, 20: 37169(R) (BMI-1774)

NICKEL
determination in blood and hair of man, activation, 20: 36728
determination in zinc sulfate and sulfide, interfering reactions in activation, 20: 36755
determination in zinc sulfate using ion exchange and activation methods, 20: 36756
development for SEFOR core materials, 20: 38531 (GEAP-5133)
effects on determination of iridium in ores by neutron activation analysis, 20: 36751
gamma reactions (γ,α) at 31 Mev, alpha spectra from, (E), 20: 38037
gamma reactions at 6.13 Mev, pair-production cross sections for, (E), 20: 37746
laser beam reactions with, uv spectra from plasma produced from, (E), 20: 38300
neutron absorption cross section in pitchblende, thermal, 20: 37994
photoelectrons from magnetized crystals of, polarization of, (E), 20: 37475
radiation effects on electric conductivity and magnetism of, electron, 20: 37297
radiation effects on diffusion in copper at 200 to 520°C, alpha, 20: 37300
radioinduced interstitial and vacancy clusters in, neutron, (E), 20: 38367
reactions with liquid sodium at high temperatures, 20: 38499 (ANL-7120, pp 839-47)
reactions with sulfur-bearing alumina at high temperatures, 20: 37168(R) (BMI-1771)
reactions with sulfur-bearing alumina at high temperatures, 20: 37169(R) (BMI-1774)
separation from metal mixtures by thin layer chromatography, 20: 36753
separation of, from thallium by ion-exchange chromatography, 20: 36935
tensile properties of 201, effects of intergranular changes on, 20: 37169(R) (BMI-1774)

NICKEL ALLOYS
effects of beryllium additions on, 20: 37275
Ce–Ni, crystal structure of intermetallic compounds in, 20: 37243
Cr–Co–Fe–Mn–Mo–Ni, corrosion of Vitallium, by boiling hydrofluoric

acid–nitric acid solutions, 20: 37169(R) (BMI-1774)
Cr–Co–Fe–Mn–Mo–Ni–Ti, corrosion of Hanford 22, by boiling hydrofluoric acid–nitric acid solutions, 20: 37169(R) (BMI-1774)
Cr–Co–Fe–Mo–Ni, corrosion of Haynes 21, by boiling hydrofluoric acid–nitric acid solutions, 20: 37169(R) (BMI-1774)
Cr–Co–Fe–Mn–Mo–Ni–Ti, corrosion of Hanford 23 and 24, by boiling hydrofluoric acid–nitric acid solutions, 20: 37169(R) (BMI-1774)
Cr–Cu–Fe–Mn–Mo–Ni–Ti, corrosion of Hanford 21, by boiling hydrofluoric acid–nitric acid solutions, 20: 37169(R) (BMI-1774)
Cr–Cu–Fe–Mn–Mo–Ni, corrosion of Illium R, by boiling hydrofluoric acid–nitric acid solutions, 20: 37169(R) (BMI-1774)
Cr–Fe–Mn–Mo–Ni–Ti, corrosion of Hanford 20, by boiling hydrofluoric acid–nitric acid solutions, 20: 37169(R) (BMI-1774)
Cr–Fe–Mn–Mo–Ni–Ti, corrosion of Hanford 17, by boiling hydrofluoric acid–nitric acid solutions, 20: 37169(R) (BMI-1774)
Cr–Fe–Mn–Ni, corrosion of corronel 230, by boiling hydrofluoric acid–nitric acid solutions, 20: 37168(R) (BMI-1771)
Cr–Fe–Mn–Ni, corrosion of corronel 230, by boiling hydrofluoric acid–nitric acid solutions, 20: 37169(R) (BMI-1774)
Cr–Ni, corrosion of Blaw Nox NA 55 and NA 64 by boiling hydrofluoric acid–nitric acid solutions, 20: 37169(R) (BMI-1774)
Dy–Ni, crystal structure of intermetallic compounds in, 20: 37243
Er–Ni, crystal structure of intermetallic compounds in, 20: 37243
Gd–Ni, crystal structure of intermetallic compounds in, 20: 37243
Ho–Ni, crystal structure of intermetallic compounds in, 20: 37243
Lu–Ni, magnetic properties of $LuNi_5$, 20: 37279
Mo–Ni, thermal capacity data and order-disorder reactions in, 20: 37278
Nd–Ni, crystal structure of intermetallic compounds in, 20: 37243
Ni–Nb–Zr, hydrogen embrittlement of, review of, 20: 37187
Ni–Pr, crystal structure of intermetallic compounds in, 20: 37243
Ni–rare earth, crystal structure of intermetallic compounds in, 20: 37243
Ni–rare earths, magnetic properties of $LaNi_2$ series, 20: 37279
Ni–Sm, crystal structure of intermetallic compounds in, 20: 37243
Ni–Tb, crystal structure of intermetallic compounds in, 20: 37243
Ni–Y, crystal structure of intermetallic compounds in, 20: 37243
Ni–Zn, critical temperature of superconducting, transition-metal impurity effects on depression of, (E), 20: 37955

NICKEL CHLORIDES
reactions with isopropylamine, thermogravimetric study of, 20: 36853

NICKEL COMPLEXES
with tetraphenylporphine in dioxane, gamma radiolysis of, 20: 36889

NICKEL(II) COMPLEXES
with salicylaldehyde and its derivatives, magnetic moments of, 20: 36823

NICKEL IONS
effects on copper determination, 20: 36726

NICKEL ISOTOPES
binding energies of even-even, calculations using shell model with reaction matrix, (T), 20: 38066

NICKEL ISOTOPES Ni-58
deuteron elastic scattering at 13.6 Mev, differential cross sections for, (E), 20: 38128
energy levels of, energy calculations using shell model with reaction matrix, (T), 20: 38066
proton elastic scattering at 49 Mev, angular distribution of polarization in, (E), 20: 38049
proton inelastic scattering at 9.10 to 9.55 Mev, spins of levels from, (E), 20: 38181
proton reactions (p,n) with, thresholds for, (E), 20: 38053
proton reactions (p,n) with, threshold energy for, (E), 20: 38054

NICKEL ISOTOPES Ni-59
energy levels of, energy calculations using shell model with reaction matrix, (T), 20: 38066

NICKEL ISOTOPES Ni-60
deuteron elastic scattering at 13.6 Mev, differential cross sections for, (E), 20: 38128
energy levels of, energy calculations using shell model with reaction matrix, (T), 20: 38066
helium-4 reactions with, formation and decay of zinc-64 in, 20: 38152
proton elastic scattering at 49 Mev, angular distribution of polarization in, (E), 20: 38049
proton reactions (p,n) with, thresholds for, (E), 20: 38053
proton reactions (p,n) with, threshold energy for, (E), 20: 38054

NICKEL ISOTOPES Ni-61
deuteron reactions at 10 to 20 Mev, excitation functions for, (E), 20: 38148
energy levels of, energy calculations using shell model with reaction matrix, (T), 20: 38066
helium-3 reactions with, formation and decay of zinc-64 in, 20: 38152

NICKEL ISOTOPES Ni-62
deuteron elastic scattering at 13.6 Mev, differential cross sections for, (E), 20: 38128
energy levels of, energy calculations using shell model with reaction matrix, (T), 20: 38066
proton reactions (p,n) with, thresholds for, (E), 20: 38053
proton reactions at 20 to 50 Mev, copper-63 compound nucleus formation in, (E), 20: 38147

NICKEL ISOTOPES Ni-63
diffusion in alpha-irradiated copper, 20: 37300
energy levels of, energy calculations using shell model with reaction matrix, (T), 20: 38066

NICKEL ISOTOPES Ni-64
deuteron elastic scattering at 13.6 Mev, differential cross sections for, (E), 20: 38128
energy levels of, energy calculations using shell model with reaction matrix, (T), 20: 38066

NICKEL ISOTOPES Ni-65
energy levels of, energy calculations using shell model with reaction matrix, (T), 20: 38066

NICKEL OXIDES
radiation effects on catalytic activity, surface excess oxygen, and electric conductivity of, gamma, 20: 36885
separation from uranía in organic slurries, centrifugal, 20: 36933

NICKEL SULFATES
radiation effects on electric conductivity of solutions of, gamma, 20: 36912
radiolysis of hydrated, gamma, 20: 36903

NIOBIUM
analysis for copper by absorption spectroscopy, effects of ions on, 20: 36726
coating with niobium disilicide, growth kinetics and diffusion reactions of, 20: 37190
creep-rupture and tensile properties of, effects of nitrogen on, 20: 37218
crystal structure of, determination by phonon dispersion, 20: 37273
determination of, using Arsenazo III, photometric, 20: 36778
deuteron reactions (d,n) with, cross sections and mechanism of, (E), 20: 38159
effects on crystal structure and properties of thoria-tungsten cermets, 20: 37185
neutron total cross sections at high energies, fluctuations in, 20: 38173
reactions with liquid sodium at high temperatures, 20: 38499 (ANL-7120, pp 839-47)
separation from hydrofluoric acid solutions by solvent extraction using dialkyl alkylphosphonates, 20: 36941
separation from protactinium by solvent extraction using isoamyl alcohol, 20: 36940
separation from water by foaming, 20: 36934
superconductivity in, nuclear spin-lattice relaxation time for, (E), 20: 37941

NIOBIUM ALLOYS
tensile properties of, effects of beryllium and zirconium on, 20: 37245
Al–Nb, properties of intermetallic compound, 20: 37260
Be–Cr–Nb, tensile properties of, 20: 37245
Be–Nb–W, tensile properties of, 20: 37245
Cr–Nb, phase studies of intermetallic compound, 20: 37239
Mo–Nb, crystal structure of, determination by phonon dispersion, 20: 37273
Nb–Re–Zr, oxidation by oxygen at 1000°C, kinetics and microstructures of, 20: 37193
Nb–Ta, shear properties of single crystal, effects of composition on, 20: 37215
Nb–V–Ti, oxidation by air at 900 to 1200°C, kinetics and mechanisms of, 20: 37191
Nb–W, tensile properties of, 20: 37245
Nb–W–Zr, tensile properties of, 20: 37245
Nb–Zr, current losses and magnetic field aberrations from high-field superconducting wires of, in adiabatic demagnetization apparatus, 20: 37970
Nb–Zr, development as fuel jacket material for fast reactors, 20: 38465 (ANL-7120, pp 289-300)
Nb–Zr, heat treatment effects on texture of, 20: 37198
Nb–Zr, hydrogen embrittlement of, review of, 20: 37187
Nb–Zr, mechanical properties of, effects of composition and heat treatments on, 20: 37236
Nb–Zr, oxidation by oxygen at 1000°C, kinetics and microstructures of, 20: 37193
Nb–Zr, phase transformations of, factors affecting, 20: 37234
Nb–Zr, plastic flow of, determination by hardness, 20: 37230
Nb–Zr, reactions with liquid sodium at high temperatures, 20: 38499 (ANL-7120, pp 839-47)
Nb–Zr, reactions with uranium mononitride at high temperatures, 20: 37168(R) (BMI-1771)
Nb–Zr, reactions with plutonium nitride and uranium nitride at high temperatures, 20: 37169(R) (BMI-1774)
Nb–Zr, superconducting properties in strong d-c magnetic fields, (E), 20: 37950

Nb–Zr, transformation temperatures of, effects of cooling rates on, 20: 37233
Nb–Zr, wetting by sodium, effects of temperature on, 20: 37168(R) (BMI-1771)
Ni–Nb–Zr, hydrogen embrittlement of, review of, 20: 37187

NIOBIUM FLUORIDES
preparation and properties of, 20: 36950
reactions with bromides, chlorides, and fluorides, 20: 36804

NIOBIUM ISOTOPES Nb-95
dispersion from fallout in seawater, 20: 37037
yields in proton fission of uranium-238 at 7.1, 9.4, and 12.0 Mev, 20: 37995

NIOBIUM ISOTOPES Nb-96
yields of, from proton fission of uranium-238 at 12 Mev, 20: 37995

NIOBIUM NITRIDES
mechanical and thermodynamic properties of, effects of zirconium on, 20: 37274

NIOBIUM OXIDES
crystal structure of monoclinic $Nb_{12}O_{29}$, 20: 36790
effects on diffusion in uranium dioxide, mechanism of, 20: 37256
preparation and properties of suboxides, 20: 36825
separation from urania in organic slurries, centrifugal, 20: 36933

NIOBIUM SILICIDES
growth on niobium surfaces, kinetics of diffusion reactions in, 20: 37190
Nb_5Si_3–W_5Si_3, oxidation and thermal stability of, at high temperatures, 20: 37262
$NbSi_2$–WSi_2, oxidation and thermal stability of, at high temperatures, 20: 37262

NIOBIUM SYSTEMS
B–Nb–W, phase studies of, 20: 37261
C–Nb–W–Zr, tensile properties of D-43, effects of brittle coatings on, 20: 37276
Nb–O, partial pressures of oxides formed in solid solutions of, 20: 36836
Nb–O, solid-solution clustering of oxygen in, measurements of, 20: 37213
Nb–O, solid-solution clustering of oxygen in, mechanisms of, 20: 37214
Nb–O–Ti, crystal structure and superconductivity at 4.2°K, effects of fabrication and heat treatments on, 20: 37267

NITRATE IONS
effects on copper determination, 20: 36726

NITRATES
Cl^-–NO_3^-–UO_2SO_4, ion exchange equilibria in, 20: 36931

NITRIC ACID
separation of thorium from, by solvent extraction using diisopentyl methylphosphonate in benzene, tributyl phosphate, and xylene solutions, 20: 36942
solvent properties of, for plutonium, 20: 36928
HF–HNO_3, corrosive effects on corronel 230, 20: 37168(R) (BMI-1771)
HF–HNO_3, effects on corrosion resistant alloys, 20: 37169(R) (BMI-1774)

NITRITES
effects on mutation induction in Schizosaccharomyces, protective effects of chloramphenicol against, 20: 36653

NITROGEN
boiling data for, nucleate and film, 20: 36993
determination in diamonds by photoactivation, 20: 36746
effects on creep-rupture and tensile properties of niobium, 20: 37218
effects on properties of chromium-yttrium alloys, 20: 37168(R) (BMI-1771)
electric discharge in, electron velocity distribution in low-pressure, (E), 20: 38213
electric discharges in beams of condensed, plasma properties from, 20: 38247
energy level transition probabilities and lifetimes in, 20: 37438
ion wave propagation in weakly ionized plasma of, damping and phase velocity of, (E), 20: 38294
neutron absorption cross section in pitchblende, thermal, 20: 37994
positron annihilation in, (E), 20: 37810
radiation doses to tissues from, in solar particle beams in space, 20: 37023 (N-65-33865)
reactions with beryllium in group VIII transition metal alloys, 20: 37275
reactions with plutonium dioxide and uranium dioxide, effects of carbon on, 20: 37207
solubility in chromium-base chromium–yttrium alloys, 20: 37169(R) (BMI-1774)
spectra lines from ion excited, rotational structure of, 20: 37471
use as carrier in plasmochemistry, 20: 38314

NITROGEN IONS
energy level transition probabilities and lifetimes in, 20: 37438
polarizability and shielding factor for, dipole, (T), 20: 37440

NITROGEN ISOTOPES N-13
energy levels, (E), 20: 38053

NITROGEN ISOTOPES N-14
deuteron reactions (d,n) at 1.173, 1.797, and 2.098 Mev, angular distributions and excitation functions for, (E), 20: 38144
energy level at 7.03 Mev, properties of, (E), 20: 38083
energy level excitation in meson ($\pi^{\pm}$) reactions ($\pi^{\pm}$,2n) with oxygen-16, (E), 20: 38070
energy level lifetimes from tritium (C-12,nγ) reactions at 12 and 17.75 Mev, 20: 38008(R) (AECL-2595)
energy levels at 5.10 and 5.83 Mev, lifetimes and gamma decay strengths of, (E), 20: 38075
energy levels of, shell-model potential parameters for low-lying, (T), 20: 38145
meson ($\pi^{\pm}$) reactions (π^-,2n) and (π^+,2p) with, carbon-12 energy level excitation in, (E), 20: 38070
mesons (π^-) reactions with, charge exchange in, (E), 20: 37740 (JINR-P-2780)
neutron reactions (n,d) at 14 Mev, (E), 20: 38150

NITROGEN ISOTOPES N-15
determination in 0.38 to 20.0 percent range, spectrographic method for, 20: 36772
neutron reactions (n,d) at 14 Mev, (E), 20: 38150
proton reactions with, 3- continuum states of oxygen-16 from, (T), 20: 38102

NITROGEN MUSTARDS
effects of tritium-labeled, on inoperable tumors, 20: 36705

NITROGEN OXIDES
effects on quenching of energy spectra in determination of carbon-14, sulfur-35, and tritium, 20: 36771
spectra from 13-kev electron excited, emission, 20: 37466(T)

NITROUS ACID
formation by radiolysis of aqueous benzene, 20: 36881

NUCLEAR AIRCRAFT
characteristics of surface effect ships, 20: 38526
characteristics of lighter than air vehicles, 20: 38526

NUCLEAR BATTERIES
performance of krypton-85, 20: 37159

NUCLEAR EMULSIONS
cosmic nucleon interactions at 25 and 10^3 Bev in, isobar production from, (T), 20: 37675
cosmic proton elastic scattering by nuclei at 3 Tev in, cross section upper limit for elastic, (E), 20: 37666
development as detector for high-energy accelerator experiments, 20: 37077 (UCR-34P107-34)
elementary-particle interactions in, at high energies, 20: 38168
meson (π^-) reactions at 50 to 176 Mev, total cross sections for double charge-exchange, (E), 20: 38012 (JINR-P-2806)
sensitivity of, latent image parameters for, 20: 37121
silver bromide electron energy sensitivity in, threshold for, 20: 37122

NUCLEAR ISOMERS
photoproduction of, use in gamma dosimetry, 20: 37079
spins of three-particle states in spherical, with odd A, 20: 38136

NUCLEAR MAGNETIC RESONANCE
book: *Formula Index to NMR Literature Data. Vol. 2: 1961–1962 References*, 20: 36842

NUCLEAR MATERIALS MANAGEMENT
methods for, economics of, 20: 38416

NUCLEAR MODELS
reaction matrix in Brueckner, method for calculation of, 20: 38160
review, 20: 38118
review of rotational, 20: 38164

NUCLEAR MODELS (COLLECTIVE)
calculations using variational method, (T), 20: 38108
formulation of breathing-mode, (T), 20: 38170

NUCLEAR MODELS (OPTICAL)
neutron states in deformed optical potential, 20: 38126

NUCLEAR MODELS (SHELL)
potential parameters for calculations using, 20: 38145
use in description of nuclear analog states, (T), 20: 38025
use with reaction matrix in calculations of binding energies and excitation energies of nickel isotopes, (T), 20: 38066

NUCLEAR PHYSICS
data analysis using on-line PDP-7 computer, 20: 38176
research at CERN, 1965, 20: 37308(R) (NP-16226)
research on, using isotopic composition of extraterrestrial and terrestrial material, 20: 37369

NUCLEAR POWER
development in Soviet Union, economic aspects of, 20: 38512
economics and prospects of, 20: 38487 (AECL-2584)

NUCLEAR POWER PLANTS
economic aspects of, 20: 36945
economics of, comparison with fossil-fuel and hydro plants, 20: 38511
economics of, comparison with coal- and oil-fired power plants, 20: 38520

efficiency using gas turbines, 20: 38513
instrumentation and control of, feasibility of unified digital system for, 20: 38508 (NYO-2764-2)
radiological safety analysis computer program, 20: 37167 (IDO-17151)
turbine design and performance, 20: 38521
NUCLEAR QUADRUPOLE RESONANCE
theory for nuclei in solids, 20: 38019
NUCLEAR REACTIONS
angular correlations for, techniques for, 20: 38179
charged-particle absorption with formation of compound nuclei, (T), 20: 38020
gamma angular correlations from, performance of detectors for measuring, 20: 38184
matrix calculations in Brueckner theory, method for, 20: 38160
on star surfaces, effects on electromagnetic activity, 20: 37399
polarization effects in (γ,N), (T), 20: 38175
production of short-lived radioisotopes by, energy function chart for, 20: 36739
properties of stellar, 20: 37392
research review, 20: 38109
resonance behavior of isospin-forbidden, 20: 38045
structure effects in lithium-ion, with light nuclei, (T), 20: 38014
theory of direct stripping, 20: 38023
NUCLEAR SPECTRA
theory of unitary matrix ensembles, 20: 38033
NUCLEAR SPIN
of three-particle isomeric states in spherical nuclei with odd A, 20: 38136
NUCLEAR STRUCTURE
effects in lithium-ion reactions with light nuclei, (T), 20: 38014
effects on charge distribution in spherical nuclei, (T), 20: 38043
energy level identification in light nuclei by photodisintegration cross sections, 20: 38138
isotope shift of charge radius, anomalous, (T), 20: 38101
quadrupole surface resonances in spherical nuclei, 20: 38039
shell-model description of nuclear analog states, (T), 20: 38025
variational approach to collective motion, 20: 38108
NUCLEAR THEORY
effective hamiltonian for nuclear matter, 20: 38160
effects of pairing correlations and Coriolis force on E2 $\Delta K = 1$ transitions, 20: 38041
eigenfunctions for spherical and deformed Saxon-Woods potentials, 20: 38078
electric quadrupole transitions in deformed even-even nuclei, 20: 38127
energy gap in finite nuclei, 20: 38113
energy level transitions in deformed odd-mass nuclei, E1 $\Delta K = 0$, 20: 38040
neutron states in deformed optical potential, 20: 38126
nuclear particle spin effects on forces in, review of, 20: 37332
quadrupole surface resonances in spherical nuclei, 20: 38039
rotation-vibration interaction in deformed even-even nuclei, 20: 38156
variational approach to collective motion, 20: 38108
NUCLEI
alpha decay of, tunnel effect in, (T), 20: 38117
charge distribution in spherical, structure effects on, (T), 20: 38043
charge distribution in, isotopic shift of, (T), 20: 38101
charged-particle absorption with formation of compound nuclei, (T), 20: 38020
cosmic meson (μ) reactions with energy losses from relativistic, (T), 20: 37707
cosmic mesons (μ) reactions at 58 mwe underground, fast neutron differential energy spectrum from, (E), 20: 37710
cosmic shower nuclear-active component reactions with light, young-air, (E), 20: 37755
decay of compound, (T), 20: 38020
description of analog states using shell model, (T), 20: 38025
electron elastic scattering by, with a Fermi charge distribution, (T), 20: 38139
electron energy levels of, group theory classification of g^N, 20: 37437
energy level density in, methods for determining, 20: 38157
energy level identification in light, by photodisintegration cross sections, 20: 38138
energy level transitions in Coulomb excitation, angular correlations for E2 and E3, (T), 20: 38032
energy level transitions in deformed odd-mass, E1 $\Delta K = 0$, (T), 20: 38040
energy level transitions in deformed odd-mass, E2 $\Delta K = 1$, (T), 20: 38041
energy level transitions in deformed even-even, E2, (T), 20: 38127
energy level widths in, effects of cluster structure on virtual-resonance, 20: 38013
energy levels of A = 40 to 50, systematics of 3⁻ and 5⁻, (E), 20: 38100
energy levels of deformed even-even, rotation-vibration interaction in, (T), 20: 38156
energy levels of odd, energy ratios and spins of, (T), 20: 38022
energy levels of, g factor measurement by resonant scattering, (T), 20: 38079
gamma reactions (γ,n) with, polarization effects in, (T), 20: 38175
helium-3 and triton emission by, superfluid model for reduced widths for, 20: 38116
isobaric mass formula and Coulomb energies in 1p shell of, 20: 38174
lithium-ion reactions with light, structure effects in, (T), 20: 38014
meson (μ⁻) capture by protons in 2s-1d, 20: 38166
meson (π⁻) capture by complex, radiative, (T), 20: 38064
meson (π⁻) reactions at 16 Bev/c with complex, multipion resonance production from, (E), 20: 37822
meson (π⁻) reactions at 50 to 176 Mev, total cross sections for double charge-exchange, (E), 20: 38012 (JINR-P-2806)
meson reactions with, tests of unitary symmetry from, 20: 38009 (BNL-10420)
neutron scattering by, slowing down parameters and Legendre polynomial coefficients for, 20: 37988 (WAPD-TM-572)
neutron states in deformed optical potential, 20: 38126
neutron strength functions of, method for estimating, 20: 38038
neutron-proton interactions in, short-range, (T), 20: 38056
neutron-proton pairing correlations in spherical even, 20: 38177
nucleon inelastic scattering via compound nucleus mechanism, review of gamma angular distributions from, 20: 38178
nucleon interaction with complex, at high energies, (T), 20: 37790
nucleon pair correlations and final-state interactions in, 20: 38015
nucleon reactions above 10 Bev, internuclear cascade model for inelastic, 20: 38122
nucleon-nucleon interaction in, research using nucleon inelastic scattering, (T), 20: 38120
particle diffraction scattering with excitation of collective states, (T), 20: 38143
particle inelastic diffraction scattering with excitation of collective states, (T), 20: 38142
photon scattering by oriented, (T), 20: 38055
polarization in solids by solid-state effect, (E/T), 20: 38402
production and decay of heavy, research using thermonuclear explosions, (E), 20: 38093
strength parameter correlation with beta bands in even, electric monopole, (T), 20: 38180
structure of A = 37 and 38, intermediate coupling shell model for, 20: 38111
surface resonances in spherical, quadrupole, (T), 20: 38039
NUCLEI (CELLS)
radiation effects on nucleoli in tissue culture cells, uv, 20: 36592
NUCLEIC ACIDS
structure of transfer RNA, 20: 36555(R) (NYO-2643-22)
synthesis of, control mechanisms for, 20: 36555(R) (NYO-2643-22)
NUCLEON SHOWERS
calculations for meson (π⁻) reactions with emulsion nuclei at 17 Bev, (T), 20: 38060
NUCLEONS
charge distribution in meson (π)-nucleon systems, (T), 20: 37791
form factors of, effect of meson (π)-meson (π) interactions on electromagnetic, (T), 20: 37801
interactions in nuclei, pair correlations and final-state, 20: 38015
interactions with nucleons in nuclei, research using nucleon inelastic scattering, (T), 20: 38120
interactions with mesons (π), Regge-pole model for charge-exchange, 20: 37761
interactions with nucleons, $SU(12)_L$ predictions for amplitudes of, (E/T), 20: 37772
interactions with nucleons, zero-energy solution with tensor forces for, 20: 37782
interactions with complex nuclei at high energies, model for, 20: 37790
interactions with mesons (π), C, P, and T invariances in bootstrap mechanism for, 20: 37794
interactions with mesons (π), electromagnetic form factors from, (T), 20: 37801
interactions with mesons (π) at 500 to 600 Mev, amplitudes for, 20: 37803
interactions with photons at high energies, meson (ω) production in, (T), 20: 37807
interactions with mesons (π), Regge dynamics in, (T), 20: 37809
interactions with nucleons, isobaric spin dependence of, 20: 37811
pair production in photon-photon interactions, (T), 20: 37758
pairing correlations in spherical even nuclei, 20: 38177
photoproduction on nuclei, polarization effects in, (T), 20: 38175
reactions with nuclei above 10 Bev, internuclear cascade model for inelastic, 20: 38122
scattering by carbon-12 at 185 Mev, inelastic, (T), 20: 38120
scattering by even-even nuclei via compound nucleus mechanism, review of gamma angular distributions from inelastic, 20: 38178

NUCLEOPROTEINS
radiation effects on, in regenerating rat liver DNA, mechanism of x, 20: 36593
NUCLEOSIDES
radiation effects on deoxyriboside excretion in urine by dogs, pigs, and sheep, gamma, 20: 36604
NUCLEOTIDES
radiation effects on nicotinamide adenine, in rat thymocytes, x, 20: 36590

O

OCTANE, CHLORO-
yields of, from gamma-induced reactions of 1-butene and phosgene, 20: 36892
OHIO
ecology of plants of Neotoma Valley, Hocking County, 20: 36548 (TID-23036)
OILS
cost of fuel, comparison with nuclear fuels, 20: 38541
radiation effects on flotation properties of, for pure minerals and commercial ores, gamma, 20: 36893
OLEIC ACID
radiation effects on content of, in free lipid fraction in seedling bean leaves, x, 20: 36598
OLEIC ACID, SODIUM SALTS
radiation effects on flotation properties of, for pure minerals and commercial ores, gamma, 20: 36893
ONIONS
radiation effects on sprouting of, economics of, 20: 37157
OOCYTES
effects of irradiation of Drosophila, on sperm cells in succeeding generations, gamma, 20: 36625
radiosensitivity of rat, x, 20: 36632
OPTICAL SYSTEMS
design for measuring asymmetric distortions in camera lenses, 20: 37053
design of stereoscopic viewer, for measuring angles and positions in three dimensions, 20: 37052
ORES
analysis of, for chromium by neutron activation methods, 20: 36750
analysis of, for iridium by neutron activation analysis, 20: 36751
flotation of, on gamma-irradiated anionic collector agents, 20: 36893
x-ray absorption and fluorescence analysis of, instruments for automatic continuous, 20: 37152
ORGANIC COMPOUNDS
analysis of, for carbon-14 and tritium, oxygen-tube combustion method for scintillation, 20: 36723
nuclear magnetic resonance spectra of, formula index to, 20: 36842
ORGANIC COMPOUNDS, METALLO-
preparation and thermal decomposition of rare earth and transition-metal alkoxide, 20: 36851
ORGANIC COOLED REACTORS
heat transfer limitations on fuel elements, 20: 38484
ORGEL REACTOR
development, 20: 38518
OSMIUM
yields from radiolysis of osmium phthalocyanine, 20: 36886
OSMIUM ISOTOPES Os-182
energy level transitions in isomeric, (E), 20: 38027
OXAZOLE, 2,2'-*p*-PHENYLENEBIS[4-METHYL-5-PHENYL-
properties for use in liquid scintillation counters, 20: 36862
properties for use in liquid scintillation counters, 20: 36863
OXAZOLE, 2,2'-*p*-PHENYLENEBIS[5-PHENYL-
properties for use in liquid scintillation counters, 20: 36863
paraffin–2,2'-*p*-phenylenebis[5-phenyloxazole–*p*-terphenyl, scintillation efficiency, 20: 37107
OXYGEN
determination in aluminum and zirconium by helium-3 activation, 20: 36741
effects of atmosphere of, on positronium lifetime in metal oxides, (E), 20: 37819
effects on corrosion and mechanical properties of hafnium, 20: 37170
effects on iodine-131 and mercury-203 uptake by tumor tissues in man and rabbits, 20: 36576
effects on properties of chromium-yttrium alloys, 20: 37168(R) (BMI-1771)
effects on radioinduced polymerization of allyl alcohol, 20: 36880
effects on radiosensitivity of bacteria, spores, and yeasts, 20: 37144
effects on tantalum, dislocation Snoek pinning strength from, (E), 20: 38360
neutron absorption cross section in pitchblende, thermal, 20: 37994
photoionization by cosmic x rays, cross sections for interstellar K-shell, 20: 37485
positron annihilation in, (E), 20: 37810
proton elastic scattering at 1 Bev, differential cross section for, (E), 20: 38010 (BNL-10438)
radiation doses to tissues from, in solar particle beams in space, 20: 37023 (N-65-33865)
radioinduced recombination with hydrogen in presence of water vapor, gamma, 20: 36910
reactions with beryllium in group VIII transition metal alloys, 20: 37275
reactions with chromium–rhenium alloys at high temperatures, mechanisms of, 20: 37186
reactions with gadolinium oxide, homomolecular and isotopic-exchange, 20: 36826
reactions with Nb–Zr and Nb–Re–Zr alloys at 1000°C, 20: 37193
separation from iodide zirconium by zone refining, 20: 37177
use as carrier in plasmochemistry, 20: 38314
yields from radiolysis of bromates, 20: 36899
OXYGEN IONS
energy loss in dielectric media at high energies, (T), 20: 37460
polarizability and shielding factor for, dipole, (T), 20: 37440
reactions with tin, fission cross sections for, (E), 20: 38123
OXYGEN ISOTOPES O-14
beta decay of, ft value, branching ratio, and shape factor of 4.12-Mev positron transition, (E), 20: 38080
OXYGEN ISOTOPES O-16
content in minerals from iron formations in Quebec, 20: 37013
energy level transitions of, gamma energy from 3^-, (E), 20: 37126
energy levels of, 3^- continuum, (T), 20: 38102
gamma reactions (γ,N) with, polarization effects in, (T), 20: 38175
meson (π^-) capture by, radiative, (T), 20: 38064
meson ($\pi^\pm$) reactions (π^-,2n) and (π^+,2p) with, nitrogen-14 energy level excitation in, (E), 20: 38070
reactions (O-16,α) with carbon-12, magnesium-24 levels from, 20: 38008(R) (AECL-2595)
reactions (O-16,nγ) with tritium at 18 Mev, fluorine-18 level lifetimes from, 20: 38008(R) (AECL-2595)
OXYGEN ISOTOPES O-17
energy levels at 3.06 and 3.85 Mev, (E), 20: 38161
OXYGEN ISOTOPES O-18
content in minerals from iron formations in Quebec, 20: 37013
content in sea urchins, variations in, 20: 36549
content in sea urchins, environmental and genetic factors in variations in, 20: 36550
energy levels of, shell-model potential parameters for low-lying, (T), 20: 38145
OXYGEN SYSTEMS
C–O–Zr, phase studies, 20: 37264
Nb–O, partial pressures of oxides formed in solid solutions of, 20: 36836
Nb–O, solid-solution clustering of oxygen in, measurements of, 20: 37213
Nb–O, solid-solution clustering of oxygen in, mechanisms of, 20: 37214
Nb–O–Ti, crystal structure and superconductivity at 4.2°K, effects of fabrication and heat treatments on, 20: 37267
O–propane, properties for proportional detectors, 20: 37092
Ta–O, partial pressures of oxides formed in solid solutions of, 20: 36836

P

PAIR PRODUCTION
theory for, in electromagnetic cascade showers, 20: 37788
PALLADIUM
plutonium determination on plates of, by alpha counting, 20: 36736
yields from radiolysis of palladium phthalocyanine, 20: 36886
PALLADIUM ISOTOPES
production in proton reactions with lead and uranium at 3 and 28 Bev, cross sections for, (E), 20: 38098
PALLADIUM ISOTOPES Pd-109
yields from helium ion-induced fission of lead-207 at 41.1 to 26.3 Mev, 20: 37996
yields in proton fission of uranium-238 at 7.1, 9.4, and 12.0 Mev, 20: 37995
PALLADIUM ISOTOPES Pd-112
yields from helium ion-induced fission of lead-207 at 41.1 to 26.3 Mev, 20: 37996
yields in proton fission of uranium-238 at 7.1, 9.4, and 12.0 Mev, 20: 37995
PALLADIUM SYSTEMS
Al_2O_3–Pd–Ag, preparation and properties of alumina-base cermets of, 20: 37209
MgO–Pd–Ag, preparation and properties of magnesia-base cermets of, 20: 37209
Pd–Ag–ThO_2, preparation and properties of thoria-base cermets of,

20: 37209
Pd–Ag–ThO_2, preparation and properties of thoria-base cermets of, 20: 37209
Pd–Ag–ZrO_2, preparation and properties of zirconia-base cermets of, 20: 37209
PALMITIC ACID
analysis of, for carbon-14, combustion method for, 20: 36721
PARAFFIN
cosmic neutron attenuation at 60 Bev, collision mean free path and neutron-proton cross section from, (E), 20: 37670
paraffin–2,2′-*p*-phenylenebis[5-phenyloxazole–*p*-terphenyl, scintillation efficiency, 20: 37107
PARAMECIUM
radiation effects on survival of *Paramecium aurelia*, ultraviolet and x, 20: 36661
PARASITES
radiation effects on Toxoplasma cysts in human eye, laser, 20: 36683
radiation effects on host response to, x, 20: 36607(R) (TID-23114)
radiation injuries and recovery in *Hymenolepis microstoma*, x, 20: 36662
PARTICLE TRACKS
measurement of positions and angles of, design of stereoscopic viewer for, 20: 37052
measurement of, equipment for, 20: 37043
PARTICLES
ionization losses in polarized polystyrene layer, optimum thickness for relativistic, (E), 20: 37435
PEACH BOTTOM POWER REACTOR
development, 20: 38523
PEAS
effects of ethylenimine and ethylmethanesulfonate on mutation frequency, meiosis, and mitosis in, 20: 36621
effects of ethylenimine and methanesulfonate on chlorophyll and morphological mutations in varieties of, 20: 36624
mutations induced by chemicals in, 20: 36634
radiation effects on chlorophyll mutation frequency, meiosis, and mitosis in, fast neutron and gamma, 20: 36621
radiation effects on chlorophyll and morphological mutations in varieties of, gamma, 20: 36624
radiation effects on mitosis in *Pisum sativum* root tip cells, thermal neutron, 20: 36644
radioinduced mutations of, γ and fast neutron, 20: 36634
PECTINS
radioinduced decomposition of, effects of moisture levels on gamma, 20: 36879
1,5-PENTANEDIAMINE
protection against radiation damage in calf-thymus DNA, mechanism of, 20: 36665
2,4-PENTANEDIONE
effects on copper determination by absorption spectroscopy, 20: 36726
PENTANES
neutron inelastic scattering in, angular distributions from slow, (E), 20: 38001
1-PENTANOL
effects on copper determination by absorption spectroscopy, 20: 36726
2-PENTANOL
effects on copper determination by absorption spectroscopy, 20: 36726
2-PENTANONE, 4-METHYL-
effects on copper determination by absorption spectroscopy, 20: 36726
4-methyl-2-pentanone–TBP, solvent properties for uranium, 20: 36716
PERCHLORIC ACID
effects on tritium exchange between *tert*-butyl alcohol and water, 20: 36849
acetic acid–ethylene glycol–$HClO_4$, properties for etching zirconium, 20: 37227
PERMEABILITY
measurement in graphite products, methods for, 20: 37225
PERSONNEL
radiation dose models for, at nuclear rocket ground tests, 20: 37034
radiation dosimetry of, in Prague, 20: 37035
radiation effects on blood plasma proteins in, 20: 36581
radiation monitoring of medical, device for, 20: 36680
PERTURBATION THEORY
convergence of perturbation series for many-body Fermi systems, 20: 38121
use in derivation of Fermi liquid theory for electrons in solids, 20: 38403
PETROLEUM
effects of mineral oil on radioinduced polymerization of dodecyl methacrylate, 20: 36875
effects on copper determination by absorption spectroscopy, 20: 36726
effects on radioinduced polymerization of acrylonitrile–styrene mixture, 20: 36876
electric power from, cost comparison with nuclear-generated, 20: 38520
PHARMACEUTICALS
radiation processing of, to destroy microorganisms, 20: 37140
PHARMACOLOGY
book: *Yearbook of Nuclear Medicine*, Vol. I, 1966, 20: 36690
PHENANTHROLINE COMPLEXES
with iron, stability of, 20: 36716
with uranyl ions, stability of, 20: 36716
PHENOL
formation by radiolysis of aqueous benzene, 20: 36881
PHENOL, *o*-BROMO-
effects on radiosensitivity of bacteria, spores, and yeasts, 20: 37144
PHENOL, *o*-CHLORO-
effects on radiosensitivity of bacteria, spores, and yeasts, 20: 37144
PHENOL, DINITRO-
effects on rate of strontium absorption by barley, 20: 36575
formation by radiolysis of aqueous benzene, 20: 36881
PHENOL, IODO-
effects on radiosensitivity of bacteria, spores, and yeasts, 20: 37144
PHENOL, NITRO-
effects on mutarotations of β-D-fructose and α-D-glucose, 20: 36577
formation by radiolysis of aqueous benzene, 20: 36881
PHENYL SULFIDE
radioinduced radical formation in, in organic glasses at –196°C, spectra from gamma, 20: 36894
PHONONS
dispersion in molybdenum, niobium, and niobium–molybdenum alloys, lattice dynamics of, 20: 37273
neutron attenuation by, in single crystals, (T), 20: 38371
PHOSGENE
radioinduced reactions of, with 1-butene at –78 to 35°C, gamma, 20: 36892
PHOSPHATE ROCKS
separation of phosphates from, efficiency of irradiated anionic collector agents in, 20: 36893
PHOSPHATES
separation from phosphorite ores, efficiency of irradiated anionic collector agents in, 20: 36893
PHOSPHATIDES
content and composition of blood plasma, in men and rats, 20: 36606(R) (NYO-1864-23)
effects of biological stress on content in blood plasma of man, 20: 36606(R) (NYO-1864-23)
radiation effects on content in rat tissues, 20: 36606(R) (NYO-1864-23)
synthesis of phosphatidylglycerol, phosphatidylglycerophosphate, and cardiolipin, 20: 36606(R) (NYO-1864-23)
PHOSPHINES
radioinduced free radicals of, in krypton, 20: 36909
PHOSPHONATES
uses in fuel element processing by solvent extraction, 20: 36948
PHOSPHONIC ACID, ALKYL-, DIALKYL ESTER
solvent properties of, for iron, niobium rare earths, and tantalum, 20: 36941
PHOSPHONIC ACID, METHYL, DIISOAMYL ESTER
solvent properties for thorium, effects of benzene, tributyl phosphate, and xylene on, 20: 36942
PHOSPHONIC ACID, PHENYL-, OCTYL ESTER
octyl phenylphosphonate–TBP, solvent properties for americium, 20: 36937
PHOSPHOPROTEINS
radiation effects on content and metabolism of, in denerved and intact muscles in rabbits, x, 20: 36602
PHOSPHORIC ACID
Hg–H_3PO_4, reduction of irradiated potassium chloride by, preparation of sulfur-35-labeled sulfuric acid by, 20: 36920
PHOSPHORIC ACID, ALKYL ESTERS
preparation of phosphorus-32-labeled tri-*n*-octyl phosphonate, 20: 36684
PHOSPHORIC ACID, BIS(2-ETHYLHEXYL) ESTER
bis(2-ethylhexyl)phosphate–TBP, solvent properties for americium, 20: 36937
PHOSPHORS
design of plastic, for measuring beta activity in gas samples, 20: 37086
efficiency in scintillation counters, 20: 37112
light output and attenuation length of, 20: 37113
preparation and properties of *p*-bis(*o*-methylstyryl)benzene, 20: 36862
properties of *p*-bis-(*o*-methylstyryl)benzene, *p*-bis-2-(4-methyl-5-phenyloxazolyl)benzene, and *p*-bis-2-(5-phenyloxazolyi)benzene, 20: 36863
wavelength shifters in plastic, preparation of distyrylbenzene derivatives for use as, 20: 36847
wavelength shifters in plastic, preparation of anthracene derivatives for use as, 20: 36848

PHOSPHORUS
neutron absorption cross section in pitchblende, thermal, 20: 37994
separation of phosphorus-33-enriched, from radiation targets, 20: 37166
PHOSPHORUS BROMIDES
reactions with niobium and tantalum pentafluorides, 20: 36804
reactions with uranium hexafluoride, 20: 36803
PHOSPHORUS CHLORIDES
reactions with niobium and tantalum pentafluorides, 20: 36804
reactions with uranium hexafluoride, 20: 36803
PHOSPHORUS FLUORIDES
reactions with uranium hexafluoride, 20: 36803
PHOSPHORUS ISOTOPES P-30
energy level quantum numbers and transitions from silicon-29 (p,γ) reaction, (E), 20: 38062
PHOSPHORUS ISOTOPES P-31
energy levels of, from sulfur-32 (n,d) reaction at 14 Mev, 20: 38150
PHOSPHORUS ISOTOPES P-32
effects with yttrium-90 on tissue homografts in dogs by lymphatic ablation, 20: 36641
incorporation into tri-n-octyl ester of phosphoric acid for use in radiotherapy, 20: 36684
radiation effects on metabolism of, in denerved and intact muscles in rabbits, x, 20: 36602
removal from glass surfaces, factors influencing, 20: 36923
PHOSPHORUS ISOTOPES P-33
production in ORR by neutron irradiation of chlorine-36 and sulfur-33, (E), 20: 37166
PHOTOELECTRIC CELLS
calibration of photoelectric nucleus counter, pressure effects on, 20: 37094
design and performance of two-channel, for recording H_β profile on microsecond time scale, 20: 37063
PHOTOGRAPHIC EMULSIONS
preparation and properties for use in electron-microscopic autoradiography, 20: 37050
sensitivity of, latent image parameters for, 20: 37121
PHOTOGRAPHIC FILM
radiation effects on sensitivity of, 20: 36895
PHOTOGRAPHIC FILM DETECTORS
use for personnel monitoring in Prague, 20: 37035
PHOTOGRAPHY
Schlieren, of rail-tube plasmas, 20: 38287
use of high-speed, in measurement of surface motion, 20: 36959 (PNE-603F)
PHOTOMETERS
design of smoke, 20: 37169(R) (BMI-1774)
development of portable smoke, 20: 37168(R) (BMI-1771)
PHOTOMULTIPLIER TUBES
switching circuit for, design and performance of, 20: 37051
use in measurement of radiation field time evolution, 20: 37311
PHOTONS
absorption and opacity calculations for stellar, 20: 37393
density of intergalactic starlight, (T), 20: 37374
dosimetry of, use of probe method in, 20: 37081
effects on cyclomerization of 4-carbon compounds, 20: 36860 (NP-16150)
flux from stellar sources, limits for, (E), 20: 37547
interactions of, perturbation theory for, (T), 20: 37841
interactions with deuterons, nonphysical partial-wave amplitude singularities in disintegration, (T), 20: 38140
interactions with protons at 400 to 600 Mev, N* (1410) production from, (E), 20: 37752
interactions with nucleons and photons, (T), 20: 37758
interactions with protons at 1.6 to 6.0 Bev, meson (ρ^0) production cross sections for, (E/T), 20: 37766
interactions with protons, SU(3) amplitudes for meson production in, (E/T), 20: 37773
interactions with deuterons at 220 to 280 Mev, differential cross sections for meson (π^0) production in, (E), 20: 37783
interactions with nucleons at high energies, meson (ω) production in, (T) 20: 37807
production by electron-positron annihilation, Bogoliubov canonical transformation for, 20: 37757
production from cosmic particle reactions with graphite at high energies, (E), 20: 38110
reactions (γ,n) with nuclei, polarization effects in, (T), 20: 38175
reactions (γ,n), (γ,2n), and (γ,3n) with iodine-127 and praseodymium-141, cross sections for, (E), 20: 38094
reactions with hydrogen atoms, excitation and ionization in, (T), 20: 38221
scattering by oriented nuclei, (T), 20: 38055
PHTHALIC ACID, POTASSIUM SALTS
effects on mutarotations of β-D-fructose and α-D-glucose, 20: 36577
PHTHALOCYANINES
radiolysis of, yields of metal ions in, 20: 36886
PHYSICS
theory of unitary matrix ensembles, 20: 38033
PIGMENTS
melanin affinity for chloroquine in mouse skin, 20: 36564
PINCH DEVICES
design and performance of Scyllacita compact high-voltage theta, 20: 38306
design of linear, 20: 38197 (LA-3553)
design of toroidal Scyllac, 20: 38197 (LA-3553)
development for high-temperature plasma production, 20: 38335
PINCH EFFECT
current waves in lightning discharge, (T), 20: 38260
currents in linear discharge, axial pressure asymmetry from Hall, (E), 20: 38289
plasma end loss in slow theta, (E), 20: 38256
PITCHBLENDES
analysis for trace elements, estimation of ratio of induced fission vs spontaneous fission from, 20: 37994
PITUITARY GLAND
radiosensitivity effects on animals, review on, 20: 36668
PLANKTON
strontium-85 photosynthesis and uptake in freshwater, effects of light on, 20: 36568
PLANT CELLS
analysis for calcium-45 and strontium-89 in algae, liquid scintillation spectrometric, 20: 36747
PLANTS
analysis of, for carbon-14 and tritium by liquid scintillation counting, oxygen flask combustion technique for sample preparation for, 20: 36764
gamma activity in lichens and herbaceous, of Neotoma Valley, Ohio, 1962 and 1964, 20: 36548 (TID-23036)
radiation effects on lupinus seed, effects of moisture on γ, 20: 36646
radioinduced mutations in peanut, resistance to virus disease, γ, 20: 36647
radiosensitivity of sweet clover seeds, variations with experimental conditions, 20: 36658
strontium-90 content in meadow and clover hay, Germany, 1962, 20: 36671
PLASMA
acoustic and electromagnetic wave interactions in, coupling of, 20: 38232
acoustic wave propagation in warm, from vertical dipoles, 20: 38229
acoustic wave propagation in warm, from vertical dipole, 20: 38230
acoustic wave propagation in strong magneto-, (T), 20: 38303
bibliography on, 20: 38199 (MATT-400)
bibliography on high-temperature, 20: 38204 (NP-16240)
book: *Particle Kinetics of Plasmas*, 20: 38348
charged-particle density in positive column of, between coaxial cylinders, (E), 20: 38236
charged-particle motion in non-adiabatic magnetic traps, stochastic, 20: 38246
charged-particle motion in, correction to second adiabatic invariant of, (T), 20: 38275
chemical properties of low-temperature, 20: 38314
chemical reactions of nitrogen with infiltrated tungsten materials at high heat fluxes, 20: 37188
circulation in MPD cells, 20: 37724
confinement of, corrections to Chew-Goldberger-Low theory for, 20: 38271
containment and stability in negative V stellarators, 20: 38243
containment by relativistic electron coils, properties of, 20: 38210 (UCRL-12455(Rev.1))
containment of alkali-metal, field curvature effects on, (E/T), 20: 38326
containment of slow theta-pinch, end losses in, 20: 38256
containment, magnetic field design with electrolytic tank analog for, 20: 38189 (AD-636095)
currents in linear pinch, axial pressure asymmetry from Hall, (E), 20: 38289
diagnostics of ionospheric, use of Langmuir probes for determining, 20: 38309
diagnostics of isotropic plane-layer, ultrahigh-frequency, (T), 20: 38225
diagnostics of monoenergetic, spherical probe dynamics for determining, (T), 20: 38190 (AD-637513)
diagnostics of, computer use for determining, 20: 38310
diagnostics of, design and performance of microwave-cavity Q sampler for, 20: 38307
diagnostics of, electrostatic probes in, (T), 20: 38278
diagnostics of, spectral distribution of scattered laser light in, (E), 20: 38259
diagnostics of, using self-reversed contours, 20: 38265(T)

dielectric function for homogeneous, calculation of, 20: 38297
diffusion across magnetic fields, properties of, 20: 38249
diffusion across magnetic fields, computer simulation of anomalous, 20: 38328
diffusion coefficient measurement for, technique for, (E/T), 20: 38322
diffusion in E-type r-f discharges, (E), 20: 38327
diffusion in magnetic mirror machines, properties of, 20: 38313
diffusion in magnetic mirror machines, (E/T), 20: 38324
diffusion in Q-machines, (T), 20: 38203 (NP-16237)
diffusion in ring r-f discharges, anomalous, (E/T), 20: 38329
diffusion of potassium magneto-, in universal instability, 20: 38264
diffusion of, review of anomalous, 20: 38330
dispersion equation for cylindrical, derivation of, 20: 38257
electric conductivity of seeded nonequilibrium, (T), 20: 38288
electric conductivity of slab of, between juxtaposed disk electrodes, 20: 38293
electric discharges in rail-tube, Schlieren photography of, 20: 38287
electromagnetic fields in anisotropic confined, electron collision effects on, 20: 38226
electromagnetic field properties in warm cylindrical magneto-, potentials for, 20: 38302
electromagnetic wave interaction with inhomogeneous drifting, dispersion relations for, (T), 20: 38194(R) (INDEC-SR-7, pp 3.22-59)
electromagnetic wave interactions with, diagnostics from, (T), 20: 38225
electromagnetic wave propagation in gyrotropic, separation constants for, 20: 38228
electromagnetic wave propagation in warm, from vertical dipole, 20: 38229
electromagnetic wave propagation in warm, from vertical dipole, 20: 38230
electromagnetic wave propagation in, ferrite antenna windows for improving, 20: 38231
electromagnetic wave propagation in inhomogeneous, properties of, (T), 20: 38233
electromagnetic wave interactions with, electron collision frequency in, 20: 38234
electromagnetic wave reflection and transmission by moving cold, (T), 20: 38237
electromagnetic wave transmission and reflection by warm, (T), 20: 38276
electromagnetic wave interactions with classical and quantum, correlation effects in, (T), 20: 38292
electromagnetic wave interaction with ferromagnetic, (T), 20: 38354 (FTI-244/T-027)
electron and ion density in Ogra-I, increasing of, 20: 38248
electron and ion density in, microwave measurement system for, 20: 38338(P)
electron beam interactions with magneto-, collective fluctuations from, 20: 38201 (NP-16210)
electron beam interactions with, cyclotron radiation excitation from, (T), 20: 38291
electron beam interactions in inhomogeneous field-free, correlation and exchange effects from, (T), 20: 38334
electron collisions in, control for alleviation of signal degradation from, 20: 38234
electron cyclotron resonance harmonic in hydrogen ion source, 20: 38224
electron cyclotron resonance in, anisotropic velocity distribution from, 20: 38205 (NYO-3565-4)
electron density and collision frequency in inhomogeneous column, (T), 20: 38193(R) (INDEC-SR-7, pp 3.5-13)
electron density from microwave scattering, (E), 20: 38254
electron density in shock tube, design of microwave probe for determining, 20: 38305
electron density of transient, design and performance of two-channel photoelectric device for measuring, 20: 37063
electron distribution function for collision-dominated, 20: 38198 (LA-DC-8099)
electron energy levels in, theory of, 20: 37474
electron paramagnetic resonance in h-f magnetic fields, (E), 20: 38220
energy levels of, forbidden transitions in, 20: 37432
equilibrium of homogeneous, in uniform magnetic fields, (T), 20: 38343
flow modes in electric shock tubes, (E), 20: 38345
flow of solar, neutral hydrogen flux in, 20: 38298
flow of, Langmuir probe measurements of hypersonic, 20: 38261
hydromagnetic equations for collisionless, viscous, 20: 38244
hydromagnetic wave damping in collisionless, (E), 20: 38272
hydromagnetic wave propagation in anisotropic, modes for, (T), 20: 38333
interactions with ion beams, instabilities associated with, 20: 38346
ion cyclotron frequency harmonic generation in longitudinally magnetized argon, (E), 20: 38252
ion cyclotron heating in Heliotron-B, 20: 38258
ion wave propagation in weakly ionized, damping and phase velocity of, (E), 20: 38294
ion-acoustic wave, propagation and damping in, (E), 20: 38283
ionization effects in sodium–potassium seeded argon, nonequilibrium, 20: 37722(R) (N-65-30843)
ionization level of intergalactic hydrogen, (E), 20: 38218
ionization properties of potassium–sodium seeded argon, (E), 20: 38195(R) (INDEC-SR-7, pp 3.60-73)
kinetic equation for, (T), 20: 38255
kinetic temperature of intergalactic hydrogen, (E), 20: 38218
kinetic theory for, review of, 20: 38207 (PPL-AF-1)
kinetics of, book on, 20: 38348
kinetics of, short-range forces in, 20: 38212
laser beam scattering on thermal density fluctuations in, review of, 20: 38336
microwave degenerate mode coupling by magnetized, in circularly cylindrical cavity, (T), 20: 38332
microwave scattering with space-charge waves from magneto-, (E), 20: 38202 (NP-16236)
motion in stationary magnetic field, steady-state and three-dimensional, (T), 20: 38312
motion in toroidal octupole fields, equipotential surfaces of, 20: 38192 (COO-1233-32)
oscillations in bounded electron, eigenfrequencies for, (T), 20: 38245
oscillations in confined cylindrical, with hot electron current, (T), 20: 38196 (JINR-P-2783-2)
oscillations in cold, sharply bounded, properties of, 20: 38301
oscillations in hot, stability of flute, (E), 20: 38262
oscillations in low-pressure mercury discharge, electron excitation of uhf, (E), 20: 38215
oscillations in low-pressure mercury discharge, electron excitation of uhf, (E), 20: 38216
oscillations in magneto-, theory for, 20: 38200 (NP-16206)
oscillations in mercury low-pressure discharge, electron-beam excitation of uhf, 20: 38214
oscillations in, energy density of, (T), 20: 38285
oscillations in, quasi-linear approximation for turbulent, 20: 38282
oscillations of beam, in h-f electric fields, 20: 38263
particle injection into mirror-quadrupole cusp well, high-energy neutral, (T), 20: 38277
particle interactions in thermal, Saha equation for ionization energy for, 20: 38222
particle interactions in quantum Vlasov, effective, (T), 20: 38286
particle losses from, research on anomalous, (E), 20: 38320
pinch in cylindrical, separated from field by thin surface, (T), 20: 38347
power flow in waveguides filled with, (T), 20: 38239
production and containment of, process for, 20: 38337(P)
production and properties from electric discharges in hydrogen beams, 20: 38247
production and properties of shock-heated, in electromagnetic shock tubes, 20: 38344
production and purification of, apparatus for, 20: 38339(P)
production of high-density, generator for, 20: 38340(P)
production of hot-electron, in magnetic mirror traps, 20: 38211(T) (AEC-tr-6782)
production of large volume steady-state, modification of Penning discharge for, 20: 38308
radiation from, equipment development for analyzing uv, 20: 38335
radiative processes in, statistical theory of, 20: 38217
relaxation in, non-Markovian processes in theory for, 20: 38251
resonance in, sheath effects on, (T), 20: 38342
sheath formation between confining field and, (T), 20: 38347
sheath of, heat transmission in Langmuir, (T), 20: 38191 (CLM-R-61)
shock structure of solar wind, 20: 37387
shock-wave patterns in wedge flow, (T), 20: 38242
spectra from laser-produced, extreme uv, (E), 20: 38300
spectra of high-temperature, bibliography on, 20: 38204 (NP-16240)
stability and pumpout in magnetic wells, (T), 20: 38266
stability criteria for, 20: 38304
stability effect of radial density distribution of helical, (E), 20: 38270
stability in cesium discharge and thermal, low-frequency, (E), 20: 38319
stability in electron-cyclotron, (E), 20: 38274
stability in magnetic mirror machines, flute, (E/T), 20: 38323
stability in magnetic mirror machines, (E/T), 20: 38324
stability in positive column, initial, (T), 20: 38331
stability in r-f discharges, (T), 20: 38317
stability of cylindrical, in longitudinal magnetic fields, 20: 38311(T)
stability of discharge produced, research on, (E), 20: 38321
stability of focused beams of, in absorbing media, 20: 38315
stability of hydrogen, effect of impurity ions on drift, 20: 38296
stability of magnetoactive, collision effects on, (T), 20: 38253

stability of magneto-, loss-cone distribution functions for, 20: 38290
stability of positive column, helical, (E/T), 20: 38318
stability of toroidal, in model c stellarator, (E), 20: 38268
stability of weakly turbulent electron-ion, (T), 20: 38269
stability of, effects of ion temperature anisotropies on high-β pitch-angle, (T), 20: 38295
stability of, modes associated with hose and mirror, (E), 20: 38272
stability of, research on, (E/T), 20: 38317
stability of, research on, 20: 38325
stability under gravitational fields, ballooning interchange, (T), 20: 38267
stability, dispersion relation for electrostatic, 20: 38273
temperatures in argon, spectroscopic measurement of, 20: 38279
turbulence in, many-body theory for, 20: 38209 (PPL-AF-5)
use in microwave detector, 20: 37119
velocity profile of flows of, measurement using laser beam, 20: 38238
wave propagation in compressible inhomogeneous, coupled electro-acoustic and electromagnetic, (T), 20: 38227
wave propagation in hot inhomogeneous media, (T), 20: 38284

PLASMA JETS
chemical reactions in, kinetics and thermodynamics of, 20: 38314
design of x-band cyclotron-resonance, 20: 38235

PLASTICS
plastic–wood, radioinduced polymerization, 20: 37145

PLATINUM
determination in solutions, colorimetric, 20: 36725
plutonium determination on plates of, by alpha counting, 20: 36736
yields from radiolysis of platinum phthalocyanine, 20: 36886

PLATINUM ALLOYS
Al–Pt, superconductivity of Al_2Pt, 20: 37985
Pt–Sn, superconductivity of PtSn, 20: 37985

PLATINUM ISOTOPES Pt-184
energy level transitions in isomeric, (E), 20: 38027

PLOWSHARE PROJECT
cloud formation in Pre-Schooner II cratering event, 20: 36958 (PNE-511)
Dugout experiment on measurement of surface motion, 20: 36959 (PNE-603F)
heavy element production in Barbel and Par events, 20: 38093
nuclear explosion uses for excavation, 20: 36972
nuclear explosion uses for rock breaking, 20: 36974
nuclear explosions for increasing natural gas production, Gasbuggy, 20: 36973
nuclear explosions for leaching and mining in, 20: 36975
radiological surveillance of Sulky Event, 20: 36960 (PNE-717F)
seismic data from PALANQUIN event, 20: 37010 (AD-631340)

PLUTONIUM
combustion of, properties of aerosols produced in, 20: 37022 (LA-DC-6942)
cost as fuel, comparison with fossil fuels, 20: 38541
determination in solutions using gamma absorption, 20: 36767
determination of, standards for, 20: 36727
determination of, using Arsenazo III, photometric, 20: 36778
determination of, in irradiated fuels by mass spectrometry, 20: 36783
preparation and purification of, 20: 36952
production and refining of, 20: 37206
separation from dicesium plutonium hexachloride by slurry–ion exchange methods, effects of cesium on, 20: 36727
separation from irradiated fuels by fluid-bed volatility processes, 20: 36926 (K-L-6091)
separation from irradiated fuels by molten-salt fluoride volatility process, 20: 36951
separation from nitric acid solution by solvent extraction using TBP, 20: 36928
separation from plutonium–uranium fuels by solvent extraction using amines, 20: 36948
sorption by Dowex 1–X4, mechanism of, 20: 36947
use as reactor fuel, economics and potential for, 20: 38483
vapor pressure of, effusion method for measuring, 20: 37307 (LA-3509)

PLUTONIUM ALLOYS
Ce–Co–Mn–Pu, analysis for cerium and manganese by ion exchange separation and potentiometric titration, 20: 36713 (LA-3402)
Ce–Co–Pu, analysis for cerium by ion exchange separation and potentiometric titration, 20: 36713 (LA-3402)
Ce–Co–Pu, combustion of properties of aerosols produced in, 20: 37022 (LA-DC-6942)
fissium–Pu–U, development as fast reactor fuel, 20: 38465 (ANL-7120, pp 289-300)
Hg–Pu, crystal structure of intermetallic compound Pu_5Hg_{21} in, 20: 37244
Mo–Pu–U, development for SEFOR fuels, 20: 38531 (GEAP-5133)
Pu–Ti–U, development as fast reactor fuel, 20: 38465 (ANL-7120, pp 289-300)
Pu–Ti–U, melting temperatures of, 20: 38465 (ANL-7120, pp 289-300)
Pu–Ti–U, use as fuel in 1000-Mw(e) fast breeder reactor, 20: 38494 (ANL-7120, pp 94-103)
Pu–U, separation of plutonium from, by solvent extraction using amines, 20: 36948
Pu–U, use as fuel in power breeder reactors, 20: 38476 (ANL-7120, pp 751-8)
Pu–U–Zr, development as fast reactor fuel, 20: 38465 (ANL-7120, pp 289-300)
Pu–U–Zr, melting temperatures of, 20: 38465 (ANL-7120, pp 289-300)

PLUTONIUM CARBIDES
PuC–UC, compatibility with stainless steel, effects of modifying additions on, 20: 38466 (ANL-7120, pp 301-13)
PuC–UC, fabrication and properties as fast reactor fuel, 20: 38467 (ANL-7120, pp 314-27)
PuC–UC, optimization studies of, for use as fast breeder reactor fuel, 20: 38495 (ANL-7120, pp 104-23)

PLUTONIUM(VI) FLUORIDES
separation from uranium hexafluorides, 20: 36950
volatility, 20: 36951

PLUTONIUM IONS
distribution coefficients of, between nitric acid and tributyl phosphate at 20 to 30°C, 20: 36928
spectra of, effects of chemical bonding and transitions on, 20: 36845

PLUTONIUM ISOTOPES
abundance ratio in irradiated fuels, 20: 36783

PLUTONIUM ISOTOPES Pu-237
excretion in rats, effects of citrate on, 20: 37025(R) (PG-Report-705)

PLUTONIUM ISOTOPES Pu-238
nuclear strength parameter correlation with beta bands in, (T), 20: 38180

PLUTONIUM ISOTOPES Pu-239
abundance ratio to uranium-238 in irradiated fuels, 20: 36783
energy level transitions in, N subshell conversion ratios for very low-lying, (T), 20: 38182
meson (μ^-) capture by, lifetime of, (E), 20: 38114
neutron Doppler effect of, in ZPR-3 fast assemblies, (E/T), 20: 38427 (ANL-7120, pp 603-9)
production in natural uranium fuel, determination by gamma spectroscopy, 20: 37287

PLUTONIUM ISOTOPES Pu-240
effects on reactivity of large steam-cooled fast power reactors, 20: 38438 (ANL-7120, pp 815-25)
nuclear strength parameter correlation with beta bands in, (T), 20: 38180

PLUTONIUM NITRATES
analysis of, for fluoride using green CaF band spectrum, method for, 20: 36730
denitration of polymer sols of, by baking, 20: 36786 (ORNL-TM-1558)

PLUTONIUM(IV) NITRATES
activity coefficient of, effects of ionic strength on, 20: 36928

PLUTONIUM NITRIDES
preparation from plutonium dioxide, 20: 37207
PuN–UN, fabrication of test fuel elements, 20: 37168(R) (BMI-1771)
PuN–UN, fabrication of test fuel elements of, 20: 37169(R) (BMI-1774)
PuN–UN, reactions with niobium-base alloys and stainless steel at high temperatures, 20: 37169(R) (BMI-1774)
PuN–W, criticality and burnup as fast reactor fuel, 20: 38442 (BNWL-283)

PLUTONIUM OXIDES
phase equilibria, 20: 38468 (ANL-7120, pp 389-91)
PuO_2–UO_2, movement within cladding in fast reactors, 20: 38473 (ANL-7120, pp 524-33)

PLUTONIUM(IV) OXIDES
production and properties of, 20: 37206
production of hypostoichiometric, method for, 20: 37181(P)
reactions with nitrogen to prepare plutonium nitride, effects of carbon on, 20: 37207
BeO–PuO_2–ThO_2, fabrication for gas-cooled reactor fuels, processes for, 20: 37168(R) (BMI-1771)
PuO_2–UO_2, fabrication of, economics of, 20: 36945
PuO_2–UO_2, processing of irradiated stainless steel-clad, 20: 36946
PuO_2–UO_2, separation of uranium from irradiated, 20: 36946
PuO_2–UO_2, stability of solid-solution, at high temperatures, 20: 37169(R) (BMI-1774)
PuO_2–UO_2, use as fuel in power breeder reactors, 20: 38476 (ANL-7120, pp 751-8)

PLUTONIUM SUBCRITICAL EXPERIMENT
development, Jan.–Mar. 1966, 20: 38443(R) (GEAP-5148)

POLARISCOPES
design for measurement of neutron polarization, 20: 38163

POLONIUM
determination on metal plates by alpha counting, 20: 36736
evaporation and deposition of, from fused lithium chloride–potassium chloride mixture, 20: 36736
separation from protactinium by solvent extraction using isoamyl alcohol,

20: 36940
POLONIUM ISOTOPES Po-210
content in drinking waters in Great Britain, 20: 37031
content in tobacco and tobacco smoke, 20: 37030
POLONIUM ISOTOPES Po-216
content in atmosphere, diurnal oscillations of, (T), 20: 37007
POLONIUM ISOTOPES Po-218
content in atmosphere, diurnal oscillations of, (T), 20: 37007
determination in air, method for, 20: 36733
POLYMERIZATION
radioinduced graft, in gas phase, method of, 20: 36908(P)
POLYMERS
preparation and properties of imidazopyrrolones, 20: 36846 (N-66-13499)
properties of inorganic, for high temperature uses, 20: 37179
POLYSACCHARIDES
analysis of, for sulfur-35, combustion method for, 20: 36721
POPULATIONS
radiation exposure to, significance of medical, 20: 36677
PORPHINE, $\alpha, \beta, \gamma, \delta$-TETRAPHENYL-
complexes with nickel, silver, and zinc, gamma radiolysis of, 20: 36889
POSITRONIUM
lifetime in ethane and argon–propane, (E), 20: 37816
lifetime in gamma-irradiated polyethylene and Teflon, dose dependence of, (E), 20: 36896
lifetime in metal oxides, (E), 20: 37819
magnetic moment of, 20: 37750
POSITRONS
annihilation in ammonia–lithium solutions, photon momentum distribution from, (E), 20: 37774
annihilation in ammonia–lithium solutions, photon momentum distribution from, (E), 20: 37818
annihilation in beryllium, electron band gap at boundary from, (E/T), 20: 38406
annihilation in gases, (E), 20: 37810
annihilation in germanium and silicon, electron momentum distribution from, 20: 37736 (COO-1297-7)
annihilation in metal oxides, gamma angular correlations from, (E), 20: 37819
annihilation in metals, review of, 20: 37820
annihilation in sodium, angular correlation of photons from, (E), 20: 37784
annihilation with core electrons in metals, momentum distributions for, (T), 20: 37821
gyromagnetic ratio of free, measurement of, 20: 37775
interactions with electrons, Bogoliubov canonical transformation for annihilation, 20: 37757
interactions with protons at 1200 Mev, cross sections for elastic, (E), 20: 37778
interactions with electrons, W meson production in, (T), 20: 37799
lifetime distribution in Teflon, correlation with angle between annihilation gamma rays, 20: 37737 (COO-1297-8)
lifetime in gamma-irradiated polyethylene and Teflon, dose dependence of slow component of, (E), 20: 36896
lifetimes in helium gas at low temperatures, (E), 20: 37817
mass of, in sodium, (T), 20: 37815
POTASSIUM
containment of plasmas of, field curvature effects on, (E/T), 20: 38326
determination in blood and hair of man, activation, 20: 36728
determination of, in biological material by neutron activation analysis, 20: 36735
determination of, in rocks by neutron activation analysis, 20: 36752
diffusion in Q-machines, (T), 20: 38203 (NP-16237)
diffusion of magnetoplasma of, in universal instability, 20: 38264
distribution in Evian quaternary formations, 20: 37012
effects on determination of chromium in ores by neutron activation analysis, 20: 36750
gamma activity of natural, specific, (E), 20: 38107
liquid, boiling under forced convection, 20: 38415
neutron absorption cross section in pitchblende, thermal, 20: 37994
neutron elastic scattering at 14 Mev, optical model analysis of, (T), 20: 38171
photoionization of atomic beams of, polarized electrons from, (E), 20: 37475
positron annihilation with core electrons in, momentum distributions for, (T), 20: 37821
stability of magnetic mirror confined, flute, (E/T), 20: 38323
POTASSIUM ACID ARSENATES
radiation effects on, ESR studies of x, 20: 36884
POTASSIUM BROMATES
radiolysis of, gamma, neutron, and lithium-6 fission product recoil, 20: 36899
POTASSIUM BROMIDES
radioinduced defects in, annealing of gamma, 20: 36901
$BaBr_2$–KBr, phase diagrams, 20: 36787 (YALE-2723(Vol.1))
$CaBr_2$–KBr, phase diagrams, 20: 36787 (YALE-2723(Vol.1))
$CdBr_2$–KBr, phase diagrams, 20: 36787 (YALE-2723(Vol.1))
CuBr–KBr, phase diagrams, 20: 36788 (YALE-2723(Vol.2))
KBr–AgBr, phase diagrams, 20: 36787 (YALE-2723(Vol.1))
KBr–KCl, phase diagrams, 20: 36788 (YALE-2723(Vol.2))
KBr–KF, phase diagrams, 20: 36788 (YALE-2723(Vol.2))
KBr–KI, phase diagrams, 20: 36788 (YALE-2723(Vol.2))
KBr–NaBr, phase diagrams, 20: 36788 (YALE-2723(Vol.2))
KBr–NaCl, phase diagrams, 20: 36788 (YALE-2723(Vol.2))
KBr–RbBr, phase diagrams, 20: 36788 (YALE-2723(Vol.2))
KBr–$SrBr_2$, phase diagrams, 20: 36788 (YALE-2723(Vol.2))
KBr–TlBr, phase diagrams, 20: 36788 (YALE-2723(Vol.2))
LiBr–KBr, phase diagrams, 20: 36788 (YALE-2723(Vol.2))
$MgBr_2$–KBr, phase diagrams, 20: 36788 (YALE-2723(Vol.2))
$PbBr_2$–KBr, phase diagrams, 20: 36788 (YALE-2723(Vol.2))
POTASSIUM CHLORIDES
radioinduced dichroism in R-bands of spectra of, gamma, 20: 36905
reactions of irradiated, with reducing mixture, preparation of sulfur-35-labeled sulfuric acid by, 20: 36920
$AlCl_3$–KCl, phase diagrams, 20: 36787 (YALE-2723(Vol.1))
$BaCl_2$–KCl, phase diagrams, 20: 36787 (YALE-2723(Vol.1))
$BiCl_3$–KCl, phase diagrams, 20: 36787 (YALE-2723(Vol.1))
$CaCl_2$–KCl, phase diagrams, 20: 36787 (YALE-2723(Vol.1))
$CdCl_2$–KCl, phase diagrams, 20: 36787 (YALE-2723(Vol.1))
CsCl–KCl, phase diagrams, 20: 36788 (YALE-2723(Vol.2))
CuCl–KCl, phase diagrams, 20: 36788 (YALE-2723(Vol.2))
$HgCl_2$–KCl, phase diagrams, 20: 36788 (YALE-2723(Vol.2))
KBr–KCl, phase diagrams, 20: 36788 (YALE-2723(Vol.2))
KCl–AgCl, phase diagrams, 20: 36787 (YALE-2723(Vol.1))
KCl–KF, phase diagrams, 20: 36788 (YALE-2723(Vol.2))
KCl–KI, phase diagrams, 20: 36788 (YALE-2723(Vol.2))
KCl–NaCl, phase diagrams, 20: 36788 (YALE-2723(Vol.2))
KCl–RbCl, phase diagrams, 20: 36788 (YALE-2723(Vol.2))
KCl–$SrCl_2$, phase diagrams, 20: 36788 (YALE-2723(Vol.2))
KCl–TlCl, phase diagrams, 20: 36788 (YALE-2723(Vol.2))
KCl–$ZnCl_3$, phase diagrams, 20: 36788 (YALE-2723(Vol.2))
LiCl–KCl, determination of polonium in, by evaporation and deposition on metal plates, 20: 36736
LiCl–KCl, phase diagrams, 20: 36788 (YALE-2723(Vol.2))
$MgCl_2$–KCl, phase diagram, 20: 36788 (YALE-2723(Vol.2))
$PbCl_2$–KCl, phase diagrams, 20: 36788 (YALE-2723(Vol.2))
$SbCl_3$–KCl, phase diagrams, 20: 36788 (YALE-2723(Vol.2))
POTASSIUM FERROCYANIDES
molecular motion of water in trihydrates of, neutron scattering studies of, 20: 36821
POTASSIUM FLUORIDES
AlF_3–KF, phase diagrams, 20: 36787 (YALE-2723(Vol.1))
BaF_2–KF, phase diagrams, 20: 36787 (YALE-2723(Vol.1))
BeF_2–KF, phase diagrams, 20: 36787 (YALE-2723(Vol.1))
CaF_2–KF, phase diagrams, 20: 36787 (YALE-2723(Vol.1))
KBr–KF, phase diagrams, 20: 36788 (YALE-2723(Vol.2))
KCl–KF, phase diagrams, 20: 36788 (YALE-2723(Vol.2))
KF–KI, phase diagrams, 20: 36788 (YALE-2723(Vol.2))
KF–NaF, phase diagrams, 20: 36788 (YALE-2723(Vol.2))
KF–RbF, phase diagrams, 20: 36788 (YALE-2723(Vol.2))
KF–SrF_2, phase diagrams, 20: 36788 (YALE-2723(Vol.2))
KF–ZnF_2, phase diagrams, 20: 36788 (YALE-2723(Vol.2))
LiF–KF, phase diagrams, 20: 36788 (YALE-2723(Vol.2))
MgF_2–KF, phase diagrams, 20: 36788 (YALE-2723(Vol.2))
PbF_2–KF, phase diagrams, 20: 36788 (YALE-2723(Vol.2))
POTASSIUM HYDROXIDES
oxidizing effects on molybdenum, passivation mechanisms in, 20: 37184
POTASSIUM IODIDES
AlI_3–KI, phase diagrams, 20: 36787 (YALE-2723(Vol.1))
CdI_2–KI, phase diagrams, 20: 36788 (YALE-2723(Vol.2))
HgI_2–KI, phase diagrams, 20: 36788 (YALE-2723(Vol.2))
KBr–KI, phase diagrams, 20: 36788 (YALE-2723(Vol.2))
KCl–KI, phase diagrams, 20: 36788 (YALE-2723(Vol.2))
KF–KI, phase diagrams, 20: 36788 (YALE-2723(Vol.2))
KI–AgBr, phase diagrams, 20: 36787 (YALE-2723(Vol.1))
KI–AgI, phase diagrams, 20: 36787 (YALE-2723(Vol. 1))
KI–NaI, phase diagrams, 20: 36788 (YALE-2723(Vol.2))
KI–TlI, phase diagrams, 20: 36788 (YALE-2723(Vol.2))
MgI_2–KI, phase diagrams, 20: 36788 (YALE-2723(Vol.2))
POTASSIUM ISOTOPES K-40
content in Antarctic rocks, 20: 37015
content in Scottish rocks, 20: 37016
distribution in Evian quaternary formation, 20: 37012
energy level structure, (E), 20: 38028
POTASSIUM ISOTOPES K-42
beta decay of, resonance states of calcium-42 from, (E), 20: 38085

POTASSIUM ISOTOPES K-47
energy levels and ground-state mass, (E), 20: 38063
POTASSIUM SILICATES
content of, in sediments of Bay of Roquebrune, 20: 36553
POTATOES
radiation effects on sprouting of, economics of, 20: 37157
radiation effects on starch in, effects of water content on gamma, 20: 36599
POWDER COMPACTS
density and properties of submicron tungsten, 20: 37200
POWDER METALLURGY
method for production of porous tungsten, 20: 37199
properties of copper–tungsten composites, 20: 37246
POWDERS
preparation of high-purity rare earth and transition-metal oxide, methods for, 20: 36851
reactions of boron carbide–tantalum, at 1200 to 1700°C in vacuum, 20: 36809
x-ray absorption analysis of, instrument for automatic continuous, 20: 37152
POWER BREEDER REACTORS
accidents in fast, energy release and mechanical effects in maximum, (T), 20: 38434 (ANL-7120, pp 654-70)
boiling in core of, voids due to transient, 20: 38440 (ANL-7120, pp 881-9)
calculations concerning, effects of group-constant uncertainties on, 20: 38420 (ANL-7120, pp 423-33)
coolant void coefficients for, extrapolation from critical assembly measurements, 20: 38425 (ANL-7120, pp 585-97)
cooling of fast, by steam at 1200 psi, 20: 38496 (ANL-7120, pp 136-40)
core design and fuel cycle for 1000-Mw(e) metal-fueled fast, 20: 38494 (ANL-7120, pp 94-103)
design and safety of large fast, panel discussion on, 20: 38457 (ANL-7120, pp 261-85)
design and safety of 1000-Mw(e) fast, 20: 38497 (ANL-7120, pp 157-61)
design and safety of 1375-Mw(e) sodium-cooled carbide-fuel modular, 20: 38456 (ANL-7120, pp 205-29)
economic and safety aspects of vented-fuel sodium-cooled, 20: 38475 (ANL-7120, pp 540-8)
excursions in, equation of state for calculations on, 20: 38435 (ANL-7120, pp 686-91)
explosion containment in single-tank, model tests of, 20: 38458 (ANL-7120, pp 692-719)
explosion containment in, model tests of, 20: 38459 (ANL-7120, pp 720-33)
fission-product retention by sodium in vented-fuel-element, 20: 38477 (ANL-7120, pp 855-61)
fuel movement within cladding in, mixed oxide, 20: 38473 (ANL-7120, pp 524-33)
fuel optimization studies for 1000-Mw(e) fast, plutonium–uranium carbide, 20: 38495 (ANL-7120, pp 104-23)
fuels for fast, development of carbide, 20: 38466 (ANL-7120, pp 301-13)
fuels for fast, mixed plutonium–uranium-238 and uranium-233–thorium, 20: 38476 (ANL-7120, pp 751-8)
fuels for, development of metallic, 20: 38465 (ANL-7120, pp 289-300)
fuels for, development of carbide, 20: 38467 (ANL-7120, pp 314-27)
neutron Doppler coefficient calculations for, comparison of methods, 20: 38421 (ANL-7120, pp 440-8)
neutron Doppler effect calculations for, effect of collision density fluctuations on, 20: 38422 (ANL-7120, pp 449-61)
neutron Doppler effect calculations for, comparison of methods, 20: 38423 (ANL-7120, pp 462-77)
neutron Doppler effect in ZPR-3 mockup of, (E/T), 20: 38427 (ANL-7120, pp 603-9)
neutron Doppler effect for uranium-235 in, 20: 38429 (ANL-7120, pp 614-15)
neutron flux distribution in, analysis of transient, 20: 38431 (ANL-7120, pp 625-31)
neutronics calculations for 1000-Mw(e) metal-fueled fast, 20: 38493 (ANL-7120, pp 85-93)
physics parameter study of large steam-cooled fast, 20: 38438 (ANL-7120, pp 815-25)
physics parameters of 1000-Mw(e) fast ceramic, calculation of, 20: 38491 (ANL-7120, pp 24-32)
power monitoring in large, selection of points for, 20: 38432 (ANL-7120, pp 632-5)
reactivity sodium void coefficients for, comparison of calculated and experimental, 20: 38419 (ANL-7120, pp 421-2)
safety characteristics of sodium-cooled coupled fast, 20: 38437 (ANL-7120, pp 789-93)
safety of gas- and steam-cooled, during flooding, 20: 38439 (ANL-7120, pp 826-36)
safety of, relation of fuel properties to, 20: 38424 (ANL-7120, pp 497-503)
safety research program of EURATOM-CEA in fast, 20: 38492 (ANL-7120, pp 54-66)
temperature distribution in fuels, calculation of transient, 20: 38470 (ANL-7120, pp 478-85)
POWER CYCLES
efficiency of nuclear power plants using gas turbines, 20: 38513
POWER REACTORS
conference on safety, fuels, and core design in large fast, 20: 38489 (ANL-7120)
containment structure design for Belgian, Italian, Japanese, Spanish, and Swiss, 20: 38522
design and construction of KSTR, 20: 38534(R) (NP-16168(Pt.B))
design of advanced gas-cooled, 20: 38514
design, economics, and safety of 1000-Mw(e) sodium-cooled fast, 20: 38498 (ANL-7120, pp 185-204)
development and research of KSTR, 20: 38533(R) (NP-16168(Pt.A))
development in Soviet Union, economic aspects of, 20: 38512
development of heavy water, 20: 38517
development of high temperature gas-cooled, 20: 38523
economic and safety aspects of vented-fuel sodium-cooled fast, 20: 38475 (ANL-7120, pp 540-8)
economics and prospects of, 20: 38487 (AECL-2584)
economics of large-scale dual-purpose, 20: 38524
economics of, comparison with fossil-fuel and hydro plants, 20: 38511
fuel development for, evaluation of plutonium, 20: 38483
instrumentation and control systems, development of unified digital system for, 20: 38508 (NYO-2764-2)
power production by, effects of hypostoichiometric oxide fuels on, 20: 37181(P)
thermal efficiency of gas–steam cycle in MHD-coupled, 20: 38488 (AERE-R-5031)
POWER SUPPLIES
development of isotopic, 20: 37142
PRASEODYMIUM
determination in hydrochloric acid solutions, spectrographic carrier-distillation, 20: 36729
effects on crystal structure of cobalt, iron, and nickel intermetallic compounds, 20: 37243
energy levels of, ionization energies from, (T), 20: 37439
neutron absorption cross section in pitchblende, thermal, 20: 37994
neutron total cross sections at high energies, fluctuations in, 20: 38173
separation from hydrochloric acid solutions by solvent extraction using dialkyl alkylphosphonates, 20: 36941
x-ray spectra from mu-mesic atoms of, (E), 20: 38058
yields from radiolysis of praseodymium phthalocyanine, 20: 36886
PRASEODYMIUM ALLOYS
Co–Pr, crystal structure of intermetallic compounds in, 20: 37243
Fe–Pr, crystal structure of intermetallic compounds in, 20: 37243
Ge–Pr, crystal structure and magnetic properties, 20: 38369
La–Pr, superconducting transition temperature of, pressure dependence of, 20: 37965
Ni–Pr, crystal structure of intermetallic compounds in, 20: 37243
PRASEODYMIUM CARBIDES
properties at 20 to 1300°C, 20: 36811
PRASEODYMIUM CHLORIDES
reactions with isopropylamine, thermogravimetric study of, 20: 36853
PRASEODYMIUM CHROMITES
phase studies, 20: 36812
spectra of, infrared, 20: 36807
PRASEODYMIUM COMPLEXES
with tartaric acid and trihydroxyglutaric acid, stability constants for, 20: 36838
PRASEODYMIUM ETHYL SULFATES
electron paramagnetic resonance and spin-bath relaxation times of crystals of, at 1.4 to 4.2°K, 20: 36855
PRASEODYMIUM IONS
spectra of, effects of chemical bonding and transitions on, 20: 36845
PRASEODYMIUM ISOTOPES Pr-141
gamma reactions (γ,n), (γ,2n), and (γ,3n) from threshold to 33 Mev, cross sections, (E), 20: 38094
PRASEODYMIUM ISOTOPES Pr-143
energy levels of, half life of second-excited, (E), 20: 38031
PRASEODYMIUM ISOTOPES Pr-144
dispersion from fallout in seawater, 20: 37037
PRASEODYMIUM LACTATES
formation constant of, potentiometric determination of, 20: 36824
PRECIPITATION, ATMOSPHERIC
decontamination of ground-air layer radioactivity by, 20: 37005
PRESSURE
effects on thermal conductivity of hydrogen, 20: 36991
production by contained explosions, in sodium and water, 20: 38459

(ANL-7120, pp 720-33)
PRESSURE VESSELS
containment shell design for Belgian, Italian, Japanese, Spanish, and Swiss power reactors, 20: 38522
containment shells, design of prestressed concrete for gas cooled reactors, 20: 38514
development of prestressed concrete, 20: 38523
radiation effects on steels for, neutron, 20: 37286
radiation effects on reactor, neutron, 20: 37289
PRESSURIZED WATER REACTORS
containment structure designs of foreign, 20: 38522
fuel element surface heat flux in, 20: 38519
heat transfer and fluid flow characteristics of, mixing effects between parallel channels, 20: 38503(R) (EURAEC-1663)
heat transfer and fluid flow characteristics of, mixing effects between parallel channels, 20: 38504(R) (EURAEC-1664)
heat transfer and fluid flow characteristics of, mixing effects between parallel channels, 20: 38505(T) (EURAEC-1672)
PRINCETON SYNCHROTRON
magnet current regulators for, design of, 20: 37338
PROCESS HEAT REACTORS
economics of, for sea water desalination, 20: 38524
PRODUCTION REACTORS
containers for shipping uranium fuel cores for, fire resistant tests of wood, 20: 37024 (NLCO-899)
PROLINE
metabolism in rat skin collagen, isotopic dilution method for studying, 20: 36562
PROLINE, HYDROXY-
metabolism in rat skin collagen, isotopic dilution method for studying, 20: 36562
PROMETHIUM
content in African pitchblende, estimation of induced fission vs spontaneous fission from, 20: 37994
energy levels of, ionization energies from, (T), 20: 37439
neutron absorption cross section in pitchblende, thermal, 20: 37994
separation from radioactive waste solutions, 20: 38538
separation of, from other lanthanides by ion exchange using ammonium lactate, mechanism of, 20: 36939
PROMETHIUM IONS
spectra of, effects of chemical bonding and transitions on, 20: 36845
PROMETHIUM ISOTOPES Pm-147
use as beta source for x-ray spectroscopic analysis, 20: 36765
use in x-ray sources, 20: 36915 (N-66-17678)
PROMETHIUM OXALATES
crystal structure of monoclinic decahydrate of, 20: 36835
PROPANE
properties for proportional detectors, 20: 37092
Ar–propane, postronium lifetime in, (E), 20: 37816
Co_2–propane, properties for proportional detectors, 20: 37092
O–propane, properties for proportional detectors, 20: 37092
1,3-PROPANEDIONE, 1,3-DIPHENYL-
complexes with rare earths, spectrofluorometric analysis for rare earths in, 20: 36722
2-PROPANOL
effects on copper determination by absorption spectroscopy, 20: 36726
1-PROPANOL, 2,3-DIMERCAPTO-
effects on mercury-203 excretion in rats, 20: 37025(R) (PG-Report-705)
2-PROPANOL, 2-METHYL-
dehydration of, isotopic exchange studies of, 20: 36849
tritium exchange of C–H bond of, with tritiated water, effects of perchloric acid on, 20: 36849
PROPELLANTS
detonation at high altitudes in booster rocket aborts, analysis of, (T), 20: 36996(R) (SC-CR-66-2045)
PROPENE, 2-METHYL- POLYMERS
heptane–polyisobutylene, use in polymer degradation dosimeter, 20: 37117
PROPIONAMIDE, PENTAFLUORO-
radiation effects on, ESR studies of gamma, 20: 36872
PROPORTIONAL DETECTORS
development, for detection of alpha particles, 20: 37025(R) (PG-Report-705)
development, for use in carbon-14 dating, 20: 37025(R) (PG-Report-705)
performance of propane-filled, 20: 37092
use in precision long counters for determining neutron flux density, 20: 37069 (BNWL-260)
PROPULSION
feasibility of nuclear, for manned interplanetary landing mission, 20: 36999
of interstellar vehicles by x-ray laser beam, (T), 20: 36997
PROTACTINIUM
determination of, using Arsenazo III, photometric, 20: 36778
separation from metals by solvent extraction using isoamyl alcohol, 20: 36940
separation from neutron-irradiated biological materials by ion exchange, 20: 36762
separation from thorium nitrate solutions, 20: 36946
separation of trace amounts of, from molten fluoride breeder blankets, 20: 36927 (ORNL-TM-1543)
PROTACTINIUM CHLORIDES
preparation and absorption spectra of, 20: 36798
PROTACTINIUM ISOTOPES Pa-231
separation from metals by solvent extraction using isoamyl alcohol, 20: 36940
PROTEINS
effects of radiation sickness on renewal intensity and specific radioactivities of muscle and serum, in rabbits, 20: 36600
radiation effects on uptake of carbon-14-labeled acetate by muscle and serum, in rabbits, 20: 36574
radiation effects on blood plasma, in Hiroshima bomb survivors, cancer patients, and personnel, 20: 36581
radiation effects on rat, effects of serum lyophilization and tumors on whole-body x, 20: 36582
radiation effects on *Vicia faba*, cytophotometric measurements on, 20: 36588
radioinduced hydration of blood serum, α and x, 20: 36579
synthesis of, control mechanisms for, 20: 36555(R) (NYO-2643-22)
PROTON BEAMS
scattering by aluminum surfaces, feasibility of scanning by, 20: 38376
PROTONS
angular and energy distributions from photon reactions (γ,p) with calcium-40 at 28 and 60 Mev, (E), 20: 38024
binding energy in sulfur-32 from (e,e'p) reactions, (E), 20: 38016
decay of, high energy fragments from baryon nonconserving, 20: 37734 (COO-818-87)
density in ionosphere, determination by analysis of proton whistlers, (T), 20: 37885
effects on CaF_2 crystals at 15 Mev, (E), 20: 38372
effects on cesium iodides, defect luminescence from, (E), 20: 38401
effects on gallium phosphides, defect determination from hyperfine ESR structure from, (E), 20: 38399
energy and intensity of, in outer Van Allen belt, (E), 20: 37905
energy spectra of solar co-rotating, 20: 37371
flux from solar flares, tables for 1954–1964, 20: 37886
flux in solar plasma flow, 20: 38298
flux in Van Allen belts, effects of critical, (T), 20: 37910
flux of geomagnetically trapped at 0.5 to 10^5 kev, near earth, (E), 20: 37902
gyromagnetic ratio, (E), 20: 37777
interaction with mesons ($K^\pm$) and ($\pi^\pm$) at high energies, elastic, (E/T), 20: 37796
interactions with mesons (K^-) at 4.6 and 5.0 Bev/c, f^* production in, 20: 37730 (BNL-10459)
interactions with mesons (π^-) at 6 Bev/c, $\pi\pi$ resonance production in, (E), 20: 37731 (BNL-10460)
interactions with mesons ($\pi^\pm$) at 6 Bev/c, resonance production in, 20: 37732 (BNL-10461)
interactions with mesons ($\pi^\pm$) at 6 Bev/c, K^* (1425) production in, (E), 20: 37733 (BNL-10462)
interactions with antineutrinos, detection of, 20: 37735(R) (COO-818-96)
interactions with mesons (π^-) above 4 Bev, Regge shrinkage in, (T), 20: 37742 (UCRL-16293)
interactions with protons at 0.33 to 6.15 Bev, polarization parameter in, (E), 20: 37743 (UCRL-16866)
interactions with mesons (π^+) at 900 Mev, N^* (1236) and N^* (1518) production in, (E), 20: 37744 (UR-875-151)
interactions with mesons (π^+) at 900 Mev, cross sections for, (E), 20: 37744 (UR-875-151)
interactions with neutrons in nuclei, short-range, (T), 20: 38056
interactions with protons at 1.4 to 3.0 Mev, differential cross sections for, (E), 20: 38081
interactions with meson (μ^-) in 2s-1d nuclei, (T), 20: 38166
interactions with neutrons at 600 Mev, cross sections for mesons (π^-) production in, (E), 20: 38186
interactions with protons at 600 Mev, cross sections for meson (π^+) production in, 20: 38186
interactions with neutrons at 630 Mev, phase shift analysis and triple scattering parameters of, (E), 20: 37739 (JINR-E-2726)
interactions with protons at 12 Bev/c, cross sections for elastic, (E), 20: 37747
interactions with neutrons at 12 Bev/c, angular distributions for, (E), 20: 37747
interactions with photons at 400 to 600 Mev, N^* (1410) production from, (E), 20: 37752
interactions with meson (K), hyperon (Λ) and (Σ) production from,

20: 37756
interactions with photons at 1.6 to 6.0 Bev, meson (ρ^0) production cross sections for, 20: 37766
interactions with protons, kinematic enhancement of resonance production in, 20: 37769
interactions with elementary particles, kinematic enhancement of resonance production in, 20: 37769
interactions with mesons (π^+) at 8 Bev/c, cross sections for strange particle production in, (E), 20: 37770
interactions with mesons (π^-) at 12 Bev/c, production of charged bosons (1929), (2195), and (2382) in, (E), 20: 37771
interactions with photons, SU(3) amplitudes for meson production in, (E/T), 20: 37773
interactions with electrons and positrons at 1200 Mev, cross sections for elastic, (E), 20: 37778
interactions with mesons (π) at 35 and 39 Mev, charge exchange in, (T), 20: 37785
interactions with antiprotons and protons at high energies, elastic, (E/T), 20: 37796
interactions with gamma radiation at 214 and 249 Mev, angular distributions from elastic, (E), 20: 37800
interactions with protons at 655 Mev, meson (π) production in, (E/T), 20: 37802
interactions with electrons, mesons (π^+) form factors from, (E), 20: 37812
interactions with neutrons, amplitudes for Regge pole exchange model of, 20: 37862
magnetic moment in atomic hydrogen, determination of g-factor from, (E), 20: 37777
magnetic shielding constant in hydrogen and water, 20: 37777
pairing correlations with neutrons in spherical even nuclei, 20: 38177
propagation of solar, review of, 20: 37493
reactions (p,α) with carbon-12 at 11.6 Mev, differential cross sections for, (E), 20: 38051
reactions (p,d) with beryllium-9 at 40.8 Mev, excitation of single-particle beryllium-8 energy levels in, (E), 20: 38067
reactions (p,d) with helium-3, angular correlations in, (E), 20: 38129
reactions (p,γ) with silicon-29, phosphorus-30 energy levels from, (E), 20: 38062
reactions (p,γ) with sulfur-34 at 1.214 Mev, chlorine-35 energy-level quantum numbers and transitions from, (E), 20: 38071
reactions (p,γ) with sulfur-36 at 0.80 to 1.80 Mev, chlorine-37 energy levels from, (E), 20: 38185
reactions (p,nf) with uranium-238 at 7.1, 9.4, and 12.0 Mev, mass distribution of fission products from, 20: 37995
reactions (p,n) with argon-40 and chlorine-37, Q-values for, (E), 20: 38028
reactions (p,n) with chromium-53, manganese-53 energy levels from, (E), 20: 38034
reactions (p,n) with carbon-13 at 3.237 to 3.85 Mev, angular distribution and excitation function for, (E), 20: 38042
reactions (p,n) with nuclei, threshold energies for, (E), 20: 38053
reactions (p,n) with aluminum-27, carbon-13, nickel-58, and nickel-60, threshold energies for, (E), 20: 38054
reactions (p,n) with boron-10, threshold for, (E), 20: 38069
reactions (p,n) with boron-11 and carbon-13, calculations using finite-range distorted-wave Born approximation, (T), 20: 38112
reactions (p,2n) with nuclei, gamma transitions in ground state rotational bands from, 20: 38008(R) (AECL-2595)
reactions with aluminum at 600 Mev, cross sections for meson ($\pi^\pm$) production in, (E), 20: 38186
reactions with aluminum and copper single crystals at 70 to 100 kev, characteristic x ray emission from, 20: 38393
reactions with barium-132, barium-136, and barium-137 at 20 Mev, production of isomeric lanthanum-131 and lanthanum-136 in, (E), 20: 38125
reactions with beryllium at 600 Mev, cross sections for meson ($\pi^\pm$) production in, (E), 20: 38186
reactions with carbon at 600 Mev, cross sections for meson ($\pi^\pm$) production in, (E), 20: 38186
reactions with copper-63, formation and decay of zinc-64 in, 20: 38152
reactions with copper at 600 Mev, cross sections for meson ($\pi^\pm$) production in, (E), 20: 38186
reactions with elements at 100 Mev, total cross sections for, (E), 20: 38018
reactions with hydrogen atoms at 2 to 117 kev, electron transfer in, (E), 20: 37446
reactions with hydrogen atoms, cross sections for charge transfer and ionization in, (T), 20: 37454
reactions with hydrogen atoms, total cross sections for charge transfer and ionization in, (T), 20: 37455
reactions with hydrogen atoms, cross sections for ionization in, (T), 20: 37456
reactions with lead and uranium at 3 and 28 Bev, product yields with A = 100 to 117, (E), 20: 38098
reactions with lead at 600 Mev, cross sections for meson ($\pi^\pm$) production in, (E), 20: 38166
reactions with molecular nitrogen, rotational energy level distributions from, 20: 37471
reactions with nickel-62 at 20 to 50 Mev, copper-63 compound nucleus formation in, (E), 20: 38147
reactions with nitrogen-15, 3$^-$ continuum states of oxygen-16 from, (T), 20: 38102
reactions with silver at 600 Mev, cross sections for meson ($\pi^\pm$) production in, (E), 20: 38186
scattering by calcium, lead-208, nickel-58, and nickel-60 at 49 Mev, angular distribution of polarization in elastic, (E), 20: 38049
scattering by carbon-12 at 4.7 to 12.8 Mev, excitation functions for elastic and inelastic, (E), 20: 38050
scattering by carbon-12 at 2.4 to 11.6 Mev, differential cross sections for elastic, (E), 20: 38051
scattering by helium and oxygen at 1 Bev, differential cross sections for elastic, (E), 20: 38010 (BNL-10438)
scattering by nickel-58 at 9.10 to 9.55 Mev, spins of levels from inelastic, (E), 20: 38181
scattering by samarium-144 at 10.0 to 10.4 Mev, polarization in elastic, (E), 20: 38068
scattering by silicon-30 at 1 to 2 Mev, differential elastic cross section for, (E), 20: 38105
scattering by strontium-88 at 4.9 to 7.5 Mev, isobaric analog states of strontium-89 in, (E/T), 20: 38076
scattering of, by aluminum at 6.6 Mev, analysis of aluminum using inelastic, 20: 36732
transmission in perfect crystals, anomalous, (T), 20: 38387

PROTOZOA
radiation effects on survival of *Tetrahymena pyriformis*, ultraviolet and x, 20: 36661

PSEUDOUREA, 2-(2-AMINOETHYL)-2-THIO-
effects on quenching of radioluminescence in dioxane liquid scintillator, 20: 36663(T)
effects on radiation injuries in rats, mechanism of, 20: 36670
protection against radiation injuries, possible mechanism of, 20: 36663(T)

PTERIDINE, 2,4,7-TRIAMINO-6-PHENYL-
preparation of carbon-14- or tritium-labeled, method for, 20: 36922

PUERTO RICO POWER REACTOR
cost and performance data on, project completion report, 20: 38510 (ORO-649)
superheater design for, effect of two-pass flow in, 20: 38509 (ORNL-TM-1449)

PULSE ANALYZERS
design for amplitude-spectrum analysis by sections, 20: 37044

PULSE GENERATORS (ELECTRONICS)
design and performance of nanosecond, 20: 37049

PURINES
reactions with hydroxyl radicals, ESR spectral studies on, 20: 36806

6-PURINETHIOL
effects on rat offspring, 20: 36643

PYRIMIDINE
radiation effects on dimers of, in *Micrococcus radiodurans* DNA, repair mechanism in uv, 20: 36610

PYRIMIDINES
reactions with hydroxyl radicals, ESR spectral studies on, 20: 36806

PYROCATECHOL
formation by radiolysis of aqueous benzene, 20: 36881

PYROCHLORES
flotation of, on gamma-irradiated anionic collector agents, 20: 36893

PYROGALLOL
effects on radioinduced polymerization of allyl alcohol, 20: 36880

PYROXENES
oxygen-16/-18 ratio in, 20: 37013

Q

QUANTUM ELECTRODYNAMICS
electromagnetic fields in Landau gauge in, covariant quantization of, 20: 37925
theory for, formalism for space-time, 20: 37922

QUANTUM MECHANICS
book: *Quantum Mechanics*, 20: 37933(T)
density matrix in, two-particle, 20: 37829
description of nuclear collective motion using variational method, (T), 20: 38108
eigenfunctions for spherical and deformed Saxon-Woods potentials, 20: 38078
many body problem in, hierarchy for Klimontovich equation for, 20: 38209 (PPL-AF-5)

regularity conditions in relativistic, (T), 20: 37931
Schroedinger equation in, nonlinear transformation of, 20: 37926
statistical theory of optical rotation in, 20: 37927
theory of unitary matrix ensembles, 20: 38033
wave equation in complex angular momentum plane, Jost solutions of Schroedinger, (T), 20: 37836
wave propagation through potential barriers in, analysis of, 20: 37929
Wigner distribution functions in relativistic, 20: 37930
QUARTZ
acoustic wave propagation at low temperatures and above 1 Bc in crystalline, x-ray alignment technique for, 20: 38366
analysis for components of, by scattering of accelerated alpha particles, 20: 36719
oxygen-16/-18 ratios in, from iron formations in Quebec, 20: 37013
radioinduced luminescence of fused, pulsed-electron, 20: 36864
QUEBEC
rocks in, oxygen-16/-18 ratios in, 20: 37013
QUINOLINE, 7-CHLORO-4-[[4-(DIETHYLAMINO)-1-METHYLBUTYL] AMINO]-
binding to melanin in uv-irradiated mice, 20: 36564
8-QUINOLINOL
analytical use for separation of cerium, ruthenium, uranium, and zirconium by ion exchange, 20: 36754
solvent properties for copper, 20: 36726

R

RABBITS
effects of radiation sickness on renewal intensity and specific radioactivities of muscle and serum proteins in, 20: 36600
radiation effects on delayed hypersensitivity in, x, 20: 36655
radiation effects on eyes of, laser, 20: 36682
radiation effects on uptake of carbon-14-labeled acetate by muscle and serum proteins in, 20: 36574
radiation effects on content and metabolism of phosphoproteins in denerved and intact muscles in, x, 20: 36602
uptake of iodine-131 and mercury-203-labeled compounds by tumors in, in oxygen environment, 20: 36576
RADIATION
dose to women from iodine-131, effects of thyroid function on, 20: 36675
doses from rocket reactor operation, hazards analysis, 20: 38525(R) (NUS-208)
dosimetry of, properties of carbonates, thoria, and barium titanate for, 20: 36913
dosimetry of, review of principles of, 20: 37081
effects of high-energy, on inorganic substances, symposium on, 20: 36897
effects on blood cells in man, protective effects of bone marrow transplants against whole-body, 20: 36669
effects on blood plasma proteins in Hiroshima bomb survivors, cancer patients, and personnel, 20: 36581
effects on brain function in animals and man, dose effects in, 20: 36651
effects on chlorophyll mutation frequency in barley, effects of partial reparation on, 20: 36622
effects on creep of graphite, temperature effects on, 20: 37223
effects on cytokinetics and regulation of progenitor cells in bone marrow, methods for assaying, 20: 36594
effects on grain growth and melting of substoichiometric uranium oxides, 20: 38468 (ANL-7120, pp 389-91)
effects on hyperlipemia development in animals, mechanism of, 20: 36580
effects on inorganic crystals, electron spin resonance spectra of radicals from, 20: 36902
effects on leukemia development in humans in Hiroshima and Nagasaki, 1946 to 1964, 20: 36645
effects on leukemia incidence, life span, and mutation induction in mice and rats, review on low-dose, 20: 36652
effects on niobium-stabilized stainless steel, in-reactor, 20: 37284
effects on polymerization of allyl alcohol, role of solvents, inhibitors, and oxygen in, 20: 36880
effects on rats, mechanism of effects of AET on, 20: 36670
effects on solids, model for change in elastic modulus from, 20: 37296
effects on thymine metabolism in man, 20: 37025(R) (PG-Report-705)
effects on uptake of carbon-14-labeled acetate by muscle and serum proteins in rabbits, 20: 36574
effects on yeast cells, kinetic regularities in regeneration of, 20: 36642
evolution of fields of, measurement method of time, 20: 37311
production and uses of, Technical Progress Review on, Spring 1966, 20: 37136
production of transitional, from charged particle interactions with films, (E), 20: 37434
quality factors near high-energy accelerators, (E), 20: 37323
use in crosslinking polycarbonates, 20: 36907(P)
uses of, review of industrial, 20: 37140
uses of, review of trends in industrial, 20: 37142
RADIATION CHEMISTRY
radiolysis of hydrochloric acid–stannous chloride solutions, gamma, 20: 36911
RADIATION DETECTION INSTRUMENTS
calibration of photoelectric nucleus counter, pressure effects on, 20: 37094
counting rate of cosmic neutron monitor, meteorological effects on, 20: 37100
data from cosmic meson monitor, meteorological corrections for, 20: 37101
design and performance of, for detecting cosmic nucleon interactions above 10^{13} ev, 20: 37657
design and performance of multidirectional meson telescope, 20: 37095
design and performance for cosmic ray detection, 20: 37103
design and performance of neutrino detector, 20: 37104
design for ionizing particles, 20: 37080
design of installation for detecting cosmic particle interactions with matter at high energies, 20: 37684
design of, for measuring strontium-85, -89, and -90 metabolism in live mice, 20: 36556
development of portable, for monitoring alpha, beta, gamma, and neutron activity, 20: 37071 (DP-993)
performance of array of, for measuring gamma angular correlations, 20: 38184
performance of cosmic neutron monitor, barometric pressure effects on, 20: 37096
performance of cosmic neutron monitor, barometric coefficient effects on, 20: 37097
performance of cosmic neutron monitor, multiplicity effects on, 20: 37098
performance of mobile cosmic neutron monitor, altitude effects on, 20: 37099
performance of spark calorimeter for cosmic meson (μ) detection, 20: 37694
use in industry, conference on, 20: 37139 (STI-PUB-112(Vol.1))
RADIATION DETECTION INSTRUMENTS (PULSE TYPE)
design and performance of, for measuring alpha disintegration rate, 20: 37082
design of neutron, using gas scintillator, 20: 37127
design of, using plastic scintillator for measuring tritium beta radiation at surfaces, 20: 37087
recording system for, design of magnetic tape, 20: 37083
use in counting carbon-14 and tritium, external alpha or gamma source for automatic corrections in, 20: 36743
RADIATION DETECTORS
design for ionizing particles, 20: 37080
RADIATION INJURIES
diagnosis of cerebral, using gamma encephalography, 20: 36696
protection against, by AET, possible mechanism of, 20: 36663(T)
protection against, role of adrenal and pituitary glands in, 20: 36668
recovery from, in *Hymenolepis microstoma*, 20: 36662
repair of DNA, mechanisms for, 20: 36578 (ORNL-P-2240)
RADIATION MONITORING
equipment for alpha and gamma, in air, 20: 36960 (PNE-717F)
evaluation of importance of cesium-137, for meat and meat products, 20: 37039
program for, in Alaska, 20: 37042
RADIATION PROTECTION
design and physical properties of dosimeter for measurements, 20: 36680
guides, 20: 37042
legal control of patient, possibilities of, 20: 36679
measures used for, in radiobiological work at University of Munich, Germany, 20: 37040
Provisions of German Atomic Law for, 20: 36676
research in, 20: 36691
RADIATION SICKNESS
anatomy and pathology of, in pigs, 20: 36657
effects on bone marrow transplants on, in man, 20: 36669
effects on dogs, nerve trunk regeneration in relation to phase of, 20: 36614
effects on renewal intensity and specific radioactivities of muscle and serum proteins in rabbits, 20: 36600
RADIATION SOURCES
development of industrial gages using radioisotope, 20: 37149
use in industry, conference on, 20: 37139 (STI-PUB-112(Vol.1))
use of radioisotope, in industrial instruments in Soviet Union, 20: 37147
use of radioisotope, in industrial instruments, 20: 37148
use of unsealed, contamination hazards from medical, 20: 36678
RADIATION TARGETS
development of polarized, 20: 37332
preparation of chlorine-36 and sulfur-33, for production of phosphorus-33 by neutron irradiation, (E), 20: 37166
RADIO RECEIVERS

performance of, for air shower detection, 20: 37102
RADIO WAVES
absorption in magnetosphere at conjugate points, cosmic noise, 20: 37914
emission from EAS, mechanisms for, (T), 20: 37625
emission of galactic, correlations with primary cosmic electron origin, 20: 37496
emission of pulsed, from EAS at 10^{16} to 10^{17} ev, (E), 20: 37626
emission of vlf, conjugate point phenomena, 20: 37914
RADIOACTIVE CONTAMINATION
measurements in environment of IRT-1000 Reactor, 20: 38535
RADIOACTIVE MATERIALS
heat content of alpha-active pyrophoric, design of isothermal drop calorimeter for measuring, 20: 37055
RADIOACTIVE WATERS
analysis of drinking water supplies in Great Britain for radium, radon, and its decay products, 20: 37031
RADIOACTIVITY
determination of natural, in ground waters of New Hampshire and Maine, 20: 37006
measurement of distribution of, from thoron decay products, on aerosols, 20: 37027
RADIOAPPLICATORS
design of remote control Cathetron for cobalt-60 treatment of uterine cancer, 20: 36687
RADIOBIOLOGY
book: *Yearbook of Nuclear Medicine*, Vol. I, 1966, 20: 36690
LET determination of electrons for use in, 20: 36689
RADIOCHEMICAL PROCESSING PLANTS
design and operation of, for fuel element reprocessing, 20: 36949
RADIOCHEMISTRY
book: *The Radiochemical Manual*. Second Edition, 20: 36924
book: *Yearbook of Nuclear Medicine*, Vol. I, 1966, 20: 36690
RADIODIAGNOSIS
doctors in, responsibility of, 20: 36709
equipment for dental and medical, Alaska program for control of, 20: 37042
hazards of, significance of genetic, 20: 36677
method for, of growth activity of bone metastases, 20: 36701
research in, 20: 36691
RADIOGRAPHY
iridium-192 uses in, 20: 36994
radioisotope uses in, 20: 37142
RADIOISOTOPES
book: *The Radiochemical Manual*. Second Edition, 20: 36924
determination in solutions by least-squares resolution of gamma spectra, 20: 36780
distribution in water in closed vessels, 20: 36711
half lives of, chart of energy function of, 20: 36739
production and uses of, review of, 20: 37137
use in geophysics, conference on, 20: 37133 (STI-PUB-112(Vol.2))
use in industrial instruments in Soviet Union, 20: 37147
use in industrial instruments, review of, 20: 37148
use in industrial gages, development of, 20: 37149
use in industry, conference on, 20: 37139 (STI-PUB-112(Vol.1))
use in instruments and radiation sources for x-ray fluorescence analysis, 20: 37150
use in underwater beacons, 20: 37158(P)
use of unsealed, contamination hazards from medical, 20: 36678
uses in geophysics and industry, review of, 20: 37143
uses of, review of trends in industrial, 20: 37142
RADIOMETERS
calibration of, design of thermal neutron source for, 20: 37073 (NP-16201)
calibration of, use of neutron sources for, 20: 37074 (NP-16202)
calibration of, use of neutron sources for, 20: 37075 (NP-16204)
design for rocket nozzle temperature measurement, 20: 38528
RADIOMETRIC ANALYSIS
method for solutions containing fast-decaying isotopes by least-squares resolution of gamma spectra, 20: 36780
method for, of tritium-labeled biological material, 20: 36763
RADIOOPAQUE AGENTS
effects of iodated, on thyroid function, 20: 36571
effects of iodine-containing, on endocrine function and iodide uptake in human thyroid, 20: 36572
RADIOPROTECTIVE COMPOUNDS
AET mechanisms of action on cell structure, 20: 36663(T)
preparation of *Bacillus subtilis* injectant for use as, 20: 36673
RADIOSENSITIVITY
mechanisms for, effects of experimental conditions and genetic differences in plant seed, 20: 36658
of *Paramecium aurelia*, effects of division stage on, 20: 36661
RADIOSTERILIZATION
effects of, on sugar cane leafhoppers, 20: 37146
RADIOTHERAPY
development of cerebral damage from, use of gamma encephalography for detecting, 20: 36696
developments in, of brain tumors, 20: 36693
doctors in, responsibility of, 20: 36709
dose distribution in, use of electronic computers for studying, 20: 3668
dose distribution in deep, of malignant tumors, 20: 36702
effects of whole-body, low-dose, on cancerous metastases, 20: 36698
effects on blood plasma proteins in man, 20: 36581
effects on brain tumors, 20: 36694
effects on face, jaw bone, and teeth in children, 20: 36708
effects on injuries and morphological changes in brain tumors, 20: 3669
effects on metastases development, gamma and x, 20: 36697
effects on radiofibroses development in lung tissue after, of bronchial carcinomas, 20: 36703
effects on tumor cell kinetics, use of tritiated-thymidine for studying, 20: 36704
electron, material for adaptation of irradiation field in, 20: 36700
equipment for intracavitary and short-distance gamma beam, 20: 36680
equipment for, design of cesium telecurie, 20: 36710
hazards of, significance of genetic, 20: 36677
isodose curves in telecobalt, use of dose gradient lines for determining, 20: 36688
LET determination of electrons for use in, 20: 36689
problems in radium, of carcinoma of uterine cervix, 20: 36699
research in, 20: 36691
use of lasers in eye, 20: 36682
use of low-dose, for children, 20: 36707
use of radioiodine localization as indication for, of thyroid, 20: 36706
use of tritium-labeled nitrogen mustard gas derivatives for, of inoperable tumors, 20: 36705
use of, for brain tumors, operability limits as indication for, 20: 36692
RADIUM
content in drinking waters in Great Britain, 20: 37031
therapy of carcinoma of uterine cervix, dose distribution in, 20: 36699
RADIUM ISOTOPES Ra-220
measurement of radioactivity of decay products from, on aerosols, 20: 37027
RADIUM ISOTOPES Ra-226
content in Maine and New Hampshire ground waters, 20: 37006
deuteron fission at 12 Mev, energy distribution of fission fragments from, (E), 20: 38132
RADON
content in drinking waters in Great Britain, 20: 37031
RADON ISOTOPES Rn-220
content in atmosphere, diurnal oscillations of, (T), 20: 37007
RADON ISOTOPES Rn-222
content in atmosphere, diurnal oscillations of, (T), 20: 37007
content in Maine and New Hampshire ground waters, 20: 37006
RAIN WATER
analysis for strontium-90 and other radioisotopes using ion exchange, gamma spectrometric, 20: 36759
collection for strontium-90 analyses, method for, 20: 36759
decontamination apparatus for, 20: 37029
washout coefficients for stack disposal of iodine-131 vapor, 20: 37033
RARE EARTH ALLOYS
Co–rare earth, crystal structure of intermetallic compounds in, 20: 3724
Co–rare earths, magnetic properties of $LnCo_2$ series, 20: 37279
Fe–rare earth, crystal structure of intermetallic compounds in, 20: 3724
Ni–rare earth, crystal structure of intermetallic compounds in, 20: 3724
Ni–rare earths, magnetic properties of $LnNi_2$ series, 20: 37279
RARE EARTH CHROMITES
spectra of, infrared, 20: 36807
RARE EARTH COMPLEXES
with diketones, spectrofluorometric analysis for, 20: 36722
with tartaric acid and trihydroxyglutaric acid, stability constants for, 20: 36838
RARE EARTH COMPOUNDS
electronic shielding in, recoilless gamma absorption studies of, 20: 37461
RARE EARTH HALIDES
radiation effects on optical properties of, 20: 37280 (NYO-3330-11)
RARE EARTH IONS
spectra of, effects of chemical bonding and transitions on, 20: 36845
RARE EARTH OXIDES
determination in presence of alkaline earth oxides using Arsenazo, complexometric, 20: 36776
RARE EARTHS
content in African pitchblende, estimation of induced fission vs spontaneous fission from, 20: 37994
determination of, using Arsenazo III, photometric, 20: 36778
effects of presence of all, on spectrographic determination of single elements, 20: 36729
effects on crystal structure of cobalt, iron, and nickel, 20: 37243

positron annihilation in, review of, 20: 37820
separation by ion exchange using ammonium lactate, mechanism of, 20: 36939
separation from nitric acid solution by solvent extraction using tributyl phosphate, effects of ammonium nitrates on, 20: 36938
separation from radioactive waste solutions, 20: 38538
RATE METERS
design of mixed radiation Rem responding, 20: 37068 (BNL-10321)
RATS
effects of calcium, strontium, and magnesium on the inotropic action of fluoride in muscle from, 20: 36567
effects of mercaptopurine on progeny of, 20: 36643
effects of radiation-processed fruits on, 20: 37156
effects of various histamine liberators on calcification produced by various metals in, 20: 36557
manganese-54 metabolism in, 20: 36554 (LA-DC-7305)
mercury-203 excretion in, effects of BAL on, 20: 37025(R) (PG-Report-705)
metabolism of carbon-14-labeled-Tween 20 in, 20: 36921
metabolism of hydroxyproline and proline in skin collagen in, isotopic dilution method for studying, 20: 36562
phosphatide content and composition in blood, 20: 36606(R) (NYO-1864-23)
plutonium-237 excretion in, effects of citrate on, 20: 37025(R) (PG-Report-705)
radiation dose to thyroid in, from iodine-125, -129, and -131, 20: 36561
radiation effects on proteins in, effects of serum lyophilization and tumors on whole-body x, 20: 36582
radiation effects on nicotinamide adenine dinucleotide content in thymocytes in, x, 20: 36590
radiation effects on properties of DNA in tissues in, whole-body x, 20: 36591
radiation effects on DNA synthesis in regenerating liver in, mechanism of x, 20: 36593
radiation effects on aminotransferase activities in central nervous system and skeletal muscle in, neutron, 20: 36601
radiation effects on methylation of guanidinacetic acid in liver in, x, 20: 36603
radiation effects on gastric emptying in, part-body x, 20: 36628
radiation effects on glycolysis and respiration in retina in, x, 20: 36630
radiation effects on histology of spleen of, during immune response, local x, 20: 36637
radiation effects on longevity of, fast-neutron, 20: 36640
radiation effects on progeny of, x, 20: 36643
radiation effects on leukemia incidence, life span, and mutation induction in, review on low-dose x, 20: 36652
radiation effects on, comparison of gamma and x, 20: 36654
radiation effects on phosphatide content in tissues of, 20: 36606(R) (NYO-1864-23)
radiation protection of, mechanism of AET on, 20: 36670
radiosensitivity of oocytes in, x, 20: 36632
strontium-90 excretion by, effects of citrate and salicylate treatment on, 20: 37025(R) (PG-Report-705)
strontium-90 transport from blood stream into gastrointestinal tract in, 20: 36558
REACTOR CONTROL ELEMENTS
effects of boron poison pins on reactivity, 20: 38441 (BAW-3492-1 (Suppl.1))
REACTOR CONTROL RODS
corrosion and mechanical properties of hafnium, effects of oxygen on, 20: 37170
drive mechanisms for, design and operation of Fermi Fast Breeder Reactor, 20: 38501 (APDA-301)
REACTOR CONTROL SYSTEMS
development of redundant autocontrol systems, 20: 38417
development of unified digital instrumentation for, 20: 38508 (NYO-2764-2)
development of, compatibility of poison solutions and structural materials, 20: 38447 (WCAP-2867)
REACTOR COOLANTS
boiling in fast reactor cores, voids due to transient, 20: 38440 (ANL-7120, pp 881-9)
critical heat flux variation in water at high pressure, 20: 38462 (GEAP-4929)
loss during accidents, high-pressure discharge mechanisms of, 20: 36990
REACTOR COOLING SYSTEMS
coolant flow and density in steam-generating, CUSH program for analysis of, 20: 38410 (AEEW-M-474)
coolant flow and heat transfer in, mixing effects between parallel channels, 20: 38503(R) (EURAEC-1663)
coolant flow and heat transfer in, mixing effects between parallel channels, 20: 38504(R) (EURAEC-1664)
coolant flow and heat transfer in, mixing effects between parallel channels, 20: 38505(R) (EURAEC-1672)
heat transfer in, high temperature gas loop measurements, 20: 38481
REACTOR FUEL ALLOYS
chemical processing and fabrication facility for Pu–Ti–U, 20: 38494 (ANL-7120, pp 94-103)
fabrication of aluminum–uranium base, 20: 38480(R) (EUR-2522.f)
neutronics calculations for fissium and low-capture, in fast power breeder reactors, 20: 38493 (ANL-7120, pp 85-93)
radioinduced swelling of, effects of impurities on, 20: 37302
refabrication cost estimating of, by remote control, 20: 37195 (ANL-6950)
REACTOR FUEL ELEMENTS
coating rupture on, pyrolytic carbon, 20: 36955(P)
coolant flow in FFTF cermet driver, hydraulic analysis of, 20: 38479 (BNWL-264)
design of, with flexible cladding, 20: 38485(P)
fabrication of ESSOR, 20: 38480(R) (EUR-2522.f)
fabrication of graphite, by extrusion, 20: 37196
fabrication of, economics of remote, 20: 36945
fabrication of, methods and standards for, 20: 37208
failure detection in vented-fuel sodium-cooled fast reactors, 20: 38475 (ANL-7120, pp 540-8)
failure detection in sodium-cooled fast reactors, 20: 38478 (ANL-7120, pp 862-7)
fission product gas release and sheath expansion in, effects of uranium dioxide density on, 20: 37254
fission-gas bubble distribution in post-irradiation annealed UO_2, electron microscopy studies on, 20: 37255
heat transfer and fluid dynamics of finned, 20: 38481
heat transfer from, limitations on external rates of, 20: 38484
heat transfer in fog cooled, dryout measurements of, 20: 38409 (AECL-2586)
neutron thermalization in plutonium-239 bearing synthetic, 20: 38455
processing of irradiated, using treated organic solvents, 20: 36943(P)
processing of irradiated, Technical Progress Review of, Spring, 1966, 20: 36944
processing of irradiated, economic aspects of, 20: 36945
processing of irradiated graphite-matrix, 20: 36946
processing of irradiated, by solvent extraction methods, 20: 36948
processing of irradiated, by compact pyrochemical methods, 20: 36952
processing of irradiated, evaluation of remote-control systems for, 20: 36953
processing of, plant and equipment design and operation for, 20: 36949
refabrication cost estimating of metallic, by remote control, 20: 37195 (ANL-6950)
separation of plutonium and uranium from irradiated, by fluid-bed volatility processes, 20: 36926 (K-L-6091)
separation of uranium from irradiated, carbon-clad, 20: 36956(P)
shipping container for spent, criticality analysis of, 20: 38486 (ACNP-66551)
temperature distribution in clad, calculation of transient, 20: 38471 (ANL-7120, pp 486-93)
testing in FARET, core design and irradiation program for, 20: 38460 (ANL-7120, pp 766-75)
thermal expansion and failure in reactors, TREAT studies of, 20: 38474 (ANL-7120, pp 534-9)
REACTOR FUEL ELEMENTS (CERAMIC)
design for fission gas accommodation, review of, 20: 38482
fabrication of thoria–urania, method for, 20: 37211
krypton and xenon release from, during reactor operations, 20: 37303
preparation of urania powders for, method for high-density, 20: 37212(P)
radiation effects on clad, 20: 37168(R) (BMI-1771)
radiation effects on clad, 20: 37169(R) (BMI-1774)
REACTOR FUEL ELEMENTS (DISPERSION)
fabrication for gas cooled reactors, processes for, 20: 37168(R) (BMI-1771)
REACTOR FUEL ELEMENTS (THERMOELECTRIC)
design, 20: 37720 (BMWF-FBK-66-06)
REACTOR FUEL PLATES
fabrication for AARR, 20: 37168(R) (BMI-1771)
fabrication for AARR, 20: 37169(R) (BMI-1774)
REACTOR FUEL SPHERES
development of pyrolytic carbon coated, 20: 38523
fabrication of thoria–urania, method for, 20: 37211
preparation for electron microscopic examination by replication, 20: 37173
REACTOR FUEL TUBES
fabrication of graphite, by extrusion, 20: 37196
REACTOR FUELS
analysis of, for plutonium and uranium, by mass spectrometry, 20: 36783
breeding ratios of carbide and nitride, research on, 20: 37168(R) (BMI-1771)

burnup characteristics of tungsten-cermet fuels in fast compact reactors, 20: 38442 (BNWL-283)
burnup of, determination by gamma intensity, 20: 37287
cladding for, development of, 20: 37169(R) (BMI-1774)
container for shipping, wood fire resistant tests, 20: 37024 (NLCO-899)
cost of, comparison with fossil-fuels, 20: 38541
cycle costs of, optimization flowsheets for, 20: 38416
decontamination of, for nuclear rockets, 20: 37034
development for SEFOR, 20: 38531 (GEAP-5133)
development of carbide, for fast breeder reactors, 20: 38466 (ANL-7120, pp 301-13)
development of carbide, for fast reactors, 20: 38467 (ANL-7120, pp 314-27)
development of metallic, for fast reactors, 20: 38465 (ANL-7120, pp 289-300)
development of plutonium, economics and potential for, 20: 38483
fission product diffusion from urania, mechanisms at 150 to 2000°C, 20: 37290
fission product diffusion from urania, at temperatures below 1500°C, 20: 37291
fission product diffusion from, methods of determining, 20: 37292
meltdown in large cores, parameters affecting, 20: 38472 (ANL-7120, pp 514-23)
movement following cladding failure in reactors, 20: 38474 (ANL-7120, pp 534-9)
movement of mixed oxide, within cladding in fast reactors, 20: 38473 (ANL-7120, pp 524-33)
optimization studies of plutonium–uranium carbide, for fast power breeder reactors, 20: 38495 (ANL-7120, pp 104-23)
performance of hypostoichiometric oxide, 20: 37181(P)
preparation of carbonitride and nitride, fluidization processes for, 20: 36850
properties of ceramic and cermet in relation to fast-reactor safety, 20: 38424 (ANL-7120, pp 497-503)
radiation effects on carbon-coated urania, 20: 37168(R) (BMI-1771)
radioinduced swelling of, mechanisms of, 20: 37299
testing of carbide and cermet, 20: 37174
use of mixed plutonium–uranium-238 and uranium-233–thorium as, in fast breeder reactors, 20: 38476 (ANL-7120, pp 751-8)

REACTOR MATERIALS
development for SEFOR, 20: 38531 (GEAP-5133)
properties at high pressures and temperatures, review, 20: 38433 (ANL-7120, pp 641-53)
radiation effects on steel, neutron, 20: 37286
testing of carbide and cermet, 20: 37174

REACTOR MATRICES
critical mass studies of heterogeneous arrays of cylindrical voids, 20: 38532 (NASA-TN-D-3555)

REACTOR SAFETY
accident analysis for fast power reactors, maximum, (T), 20: 38434 (ANL-7120, pp 654-70)
accident analysis for 1375-Mw(e) sodium-cooled modular fast reactor, 20: 38456 (ANL-7120, pp 205-29)
accident analysis for 1000-Mw(e) fast power reactor, 20: 38497 (ANL-7120, pp 157-61)
accident analysis for 1000-Mw(e) sodium-cooled fast reactor, 20: 38498 (ANL-7120, pp 185-204)
analysis for potassium-cooled fast reactors, 20: 38415
analysis of, for nuclear rocket ground testing, 20: 37034
conference on fast reactors, Argonne National Lab., Oct. 11–14, 1965, 20: 38489 (ANL-7120)
containment systems development for, 20: 38463 (IITRI-578P22-15)
containment systems development for, 20: 36978 (NAA-SR-12001)
criteria for large steam-cooled fast power reactors, 20: 38438 (ANL-7120, pp 815-25)
excursions in fast reactors, equation of state for calculations on, 20: 38435 (ANL-7120, pp 686-91)
explosion containment in single-tank fast reactors, model tests of, 20: 38458 (ANL-7120, pp 692-719)
explosion containment in fast, model tests of, 20: 38459 (ANL-7120, pp 720-33)
fuel properties in relation to, in fast reactors, 20: 38424 (ANL-7120, pp 497-503)
in coupled fast reactor having negative Doppler and sodium void reactivity effects, 20: 38437 (ANL-7120, pp 789-93)
loss-of-coolant and ramp-reactivity-insertion calculations for fast power breeder reactor, 20: 38493 (ANL-7120, pp 85-93)
neutronic coupling effects on, in modular fast reactors, 20: 38436 (ANL-7120, pp 776-88)
of large fast power reactors, panel discussion on, 20: 38457 (ANL-7120, pp 261-85)
poison effects on, during flooding of gas- and steam-cooled fast reactors, 20: 38439 (ANL-7120, pp 826-36)
radioactivity in coolant and cover gas of vented-fuel reactors, 20: 38477 (ANL-7120, pp 855-61)
research program of EURATOM-CEA on, 20: 38492 (ANL-7120, pp 54-66)
transient calculation method for prompt critical fast reactors, 20: 38413

REACTOR SAFETY EXPERIMENTS
meltdown studies in TREAT applied to reactor accident analysis, 20: 38472 (ANL-7120, pp 514-23)
meltdown studies in TREAT, review of recent, 20: 38474 (ANL-7120, pp 534-9)
reactivity changes in Spert-IV, kinetic response to, 20: 38449
temperature distribution in TREAT, calculation by finite transformation, 20: 38471 (ANL-7120, pp 486-93)

REACTOR SHIELDING
design and performance of SNAP-8, 20: 38527
design for MCR, secondary gamma production analysis, 20: 38506 (NDA-2143-7)
design for MCR, secondary gamma production analysis, 20: 38507 (NDA-Memo-2143-11)
gamma interactions in, charge build-up from, 20: 38529

REACTOR SLURRIES
radiation testing of thoria–urania aqueous suspension, 20: 38533(R) (NP-16168(Pt.A))

REACTOR TUBES
crack propagation in Zircaloy-2, detection and mechanisms of, 20: 37172
fabrication of aluminum–Zircaloy-4, by explosive welding, 20: 37168(R) (BMI-1771)
fabrication of aluminum–Zircaloy-4, by explosive welding, 20: 37169(R) (BMI-1774)

REACTORS
calculations concerning, comparison of, 20: 38490 (ANL-7120, pp 3-23)
containment structures for, design and evaluation, 20: 38463 (IITRI-578P22-15)
design of, steady-state-coupled fluid flow and heat conduction analysis, 20: 38461 (CONF-651110-29)
kinetics of, composed of two loosely coupled cores, 20: 38454
neutron density in reflected, pulsed two-region calculations, 20: 38453
neutron diffusion in, stationary and kinetic control rod analysis, 20: 38448
neutron flux distribution in high-power slab, 20: 38452
neutron flux distributions in, void effects on, 20: 38532 (NASA-TN-D-3555)
neutron resonance absorbers in, multigroup cross sections for, (T), 20: 38451
operation in space, charge build-up from Compton scattering, 20: 38529
power level fluctuations of steady-state operating, 20: 38445 (RT-FI-(66)1)
radiological safety analysis computer program, 20: 37167 (IDO-17151)
reactivity control in, effects of boron poison pins, 20: 38441 (BAW-3492-1(Suppl.1))
reactivity of reflected, two-region model analysis, 20: 38453
reactivity response and effective absorption cross sections in, 20: 38410
shutdown of, time optimal xenon, program for, 20: 38411 (BNWL-186)

RECOIL IONS
diffusion of, in radiolysis of phthalocyanines, 20: 36886

REDOX PROCESS
ion-exchange resin compatibility in, 20: 36954
waste from, separation of aluminum nitrate nonahydrate from acid, 20: 36925 (HW-82771(Pt.3))

REFRACTORY MATERIALS
coating of metallic, materials and processes for, 20: 37192
creep in ultrahigh vacuum, design and performance of apparatus for determining, 20: 37263
thermal diffusivity at high temperatures, transient measurement of, 20: 37722(R) (N-65-30843)

RELATIVITY THEORY
cosmological models in general, singularities in SO(3,R) homogeneous, 20: 37430
electromagnetic and gravitational fields in Minkowskian metric of, 20: 37923
field equations in general, source dynamics for asymptotically flat space solutions of, 20: 37932
gravitation theory in general, quadratic lagrangians in, 20: 37918
quaternion methods in special, spinor theory for, 20: 37924

REMOTE-CONTROL EQUIPMENT
development of, for use in fuel element reprocessing, 20: 36953

RESEARCH REACTORS
development of redundant autocontrol systems, 20: 38417
fuel element fabrication for ESSOR, 20: 38480(R) (EUR-2522.f)
kinetic behavior of UTR-10, 20: 38454
radiation fields near bare, effects on plant life, 20: 36609
radioactivity in environment of IRT-1000, 20: 38535
reactivity in WWR-S, effects of resonance neutrons on, 20: 38536

RESINS
effects on iodine-131-labeled triiodothyronine metabolism in human thyroid, 20: 36573
injection into rock, control of, using radiometric surface hygrometers, 20: 37134
RESPIRATION
radiation effects on, in guinea pig and rat retina, x, 20: 36630
RHENIUM
content in African pitchblende, estimation of induced fission vs spontaneous fission from, 20: 37994
deformation twinning in single-crystal, (E), 20: 37257
effects on crystal structure and properties of thoria-tungsten cermets, 20: 37185
ionization and work functions of, critical temperatures for, 20: 37277
neutron absorption cross section in pitchblende, thermal, 20: 37994
yields from radiolysis of rhenium phthalocyanine, 20: 36886
RHENIUM ALLOYS
Cr–Re, oxidation at high temperatures, mechanisms of, 20: 37186
Nb–Re–Zr, oxidation by oxygen at 1000°C, kinetics and microstructures of, 20: 37193
Re–Ta, faulting in, effects of cold working on, 20: 37217
Re–W, faulting in, effects of cold working on, 20: 37217
Re–W, ionization and work function of, critical temperatures for, 20: 37277
RHENIUM OXIDES
formation by oxidation of chromium–rhenium alloys, mechanisms of high-temperature, 20: 37186
Dy_2O_3–ReO_2, magnetic properties and structure of compounds formed in, 20: 36784(R) (AD-636054)
Er_2O_3–ReO_2, magnetic properties and structure of compounds formed in, 20: 36784(R) (AD-636054)
Gd_2O_3–ReO_2, magnetic properties and structure of compounds formed in, 20: 36784(R) (AD-636054)
Nd_2O_3–ReO_2, magnetic properties and structure of compounds formed in, 20: 36784(R) (AD-636054)
ReO_2–Sm_2O_3, magnetic properties and structure of compounds formed in, 20: 36784(R) (AD-636054)
ReO_2–Yb_2O_3, magnetic properties and structure of compounds formed in, 20: 36784(R) (AD-636054)
ReO_2–Y_2O_3, magnetic properties and structure of compounds formed in, 20: 36784(R) (AD-636054)
RHODIUM
preparation of standard solutions of, by electrolytic dissolution for activation analysis, 20: 36775
RHODIUM ISOTOPES Rh-98
isomer formation and decay, (E), 20: 38106
RHODIUM ISOTOPES Rh-101
beta decay of, ruthenium-101 energy levels from, (E), 20: 38091
RHODIUM ISOTOPES Rh-106
dispersion from fallout in seawater, 20: 37037
RIBONUCLEASE
radiation effects on structure of, gamma, 20: 36584
RIBONUCLEIC ACID
fractionation of, 20: 36555(R) (NYO-2643-22)
radiation effects on synthesis of, uv, 20: 36555(R) (NYO-2643-22)
synthesis of, effects of virus infection on, 20: 36555(R) (NYO-2643-22)
x-ray scattering by solutions of, low-angle, (T), 20: 36586(T)
RIBONUCLEIC ACID, DESOXY-
radiation effects on calf-thymus, protective effects of disulfides against x, 20: 36665
radiation effects on properties of, in rat thymus, 20: 36591
radiation effects on regenerating rat liver synthesis of, mechanism of x, 20: 36593
radiation effects on, detection by enzymatic hydrolysis, uv, 20: 36596
radiation effects on pyrimidine dimers in *Micrococcus radiodurans*, repair mechanism in uv, 20: 36610
radiation effects on breakdown of enzymes in *Micrococcus lysodeicticus*, uv, 20: 36583
radiation injury and repair mechanisms for, 20: 36578 (ORNL-P-2240)
RICE
radiation effects on, comparison of fast neutron and gamma, 20: 36649
ROCKET MOTOR NOZZLES
temperature measurement in, radiometer for, 20: 38528
ROCKET REACTORS
control of, feasibility of Chemical Poison Loop System, 20: 38447 (WCAP-2867)
destruct of, core particle velocity estimates, 20: 38525(R) (NUS-208)
power excursions in, development of transient codes, 20: 38525(R) (NUS-208)
testing of, environmental safety aspects of, 20: 38525(R) (NUS-208)
testing of, safety aspects of ground, 20: 37034
ROCKET REACTORS (KIWI)
simulation testing of, radiometer for temperature measurement in, 20: 38528
testing of B4E, effluent release from, 20: 38525(R) (NUS-208)
ROCKETS
abort at high altitudes, analysis of, (T), 20: 36996(R) (SC-CR-66-2045)
ROCKS
age of Scottish, 20: 37016
ages of Antarctic, estimation of, 20: 37015
analysis for iron in boreholes, activation, 20: 37019
analysis for uranium using Arsenazo III, photometric, 20: 36774
analysis of, for potassium by neutron activation methods, 20: 36752
analysis of, in boreholes, activation,, 20: 37018
breaking of, use of nuclear explosions for, 20: 36974
resin injection into, control of, using radiometric surface hygrometers, 20: 37134
RODS
boiling heat transfer measurements on multirod geometries, 20: 36986 (GEAP-5073)
water boiling in bundle of, critical, (T), 20: 36992
ROOTS
iodine-131 method for measurement of extension of tree, 20: 36560
ROTORS
analysis at critical speed, rotordynamic, 20: 36977 (NAA-SR-11944)
RUBIDIUM BROMATES
radiolysis of, gamma, neutron, and lithium-6 fission product recoil, 20: 36899
RUBIDIUM BROMIDES
KBr–RbBr, phase diagrams, 20: 36788 (YALE-2723(Vol.2))
LiBr–RbBr, phase diagrams, 20: 36788 (YALE-2723(Vol.2))
PbBr–RbCl, phase diagrams, 20: 36788 (YALE-2723(Vol.2))
RbBr–AgBr, phase diagrams, 20: 36787 (YALE-2723(Vol.1))
RbBr–NaBr, phase diagrams, 20: 36788 (YALE-2723(Vol.2))
RUBIDIUM CHLORIDES
$BaCl_2$–RbCl, phase diagrams, 20: 36787 (YALE-2723(Vol.1))
$CaCl_2$–RbCl, phase diagrams, 20: 36787 (YALE-2723(Vol.1))
$CdCl_2$–RbCl, phase diagrams, 20: 36787 (YALE-2723(Vol.1))
CsCl–RbCl, phase diagrams, 20: 36788 (YALE-2723(Vol.2))
CuCl–RbCl, phase diagrams, 20: 36788 (YALE-2723(Vol.2))
KCl–RbCl, phase diagrams, 20: 36788 (YALE-2723(Vol.2))
LiCl–RbCl, phase diagrams, 20: 36788 (YALE-2723(Vol.2))
$MgCl_2$–RbCl, phase diagrams, 20: 36788 (YALE-2723(Vol.2))
PbBr–RbCl, phase diagrams, 20: 36788 (YALE-2723(Vol.2))
$PbCl_2$–RbCl, phase diagrams, 20: 36788 (YALE-2723(Vol.2))
RbCl–AgCl, phase diagrams, 20: 36787 (YALE-2723(Vol.1))
RbCl–RbF, phase diagrams, 20: 36788 (YALE-2723(Vol.2))
RbCl–$SrCl_2$, phase diagrams, 20: 36788 (YALE-2723(Vol.2))
RbCl–TlCl, phase diagrams, 20: 36788 (YALE-2723(Vol.2))
RbCl–$ZnCl_2$, phase diagrams, 20: 36788 (YALE-2723(Vol.2))
RUBIDIUM FLUORIDES
BaF_2–RbF, phase diagrams, 20: 36787 (YALE-2723(Vol.1))
CaF_2–RbF, phase diagrams, 20: 36787 (YALE-2723(Vol.1))
KF–RbF, phase diagrams, 20: 36788 (YALE-2723(Vol.2))
LiF–RbF, phase diagrams, 20: 36788 (YALE-2723(Vol.2))
MgF_2–RbF, phase diagrams, 20: 36788 (YALE-2723(Vol.2))
RbCl–RbF, phase diagrams, 20: 36788 (YALE-2723(Vol.2))
RbF–NaF, phase diagrams, 20: 36788 (YALE-2723(Vol.2))
RbF–ZnF_2, phase diagrams, 20: 36788 (YALE-2723(Vol.2))
RUBIDIUM IODIDES
RbI–AgI, phase diagrams, 20: 36787 (YALE-2723(Vol.1))
RUBIDIUM ISOTOPES Rb-86
yields of, from proton fission of uranium-238 at 12 Mev, 20: 37995
RUBIDIUM ISOTOPES Rb-87
determination in Antarctic rocks for age estimation, 20: 37015
RUBIES
radiation effects on optical properties of, 20: 37280 (NYO-3330-11)
RUTHENIUM
content in African pitchblende, estimation of induced fission vs spontaneous fission from, 20: 37994
neutron absorption cross section in pitchblende, thermal, 20: 37994
separation from cerium, uranium, and zirconium by ion exchange using 8-quinolinol, 20: 36754
separation from irradiated fuel elements by solvent extraction using tertiary amines, 20: 36948
separation from radioactive waste solutions, 20: 38538
separation from waste solutions, efficiency of cellulose–bentonite flocculation for, 20: 36929
separation from water by foaming, 20: 36934
yields from radiolysis of ruthenium phthalocyanine, 20: 36886
RUTHENIUM FLUORIDES
thermodynamic properties, 20: 36950
RUTHENIUM ISOTOPES Ru-101
energy levels, (E), 20: 38091
RUTHENIUM ISOTOPES Ru-103
dispersion from fallout in seawater, 20: 37037

RUTHENIUM ISOTOPES Ru-105
yields from helium ion-induced fission of lead-207 at 41.1 to 26.3 Mev, 20: 37996
yields in proton fission of uranium-238 at 7.1, 9.4, and 12.0 Mev, 20: 37995
RUTHENIUM ISOTOPES Ru-106
dispersion from fallout in seawater, 20: 37037
RUTILES
electric conductivity of, symposium on, 20: 37179

S

SAFETY
book: *The Radiochemical Manual*. Second Edition, 20: 36924
SAFETY HAZARDS
evaluation of, from rocket reactor tests, 20: 38525(R) (NUS-208)
SALICYLALDEHYDE
complexes with cobalt, magnetic moments of, 20: 36823
complexes with iron, magnetic moments of, 20: 36823
complexes with iron, Moessbauer spectra of, at +23, −78, and −195°C, 20: 36823
complexes with nickel, magnetic moments of, 20: 36823
SALICYLIC ACID
effects on strontium-90 excretion in rats, 20: 37025(R) (PG-Report-705)
SALT DEPOSITS
nuclear explosion in Tatum, Salmon, 20: 36962
nuclear explosion in Tatum, calculations of free-field motion for Salmon, 20: 36963
nuclear explosions in, full and partial decoupling in, (T), 20: 36964
SAMARIUM
content in African pitchblende, estimation of induced fission vs spontaneous fission from, 20: 37994
determination in complexes with diketones, spectrofluorometric, 20: 36722
determination in hydrochloric acid solutions, spectrographic carrier-distillation, 20: 36729
effects on crystal structure of cobalt, iron, and nickel intermetallic compounds, 20: 37243
energy levels of, ionization energies from, (T), 20: 37439
neutron absorption cross section in pitchblende, thermal, 20: 37994
SAMARIUM ALLOYS
Co–Sm, crystal structure of intermetallic compounds in, 20: 37243
Fe–Sm, crystal structure of intermetallic compounds in, 20: 37243
Ge–Sm, crystal structure and magnetic properties, 20: 38369
Ni–Sm, crystal structure of intermetallic compounds in, 20: 37243
SAMARIUM CHLORIDES
reactions with isopropylamine, thermogravimetric study of, 20: 36853
SAMARIUM CHROMITES
phase studies, 20: 36812
spectra of, infrared, 20: 36807
SAMARIUM COMPLEXES
with diketones, spectrofluorometric analysis for, 20: 36722
with tartaric acid and trihydroxyglutaric acid, stability constants for, 20: 36838
SAMARIUM IONS
spectra of, effects of chemical bonding and transitions on, 20: 36845
SAMARIUM ISOTOPES Sm-144
proton elastic scattering at 10.0 to 10.4 Mev, proton polarization in, (E), 20: 38068
triton reactions (t,p) at 12 Mev, samarium-146 energy levels from, (E), 20: 38052
SAMARIUM ISOTOPES Sm-145
energy level at 0.90 Mev, spin of, (E), 20: 38068
SAMARIUM ISOTOPES Sm-146
energy levels of, spin and parity of, (E), 20: 38052
SAMARIUM ISOTOPES Sm-147
hyperfine structure and nuclear moments of, 20: 37459
neutron reactions (n,α) up to 200 ev, alpha decay of samarium-148 in, (E), 20: 38072
SAMARIUM ISOTOPES Sm-148
alpha decay of excited, (E), 20: 38072
triton reactions (t,p) at 12 Mev, samarium-150 energy levels from, (E), 20: 38052
SAMARIUM ISOTOPES Sm-149
hyperfine structure and nuclear moments of, 20: 37459
neutron reactions (n,α) up to 200 ev, alpha decay of samarium-150 in, (E), 20: 38072
SAMARIUM ISOTOPES Sm-150
alpha decay of excited, (E), 20: 38072
energy levels of, spin and parity of, (E), 20: 38052
triton reactions (t,p) at 12 Mev, samarium-152 energy levels from, (E), 20: 38052
SAMARIUM ISOTOPES Sm-152
energy levels of, spin and parity of, (E), 20: 38052
nuclear strength parameter correlation with beta bands in, (T), 20: 38180
triton reactions (t,p) at 12 Mev, samarium-154 energy levels from, (E), 20: 38052
SAMARIUM ISOTOPES Sm-153
yields in proton fission of uranium-238 at 7.1, 9.4, and 12.0 Mev, 20: 37995
SAMARIUM ISOTOPES Sm-154
electron tunneling in, quantum mechanical fluctuation effects on, 20: 38408
energy levels of, spin and parity of, (E), 20: 38052
energy levels of, properties of, 20: 38408
triton reactions (t,p) at 12 Mev, samarium-156 energy levels from, (E), 20: 38052
SAMARIUM ISOTOPES Sm-156
energy levels of, spin and parity of, (E), 20: 38052
SAMARIUM OXALATES
crystal structure of monoclinic decahydrate of, 20: 36835
SAMARIUM OXIDES
ReO_2–Sm_2O_3, magnetic properties and structure of compounds formed in, 20: 36784(R) (AD-636054)
Sm_2O_3–SiO_2, preparation, properties, and structure of $Sm_4(SiO_4)_3$ in, 20: 36784(R) (AD-636054)
SAND DOLLARS
carbon isotope variations in, 20: 36549
carbon isotopic variations in, environmental and genetic factors, 20: 36550
oxygen isotope variations in, 20: 36549
SAP (SINTERED ALUMINUM PRODUCTS)
fabrication for nuclear uses, 20: 37210
reactions with urania at 600°C, 20: 37203
SARCOMAS
radiotherapy of, low-dose x, 20: 36698
SCANDIUM
determination of, using Arsenazo III, photometric, 20: 36778
separation from hydrochloric acid solutions by solvent extraction using dialkyl alkylphosphonates, 20: 36941
SCANDIUM ISOTOPES Sc-42
energy levels of, shell-model potential parameters for low-lying, (T), 20: 38145
SCANDIUM ISOTOPES Sc-45
energy level at 12.4 kev, K-conversion coefficient for, (E), 20: 38087
SCANDIUM ISOTOPES Sc-49
energy levels and ground-state mass, (E), 20: 38063
SCANDIUM OXIDES
Fe_2O_3–MnO_x–Sc_2O_3, phase studies of solid solutions in, 20: 36839
SCANDIUM SILICIDES
preparation of, method for, 20: 37176
SCATTERING
angular correlations for E2 and E3 transitions in Coulomb excitation, (T), 20: 38032
density matrix for two-particle, 20: 37829
model for high-energy, modified single-particle exchange, 20: 37862
potential, approximation method for phase shifts in, 20: 37852
potential, Moller operators for singular, 20: 37831
S matrix for, U(12) symmetry and unitarity condition for, 20: 37855
S-matrix for quantum, structure of, 20: 37854
S-matrix in complex angular momentum plane, dispersion relations for, (T), 20: 37836
theory of diffraction, with excitation of collective nuclear states, 20: 38143
theory of high-energy, lectures on, 20: 37826 (NP-16231)
theory of inelastic diffraction, with excitation of collective nuclear states, 20: 38142
SCINTILLATION DETECTORS
construction of gas, for neutron counter, 20: 37127
design and performance of, based on medicinal paraffin, 20: 37112
development, for use as neutron dosimeters, 20: 37025(R) (PG-Report-705)
performance of liquid, 20: 37107
performance of, for measuring beta activity in tritiated surface films, 20: 36738
pulse-shape discrimination of, for cosmic ray studies, 20: 37111
standardization of liquid, method for external, 20: 37085
SCOTLAND
rocks in, estimation of ages of, 20: 37016
SCREENS
performance testing of sieve trays for GS heavy water process, 20: 37160 (DP-1025)
SEA URCHINS
carbon isotope variations in, 20: 36549
carbon isotopic variations in, environmental and genetic factors, 20: 36550

oxygen isotope variations in, 20: 36549
oxygen isotopic variations in, environmental and genetic factors, 20: 36550

SEA WATER
chemical composition of sediments of Bay of Roquebrune, 20: 36553
desalination of, economics of large-scale nuclear plants for, 20: 38524
fallout dispersion in, 20: 37037
level of Pleistocene, determination of, from fossil coral age, 20: 37014

SEDIMENTARY DEPOSITS
analysis for potassium by scintillation counting, 20: 37012

SEED
effects of diethyl pyrocarbonate on cells and growth of barley, 20: 36589
effects of free lipid fraction from irradiated seedling bean leaves on wheat, toxic, 20: 36598
radiation effects on chromosomes in barley, effects of diethyl pyrocarbonate on fast-neutron and gamma, 20: 36589
radiation effects in cotton species *Gossypium barbadense*, 20: 36623
radiosensitivity of *Lupinus angustifolius* L., effect of moisture content on γ, 20: 36646

SEEDLINGS
radiation effects on fatty acid content in free lipid fraction of leaves of bean, x, 20: 36598
survival of wheat, following gamma radiation, 20: 36650

SEISMIC WAVES
amplitude and travel-time spectra of, analysis of, for Salmon explosion, 20: 36968
amplitudes and travel times from Salmon explosion, 20: 36967
amplitudes for decoupled sources, first-zone P, 20: 36966
measurement in southern Mississippi, crustal structure determinations from, 20: 36965
propagation from Salmon explosion, 20: 36962
propagation from Salmon explosion, time dependence of, (T), 20: 36963

SEISMOLOGY
data from PALANQUIN underground explosion, 20: 37010 (AD-631340)

SELENIUM
effects on determination of iridium in ores by neutron activation analysis, 20: 36751

SELENIUM FLUORIDES
reactions with vanadium pentafluoride, 20: 36804

SEMICONDUCTOR DETECTORS
design and performance of, for use in 4π beta spectrometers, 20: 37125
performance of germanium, for measuring gamma angular correlations, 20: 38184
performance of silicon telescope, for charge and energy spectrometry of cosmic particles, 20: 37575
response of lithium-drifted germanium, for gamma rays, 20: 37126
timing circuits for, design of, 20: 38161
use of lithium-drifted germanium, in neutron capture gamma spectroscopy, 20: 37072 (KFK-429)

SEMICONDUCTORS
electron momentum distribution in germanium and silicon, positron annihilation method for determining, 20: 37736 (COO-1297-7)
properties of, transmuted center Fermi level spectroscopy, for determining, (T), 20: 38407
radiation effects on antimony–indium, gamma and neutron, 20: 37295

SEPARATION PROCESSES
development of aqueous, for irradiated fuels, review of, 20: 36947
for cerium purification, 20: 36936

SHALES
radioactive waste disposal in, by hydraulic fracturing, 20: 38538

SHEEP
radiation effects on Dische-positive material in blood and urine in, gamma, 20: 36604

SHELLS
stress distribution in heated spherical, theoretical analysis, 20: 36957 (DRI-2327)

SHIELDED CONTAINERS
spent fuel shipping cask criticality analysis, 20: 38486 (ACNP-66551)

SHIELDING
calculations, computer use for, 20: 38350 (ORNL-P-2310)
electronic, of rare earths, recoilless gamma absorption studies of, 20: 37161
method of, in waste disposal, 20: 38539(P)

SHIELDING MATERIALS
use of Plastilin for electron therapy discrimination, 20: 36700

SHIPPING
container for fuel cores, fire resistance tests of wood, 20: 37024 (NLCO-899)

SHIPPINGPORT ATOMIC POWER STATION, PENNA.
environs monitoring, 1965, 20: 37026 (PNRO-SMD-137)

SHOCK TUBES
development of electromagnetic, for high-temperature, dense plasma production, 20: 38335
electron density distribution in, microwave probing technique for measuring, 20: 38305
magnetohydrodynamic experiments in low-attenuation electromagnetic, 20: 37882
plasma flow modes in electric, (E), 20: 38345
plasmas in electromagnetic, production and properties of shock-heated, 20: 38344

SHOCK WAVES
equations of state in, 20: 38433 (ANL-7120, pp 641-53)
interactions with gases, effect of line radiation on precursor ionization in, 20: 37881
magnetohydrodynamic, in solar wind, 20: 37387
production from solar corona discharges, effects on cosmic activity, 20: 37486
propagation from Salmon explosion, 20: 36962
propagation from Salmon explosion, time dependence of, (T), 20: 36963
propagation in air, charged particle density and temperature in front of, 20: 37880

SILANE
tetramethyl-, radiolysis of solid, yields and mechanisms in, 20: 36883

SILICIDES
properties of, for high-temperature coatings, 20: 37192

SILICON
deposition on sintered molybdenum powder for oxidation protection, 20: 37204
determination in coal using neutron activation, system for continuous on-line, 20: 36769
determination in sputum of tubercular and silicotic patients by activation methods, 20: 36542
effects on determination of chromium in ores by neutron activation analysis, 20: 36750
effects on radioinduced swelling in uranium, 20: 37302
electron momentum distribution in, positron annihilation method for determining, 20: 37736 (COO-1297-7)
neutron absorption cross section in pitchblende, thermal, 20: 37994
neutron total cross sections at high energies, fluctuations in, 20: 38173
performance of telescope detectors of, for charge and energy spectrometry of cosmic particles, 20: 37575
radiation effects on MOS transistors of, positive charge distribution in dielectric layer from x, (E), 20: 37130
radiation effects on insulated-gate FET transistors on substrate of, photocurrent contribution to drain current from, 20: 37132
radiation effects on, transient annealing from neutron, 20: 37129 (SC-DC-66-1820)

SILICON CARBIDES
preparation and properties for protective coatings on molybdenum and tungsten, 20: 37189
preparation of pyrolytic, symposium on, 20: 37179
sintering of, symposium on, 20: 37179
surface friction of, symposium on, 20: 37179

SILICON CHLORIDES
reactions with uranium hexafluoride, 20: 36803

SILICON HYDRIDES
radioinduced free radicals of, in krypton, 20: 36909

SILICON IONS
effects on formation of single-crystal beryllium oxide, 20: 36814

SILICON ISOTOPES Si-27
energy levels, (E), 20: 38053

SILICON ISOTOPES Si-28
deuteron reactions (d,pγ) at 4 to 6 Mev, angular correlations of, (E/T), 20: 38086
meson (μ^-) capture by protons in, rate of, 20: 38166
neutron reactions (n,α) at 12 to 23 Mev, (E), 20: 38036

SILICON ISOTOPES Si-29
energy levels at 1.28 and 2.05 Mev, (E/T), 20: 38086
neutron reactions (n,α) at 12 to 23 Mev, (E), 20: 38036
proton reactions (p,γ) with phosphorus-30 energy levels from, (E), 20: 38062

SILICON ISOTOPES Si-30
proton differential elastic scattering cross section at 1 to 2 Mev, (E), 20: 38105

SILICON NITRIDES
surface friction of, symposium on, 20: 37179

SILICON OXIDES
analysis for sodium, MOS and radiochemical, 20: 36744
effects on rate of polymerization of allyl alcohol, 20: 36880
heating of, effects on charge distributions in, 20: 37285
radiation effects on charge distributions in, uv and x, 20: 37285
reactions with lanthanum and neodymium oxides in solid state, 20: 36840
vaporization of, thermodynamics of, 20: 36841
$(NH_4)_2CO_3$–$MgCl_2$–SiO_2–$UO_2(NO_3)_2$, reactions in, silicate formation in, 20: 36797

$(NH_4)_2CO_3$–SiO_2–$UO_2(NO_3)_2$, reactions in, silicate formation in, 20: 36797
Sm_2O_3–SiO_2, preparation, properties, and structure of $Sm_4(SiO_4)_3$ in, 20: 36784(R) (AD-636054)

SILICON SYSTEMS
Al_2O_3–NaF–Si, properties as coating for D-43 and TZM alloys, 20: 37276

SILICOORGANIC COMPOUNDS
methyl trichlorosilane, pyrolysis to silicon carbide for refractory metal coatings, 20: 37189
radiation effects on, EPR study of electron, 20: 36883

SILTS
chemical composition of, in Bay of Roquebrune, 20: 36553
content of suspended sediment in river waters, radiometric instrument for measuring, 20: 37057
density measurements of, using gamma sources, instrument for, 20: 37150

SILVER
alpha reactions (α,n) at 17 Mev, level density parameters from, (E), 20: 38115
content in African pitchblende, estimation of induced fission vs spontaneous fission from, 20: 37994
diffusion in beryllium at 656 to 900°C, 20: 37250
effects on determination of iridium in ores by neutron activation analysis, 20: 36751
effects on sorptive properties of iron oxide for iodine-131, 20: 36800
electron plasma losses at 3.6 ev in foils of, foil-thickness and temperature dependence of, (E), 20: 38400
gamma reactions at 6.13 Mev, pair-production cross sections for, (E), 20: 37746
meson (π^-) reactions at 17 Bev in nuclear emulsions, (T), 20: 38060
neutron absorption cross section in pitchblende, thermal, 20: 37994
plutonium determination on plates of, by alpha counting, 20: 36736
proton reactions at 600 Mev, cross sections for meson ($\pi^\pm$) production in, 20: 38186
separation of, from thallium by ion-exchange chromatography, 20: 36935
stopping power for lead-208 alpha recoil nuclei, (E), 20: 37470

SILVER ALLOYS
effects of beryllium additions on, 20: 37275

SILVER BROMIDES
sensitivity of emulsion microcrystals of, for electrons, 20: 37122
AgBr–AgCl, phase diagrams, 20: 36787 (YALE-2723(Vol.1))
AgBr–AgI, phase diagrams, 20: 36787 (YALE-2723(Vol.1))
AgBr–NaBi, phase diagrams, 20: 36787 (YALE-2723(Vol.1))
AgBr–TlBr, phase diagrams, 20: 36787 (YALE-2723(Vol.1))
$CdBr_2$–AgBr, phase diagrams, 20: 36787 (YALE-2723(Vol.1))
CuBr–AgBr, phase diagrams, 20: 36787 (YALE-2723(Vol.1))
KBr–AgBr, phase diagrams, 20: 36787 (YALE-2723(Vol.1))
KI–AgBr, phase diagrams, 20: 36787 (YALE-2723(Vol.1))
LiBr–AgBr, phase diagrams, 20: 36787 (YALE-2723(Vol.1))
RbBr–AgBr, phase diagrams, 20: 36787 (YALE-2723(Vol.1))

SILVER CHLORIDES
AgBr–AgCl, phase diagrams, 20: 36787 (YALE-2723(Vol.1))
AgCl–AgI, phase diagrams, 20: 36787 (YALE-2723(Vol.1))
AgCl–NaCl, phase diagrams, 20: 36787 (YALE-2723(Vol.1))
AgCl–TlCl, phase diagrams, 20: 36787 (YALE-2723(Vol.1))
$CaCl_2$–AgCl, phase diagrams, 20: 36787 (YALE-2723(Vol.1))
$CdCl_2$–AgCl, phase diagrams, 20: 36787 (YALE-2723(Vol.1))
CsCl–AgCl, phase diagrams, 20: 36787 (YALE-2723(Vol.1))
CuCl–AgCl, phase diagrams, 20: 36787 (YALE-2723(Vol.1))
HgI_2–AgCl, phase diagrams, 20: 36787 (YALE-2723(Vol.1))
$InCl_3$–AgCl, phase diagrams, 20: 36787 (YALE-2723(Vol.1))
KCl–AgCl, phase diagrams, 20: 36787 (YALE-2723(Vol.1))
LiCl–AgCl, phase diagrams, 20: 36787 (YALE-2723(Vol.1))
$MgCl_2$–AgCl, phase diagrams, 20: 36787 (YALE-2723(Vol.1))
$PbCl_2$–AgCl, phase diagrams, 20: 36787 (YALE-2723(Vol.1))
RbCl–AgCl, phase diagrams, 20: 36787 (YALE-2723(Vol.1))

SILVER COMPLEXES
with tetraphenylporphine in dioxane, gamma radiolysis of, 20: 36889

SILVER FLUORIDES
AgF–ZnF_2, phase diagrams, 20: 36787 (YALE-2723(Vol.1))

SILVER IODIDES
AgBr–AgI, phase diagrams, 20: 36787 (YALE-2723(Vol.1))
AgCl–AgI, phase diagrams, 20: 36787 (YALE-2723(Vol.1))
AgI–NaI, phase diagrams, 20: 36787 (YALE-2723(Vol.1))
CuI–AgI, phase diagrams, 20: 36787 (YALE-2723(Vol.1))
KI–AgI, phase diagrams, 20: 36787 (YALE-2723(Vol.1))
LiI–AgI, phase diagrams, 20: 36787 (YALE-2723(Vol.1))
PbI_2–AgI, phase diagrams, 20: 36787 (YALE-2723(Vol.1))
RbI–AgI, phase diagrams, 20: 36787 (YALE-2723(Vol.1))

SILVER ISOTOPES Ag-107
neutron reactions (n,α) at 12 to 23 Mev, (E), 20: 38036

SILVER ISOTOPES Ag-108
energy level of, low-lying, (E), 20: 38135

SILVER ISOTOPES Ag-110
tracer use for silver diffusion in beryllium, 20: 37250

SILVER ISOTOPES Ag-111
yields from helium ion-induced fission of lead-207 at 41.1 to 26.3 Mev, 20: 37996
yields in proton fission of uranium-238 at 7.1, 9.4, and 12.0 Mev, 20: 37995

SILVER ISOTOPES Ag-113
yields from helium ion-induced fission of lead-207 at 41.1 to 26.3 Mev, 20: 37996
yields in proton fission of uranium-238 at 7.1, 9.4, and 12.0 Mev, 20: 37995

SILVER SYSTEMS
Al_2O_3–Ag, preparation and properties of alumina-base cermets of, 20: 37209
Al_2O_3–Pd–Ag, preparation and properties of alumina-base cermets of, 20: 37209
Ca–NaCl–Ag, radioinduced color centers in, x, 20: 38396
MgO–Pd–Ag, preparation and properties of magnesia-base cermets of, 20: 37209
NaCl–Ag, radioinduced color centers in, x, 20: 38396
Pd–Ag–ZrO_2, preparation and properties of zirconia-base cermets of, 20: 37209

SINGLE CRYSTALS
deformation of alpha-phase zirconium alloy, effects of preferred orientation on, 20: 37226
dislocations in dimolybdenum carbide, effects of structure and annealing on, 20: 37247
hydride orientation in zirconium, effects of stress on, 20: 37269
neutron attenuation by phonons in, (T), 20: 38371
strength of niobium–tantalum alloy, 20: 37215

SKELETON
radiation effects on aminotransferase activities in muscle in rat, neutron, 20: 36601

SKIN
effects of various histamine liberators on calcification produced by various metals in rat, 20: 36557
metabolism of hydroxyproline and proline in collagen of rat, isotopic dilution method for studying, 20: 36562
radiation effects on skin pigments as used in study of melanin affinity for chloroquine, uv, 20: 36564
radiation effects on collagen in kangaroo and mouse, uv, 20: 36595

SMOKES
detection of, development of photometer for, 20: 37168(R) (BMI-1771)
detection of, photometer design for, 20: 37169(R) (BMI-1774)
polonium-210 content in tobacco, 20: 37030

SNOW
washout coefficients for stack disposal of iodine-131 vapor, 20: 37033

SODIUM
combustion of, properties of aerosols produced in, 20: 37022 (LA-DC-6942)
determination in silicon oxides, MOS and radiochemical, 20: 36744
effects on determination of chromium in ores by neutron activation analysis, 20: 36750
energy levels of ionized, forbidden transitions in, 20: 37432
explosions in, pressure produced by contained, 20: 38459 (ANL-7120, pp 720-33)
expulsion into air, equipment and method for study of, 20: 38500 (ANL-7120, pp 868-72)
fission-product retention by, in vented-fuel reactors, 20: 38477 (ANL-7120, pp 855-61)
neutron absorption cross section in pitchblende, thermal, 20: 37994
positron annihilation in, angular correlation of photons from, (E), 20: 37784
positron annihilation with core electrons in, momentum distributions for, (T), 20: 37821
positron effective mass in, (T), 20: 37815
reactions of liquid, with reactor materials at high temperatures, 20: 38499 (ANL-7120, pp 839-47)
reactivity void coefficients in fast reactors, 20: 38418 (ANL-7120, pp 413-20)
reactivity void coefficients of, calculation of, 20: 38419 (ANL-7120, pp 421-2)
reactivity void coefficients of, in ZPR-6, 20: 38426 (ANL-7120, pp 598-602)
wetting of niobium-zirconium alloys, effects of temperature on, 20: 37168(R) (BMI-1771)
wetting of uranium nitride, temperature effects on, 20: 37168(R) (BMI-1771)

SODIUM BROMATES
radiolysis of, gamma, neutron, and lithium-6 fission product recoil, 20: 36899

SODIUM BROMIDES

AgBr–NaBi, phase diagrams, 20: 36787 (YALE-2723(Vol.1))
$BaBr_2$–NaBr, phase diagrams, 20: 36787 (YALE-2723(Vol.1))
$CaBr_2$–NaBr, phase diagrams, 20: 36787 (YALE-2723(Vol.1))
$CdBr_2$–NaBr, phase diagrams, 20: 36787 (YALE-2723(Vol.1))
CsBr–NaBr, phase diagrams, 20: 36788 (YALE-2723(Vol.2))
KBr–NaBr, phase diagrams, 20: 36788 (YALE-2723(Vol.2))
LiBr–NaBr, phase diagrams, 20: 36788 (YALE-2723(Vol.2))
$MgBr_2$–NaBr, phase diagrams, 20: 36788 (YALE-2723(Vol.2))
NaBr–NaCl, phase diagrams, 20: 36788 (YALE-2723(Vol.2))
NaBr–NaF, phase diagrams, 20: 36788 (YALE-2723(Vol.2))
NaBr–NaI, phase diagrams, 20: 36788 (YALE-2723(Vol.2))
NaBr–$SrBr_2$, phase diagrams, 20: 36788 (YALE-2723(Vol.2))
NaBr–TlBr, phase diagrams, 20: 36788 (YALE-2723(Vol.2))
$PbBr_2$–NaBr, phase diagrams, 20: 36788 (YALE-2723(Vol.2))
RbBr–NaBr, phase diagrams, 20: 36788 (YALE-2723(Vol.2))

SODIUM CARBONATES
content of, in sediments of Bay of Roquebrune, 20: 36553
development for SEFOR core materials, 20: 38531 (GEAP-5133)

SODIUM CHLORIDES
analysis of, method for evaluation of random errors in activation, 20: 36734
radiation effects on coloration and d-c conductivity in pure and doped, x, (E), 20: 38373
AgCl–NaCl, phase diagrams, 20: 36787 (YALE-2723(Vol.1))
$AlCl_3$–NaCl, phase diagrams, 20: 36787 (YALE-2723(Vol.1))
$BaCl_2$–NaCl, phase diagrams, 20: 36787 (YALE-2723(Vol.1))
$BeCl_2$–NaCl, phase diagrams, 20: 36787 (YALE-2723(Vol.1))
$CaCl_2$–NaCl, phase diagrams, 20: 36787 (YALE-2723(Vol.1))
Ca–NaCl–Ag, radioinduced color centers in, x, 20: 38396
$CdCl_2$–NaCl, phase diagrams, 20: 36787 (YALE-2723(Vol.1))
CsCl–NaCl, phase diagrams, 20: 36788 (YALE-2723(Vol.2))
$HgCl_2$–NaCl, phase diagrams, 20: 36788 (YALE-2723(Vol.2))
$InCl_3$–NaCl, phase diagrams, 20: 36788 (YALE-2723(Vol.2))
KBr–NaCl, phase diagrams, 20: 36788 (YALE-2723(Vol.2))
KCl–NaCl, phase diagrams, 20: 36788 (YALE-2723(Vol.2))
LiCl–NaCl, phase diagrams, 20: 36788 (YALE-2723(Vol.2))
$MgCl_2$–NaCl, phase diagrams, 20: 36788 (YALE-2723(Vol.2))
NaBr–NaCl, phase diagrams, 20: 36788 (YALE-2723(Vol.2))
NaCl–Ag, radioinduced color centers in, x, 20: 38396
NaCl–UO_2, fission product recoil ranges in, 20: 37997

SODIUM FLUORIDES
AlF_3–NaF, phase diagrams, 20: 36787 (YALE-2723(Vol.1))
Al_2O_3–NaF–Si, properties as coating for D-43 and TZM alloys, 20: 37276
BaF_2–NaF, phase diagrams, 20: 36787 (YALE-2723(Vol.1))
BeF_2–NaF, phase diagrams, 20: 36787 (YALE-2723(Vol.1))
CaF_2–NaF, phase diagrams, 20: 36787 (YALE-2723(Vol.1))
$CdCl_2$–NaF, phase diagrams, 20: 36787 (YALE-2723(Vol.1))
CsF–NaF, phase diagrams, 20: 36788 (YALE-2723(Vol.2))
KF–NaF, phase diagrams, 20: 36788 (YALE-2723(Vol.2))
LiF–NaF, phase diagrams, 20: 36788 (YALE-2723(Vol.2))
MgF_2–NaF, phase diagrams, 20: 36788 (YALE-2723(Vol.2))
NaBr–NaF, phase diagrams, 20: 36788 (YALE-2723(Vol.2))
NaF–NaI, phase diagrams, 20: 36788 (YALE-2723(Vol.2))
NaF–SrF_2, phase diagrams, 20: 36788 (YALE-2723(Vol.2))
NaF–ZnF_2, phase diagrams, 20: 36788 (YALE-2723(Vol.2))
PbF_2–NaF, phase diagrams, 20: 36788 (YALE-2723(Vol.2))
RbF–NaF, phase diagrams, 20: 36788 (YALE-2723(Vol.2))

SODIUM HYDROXIDES
effects on mutarotations of β-D-fructose and α-D-glucose, 20: 36577
radiation effects on normal and deuterated at 77°K, gamma, 20: 36871

SODIUM IODIDES
spectra from thallium-activated, low-temperature, 20: 37441(T)
AgI–NaI, phase diagrams, 20: 36787 (YALE-2723(Vol.1))
CdI_2–NaI, phase diagrams, 20: 36788 (YALE-2723(Vol.2))
KI–NaI, phase diagrams, 20: 36788 (YALE-2723(Vol.2))
methanol–NaI, properties for oxide particle suspension in centrifuges, 20: 36933
MgI_2–NaI, phase diagrams, 20: 36788 (YALE-2723(Vol.2))
NaBr–NaI, phase diagrams, 20: 36788 (YALE-2723(Vol.2))
NaF–NaI, phase diagrams, 20: 36788 (YALE-2723(Vol.2))
PbI_2–NaI, phase diagrams, 20: 36788 (YALE-2723(Vol.2))

SODIUM IONS
effects on formation of single-crystal beryllium oxide, 20: 36814

SODIUM ISOTOPES Na-23
performance as solar neutrino detector, 20: 37793

SODIUM OXIDES
B_2O_3–Eu_2O_3–Na_2O, spectra at liquid nitrogen temperature and room temperature, absorption and emission, 20: 36813

SODIUM PERCHLORATES
solvent properties of solutions of, for zirconium hydroxide, 20: 36789

SODIUM PHOSPHATES
radiation effects on pure and sodium sulfate-doped, ESR studies of gamma, 20: 36870

SODIUM SULFATES
analysis of, for sulfur-35, combustion method for, 20: 36721
effects on ESR spectra of irradiated sodium polyphosphates, 20: 36870
radiolysis of anhydrous and hydrated, gamma, 20: 36903

SODIUM TUNGSTATES
$Nd_2(WO_4)_3$–Na_2WO_4, phase diagrams, 20: 37241

SODIUM VANADATES
reactions with thorium salts, electrometric study of, 20: 36822

SOILS
analysis for uranium using Arsenazo III, photometric, 20: 36774
cesium-137 transfer from, to dairy cattle feeds, 20: 37038
density measurement of, using gamma back-scattering, gage response in, 20: 37020
isotopic exchange in suspensions of, method for continuous recording of, 20: 36793
strontium-90 content of, Neotoma Valley, Ohio, 1958 through 1964, 20: 36548 (TID-23036)

SOLAR BATTERIES
radiation effects on silicon, transient annealing from neutron, 20: 37129 (SC-DC-66-1820)

SOLAR FLARES
configuration of proton-emitting, (T), 20: 37346
data compilation for 1954–1964, 20: 37886
effects on cosmic ray energy and intensity, (E), 20: 37537
magnetic disturbances during, relation of auroral displays to, 20: 37887
magnetic disturbances during, relation of auroral displays to, 20: 37888
properties of four related, on Sept. 1957, (E), 20: 37347
proton doses from, properties of, 20: 37915
radiation hazards to astronauts from, 20: 36627
x-ray spectra from, 20: 37360

SOLAR RADIATION
cosmic ray friction effects on solar wind, model for, 20: 37372
detection of neutrino, by capture in chlorine 37, (T), 20: 37366
effects of solar wind on cosmic ray intensity variations, (T), 20: 37517
effects on comet structure, 20: 37386(T)
energy spectra and intensity time dependence of proton, in stratosphere, (E), 20: 37536
energy spectra of helium ion and proton, in co-rotation with sun, 20: 37371
flux of neutron, at 20 to 160 Mev, (E), 20: 37375
flux of nuclei ($Z \geq 3$) in, (E), 20: 37567
geomagnetic cavity in solar wind, neutral point of, (T), 20: 37895
intensity modulation in interplanetary space, (T), 20: 37542
intensity of solar wind, correlations with cosmic ray 27-day intensity modulation, (E), 20: 37528
intensity of, Mariner IV data on, 20: 37341 (N-66-17354)
interaction with solar magnetic field, (T), 20: 37349
magnetohydrodynamic discontinuities in solar wind, 20: 37387
measurement of, Mariner IV instrumentation for, 20: 37341 (N-66-17354)
model of solar wind, viscous, (T), 20: 37350
propagation of proton, review of, 20: 37493
research on neutrino, using isotopic composition of solar material, 20: 37369
velocity of solar wind, correlations with cosmic ray rigidity spectrum, (E), 20: 37533

SOLID SOLUTIONS
clustering of oxygen in niobium–oxygen, measurements of, 20: 37213
clustering of oxygen in niobium–oxygen, mechanism of, 20: 37214

SOLIDS
electron interactions in, Fermi liquid theory for, 20: 38403
nuclear quadrupole resonance in, (T), 20: 38019
radioinduced defects in, model for change in elastic modulus from, 20: 37296

SOLUTIONS
analysis for plutonium and uranium using gamma absorption, 20: 36767
analysis for radioisotopes by least-squares resolution of gamma spectra, 20: 36780

SOLVENT EXTRACTION PROCESSES
development of, for processing irradiated fuel elements, 20: 36948

SOUTHWEST EXPERIMENTAL FAST OXIDE REACTOR
core materials for, description of, 20: 38531 (GEAP-5133)
fuel materials for, description of, 20: 38531 (GEAP-5133)

SPACE
cosmic and solar radiation modulation in interplanetary, (T), 20: 37542
dust particles in interplanetary, charged, 20: 37913(T)
effects of interplanetary, on cosmic ray modulation, 20: 37497
gas expansion in intergalactic, relativistic, (T), 20: 37503
magnetic field structure in interplanetary, review of, 20: 37898
radiation doses to tissues from alpha particles and heavy nuclei in solar particle beams in, 20: 37023 (N-65-33865)

SPACE FLIGHT
feasibility of nuclear-propelled manned interplanetary landing mission, 20: 36999
radiation hazards to astronauts from highly ionizing radiation, 20: 36627
SPACE VEHICLES
carbon dioxide sensor for Gemini, 20: 37064
instrumentation for Mariner IV, operation and sensitivity of, 20: 37341 (N-66-17354)
lifting surfaces for re-entry of, properties of infiltrated tungsten for, 20: 37188
power sources for large payloads, 20: 36998
propulsion by coherent x-rays, (T), 20: 36997
reactor operation in, charge build-up in, (T), 20: 38529
SPARK CHAMBERS
current splitting in divided-electrode, 20: 37109
design and performance of, review on, 20: 37043
efficiency of large-gap neon-filled, at 600 mm Hg, 20: 37088
performance of helium- and neon-filled streamer, 20: 37110
performance using vidicon techniques for charged particle counting, 20: 37114
sparking efficiency and threshold voltage, 20: 37105
SPECIFIC HEAT
measurement from 250 to 1000°C, calorimeter for, 20: 37278
SPECTROMETERS
design and performance of electronic digital, for experimental nuclear physics, 20: 37128
SPERM
radiation effects on Drosophila, in succeeding generations after oocyte exposure, gamma, 20: 36625
SPINELS
preparation and properties of, symposium on, 20: 37179
SPLEEN
analysis of, for carbon-14 and tritium by scintillation counting, combustion method for, 20: 36721
radiation effects on hematopoietic response in guinea pig, effects of unilateral limb shielding on gamma, 20: 36611
radiation effects on histology of rat, during immune response, local x, 20: 36637
radiation effects on homografts of, in dogs by lumphatic ablation, 20: 36641
SPORES
radiosensitivity of, effects of chemicals on, 20: 37144
STACK DISPOSAL
washout coefficients for iodine-131 vapor, rain and snow, 20: 37033
STAINLESS STEEL
compatibility of 316, with cadmium sulfate, 20: 38447 (WCAP-2867)
compatibility with mixed carbide fast breeder reactor fuels, 20: 38466 (ANL-7120, pp 301-13)
compatibility with mixed-carbide fast reactor fuels, 20: 38467 (ANL-7120, pp 314-27)
corrosion by water, gamma radiation effects on, 20: 37182
corrosion of types 309S, 310, and 446, by boiling hydrofluoric acid–nitric acid solutions, 20: 37169(R) (BMI-1774)
dissolution of, operation of pilot plant for electrolytic, 20: 36949
fabrication and testing for reactor uses, 20: 37174
performance as fuel jacket material for fast reactors, 20: 38465 (ANL-7120, pp 289-300)
radiation effects on austenitic, 20: 37174
radiation effects on type 347, neutron, 20: 37168(R) (BMI-1771)
radiation effects on type 347, neutron, 20: 37169(R) (BMI-1774)
radiation effects on tensile properties of niobium-stabilized, in-reactor, 20: 37284
radiation effects on mechanical properties of types 17-4PH, AM-350, A-236, 405, and 406, neutron, 20: 37286
reactions with plutonium nitride and uranium nitride at high temperatures, 20: 37169(R) (BMI-1774)
reactions with uranium mononitride at high temperatures, 20: 37168(R) (BMI-1771)
B–stainless steel, ductility of, effects of ultrasound on, 20: 37221
stainless steel–UO_2, fabrication of fuel plates from, 20: 37168(R) (BMI-1771)
STARCHES
radiation effects on potato, effects of water content on gamma, 20: 36599
STARS
age determination of A, B, and F, 20: 37417
contraction of, properties of, 20: 37396
cooling and detectability of neutron, 20: 37355
cosmic ray origin in supernova, (T), 20: 37498
cosmic-ray emission from radio source, 20: 37490
dynamics of dense photon, 20: 37357
element abundance determination in CH, 20: 37424
element abundance differences among population I, 20: 37425
element abundance in peculiar A, 20: 37426
element abundances in, determination of, 20: 37422
element transport in, from neutron capture, 20: 37423
energy transport in, by turbulent convection, 20: 37394
evolution and structure of, analytical models for, 20: 37391
evolution of binary, 20: 37429
evolution of one solar mass, 20: 37401
evolution of seven solar mass, 20: 37405
evolution of three solar mass, 20: 37402
evolution of, advanced stages in, 20: 37404
evolution of, calculation of main-sequence, 20: 37400
evolution of, contraction phase of, 20: 37397
evolution of, nucleosynthesis in, 20: 37392
evolution of, role of magnetic activity in, 20: 37399
evolution of, schematic pre-main-sequence, 20: 37398
evolution of, survey on, 20: 37367
expansion of, moment of inertia variations in, 20: 37384(T)
explosion of type II supernova, properties of, 20: 37407
light curve of Nova Herculis 1934, comparison with lightning current, (T), 20: 38260
lithium depletion in main-sequence, 20: 37421
mass determination of hot isothermal white dwarfs, critical, (T), 20: 37383(T)
mass loss from red giants, 20: 37415
mass loss from T Tauri, 20: 37414
mass-luminosity relation for, 20: 37427
model for neutron, effects of nuclear forces on, 20: 37356
model for superstars and galactic evolution, scintillation, 20: 37358
neutrino emission from collapsing, methods for observing, 20: 37379
neutrino emission from neutron, properties of, 20: 37355
neutrino processes in pre-supernova evolution, 20: 37406
nuclear reactions on surface of, effects on electromagnetic activity, 20: 37399
nuclear reactions in interiors of, at $(5 \text{ to } 30) \times 10^6$ °K, (T), 20: 37377
origin of matter in steady-state universe, quasars as, 20: 37361
photometry of B-type, 20: 37418
photon density from intergalactic, (T), 20: 37374
photon flux from, limits for high energy, (E), 20: 37547
properti es of field horizontal branch and RR Lyrae, 20: 37419
properties of quasi-stellar objects and radio sources, 20: 37370
properties of quasi-stellar radio sources, optical, 20: 37382(T)
properties of, survey on, 20: 37367
pulsations from, excitation and growth of, 20: 37412
pulsations from, properties of, 20: 37413
radiations from, origin of microwave background, 20: 37362
rotation effects on electromagnetic activity, 20: 37399
rotation of neutron, 20: 37363
spectra of T Tauri, uv excess in, 20: 37420
spectrum of 3C9, for intergalactic molecular hydrogen extinction, (E), 20: 37353
stability of Cepheid, models for, 20: 37411
structure of, photon absorption and opacity calculations for determining, 20: 37393
temperature of white dwarfs, cooling of, 20: 37408
x-ray source, spectra of 20- to 58-kev, (E), 20: 37376
STATISTICS
formalism of quantum, for optical rotation, 20: 37927
STEAM
reactions with uranium hexafluoride to prepare uranium dioxide, 20: 37205
STEEL
neutron scattering by cylinders of, spectra from fast, (E/T), 20: 38007
radiation effects on types Hy-80, A212B, A302B, and A336, neutron, 20: 37286
reactions with liquid sodium at high temperatures, 20: 38499 (ANL-7120, pp 839-47)
testing of, use of iridium-192 in radiographic, 20: 36994
STELLARATORS
plasma stability in negative V, 20: 38243
STELLARATORS (C)
plasma excitation and ionization in, neon ion, 20: 38250
plasma fluctuations and control of pumpout in, (T), 20: 38266
plasma stability in, toroidal, (E), 20: 38268
STIBINES
radioinduced free radicals of, in krypton, 20: 36909
STOMACH
radiation effects on emptying in rat, part-body x, 20: 36628
STRANGE PARTICLES
production in meson (π^+) interactions with protons at 8 Bev/c, cross sections for, (E), 20: 37770
STRATOSPHERE
cosmic and solar radiation intensity in, (E), 20: 37536
cosmic-ray intensity variations in, cyclic, (E), 20: 37532
cosmic-ray intensity in, temperature dependence of, (E), 20: 37591

cosmic-ray flux variation in, height dependence of, (E), 20: 37552
particle flux in, increases of ionizing, (E), 20: 37907

STREPTOMYCES
use in biosynthesis of tritium-labeled actinomycins, 20: 36545

STRONTIUM
absorption by barley, genotype effect on rate of, 20: 36575
content in African pitchblende, estimation of induced fission vs spontaneous fission from, 20: 37994
determination of, using Arsenazo III, photometric, 20: 36778
effects on inotropic action of fluoride in rat ventricle, 20: 36567
neutron absorption cross section in pitchblende, thermal, 20: 37994
ranges of recoil, in sodium chloride–uranium dioxide mixtures, 20: 37997
separation from radioactive waste solutions, 20: 38538
separation from water by foaming, 20: 36934
separation of, from thallium by ion-exchange chromatography, 20: 36935

STRONTIUM BROMATES
radiolysis of, gamma, neutron, and lithium-6 fission product recoil, 20: 36899

STRONTIUM BROMIDES
$BaBr_2$–$SrBr_2$, phase diagrams, 20: 36787 (YALE-2723(Vol.1))
KBr–$SrBr_2$, phase diagrams, 20: 36788 (YALE-2723(Vol.2))
LiBr–$SrBr_2$, phase diagrams, 20: 36788 (YALE-2723(Vol.2))
NaBr–$SrBr_2$, phase diagrams, 20: 36788 (YALE-2723(Vol.2))
$SrBr_2$–SrI_2, phase diagrams, 20: 36788 (YALE-2723(Vol.2))

STRONTIUM CARBONATES
thermoluminescence properties of, for use as radiation dosimeter, 20: 36913

STRONTIUM CHLORIDES
$BaCl_2$–$SrCl_2$, phase diagrams, 20: 36787 (YALE-2723(Vol.1))
$CaCl_2$–$SrCl_2$, phase diagrams, 20: 36787 (YALE-2723(Vol.1))
$CdCl_2$–$SrCl_2$, phase diagrams, 20: 36787 (YALE-2723(Vol.1))
CsCl–$SrCl_2$, phase diagrams, 20: 36788 (YALE-2723(Vol.2))
KCl–$SrCl_2$, phase diagrams, 20: 36788 (YALE-2723(Vol.2))
LiCl–$SrCl_2$, phase diagrams, 20: 36788 (YALE-2723(Vol.2))
$MgCl_2$–$SrCl_2$, phase diagrams, 20: 36788 (YALE-2723(Vol.2))
$PbCl_2$–$SrCl_2$, phase diagrams, 20: 36788 (YALE-2723(Vol.2))
RbCl–$SrCl_2$, phase diagrams, 20: 36788 (YALE-2723(Vol.2))
$SrCl_2$–SrF_2, phase diagrams, 20: 36788 (YALE-2723(Vol.2))
$SrCl_2$–TlCl, phase diagrams, 20: 36788 (YALE-2723(Vol.2))
$SrCl_2$–$ZnCl_2$, phase diagrams, 20: 36788 (YALE-2723(Vol.2))

STRONTIUM FLUORIDES
BaF_2–SrF_2, phase diagrams, 20: 36787 (YALE-2723(Vol.1))
BeF_2–SrF_2, phase diagrams, 20: 36787 (YALE-2723(Vol.1))
CaF_2–SrF_2, phase diagrams, 20: 36787 (YALE-2723(Vol.1))
KF–SrF_2, phase diagrams, 20: 36788 (YALE-2723(Vol.2))
LiF–SrF_2, phase diagrams, 20: 36788 (YALE-2723(Vol.2))
NaF–SrF_2, phase diagrams, 20: 36788 (YALE-2723(Vol.2))
$SrCl_2$–SrF_2, phase diagrams, 20: 36788 (YALE-2723(Vol.2))

STRONTIUM IODIDES
$BaBr_2$–SrI_2, phase diagrams, 20: 36787 (YALE-2723(Vol.1))
BaI_2–SrI_2, phase diagrams, 20: 36787 (YALE-2723(Vol.1))
$SrBr_2$–SrI_2, phase diagrams, 20: 36788 (YALE-2723(Vol.2))

STRONTIUM ISOTOPES
purification of electromagnetically separated, 20: 37163

STRONTIUM ISOTOPES Sr-85
determination of, with calcium-45 in whole algae cells, liquid scintillation spectrometric, 20: 36747
metabolism in live mice, design of radiation detectors for measuring, 20: 36556
photosynthesis and uptake of, in freshwater plankton, effects of light on, 20: 36568

STRONTIUM ISOTOPES Sr-86
energy levels of, shell-model potential parameters for low-lying, (T), 20: 38145

STRONTIUM ISOTOPES Sr-87
determination in Antarctic rocks for age estimation, 20: 37015
neutron reactions (n,γ) at thermal energies, strontium-88 neutron binding energy and energy levels from, (E), 20: 38141

STRONTIUM ISOTOPES Sr-88
binding energy from strontium-87 neutron capture, neutron, (E), 20: 38141
energy levels from strontium-87 neutron capture, (E), 20: 38141
proton elastic and inelastic scattering at 4.9 to 7.5 Mev, isobaric analog states of strontium-89 in, (E/T), 20: 38076

STRONTIUM ISOTOPES Sr-89
distribution in sea water, from waste disposal, 20: 38537
energy levels of, analogs in yttrium-89, 20: 38076
metabolism in live mice, design of radiation detectors for measuring, 20: 36556
separation from waste solutions using humic acid column, 20: 36930
yields in proton fission of uranium-238 at 7.1, 9.4, and 12.0 Mev, 20: 37995

STRONTIUM ISOTOPES Sr-90
content in hay in Germany, 1962, 20: 36671
content in milk, Germany, 1962 through 1964, 20: 36674
content in soil of Neotoma Valley, Ohio, 1958 through 1964, 20: 36548 (TID-23036)
determination in rain water using ion exchange, gamma spectrometric, 20: 36759
distribution in sea water, from waste disposal, 20: 38537
excretion in rats, effects of citrate and salicylate treatments, 20: 37025(R) (PG-Report-705)
metabolism in live mice, design of radiation detectors for measuring, 20: 36556
separation from rain water, 20: 37029
separation of, from fission products in nitric acid solutions, chromatographic, 20: 36748
transport from blood stream into gastrointestinal stream in rats, 20: 36558
use in x-ray sources, 20: 36915 (N-66-17678)

STRONTIUM ISOTOPES Sr-91
yields from helium ion-induced fission of lead-207 at 41.1 to 26.3 Mev, 20: 37996
yields in proton fission of uranium-238 at 7.1, 9.4, and 12.0 Mev, 20: 37995

STRONTIUM ISOTOPES Sr-92
yields from helium ion-induced fission of lead-207 at 41.1 to 26.3 Mev, 20: 37996

STRONTIUM TITANATES
superconducting critical fields and magnetization of niobium-doped, (E), 20: 37953

STRUCTURES
leakage from, measurement of rate of, 20: 36978 (NAA-SR-12001)

STYRENE
acrylonitrile–styrene, radiochemical grafting of, on polyvinyl chloride at 0 to 50°C, 20: 36877
acrylonitrile–styrene, radioinduced polymerization of, at −78, 0, and 50°C, effects of dimethylformamide and oil on, 20: 36876
acrylonitrile–styrene, radioinduced grafting on polytetrafluoroethylene, effects of monomer diffusion rate on, 20: 36878

STYRENE POLYMERS
particle ionization losses in polarized layer of, optimum thickness for relativistic, (E), 20: 37435

SULFATE IONS
effects on copper determination, 20: 36726

SULFIDES
electric and thermal conductivity of metal, symposium on, 20: 37179

SULFUR
content in African pitchblende, estimation of induced fission vs spontaneous fission from, 20: 37994
determination of, using Arsenazo III, photometric, 20: 36778
gamma reactions (γ,α) at 31 Mev, alpha spectra from, (E), 20: 38037
neutron absorption cross section in pitchblende, thermal, 20: 37994
neutron total cross sections at high energies, fluctuations in, 20: 38173
reactions with beryllium in group VIII transition metal alloys, 20: 37275

SULFUR FLUORIDES
reactions with vanadium pentafluoride, 20: 36804

SULFUR ISOTOPES
distribution in ore, determination of deposit genesis from, 20: 37011

SULFUR ISOTOPES S-32
electron reactions (e,e′p) at 408 Mev, proton binding energies from, (E), 20: 38016
neutron reactions (n,d) at 14 Mev, (E), 20: 38150
use in determination of ore deposit genesis, 20: 37011

SULFUR ISOTOPES S-33
neutron reactions (n,p), phosphorus-33 production in, (E), 20: 37166

SULFUR ISOTOPES S-34
neutron reactions (n,d) at 14 Mev, (E), 20: 38150
proton reactions (p,γ) at 1.214 Mev, chlorine-35 energy-level quantum numbers and transitions from, 20: 38071
use in determination of ore deposit genesis, 20: 37011

SULFUR ISOTOPES S-35
determination of, in biological and organic materials, combustion method for, 20: 36721
determination of, instrumentation effects on quenching of energy spectrum in, 20: 36771

SULFUR ISOTOPES S-36
proton reactions (p,γ) at 0.80 to 1.90 Mev, chlorine-37 energy levels from, (E), 20: 38185

SULFUR MINERALS
genesis of, determination by abundance of stable isotopes, 20: 37011

SULFUR OXIDES
effects on quenching of energy spectra in determination of carbon-14, sulfur-35, and tritium, 20: 36771

SULFURIC ACID
determination of, by backscattering of beta particles, 20: 36770
effects on mutarotations of β-D-fructose and α-D-glucose, 20: 36577

oxidizing effects on molybdenum, passivation mechanisms in, 20: 37184
preparation of carrier-free sulfur-35-labeled, from neutron-irradiated potassium chloride, 20: 36920
SUN
activity of, correlations with cosmic ray rigidity spectrum, (E), 20: 37543
activity of, effects on primary cosmic ray intensity, 20: 37509
activity of, effects on cosmic alpha flux, (E), 20: 37556
activity variations of, periodicity of parameters for diurnal, (E), 20: 37373
atmosphere of, dynamics of, 20: 37389
book: *Introduction to Solar Terrestrial Relations*, 20: 37916
chromosphere of, structure of, 20: 37912
corona of, simulation device for, 20: 38335
coronal condensations, abundance of calcium and iron in, (E), 20: 37348
effects on cosmic radiation intensity, determination from cosmic electron energy spectra, 20: 37499
effects on cosmic ray modulation, 20: 37545
effects on primary cosmic ray spectra, modulation at low rigidities from, (E), 20: 37584
energy generation by, proton-proton chain and CNO-cycle contributions to, 20: 37366
evolution from pure-hydrogen galaxie, 20: 37409
evolution of, contraction phase of, 20: 37397
neutrino emission by, flux at earth from, (T), 20: 37366
neutrino flux from, (T), 20: 37377
spot activity on, properties of, (T), 20: 37385(T)
spot configuration and proton emission, (T), 20: 37346
spot number correlations with cosmic neutron intensity variation, relative, (E), 20: 37524
spot opacity properties, (T), 20: 37354
spots on, gaseous pressure in, 20: 37343
spots on, umbra intensity of, 20: 37364
structure parameters of, neutrino spectroscopy method for determining, 20: 37378
temperature of interior of, methods using solar neutrino detection for determining, 20: 37380
SUPERCONDUCTIVITY
of tantalum–titanium wires, effects of crystal structure on, 20: 37268
theory for, strong electron-phonon coupling in pairing, 20: 37952
theory of, characteristic features of, 20: 37967
SUPERCONDUCTORS
acoustic wave attenuation in type-II, near transition temperature, (T), 20: 37948
critical field and transition temperature of indium, in porous glass, (E), 20: 37949
critical field and magnetization of molybdenum–titanium alloy, Pauli spin and spin-orbit effects on, (E), 20: 37951
critical fields and magnetization of niobium-doped strontium titanate, (E), 20: 37953
critical temperature of, transition-metal impurity effects on depression of, (E), 20: 37955
critical temperature in thin film, review of, 20: 37976
current density in niobium–oxygen–titanium, effects of processing on, 20: 37267
current distribution in coils of, optimum, (T), 20: 37971
current losses and magnetic field aberrations from high-field wires of, in adiabatic demagnetization apparatus, 20: 37970
current losses in type II, calculation of a-c, 20: 37969
electric conductivity of lead–indium, effect of transport-current polarity on, (E), 20: 37945
electric conductivity of type II, (T), 20: 37979
electron decay rate in, injected, 20: 37984
electron tunneling in junctions of, design and performance of system for measuring small nonlinearities in, 20: 37973
electron tunneling in, review of Josephson, 20: 37975
electron tunneling in coupled, quantum effects of, 20: 37986
energy gap parameter of, nonmagnetic impurity effects on anisotropy of, (T), 20: 37958
magnetic field effects on performance of type II, 20: 37942
magnetic flux motion in lead and indium–lead, induced voltage from, (E/T), 20: 37966
magnetic flux pumps of, processes in, (T), 20: 37977
magnetic flux trapping at 10 to 1000 Mc in, (E/T), 20: 37954
magnetic properties of type-II, Pauli paramagnetism effects on, (T), 20: 37956
magnetization of aluminum–magnesium, (E), 20: 37935 (CEA-R-2906)
nuclear spin-lattice relaxation time in type II, (E), 20: 37941
paramagnetic limit in type II, (T), 20: 37936 (CLM-R-60)
properties of indium–tin and tin, 20: 37271
properties of niobium–zirconium alloy, in strong d-c magnetic fields, (E), 20: 37950
pulse transmission properties of subminiature coaxial delay lines of, high-voltage, (E), 20: 37939
stability of ideal film, with current, (T), 20: 37938
structure of mixed-state in vanadium, NMR and relaxation studies of, 20: 37963
thermal conductivity of indium–lead, temperature dependence of, (E), 20: 37940
transition temperature of zinc, isotope effects on, (E), 20: 37959
transition temperatures for thin film, properties of, 20: 37980
ultrasonic attenuation in gapless, coefficient for transverse, (T), 20: 37957
use in large high-field magnets, 20: 37934 (BNL-10380)
vortex pairs in, lifetime of, (T), 20: 37944
SUPERFLUIDITY
properties of helium II, rotational, 20: 37987
properties of liquid helium II, review of, 20: 37974
rotation of Fermi systems, 20: 37473
SUPERHEATERS (NUCLEAR)
design of BONUS, effect of two-pass flow on, 20: 38509 (ORNL-TM-1449)
SURFACE WATERS
sediment content of river, radiometric instrument for measuring, 20: 37057
SUSPENSIONS
isotopic exchange in, method for continuous recording of, 20: 36793
x-ray fluorescence analysis of aqueous, instrument for automatic continuous, 20: 37152
SWEDEN
x-ray standards in, 20: 37078
SWINE
effects of radiation-processed fruits on, 20: 37156
radiation effects on anatomy and pathology in, whole-body gamma, 20: 36657
radiation effects on Dische-positive material in blood and urine in, gamma, 20: 36604
radiation sickness in, anatomy and pathology of, 20: 36657
SWITCHES
design and performance of radiation-sensitive, 20: 37062
SYNCHROCYCLOTRONS
beam current of JINR, effect of electrostatic focusing on proton, 20: 37328
beam intensity and space charge limit of, method for increasing, 20: 37320 (CONF-660510-19)
research program at CERN, during 1965, 20: 37308(R) (NP-16226)
SYNCHROTRONS
magnetic fields in elliptic vacuum chambers of, calculations for, 20: 37318 (BNL-10436)
research program at CERN proton, 1965, 20: 37308(R) (NP-16226)
storage rings for CERN, design and development of intersecting, 20: 37325
storage rings for CERN, research on intersecting, 20: 37327
storage rings for CERN, design and development of intersecting, 20: 37326
SYSTEMS FOR NUCLEAR AUXILIARY POWER
insulation for, development of fibrous-type, 20: 36983(R) (ALO-3633-1)
SYSTEMS FOR NUCLEAR AUXILIARY POWER (SNAP-2)
rotordynamic analysis of, Combined Rotating Unit-V, 20: 36977 (NAA-SR-11944)
SYSTEMS FOR NUCLEAR AUXILIARY POWER (SNAP-8)
operation experience, 20: 38527
shielding design for, 20: 38527

T

TANTALUM
analysis for copper by absorption spectroscopy, effects of ions on, 20: 36726
coating with tantalum disilicide, growth kinetics and diffusion reactions of, 20: 37190
dislocations in, magnitude of Snoek pinning of oxygen-induced, (E), 20: 38360
effects on crystal structure and properties of thoria-tungsten cermets, 20: 37185
evaporation in vacuum at 2063 to 3203°K, effects of pressure on, 20: 36834
magnetic flux trapping at 10 to 1000 Mc in superconducting, (E/T), 20: 37954
neutron total cross sections at high energies, fluctuations in, 20: 38173
reactions with boron carbide at 1200 to 1700°C, 20: 36809
separation from hydrofluoric acid solutions by solvent extraction using dialkyl alkylphosphonates, 20: 36941
TANTALUM ALLOYS
creep at ultrahigh vacuum, design and performance of apparatus, 20: 37263
Al–Ta, properties of intermetallic compound, 20: 37260

Nb–Ta, shear properties of single crystal, effects of composition on, 20: 37215
Re–Ta, faulting in, effects of cold working on, 20: 37217
Ta–Ti, superconductivity at 4.2°K, effects of crystal structure on, 20: 37268

TANTALUM BORIDES
production by reactions of boron carbide–tantalum powders at 1200 to 1700°C, 20: 36809

TANTALUM FLUORIDES
reactions with bromides, chlorides, and fluorides, 20: 36804

TANTALUM IONS
effects on copper determination, 20: 36726

TANTALUM ISOTOPES Ta-181
neutron reactions (n,α) at 12 to 23 Mev, (E), 20: 38036

TANTALUM ISOTOPES Ta-182
diffusion in titanium, environmental effects on, 20: 37175
gamma spectra, (E), 20: 38158
internal conversion electron spectrum above 5 kev, (E), 20: 38134
tracer uses for vaporization of tantalum in vacuo, 20: 36834

TANTALUM ISOTOPES Ta-183
decay scheme, (E), 20: 38104
energy level studies through beta decay of tantalum-183, (E), 20: 38104

TANTALUM ISOTOPES Ta-185
tracer uses for vaporization of tungsten in vacuo, 20: 36834

TANTALUM SILICIDES
growth on tantalum surfaces, kinetics of diffusion reactions in, 20: 37190

TANTALUM SYSTEMS
C–Ta–Zr, phase studies, 20: 37270
Ta–O, partial pressures of oxides formed in solid solutions of, 20: 36836

TAPEWORMS
life cycle and pathological effects in intermediate and final hosts, 20: 36607(R) (TID-23114)
radiation effects on host response to, x, 20: 36607(R) (TID-23114)

TARTARIC ACID
complexes with rare earths, stability constants for, 20: 36838

TECHNETIUM
content in African pitchblende, estimation of induced fission vs spontaneous fission from, 20: 37994
neutron absorption cross section in pitchblende, thermal, 20: 37994
separation from neutron-irradiated biological materials by ion exchange, 20: 36762

TECHNETIUM ISOTOPES Tc-99
incorporation in albumin for use in scintiscanning of lungs, 20: 36919

TEETH
effects of radiotherapy of face on, in children, 20: 36708

TELEVISION EQUIPMENT
performance of vidicon tubes with spark chambers for charged particle counting, 20: 37114

TELLURIC ACID
preparation of, for use in production of iodine-131 by neutron irradiation, 20: 36917

TELLURIUM
effects on determination of iridium in ores by neutron activation analysis, 20: 36751
Mössbauer effect of tin-119 in, (T), 20: 38375
x-ray spectra from mu-mesic atoms of, (E), 20: 38058
yields from radiolysis of tellurium phthalocyanine, 20: 36886

TELLURIUM ISOTOPES Te-121
decay scheme, (E), 20: 38188

TELLURIUM ISOTOPES Te-127
decay scheme, (E), 20: 38188

TEMPERATURE
effects on Doppler coefficient for fast reactors, 20: 38421 (ANL-7120, pp 440-8)
effects on errors in measurement of building leakage, 20: 36978 (NAA-SR-13001)
effects on iodine-131-labeled triiodothyronine metabolism in human thyroid, 20: 36573
effects on neutron Doppler effect in ZPR-6, 20: 38428 (ANL-7120, pp 610-13)
effects on radioinduced creep of graphite, 20: 37223
effects on rate of strontium absorption by barley, 20: 36575
effects on reactivity of uranium-235 and uranium-238 in fast-neutron spectra, 20: 38429 (ANL-7120, pp 614-15)
effects on thermal conductivity of hydrogen, 20: 36991

TERBIUM
determination in complexes with diketones, spectrofluorometric, 20: 36722
determination in hydrochloric acid solutions, spectrographic carrier-distillation, 20: 36729
effects on crystal structure of cobalt, iron, and nickel intermetallic compounds, 20: 37243
neutron absorption cross section in pitchblende, thermal, 20: 37994

TERBIUM ALLOYS
Co–Tb, crystal structure of intermetallic compounds in, 20: 37243
Fe–Tb, crystal structure of intermetallic compounds in, 20: 37243
Ge–Tb, crystal structure and magnetic properties, 20: 38369
Ni–Tb, crystal structure of intermetallic compounds in, 20: 37243

TERBIUM CHROMITES
spectra of, infrared, 20: 36807

TERBIUM COMPLEXES
with diketones, spectrofluorometric analysis for, 20: 36722
with tartaric acid and trihydroxyglutaric acid, stability constants for, 20: 36838

TERBIUM HYDROXIDES
preparation and crystal structure of, 20: 36791

TERBIUM IONS
spectra of, effects of chemical bonding and transitions on, 20: 36845

TERBIUM ISOTOPES Tb-159
energy levels of, energy ratios and spins of, (E/T), 20: 38022
proton reactions (p,2n) with, gamma transitions in ground state rotational bands from, 20: 38008(R) (AECL-2595)

TERBIUM PHOSPHIDES
crystal structure, 20: 38370
electric conductivity and magnetic susceptibility, 20: 38370

TERPHENYL
alpha and beta reactions with, decay of scintillations from, 20: 37305
paraffin–2,2′-*p*-phenylenebis[5-phenyloxazole–*p*-terphenyl, scintillation efficiency, 20: 37107

TETRAZOLIUM COMPOUNDS
analytical use in colorimetric determination of cerium, gold, and platinum, 20: 36725

THALLIUM
separation of, from other metals by ion-exchange chromatography, 20: 36935
x-ray spectra from mu-mesic atoms of, (E), 20: 38058

THALLIUM BROMIDES
AgBr–TlBr, phase diagrams, 20: 36787 (YALE-2723(Vol.1))
KBr–TlBr, phase diagrams, 20: 36788 (YALE-2723(Vol.2))
NaBr–TlBr, phase diagrams, 20: 36788 (YALE-2723(Vol.2))
$PbBr_2$–TlBr, phase diagrams, 20: 36788 (YALE-2723(Vol.2))
TlBr–TlCl, phase diagrams, 20: 36788 (YALE-2723(Vol.2))
TlBr–TlI, phase diagrams, 20: 36788 (YALE-2723(Vol.2))

THALLIUM CHLORIDES
AgCl–TlCl, phase diagrams, 20: 36787 (YALE-2723(Vol.1))
$BaCl_2$–TlCl, phase diagrams, 20: 36787 (YALE-2723(Vol.1))
$CaCl_2$–TlCl, phase diagrams, 20: 36787 (YALE-2723(Vol.1))
$CdCl_2$–TlCl, phase diagrams, 20: 36787 (YALE-2723(Vol.1))
CsCl–TlCl, phase diagrams, 20: 36788 (YALE-2723(Vol.2))
CuCl–TlCl, phase diagrams, 20: 36788 (YALE-2723(Vol.2))
$HgCl_2$–TlCl, phase diagrams, 20: 36788 (YALE-2723(Vol.2))
$InCl_3$–TlCl, phase diagrams, 20: 36788 (YALE-2723(Vol.2))
KCl–TlCl, phase diagrams, 20: 36788 (YALE-2723(Vol.2))
LiCl–TlCl, phase diagrams, 20: 36788 (YALE-2723(Vol.2))
$MgCl_2$–TlCl, phase diagrams, 20: 36788 (YALE-2723(Vol.2))
$PbCl_2$–TlCl, phase diagrams, 20: 36788 (YALE-2723(Vol.2))
RbCl–TlCl, phase diagrams, 20: 36788 (YALE-2723(Vol.2))
$SrCl_2$–TlCl, phase diagrams, 20: 36788 (YALE-2723(Vol.2))
TlBr–TlCl, phase diagrams, 20: 36788 (YALE-2723(Vol.2))
TlCl–$SnCl_2$, phase diagrams, 20: 36788 (YALE-2723(Vol.2))
TlCl–TlI, phase diagrams, 20: 36788 (YALE-2723(Vol.2))
TlCl–$ZnCl_2$, phase diagrams, 20: 36788 (YALE-2723(Vol.2))

THALLIUM FLUORIDES
thermodynamic properties, 20: 36950

THALLIUM IODIDES
KI–TlI, phase diagrams, 20: 36788 (YALE-2723(Vol.2))
TlBr–TlI, phase diagrams, 20: 36788 (YALE-2723(Vol.2))
TlCl–TlI, phase diagrams, 20: 36788 (YALE-2723(Vol.2))

THERMAL INSULATION
development and evaluation of fibrous-type, for radioisotope power systems, 20: 36983(R) (ALO-3633-1)

THERMIONIC CELLS
design of cesium-plasma, 20: 38340(P)
design of magnetically channeled plasma diode, 20: 37729(P)
design of nuclear-fueled, 20: 37720 (BMWF-FBK-66-06)
development of reservoirless, for use in space, 20: 37725
emitter surface properties of plasma diode, 20: 37722(R) (N-65-30843)
plasma electron and ion collisions in, computer simulation methods for, 20: 37726
uses as power supplies in space vehicles, 20: 36998

THERMODYNAMICS
theory of unitary matrix ensembles, 20: 38033

THERMOELECTRIC CELLS
uses as power supplies in space vehicles, 20: 36998

THERMONUCLEAR EXPLOSIONS

production of heavy nuclides in Barbel and Par events, (E), 20: 38093
THERMONUCLEAR REACTIONS
cross sections for helium-3–helium-3, at 0.5 to 1.7 Mev, (E), 20: 38131
THERMONUCLEAR REACTORS
design for plasma production, compression, and containment, 20: 38337(P)
design of toroidal, for research, 20: 38341(P)
plasma containment in Astron, properties of relativistic electron coil, 20: 38210 (UCRL-12455(Rev.1))
plasma density in Ogra-I, increasing of, 20: 38248
THICKNESS GAGES
design of digital radiometric, for discontinuous sheets and tube walls, 20: 37058
design of, using x-ray fluorescence for measurements on metal coatings, 20: 37151
use of radiometric, in industry, 20: 37148
THIOCYANATES
effects on metabolism of iodine-131 and iodine-125 in cows, 20: 36563
THORIUM
analysis of irradiated, for cesium-137 using ion exchange on ring oven, spectrometric, 20: 36758
content in African pitchblende, estimation of induced fission vs spontaneous fission from, 20: 37994
determination in presence of lead and uranium, photometric, 20: 36773
determination of, use of melanoxetin in spectrophotometric, 20: 36742
determination of, by titration using sodium vanadate, 20: 36822
neutron absorption cross section in pitchblende, thermal, 20: 37994
phase transformation of, effects of rare earths on, 20: 37242
separation from lead by electrolytic precipitation, 20: 36773
separation from nitric acid solutions using diisopentyl methylphosphonate in benzene, tributyl phosphate, and xylene, 20: 36942
separation from protactinium by solvent extraction using isoamyl alcohol, 20: 36940
separation of, from thallium by ion-exchange chromatography, 20: 36935
use of, as reactor fuel, facility for studying, 20: 36949
THORIUM ALCOHOLATES
preparation of, and thermal decomposition to oxide coatings and powders, 20: 36851
THORIUM ALLOYS
Er–Th, phase studies of, 20: 37242
Gd–Th, phase studies of, 20: 37242
Ho–Th, phase studies of, 20: 37242
Lu–Th, phase studies of, 20: 37242
Nd–Th, phase studies of, 20: 37242
Th–U, use as fuel in power breeder reactors, 20: 38476 (ANL-7120, pp 751-8)
THORIUM CARBIDES
coating of particles of, with carbon, 20: 37206
phase studies, 20: 37206
phase studies, 20: 37265
production of, by sol-gel process, 20: 37206
ThC–UC, preparation, 20: 37206
THORIUM CHLORIDES
hydrolysis of solutions of, equilibrium ultracentrifugation following, 20: 36802
THORIUM COMPLEXES
with melanoxetin, preparation and properties, 20: 36742
THORIUM FLUORIDES
BeF_2–LiF–ThF_4, separation of protactinum from molten, 20: 36927 (ORNL-TM-1543)
LiF–ThF_4, separation of protactinium from molten, 20: 36927 (ORNL-TM-1543)
THORIUM FORMATES
preparation and properties of trihydrate of, 20: 36795
THORIUM HYDROXIDES
thermal decomposition of, oxide preparation by, 20: 36843
THORIUM ISOTOPES Th-230
nuclear strength parameter correlation with beta bands in, (T), 20: 38180
THORIUM ISOTOPES Th-232
nuclear strength parameter correlation with beta bands in, (T), 20: 38180
THORIUM NITRATES
reactions with vanadates, electrometric study of, 20: 36822
separation of protactinium from, 20: 36946
thermal decomposition of, oxide preparation by, 20: 36843
THORIUM OXALATES
thermal decomposition of, oxide preparation by, 20: 36843
THORIUM OXIDES
preparation and sorptive properties of, 20: 36843
thermoluminescence properties of, for use as radiation dosimeter, 20: 36913
THORIUM(IV) OXIDES
production of hypostoichiometric, method for, 20: 37181(P)
production of, by sol-gel process, 20: 37206
BeO–PuO_2–ThO_2, fabrication for gas-cooled reactor fuels, processes for, 20: 37168(R) (BMI-1771)
Pd–Ag–ThO_2, preparation and properties of thoria-base cermets of, 20: 37209
ThO_2–UO_2, fabrication into fuel spheres, method for, 20: 37211
ThO_2–UO_2, radiation testing of aqueous fuel suspensions of, 20: 38533(R) (NP-16168(Pt.A))
ThO_2–UO_2, use as fuel in power breeder reactors, 20: 38476 (ANL-7120, pp 751-8)
ThO_2–W, crystal structure and properties of tungsten-base, effects of hafnium, molybdenum, niobium, rhenium, and tantalum on, 20: 37185
ThO_2–W–Zr, crystal structure and properties of tungsten-base, 20: 37185
W–ThO_2, chemical reactions with nitrogen plasmas and subsonic air at high heat fluxes, 20: 37188
THORIUM PERCHLORATES
hydrolysis of solutions of, equilibrium ultracentrifugation following, 20: 36802
THORIUM SYSTEMS
C–Th, phase studies, 20: 37265
THORIUM VANADATES
preparation and properties of, electrometric study of, 20: 36822
THULIUM
determination in hydrochloric acid solutions, spectrographic carrier-distillation, 20: 36729
energy levels of, ionization energies from, (T), 20: 37439
neutron absorption cross section in pitchblende, thermal, 20: 37994
separation of, from other lanthanides by ion exchange using ammonium lactate, mechanism of, 20: 36939
THULIUM CHROMITES
spectra of, infrared, 20: 36807
THULIUM HYDROXIDES
preparation and crystal structure of, 20: 36791
THULIUM IONS
spectra of, effects of chemical bonding and transitions on, 20: 36845
THULIUM ISOTOPES Tm-169
proton reactions (p,2n) with, gamma transitions in ground state rotational bands from, 20: 38008(R) (AECL-2595)
THYMIDINE
use of tritiated, for studying tumor cell kinetics in radiotherapy, 20: 36704
THYMINE
radiation effects on metabolism in man, 20: 37025(R) (PG-Report-705)
reactions with hydroxyl radicals, ESR spectral studies on, 20: 36806
THYMUS GLAND
radiation effects on nicotinamide adenine dinucleotides content in rat thymocytes, x, 20: 36590
radiation effects on properties of DNA in rat, whole-body x, 20: 36591
radiation effects on hematopoletic response in guinea pig, effects of unilateral limb shielding on gamma, 20: 36611
radiation effects in producing leukemia originating in mouse, x, 20: 36613
THYROID GLAND
effects of function of, on radiation burden from iodine-131 in women, 20: 36675
effects of iodated x-ray contrast media on, secondary, 20: 36571
effects of iodine-containing x-ray contrast media on endocrine function and iodide uptake in human, 20: 36572
metabolism of iodine-131-labeled triiodothyronine in human, factors affecting, 20: 36573
radiation dose to rat, from iodine-125, -129, and -131, 20: 36561
radiotherapy of, use of radioiodine localization as indication for, 20: 36706
THYRONINE, TRIIODO-
metabolism in mice, autoradiography of, 20: 36570
metabolism of iodine-131-labeled, in human thyroid, factors affecting, 20: 36573
THYROXINE
metabolism in mice, autoradiography of, 20: 36570
TIMING CIRCUITS
design for semiconductor detectors, 20: 38161
design of encoder, for neutron time-of-flight measurements, 20: 37067 (AECL-2578)
TIN
determination of stannic, in presence of stannous, 20: 36911
gamma spectra from tin-119 in, at 2 to 6°K, 20: 37271
magnetic flux trapping at 10 to 1000 Mc in superconducting copper-doped, (E/T), 20: 37954
oxygen ion fission of, cross sections for, (E), 20: 38123
properties of superconducting, 20: 37271
separation from antimony and arsenic by thin layer chromatography, 20: 36753
yields of stannic, from gamma radiolysis of hydrochloric acid–stannous

chloride solutions, 20: 36911

TIN ALLOYS
Au–Sn, superconductivity of Au_5Sn and AuSn, 20: 37985
Bi–Sn, Hall effect in quenched films of, below 47°K, 20: 38384
In–Sn, gamma spectra from tin-119 in, at 2 to 6°K, 20: 37271
In–Sn, magnetic flux trapping at 10 to 1000 Mc in superconducting, (E/T), 20: 37954
In–Sn, properties of superconducting, 20: 37271
Ir–Sn, superconductivity of $IrSn_2$, 20: 37985
Mn–Sn, critical temperature of superconducting, transition-metal impurity effects on depression of, (E), 20: 37955
Pt–Sn, superconductivity of PtSn, 20: 37985

TIN BROMIDES
tin-119 quadrupole interactions in, Moessbauer-effect studies of, 20: 36816
$AlBr_3$–$SnBr_3$, phase diagrams, 20: 36787 (YALE-2723(Vol.1))
$AsBr_3$–$SnBr_3$, phase diagrams, 20: 36787 (YALE-2723(Vol.1))
$BiBr_3$–$SnBr_4$, phase diagrams, 20: 36787 (YALE-2723(Vol.1))
$SbBr_3$–$SnBr_4$, phase diagrams, 20: 36788 (YALE-2723(Vol.2))
$SnBr_4$–SnI_4, phase diagrams, 20: 36788 (YALE-2723(Vol.2))

TIN CHLORIDES
$CaCl_2$–$SnCl_2$, phase diagrams, 20: 36787 (YALE-2723(Vol.1))
$CdCl_2$–$SnCl_2$, phase diagrams, 20: 36787 (YALE-2723(Vol.1))
CuCl–$SnCl_2$, phase diagrams, 20: 36788 (YALE-2723(Vol.2))
HCl–$SnCl_2$, radiolysis of aqueous solutions of, gamma, 20: 36911
$InCl_3$–$SnCl_2$, phase diagrams, 20: 36788 (YALE-2723(Vol.2))
LiCl–$SnCl_2$, phase diagrams, 20: 36788 (YALE-2723(Vol.2))
$MgCl_2$–$SnCl_2$, phase diagrams, 20: 36788 (YALE-2723(Vol.2))
$PbCl_2$–$SnCl_2$, phase diagrams, 20: 36788 (YALE-2723(Vol.2))
$SbCl_3$–$SnCl_4$, phase diagrams, 20: 36788 (YALE-2723(Vol.2))
$SnCl_2$–$ZnCl_2$, phase diagrams, 20: 36788 (YALE-2723(Vol.2))
TlCl–$SnCl_2$, phase diagrams, 20: 36788 (YALE-2723(Vol.2))

TIN COMPLEXES
tin-119 quadrupole interactions in, Moessbauer-effect studies of, 20: 36816

TIN COMPOUNDS
tin-119 quadrupole interactions in, Moessbauer-effect studies of, 20: 36816

TIN HYDRIDES
radioinduced free radicals of, in krypton, 20: 36909

TIN IODIDES
AlI_3–SnI_4, phase diagrams, 20: 36787 (YALE-2723(Vol.1))
InI_3–SnI_2, phase diagrams, 20: 36788 (YALE-2723(Vol.2))
$SnBr_4$–SnI_4, phase diagrams, 20: 36788 (YALE-2723(Vol.2))

TIN IONS
effects on copper determination, 20: 36726

TIN ISOTOPES Sn-112
helium-3 reactions (He-3,d) at 18 Mev, antimony-113 energy levels from, (E), 20: 38073

TIN ISOTOPES Sn-114
helium-3 reactions (He-3,d) at 18 Mev, antimony-115 energy levels from, (E), 20: 38073

TIN ISOTOPES Sn-116
helium-3 reactions (He-3,d) at 18 Mev, antimony-117 energy levels from, (E), 20: 38073

TIN ISOTOPES Sn-118
helium-3 reactions (He-3,d) at 18 Mev, antimony-119 energy levels from, (E), 20: 38073

TIN ISOTOPES Sn-119
gamma radiation from, resonance absorption of 23.8 kev, 20: 37271
Mössbauer effect of, in tellurium, (T), 20: 38375
nuclear magnetic moments of, in tin compounds, Moessbauer-effect studies of, 20: 36816

TIN ISOTOPES Sn-120
energy levels, (E), 20: 38058
helium-3 reactions (He-3,d) at 18 Mev, antimony-121 energy levels from, (E), 20: 38073

TIN ISOTOPES Sn-122
energy levels, (E), 20: 38058
helium-3 reactions (He-3,d) at 18 Mev, antimony-123 energy levels from, (E), 20: 38073

TIN ISOTOPES Sn-123
decay scheme, (E), 20: 38188

TIN ISOTOPES Sn-124
helium-3 reactions (He-3,d) at 18 Mev, antimony-125 energy levels from, (E), 20: 38073

TIN ISOTOPES Sn-125
decay scheme, (E), 20: 38188

TIN OXIDES
reactions with lanthanum and neodymium oxides in solid state, 20: 36840
tin-119 quadrupole interactions in, Moessbauer-effect studies of, 20: 36816

TISSUE HOMOGENATES
luminescence of, from biochemical reactions, 20: 36547

TISSUES
book: *Yearbook of Nuclear Medicine*, Vol. I, 1966, 20: 36690
radiation doses to, during deep therapy of malignant tumors, 20: 36702
radiation doses to, from alpha particles and heavy nuclei in solar particle beams in space, 20: 37023 (N-65-33865)
radiation effects on anatomy and pathology of swine, whole-body gamma, 20: 36657
radiation effects on properties of DNA in rat, whole-body x, 20: 36591

TITANIUM
determination in iron oxides by activation methods, 20: 36760
laser beam reactions with, uv spectra from plasma produced from, (E), 20: 38300
neutron absorption cross section in pitchblende, thermal, 20: 37994
neutron total cross sections at high energies, fluctuations in, 20: 38173
reactions with liquid sodium at high temperatures, 20: 38499 (ANL-7120, pp 839-47)
separation from protactinium by solvent extraction using isoamyl alcohol, 20: 36940
tantalum-182 diffusion in, environmental effects on, 20: 37175

TITANIUM ALCOHOLATES
preparation of, and thermal decomposition to oxide coatings and powders, 20: 36851

TITANIUM ALLOYS
Al–Ti, properties of intermetallic compound, 20: 37260
Cr–Co–Fe–Mn–Mo–Ni–Ti, corrosion of Hanford 22, by boiling hydrofluoric acid–nitric acid solutions, 20: 37169(R) (BMI-1774)
Cr–Co–Fe–Mn–Mo–Ni–Ti, corrosion of Hanford 23 and 24, by boiling hydrofluoric acid–nitric acid solutions, 20: 37169(R) (BMI-1774)
Cr–Cu–Fe–Mn–Mo–Ni–Ti, corrosion of Hanford 21, by boiling hydrofluoric acid–nitric acid solutions, 20: 37169(R) (BMI-1774)
Cr–Fe–Mn–Mo–Ni–Ti, corrosion of Hanford 20, by boiling hydrofluoric acid–nitric acid solutions, 20: 37169(R) (BMI-1774)
Cr–Fe–Mn–Mo–Ni–Ti, corrosion of Hanford 17, by boiling hydrofluoric acid–nitric acid solutions, 20: 37169(R) (BMI-1774)
Mo–Ti, critical field and magnetization of superconducting, Pauli spin and spin-orbit effects on, (E), 20: 37951
Mo–Ti–Zr, tensile properties of TZM, effects of brittle coatings on, 20: 37276
Nb–V–Ti, oxidation by air at 900 to 1200°C, kinetics and mechanisms of, 20: 37191
Pu–Ti–U, development as fast reactor fuel, 20: 38465 (ANL-7120, pp 289-300)
Pu–Ti–U, melting temperatures of, 20: 38465 (ANL-7120, pp 289-300)
Pu–Ti–U, use as fuel in 1000-Mw(e) fast breeder reactor, 20: 38494 (ANL-7120, pp 94-103)
Ta–Ti, superconductivity at 4.2°K, effects of crystal structure on, 20: 37258
Ti–V, reactions with liquid sodium at high temperatures, 20: 38499 (ANL-7120, pp 839-47)
Ti–V, use as fuel element cladding material in 1000-Mw(e) fast breeder reactor, 20: 38494 (ANL-7120, pp 94-103)

TITANIUM CHLORIDES
reactions with niobium and tantalum pentafluorides, 20: 36804
reactions with uranium hexafluoride, 20: 36803
diethyl aluminum chloride–$TiCl_4$, catalytic effects on ethylene polymerization, deuterium and hydrogen exchange reactions during, 20: 36827

TITANIUM IONS
effects on copper determination, 20: 36726

TITANIUM ISOTOPES Ti-45
nuclear magnetic moments, (E/T), 20: 38089
nuclear spin, (E/T), 20: 38089

TITANIUM ISOTOPES Ti-50
alpha inelastic scattering at 31 Mev, (E), 20: 38100
energy level systematics, determination using alpha inelastic scattering at 31 Mev, 20: 38100
triton reactions (t,α) and (t,p) at 7.5 Mev, scandium-49 and titanium-52 energy levels and masses from, (E), 20: 38063

TITANIUM ISOTOPES Ti-52
energy levels and ground-state mass, (E), 20: 38063

TITANIUM OXIDES
effects on sintering behavior of urania powders, 20: 37202
reactions with lanthanum and neodymium oxides in solid state, 20: 36840
separation from urania in organic slurries, centrifugal, 20: 36933

TITANIUM SYSTEMS
C–Mo–Ti–Zr, crack formation in Mo-3 alloy ingots, effects of molybdenum capping on, 20: 37219
Nb–O–Ti, crystal structure and superconductivity at 4.2°K, effects of fabrication and heat treatments on, 20: 37267

TOBACCO

polonium-210 content in, 20: 37030
TOLUENE
radiolysis of, in tritiated water, hydrogen–tritium exchange in gamma, 20: 36868
α-TOLUENETHIOL
radioinduced radical formation in, in organic glass at −196°C, gamma, 20: 36894
TRACER TECHNIQUES
development and uses of, review of, 20: 37142
for nickel diffusion in copper, 20: 37300
theory development for, review of, 20: 36544
TRACER TECHNIQUES (BIOLOGY)
evaluation of carbon-14 and tritium for measuring glucose production in dogs, 20: 36565
TRACER TECHNIQUES (BOTANY)
method for tree root extension measurement using iodine-131 in longleaf pines in North Carolina, 20: 36560
TRACER TECHNIQUES (CHEMISTRY)
for cesium sorption by graphite, 20: 36799
for vaporization studies of molybdenum, tantalum, and tungsten, 20: 36834
TRACER TECHNIQUES (MEDICINE)
book: *Yearbook of Nuclear Medicine*, Vol. I, 1966, 20: 36690
TRACER TECHNIQUES (METALLURGY)
for diffusion of iron and silver in beryllium, 20: 37250
for self diffusion in lead, 20: 37272
for self-diffusion in beryllium, 20: 37249
TRANSISTORS
radiation effects on MOS, positive charge distributions in dielectric layer from x, (E), 20: 37130
radiation effects on insulated-gate FET, gain and drain current from gamma, 20: 37132
radiation effects on silicon, transient annealing from neutron, 20: 37129 (SC-DC-66-1820)
TRANSITION METAL ALLOYS
effects of beryllium additions on group I and VIII alloys of, review on, 20: 37275
with aluminum, properties of intermetallic compound, 20: 37260
TRANSITION METALS
solubility of beryllium in group VIII, 20: 37275
TREES
carbon-14 content in, cosmic ray secular variation determination from, (E), 20: 37602
iodine-131 tracer technique for measurement of root extension in pine, 20: 36560
radiation effects on aging and autumnal events in, γ and neutron, 20: 36609
radiosensitivity of southeastern, predicted seasonal, 20: 36551
TRINO POWER REACTOR
containment structure design, 20: 38522
TRITIUM
beta activity from, design of counter using plastic scintillator for measuring, 20: 37087
beta activity from, limitations in liquid scintillation emulsion counting of, 20: 36720
beta activity in liquid phosphors of, performance of surface roughened glass vessels for measuring, 20: 37084
carbon-12 reactions (C-12,pγ) at 22 Mev, carbon-14 level lifetimes from, 20: 38008(R) (AECL-2595)
carbon-12 reactions (C-12,nγ) at 12 and 17.75 Mev, nitrogen-14 level lifetimes from, 20: 38008(R) (AECL-2595)
content in water vapor in atmosphere, method for measuring, 20: 37028
determination by liquid scintillation counting, use of external alpha or gamma source in automatic corrections in, 20: 36743
determination of, in biological and organic materials, combustion method for, 20: 36721
determination of, in organic compounds, oxygen-tube combustion method for scintillation, 20: 36723
determination of, in plant tissue by liquid scintillation counting, oxygen flask combustion technique for sample preparation for, 20: 36764
determination of, instrumentation effects on quenching of energy spectrum in, 20: 36771
deuteron reactions (d,n) with, angular distribution of neutron polarization in, (E), 20: 38163
effects in cyclophosphamide and endoxan on inoperable tumors, 20: 36705
emission in nuclear transitions superfluid model for reduced widths for, 20: 38116
exchange between tritiated water and C–H bond of *tert*-butyl alcohol, catalytic effect of perchloric acid on, 20: 36849
incorporation in actinomycins, biosynthetic procedure for, 20: 36545
incorporation in ethyl, isopropyl, and methyl esters of methanesulfonic acid, 20: 36916
incorporation in 2,4(7-triamino-6-phenylpteridine, method for, 20: 36922
oxygen-16 reactions (O-16,nγ) at 18 Mev, fluorine-18 level lifetimes from, 20: 38008(R) (AECL-2595)
radiation effects on exchange between tritiated water and benzene or toluene, 20: 36868
tracer use for measuring glucose production in dogs, 20: 36565
use in isotopic dilution studies on metabolism in rat skin collagen, 20: 36562
uses in carbon dioxide sensor for Gemini spacecraft, 20: 37064
TRITIUM COMPOUNDS
beta activity in surface films of, scintillation method for measuring, 20: 36738
TRITONS
effects on alkali metal and alkaline earth bromates, 20: 36899
reaction (t,p) with copper-63 and copper-65 at 12 Mev, copper-65 and copper-67 energy levels from, (E), 20: 38035
reactions (t,α) and (t,p) with calcium-48 and titanium-50 at 7.5 Mev, (E), 20: 38063
reactions (t,α) with deuterium at 0.115 to 1.650 Mev, differential cross sections for, (E), 20: 38130
TRYPSIN
analytical use for determination of silicon in sputum by activation methods, 20: 36542
effects on dose response in irradiated hamster and HeLa cells after plating and trypsinization, 20: 36664
TUBERCULOSIS
antigen test for, using iodine-131, 20: 36681
diagnosis of, by determination of silicon content in sputum by activation analysis, 20: 36542
TUBES
fabrication of Zircaloy-2, effects on crystal structure of, 20: 37237
flow of two-phase mixtures through, liquid volume fraction measurements in upward adiabatic, 20: 36985 (EURAEC-1088)
flow upward in, hydrodynamic characteristics of bubbly, 20: 36988 (TID-23261)
TUMORS
effects on radiation effects on proteins in rats, 20: 36582
radiation effects on viability of Ehrlich ascites, use of dyes for assaying, x, 20: 36631
radiotherapy of, dose distribution in deep, 20: 36702
radiotherapy of, use of tritiated-thymidine for studying cell kinetics in, 20: 36704
radiotherapy of, using tritium-labeled nitrogen mustard gas derivatives, 20: 36705
uptake of iodine-131 and mercury-203-labeled compounds in oxygen environment from hydrogen peroxide breakdown, 20: 36576
TUNGSTEN
atom reactions with, electron ejection from helium and neon, (E), 20: 37450
chemical reactions with nitrogen plasmas and subsonic air at high heat fluxes, 20: 37188
chemical reactions of brass-infiltrated, with nitrogen plasmas and subsonic air at high heat fluxes, 20: 37188
chemical reactions of silver-infiltrated, with nitrogen plasmas and subsonic air at high heat fluxes, 20: 37188
chemical reactions of aluminum–tin alloy-infiltrated, with nitrogen plasmas and subsonic air at high heat fluxes, 20: 37188
chemical reactions of copper silicide-infiltrated, with nitrogen plasmas and subsonic air at high heat fluxes, 20: 37188
compaction of powdered, high-pressure methods for, 20: 37200
electron emission from barium- and cesium-surrounded models for, (T), 20: 37431(R) (INDEC-SR-7, pp 3.76-111)
evaporation in vacuum at 2063 to 3203°K, effects of pressure on, 20: 36834
ionization and work functions of, critical temperatures for, 20: 37277
laser beam reactions with, ion emission from, 20: 37298
preparation and properties of powder-compact plates of, for ionizers, 20: 37199
protection against oxidation, silicon carbide coatings for, 20: 37189
separation from neutron-irradiated biological materials by ion exchange, 20: 36762
tensile properties of wires of, at 1200 to 2000°F, 20: 37251
yields from radiolysis of tungsten phthalocyanine, 20: 36886
TUNGSTEN ALLOYS
Be–Nb–W, tensile properties of, 20: 37245
Cr–Co–Fe–W, corrosion of Rexalloy 33, by boiling hydrofluoric acid–nitric acid solutions, 20: 37169(R) (BMI-1774)
Cu–W, properties of tungsten-strengthened composite, 20: 37246
Nb–W, tensile properties of, 20: 37245
Nb–W–Zr, tensile properties of, 20: 37245
Re–W, faulting in, effects of cold working on, 20: 37217
Re–W, ionization and work function of, critical temperatures for,

20: 37277
TUNGSTEN FLUORIDES
reactions with uranium hexafluoride, 20: 36803
TUNGSTEN IONS
effects on copper determination, 20: 36726
TUNGSTEN ISOTOPES W-180
energy level transitions in isomeric, (E), 20: 38027
TUNGSTEN ISOTOPES W-182
energy level at 1.2895 Mev, magnetic moment of, (E), 20: 38134
TUNGSTEN OXIDES
Nd_2O_3–WO_3, phase diagrams, 20: 37240
TUNGSTEN SILICIDES
Nb_5Si_3–W_5Si_3, oxidation and thermal stability of, at high temperatures, 20: 37262
$NbSi_2$–WSi_2, oxidation and thermal stability of, at high temperatures, 20: 37262
TUNGSTEN SYSTEMS
B–Nb–W, phase studies of, 20: 37261
C–Nb–W–Zr, tensile properties of D-43, effects of brittle coatings on, 20: 37276
LaB_6–W, physical properties and work function of, 20: 37258
PuN–W, criticality and burnup as fast reactor fuel, 20: 38442 (BNWL-283)
ThO_2–W, crystal structure and properties of tungsten-base, effects of hafnium, molybdenum, niobium, rhenium, and tantalum on, 20: 37185
ThO_2–W–Zr, crystal structure and properties of tungsten-base, 20: 37185
UO_2–W, criticality and burnup as fast reactor fuel, 20: 38442 (BNWL-283)
W–ThO_2, chemical reactions with nitrogen plasmas and subsonic air at high heat fluxes, 20: 37188
TURBINES
design and performance of, for nuclear power plants, 20: 38521
efficiency of nuclear power plants using gas-driven, 20: 38513
TWEEN 20
metabolism of carbon-14-labeled, in rats, 20: 36921
preparation of carbon-14-labeled, methods for, 20: 36921

U

ULTRASONICS
effects on ductility of boron-bearing stainless steel, 20: 37221
ULTRAVIOLET RADIATION
effects on blood serum proteins, chemical, 20: 36579
effects on charge distributions in silicon oxides, 20: 37285
effects on collagen, determination by magnetic resonance spectroscopy, 20: 36585
effects on cytoplasmic mutant of *Aspergillus nidulans*, 20: 36629
effects on DNA, detection by enzymatic hydrolysis, 20: 36596
effects on DNA, repair mechanisms for, 20: 36578 (ORNL-P-2240)
effects on *E. coli* cultures, increased number of virus-producing cells and other mutants from, 20: 36617
effects on enzymatic breakdown in DNA from *Micrococcus lysodeicticus*, 20: 36583
effects on function of basic cerebral nervous processes in man, 20: 36626
effects on hydration and dehydration of uridine and its derivatives, 20: 36597
effects on kangaroo and mouse skin collagen, 20: 36595
effects on luminescence intensity of anthracene, 20: 37131
effects on mutation induction in synchronous populations of *Streptococcus faecalis*, chromosome mapping by, 20: 36635
effects on mutation induction in bacteriophage T4, 20: 36636
effects on mutation induction in Schizosaccharomyces, environmental effects on, 20: 36653
effects on nucleoli in tissue culture cells, 20: 36592
effects on phthalocyanines, 20: 36886
effects on pyrimidine dimers in *Micrococcus radiodurans* DNA, repair mechanism in, 20: 36610
effects on RNA synthesis, 20: 36555(R) (NYO-2643-22)
effects on skin pigments in mice, 20: 36564
effects on survival of *Paramecium aurelia* and *Tetrahymena pyriformis*, 20: 36661
emission from plasma, equipment development for analyzing, 20: 38335
ULTRAVIOLET SPECTROSCOPY
of irradiated polyethylene, 20: 36857 (COO-1088-21)
UNDERGROUND EXPLOSIONS
cloud formation in Pre-Schooner II cratering event, 20: 36958 (PNE-511)
earth motion in row-charge, 20: 36959 (PNE-603F)
properties of Salmon, 20: 36962
seismic data from PALANQUIN event, 20: 37010 (AD-631340)
use for leaching and mining, in Plowshare project, 20: 36975
use of nuclear, to increase productivity of natural gas wells, 20: 36961 (UCRL-12229)
UNDERWATER EXPLOSIONS
calculations for Salmon, free-field motion from, 20: 36963
decoupling in salt cavities for, seismic displacement potentials for full and partial, (T), 20: 36964
electric transients during, source mechanisms for, 20: 36971
environment from Salmon, post-explosion, 20: 36970
epicenter of Salmon, determination of, 20: 36969
ground motion from Salmon, calculations for free field, 20: 36963
seismic wave amplitudes and travel times from Salmon, 20: 36967
seismic wave amplitude and travel-time spectra from Salmon, analysis of, 20: 36968
seismic waves from decoupled, amplitudes for first-zone P, 20: 36966
uses for excavation, 20: 36972
uses for increasing production of natural gas, 20: 36973
uses for rock breaking, 20: 36974
water wave generation by, simulation of nuclear, 20: 37306 (AD-636408)
URACIL
reactions with hydroxyl radicals, ESR spectral studies on, 20: 36806
URANIUM
analysis of irradiated, for cesium-137 using ion exchange on ring oven, spectrometric, 20: 36758
analysis of, for chromium copper, and manganese by activation methods, 20: 36715
content in African pitchblende, estimation of induced fission vs spontaneous fission from, 20: 37994
cost as fuel, comparison with fossil fuels, 20: 38541
determination in minerals, rocks, and soils using Arsenazo III, photometric, 20: 36774
determination in presence of lead and thorium, photometric, 20: 36773
determination in solutions using gamma absorption, 20: 36767
determination of trace amounts of, separation processes in, 20: 36717
determination of, using arsenazo, cation interference in spectrophotometric, 20: 36716
determination of, using Arsenazo III, photometric, 20: 36778
determination of, in irradiated fuels by mass spectrometry, 20: 36783
fluorination with bromine fluorides, 20: 36950
grain growth in alpha–, 20: 37222
neutron absorption cross section in pitchblende, thermal, 20: 37994
proton reactions at 3 and 28 Bev, A = 100 product yields in, (E), 20: 38098
radioinduced swelling in, mechanisms of, 20: 37299
radioinduced swelling of Zircaloy-clad at 500°C, effects of aluminum, iron, and silicon additions on, 20: 37302
reactions with liquid sodium at high temperatures, 20: 38499 (ANL-7120, pp 839-47)
reactivity of, effects of expansion on, 20: 38428 (ANL-7120, pp 610-13)
separation from cerium, ruthenium, and zirconium by ion exchange using 8-quinolinol, 20: 36754
separation from fission products and neptunium by ion exchange using 8-quinolinol, 20: 36754
separation from graphite-matrix fuels, 20: 36946
separation from irradiated fuels by fluid-bed volatility processes, 20: 36926 (K-L-6091)
separation from irradiated fuels by volatility processes, 20: 36950
separation from irradiated aluminum–uranium fuels by molten-salt fluoride volatility process, 20: 36951
separation from irradiated fuels by pyrochemical methods, 20: 36952
separation from lead by electrolytic precipitation, 20: 36773
separation from metal mixtures by thin layer chromatography, 20: 36753
separation from plutonium dioxide–uranium dioxide fuels, 20: 36946
separation from protactinium by solvent extraction using isoamyl alcohol, 20: 36940
separation from sulfate solutions by ion exchange, 20: 36931
separation of, from aqueous alkalized solutions by solvent extraction using hexane–TBP, 20: 36932
separation of, from thallium by ion-exchange chromatography, 20: 36935
separation of, from pyrolytic carbon-clad fuel, 20: 36956(P)
separation of, from fission products by solvent extraction with TBP and cyclohexane, 20: 36714
separation of, from impurities by solvent extraction using tributyl phosphate–4-methyl-2-pentanone, 20: 36716
separation of, from nitrate solutions by solvent extraction using ethyl acetate–tributyl phosphate, 20: 36717
separation of, from aqueous solutions by solvent extraction using benzene and tributyl phosphate, 20: 36718
separation of, from aqueous solutions by solvent extraction using cyclohexane and tributyl phosphate, 20: 36718
URANIUM ALLOYS
Al–U, fabrication of ESSOR fuel elements of, 20: 38480(R) (EUR-2522.f)
Al–U, separation of uranium from irradiated, by molten-salt fluoride volatility process, 20: 36951
Fe–U, effects on compatibility of mixed carbide reactor fuels with

stainless steel, 20: 38466 (ANL-7120, pp 301-13)
fissium–Pu–U, development as fast reactor fuel, 20: 38465 (ANL-7120, pp 289-300)
Mo–Pu–U, development for SEFOR fuels, 20: 38531 (GEAP-5133)
Mo–U, radioinduced swelling of Zirculoy-clad, at 500°C, 20: 37302
Pu–Ti–U, development as fast reactor fuel, 20: 38465 (ANL-7120, pp 289-300)
Pu–Ti–U, melting temperatures of, 20: 38465 (ANL-7120, pp 289-300)
Pu–Ti–U, use as fuel in 1000-Mw(e) fast breeder reactor, 20: 38494 (ANL-7120, pp 94-103)
Pu–U, separation of plutonium from, by solvent extraction using amines, 20: 36948
Pu–U, use as fuel in power breeder reactors, 20: 38476 (ANL-7120, pp 751-8)
Pu–U–Zr, development as fast reactor fuel, 20: 38465 (ANL-7120, pp 289-300)
Pu–U–Zr, melting temperatures of, 20: 38465 (ANL-7120, pp 289-300)
Th–U, use as fuel in power breeder reactors, 20: 38476 (ANL-7120, pp 751-8)
U–Zr, solubility in hydrofluoric acid, 20: 36946

URANIUM BORIDES
electron emission from thermionic, (E), 20: 37723

URANIUM CARBIDES
fluorination, 20: 36950
PuC–UC, compatibility with stainless steel, effects of modifying additions on, 20: 38466 (ANL-7120, pp 301-13)
PuC–UC, fabrication and properties as fast reactor fuel, 20: 38467 (ANL-7120, pp 314-27)
PuC–UC, optimization studies of, for use as fast breeder reactor fuel, 20: 38495 (ANL-7120, pp 104-23)
ThC–UC, preparation, 20: 37206

URANIUM CARBONITRIDES
preparation from urania fluidization processes for, 20: 36850

URANIUM CHLORIDES
polarographic behavior of, in dimethylformamide and dimethyl sulfoxide, 20: 36745

URANIUM COMPOUNDS
analysis for impurities by neutron activation analysis, 20: 36714

URANIUM(IV) FLUORIDES
separation from plutonium hexafluorides, 20: 36950

URANIUM(VI) FLUORIDES
preparation and properties of, specifications for, 20: 36945
reactions with bromides, chlorides, and fluorides, 20: 36803
reactions with steam to prepare uranium dioxide, 20: 37205
volatility, 20: 36951

URANIUM IONS
spectra of, effects of chemical bonding and transitions on, 20: 36845

URANIUM ISOTOPES
separation by photochemical methods, 20: 37164

URANIUM ISOTOPES U-232
nuclear strength parameter correlation with beta bands in, (T), 20: 38180

URANIUM ISOTOPES U-234
nuclear strength parameter correlation with beta bands in, (T), 20: 38180

URANIUM ISOTOPES U-235
burnup in natural uranium fuel, determination by gamma spectroscopy, 20: 37287
consumption rate in reactor fuels, 20: 36783
decay constant of isomeric, effect of chemical state on, (E), 20: 38090
neutron Doppler effect in, activation measurements of, 20: 38430 (ANL-7120, pp 616-24)
reactivity in fast-neutron spectra, expansion and temperature effects on, 20: 38429 (ANL-7120, pp 614-15)
reactivity of, effects of expansion and temperature on, 20: 38428 (ANL-7120, pp 610-13)
separation in gaseous diffusion plants, tables of 10-10 uranium unit cost components, 20: 37161 (K-OA-1313)

URANIUM ISOTOPES U-236
production in reactor fuels, 20: 36783

URANIUM ISOTOPES U-238
abundance ratio to plutonium-239 in irradiated fuels, 20: 36783
neutron Doppler effect of, in ZPR-3 fast assemblies, (E/T), 20: 38427 (ANL-7120, pp 603-9)
neutron Doppler effect in, effects of temperature on, 20: 38428 (ANL-7120, pp 610-13)
neutron Doppler effect in, activation measurements of, 20: 38430 (ANL-7120, pp 616-24)
nuclear strength parameter correlation with beta bands in, (T), 20: 38180
proton fission at 7.1, 9.4, and 12.0 Mev, mass and nuclear charge distributions in, 20: 37995
reactivity in fast-neutron spectra, temperature effects on, 20: 38429 (ANL-7120, pp 614-15)

URANIUM NITRIDES
preparation from uranium dioxide, 20: 37207
preparation from urania, fluidization processes for, 20: 36850
radiation effects on thermal conductivity and thermal expansion of, 20: 37168(R) (BMI-1771)
radiation effects on thermal conductivity of, 20: 37169(R) (BMI-1774)
reactions with niobium-zirconium alloys at high temperatures, 20: 37168(R) (BMI-1771)
reactions with stainless steel at high temperatures, 20: 37168(R) (BMI-1771)
wetting by sodium, temperature effects on, 20: 37168(R) (BMI-1771)
PuN–UN, fabrication of test fuel elements, 20: 37168(R) (BMI-1771)
PuN–UN, fabrication of test fuel elements of, 20: 37169(R) (BMI-1774)
PuN–UN, reactions with niobium-base alloys and stainless steel at high temperatures, 20: 37169(R) (BMI-1774)

URANIUM OXIDES
phase equilibria, 20: 38468 (ANL-7120, pp 389-91)
production, 20: 37205
radiation effects on grain growth and melting of substoichiometric, 20: 38468 (ANL-7120, pp 389-91)
reactivity of, effects of expansion, isotopic composition, and temperature on, 20: 38428 (ANL-7120, pp 610-13)

URANIUM(IV) OXIDES
conversion to uranium carbonitrides and uranium nitrides, fluidization processes for, 20: 36850
crystal structure above 145°C, phases in, (E), 20: 36832
diffusion in, effects of oxide impurities on, 20: 37256
diffusion of xenon in, effects of trapping sites on, 20: 37293
effects of density of, on fission product gas release and sheath expansion in fuel elements, 20: 37254
fission gas emission at 800 to 1600°C, effect of neutron flux on, 20: 38464 (AERE-M-1607)
fission product diffusion from, mechanisms at 150 to 2000°C, 20: 37290
fission product diffusion from, mechanisms at temperatures below 1500°C, 20: 37291
fission product gas behavior in, effect on fuel element design, 20: 38482
fission-gas bubble distribution in post-irradiation annealed, electron microscopy studies on, 20: 37255
krypton and xenon release from, during reactor operations, 20: 37303
magnetic phase change in, from far-infrared absorption spectra, 20: 38383
melting points of hypostoichiometric urania, 20: 37220
preparation of compactible high-density, method for, 20: 37212(P)
processing of irradiated, by chloride and fluoride volatility methods, 20: 36950
production by reduction of higher oxides or conversion of hexafluoride, 20: 37205
production of hypostoichiometric, method for, 20: 37181(P)
radiation effects on carbon-coated particulate, 20: 37168(R) (BMI-1771)
radioinduced swelling in, mechanisms of, 20: 37299
reactions with liquid sodium at high temperatures, 20: 38499 (ANL-7120, pp 839-47)
reactions with nitrogen to prepare uranium nitride, effects of carbon on, 20: 37207
reactions with powdered aluminum at 600°C, 20: 37203
reactions with sintered aluminum at 600°C, 20: 37203
separation from metal oxides in organic slurries, centrifugal, 20: 36933
sintering of powdered, effects of metal oxide additions on, 20: 37202
temperature distribution in, calculation of transient, 20: 38470 (ANL-7120, pp 478-85)
thermal conductivity of hypostoichiometric, 20: 37181(P)
CeO_2–UO_2, radiation effects on clad, 20: 37168(R) (BMI-1771)
CeO_2–UO_2, segregation due to temperature gradients in, 20: 38469 (ANL-7120, pp 400-9)
NaCl–UO_2, fission product recoil ranges in, 20: 37997
PuO_2–UO_2, fabrication of, economics of, 20: 36945
PuO_2–UO_2, movement within cladding in fast reactors, 20: 38473 (ANL-7120, pp 524-33)
PuO_2–UO_2, processing of irradiated stainless steel-clad, 20: 36946
PuO_2–UO_2, separation of uranium from irradiated, 20: 36946
PuO_2–UO_2, stability of solid-solution, at high temperatures, 20: 37169(R) (BMI-1774)
PuO_2–UO_2, use as fuel in power breeder reactors, 20: 38476 (ANL-7120, pp 751-8)
stainless steel–UO_2, fabrication of fuel plates from, 20: 37168(R) (BMI-1771)
ThO_2–UO_2, fabrication into fuel spheres, method for, 20: 37211
ThO_2–UO_2, radiation testing of aqueous fuel suspensions of, 20: 38533(R) (NP-16168(Pt.A))
ThO_2–UO_2, use as fuel in power breeder reactors, 20: 38476 (ANL-7120, pp 751-8)
UO_2–W, criticality and burnup as fast reactor fuel, 20: 38442 (BNWL-283)
UO_2–ZrO_2, radiation effects on calcia-stabilized clad, 20: 37168(R) (BMI-1771)
UO_2–ZrO_2, radintion effects on calcia-stabilized clad, 20: 37169(R)

(BMI-1774)
URANIUM SILICATES
formation of, in silica solution, effect of insoluble uranyl ions on, 20: 36797
URANIUM SILICIDES
radioinduced swelling of Zircaloy-clad, at 500°C, 20: 37302
URANYL COMPOUNDS
polarographic behavior of, in dimethylformamide and dimethyl sulfoxide, 20: 36745
URANYL IONS
complexes with arsenazo, stability of, 20: 36716
complexes with phenanthroline, stability of, 20: 36716
incorporation of insoluble, in calcium and iron carbonates, 20: 36796
incorporation of insoluble, during silicate formation, 20: 36797
URANYL NITRATES
$(NH_4)_2CO_3$–$MgCl_2$–SiO_2–$UO_2(NO_3)_2$, reactions in, silicate formation in, 20: 36797
$(NH_4)_2CO_3$–SiO_2–$UO_2(NO_3)_2$, reactions in, silicate formation in, 20: 36797
URANYL SULFATES
Cl^-–NO_3^-–UO_2SO_4, ion exchange equilibria in, 20: 36931
UREA, 1-[3-(CHLOROMERCURI)-2-METHOXYPROPYL]-
uptake of mercury-203-labeled, by tumor tissues in oxygen environment in man and rabbits, 20: 36576
UREA COMPLEXES
effects of nitrosomethylurea on peas, genetic, 20: 36634
URIDINE
radiation effects on hydration and dehydration reactions of, uv, 20: 36597
URIDYLIC ACID
radiation effects on hydration and dehydration reactions of, uv, 20: 36597
URINE
analysis of, for tritium, combustion method for, 20: 36721
radiation effects on deoxyriboside excretion in dog, pig, and sheep, gamma, 20: 36604
UTERUS
radiotherapy of cancer of, remote control cobalt-60 unit for, 20: 36687
radiotherapy of carcinomas of, dose distribution in radium, 20: 36699

V

VACUUM SEALS
design of flange-aluminum foil gasket for ultra-high vacuum use, 20: 37000 (UCID-4548(Rev.4))
VAN ALLEN RADIATION BELTS
charged-particle distribution in, review of, 20: 37911
electron and proton energy and intensity in outer, (E), 20: 37905
electron distributions in, spikes in energetic, (E), 20: 37903
origin and formation of, charged particle drift mechanism for, (T), 20: 37909
particle diffusion, acceleration, and losses in, equatorial orbit study of, 20: 37489
properties of, review of, 20: 37489
stability of, electron and proton critical flux effects on, (T), 20: 37910
structure of, review of, 20: 37899
VAN DE GRAAFF ACCELERATORS
beam injection system for, design of nanosecond ion pulsed for, 20: 37337
voltage calibration of 400-kv, technique for rapid, 20: 37331
VANADIUM
effects on crystal field properties of zirconium oxide, 20: 36854
neutron absorption cross section in pitchblende, thermal, 20: 37994
reactions with liquid sodium at high temperatures, 20: 38499 (ANL-7120, pp 839-47)
separation of, from thallium by ion-exchange chromatography, 20: 36935
superconducting mixed-state structure in, NMR and relaxation studies of, 20: 37963
VANADIUM ALLOYS
development as fuel jacket material for fast reactors, 20: 38465 (ANL-7120, pp 289-300)
Al–V, properties of intermetallic compound, 20: 37260
Ga–V, critical field of superconducting V_3Ga, (T), 20: 37936 (CLM-R-60)
Nb–V–Ti, oxidation by air at 900 to 1200°C, kinetics and mechanisms of, 20: 37191
Ti–V, reactions with liquid sodium at high temperatures, 20: 38499 (ANL-7120, pp 839-47)
Ti–V, use as fuel element cladding material in 1000-Mw(e) fast breeder reactor, 20: 38494 (ANL-7120, pp 94-103)
VANADIUM FLUORIDES
reactions with chlorides, fluorides, and sulfides, 20: 36804
VANADIUM IONS
effects on copper determination, 20: 36726
VANADIUM ISOTOPES V-51
carbon-12 reactions up to 120 Mev, copper-63 compound nucleus formation in, (E), 20: 38147
nuclear quadrupole moment of, (E), 20: 38026
spin-lattice relaxation in superconducting vanadium silicide at low temperatures, 20: 37964
VANADIUM OXIDES
effects on sintering behavior of urania powders, 20: 37202
VANADIUM SILICIDES
vanadium-51 spin-lattice relaxation at low temperatures in superconducting, 20: 37964
VAPOR PRESSURE
molecular effusion method for measuring, 20: 37307 (LA-3509)
of reactor fuel materials, equations for, 20: 38433 (ANL-7120, pp 641-53)
VELA PROJECT
seismic data from PALANQUIN event, 20: 37010 (AD-631340)
VESPIDAE
radiation effects on genetic variability in Habrobracon, gamma, 20: 36659
VESSELS
design for use in measurement of leakage rate, 20: 36978 (NAA-SR-12001)
fire resistance tests of wood containers for shipping fuel cores, 20: 37024 (NLCO-899)
VINYL COMPOUNDS
graft-copolymerization of, with cellulose esters, 20: 36906(P)
VIRUSES
effects on RNA synthesis in cultured cells, 20: 36555(R) (NYO-2643-22)
radiation effects on DNA in, repair mechanisms for uv and x, 20: 36578 (ORNL-P-2240)
VISUAL PURPLE
luminescence in, relation of x-ray visibility to, 20: 36587(T)
VITAMIN K
effects on radiosensitivity of bacteria, spores, and yeasts, 20: 37144
VOLATILITY SEPARATION PROCESSES
development of fluid-bed, for processing irradiated fuels, 20: 36926 (K-L-6091)
development of, for treatment of irradiated fuels, 20: 36950

W

WASTE DISPOSAL
book: *The Radiochemical Manual*. Second Edition, 20: 36924
ground storage method of, 20: 38539(P)
marine, physicochemical properties of cesium-137, cobalt-60, strontium-89, and strontium-90 in, 20: 38537
methods of, technical progress review of, 20: 38538
WASTE PROCESSING
calcination methods of, fluid-bed, 20: 38538
conversion to glasses, 20: 38538
incorporation in asphalt for, 20: 38538
ion-exchange methods of, for low- and intermediate-level-activity wastes, 20: 38538
methods of, technical progress review of, 20: 38538
WASTE SOLUTIONS
hazards of, from medical use of unsealed radioactive sources, 20: 36678
ruthenium separation from, by cellulose–bentonite flocculation, 20: 36929
separation of aluminum nitrate nonahydrate from Redox acid, by crystallization techniques, 20: 36925 (HW-82771(Pt.3))
separation of barium-137, cesium-137, cobalt-60, and strontium-89 from, using coal humic acid column, 20: 36930
WATER
boiling in rod bundles, critical, (T), 20: 36992
cerium compound absorption spectra in, 20: 36831
content in cereals, determination of, using neutron thermalization, 20: 37154
corrosive effects on stainless steel, gamma radiation effects on, 20: 37182
cosmic meson (μ) reactions with, energy losses from relativistic, (T), 20: 37707
decontamination of, by sorption of iodine-131 on hydrated ferric oxide containing silver, 20: 36800
effects of flooding, on reactivity of gas- and steam-cooled fast reactors, 20: 38439 (ANL-7120, pp 826-36)
effects on gamma radiation effects on potato starch, 20: 36599
effects on radioinduced decomposition of pectins, 20: 36879
effects on radioinduced polymerization of allyl alcohol, 20: 36880
explosions in, pressure produced by contained, 20: 38459 (ANL-7120, pp 720-33)
flow through tube apertures at high pressures, analyses of, 20: 36990
mixing with air, tracer study of, 20: 36989 (WAPD-TM-492)
molecular motion in, neutron scattering studies of, 20: 36821

neutron distribution along cylindrical ducts in, fission, (E), 20: 38351
neutron scattering by, hindered-translator model for one-particle motions in slow, 20: 37999
radioisotope distribution in, in closed vessels, 20: 36711
separation of fission products from, by foaming, 20: 36934
sorption by thorium oxides, 20: 36843
air–water, bubbly flow upward in tubes, hydrodynamic characteristics of, 20: 36988 (TID-23261)
CCl_4–TBP–H_2O, azeotropic distillation of, 20: 36731
dioxane–H_2O, cerium compound absorption spectra in, 20: 36831
TBP–H_2O, cerium compound absorption spectra in, 20: 36831
WATER-d_2
analysis for hydrogen by thermal neutron transmission, 20: 36740
effects on reactivity of large steam-cooled fast power reactors, 20: 38438 (ANL-7120, pp 815-25)
production of, by GS process, performance testing of sieve trays for, 20: 37160 (DP-1025)
radiation effects on deuterium exchange with benzene, cyclohexane, and *n*-hexane, gamma, 20: 36866
WATER-t
content in atmosphere, 20: 37028
radioinduced tritium exchange with benzene and toluene, 20: 36868
WATER-t_2
content in atmosphere, 20: 37028
tritium exchange with *tert*-butyl alcohol, effects of perchloric acid on, 20: 36849
WATER COOLED REACTORS
coolant void coefficients for steam-cooled fast, extrapolation from critical assembly measurements, 20: 38425 (ANL-7120, pp 585-97)
fuel element dryout heat flux in, 20: 38409 (AECL-2586)
heat transfer limitations on fuel elements, 20: 38484
performance of steam-cooled fast power breeder, at 1200 psi, 20: 38496 (ANL-7120, pp 136-40)
physics parameter study of large steam-cooled fast power, 20: 38438 (ANL-7120, pp 815-25)
reactivity changes in, kinetic response prediction for, 20: 38449
safety of steam-cooled fast, during flooding, 20: 38439 (ANL-7120, pp 826-36)
WATER MODERATED REACTORS
coolant density profile in, computer program for, 20: 38450
neutron flux distribution in, computer program for, 20: 38450
reactivity changes in, kinetic response prediction for, 20: 38449
WATER SUPPLIES
radioactivity of Maine and New Hampshire, 20: 37006
research on underground, using gamma and neutron scattering, 20: 37135
WATER VAPOR
effects on radioinduced recombination of hydrogen and oxygen, 20: 36910
tritium content in atmospheric, method for measuring, 20: 37028
WATER WAVES
propagation from underwater nuclear explosions, simulation of, 20: 37306 (AD-636408)
WELDING
methods for fuel element cladding and end caps, 20: 37208
methods for pressure tubes, explosive, 20: 37168(R) (BMI-1771)
methods for pressure tubes, explosive, 20: 37169(R) (BMI-1774)
WELL LOGGING
analysis of iron-bearing ores and rocks in boreholes, activation, 20: 37019
analysis of rocks in boreholes, activation, 20: 37018
instruments and techniques for, radiometric, 20: 37060
neutron source for pulsed neutron-neutron, in gas and oil wells, 20: 37017
soil density and moisture measurements using gamma and neutron scattering, 20: 37135
WELLS
productivity of natural gas, improvement by underground nuclear explosions, 20: 36961 (UCRL-12229)
WHEAT
effects of free lipid fraction from irradiated seedling bean leaves on seed of, toxic, 20: 36598
radiation effects on mutations in embryos of, gamma, 20: 36650
radioinduced mutations in, fast neutron and gamma, 20: 36620
radiosensitivity of, effects of polyploidy on gamma, 20: 36648
WHISTLERS
analysis of proton, for density determination in ionosphere, (T), 20: 37885
WIND
equations for inrush, development of, 20: 36995 (AD-636794)
WIRES
superconductivity of niobium–oxygen–titanium, effects of crystal structure on, 20: 37267
superconductivity of tantalum–titanium, effects of crystal structure on, 20: 37268
tensile properties of tungsten, at 1200 to 2500°F, 20: 37251
WOOD
plastic–wood, radioinduced polymerization, 20: 37145
WORMS
chromium distribution in polychaete, 20: 36552
radiation effects on embryos of blindworm, x, 20: 36615

X

X RADIATION
absorption of cosmic, by interstellar and intergalactic matter, 20: 37485
auroral zone, conjugate balloon observations, 20: 37914
dose estimations for, current intensity and flux in, 20: 37091
dosimetry of, Finnish and Swedish standard chambers for, 20: 37078
effects in producing lymphomatoses of thymic origin in mice, 20: 36613
effects on aging of chicken embryos, 20: 36605(R) (COO-1119-5)
effects on blood plasma proteins in Hiroshima bomb survivors, cancer patients, and personnel, 20: 36581
effects on blood serum proteins, chemical, 20: 36579
effects on calcium–sodium chloride–silver crystals, color centers from, 20: 38396
effects on calf-thymus DNA, protective effects of disulfides against, 20: 36665
effects on cerebral cortex of monkeys, 20: 36656
effects on charge distributions in silicon oxides, 20: 37285
effects on collagen, determination by magnetic resonance spectroscopy, 20: 36585
effects on coloration and d-c conductivity of pure and doped sodium chloride crystals, 20: 38373
effects on content and metabolism of phosphoproteins in denerved and intact muscles in rabbits, 20: 36602
effects on delayed hypersensitivity in guinea pigs and rabbits, 20: 36655
effects on DNA synthesis in regenerating rat liver, mechanism of, 20: 36593
effects on DNA, repair mechanisms for, 20: 36578 (ORNL-P-2240)
effects on egg-to-adult viability in *D. melanogaster*, 20: 36618
effects on embryos of blindworm, 20: 36615
effects on fatty acid content in free lipid fraction beam leaves, 20: 36598
effects on frozen iron sulfate solutions, 20: 36867
effects on gastric emptying in rats, part-body, 20: 36628
effects on glycolysis and respiration in guinea pig and rat retina, 20: 36630
effects on growth of lymphoma cells by exposure of culture medium, 20: 36633
effects on hamster and HeLa cells after plating and trypsinization, dose response in, 20: 36664
effects on histology of rat spleen during immune response, local, 20: 36637
effects on host response to tapeworms, 20: 36607(R) (TID-23114)
effects on *Hymenolepis microstoma*, 20: 36662
effects on kidney tissues and renal clearance of mice, 20: 36608
effects on light-sensitivity of film, 20: 36895
effects on methylation of guanidinacetic acid in rat liver, 20: 36603
effects on mice, protective effects of *Bacillus subtilis* preparations against, 20: 36673
effects on MOS transistors, positive charge distributions in dielectric layer from, (E), 20: 37130
effects on mutation induction in Schizosaccharomyces, environmental effects on, 20: 36653
effects on nicotinamide adenine dinucleotides content in rat thymocytes, 20: 36590
effects on nuclear proteins in *Vicia faba*, cytophotometric measurements on, 20: 36588
effects on phosphatide content in rats, 20: 36606(R) (NYO-1864-23)
effects on photoconductivity of anthracene, 20: 36873
effects on phthalocyanines, 20: 36886
effects on plants, leaves and leaf extracts premature aging and autumnal events, 20: 36609
effects on point defects in plastically deformed lithium fluoride at low temperature, 20: 38368
effects on potassium dihydrogen arsenate, ESR studies of, 20: 36884
effects on properties of DNA in rat tissues, whole-body, 20: 36591
effects on proteins in rats, effects of serum lyophilization and tumors on whole-body, 20: 36582
effects on rat offspring, 20: 36643
effects on rat oocytes, 20: 36632
effects on rats, biological, 20: 36654
effects on seeds of sweet clover and barley, importance of experimental conditions on, 20: 36658
effects on somatic crossing over in *D. melanogaster*, effects of age on location of, 20: 36619

effects on surface area of calcium oxide, 20: 36904
effects on survival of *Paramecium aurelia* and *Tetrahymena pyriformis*, 20: 36661
effects on thermal decomposition of mercury oxalate, 20: 36898
effects on viability of Ehrlich ascites tumor cells, use of dyes for assaying, 20: 36631
emission by californium-252 fission fragments, (E), 20: 38095
energy spectra and flux of primary cosmic, at 20 to 50 kev, (E), 20: 37580
energy spectra of galactic, interpretation of, 20: 37488
energy spectra of isotropic galactic, (E), 20: 37500
monitoring in personnel in Prague, use of film dosimeters for, 20: 37035
scattering by RNA molecules in solution, low-angle, (T), 20: 36586(T)
scattering from crushed coal, determination of ash content by back-, 20: 37153
sources of 20 to 58 kev, stellar, (E), 20: 37376
spectra from solar flares, 20: 37360
use for propulsion of interstellar vehicles, (T), 20: 36997
use for quartz crystal alignment for acoustic wave propagation at low temperatures, 20: 38366
use of low-dose, for therapy in children, 20: 36707
visibility of, relation of rhodopsin luminescence to, 20: 36587(T)

X-RAY-ABSORPTION ANALYSIS
of powdered minerals and ores, instrument for automatic continuous, 20: 37152

X-RAY EQUIPMENT
dental and medical, Alaska program for control of, 20: 37042
design and performance of specimen-testing, with temperature control using gas streams, 20: 37047
design of, for x-ray spectroscopic analysis using promethium-147 beta source, 20: 36765

X-RAY FLUORESCENCE ANALYSIS
development of instruments and radiation sources for, 20: 37150
of aqueous suspensions of minerals and ores, instrument for automatic continuous, 20: 37152
use for thickness measurements on metal coatings, 20: 37151
use in continuous analysis of gas mixtures, 20: 36766

X-RAY SOURCES
design and uses of beta-excited, 20: 36915 (N-66-17678)
development of radioisotope, for x-ray fluorescence analysis, 20: 37150

X-RAY SPECTROMETERS
coincidence circuits for, design and performance of, 20: 37093

XANTHATES
radiation effects on flotation properties of, for pure minerals and commercial ores, gamma, 20: 36893

XANTHINES
reactions with hydroxyl radicals, ESR spectral studies on, 20: 36806

XENON
diffusion in uranium dioxide, effects of oxide impurities on, 20: 37256
diffusion in urania, effects of trapping sites on, 20: 37293
xenon-131 NMR in liquid and solid, at 4.2 to 250°K, (E), 20: 38404
xenon-131 quadrupole relaxation time in liquid and solid, temperature dependence of, (T), 20: 38392

XENON IONS
sputtering on copper at 100 kev to 1 Mev, 20: 37468

XENON ISOTOPES Xe-131
energy level at 364 kev, half life of, (E), 20: 38031
energy levels of, energy ratios and spins of, (E/T), 20: 38022
nuclear magnetic resonance in liquid and solid xenon at 4.2 to 250°K, (E), 20: 38404
nuclear quadrupole relaxation time in liquid and solid xenon, temperature dependence of, 20: 38392
spin lattice relaxation time in solid xenon, (E/T), 20: 38404

XENON ISOTOPES Xe-133
release from irradiated uranium dioxide, apparent diffusion coefficient, 20: 38464 (AERE-M-1607)

XENON ISOTOPES Xe-134
diffusion from BeO–UO_2 and UO_2 fuel elements during reactor operation, 20: 37303

XENON ISOTOPES Xe-135
energy levels, (E), 20: 38099

XENON ISOTOPES Xe-136
deuteron reactions (d,ρ) and (d,t) at 15 Mev, xenon-135 and xenon-137 energy levels from, (E), 20: 38099

XENON ISOTOPES Xe-137
energy levels, (E), 20: 38099
half life measurement, 20: 38017

XENON ISOTOPES Xe-138
half life measurement, 20: 38017

XENON ISOTOPES Xe-139
half life measurement, 20: 38017

XENON ISOTOPES Xe-140
half life measurement, 20: 38017

XYLENE
effects on solvent properties of diisopentyl methylphosphonate for thorium in nitric acid solutions, 20: 36942

Y

YEASTS
radiation effects on, in fruit juices, 20: 37156
radiation effects on, kinetic regularities in regeneration of, 20: 36642
radiosensitivity of, effects of chemicals on, 20: 37144

YTTERBIUM
determination in hydrochloric acid solutions, spectrographic carrier-distillation, 20: 36729
energy levels of, ionization energies from, (T), 20: 37439
neutron absorption cross section in pitchblende, thermal, 20: 37994

YTTERBIUM ACETATES
dissociation constants of, electrolytic, 20: 36830

YTTERBIUM ALCOHOLATES
preparation of, and thermal decomposition to oxide coatings and powders, 20: 36851

YTTERBIUM ALLOYS
La–Yb, superconducting transition temperature of, pressure dependence of, (E/T), 20: 37965
Sb–Yb, crystal structure of $YbSb_2$ in, 20: 37238

YTTERBIUM CHROMITES
spectra of, infrared, 20: 36807

YTTERBIUM COMPLEXES
with tartaric acid and trihydroxyglutaric acid, stability constants for, 20: 36838

YTTERBIUM HYDROXIDE OXIDES
preparation and crystal structure of, 20: 36791

YTTERBIUM IONS
electron paramagnetic resonances in cesium oxide single crystals at 10 Bc, (E), 20: 38391
spectra of, effects of chemical bonding and transitions on, 20: 36845

YTTERBIUM ISOTOPES Yb-168
energy level transitions from thulium-169 (p,2n) reactions, ground state rotational, 20: 38008(R) (AECL-2595)

YTTERBIUM ISOTOPES Yb-171
hyperfine structure in cesium oxide single crystals at 10 Bc, EPR determination of, (E), 20: 38391

YTTERBIUM ISOTOPES Yb-173
hyperfine structure in cesium oxide single crystals at 10 Bc, EPR determination of, (E), 20: 38391

YTTERBIUM OXIDES
ReO_2–Yb_2O_3, magnetic properties and structure of compounds formed in, 20: 36784(R) (AD-636054)

YTTERBIUM SULFATES
dissociation constants of, electrolytic, 20: 36830

YTTRIUM
determination in hydrochloric acid solutions, spectrographic carrier-distillation, 20: 36729
deuteron reactions (d,n) with, cross sections and mechanism of, (E), 20: 38159
effects on crystal structure of cobalt, iron, and nickel intermetallic compounds, 20: 37243
neutron absorption cross section in pitchblende, thermal, 20: 37994
neutron total cross sections at high energies, fluctuations in, 20: 38173
separation from hydrochloric acid solutions by solvent extraction using dialkyl alkylphosphonates, 20: 36941
separation from water by foaming, 20: 36934
yields from helium ion-induced fission of lead-207 at 41.1 to 26.3 Mev, 20: 37996

YTTRIUM ALCOHOLATES
preparation of, and thermal decomposition to oxide coatings and powders, 20: 36851

YTTRIUM ALLOYS
Co–Y, crystal structure of intermetallic compounds in, 20: 37243
Cr–Y, properties of chromium-base, effects of interstitial nitrogen and oxygen on, 20: 37168(R) (BMI-1771)
Cr–Y, solubility of nitrogen in chromium-base, 20: 37169(R) (BMI-1774)
Fe–Y, crystal structure of intermetallic compounds in, 20: 37243
Ni–Y, crystal structure of intermetallic compounds in, 20: 37243

YTTRIUM BORIDES
crystal structure and thermionic properties of, (E), 20: 38359
mechanical properties of, (E), 20: 38359

YTTRIUM CARBIDES
properties at 20 to 1300°C, 20: 36811

YTTRIUM CHLORIDES
reactions with isopropylamine, thermogravimetric study of, 20: 36853

YTTRIUM CHROMITES
phase studies, 20: 36812

spectra of, infrared, 20: 36807
YTTRIUM FLUORIDES
thermodynamic properties, 20: 36950
YTTRIUM ISOTOPES Y-90
effects with phosphorus-32 on tissue homografts in dogs by lymphatic ablation, 20: 36641
energy levels of, shell-model potential parameters for low-lying, (T), 20: 38145
separation from rain water, 20: 37029
YTTRIUM OXIDES
effects on diffusion in uranium dioxide, mechanism of, 20: 37256
reactions with lanthanum and neodymium oxides in solid state, 20: 36840
ReO_2–Y_2O_3, magnetic properties and structure of compounds formed in, 20: 36784(R) (AD-636054)
YTTRIUM SILICIDES
preparation of, method for, 20: 37176
YTTRIUM SYSTEMS
calcium oxalate–Y, precipitation reactions in, distribution coefficients of, 20: 36794
YUGOSLAVIA
radioisotope production and uses in, 20: 37137

Z

ZERO POWER REACTOR (MARK II)
criticality studies in, 20: 38532 (NASA-TN-D-3555)
ZINC
content of, in sediments of Bay of Roquebrune, 20: 36553
determination in blood and hair of man, activation, 20: 36728
effects on discontinuous precipitation in beryllium–copper alloys, 20: 37253
gamma reactions (γ,α) at 31 Mev, alpha spectra from, (E), 20: 38037
laser beam reactions with, uv spectra from plasma produced from, (E), 20: 38300
neutron total cross sections at high energies, fluctuations in, 20: 38173
separation from metal mixtures by thin layer chromatography, 20: 36753
separation from neutron-irradiated biological materials by ion exchange, 20: 36762
separation of, from thallium by ion-exchange chromatography, 20: 36935
superconducting transition temperature of, isotope effects on, (E), 20: 37959
yields from radiolysis of zinc phthalocyanine, 20: 36886
ZINC ALLOYS
Co–Zn, critical temperature of superconducting, transition-metal impurity effects on depression of, (E), 20: 37955
Cr–Zn, superconducting critical temperature of, transition-metal impurity effects on depression of, (E), 20: 37955
Fe–Zn, critical temperature of superconducting, transition-metal impurity effects on depression of, (E), 20: 37955
Mn–Zn, superconducting critical temperature of, transition-metal impurity effects on depression of, (E), 20: 37955
Ni–Zn, critical temperature of superconducting, transition-metal impurity effects on depression of, (E), 20: 37955
ZINC BROMIDES
$CdBr_2$–$ZnBr_2$, phase diagrams, 20: 36787 (YALE-2723(Vol.1))
ZINC CARBONATES
thermoluminescence properties of, for use as radiation dosimeter, 20: 36913
ZINC CHLORIDES
effects as calcergen, relation to histamine liberator: in rats, 20: 36557
$BaCl_2$–$ZnCl_2$, phase diagrams, 20: 36787 (YALE-2723(Vol.1))
$CaCl_2$–$ZnCl_2$, phase diagrams, 20: 36787 (YALE-2723(Vol.1))
$CdCl_2$–$ZnCl_2$, phase diagrams, 20: 36787 (YALE-2723(Vol.1))
$CuCl$–$ZnCl_2$, phase diagrams, 20: 36788 (YALE-2723(Vol.2))
$HgCl_2$–$ZnCl_2$, phase diagrams, 20: 36788 (YALE-2723(Vol.2))
$InCl_3$–$ZnCl_2$, phase diagrams, 20: 36788 (YALE-2723(Vol.2))
KCl–$ZnCl_2$, phase diagrams, 20: 36788 (YALE-2723(Vol.2))
$MgCl_2$–$ZnCl_2$, phase, 20: 36788 (YALE-2723(Vol.2))
$PbCl_2$–$ZnCl_2$, phase diagrams, 20: 36788 (YALE-2723(Vol.2))
$RbCl$–$ZnCl_2$, phase diagrams, 20: 36788 (YALE-2723(Vol.2))
$SnCl_2$–$ZnCl_2$, phase diagrams, 20: 36788 (YALE-2723(Vol.2))
$SrCl_2$–$ZnCl_2$, phase diagrams, 20: 36788 (YALE-2723(Vol.2))
$TlCl$–$ZnCl_2$, phase diagrams, 20: 36788 (YALE-2723(Vol.2))
ZINC COMPLEXES
with tetraphenylporphine in dioxane, gamma radiolysis of, 20: 36889
ZINC FLUORIDES
AgF–ZnF_2, phase diagrams, 20: 36787 (YALE-2723(Vol.1))
KF–ZnF_2, phase diagrams, 20: 36788 (YALE-2723(Vol.2))
LiF–ZnF_2, phase diagrams, 20: 36788 (YALE-2723(Vol.2))
NaF–ZnF_2, phase diagrams, 20: 36788 (YALE-2723(Vol.2))
RbF–ZnF_2, phase diagrams, 20: 36788 (YALE-2723(Vol.2))
ZINC IONS
effects on copper determination, 20: 36726
reactions in copper at 150 kev, thermal annealing of damage from, 20: 38378
ZINC ISOTOPES Zn-64
formation and decay in compound-nucleus reactions, 20: 38152
ZINC ISOTOPES Zn-65
uptake from infected intestine of chickens, 20: 36566
ZINC ISOTOPES Zn-71
yields from helium ion-induced fission of lead-207 at 41.1 to 26.3 Mev, 20: 37996
ZINC ISOTOPES Zn-72
yields from helium ion-induced fission of lead-207 at 41.1 to 26.3 Mev, 20: 37996
ZINC OXIDES
effects on rate of polymerization of allyl alcohol, 20: 36880
positronium lifetime in, (E), 20: 37819
radiation effects on, electron and neutron, 20: 37281
ZINC SULFATES
analysis for cobalt, iron, and manganese using ion exchange chromatography and activation methods, 20: 36757
analysis for copper and nickel using ion exchange and activation methods, 20: 36756
analysis for metals, interfering reactions in activation, 20: 36755
radiation effects on electric conductivity of solutions of, gamma, 20: 36912
radiolysis of hydrated, gamma, 20: 36903
ZINC SULFIDES
analysis for cobalt, iron, and manganese using ion exchange chromatography and activation methods, 20: 36757
analysis for metals, interfering reactions in activation, 20: 36755
radiation effects on electric conductivity and Hall effect in monocrystals of, fast-neutron, 20: 36865
ZIRCALOY-2
compatibility with cadmium sulfate, 20: 38447 (WCAP-2867)
crack propagation in pressure tubes of, detection and mechanisms of, 20: 37172
crystal structure of thin-walled tubes of, effects of fabrication on, 20: 37237
fabrication effects on mechanical properties of, 20: 37232
fracture transition temperatures of, review of effects of hydrogen and grain size on, 20: 37187
heat treatment effects on texture of, 20: 37198
mechanical properties of alpha-phase, effects of preferred orientation on, 20: 37226
mechanical properties of, effects of preferred orientation on, 20: 37232
plastic flow of, determination by hardness, 20: 37230
ZIRCALOY-4
fabrication into aluminum-lined tubes of, by explosive welding, 20: 37168(R) (BMI-1771)
fabrication into aluminum-lined tubes of, by explosive welding, 20: 37169(R) (BMI-1774)
fatigue at 1175°R of cold-worked, mechanisms of, 20: 37235
ZIRCONIUM
analysis for oxygen by helium-3 activation, 20: 36741
crystal structure of, determination by polarized-light microscopy, 20: 37266
determination of, using Arsenazo III, photometric, 20: 36778
deuteron reactions (d,n) with, cross sections and mechanism of, (E), 20: 38159
dislocations in, etching method for, 20: 37227
effects on crystal structure and properties of thoria-tungsten cermets, 20: 37185
effects on mechanical and thermodynamic properties of niobium nitrides, 20: 37274
effects on tensile properties of niobium alloys, 20: 37245
embrittlement of alpha-, review of effect of hydrogen on, 20: 37187
fracture at 78, 197, and 373°K, mechanisms of, 20: 37231
hydride orientation in single-crystal tensile specimens of, effects of stress on, 20: 37269
mechanical properties of annealed, rolled-plate at room temperature, effects of prestrain at 77°K on, 20: 37228
neutron absorption cross section in pitchblende, thermal, 20: 37994
neutron total cross sections at high energies, fluctuations in, 20: 38173
plastic deformation of foils of, analysis by electron microscopy, 20: 37248
plastic flow of, determination by hardness, 20: 37230
reactions with liquid sodium at high temperatures, 20: 38499 (ANL-7120, pp 839-47)
separation from cerium, ruthenium, and uranium by ion exchange using 8-quinolinol, 20: 36754
separation from protactinium by solvent extraction using isoamyl alcohol, 20: 36940
separation from water by foaming, 20: 36934

superconductivity of high-pressure form of, 20: 37985
yield point of polycrystalline alpha-phase, mechanisms affecting, 20: 37229
yields from radiolysis of zirconium phthalocyanine, 20: 36886
zone refining of, redistribution of iron and oxygen during, 20: 37177

ZIRCONIUM ALLOYS
mechanical properties of alpha-phase, effects of preferred orientation on, 20: 37226
production of corrosion-resistant, method for, 20: 37194(P)
Al–Zr, properties of intermetallic compound, 20: 37260
Cu–Zr, oxidation by carbon monoxide at high temperatures, mechanisms of, 20: 37183
Ho–Zr, fracture at 78, 197, and 373°K, mechanisms of, 20: 37231
Mg–Zr, recrystallization grain growth of, effects of hydration on, 20: 37252
Mo–Ti–Zr, tensile properties of TZM, effects of brittle coatings on, 20: 37276
Nb–Re–Zr, oxidation by oxygen at 1000°C, kinetics and microstructures of, 20: 37193
Nb–W–Zr, tensile properties of, 20: 37245
Nb–Zr, current losses and magnetic field aberrations from high-field superconducting wires of, in adiabatic demagnetization apparatus, 20: 37970
Nb–Zr, development as fuel jacket material for fast reactors, 20: 38465 (ANL-7120, pp 289-300)
Nb–Zr, heat treatment effects on texture of, 20: 37198
Nb–Zr, hydrogen embrittlement of, review of, 20: 37187
Nb–Zr, mechanical properties of, effects of composition and heat treatments on, 20: 37236
Nb–Zr, oxidation by oxygen at 1000°C, kinetics and microstructures of, 20: 37193
Nb–Zr, phase transformations of, factors affecting, 20: 37234
Nb–Zr, plastic flow of, determination by hardness, 20: 37230
Nb–Zr, reactions with liquid sodium at high temperatures, 20: 38499 (ANL-7120, pp 839-47)
Nb–Zr, reactions with uranium mononitride at high temperatures, 20: 37168(R) (BMI-1771)
Nb–Zr, reactions with plutonium nitride and uranium nitride at high temperatures, 20: 37169(R) (BMI-1774)
Nb–Zr, superconducting properties in strong d-c magnetic fields, (E), 20: 37950
Nb–Zr, transformation temperatures of, effects of cooling rates on, 20: 37233
Nb–Zr, wetting by sodium, effects of temperature on, 20: 37168(R) (BMI-1771)
Nd–Zr, fracture at 78, 197, and 273°K, mechanisms of, 20: 37231
Ni–Nb–Zr, hydrogen embrittlement of, review of, 20: 37187
Pu–U–Zr, development as fast reactor fuel, 20: 38465 (ANL-7120, pp 289-300)
Pu–U–Zr, melting temperatures of, 20: 38465 (ANL-7120, pp 289-300)
U–Zr, solubility in hydrofluoric acid, 20: 36946

ZIRCONIUM BORIDES
conversion of ZrB_{12} to ZrB_2, kinetics and mechanisms of, 20: 36810
preparation by slip casting, method for, 20: 37201

ZIRCONIUM FLUORIDES
purification, 20: 36950

ZIRCONIUM HYDRIDES
crystal orientation in single-crystal zirconium, effects of stress on, 20: 37269
effects on average thermal-neutron capture cross sections of media, (T), 20: 37991

ZIRCONIUM HYDROXIDES
solubility in sodium perchlorate solutions, 20: 36789

ZIRCONIUM IONS
effects on copper determination, 20: 36726

ZIRCONIUM ISOTOPES
purification of electromagnetically separated, 20: 37163

ZIRCONIUM ISOTOPES Zr-90
alpha elastic and inelastic scattering at 65 Mev, differential cross sections for, (E/T), 20: 38092
alpha reactions (α,He-3) at 65 Mev, (E/T), 20: 38092
deuteron reactions (d,p) at 2.7 to 3.6 Mev, proton angular distributions from, (E), 20: 38096
energy levels of, shell-model potential parameters for low-lying, (T), 20: 38145
neutron strength functions of, calculation of, 20: 38038

ZIRCONIUM ISOTOPES Zr-91
alpha elastic and inelastic scattering at 65 Mev, differential cross sections for, (E/T), 20: 38092
alpha reactions (α,He-3) at 65 Mev, (E/T), 20: 38092

ZIRCONIUM ISOTOPES Zr-92
alpha elastic and inelastic scattering at 65 Mev, differential cross sections for, (E/T), 20: 38092
alpha reactions (α,He-3) at 65 Mev, (E/T), 20: 38092
neutron strength functions of, calculation of, 20: 38038

ZIRCONIUM ISOTOPES Zr-94
neutron strength functions of, calculation of, 20: 38038

ZIRCONIUM ISOTOPES Zr-95
dispersion from fallout in seawater, 20: 37037
yields in proton fission of uranium-238 at 7.1, 9.4, and 12.0 Mev, 20: 37995

ZIRCONIUM ISOTOPES Zr-96
neutron strength functions of, calculation of, 20: 38038

ZIRCONIUM ISOTOPES Zr-97
yields from helium ion-induced fission of lead-207 at 41.1 to 26.3 Mev, 20: 37996
yields in proton fission of uranium-238 at 7.1, 9.4, and 12.0 Mev, 20: 37995

ZIRCONIUM OXIDES
crystal field properties of, effects of chromium and vanadium on, 20: 36854
deposition on graphite by alkoxide decomposition, 20: 36851
effects on corrosion resistance of copper–zirconium alloys, 20: 37183
production of hypostoichiometric dioxide, methods for, 20: 37181(P)
reactions with lanthanum and neodymium oxides in solid state, 20: 36840
vaporization of, thermodynamics of, 20: 36841
Eu_2O_3–ZrO_2, phase studies, 20: 36815
Pd–Ag–ZrO_2, preparation and properties of zirconia-base cermets of, 20: 37209
UO_2–ZrO_2, radiation effects on calcia-stabilized clad, 20: 37168(R) (BMI-1771)
UO_2–ZrO_2, radiation effects on calcia-stabilized clad, 20: 37169(R) (BMI-1774)

ZIRCONIUM SYSTEMS
C–Mo–Ti–Zr, crack formation in Mo-3 alloy ingots, effects of molybdenum capping on, 20: 37219
C–Nb–W–Zr, tensile properties of D-43, effects of brittle coatings on, 20: 37276
C–O–Zr, phase studies, 20: 37264
C–Ta–Zr, phase studies, 20: 37270
ThO_2–W–Zr, crystal structure and properties of tungsten-base, 20: 37185

REPORT NUMBER INDEX

Reports, conference papers and proceedings, numbered translations, and patents abstracted during the period are included in this index. Each item is listed by report number; this is followed by the abstract number and a brief notation regarding public availability. The index entries show which reports are on file in the depository libraries, which reports have been published in open-literature journals (journal citation given), and which reports can be purchased (source and price). Whenever a report is identified by more than one number, cross references from secondary to primary report numbers are cited.

The report number codes apply to AEC reports unless designated otherwise. Non-AEC reports are identified by parenthetical notes after the report codes; e.g., (non-AEC), (British), (Canadian), (French). The note (Misc.) identifies those codes used for both USAEC and non-AEC reports. Patents are listed under the heading "PATENTS"; the country of origin is included in parentheses.

A comprehensive listing of both AEC and non-AEC report codes is contained in TID-85(5th Rev.), *Report Number Series Used by the Division of Technical Information in Cataloging Reports*. This information is also included in the Cumulative Report Number Index (issued annually).

Public Availability of USAEC Reports

All USAEC reports abstracted in *NSA* are available to the public through one or more of the following sources:

(1) Depository libraries in the United States, in other countries, and in international agencies. A list of these depositories appears on the inside covers of each issue of *NSA*.

(2) Scientific and technical journals or other publications.

(3) Microcard Editions, Inc., in Microcard and micronegative form. Orders and inquiries should be sent to: Accounting and Shipping Department, West Salem, Wisconsin 54669.

(4) Clearinghouse for Federal Scientific and Technical Information, U. S. Department of Commerce, Springfield, Virginia 22151.

(5) Superintendent of Documents, U. S. Government Printing Office, Washington, D. C. 20402.

Public Availability of Non-AEC Reports

U. S. Reports. Many reports of U. S. Government agencies are available to the public from the Clearinghouse for Federal Scientific and Technical Information (CFSTI). This availability is given when known. Such reports should be ordered by AD number or NASA-N number. If availability is not shown, inquiries may be directed to CFSTI. In the case of NP numbers, inquiries should be by title and author.

Non-U. S. Reports. Many reports of atomic energy establishments of other countries are deposited in the libraries listed on the inside covers of each issue of *NSA*.

Additionally, the following have made their reports available as indicated.

AUSTRALIA

Australian Atomic Energy Commission Research Establishment. Available upon request from the Library, Australian Atomic Research Establishment, Private Mail Bag, Sutherland, New South Wales, Australia.

BELGIUM

Centre d'Étude de l'Énergie Nucléaire. Available upon request to individuals and organizations, from the Centre d'Étude de l'Énergie Nucléaire (CEN), 31, Rue Belliard, Bruxelles, Belgium.

CANADA

Atomic Energy of Canada Limited. For sale by the Technical Information Officer, Atomic Energy of Canada Limited, Chalk River, Ontario, Canada. Copies are also deposited in libraries in the United Kingdom.

National Research Council of Canada. Available from the National Research Council of Canada, Ottawa 2, Ontario, Canada.

DENMARK

Atomic Energy Commission Research Establishment, Risø. Available on exchange from the Library, Danish Atomic Energy Commission, Risø, Roskilde, Denmark. Also for sale by Jul. Gjellerup, Booksellers, 87 Sölvgade, København K., Denmark.

Danatom. Available on loan from Research Establishment, Risø, Roskilde, Denmark. Copies are available from Danatom, Aurehøjvej 2, Hellerup, Denmark.

EURATOM

Reports from the Commission of the European Atomic Energy Community are available from: Presses academiques europeennes, 98, chaussee de Charleroi, Brussels 6, Belgium; and Office central de vente des publications des Communautes eurodeennes 2, place de Metz, Luxemburg.

FRANCE

Commissariat à l'Énergie Atomique. Inquiries for reports numbered 1-2199 should be addressed to Commissariat à l'Énergie Atomique, Service Central de Documentation, Centre d'Études Nucléaires de Saclay, Boite Postale No. 2, Gif-sur-Yvette (S. et O.), France. Reports numbered 2200 and above are available from La Documentation Francaise, 16 Rue Lord-Byron, Paris VIII, France.

Service Central de Protection contre les Rayonnements Ionisants. Copies are available from Ministère de la Santé Publique, Service Central de Protection contre les Rayonnements Ionisants, B. P. n° 35–LE VESINET (S. et O.), France.

GERMANY

Deutsches Elektronen-Synchrotron DESY. Copies are available from Deutsches Elektronen-Synchrotron Desy, Dokumentation, 2000 Hamburg-Gr. Flottbek 1, Notkestieg 1, Germany.

Gesellschaft für Kernforschung mbH (KFK). Copies are available from Gesellschaft für Kernforschung mbH, 75 Karlsruhe, Postfach 947, Germany. Copies are also deposited in many national nuclear centers in the world.

Kernforschungsanlage. Copies may be ordered from Zentralbibliothek der Kernforschungsanlage Jülich, Jülich, Bundesrepublik Deutschland.

Hahn-Meitner-Institute für Kernforschung. Available without charge from Hahn-Meitner-Institute für Kernforschung Berlin, Bibliothek, Glienicker Strasse 100, 1 Berlin

39, Germany. Copies are deposited in many national nuclear centers in the world.

Johann-Wolfgang-Goethe Universität, Frankfurt Am Main, Institut für Kernphysik, (IKF). Copies are available from Gmelin Institut, 40-42 Varrentrappstrasse, Frankfurt (Main), West Germany.

ISRAEL

Israel Atomic Energy Commission. Available without charge from Ministry of Defence/Atomic Energy Commission, Soreq Research Establishment, Yavne, Israel. Copies are deposited in libraries in Israel and in other countries.

ITALY

Centro Informazioni Studi Esperienze (CISE). For sale at CISE Press Office, Casella Postale 3986, Milano, Italy. Copies are deposited in libraries in Italy.

Comitato Nazionale per l'Energia Nucleare. Copies are available from Comitato Nazionale per l'Energia Nucleare, Divisione Affari Internazionali e Studi Economici, Ufficio Pubblicazioni, Via Belisario, 15, Roma, Italy.

JAPAN

Japan Atomic Energy Research Institute (JAERI). Available from the Staff Supply Cooperative of Japan Atomic Energy Research Institute (JAERI), 1-1 Tamura-Cho, Shiba, Minato-Ku, Tokyo, Japan. Copies are deposited in depositories in Tokyo, Nagoya, and Osaka.

Nagoya University. Copies are available from Research Information Center, Institute of Plasma Physics, Nagoya University, Nagoya, Japan.

University of Tokyo. Available free of charge from Institute for Nuclear Study, University of Tokyo, Tanashi-Machi, Kitatama-gun, Tokyo, Japan.

NETHERLANDS

Reactor Centrum Nederland. For sale by Reactor Centrum Nederland, 112 Scheveningseweg, 's-Gravenhage, The Netherlands. Copies are deposited in university libraries in Holland and in many national nuclear centers in the world.

NEW ZEALAND

Institute of Nuclear Sciences. Copies are available from Librarian, Institute of Nuclear Sciences, D.S.I.R., Private Bag, Lower Hutt, New Zealand. Copies are deposited in other countries.

NORWAY

Forsvarets Forskningsinstitutt. Copies available from Norwegian Defence Research Establishment, Library, P. O. Box 25, Kjeller, Norway.

Institutt for Atomenergi. "KR" reports are available on an exchange basis from the Library, Institutt for Atomenergi, Box 40, Kjeller, Norway. Other series are not generally available to the public.

Norwegian Reactor School. Copies are available from The Library, Institutt for Atomenergi, P. O. Box 40, Kjeller, Norway.

PAKISTAN

Atomic Energy Center. Copies are available from Atomic Energy Center, P. O. Box 658, Lahore, (West Pakistan).

POLAND

Reports of the Polish nuclear institutes are published by the Nuclear Energy Information Center of the Government Commissioner for Use of Nuclear Energy. Copies are available from Ośrodek Informacji o Energii Jądrowej, Warszawa, PKiN, Poland.

SPAIN

Junta de Energia Nuclear. "JEN" reports are available without charge from Servicio de Documentation, Junta de Energia Nuclear, Ciudad Universitaria, Madrid (3), Spain.

SWEDEN

Aktiebolaget Atomenergi. "AE" reports are for sale from Aktiebolaget Atomenergi, Library Section, Box 43041, Stockholm 43, Sweden. Bibliographies and literature surveys of the VDDIT- series may be obtained from Aktiebolaget Atomenergi, Information Office, Scientific and Technical Information, Box 43041, Stockholm 43, Sweden. Other series are not generally available to the public. Organizations in the atomic energy field may obtain copies from Aktiebolaget Atomenergi. Microcopy of AE reports is available from the International Documentation Centre, Tumba, Sweden.

SWITZERLAND

CERN European Organization for Nuclear Research. Available without charge from CERN European Organization for Nuclear Research, Geneva 23, Switzerland. Copies are deposited in libraries in 13 countries.

Eidgenössisches Institut für Reaktorforschung. "EIR" reports are available from Eidgenössiches Institut für Reaktorforschung, c/o Bibliothek, Würenlingen/Ag, Switzerland.

TURKEY

Turkish Atomic Energy Commission. Copies are available free of charge from T.A.E.C., Çekmece Nuclear Research Center, P. O. Box 1, Airport, Istanbul, Turkey.

UNITED KINGDOM

United Kingdom Atomic Energy Authority. Some reports are for sale in the United States by the British Information Service (BIS), 845 Third Avenue, New York, N. Y. 10022. United Kingdom reports generally may be purchased from Her Majesty's Stationery Office, London. Copies not for sale by Her Majesty's Stationery Office may be purchased in microcopy form from Micro Methods Limited, East Ardsley, Wakefield, Yorks, England. Report copies are deposited in a large number of libraries in England, depositories of the USAEC in the United States and abroad, and in most national nuclear centers throughout the world.

Conferences

Published conference proceedings as well as individual unpublished papers from conferences are included in this index. A CONF number is assigned to the conference if published proceedings are received and also if only a single paper is received. The base number used is year-month-sequence. Thus, the number CONF-650101 would indicate that the conference was held in 1965, in January, and that this was the first January 1965 conference so received. This number would be assigned to complete published proceedings, or if individual papers are received, the base number would be extended to include a paper number, i.e., CONF-650101-1. As additional papers are received, they will be assigned consecutive numbers in the series, CONF-650101-1, 2, 3, 4, etc. This numbering system ensures that all papers received from a conference will be associated with that conference in this index.

If published proceedings are received after the receipt of individual papers, the complete proceedings will be abstracted and the abstract number will appear in this index with the base CONF number.

Abbreviations Used in Availability Column

AECL	For sale by Atomic Energy of Canada Ltd., Chalk River, Ontario, Canada.
BIS	For sale by British Information Service, 845 Third Avenue, New York, N. Y. 10022
CFSTI	For sale by the Clearinghouse for Federal Scientific and Technical Information, U. S. Department of Commerce, Spring-

field, Virginia 22151. The symbol "cy" indicates that the format of the item sold may be either a printed document or a photographic reproduction (two-thirds of original size) depending upon the availability of printed stock. The indicated price is for either format. The symbol "mn" is used to indicate that copy is also available in the form of micronegatives (microfiche).

Dep. AEC reports: Full-size copy is on deposit in the depository libraries both inside and outside the United States. These reports are also for sale by Microcard Editions, Inc., Accounting and Shipping Department, West Salem, Wisconsin 54669.

Non-AEC reports: Full-size copy on deposit in the depository libraries in the United States only.

Dep.(mc) Same as for Dep., except copy is in Microcard form.

Dep.(mn) Same as for Dep., except copy is in micronegative (microfiche) form.

DSIR For sale by the National Lending Library for Science and Technology (D.S.I.R.), Boston Spa, Yorkshire, England.

DTI Extension Available from the U. S. Atomic Energy Commission, Division of Technical Information Extension, P. O. Box 62, Oak Ridge, Tennessee 37830.

EM Blueprints and microcopy of AEC engineering drawings are available from Clearinghouse for Federal Scientific and Technical Information, U. S. Department of Commerce, Springfield, Virginia 22151. Current prices of the CAPE- packages may be obtained from this address. TID-4100, available from the Division of Technical Information Extension, P. O. Box 62, Oak Ridge, Tennessee 37831, contains information on all the CAPE- packages for sale.

Gmelin Available at a nominal charge and under the AED- number shown from Atomic Energy Documentation Center, Gmelin Institute, 40-42 Varrentrappstrasse Frankfurt (Main), West Germany.

GPO For sale by the Superintendent of Documents, Government Printing Office, Washington, D. C. 20402.

HMSO Her Majesty's Stationery Office, London.

IAEA Available from the International Atomic Energy Agency, Vienna, Austria, and from its sales agencies in various countries throughout the world. A list of these agencies is found in each STI/DOC and STI/PUB publication.

JCL For sale by the Special Libraries Association Translation Center, John Crerar Library, 35 West 33rd Street, Chicago, Illinois 60616.

LC For sale by the Library of Congress, Photoduplication Service, Washington, D. C. 20540.

NAS National Academy of Sciences, National Research Council, Washington, D. C. 20418.

NRC For sale by the National Research Council of Canada, Ottawa, Ontario, Canada.

ORAU Available on interlibrary loan from the Library, Oak Ridge Associated Universities, Post Office Box 117, Oak Ridge, Tennessee 37830.

ORINS See ORAU.

UKAEA, London Available from United Kingdom Atomic Energy Authority, 11 Charles II Street, London, S. W. 1.

UN United Nations Bookshop, United Nations Headquarters, New York, New York.

USGS Available free of charge from the U. S. Geological Survey, Washington, D. C. 20242.

ZLDI Zentralstelle Für Luftfahrtdokumentation Und-Information, Maria-Theresia-Strasse 21, Munich 27, Germany.

[The symbols "ph," "mf," and "fs" are used to designate that copy is available only in photostat, microfilm, or facsimile form. The symbol "mn" is used to designate that copy is available in micronegative (microfiche) form. The symbol "cy" is used to designate full size or photographically enlarged copy (two-thirds of original size).]

Report No.	Abstract No.	Availability
ACNP–	**(Misc.)**	
66551	20-38486	Dep. mn. CFSTI $2.00 cy, $0.50 mn
AD–	**(Misc.)**	
631340	20-37010	CFSTI $2.00 cy, $0.50 mn
636054	20-36784	CFSTI $2.00 cy, $0.50 mn
636095	20-38189	CFSTI $1.00 cy, $0.50 mn
636408	20-37306	CFSTI $3.00 cy, $0.50 mn
636788	20-38349	CFSTI $2.00 cy, $0.50 mn
636794	20-36995	CFSTI $2.00 cy, $0.50 mn
637513	20-38190	CFSTI $5.00 cy, $1.00 mn
AEC-tr–	**(For complete listing see TID-4025)**	
6782	20-38211	Dep. mn. CFSTI $2.00 cy, $0.50 mn. JCL $4.60 fs, $1.43 mf
AECL–	**(Canadian)**	
2536	20-37066	Dep. mn. AECL $1.00
2578	20-37067	Dep. mn. AECL $1.00
2584	20-38487	Dep. mn. AECL $0.50
2586	20-38409	Dep. mn. AECL $1.00
2595	20-38008	Dep. mn. AECL $1.50
AED-C–	**(Non-AEC)**	
05-05	20-37138	Dep. mn
AEEW-M–	**(British)**	
474	20-38410	Dep. BIS $1.40. HMSO 7s.
AEEW-R–	**(British)**	
396	20-38417	Chartered Mech. Eng., 12: 603(1965)
AERE-M–	**(British)**	
1607	20-38464	Dep. mn
AERE-R–	**(British)**	
4650	20-36850	pp 1-18 of Special Ceramics 1964
4952	20-37299	See CONF-650904-12
4970	20-37255	Nucl. Appl., 2: 123-30(1966)
5031	20-38488	Dep. BIS $1.10. HMSO 5s. 6d.
AFCRL–	**(Non-AEC)**	
66-328	20-38189	See AD-636095
ALO–		
3633-1	20-36983	Dep. mn. CFSTI $5.00 cy, $1.00 mn
ANL–		
6950	20-37195	Dep. mn. CFSTI $2.00 cy, $0.50 mn
7120	20-38489	Dep. mn. CFSTI $9.25 cy, $3.75 mn
APDA–	**(Misc.)**	
301	20-38501	Dep. mn. CFSTI $6.00 cy, $1.25 mn
ARL–	**(Non-AEC)**	
66-0024	20-38190	See AD-637513
BAW–	**(Misc.)**	
3492-1(Suppl.1)	20-38441	Dep. mn. CFSTI $2.00 cy, $0.50 mn
BMI–	**(Misc.)**	
1771	20-37168	Dep. mn. CFSTI $2.00 cy, $0.50 mn
1774	20-37169	Dep. mn. CFSTI $2.00 cy, $0.50 mn
BMwF-FBK–	**(German)**	
66-06	20-37720	Dep. mn
BNL–		
963	20-36984	Dep. mn. CFSTI $2.00 cy, $0.50 mn
9900	20-37925	Progr. Theoret. Phys. (Kyoto), 35: 1111-16(1966)
9996	20-38095	Phys. Rev., 148: 1206-20(1966)
10014	20-38098	Phys. Rev., 148: 1235-40(1966)
10050	20-38048	Nucl. Phys., 86: 102-12(1966)
10060	20-37946	Phys. Rev., 148: 138-45(1966)
10105	20-36821	J. Chem. Phys., 45: 1312-17(1966)
10143	20-37313	Dep. mn. CFSTI $1.00 cy, $0.50 mn
10148	20-37314	Dep. mn. CFSTI $1.00 cy, $0.50 mn
10178	20-38087	Phys. Rev., 148: 1148-50(1966)
10321	20-37068	Dep. mn. CFSTI $1.00 cy, $0.50 mn
10323	20-37315	Dep. mn. CFSTI $1.00 cy, $0.50 mn
10324	20-37316	Dep. mn. CFSTI $1.00 cy, $0.50 mn
10341	20-37317	Dep. mn. CFSTI $1.00 cy, $0.50 mn
10380	20-37934	Dep. mn. CFSTI $1.00 cy, $0.50 mn
10387	20-37823	Dep. mn. CFSTI $2.00 cy, $0.50 mn
10420	20-38009	Dep. mn. CFSTI $1.00 cy, $0.50 mn
10436	20-37318	Dep. mn. CFSTI $1.00 cy, $0.50 mn
10438	20-38010	Dep. mn. CFSTI $1.00 cy, $0.50 mn
10459	20-37730	Dep. mn. CFSTI $1.00 cy, $0.50 mn
10460	20-37731	Dep. mn. CFSTI $1.00 cy, $0.50 mn
10461	20-37732	Dep. mn. CFSTI $1.00 cy, $0.50 mn
10462	20-37733	Dep. mn. CFSTI $1.00 cy, $0.50 mn
BNWL–		
186	20-38411	Dep. mn. CFSTI $2.00 cy, $0.50 mn
260	20-37069	Dep. mn. CFSTI $3.00 cy, $0.75 mn
264	20-38479	Dep. mn. CFSTI $3.00 cy, $0.75 mn
283	20-38442	Dep. mn. CFSTI $2.00 cy, $0.50 mn
BNWL-SA–		
180	20-37230	Electrochem. Technol., 4: 313-17(1966)
247	20-38353	Dep. mn. CFSTI $1.00 cy, $0.50 mn
537	20-37070	Dep. mn. CFSTI $1.00 cy, $0.50 mn
540	20-37220	J. Amer. Ceram. Soc., 49: 395-6(1966)
CAR–		
882-19	20-37824	Dep. mn. CFSTI $5.00 cy, $1.00 mn
CEA-R–	**(French)**	
2906	20-37935	Dep. mn
2976	20-37319	Dep. mn
CISE-R–	**(Italian)**	
105	20-36985	See EURAEC-1088
CLM-R–	**(British)**	
60	20-37936	Dep. mn. BIS $0.30
61	20-38191	Dep. mn. BIS $0.30. HMSO 1s. 9d.
CONF-620502–	**20-36691**	**(43rd Meeting of the German X-Ray Society, Cologne, Germany, May 7–10, 1962) Strahlentherapie, Sonderbaende, 52: 1-372(1963)**
CONF-631114–	**20-37390**	**(Conference on Stellar Evolution, New York, Nov. 13–15, 1963) $19.50**
CONF-640715–	**20-37179**	**(Symposium on Special Ceramics, Stoke-on-Trent, England, July 8–10, 1964) 90s.**
CONF-650405–	**(International Conference on Modern Trends in Activation Analysis, College Station, Tex., Apr. 19–22, 1965)**	
23	20-36782	ORAU. Gmelin, AED-CONF-65-040-36
26	20-36781	ORAU. Gmelin, AED-CONF-65-040-37
CONF-650602–	**(American Nuclear Society 11th Annual Meeting, Gatlinburg, Tenn., June 20–24, 1965)**	
84	20-37303	ORAU. Gmelin, AED-CONF-65-125-119
86	20-36783	ORAU. Gmelin, AED-CONF-65-125-127
CONF-650631–	**(International Powder Metallurgical Conference, New York, June 14–17, 1965)**	
4	20-37210	ORAU. Gmelin, AED-CONF-65-194-4
CONF-650632–	**(7th Biennial Conference on Carbon, Cleveland, June 21–25, 1965)**	
1	20-36799	See GA-6415
2	20-37196	See GA-6439
CONF-650637–	**(International Conference on Luminescent Dosimetry, Palo Alto, Calif., June 21–23, 1965)**	
9	20-36913	ORAU. Gmelin, AED-CONF-65-151-13
CONF-650707–	**20-21164**	**(IEEE Annual Conference on Nuclear and Space Radiation Effects, Ann Arbor, Mich., July 12–15, 1965) Trans. Nucl. Sci., NS-12: 1-155(1965)**
20	20-37132	ORAU. Gmelin, AED-CONF-65-152-23
22	20-38405	ORAU. Gmelin, AED-CONF-65-152-24
23	20-37062	ORAU
CONF-650719–	**(4th Annual Reliability and Maintainability Conference, Los Angeles, July 28–30, 1965)**	

Report No.	Abstract No.	Availability
2	20-37192	ORAU. Gmelin, AED-CONF-65-190-3
CONF-650721–	**(Positron Annihilation Conference, Detroit, July 27–29, 1965)**	
6	20-37819	ORAU. Gmelin, AED-CONF-65-211-7
7	20-37816	ORAU. Gmelin, AED-CONF-65-211-3
8	20-37815	ORAU. Gmelin, AED-CONF-65-211-2
9	20-37821	ORAU. Gmelin, AED-CONF-65-211-6
10	20-38406	ORAU. Gmelin, AED-CONF-65-211-8
11	20-37820	ORAU. Gmelin, AED-CONF-65-211-4
12	20-37818	ORAU. Gmelin, AED-CONF-65-211-5
13	20-37817	ORAU. Gmelin, AED-CONF-65-211-13
16	20-36896	ORAU. Gmelin, AED-CONF-65-211-16
CONF-650802–	**(Cryogenic Engineering Conference, Houston, Tex., Aug. 23–25, 1965)**	
13	20-36993	ORAU. Gmelin, AED-CONF-65-193-23
CONF-650804–	**(5th Rare Earth Research Conference, Ames, Iowa, Aug. 30–Sept. 1, 1965)**	
24	20-36845	ORAU. Gmelin, AED-CONF-65-208-24
CONF-650813–	**(6th Biennial Gas Dynamics Symposium, Evanston, Ill., Aug. 27, 1965)**	
2	20-37986	ORAU. Gmelin, AED-CONF-65-216-7
CONF-650827–	**(Western Electronics Show and Conference, San Francisco, Aug. 24–27, 1965)**	
2	20-37124	ORAU. Gmelin, AED-CONF-65-213-2
CONF-650829–	**(American Society of Corrosion Engineers, Power Division Specialty Conference, Denver, Aug. 18–20, 1965)**	
2	20-38522	ORAU. Gmelin, AED-CONF-65-238-1
CONF-650838–	**(American Assn. for the Advancement of Science, 16th Alaska Science Conference, Juneau, Alaska, Aug. 30–Sept. 1, 1965)**	
1	20-37042	ORAU. Gmelin, AED-CONF-65-241-1
CONF-650904–	**(Symposium on Radiation Effects, Asheville, N. C., Sept. 8–10, 1965)**	
12	20-37299	ORAU. Gmelin, AED-CONF-65-226-7
13	20-37302	ORAU. Gmelin, AED-CONF-65-226-4
CONF-650922–	**20-17156**	**(1st International Symposium on Magnet Technology, Stanford, Calif., Sept. 8–10, 1965) Dep. mn. CFSTI $8.50 cy, $3.50 mn**
21	20-36982	ORAU. Gmelin, AED-CONF-65-285-3
22	20-37338	ORAU. Gmelin, AED-CONF-65-285-2
CONF-650927–	**(American Physical Society, Honolulu, Hawaii, Sept. 2–4, 1965)**	
6	20-37822	ORAU. Gmelin, AED-CONF-65-222-36
8	20-38334	ORAU. Gmelin, AED-CONF-65-222-30
11	20-37063	ORAU. Gmelin, AED-CONF-65-222-19
25	20-37277	ORAU. Gmelin, AED-CONF-65-222-49
28	20-38333	ORAU. Gmelin, AED-CONF-65-222-59
CONF-650932–	**20-34803**	**(Symposium on the Inelastic Scattering of Neutrons by Condensed Systems, Upton, N. Y., Sept. 1965) See BNL-940**
7	20-38005	ORAU. Gmelin, AED-CONF-65-292-3
10	20-38004	ORAU. Gmelin, AED-CONF-65-292-10
CONF-650948–	**(9th International Conference on Cosmic Rays, London, Sept. 6–17, 1965)**	
Vols. 1 & 2	20-37492	London, The Institute of Physics and The Physical Society, 1966. 10 Pound, 10s.
2	20-37713	pp 1041-4 of Proceedings of the Ninth International Conference on Cosmic Rays. Vol. 2
CONF-650961–	**(American Geophysical Union, 5th Western National Meeting, Dallas, Sept. 1–3, 1965)**	
6	20-37917	ORAU. Gmelin, AED-CONF-65-224-13
CONF-651009–	**20-38489**	**(Conference on Safety, Fuels and Core Design in Large Fast Power Reactors, Argonne, Oct. 11–14, 1965) See ANL-7120**
CONF-651015–	**(American Physical Society Meeting, Chicago, Oct. 7, 1965)**	
11	20-37126	ORAU. Gmelin, AED-CONF-65-312-28
13	20-38407	ORAU. Gmelin, AED-CONF-65-312-30
14	20-37125	ORAU. Gmelin, AED-CONF-65-312-36
CONF-651017–	**20-25495**	**(Electrochemical Society Meeting, Buffalo, Oct. 10–14, 1965) Electrochem. Technol., 4: 77-162(1966)**
Pt. 3	20-37171	Electrochem. Technol., 4: 289-377(1966)
CONF-651019–	**(15th Canadian Chemical Engineering Conference, Quebec City, Canada, Oct. 25, 1965)**	
4	20-37211	ORAU
5	20-38484	ORAU. Gmelin, AED-CONF-65-294-8
CONF-651023–	**(Symposium on Radioisotope Instruments in Industry and Geophysics, Warsaw, Oct. 18–22, 1965)**	
Vol.1	20-37139	See STI-PUB-112(Vol.1)
Vol.2	20-37133	See STI-PUB-112(Vol.2)
CONF-651025–	**(Symposium on Physical Metallurgy of Refractory Metals, French Lick, Ind., Oct. 3–5, 1965)**	
13	20-37274	ORAU. Gmelin, AED-CONF-65-375-18
CONF-651049–	**(IEEE Thermionic Conversion Specialist Conference, San Diego, Calif., Oct. 25–27, 1965)**	
20	20-37726	ORAU. Gmelin, AED-CONF-65-324-21
CONF-651062–	**(Metallurgical Society Fall Meeting, Detroit, Oct. 17–21, 1965)**	
2	20-37276	ORAU. Gmelin, AED-CONF-65-325-4
3	20-37275	ORAU. Gmelin, AED-CONF-65-325-5
4	20-37304	ORAU. Gmelin, AED-CONF-65-325-12
CONF-651071–	**(American Nuclear Society, New York State Inter-sectional Meeting, Buffalo, Oct. 23, 1965)**	
1	20-38523	ORAU. Gmelin, AED-CONF-65-356-2
CONF-651110–	**(American Society of Mechanical Engineers, Annual Winter Meeting, Chicago, Nov. 7–11, 1965)**	
29	20-38461	Dep. mn. CFSTI $1.00 cy, $0.50 mn
CONF-651118–	**(American Physical Society, Gatlinburg, Tenn., Nov. 11–13, 1965)**	
6	20-38184	ORAU. Gmelin, AED-CONF-65-329-2
7	20-38180	ORAU. Gmelin, AED-CONF-65-329-5
8	20-38179	ORAU. Gmelin, AED-CONF-65-329-12
12	20-38181	ORAU. Gmelin, AED-CONF-65-329-7
13	20-38178	ORAU. Gmelin, AED-CONF-65-329-10
14	20-38182	ORAU. Gmelin, AED-CONF-65-329-16
CONF-651126–	**(American Physical Society, 7th Annual Meeting of the Division of Plasma Physics, San Francisco, Nov. 8–11, 1965)**	
2	20-38332	ORAU. Gmelin, AED-CONF-65-353-1
CONF-651132–	**(Atomic Industrial Forum, 12th Annual Conference, Washington, D. C., Nov. 17, 1965)**	
3	20-36999	ORAU. Gmelin, AED-CONF-65-337-28
4	20-38541	ORAU. Gmelin, AED-CONF-65-337-22
5	20-38416	ORAU. Gmelin, AED-CONF-65-337-21
6	20-38524	ORAU. Gmelin, AED-CONF-65-337-3
CONF-651147–	**20-36897**	**(American Society for Testing Materials, 5th Pacific Area National Meeting, Seattle, Oct. 31–Nov. 5, 1965) Amer. Soc. Test. Mater., Spec. Tech. Pub., No. 400, 1-170(1966)**
CONF-651213–	**(American Physical Society, Winter Meeting in the West, Los Angeles, Dec. 20–22, 1965)**	
14	20-37929	ORAU. Gmelin, AED-CONF-65-400-30
CONF-660107–	**(American Physical Society Meeting, New York, Jan. 26–29, 1966)**	
51	20-38188	ORAU. Gmelin, AED-CONF-66-003-121
52	20-38173	ORAU. Gmelin, AED-CONF-66-003-114
53	20-38185	ORAU. Gmelin, AED-CONF-66-003-120
56	20-38177	ORAU. Gmelin, AED-CONF-66-003-132
58	20-38183	ORAU. Gmelin, AED-CONF-66-003-129

Report No.	Abstract No.	Availability
CONF-660204–		(American Nuclear Society Meeting, San Diego, Calif., Feb. 7–9, 1966)
17	20-38006	ORAU. Gmelin, AED-CONF-66-017-17
19	20-38455	ORAU. Gmelin, AED-CONF-66-017-14
CONF-660207–		(Radioisotope Applications in Aerospace Symposium, Dayton, Ohio, Feb. 15–17, 1966)
15	20-37064	ORAU. Gmelin, AED-CONF-66-011-17
CONF-660209–		(Conference on Intermediate Energy Physics, Williamsburg, Va., Feb. 9–11, 1966)
15	20-38186	ORAU. Gmelin, AED-CONF-66-023-18
17	20-37479	ORAU. Gmelin, AED-CONF-66-023-15
CONF-660212–		(Radiation Research Society. 14th Annual Meeting, Coronado, Calif., Feb. 13–16, 1966)
10	20-36576	ORAU. Gmelin, AED-CONF-66-016-10
CONF-660217–		(Symposium on Interdisciplinary Aspects of Radiative Energy Transfer, Philadelphia, Feb. 24–26, 1966)
4	20-38335	ORAU. Gmelin, AED-CONF-66-013-8
5	20-37881	ORAU. Gmelin, AED-CONF-66-013-9
CONF-660301–		(IEEE International Convention, New York, Mar. 21–25, 1966)
4	20-37727	ORAU. Gmelin, AED-CONF-66-052-3
CONF-660306–		(American Physical Society, Conference on Isobaric Spin, Tallahassee, Mar. 17–19, 1966)
11	20-37811	ORAU. Gmelin, AED-CONF-66-048-7
12	20-38174	ORAU. Gmelin, AED-CONF-66-048-8
CONF-660327–		(American Physical Society Meeting, Durham, N. C., Mar. 28–31, 1966)
2	20-38176	ORAU. Gmelin, AED-CONF-66-050-9
CONF-660411–		(American Physical Society Meeting, Washington, D. C., Apr. 25–28, 1966)
4	20-37812	ORAU. Gmelin, AED-CONF-66-060-16
5	20-37987	ORAU. Gmelin, AED-CONF-66-060-22
6	20-37813	ORAU. Gmelin, AED-CONF-66-060-31
9	20-38172	ORAU. Gmelin, AED-CONF-66-060-9
10	20-38408	ORAU. Gmelin, AED-CONF-66-060-7
11	20-38175	ORAU. Gmelin, AED-CONF-66-060-3
12	20-37814	ORAU. Gmelin, AED-CONF-66-060-30
13	20-38170	ORAU. Gmelin, AED-CONF-66-060-4
15	20-37273	ORAU. Gmelin, AED-CONF-66-060-46
33	20-37481	See COO-818-86
35	20-38187	ORAU. Gmelin, AED-CONF-66-060-117
CONF-660415–		(22nd Annual Conference of the National Assn. of Corrosion Engineers, Miami Beach, Apr. 1966)
2	20-37193	ORAU. Gmelin, AED-CONF-66-071-3
CONF-660420–		(International Conference on Two-Body Problems at High Energy, Stony Brook, N. Y., Apr. 22–23, 1966)
2	20-37743	See UCRL-16866
CONF-660426–		(8th Annual Symposium on Electron and Laser Beam Technology, Ann Arbor, Mich., Apr. 6–8, 1966)
1	20-37339	ORAU. Gmelin, AED-CONF-66-073-1
CONF-660430–		(Ohio Academy of Science, 75th Annual Meeting, Columbus, Ohio, Apr. 21–23, 1966)
4	20-38171	ORAU. Gmelin, AED-CONF-66-149-1
CONF-660436–		(Intermag Conference, Stuttgart, Germany, Apr. 1966)
1	20-37934	See BNL-10380
CONF-660438–		(International Quantum Electronics Conference, Phoenix, Ariz., Apr. 12–15, 1966)
3	20-38336	ORAU. Gmelin, AED-CONF-66-078-8
4	20-37298	ORAU. Gmelin, AED-CONF-66-078-7
CONF-660442–		(European Nuclear Energy Agency Seminar-Workshop on Computer Programs for Shielding Calculations, Ispra, Italy, Apr. 26–29, 1966)
1	20-38350	See ORNL-P-2310
CONF-660510–		(International Conference on Isochronous Cyclotrons, Gatlinburg, Tenn., May 2–5, 1966)
19	20-37320	Dep. mn. CFSTI $1.00 cy, $0.50 mn
CONF-660536–	20-38316	(Conference on Plasma Instabilities and Anomalous Transport, Coral Gables, Fla., May 2–4, 1966) $4.00
CONF-660540–		(Conference on Non-Compact Groups in Particle Physics, Milwaukee, Wis., May 4–6, 1966)
2	20-37823	See BNL-10387
CONF-660609–		(International Symposium on Food Irradiation Meeting, Karlsruhe, Germany, June 6–10, 1966)
12	20-37157	ORAU
13	20-37155	ORAU
29	20-37156	ORAU
CONF-660611–		(Society of Applied Spectroscopy Meeting, Chicago, June 14–15, 1966)
4	20-37480	ORAU. Gmelin, AED-CONF-66-172-1
CONF-660614–		(3rd International Congress on Radiation Research, Cortina, Italy, June 1966)
3	20-36857	See COO-1088-21
CONF-660620–		(International Symposium on Regulatory Mechanisms in Nucleic Acid and Protein Biosynthesis, Lunteren, Netherlands, June 5–10, 1966)
1	20-36578	See ORNL-P-2240
CONF-660621–		(Health Physics Society, 11th Annual Meeting, Houston, Tex., June 27–30, 1966)
9	20-37068	See BNL-10321
CONF-660625–		(IAEA Panel Meeting, Vienna, Austria, June 6–10, 1966)
2	20-37072	See KFK-429
CONF-660633–		(American Physical Society, Division of Plasma Physics, Minneapolis, Minn., June 1966)
1	20-38192	See COO-1233-32
CONF-660705–		(IEEE Annual Conference, Palo Alto, Calif., July 18–22, 1966)
1	20-37129	See SC-DC-66-1820
CONF-660713–		(6th International Symposium on Corpuscular Photography, Florence, Italy, July 19–23, 1966)
1	20-37077	See UCR-34P107-34)
CONF-660714–		(Institute for Defense Analysis Meeting, Santa Barbara, Calif., July 18–Aug. 10, 1966)
1	20-38198	See LA-DC-8099
CONF-660807–		(Symposium on Neutron Monitoring for Radiological Protection, Vienna, Austria, Aug. 29, 1966)
1	20-37070	See BNWL-SA-537
CONF-660808–		(13th International Conference on High Energy Physics, Berkeley, Calif., Aug. 31–Sept. 7, 1966)
1	20-37731	See BNL-10460
2	20-37732	See BNL-10461
3	20-37733	See BNL-10462
4	20-37730	See BNL-10459
CONF-660904–		(9th Air Cleaning Conference, Boston, Mass., Sept. 13–16, 1966)
1	20-37022	See LA-DC-6942
3	20-36976	See DP-MS-66-45
CONF-660905–		(36th International Congress on Industrial Chemistry, Brussels, Belgium, Sept. 13, 1966)
1	20-36926	See K-L-6091
CONF-660906–		(International Conference on Nuclear Physics, Gatlinburg, Tenn., Sept. 12–17, 1966)
7	20-38010	See BNL-10438
CONF-660907–		(American Chemical Society Meeting, New York, Sept. 11–16, 1966)
1	20-36785	See ORNL-P-2202
CONF-660911–		(Conference on Radiation Measurements in Nuclear Power, Berkeley, England, Sept. 12–16, 1966)

Report No.	Abstract No.	Availability
2	20-37076	See SC-DC-66-1512
CONF-660913–	**(International Conference on Nuclear Physics, Berkeley, Calif., Sept. 12–17, 1966)**	
1	20-38009	See BNL-10420
COO–		
7-395	20-38077	Phys. Rev., 148: 998-1002(1966)
818-86	20-37481	Dep. mn. CFSTI $1.00 cy, $0.50 mn
818-87	20-37734	Dep. mn. CFSTI $3.00 cy, $0.75 mn
818-96	20-37735	Dep. mn. CFSTI $2.00 cy, $0.50 mn
1088-21	20-36857	Dep. mn. CFSTI $2.00 cy, $0.75 mn.
1098-14	20-37959	Phys. Rev. Lett., 17: 255-7(1966)
1119-5	20-36605	Dep. mn. CFSTI $3.00 cy, $0.50 mn
1198-331	20-37970	Rev. Sci. Instrum., 37: 1024-9(1966)
1198-371	20-37961	Phys. Rev. Lett., 17: 367-72(1966)
1233-32	20-38192	Dep. mn. CFSTI $1.00 cy, $0.50 mn
1297-7	20-37736	Dep. mn. CFSTI $3.00 cy, $0.75 mn
1297-8	20-37737	Dep. mn. CFSTI $3.00 cy, $0.75 mn
DC-TN–	**(Non-AEC)**	
1050-1	20-36995	See AD-636794
DL–	**(Canadian)**	
69	20-38487	See AECL-2584
DOCKET	**(Misc.)**	
50-235	20-38530	See GA-6078
DP–		
993	20-37071	Dep. mn. CFSTI $1.00 cy, $0.50 mn
1025	20-37160	Dep. mn. CFSTI $3.00 cy, $0.75 mn
DP-MS–		
66-45	20-36976	Dep. mn. CFSTI $1.00 cy, $0.50 mn
DRI–	**(Misc.)**	
2327	20-36957	Dep. mn. CFSTI $3.00 cy, $0.75 mn
DSR–	**(Misc.)**	
5003	20-36988	See TID-23261
DUBNA REPORTS	**(Russian)**	
See JINR (Russian)		
ECOM–	**(Non-AEC)**	
01304-4	20-36784	See AD-636054
EGG–		
1183-1164	20-37939	J. Appl. Phys., 37: 3297-3300(1966)
ELI–	**(Canadian)**	
70	20-37066	See AECL-2536
EUR–	**(European Atomic Energy Community)**	
2040	20-36985	See EURAEC-1088
2522.f	20-38480	Dep. mn
2854	20-38502	See EURAEC-1662
2855	20-38503	See EURAEC-1663
2856	20-38504	See EURAEC-1664
2864	20-38505	See EURAEC-1672
EURAEC–		
1088	20-36985	Dep. mn. CFSTI $4.00 cy, $0.75 mn
1657	20-36986	See GEAP-5073
1658	20-38443	See GEAP-5148
1662	20-38502	Dep. mn. CFSTI $2.00 cy, $0.50 mn
1663	20-38503	Dep. mn. CFSTI $2.00 cy, $0.50 mn
1664	20-38504	Dep. mn. CFSTI $2.00 cy, $0.50 mn
1672	20-38505	Dep. mn. CFSTI $1.00 cy, $0.50 mn
FTI–	**(Non-AEC)**	
244/T-027	20-38354	Dep. mn.
GA–	**(Misc.)**	
6078	20-38530	Dep. mn. CFSTI $3.00 cy, $0.75 mn
6415	20-36799	Carbon, 4: 99-106(1966)
6439	20-37196	Carbon, 4: 51-8(1966)
6946	20-38266	Phys. Fluids, 9: 1437-41(1966)
GEAP–	**(Misc.)**	
4929	20-38462	Dep. mn. CFSTI $2.00 cy, $0.50 mn
5073	20-36986	Dep. mn. CFSTI $3.00 cy, $0.75 mn
5133	20-38531	Dep. mn. CFSTI $2.00 cy, $0.50 mn
5148	20-38443	Dep. mn. CFSTI $1.00 cy, $0.50 mn
HW–		
82771(Pt.3)	20-36925	Dep. mn. CFSTI $2.00 cy, $0.50 mn
I–	**(Misc.)**	
A2049-27	20-36980	See TID-23270
IC–	**(Misc.)**	
66/89	20-37738	Dep. mn
IDO–		
17151	20-37167	Dep. mn. CFSTI $6.00 cy, $1.25 mn
IFA-CR–	**(Rumanian)**	
73	20-36858	Dep. mn
IITRI–	**(Misc.)**	
578P22-15	20-38463	Dep. mn. CFSTI $4.00 cy, $0.75 mn
INDEC-SR–	**(Non-AEC)**	
5	20-37722	See N-65-30843
7	20-37721	
IPST-Cat.–	**(Russian)**	
1429	20-37745	For translation see TT-65-50130
IS–		
1335	20-36712	Dep. mn. CFSTI $4.25 cy, $1.75 mn
ITEF–	**(Russian)**	
355	20-38355	Dep. mn
406	20-38412	Dep. mn
JINR–	**(Russian)**	
E-2726	20-37739	Dep. mn
P-2699	20-38444	Dep. mn
P-2780	20-37740	Dep. mn
P-2783-2	20-38196	Dep. mn
P-2788	20-37741	Dep. mn
P-2805	20-38011	Dep. mn
P-2806	20-38012	Dep. mn
JNPC-RKWP–	**(British)**	
P344	20-38446	See TRG-Report-1138
K-L–		
6091	20-36926	Dep. mn. CFSTI $2.00 cy, $0.50 mn
K-OA–		
1313	20-37161	Dep. mn. CFSTI $3.00 cy, $0.75 mn
KFK–	**(German)**	
429	20-37072	Dep. mn
LA–		
3402	20-36713	Dep. mn. CFSTI $1.00 cy, $0.50 mn
3509	20-37307	Dep. mn. CFSTI $4.00 cy, $1.00 mn
3510	20-38356	Dep. mn. CFSTI $5.00 cy, $1.00 mn
3553	20-38197	Dep. mn. CFSTI $2.00 cy, $0.50 mn
LA-DC–		
6942	20-37022	Dep. mn. CFSTI $1.00 cy, $0.50 mn
7305	20-36554	Dep. mn. CFSTI $2.00 cy, $0.50 mn
7382	20-37224	Carbon, 4: 81-4(1966)
7467	20-38306	Rev. Sci. Instrum., 37: 1065-8(1966)
7750	20-37873	Phys. Rev., 148: 108-24(1966)
7836	20-38097	Phys. Rev., 148: 1226-34(1966)
7991	20-38063	Phys. Lett., 22: 162-4(1966)
8099	20-38198	Dep. mn. CFSTI $2.00 cy, $0.50 mn
MATT–		
380	20-38243	J. Nucl. Energy, Pt. C, 8: 361-72(1966)
400	20-38199	Dep. mn. CFSTI $3.00 cy, $0.75 mn
433	20-38283	Phys. Fluids, 9: 1605-6(1966)
434	20-38250	J. Opt. Soc. Amer., 56: 1179-88(1966)
MIT–	**(Misc.)**	
2098-250	20-37773	Phys. Lett., 22: 239-40(1966)

Report No.	Abstract No.	Availability
N–	**(Misc.)**	
65-30843	20-37722	CFSTI $3.00 cy, $0.75 mn
65-31239	20-37825	Dep. mn
65-33865	20-37023	CFSTI $1.00 cy, $0.50 mn
66-13499	20-36846	CFSTI $1.00 cy, $0.50 mn
66-17354	20-37341	CFSTI $1.00 cy, $0.50 mn
66-17678	20-36915	CFSTI $1.50 cy, $1.25 mn
NAA-SR–		
11944	20-36977	Dep. mn. CFSTI $2.00 cy, $0.50 mn
11949	20-36987	Dep. mn. CFSTI $3.00 cy, $0.75 mn
12001	20-36978	Dep. mn. CFSTI $1.00 cy, $0.50 mn
NASA-CR–	**(Misc.)**	
54995	20-38447	See WCAP-2867
64303	20-37722	See N-65-30843
64997	20-37023	See N-65-33865
70375	20-37341	See N-66-17354
NASA-TM–	**(Misc.)**	
X-57034	20-36846	See N-66-13499
X-57037	20-36859	See N-66-13497
NASA-TN–	**(Misc.)**	
D-3555	20-38532	CFSTI $1.00 cy, $0.50 mn
NDA–	**(Misc.)**	
2143-7	20-38506	Dep. mn. CFSTI $2.00 cy, $0.50 mn
NDA-Memo–	**(Misc.)**	
2143-11	20-38507	Dep. mn. CFSTI $1.00 cy, $0.50 mn
NLCO–		
899	20-37024	Dep. mn. CFSTI $1.00 cy, $0.50 mn
NP–	**(AEC File No. for Non-AEC Reports)**	
16150	20-36860	Dep. mn
16168(Pt.A)	20-38533	Dep. mn
16168(Pt.B)	20-38534	Dep. mn
16201	20-37073	Dep. mn
16202	20-37074	Dep. mn
16204	20-37075	Dep. mn
16205	20-37321	Dep. mn
16206	20-38200	Dep. mn
16210	20-38201	
16226	20-37308	Dep. mn
16231	20-37826	
16236	20-38202	
16237	20-38203	
16240	20-38204	National Bureau of Standards Free
NSAM–	**(Non-AEC)**	
933	20-37023	See N-65-33865
NUS–	**(Misc.)**	
208	20-38525	Dep. mn. CFSTI $3.00 cy, $0.75 mn
NYO–		
1864-23	20-36606	Dep. mn. CFSTI $1.00 cy, $0.50 mn
1932-106	20-37782	Proc. Phys. Soc. (London), 88: 909-13 (1966)
2643-22	20-36555	Dep. mn. CFSTI $3.00 cy, $0.50 mn
2764-2	20-38508	Dep. mn. CFSTI $7.00 cy, $1.75 mn
3038-1	20-37604	pp 609-15 of Proceedings of the Ninth International Conference on Cosmic Rays. Vol. 2
3330-11	20-37280	Dep. mn. CFSTI $4.00 cy, $0.75 mn
3525-7	20-38085	Phys. Rev., 148: 1133-6(1966)
3565-4	20-38205	Dep. mn. CFSTI $1.00 cy, $0.75 mn
ORNL–		
3972	20-36979	Dep. mn. CFSTI $1.00 cy, $0.50 mn
ORNL-P–	**(Misc.)**	
1203	20-38096	Phys. Rev., 148: 1221-6(1966)
1539	20-38206	Dep. mn. CFSTI $1.00 cy, $0.50 mn
1622	20-36568	Nature, 211: 96-7(1966)
1635	20-36610	Biochim. Biophys. Acta, 123: 26-33(1966)
1675	20-37232	Electrochem. Technol., 4: 322-9(1966)
1763	20-38274	Phys. Fluids, 9: 1498-1503(1966)
1870	20-36551	Radiat. Bot., 6: 307-11(1966)
1914	20-37919	J. Chem. Phys., 45: 1142-4(1966)
1947	20-38391	Phys. Rev., 148: 350-2(1966)
1979	20-36802	Inorg. Chem., 5: 1337-44(1966)
2016	20-37266	Trans. Met. Soc. AIME, 236: 1104-6(1966)
2019	20-38364	J. Appl. Phys., 37: 3145-52(1966)
2066	20-38291	Phys. Rev., 148: 97-103(1966)
2092	20-38092	Phys. Rev., 148: 1174-91(1966)
2202	20-36785	Dep. mn. CFSTI $1.00 cy, $0.50 mn
2240	20-36578	Dep. mn. CFSTI $2.00 cy, $0.50 mn
2270	20-37175	Phys. Status Solidi, 16: K63-5(1966)
2310	20-38350	Dep. mn. CFSTI $1.00 cy, $0.50 mn
ORNL-TM–		
1449	20-38509	Dep. mn. CFSTI $1.00 cy, $0.50 mn
1543	20-36927	Dep. mn. CFSTI $2.00 cy, $0.50 mn
1558	20-36786	Dep. mn. CFSTI $1.00 cy, $0.50 mn
ORO–		
649	20-38510	Dep. mn. CFSTI $5.00 cy, $1.00 mn
2915-60	20-38064	Phys. Lett., 22: 164-6(1966)
PAEC(A)IN–	**(Philippines)**	
652	20-38540	Dep. mn
PATENTS	**(Canadian)**	
733,890	20-37181	
PATENTS	**(German)**	
1,213,629	20-37194	
1,216,447	20-38337	
1,219,255	20-36779	
PATENTS	**(Japanese)**	
1965-6680	20-36943	
1965-8911	20-36906	
1965-9630	20-36907	
1965-9964	20-36908	
1965-19193	20-36914	
PATENTS	**(U. S.)**	**($0.50 each, U. S. Patent Office)**
3,254,564	20-37340	
3,258,401	20-38341	
3,258,618	20-37728	
3,258,633	20-38340	
3,260,466	20-36955	
3,260,574	20-36956	
3,262,274	20-38539	
3,262,760	20-37212	
3,262,860	20-38485	
3,263,082	20-37021	
3,265,152	20-37158	
3,265,583	20-38339	
3,265,967	20-38338	
3,267,307	20-37729	
3,268,758	20-37065	
PG-Report–	**(British)**	
705	20-37025	Dep. BIS $0.30, HMSO 1s. 6d.
PNE–		
511	20-36958	Dep. mn. CFSTI $1.50 cy, $0.50 mn
603F	20-36959	Dep. mn. CFSTI $2.00 cy, $0.75 mn
717F	20-36960	Dep. mn. CFSTI $2.00 cy, $0.75 mn
PNRO-SMD–		
137	20-37026	Dep. mn. CFSTI $2.00 cy, $0.50 mn
PPL-AF–	**(Non-AEC)**	
1	20-38207	
2	20-37865	
4	20-38208	
5	20-38209	
PR-P–	**(Canadian)**	
67	20-38008	See AECL-2595
R–	**(Misc.)**	
424	20-37306	See AD-636408
RLO–		
1388-1	20-38080	Phys. Rev., 148: 1024-30(1966)
1921-7	20-38088	Phys. Rev., 148: 1151-6(1966)
1921-8	20-38029	Nucl. Phys., 85: 513-18(1966)

Report No.	Abstract No.	Availability
RT-FI–	**(Italian)**	
(66)1	20-38445	Dep. mn
SC-CR–		
66-2045	20-36996	Dep. mn. CFSTI $2.00 cy, $0.50 mn
66-2057	20-36957	See DRI-2327
SC-DC–		
66-1512	20-37076	Dep. mn. CFSTI $1.00 cy, $0.50 mn
66-1820	20-37129	Dep. mn. CFSTI $2.00 cy, $0.50 mn
SLAC-PUB–		
166	20-37046	J. Appl. Phys., 37: 3321-2(1966)
STI-PUB.–	**(International Atomic Energy Agency)**	
112(Vol.1)	20-37139	IAEA: $12.00; S252,-; £3.12.0; F Fr 48,-; DM 42,-
112(Vol.2)	20-37133	IAEA: $10.00; S210,-; £3.0.0; F Fr 40,-; DM 35,-
TH–	**(Non-AEC)**	
101	20-37825	See N-65-31239
TID–		
22346	20-38051	Nucl. Phys., 86: 130-44(1966)
22348	20-38050	Nucl. Phys., 86: 119-29(1966)
22721	20-37054	Rev. Sci. Instrum., 37: 1014-18(1966)
22778	20-38054	Nucl. Phys., 86: 187-92(1966)
22818	20-38053	Nucl. Phys., 86: 167-86(1966)
23036	20-36548	Dep. mn. CFSTI $2.00 cy, $0.50 mn
23114	20-36607	Dep. mn. CFSTI $1.00 cy, $0.50 mn
23261	20-36988	Dep. mn. CFSTI $4.00 cy, $1.00 mn
23270	20-36980	Dep. mn. CFSTI $3.00 cy, $0.50 mn
TRG–	**(Misc.)**	
66-22	20-38441	See BAW-3492-1(Suppl.1)
TRG-Report–	**(British)**	
1049	20-37236	Electrochem. Technol., 4: 358-65(1966)
1138	20-38446	Dep. BIS $1.70. HMSO 8s. 6d.
TT–	**(Canadian)**	
65-50130	20-37745	CFSTI $8.20 cy, $2.25 mn
UCID–		
4548(Rev.4)	20-37000	Dep. mn. CFSTI $1.00 cy, $0.50 mn
UCR–		
34P107-34	20-37077	Dep. mn. CFSTI $1.00 cy, $0.50 mn
UCRL–		
7701	20-38094	Phys. Rev., 148: 1198-1205(1966)
7701(Rev.1)	20-38094	See UCRL-7701
12229	20-36961	Dep. mn. CFSTI $1.00 cy, $0.50 mn
12455(Rev.1)	20-38210	Dep. mn. CFSTI $1.00 cy, $0.50 mn
14280(Rev.1)	20-36970	J. Geophys. Res., 71: 3507-21(1966)
14330	20-36975	World Mining, 18: No. 10, 53-63(1965)
14365	20-37827	Dep. mn. CFSTI $1.00 cy, $0.50 mn
14468	20-38273	Phys. Fluids, 9: 1496-7(1966)
14500	20-38093	Phys. Rev., 148: 1192-8(1966)
14502(Rev.1)	20-37200	Int. J. Powder Met., 2: No. 3, 49-57(1966)
14695	20-38393	Phys. Rev., 148: 413-19(1966)
14731	20-38082	Phys. Rev., 148: 1063-71(1966)
16042(Rev.)	20-37483	J. Geophys. Res., 71: 3817-34(1966)
16163	20-38027	Nucl. Phys., 85: 481-503(1966)
16260(Rev.)	20-37053	Rev. Sci. Instrum., 37: 1007-10(1966)
16293	20-37742	Dep. mn. CFSTI $1.00 cy, $0.50 mn
16610	20-38275	Phys. Fluids, 9: 1503-13(1966)
16687	20-36619	Genetics, 54: 267-76(1966)
16752	20-36805	Inorg. Chem., 5: 1466-8(1966)
16866	20-37743	Dep. mn. CFSTI $1.00 cy, $0.50 mn
UJV–	**(Czechoslovakian)**	
1553	20-36861	Dep. mn
UR–		
875-110	20-37830	Ann. Phys. (N. Y.), 38: 377-91(1966)
875-151	20-37744	Dep. mn. CFSTI $4.00 cy, $1.00 mn
875-150	20-37772	Phys. Lett., 22: 236-8(1966)
WAPD-T–		
1859	20-37289	Nucl. Appl., 2: 106-15(1966)
WAPD-TM–	**(Misc.)**	
492	20-36989	Dep. mn. CFSTI $2.00 cy, $0.50 mn
572	20-37988	ORAU
573	20-37989	Dep. mn. CFSTI $1.00 cy, $0.50 mn
WCAP–	**(Misc.)**	
2867	20-38447	
WW–	**(Dutch)**	
015-R95	20-38503	See EURAEC-1663
016-R93	20-38502	See EURAEC-1662
WWO–	**(Misc.)**	
15-R96	20-38504	See EURAEC-1664
15-R100	20-38505	See EURAEC-1672
Y–		
1546	20-36981	Dep. mn. CFSTI $1.00 cy, $0.50 mn
YALE–		
2723-1(Vol.1)	20-36787	Dep. mn. CFSTI $7.00 cy, $1.50 mn
2723-1(Vol.2)	20-36788	Dep. mn. CFSTI $7.00 cy, $1.75 mn

DEPOSITORIES OF USAEC REPORTS

In Countries Other than the U.S.

ARGENTINA
Buenos Aires, Comisión Nacional de Energía Atómica
AUSTRALIA
Canberra, Australian National Library
Sutherland, New South Wales, Australian Atomic Energy Commission
AUSTRIA
Vienna, Zentral Bibliothek der Physikalischen Institute der Universität
BELGIUM
Mol-Donk, Centre d'Etude de l'Energie Nucleaire
BOLIVIA
La Paz, Comisión Nacional de Energia Nuclear
BRAZIL
Rio de Janeiro, Instituto Brasileiro de Bibliografia e Documentacao
São Paulo, Instituto de Energia Atomica, Cidade Universitaria São Paulo
BURMA
Rangoon, Union of Burma Applied Research Institute, Atomic Energy Center Library
CANADA
Hamilton, McMaster University
Ottawa, National Research Council Library
Vancouver, University of British Columbia
CHILE
Santiago, Departamento de Fisica, Universidad de Chile
CHINA
Hsinchu, Taiwan, Free China, National Tsing Hua University
COLOMBIA
Bogota, Instituto De Asuntos Nucleares
COSTA RICA
San Pedro, University of Costa Rica Library
DENMARK
Risö, Danish Atomic Energy Commission
ECUADOR
Quito, Escuela Politécnica Nacional
EL SALVADOR
San Salvador, Universidad de El Salvador, Biblioteca de Energia Nuclear
FINLAND
Helsinki, Teknillisen Korkeakoulun Kirjasto
FRANCE
Gif-sur-Yvette, Centre d'Etudes Nucléaires de Saclay
Paris, Académie des Sciences
GERMANY
Berlin, Hahn-Meitner-Institut für Kernforschung Berlin
Frankfurt/Main, Gmelin-Institut
Munich, Technische Hochschule, Bibliothek
GHANA
Accra, University College of Ghana
GREECE
Athens, Nuclear Research Center "Democritus"
GUATEMALA
Guatemala, Comisión Nacional de Energía Nuclear
INDIA
Bombay, Department of Atomic Energy
IRAN
Tehran, Tehran University Nuclear Centre
IRAQ
Baghdad, Iraqi Atomic Energy Commission
IRELAND
Dublin, University College
ISRAEL
Rehovoth, Israel Atomic Energy Commission
ITALY
Rome, Centro di Studi Nucleari della Casaccia
Rome, Comitato Nazionale per l'Energia Nucleare
JAPAN
Tokyo, National Diet Library
KOREA
Seoul, Office of Atomic Energy
LEBANON
Beirut, Lebanese National Council for Scientific Research
LUXEMBOURG
Luxembourg, Ministry of Transport and Electricity
MALAYSIA
Kuala Lumpur, University of Malaysia
MEXICO
Mexico, D.F., Comisión Nacional de Energía Nuclear
NETHERLANDS
The Hague, Reactor Centrum Nederland
NEW ZEALAND
Lower Hutt, Institute of Nuclear Sciences
NIGERIA
Ibadan, University of Ibadan
NORWAY
Lillestrom, Institutt för Atomenergi
PAKISTAN
Lahore, West Pakistan, Atomic Energy Centre
PERU
Lima, Junta de Control de Energia Atomica
PHILIPPINE REPUBLIC
Manila, Philippine Atomic Energy Commission
POLAND
Warsaw, Biura Pelnomocnika Rzadu do Spraw Wykorzystania Energii Jadrowej
PORTUGAL
Sacavem, Junta de Energía Nuclear
REPUBLIC OF SOUTH AFRICA
Pretoria, Atomic Energy Board Library
REPUBLIC OF THE CONGO
Leopoldville, Université Lovanium
SPAIN
Madrid, Junta de Energía Nuclear, Biblioteca Documentación y Publicaciones, Ciudad Universitaria
SWEDEN
Nyköping, Aktiebolaget Atomenergi
SWITZERLAND
Zürich, Eidgenössische Technische Hochschule, Bibliothek
THAILAND
Bangkok, Office of the Thai Atomic Energy Commission, Department of Science
TURKEY
Ankara, Turkish Atomic Energy Commission, Atomic Energy Library
UNITED ARAB REPUBLIC
Cairo, Atomic Energy Commission
UNITED KINGDOM
Birmingham, Central Library
Boston Spa, National Lending Library for Science and Technology
Kingston upon Hull, Central Library
Liverpool, Central Library
London, Central Library, Acton
London, National Reference Library
London, Science Museum Library, South Kensington
Manchester, Central Library
Newcastle upon Tyne, Central Library
Nottingham, Central Library
Sheffield, Central Library
URUGUAY
Montevideo, Comision Nacional de Energia Atomica
VENEZUELA
Caracas, Instituto Venezolano de Investigaciones Científicas
VIET-NAM
Saigon, Atomic Energy Office
YUGOSLAVIA
Belgrade, Federal Commission for Nuclear Energy

In International Agencies

AUSTRIA
Vienna, International Atomic Energy Agency
BELGIUM
Brussels, La Bibliotheque EURATOM
FRANCE
Paris, European Nuclear Energy Agency, O.E.C.D.
ITALY
Ispra, EURATOM Research Center
SWITZERLAND
Geneva, United Nations Library

UNITED STATES
GOVERNMENT PRINTING OFFICE
DIVISION OF PUBLIC DOCUMENTS
WASHINGTON, D.C. 20402

OFFICIAL BUSINESS

POSTAGE AND FEES PAID
U.S. GOVERNMENT PRINTING OFFICE

TECHNICAL PROGRESS REVIEWS

The Division of Technical Information, U. S. Atomic Energy Commission, also publishes the Technical Progress Reviews, a series of five quarterly journals on nuclear technology. These journals, compiled by specialists and recognized authorities, summarize, evaluate, and reference the progress of development in five important fields.

Isotopes and Radiation Technology P. S. Baker, A. F. Rupp, and associates, Oak Ridge National Laboratory. Reviews AEC-sponsored projects and related significant worldwide developments in radioisotopes and radiation technology.

Nuclear Safety Wm. B. Cottrell, W. H. Jordan, and associates, Oak Ridge National Laboratory. Covers topics relevant to the analysis and control of hazards associated with nuclear reactors and with operations involving fissionable materials and the products of nuclear fission.

Power Reactor Technology Argonne National Laboratory. Reviews research, development, design practices, and operating experiences associated with power reactors, including aerospace applications.

Reactor Fuel Processing Stephen Lawroski and associates, Argonne National Laboratory. Reviews all aspects of the fuel-processing field, including aqueous and nonaqueous processing and waste disposal.

Reactor Materials R. W. Dayton, E. M. Simons, and associates, Battelle Memorial Institute. Covers the properties, behavior, and fabrication processes of materials used in nuclear reactors and associated equipment.

Availability

SUBSCRIPTION RATE: The Technical Progress Reviews may be purchased from the Superintendent of Documents, U. S. Government Printing Office, Washington, D. C. 20402, at $2.50 per year for each subscription or $0.70 per issue.

POSTAGE: Postpaid within the United States, Canada, Mexico, and all Central and South American countries except Argentina, Brazil, British and French Guiana, Surinam, and British Honduras. For these Central and South American countries and all other countries, add $0.75 per year or $0.20 per single issue.

REMITTANCE: Payment should be by check, money order, or document coupons and MUST accompany order. Remittances from foreign countries should be made by international money order or draft on an American bank payable to the Superintendent of Documents or by UNESCO book coupons.